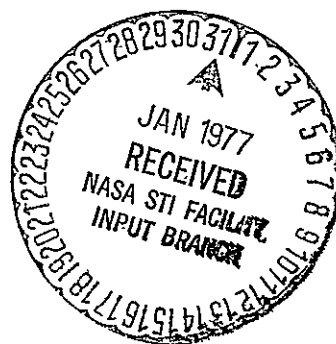


INITIAL TECHNICAL, ENVIRONMENTAL AND ECONOMIC EVALUATION OF SPACE SOLAR POWER CONCEPTS

VOLUME II - DETAILED REPORT

(NASA-TM-X-74310) INITIAL TECHNICAL ENVIRONMENTAL, AND ECONOMIC EVALUATION OF SPACE SOLAR POWER CONCEPTS. VOLUME 2: DETAILED REPORT (NASA) 908 p HC A99/MF A01
N77-16443
Unclas
CSCI 10A G3/44 11523

AUGUST 31, 1976



National Aeronautics and Space Administration
LYNDON B. JOHNSON SPACE CENTER
Houston, Texas

INITIAL TECHNICAL, ENVIRONMENTAL AND ECONOMIC
EVALUATION OF SPACE SOLAR POWER CONCEPTS

Lyndon B. Johnson Space Center
Houston, Texas

VOLUME I - SUMMARY

VOLUME II - DETAILED REPORT

INITIAL TECHNICAL, ENVIRONMENTAL AND ECONOMIC
EVALUATION OF SOLAR POWER SATELLITES

VOLUME II - DETAIL REPORT

- I. INTRODUCTION
- II. SUMMARY AND CONCLUSIONS
- III. PROGRAM REQUIREMENTS
 - A. Projected Energy Demand
 - B. Implementation Scenarios
- IV. POWER STATION
 - A. System Analysis
 - 1. Efficiencies
 - 2. MPTS/MRCS Analysis
 - 3. Orbit Considerations
 - 4. Configurations
 - 5. Mass Properties
 - B. Solar Energy Collection System
 - 1. Solar Array
 - a. Solar Cell Technology
 - b. Solar Cell Blankets and Concentrators
 - c. Alternate Energy Conversion Concepts
 - 2. Power Distribution
 - 3. Structure
 - 4. Attitude and Orbit Control
 - 5. Instrumentation, Control and Communications
 - 6. Maintenance Station
 - C. Microwave Power Transmission System
 - 1. Antenna Array
 - 2. Microwave Generators
 - a. Microwave Generators
 - b. Radio Frequency Interference

3. Subarrays
4. Phase Control
5. Pointing Control
6. Power Distribution
7. Structure
8. Rotary Joint
9. Thermal Control

D. Microwave Reception and Conversion System

1. Rectenna
 - a. Rectenna
 - b. Structural Support and Ground Preparation
2. Grid Interface

E. Operations

F. Unit Costs

APPENDIX - Comparison Study of Thermal Engine (Brayton Cycle)
and Photovoltaic SPS Design Concepts

V. SPACE CONSTRUCTION AND MAINTENANCE SYSTEM

A. System Requirements and Analysis

APPENDIX 1 - Construction Studies

APPENDIX 2 - Consideration of Joining Processes for Construction

APPENDIX 3 - Proposed Construction Experiment for Shuttle OFT Flight

B. Construction Base

1. Construction and Manufacturing Facility
2. Orbital Construction and Support Equipment
3. Logistics Facility
4. Integration Management Facility
5. Crew Habitability Facilities
6. Construction Base Configuration Evaluation

C. Construction Operations

APPENDIX 1 - SPS Orbital Construction Organization

VI. SPACE TRANSPORTATION SYSTEMS

A. System Requirements and Analysis

B. Heavy Lift Launch Vehicles

1. Summary
2. Modified Single Stage to Orbit Vehicles
3. Winged Launch Vehicle
4. Two Stage Ballistic Vehicle

C. Personnel and Priority Cargo Vehicle

D. Cargo Orbital Transfer Vehicle

E. Personnel Orbital Transfer Vehicles

F. Summary of Projected Transportation System Characteristics

VII. INTEGRATED OPERATIONS

A. System Requirements and Analysis

B. Program Model

C. Mission Management Concept

D. Mission Management Functions

E. Key Considerations and Areas for Further Investigation

VIII. ENVIRONMENTAL CONSIDERATIONS

A. Methodology

B. Environmental Questions

C. Comparisons with Conventional Systems

IX. MANUFACTURING CAPACITY, NATURAL RESOURCES, TRANSPORTATION AND ENERGY CONSIDERATIONS

A. Requirements

B. Manufacturing Capacity

C. Natural Resources

D. Surface Transportation

E. Energy Payback

APPENDIX - Material Summary

X. PROGRAM DEVELOPMENT PLAN

- A. Program Phasing
- B. System Development and Exploration
- C. Technology Advancement Phase
- D. System Development
- E. Program Costs

XI. PROGRAM COST AND ECONOMIC ANALYSIS

- A. Methodology
- B. SPS Costs
- C. Comparison with Conventional and Other Advanced Systems
- D. Summary Remarks

APPENDIX A - Terrestrial Solar Power

APPENDIX B - Cost Sensitivity Analysis

INITIAL TECHNICAL, ENVIRONMENTAL AND ECONOMIC
EVALUATION OF SPACE SOLAR POWER CONCEPTS

VOLUME II - DETAILED REPORT

I. INTRODUCTION

The requirements for energy in the U.S. and the world will continue to increase to support a growing population and to improve the quality of life for that population. Projections indicate the U.S. requirements will grow by a factor of two to three between now and the Year 2000.

The manner in which we will meet this requirement is not clear. Oil and gas are expected to be depleted within decades. Fuel for the present class of nuclear reactor systems will also be depleted in the same timeframe. The breeder reactor system, when successfully developed, will greatly extend the natural fuel resource but presents continuing safety and environmental concerns, not the least of which is the disposal of nuclear waste as it accumulates from large-scale nuclear energy production. Fusion reactor systems also have potential, but these require significant scientific advances. Coal resources appear sufficient for several hundreds of years. The environmental concerns associated with mining coal, and the subsequent problems or costs in reducing air pollution to an acceptable level during its use, are well known. The logistics of a greatly expanded coal industry is also a significant although not unsolvable consideration.

In view of the problems or concerns related to obtaining the required energy from oil, gas, nuclear and coal sources, the nation is actively pursuing alternate sources of energy for the future. Solar energy is an obvious candidate for consideration. Solar energy is inexhaustible and clean and the increasing costs of other sources will make solar energy more attractive in the future. The use of solar energy collected on the earth has several basic limitations, however, which will tend to inhibit its widespread use. At any given location on the earth, a solar collector will be limited by such factors as the day-night cycle, cloud cover and atmospheric attenuation. The day-night cycle particularly requires the use of expensive storage capacity or limits the solar application by requiring additional power sources.

A concept has been presented ("Power from the Sun: Its Future," Dr. Peter E. Glaser, Amer. Assn. Advan. Sci., Vol. 162, 22 November 1968, pp. 857-61) which is intended to alleviate limitations associated with the collection of solar energy on earth. This concept involves placing large solar power satellites in geosynchronous orbit and beaming microwave energy down to collection stations on the earth. Some of the advantages of this concept are that the satellite is in near-continuous

sunlight which is not attenuated by the atmosphere; no electrical storage facilities are required; the land use requirement is reduced by a factor of 5 to 10; and the ground power output can be located near the user rather than in desert-type regions.

The space concept, while having advantages, also introduces new requirements. These include the need for transportation of the power station into space and the transmission of power from space to earth by microwave radiation.

Several studies conducted in the past few years have been directed toward exploring the feasibility of the concept. The results of these studies have generally been favorable, while reflecting a need for significant technological advancement if the concept is to be economically competitive with ground-based systems.

Critical areas were identified during the course of these studies and research and development programs have begun to be formulated to investigate these areas. A particular effort was conducted at the Johnson Space Center during the summer of 1975 to evaluate the need and feasibility of a Space Solar Power Development Laboratory. The study was done in support of the NASA "Outlook for Space" study and was documented in JSC-09991. Possible requirements for a development laboratory or "pilot plant" type solar power satellite were evaluated and the technical feasibility of such a plant was established.

In view of past study results, the six-week study, and the conclusions of the "Outlook for Space" study, it was decided to implement at JSC a more detailed study of the Space Power Concept. This document (Volume II) contains the detailed results of that study. Volume I presents a summary of the study results. The study was conducted between September 1975 and June 1976, by JSC personnel. The principle authors of each sub-section are identified by name and JSC organization.

The general objectives of Solar Power Satellite (SPS) studies include:

1. Establishment of realistic technical and economic design criteria and requirements for a full scale SPS.
2. Definition of technology development and flight test programs necessary to achieve the optimum SPS design.
3. Comparison of the SPS with other energy generation options to establish the relative economic, environmental, and social advantages/disadvantages of the SPS concept.

These objectives are quite broad and definitive answers will require a number of years of study augmented by technology efforts in a number of areas. Nevertheless, the present study provides further insight into a

number of aspects of the concept and provides a point of departure for further work. The summary (Volume I) presents a number of preliminary conclusions and a synopsis of the more detailed studies which are presented in Volume II.

Certain programmatic guidelines were chosen to initiate the study based on deployment of the first operational SPS as early as 1990.

a. Program plans and technology projections will be developed based on deployment of the first operational SPS as early as 1990.

b. The capability will be provided as early as 1995 to deploy two to four SPS per year.

c. Dedicated transportation systems will be developed and optimized specifically for use in deploying and operating the SPS network.

d. Materials used in fabricating and operating an SPS will be obtained only from the earth.

e. The SPS will be deployed in appropriate geosynchronous orbits only.

f. The lifetime of an SPS will nominally be 30 years although liberal refurbishment/replacement of parts may be assumed.

g. The SPS will be designed in a manner to optimize participation of man in its fabrication, assembly, and operation.

h. Availability of scarce resources will be a major consideration in projecting technologies to be used in fabricating the SPS network.

i. Energy as well as economic payback will be assessed in determining the SPS development strategy.

j. Aspects of social and environmental impact will be assessed.

k. Assembly fabrication strategies for SPS will be developed such as to minimize overall costs.

The first two guidelines were modified slightly as the study progressed in that various scenarios were defined and evaluated.

Available resources defined the scope and depth of the study. For example, the study was primarily limited to consideration of the photovoltaic concept for solar energy collection and conversion. Similarly, the more detailed design studies were limited to consideration of silicon solar cells. Given these restrictions, a range of power station sizes and weights were determined based on conservative and optimistic estimates of collection, conversion, transmission and receiving efficiencies.

Analyses and/or design studies were conducted for each element of the systems to varying degrees. These studies included several satellite configurations, construction concepts, crew requirements, alternate microwave generator concepts, rotary joint designs, attitude and control concepts, and structural designs.

Several program scenarios were developed which defined the number and schedule of space power satellites required to provide varying percentages of the nation's energy needs in the 1995-2025 period.

Satellite weights were then coupled with the number and schedules of satellites required to define a range of transportation requirements. These requirements were used to guide the study of various transportation elements and to estimate integrated transportation requirements such as fleet size. Transportation elements for which specific studies were conducted included multi-stage winged and ballistic heavy lift launch vehicles, and of a variety of orbital transfer vehicle thrusters, and personnel launch and transfer vehicle designs.

In a similar manner, the satellite and transportation system characteristics, number and schedule were used as a basis to estimate the cost of DDT&E, total program, and mills per kilowatt hour. Preliminary estimates are also provided of natural resource requirements and pollutants emitted from processing and launch operations. Estimates of energy payback are also presented.

Figure I-1 presents the task structure that was used in the study effort. Both Volume I and Volume II are organized according to this task structure.

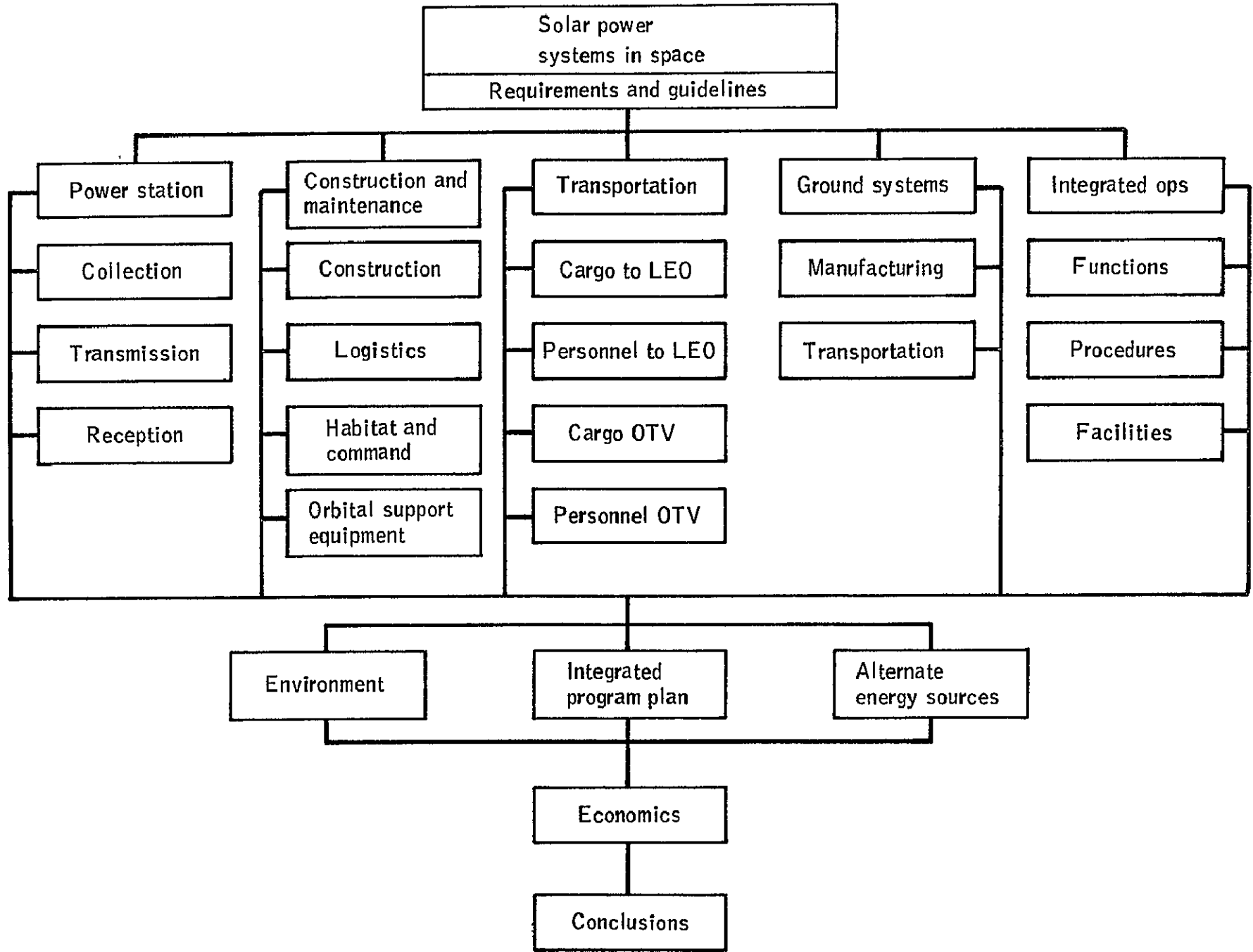


Figure I-1. - Study task structure.

II. CONCLUSIONS

The scope and complexity of the satellite power concept coupled with the limited depth of the present study would make it inappropriate to draw absolute conclusions. However, the SPS concept appears to be technically feasible in that no design or operational problems were encountered that did not appear amenable to solution. The economic viability of the system appears promising but is obviously dependent upon a combination of technology advancement and/or the costs of competitive sources.

Within the limitations of the study and based on a variety of assumptions and/or estimates, the following preliminary conclusions are presented.

1. The maximum power output of an individual microwave transmission link to earth is about 5 GW and the transmitting antenna diameter is about 1 km, based on the following assumptions;

- o An operating frequency of 2.45 GHz
- o A maximum allowable power density at the ionosphere of 23 mW/cm^2
- o A maximum allowable antenna waveguide temperature of 485°K resulting in a power density at the antenna of 21 Kw/m^2
- o A 10 db Gaussian taper of the microwave beam

2. The estimated mass of a 10 GW SPS (incorporating solar energy converters sufficient for two 5-GW microwave power transmission systems) is between 47×10^6 and 124×10^6 kg, based on the following assumptions:

- o Silicon cell arrays with an efficiency of 15 to 17 percent at 30°C and a concentration ratio of 2.
- o An overall system conversion and transmission efficiency range of 4.2 to 8.0 percent
- o A weight growth of 50 percent over present estimates

The resulting solar array areas ranged from 96 to 183 km^2 .

3. The silicon solar cell arrays make up well over half the weight and cost of the satellite. Consequently, additional effort on solar arrays offers the most potential for overall system improvement, particularly with respect to new approaches which could result in significant weight reduction.

4. Considerations of the structure indicated that minimum weight can be achieved if design loads are limited to those encountered on orbit and after construction. If this is done, the structure can be held at a very small percentage ($<5\%$) of the SPS weight. The major factors in design will not be weight but the development of techniques for automated on-orbit construction and for conducting large electrical currents.

5. Development of automated construction techniques is complex and requires a great deal of further effort. A preliminary task evaluation based on a conceptual construction technique suggests that as many as 600 personnel may be required in space to construct an SPS in one year, with minor variations expected in personnel required due to configuration and construction location. Placing and supporting these personnel in orbit is a relatively small factor in the overall transportation requirement.

6. Past studies have indicated an apparent performance advantage of constructing, assembling, or deploying all or a portion of the solar arrays in low earth orbit and then utilizing solar energy with electric thrusters to propel the system or major elements thereof to geosynchronous orbit. The present study concludes that this area needs further study with full consideration given to the following factors:

- o Degradation of the exposed solar arrays during transit
- o Protection of unused arrays during transit
- o Earth shadowing during portions of transit possibly requiring non-solar propulsion
- o Docking and assembly of large SPS sections at geosynchronous orbit and resulting impact on structural design
- o Relative simplicity of chemical stages for transfer of "containerized" packages to geosynchronous orbit
- o Radiation conditions at geosynchronous orbit

7. The SPS in equatorial orbit will be eclipsed both by the earth and by other satellites. These eclipses result in as many as three brief (up to 75 min) power outages per day for two six-week periods per year although less than 1% of the available energy is lost. The SPS/grid system must be designed to accommodate these outages.

8. Conceptual designs and characteristics were developed for two-stage winged and ballistic heavy lift launch vehicles of varying payload capability. While the ballistic systems are much smaller and lighter, recovery and reusability will be key issues in establishing the desired configuration.

9. Heavy lift launch vehicle design considerations established hydrocarbon fuel rather than hydrogen as the choice for first stage propellant because of its greater energy density.

10. Considerations of I_{sp} and confidence in technical development of candidate electric engines indicate that the MPD arcjet engine appears

to be the best choice for self-powered orbital transfer. These engines are also suitable for subsequent use as thrusters for the SPS attitude control system.

11. The high-launch rates required indicate that launch window and related operational considerations may become significant factors. Launch latitudes near the equator greatly expand the launch window and offer performance advantages.

12. Based on varying assumptions as to performance, construction, location, orbital transfer modes and reusability, achievable transportation costs to geosynchronous orbit are estimated to range from \$71 to \$294 per kilogram. The major contributor to the total transportation costs for a given program was the cost of transporting the necessary material to low earth orbit.

13. The cost of producing electricity from solar power satellites as described herein is estimated to be in the range of 29 to 115 mills/kWhr. This range of estimates is based on the following assumptions:

- o An implementation of 112 10-GW satellites over a 30-year period
- o A range of satellite weights and transportation costs as indicated earlier
- o A design, development, test and evaluation (DDT&E) cost
- o A space hardware repair/replacement rate of 1% annually
- o Plant factor of 92 percent allowing for eclipses and maintenance time
- o Return on capital investment of 15 percent

14. The cost of producing electricity with conventional (nuclear and fossil) plants is predicted to be in the 30 to 60 mills/kWh range, in the 1995 time period, depending upon the cost, fuel, and type of power plant. The cost of producing electricity with potential ground-based power plant concepts (ground solar, geothermal, wind) are estimated to be from 28 to 121 mills/kWh.

15. The introduction of SPS in lieu of meeting an equivalent portion of the nation's energy needs with new nuclear and coal-burning electrical power plants will result in significant reduction in emissions (particulates, NO_x, SO_x, nuclear waste).

16. The microwave power density at the edge of the rectenna (1 mW/cm²) is about one-tenth of the present U.S. standard for human exposure. The

system is fail-safe in that the beam would be dispersed to harmless intensity levels should be microwave beam pointing control fail.

17. Implementation of SPS on a large scale would create an increased demand for resources such as aluminum and rocket propellant gases (hydrogen and argon). Also, production capacity would have to be substantially increased in the areas of solar cells and reduction of arsenic from oxides (for the manufacture of gallium arsenide diodes). However, there does not appear to be any critical shortages of resources for SPS construction based on world reserves.

III. PROGRAM REQUIREMENTS

Tony E. Redding and Barry M. Wolfer
Urban Systems Project Office

A. Projected Energy Demand

Projections of the nation's electrical energy demand have been made by the FPC (Federal Power Commission), the ERDA (Energy Research and Development Administration) and other federal agencies and private organizations. Figure III-1 shows the FPC and ERDA projections for electrical energy demand through 1990 and 2000, respectively. The FPC projection through 1990 is given in the 1970 Federal Power Survey Report, Volume 1. The ERDA projection (given in ERDA-48, Volume 1, June 1975) involves six different technological development scenarios and their resulting electrical demands. The highest electricity generation scenario presented by ERDA is based on intensive electrification and it has a 4.4 percent per year growth rate in the year 2000. The lowest electricity generation scenario is based on improved efficiencies in end use and it has a 1.4 percent year growth rate in the year 2000. The FPC projection, which is higher than any of the ERDA projections, has an annual growth rate of about 6.0 percent per year in 1990. Because it represents the most severe requirements in terms of capacity needs and growth rate, the FPC projection was used as a basis for evaluating the potential of the SPS (Solar Power Satellite) system.

B. Implementation Scenarios

Effective use of solar power implies that SPS must produce a significant portion of the future electrical energy demand. Therefore, scenarios of SPS implementation rates were developed that would provide 25 percent of the new capacity by 2015 (scenario A), 50 percent of the new capacity by 2010 (scenario B), and all of the new capacity by 2005 (scenario C). The new capacity requirements are based on extrapolation of the FPC projection from 1990 to 2025 as shown in figure III-1. Figure III-1 shows the cumulative new capacity (GW) addition for each of these scenarios and the resultant electrical energy (GWH) provided by SPS each year until 2025. Scenario B was used as an illustrative example by which to examine the SPS program in terms of its technical requirements and resulting economic analysis. This scenario results in providing a significant quantity of the total electrical energy by 2025 (31 percent based on FPC projection and 50 percent based on the highest ERDA projection). The SPS installed capacity by 2025 would be 1120 GW or about 30 percent of the FPC total. Based on a 10 GW SPS power output, as described in Section IV, a total of 112 satellites will be required to accomplish Scenario B.

Figure III-2 shows a year-by-year summary of 10 GW SPS installations for the three scenarios over the 30 year implementation period. Note that in Scenario B, the SPS installation rate reaches 7 per year in 2023.

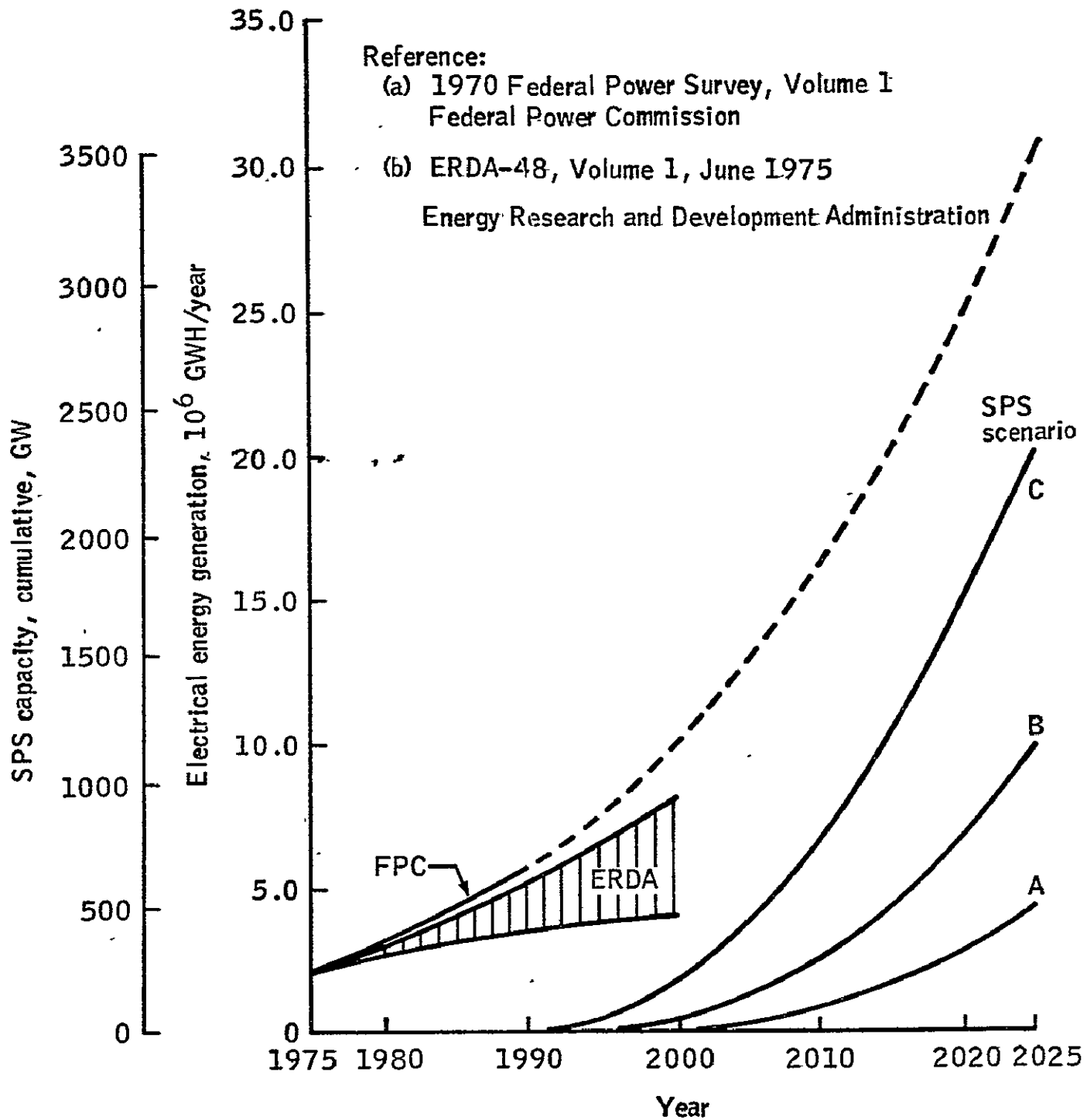


Figure III-1.- Projections of U.S. electrical energy requirements and possible SPS implementation scenarios.

FIGURE 111-2 POTENTIAL SPS SCENARIOS

	1988	1990	1995	2000	2005	2010
SCENARIO A				1 1	1	1 1 1 1 2
CUM TOTAL				1 2 3	4 5 6 7 9	
SCENARIO B			1 1 1 1	1 1 2 2 2	2 3 3 3 3	
CUM TOTAL			1 2 3 4	5 6 8 10 12	14 17 20 23 26	
SCENARIO C		1 1 1 1 2	2 2 2 3 3	3 4 4 5 5	6 7 7 8 8	
CUM TOTAL		1 2 3 4 6	8 10 12 15 18	21 25 29 34 39	45 52 59 67 75	

	2010	2015	2020	2025
SCENARIO A	2 2 2 2 2	3 3 3 3 3	3 3 3 3 4	
CUM TOTAL	11 13 15 17 19	22 25 28 31 34	37 40 43 46 50	
SCENARIO B	4 4 5 5 5	6 6 6 6 6	6 6 7 7 7	
CUM TOTAL	30 34 39 44 49	55 61 67 73 79	85 91 98 105 112	
SCENARIO C	9 9 9 10 11	11 12 12 12 12	13 13 13 13 14	
CUM TOTAL	84 93 102 112 123	134 146 158 170 182	194* 205* 215* 224* 232*	

*THESE NUMBERS ACCOUNT FOR REPLACING SPS'S AFTER 30 YEARS

A: LATE FULL SCALE PROTOTYPE, SLOW BUILDUP TO 25% OF MARKET BY 2015

B: MID FULL SCALE PROTOTYPE, MODERATE BUILDUP TO 50% OF MARKET BY 2010

C: EARLY FULL SCALE PROTOTYPE, FAST BUILDUP TO MARKET SATURATION BY 2005

IV. POWER STATION

A. SYSTEM ANALYSIS

IV-A-1. Efficiencies

L. E. Livingston
Spacecraft Design Div.

Three estimates were made of the efficiency of each step in the power collection and transmission process: a minimum, which could be achieved by 1995 with virtual certainty; a maximum, the best that could realistically be expected under the most favorable circumstances; and a nominal or reference, representing the value most likely to be achieved. These are summarized in figure IV-A-1-1, together with the corresponding power levels at each stage for 5 GW DC output from the power interface.

Since these estimates were required for subsystem sizing, they were made early in the study. Subsequent work (cf. section IV-A-2) has changed some estimates by several percentage points; these are shown in figure IV-A-1-1 for comparison. However, the "initial reference" data in figure IV-A-1-1 have been used, for the sake of consistency, in all sizing exercises. These changes would reduce the total solar input, and consequently the total array area, about 10 percent from the example configurations discussed in the rest of this report. Insufficient time was available to repeat all the subsystem calculations in detail, and no attempt was made to do so.

<u>Power, GW*</u>	<u>Efficiencies</u>		<u>Revised Estimate</u>
	<u>Initial Estimates</u>		
	<u>Reference</u>	<u>(Min - Max)</u>	
Solar energy			
↓ 93.06 (118.70 - 62.36)			
Photovoltaic conversion	.103	(.103 - .116)	.103
↓ 9.59 (12.23 - 7.24)			
Spacecraft power distribution	.92	(.85 - .93)	.92
↓ 8.82 (10.39 - 6.73)			
Antenna power distribution	.96	(.94 - .97)	.98
↓ 8.47 (9.77 - 6.53)			
DC-RF conversion	.87	(.85 - .94)	.87
↓ 7.37 (8.31 - 6.14)			
Phase control	.95	(.90 - .96)	†
↓ 7.00 (7.48 - 5.89)			
Waveguides (I ² R)	.99	(.99 - .99)	.98
↓ 6.93 (7.40 - 5.83)			
Mechanical alignment	.97	(.97 - .99)	.98
↓ 6.72 (7.18 - 5.77)			
Atmosphere	.96	(.92 - .98)	.98
↓ 6.45 (6.60 - 5.66)			
Energy collection	.90	(.90 - .95)	.88
↓ 5.81 (5.94 - 5.38)			
RF-DC conversion	.87	(.85 - .94)	.90
↓ 5.05 (5.05 - 5.05)			
Power interface	.99	(.99 - .99)	.99
↓ 5.00			
DC power to grid			
Overall	.054	(.042 - .080)	.060

* Power levels are given in the same order as corresponding efficiencies

† 'Included in "energy collection"

Figure IV-A-1-1.- SPS efficiencies.

INTRODUCTION

The initial task in the Satellite Power Station study was to determine an appropriate sizing for the overall satellite system. The station consists of large solar arrays converting solar energy to DC electricity by the photovoltaic process. This electrical energy is transmitted back to the earth using a high power microwave transmission system. The microwave system, consisting of DC-RF amplifiers, a large planar phased array, and a ground antenna/rectifier scheme (rectenna), must be capable of operating at a high efficiency over a 30 year lifetime with a low failure rate. The microwave energy is rectified back to DC electricity in the rectenna and then collected and carried via buss bars to a power distribution interface with commercial landlines. The output DC power from the solar power station will be defined at a collection point near the ground rectenna, prior to any signal conditioning or DC/AC conversion.

IV.A.2(a) SYSTEM SIZING

The physical size and power capabilities for the Satellite Power Station (SPS) are dependent upon: (1) the amount of DC output power at the ground rectenna, (2) the transmit antenna size, and (3) the system efficiencies. The tradeoffs for defining these system requirements are as follows:

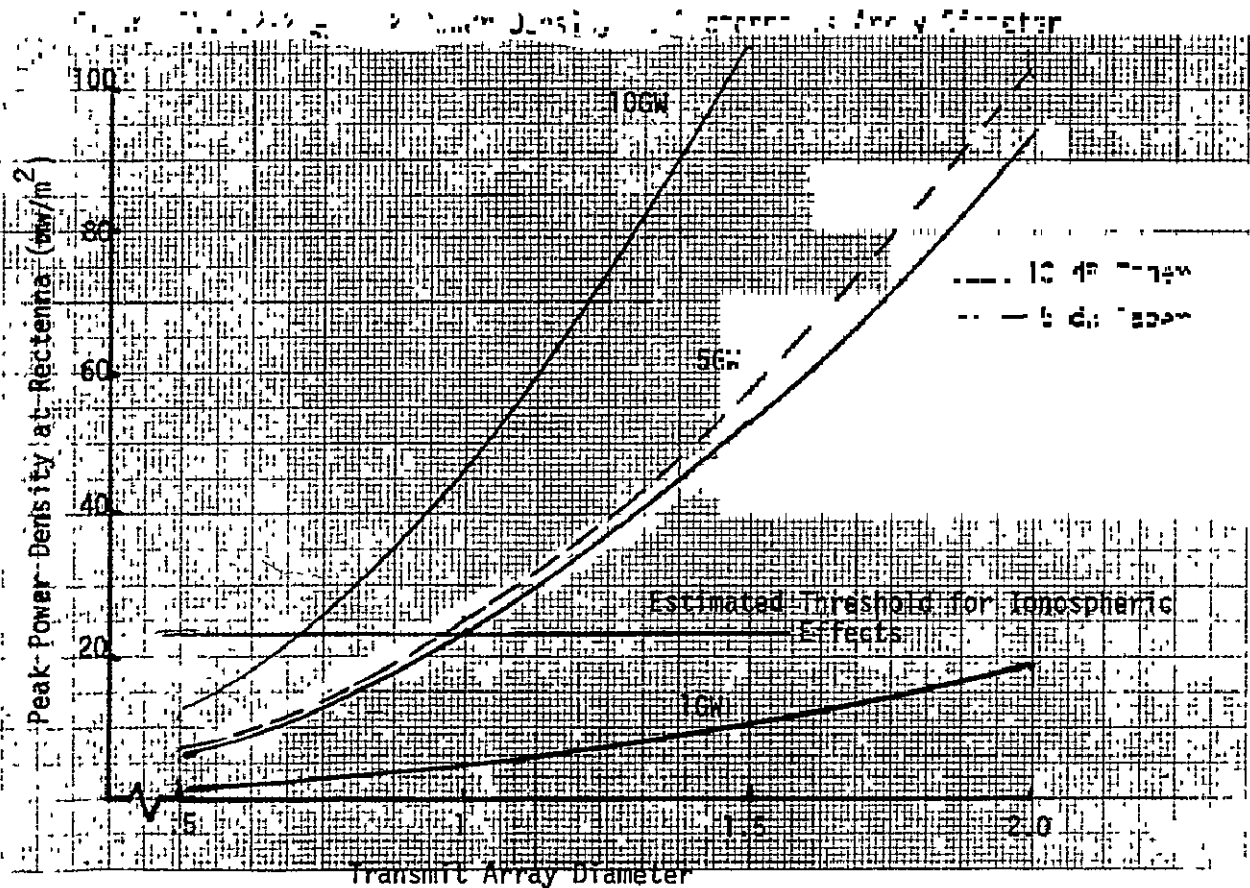
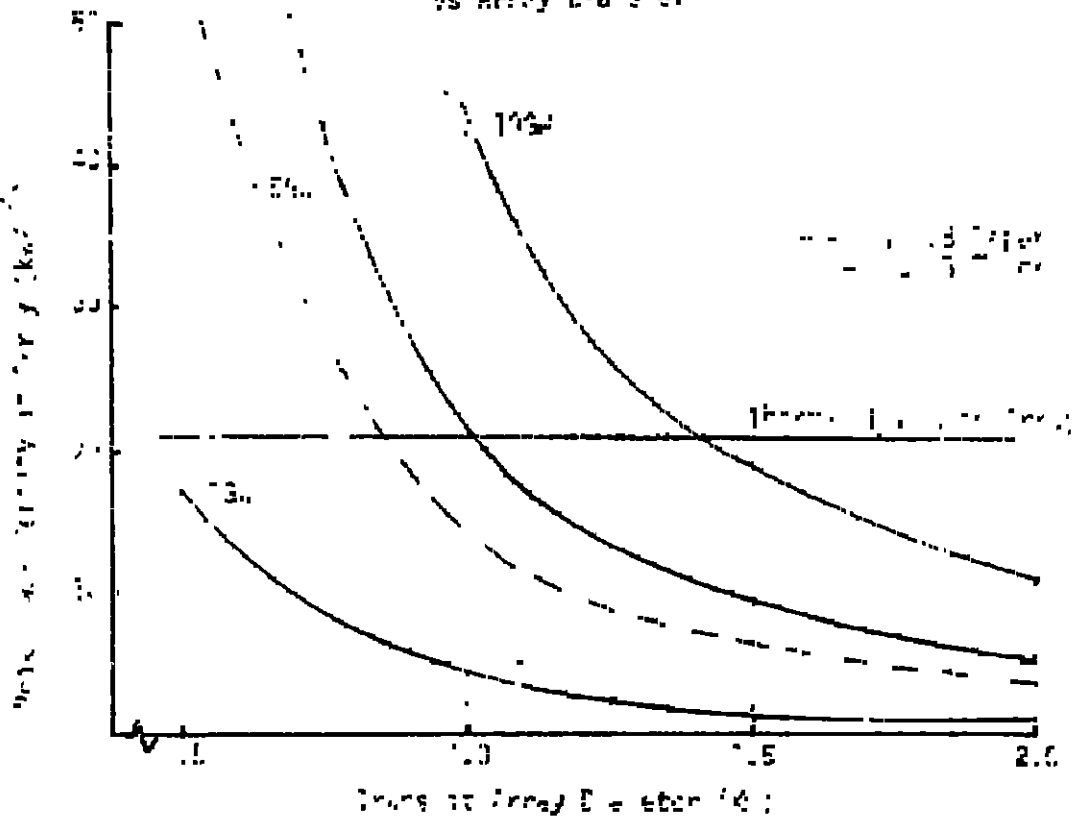
(1) Amount of DC power out of rectenna - Three output power levels, 1GW, 5GW, and 10GW, were studied. Raytheon (ref. 1) and Lewis Research Center (ref. 2) indicate there may be some cost advantages in going to high power systems. The allowable output power level is also dependent upon the size of the microwave transmit array antenna in the SPS as discussed below.

(2) Tradeoffs of SPS transmit antenna size - The size of planar phased array in the satellite is primarily dependent upon four factors:

(a) Thermal constraints within the antenna - At the center of the phased array, temperature limitations due to heat radiated by the DC to RF converters determine a minimum size for the antenna. The maximum power density (on boresight) at the transmit antenna is given as a function of array diameter in Figure IV.A.2-1. A 10 dB taper aperture illumination for a 5GW system will just meet the thermal limitations for the antenna. (The 10 dB taper illumination rather than a 5 dB taper was selected because of increased collection efficiency at the rectenna as will be discussed later.) For the model configuration, the maximum power density at boresight will be 20.88 KW/m² when using a 1 km array 5GW system. This density level gives a temperature of 450° - 485°K at the antenna for a DC to RF amplifier conversion efficiency of 85-90%. This temperature is an upper limit

ORIGINAL PAGE IS
OF POOR QUALITY

Figure IV.A.2-1 Peak Power Density at Transmit Array
vs Array Diameter



for aluminum waveguides. The klystrons are mounted behind the waveguides and radiate thermally outward via graphite radiators or heat pipes. However, the area between the waveguides and the thermal radiators for the klystrons will act as an oven and operate in the 450-485° temperature range. Therefore, a 1 km or larger transmit antenna is needed for a 5GW 10 dB Gaussian taper illumination.

(b) Microwave power density limitations in the ionosphere - As the antenna array size increases, the maximum power density transmitted through the ionosphere increases. Previous studies (ref. 1, 3) indicate that non-linear interactions between the ionosphere and the power beam begin to occur at some threshold power density level which is dependent upon the operating frequency. This threshold level is 23 mw/cm² for the model SPS system using an operating frequency of 2.45 GHz. This places a maximum size on the antenna for a given power output at the rectenna.

The maximum power density at the rectenna as a function of transmit array size is given in Figure IV.A.2-2. Three output DC power levels, 1GW, 5GW, and 10GW, at the rectenna are shown, together with a 5 dB and 10 dB Gaussian taper for the 5GW system. These curves indicate that a 1 km array, 10 dB taper, 5GW system is at the maximum power density level set by the ionospheric interaction limit of 23 mw/cm². However, this 23 mw/cm² density level can only be considered a guideline, not an absolute requirement. There is not sufficient experimental data available to accurately predict the exact threshold level.

(c) Maximum output power - If Figures IV.A.2-1 and -2 are superimposed such that the power density limits coincide (Figure IV.A.2-3), it may readily be determined whether a given combination of output power and transmitting antenna diameter exceed either of the two limits. For example, 6GW output and 0.8 km diameter fall within the ionosphere limit but greatly exceed the transmitting antenna thermal limit. Since the only issue is whether an operating point falls above or below the limit line, the relative sizes of the vertical scales are unimportant for this superposition.

For the limits used here, the maximum output power is 5GW and the corresponding antenna diameter is 1.0 km. A high output power has a number of economic and operational advantages discussed elsewhere in this report; consequently, the maximum of 5GW output power, together with 1.0 km transmitting antenna diameter, has been used for sizing purposes throughout this study.

These results will change if the maximum power densities are revised. For example, if the transmitter limit were 25 kw/m² and the ionosphere limit 40 mw/cm², the maximum output power would be 7.1GW and the antenna diameter 1.1 km.

(d) Rectenna size - As the transmit array size increases, the beamwidth of the main lobe decreases in proportion to the array area, which causes the rectenna size (and cost) to decrease. The tradeoffs of

Figure IV.A.2-3 - Thermal and Ionospheric Constraints on DC Output Power

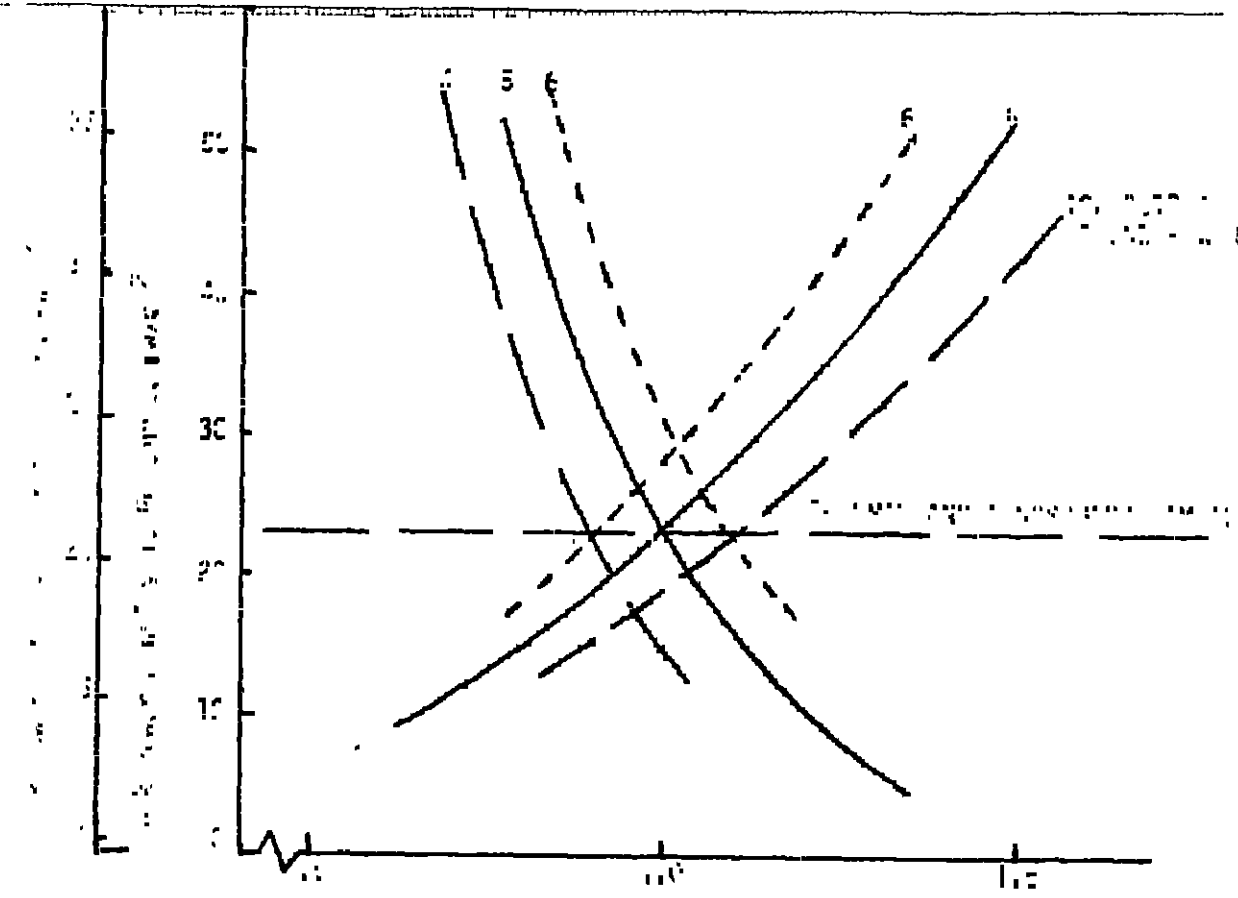
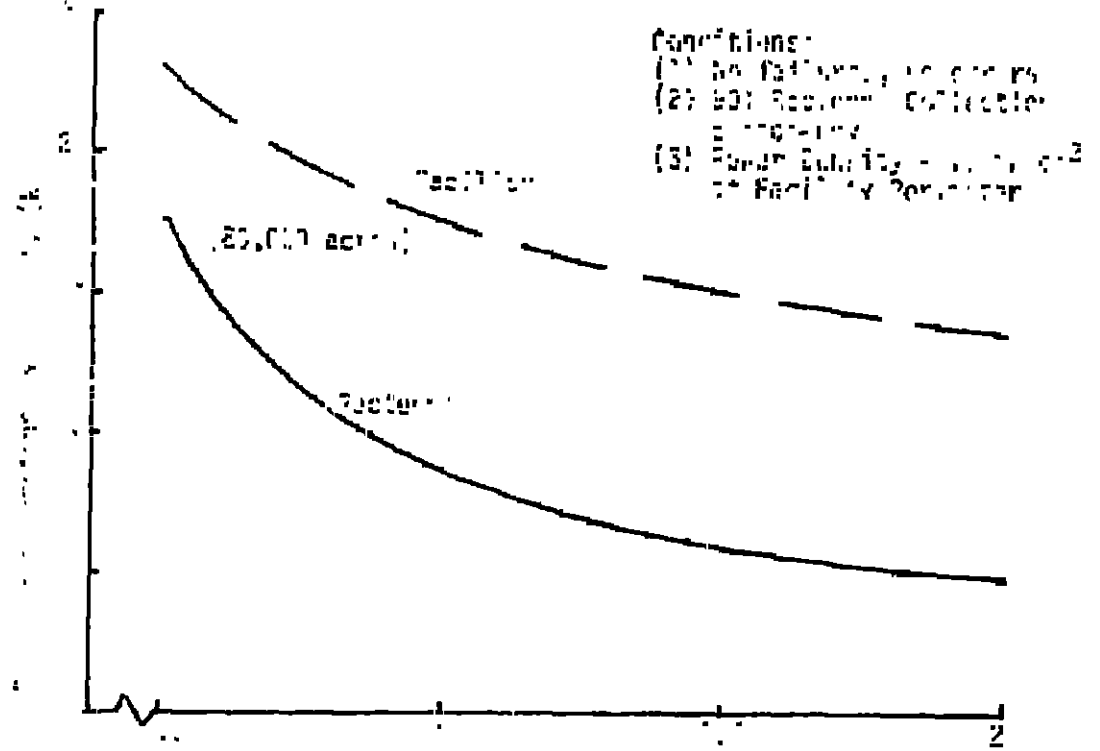


Figure IV.A.2-4 - Ionospheric System Size vs. Transmitted Power



ORIGINAL PAGE IS
 OF POOR QUALITY

rectenna size are shown in Figure IV.A.2-4. The rectenna size is that required for a 90% flux intercept efficiency, or collection efficiency. The ground facility, which is the area fenced off for the rectenna system, was arbitrarily chosen to intercept all power density levels out to .05 mw/cm². This density level example is 200 times more stringent than the 10 mw/cm² radiation standard set by the United States; however, it is 5 times greater than the .01 mw/cm² USSR standard. The exact power density standard to use is not known at this time and should be one objective of a microwave radiation study. However, it is felt that the SPS density limit will be somewhere between the present USA and USSR standards. Since the radiation will be continuous, the SPS standard may be closer to the USSR limit. The facility required for a 1 km transmit array covers 80,000 acres - a large land area.

In summary, the 1 km transmit array, together with a 10 dB Gaussian taper illumination for a 5GW system, was chosen as the model configuration for three reasons: (1) the system operates just below the 23 mw/cm² threshold level expected for nonlinear ionosphere interactions, (2) the power density at the transmit array is at the 21 kw/m² limit due to thermal constraints for the waveguides and klystrons, and (3) a size/cost tradeoff for the rectenna and transmit array has a broad minima at a 1.0 km array diameter.

IV.A.2(b) IONOSPHERIC EFFECTS

The microwave beam/ionospheric interactions can be divided into two categories: the ionospheric effects on the beam and the beam effects on the ionosphere. Previous work by Raytheon (ref. 1) indicates the ionospheric effects on the beam, such as phase dispersions, beam displacement, and power absorption, will be minimal. However, the beam perturbations to the ionosphere must be considered when sizing the SPS power. As the microwave power density increases above a threshold level, nonlinear interactions between charged particles in the ionosphere and the power beam begin to occur. This threshold level has been postulated to be approximately 23 mw/cm² for a 2.45 GHz frequency, which is close to the peak density expected for a 5GW system.

When the microwave power approaches the threshold level, the ionosphere will be perturbed as shown in Figure IV.A.2-5. In the "F" layer there will be heating and expansion with a corresponding reduction in the electron/ion density. A "hole" will be punctured in the "F" layer due to the reduction in electron/ion concentration. The neutral particles however will not be appreciably affected by the heating, and their concentration will remain the same. These particles, i.e., the electrons, ions, and neutrons are moving through the ionosphere at some velocity - estimated to be 50 meters/second (ref. 4). Thus, as these particles sweep pass the "hole" region, they will slowly diffuse back until the normal equilibrium density level is again reached. Rough calculations indicate the "hole" will be closed within five minutes, or about 15 km, after the particles leave the heated region. In the "D" region the microwave heating slows the electron/ion recombination rate and the density may actually increase. There will be no

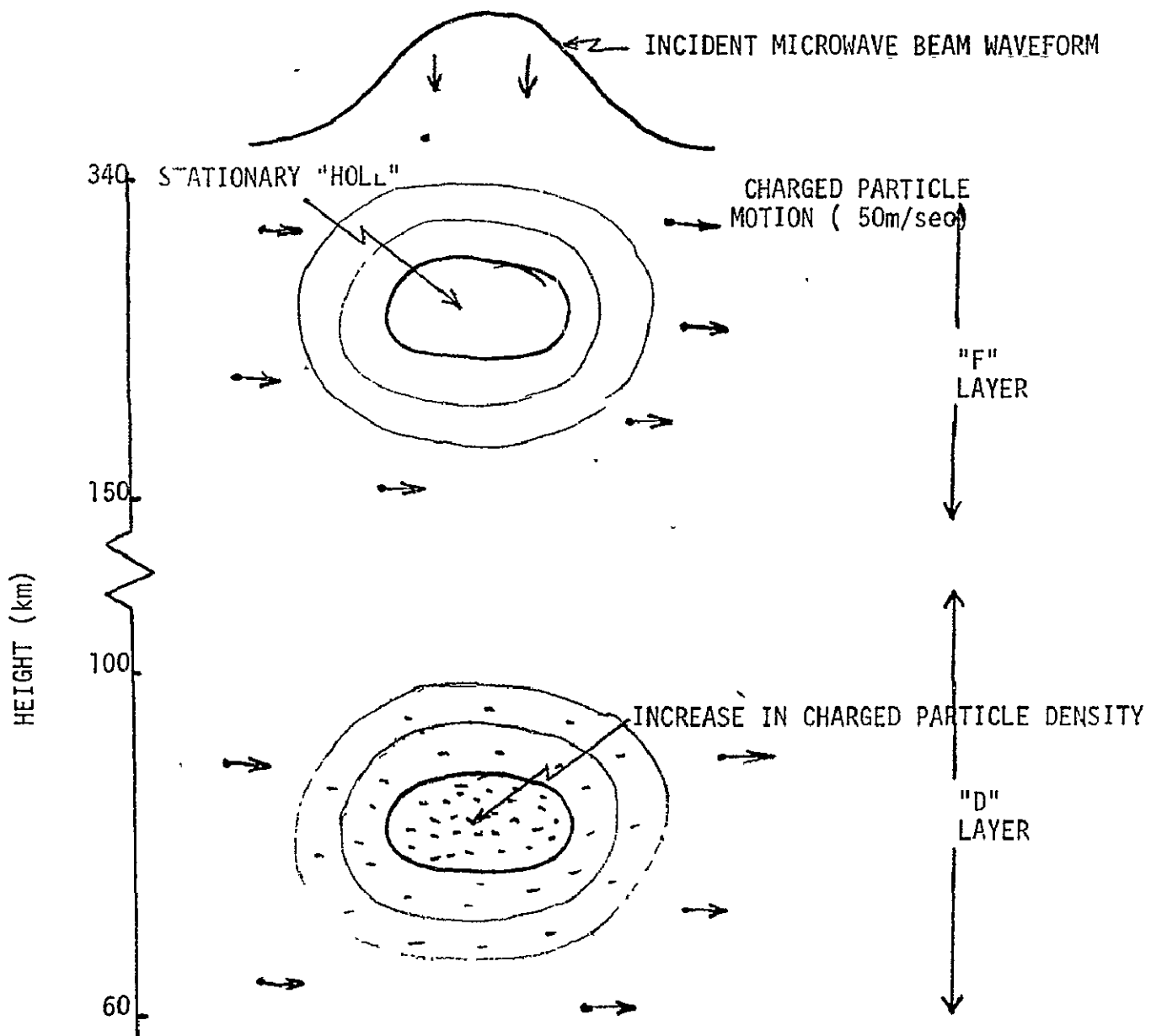


Figure IV.A.2-5 -Changes in electron/ion density for microwave power densities above the threshold level.

change on neutral particle concentration as was the condition in the "F" region. As the ionosphere drifts out of the heated region, the temperature will almost instantaneously decrease to normal (within a few milliseconds) but the time required for the density to return to normal will be longer (10-to 20-minutes).

There should be no change in solar ray absorption by the ionosphere since the neutral particles rather than the electrons and ions, absorb solar radiation. As mentioned previously, the density of the neutral particles remains constant in the hole region.

The main problems associated with nonlinear heating and hole creation are possible disruptions in HF, VHF communication systems, and VLF navigation systems due to additional RFI and multipath degradations. The power density levels at which nonlinear effects in the ionosphere begin to occur have not been measured at S-band frequencies and can only be speculated upon. There are a number of possible ground-based tests which can provide information on the nonlinear effects and determine at what power levels these effects actually occur. However, for the model configuration the $23\text{mw}/\text{cm}^2$ was taken as the upper bound for the power density level and consequently, was a factor in selecting 5GW as the output DC power.

IV.A.2 (c) NOMINAL EFFICIENCIES FOR SYSTEM SIZING

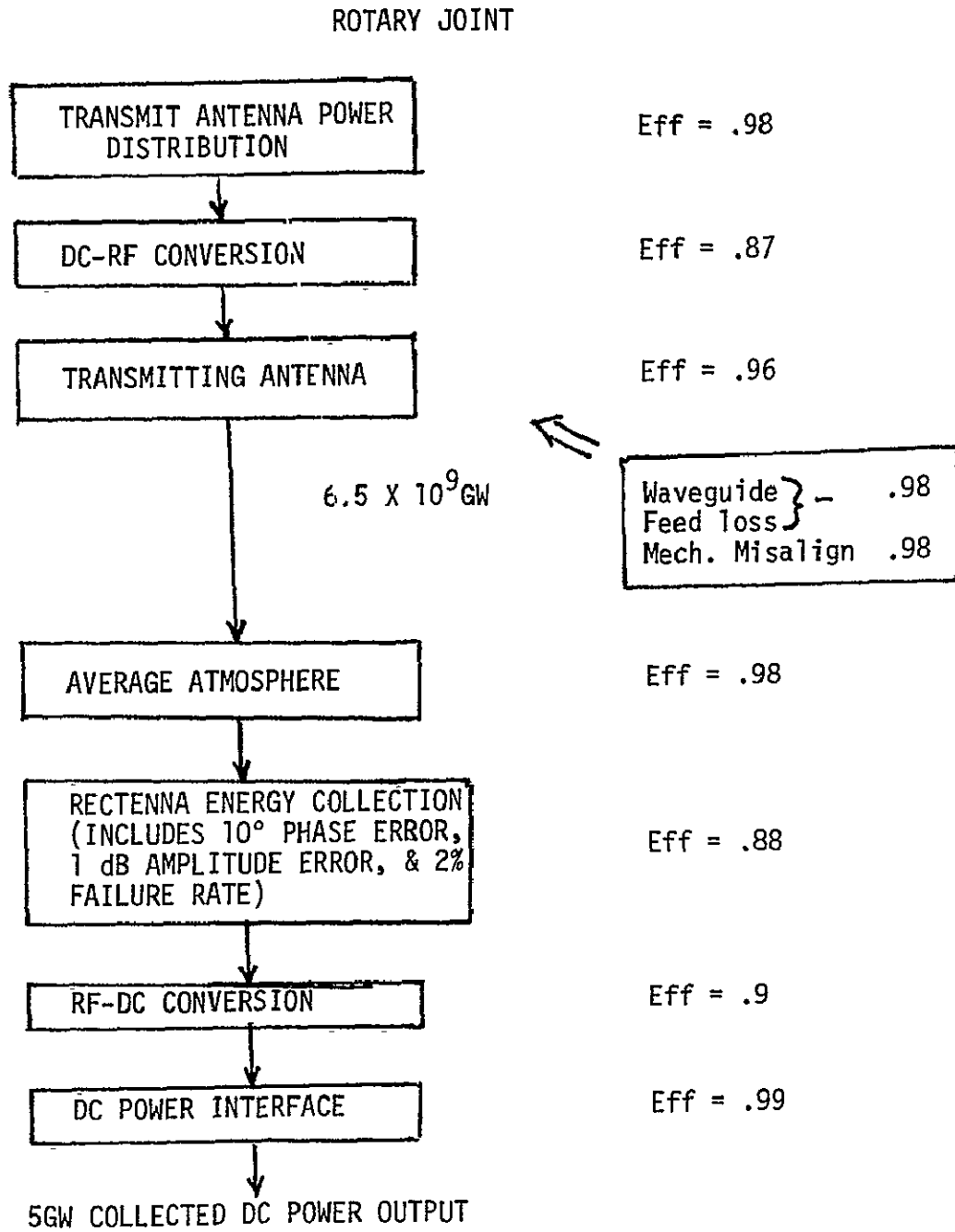
After the DC output power at the rectenna and the transmit array size are selected, then representative values for efficiencies for each of the subsystems in the SPS are determined. The nominal system efficiency from the RF radiated output of the transmit antenna to the collected DC power at the rectenna is specified to be 76%. Using this efficiency and the 5GW DC output power, the RF power radiated from the transmit antenna is 6.5GW. The microwave system performance curves given in this report are all based upon 6.5GW radiated RF power. The nominal efficiencies for the microwave subsystems and their associated power levels are given in Figure IV.A.2-6.

The total microwave system efficiency (nominal) from the DC output of the rotary joint to the collected DC output of the rectenna is 63%. Details on the efficiency tolerances for the total SPS system are given later in the text.

IV.A. (d) FREQUENCY SELECTION

A frequency of 2.45 GHz was chosen for the JSC system, which is the same as that used in the Raytheon/Lewis studies (ref. 1, 2). The 2.45 GHz is at the center of a 100 MHz band reserved for government and non-government industrial, scientific, and medical use. This band has the advantage in that any radio communication services operating within the 2450 ± 50 MHz limits must accept any harmful interference that may be experienced from the operation of industrial, scientific and medical equipment. That is, as long as the microwave energy is confined to this frequency band, there will be no interference problems. Other advantages of this frequency include low atmospheric attenuation even in the presence

Figure IV.A.2-6 - Nominal Efficiencies for the Microwave System



of rain and good operating efficiencies for the microwave components. However, there is one reason for considering a higher frequency such as 3.0 GHz. Since the effective gain of the transmit antenna is proportional to λ^2 (the wavelength squared), a 44% increase in gain is achieved for the same 1 km array by going to 3.0 GHz rather than 2.45 GHz. Such a change in frequency would require approval by the ICCR (International Radio Consultative Committee) which meets again in 1979.

IV.A.2(e) ANTENNA APERTURE ILLUMINATION

In order to achieve a high transmission efficiency, the transmit antenna must have an aperture distribution across the array surface which maximizes the amount of RF power intercepted by the ground rectenna. The previous work by Raytheon and JPL (ref. 1, 5) has shown that a truncated Gaussian taper is a good approximation for an optimum aperture distribution. This illumination function has the form

$$E(r) = e^{-.115 \text{ dB} \left(\frac{r}{r_0}\right)^2}$$

where dB - is the amount of taper from the center to the edge of the array

r - is the radial position across the array

r_0 - is the radius of the circular transmit array.

The mainbeam pattern and sidelobe characteristics of the antenna will vary with amount of edge taper as shown in Figure IV.A.2-7. A uniform illumination, that is 0dB taper, has a narrow mainbeam and the maximum density at boresight (center of rectenna). Increasing the amount of taper produces a lower boresight density, a wider mainlobe, and lower sidelobes. These power density curves are for a 1 km transmit array with no phase or amplitude errors and no failures.

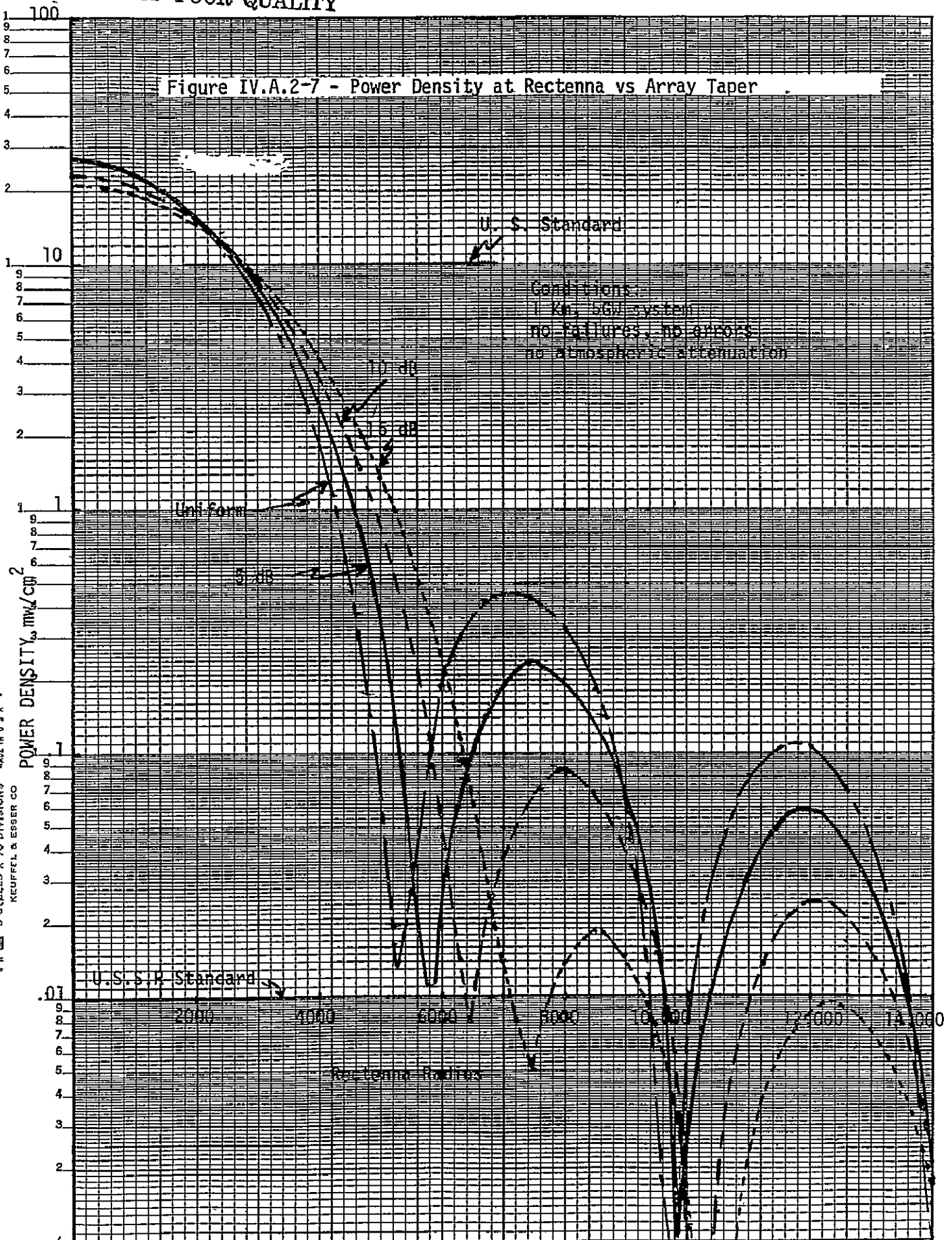
The rectenna collection efficiency, that is, the amount of flux density intercepted by the rectenna, is shown in Figure IV.A.2-8 for the same taper configurations. As would be expected, the collection efficiency for a given rectenna radius increases with the amount of taper. The model configuration has a 10 dB taper which means that the power density at the center of the array is 10 times that at the edge. For the no error/no failure conditions the 10 dB taper system gives a 90% collection efficiency at a radius of 4300 meters.

IV.A.2(f) STEP-TAPER ANALYSES

The 10 dB Gaussian taper will not be a continuous function across the array surface; rather it will be a physically-realizable quantized approximation. Three configurations, 5 step, 8 step, and 10 step approximations were investigated. Minimizing the number of steps

ORIGINAL PAGE IS
OF POOR QUALITY

Figure IV.A.2-7 - Power Density at Rectenna vs Array Taper



KEUFEEL & ESSER CO
SEMI-LOGARITHMIC 46 6213
5 CYCLES X 70 DIVISIONS
MADE IN U.S.A.

Figure IV.A.2-8 - Rectenna Collection Efficiency vs Array Taper

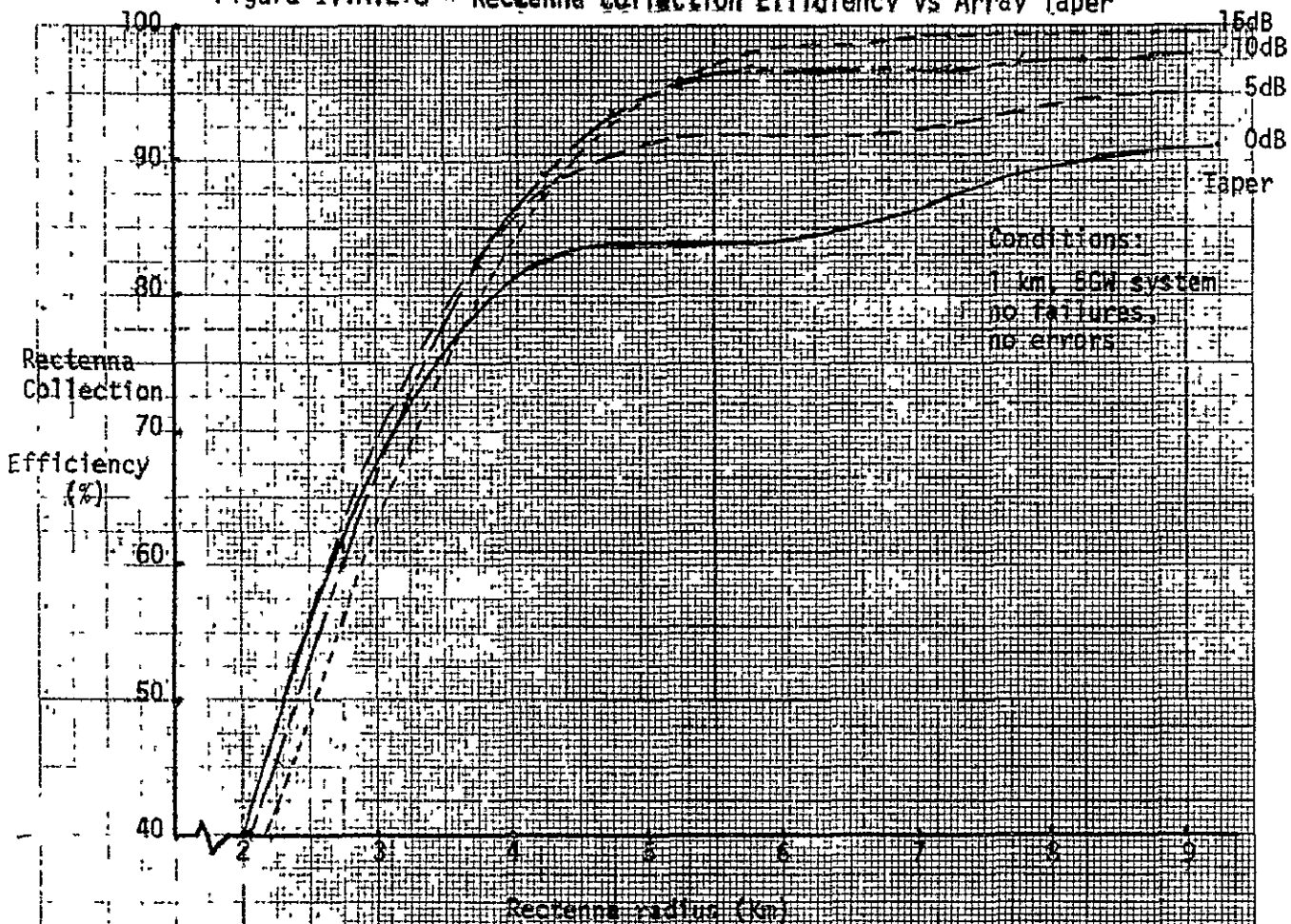
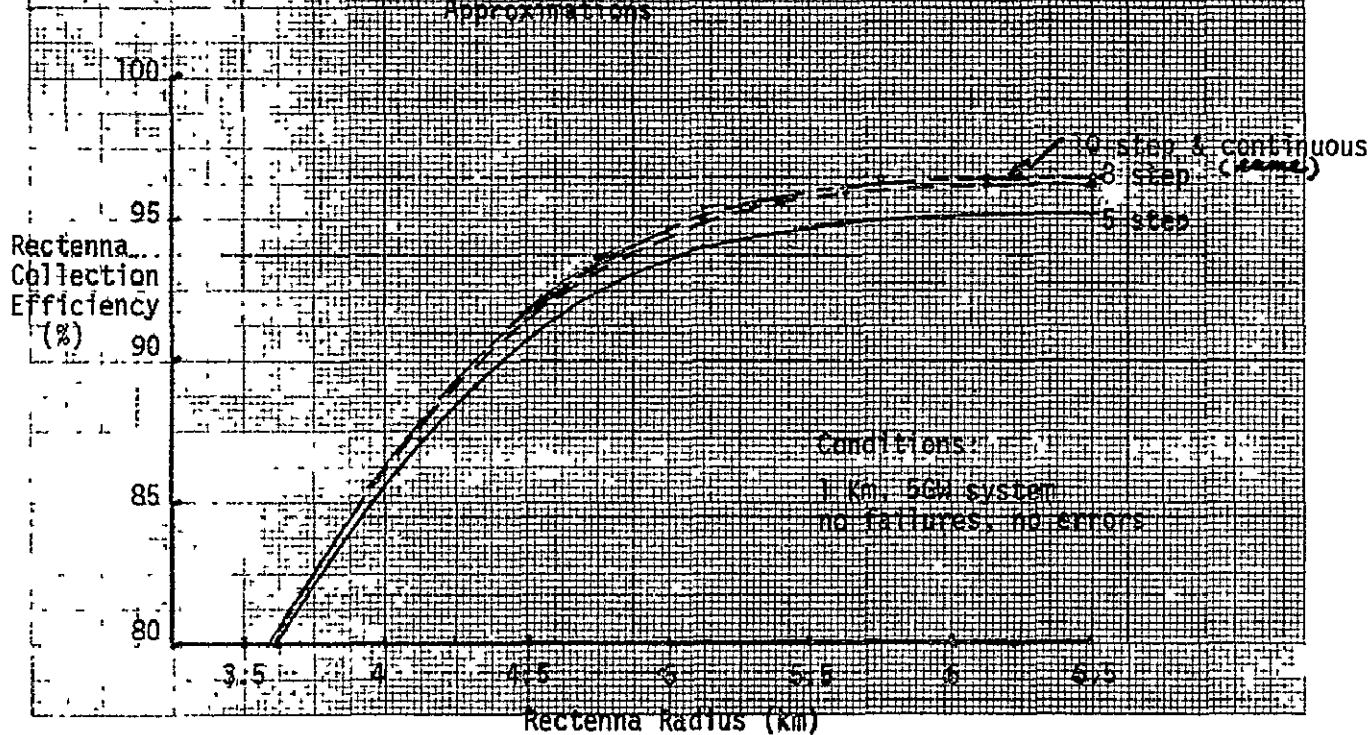


Figure IV.A.1-9 - Rectenna Collection Efficiency vs Step Taper Approximations



simplifies the antenna design at the cost of decreased collection efficiency at the rectenna. The steps are quantized in equal power increments according to the relationship (ref. 1),

$$\text{Power (r)} = \frac{1}{N} I \left[N \left(e^{-1.15 \left(\frac{r}{r_0} \right)^2} \right)^2 + .5 \right] \quad (2)$$

where N - is the number of steps

I - is the lowest integer

The collection efficiencies for the 5, 8, and 10 step quantizations are compared to the continuous distribution in Figure IV.A.2-9. There are only small differences between the collection efficiencies of these three step approximations, which is in contrast to previous results (ref. 1). However, since the revenue return over the 30-year lifetime of the SPS is \$524 X 10⁶ per 1% collection efficiency (based upon a charge rate of 40 mils per kilowatt-hour), the model configuration will have a 10 step approximation. The 10 step function gives about 1% greater efficiency than the 5 step and the extra \$524 X 10⁶ revenue justifies the slightly greater complexity of the antenna.

The configuration of the 10 step taper is shown below in Figure IV.A.2-10. The amount of power radiated per subarray is lowered progressively outward from the center of the total array by reducing the number of klystrons per subarray. There is a maximum of 42 klystrons/subarray at the center of the array and a minimum of 6 klystrons/subarray at the edge.

A diagram of the normalized power density at the array as a function of radius is shown in Figure IV.A.2-11. There are equal power increments between each step except at the center and end of the array. This is the configuration used in the design of the DC power distribution for the antenna.

IV.A.2(g) SUBARRAY SIZE TRADEOFFS

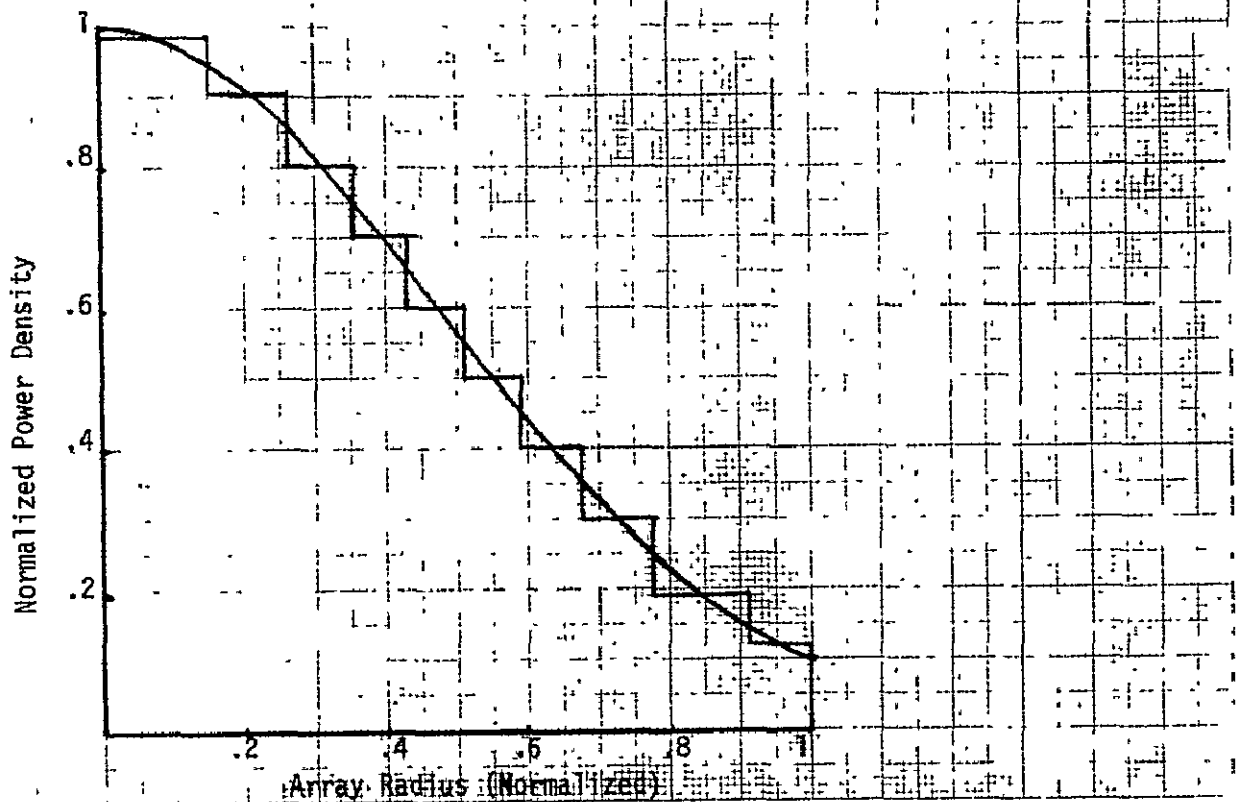
The 1 km transmit array is composed of smaller subarrays, each phased together with a feedback reference signal from the ground. Each subarray can be considered an individual antenna, the gain and beamwidth of which is determined by its size. The previous work (ref. 1) used an 18m X 18m subarray. However, the 18m X 18m subarray had such a narrow beamwidth that active positioning devices, i.e., motor-driven screwjacks, were needed in order to mechanically compensate for small misalignments in the antenna. These misalignments were caused by thermal warping of the antenna, tilting of the individual subarrays, etc. Smaller subarrays have the advantage of wider beamwidths, and hence, reduced mechanical alignment requirements. However, the phase control costs increase since each subarray has its own receiver and phasing electronics.

Figure IV.A.2-10 - Ten-Step Quantization of 10 dB Gaussian Taper

Normalized Radius	Power Density (kw/m ²)	Klystrons Per Subarray	Current per Subarray (amps)	Power per 10m X 10m Subarray (10 ⁶ w)
.15	20.88	42	53	2.088
.25	19.16	38	48	1.916
.353	16.97	34	43	1.697
.43	14.88	30	38	1.488
.51	12.73	25	31	1.27
.59	10.55	21	26	1.05
.675	8.43	17	21	.84
.775	6.31	13	16	.63
.91	4.13	8	10	.41
1.0	2.59	6	8	.26

Condition: 6.5×10^9 watts radiated out of antenna;
 Klystrons - 50 Kw, 40 Kv, 1.25 amps/unit

Figure IV.A.2-11 - Normalized Power Density as a Function of Radius



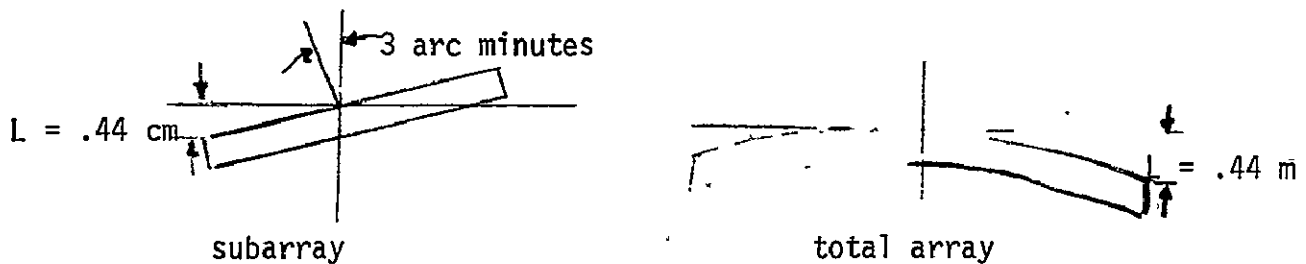
The effective subarray antenna gains as a function of the tilt angle, or mechanical misalignment, are shown in Figure IV.A.2-12. Three subarray sizes, 4, 10 and 18 meters, were studied. A 2% loss in antenna efficiency was allocated for mechanical misalignments which corresponds to 8.0, 3.2, and 1.9 arc minutes for the 4, 10 and 18 meter square subarrays.

The total cost of the transmit antenna as a function of subarray size is shown in Figure IV.A.2-13. The transmit antenna is a 1 km, 5GW system -- the only change is the \$64,000 cost for the phasing electronics associated with each subarray. The curve which is calculated using the relationship

$$\text{antenna cost} = \underset{\substack{\uparrow \\ \text{fixed cost - independent of subarray size}}}{\$1165 \times 10^6} + \$64,000/\text{subarray (\# of subarrays)} \quad (3)$$

indicates that small subarrays are impractical due to the large increase in cost. A 4m X 4m subarray configuration cost $\$2.7 \times 10^9$ more than a 10m X 10m system.

Therefore, the model system uses a 100 m² subarray (approximately 10m X 10m) which is a compromise between the more stringent alignment requirements for larger subarrays and the increased cost of smaller subarrays. The total number of these subarrays within the 1 km total array is 7,850. The mechanical alignment requirement is + 3 arc minutes, giving a 2% loss in antenna efficiency. The corresponding misalignment tilt in length is .44 cm for the subarray and .44m for the total array.



The stringent mechanical alignment requirement for the subarrays is the tilt angle from boresight to the ground; the vertical displacement of the subarrays with respect to each other is not that critical since the electronic phasing can compensate for different path lengths to the ground.

IV.A.2(h) BASIC SYSTEM PERFORMANCE REQUIREMENTS

The preceding analysis has considered only a perfect antenna; the degradations associated with phase and amplitude errors, together with failure rates, will now be determined.

Figure IV.A.2-12 - Effective Subarray Antenna Gain Versus Tilt Angle

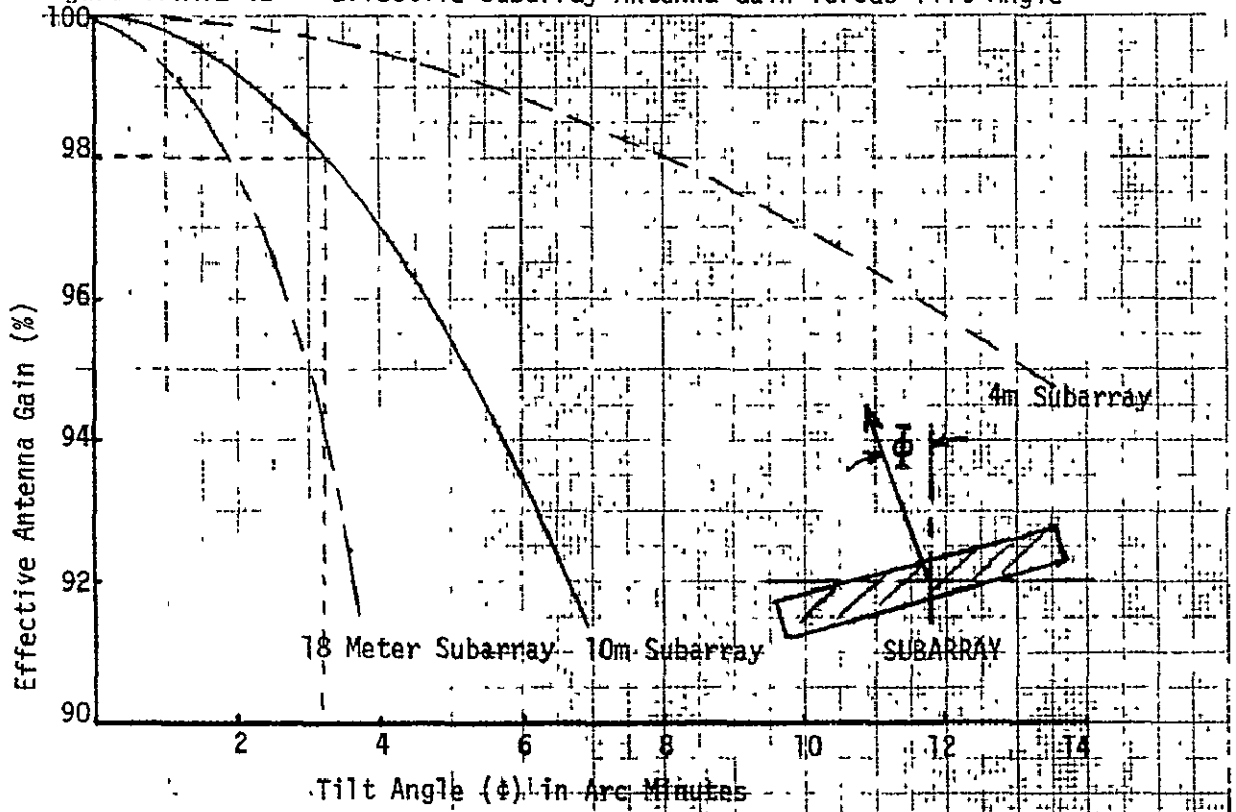
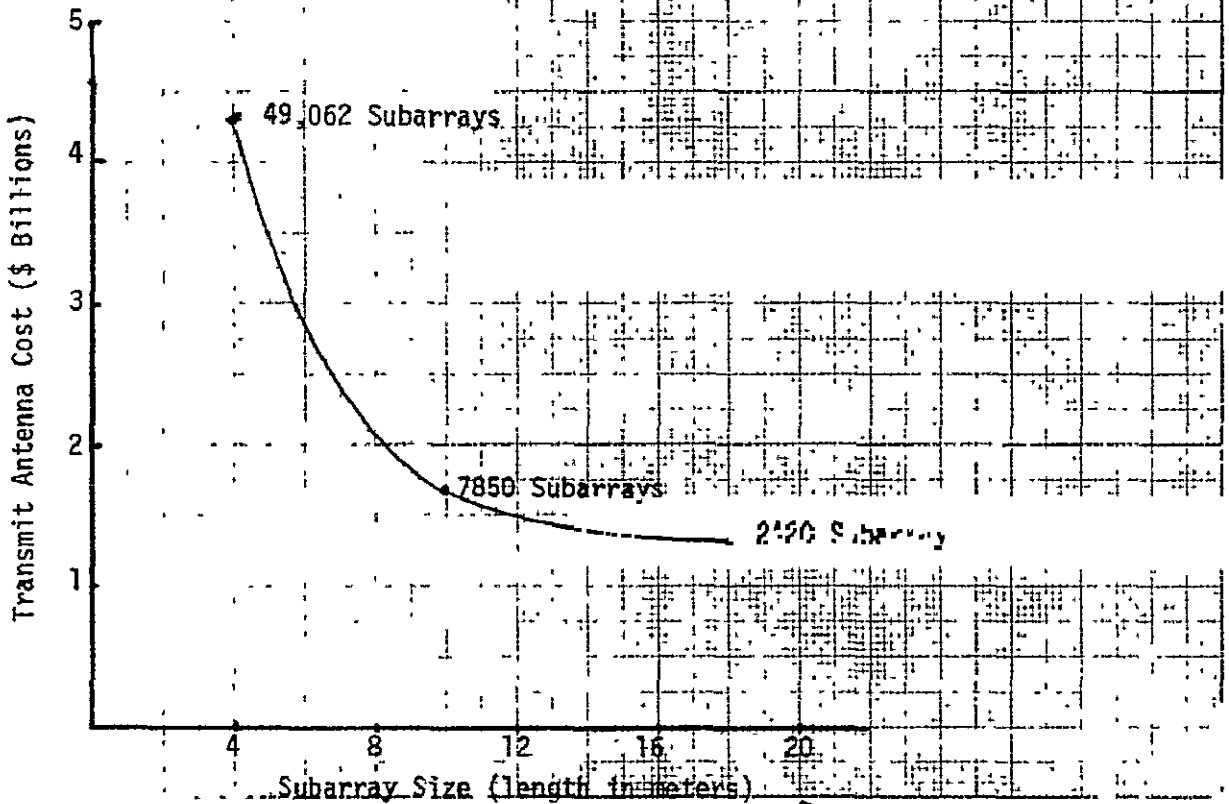


Figure IV.A.2-13 - Transmit Antenna Cost Versus Subarray Size



(1) Random Phase Error - A Gaussian distribution phase error with selected standard deviations will be applied to each subarray. These phase errors are due to noise in the phase lock loop reference in the subarray's RF receiver, phase shifts in the klystrons, errors in the calibrated path lengths of the phase reference distribution system, etc. The rectenna collection efficiency for 0° , 7° , 14° , and 20° phase errors are shown in Figure IV.A.2-14. There are no amplitude errors nor failures in these calculations. For a 5000 meter rectenna radius, the efficiency loss as compared to a 0° phase error system varies from 1% for a 7° error to 10% for a 20° error. The model configuration is specified to have a 10° error.

(2) Amplitude Tolerance - A Gaussian distribution amplitude illumination error with selected standard deviations will be applied to each subarray. The amplitude errors are due to variations in klystron outputs, losses in the feeds and in the waveguides, etc. The rectenna collection efficiency for 0, ± 1 dB, and ± 2 dB amplitude errors are shown in Figure IV.A.2-15. There are no phase errors or failures in the data. For a 5000 meter rectenna radius, the efficiency loss for a ± 1 dB amplitude error (the model configuration) is only .5%.

(3) Failure Rates - Random failure rates of selected percentages are now applied to the entire transmit array. The failures would be due to the failures in the 130,000 klystrons, the 7,850 RF receivers and phase control circuits, and possibly in DC power distribution system in the antenna.

The rectenna collection efficiency for 0, 2%, 5%, and 10% random failure rates are shown in Figure IV.A.2-16. There are no phase or amplitude errors for this data. Collection efficiency is very sensitive to random failures, with about a 2% drop in efficiency for each 1% failure rate. This corresponds to a loss in revenue over a 30-year life time of over \$1 billion for each 1% failure rate. A reasonable goal is 2% failure rate for the model configuration.

(4) Combined Phase Errors and Failure Rates - When there are both phase errors and failures in the antenna, the loss in rectenna collection efficiency is compounded. This data are given in Figure IV.A.2-17 for various combined phase error and failure rates. No amplitude errors are present.

(5) System Performance with Specified Parameters - The model configuration has an error budget of 10° phase error, ± 1 dB amplitude error and a 2% random failure rate. The rectenna collection efficiency for this configuration as shown in Figure IV.A.2-18 is 88% for a 5000 meter rectenna radius. This is the collection efficiency used when calculating the total DC output power.

The power density at the rectenna for the baseline configuration is shown in Figure IV.A.2-19. The density varies from approximately 22 mw/cm² at the center of the rectenna to .9 mw/cm² at the edge.

Figure IV.A.2-14 - Rectenna Collection Efficiency vs Phase Error

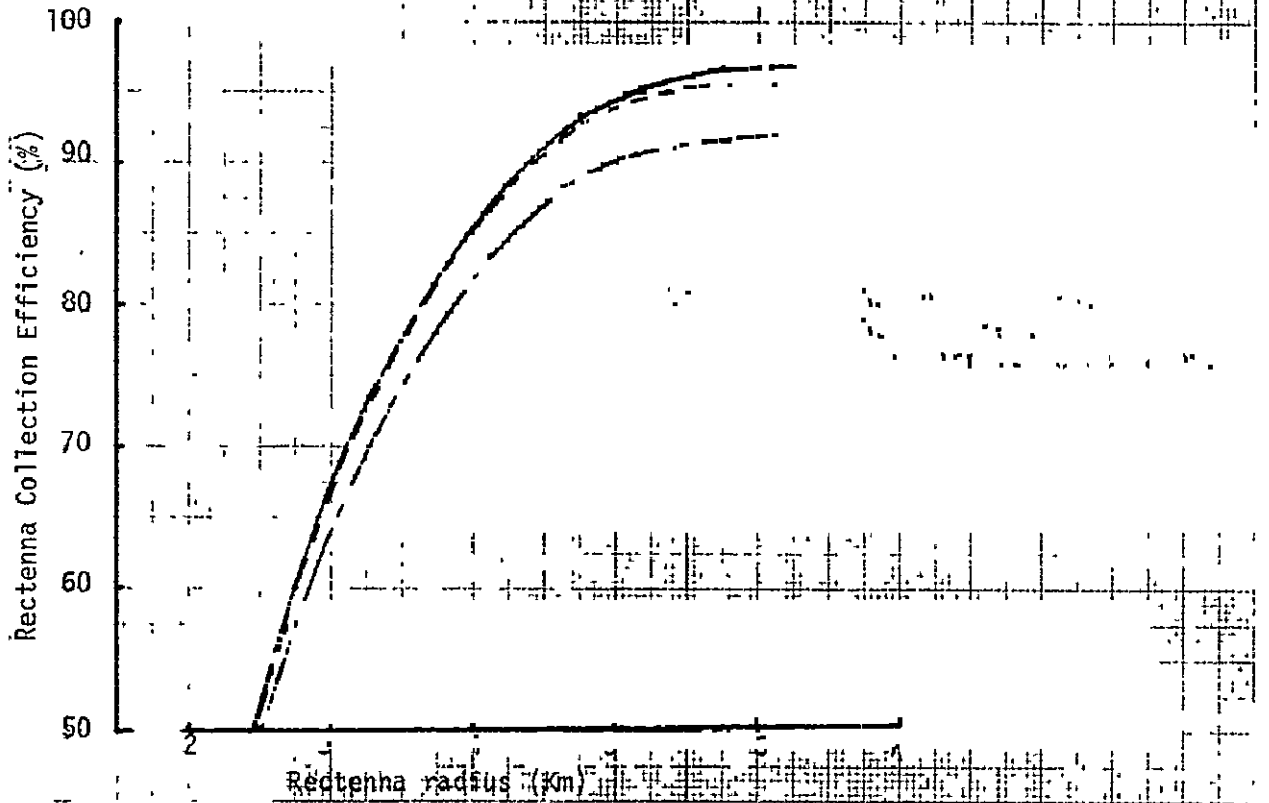
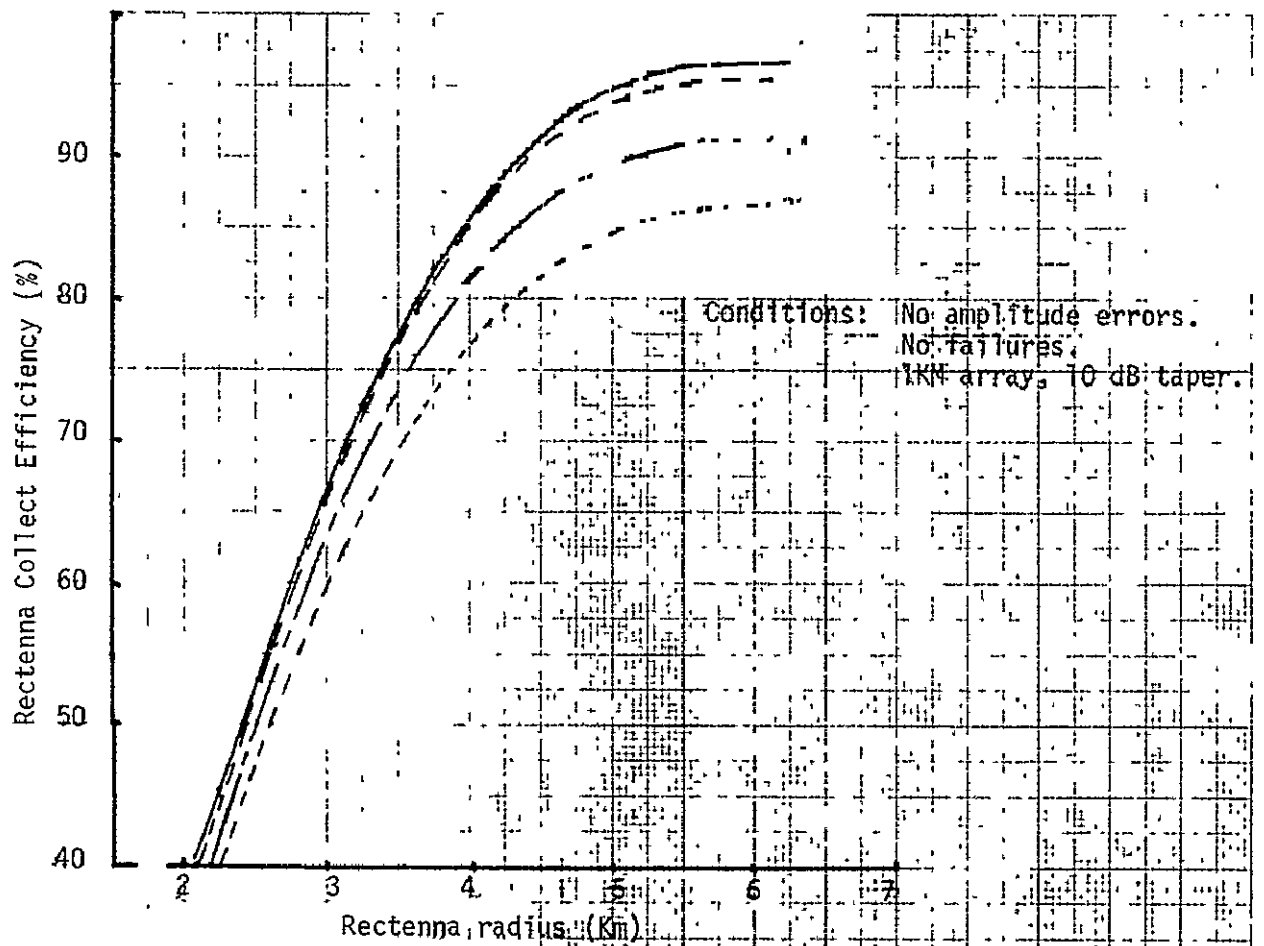


Figure IV.A.2-15 - Rectenna Collection Efficiency vs Amplitude Error

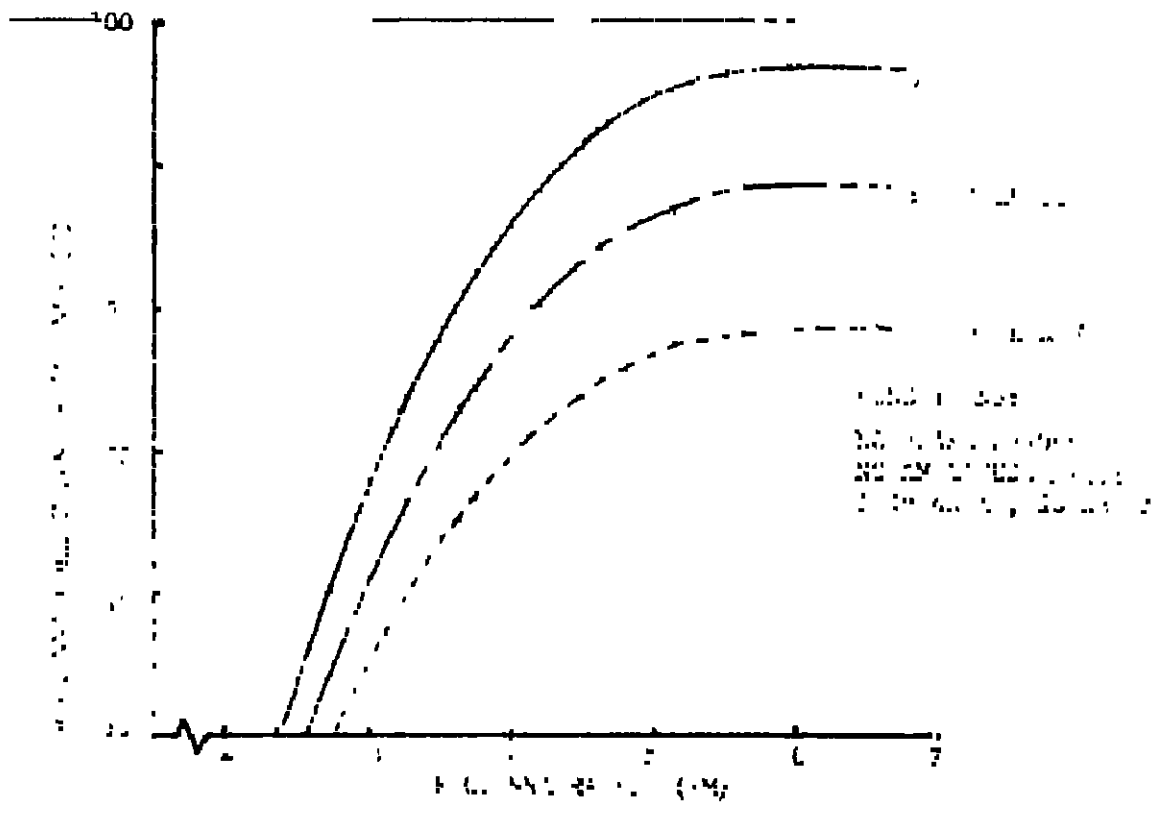
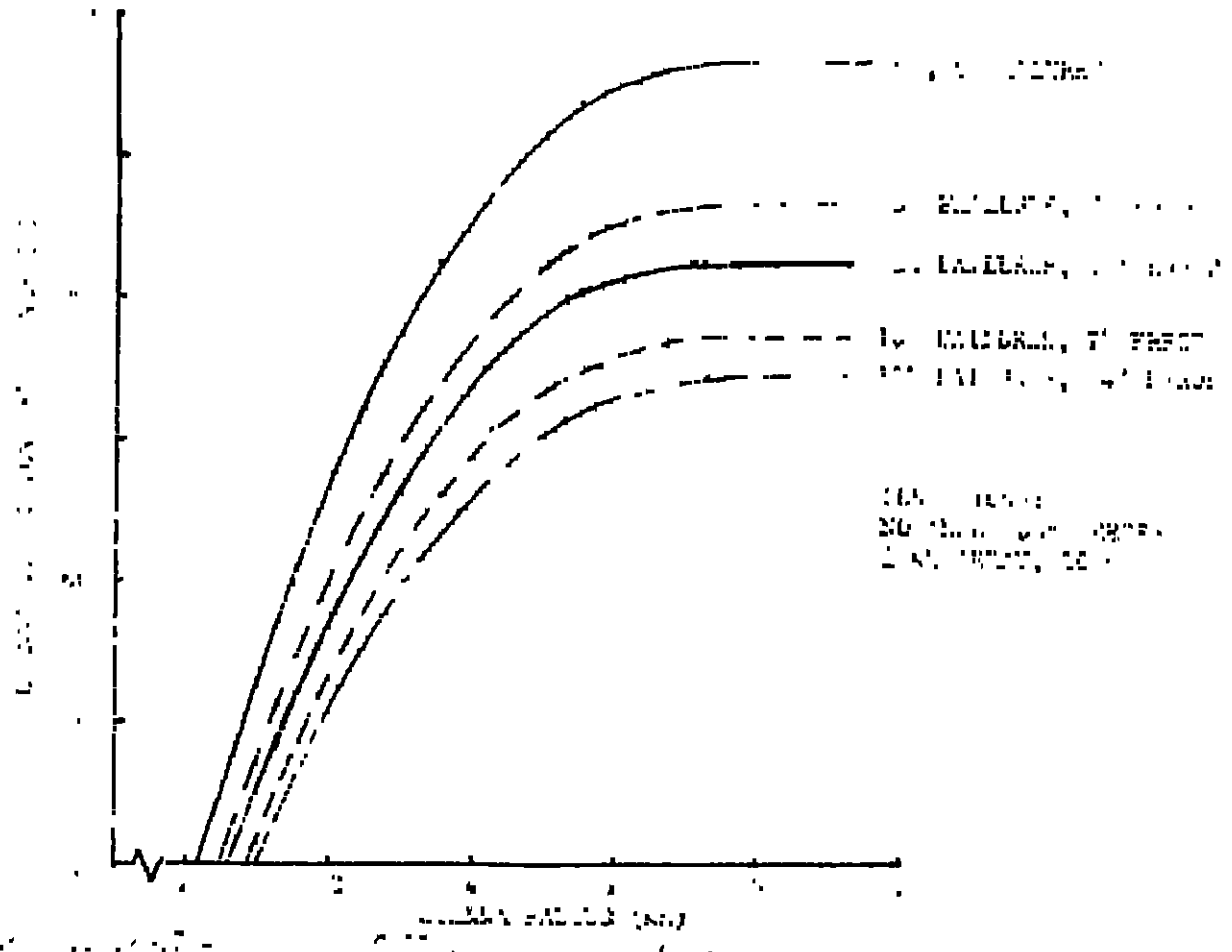


Figure 1. Conversion percentage vs. time for various conditions.



F1

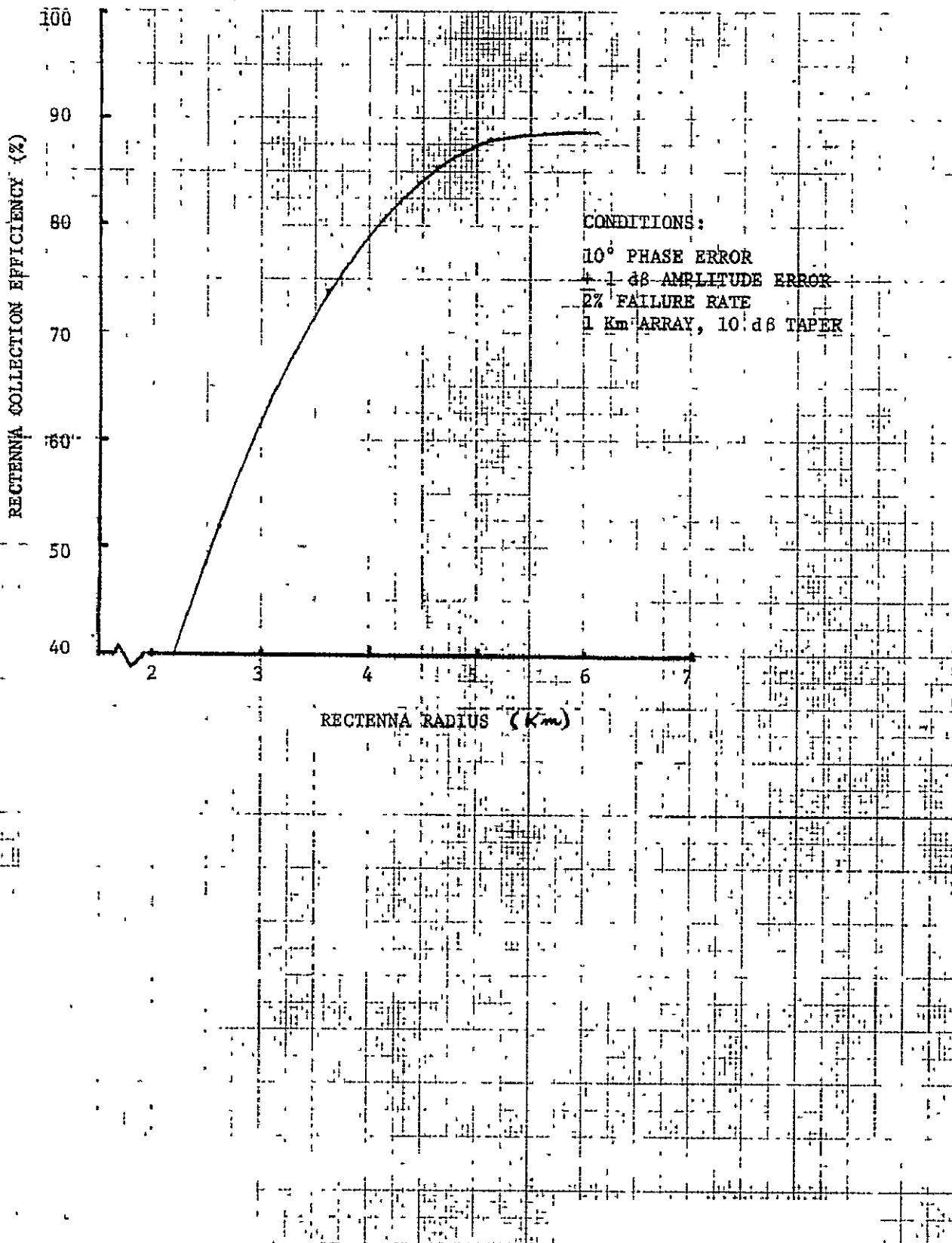
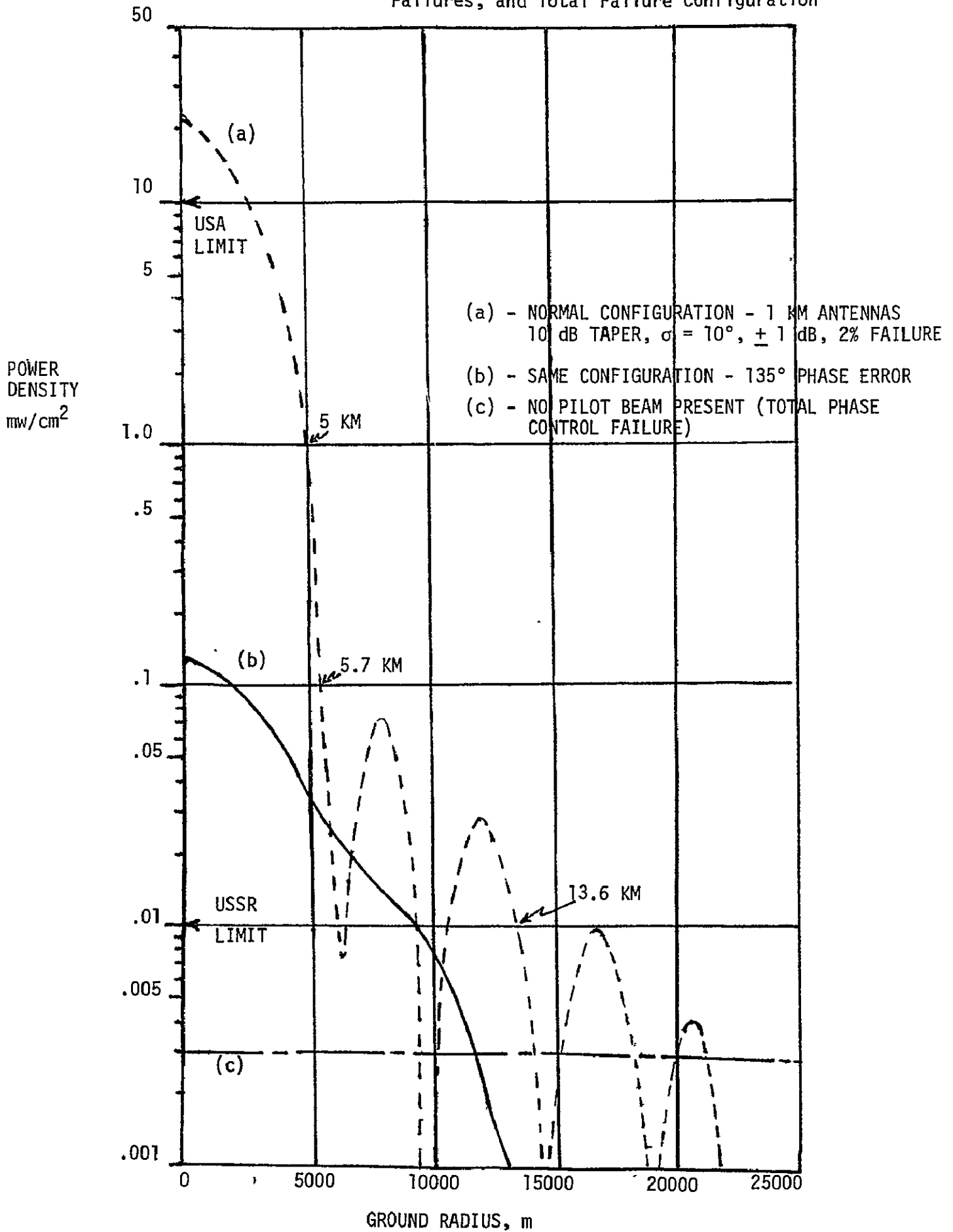


Figure IV.A.2-18 - Rectenna Collection Efficiency for Baseline Configuration

Figure IV.A.2-19 - Power Density at Rectenna for Normal, Partial Failures, and Total Failure Configuration



IV.A.2(i) NOMINAL WEIGHT AND COST SUMMARY FOR THE MICROWAVE SYSTEM SIZING

The nominal weights and costs for the 5GW microwave system with the 1 km transmit array are summarized below. The transportation cost is assumed to be \$164/kg. No construction costs are included.

Transmit Antenna

Subsystem	Cost	Weight	Transportation Cost	Total Cost
Klystrons (130,000 units)	\$260X10 ⁶	4.42X10 ⁶	\$725X10 ⁶	\$985X10 ⁶
Subarray Phase & Control System (using cables)	\$22X10 ⁶	.147X10 ⁶	\$24.1X10 ⁶	\$46.1X10 ⁶
Subarray Receivers/ Transmitters (for 8.750 subarrays with redundant units)	\$471X10 ⁶	.028X10 ⁶	\$4.59X10 ⁶	\$475.6X10 ⁶
DC Power Distribution (lateral system - 40Kv)	\$3X10 ⁶	.084X10 ⁶	\$13.8X10 ⁶	\$16.8X10 ⁶
Attitude Sensors & Command System	\$5X10 ⁶	.002X10 ⁶	\$.328X10 ⁶	\$5.3X10 ⁶
Waveguides (.55mm aluminum)	\$115X10 ⁶	1.66X10 ⁶	\$272X10 ⁶	\$387X10 ⁶
Structure (primary, secondary structures, thermal control - excluding rotary joint)	\$60X10 ⁶	1.04X10 ⁶	\$170.5X10 ⁶	\$230.5X10 ⁶
TOTAL WEIGHT		7.38X10 ⁶ kg		
TOTAL COST				\$2146X10 ⁶

Cost/size relationship; total cost = \$985X10⁶ + \$1479/m² X array area,

Ground Systems - (excluding DC bus bars)

Rectenna is 10 km in diameter;

Subsystem	Quantity Required	Cost
Rectenna		
Dipole	14,500X10 ⁶ (185/m ²)	\$217X10 ⁶ (.015 each)
Circuit and Diode Assembly	14,500X10 ⁶	\$217X10 ⁶ (.015 each)
Land & Preparation	17.6 km diameter (80,000 acres)	\$210X10 ⁶ (\$2,500/acre cost \$1,000/acre preparation)
Ground Command and Pilot System		\$50X10 ⁶
Support Structure and Assembly (for 78.5X10 ⁶ m ²)		\$589X10 ⁶ (\$30,000/acre or \$7.50/m ²)
TOTAL COST		\$1292X10 ⁶

The \$1.29X10⁹ cost for the rectenna and facility is heavily dependent upon the diode and assembly cost/unit. A large variation in the \$.015/unit cost could significantly change the rectenna cost.

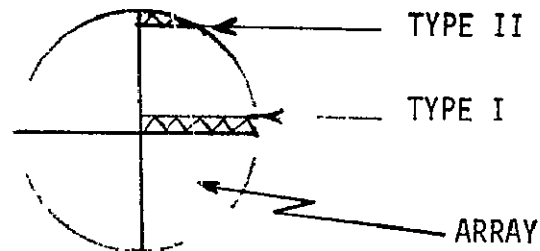
IV.A.2(j) FAILURE MODE ANALYSIS

Studies were made into three types of discrete failures in the transmit antenna (1) a partial breakdown in the phase control system, (2) a total breakdown of the phase control system, and (3) a partial breakdown in the DC power distribution system.

If the feedback phase control to the subarrays has large errors induced into the system, the subarrays no longer add in-phase to create a high power, narrow beam signal. Each subarray may act as an individual antenna, radiating its energy to the earth as a wide beamwidth signal. The power density at the rectenna for a large phase error of 135° is shown in Figure IV.A.2-19. The power density into and around the rectenna decreases by a factor of 100 within the main beam when compared to a properly phased-signal. Comparative sidelobe levels will increase with distance from the rectenna.

A total breakdown of the phase control system, as would happen if the pilot beam from the ground was interrupted, is also shown in Figure IV.A.2-19. The power density is reduced to $.003 \text{ mw/cm}^2$, well below even the stringent USSR microwave limits. There should not be any health hazards if the phase control system fails completely.

Two types of failures within the lateral DC power distribution system were investigated. Referring to the diagram below, switching failures in the lateral system



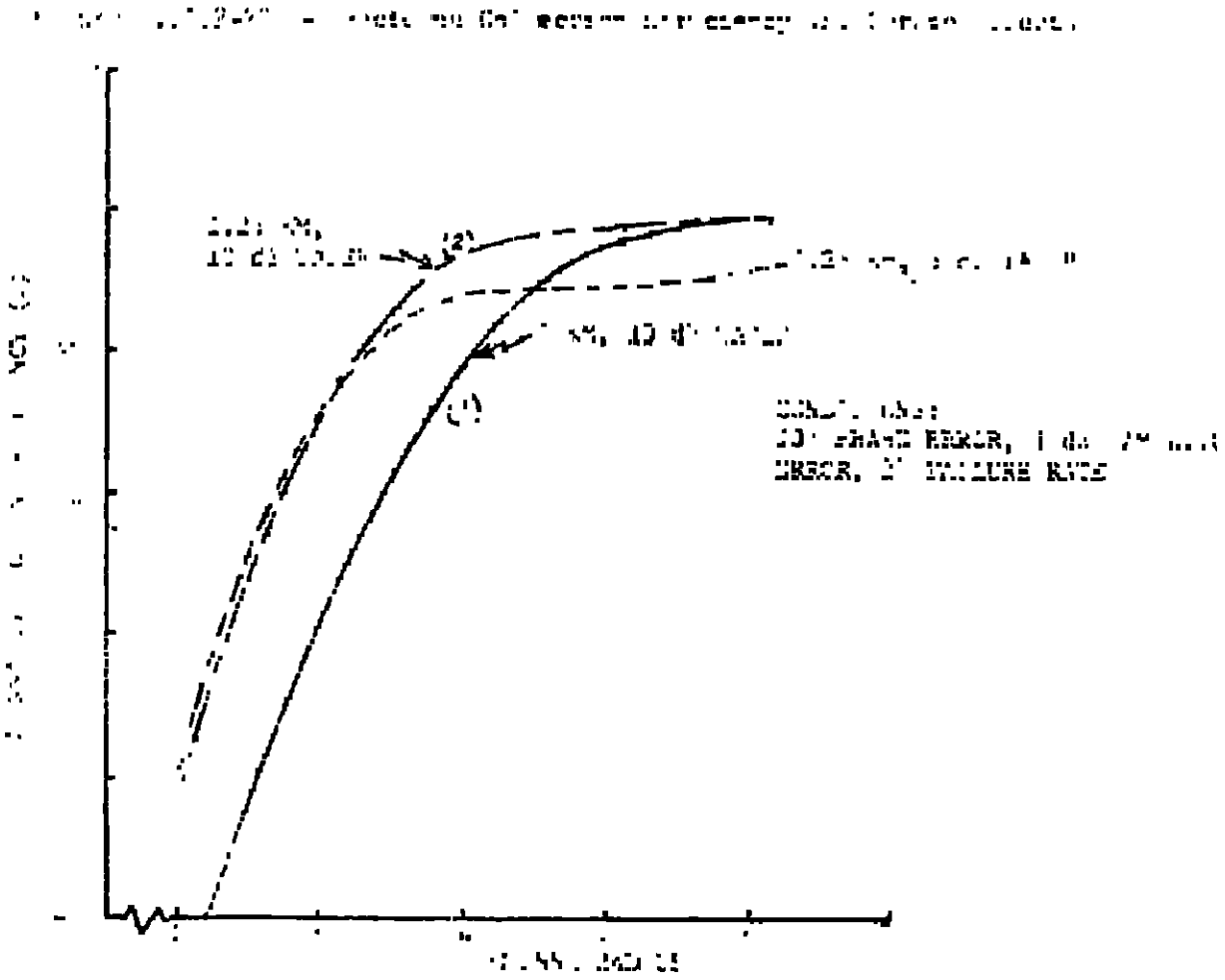
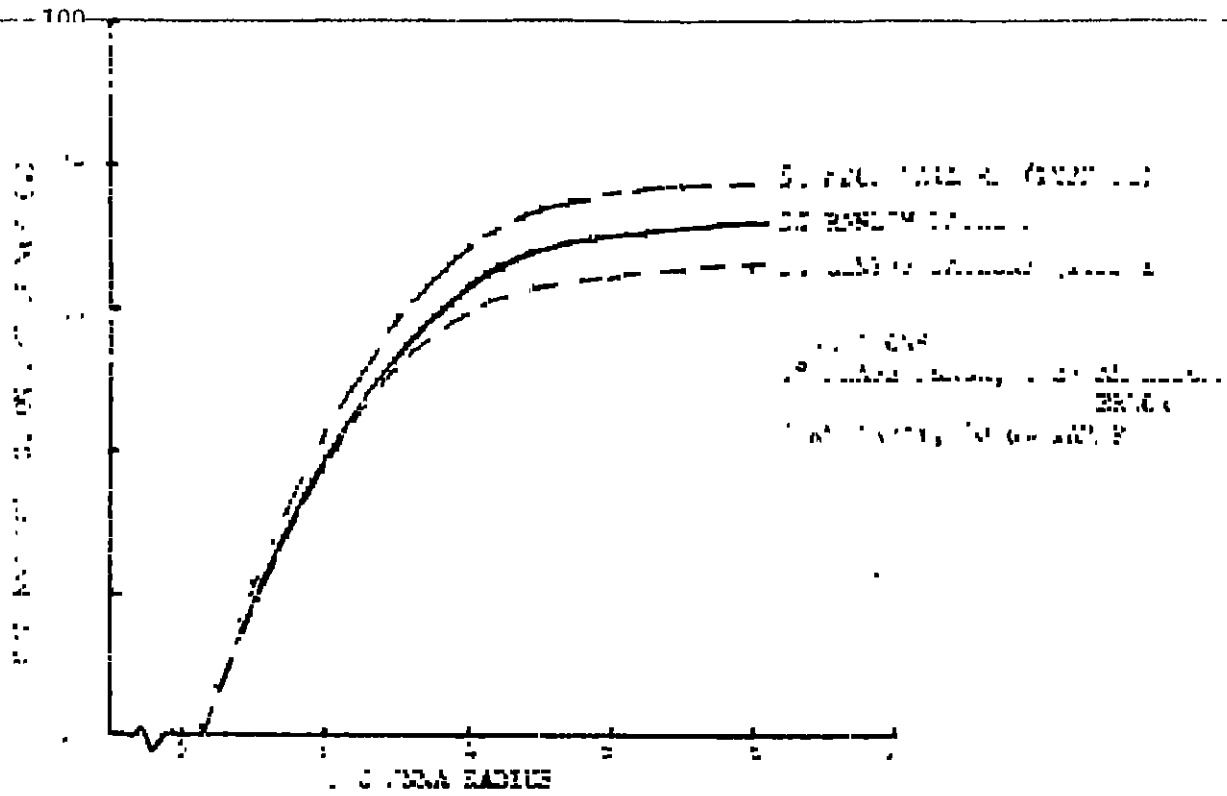
near the center of the array (called Type I) and near the edge of the array (Type II) are shown. In each case a 5% loss in the number of radiating subarrays is assumed. The rectenna collection efficiency for these two types of failures are compared with a 5% random failure in Figure IV.A.2-20. As would be expected, the 5% discrete loss at the center of the array has the greatest loss in efficiency while the 5% loss at the edge has the minimum loss. The subarrays at the edge of the array have only 1/10 the radiated power of those in the center, and hence, do not appreciably affect the efficiency.

IV.A.2(k) CONTINGENCY ISSUES

Some studies have been done into the solutions of possible system problem areas. These include:

(1) What can be done if the phase, amplitude, or failure rate requirements are too stringent, or the subarray misalignment tolerances cannot be met?

One solution is to increase the size of the transmit array. The rectenna collection efficiency for 1.25 km antenna is compared to the 1 km, model antenna in Figure IV.A.2-21. Both curves have the same error budget, 10° phase error, $+1 \text{ dB}$ amplitude error, and 2% failure rate. For the 10 dB taper curves, (1) and (2), the 1.25 km antenna gives 5-7% greater efficiency in the mainbeam and can compensate for greater errors or failure rates. Referring back to Section IV.A.2(i), the increase in transmit array cost for going to a 1.25 km diameter is $\$700 \times 10^6$, which is the equivalent in revenue cost ($\$522 \times 10^6$ per 1% collection efficiency) of 1.4% in collection efficiency. Thus, for a cost viewpoint, if the collection efficiency drops because of projected increases in the errors or failure rates, a larger transmit antenna may be justified.



(2) What should be done if thermal radiation problems at the center of the transmit array cannot be solved without using complex, active cooling systems?

One solution is to reduce the taper to 5 dB and increase the antenna size. The collection efficiency for a 1.25 Km, 5 dB taper antenna is shown in Figure IV.A.2 -21. It would be more desirable to increase the diameter to 1.25 Km and keep the 10 dB taper. The data given in Figure IV.A.2-1 indicates the boresight power density would decrease approximately 30% by going to the larger diameter and keeping the 10 dB taper.

(3) Klystron versus amplitrons - The model configuration uses 50 Kw klystrons for the power converters in contrast to previous studies which employed 5 Kw amplitrons. It is felt that klystrons would have a higher reliability. From a system viewpoint, there are two critical issues which may determine whether amplitrons or klystrons should be used. There are (1) high efficiency with reduced power - the DC input power to the transmit antenna will decrease by about 30% over the 30-year lifetime. As the current slowly decreases to 70% of its initial value into the power converters, the klystron or amplitron must maintain a high DC-to-RF conversion efficiency. One method to reduce this 30% reduction is to add solar cell arrays periodically to the SPS. (2) High reliability - the rectenna collection efficiency is very dependent upon the failure rate. The % collection efficiency as a function of failure rate for a transmit antenna with 10° phase error and ± 1 dB amplitude error is shown in Figure IV.A.2-22. The slope of the curve gives a 2% loss in efficiency for each additional 1% failure rate. As discussed previously, this is one billion dollars loss in revenue over the 30-year life for 1% failure rate. Thus, the power converters must operate efficiently and reliably in a high temperature environment.

IV.A.2(1) BASIC MICROWAVE SYSTEM PERFORMANCE SUMMARY

The performance characteristics and requirements for the model microwave system may be summarized as follows:

- (1) Output DC power - 5GW at the rectenna
- (2) Transmit Array size - 1 km in diameter
- (3) Array aperture illumination - a 10 step, truncated Gaussian amplitude distribution with a 10 dB edge taper
- (4) Subarray size - 100 m^2 (approximately 10m X 10M)
- (5) Number of subarrays - 7,850
- (6) Error budget -
 - Total RMS phase error for each subarray - 10° (for the phase control system)
 - Amplitude tolerance across subarray - ± 1 dB
 - Failure rate (total) - 2% over 30 year lifetime

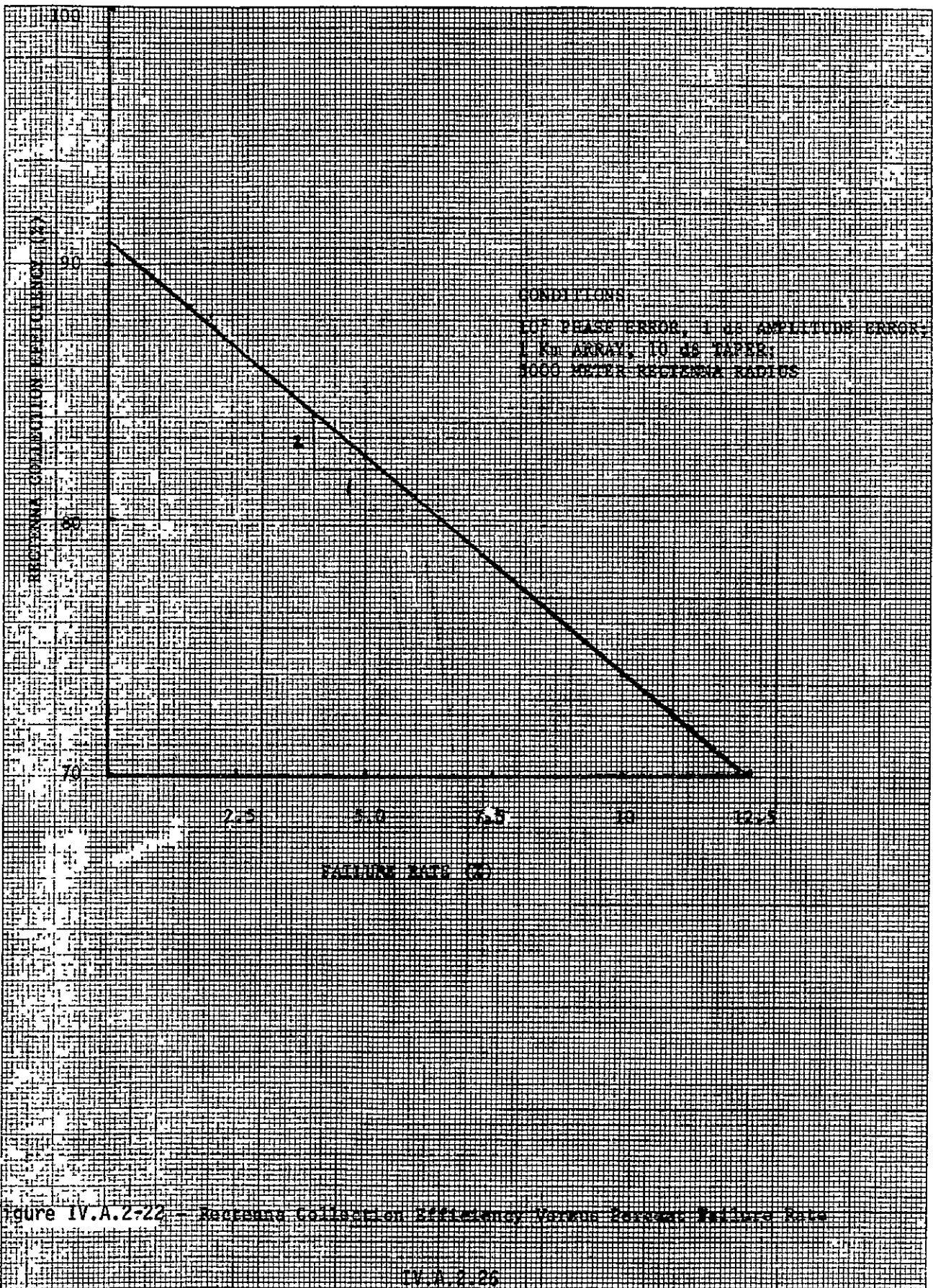


Figure IV.A.2-22 - Receiver Collection Efficiency Versus Receiver Failure Rate

IV.A.2-26

ORIGINAL PAGE IS
 OF POOR QUALITY

- (7) Power converters - 50 kw klystrons
- (8) Phase control - An active, retrodirective array with a phasing system using transmission lines combined with a subarray-to-subarray phase transfer scheme.
- (9) Antenna radiators - slotted waveguides
- (10) DC power distribution system - lateral configuration; 40 KV
- (11) Antenna mechanical alignment requirements - ± 3 arc minutes for a 2% loss in effective antenna gain
- (12) Rectenna dimensions - 10 km X 13 km (for a 36° latitude)
- (13) Rectenna collection efficiency - 88% using the specified error budget
- (14) Ground facility dimensions - 17 km by 23 km (for the .05 mw/cm² power density limit taken as the example)
- (15) Power density at center of rectenna - 22 mw/cm²
- (16) Power density at edge of rectenna - .9 mw/cm²
- (17) Power density at edge of ground facility - .05 mw/cm²
- (18) Rectenna cost - \$1.29 X 10⁹
- (19) Transmit array cost - \$2.146 X 10⁹
- (20) Transmit array weight - 7.38 X 10⁶ kg
- (21) Total microwave system efficiency (nominal) 63% (from DC output at rotary joint in transmit array to collected DC output of rectenna).

} atmospheric
attenuation
included

REFERENCES

1. Maynard, O.E.; Brown, W. C.; Edwards, A.; Haley, J. T.; Metz, G.; Howell, J. M.; Nathan, A., "Microwave Power Transmission System Studies" NASA CR-134886, Contract NAS 3-17835. Raytheon Company, Sudbury, Mass., December 1975.
2. G. H. Stevens and R. Schu, "Some Requirements of a Space to Earth Microwave Power Transmission Link" Lewis Research Center Report, 1975.
3. Meltz, G., et al., "Ionospheric Heating By Powerful Radio Waves" Radio Science, Vol. 9, pp. 1049-1063, November 1974.
4. Gordan, William, "Private Communication" April 1976.
5. "Microwave High Power Transmission - Final Report", Jet Propulsion Laboratory, #434-41001-0-330, 1974

IV-A-3. Orbit Considerations

a. Perturbations

V. R. Bond
Mission Planning & Analysis Div.

The tacit assumption is made in the discussion of a geosynchronous satellite that it is in orbit at a precise constant distance (42, 241 km) from the center of the earth and in the plane of the earth's equator. At this radius, the angular rate of the satellite is equal to the rotational rate of the earth. The satellite will therefore remain over the same point on the earth's equator, having the appearance of being fixed relative to this point.

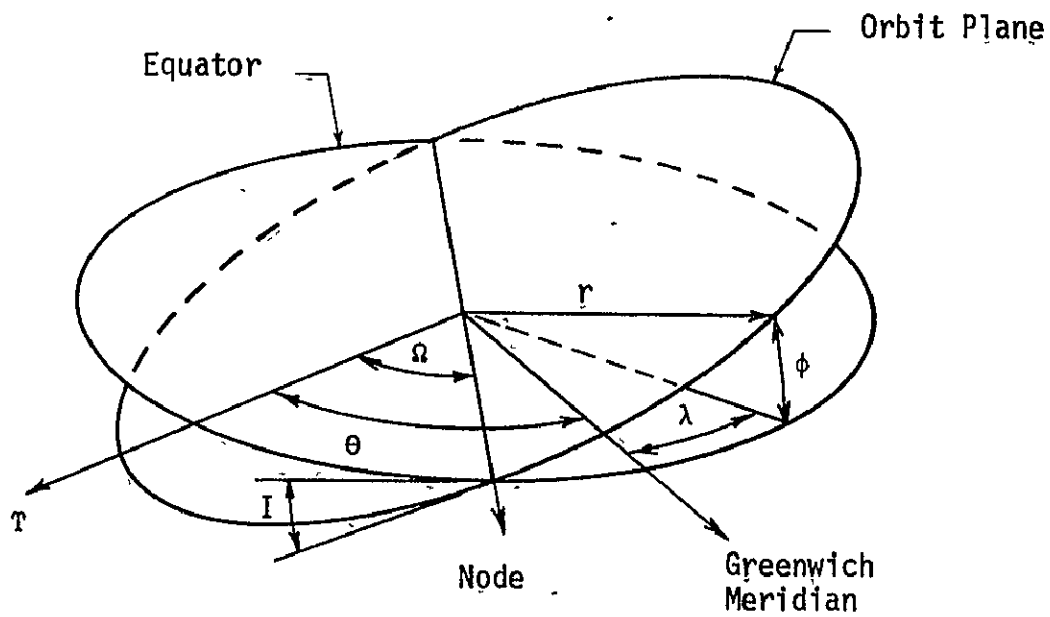
This is a rather idealized view and would be true if the earth were a homogeneous sphere and if the earth were the only gravitational body in the universe. Actually, since the earth is not a homogeneous sphere and since it is perturbed by other gravity sources (mainly the sun and moon) and since the effects due to solar pressure are not negligible (on a satellite of substantial size), the motion is much more complicated than that described for the idealized situation above. But these perturbative effects* are fortunately for the most part uncoupled and may be analyzed somewhat independently. They are of approximately the same order of magnitude at the satellite radius and will be discussed in the order (1) luni-solar (moon and sun); (2) solar pressure; and (3) equatorial ellipticity (J_{22}).

(1) Luni-Solar (Sun and Moon Effects)

The luni-solar perturbations have substantial effects only upon the node Ω and the inclination I of the orbit. These angles can be understood by referring to figure IV-A-3-1. The node Ω is the angle measured from a fixed direction in space (a line from the center of the earth to the point where the sun crosses the earth's equator from south to north--the vernal equinox). The inclination I is the angle between the earth's equator and the satellite orbit. Table IV-A-3-1 shows some representative values of the inclination after two years and 26.5 years for different values of the initial inclination. The important point is that the inclination I has a period of 53 years and that the maximum value of I depends upon the initial values of I and Ω . For example, the first row of table IV-A-3-1 shows that an orbit initially in

*For the solar power station there may be other forces which should be considered. For example, the induced thrust due to the emission of microwave energy from the antenna.

IV-A-3-2



- θ = R.A. of Greenwich
- ϕ = Latitude
- λ = Longitude
- r = Radius
- τ = Fixed Direction (Vernal Equinox)

Figure IV-A-3-1. Orbit Geometry

Table IV-A-3-1. Variation of Inclination

<u>I_0</u>	<u>Ω_0</u>	<u>I (2 yrs)</u>	<u>Max. I (26.5 yrs)</u>
0°	undef.	1.73°	14.7°
1°	270°	.74°	14.9°
1°	90°	2.00°	15.0°
7.3°	180°	8.00°	29.4°
7.3°	0°	7.30°	7.3° (const)

IV-A-3-3

the earth equatorial plane ($I_0 = 0$, Ω_0 undefined) will attain a maximum I of 14.7 degrees after 26.5 years. However, the last row shows that an orbit with initial $I = 7.3$ degrees and initial $\Omega = 0$ has a constant orientation in space. For $e = 0$, the satellite longitude λ remains constant but the latitude varies between ± 7.3 degrees each day.

(2) The Solar Pressure Effects

The solar pressure effects depend upon the area and weight of the satellite. The results of this section are consistent with the area and weight data stated elsewhere in this document.

The effects of solar pressure are very complex to analyze and the studies are not yet complete. However, the significant effects are a growth in eccentricity, e , and a rotation of the line of apsides. In the idealized case, $e = 0$, but the solar pressure causes an increase in this value to 0.068 in the first year. During the first few years, there is a periodic oscillation in e between 0 and 0.068. However, numerical studies indicate that for certain initial conditions there is a long term growth of the mean value of e . Further studies should reveal whether this growth in e is truly secular (increasing without bound) or is simply a longer periodic motion.

It also appears that the maximum e can be reduced by choosing an intermediate initial value of e and a suitable perigee location. This possibility also requires more detailed study.

The principal result of the periodic (one year) variation in eccentricity is a daily longitude oscillation $\Delta\lambda$ about the mean value of the longitude λ . For small I (up to about 10 degrees), $\Delta\lambda \approx \pm 2e$ (radians); for $e = 0.068$, the variation in longitude is ± 7.87 degrees.

(3) Equatorial Ellipticity Effects

This perturbation arises from the fact that the earth is not symmetrical about its spin axis. A slice of the earth perpendicular to the spin axis has an elliptical shape. This corresponds to the J_{22} tesseral term in the earth's potential expansion. Mathematically the problem has four stationary solutions. Two of these solutions are stable and two are unstable. The stable solutions represent points above the equator at about 120°W and 60°E on the minor axis of the equatorial ellipse; the unstable solutions represent points at 30°W and 150°E (see figure IV-A-3-2) on the major axis of the equatorial ellipse.

If at a stable point initially, a satellite will tend to remain; if disturbed somewhat it will librate about the stable point. The period of libration is a function of the initial displacement from the stable point (see figure IV-A-3-3). For example, a displacement in longitude of 60° from a stable point results in a libration period of about 1000 days.

IV-A-3-5

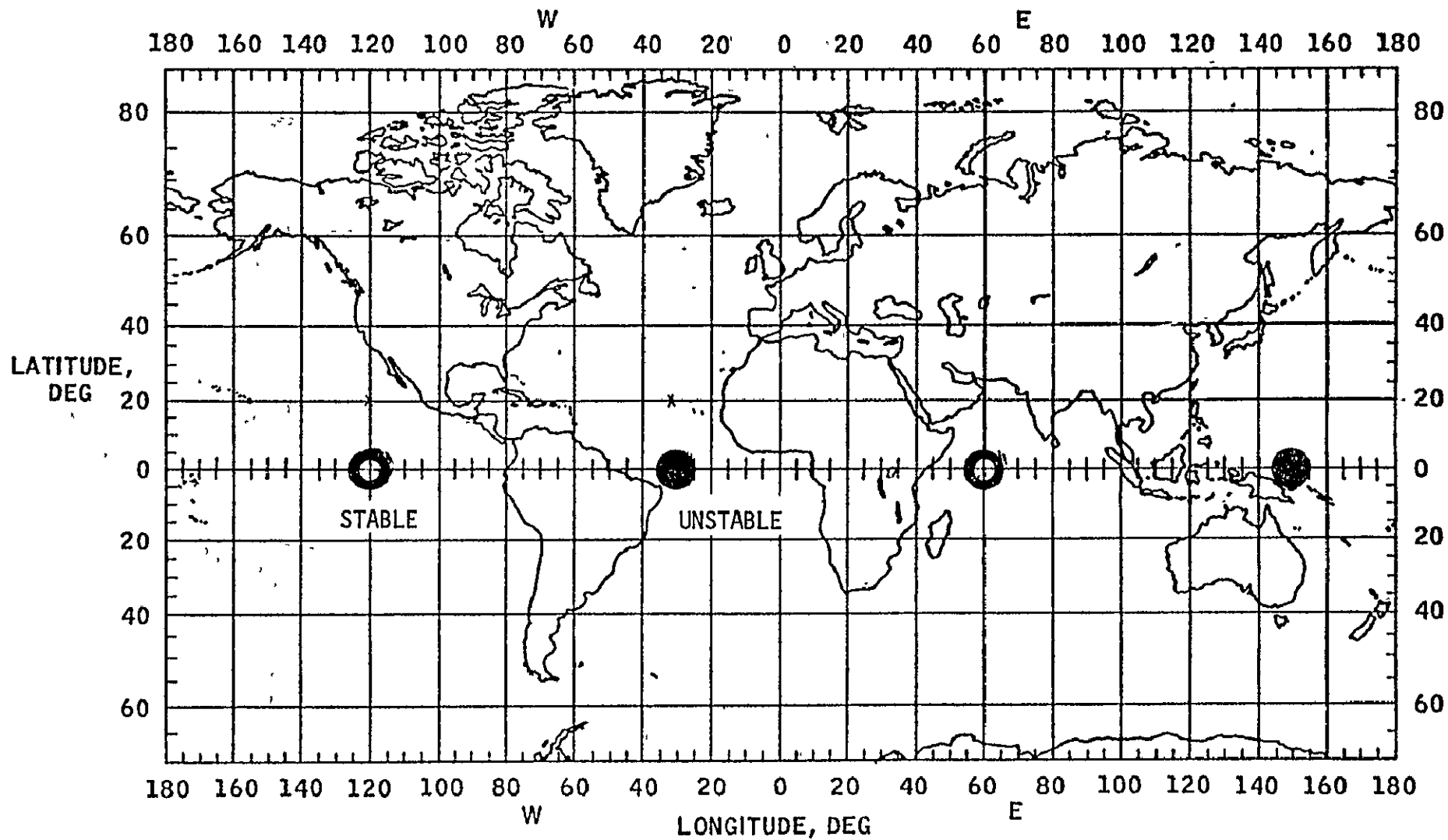


Figure IV-A-3-2. Stable and Unstable Points

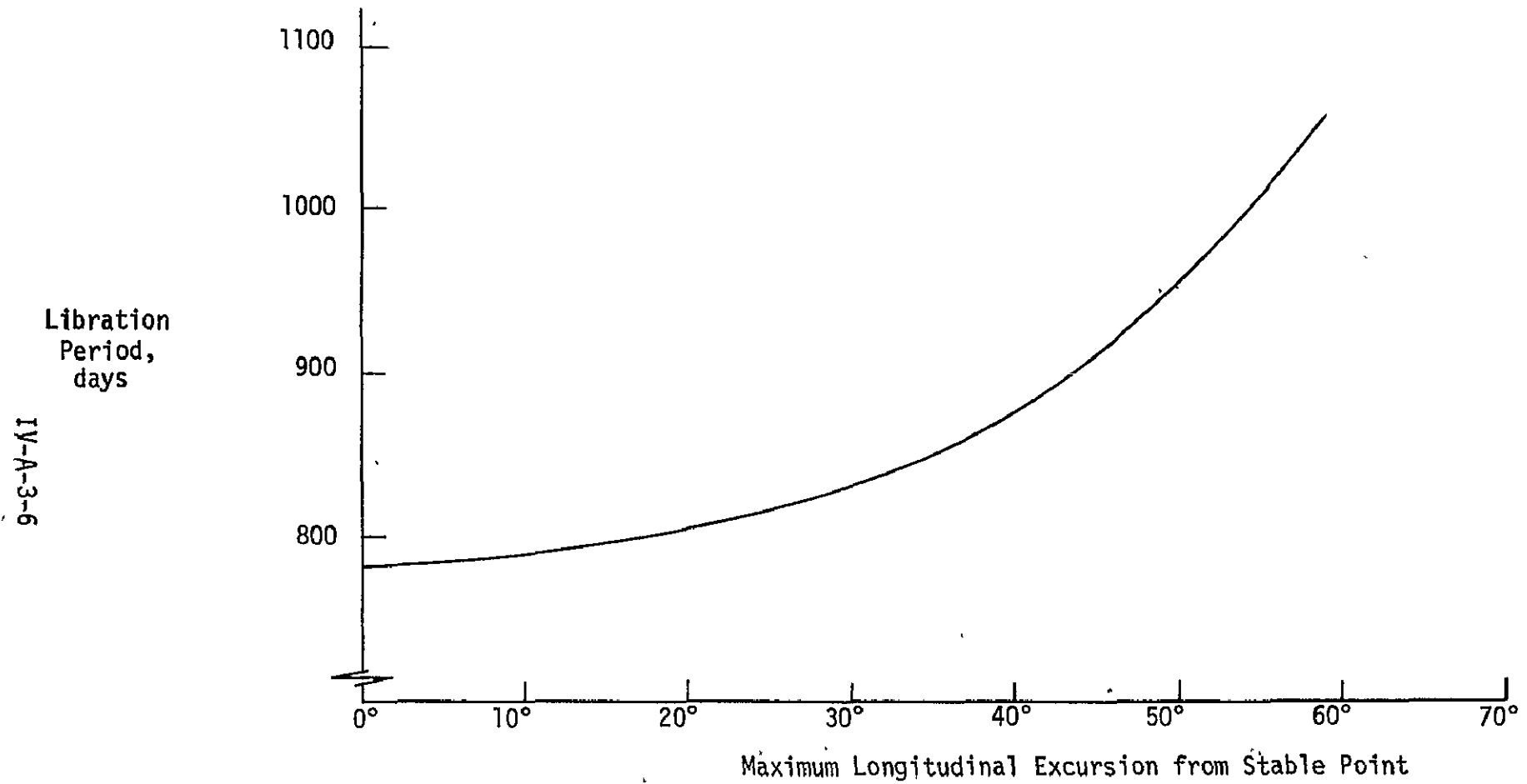


Figure IV-A-3-3. Libration Periods of 24-Hour Satellites

If at an unstable point initially, a satellite will tend to drift away and never return to the initial point.

Since there are only two points where long term stability is achievable, the distribution of geosynchronous satellites about the earth will be limited to these two areas unless station-keeping is permitted. The accumulated delta V requirements for one year for nulling out the ellipticity effects is only one or two feet per second.

(4) Conclusions and Recommendations

The perturbations on a geosynchronous satellite are due to the luni-solar gravitational forces, the solar pressure, and the gravitational force due to the ellipticity of the earth's equator.

The luni-solar effects produce a periodic variation in the inclination of 53 years. By choosing an inclination of 7.3 degrees with a node of zero, an orbital plane fixed in space is obtained.

The solar pressure produces a one year periodic variation in the orbital eccentricity e . For e initially zero, the maximum value of e is 0.068. A non-zero e causes a daily oscillation in longitude of $+2e$ (radians). There is some evidence that the perturbation in eccentricity grows with time. Further studies are required in this area.

The earth's equator can cause large variations in longitude. Unless placed near one of the two stable libration points, the drifts in longitude can become quite large, but periodic.

A detailed analysis for the best approach in correcting these effects is recommended. This analysis should also include perturbations not considered here such as the induced thrust due to the emission of the microwave energy.

b. Non-Ideal Orbits

L. E. Livingston
Spacecraft Design Div.

In the ideal case, the SPS would be placed in a stationary (synchronous, zero-eccentricity, zero-inclination) orbit at a longitude equal to that of the rectenna. A synchronous period can be achieved and maintained without difficulty. However, as discussed in the preceding section, eccentricity and inclination can be held at zero, and longitude at any desired value, only by active stationkeeping. This section discusses some of the ramifications of departures from the ideal orbit.

Eccentricity

The most obvious effect of eccentricity is a daily cyclic variation in the distance from the antenna to the rectenna, which causes

a variation in power density on the rectenna and consequently a variation in power output. This is illustrated in figure IV-A-3-4, which presents output as a function of time and rectenna latitude for an eccentricity of 0.04. This eccentricity is thought to be an achievable peak value (with suitable initial conditions) and has been used for the following analyses. The plots assume an SPS designed for 5 GW rectenna output at 40° latitude in a circular orbit. Total variation in output is roughly 100 MW from maximum to minimum, or about 2 percent. The variation is greater at higher latitudes.

The azimuth and angle of incidence of the microwave beam also vary and influence the power density distribution over the rectenna. The effect appears to be minor for small longitude differences between satellite and rectenna (but not for large differences: see "Longitude Offset" below).

Orbit eccentricity has two effects, essentially independent, on transmitting antenna motion. In a circular orbit, the antenna would rotate continuously at constant angular velocity about an axis perpendicular to the orbit plane (POP). However, the varying orbital velocity of the SPS and the resulting daily oscillation in longitude require a deviation from constant velocity about this axis. The departure from uniform motion is shown in figure IV-A-3-5. Peak angular acceleration of the antenna is about 4.8×10^{-10} rad/s² for an eccentricity of 0.04, zero inclination and rectenna latitude of 40°; it is approximately proportional to eccentricity and varies only slightly with latitude.

The second effect of eccentricity on antenna motion is a variation in elevation angle above the orbit plane, caused by the variation of the satellite radius vector; the amount is illustrated in figure IV-A-3-6 for an eccentricity of 0.04. The amount of variation is greater for higher rectenna latitudes and for higher eccentricities. For 40° latitude and 0.04 eccentricity, maximum angular acceleration is about 5.2×10^{-11} rad/s².

Collision avoidance may be the most important problem with eccentric orbits. Relative to a coordinate system fixed in the earth, a satellite in an eccentric synchronous orbit follows an approximately elliptical path whose major axis is $4ae$, where a is the semimajor axis of the orbit (42164 km) and e is the eccentricity. It follows the same path relative to a satellite in a stationary (synchronous, zero-eccentricity, zero-inclination) orbit.

If 112 satellites are distributed uniformly between the longitudes of Maine and Oregon, the average separation is 0.5° of longitude or 368 km at synchronous altitude. If the difference in eccentricities of two adjacent satellites was as much as 0.0045, their orbits would intersect. Since the expected eccentricity of the SPS orbit is

System designed for 5 GW output at zero eccentricity and 40° latitude

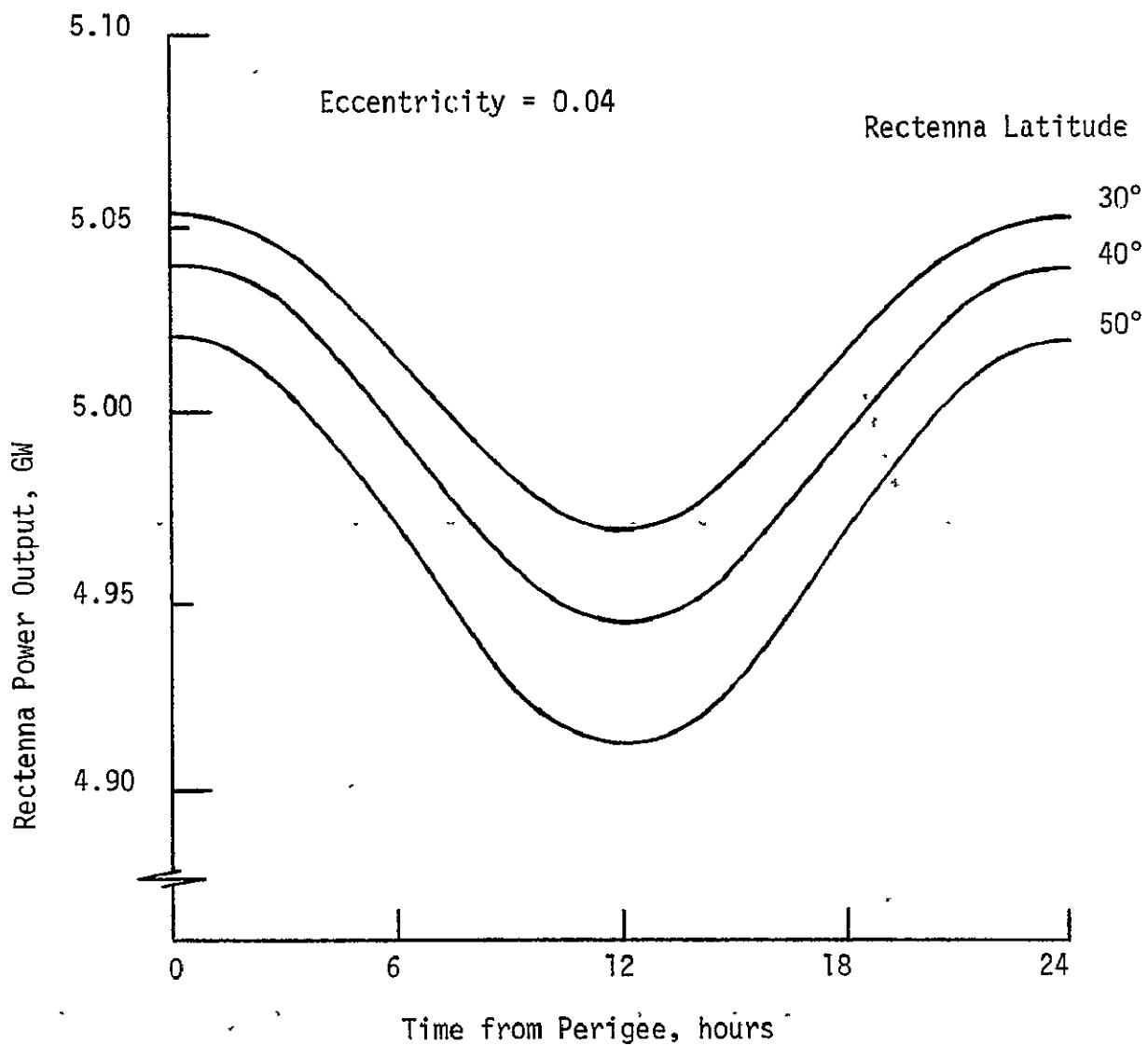


Figure IV-A-3-4. Power Output Variation in Eccentric Orbit

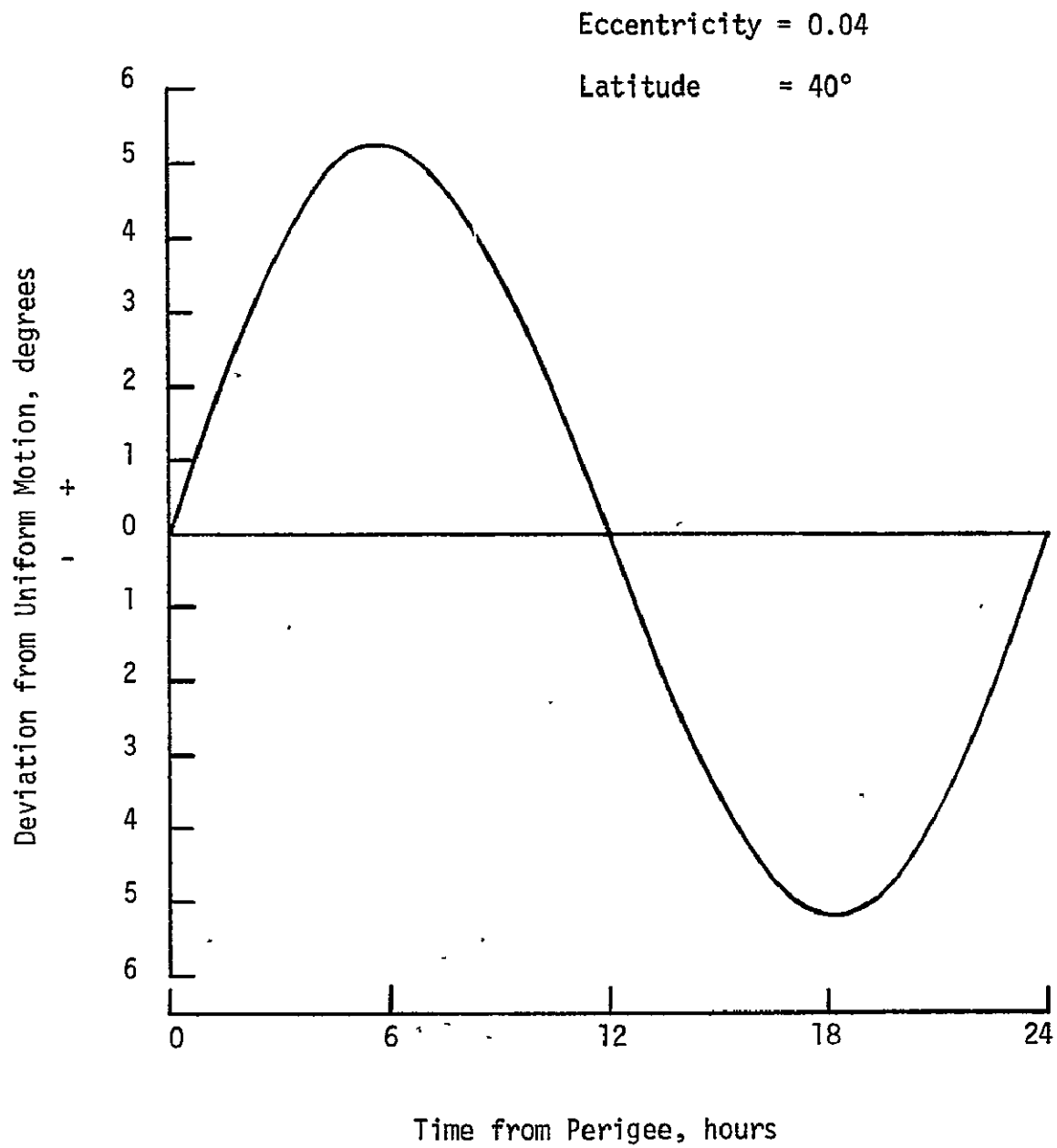


Figure IV-A-3-5. Antenna Rotation

Eccentricity = 0.04

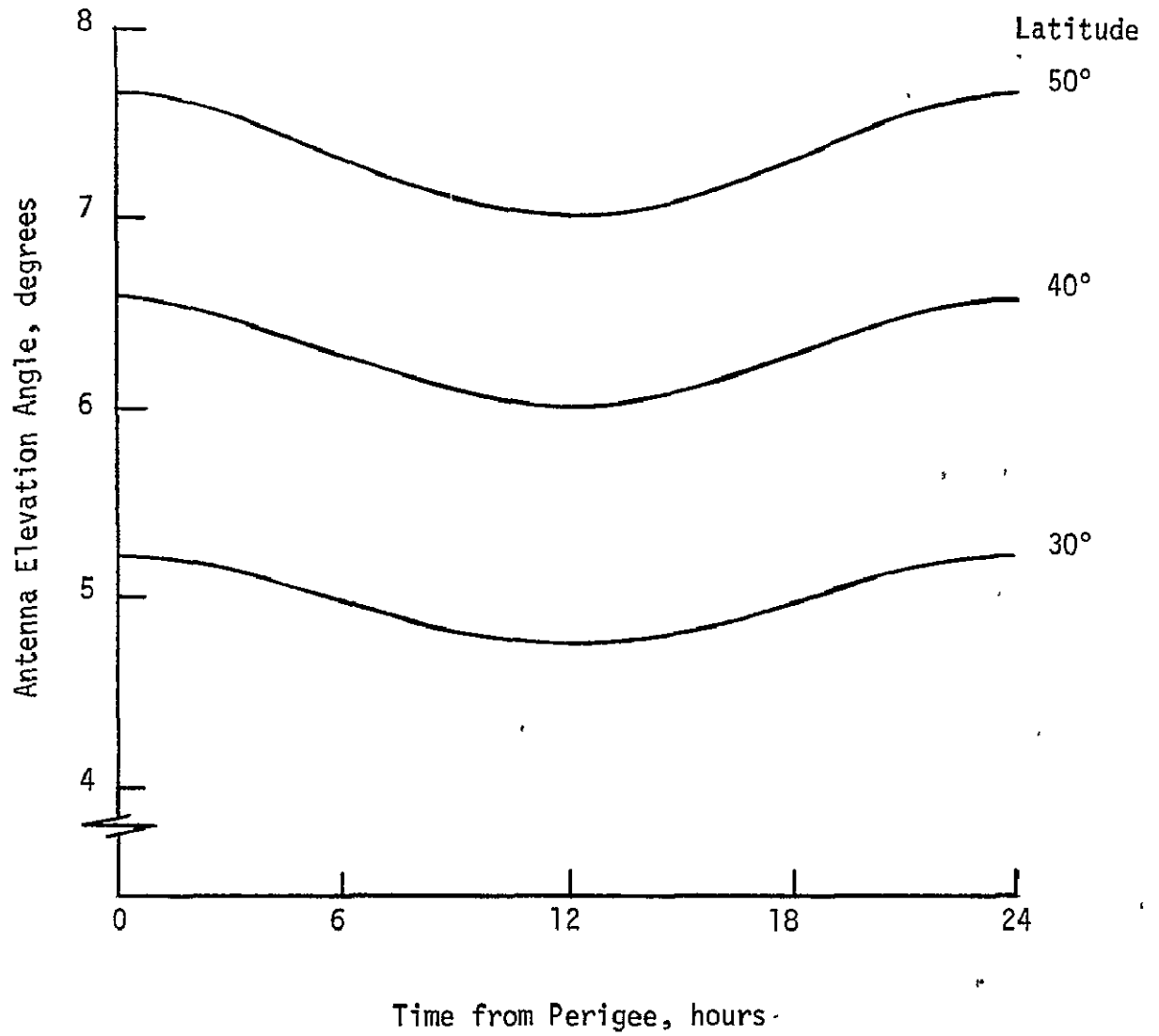


Figure IV-A-3-6. Antenna Elevation Angle

IV-A-3-11

at least ten times this figure, and since the several dozen present synchronous satellites are all in nearly circular orbits, with eccentricities generally less than 0.001, the possibility of collision cannot be neglected. This is particularly true because the SPS program would be the first instance of a large number of satellites being separated by distances only ten or 20 times the dimensions of the satellites.

Probabilities of collision have not been calculated, but the possibility should be considered that eccentric orbits for the SPS's would require all other synchronous satellites within the conflicting range of longitudes to be physically removed from orbit and their functions performed by equipment incorporated (on a "piggy-back" basis) into one or more SPS's. Whether the eccentricity of the SPS orbit is held at zero or permitted to vary, it appears probable that all orbits, SPS and others alike, must be actively controlled to a common eccentricity in order to achieve an acceptably low risk of collision.

Inclination

Consideration of the effects of an inclined orbit has been limited in this study to a single inclination of 7.3° , based on the assumption that the orbit will either be held at zero or, to save propellant, placed in the 7.3° , constant-inclination orbit discussed in IV-A-3-a.

The major effect of an inclined orbit is a daily variation in the angle of incidence of the microwave beam on the rectenna, amounting to roughly 16° (figure IV-A-3-7). This increases rectenna cost in two ways. First, since the major axis of the elliptical area illuminated by the beam is equal to the beam diameter divided by the cosine of the maximum angle of incidence, the land area to be acquired is greater. Second, if the rectenna utilizes the sawtooth configuration commonly assumed (for simplicity of construction, maintenance, etc.), a varying angle of incidence requires more rectenna elements than would a constant angle of incidence, because some of the elements are shadowed by other elements during part of the daily cycle (see figure IV-A-3-8). The magnitude of these effects is summarized in figure IV-A-3-9 as a function of rectenna latitude. These curves indicate only the additional ground area and rectenna elements necessary to intercept the beam as the angle of incidence varies. Variations in azimuth of several degrees will occur and will add still more to the area required, but this has not been evaluated numerically. Variations in power density at a given location on the rectenna will adversely affect efficiency; this has also not been evaluated.

The variation in range, and hence in power output, because of the eccentric orbit is increased somewhat if the inclination is not zero. At a rectenna latitude of 40° and eccentricity of 0.04, for example, total variation in output is 1.9% at zero inclination and 2.0 to 2.6%, depending on perigee orientation, at 7.3° inclination.

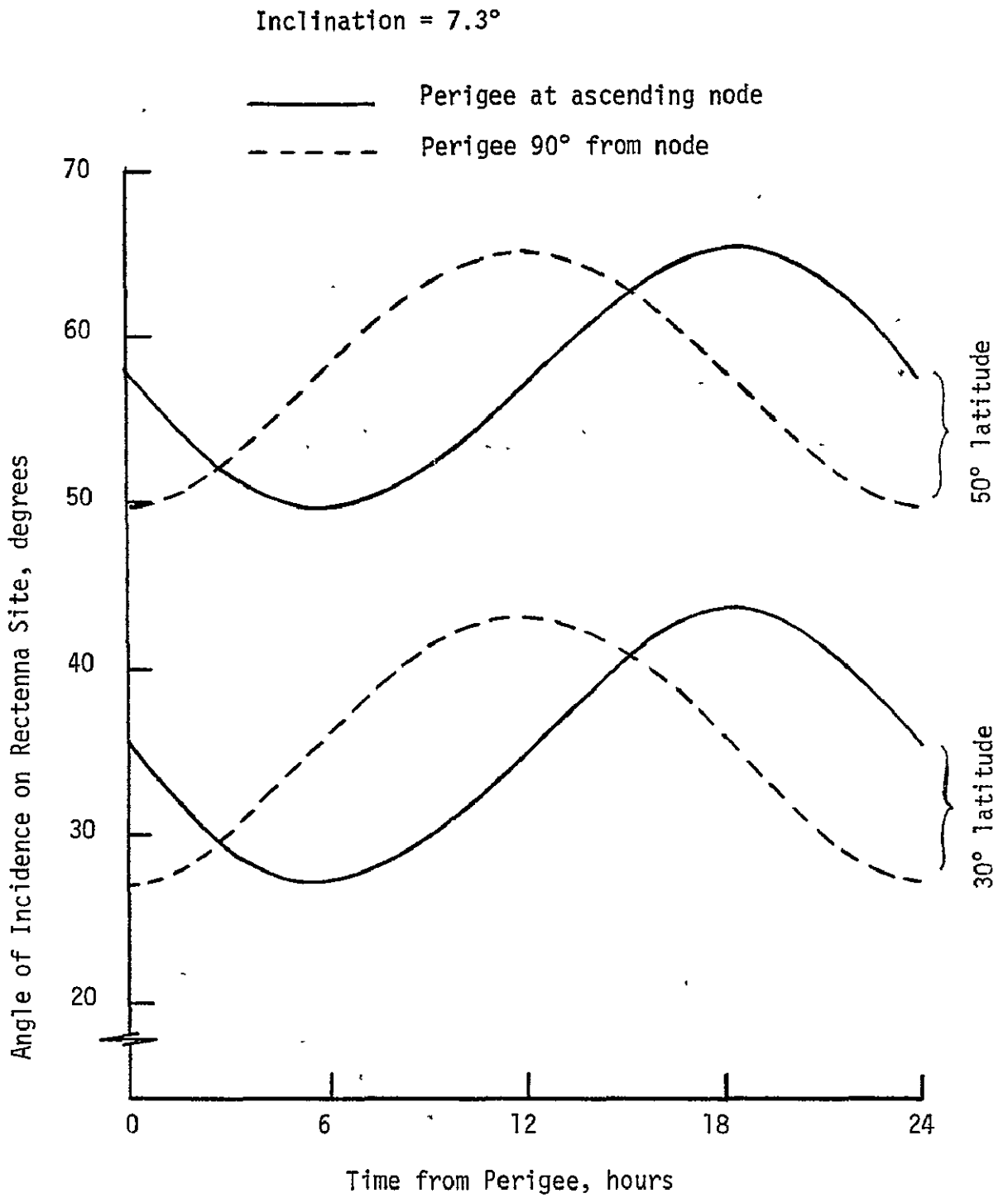


Figure IV-A-3-7. Variation in Angle of Incidence (Inclined Orbit)

IV-A-3-14

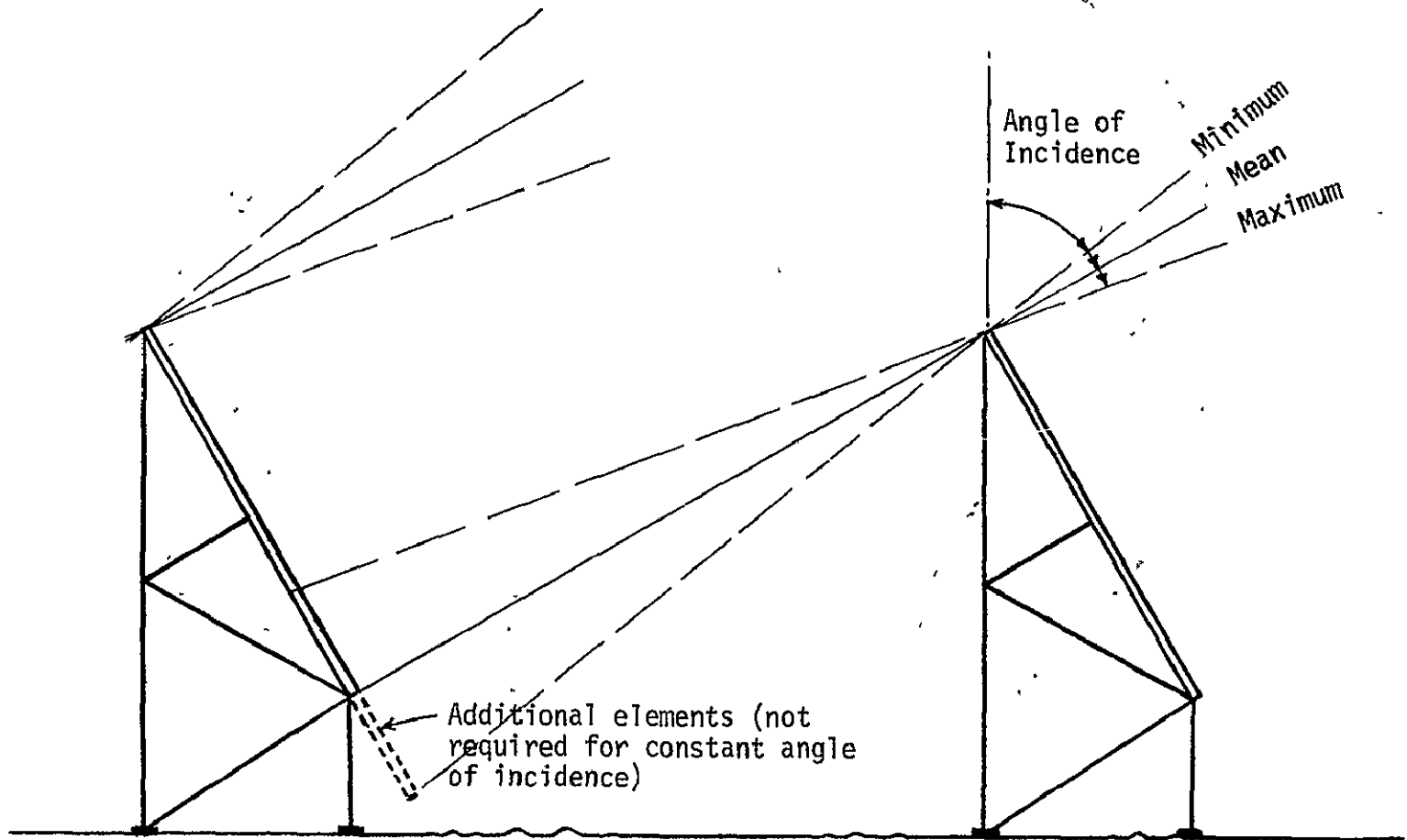


Figure IV-A-3-8. Additional Rectenna Elements for Variable Angle of Incidence

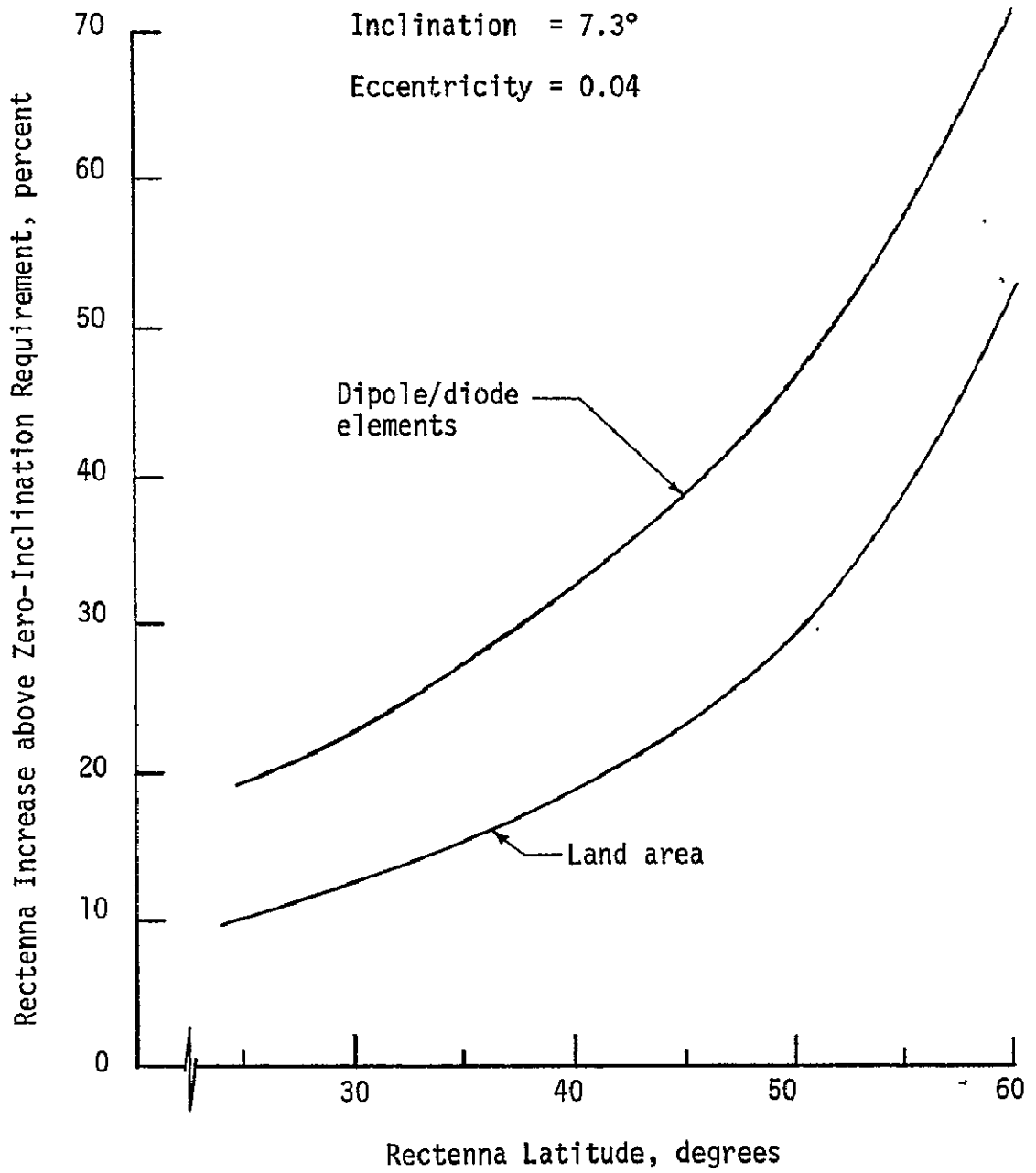


Figure IV-A-3-9. Increased Rectenna for Non-Zero Inclination

Antenna joint accelerations are also slightly higher for inclined orbits, but the increase over that for a zero-inclination, equal-eccentricity orbit is not significant.

Longitude Offset

Ideally, the average longitude of the SPS (i.e., the longitude at perigee and apogee) is the same as the longitude of the rectenna. In practice, however, the satellites must be spaced in longitude as uniformly as possible, while rectenna locations will be determined by energy consumption distribution, land availability, etc. Thus, some longitude offset will in general be unavoidable.

As with orbit inclination, the principal impact of a longitude offset is on the angle of incidence at the rectenna. This is illustrated in figure IV-A-3-10 for 40° latitude and 0.04 eccentricity. The increase is small up to about 10° offset, and increases rapidly thereafter. The variation in angle of incidence (due to eccentricity) also becomes greater, so that the rectenna not only covers more area but also requires more dipole elements for the same reason discussed under inclination, although the effect is not as severe. The increases in both angle of incidence and variation of angle become rapidly greater at higher latitudes. Hence, high-latitude rectennas should be given preference in SPS longitude assignments.

Range also increases with longitude offset, causing a slight power loss if the SPS and rectenna are held constant. However, the loss is only about 1% at an offset of 40° (see figure IV-A-3-11).

c. Eclipses

L. E. Livingston
Spacecraft Design Division

An SPS in synchronous equatorial orbit experiences solar eclipses by the earth, the moon, and other SPS. Eclipses by the earth and by other satellites differ in several respects; both must be considered during design and are discussed below. Eclipses by the moon are less important. They are similar in character to eclipses by the earth, but are generally shorter in duration, less severe, and much less frequent. A detailed examination has, therefore, not been made, although it is conceivable that a combination of exceptional circumstances could occasionally produce an eclipse by the moon that exceeded the range of effects of earth and satellite eclipses.

Eclipse by Earth

These eclipses occur daily when the sun is sufficiently close to the orbit plane for the earth's shadow to fall on the orbit. Assuming a zero-inclination orbit, this happens at the equinoxes. There are approximately 43 eclipses centered around the spring equinox and

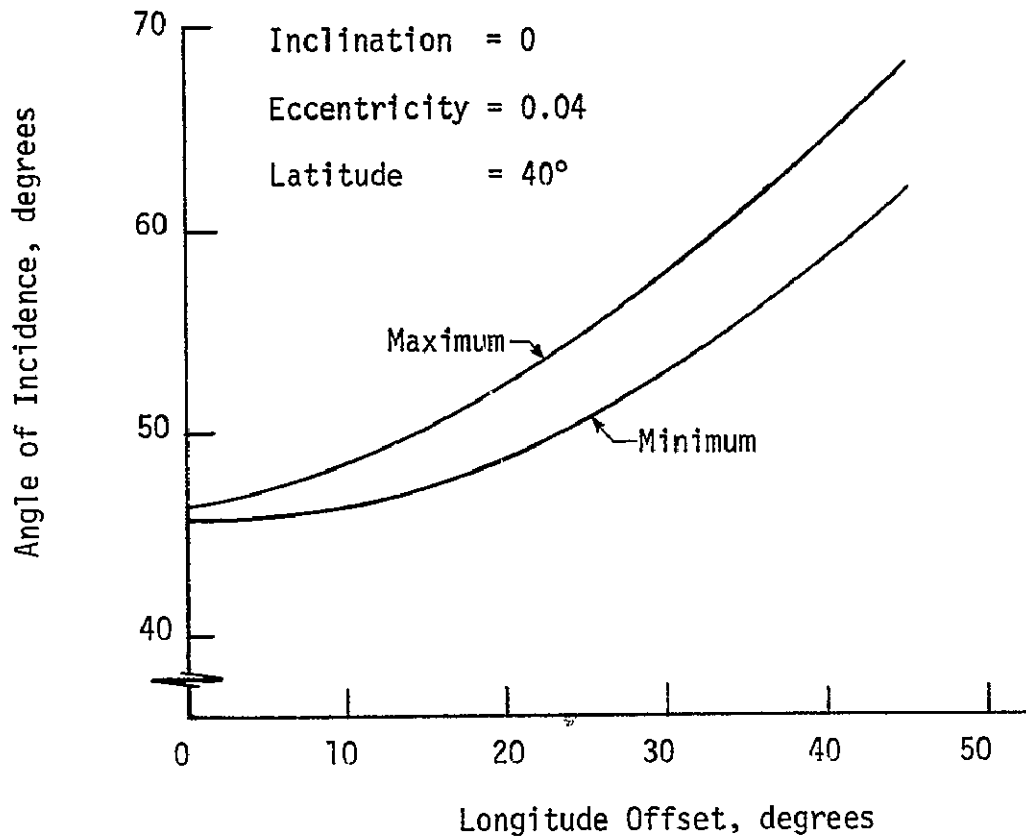


Figure IV-A-3-10. Angle of Incidence vs. Longitude Offset

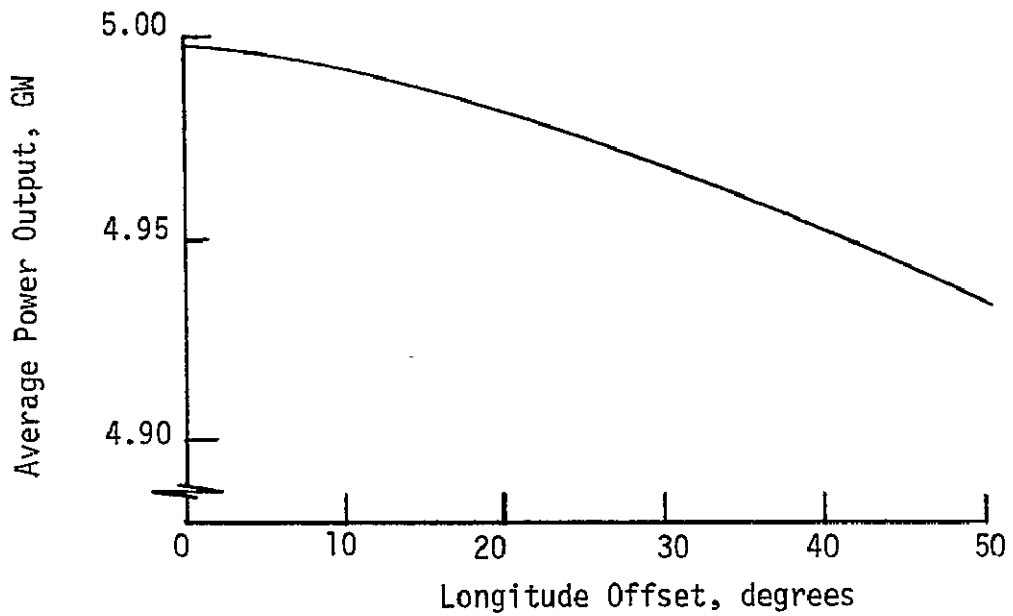


Figure IV-A-3-11. Power Output vs. Longitude Offset

44 in the fall. Maximum duration is about 75 minutes for an eccentricity of 0.04 with perigee toward the sun. Other perigee positions reduce the time slightly; higher eccentricities increase it. Duration varies from day to day as the earth's shadow moves across the orbit (figure IV-A-3-12).

With the exception of the first and last day or two of each series, the eclipse is total. Minimum time in the penumbra is about 2.3 minutes and occurs at the beginning and end of the maximum duration eclipse (see figure IV-A-3-12). Since the width of the penumbra is roughly 400 km and the array is less than 30 km in its longest dimension, the illumination gradient over the array is slight at any instant of time.

Power loss due to eclipse by the earth is 0.97% of the total output averaged over a year if the SPS can begin transmitting at full power as soon as it emerges from the eclipse. This figure must be increased to account for any start-up time that may be required. The impact on the ground distribution system is lessened by the fact that the eclipse occurs at about local midnight, when demand is relatively low. However, electrical energy storage must be provided to operate spacecraft systems during the eclipse. For the high-performance reaction control systems, with average power requirements in the multi-megawatt range, this can be a significant item (see section IV-B-4).

At an average longitude separation of 0.5° (see following section), as many as 38 satellites will be in the earth's shadow at one time. If each SPS is located as close as possible to its rectennas to minimize losses, eclipse by the earth will tend to cause simultaneous loss of all satellite-produced power to large sections of the country. Some losses due to longitude offset may be preferable to such concentrated outages.

Eclipse by Other Satellites

The number of satellites contemplated by the SPS program will require close spacing between satellites. As noted in section IV-A-3-b, 112 satellites between the longitudes of Maine and Oregon would be separated by about 0.5° of longitude, or 368 km at synchronous altitude. At this distance, an SPS can be significantly eclipsed by its neighbors when the sun is in or near the orbit plane.

The eclipse occurs where the solar vector is tangent to the orbit or, roughly, at 6:00 a.m. and 6:00 p.m. rectenna time. In an eccentric orbit, the morning eclipse is later and the evening eclipse earlier. The easternmost satellite, of course, will not be eclipsed in the morning (figure IV-A-3-13), nor the westernmost in the evening. The duration and overall intensity of the eclipse are illustrated in figure IV-A-3-14 for several dates before or after the equinox. The

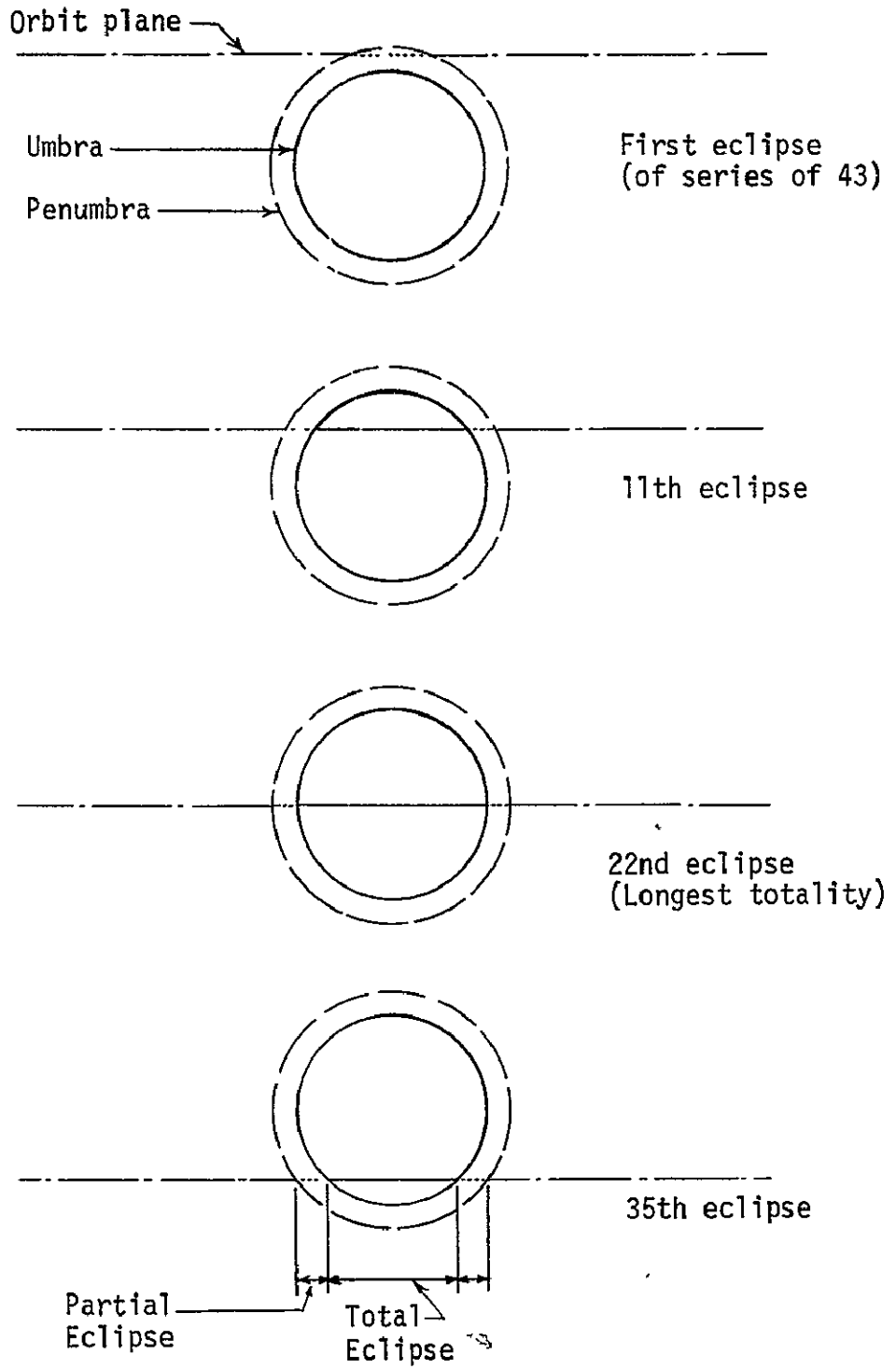


Figure IV-A-3-12. SPS Eclipse by Earth

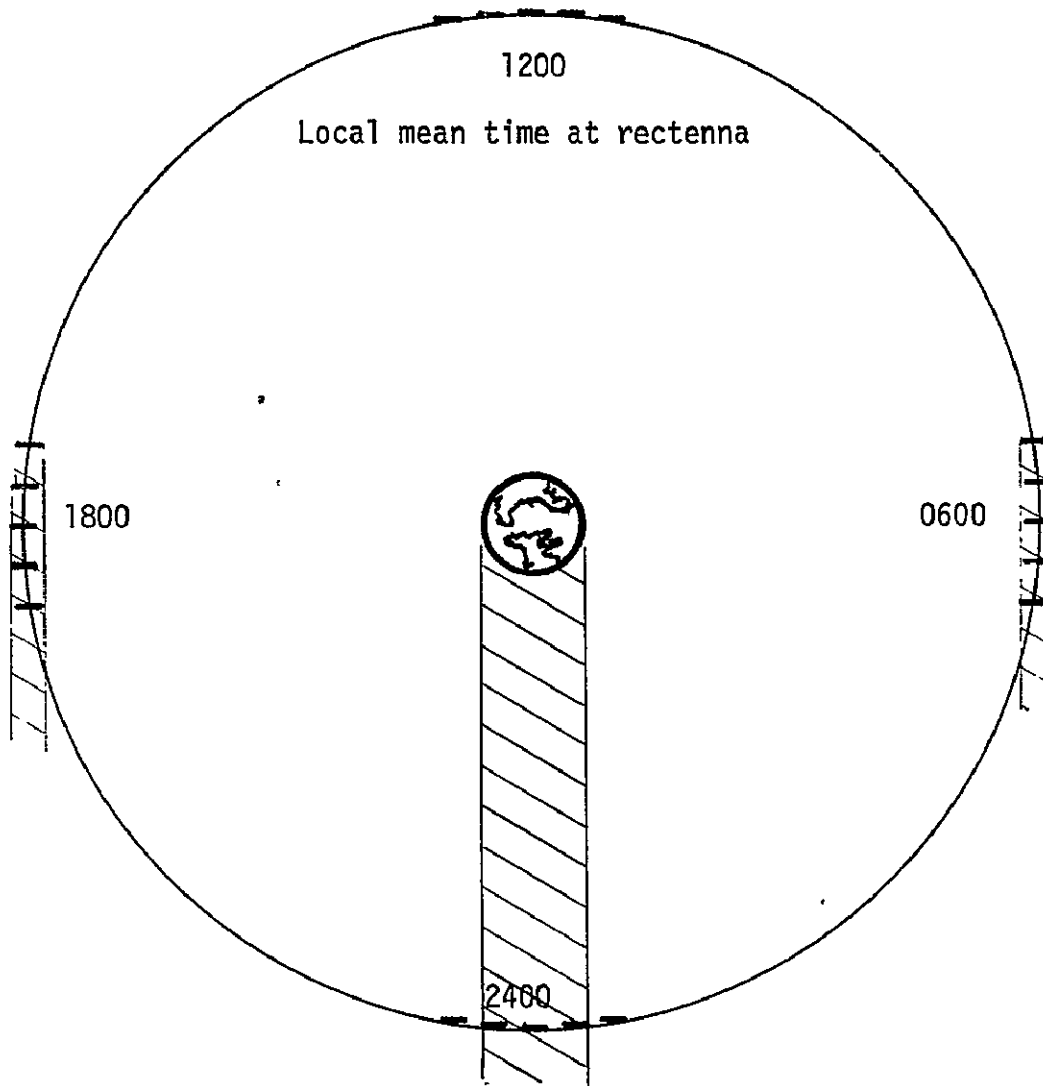


Figure IV-A-3-13. SPS Eclipses

IV-A-3-21

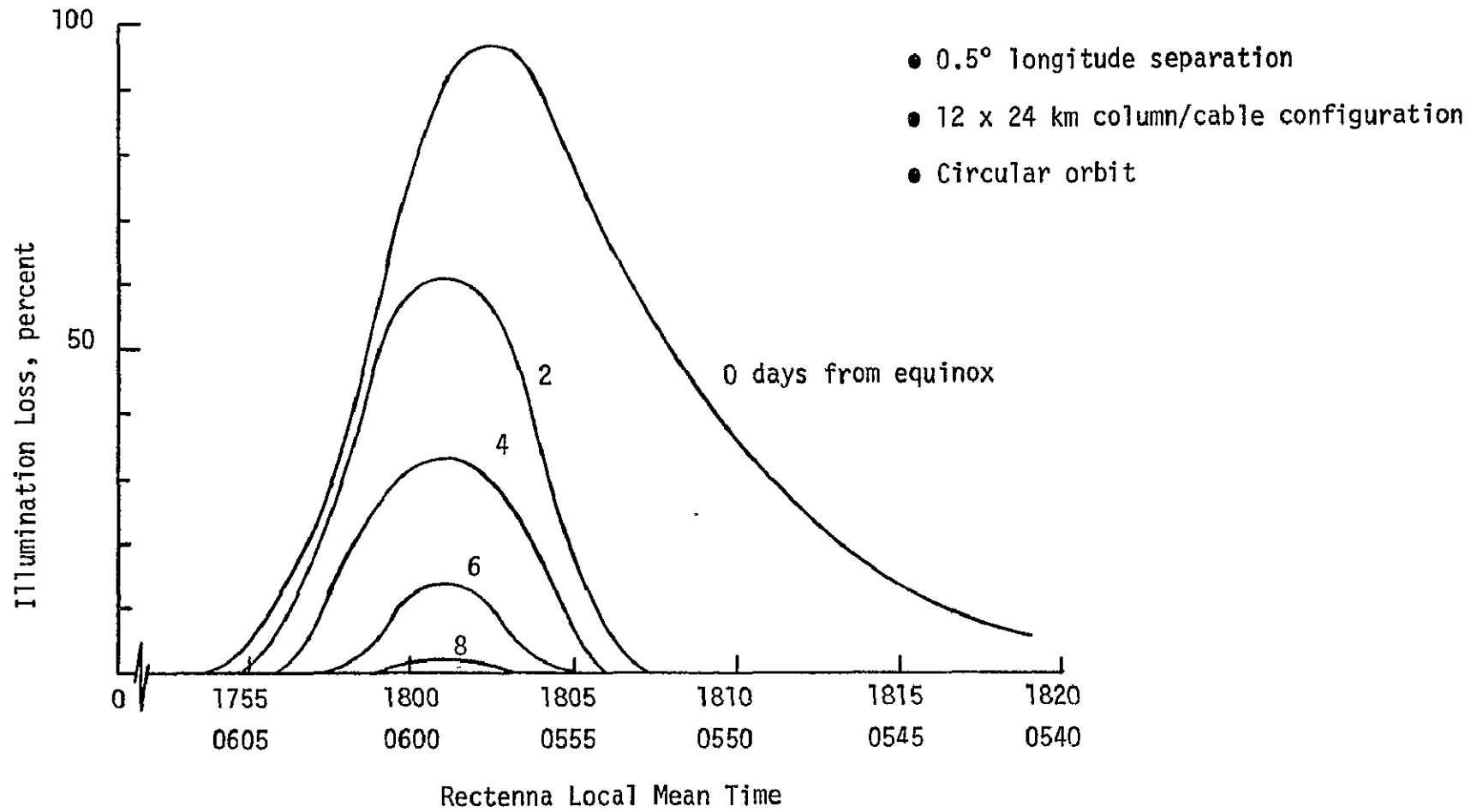


Figure IV-A-3-14. Illumination Loss from Eclipse by SPS

"percentage of occultation" refers to the total amount of sunlight falling on the array. As discussed below, this is not necessarily a measure of useful power output.

It is assumed for these calculations that all satellites are in precisely the same orbit, presenting an appearance similar to figure IV-A-3-15 if viewed from the center of the eclipsed satellite. In practice, such precision may not be achieved. An inclination difference of $.033^\circ$, for example, would displace a satellite 24 km perpendicular to the orbit plane, shifting by about 12 days the eclipses of a satellite at 0.5° longitude separation. The overall result of such staggered eclipses would be less power loss on any given day, more days with some loss, and slightly more total loss per year. In the worst case, however, total power loss is less than 0.1% of the annual output.

Going one step farther, an inclination difference of 0.22° with the line of nodes toward the sun would elevate the satellite 23.5° above the equator as seen from the next satellite in line, eliminating all eclipses by that satellite. The impact of eclipses by other satellites could be greatly reduced in this way, since the nearest satellite causes most of the shadowing (figure IV-A-3-16). However, the orbit maintenance problem would become more complex, particularly since both lunar/solar perturbations and nodal regression due to the earth's oblateness would adversely affect the desired orbits.

A more serious question is the relative sharpness of the shadow. The width of the penumbra is proportional to the spacing between satellites; at 0.5° spacing, it is only about 3.4 km wide. Since the array is much larger than this, the illumination intensity can vary over the array from full sun to total darkness (figure IV-A-3-17). If cooling rates are comparable to the maximum duration of the eclipse (15 to 20 minutes), differential contraction could produce thermal stresses and distortion. The severity of this problem is a function of configuration and materials; the column/cable configuration, for example, can be expected to experience greater stresses than a non-redundant truss structure (which could distort without developing internal stresses). However, the need for some tension in the solar cell blankets and concentrators, together with the limited choice of materials for these items, may make some thermal stresses unavoidable in any structural concept.

Variable SPS Orbits for Eclipse Avoidance

It is conceivable that the power interruptions caused by eclipses could be eliminated by changing the orbit of the satellite from time to time so as to maintain continuous illumination. The following discussion explores this possibility in detail.

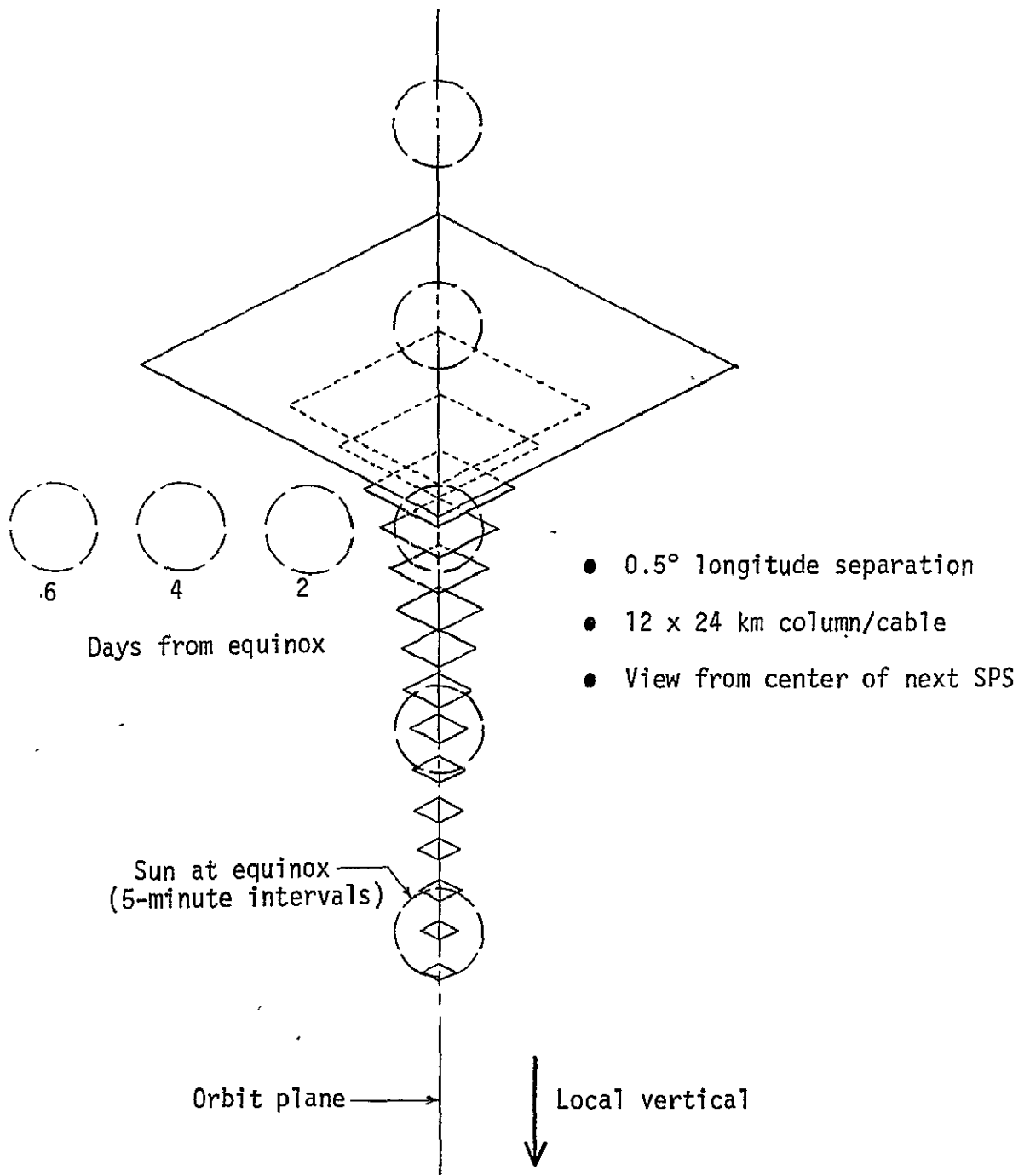


Figure IV-A-3-15. Eclipse by Other SPS

IV-A-3-24

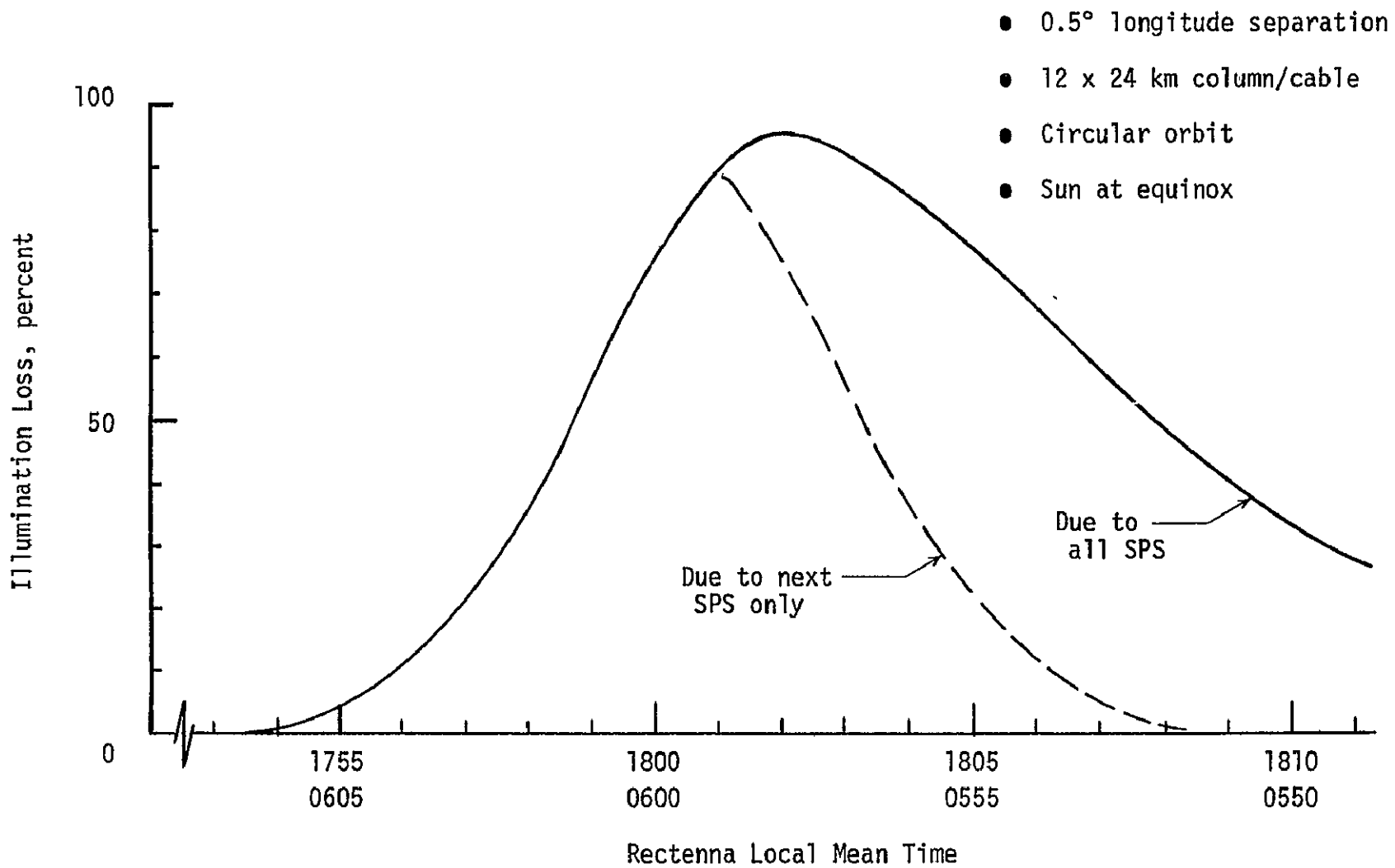


Figure IV-A-3-16. Eclipse by Adjacent SPS

- 0.5° longitude separation
- 12 x 24 km column/cable

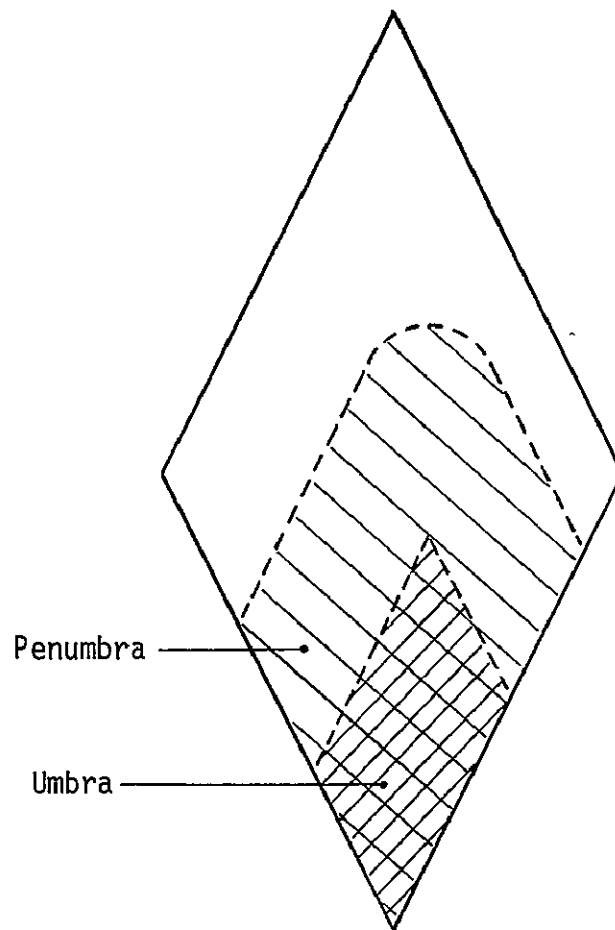


Figure IV-A-3-17. Shadow Size from Adjacent SPS

There is no eclipse if β , the angle between the solar vector and the orbit plane, is large enough (see figure IV-A-3-18). For a synchronous orbit with an eccentricity of 0.04, the minimum β is 8.54° at apogee and 9.26° at perigee. These must be measured at the sun's lower limb if all partial eclipses are to be avoided, and must therefore be increased by 0.27° (the sun's maximum semidiameter) to obtain the correct angle to the center of the sun. The minimum β is then 8.81° to 9.53° . The higher value will be used here for conservatism; the conclusions would be the same for either figure. The minimum β for avoidance of eclipse by other satellites is substantially less than for earth eclipses. The satellite eclipse problem need not be considered separately, therefore.

It is convenient to specify the orientation of the orbit plane by the projection on the celestial sphere of the normal to the orbit plane. There will be no eclipse if the normal is at least 9.53° from the locus of points 90° from the sun. Thus, the region up to 9.53° on each side of the great circle 90° from the sun is an "eclipse zone" (figure IV-A-3-19). If the normal to the orbit plane is within this zone, an eclipse will occur; if the normal is outside the zone, there will be no eclipse.

The eclipse zone rotates with the sun. Since polarity is immaterial, its period is six months (neglecting the eccentricity of the earth's orbit, which is also not pertinent to this question). The monthly movement of the zone is illustrated in figure IV-A-3-20, which represents a view from the north pole. Because of the obliquity of the ecliptic (23.5°), the motion is not symmetrical with respect to the pole.

Referring to figure IV-A-3-20, it can be seen that the orbit can be kept out of the eclipse zone in two ways. The first, with the normal to the orbit plane indicated by circles, is to adjust the inclination of the orbit so that the normal always remains on the same side of the eclipse zone. The second, with the normal denoted by triangles, is to make a large plane change maneuver every six months (March and September) so as to move the orbit normal across the eclipse zone. This maneuver must be completed in less than one orbit if no eclipses whatever are to be permitted.

The first approach requires relatively gradual plane changes, although the total amount is large. As shown in figure IV-A-3-20, the total plane change is on the order of $90^\circ/\text{year}$. For a mass of 82000 M.T. and specific impulse of 98 km/s, the propellant required is roughly 4×10^6 kg/year. The principal difficulty, however, is the maximum inclination of 33° (June). As noted on page IV-A-3-12, non-zero inclinations cause a large variation in the angle of incidence of the microwave beam at the rectenna, the total excursion being about twice the inclination.

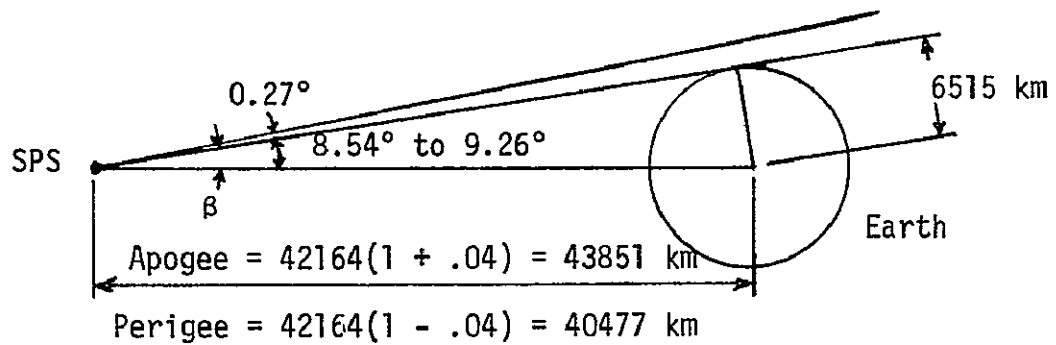


Figure IV-A-3-18. - Minimum β for no eclipse

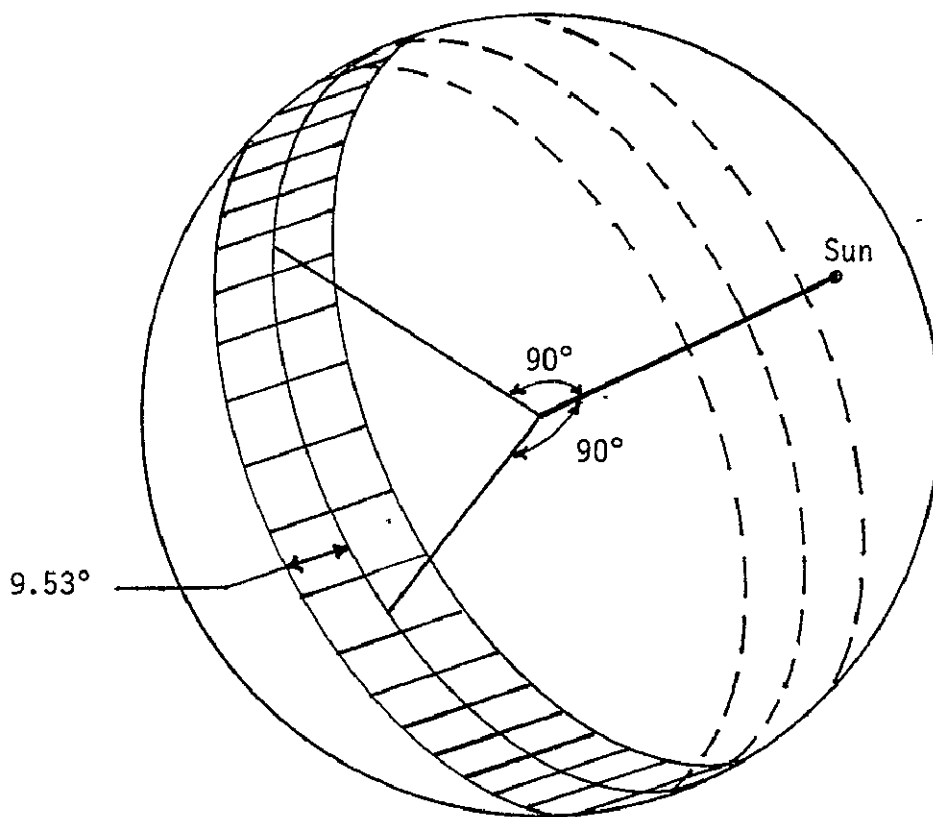


Figure IV-A-3-19. - "Eclipse zone"

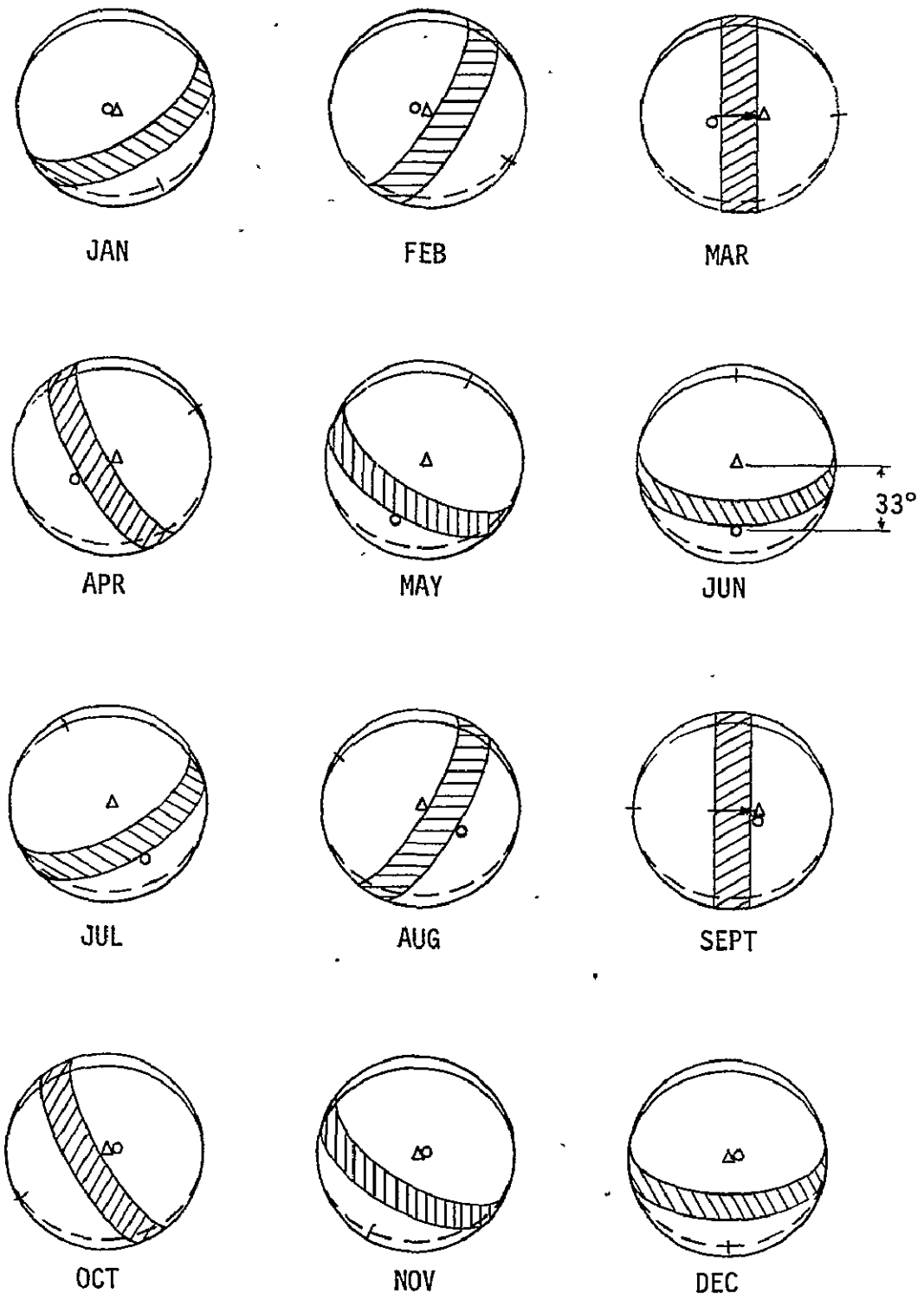


Figure IV-A-3-20. - Annual motion of eclipse zone

In the present case, the angle of incidence at 40° rectenna latitude will vary from about 8° to 82° daily at maximum inclination. There is also a substantial variation in azimuth of the beam. The resulting variation in the "footprint" of the microwave beam is illustrated in figure IV-A-3-21 for a typical case. The enormous increase in land area and rectenna elements required, even aside from large atmospheric losses and the difficulty of configuring a given section of the rectenna to perform efficiently over a wide range of power densities, appear to make this approach totally unacceptable.

The second approach need go no higher than 9.5° inclination (in March and September). While representing a substantial penalty in land and rectenna elements (see page IV-A-3-15 for data for 7.3°), it is a great improvement over 33°. The difficulty here is the time constraint on the plane change, viz., 19° in less than 24 hours. At synchronous orbit, this involves a minimum delta-V (impulsive) of 1020 m/s. Even if the maneuver could be spread over, say, 4/5 of an orbit without penalty, the acceleration would be about 0.0015 g. At a somewhat more plausible figure of a tenth of an orbit, the acceleration would be 0.012 g, requiring a thrust of about 10^7 N (2.2×10^6 lb). To design the SPS to these loads appears prohibitively heavy, aside from the propellant required (about 3.6×10^6 kg/year) and the cost of the thrusters. Note that it will be necessary to maneuver all satellites simultaneously or nearly so; moving propulsion modules from one SPS to another to reduce propulsion system investment is therefore not possible.

In summary, maneuvering solar power satellites so as to avoid eclipses by the earth appears to be completely out of the question. It will be necessary, therefore, to accept outages resulting from eclipses or to provide energy storage or standby generators to fill the gaps.

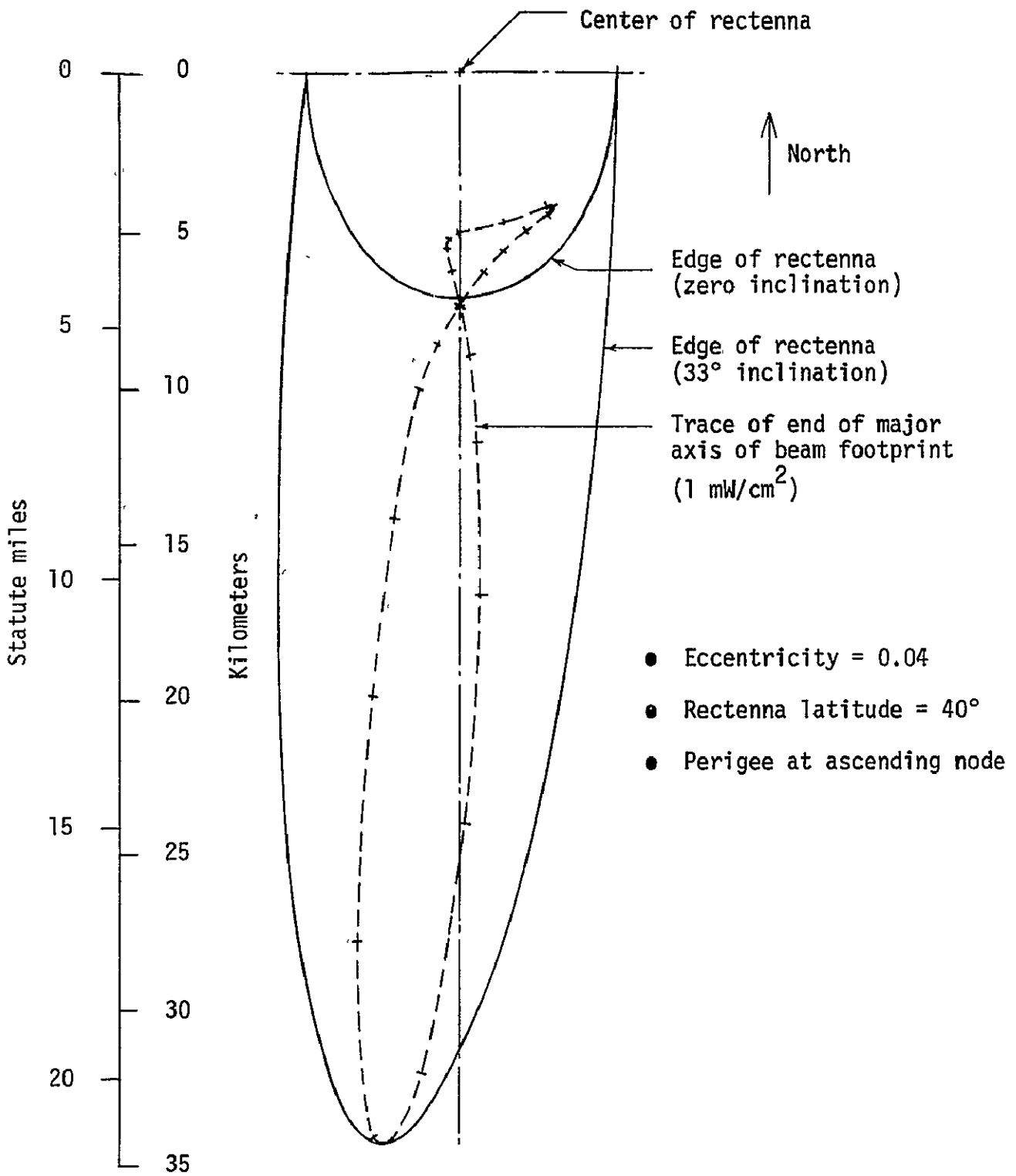


Figure IV-A-3-21. - Rectenna size for 33° inclination

A number of SPS configurations have been studied and a variety of possible arrangements are illustrated in Figures IV-A-4-1 through 13. These figures illustrate the major components of the SPS, which are the solar array, the antenna, and the rigidizing structure.

During configuration design, consideration was given to the following basic requirements:

(1) Minimize external disturbing forces, primarily gravity gradient forces, by providing an inertially balanced structure (i.e., for solar orientation $I_x = I_y = I_z$; for perpendicular to the orbit plane (P.O.P.) orientation $I_x = I_z$). For a discussion of external disturbing forces see Section IV-B-4.

(2) Locate the antenna or antennas so that pointing requirements are most readily satisfied and forces acting on the antenna/antennas are symmetrical with respect to the SPS center of mass.

(3) Select a geometric shape and arrangement which can be fabricated and assembled with a minimum amount of complexity. The configuration should be such to allow efficient fabrication in space by the use of automatic machinery.

(4) For a discussion of the primary and secondary structure of large satellites in orbit see Section IV-B-3.

Figure IV-A-4-1: Configuration 76B-2 illustrates an arrangement which is counterweighted to achieve equal mass moments of inertia about two axes ($I_x = I_z$). The solar array is oriented perpendicular to the orbit plane. The structure for this configuration consists of three major compression column members stabilized with cables. This configuration has two antennas, each beaming one half the power towards its own separate ground based rectenna. Two antennas are required for a symmetrical arrangement to avoid unbalanced torques. It appears that the shape of this configuration will require a more complex technique for the fabrication and assembly than some of the other geometric shapes, namely rectangular or square.

Figure IV-A-4-2 (Config. 76D-1): This configuration is similar to configuration 76B-2 except that the array is solar oriented and is configured to provide equal mass moments of inertia about the three primary axes, using counterweights. Solar orientation allows a 4% smaller area for the same power output.

Figure IV-A-4-3 & 4 (Config. 76J): In this configuration the array is oriented perpendicular to the orbit plane. This orientation allows a simpler antenna axes arrangement. The structural concept is similar to the previous configurations (76B-2 and 76D-1) except this

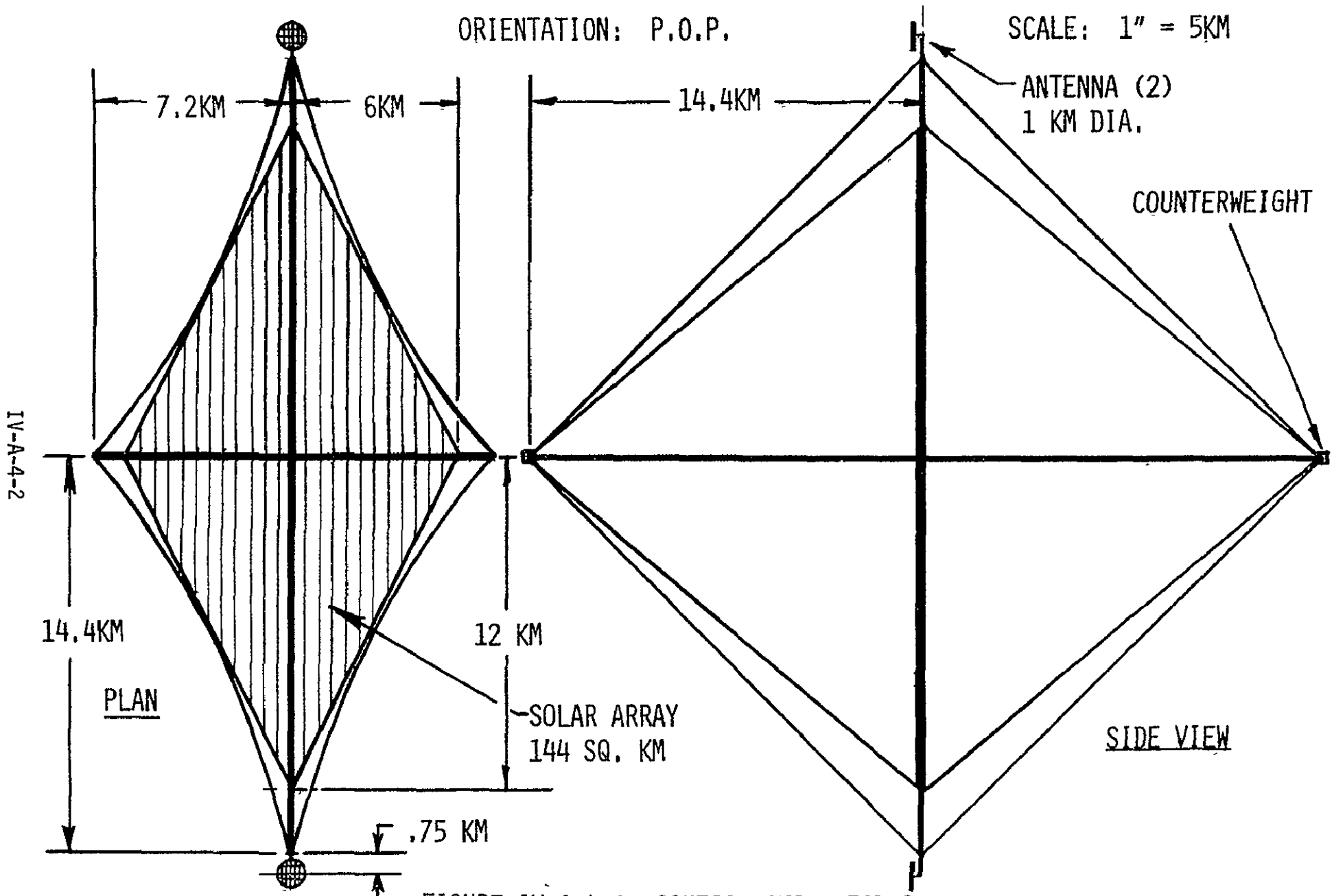


FIGURE IV-A-4-1 CONFIGURATION 76B-2

ORIENTATION: SOLAR

SCALE: 1 IN = 6 KM

IV-A-4-3

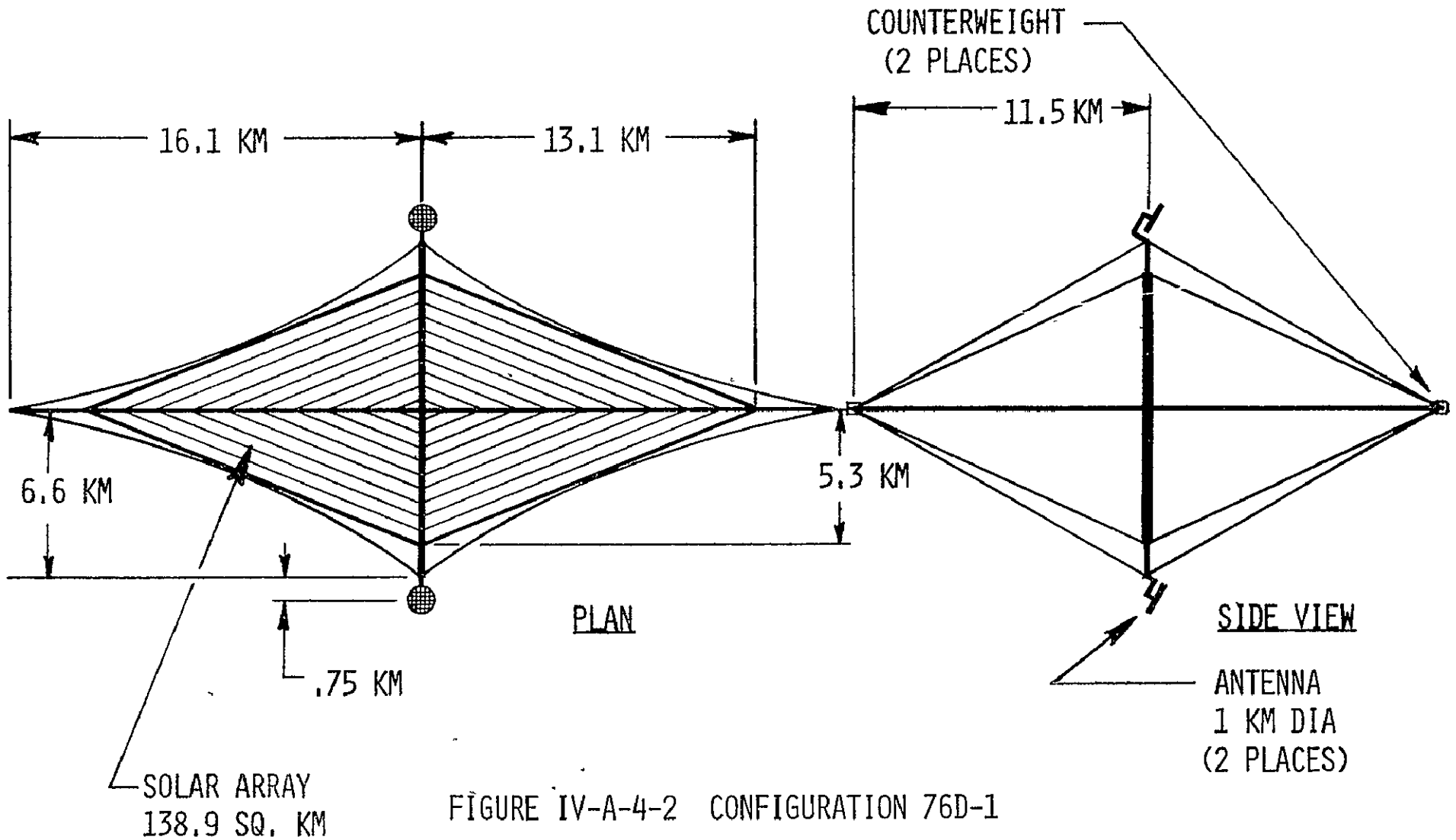


FIGURE IV-A-4-2 CONFIGURATION 76D-1

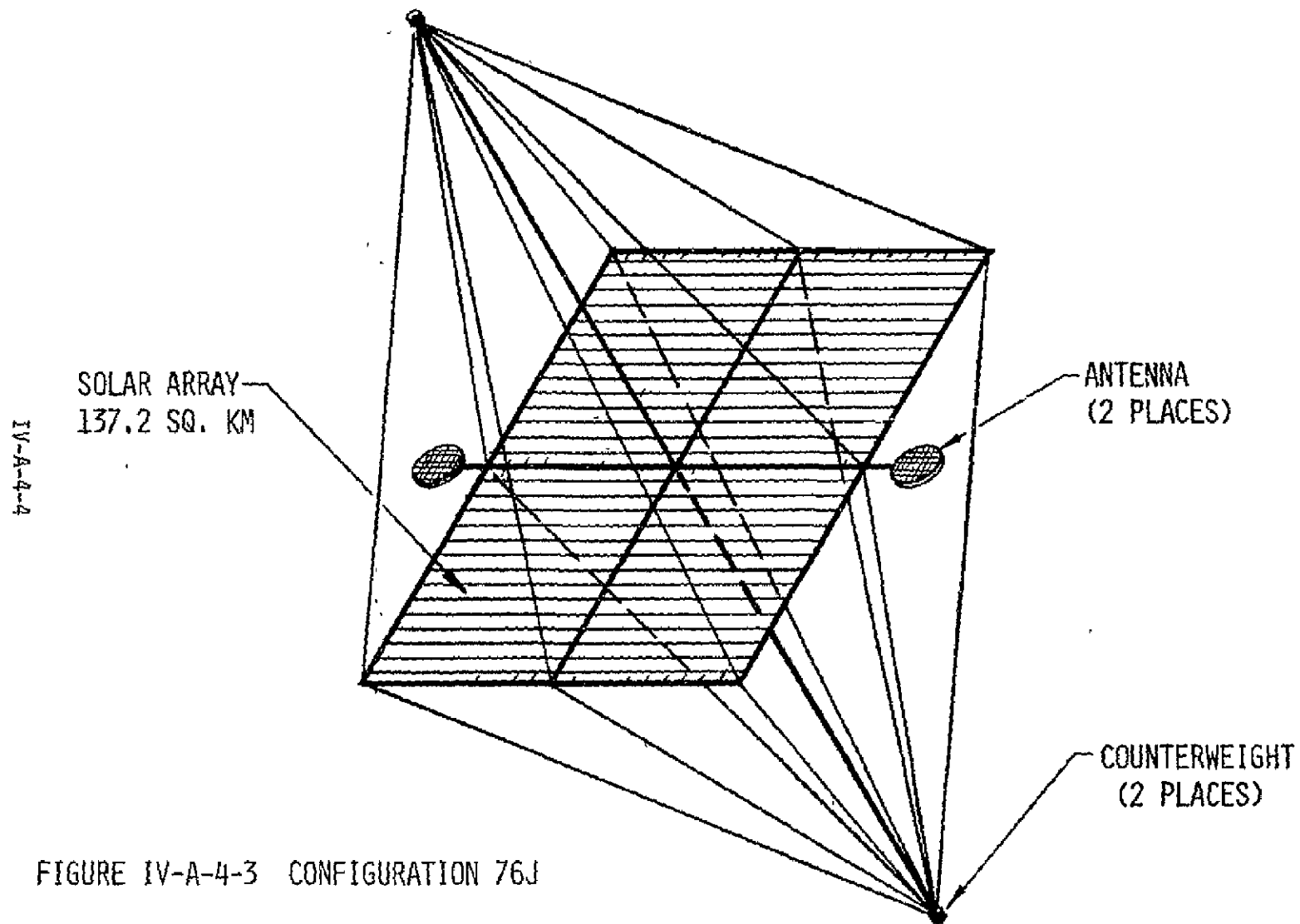


FIGURE IV-A-4-3 CONFIGURATION 76J

ORIENTATION: POP

SCALE: 1" = 5 KM

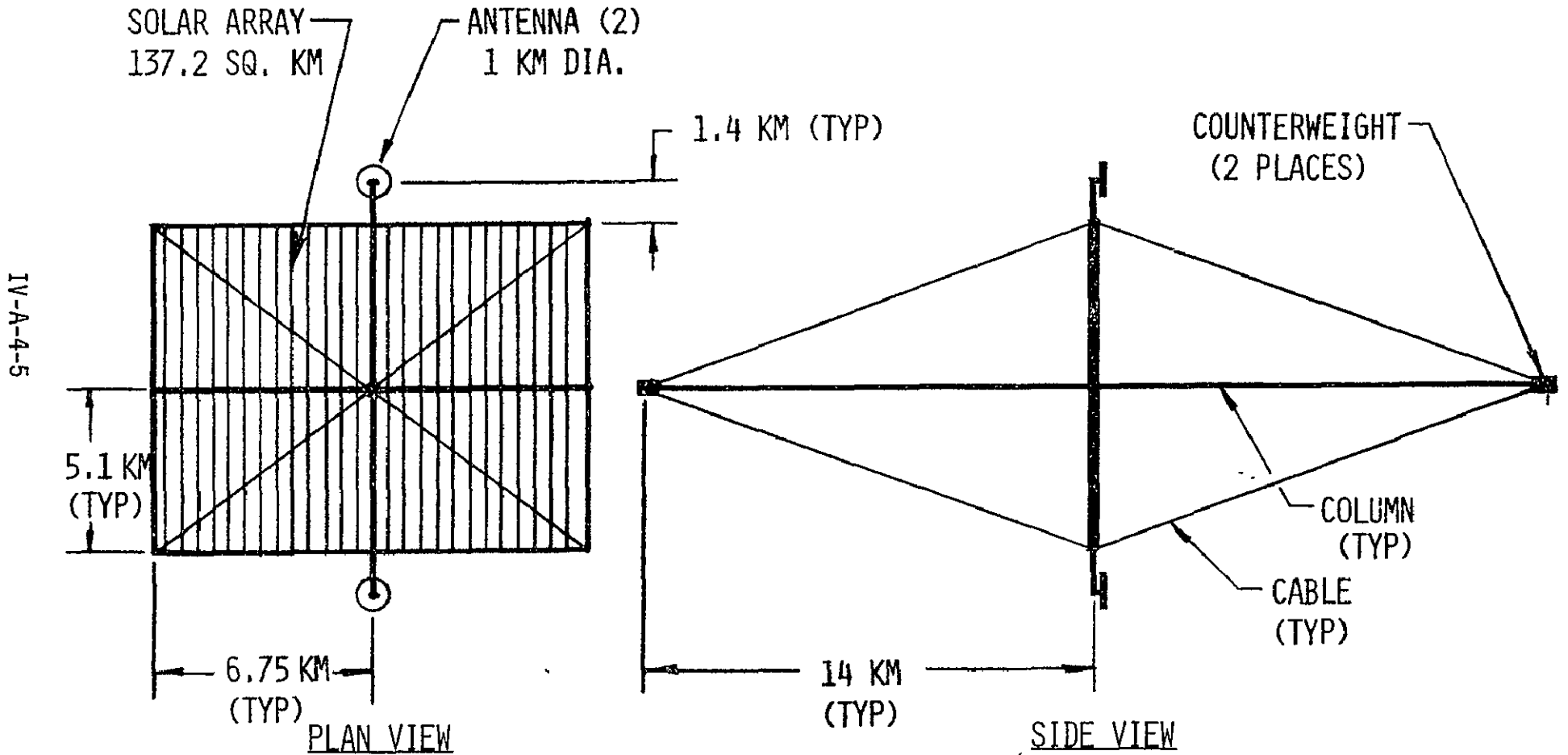


FIGURE IV-A-4-4 CONFIGURATION 76J

concept has seven major compression columns. The rectangular shape appears to be more suited to automatic fabrication and assembly in orbit than the diamond shape. Counterweights are used to obtain equal moments of inertia about the three primary axes, like config. 76D-1. This configuration cannot operate as a solar oriented SPS, because the antennas would periodically beam through the corners of the solar array.

Figure IV-A-4-5 & 6 (Config. 76K): This configuration is the same as Config. 76J except for different dimensions for the rectangular shape, which are optimized for minimum counterweight to have equal moments of inertia about two axes.

Figure IV-A-4-7 (Config. 76L): This configuration is oriented perpendicular to the orbit plane and has a single antenna located between two rectangular arrays. Total power output is one half that of the previously discussed two antenna arrangements. The structure for each array consists of compression columns supported with tension lines. A continuous beam spans the total length, connects the two arrays and provides a support axis for the centrally located antenna.

Figure IV-A-4-8 & 9 (Config. 76M & 76N): Configuration 76M and N are oriented perpendicular to the orbit plane and have a single centrally located antenna. The only difference in these two concepts is the detail arrangement of the solar cell/reflector system as illustrated. Neither of these concepts use counterweights, but achieve equal moments of inertia ($I_x = I_z$) about two axes by arrangement of the structure and array (one half the array area on each side of the neutral axis as illustrated).

Figure IV-A-4-10 (Config. 76P): This configuration is oriented perpendicular to the orbit plane and has a single centrally located antenna. Structural rigidity for this concept is achieved through the use of compression columns and tension lines. Counterweights are used to obtain equal moments of inertia about two axes. In this concept the solar cells occupy the central portion of the array and the solar collectors are located on the sides.

Figure IV-A-4-11 (Config. 76R): Configuration 76R is oriented perpendicular to the orbit plane and has an antenna located at each end of the structure as illustrated. The structure for this concept is simply a three dimensional rectangular truss system 5 km x 28 km of constant thickness. This concept does not have equal moments of inertia about the mutually orthogonal axes; and, therefore, will require almost continuous reaction control thrust to counteract gravity gradient torques. Of all the configurations, this one seems to be the simplest to fabricate and assemble. It seems quite feasible to construct this configuration efficiently with a single operation output from an automatic machine or factory in orbit.

Figure IV-A-4-12 (Config. 76-S): This configuration is similar to 76R except the structural concept is different and would probably be

more difficult to construct. The solar cells are located in the center of the .56 km thick cross section. The center of gravity for this arrangement is more or less centrally located.

Figure IV-A-4-13 (Config. 76-T): This configuration is basically the same as 76R but is designed to have greater stiffness and a fewer number of beam elements (five beams) which should result in a structure which is simpler to fabricate using automatic machinery.

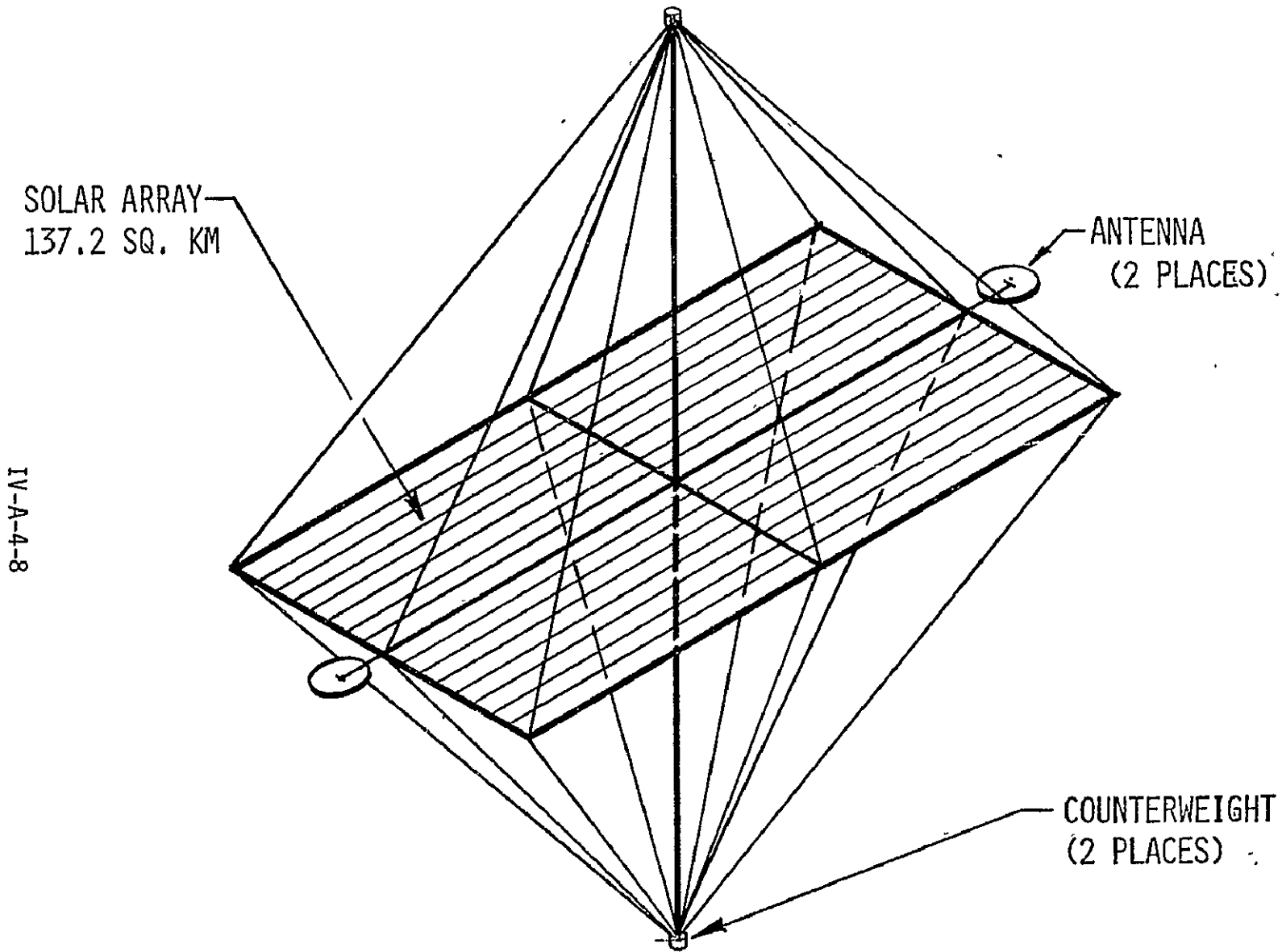


FIGURE IV-A-4-5 CONFIGURATION 76K

ORIENTATION: POP

SOLAR
ARRAY
137.2 SQ. KM

SCALE: 1" = 5 KM

ANTENNA (2)
1 KM DIA.

1.05 KM
(TYP)

COUNTERWEIGHT
(2 PLACES)

IV-A-4-9

8.28 KM
(TYP)

4.14 KM
(TYP)

COLUMN
(TYP)

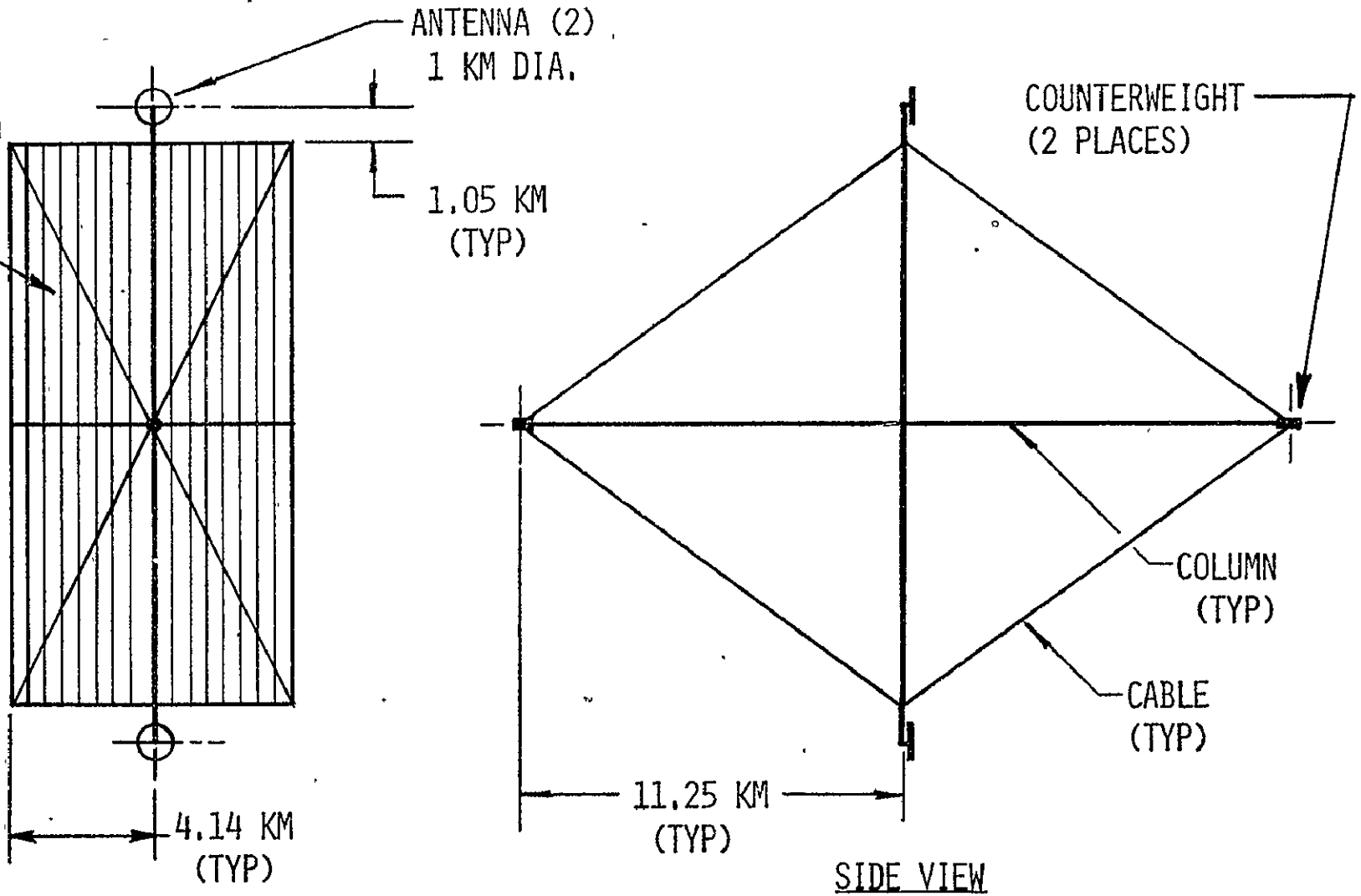
CABLE
(TYP)

11.25 KM
(TYP)

SIDE VIEW

PLAN VIEW

FIGURE IV-A-4-6 CONFIGURATION 76K



ORIENTATION: POP

SCALE: 1" = 40 KM

IV-A-4-10

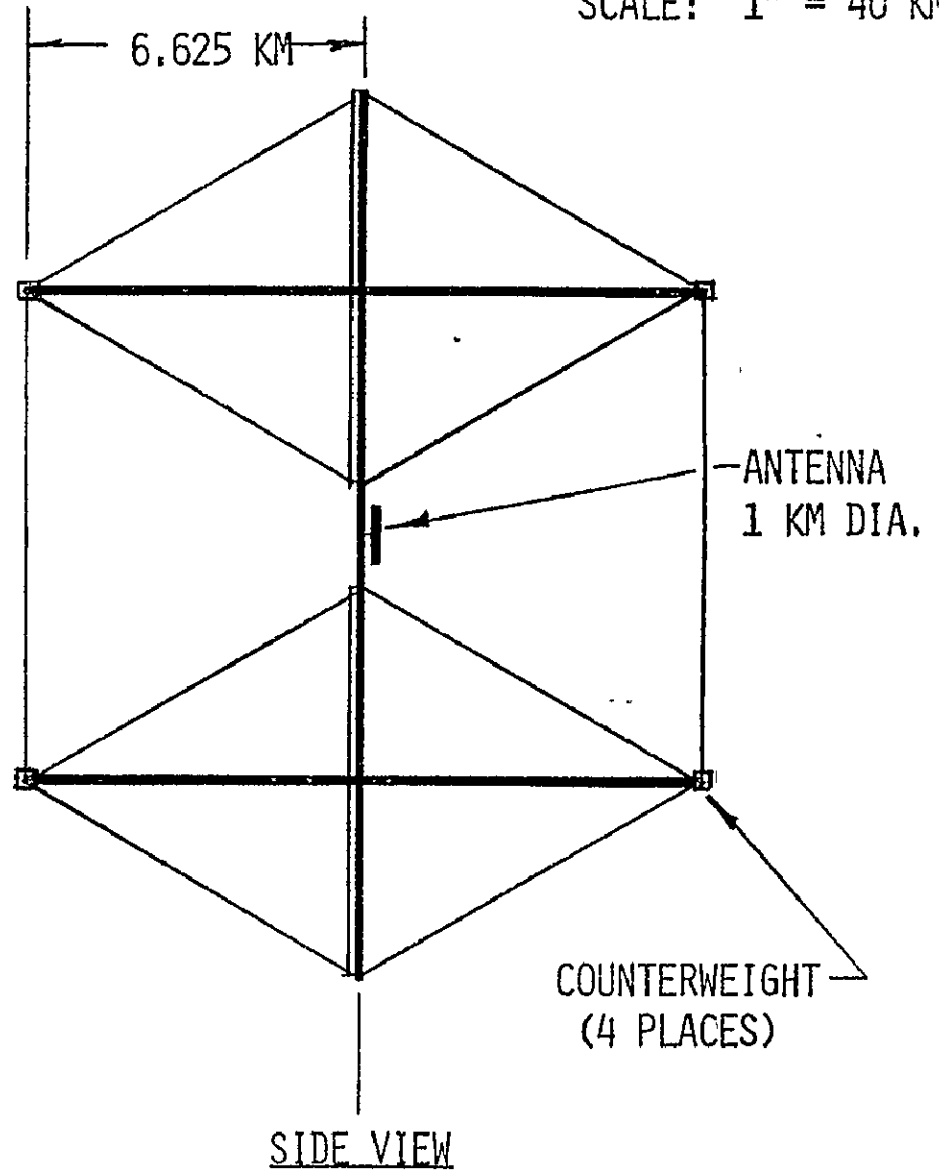
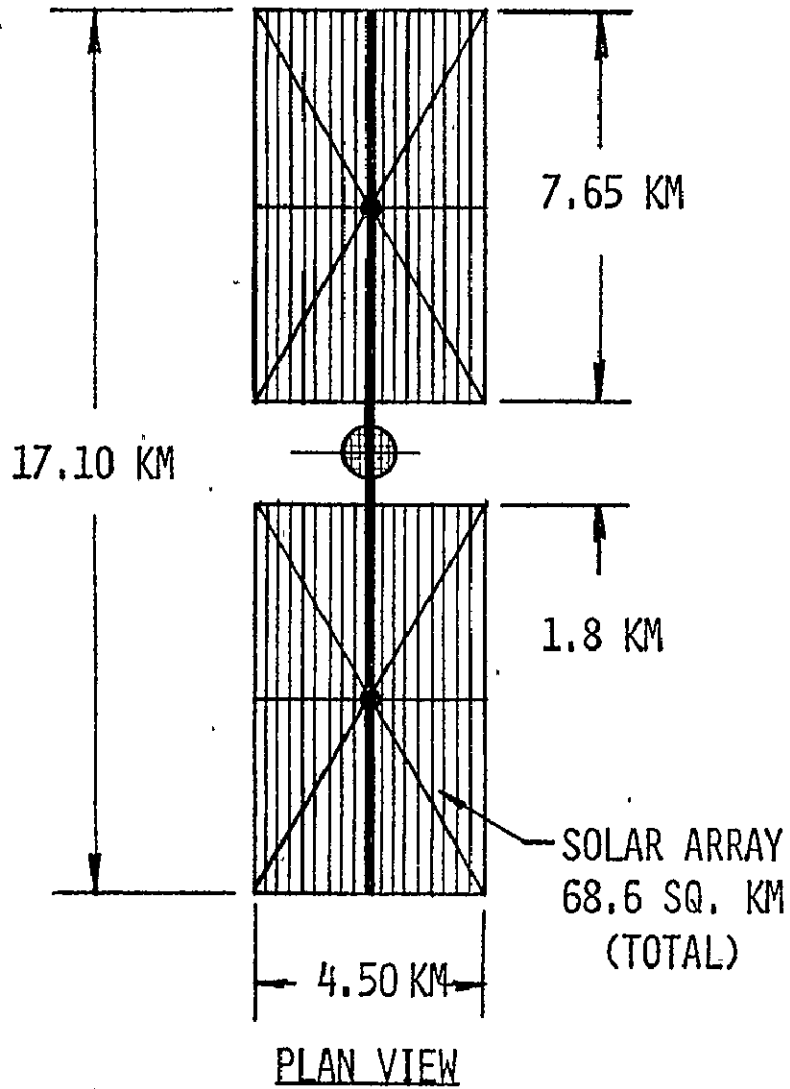


FIGURE IV-A-4-7 CONFIGURATION 76L

IV-A-4-11

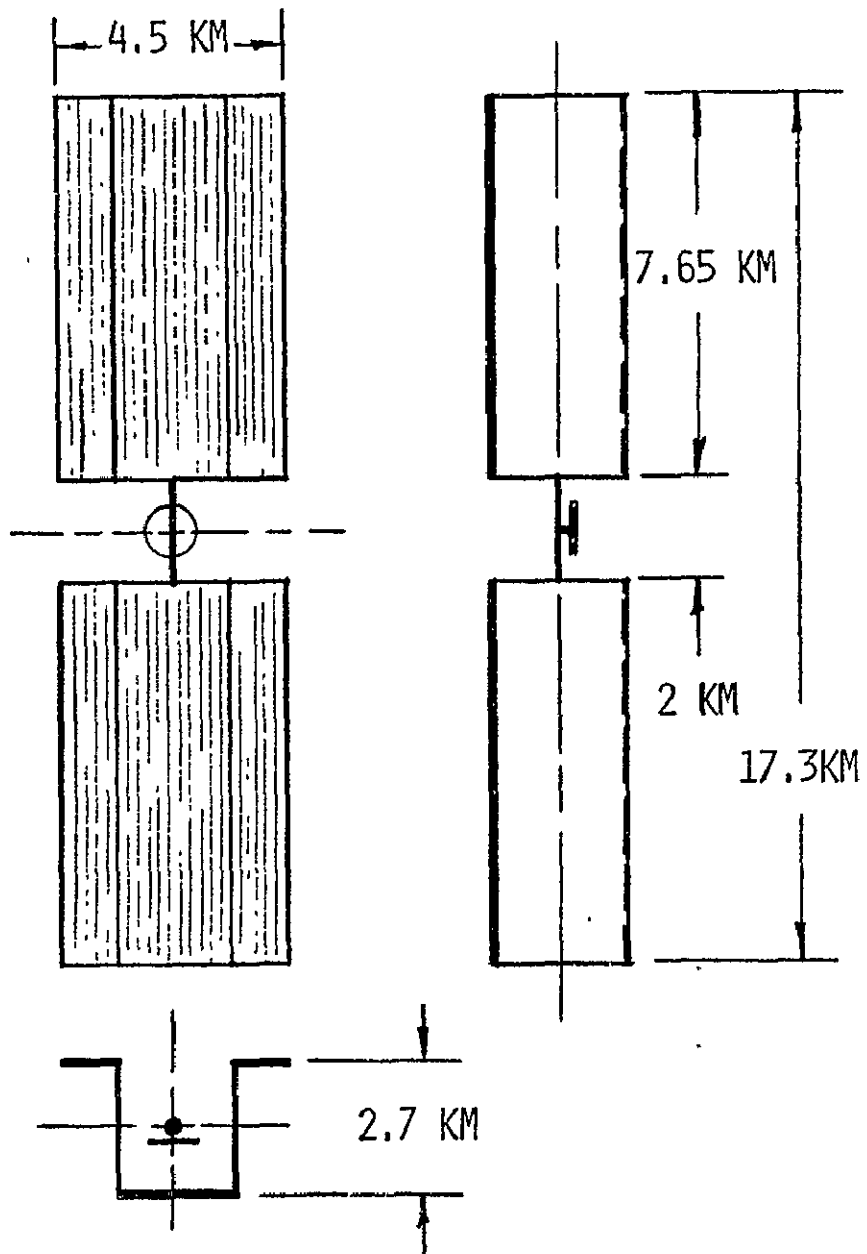


FIGURE IV-A-4-8 CONFIGURATION 76M

SCALE: 1" = 4 KM

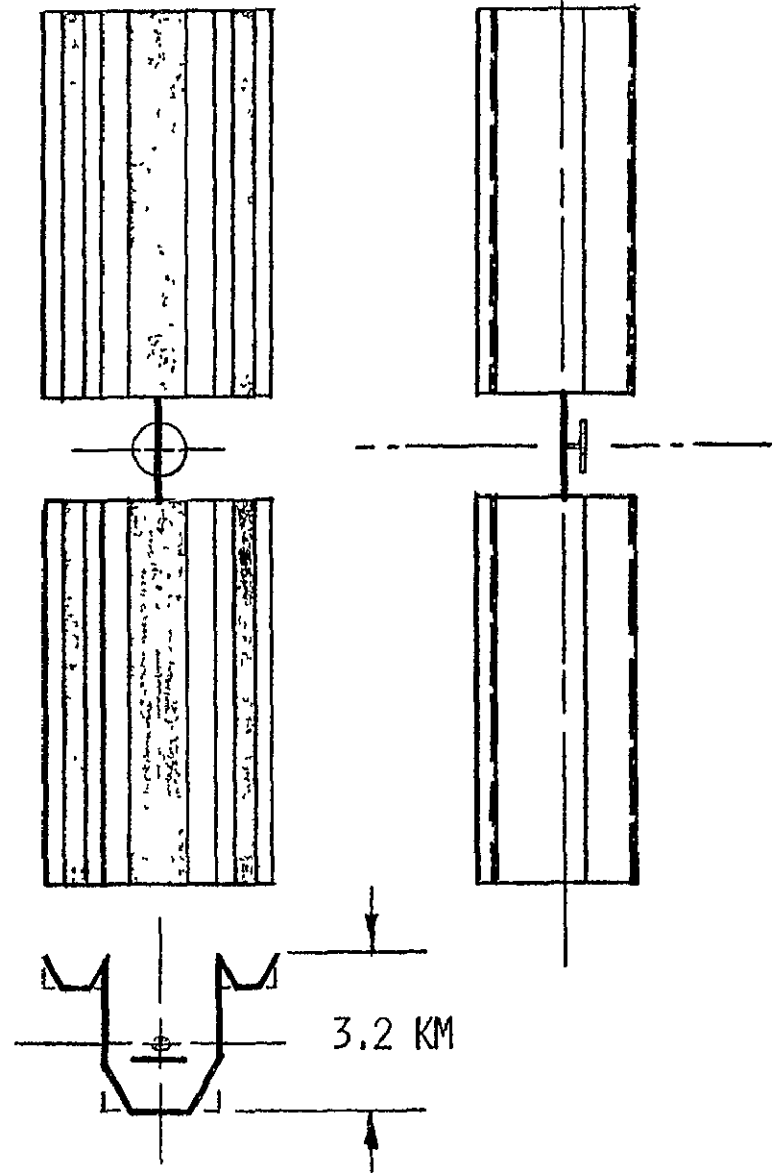


FIGURE IV-A-4-9 CONFIGURATION 76N

IV-A-4-12

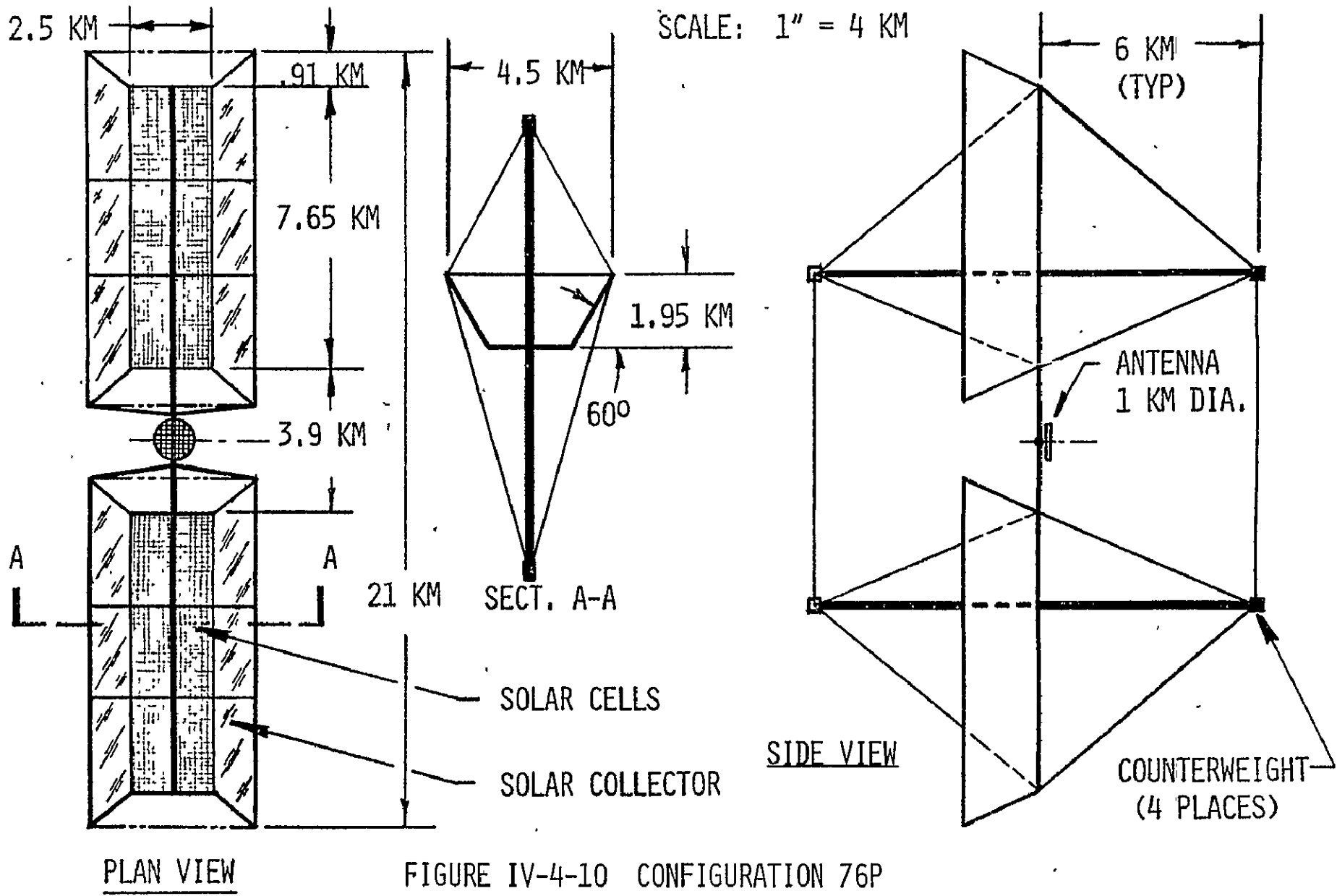
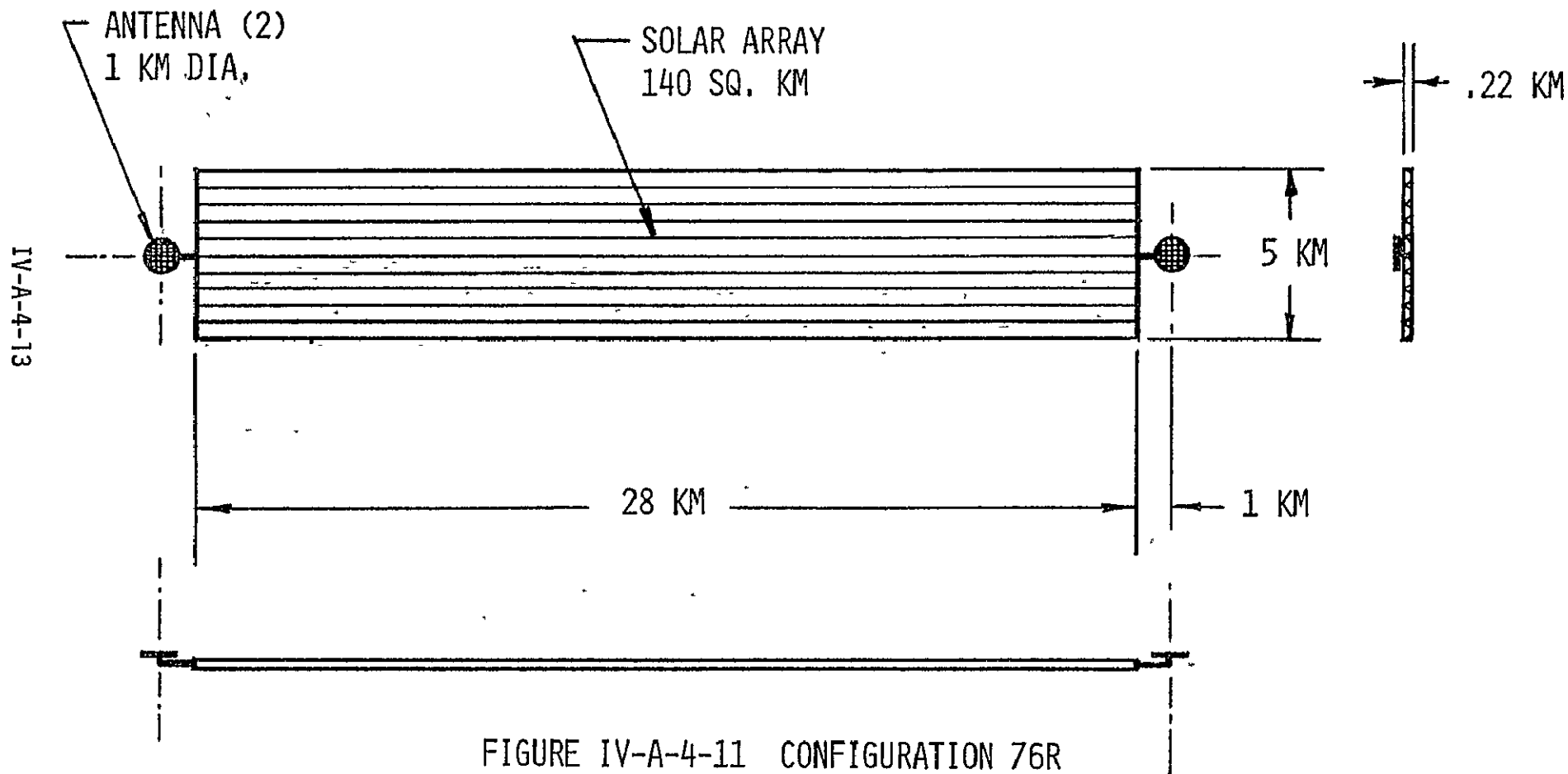


FIGURE IV-4-10 CONFIGURATION 76P

ORIENTATION: P.O.P.

SCALE: 1" = 5 KM



ORIENTATION: P.O.P.

SCALE 1" = 5 KM

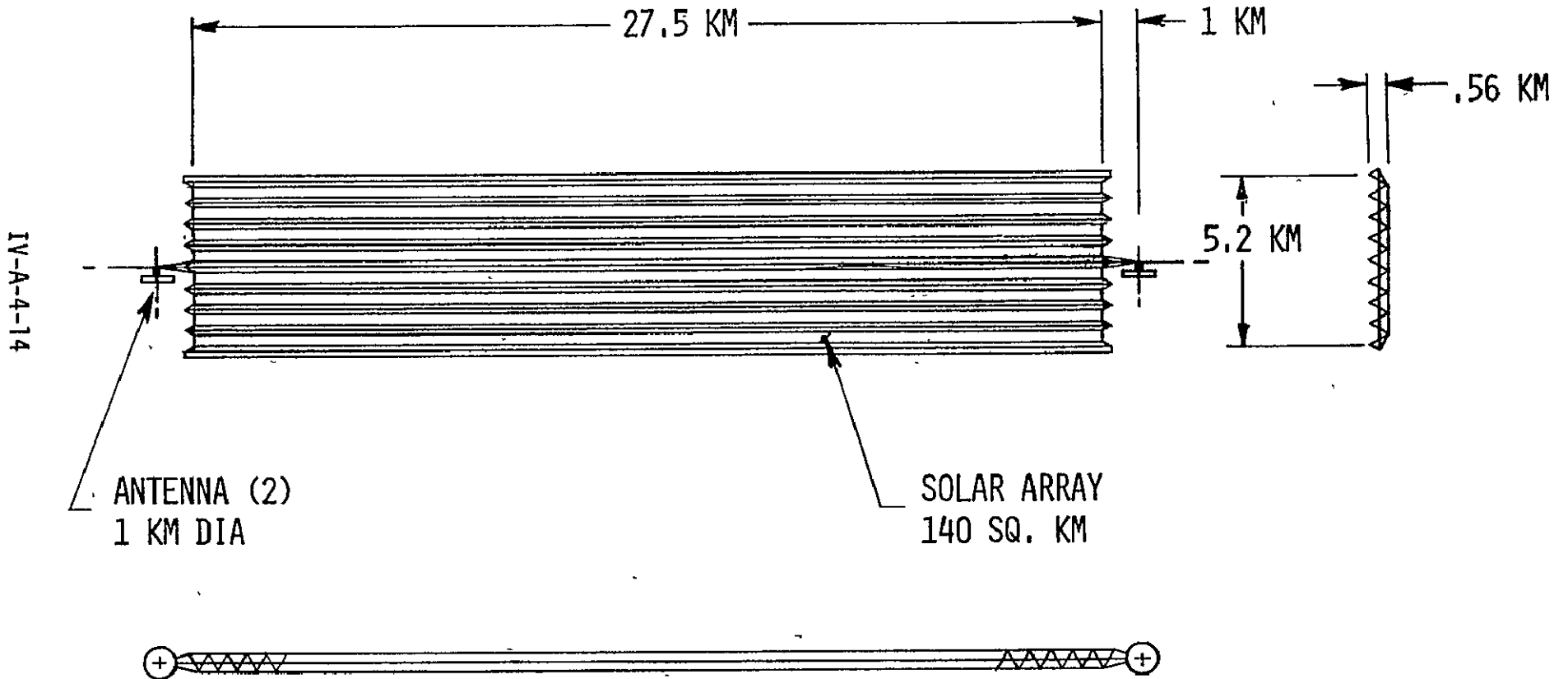


FIGURE IV-A-8-12 CONFIGURATION 76-S

SCALE 1" = 5 KM

ORIENTATION: P.O.P.

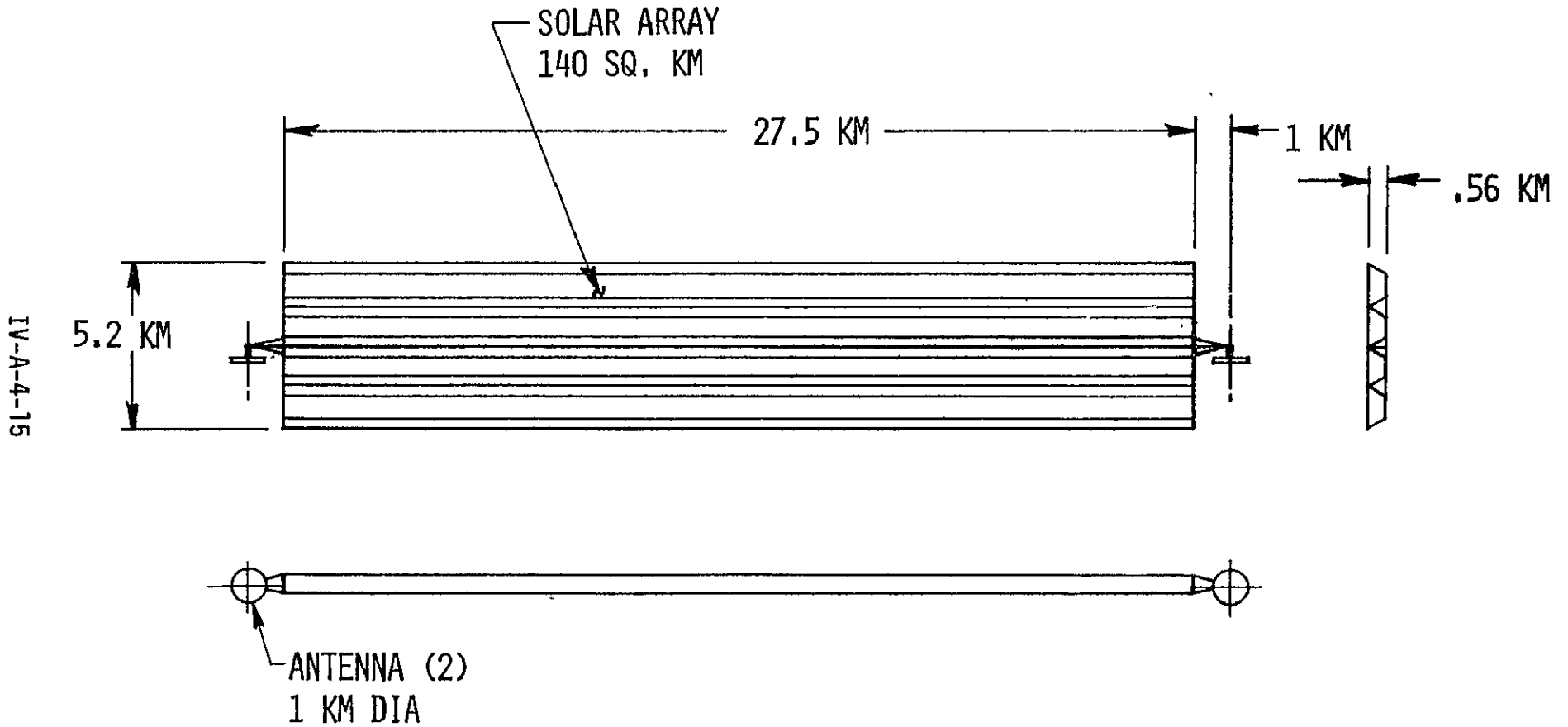


FIGURE IV-A-4-13 CONFIGURATION 76-T

a. Weight Growth

Weight growth occurs through the various phases of every major program. For all aerospace vehicles, the usual range of weight growth is between 5 and 50 percent, represented by low-risk design aircraft and complex, advanced spacecraft respectively.

The value of 50 percent weight growth has been chosen because of the advanced nature of the SPS. Although it is reasonable to assume that advancements will be made in materials and design and fabrication techniques, these advancements will be more than offset by the inexorable weight growth that occurs based on historical data.

Figure IV-A-5-1 shows the general pattern of weight growth for various aerospace vehicles from program beginning to end. It should be noted that the data used to develop these curves is from the acquisition phase of the vehicle programs; zero percent growth coincides with the original specification weight or control weight. This is because the weight growth during the definition phase is not sufficiently documented to be shown. In many cases, however, the weight growth during the definition phase has been substantial and had a definite impact on the total weight growth.

The Mercury spacecraft as shown in figure IV-A-5-1 grew about 30 percent throughout the acquisition phase. The Gemini spacecraft is generally considered a second-generation vehicle based on Mercury although it still grew about 18 percent. The Apollo Command Module grew over 50 percent primarily because of new technology that had to be developed to go into and return from deep space. It should be pointed out that the above three spacecraft represent essentially all dry weight so that it was not the addition of propellant that caused the weight growths. The Apollo Lunar Module grew over 20 percent in dry weight and over 50 percent in gross weight. However, a substantial portion of the gross weight growth was caused by increases in propellant.

Aircraft appear to have the lowest average weight growth of aerospace vehicles. The low average value of 5 percent is primarily due to the low level of advanced technology required as well as established design techniques. This has been a big factor in the design and fabrication of the Space Shuttle Orbiter to date. Although a 10 percent weight growth was chosen for the Space Shuttle Orbiter, it appears that this will be exceeded.

The shaded values of figure IV-A-5-1 represent an average of around 40 percent growth. Since the SPS is still in the definition phase, an additional 10 percent for a total of 50 percent weight growth allowance is felt to be realistic at least until the acquisition phase is begun.

DATA POINTS:

1. MERCURY
2. GEMINI
3. APOLLO COMMAND MODULE
4. APOLLO LUNAR MODULE
5. AIRCRAFT

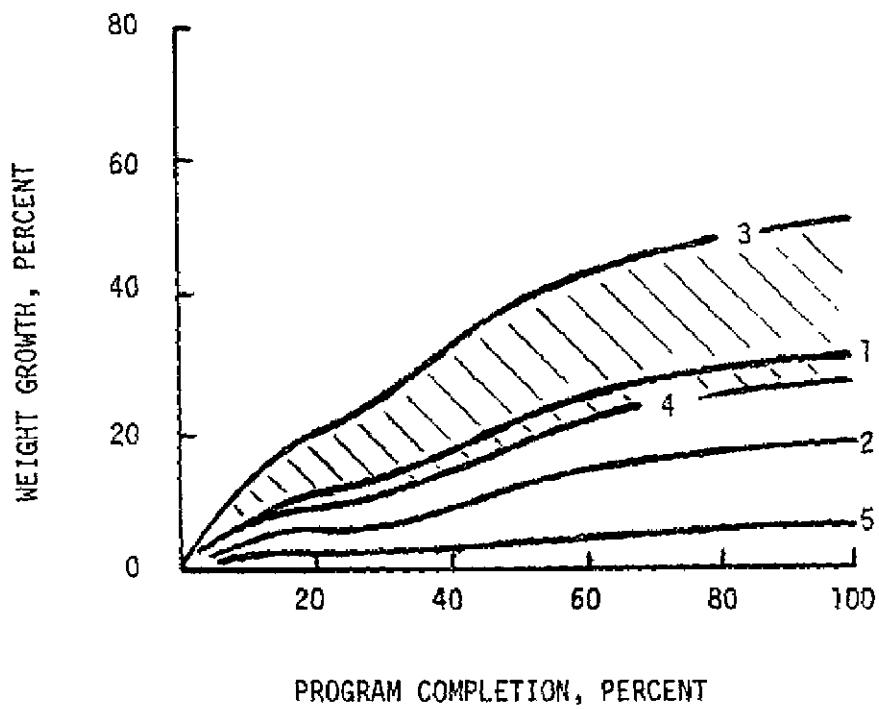


FIGURE IV-A-5-1. AEROSPACE VEHICLE WEIGHT GROWTH

b. Weight Estimates

In order to encompass the greatest conceivable range of weights for the operational satellite, nine estimates were made for each of two example configurations based on nominal and extreme values of solar array area and subsystem unit weights. Estimates for the column/cable configuration are given in tables IV-A-5-1, -2, and -3 and for the truss configuration in tables IV-A-5-4, -5, and -6.

The column/cable configuration which has been used for estimating purposes is illustrated in figure IV-A-4-1. Dimensions for the three overall efficiencies of section IV-A-2 are as follows:

Efficiency (overall)		.080	.054	.042
Area, km ²		96.1	143.4	182.9
a	} m	5904	7212	8145
b		11808	14424	16290
c		11808	14424	16290
d		4932	6025	6804
e		9865	12050	13609
r		750	750	750

Dimensions for the truss configuration (figure IV-A-4-13) are:

Efficiency (overall)		.080	.054	.042
Area, km ²		96.1	143.4	182.9
a	} m	3991	5211	6129
b		24080	27517	29841
c		432	564	663
r		974	1041	1092

Table IV-A-5-1. Column/Cable Configuration Mass Summary (Nominal Unit Masses)

COMPONENT	METRIC TONS (KG/1000)			REMARKS	
	MIN.	REF.	MAX.		
1.0 SOLAR ENERGY COLLECTION SYSTEM	(25924)	(39171)	(50479)		
1.1 PRIMARY STRUCTURE	182	222	251	3.08 kg/m column length	
1.2 SECONDARY STRUCTURE	140	209	267		
1.3 MECHANICAL SYSTEMS	40	40	40		
1.4 MAINTENANCE STATION	85	85	85	1000 m ³ enclosed volume	
1.5 CONTROL	280	313	343	200 M.T. dry wt. + 1 yr. propellant	
1.6 INSTRUMENTATION/COMMUNICATIONS	4	4	4		
1.7 SOLAR CELL BLANKETS	19218	28677	36576	0.4 kg/m ²	
1.8 SOLAR CONCENTRATORS	3843	5735	7315	0.04 kg/m ²	
1.9 POWER DISTRIBUTION	2132	3886	5598		
2.0 MICROWAVE POWER TRANSMISSION SYSTEM	(13304)	(15371)	(16765)		
2.1 PRIMARY STRUCTURE	392	392	392		
2.2 SECONDARY STRUCTURE	518	518	518		
2.3 SUBARRAY STRUCTURE	300	300	300		
2.4 THERMAL CONTROL	23	23	23		
2.5 MECHANICAL SYSTEMS	30	30	30		
2.6 ROTARY JOINTS	635	635	635		
2.7 POINTING CONTROL	100	100	100		
2.8 POWER DISTRIBUTION	127	167	197		
2.9 PHASE CONTROL	358	358	358		
2.10 MICROWAVE GENERATORS	6819	8846	10210		
2.11 WAVEGUIDES	4002	4002	4002		
	SUB TOTAL	39228	54542	67244	
	GROWTH	19614	27271	33622	50%
	TOTAL	58842	81813	100866	

IV-A-5-4

Table IV-A-5-2. Column/Cable Configuration Mass Summary (Minimum Unit Masses)

COMPONENT	METRIC TONS (KG/1000)			REMARKS
	MIN.	REF.	MAX.	
1.0 SOLAR ENERGY COLLECTION SYSTEM	(20914)	(31556)	(40624)	
1.1 PRIMARY STRUCTURE	164	200	226	Nominal -10%
1.2 SECONDARY STRUCTURE	126	188	240	" "
1.3 MECHANICAL SYSTEMS	30	30	30	
1.4 MAINTENANCE STATION	70	70	70	
1.5 CONTROL	217	248	277	Nominal dry wt. -25%
1.6 INSTRUMENTATION/COMMUNICATIONS	3	3	3	
1.7 SOLAR CELL BLANKETS	14893	22224	28346	0.31 kg/m ²
1.8 SOLAR CONCENTRATORS	3843	5735	7315	0.04 kg/m ²
1.9 POWER DISTRIBUTION	1568	2858	4117	
2.0 MICROWAVE POWER TRANSMISSION SYSTEM	(10625)	(12278)	(13393)	
2.1 PRIMARY STRUCTURE	353	353	353	Nominal -10%
2.2 SECONDARY STRUCTURE	466	466	466	" "
2.3 SUBARRAY STRUCTURE	270	270	270	" "
2.4 THERMAL CONTROL	21	21	21	" "
2.5 MECHANICAL SYSTEMS	27	27	27	" "
2.6 ROTARY JOINTS	363	363	363	
2.7 POINTING CONTROL	80	80	80	Nominal -20%
2.8 POWER DISTRIBUTION	102	134	158	" "
2.9 PHASE CONTROL	286	286	286	" "
2.10 MICROWAVE GENERATORS	5455	7076	8167	" "
2.11 WAVEGUIDES	3202	3202	3202	" "
SUB TOTAL	31539	43834	54017	
GROWTH	15770	21917	27009	50%
TOTAL	47309	65751	81026	

IV-A-5-5

Table IV-A-5-3. Column/Cable Configuration Mass Summary (Maximum Unit Masses)

IV-A-5-6

COMPONENT	METRIC TONS (KG/1000)			REMARKS	
	MIN.	REF.	MAX.		
1.0 SOLAR ENERGY COLLECTION SYSTEM	(31372)	(48018)	(62434)		
1.1 PRIMARY STRUCTURE	218	266	301	Nominal +20%	
1.2 SECONDARY STRUCTURE	168	251	320	" "	
1.3 MECHANICAL SYSTEMS	50	50	50		
1.4 MAINTENANCE STATION	100	100	100		
1.5 CONTROL	393	439	479	Nominal dry wt. +50%	
1.6 INSTRUMENTATION/COMMUNICATIONS	5	5	5		
1.7 SOLAR CELL BLANKETS	22100	32979	42062	0.46 kg/m ²	
1.8 SOLAR CONCENTRATORS	3843	5735	7315	0.04 kg/m ²	
1.9 POWER DISTRIBUTION	4495	8193	11802		
2.0 MICROWAVE POWER TRANSMISSION SYSTEM	(16218)	(18730)	(20427)		
2.1 PRIMARY STRUCTURE	470	470	470	Nominal +20%	
2.2 SECONDARY STRUCTURE	622	622	622	" "	
2.3 SUBARRAY STRUCTURE	360	360	360	" "	
2.4 THERMAL CONTROL	25	25	25	" +10%	
2.5 MECHANICAL SYSTEMS	36	36	36	" +20%	
2.6 ROTARY JOINTS	907	907	907		
2.7 POINTING CONTROL	130	130	130	Nominal +30%	
2.8 POWER DISTRIBUTION	254	334	394	" +100%	
2.9 PHASE CONTROL	430	430	430	" +20%	
2.10 MICROWAVE GENERATORS	8182	10614	12251	" "	
2.11 WAVEGUIDES	4802	4802	4802	" "	
	SUB TOTAL	47590	66748	82861	
	GROWTH	23795	33374	41431	50%
	TOTAL	71385	100122	124292	

Table IV-A-5-4. Truss Configuration Mass Summary (Nominal Unit Masses)

IV-A-5-7

COMPONENT	METRIC TONS (KG/1000)			REMARKS
	MIN.	REF.	MAX.	
1.0 SOLAR ENERGY COLLECTION SYSTEM	(27164)	(40869)	(52690)	1000 m ³ enclosed volume 200 M.T. dry wt. + 1 yr. propellant 0.4 kg/m ² 0.04 kg/m ²
1.1 PRIMARY STRUCTURE	1852	2764	3525	
1.2 SECONDARY STRUCTURE	140	209	267	
1.3 MECHANICAL SYSTEMS	40	40	40	
1.4 MAINTENANCE STATION	85	85	85	
1.5 CONTROL	304	355	398	
1.6 INSTRUMENTATION/COMMUNICATIONS	4	4	4	
1.7 SOLAR CELL BLANKETS	19218	28677	36576	
1.8 SOLAR CONCENTRATORS	3843	5735	7315	
1.9 POWER DISTRIBUTION	1678	3000	4480	
2.0 MICROWAVE POWER TRANSMISSION SYSTEM	(13304)	(15371)	(16765)	50%
2.1 PRIMARY STRUCTURE	392	392	392	
2.2 SECONDARY STRUCTURE	518	518	518	
2.3 SUBARRAY STRUCTURE	300	300	300	
2.4 THERMAL CONTROL	23	23	23	
2.5 MECHANICAL SYSTEMS	30	30	30	
2.6 ROTARY JOINTS	635	635	635	
2.7 POINTING CONTROL	100	100	100	
2.8 POWER DISTRIBUTION	127	167	197	
2.9 PHASE CONTROL	358	358	358	
2.10 MICROWAVE GENERATORS	6819	8846	10210	
2.11 WAVEGUIDES	4002	4002	4002	
SUB TOTAL	40468	56240	69455	
GROWTH	20234	28120	34728	
TOTAL	60702	84360	104183	

Table IV-A-5-5. Truss Configuration Mass Summary (Minimum Unit Masses)

IV-A-5-8

COMPONENT	METRIC TONS (KG/1000)			REMARKS
	MIN.	REF.	MAX.	
1.0 SOLAR ENERGY COLLECTION SYSTEM	(21443)	(32136)	(41170)	
1.1 PRIMARY STRUCTURE	1667	2488	3173	Nominal -10%
1.2 SECONDARY STRUCTURE	126	188	240	" "
1.3 MECHANICAL SYSTEMS	30	30	30	
1.4 MAINTENANCE STATION	70	70	70	
1.5 CONTROL	236	278	313	Nominal dry wt. -25%
1.6 INSTRUMENTATION/COMMUNICATIONS	3	3	3	
1.7 SOLAR CELL BLANKETS	14893	22224	28346	0.31 kg/m ²
1.8 SOLAR CONCENTRATORS	3843	5735	7315	0.04 kg/m ²
1.9 POWER DISTRIBUTION	575	1120	1680	Concentrators plus buses at ends
2.0 MICROWAVE POWER TRANSMISSION SYSTEM	(10625)	(12278)	(13393)	
2.1 PRIMARY STRUCTURE	353	353	353	Nominal -10%
2.2 SECONDARY STRUCTURE	466	466	466	" "
2.3 SUBARRAY STRUCTURE	270	270	270	" "
2.4 THERMAL CONTROL	21	21	21	" "
2.5 MECHANICAL SYSTEMS	27	27	27	" "
2.6 ROTARY JOINTS	363	363	363	
2.7 POINTING CONTROL	80	80	80	
2.8 POWER DISTRIBUTION	102	134	158	Nominal -20%
2.9 PHASE CONTROL	286	286	286	" "
2.10 MICROWAVE GENERATORS	5455	7076	8167	" "
2.11 WAVEGUIDES	3202	3202	3202	" "
SUB TOTAL	32068	44414	54563	
GROWTH	16034	22207	27282	50%
TOTAL	48102	66621	81845	

Table IV-A-5-6. Truss Configuration Mass Summary (Maximum Unit Masses)

IV-A-5-9

COMPONENT	METRIC TONS (KG/1000)			REMARKS
	MIN.	REF.	MAX.	
1.0 SOLAR ENERGY COLLECTION SYSTEM	(31452)	(47395)	(60936)	
1.1 PRIMARY STRUCTURE	2222	3317	4230	Nominal +20%
1.2 SECONDARY STRUCTURE	168	251	320	" "
1.3 MECHANICAL SYSTEMS	50	50	50	
1.4 MAINTENANCE STATION	100	100	100	
1.5 CONTROL	419	478	527	
1.6 INSTRUMENTATION/COMMUNICATIONS	5	5	5	
1.7 SOLAR CELL BLANKETS	22100	32979	42062	0.46 kg/m ²
1.8 SOLAR CONCENTRATORS	3843	5735	7315	0.04 kg/m ²
1.9 POWER DISTRIBUTION	2545	4480	6327	No benefit from concentrators
2.0 MICROWAVE POWER TRANSMISSION SYSTEM	(16218)	(18730)	(20427)	
2.1 PRIMARY STRUCTURE	470	470	470	Nominal +20%
2.2 SECONDARY STRUCTURE	622	622	622	" "
2.3 SUBARRAY STRUCTURE	360	360	360	" "
2.4 THERMAL CONTROL	25	25	25	" +10%
2.5 MECHANICAL SYSTEMS	36	36	36	" +20%
2.6 ROTARY JOINTS	907	907	907	
2.7 POINTING CONTROL	130	130	130	
2.8 POWER DISTRIBUTION	254	334	394	Nominal +100%
2.9 PHASE CONTROL	430	430	430	" +20%
2.10 MICROWAVE GENERATORS	8182	10614	12251	" "
2.11 WAVEGUIDES	4802	4802	4802	" "
SUB TOTAL	47670	66125	81363	
GROWTH	23835	33063	40682	50%
TOTAL	71505	99188	122045	

These solar array areas are based on the efficiencies given in section IV-A-2 and a solar constant of 1353 W/m^2 , but have been increased 4.3 percent to allow for losses due to orientation perpendicular to the orbit plane (POP) so that the annual average DC output power is 5 GW per rec-tenna. This means that maximum output is 5.2 GW, which slightly exceeds the transmitter and ionosphere power density limits of section IV-A-1. It is assumed that the uncertainty associated with these limits is great enough that a problem will not exist.

The unit weight basis, where available, is given in the tables. For a given unit weight, secondary structure (item 1.2) was assumed proportional to array area and array power distribution (1.9) proportional to the $3/2$ power of area. Antenna power distribution (2.7) and microwave generators (2.9) were assumed to be proportional to the power level at those stages of the transmission process.

Totals have been increased by 50 percent to account for probable growth.

The variation of weight with efficiency and unit weights can be more easily visualized by reference to figure IV-A-5-2, although the apparently large range of weights is misleading for several reasons. First, it is unlikely that all efficiencies will be at the minimum, or at the maximum, simultaneously. Thus, the probable range of overall efficiency is narrower than shown. Second, a similar argument can be made for unit weights, although perhaps less convincingly. Finally, high efficiencies are, in general, not achieved concurrently with low unit weights, so that the lower left and upper right corners of the region are relatively unlikely to occur.

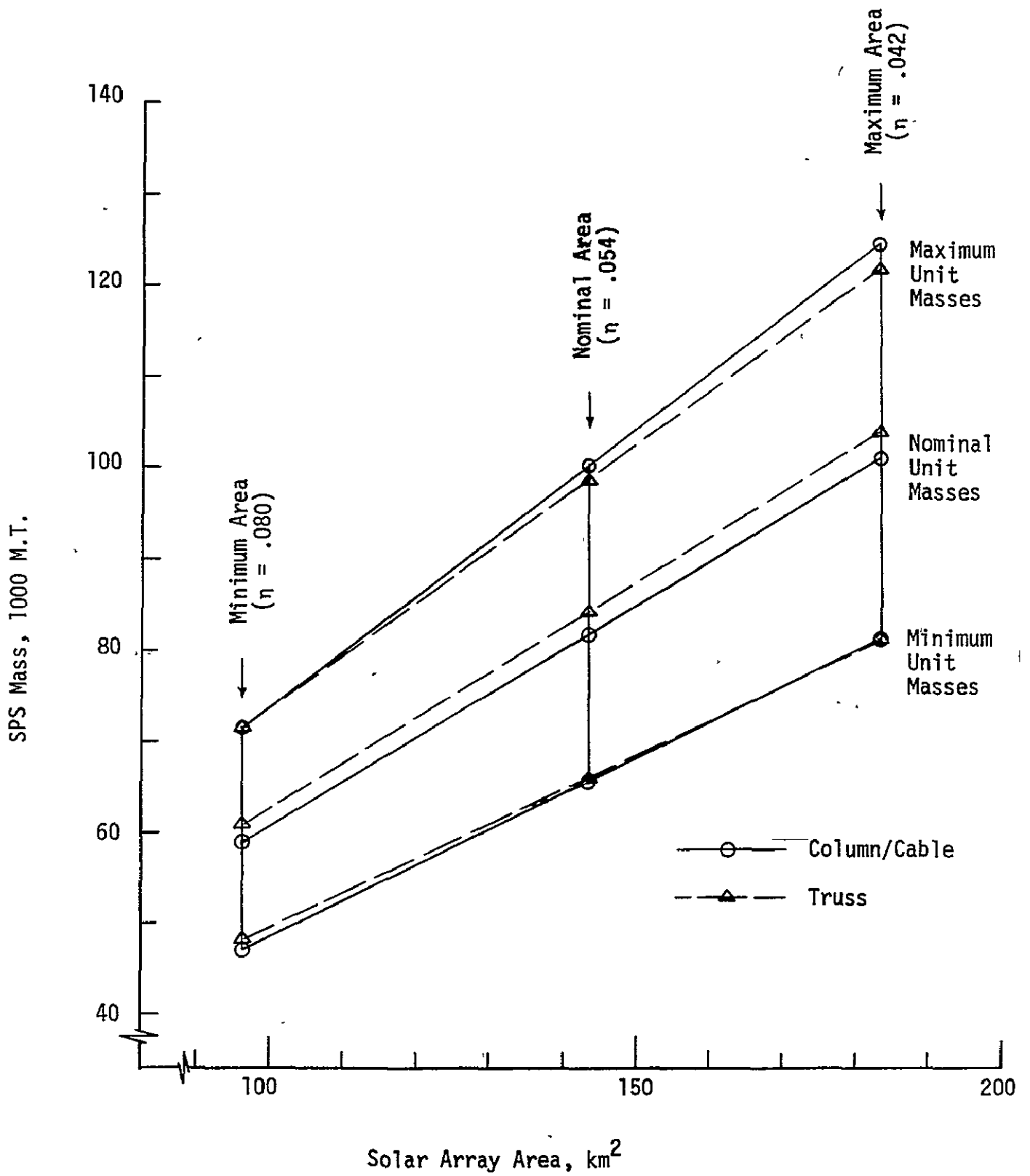


Figure IV-A-5-2. SPS Mass Range

IV-B. SOLAR ENERGY COLLECTION SYSTEM

S. Gaudiano, F. L. Baiamonte
Experiment Systems Division

1. Solar Array

IV.B.1.a SOLAR CELL TECHNOLOGY

(1) INTRODUCTION

One of the most fundamental and necessary elements of the SPS is the solar cell, a photovoltaic device which converts incident radiation from the sun into electrical energy. Solar arrays comprise the largest and heaviest portion of the SPS. It is therefore necessary that there be a clear understanding of this device since improvements within it radically affect the configuration of the SPS design and its cost. This section of the report involves the technological factors associated with the cells including their operational limitations, materials, and fabrication techniques. The discussion is based on the use of silicon as the primary solar cell semiconductor material, but also includes comparisons with other candidate materials such as gallium arsenide and cadmium sulfide where applicable.

(2) THEORY OF OPERATION

A semiconductor material is a poor conductor of electricity which has a conductivity greater than insulators but less than metals (figure IV.B.1.a.1). Its conductivity ranges from approximately 10^{-6} (ohm-cm) $^{-1}$ to 10^6 (ohm-cm) $^{-1}$. The energy gap between the valence band and the conduction band is small enough (figure IV.B.1.a.2) such that an appreciable number of thermally excited electrons from the valence band can move into the conduction band. The electrons which are excited to the conduction band leave an empty state in the valence band which is referred to as a hole. Further, there may be nonsemiconductor atoms present with energy levels in the forbidden band, near the conduction band, which can donate an electron to the conduction band.

The electrical characteristics of the semiconductor can be altered by doping it with impurity atoms having the desired electrical properties. If the semiconductor contains more electrons than holes, it is said to be n-type, and if there are more holes than electrons, it is said to be p-type.

The electrochemical potential for charged carriers in p-type semiconductors differs from n-type semiconductors. It is this potential difference which gives rise to an electric field between n-type and p-type regions in a semiconductor material. Electrons in the p-type material are swept by the built-in field of the junction to the n-type material, and since the holes are of opposite charge, they flow to the p-type silicon.

As radiant (photon) energy impinges upon the semiconductor, electron-hole pairs are generated and they migrate through the semiconductor until they are either collected or recombine with other holes

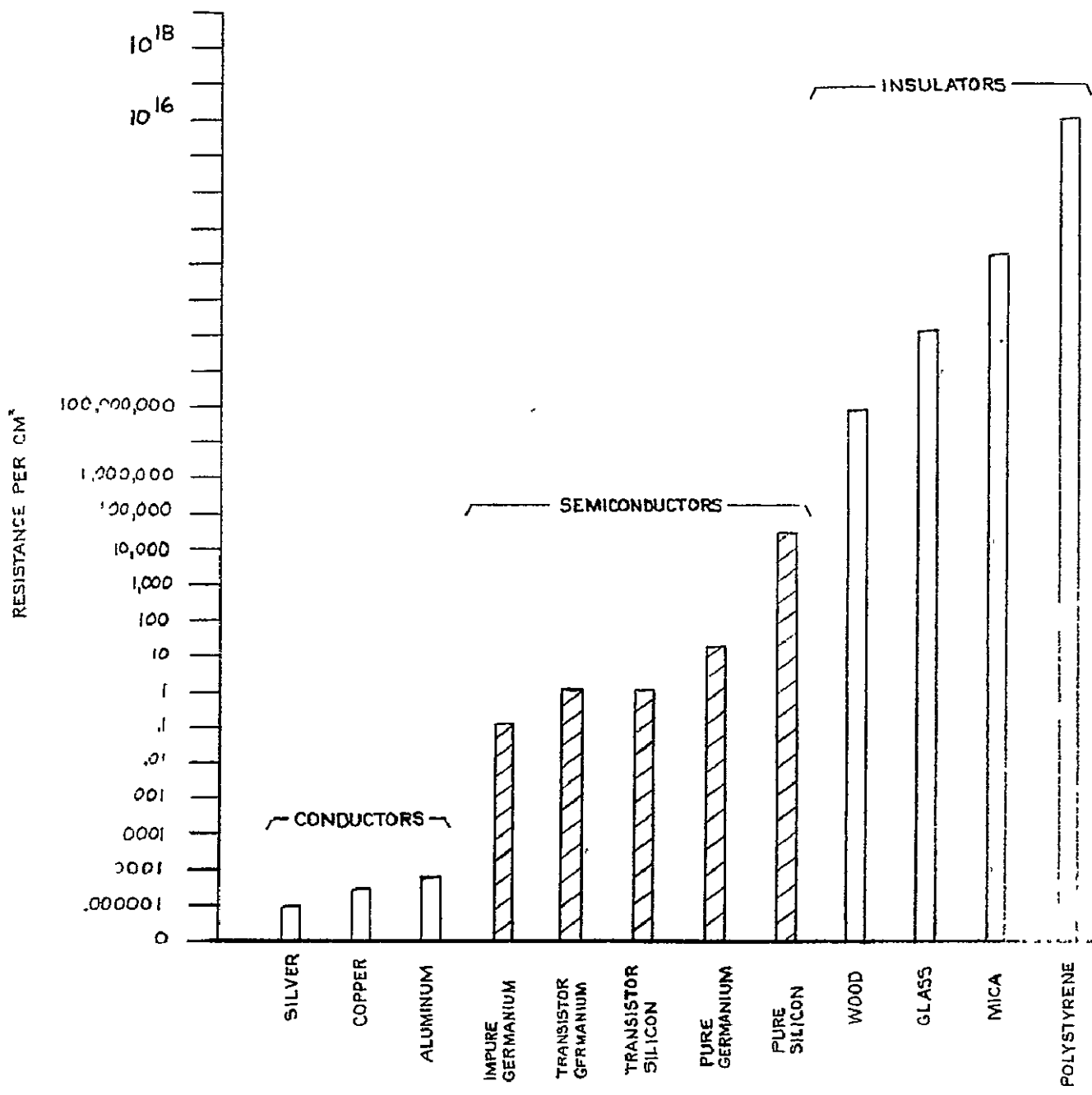
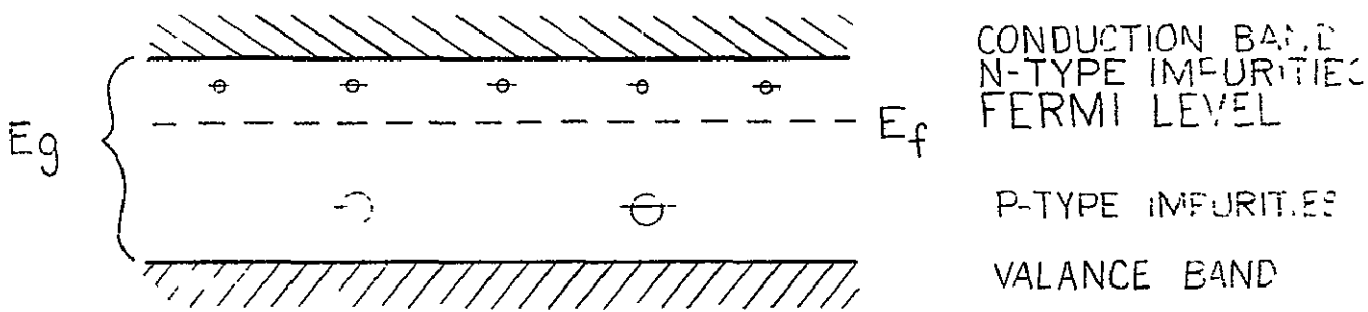


CHART OF RESISTANCE PER cm^2 OF CONDUCTORS, SEMICONDUCTORS, AND INSULATORS

FIGURE IV.B.1.a.1

IV.B.1.a.2



CONDUCTION BAND
 N-TYPE IMPURITIES
 FERMI LEVEL

P-TYPE IMPURITIES

VALANCE BAND

ENERGY DIAGRAM OF IMPURITIES IN SILICON

FIGURE IV.B.1.a.2

IV.B.1.a.3

or electrons. If a minority carrier enters the region of an n-p junction, it is swept across by the electric field, separated from its counterpart, and is said to be collected (figure IV.B.1.a.3). The collected electrical carriers (electrons and holes) flow from the semiconductor to metal contacts on the front and back of the device and provide power to an external load.

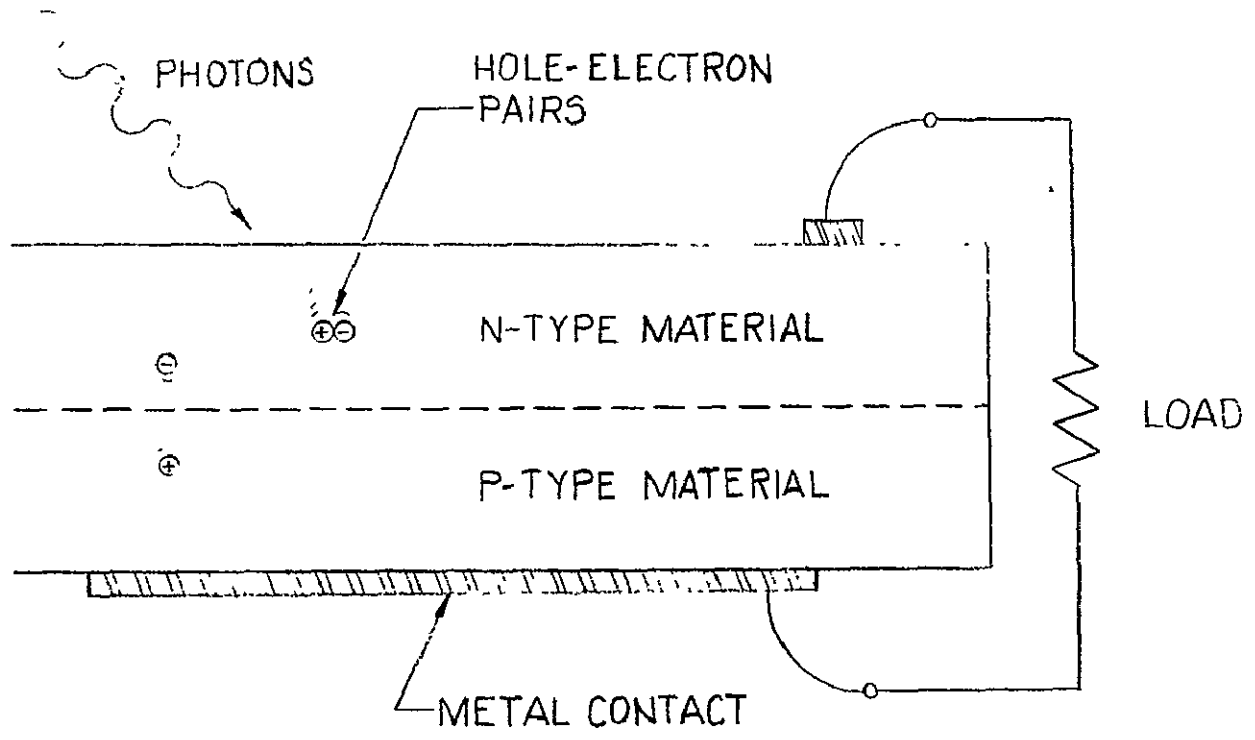
The distance a hole or electron travels before it interacts with other atoms is defined as its diffusion length. The objective is to generate electrons or holes such that they are near enough to the n-p junction to be collected before they are recombined. If this is not accomplished, the holes and electrons will be recombined, which releases heat to the semiconductor material instead of producing electrical energy and results in a net loss of efficiency. The recombination centers are impurities and crystal defects within and on the surface of the semiconductor material.

(3) SOLAR CELL EFFICIENCY CONSIDERATIONS

The efficiency (η) of a solar cell is the ratio of the electrical power output to the incident solar energy impinging upon its surface. There are many characteristics which contribute to solar cell inefficiencies and include absorption coefficients, specular reflections, temperature, electrode masking, ohmic resistance, and radiation effects, among others. The sun provides 1353 W/m^2 of radiant energy in outer space (AMO-air mass zero), and it is distributed over the spectrum which is shown in figure IV.B.1.a.4. However, only a small portion of this energy is available for conversion to electricity by solar cells because of limitations in the spectral response of available semiconductor materials. Figure IV.B.1.a.5 shows a comparison of the response of silicon, gallium arsenide, and cadmium sulfide with the AMO solar spectrum. Note that in each case, the peaked response of the materials does not coincide with that of the sun. Thus, complete absorption of all of the available energy is not possible.

In an effort to improve the efficiency of the silicon solar cell, certain modifications have been made to its physical structure. These modifications enable the cell to make greater use of the light in the short wavelength end of the solar spectrum and to increase the total light absorption at all frequencies. Figure IV.B.1.a.6 shows a response comparison of two recent solar cell developments which have a substantially higher efficiency than does a conventional cell. The violet cell obtains its name because it has a significantly improved response in the violet region. CNR (Comsat Non-Reflective) cell also has this characteristic, plus a special surface treatment which reduces reflected light to almost zero.

The maximum theoretical efficiency for silicon solar cells is predicted to be approximately 22% at 298K. Special small-area experimental silicon cells have achieved 19.7% under laboratory conditions. The conventional silicon cells in production volumes have an



SOLAR CELL

FIGURE IV.B.1.a.3

IV.B.1.a.5

IV.B.1.a.6

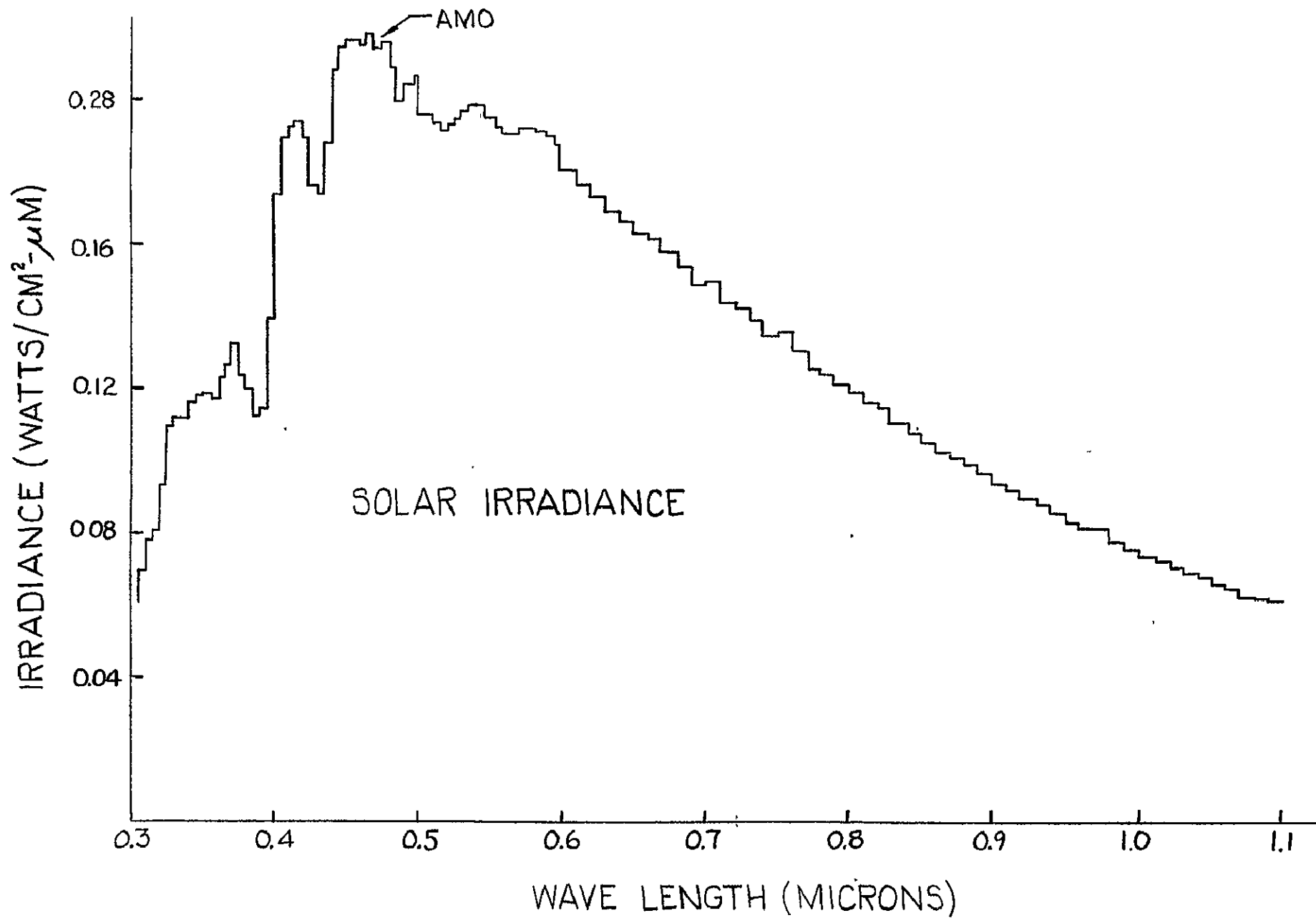


FIGURE IV.B.1.a.4

IV.B.1.a.7

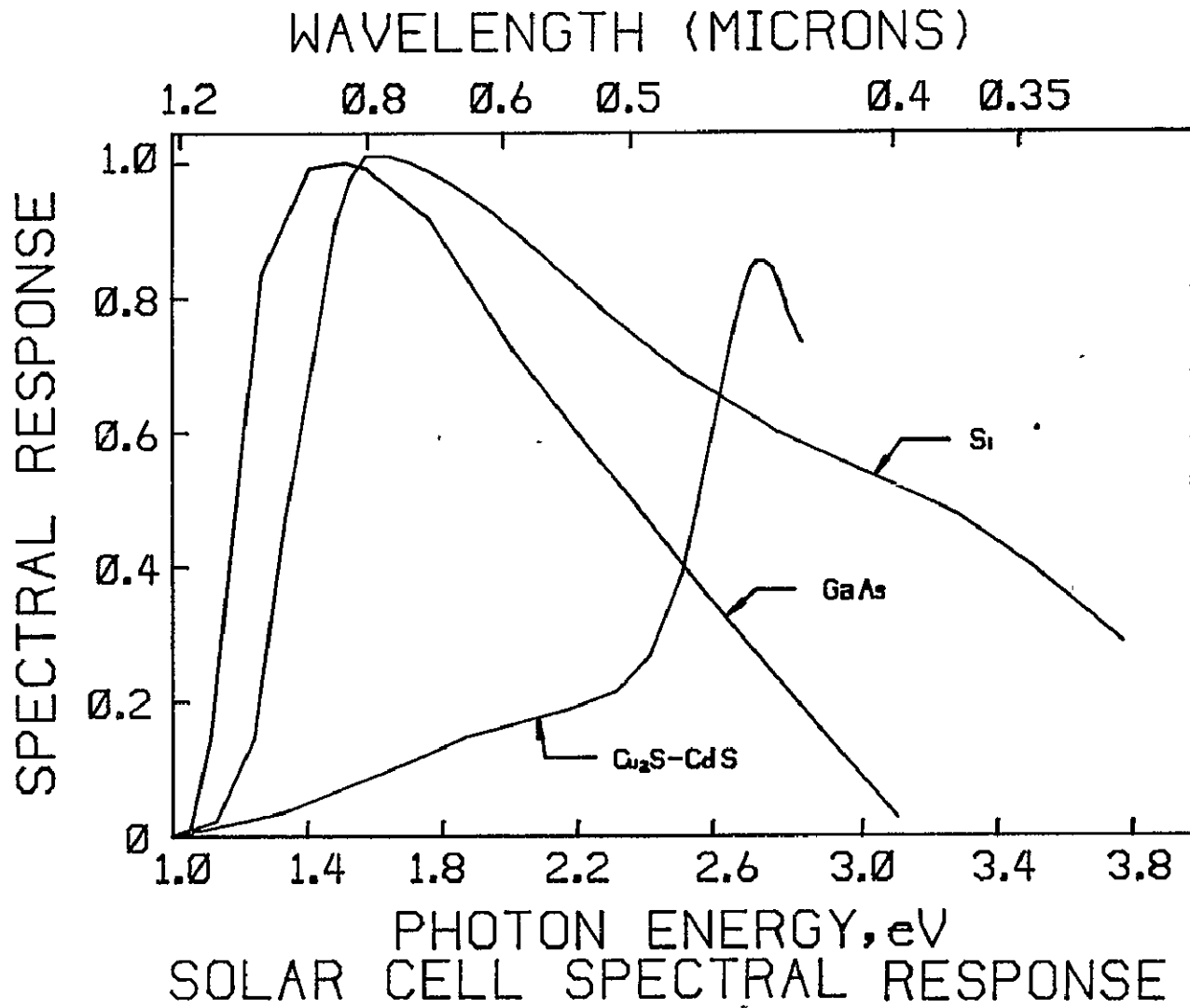


FIGURE IV.B.1.a.5

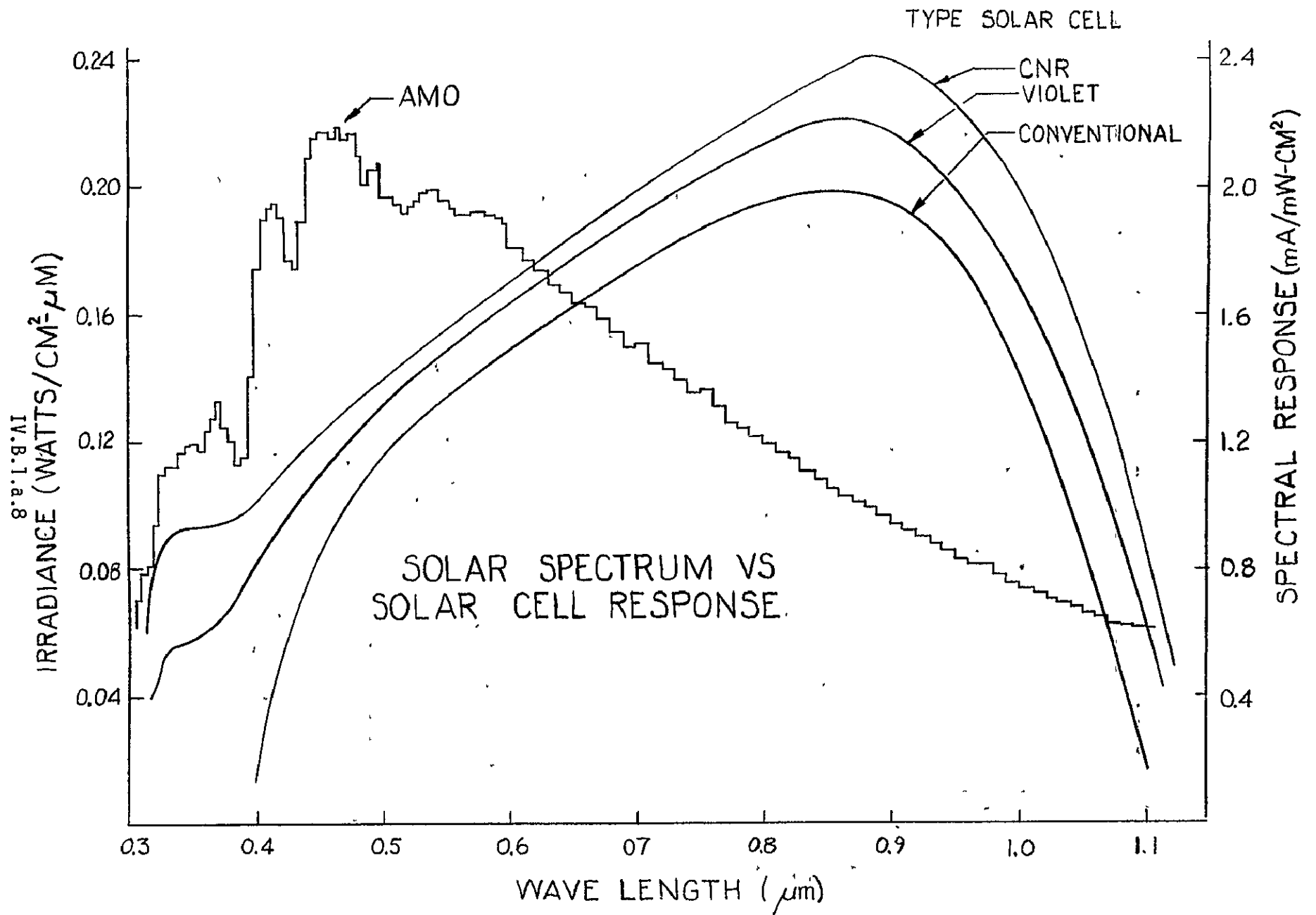


FIGURE IV.B.1.a.6

efficiency between 10 and 12%, whereas violet cells produced in large batches have an efficiency of 14%.

Light reflection is another loss mechanism in solar cells. The index of refraction of a vacuum is one and that of polished silicon is 3.4. This mismatch in reflective indices gives rise to high reflection losses. To minimize this effect, an antireflective transparent coating is usually applied to the front surface of the cell. This reduces the loss to less than 10%, which is acceptable for typical applications. In order to improve the cell further, special surface texturing treatments are required. In the case of silicon, preferential etches are applied which form pyramids approximately 2000-6000 nm in height. Light is reflected off the angular surfaces of these pyramids several times until almost all of it is absorbed (figure IV.B.1.7), hence the name, a "black" cell. The reflection of a black cell is less than 5%, and they have had average efficiencies of approximately 15% in test runs of 1000 units.

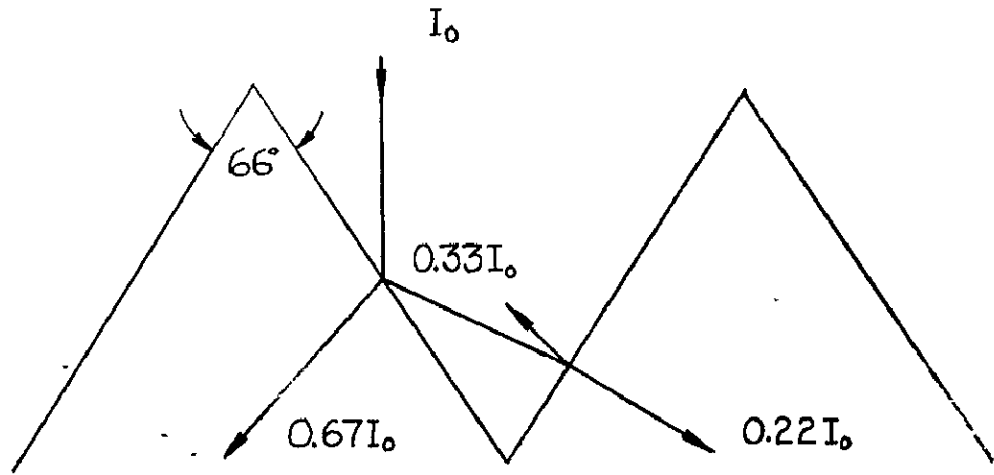
Pyramid-like structures form in silicon because it has a face-centered cubic structure. When oriented in certain planes, the corners of the crystals appear prominently when the silicon is exposed to certain preferential etches. Deep groove-like structures are also possible with etchants as well as with ion milling techniques. The adaptability of these surface antireflective techniques to nonsilicon materials has yet to be demonstrated.

All incident energy which cannot be converted by the solar cell into electrical energy is absorbed as heat, which also constitutes a loss. As the temperature of the semiconductor material increases, its conversion efficiency decreases. The effect of efficiency decrease with temperature for each of the three materials is shown in figure IV.B.1.a.8. As in the previous figure, gallium arsenide exhibits superior characteristics over that of either silicon or cadmium sulfide.

The current collection electrode on the top surface of the solar cell represents another loss in efficiency because it masks a finite portion of the conversion area from incident radiation. This electrode typically has a comb or tree-shaped design so that current flow in any one area of the cell is reduced to a minimum. The greater the amount of current that must flow through the semiconductor material, the greater will be the I^2R losses (heat). A compromise in electrode area and I^2R losses is reached around 5% of the active area of the cell.

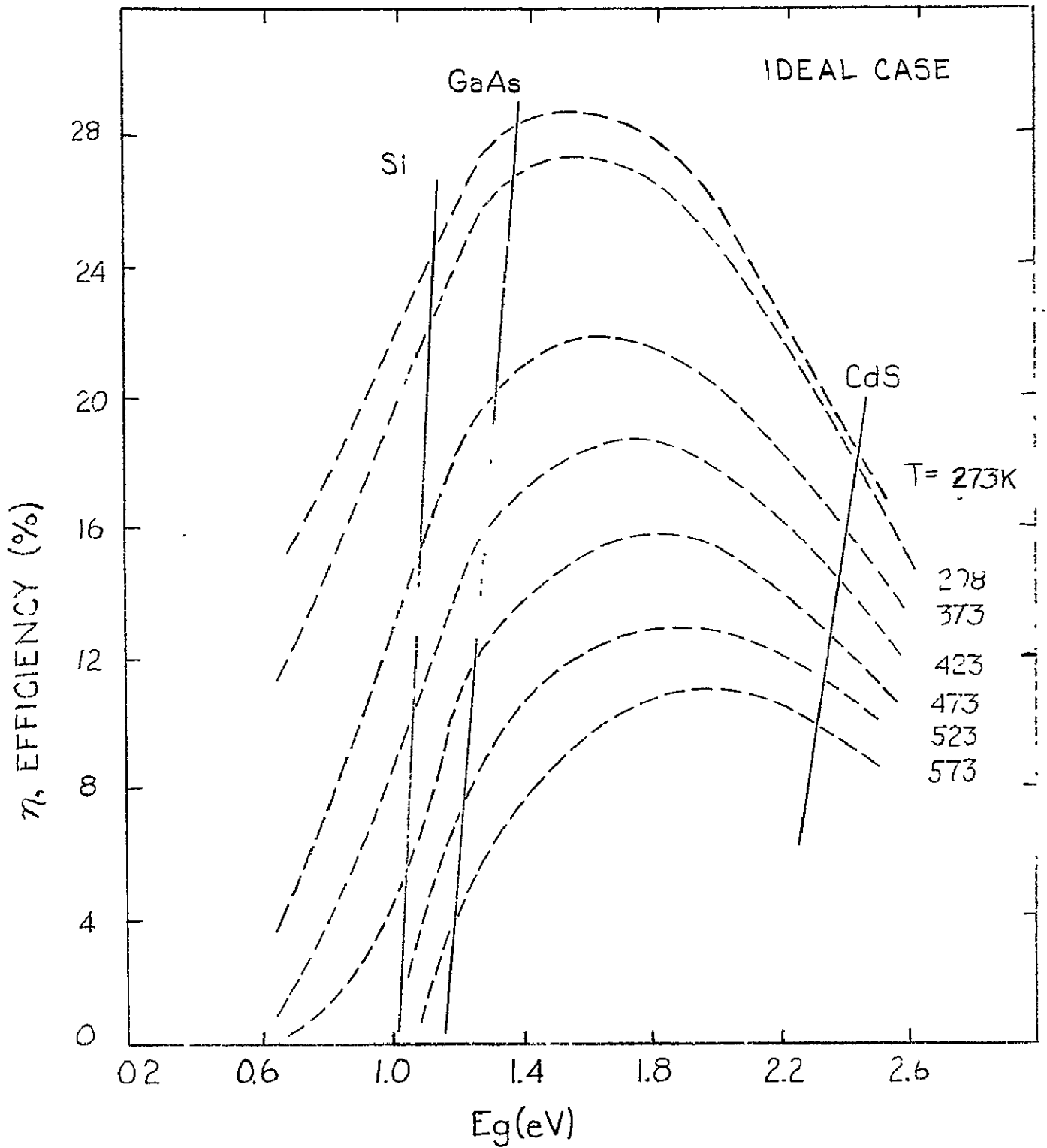
In addition to loss in the bulk material as a result of lateral current flow, solar cells also have I^2R losses associated with the metallic electrodes themselves and with a contact resistance to the semiconductor. Although the resistance is small, it is nevertheless in series with the current flow at all times and causes an I^2R loss in the cell.

IV.B.1.a.10



OPTICAL PATH ON A COMSAT BLACK CELL

FIGURE IV.B.1.a.7



THEORETICAL SOLAR CELL EFFICIENCY

FIGURE IV.B.1.a.8

The primary cause of solar cell efficiency degradation in space is proton and electron radiation. Incident protons and electrons produce crystal lattice defects in the semiconductor material, which in turn, act as recombination centers for holes and electrons (figure IV.B.1.a.9). Thin cells are less susceptible to radiation damage than are thick cells, but there is a limitation on how thin a cell can be. The absorption of light in silicon, for example, is less than that of other semiconductors. As a result, its thickness must be greater than 0.100 mm or the efficiency will be too low to be of practical value. Figure IV.B.1.a.10 shows efficiency degradation as a function of thickness for two types of silicon material. Other materials, such as gallium arsenide, have a much higher absorption coefficient and require only a 0.005 mm thickness.

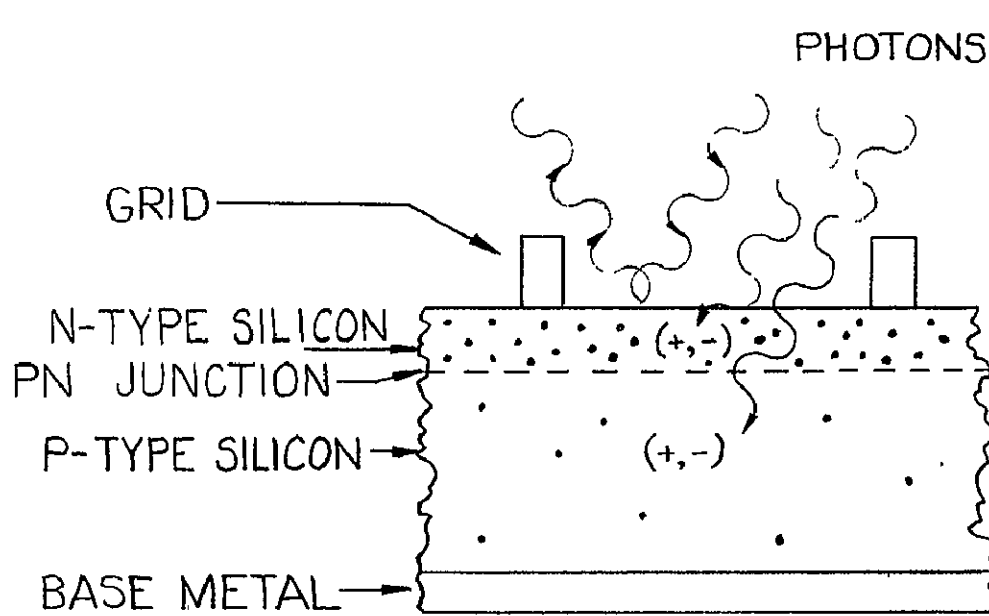
In order to protect the solar cell from radiation, a 0.150-0.300 mm cover glass is usually mounted on top of the cell. This adds some absorption losses, and of course, reduces cell efficiency. More importantly, however, it generally doubles the cell's weight. Since weight is a critical parameter in the SPS's solar cell arrays, a thin film of durable translucent plastic is being proposed instead of the cover glass. It would provide the same protection as the glass, have slightly greater absorption loss, and would be much lighter.

(4) ALTERNATE SOLAR CELL MATERIALS

The problems of marginal efficiency, efficiency degradation with temperature, thickness limitations, susceptibility to radiation damage, and high cost have prompted researchers to have interests in photovoltaic materials other than silicon. Alternative materials are listed in figure IV.B.1.a.7, but of this group, only two, cadmium sulfide and gallium arsenide, have been studied extensively. The balance have various physical problems which limit their usefulness.

Cadmium sulfide has been known as a photosensitive material for several decades. It was actively studied by the NASA/Lewis Research Center as a photovoltaic converter during the 1960's. Their interest stemmed from a desire to have a flexible solar cell array that could be rolled into a dense form for storage. It was found that polycrystalline cells could be fabricated on both thin metal foils and metallized plastic films. However, the best efficiency that could be obtained was about 8%, and this tended to degrade to a somewhat lower value with time. The cells were also very susceptible to the effects of moisture which required them to be hermetically sealed. The low efficiency and moisture degradation problem eventually caused the effort to be abandoned in favor of silicon.

It is interesting to note that there is a greater potential for space manufacturing of cadmium sulfide solar cells than either silicon or gallium arsenide. The high vacuum environment is a convenient advantage because the cells are typically manufactured by a vacuum deposition process. This is not necessarily a simple technique to perform

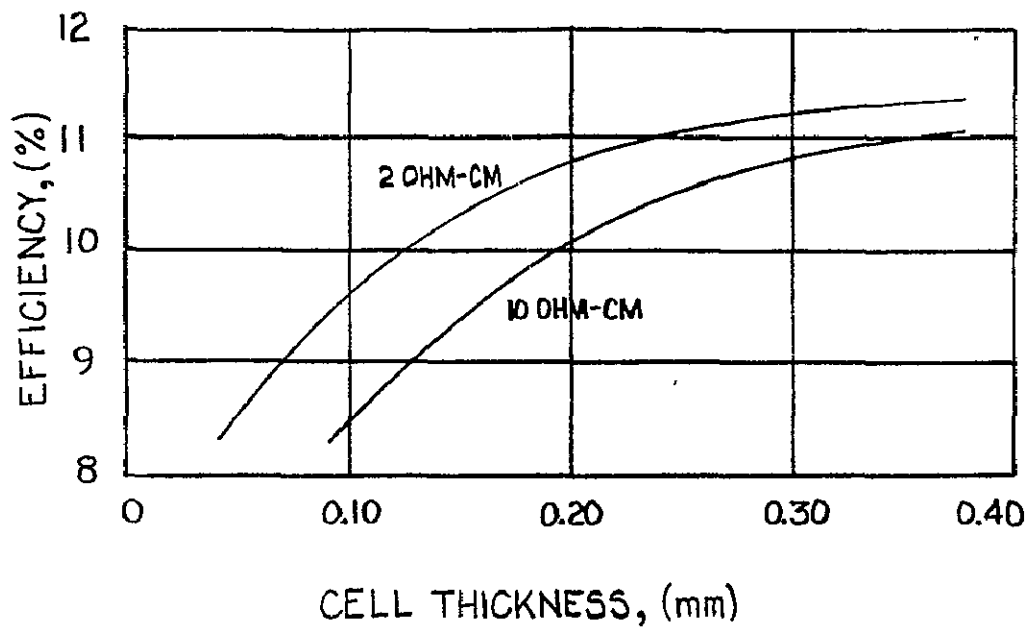


LOSS MECHANISMS

- REFLECTION
- RECOMBINATION
- CONTACT RESISTANCE
- BULK RESISTANCE

SOLAR CELL LOSS MECHANISMS

• FIGURE IV.B.1.a.9



SOLAR CELL EFFICIENCY VS CELL THICKNESS

FIGURE IV.B.1.a.10

because cadmium sulfide tends to fractionate into its elemental components when heated. The resulting film suffers from a stoichiometric imbalance of these components and, therefore, reduces efficiency. Closely controlled co-evaporation of cadmium and sulfur, to form the cadmium sulfide compound on a substrate, is possibly an answer to the fractionation problem. Since cadmium sulfide cells have already been manufactured on metallized plastic, and since the same material will be used in the SPS arrays, it seems logical to expect that the cells could be manufactured as part of the array blankets in one continuous process. This could be done with a high degree of automation and, therefore, a minimum of manpower.

The deposited compound film is presently treated with a copper bearing solution to obtain efficient photovoltaic conversion. This results in an internal self-destruction mechanism and partly accounts for the efficiency degradation with time and humidity. The use of electronic ion implantation, instead of wet chemical activators, could eliminate this problem and is also naturally suited to the high vacuum environment of space.

Renewed interest in cadmium sulfide has been generated in this country and in Europe as a low-cost, large-area power source for consumer applications. At least one major U.S. petroleum company is sponsoring high-level development programs and research is in progress at various universities to understand the basic operation of the cell. No new breakthroughs in efficiency have been announced as of yet, but the researchers are optimistic about success.

Gallium arsenide is the most serious contender to displace silicon as the prime photovoltaic material in the future. Its advantages of higher efficiency, lower temperature sensitivity, and radiation hardness have been mentioned previously and are essential to the success of the SPS. Experimental solar cells of aluminum-gallium-arsenide have demonstrated efficiencies greater than the best production silicon cell.

While gallium arsenide has a number of advantages over silicon, it also has a number of significant disadvantages. It is a binary compound instead of a single element, and is therefore more difficult to process in large defect-free crystals. Like cadmium sulfide, gallium arsenide has been known for a long time, but the major development work on it has only been done since 1970. Since that time, the demand for it has grown substantially as digital readouts for electronic hand calculators and electronic wristwatches. These applications remain the single largest use for the material, and the growth is expected to continue unabated.

Gallium arsenide solar cells are not yet in production, but recent announcements by two companies are encouraging and at least a limited production line is expected within the next two years.

Polycrystalline silicon is also being studied as a material for producing large quantities of solar cells by automated processing and at low cost. The concept is based on depositing the semiconductor material on a continuous and inexpensive substrate. This technique would eliminate the energy and cost intensive processes which are presently used to fabricate thin solar cells of crystalline silicon.

Work on polycrystalline silicon solar cells has only been pursued actively since 1975, and the efforts to date have been devoted to understanding the fundamental operation of the device. However, efficiencies between 4 and 6% have been reported. As expected, a wide variety of problems confront polycrystalline silicon researchers and include high recombination losses, expansion coefficient mismatches, preferential doping at grain boundaries, and backside electrode connections.

The recombination loss at crystallite grain boundaries is the most critical parameter of a polycrystalline silicon solar cell. The belief is that if the crystallites can be made large enough, then the major portion of current flow will be vertically rather than horizontally, and efficiency will be preserved. Methods proposed for achieving this include melting and resolidification using electron beams or lasers.

The substrate is critical in a polycrystalline silicon solar cell because it affects the structure and composition of the film. Furthermore, depending on how the film is deposited, it must be capable of withstanding high temperatures. Thus far, steel, carbon, and sapphire have been used in experimental cells and aluminum has been proposed.

Thin crystalline films of silicon are routinely grown on synthetic sapphire by epitaxial deposition processes for the integrated circuit industry. The technique is successful because the crystal lattice spacing is very close to that of silicon and, therefore, large areas of relatively defect-free films can be formed. A similar process for gallium arsenide is not known to exist. Silicon has also been deposited in the amorphous state which does not have crystalline structure or crystallite boundaries. The expected efficiencies for such cells is as high as 10%. If the size of the crystallites is larger than the thickness of the solar cells, most of the electrical carriers can be collected without encountering grain boundaries. A method has been developed by Solarex which involves casting silicon so that large crystallites on the order of a millimeter are formed. Solarex has announced a cell made by this process with a 10% efficiency.

Since solar cell weight is an important factor in the design of the SPS arrays, it is worthwhile to analyze its effects in thin-film solar cells. Data has been shown previously that the minimum thickness for a crystalline silicon solar cell is 0.100 mm. In the case of silicon, the minimum weight has been reached. Even if a polycrystalline silicon

cell of equal efficiency could be produced, it would weigh more than its crystalline equivalent by the weight of the supporting substrate, assuming the silicon thickness was equal. Only gallium arsenide, whose minimum absorption thickness is less than silicon, has the potential for weight savings, and it is not as great as one might expect. Gallium arsenide has a specific gravity of 5.32 compared to silicon which is 2.34. Thus, a film of gallium arsenide cannot exceed 0.044 mm or it will weigh as much as silicon. Since only 0.005-0.010 mm are theoretically required, the difference in mass is all that is possible for the substrate. This significantly restricts the choice of substrate materials to lightweight materials.

(5) MATERIAL AVAILABILITY AND PROCESSING

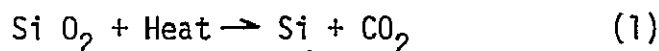
The solar array of each 5GW SPS will have a total area of approximately $71.7 \times 10^6 \text{m}^2$ of which half or $35.8 \times 10^6 \text{m}^2$ will be active. The large quantities of materials required raise questions concerning the availability of the materials required for an SPS, the required production manufacturing facilities, and cost. This section analyzes these questions for silicon, gallium arsenide, and cadmium sulfide.

(a) SILICON

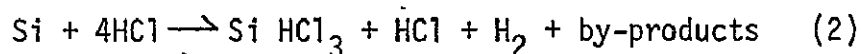
Silicon is derived from silica ores (sand), and thus there is an abundant supply of the element in the earth's crust. The steel industry uses over 90×10^3 metric tons of metallurgical grade silicon (98% pure) per year. Table IV.B.1.a.1 is a listing of the 1975 production of semiconductor grade silicon by the major U.S. and world manufacturers and shows that their output would have to be increased by more than an order of magnitude to be adequate just for finished cells. At present, their production output is used almost solely for electronic device fabrication.

[1] PRODUCTION OF HIGH PURITY SILICON

Silicon dioxide, in the form of silica ore, is mixed with carbon and heated in an arc furnace (Figure IV.B.1.a.11) to produce a metallurgical grade of silicon (99% Si). The reaction is described by the following reaction.



The metallurgical grade of silicon must be purified in order to obtain semiconductor grade material. The preferred method of obtaining high purity silicon involves converting silicon into trichlorosilane according to the following reaction:



In order to eliminate the by-products of the process and improve the purity, the trichlorosilane is distilled. Liquid

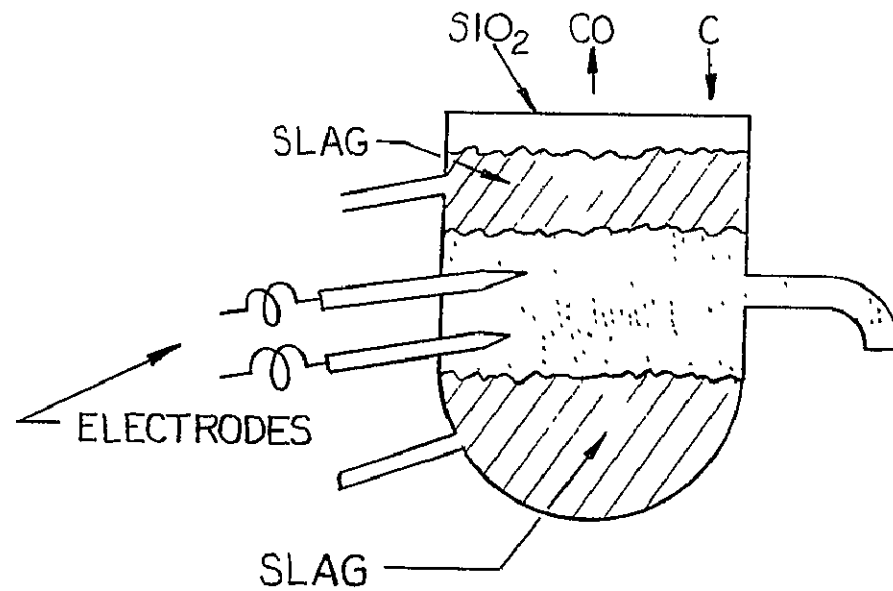
TABLE IV.B.a.1

ANNUAL PRODUCTION (1975) OF POLYCRYSTALLINE SILICON

<u>MANUFACTURERS</u>	<u>PRESENT PRODUCTION</u>	<u>MAXIMUM PRODUCTION</u>	<u>SURPLUS CAPABILITY</u>
DOW CORNING	330 TONS (1)		
MONSANTO	330 TONS	450 TONS	120 TONS
TEXAS INSTRUMENTS	330 TONS (1)		
WACKER (GERMANY)	563 TONS	UNKNOWN	
	<hr/>		
TOTAL	1153 TONS		

(1) EXPANSION PLANS WERE TERMINATED. WOULD HAVE ADDED AN ADDITIONAL 290 TONS EACH TO 1975 PRODUCTION. EXPANSION PLANS ARE EXPECTED TO BE REACTIVATED DURING 1978 - 1980 TIME FRAME.

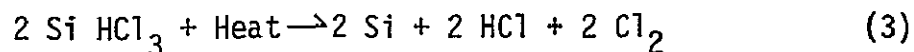
IV.B.1.a.19



REDUCTION SILICON
DIOXIDE

FIGURE IV.B.1.a.11

trichlorosilane is converted into solid polycrystalline semiconductor grade (99.999% Si) by a thermoelectric decomposition (Figure IV.B.1.a.12) process described by the following:



It should be noted that over 200 possible reactions exist for producing silicon material. Twenty of these are analyzed under contract to the ERDA (Energy Resource and Development Administration). Of this group, three appear to be the most promising and include the technique previously described.

[2] CRYSTAL GROWTH

Single crystal material is necessary to maximize the efficiency of silicon solar cells. Single crystal silicon ingots are grown from the high purity polysilicon. There are innumerable methods of growing single crystal silicon ingots of which many are simply modifications of each other. The most widely used method is the Czochralski method which uses a rotating crucible of molten silicon. A counter rotating crystal is dipped into the crucible and then slowly withdrawn from the molten liquid (Figure IV.B.1.a.13). The silicon adheres to the seed crystal and solidifies as the crystal is withdrawn from the melt. In this manner an ingot is "pulled" and retains the orientation of the seed.

Another method which is sometimes used to produce ingots is the float zone technique (Figure IV.B.1.a.14) which employs a long vertical polycrystalline cylinder of silicon. In this process a small section of the polycrystalline silicon cylinder is melted and allowed to solidify. A seed crystal is placed at the top of the melt, and an r-f induction coil is moved slowly from the top of the cylinder downwards to melt the silicon. As the melted section cools, it crystallizes in the orientation of the single crystal. This method has the advantage that there is no crucible in contact with the silicon, therefore less contamination and defects within the crystal. Because of this fact, zone refined silicon is more radiation resistant than Czochralski silicon. However, today's Czochralski crystal pullers produce large volumes of ingots with few defects and are the most commonly used method of growing silicon ingots. The crystal growing process produces a single crystal ingot up to 0.075 meters in diameter and more than one meter in length.

[3] WAFER FABRICATION

The silicon ingot is sliced perpendicular to its length near each end to form a cylindrical shape. A grinding operation is then used to eliminate the surface irregularities which resulted during the crystal growing operation. Next, the cylinder of

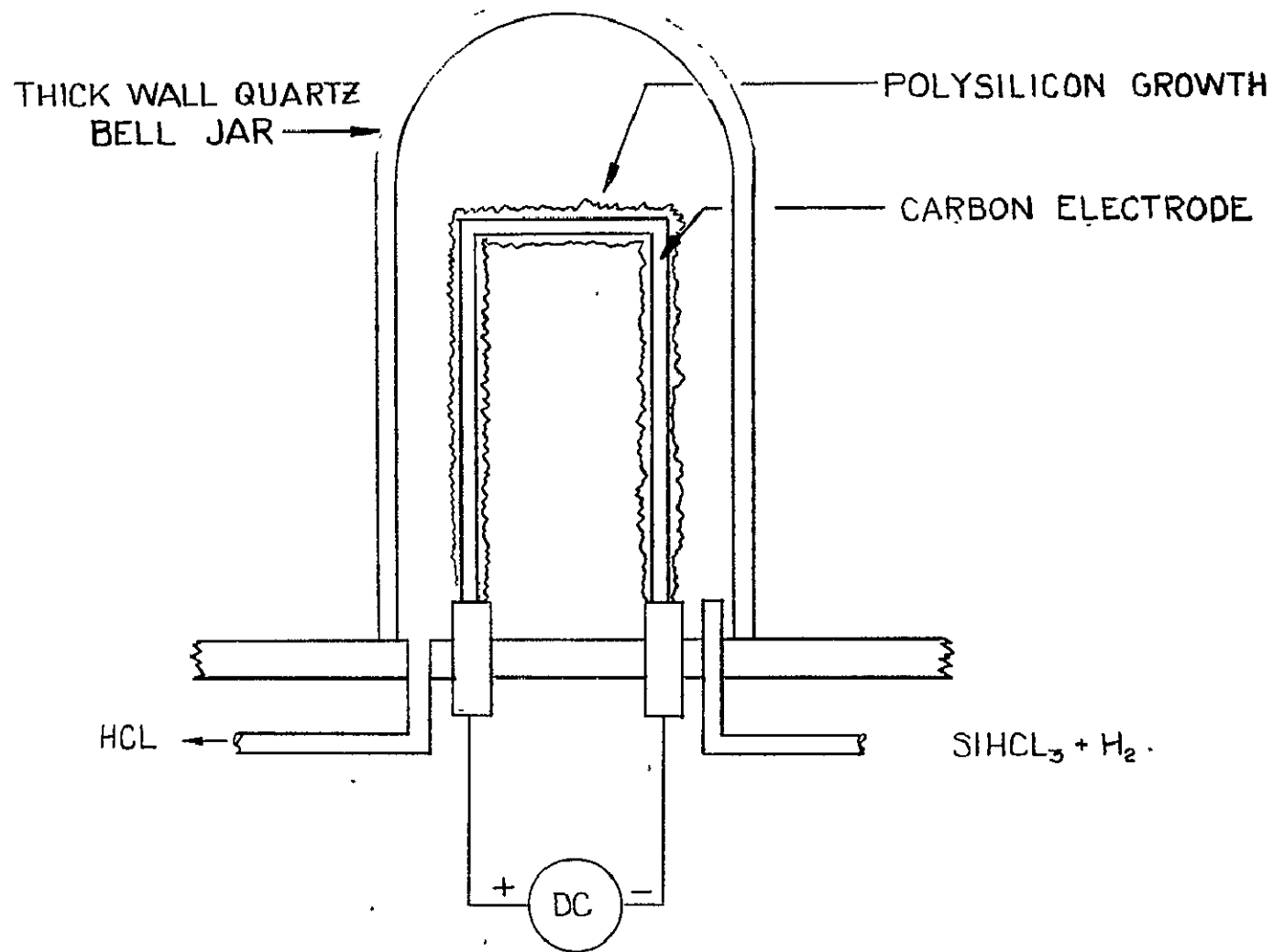
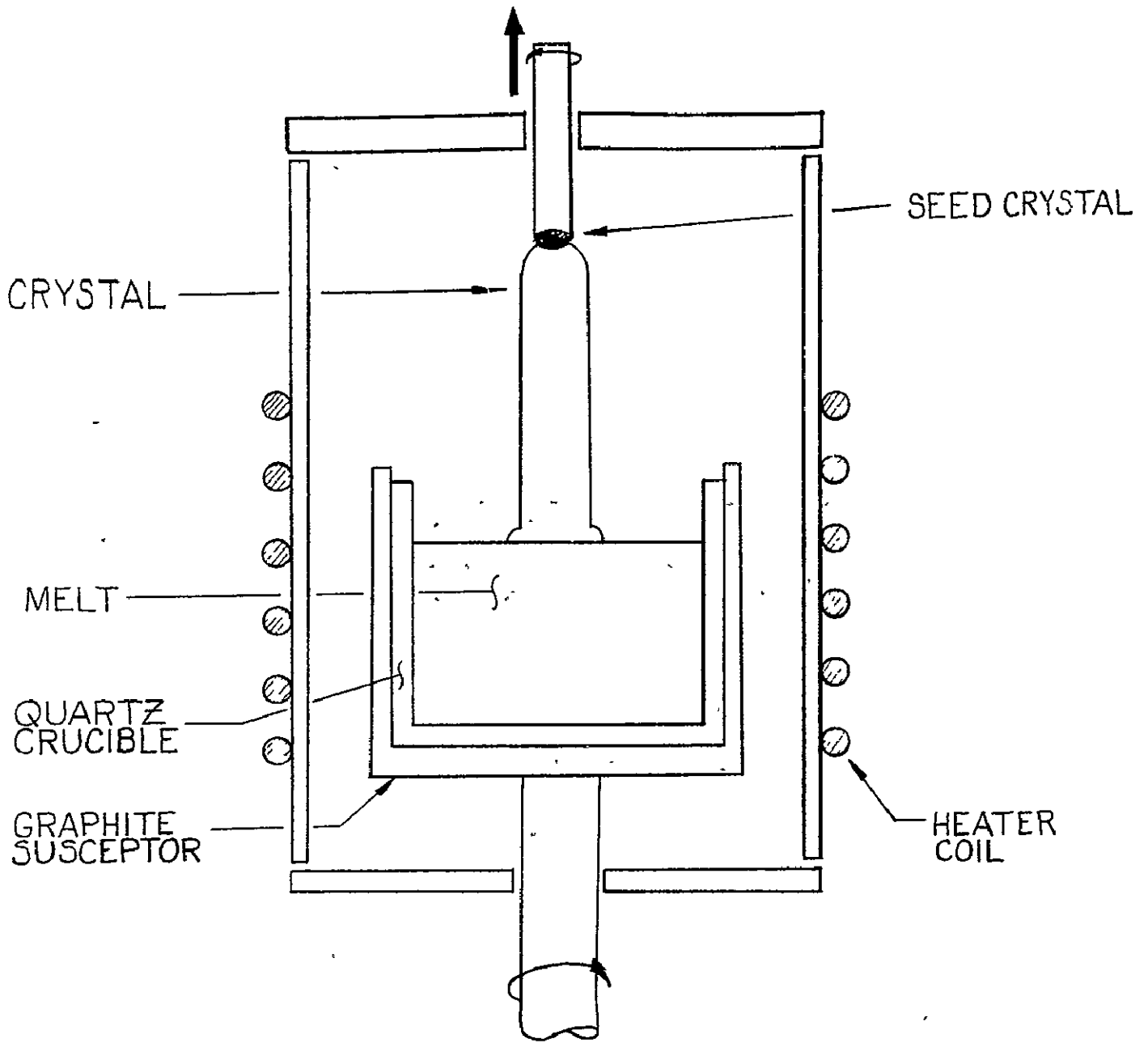


FIGURE IV.B.1.a.12- DECOMPOSITION OF TRICHLOROSILANE



CZOCHEKRALSKI METHOD

FIGURE IV.B.1.a.13

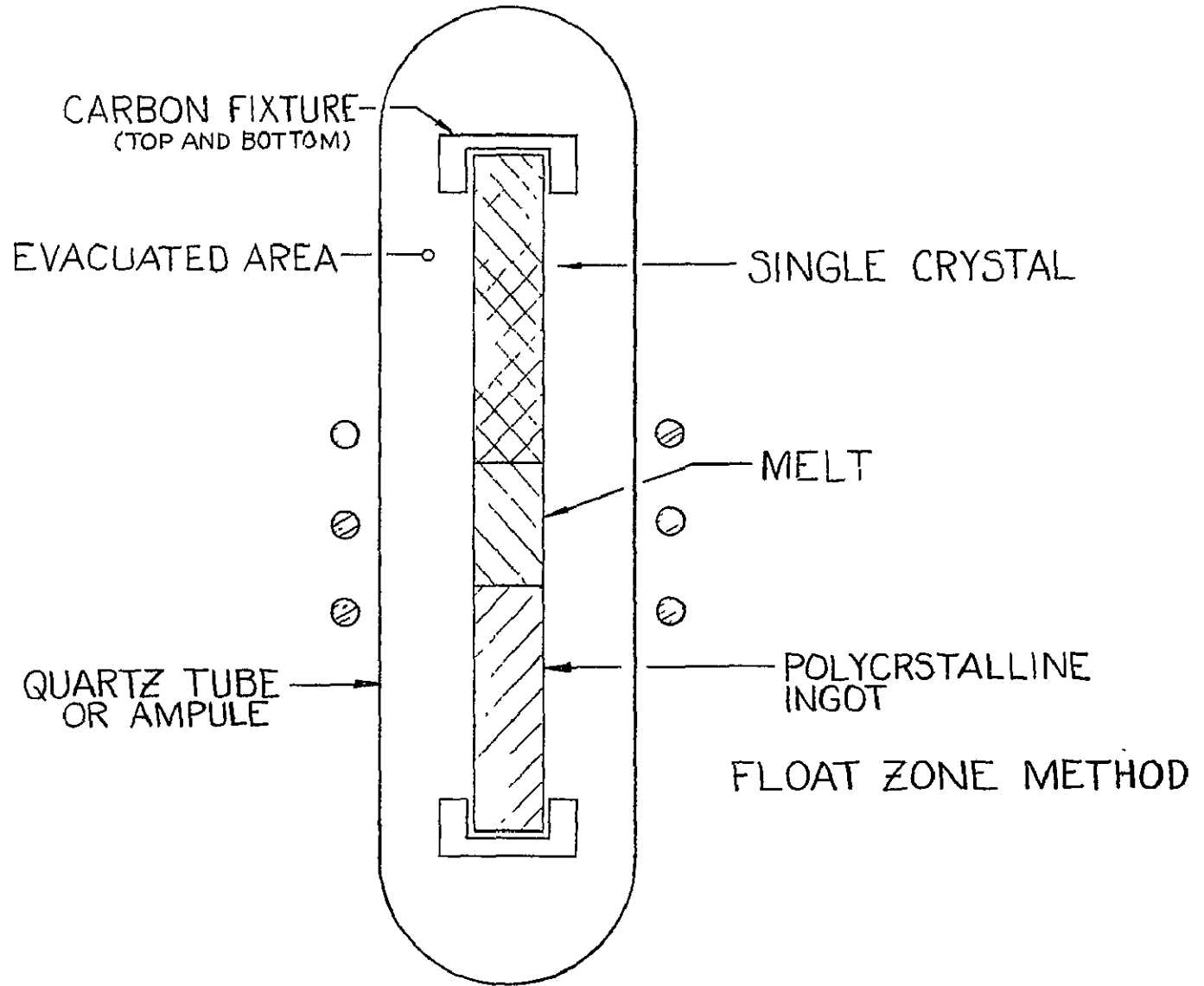


FIGURE IV.B.1.a.14 - FLOAT ZONE METHOD

silicon is sliced repeatedly with a centerless diamond saw to produce individual wafers (Figure IV.B.1.a.15). The saw kerf may be as much as 0.500 mm and is a function of the diameter of the wafer. The wafers are typically rough cut at 0.250 mm minimum to minimize breakage from saw vibrations. Handling losses require that the wafers from large diameter ingots be cut proportionally thicker. Thin wafers are obtained by lapping the 0.250 mm wafers down to the desired thickness. Because of these factors, the solar cell area per unit weight of silicon ingot does not increase by producing wafers thinner than 0.750 mm although thinner wafers are required to minimize the weight of the solar arrays of the satellite power system.

[4] SILICON LOSS/RECLAMATION

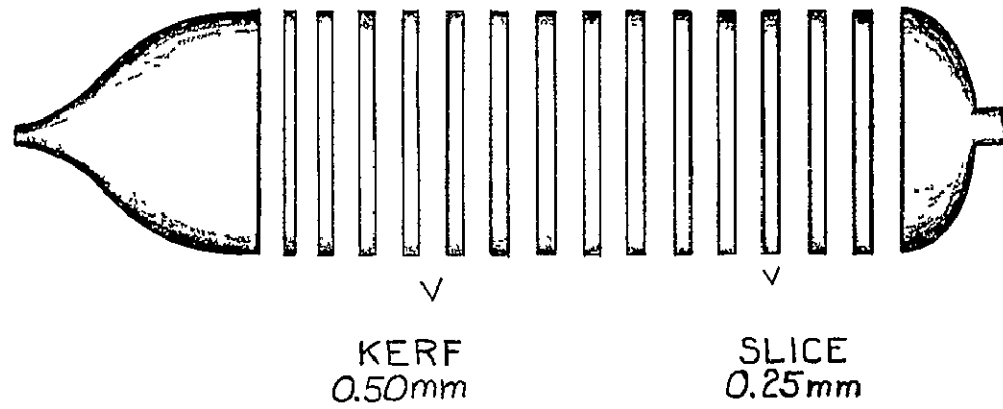
The end pieces of the silicon ingot which were cut off are reused since they represent a significant amount of pure material. Such is not the case with the dust from the sawing operation because its surface is quickly oxidized. Reclamation of the dust has not been economically feasible thus far but will be in the future. The kerf loss for a 0.500 mm saw cut amounts to 66 percent of the volume of the cylinder of silicon. Lapping and polishing the wafers down to 0.100 mm results in the loss of another 20 percent of volume. When the rectangular cells are fabricated from round wafers, a further decrease in volume from edge loss is another factor. Figure IV.B.1.a.16 shows that 30 percent of each wafer, which will be diced onto 20 mm x 20 mm solar cell blanks, is lost because of this reason. This further reduces the maximum useful volume of an ingot to only 9.3 percent. To this must be added additional unrecoverable losses from handling, testing, etc. A complete listing of the ingot losses is shown in Table IV.B.1.a.2. It is clear that while the ingot process can produce excellent quality wafers, in its present state-of-the-art it is not amenable to the low-cost, high-volume production of silicon necessary for the SPS.

(b) SILICON SHEETS

There has been a considerable effort to develop methods of growing silicon in thin sheets. The advantage of such a method would be the elimination of sawing, lapping, and polishing operations which are necessary for the silicon blanks. The process could be a continuous flow, and it has been estimated that a cost reduction of 10 to 100 times could be realized if it is successful.

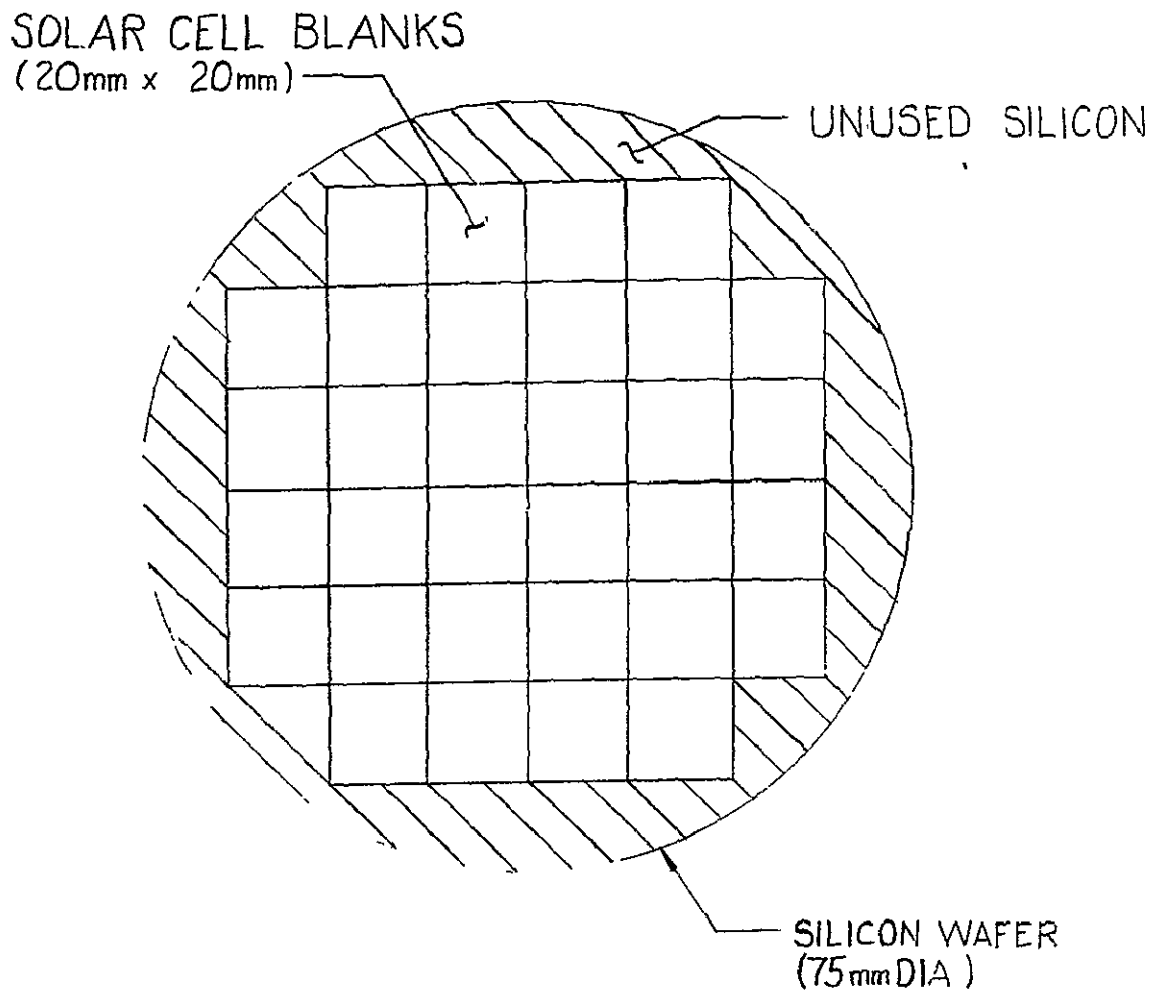
One of the oldest sheet growth processes is the dendritic web technique (Figure IV.B.1.a.17). In this method, a molten film of silicon is pulled from the melt by being suspended between two dendrites. So far, this method has produced a better crystal structure with fewer defects than other silicon sheet processes. However, its growth rate is slower than the EFG (edge-defined film-fed growth) described below and the webs are somewhat thicker.

INGOT SLICING LOSS



IV.B.1.a.25

FIGURE IV.B.1.a.15



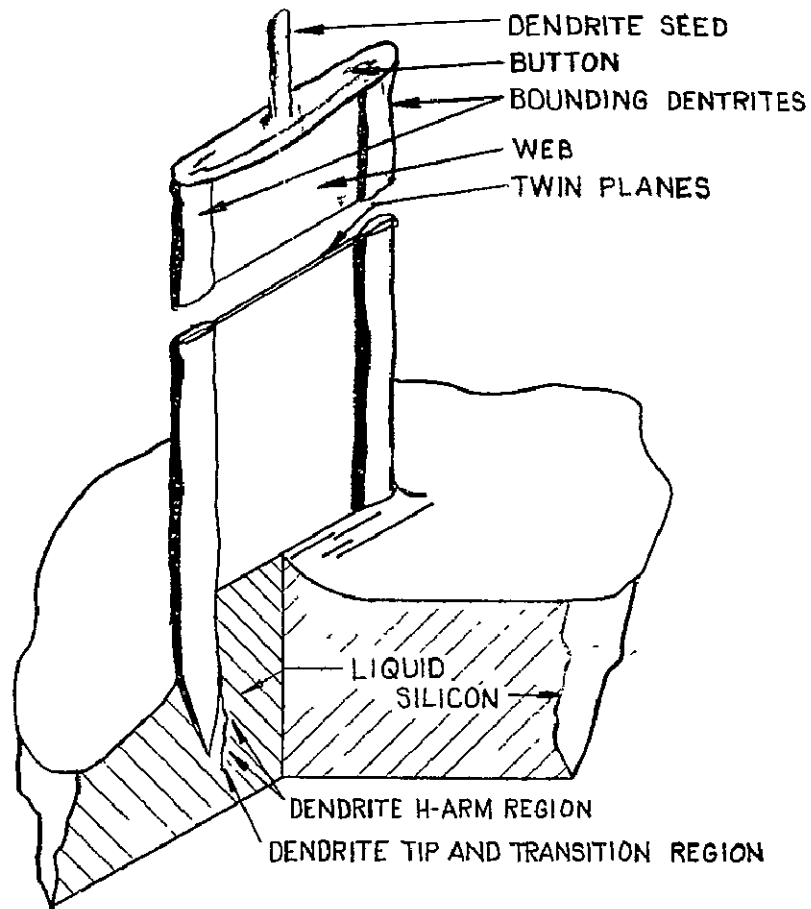
SOLAR CELL BLANKS FROM SILICON WAFER

FIGURE IV.B.1.a.16

TABLE IV.B.1.a.2

INGOT LOSSES BY VOLUME

<u>OPERATION</u>	<u>INGOT LOSS (%)</u>
SAWING	66
LAPPING	16
POLISHING	4
DICING	4.7
BREAKAGE	1.3
	<hr/>
	92%



DENDRITIC WEB GROWTH

FIGURE IV.B.1.a.17

The EFG employs drawing (Figure IV.B.1.a.18) a ribbon of silicon through a carbon die which is fed by capillary action. The problem with the EFG method is that molten silicon which reacts with almost all substances combines with the die material. Carbon has been the most successful material used to date. However, even with it, the surface of the ribbons has pieces of silicon carbide imbedded in it. Also, there are numerous lattice defects in the crystal's surface and the general problem of twinning.

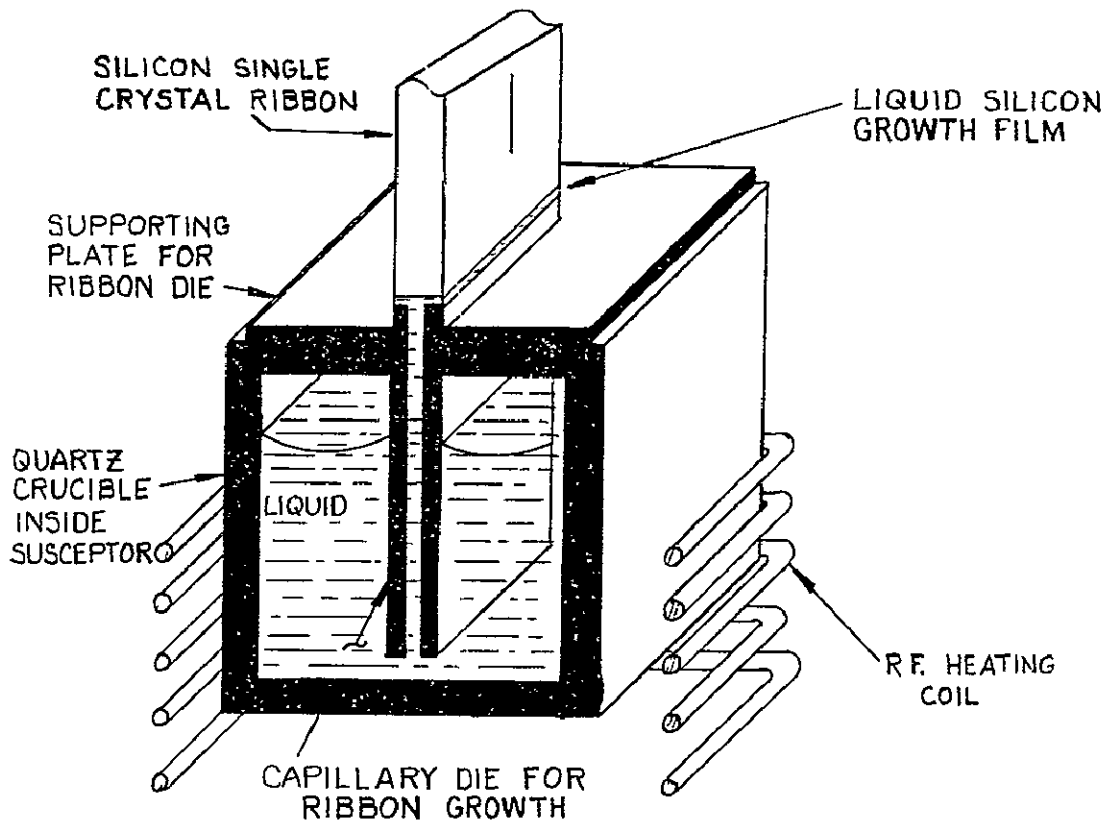
Several other methods of fabricating silicon sheets are being studied under ERDA/JPL contracts. One such method involves producing silicon on a (Figure IV.B.1.a.19) molten layer of tin similar to the process which is used to produce plate glass. Another technique being investigated is dipping (Figure IV.B.1.a.20) in which a carbon coated ceramic sheet is dipped into molten silicon and then withdrawn. The resulting sheet is hoped to have a single crystalline layer of silicon on its surface. Another proposed method of forming silicon sheets involves forming a silicon plate between two rollers (Figure IV.B.1.a.21). The thick slab of silicon is heated to its elastic temperature as it is squeezed between the rollers into a thin sheet. It is doubtful that the resultant material will be a single crystal which is necessary for high efficiency solar cells. It is also believed to suffer from similar reaction problems as the EFG technique.

(c) GALLIUM ARSENIDE

While the earth's crust contains an abundant supply of gallium (15 ppm), gallium does not occur in concentrated quantities but as a trace element in ores of Al, Zn, Cu, and coal. At present gallium is obtained from bauxite which has an average concentration of 50 ppm as a by-product in the production of aluminum. The recovery process is inefficient and yields 1 percent of the gallium present. Present estimates indicate that the process can be improved to recover as much as 30 percent of the gallium present. Improvement of the process will increase initially the cost of gallium from a recent price of \$600/kg.

Mineral producers regard the production statistics of gallium as proprietary data and therefore production data is estimated (Table IV.B.1.a.3). Current estimates place the U.S. production of gallium in excess of one ton and world production at more than 12 tons. With the increased usage and expanding market in GaAs light emitting diodes, the production and consumption are continually increasing. From the known reserves of bauxite, the U.S. reserves of gallium are estimated to be from 2,700 to 8,400 tons, and the world reserves are 115,000 tons.

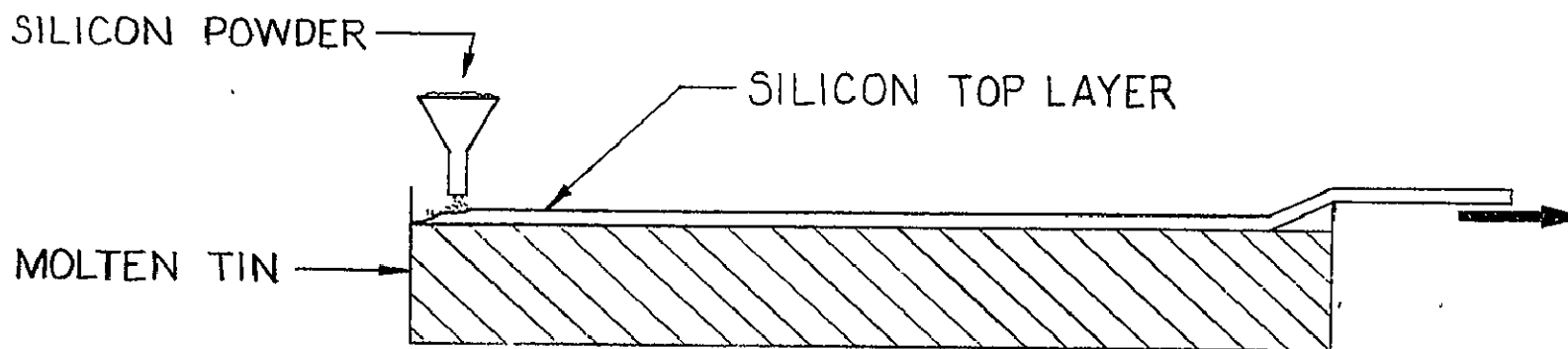
Therefore, a more precise estimate of the gallium required for a GaAs solar cell array will require sufficient research and development to define an acceptable GaAs cell. The preliminary



EDGE-DEFINED, FILM-FED GROWTH
 (EFG) OF SILICON RIBBON

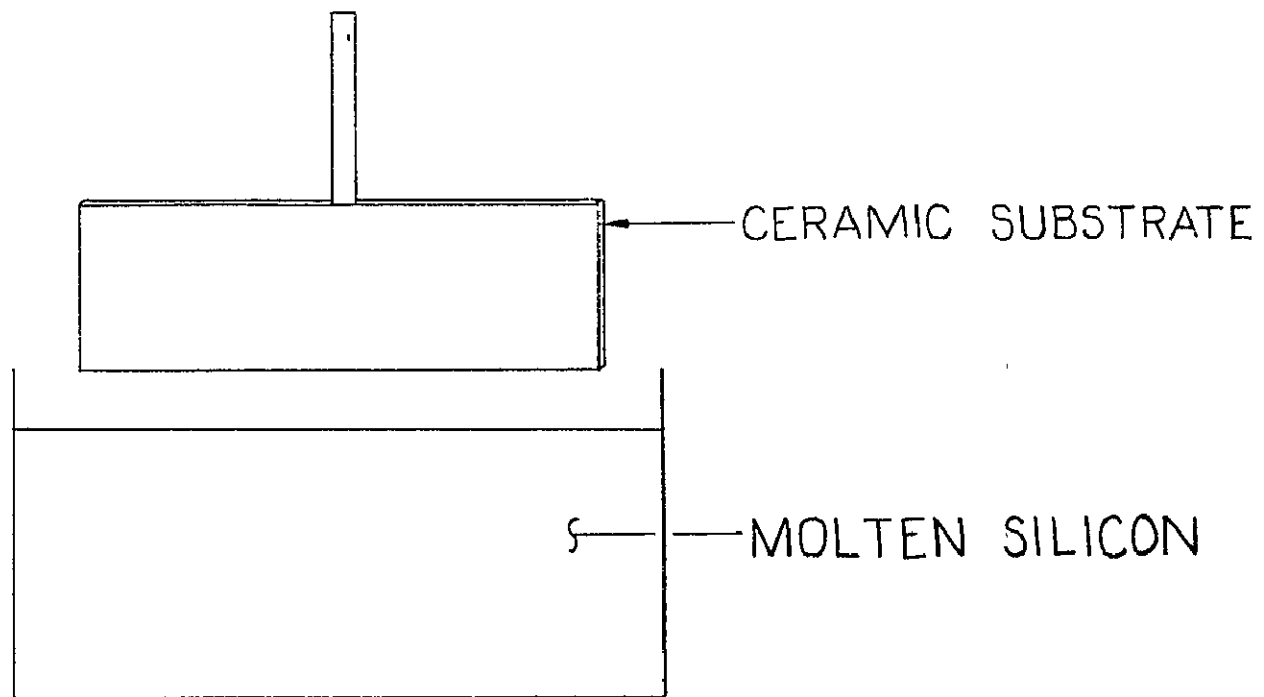
FIGURE IV.B.1.a.18

IV.B.1.a.31



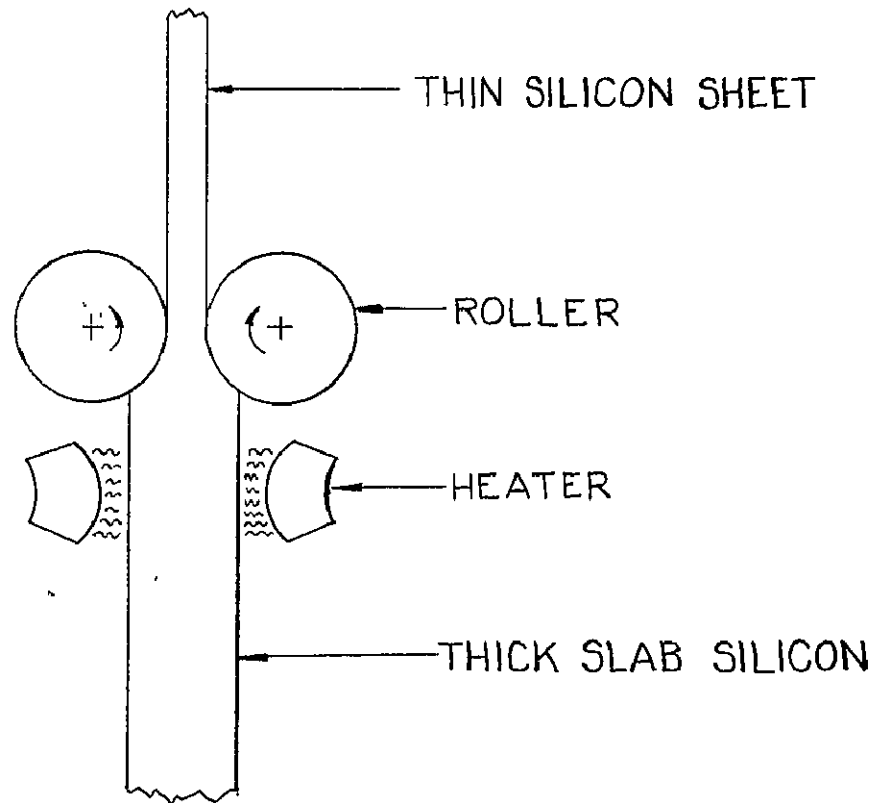
FLOATING SUBSTRATE

FIGURE IV.B.1.a.19



DIPPING PROCESS

FIGURE IV.B.1.a.20



ROLLING SILICON INTO A THIN SHEET

FIGURE IV.B.1.a.21

TABLE IV.B.1.a.3

GALLIUM ARSENIDE MATERIAL AVAILABILITY IN METRIC TONS

<u>MATERIAL</u>	<u>IMPORTED</u>	<u>DOMESTIC</u>
GALLIUM	6.08 (1972)	(UNKNOWN)
ARSENIC	605 (1972)	(UNKNOWN)
GALLIUM ARSENIDE	(UNKNOWN)	15 (1975)

AMOUNT OF GALLIUM ARSENIDE REQUIRED FOR ONE SPS ARRAY - 23,900 TONS

IV. B. 1. a. 34

results (Figure IV.B.1.a.22) indicate that a very high concentration ratio is desirable, and a substrate other than GaAs is needed. Also, further research is needed in the recovery of gallium.

The technology of gallium arsenide is not as well developed as silicon. Some of the immediate areas which must be explored are (1) methods of extracting large quantities of gallium from bauxite, (2) reducing the cost of gallium, (3) elimination of the gallium arsenide substrate, and (4) the development of concentrators for the use in space with ratios greater than 10.

Arsenic is a by-product from processing metal based ores such as copper, lead, and iron. Roasting the ores produces volatile oxides which are collected as flue dusts. The flue dusts are purified to obtain white arsenic (As_2O_3) or reduced with carbon to yield arsenic metal. In general, these processes are well developed and, for the most part, arsenic is considered a troublesome by-product.

Arsenic production consists of approximately 97 percent white arsenic and 3 percent metallic oxide. The U.S. imports approximately 16,000 tons of (Figure IV.B.1.a.23) white arsenic and 600 tons of metallic arsenic. The price of white arsenic fluctuates from \$2 to \$4 per kg (1972).

The availability of arsenic or refining it does not appear as a significant problem for the SPS. At most, facilities will have to be increased to reduce white arsenic to arsenic metal. Gallium will be the key element in fabricating GaAs solar cells.

The availability of gallium arsenide solar cells for the SPS arrays is as dependent on the availability of large scale raw material processing facilities and techniques as much as it is on the basic elements to make the compound. At present, vast sums are being spent each year by the ERDA to improve the supply of device-grade silicon and to lower its price. These improvements are being made in a material technology that is already mature and has more than two decades of manufacturing experience behind it. It also has a number of vendors who are producing it in large quantities now, and have a capability to expand their operations in the future.

With respect to the control of surface states and bulk impurities, gallium arsenide has not been developed to the level of silicon technology. Many researchers believe that the recent developments in epitaxial methods of growing heterojunctions in semiconductors will lead to gallium arsenide devices which are superior to silicon devices.

The SPS array requirements could be enough of a special need to justify such an independent effort because of the weight

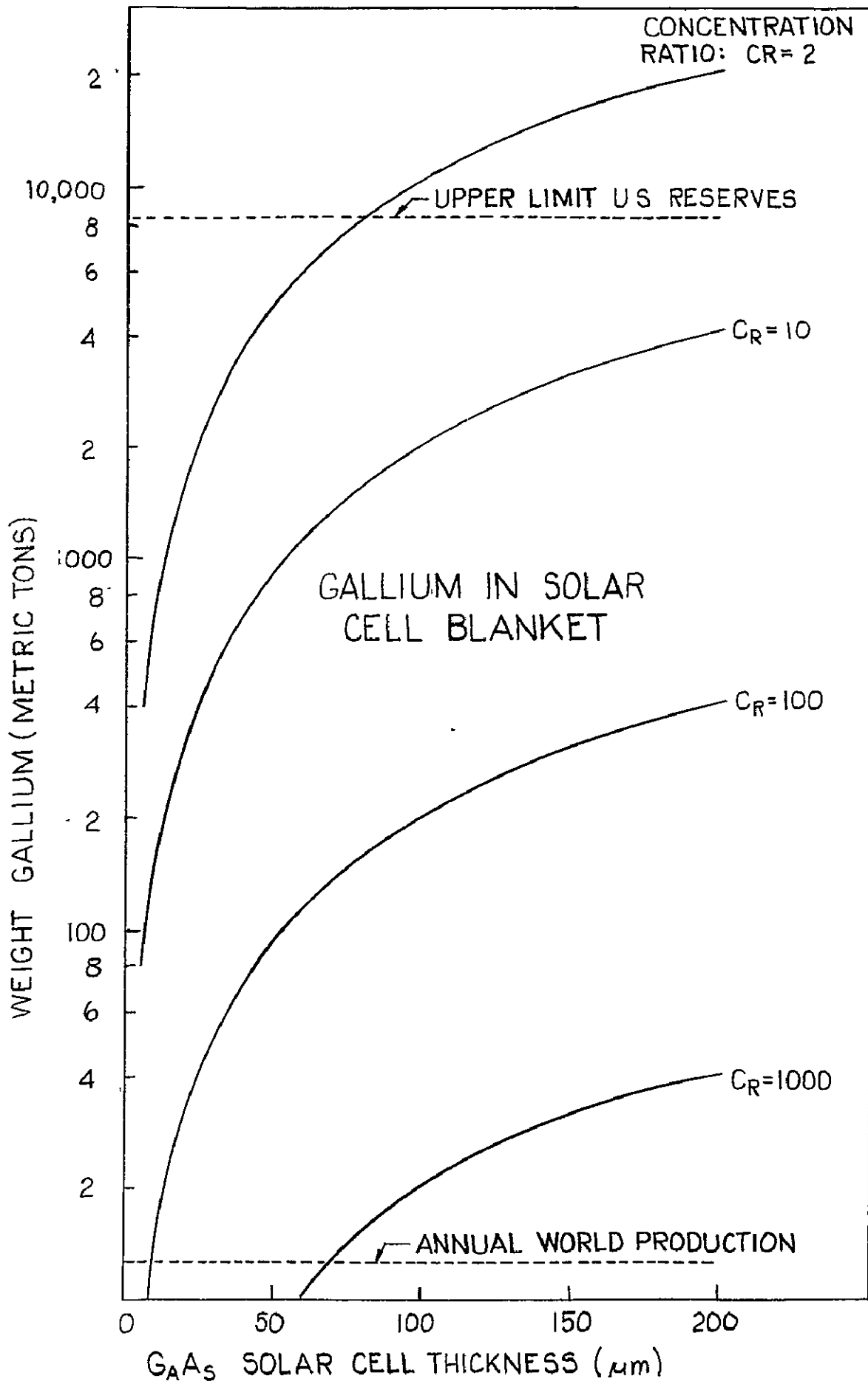


FIGURE IV.B.1.a.22

IV.B.1.a.37

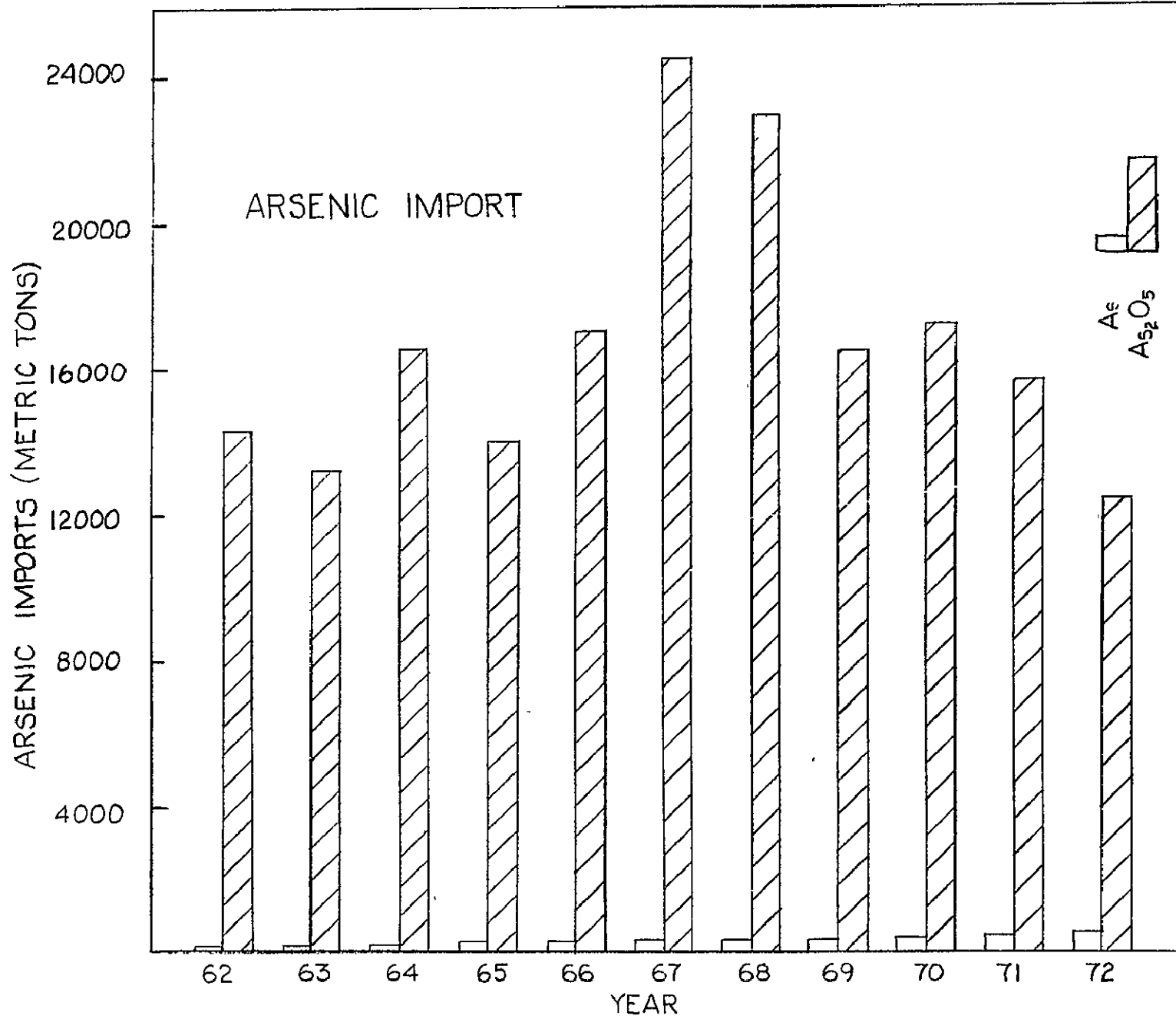


FIGURE IV.B.1.a.23

criticality. It should be realized, however, that much more than a comparable amount of funding would be required for gallium arsenide than for silicon because, by comparison, the former is not nearly as advanced in technology. Though similar as far as its operation in a solar cell is concerned, gallium arsenide has entirely different properties and requires unique manufacturing techniques. At present, the only significant manufacturing capability in gallium arsenide exists in one U.S. company. Expanding this effort into a dedicated large-scale production would put industry on a new learning curve that would invariably cause major problems. Furthermore, the time in which to accomplish this mammoth feat, for the quantity of cells that would be required, is extremely short. For silicon, however, it would mean only that the companies who are presently manufacturing integrated circuits would expand their already familiar operations to include solar cells.

The cost of gallium arsenide solar cells will never be as low as silicon because of the reasons already stated. However, the cost would not have to be the same to be competitive from a system performance point of view. A reduction in system weight could be an important factor in offsetting the higher initial cost of the cells. The same can also be said concerning minimizing radiation degradation and increasing life in orbit. Too much uncertainty exists at this time to predict what the break-point in cell cost would have to be to make the use of gallium arsenide cells feasible in the SPS arrays.

(d) CADMIUM SULFIDE

A 5 GW SPS solar array fabricated with 0.025 mm cadmium sulfide solar cells which have a 7.11 percent efficiency at 373 K would require an active area of $51.1 \times 10^6 \text{ m}^2$. Since the specific gravity of cadmium sulfide is 4.84, the array would contain 6286 tons of cadmium sulfide. This corresponds to 4903 tons of cadmium and 1383 tons of sulfur. During 1972, 3640 tons of cadmium and over 7×10^6 tons of sulfur were produced in the U.S. While there is an ample supply of sulfur, the production of cadmium would have to be increased. The estimated U.S. reserves of cadmium are 2×10^5 tons.

(6) SOLAR CELL FABRICATION

In principle, a silicon solar cell is merely a p-n junction diode. The junction gives rise to a potential barrier, and the associated electric field separates the hole-electron pairs, which are generated by incident photon radiation, into a unidirectional electrical current. For silicon, the semiconductor bandgap is 1.1 electron volts. However, the effective potential difference across the junction barrier is 0.55-0.60 volts. P-N junctions are formed by diffusing a n-type dopant into a silicon wafer that has been doped uniformly with p-type dopants. The conventional silicon solar cell is fabricated by taking a p-type solar cell blank and diffusing phosphorous

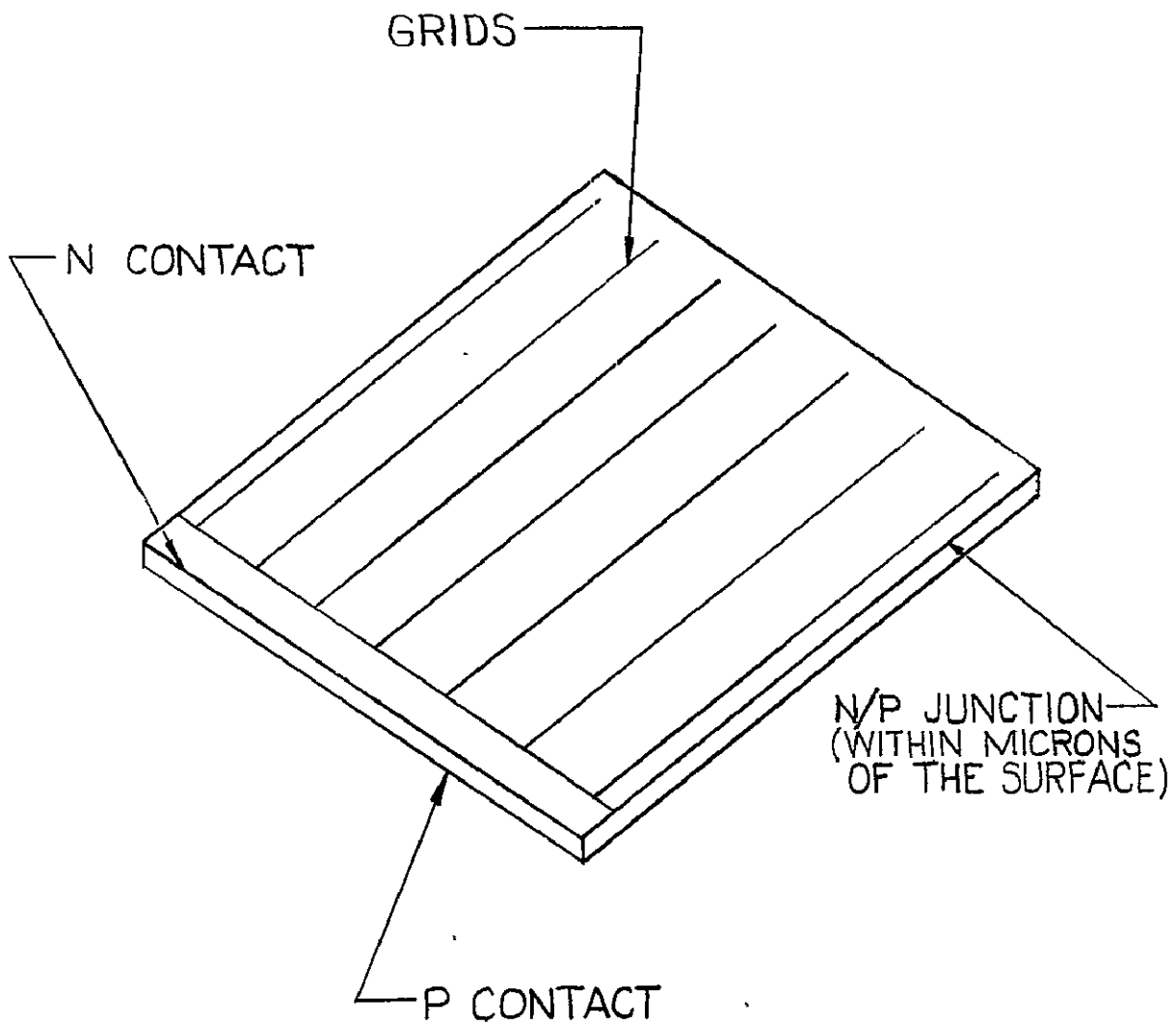
into its upper surface from 150 nm to 300 nm deep. The process involves the use of special furnaces which operate around 1273K and take about one hour.

(a) ELECTRICAL CONNECTIONS/ANTIREFLECTION COATINGS:

Electrical connections are formed on a solar cell by depositing various metals on the front and backside. A comb or tree pattern is placed on the surface (Figure IV.B.1.a.24), and the backside is completely covered unless wraparound electrodes are used. The metal coatings are sintered onto the silicon to minimize the contact resistance and improve adhesion. A common metallization system uses a titanium, platinum, and silver combination for the grid electrodes. The back surface is coated with the same metallization or another metal such as aluminum or a combination of nickel and copper.

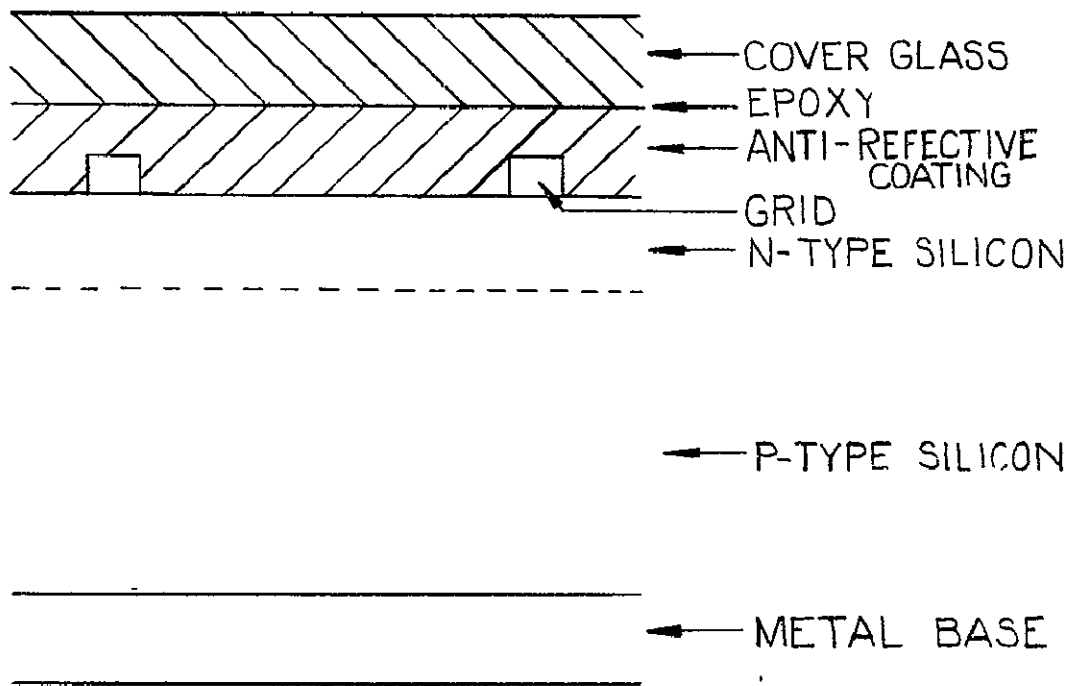
Antireflective coatings of Ta_2O_5 or SiO_2 are applied by vacuum deposition and are necessary to maintain the efficiency of the cell. Polished silicon normally reflects as much as 30 percent of the light which strikes its surface, and the coating reduces this to about 5-10 percent. More effective light energy capture methods have been developed in the laboratory and can reduce the reflection to almost zero. However, these techniques involve wet chemical techniques. A high-quality cover glass is usually cemented to the (Figure IV.B.1.a.25) top surface of the cell to provide protection from proton and electron radiation.

The violet cell is very similar to the conventional cell and differs mainly by having a shallower N-P junction (150 nm versus 300 nm) and an antireflective coating of Ta_2O_5 (Figure IV.B.1.a.26). The antireflective coating of a violet cell is thinner than that of the conventional cell so that it will be more responsive in the ultraviolet or blue region of the solar spectrum. The solar cell design used on the SPS will probably correspond to the violet cell. Its efficiency at present is approximately 14 percent and is projected to be 16 percent or better in the future. This cell is also being space qualified, whereas many of the other special cells are still in the laboratory stage of development.



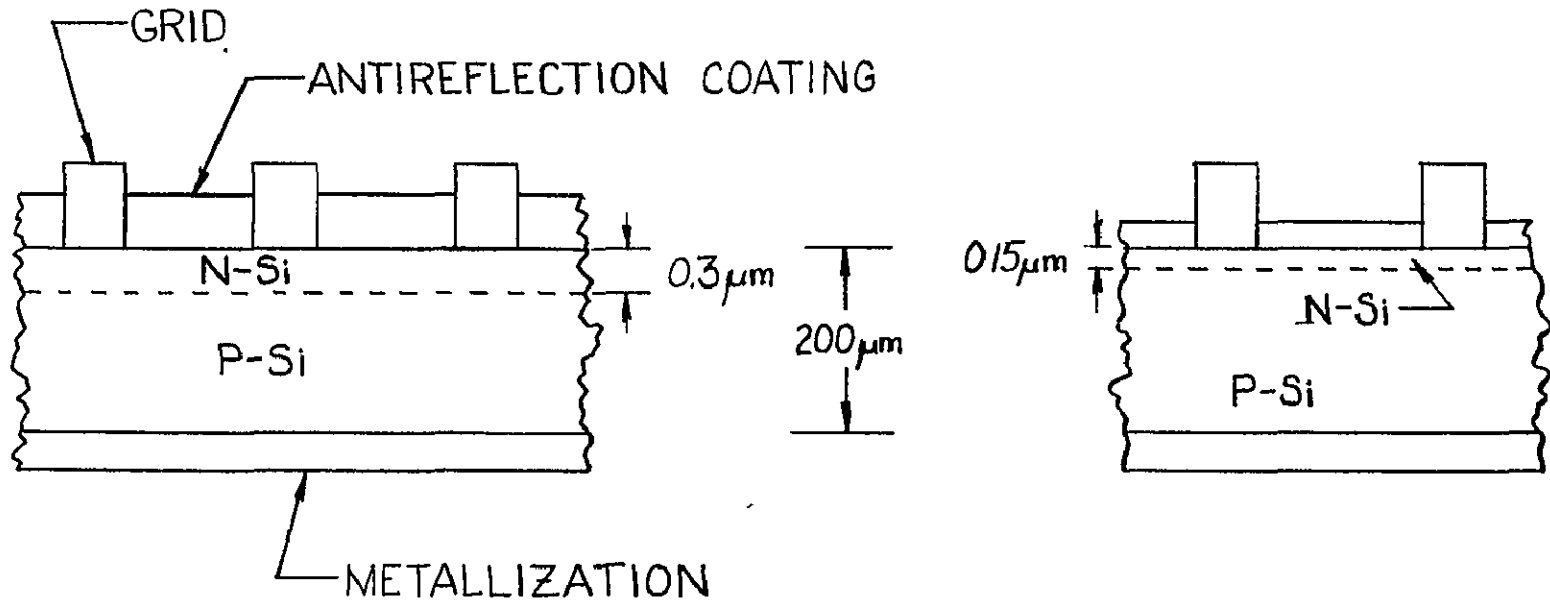
TYPICAL SOLAR CELL

FIGURE IV.B.1.a.24



SILICON SOLAR CELL

FIGURE IV.B.1.a.25



CONVENTIONAL CELL

VIOLET CELL

SOLAR CELLS

FIGURE IV.B.1.a.26

BIBLIOGRAPHY

1. Hovel, Harold J., Solar Cells, Academic Press, New York, 1975
2. Conference Record of the Eleventh IEEE Photovoltaic Specialists Conference, May 6-8, 1975, Institute of Electrical and Electronics Engineers, Inc.
3. Conference Record of the Tenth IEEE Photovoltaic Specialists Conference, November 13-15, 1973, Institute of Electrical and Electronics Engineers, Inc.
4. Proceedings of the First ERDA Semiannual Solar Photovoltaic Conversion Program Conference, July 22-25, 1975, Jet Propulsion Laboratory
5. European Cooperation Space Environment Committee, Solar Cells, Gordon and Breach Science Publishers, New York, 1971
6. Wysocki, Joseph J. and Paul Rapport, "Effect of Temperature on Photovoltaic Solar Energy Conversion," J. Applied Physics 31, pp. 571-578, March 1960
7. Loferski, J. J. and J. J. Wysocki, "Spectral Response of Photovoltaic Cells," RCA Review 22, pp. 38-56, March 1961.
8. Rapport, Paul, "The Photovoltaic Effect and Its Utilization," RCA Review 20, pp. 373-397, September 1959.
9. Terman, L. M., "Spectral Response of Solar Cell Structures," Solid State Electronics 2, pp. 1-7, 1961.
10. "Solar Electromagnetic Radiation", NASA SP-8005, Federal Scientific and Technical Information, Springfield, VA.
11. Thekaekzra, M. P., "Solar Energy Outside the Earth's Atmosphere," Solar Energy 14, pp. 109-127, (1973)
12. Kondrat'ev, K. Ya, Ed., Radiation Characteristics of the Atmosphere and the Earth's Surface, pp. 248-328, NASA TT F-678 (TT71-58003), Gidrometeorologicheskoe Press, Leningrad, 1969.
13. Bureau of Mines, Minerals Year Book, 1972, Volume 1, U. S. Government Printing Office
14. Gooch, C. H., Ed., Gallium Arsenide Lasers, "The Preparation and Properties of Gallium Arsenide" by M. C. Rowland, pp. 133-192, John Wiley & Sons

IV-B-1b. Solar Cell Blankets and Concentrators - James L. Cioni
Propulsion and Power Div.
Concept Derivation

In deriving a reference configuration for the photovoltaic blankets and the concentrators, two basic approaches were employed. First, a series of parametric analyses were performed to determine the sensitivity of the system to configuration and basic device performance characteristics. Second, an assessment was made to determine what levels of technological achievement are necessary or probable between now and the 1990's time frame of the subject SPS. Among the set of parametric analyses first performed were analyses dealing with temperature and relative performance associated with various levels of solar concentration. From these relative performance results, a configuration was established for which sizing and performance analyses could be performed.

In establishing the final reference system for the study, the driving guideline was to minimize the impact on total system cost. To arrive at such a point the system analyses had to be iterated several times since the relative contributions to cost from (a) hardware development and manufacturing cost, (b) transportation cost associated with weight and volume of the hardware, and (c) operations and maintenance costs were unknown.

In arriving at the system parameters (weight, performance, and cost) an attempt was made to choose levels of achievement that are within the realm of reason, though significantly advanced in today's content. Thus, in any specific area it might be possible to predict higher potential for achievement.

Parametric Performance

Past experience in photovoltaics leads to the assumption that there are two potentially viable candidate photovoltaic devices to use in a concentrated solar array. The two, silicon and gallium arsenide solar cells, have potential for high efficiency and long life on an orbital station. The first step was to make relative comparisons of these two types of solar arrays. Figures IV-B-1a-1, 2, 3 show the relative characteristics derived in the study to compare and contrast Si and GaAs arrays. The derivation of the figures is based on the following assumptions:

1. GaAs and Si solar cell blankets behave the same thermally; i.e., for a given concentration ratio the equilibrium temperature will be the same.
2. The basic blanket mass per unit area for each type cell would be the same and the blankets would be of the same construction type.
3. High volume production Si cells will be less efficient than GaAs cells under the same production levels. (Si = 16% GaAs = 20%).

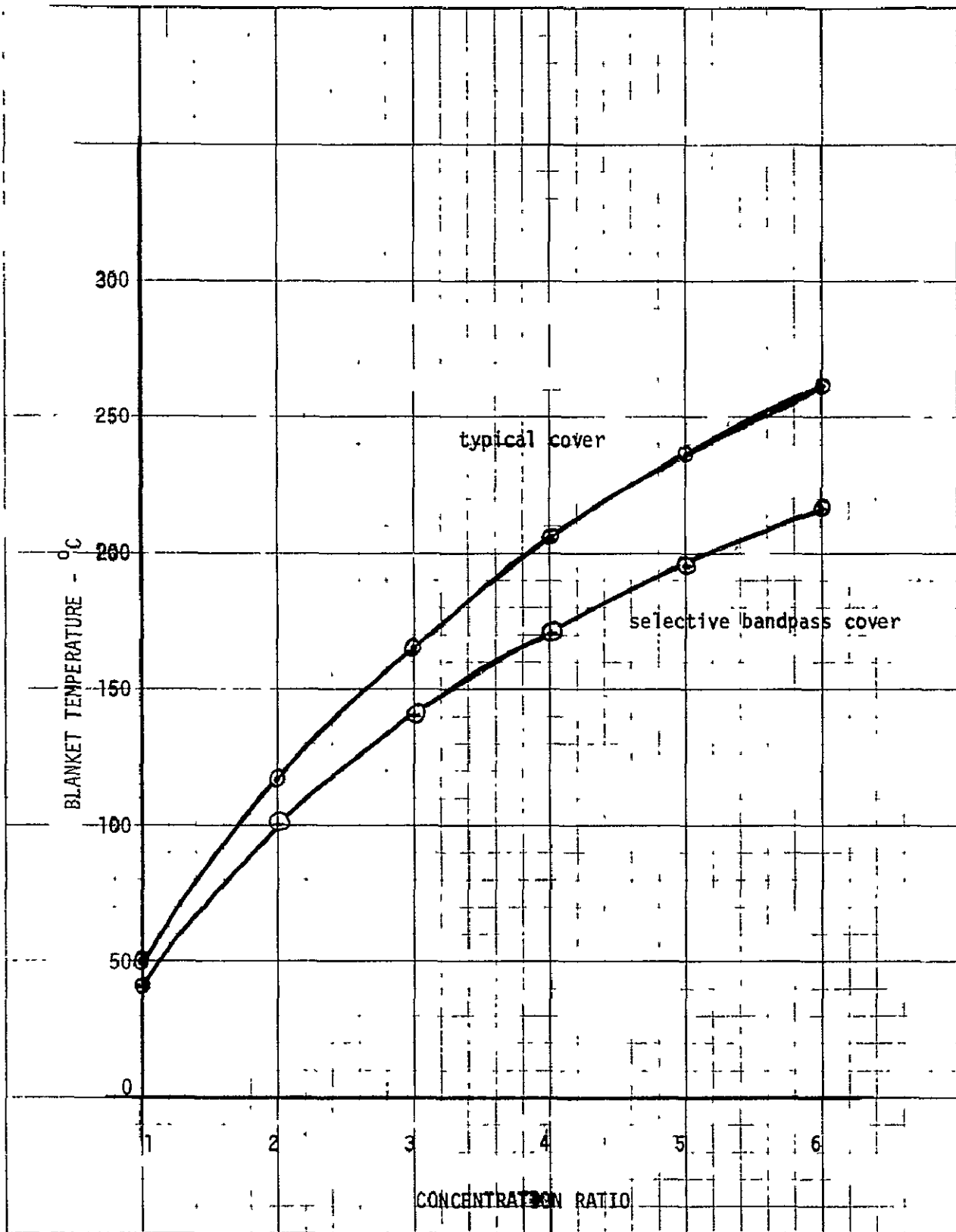


FIGURE IV-B-1b-1. SOLAR BLANKET TEMPERATURE VS. CONCENTRATION RATIO
IV-B-1b-2

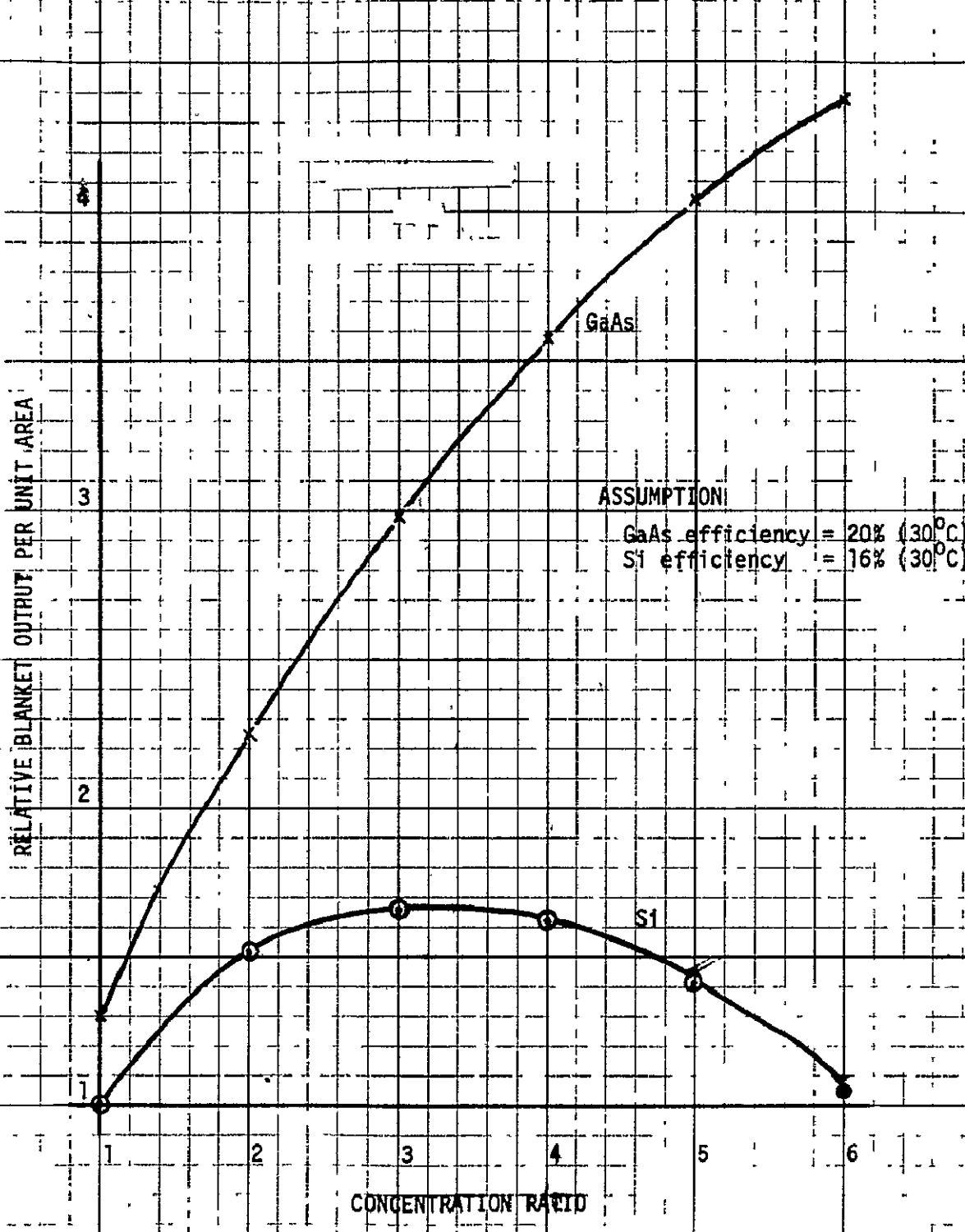
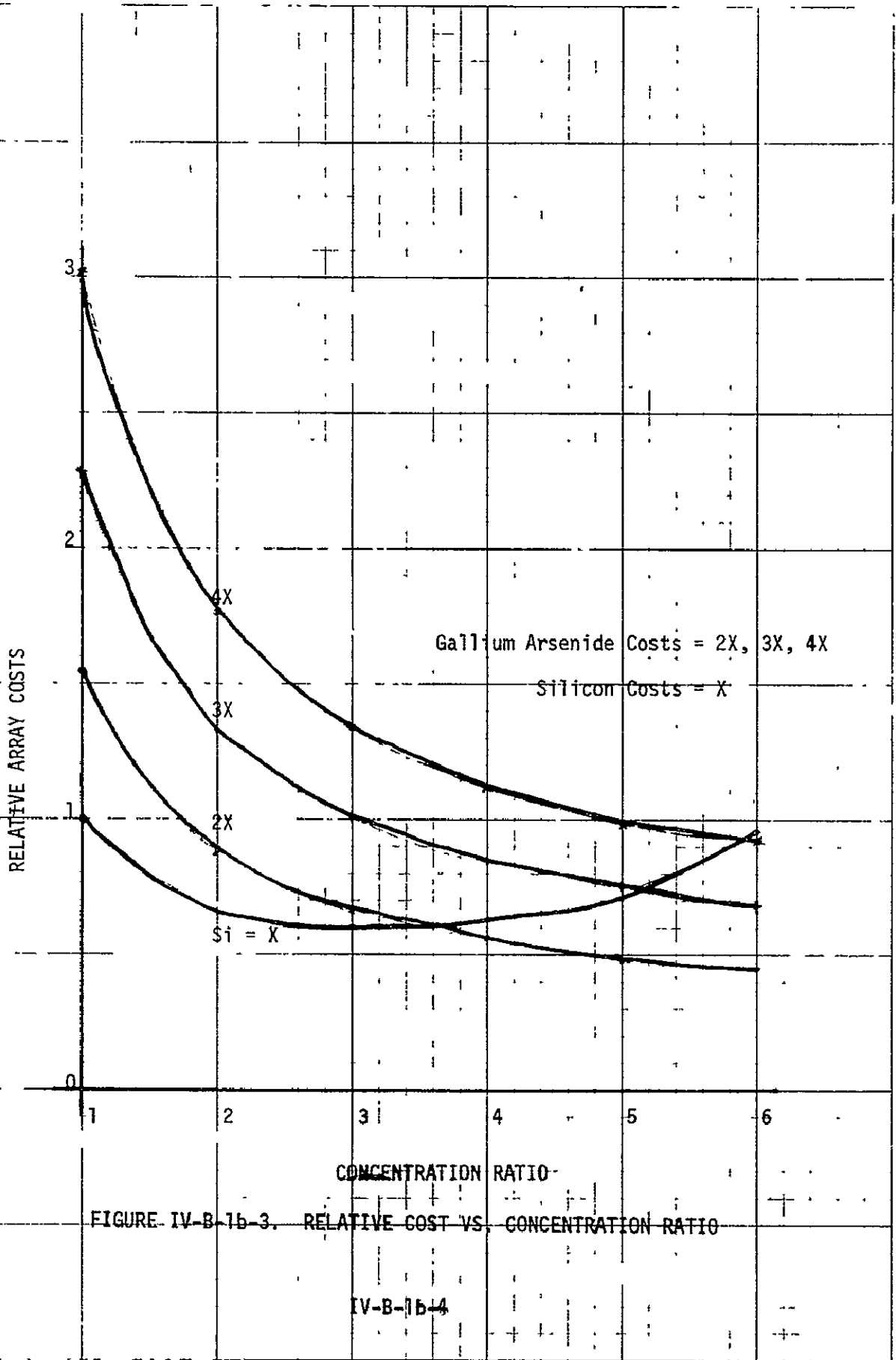


FIGURE IV-B-1b-2. RELATIVE BLANKET OUTPUT PER UNIT AREA
 VS. CONCENTRATION RATIO

IV-B-1b-3



4. GaAs cells are less sensitive to reduction in performance due to increased temperature (.45%/°C,Si and .25%/°C,GaAs).

5. The ultimate minimum cost for GaAs solar cells is significantly greater than that of silicon.

6. Some degree of spectral selectivity will be employed to minimize the steady state temperature of the solar blankets under all levels of concentration.

7. Blanket heat rejection will be performed passively.

From the figures, one can readily see the benefits to be derived from a GaAs array as characterized herein. The reduced thermal sensitivity allows significant performance gains with higher concentration and reduced active solar cell blanket area. However, if solar array cost is to be a major drive (which it most probably will be) it is readily seen in the cost curve that even under the most optimistic relative cost picture, a GaAs array must employ concentration ratios greater than 6X to effect the same array cost as a silicon array which has a 2X concentration ratio.

Early in the activity it was decided that the desired system would minimize complexity. This then eliminates high concentration ratios on two counts: 1) The geometric arrangement necessary to achieve concentration ratios beyond 2X - 2.5X. For flat reflector, trough concentrators, concentration ratios higher than this range require more than a two sided concentrator or can lead to complex curved shapes. The more complex the concentrator geometry, the less forgiving it becomes to even minor misalignments of the whole array. It would also make more complex the highly automated system assembly process being envisioned for the SPS. 2) It is desirable to stay away from a system that requires any form of active cooling of the solar blanket. For an assembly of silicon cells, active cooling becomes a necessity in the region near 3X concentration; for GaAs this occurs near 10X concentration. Therefore, an array of silicon solar cells with a concentration of approximately 2X was chosen as the reference for this activity.

Solar Array Blanket

The basic solar array blankets used in the reference configuration of the SPS are flexible substrate arrays typical of current advanced array hardware. Programs are currently generating a body of applicable data and experience are under contract both within NASA (Space Station and SEPS Solar Arrays) and the Air Force (FRUSA and Hardened FRUSA).

The required volume of production and minimal production cost of an SPS array necessitates significantly different production techniques from even the most advanced production today. The whole process will be one

in which man is virtually completely out of the loop except in a monitoring role. The lightweight, flexible solar arrays which represent the best of today's technology are very similar in concept to those which will be necessary for the SPS application. The major differences lie in weight and cost of the blankets. The lightest blanket available in today's designs are 0.95 Kg/M^2 ($0.20\#/ft^2$) and cost $\$20K-\$40K/M^2$. The blankets for the SPS must weigh on the order of $.4 \text{ Kg/M}^2$ ($0.08\#/ft^2$) or less and cost 1/500 to 1/1000 as much as today's cheapest space quality solar arrays. The only way to achieve this level of cost reduction (given an inexpensive solar cell) is through an automated continuous process. This process will be more akin to newspaper printing than today's production techniques. The process will employ rolls of substrate material moving continuously through the various processes with a finished product coming out in a package suitable for launching to the SPS assembly site.

The basic construction of the blankets is shown in Figure IV-B-1-b-4. The concept involves a patterned interconnect (conductor) system of aluminum or copper (or other suitable material) laminated between two thin layers of Kapton. A pattern of holes in the top layer of Kapton will expose the interconnect pattern. The solar cells will be laid onto the upper Kapton layer and welded through the hole pattern to the interconnect. Via this method the cells are electrically and mechanically attached to the blanket, no cell to substrate adhesive is needed. Finally, the cells will be covered with a plastic material (e.g., FEP Teflon or similar material) either singly or in groups.

Solar Cells

The solar cells used in the reference configuration are wraparound contact cells; i.e., both positive and negative contacts are on the back side of the cell. With this type of cell several benefits are realized. 1) The whole top of the cell can be covered with the cell cover with no gap for the looped top interconnector. 2) Both positive and negative contact welds can be made simultaneously and 3) all inspections (manual or automatic) are performed from the back side. Such cells as these have been in development for several years. They were, in fact, the baseline solar cell on JSC's large space station solar array (1970-73) as well as MSFC's SEPS array.

The solar cells in the reference system design are very thin in order to reduce basic blanket weight. Current production solar cells are from $200 \mu\text{M}$ (8 mils) to $300 \mu\text{M}$ (12 mils). The cells in the SPS reference are $100 \mu\text{M}$ (4 mils) in thickness and might possibly be as thin as $50 \mu\text{M}$ (2 mils). In today's production methods it is extremely difficult to manufacture a cell of $100 \mu\text{M}$ thickness. Breakage of cells this thin would be very high with today's hand manufacturing. Most probably a high volume, automated production system could cope with the thin cells since machines can be programmed for a more delicate touch than can a human being.

The physical dimensions of the cells used in the reference design are typically 4 cm x 4 cm. However, the physical dimensions which will be ultimately available are relatively unimportant. The major determinant will be 1) what size cell can be conveniently produced in the still to be developed continuous process and 2) what size is less susceptible to mechanical damage in the SPS application.

Solar Cell Covers

The covers to be used in this application serve two primary purposes. 1) They provide protection from charged particle radiation and 2) they provide a selective band pass filter to minimize incidence on the solar cell of light at wavelengths to which the solar cell is less sensitive from a power generation standpoint. The covers in this reference system are thin ($\sim 25 \mu\text{M}$) since the radiation environment is not a severe one. In the reference system, a plastic cover is desired which can be heat sealed or otherwise attached to the cell without the addition of an adhesive layer.

Interconnect Material

Several choices are available for interconnect material. Major among these are silver, copper, and aluminum. The lightest weight system would be aluminum; however, copper offers distinct advantages. The interconnect system in this application will be designed to withstand the severe thermal cycling environment imposed by a geostationary orbit, without imposing major stresses on the solar cells and the welds themselves. This will be accomplished by designing a pattern of stress loops in the pattern. The use of stress loops adds to the effective conductor length within the blanket and thus adds weight. This could be avoided only if the entire blanket assembly, including substrate, interconnect, and solar cells could be fabricated of materials with a good (nearly perfect) match of thermal expansion characteristics. The interconnect pattern will be generated via photo repeat techniques and will be mechanically or chemically formed.

Substrate Materials

The basic substrate to be used will be a plastic membrane system probably thin ($12.5 \mu\text{M}$) Kapton laminate with a material like FEP Teflon as the adhesive layer bounding the interconnect. Reinforcing can be provided by framing each module section with fiberglass in the outer edge of the laminate. This type of construction is currently being used in all advanced, flexible solar array work. Much long term testing has been performed to characterize these materials at elevated temperatures under mechanical stress.

Concentrator/Reflector

The concentrators used in the reference system are Kapton 12.5 μM thick with a highly reflective layer of aluminum 10 μM thick. It was assumed that the reflectivity of the concentrator will be 0.85. Thus, to achieve an actual concentration ratio of 2X, a geometric ratio on the order of 2.15X will be required.

Reference System Performance

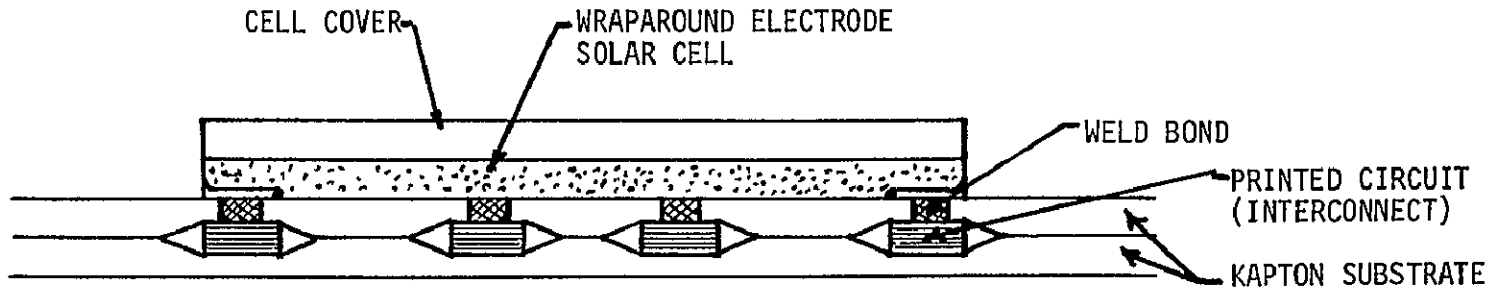
Reference system performance as shown in Table IV-B-1-b-1 is based on the use of an average 16% efficient (30°C) silicon solar cell. The predicted steady state temperature of 100°C under a concentration ratio of 2X as selected for the reference system. At this temperature the basic cell efficiency is predicted to be approximately 11%. With build-up and other system losses the realized performance will be approximately 10.3%. Each cell will have an output voltage at maximum power on the order of 0.32 volts and a 4 cm x 4 cm cell will have a current output of approximately 1.4 amps/cell (in 2X concentrated system) that will yield approximately 240 watts/M² of active blanket area.

Weights (Blanket and Concentrator)

Table IV-B-1-b-1 shows a breakdown of blanket and concentrator weights for the reference system on a per unit and system basis. Also shown are the impacts of cell and cover thickness variances. From this table it is seen that the reference weight of approximately 0.4 Kg/M² for the blanket is not the absolute minimum achievable should a thinner solar cell be available in the SPS time frame. In this study it is considered that the minimum achievable solar cell blanket weight is something in excess of 0.31 Kg/M² and that a reasonable maximum would approach 0.5 Kg/M². The concentrator material previously described will have a weight/unit area (actual area) on the order of 0.04 Kg/M².

Degradation

Two major causes of solar blanket degradation are expected -- radiation damage and damage due to thermal cycling. The radiation environment associated with geosynchronous orbits is not too severe. Thermal cycling degradation will possibly be greater than radiation unless a blanket system design can be devised which accommodates the severe thermal cycles. In flexible substrate arrays of the type to be used in the SPS the thermal time constants will be very short. It is conceivable that the blanket will swing from its steady state temperature of 100°C to a low level (-100°C) in approximately one minute. Under these conditions tremendous stresses can be generated in the interconnect, cell, weld, and cover interfaces. If, through design, these can be dealt with, the total expected degradation of the array should be on the order of that currently experienced by satellites in geosynchronous orbits; i.e., approximately 6% in first five years and probably 1%/year thereafter. (31% in 30 years.)



Cover	25.4 μM	Plastic Film (e.g. FEP Teflon)
Solar Cell	100 μM	Silicon Cell With Wraparound Electrode (typ 4cm X 4cm)
Kapton	12.7 μM	(each for two layers)
Adhesive	12.7 μM	(each for two layers)
Printed Circuit Interconnect	25.4 μM	Copper or Aluminum

FIGURE IV-B-1b-4, ARRAY BLANKET LAMINATE

Costs

The basis used herein was to work from the ERDA effort to develop high volume, low cost silicon cells for terrestrial applications. The ERDA program will achieve a high volume production by 1985 of 10% (AM1) solar cells at a cost of \$500/Kw. The SPS program will be able to build from the ERDA work and have approximately ten additional years to pursue the solar cells necessary for the SPS. It therefore seems probable that with the additional ten years to pursue high efficiency improvements that \$500/Kw for the SPS is a reasonable goal for which to strive. If the ERDA goal can be achieved by 1985, a high probability exists that the SPS goal can also be met.

Technology Status

Current Technology

Solar Array Blanket - Over the past several years much work has been done in this country toward development of flexible substrate, light-weight solar arrays. Early hardware in those development programs weighed on the order of 1.7 Kg/M². These arrays used Kapton, fiberglass and other materials being considered in the context of the SPS. The solar cells were 200-300 μ M thick and used soldered interconnect systems. Some of the designs did not use the laminated interconnect system being referenced herein. The latest versions of this hardware being developed within NASA weighs less than 1 Kg/M² and makes use of cells which are 200 μ M thick. Also, they use 12.5 μ M thick Kapton (presently thinnest available). As can be seen in the weight table (Table IV-B-1-b-1), the major effort in weight reduction achievement will of necessity come from the use of a thin solar cell and cover. It is felt that the work going on in continuous thick film single crystal silicon solar cells offers hope of achieving a 100 μ M cell for this application. Probably, however, special emphasis will be necessary to guide the goals of such a program to also meet the high efficiency needed. The efficiency achievement, which will need to be interlocked with the high volume production of thin cells, are being pursued presently in both private and government labs. Work involving wraparound contacts, spray-on contacts, integral covers and the like all are making significant progress today. This gives confidence that with proper guidance the next 15 to 20 years can realize the necessary achievements.

An area where work must be initiated is in the area of concentrator development. If the achievable reflectivity is considerably lower than reference, a more complex geometry for the reflector will be necessary (or more solar blanket added). In addition, the lifetime in orbit and surface quality relationships must be developed. This can only be done through in-space flight experiments.

The determination of thermal cycling degradation also must be pursued. A certain body of analytical work has been done which can be coupled

Blanket (240 watts/M² at 2X concentration)

solar cells
Eff. 16% AMO*, 30°C
11% AMO, 100°C

Mass/unit area
cells 265 gm/M²
cover 55 gm/M²

Substrate
Kapton 36 gm/M²
Teflon 55 gm/M²
Interconnect
(Aluminium) 10 gm/M²

Concentrator 2.16:1 (to obtain 2X)

Reflectivity 0.85

mass/unit area 40 gm/M²

Kapton 18 gm/M² (12.7 μM)
Aluminum 22 gm/M² (10 μM)

For 5 GW Station (9.6 GW gross output)

Blanket Area 40 X 10⁶ M²

Blanket Weight 16 X 10⁶ Kg

Concentrator 80 X 10⁶ M²

Concentrator Wt 4 X 10⁶ Kg

Total Array Weight (Blanket + Concentrator)

20 X 10⁶ Kg

* Air Mass Zero (sunlight spectrum and intensity outside earth's atmosphere at 1 Au)

TABLE IV-B-1b-1. BLANKET WEIGHT/PERFORMANCE SUMMARY

with ground test in some of the facilities where sophisticated thermal cycling test can be performed to screen likely approaches and materials. However, for the ultimate proof, extensive flight experimentation will be necessary.

References

1. Space Station Solar Array Technology Evaluation Program - First Topical Report - LMSC-A981486, December 1970 (Revised by LMSC-D159124).
2. Space Station Solar Array Technology Evaluation Program - Second Topical Report - LMSC-A995719, November 1971.
3. Design Data Handbook for Flexible Solar Array Systems - MSC07161 (LMSC-D159618), March 1973.
4. Final Report - Solar Array Flexible Substrate Design Optimization, Fabrication, Delivery, and Test Evaluation Program - LMSC-D384284, March 1975.
5. Glaser, P. E., et al, Feasibility Study of a Satellite Solar Power Station - NASA CR-2357, February 1974.
6. Satellite Solar Power Station - Solar Photovoltaic Array Report - Spectrolab Report Q-71098, November 1971.
7. A. F. Forestiori, (LeRC) Personal Communication (Si Solar Cell Developments)
8. E. Conway (LRC), Personal Communication (GaAs Solar Cell Developments)
9. High Efficiency Solar Cell Development - NAS5-20652 - Optical Coating Laboratory, Inc.
10. Development of a High Efficiency Thin Silicon Solar Cell - JPL Contract No. 954290 - Solarex Corporation
11. A Program Continuation to Develop Processing Procedures for Advanced Silicon Solar Cells - Contract NAS3-17350, Spectrolab - January 1975 - March 1976.
12. Feasibility Study of a 200 Watt per Kilogram Lightweight Solar Array System - JPL Contract 954393 - GE No. 76SDS4214, April 1976.

IV-B-1-c-1.0 Introduction

The reference JSC SPS design concept uses silicon solar cells for solar energy collection and conversion to electricity. There are, however, several other energy conversion system candidates that are potentially attractive for SPS application. One of the more promising alternate concepts, advanced by The Boeing Company, utilizes a solar concentrator-closed Brayton cycle system for power generation.

To gain additional perspective into energy conversion alternatives, a study was conducted to define and evaluate candidate concepts. In the following text, a discussion of "thermal engine" power conversion systems and other thermal system concepts is presented, with emphasis on the closed Brayton or Joule cycle. This is followed by an evaluation of the proposed Boeing closed Brayton cycle design concept.

IV-B-1-c-2.0 Alternate Power Conversion Systems

2.1 Introduction

This section consists of a survey of available thermal engine (dynamic) system concepts, and it includes an evaluation of the Boeing (Brayton cycle) system.

2.2 Background and Related Work

An alternative concept to the Glaser photovoltaic system^{1*} is a thermal engine system consisting essentially of solar reflectors, energy absorbers, dynamic converters, and a heat rejection subsystem (radiators). This alternative to photovoltaics is being pursued primarily due to the inherently higher conversion efficiency of the heat engine system (as high as 40%), which results in reduced area required for the solar reflector, and also because the generation of a.c. power in large quantities reduces conductor weight significantly. There are other advantages and disadvantages of this system which will be discussed in more detail in the text of this report.

Early comparison studies of nuclear turboelectric power plants operating on both the Brayton and Rankine cycle principles resulted in more favorable acceptance of the Rankine cycle system due to its smaller radiator area and lighter weight at peak cycle temperatures (at that time 1150-1250°F). Several Rankine-cycle space power systems received major development emphasis, among them the solar Sunflower and ASTEC systems, and the nuclear SNAP systems (e.g., SNAP-2, SNAP-8, and SNAP-50).² For the short-duration missions (compared to SPS) being considered for early missions,

*Superscripted numbers refer to similarly numbered references at the end of this report.

the Rankine cycle system concept with either organic working fluids for lower-temperature operations (approximately 700°F), or liquid metals (mercury, NaK, or potassium) for higher temperatures, was indeed attractive.

Unlike ground-based power systems, space systems must dissipate waste heat by radiation, which makes size and weight a function of the fourth power of the radiating temperature. Since the radiator is the heaviest component of the system, power plant weight can be minimized by designing a minimum-area radiator system. This can only be done by raising the radiating temperature. Thus to capture as large a portion of Carnot (ideal) cycle efficiency as possible, a high turbine inlet temperature is desirable.

Technology advances brought about by intensive development efforts continued over the years to improve Rankine cycle systems. However, as longer missions were planned, the advantages of the Rankine cycle were diminished by problems such as decomposition of the working fluid in organic Rankine cycle systems, and internal corrosion in the liquid metal systems. These problems are sharply accelerated by elevated temperatures and long-duration operational requirements. As developmental problems in extending Rankine cycle technology persisted, the Brayton cycle began to look more attractive. Early applications of open-cycle Brayton systems came in the aircraft and utility industries. Extensive research and development programs on compressors and turbines for aircraft propulsion have been conducted for over 35 years. Early gas turbine work in the utility industry concentrated on airbreathing gas turbines for peakload power plants, and later for base-load and hybrid (Brayton peakload, Rankine base-load) systems. Work on closed Brayton cycle space power systems above one kilowatt for extended mission durations (months or years) began in the late 1950's and has progressed to its present high degree of sophistication in component and system technology. The closed Brayton cycle has also found application in the marine industry, rails, vehicular transportation, and propulsion. Government contracts (with one company³ (1963-1974) totaled more than twenty million dollars. The Federal Republic of Germany presently has five closed Brayton plants in operation⁴, the largest of which is at Gelsenkirchen with a continuous output of 17.25 megawatts and a 30 percent overall thermal efficiency. This plant has operated for a total of 48,000 hours as of May 31, 1975. An earlier plant built at Ravensburg (2.3 megawatts, 25% efficiency) had 110,000 hours of operation on May 31, 1975.

Thus it is evident that there is ample conversion system technology to draw upon for the design of the SPS. However, while the conversion device is the heart of the system, two other essential components are the reflector-absorber subsystem and the heat rejection subsystem. Figure IV-B-1-c-1 schematically illustrates these subsystems for the SPS application.

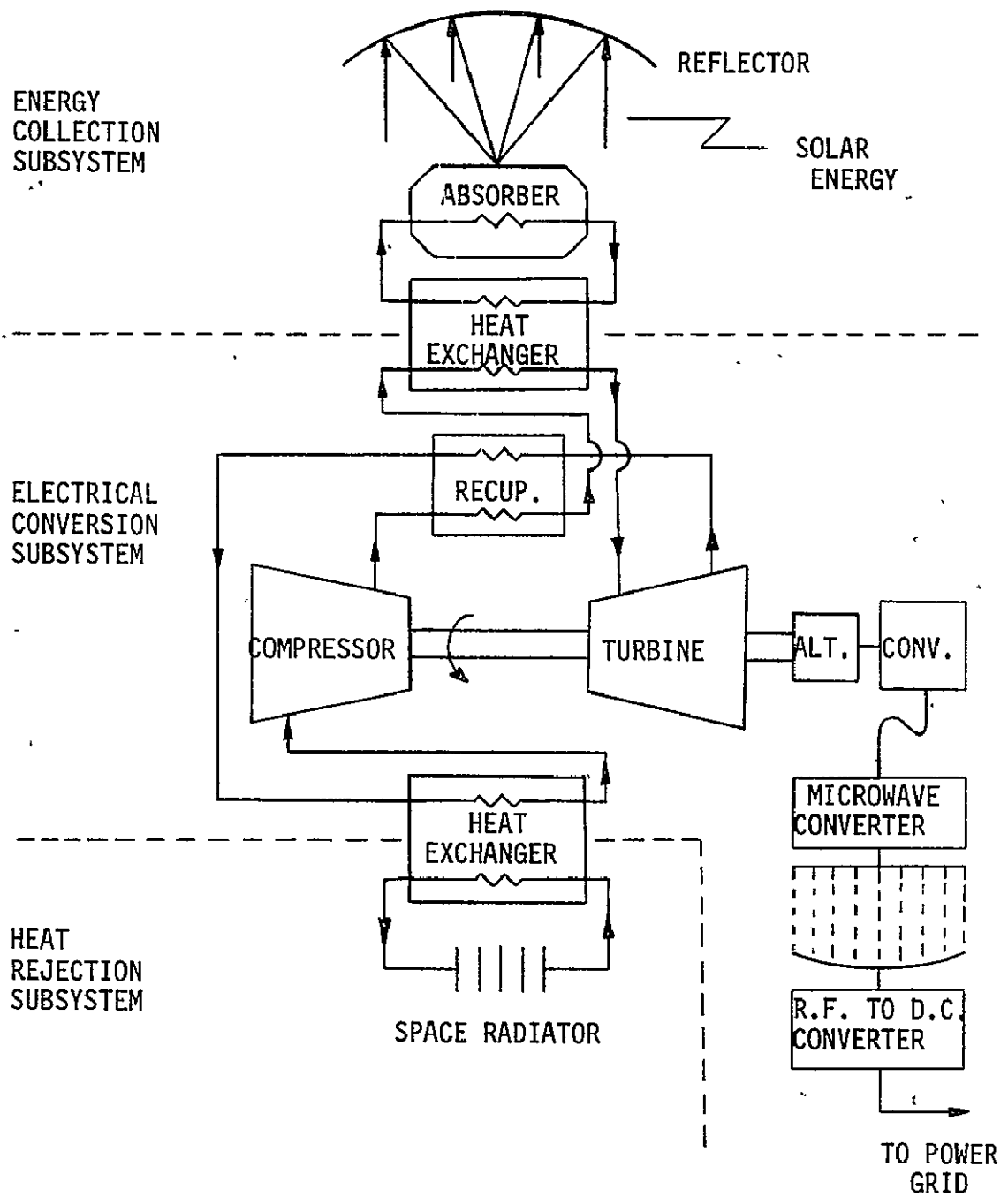


FIGURE IV-B-1-c-1, CLOSED BRAYTON CYCLE SOLAR CONVERSION SYSTEM

IV-B-1-c-3

In providing a radiator system for the thermal engine concept, several design choices must be made early in the design program including: (1) Will the cycle working fluid be used as the radiator fluid also (direct radiator) or will a secondary coolant loop with an interface heat exchanger be provided? With the Rankine cycle the direct method would involve a condensing radiator, whereas with the Brayton cycle a gas radiator would be required for direct radiation; (2) Will the radiator reject heat from one or both sides?; (3) Long-term meteoroid protection of the fluid tubes must be provided for reliability purposes; (4) An extremely reliable fluid pump is required for extended operation. These questions will be discussed in more detail in the text of the report, but it should be noted here that whatever concepts are selected, the design of the heat rejection system in principle involves no major technological breakthroughs. The design of space radiators is a well-known technology, and techniques abound for this task (see, for example, refs. 5 and 6). Extreme care in designing the radiator subsystem is required, however, as this is the heaviest single component of the system.

From a technological standpoint, the weakest component of the thermal engine system is the reflector-absorber subsystem. Both the reflector and absorber systems will require technological innovations to effect proper collection, concentration and absorption into the working fluid of the vast amount of solar energy required to power the system. Since weight is at a premium and the collector is the largest-area component, an extremely lightweight reflector system is needed with a reasonable reflectivity and concentration ratio. Since the absorber must operate at temperatures higher than the turbine inlet temperature, precautions must be taken to obtain a high-thermal-efficiency absorber with a minimum of re-radiation, reflection, and other heat losses.

The one most significant technology breakthrough required for feasibility of the entire concept (be it the photovoltaic or the thermal engine) is the problem of how to design, erect and maintain large structures in space. This problem is addressed in another section of the report and will not be discussed here. From the thermal engine standpoint, however, the problem affecting all subsystems and components is one of a "scale-up" nature from the size of existing devices to the very large sizes (even with modularization) required for the SPS.

In summary, from a purely technological standpoint, there appears to be no inherently insurmountable problem with the thermal engine concept, although many engineering problems will need to be solved to make the concept a workable system. This report will discuss these engineering problems and will evaluate where possible the solution proposed by the Boeing Company, as well as compare the thermal engine and photovoltaic concepts. It should be emphasized that in this brief study only an evaluation and discussion of concept is possible, since sufficient design details are not available at this point in time.

2.3 Requirements

With each new stage of concept evolution, more numerous and more detailed requirements arise. Currently, only these general guidelines are considered:

(1) Each SPS power satellite shall produce 10 Gwe. Systems may be modularized if necessary to meet this requirement.

(2) The operating life of an SPS satellite shall be 30 years. Components shall either be designed to operate the full 30-year period, or a maintenance and/or replacement schedule shall be established.

(3) The system shall be capable of withstanding the brief semi-annual earth occultation periods. During these periods, the system shall not be required to produce electrical power.

(4) A Heavy Lift Launch Vehicle (HLLV) with a payload weight limitation of 10^6 pounds shall be provided to lift the system into a low earth orbit (LEO) from which it can be propelled to geosynchronous earth orbit (GEO). The system shall be capable of being assembled in orbit (either full assembly in geosynchronous orbit, or partial assembly in LEO to provide electrical power for propulsion to GEO).

Requirements relative to the thermal engine system are that it shall include a solar energy collector and absorber subsystem, an energy conversion subsystem, and a heat rejection subsystem. Interface requirements at the structural, microwave and environmental system interfaces shall be specified in more detail during concept evolution.

2.4 Options

Several system design options are being considered, each relative to its appropriate subsystem. These include:

(1) Energy collector-absorber device. Several collector concepts are under consideration, including inflatable, inflatable rigidized, Fresnel, and faceted. Absorber variations include designs for flowing the working fluid directly through the absorber, or provisions for a secondary, high-temperature fluid loop with an interface heat exchanger.

(2) Conversion device. Both Rankine and Brayton cycle systems are candidates; other conversion systems are also discussed.

(3) Heat rejection device. The two primary options in this subsystem are (1) gas-vs-liquid radiator, and (2) conventional-vs-electromagnetic (EM) pump in the case of a liquid metal coolant loop.

These options are discussed in this report, and evaluations of the proposed Boeing system are made wherever sufficient data exists.

2.5 Comparison of Conversion System Concepts

2.51 Working Fluid Cycles .

2.511 The Rankine Cycle

Temperature-entropy diagrams for two different types of Rankine cycle working fluids are shown in Figure IV-B-1-c-2; The difference between the two fluid types is basically in the shape of the saturated vapor line. Both of these cycles have saturated vapor at the turbine inlet; however, the Type-A fluid expands in the turbine through the "wet" region, whereas the Type-B fluid expands in the superheat region. Examples of a Type-A fluid are water, ammonia, and the liquid metals (sodium, rubidium, mercury, etc.). Examples of a Type-B fluid are many of the freons, Diphenyl, Dowtherm A, etc. A comparison of the Carnot cycle with that of a typical Rankine cycle with a Type-A fluid is shown in Figure IV-B-1-c-2b.

Since any space (as opposed to terrestrial) working fluid cycle must operate with as high a radiator temperature as possible to minimize system weight, it is necessary to elevate peak cycle temperature to as high a temperature as can be tolerated within material limitations in order to maximize cycle efficiency. Thus while ground-based steam power systems operate typically below 1200F, space power systems may operate as high as 2000F.

While the organic or Type-B fluids have been considered for certain space applications, e.g., the ORACLE (Organic Rankine Cycle) program, two problems exist which make their use difficult for SPS. First, at the high temperatures required, peak cycle pressures for these fluids are much greater than those for the liquid-metal systems, resulting in a larger system weight. Secondly, organic fluids can only be used at temperatures below approximately 700F for extended-duration missions due to decomposition of the working fluid. This reduced working fluid temperature would result in even further additional system weight.

Thus Rankine cycle working fluids are essentially limited to Type-A fluids, meaning for the most part water, ammonia, or the liquid metals. Fluids such as water and ammonia have high vapor pressures at peak temperatures and would increase system weight substantially. For example, whereas peak pressures in terrestrial steam systems are on the order of 10^3 psia, they are generally an order of magnitude lower for space systems. On the other hand, while system operating pressures are low for liquid metal systems, corrosion is enhanced at elevated temperatures, and in view of the 30-year life requirement of the SPS, this is the biggest single disadvantage of the Rankine cycle.

In addition to the various working fluid types, the cycles differ in their heat rejection methods. Figure IV-B-1-c-3 illustrates the direct and indirect cycles. In the direct cycle a condensing radiator is employed

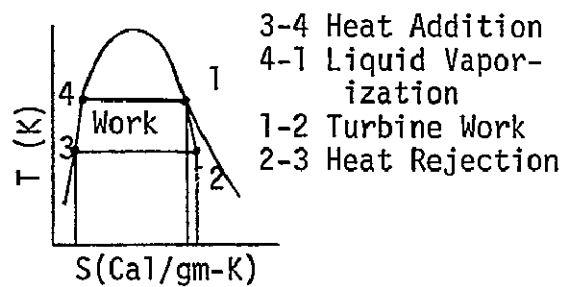
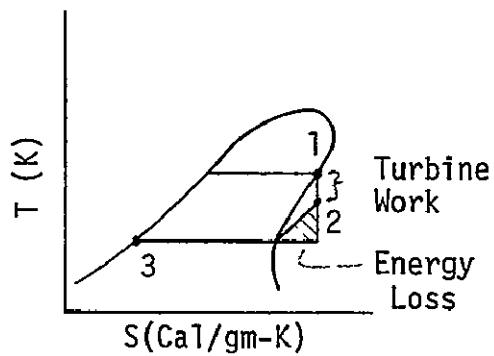
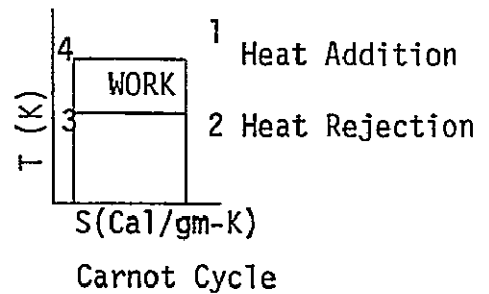
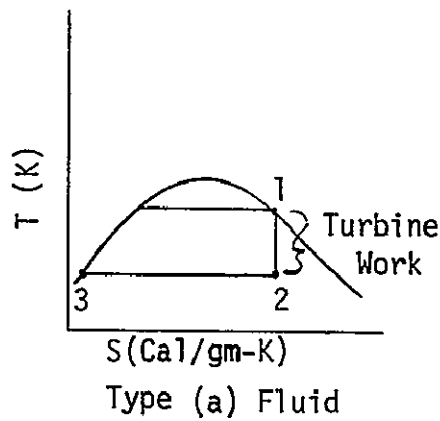


Fig. IV-B-1-c-2a. Ideal Cycles for Type (a) and (b) Fluids

Fig. IV-B-1-c-2b. Carnot Cycle Compared to an Actual Cycle for a Typical Type (a) Fluid

Figure IV-B-1-c-2. Theoretical Rankine Cycles

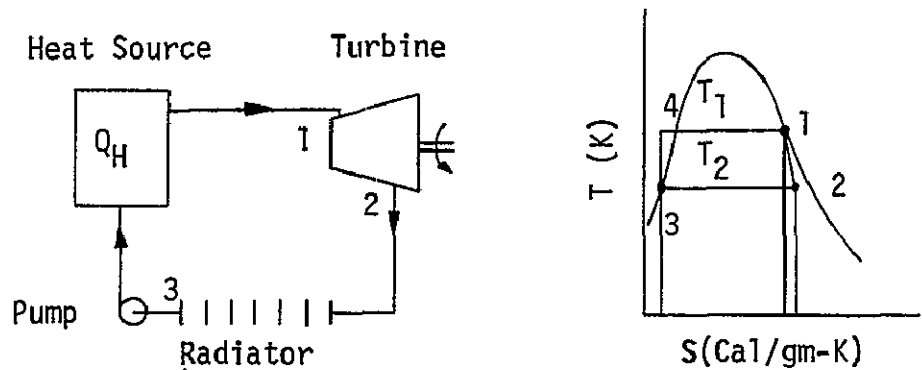


Fig. IV-B-1-c-3a. Direct Cycle

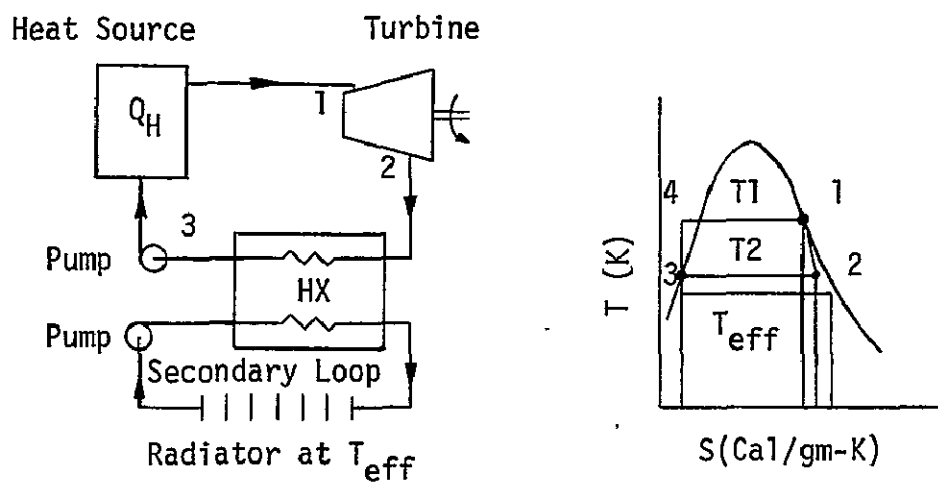


Fig. IV-B-1-c-3b. Indirect Cycle

Figure IV-B-1-c-3. Direct and Indirect Rankine Cycles

to directly reject heat to space at essentially a constant temperature. The indirect cycle avoids the zero-g condensing radiator by using a secondary fluid loop with an intermediate heat exchanger. Many Type-A Rankine cycles use superheated vapor at the turbine inlet to increase turbine efficiency by eliminating liquid particles in the turbine. Erosion of turbine blades is largely caused by liquid particles striking the leading edge of the blades.

For application of the Rankine cycle to the SPS, four main technology areas must be carefully considered: (1) Materials problems due to corrosion at high temperatures, (2) turbine-blade erosion; (3) thermal design considerations and stability of compact once-through boilers; (4) pump technology. While considerable progress has been made in the field of high-temperature materials over the years, corrosion in the presence of liquid metals is still a major problem, and it is not presently expected that corrosion rates can be minimized over the next several years to meet the 30-year life requirement and make the high-temperature liquid metal Rankine cycle system a viable candidate for the SPS.

2.512 The Brayton Cycle

Because of problems such as those discussed above, space power system designers turned to single-phase working fluid cycles which could provide a net usable output power after satisfying compression penalties. This work led to the closed Brayton cycle as the promising gas cycle for space applications, as discussed earlier.

A thermodynamic diagram for the various processes in the closed-cycle Brayton system is shown in Figure IV-B-1-c-4a. After expanding polytropically through the turbine, the working gas then exchanges heat with fluid leaving the compressor in the recuperator (recuperation increases cycle efficiency) before entering a waste-heat exchanger. After rejection of energy to a heat sink, the working fluid is then compressed in stages, with intercooling between stages, before flowing through the low-temperature side of the recuperator and on to the heat source. A schematic of the system is shown in Figure IV-B-1-c-4b. The following discussion of the characteristics of the closed Brayton cycle system is presented to give the reader a basic understanding of this system before evaluating the Boeing concept.⁷

In addition to a long and successful development history and a continually increasing "state of technology," the closed Brayton cycle is attractive for extended space missions such as the SPS for two reasons. The inert gas working fluid (1) precludes internal system corrosion, thus alleviating the peak cycle temperature limitations from the aspect of chemical combinatorial effects of the working fluid with component materials; (2) eliminates problems associated with two-phase fluids such as turbine erosion, pump cavitation, and low-gravity boiling and condensing. Furthermore, gas bearing technology is well-developed for Brayton systems,

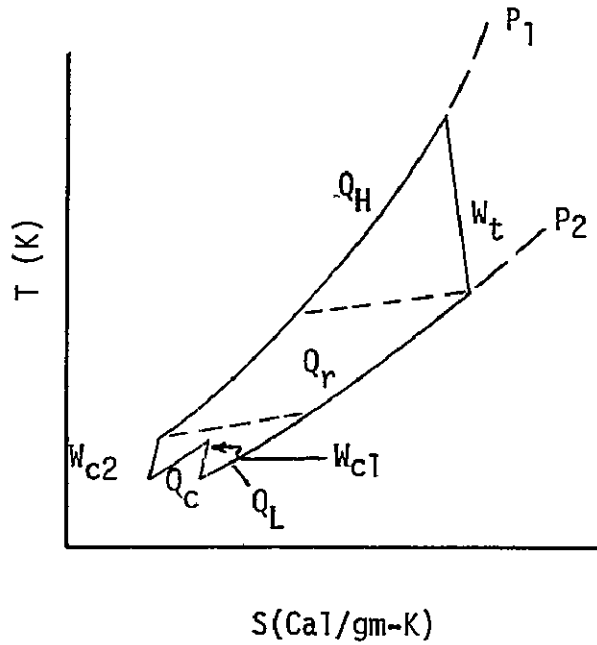


Fig. IV-B-1-c-4a, Temperature-Entropy Diagram for a Closed Brayton Cycle

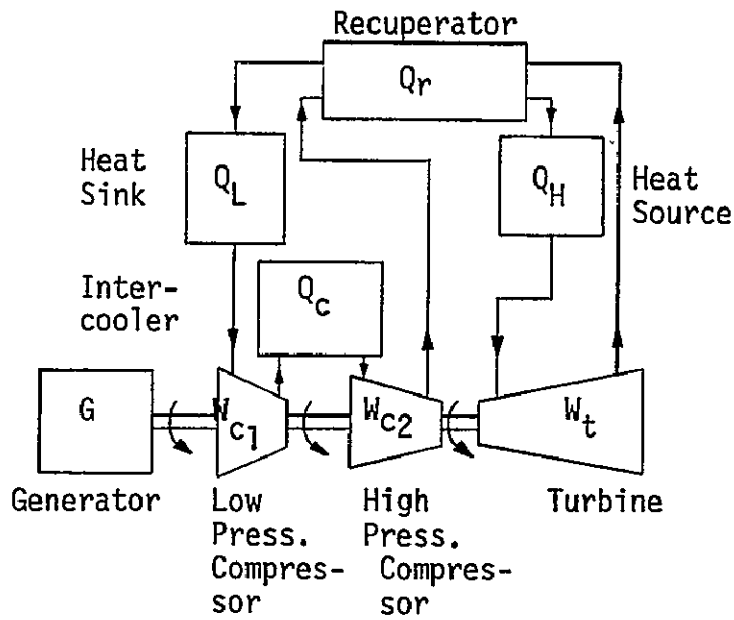


Fig. IV-B-1-c-4b, Closed Brayton Cycle System

Figure IV-B-1-c-4. T-S and Schematic Diagrams for a Closed Brayton Cycle System

and thus the working fluid serves as a lubricant for all rotating components, eliminating cross-leakage effects in conventionally lubricated systems.

The cycle efficiency for a Brayton system is a function primarily of the peak cycle, or turbine inlet, temperature and the system pressure ratio, as shown for a typical Brayton system⁸ in Figure IV-B-1-c-5. These calculations assume efficiencies of 88% and 90%, respectively, for the compressor and turbine, with a recuperator effectiveness of 0.90. The figure illustrates that for a given turbine inlet temperature, an optimum pressure ratio (ratio of turbine inlet to compressor inlet pressure) exists for maximum efficiency. Absolute pressure levels are determined by size and weight tradeoffs. Higher pressures reduce heat exchanger size, but the weight of other system components increases due to structural considerations.

The type of working fluid used in the cycle affects the number of stages required for the turbine and compressor, as well as heat exchanger size. These effects are illustrated in Figure IV-B-1-c-6. Figure IV-B-1-c-6a illustrates the decrease in the required number of stages for molecular weights from 4 (helium) to 40 (argon). Mixtures of these two gases (or other gases) will yield molecular weights between these two extremes. The main point of this figure is that turbine and compressor size and weight will decrease with increasing molecular weight of the working fluid. Figure IV-B-1-c-6b shows how relative recuperator size (the recuperator is the largest heat exchanger in the system) increases with molecular weight.

As stated previously, recuperation increases overall cycle efficiency. However, to accomplish this, certain penalties associated with a recuperative heat exchanger must be paid. These penalties in efficiency and size (which are analogous to weight) are shown in Figure IV-B-1-c-7. Figure IV-B-1-c-7a indicates a rate of 1% decrease in cycle efficiency for a two percent rise in recuperator pressure loss. While it is desirable to keep the pressure loss as low as possible in the recuperator for cycle efficiency reasons, this can only be accomplished by making the heat exchanger larger, as shown in Figure IV-B-1-c-7b. Thus it is seen that careful system tradeoffs are necessary to achieve optimum cycle performance.

Recuperator performance (heat exchanger effectiveness) is also an important parameter, and it too has an effect on cycle efficiency. This effect is shown in Figure IV-B-1-c-8a, where it is seen that a decrease in recuperator effectiveness is accompanied by a corresponding decrease in cycle efficiency (recuperator effectiveness values for typical space power systems are in the 0.90 region). The figure also illustrates how the optimum cycle pressure ratio decreases with an increase in effectiveness. Figure IV-B-1-c-8b shows the relative variation of recuperator size with effectiveness and illustrates the extreme weight penalty which must be paid for effectiveness values approaching 1.0.

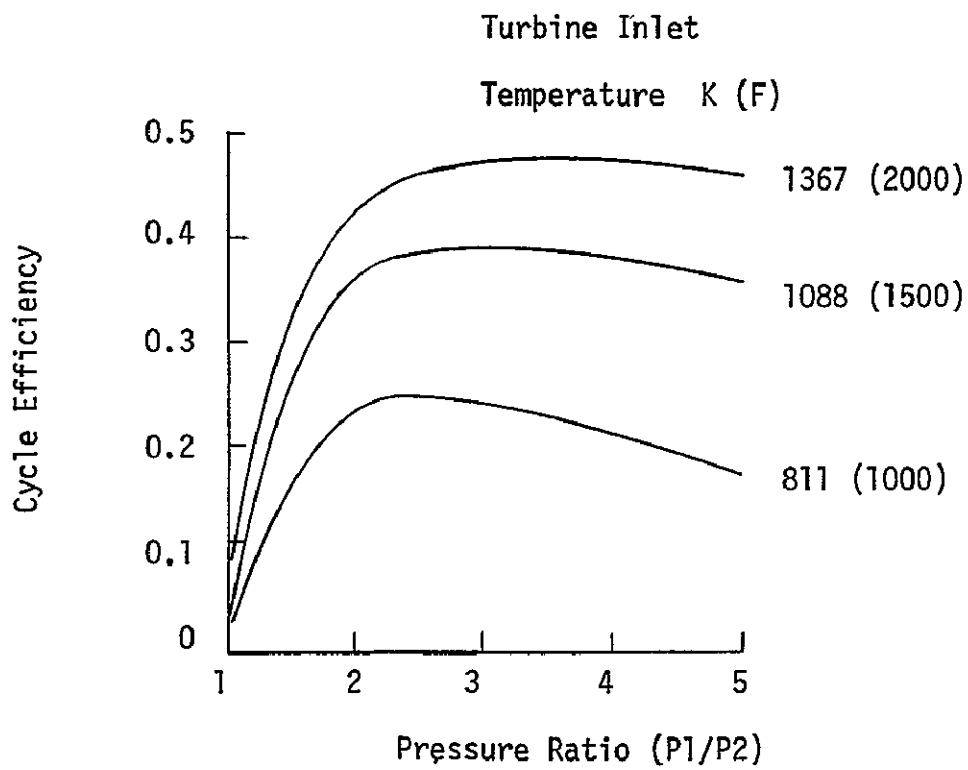


Figure IV-B-1-c-5. Closed Brayton Cycle Plant Performance
 Compressor Polytropic Efficiency .88
 Turbine Polytropic Efficiency .90
 Recuperator Effectiveness .90

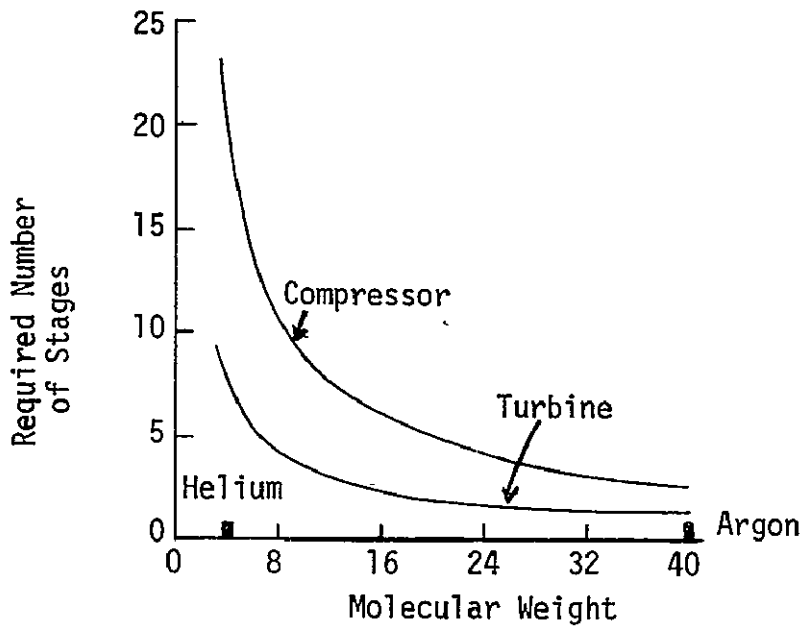


Fig. IV-B-1-c-6a. Effect of Working Fluid on the Required Number of Stages

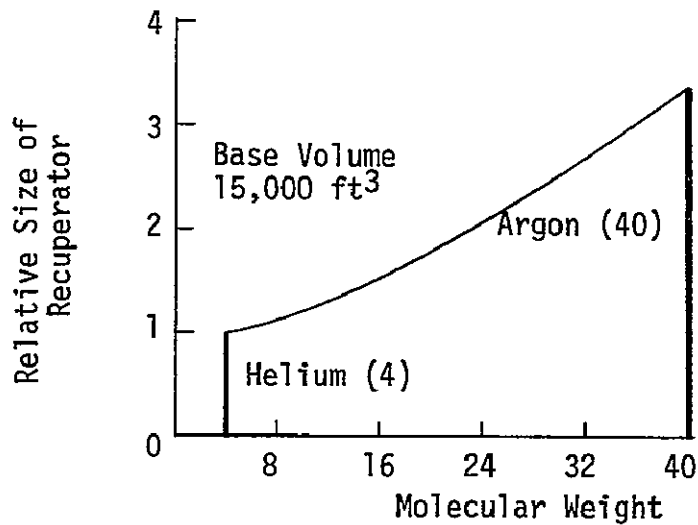


Fig. IV-B-1-c-6b. Effect of Working Fluid on Recuperator Size: Effectiveness = .90

Figure IV-B-1-c-6. Effect of Working Fluid on Recuperator Size and Cycle Efficiency

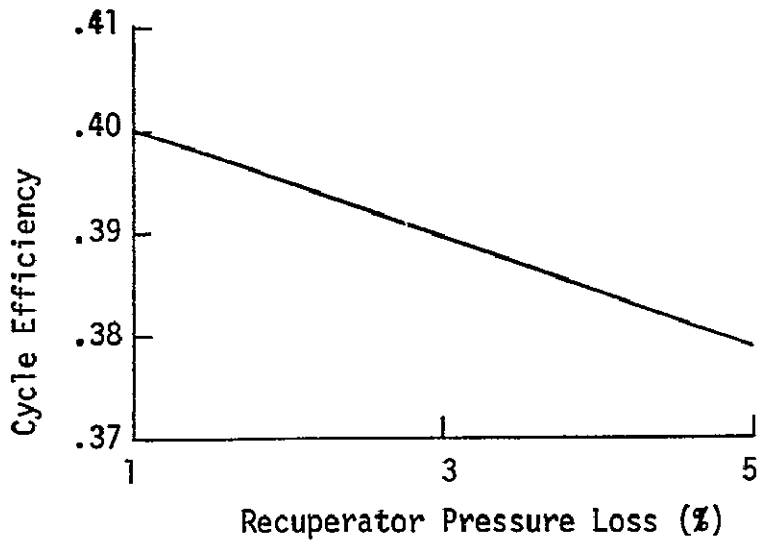


Fig. IV-B-1-c-7a. Effect of Recuperator Pressure Loss on Cycle Performance

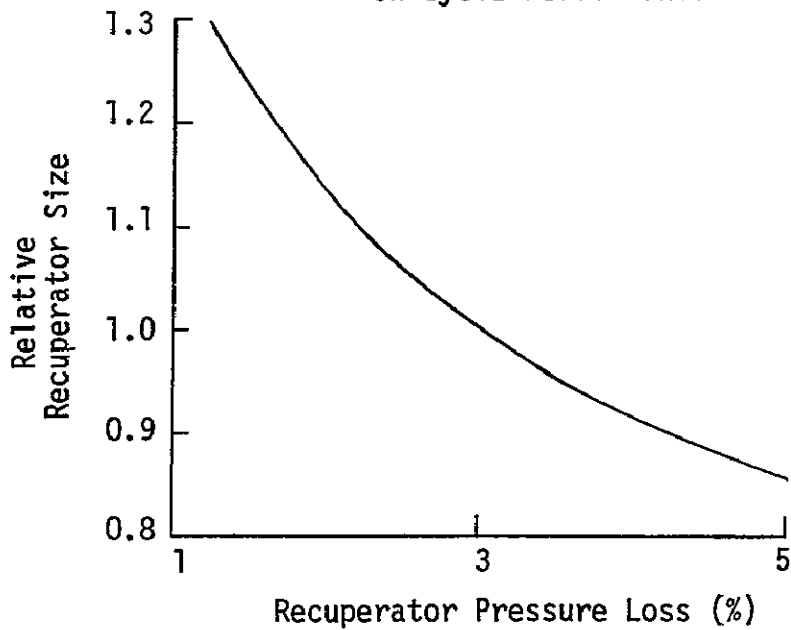


Fig. IV-B-1-c-7b. Effect of Recuperator Pressure Loss on Size of Recuperator

Figure IV-B-1-c-7. Effect of Recuperator Pressure Loss on Recuperator Size and Cycle Efficiency

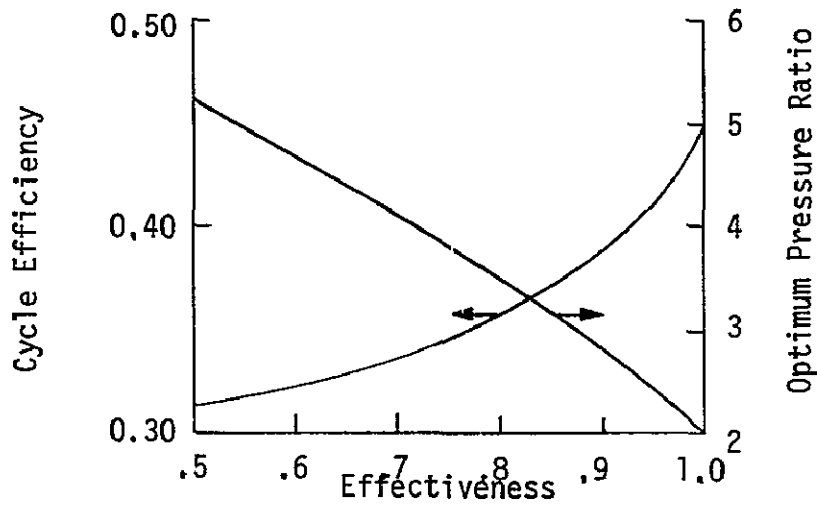


Fig. IV-B-1-c-8a. Influence of Effectiveness on Cycle Performance

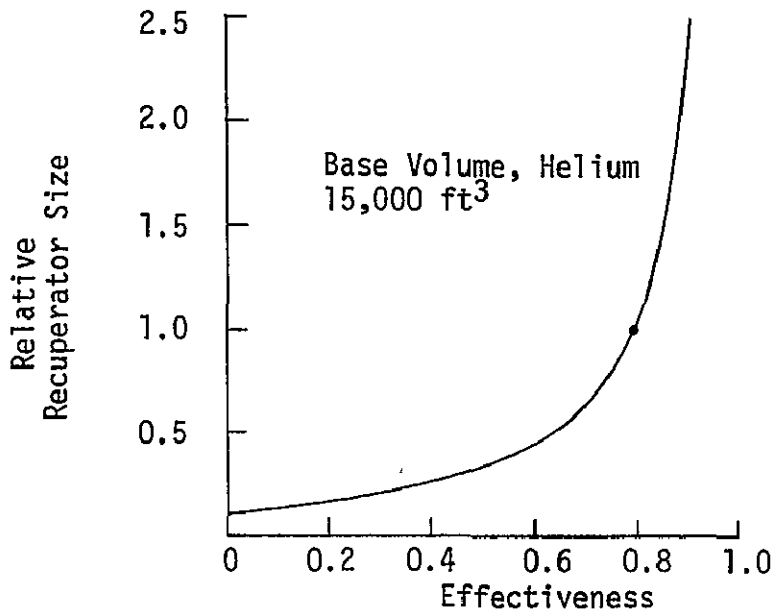


Fig. IV-B-1-c-8b. Influence of Effectiveness on Recuperator Size

Figure IV-B-1-c-8. Influence of Recuperator Effectiveness on Design Parameters

2.52 Other Thermal System Concepts

In addition to the working fluid cycles, two other conversion concepts were considered in the study.

The thermionic concept is based on the phenomenon of electron emission from a high-temperature (approximately 3000F) electrode across a gap filled with cesium vapor to enhance the flow of electrons, with collection at a low-temperature electrode. The efficiency of the device is a function of emitter temperature, and efficiencies of 7 to 10% can be achieved with an emitter operating at 2500°F, as compared to 14 to 17% efficiency at 3000°F. Some research has been initiated to try to reduce emitter temperatures without lowering efficiency, and progress has been made by orienting the crystal axes of the tungsten electrodes in certain ways. For a given efficiency, this has allowed a reduction in emitter temperature of 200 to 300°F, but not under 2200°F. Several converters have been operating for periods over one year, but consistent results have not been achieved. The main problems with this concept are: (1) very high temperatures are required to produce efficiencies of only half that of the Brayton cycle, and these temperatures are too high for the 30-year life requirement of the SPS; (2) the gap between electrodes must be very small (0.01 inch) which presents a significant thermo-structural problem; (3) it is difficult to control the vapor pressure of the cesium at the required level; and (4) cesium leakage further complicates the system. For these reasons this system will not be further considered in the study.

Another concept considered briefly was the magnetohydrodynamic (MHD) generator, a high-temperature conversion device using an electrically conducting fluid (liquid metal, liquid metal vapor, or a gas) which is ionized and flows through a channel at right angles to an applied magnetic field, producing a voltage across the channel. Highest efficiencies reached so far with liquid metal systems have been 56% (generator only) on a small liquid metal unit, with projected generator efficiencies of 70-75% for large generators, but present systems have an overall efficiency of less than 10% at a peak temperature of 2000°F. A problem with achieving acceptable electrical conductivity exists with the gas systems. The life limiting component is the current-carrying channel. Also, more work is needed to improve the electrical conductivity of the fluid by electron acceleration techniques. Another problem for space units is the high strength of magnetic field required. This involves the use of large magnets and heavy supports. The development state of the MHD concept is not considered sufficiently advanced to merit further consideration in this study.

2.6 Reflector-Absorber Subsystems

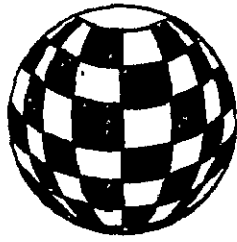
While analysis techniques are available for the design of solar reflector-absorber subsystems⁹, much development work remains to be done in these two related areas. The intent of this section is not to concentrate on

these techniques as this subject is extremely complex and involved, but rather, to describe several concepts which should be considered in system selection.

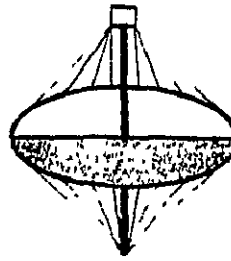
Absorber design techniques are directed mainly toward decreasing radiation and reflection losses through the aperture, as well as minimizing losses through the walls and structure of the absorber. Proper absorption of the high heat fluxes involved and transfer of energy to the working fluid are accomplished through judicious system geometry choices and proper selection of materials. The cavity-type absorber is the only type considered in this investigation, as it provides significantly higher thermal efficiency than any other type due to reduced reflection and re-radiation losses, and it allows the achievement of the high heat flux requirements and control of same within the cavity. The cavity walls are insulated (the Boeing concept uses Alumina/Silica fiber insulation¹⁰), and the working fluid is pumped through columbium tubing within the absorber. Use of refractory metals is common in absorbers of this type. Future technological breakthroughs are predicated on the use of ceramic materials in the cavity to allow even higher cycle temperatures (contingent upon advances in high-temperature turbocomponent technology).

The solar reflector, while integrally related to the high-temperature absorber in its design, is the lowest temperature component of the system. The higher its reflectivity, the lower its operating temperature. The small amount of heat absorbed in the reflector system is radiated directly to space while the reflector concentrates large amounts of energy toward the aperture of the absorber. For this application the perfect reflector or concentrator, of course, is a parabola, and thus all concentrator designs must approach a paraboloidal geometry to achieve the high temperatures required for the thermal engine system. While rigid collectors of high optical quality are preferred, structural problems limit the degree of rigidity which can be achieved, and weight considerations force the designer to accept reflector materials such as the Boeing aluminized plastic film with optical qualities inferior to those of a good silvered mirror¹⁰.

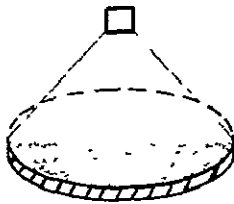
Several reflector configurations were examined in the study, including inflatable, inflatable rigidized, petal, and faceted types. These configurations are shown in Figure IV-B-1-c-9. Figure IV-B-1-c-9a shows a spherical collector which is inflated with a gas at a very low pressure. The power conversion device and spherical absorber are mounted at the center of the sphere. This system requires no attitude control, as it gathers and concentrates sunlight in any orientation. Solar energy penetrates the transparent sections, while the opaque sections have an internal reflective coating to focus the solar energy toward the center of the sphere. Problems with this concept are (1) inflation gas leakage; (2) spherical absorber design problems; (3) remote radiator location on opaque sections, with associated installation problems after inflation is accomplished; and most importantly (4) achievable concentration ratios are low.



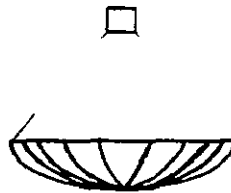
(a) Inflatable, Spherical



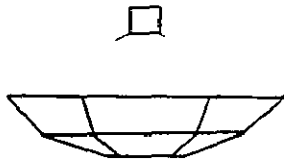
(b) Inflatable, Spherical Distorted



(c) Inflatable Rigidized



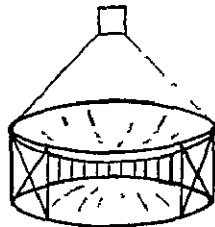
(d) Petal Type



(e) Faceted, Paraboloid Approximation



(f) Faceted, Fresnel



(g) Drum, Tensioned Net

Figure IV-B-1-c-9. Solar Reflector Concepts

Figure IV-B-1-c-9b shows a modified inflatable concept in which an essentially parabolically patterned system is inflated and subsequently distorted with tension wires attached to a mainframe to fine-tune the system toward a more perfect paraboloidal shape. The top half of the system is transparent, and the bottom half is coated with a reflective substance. Advantages of this system include a higher concentration ratio than the inflatable spherical system with less overall complexity. Problems exist, however, with orientation of the overall structure and inflation gas leakage. Also, some losses are involved due to reflection of incident solar energy off the transparent surface. Figure IV-B-1-c-9c shows a parabolically patterned reflector system which is rigidized in space. Unless an extremely lightweight foam or other rigidizing material is used, the weight of the rigidizing material would cause the large-area collector system to be excessively heavy. Figure IV-B-1-c-9d shows a petal-type reflector which is a fairly high-precision system requiring a rigid mainframe support structure. The petal-type system was not seriously considered due to the extremely large weight penalty associated with providing a structure rigid enough to insure adequate solar concentration.

Figure IV-B-1-c-9e shows a faceted collector of paraboloidal approximation. This is the Boeing concept. Each flat-plate facet is approximately one fourth of an acre in area and is individually steered providing a high degree of system redundancy. Figure IV-B-1-c-9f is essentially the same concept, except that all the facets are mounted in a common plane. Although this concept was first considered for simplicity of construction, it is judged to be inferior to the concept of Figure IV-B-1-c-9e due to shadowing effects as well as its lack of structural rigidity. Figure IV-B-1-c-9g shows a drum configuration with a pair of tensioned nets approximating a paraboloid of revolution. The aluminized thin-film facets would be mounted on the concave side of one of the tensioned nets. This system may or may not need individual facet steering provisions, but in any case is expected to save a considerable amount of weight in reduced mainframe structure.

2.7 Heat Rejection Subsystems

The dissipation of waste heat from any space system requires rejection to the space environment. Intermediate devices such as heat pipes may be used to transfer the waste heat with a minimum temperature drop to the radiator system, but the radiating surface itself cannot be eliminated. For this reason it is essential to design into the radiator system the highest possible effectiveness. The effectiveness of a space radiator is the ratio of the amount of heat actually rejected from the radiator to the amount of heat which could be rejected from a fin or plate radiating isothermally to space at the inlet fluid temperature (i.e., no temperature gradients exist in the plate). A high effectiveness is important since the radiator is the heaviest single component of the thermal engine system. Many parameters are involved in the design of a fin-tube radiator system, such as fluid temperature levels, the nature of the space environment (dictated by orbital attitude, surrounding

planets, and the geometry of the orbital system), meteoroid protection requirements, surface coating properties, material properties of the fins and tubes, properties of the heat transport fluid, transport rates, etc. Fortunately, radiator-design techniques are well-developed, and extensive computer codes exist for the design of any type system required. An interesting consideration, however, is to simplify the problem to get an idea of the area required, for example, for the Brayton cycle system, by deriving for geosynchronous orbit the "equivalent sink temperature," which is the apparent environment temperature for radiation "seen" by an isothermal plane of given surface coating properties in a given orbital attitude. This equivalent sink temperature is derived for two panel attitude configurations as shown in Figure IV-B-1-c-10. The first is for a panel whose normal vector is parallel to the sun vector. The normal for the second configuration is perpendicular to the sun vector. In both cases the radiator panel will always be facing away from direct solar incidence, and the panel will always be irrotational with respect to its own axis since the SPS reflectors are precisely oriented to the sun at all times. The equivalent sink temperature variations for these two configurations in geosynchronous orbit are shown in Figure IV-B-1-c-11, for (α_s/ϵ) (ratio of solar absorptivity to thermal emissivity for the surface coating) values from 0 to 1. A good radiator surface coating will have a low solar absorptivity with a high thermal emissivity. The Apollo radiator coating had an (α_s/ϵ) ratio of (0.18/0.92), or about 0.2. As the coating degrades in orbit, its solar absorptivity rises, making it a less effective barrier to sunlight reflected off the earth. The influence of solar absorptivity becomes less important as radiator operating temperature increases. Thus solar absorptivity for the Apollo radiator panels (operating temperature on the order of 100F) is much more critical than it would be for the Brayton cycle radiator, which would operate at 300 to 500°F. One early radiator concept for the Brayton system assumed an integrated reflector-radiator wherein the radiator panels were mounted on the back side of the reflector to reduce structural requirements. In this case the curves of configuration (a) are applicable in Figure IV-B-1-c-11. In this configuration, however, the radiator is very far from the conversion system, which causes increased pressure drop and pumping power problems. While these problems would be serious for a gas radiator system, they may be offset for a liquid system by the weight saving effected through integration of these two large-area system components. The maximum equivalent sink temperature for this configuration is approximately 220°R for $(\alpha_s/\epsilon) = 1.0$. This maximum sink temperature occurs when the SPS is in line with the earth-sun vector ($\theta=0^\circ$). The curves of configuration (b) correspond to the present Boeing radiator system concept, and in this case the maximum equivalent sink temperature is approximately 190°R. This maximum occurs when the SPS is 60° removed from the earth-sun vector.

The required radiator area for a radiator with a thermal emissivity of 0.85 and a varying solar absorptivity (from 0.25 for a new surface to 0.85 for a degraded surface) for radiator effectiveness values of 0.7

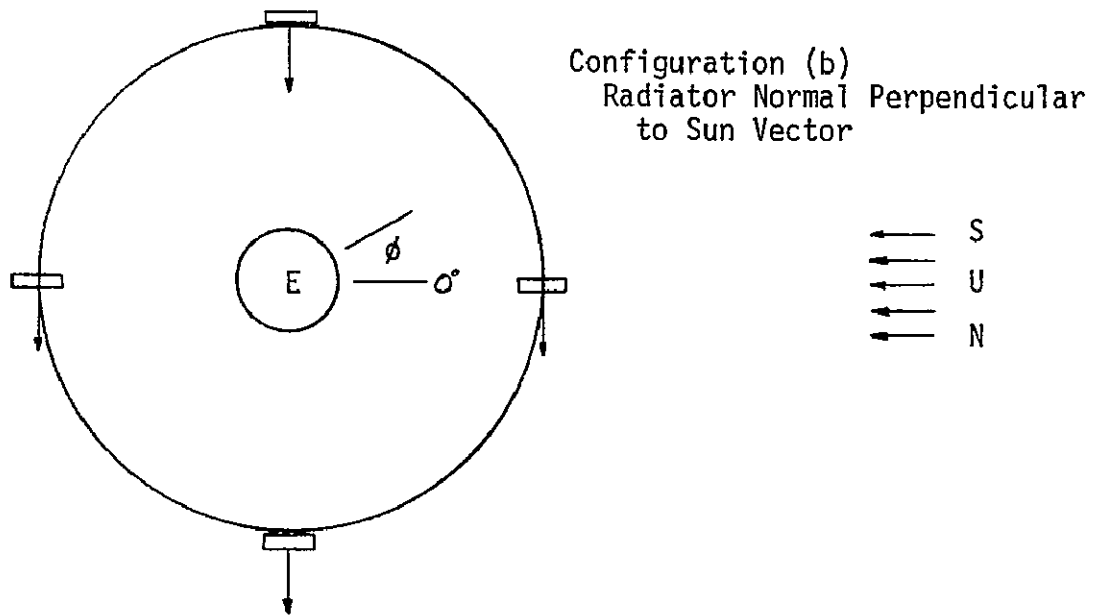
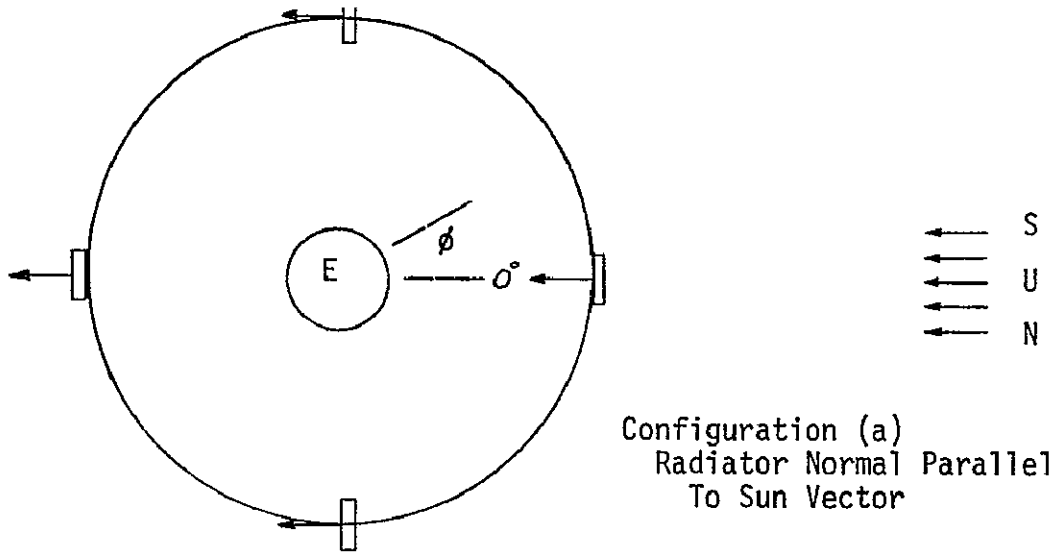
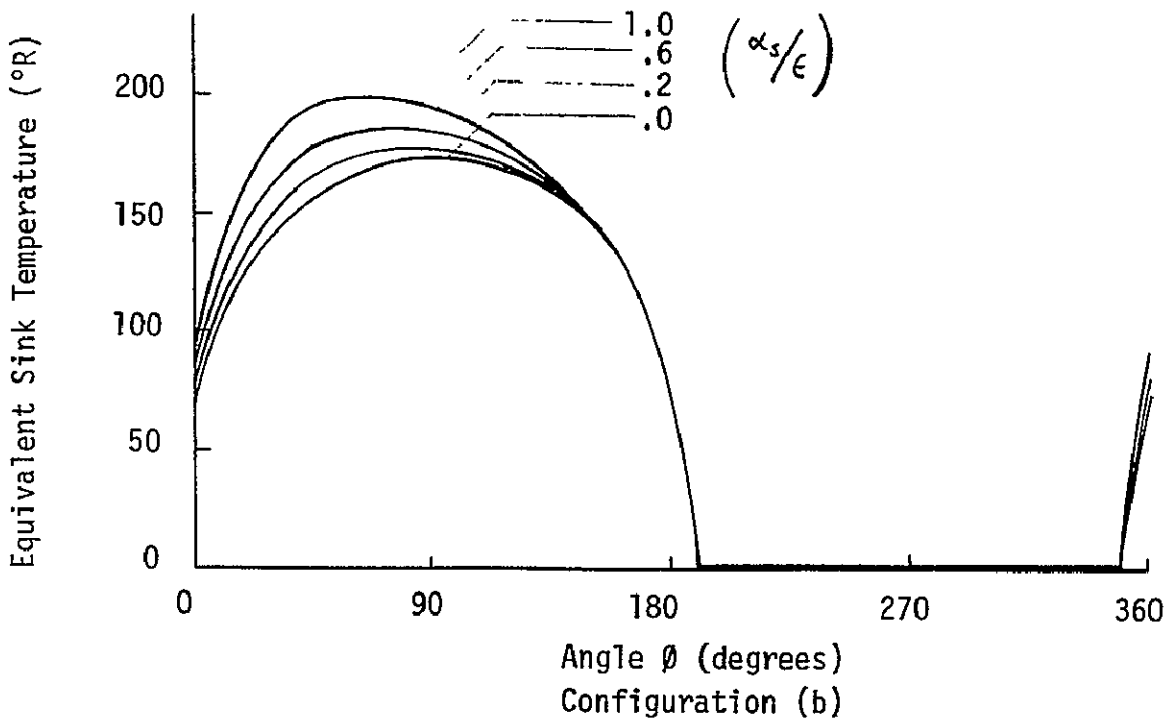
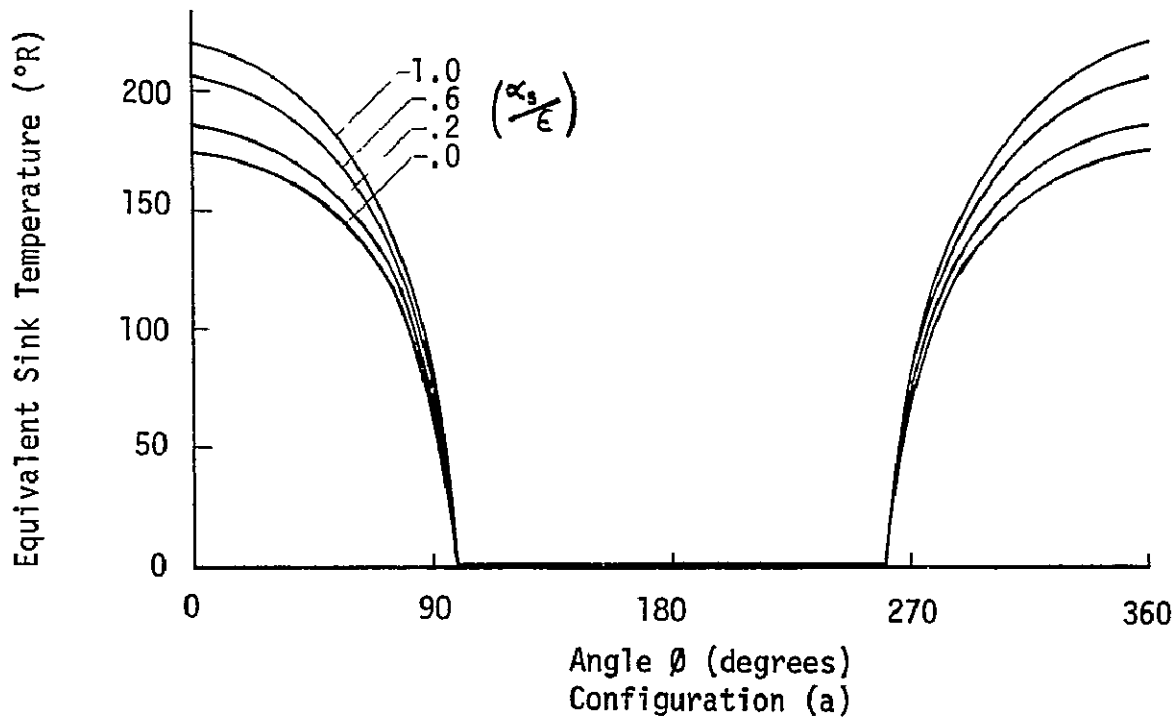


Figure IV-B-1-c-10. SPS Radiator Orientations



Note: These Configurations Correspond to Preceding Figure IV-B-1c-10.

Fig. IV-B-1-c-11. Equivalent Sink Temperature vs.
Position in Orbit

to 0.9, is shown in Figure IV-B-1-c-12. The orbital attitude of Figure IV-B-1-c-10a is assumed. This figure shows that for an average radiator temperature of 450°F (assuming radiator fluid enters at 550°F and leaves at 350°F), and an effectiveness of 0.8, the required area per unit of heat rejection is approximately $1.25 \times 10^{-3} \text{ft}^2/\text{Btu hr}$ (one side radiating). This area can be decreased, though not by a direct factor of 2, by using a radiator which dissipates heat from two sides. The effect of surface degradation from solar absorptivity of 0.25 to 0.85 is insignificant at these radiating temperatures.

2.8 The Boeing Brayton System Concept

2.81 System Description

Boeing has studied several system concepts including both the photovoltaic and Brayton cycle systems. The basic dynamic conversion concept studied by the Boeing Company involves the use of a closed Brayton cycle system, a solar collector-absorber system, and a space radiator in conjunction with the microwave sending and receiving systems. The system would be boosted into a low earth orbit (LEO), there to be partially assembled for the trip (using solar-powered electric thrusters) to geosynchronous earth orbit (GEO), where final assembly would be completed.

Figure IV-B-1-c-13 illustrates the fully deployed system. The four modules each consist of a mainframe structure formed from fold-out trusses. This primary structure supports the reflector, absorber, conversion units, and radiator system.

2.811 Solar Concentrator

The reflector, or concentrator, is made up of many individual flat facets, each driven by servoactuators mounted in the hub of each facet. Each facet is controlled about two axes, and control to within $\pm 5^\circ$ is required. A typical reflecting facet is shown in Figure IV-B-1-c-14. The plastic film reflector material is mounted on a tensioned stretch rack, the free edges of which are scalloped to provide a smoother surface.

2.812 Cavity Absorber

The approximately spherical cavity absorber is the highest-temperature component of the system. As such, its walls are covered with a 25 cm. thickness of alumina-silica insulation. This insulation is in turn covered with a titanium skin and stiffening frame. The inner walls are made of columbium and contain tubing for the Brayton cycle working fluid. The hottest temperature in the cavity is 1533K (2300F) and the fluid tube temperature varies from 980K (1300F) at the inlet to 1311K (1900F) at the outlet. In the event of a no-flow situation within the tubes, the facets are automatically turned away from the aperture. The four thermal loss sources of the absorber are re-reflection at the inner walls through the aperture, re-radiation through the aperture, back-side radiation from the outer walls, and conduction through the support

REQUIRED RADIATOR AREA
 PER UNIT HEAT REJECTED
 AS A FUNCTION OF RADIATOR TEMPERATURE
 FOR AN EQUIVALENT SINK TEMP. OF 220°R

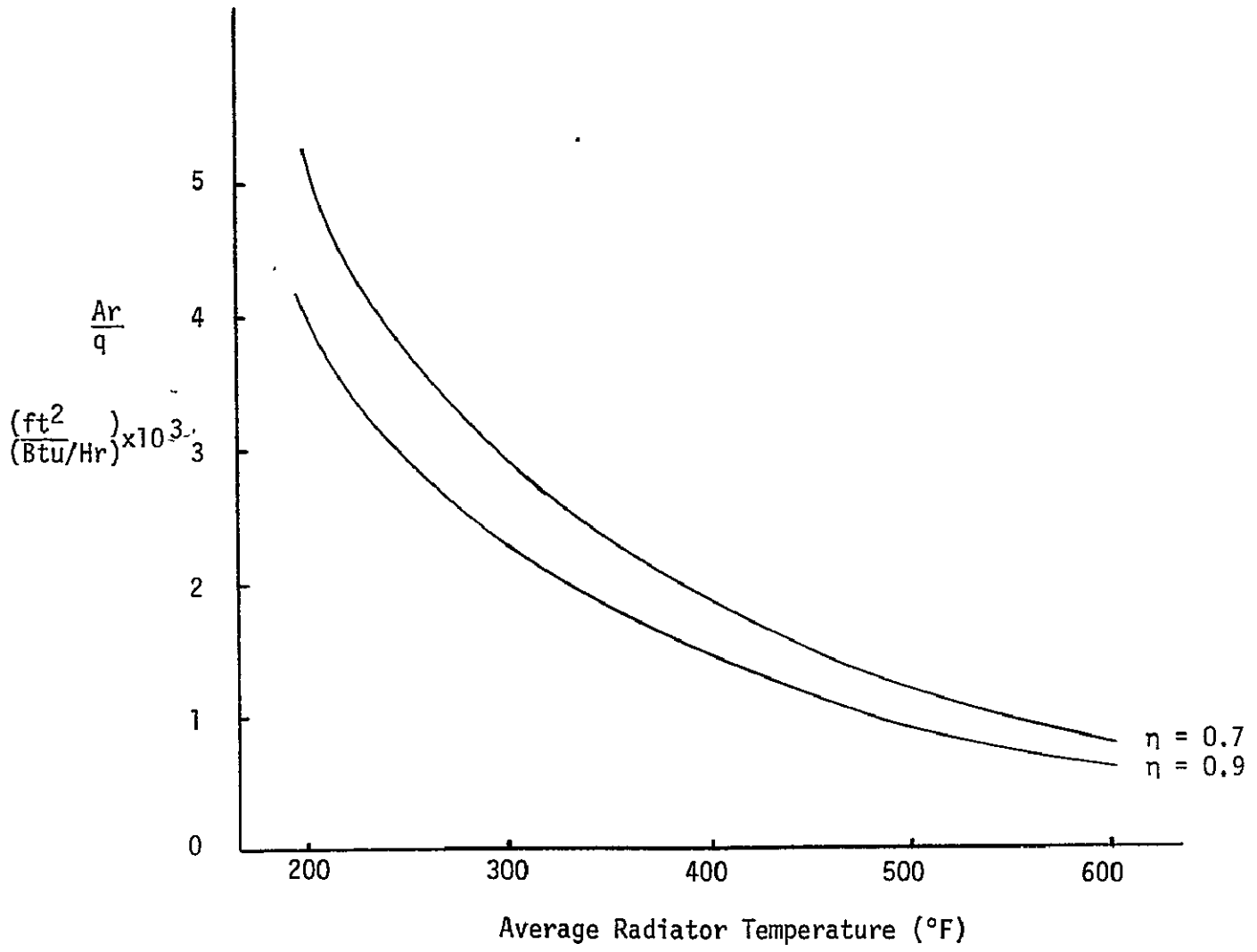


Figure IV-B-1-c-12

IV-B-1-c-25

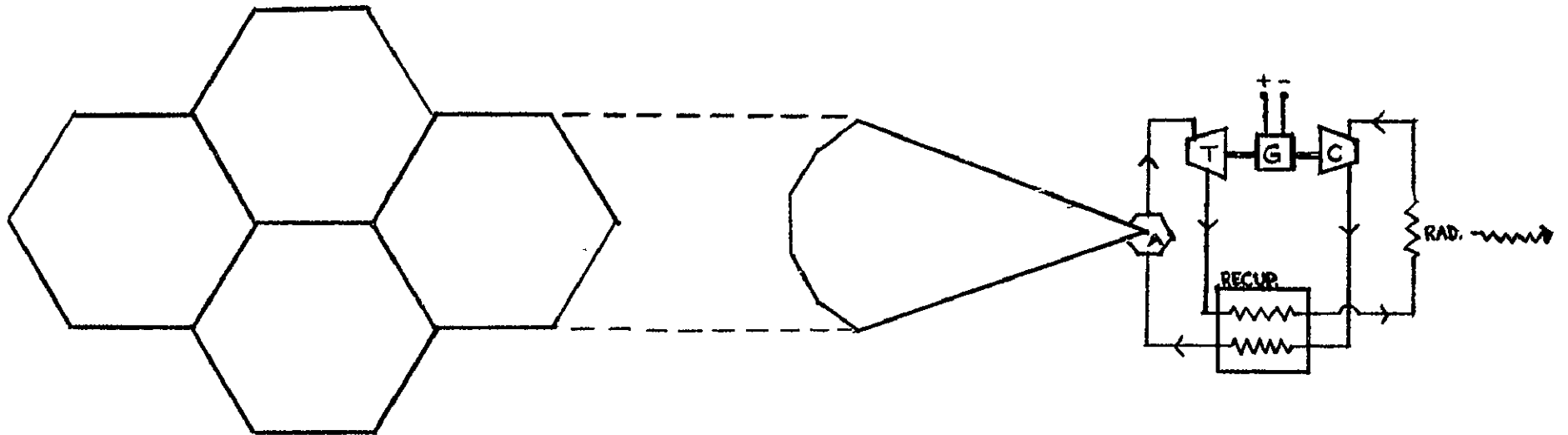


Figure IV-B-1-c-13. Schematic of Boeing Thermal Engine

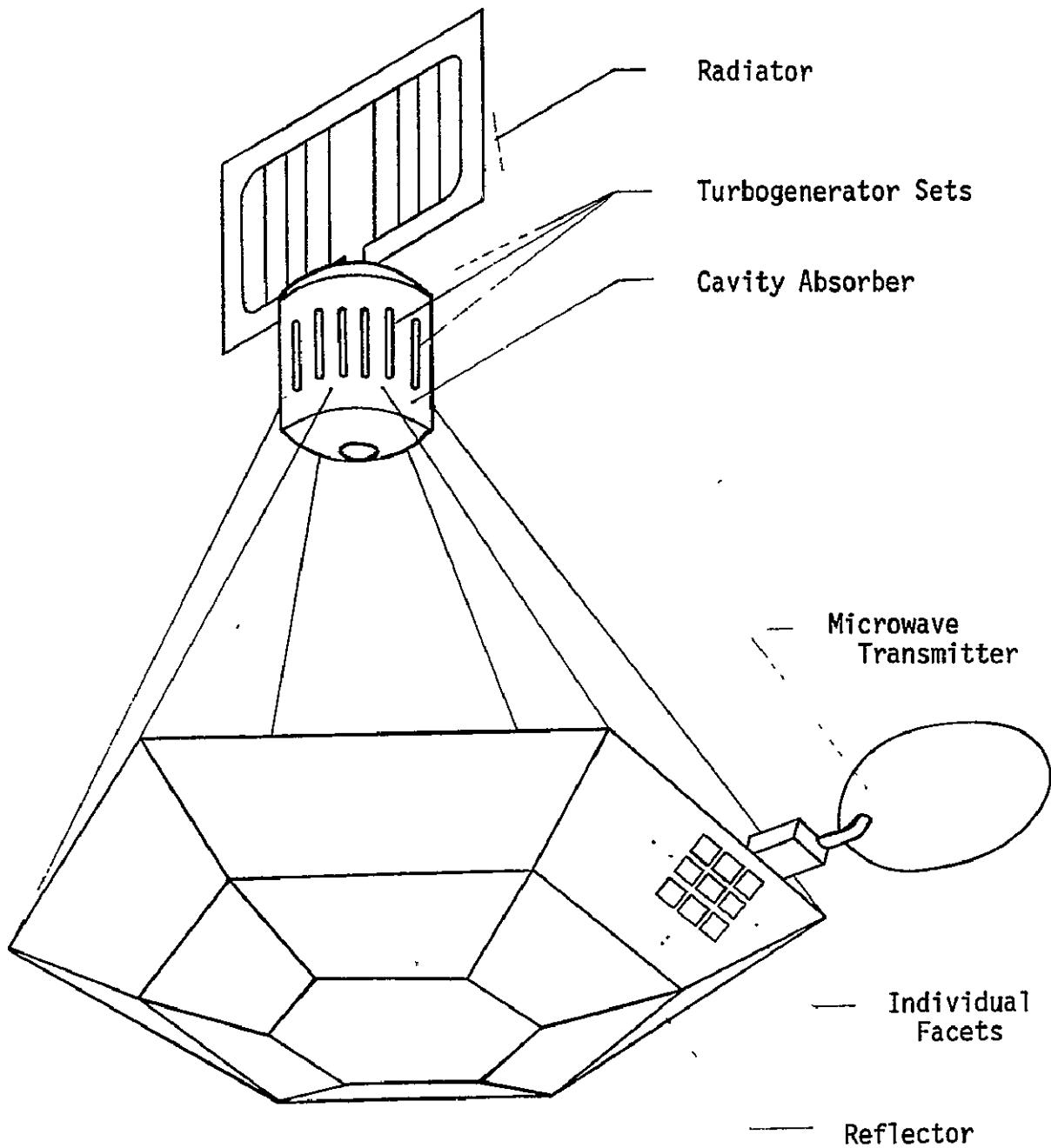


Figure IV-B-1-c-14. Typical Thermal Engine

mounts. The overall thermal efficiency of the absorber is estimated by Boeing to be 87%. In addition to reflector (facet) efficiency and absorber efficiency, a concentration penalty is involved due to the fact that the facets are flat and the surface is not a perfect mirror (the reflected energy is somewhat diffuse). Thus a "concentration efficiency" of 0.69 is used in reflector-absorber system calculations.

2.813 Thermal Engine/Generator/Radiator

The turbine, compressor and generator are mounted on a common shaft supported by gas bearings. Each turboset generates 300 Mwe. The recuperator and heat rejection heat exchanger are mounted together on the engine pallet in the latest conceptual design, which uses a liquid metal radiator fluid loop with conventional fluid pumps (liquid metals are acceptable at the low-temperature side of the cycle).

2.82 Design Characteristics

A summary of the design characteristics of the system is presented in Table IV-B-1-c-1.

Figure IV-B-1-c-15 summarizes the efficiency chain for the system, indicating an overall system efficiency from solar input to generator output of 18.3% based on 1984 technology. Using this efficiency chain, an overall energy balance for the system is shown in Figure IV-B-1-c-16. This system is designed to beam microwave energy to earth through a 1000-meter diameter transmitting antenna, where the microwave energy is then recon-verted to a net usable 10 GWe which is fed into the terrestrial grid.

2.83 Transport and Assembly Considerations

The subject of transport systems is dealt with in much detail in other sections of this report, but this section deals only with the concepts of transport and assembly as applied to the Brayton cycle conversion system.

Several concepts are currently under study for transportation and orbital assembly of the thermal engine system. One concept consists of the use of a heavy lift launch vehicle (HLLV) to get the system into low earth orbit (LEO), where it is partially assembled to provide some fraction of its total rated output to power a system of electric thrusters. Other concepts involve the use of hybrid chemical-electrical propulsion systems from LEO to GEO. But regardless, all concepts use the HLLV, a high-launch-rate/low-cost vehicle with a payload capability of between 500,000 and 1,000,000 lbs. One 300 MW turbo-compressor-alternator package would weigh close to 1,000,000 lbs implying 48 launches into LEO for the turbo units. It would then take about twice as many launches as this to get the rest of the system into LEO (heat exchangers, absorber, reflectors, auxiliaries).

TABLE IV-B-1-c-1. DESIGN CHARACTERISTICS OF BOEING BRAYTON SPS

Solar Concentrator

Effective Concentration Ratio		1,000-2,000
No. Modules		4
No. Facets per Module		10,000-25,000
Area of One Facet, m ² (ft ²)		App. 339 (app. 3650)
Facet Efficiency		0.79 (near-term) 0.84 (advanced-1984)
Module Area m ² (ft ²)	0.85 x 10 ⁶ (9.1 x 10 ⁶) 1.42 x 10 ⁶ (15.29 x 10 ⁶)	(projected) (actual)

Cavity Absorber

Maximum Diameter, m (ft)	85 (325)
Aperture Diameter, m (ft)	52 (171)
Thermal Efficiency	0.87
Maximum Temperature, K (F)	1533 (2300)

Thermal Engine/Generator

Generator Output Power, Mwe (900 Hz)	300
No. Generators Per Module or Pallet	12
Total Busbar Power, Gwe	14.4

Note: (1) Busbar power for this Boeing concept is higher than the 10 GWe used in the JSC study.

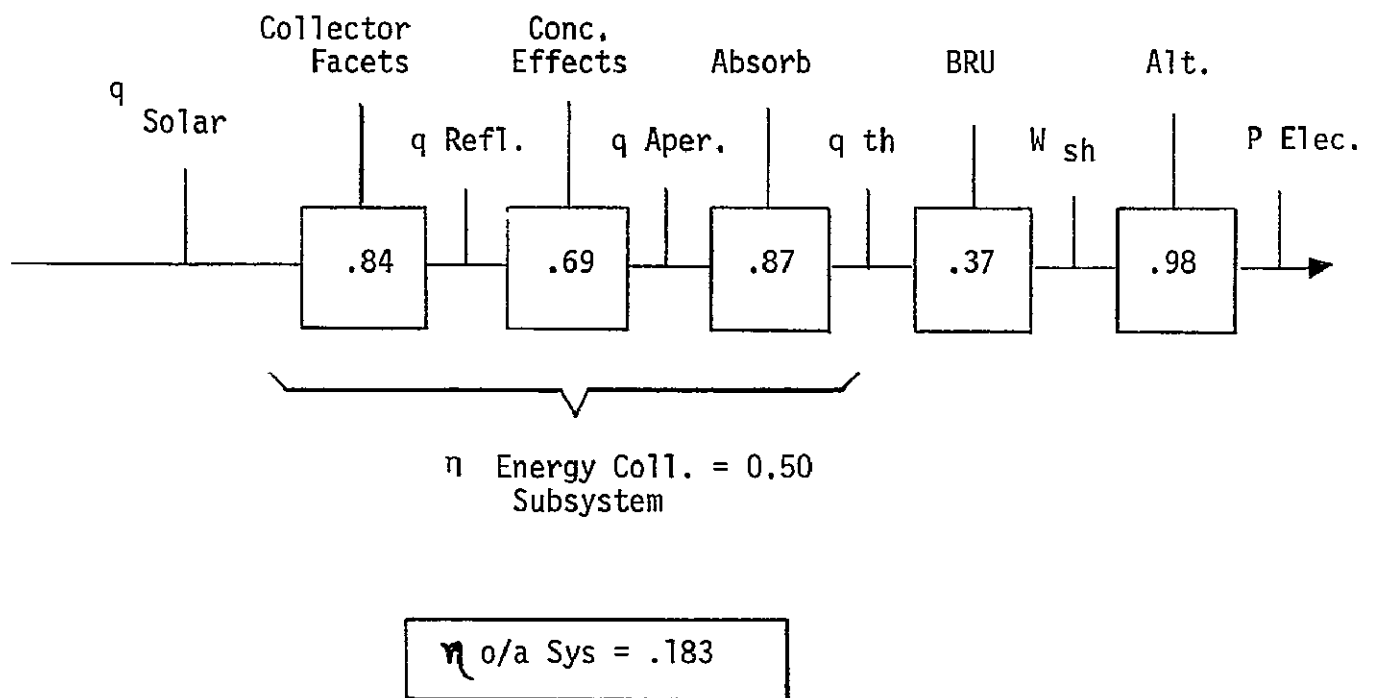


Figure IV-B-1-c-15. System Efficiency Assessment

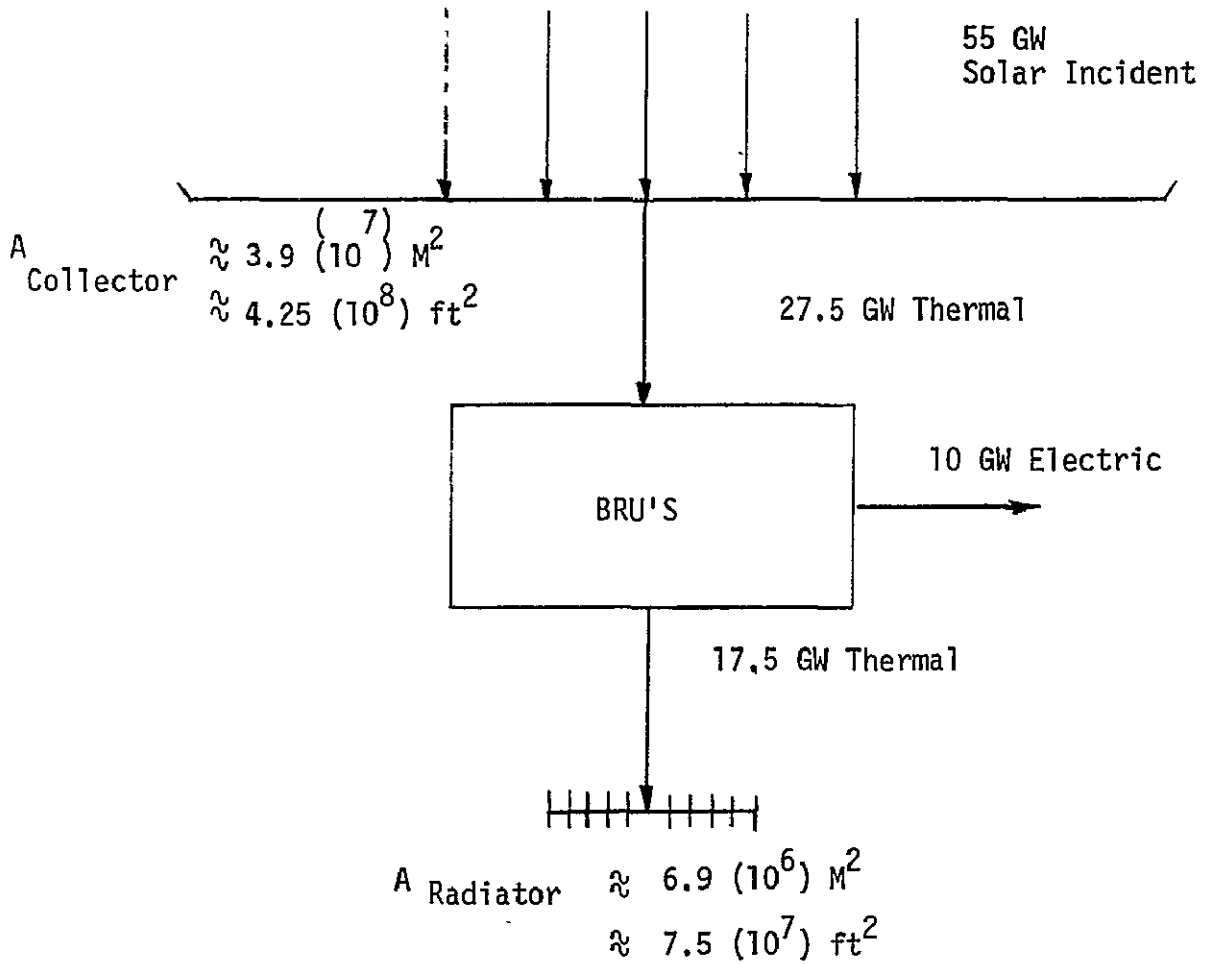


Figure IV-B-1-c-16. Overall System Energy Balance

Whether partial assembly in LEO or total assembly in GEO occurs, the system will have to be constructed in modular fashion so that as little difficulty as possible is encountered during assembly, and so that maximum transport efficiency can be achieved. This means the designer's attention must be focused on as high-density a package as possible for the collector and the radiator subsystems.

Assembly operations would be conducted by meeting each load at some distance from the station with a manned tug which would bring the load to the station and dock with it. The load would then be transferred to a predetermined location on the assembly frame and secured. After build-up of the absorber cavity, with the turbo packages mounted on it, collapsible frames would be extended to serve as a base for radiator system mounting. From the nucleus containing over 50 percent of the weight of the system, collapsed support arms are extended from the cavity for construction of the reflector subsystem, the lightest, but largest, component of the system. The four modules would be attached one to another as they are completed, and the microwave system(s) would then be assembled on the module periphery. One power satellite per year would be constructed in this manner. An orbital assembly crew supported by a space station would accomplish the assembly task. Orbital assembly benefits include the absence of large gravity loads and the advantage of being able to use vacuum processes such as electron beam welding without vacuum facilities. However, problems exist, too, with orbital assembly, mainly those of earth eclipse and gravity gradient forces.

2.84 Operations and Maintenance Aspects

Once the start sequence is initiated for the system, the turboalternators are never shut down. During periods of full sunlight (over 99% of the time), each turbogenerator produces a constant 300 Mwe. During eclipse periods (less than 1% of the time) turbopackage spinning reserve is relied upon, with thermal storage if required, to keep the shaft turning. This is to avoid start-up and shut-down of the gas bearing system, which can be done (even easier in low gravity), but which limits the life of the system. The radiator system would either have to be shuttered, which seems impractical for such a large-area system; or the fluid would be allowed to freeze; or, thermal storage for the heat rejection system could be provided.

A small amount of parasitic power would be required to operate the individual facet servos, and in the event of a fluid loop failure, the reflector facets would automatically be defocused to protect the absorber.

Make-up fluids would be supplied to the system from a tank farm attached to the station, and surface coating refurbishment or replacement would be performed by a support crew, which would also monitor system performance from a central power plant control facility and provide other maintenance functions as required.

* Latest investigation indicates that the size of the turbomachinery is such that much lower operating speeds than originally envisioned would be necessary - in which case conventional bearings may be preferable.

2.85 System Weights

A weight summary for the orbital Brayton cycle system is presented in Table IV-B-1-c-2.

2.9 Evaluation of the Boeing Brayton Concept

The two most significant challenges associated with the overall SPS concept are found in transporting the system to its ultimate geosynchronous destination and assembly of the system in space. As the subjects of transport and assembly are covered in other sections of this report, and since the Boeing concepts in these areas are still evolving, no evaluation of the Boeing transport and assembly concepts, except as related to the conversion system, is presented in this section. As such, the evaluation is essentially confined to the conversion system and its components.

Of all the reflector-concentrator concepts considered adaptable for SPS purposes (see Figure IV-B-1-c-9), individually steered flat facets such as Boeing has proposed appear to be the most feasible from the combined standpoints of efficiency, attitude control, redundancy, and life requirements. The system analysis is not yet sufficiently advanced to know with certainty the optimal number of individual facets required. From a thermal efficiency standpoint, the larger the number of facets, the better, as this more closely approximates a parabola; however, there are other considerations such as weight, packaging, assembly, cost, etc., which must be included in the final analysis. These same considerations, coupled now with reflector/concentrator inertial and attitude constraints, are important in the selection of the optimum number of modules (Boeing has chosen four). Thus, while it is too early for a quantitative decision on these items, qualitatively it is that the concept is viable. A particular area requiring further investigation is the three-dimensional aspect of the Boeing reflector/concentrator, particularly in regard to structural rigidity.

Reflector efficiency is a function of the reflectivity of the surface, geometrical imperfections, faceted construction, alignment, and degradation with time due to meteoroid punctures, high-energy particle sputtering, and low energy proton entrapment leading to bubble formation. While the reflectivity of a highly polished silvered mirror surface approaches 1.0, with polished aluminum somewhat lower at about 0.95, the aluminized plastic film proposed for the SPS has a reflectivity of between 0.85 and 0.91 (the Boeing study assumes 0.89, 1984 technology). The assumed reflectivity is reasonable, but very little is known about degradation over the 30-year lifetime of the system. Boeing states that "fortunately geosynchronous orbit lies within the bowshock of the earth, so that the low energy protons of the solar wind are not a problem. The high energy protons of the Van Allen belts will probably pass through the reflector with no effect other than sputtering. Surface erosion rates between

TABLE IV-B-1-c-2, BOEING THERMAL ENGINE SYSTEM WEIGHTS (14.4 GW System)

<u>SYSTEM WEIGHTS</u>		<u>WEIGHT, 10⁶ LB.</u>
<u>ITEM</u>		
Cavity Absorbers		
Heat Exchangers	7.10	
Wall Panels	0.94	
Insulation	1.38	
		<hr/>
		9.42
Radiators		42.00
Thermal Engines		30.29
Generators		15.14
Concentrators		38.76
Antenna		4.00
Misc. (ACS, ECS, Etc.)		<u>1.40</u>
		141.01

All weights include 20% Contingency/Growth Factor

2×10^{-8} and 0.85×10^{-10} cm^2/day have been predicted, corresponding to useful lifetime of an optical surface of between one year and 200 years, with a 'best estimate' of ten years, which we use here." Consequently, the Boeing reflector design consists of three layers of aluminized plastic film, the first two layers of which are to be discarded after ten years each of use. It is felt that the area of reflector subsystem design, with particular emphasis on long-term degradation, is one of the more critical areas in the entire thermal engine concept, and very little knowledge has been accumulated in this regard to date. This data is urgently needed. Additionally, Boeing uses (based on a 32 ft^2 facet experiment) a reduction in efficiency of 2% due to edge scalloping (to reduce surface waviness), 2% for gaps between facets, and 1% for pointing error and facet failures. These values are shown in Table IV-B-1-c-3. Without further experimentation it is difficult to argue with these numbers, except to say that facet failures alone could account for more than a 1% loss, hence the reflector should be overdesigned from an area standpoint to account for some preplanned number of facet failures (higher than 1%) over the 30-year lifetime of the system. A final point on the reflector is that much work is still required to determine (1) the range of control required for each facet due not only to relative movement between the solar vector and the main axis of the reflector, but also due to relative movement between the reflector and the absorber because of structural stiffness (or lack of), and (2) required pointing accuracy of the reflector.

Another most critical technology area in the system design is the thermal absorber, due to the fact that it is the highest-temperature component of the system. Some technology is available for small space units and larger terrestrial units, but much work remains to be done. Design optimization of very large absorbers on the order of the SPS has just begun at Boeing, but analyses must be refined to include the combined effects on system efficiency of such factors as geometrical configuration, absorption qualities, surface radiation, etc. Until such data becomes available, the assumed Boeing overall thermal efficiency of 0.87 cannot be disputed.

The technology of the Brayton thermal engine is the most extensive and well-developed of all components of the electrical conversion system. Literally tens of thousands of hours of operation have been achieved on entire Brayton systems as well as individual components, these systems including large terrestrial Brayton systems for the utilities industry. The choice of the Brayton cycle, it is felt, over the Rankine and other conversion methods for this application is a wise one. As discussed earlier, Rankine cycle technology trails that of the Brayton, and due to the ever-present corrosion problem in high-temperature liquid metal systems, inherent limitations constrain Rankine cycle systems for this application. Cycle efficiencies depend primarily on turbine inlet temperature and compressor/turbine efficiencies since other parameters such as heat rejection temperature and pressure ratio are dictated by weight and other considerations. The Boeing Brayton system baselines a 1900F

TABLE IV-B-1-c-3. Boeing-Assumed Facet Efficiency Summary

CONTRIBUTING FACTOR	NEAR TERM	ADVANCED (1984)
1) Edge Scalloping*	0.98	0.98
2) Gaps between facets	0.97	0.98
3) Specular Reflection**	0.85	0.89
4) Pointing Error, Failures	0.98	0.99
	0.79	0.84
TOTAL		

* Scalloping controls wrinkles and is helpful in reducing diffusivity.

** Energy collected within a 1° total cone angle when illuminated by a 0.50° total cone angle source.

C-3

turbine inlet (1984 technology), which is near the upper temperature limit for the superalloys. The Oberhausen Brayton unit in Europe has been in operation for 11 years with a turbine inlet temperature of 1310F and air as the working fluid. With an inert gas working fluid it is felt that the Oberhausen technology could be extrapolated to build an SPS turbine with a 1600F inlet temperature. Increases in materials technology would be required for a 1900F turbine, particularly since the absorber would have to operate at 2300F, but it is not unreasonable to assume, based on past technology increases, that technology advances in superalloys and refractories will occur within the next ten years, which will make the 1900F turbine inlet reasonable for the SPS. Small gains in absorber efficiency, coupled with advanced aerodynamic turbine and compressor design techniques, will contribute to an increase in overall system efficiency. More exotic schemes such as cooling of turbine blades, ceramic turbine parts, and advanced recuperator materials are also possibilities for the future.

The Boeing-study-assumed turbo-compressor-generator package size of approximately 300 MW per unit is consistent with NASA projections for maximum payload weight in the HLLV (1,000,000 lbs) and is based on a specific weight for the machine of 3.3 lb/kW.

The heat rejection concept originally proposed by Boeing was a gas radiator system in which the working fluid was piped directly to the radiator panels where heat pipes were employed to distribute heat to the fins. The gas radiator was favored because even though the pressurized gas tubes were somewhat larger and heavier than liquid tubes, the heavy interface heat exchanger involved with the use of the liquid loop was avoided. However, as preliminary design studies progressed, it became evident that since the recuperator had to essentially be in a pressure vessel, a liquid loop would not be as heavy as originally thought since the interface heat exchanger could be included in that same pressure vessel. When this was realized, the liquid radiator system began to look more attractive from standpoints other than weight, such as working fluid pressure drop and meteoroid protection. To meet SPS life requirements, a liquid metal, as opposed to a conventional organic fluid, was chosen. Further, conventional electrically driven fluid pumps were baselined to flow the liquid through the radiator system. It is felt that the liquid radiator system is a good choice. Abundant technology on fin-tube space radiator systems exists, and scale-up to the order of the SPS involves only problems of engineering design and not new technology. Adequate surface coatings for the 30-year life requirement may be a problem. Excellent radiator surface coatings are presently available for space radiator systems, but 30-year endurability has not been proven. In the event a chosen coating has life limitations; e.g., due to damage by ultraviolet radiation, a coating maintenance program would be considered, and this is not an insurmountable problem. Statistical data on meteoroid damage is available, but more data is needed at geosynchronous altitude. This, too, will be available in time, and meteoroid protection to accommodate these environmental conditions is an engineering design, and not a technology problem.

The choice of a liquid metal heat transport fluid over a conventional organic fluid in the radiator is a necessary one due to the inherent life limitation of the conventional fluids, a problem which is aggravated by temperature. The temperature of the fluid in the radiator must be held fairly high (350 to 550F) to reduce this major weight component. Although liquid metals should be used only if no other fluids are adequate, this choice seems best at present for the thermal engine. The corrosion problem does not exist at the low-temperature end of the cycle as it does at the upper end. The final fluid choice need not be made now, although if freezing turns out not to be a problem during periods of eclipse, the familiar NaK-78 may be a good selection. If freezing is a problem, some mixture such as Cesium-Nak could be used to lower the freezing point of the fluid. The Boeing study to date makes no mention of thermal storage requirements (if any) for eclipse periods, and this problem must be addressed. During the semi-annual eclipse periods, the rotating turbo-machinery would probably be kept spinning to avoid start-up and shut-down damage to the bearings. The turbogenerator set would thus act as a flywheel energy storage system whose stored energy would be released to supply bearing and windage losses in a no-load condition. Spinning reserve for a large gas turbine system such as this is expected to be below 4% of output power. If this spinning reserve is not sufficient for the maximum 75 min/day eclipse period, then supplementary heat storage would have to be provided. During the no-load condition, unless the radiating surfaces of the heat rejection subsystem are covered in some manner, the radiator will continue to reject large amounts of energy to space. If it is determined that freezing in the radiator cannot be tolerated, then significant thermal storage material will have to be included as an integral part of the radiator design. If freezing can be permitted, then by judicious choice of the heat transport fluid and careful consideration of the thermostructural design of the heat rejection system, the radiator can be made much lighter and more compact. Since the radiator is the heaviest component of the system, its optimization is very important. The Boeing work available to date makes no mention of any of these important aspects of radiator design. Furthermore, it is felt that the conventional fluid pump in the radiator loop is not adequate. For lifetimes on the order of the SPS requirement, conventional pump components are much inferior to the electromagnetic (EM) pump. Although the EM pump has a much lower efficiency than that of a conventional fluid pump, the life requirement in this case would be foremost, and the EM pump, with no moving parts, is considered the only type capable of meeting the life requirement.

A final consideration in evaluating the Boeing study is its lack of mention of the use of cryogenically cooled superconducting generators and superconducting cables for power transmission to the microwave system. While still in a very early development state, a closed-cycle superconducting system for both electrical power generation and transmission, even with its associated liquefaction plant, has an enormous weight-saving

potential for a system as large as the SPS. The proposed generators weigh approximately 1.6 lb/kW. Cryogenic superconducting generators could reduce this specific weight to at least 50% of that of the proposed generators.¹¹

IV-B-1-c-3.0 Conclusions and Recommendations

The preceding analysis indicates that a number of "thermal engine" conversion concepts are potentially available; however, the closed Brayton cycle stands out as the most promising option.

Of the several reflector concepts discussed, the faceted and the tensioned net systems appear most attractive. Much analysis remains to be done on the reflector and cavity-type absorber as these are the components for which the least work has been done to date.

A heat rejection system comprised of a fin-tube radiator coupled to a Brayton cycle heat exchanger through a low-temperature liquid metal fluid loop powered by an electromagnetic pump appears feasible for satisfying SPS requirements. Much work remains on devising new methods of weight optimization for the radiator, as this is the heaviest single component of the system.

In view of its favorable characteristics for SPS application, the closed Brayton cycle system approach should be pursued in parallel with photovoltaic system studies.

References

1. Peter E. Glaser, "The Satellite Solar Power Station - A Focus for Future Space Activities," Presentation to the Subcommittee on Space Science and Applications of the Committee on Science and Technology, U.S. House of Representatives, July 22, 1975.
2. H. M. Dieckamp, Nuclear Space Power Systems (published by Atomics International, Canoga Park, California, September 1967), p.24.
3. The Garrett Corporation, "Closed Cycle Gas Turbine Status," MS3736-0, June 1975.
4. K. Bammert and G. Groschup, "Status Report on Closed-Cycle Power Plants in the Federal Republic of Germany," paper presented at 21st Annual International Gas Turbine Conference, March 21-25, 1976, New Orleans, U.S.A.
5. W. Z. Black and W. Wulff, "Study of Design Parameters of Space Base and Space Shuttle Heat Rejection Systems," Contract NAS9-10415, February 1971.
6. D. B. Mackay, Design of Space Powerplants, p. 221 ff.
7. G. R. Woodcock and D. L. Gregory, "Derivation of a Total Satellite Energy System," AIAA paper 75-640, April 24, 1975.
8. Selected Technology for the Electric Power Industry, NASA SP-5057, September 1968.
9. Combustion and Propulsion, Sixth Agard Colloquium; Energy Sources and Energy Conversion; Cannes, France; March 16-20, 1964; "Solar Collector Limitations," by Schrenk, and "Limitations des Collecteurs Solaires," by Trombe and Grives.
10. G. R. Woodcock and D. L. Gregory, "Orbital Solar Energy Technology Advances," Record of the Tenth Intersociety Energy Conversion Engineering Conference (Energy 10), Newark, Delaware, August 1975.
11. Appleton, A. and Anderson, A., in Proc. of 1972 App. Supercond. Conf., Annapolis, Md., IEEE Pub. 72CH0682-5-TABSC (1972).

IV Power Station System
B. Collection Module Photovoltaic
(2) Power Distribution

R. C. Kennedy
Control Systems Development Division

Introduction

The collection module distribution system as discussed here includes the power busses and any regulation and control equipment external to the solar cell blankets. Its primary function is to provide the conductive path between the blanket modules and the transmitting antenna gimbal joint. Conceptually, the system will comprise a matrix of large continuous conductor busses with a maximum current level of several hundred thousand amperes at the gimbal. Any switching or power regulation required of the distribution system will be done at the interface where the blanket modules feed to the busses. Amperage levels at this interface will be only a few thousand amperes. No switching or other power control will be attempted on the main busses.

The nominal operating voltage for the station was arbitrarily set at 40 KV. Previous studies chose a 20 KV level presumably to match the operating voltage of the Amplitron DC-RF converter. In this study, the Klystron was the preferred converter and is directly compatible with the selected operating voltage. It remains the subject of much research and analysis to determine if 40 KV, or even 20 KV, is a practical operating voltage of the station. The plasma environment, both natural and artificial, surrounding the station will interact with unprotected busses and result in power losses (leakage) and, under adverse conditions, breakdown may occur causing potentially dangerous arcing between conductors. The quantitative assessment of plasma effects is beyond the scope of this study and, except for recognition of the problem, will not be treated further.

Conventional metallic conductor material was selected for the bus structure. Cryogenic superconductor systems were not seriously considered because of the complexity and reliability of the refrigeration system. Weight trades were not conducted, but it is thought that the overall cryogenic superconductor system would show only a marginal advantage. The eventual development of room temperature superconductors has been speculated upon, but there is no evidence that technology will produce usable materials for application to this program.

The product of electrical resistivity and weight density was used as a figure of merit to select the conductor material. The following table shows this parameter for candidate conventional materials at room temperatures.

TABLE IV-B-2-1

<u>Material</u>	<u>$\sigma(\text{ohm-cm}^2/\text{cm}) \times \rho(\text{gm/cm}^3) \times 10^8$</u>
Pure aluminum	1993
Structural aluminum	2900
Copper	4235
Silver	4530

This table shows that pure aluminum is the most weight-efficient material to use as a conductor to minimize resistive losses. A similar figure of merit combining density and thermal conductivity would show that aluminum is superior for passive radiative cooling.

Based on the above, pure aluminum has been selected as the nominal conductor material with structural (6061) aluminum to be used if the electrical busses are integrated with a load-carrying structure. The desirability of integrating the distribution system with the structure or other subsystem components needs to be evaluated at the configuration synthesis level since it is not clear, at this point, that the advantages outweigh the problems associated with the integration. A key will be the weight savings which can be obtained by integration. If only a small percentage of the total configuration weight can be saved, it may be more appropriate to minimize the integration aspects until more of the total problem is understood.

System Conductor Weight

The technique used to establish the overall bus system weight was to find an "optimum" current density (amperage per cross-sectional area of conductor) which would minimize the bus weight relative to resistance (I^2R) losses. That is, for a given current flow, the weight of conductor material (W_B) can be reduced by permitting larger current densities with attendant increases in temperature and I^2R losses. Temperature considerations aside, a convenient method of rapidly arriving at an acceptable current density is to assume that the power losses will have to be made up by additional solar array area and that the area will weigh K gm/watt. The additional weight (W_A) to compensate for the I^2R losses will be:

$$W_A = K (\text{power loss}) = K\sigma\epsilon LI$$

- where σ = resistivity
- L = bus length
- ϵ = current density
- I = amperage

and the total equivalent weight (W_E) is

$$\begin{aligned} W_E &= W_B + W_A \\ &= LI (\rho/\epsilon + K\sigma\epsilon) \end{aligned}$$

Differentiating and solving for the value of ϵ to minimize W_E yields

$$\epsilon = \sqrt{\rho/K\sigma}$$

Note that this parameter is independent of the configuration geometry.

For pure aluminum at 100°F, and with a solar array weight-to-power ratio of 2.13 gm/watt, the resulting current density is 558 amp/cm². This value was used to design the bus structure, and for a given bus configuration and geometry, a quick check of the cooling was made to insure that the system would run at, or below, the design temperature.

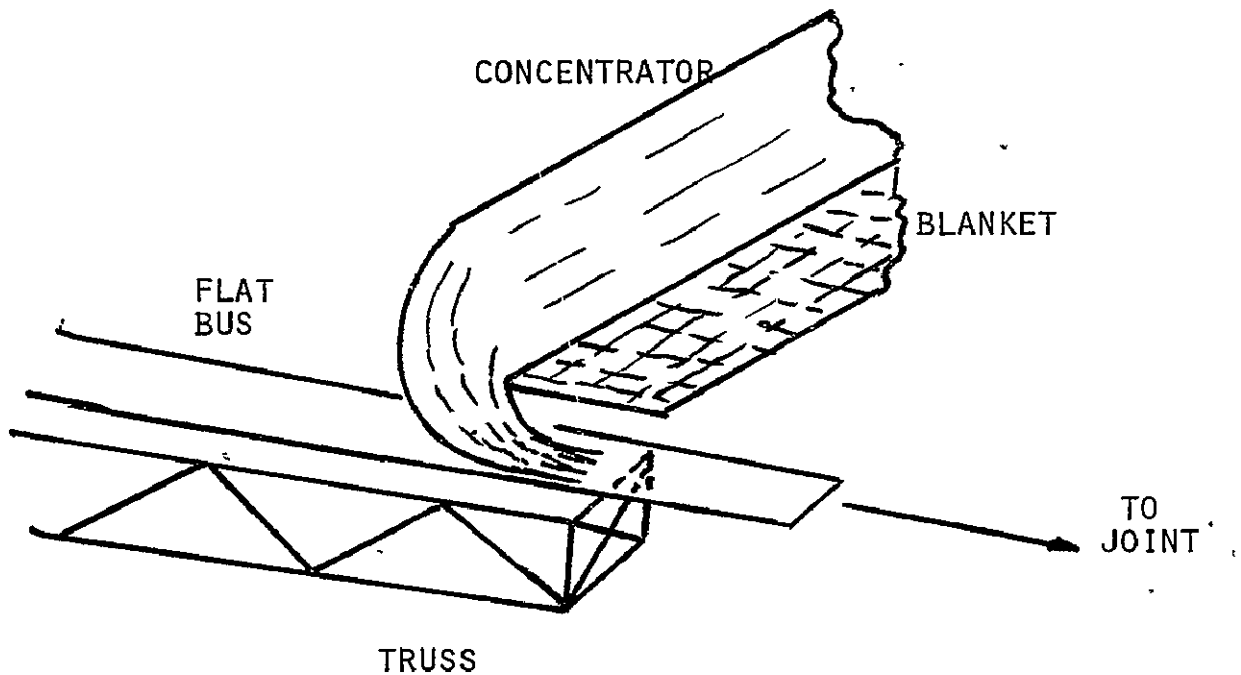
Conductor Bus Design Concepts

The preceding section developed the distribution bus system based on the assumption of constant current density which specifies the amount of material required for the conduction of electricity. The geometrical shape of the conductor is largely a thermal problem. The ideal geometry is a thin flat sheet since it maximizes the radiative surface area to cross-section area. Alternately, large diameter thin-walled tubes are attractive if the bus is to become a structural member.

The thin flat sheet geometry leads to the consideration of using the aluminum solar array concentrators as conductors. A one-half mil thickness will provide sufficient cross-section to maintain the current density at the specified level for the configurations analyzed and are ideally oriented for passive cooling. While this concept offers a significant weight savings, several problems require additional research. For example, it may be difficult to maintain uniform current distribution and uniform resistivity throughout the conductor. Nonuniform effects could cause localized heating and adverse distortion of the reflective surface. A design compromise may be possible which would increase the thickness beyond that required for a concentrator in order to provide better electrical, thermal, and mechanical properties.

If the "conductive foil" concept proves valid, the flat sheet geometry can be extended to the main bus system carrying power to the transmitting antenna. If the load-carrying structural truss cross-section is square or rectangular, the flat sheet conductors would be attached to the sides of the load-carrying structural truss. The juncture between the concentrator and the main bus is a curved sheet extension of the reflector surface transitioning smoothly to the main bus for electrical continuity

(see sketch). Near the antenna, the main busses would have to be formed into a "funnel" shape terminating in a cylindrical tube to conform to the rotary joint design.



SKETCH

The extent of insulation required has not been established. It will undoubtedly be required on busses at different potentials in the near proximity to each other. The major uncertainty is the insulation required to protect against plasma effects. If this proves to be necessary, it will mean a major weight penalty since it will be required over much of the distribution system. Insulation of the conductors will also aggravate the thermal problem and may require active cooling. Punctures from meteorites will also cause leakage paths. Lewis Research Center personnel who have been studying this problem indicate that, due to a "funneling" effect, the severity of the leakage may be much more than anticipated from small pin-hole size punctures.

Configuration Weight/Performance Summary

System weights were calculated for the configuration shown in figure IV-B-2-1. In this concept, the concentrators are along the vertical and the solar array channels are 0.5 km wide. The nominal operating voltage is

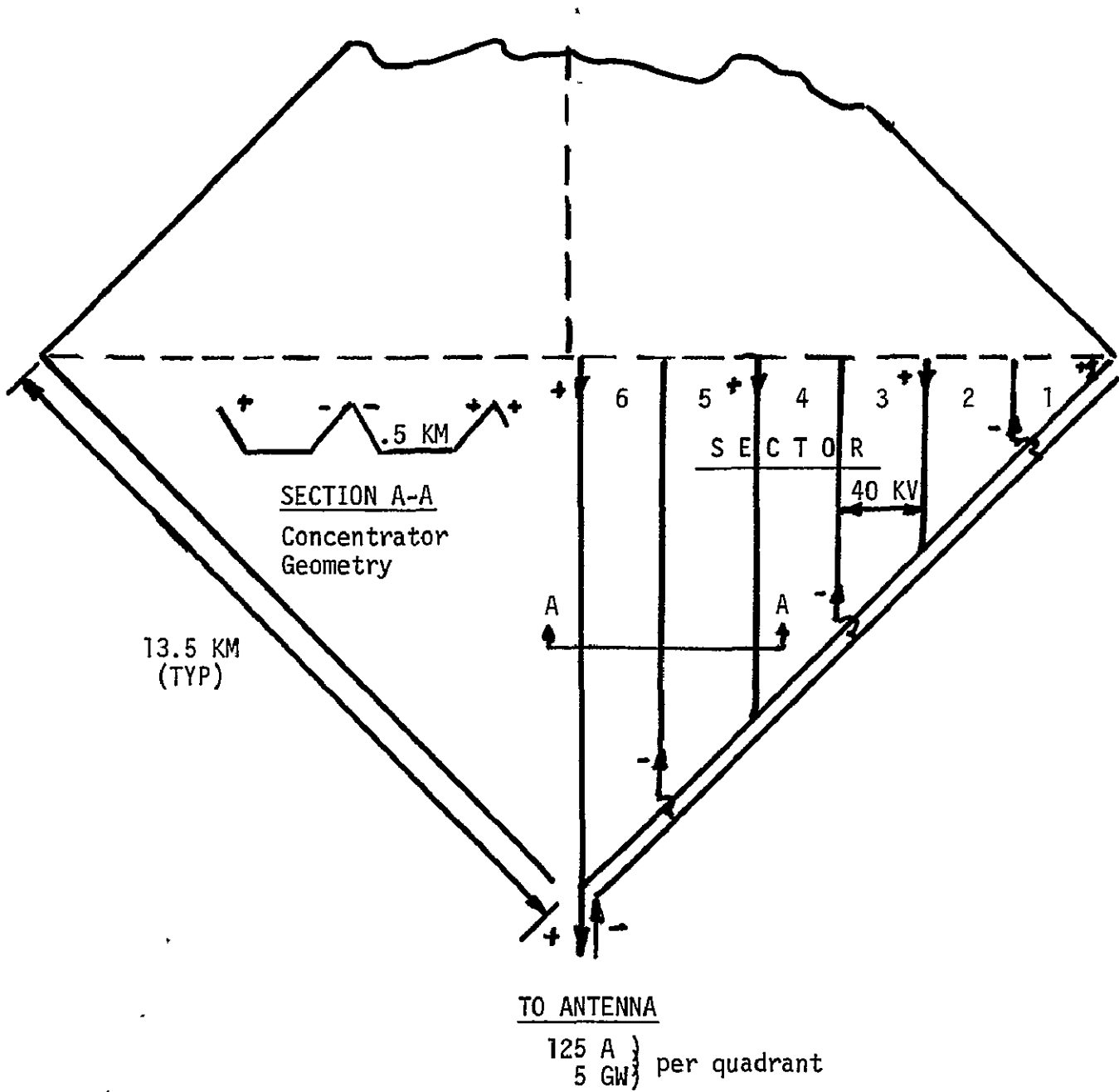


Figure IV-B-2-1. Circuit Schematic for Single Quadrant

40 KV and develops approximately 5 GW from each quadrant of the station (10 GW per antenna). Power is collected from the solar arrays by a series of busses along the vertical. These feed a main diagonal bus for transmission to the antenna. Return lines parallel the collector lines.

With solar array performance of 250 watts/meter² (concentration ratio of 2), the following table shows the ideal power output and maximum amperage for each sector indicated on the figure.

<u>Sector</u>	<u>Power Out (Watts x 10⁶)</u>	<u>Max Amps x 10³</u>
1	192	4.8
2	449	11.2
3	704	17.6
4	962	24.1
5	1217	30.4
6	1475	36.9
	<hr/> 5000	<hr/> 125.0

Distribution bus weights (W_B) are calculated for aluminum using the constant current density previously determined:

$$W_B = \rho/\epsilon \sum_{i=1}^{i=n} L_i I_i$$

where $L_i I_i$ is the current length for the (n) individual conductors.

The busses which collect power from the solar arrays are assumed to have a linearly increasing current from zero to the maximum value at the main bus juncture. The main bus is assumed to have a step increase in cross-section area at the junctures in order to maintain constant current density.

Total configuration system weights are as follows:

<u>Component</u>	<u>Weight (Kgm x 10⁶)</u>
Diagonal busses	2.06
Main busses	1.75
Insulation, control equipment (2% of conductor weight)	0.08
	<hr/> 3.89

This weight is on the order of 7 percent of total configuration weight. If means can be found to use the concentrators as conductors, this will reduce to 3-4 percent. Total power loss (I^2R losses only) are about

1700 MW. With a nominal 20 GW being developed, the system transmission efficiency is 92 percent. Switching and other control equipment will operate at 95-99 percent.

Technology Status

Other than the previously mentioned unknowns regarding the effect of the plasma environment on system operation, the principal technology issues are the methods of power switching and power transfer across the rotating joint. The conductor bus system does not appear to present a major obstacle although the concept of using thin, flat conductors needs additional research and concept verification.

The switch problem stems from the operation at extremely high power levels and the characteristic of the d.c. current not passing through zero (as with alternating current) at the switching point. Ground switching systems utilize a variety of techniques to extinguish arcs during contact opening with the most popular techniques being oil cooling and magnetic blowout. The latter places a magnetic field across the superheated ionized path to lengthen the arc distance and displace it to a cooler region. Neither technique is particularly attractive for this application.

Solid-state technology offers the best potential, but currently available switches are limited to a few hundred amps at a few thousand volts. However, developmental programs are underway, for d.c. ground system applications, which have switched currents of 2000 amps at voltage levels above 100 KV. The basis for the switching technique is to momentarily shunt the current to a resistive bank while the interrupter switch is activated. This and other similar techniques should provide the basic technology around which a device for specific SPS application can be tailored.

The joint design employs conventional slip rings for power transfer. If the current density across the gap is maintained at less than 300 amps per square inch, the slip ring approach should be (electrically) satisfactory. Mechanically and thermally the joint presents a severe design problem. It is proposed that the complete joint system stand alone as a technology item and that new power transfer technologies such as liquid metals be addressed as components of the joint technology program.

Finally, the analysis of electromagnetic field effects can be properly categorized as a technology item. Although the basic field mechanisms are understood, the rigorous analysis of the effects will require extensive math modeling and simulation. Of interest are effects which cause a redistribution of current within the conductor from either its own field or proximity fields of other conductors. Nonuniform current densities will cause additional resistive losses and localized heating. Mechanical stress and force interactions between closely spaced conductors need to be analyzed in some detail to insure that the distribution system

is mechanically, as well as electrically, sound. Finally, the interaction of the overall station field with the external Earth magnetic field requires analysis to assess the disturbance torques which will have to be accommodated in the design of the control system.

IV-B-3. Structure

a. Introduction

Objective consideration of the concept of solar power stations in space involves many scientific principles, and requires an awareness of current and feasible technology, experience in the practical aspects of accomplishing major endeavors, and the perspectives of future energy demands and the economic validity of alternative approaches. In considering the structure for a solar power station, it is essential to dispose of preconceived ideas of structures based on terrestrial experience, and to focus instead on concepts which address the design requirements. Some background information is available from studies performed by Arthur D. Little Inc., the Boeing Company, and the JSC Pilot Plant Study (reference 1-3).

The geosynchronous orbit environment is characterized by a hard vacuum, the energy and mass fluxes from the sun, and the earth's gravitational field, magnetic field and thermal radiation. Operating loads on the primary structure are markedly low thereby increasing the significance of transportation, assembly and maintenance loads. The large scale of a solar power station emphasizes potential dynamic characteristics which must be addressed in the design of its structure. In addition, since local temperatures are established almost entirely by radiation exchange, the design of structural elements and their thermal control are intimately coupled.

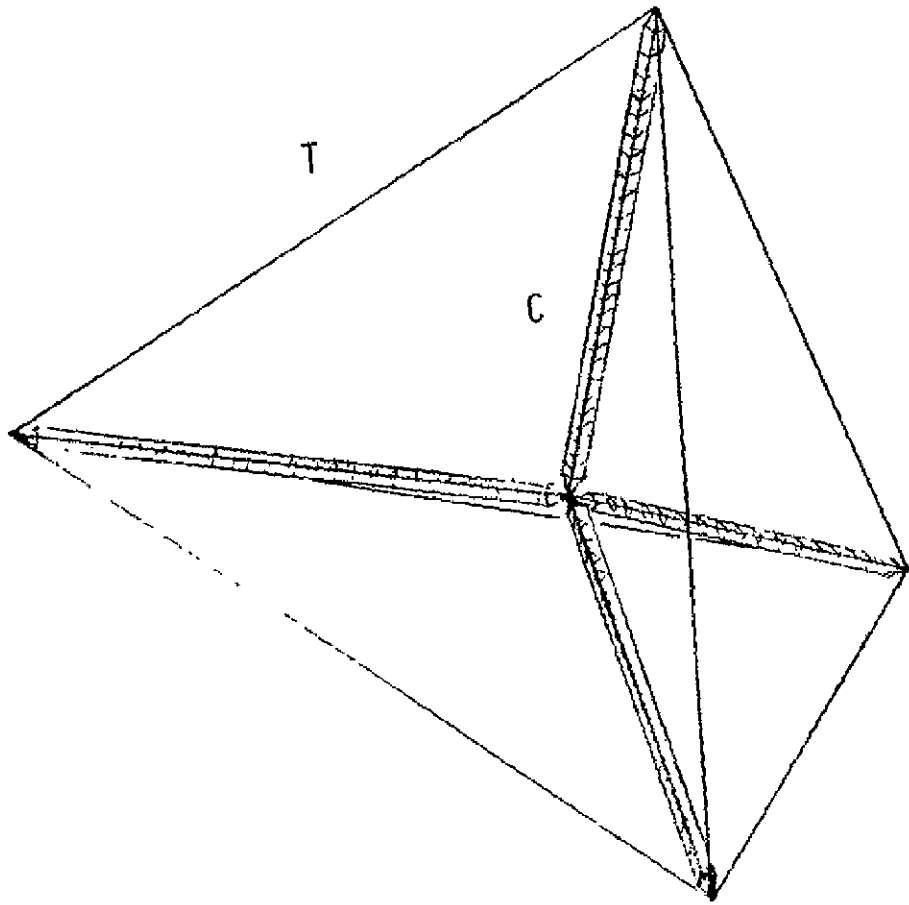
The general requirements of the structure are: (1) maintain the overall and local integrity of the configuration to collect or focus the relatively diffuse solar energy flux (1.4 GW/km^2) and (2) minimize capital investment through a light-weight system which offers an ease of construction for both the structure and the array. This leads to an ironical statement of the structural requirements: structural stiffness and conceptual flexibility. The lifetime of the structure is a materials requirement to withstand the ultraviolet and hard radiation environment and the thermal transients associated with occultation.

The vast size of the solar power station array and the general structural requirements lead directly to an open structure for light-weight and to a three-dimensional structure for stiffness. Within this category, two structural concepts have been investigated: one providing a maximum concentration of load paths and a second possessing a minimum concentration of load paths. Both concepts achieve a light-weight structure within the limitation of large scale, low loads, minimum gauge considerations and high structural efficiency.

The first and lightest structural concept makes maximum use of the most efficient structural element, the cable, and a minimum use of buckling limited compression members. The lightest structural configuration using this concept to provide three-dimensional stiffness (over a given cross-sectional area) is a tetrahedron formed by tension lines and held in place by four compression members extending from the centroid to each vertex. This configuration is shown schematically in figure IV-B-3-1. This structural concept and the idea of minimizing gravity gradient torque has led to the column/cable configuration shown in figure IV-B-3-2. The secondary structure for this configuration is conceptually a three-dimensional spider web of tension lines to maintain local configurational integrity, overcome electrical current interaction forces, and to provide sufficient membrane stress for dynamic stability of the array.

The second structural concept possesses a uniform pattern of structural "hard points" characterized by a "planar" truss. The distributed solar

IV-B-3-2



$$\text{BASE AREA} = \frac{16C^2}{9\sqrt{3}} = \frac{\sqrt{3}}{4} T^2$$

FIGURE IV-B-3-1 OPTIMUM STRUCTURAL CONFIGURATION FOR THREE-DIMENSIONAL STIFFNESS

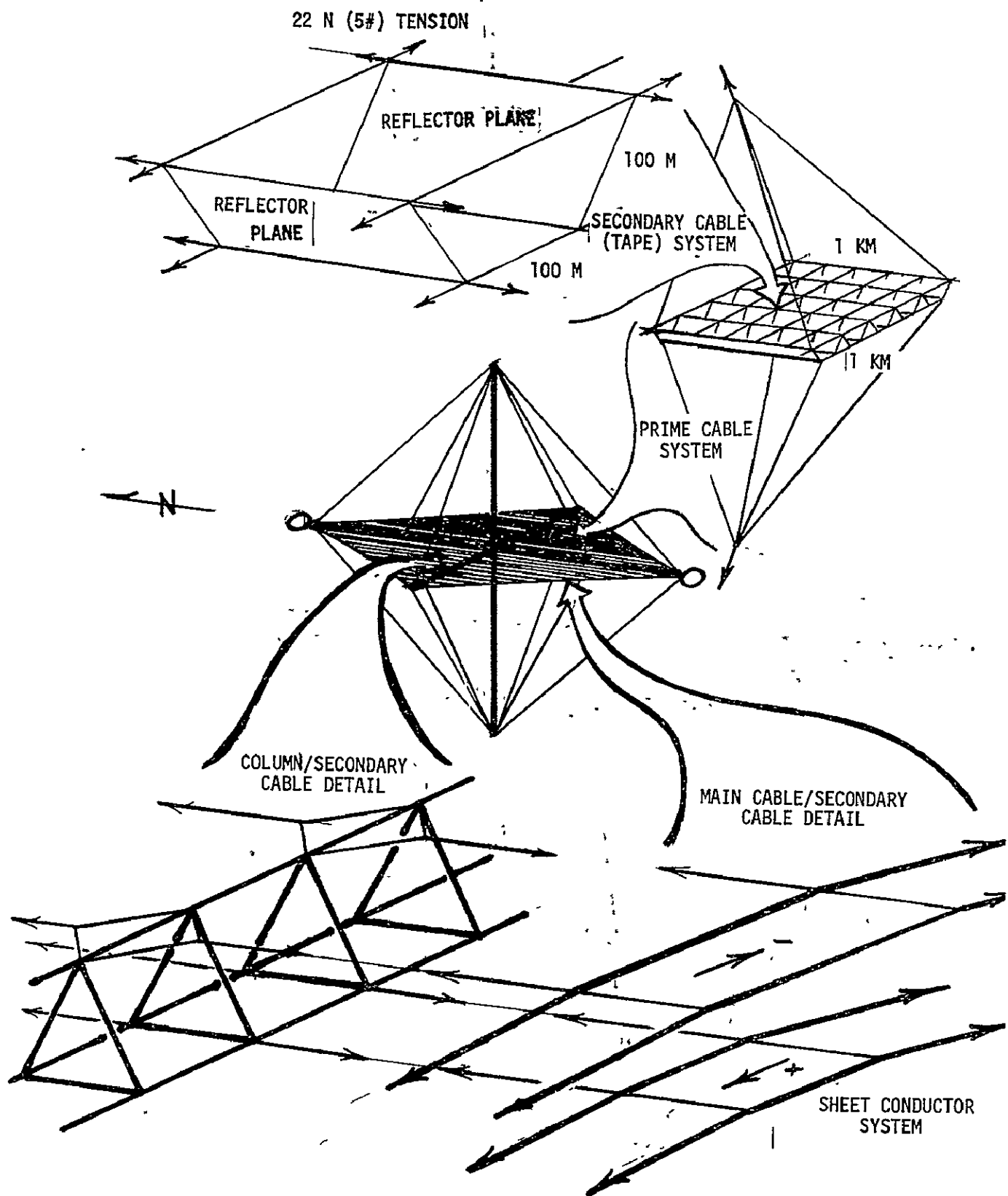


FIGURE IV-B3-2 COLUMN/CABLE CONFIGURATION
IV-B-3-3

cell array is thus provided short load paths for inertial loadings. The limits of dynamic stability for the overall array establish the planar truss compressive element design. This is a less efficient structural concept from the standpoint of structural weight alone; however, potential advantages exist for the power distribution system and for assembly efficiency due to the repetitiveness of the configuration. This is similar to the structural design approach used in the A. D. Little SSPS study (reference 1) and forms the basis for the "truss" configuration shown in figure IV-B-3-3.

Although weight is a prime cost driver for the SPS structure, the column/cable and truss configuration structural weights are respectively less than 1 percent and 3 percent of the total system weights. Therefore, it is plausible that total system costs may be lower with a less efficient but more versatile structure. Requirements of transportation, assembly, quality control, manufacturing, etc. may add structural weight but lower overall costs.

The technology relationship between SPS structure and aircraft structure can be likened to the relationship between aircraft structure and the structure of a bridge. The structure for a solar power station will be totally different from conventional aircraft or spacecraft design. However, there are no major technological problems in the array structure which cannot be solved through development and test programs demonstrating construction, assembly, and material qualifications prior to SPS initiation.

b. Loads, Environment, and Dynamics

There are three primary natural loads to consider for a large satellite in geosynchronous orbit:

Gravity gradient forces on a system oriented perpendicular to the orbit plane cause a torque about the axis normal to the orbit plane which is cyclic over a 12-hour period. For a truss configuration sized for a 10 GW ground output, this torque would have a maximum magnitude of about 1.2-million N-m over the period, requiring a maximum control force of about 100 N applied out at the corners of the array. The gravity gradient also produces a 12-hour cycle of tensile force in the array which peaks at about 50 N. Attitude control is simplified if the moments of inertia about orthogonal axis are equal. The gravity gradient tends to stabilize the configuration in the direction of the maximum moment of inertia.

If it turns out that initial construction in a lower orbit is less costly than geosynchronous construction, gravity gradient torques are more troublesome if allowed to exist, since torques are about 230 times as great at 500 km as they are at geosynchronous altitude. Consequently, the station would probably be held horizontally during construction, minimizing or eliminating torques from this source.

Solar radiation pressure causes an evenly distributed force of about 600 N on a satellite of this size, but it results primarily in a perturbation to the orbit, tending to make the orbit slightly eccentric. However, because of the tremendous difference in area/mass ratios of the solar array and antenna, solar pressure would cause a shear force of about 90 N maximum between the array and the antenna. In addition, substantial torques can be created if the center of mass and the center of pressure are not coincident in the system.

Solar and lunar gravity and the earth's equatorial ellipticity cause substantial orbit perturbations but do not create any significant structural loads. Atmospheric drag at geosynchronous altitude is negligible. Drag,

IV-B-3-5

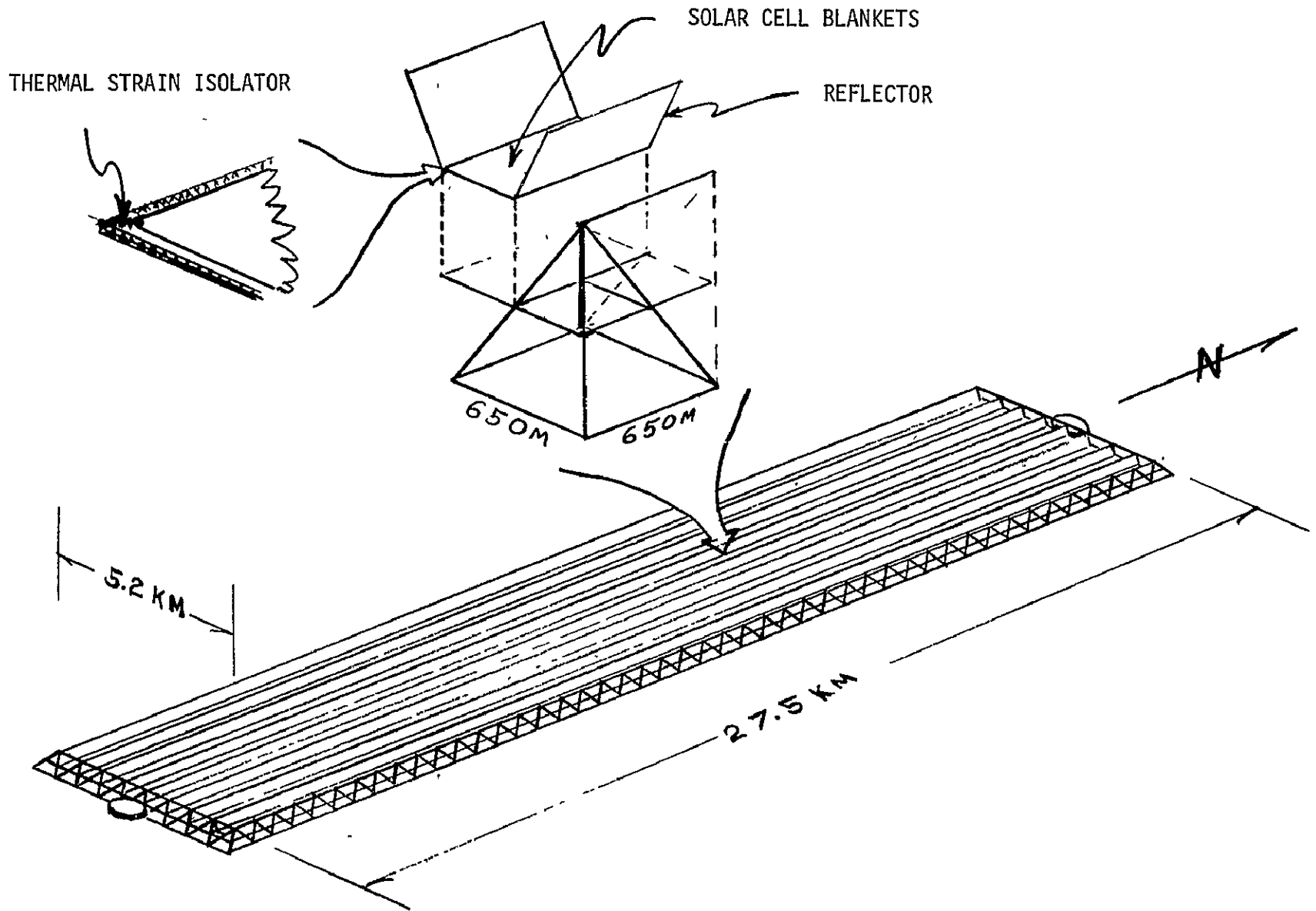


FIGURE IV B3-3 THE "TRUSS" CONFIGURATION

however, is a major consideration for low orbit construction. Fortunately, a gravity-gradient orientation (which is required to eliminate enormous torques) can also be a low-drag orientation. Drag force at 500 km is on the order of 400 N for a 10 GW output station oriented horizontally with solar concentrators "into the wind."

There are several induced loads on the structure, most of which are caused by the following:

Control system inputs to thrusters are required for attitude control and orbit correction. Thrust loads of 100 to 300 N are expected to be maximum, depending upon how the satellite is oriented for operation.

Current loop/magnetic field interaction is a function of current conductor configuration with torque proportional to the loop area and current. With particular conductor path design, this torque can be made zero. However, it may be possible to use these forces to advantage by integrating them, with proper switching, into the control system as a partial substitute for some of the required control forces. If the total system current was routed around the exterior of the configuration, torques could be obtained about an east-west or about a radial axis of approximately 10-million N-m. In low earth orbit, the magnetic field is around 200 times as high as it is in geosynchronous orbit. Therefore, for construction and initial operation for transfer from 500 km, the current loop/magnetic interaction is proportionately more significant.

Interaction between conductors is also configuration dependent. The resulting forces are proportional to the square of the current and inversely proportional to the distance separating the conductors. These forces can be held to reasonable levels with proper power distribution design; i.e., by a large number of conductors spaced as far apart as possible and/or by a high voltage low current power distribution system.

Antenna recoil is the reaction force due to microwave transmission from the antenna. Force is proportional to power transmittal and is about 22 N for each antenna.

Due to the solar radiation pressure, antenna motion will not be a uniform one rev/day since the orbit is not circular. Peak torque from this motion will be about 240 N-m for an expected eccentricity of 0.04.

Transient thermal gradients will occur during occultation by the earth for up to 1 1/4 hours daily for six weeks around the spring and fall equinoxes. In addition, when these satellites are deployed in numbers large enough to place them as close as a degree apart, the satellites will partially shadow each other for 10 to 15 minutes twice each day near the equinoxes and these occultations will not be uniform over the array (as discussed in IV-A-3).

The environment of the solar array consists of a hard vacuum with thermal radiation, primarily from the sun, the solar wind, and the earth's magnetic field.

The sun emits thermal radiation with a spectral distribution characteristic of a black body at about 6000°K with a peak flux in the visible range. Due to the large distance between the sun and the earth, the magnitude of this thermal flux is about 1.4 GW/km². This energy flux is characteristic of a local black body at about 400°K. In this environment with the reference array configuration exhibiting a concentration factor of two solar fluxes to the solar cells, the solar cells will operate at about 100°C to 125°C. The reflectors on the other hand will operate at about -40°C to 0°C depending on whether

the reflectors have both sides or one side coated with high emissivity material. During nominal operation, the only obvious influence of the solar flux is the potential ultraviolet degradation of exposed materials and coatings.

Fortuitously, the solar cells and reflectors have about the same characteristic decay time (about 12 seconds) to a step function occultation. Although the structural decay times are quite variable, a typical characteristic decay time is on the order of five minutes. Therefore, the solar cells and reflectors will virtually track the sun set and sun rise; however, the structure will lag somewhat in response. Significant differences between thermal strains must be accommodated either through detailed design features or preferably through strain allowances afforded by the structural configuration. Thermal strain between the nominal operating condition and the assembly environment must be accommodated by the assembly process.

The solar wind pressure is three orders of magnitude below the light pressure, but this hard radiation energy flux is seven orders of magnitude below the thermal radiation energy flux. The solar wind influences the earth's magnetic field causing daily fluctuations relative to the SPS and sporadic fluctuations which are not well understood. Also, the charged particle flux can degrade material characteristics such as surface reflectivity.

The structural requirement of maintaining configuration integrity within potential dynamic motion is more restrictive than the requirements for either the static loads or the environment. Proximity of the system frequency to any excitation frequency establishes the ratio of the system kinetic energy relative to the potential energy characterized by the stress and displacement of the structure.

The most significant dynamic loading frequencies to the large array are the twice daily (2.3×10^{-5} Hz) and daily gravity gradient loading cycles. The orbit fluctuations of 8000 km (due to the solar pressure) and the magnetic field fluctuations occur on a daily cycle. To keep the dynamic motions of the overall station to a reasonable level, a minimum natural frequency criterion of 2.3×10^{-4} Hz was selected. This establishes a membrane tension level in the cable/column array of about .25 N/m. The minimum structural thickness of the "truss" configuration is on the order of 600 meters. The natural frequency of any configuration is directly proportional to the ratio of its shortest dimension to its longest dimension. In absolute terms, the natural frequency is inversely proportional to a characteristic dimension.

It is estimated that the control system will provide loads at frequencies which will not exceed .2 Hz. This is orders of magnitude above the fundamental or low order array frequencies; however, potential interactions between the control system and individual or small groups of structural elements exist.

c. Structural Configurations

General: The design of a solar power station must primarily address the financial investment required to obtain a flow of electrical energy into the existing ground network. The selection of an SPS configuration should be based on a cost optimization obtained through a proper balance of total system weight, transportation requirements, maintenance characteristics, and the total time from investment to electrical power production. Total time includes the time from the commitment of resources through processing, transport, assembly, checkout, and operation.

The structural weight for the solar cell array concept employed in this study is less significant to the baseline selection process than other systems (solar cell blankets, reflectors, power distribution system, and attitude control system). This may not be the case for other concepts (particularly those which might require large concentrations of the solar flux) such as the Brayton cycle "Power Sat" approach proposed by Boeing (reference 2) or selective spectral reflection concepts which may enhance the performance of solar cells. The significance of the structural configuration is far greater with respect to factors such as attitude control, assembly, electrical conduction lengths and simplicity of design than it is from the standpoint of weight. The station weight is driven primarily by the large number of small "light" components as opposed to the small number of "heavy" components.

The structural requirements, low loads, and minimum gauge considerations lead to the idea of few large structural members. The large members minimize the significance of joints and can provide the three-dimensionality required for dynamic stability. Consideration of the low loads, low thermal expansion, and stiffness requirements lead to the selection of graphite as a reference material for the SPS structure. The column buckling limits shown as a dashed curve in figure IV-B-3-4 were used to size compression members as will be discussed below.

Cable/Column Configuration: The cable/column configuration shown in figure IV-B-3-2 enables a concentration of all the array compression loading into only six main columns. All other significant structural members of the array are cables as illustrated. Twelve main tension cable systems join the columns to form an overall rigid structure. Less than 3000 N (600#) tension is required in these main cables to provide dynamic stability of the array (0.25 N-m membrane tension). The solar cells and reflectors are basically suspended by cables (or tapes to facilitate attachment to cell and reflector substrates) in 200 m by 200 m units. The tension in the cables supporting the solar cell/reflector unit is 22 N (5#). These units are suspended in 1 km² modules which are guyed to the columns as illustrated in figure IV-B-3-2. Electrical conduction outside the cell blankets is handled by the reflector sheets (for low temperature and therefore low resistance). Electrical transmission to the antenna is in conductor sheets suspended along the main cable system at the outer edge of the array.

This configuration was sized for delivery of 10 GW on the ground. Two antennas are provided for 5 GW transmission to two separate locations. This also affords symmetry to the configuration for attitude control. The control system could utilize thrusters at the exterior tips of each column or a combination of thrusters and current loop control via the exterior main cables. The latter system would eliminate the need for thrusters in the vicinity of the antenna.

The six columns are segmented into 3.6 km lengths and guyed with intermediate main cables for static elastic stability of the configuration (stays may be required for torsional stability). The columns are tiered as illustrated in figure IV-B-3-5 and contain bracing cables (not shown). Although these bracing cables are less than 10 percent of the column weight, strict control of the tension in these cables is required for the static elastic stability of the trusses and columns. The cylindrical tube elements must be opaque (open) to thermal radiation to prevent thermal distortion. The compression element, bracing requirements, and guying requirements for the graphite composite columns were determined from a length to radius of gyration (L/ρ) of 100 as indicated in

IV-B-3-9

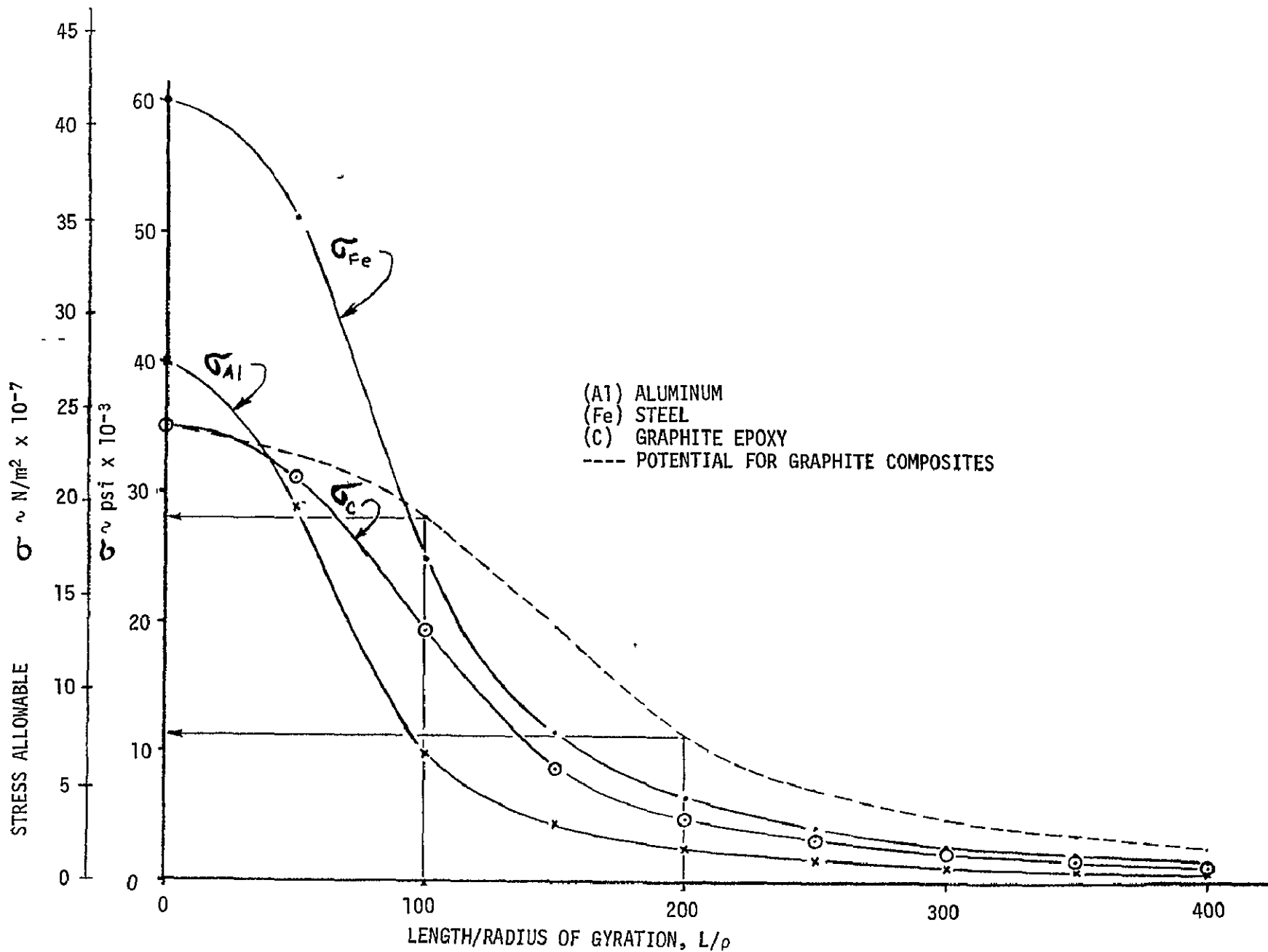


FIGURE IV-B-3-4 JOHNSON-EULER COLUMN ALLOWABLE STRESSES

MATERIAL: GRAPHITE COMPOSITE
 STRUCTURAL CONFIGURATION: SIMPLE, COMMON ELEMENTS, CABLE STIFFENED

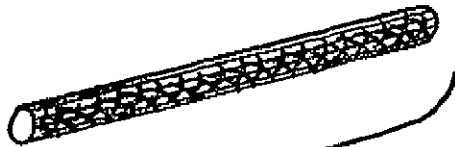
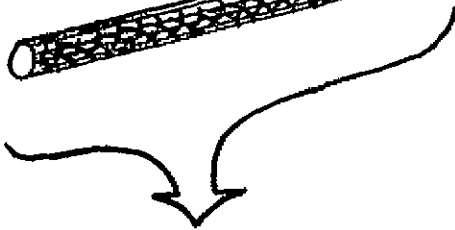
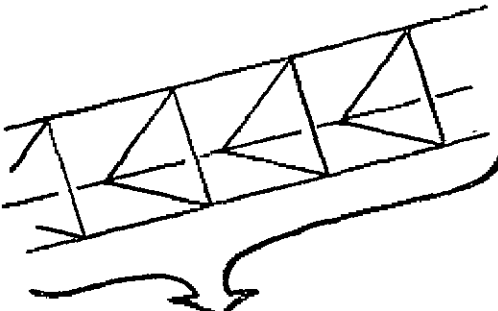
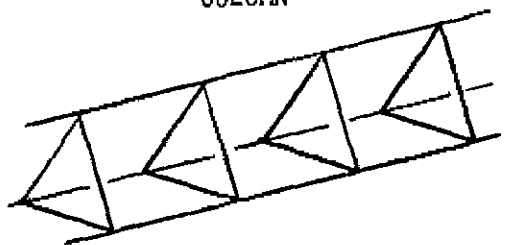
<u>ELEMENT</u>	<u>DIMENSIONS</u>	<u>NUMBER</u>	<u>WEIGHT/ELEMENT</u>	<u>MAX. LOAD</u>
 THERMALLY OPAQUE TUBE	6.9 cm DIAMETER .1778 mm (7 MIL) THICK 2.45 m LONG (D/t ~ 390, L/ρ ~ 100)	1,062,720 (246/TRUSS)	0.072 Kg/TUBE	8,200 N
 TRUSS				
 COLUMN	2.45 m WIDE 100 m LONG L/ρ ~ 100	4320 (216/COLUMN)	0.18 Kg/M 17.67 Kg/TRUSS	34,000 N
	100 m WIDE 3600 m LONG L/ρ ~ 90	20	1.06 Kg/M 3814 Kg/TRUSS <hr/> 76,000 Kg X2 FOR JOINTS DIAGONAL BRACING = 152,000 Kg (335,000 #)	100,000 N (NOMINAL) (7,000 N LOAD)

FIGURE IV-B-3-5 - EXAMPLE COLUMN FOR COLUMN/CABLE CONFIGURATION

figures IV-B-3-4 and 5. Detailed dynamic and thermal analyses have not been performed; however, the columns could withstand 15 times the anticipated static loads. All structural weights for the cable/column configuration were multiplied by two to allow for joints, cross bracing, fittings and our lack of experience with such a structure. To re-emphasize the importance of cost, it should be noted here that a less precise, heavier, but less sensitive column (lower L/ρ) may be desirable. This can only be ascertained in the detailed design stage.

Truss Configuration: The "truss" configuration shown in figure IV-B-3-3 is sized for the same electrical power and microwave transmission parameters as the cable/column configuration. This planar truss is a three-dimensional structure composed of axial load carrying members. These members are arranged in repeating pyramidal modules as illustrated in figure IV-B-3-3. This structure does not "shadow" any of the solar cells or reflectors. Thus, the structure is continuous at full depth as required for dynamic stability in the "long" dimension (27.5 km) and at half depth beneath the solar cells. Although optical shadowing is not significant for the dimensions involved, a full depth structure is not required for dynamic stability in the transverse direction (5.2 km).

The planar truss possesses hard points at the intersection of each member. Thus, a distributed mass (such as the solar cell blanket) is afforded a relatively short and direct load path. The redundant nature of the planar truss offers a failsafe structure in the event of individual member failure. To accommodate an occultation, however, thermal strain relief connectors would be required between the solar blanket or reflectors and the hard points.

Progression in the technology of lightweight structures generally assumed that elastic buckling did not occur during the life cycle of a structure. The ultra light structure required for the truss type configurations of the SPS cannot be realized with conventional aerospace structural technology. This is understood in engineering terms by reference to the elastic buckling curves for columns, figure IV-B-3-4. The SPS truss structure may operate at compressive stresses near the buckling stress. Although elastic buckling might occur from unique loadings (e.g., construction, maintenance) the structure would return to an operational shape on removal of the unique loading. The deformation of a venetian blind is an example of this type of structure. The truss structure in the Glaser concept is built up from venetian blind type elements as suggested by the Grumman Aerospace Corporation (reference 4). It should be noted that the concept of allowing local elastic buckling is not possible for the cable/column configuration where buckling would be a failure.

The planar truss module shown in figure IV-B-3-3 is built up from compression elements as given in figure IV-B-3-6. A venetian blind type element was designed for an L/ρ of 200. This 25 cm long element has a cross-section formed from a parabola segment with a height of 0.3 cm and a 5 cm width. A graphite composite material of .127 mm (5 mil) thickness is suggested. Despite the seeming frailty of this venetian blind type element, incorporation in a three-dimensional form will result in a more than adequate structure for the low anticipated loadings. It should be noted that based on the two examples calculated (figures IV-B-3-5 and 6) a rather long space truss or column can be obtained at roughly 1 kg/m mass per unit length. This truss member may be used with minor modifications in a number of configurations. The 16 m wide truss can be 1 km long with an L/ρ of 200. This provides a 1 km size pyramidal module for

MATERIAL: GRAPHITE COMPOSITE
 STRUCTURAL CONFIGURATION: SIMPLE ELASTIC ELEMENTS

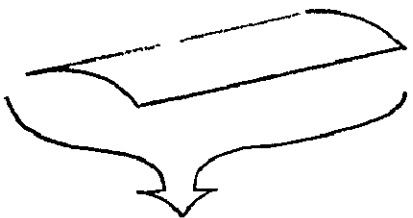
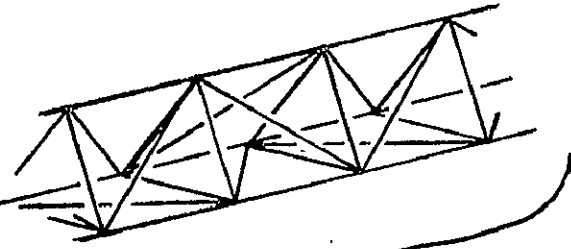
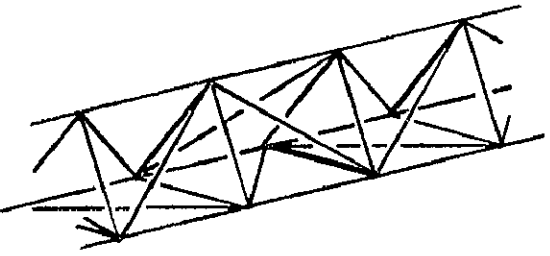
<u>ELEMENT</u>	<u>DIMENSIONS</u>	<u>NUMBER</u>	<u>WEIGHT</u>	<u>MAX. LOAD</u>
ELASTIC MEMBER				
	.1270 mm (5 mil) THICK 3 mm HIGH 5 cm WIDE 25 cm LONG 35 cm LONG $L/\rho \leq 200$	538,560,000 269,280,000 (MADE FROM CONTINUOUS TAPES)	0.0024 Kg 0.0034 Kg	440 N
FIRST TRUSS	25 cm WIDE 16 m LONG 23 m LONG $L/\rho \sim 200$	816,000 408,000	0.0996 Kg/m 1.60 Kg 2.27 Kg	2,640 N
				
SECOND TRUSS	16 m WIDE 650 m LONG 365 m LONG 325 m LONG 160 m LONG $L/\rho \leq 200$	1,100 1,770 2,200 565	1.028 Kg/m 670 Kg 375 Kg 335 Kg 170 Kg	15,840 N
				
			2,237,540 Kg	
			X 1.25 FOR JOINTS, FITTINGS = 2,796,925 Kg	
			(6,153,235 #)	

FIGURE IV-B-3-6 - EXAMPLE TRUSSES FOR 10 GW "TRUSS" CONFIGURATION

use in a modified Glaser type configuration as shown in figure IV-B-3-7. This is a 5 GW configuration with a centrally located microwave antenna. The number of structural members requiring dielectric material has been reduced to just the outside members. This is in contrast to the original Glaser structure in which all longitudinal members were carried into the transmission space. The deepening of the structure makes this possible with no increase in weight. The linear amount of truss required in this planar truss structure is constant and independent of depth. The added number of joints in a shallow structure increases the structural weight and provides less stiffness.

The antenna cradle for this 5 GW configuration is shown in figure IV-B-3-8. Translational inertia from rotation of the microwave antenna should be kept to a minimum during normal operations. The function of this cradle is to allow 360° rotation without translational movement. Two pivot points allow rotation about the X axis for adjustment to rectenna latitude. A rotary joint on either end of the cradle allows continuous rotation and passage of electrical current.

A large variety of structural configurations is possible through a combination of these two structural concepts. For example, the "picnic table" configuration shown in figure IV-B-3-9 could use a combination of distributed and concentrated load paths to achieve an isotropic moment of inertia tensor. This would minimize attitude control problems and be amenable to current loop control about two axes.

d. Technology and Testing Requirements

The design, development, transport, fabrication and assembly of a solar power station structure requires a refined blend of analysis and testing. Although this represents a technological challenge, it can also be viewed as a logical development proceeding from the technology foundation associated with current aircraft and space vehicles. The main difficulty associated with the design and development of a structure for the solar power station, as currently envisioned, is the impossibility of ground test simulation. The measurement of even tolerance capability for a structural element is not possible in the earth's gravitational environment.

The situation is somewhat analogous to the impossibility of experimentally duplicating the reentry flow field environment for a spacecraft such as the Space Shuttle Orbiter. In this case, a numerical flow field analysis, which was calibrated by comparison of wind tunnel data and numerical analysis of wind tunnel flow fields, is used to establish the design environment for the Orbiter. By analogy, numerical analysis of the SPS structural design characteristics can be calibrated through carefully planned orbital tests and associated measurements and then applied with confidence to the final design. Necessary elements to this process are the adequate comprehension of the material characteristics, fabrication and assembly limitations, the detailed loads and temperature distribution, and integrated analyses of other significant subsystems such as the control system, power distribution system, and the electronic components. To support this design and development process, a synergetic balance of analysis and test requirements is needed.

e. Consideration of Materials for Solar Power Stations

Introduction: In considering candidate materials suitable for use in the SPS, one must first consider the environmental extremes and load requirements of the system. These requirements are related to the following major parameters:

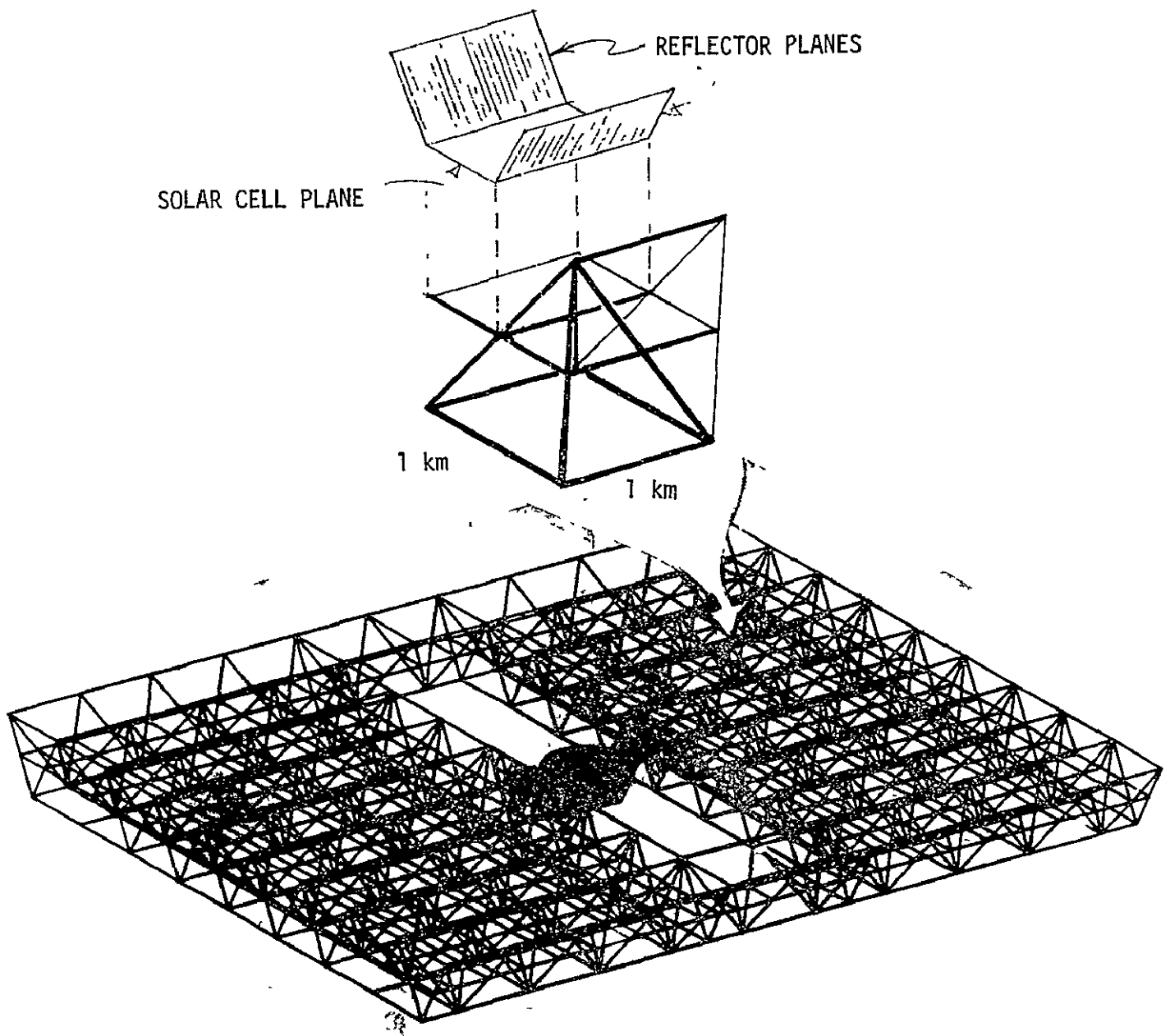


FIGURE IV-B3-7 5 GW ARRAY

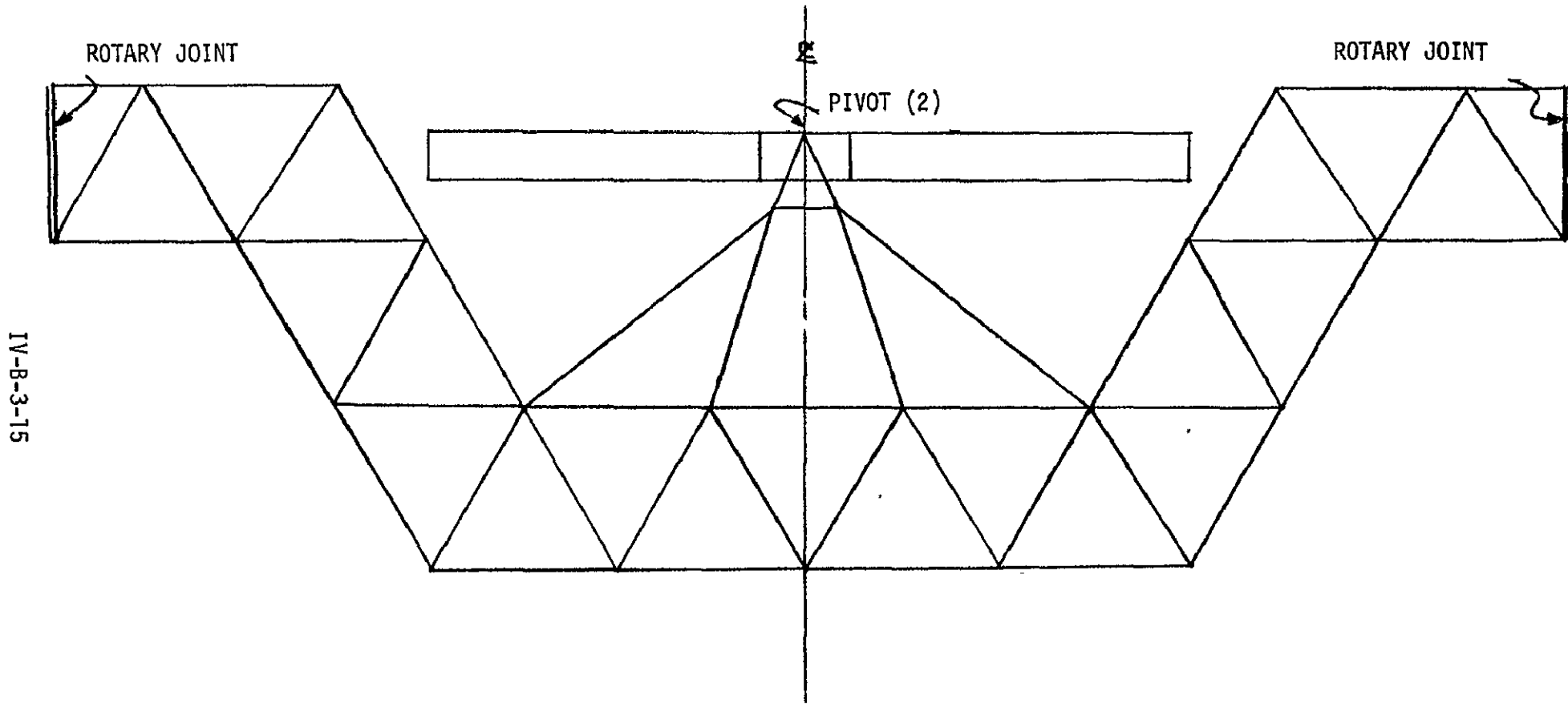


FIGURE IV-B-3-8 MOVABLE SUPPORT STRUCTURE FOR 5 GW ARRAY

IV-B-3-16

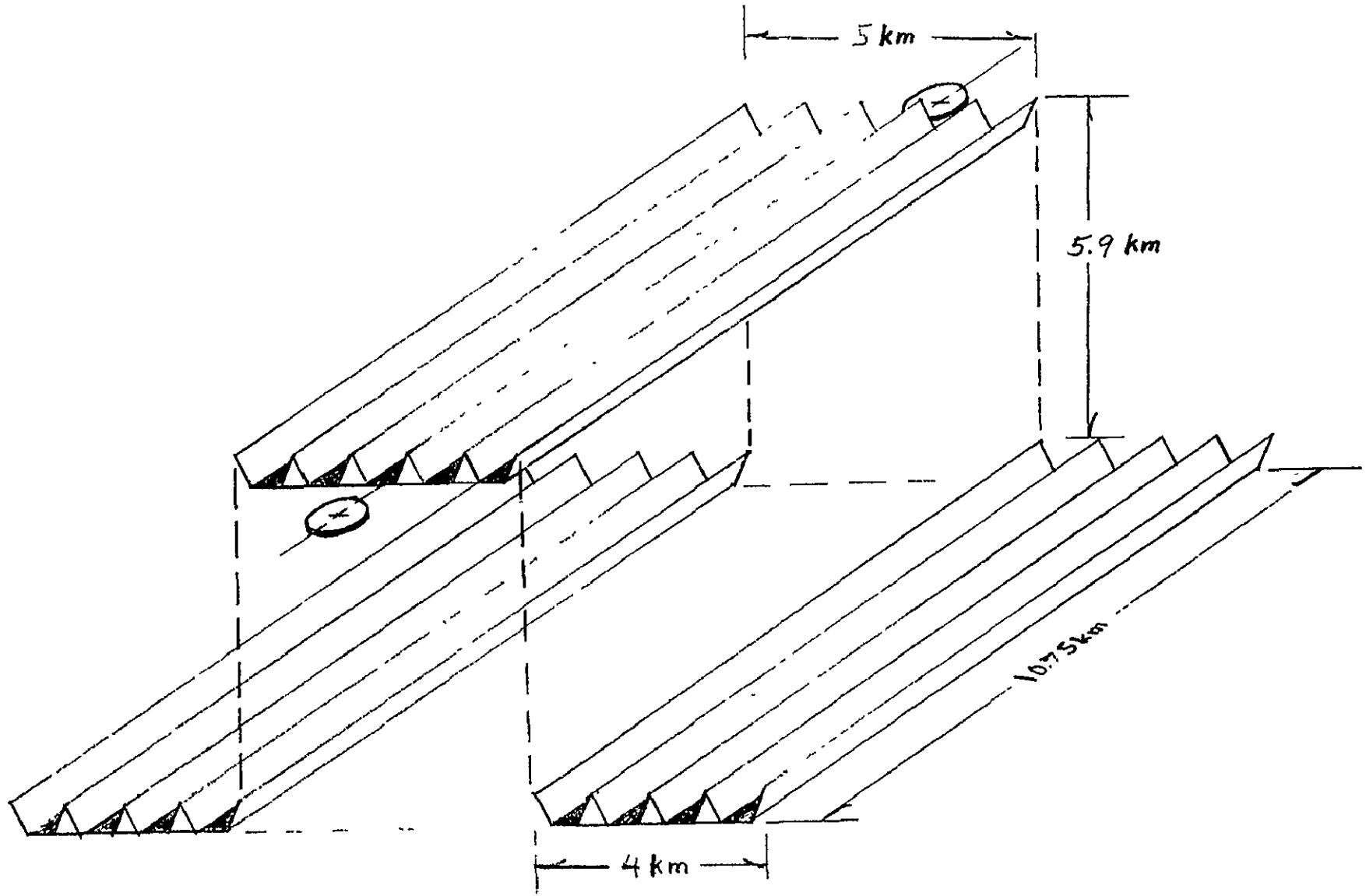


FIGURE IV-B3-9 "PICNIC TABLE" CONFIGURATION

1. Vacuum exposure
2. Radiation effects
3. Temperature extremes (6°K to 500°K)
4. High fabrication loads during construction; Low operational loads after construction
5. Orbital fabrication techniques
6. Thirty-year operational life

In general, materials used in the SPS fall into two general categories, structural and nonstructural. The structural materials make up the framework, trusses, cables, etc., which support the solar cell arrays and antenna elements. The nonstructural materials include solar concentrators (reflectors), solar cells, antenna wave guides, etc., which are necessary for the operation of the system. In the SPS configurations evaluated in this study, the structural materials actually account for less than 3 percent of the total SPS weight.

The general characteristics of both structural and nonstructural materials evaluated in this study are discussed below in more detail.

Environmental Effects: In evaluating materials for the SPS, environmental effects arising from vacuum, radiation and high and low temperatures are of primary consideration. For the screening of generic classes of materials, changes in properties were considered acceptable if the change was reasonably well characterized for the environment, if the material retained useful engineering properties with the effects of the environment considered, and if the change was reversible. An example of an environmentally-caused change would be loss in ductility with low temperatures. Aluminum alloys are well characterized at temperatures as low as liquid helium (4°K). Several alloys are considered acceptable for use in structural applications at these temperatures even though the loss of ductility at the cryogenic temperature is significant. These alloys are considered acceptable because:

1. The change has been quantitatively determined with a reasonably good data base.
2. The remaining ductility is enough to be useful in an efficient structural design.
3. The change is reversible; i.e., on warming, the ductility returns to the material and the degradation is neither additive nor accumulative.

Another example is in the area of plastic films. Here, the polyimide films such as Kapton (H-film) become brittle at low temperatures; but, again, enough ductility remains at temperatures as low as 77°K to make the material useful for this temperature range. The ductility of this material also returns with increasing temperature and no permanent damage would be anticipated.

Using criteria similar to these examples, various candidate materials were examined for application in the SPS environment.

Structural Materials:

1. Aluminum Alloys

Approximately 4 to 6 million pounds of structural materials are required in the fabrication of one SPS. Aluminum alloy, because of its availability and low cost, would probably be the best choice if the SPS was required for construction today. Aluminum can be packaged in sheet rolls, transported to orbit, and fabricated to meet most structural design requirements. Aluminum exhibits excellent stability for the space environments, and its mechanical and physical properties are well characterized. One potential problem with aluminum

is that its relatively high coefficient of thermal expansion could lead to problems in maintaining the proper "flatness" required for supporting the solar collecting and microwave transmitting elements. Another possible disadvantage for using aluminum, especially in the 1995 time frame, is that electric power is the primary energy source in converting aluminum containing ores to pure aluminum metal.

2. Graphite Composites

Recent development and promising future development of high modulus and high strength graphite fibers tend to favor the use of graphite composites for the major structural elements of SPS. Graphite composites with an epoxy matrix for "normal" environmental temperature exposure, or polyimide matrix for high temperature use, are being used more frequently in aerospace primary structure applications. Graphite has a favorable low coefficient of thermal expansion, can be packaged in "prepreg" tape form with its matrix material, transported to orbit, and used to fabricate almost any required structural beam shape during SPS assembly. An alternate to the use of uncured "prepreg" tapes is to use cured graphite reinforced thermoplastic rolls or sheet materials which offer possible advantages in fabrication and joining techniques (see Appendix V-A-2). Two concerns which probably require additional evaluation are possible radiation damage (to matrix) and low temperature effects on composite mechanical properties, although existing development programs indicate neither concern is unsurmountable. A potential concern is the availability of carbon-base raw materials for use in the production of the graphite and matrix materials in the 1995 time period. Presently, graphite composites are produced from petroleum base raw materials, although recent advances in low cost "pitch" raw materials for graphite promise to be suitable substitutes. Additional study/evaluation is required in this area to fully assess the possible impact on graphite composite materials used in the SPS construction.

3. Cable Materials

The primary potential use of stainless steel in the SPS would be for tension cables. Stainless steel wire can be cold drawn to very high tensile strengths and woven into cables to meet design requirements. The major disadvantages of steel (high density and moderately high coefficient of thermal expansion) tend to negate any real advantage of using steel cables in the SPS.

Kevlar 49 fiber (polyimide) is considered to be an alternate candidate for the tension cable because of its high tensile properties. However, its moderately high negative coefficient of thermal expansion could cause serious problems if not properly corrected by design. Kevlar 49 also has only moderate resistance to radiation damage; therefore, a useful life of thirty years is doubtful. Protective coatings with sleeving materials would probably be required, or periodic cable replacement could be necessary.

A potential use of graphite fiber or graphite composite tension cables is being considered. Since the previous use of graphite in cable systems is limited, development programs will probably be required to establish fabrication and application characteristics.

4. Metal Matrix Composites

Although not studied in detail, boron filament/aluminum matrix composites should be considered for use in SPS construction. Boron/aluminum composites perhaps best resist all of the environmental extremes, including radiation and low temperature effects. Another advantage of its use is the possibility of using the boron/aluminum structure for conducting electricity from the solar cells to the antenna, thereby eliminating nonstructural conducting

wire used for that sole purpose. Two disadvantages of boron/aluminum use are its relative high cost and difficulty in fabricating non-tubular structural shapes.

Nonstructural Materials

1. Solar Concentrator Materials

Two materials are considered for use as the solar concentrators (reflectors), aluminized Mylar and aluminized Kapton. Both materials exhibit similar properties except that the Kapton (polyimide) is better for high temperature use than the Mylar (polyester). The concentrator temperature is expected to reach 300°K maximum, and either material should be satisfactory at that level. Both materials can be fabricated on earth in rolls, and transported to orbit for assembly on the SPS structure. One possible concern is the brittle low temperature properties of the materials, which might require special assembly procedures to insure that concentrators are "warm" enough to install without breakage. The use of Kapton favors lower temperature installation.

Another consideration meriting additional study is the possibility of utilizing the space vacuum to vapor deposit the reflective aluminum on the Mylar or Kapton surfaces. All advantages/disadvantages of this approach have not been fully evaluated.

2. Coatings

Thermal control coatings used in manned spacecraft systems are candidates, but they may not survive combined radiation and vacuum environment for extended periods of time required by the SPS. This class of materials will require testing and likely require development to find acceptably reliable coatings. Evaluation of coatings in use in current unmanned planetary spacecraft such as Mariner and Pioneer will provide significant insight into potential systems for the SPS applications.

3. Elastomers and Adhesives

The need for seals and soft surfaces at low temperatures will require some development since few commercial materials will retain enough flexibility at temperatures below 116°K to perform satisfactorily. Silicones, Vitons, and fluoropolymers represent the best systems for immediate considerations. Thermal control systems may be needed for critical systems to prevent leakage or wear in these applications.

It is anticipated that adhesive bonding will be a required joining/repair technique for much of the SPS. Structural adhesives are available for use from 127°K to 500°K. Joining of graphite composite members can be done with suitable adhesives, or by special fabrication techniques with graphite composite tapes. Specialized joints requiring multiple connection of several structural members might require reinforcement guide joints which are fabricated on earth and carried into orbit for assembly.

4. Other Nonstructural Materials

The other major nonstructural materials proposed on SPS are the electrical conductors (EC Aluminum), solar cells (silicon), and antenna wave guides (aluminum). The wave guides are hollow rectangular tubes with close accuracy slots required on the microwave transmission face. The exact construction techniques required to produce the wave guides should be further evaluated to insure the feasibility of the proposed design.

One area requiring additional study is the materials problems associated with the SPS power distribution system. The effective joining of the

aluminum transmission lines is necessary to minimize line size and weight requirements and still maintain the necessary electrical conductivity for efficient energy transmission. Coatings may also be required on electrical transmission lines to provide the necessary thermal control properties to maintain sufficiently low temperatures.

Summary: In considering the candidate materials from which the SPS may be constructed, there does appear to be an adequate technology base present as a beginning. The use of graphite composite materials for the primary structure appear to be promising. The unknown of a thirty-year life in a space environment does raise questions since the material is relatively new. Aluminum alloys, on the other hand, have an extensive history of use in previous years which add confidence that aluminum will do the job. The fact that the 30-year operational stresses on the SPS will be primarily the result of thermal cycles and thermal gradients tend to favor a materials with a low coefficient of thermal expansion, such as graphite composites. As a result, graphite composites appear to meet the major requirements of the SPS structural members, although a thorough evaluation of radiation damage, outgassing and thermal effects is needed to prove the usefulness of these materials. Available data indicate these problems may be overcome and lend optimism that in-space fabrication techniques may be simpler than with metals.

Nonmetallic films and fibers for supporting solar cells appear to be available providing the design does not introduce local loads at low temperature where low temperature brittleness could lead to failure. Adhesive films provide simple techniques for joining and repair.

Existing materials for low temperature, vacuum stable seals and elastomers may not be satisfactory. This may require material development or thermal control techniques for successful application.

Many specific materials problems will surface when the design matures. Overviews such as this summary should be evaluated in this light. It is concluded that a sufficient number of candidate materials exist to warrant further design study so that development problems can be defined and solved prior to SPS initiation and commitment.

f. References

1. Glaser, Peter E., et al: Feasibility Study of a Satellite Solar Power Station, NASA CR-2357, February 1974.
2. Woodcock, G. R. and Gregory, D. L.: Derivation of a Total Satellite Energy System, AIAA paper 75-640, AIAA/AAS Solar Energy for Earth Conference, Los Angeles, April 24, 1975.
3. JSC Six-Week Study, Space Solar Power Development Laboratory, NASA JSC-09991.
4. Quinn, R.: Selection of the Baseline Attitude Control System for the SSPS and a Stability and Performance Analysis of the Elastic Coupling Between the Control System and the Spacecraft's Structural Modes, Grumman Aerospace Corporation, Bethpage, New York, ASP-611-M-1009 (NASA 74X76993).

IV-B-4. Attitude and Orbit Control

The control system must compensate for all forces acting on the SPS, both orbit perturbations and attitude disturbances. Orbit perturbations are analyzed in section IV-A-3. The reaction control system discussion in this section includes both orbit maintenance and attitude control requirements.

a. Attitude Disturbances

L. E. Livingston
Spacecraft Design Div.

Synchronous Orbit

The most important torque acting on the SPS is that produced by gravity/centrifugal gradients. For a flat solar-oriented array, there are two principal components (see figure IV-B-4-1). The first component acts about an axis normal to the orbit plane and tends to align the plane of the array with local vertical. It is cyclic with a period equal to half the orbital period. Numerically, for a circular, synchronous orbit

$$T = 8.0 \times 10^{-9} (I_z - I_x) \sin 2\theta$$

where I_z and I_x are expressed in kg-m^2 and T in N-m. The peak torque for a square array of 137.5 km^2 and 35000 M.T. is about 3.2×10^6 N-m. The second component acts about the line of intersection of the array and the orbit plane. Its magnitude is $10.6 \times 10^{-9} (I_z - I_y) \sin 2\beta$ in position 1 (X-axis perpendicular to radius vector) and $2.7 \times 10^{-9} (I_z - I_y) \sin 2\beta$ in position 2 (X-axis parallel to radius vector). Since β reaches an extreme value of 23.5° , maximum torques are 3.1×10^6 N-m and 0.8×10^6 N-m in positions 1 and 2, respectively.

Solar radiation pressure of about 600 N will produce a constant torque if the center of mass and center of pressure are not coincident.

Microwave recoil of 22 N per antenna will produce a torque, varying in direction with antenna orientation, if the antennas are not balanced with respect to the mass center of the SPS.

If the eccentricity of the orbit is not zero, the antenna angular velocity will not be constant. For the expected eccentricity of 0.04 and an 8×10^6 kg antenna, peak torque will be about 240 N-m. Variation is roughly sinusoidal with a period of one day.

If a current loop is formed by large separation of positive and negative conductors, interaction with the earth's magnetic field will produce a torque on the SPS. With a total current of 450,000 A, the magnitude of the torque can be as high as 50,000 N-m per square kilometer of current loop area.

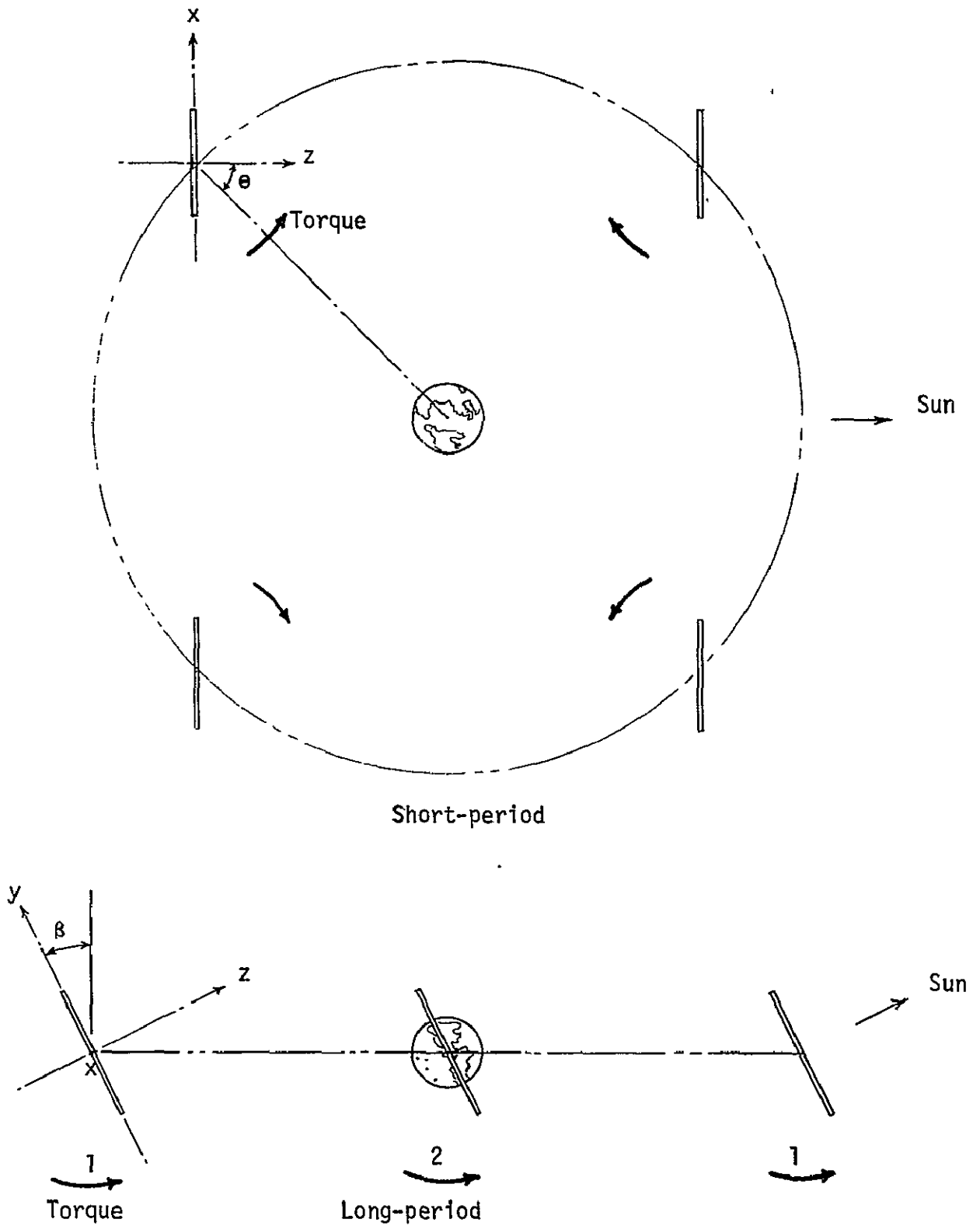


Figure IV-B-4-1. Gravity Gradient Torques

Low Orbit

Gravity gradient torque is the predominant attitude disturbance in low orbit. At 500 km altitude, its magnitude is 230 times that in synchronous orbit. Thus, a square array (137.5 km², 35000 M.T.) would require a maximum RCS thrust of 125,000 N to move from a stable to an unstable attitude. This would be the case, for example, if the array were constructed in a stable attitude (vertically oriented) and rotated to an unstable attitude (horizontal) for transfer to synchronous orbit. The same peak torque would be necessary if a solar orientation were maintained for maximum power output during self-powered transfer.

Aerodynamic torque will be important only if the center of mass and center of pressure are not coincident. Even the maximum plausible offset, however, cannot produce torques of the same magnitude as gravity gradient.

Since solar radiation pressure is about 5 percent of aerodynamic drag at 500 km, it does not contribute appreciably to the stabilization problem in low orbit. Antenna loads are absent because the antennas are inoperative.

Current loop/magnetic field interactions can exist only during self-powered transfer.

b. Orientation Considerations

As noted in the preceding section, a large, flat, solar-oriented array experiences substantial gravity gradient torques. These can be counteracted by a reaction control system. For the example square array, the propellant penalty is 110,000 kg per year to compensate for the cyclic torque and 68,000 kg per year for the long-term torque, assuming a specific impulse of 98,000 m/s (10,000 lb-s/lb). In addition to the cost of resupplying the propellant, the cloud of material surrounding the SPS will be increased to some extent by the expended propellant. It appears worthwhile, then, to explore ways of reducing propellant requirements.

Since the first torque is cyclic with a reasonable period, control moment gyros (CMG) seem worth considering. However, using the same example as before, scaling up the rotor of the Skylab ATM gyro (same material and geometry) results in a rotor mass of 10⁷ kg without considering mounting, actuators, etc. This is three times as great as the propellant supply for 30 years. Aside from the difficulty of achieving a 30-year lifetime, CMG technology would have to advance at least an order of magnitude to be weight-competitive.

(1) Column/Cable Configuration

An alternative approach is to eliminate the torque. This can be done for the short-term torque by making $I_x = I_z$ by adding counterweights. Counterweights are attractive for configurations such as the column/cable (figure IV-B-4-2) because they can be placed on existing structure with minimum penalty. The RCS and the maintenance station, in fact, can serve as part of the counterweight.

The total counterweight mass required is shown in figure IV-B-4-3 for various height/width (b/a) ratios, assuming dimensions b and c are equal. A long, slender configuration requires less counterweight, but at the expense of additional bus weight along the outer edges of the array. A rough analysis indicates a weight-optimized b/a ratio of about 2.3. If this ratio is set at 2 to facilitate use of uniform segments in all columns, total counterweight mass is 1.07×10^6 kg. If RCS were used to counteract gravity gradient torque on the same configuration, peak thrust (total at both ends of the Z-axis column) would be 123 N, and the average thrust 78 N. At a specific impulse of 98,000 m/s, propellant requirements would be 25,200 kg per year, or 907,000 kg over 30 years with 20 percent allowance for tanks. Since all of this propellant need not be launched at the outset, counterweights appear advantageous only if a high specific impulse cannot be achieved, or if contamination considerations force propellant consumption to an absolute minimum.

The long-term torque can be handled similarly by making all three moments of inertia equal. This can be accomplished by a suitable choice of the ratio b/a, which in effect uses the solar array itself to counterbalance the antennas. If the mass of each antenna is 8.125×10^6 kg, the parameters used in the previous example require that $b/a = 0.407$. Referring to figure IV-B-4-4, it may be seen that the counterweight mass increases substantially for small b/a unless the column height is very large. However, interference with the microwave beam limits the height of the column in relation to dimension "b". If the southerly antenna is aimed at 40°N. latitude, the maximum value of c is 1.748b (see figure IV-B-4-5). Minimum counterweight mass for $I_x = I_y = I_z$ is then 7.7×10^6 kg, an increase of 6.6×10^6 kg over that required for two-axis equalization. Such a penalty is not justifiable, and this concept was dropped.

For the long-term torque, it is also possible to align the spacecraft principal axes with local vertical and the flight path, reducing the $(\sin 2\theta)$ term to zero. This is applicable to the long-term torque because the angle varies through a limited range ($\pm 23.5^\circ$), making it possible to maintain a reasonably good solar attitude. If the power output is proportional to the cosine of the angle of incidence, the maximum loss is 8.3 percent (at the solstices) and the annual average loss

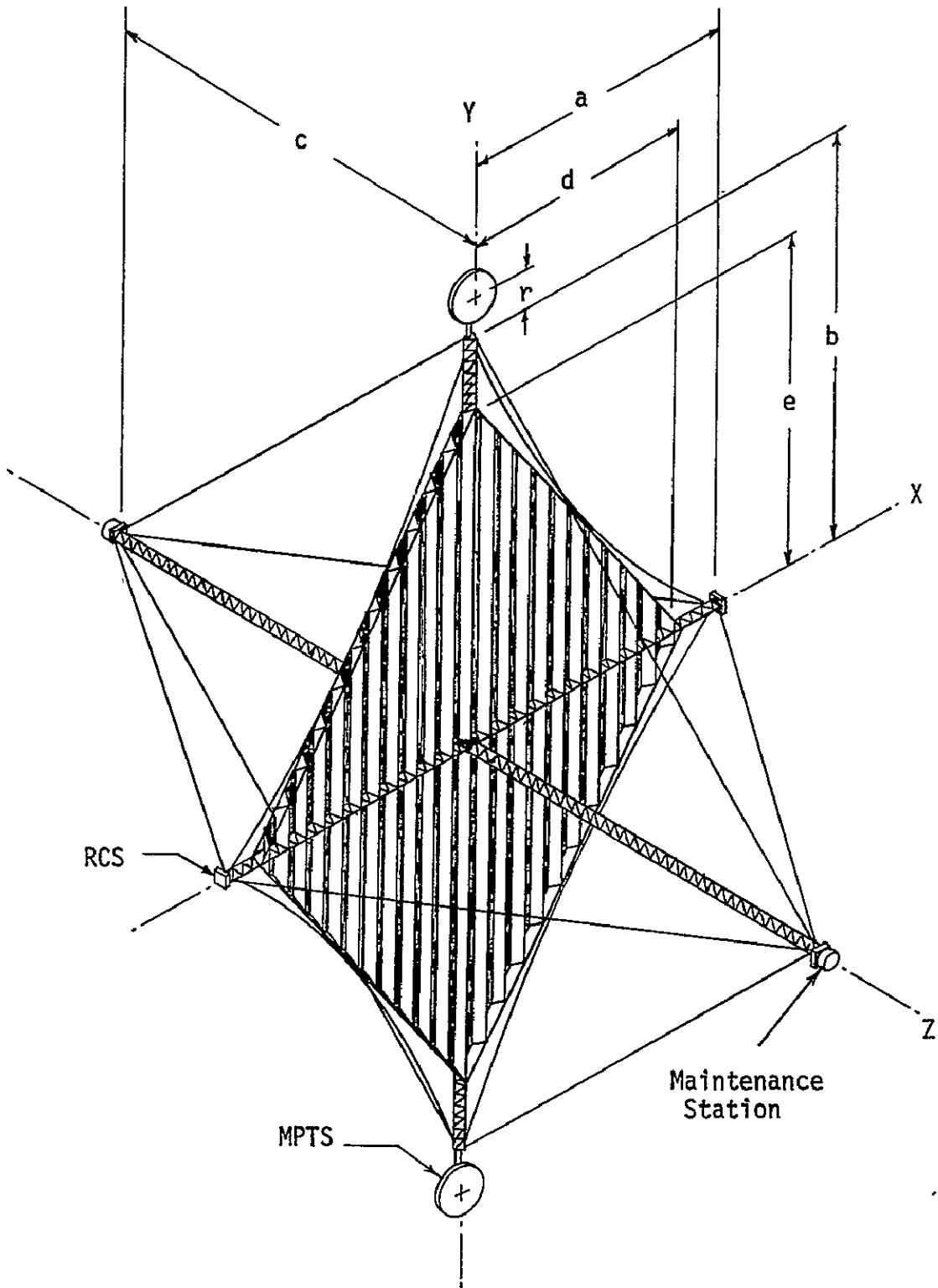


Figure IV-B-4-2. Column/Cable Configuration

IV-B-4-5

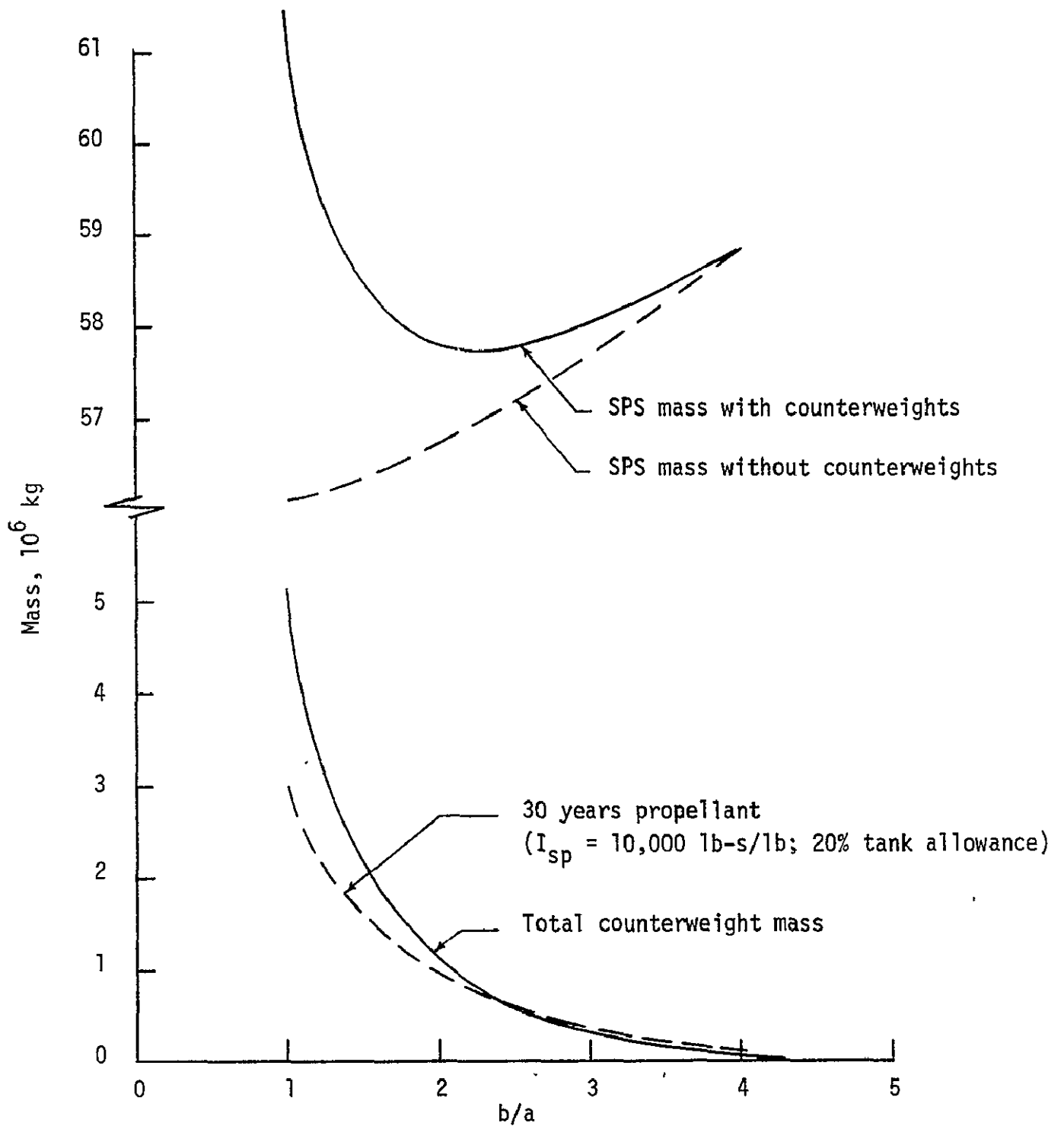


Figure IV-B-4-3. Short-period Gravity Gradient Compensation
(Column/Cable Configuration)

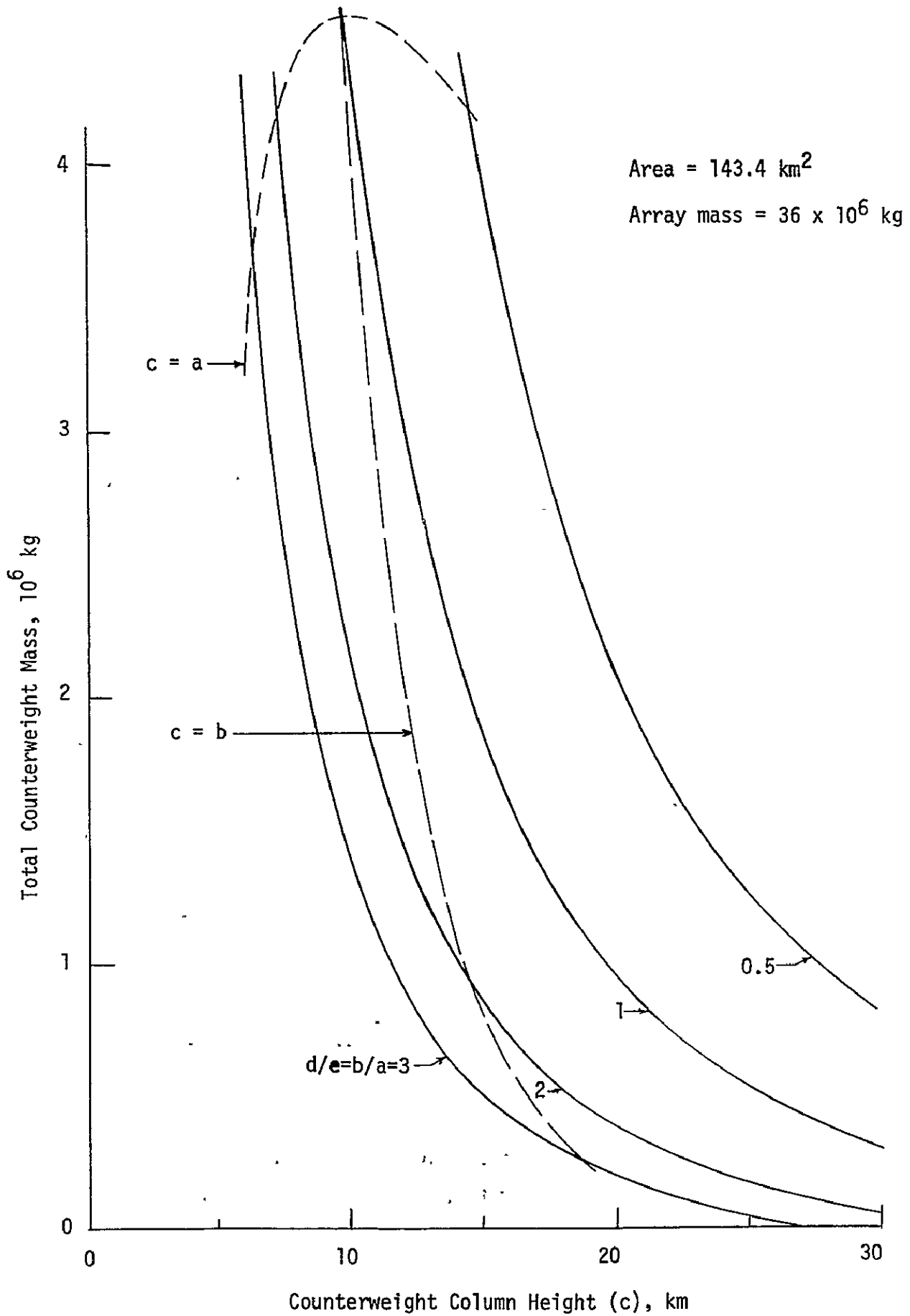
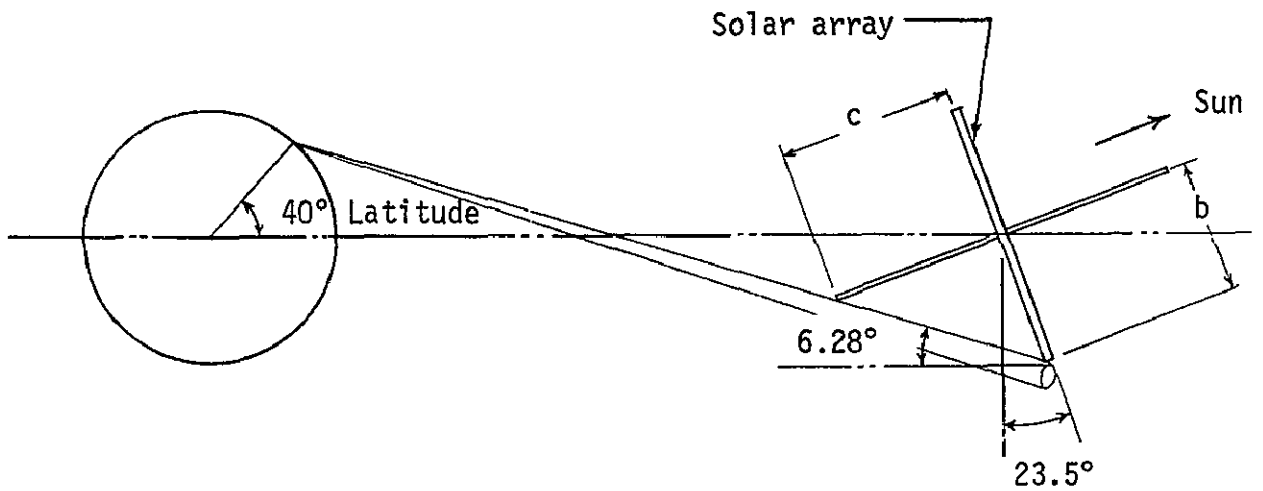


Figure IV-B-4-4. Counterweight Mass (Column/Cable)



$$c/b = \tan (90^\circ - 6.28^\circ - 23.5^\circ)$$

$$= 1.748$$

Figure IV-B-4-5. Counterweight Column Height Limit

about 4.1 percent. Since the sun's average position is in the orbit plane, the array should be oriented perpendicular to the orbit plane (POP).

Lateral misalignment relative to the concentrator troughs results in losses much higher than the simple cosine relation of a flat array (figure IV-B-4-6). POP orientation of the array, therefore, requires that the concentrators also be POP rather than the more convenient diagonal mounting that was possible with solar orientation (figure IV-B-4-7).

To maintain the same average power output, the solar array must be enlarged to compensate for the loss due to POP orientation. This penalty is 1.48×10^6 kg for solar cells, concentrators and supporting structure. An additional penalty arises from the considerably greater length of power bus required, as illustrated in figure IV-B-4-7; this is estimated at 2.07×10^6 kg. On the other hand, solar orientation with $b/a = 2$ would require an additional 300,000 kg of propellant per year ($I_{sp} = 98,000$ m/s) compared to POP orientation. Over a 30-year life, therefore, the POP orientation offers a substantial weight savings.

The preceding discussion implicitly assumed that no other disturbances acted on the SPS. In reality, this will not be the case. Antenna tilt for non-zero rectenna latitudes will produce a gravity gradient torque on the antenna, non-uniform mass distribution can produce a radiation pressure torque, and random and second-order disturbances will have a virtually unpredictable effect. Accordingly, provision must be made to maintain the desired attitude within some deadband.

Since the Y axis (minimum moment of inertia) is POP, the attitude is unstable. For the column/cable configuration, the average torque is $1.04 \times 10^6 \theta$ N-m, where θ is the departure of the Y axis from POP in degrees (θ small). The thruster moment arm for this configuration is 7212 m about the Z axis and 14424 m about the X axis. The thrust required is then 144 θ N or 72 θ N for the Z and X axes, respectively. Assuming the same error about both axes and a specific impulse of 98,000 m/s, total propellant required is 70,000 θ kg per year, where θ is the average error angle. Clearly, it is desirable to keep θ as small as possible; a target of 0.2 degree appears reasonable and has been used for propellant budgeting purposes.

In summary, the preferred attitude for the column/cable configuration is POP to eliminate long-term torque combined with a relatively slender configuration (long axis POP) to minimize short-term torque. Short-term torque will be counteracted by propulsion or counterweights, depending on the specific impulse that can be achieved.

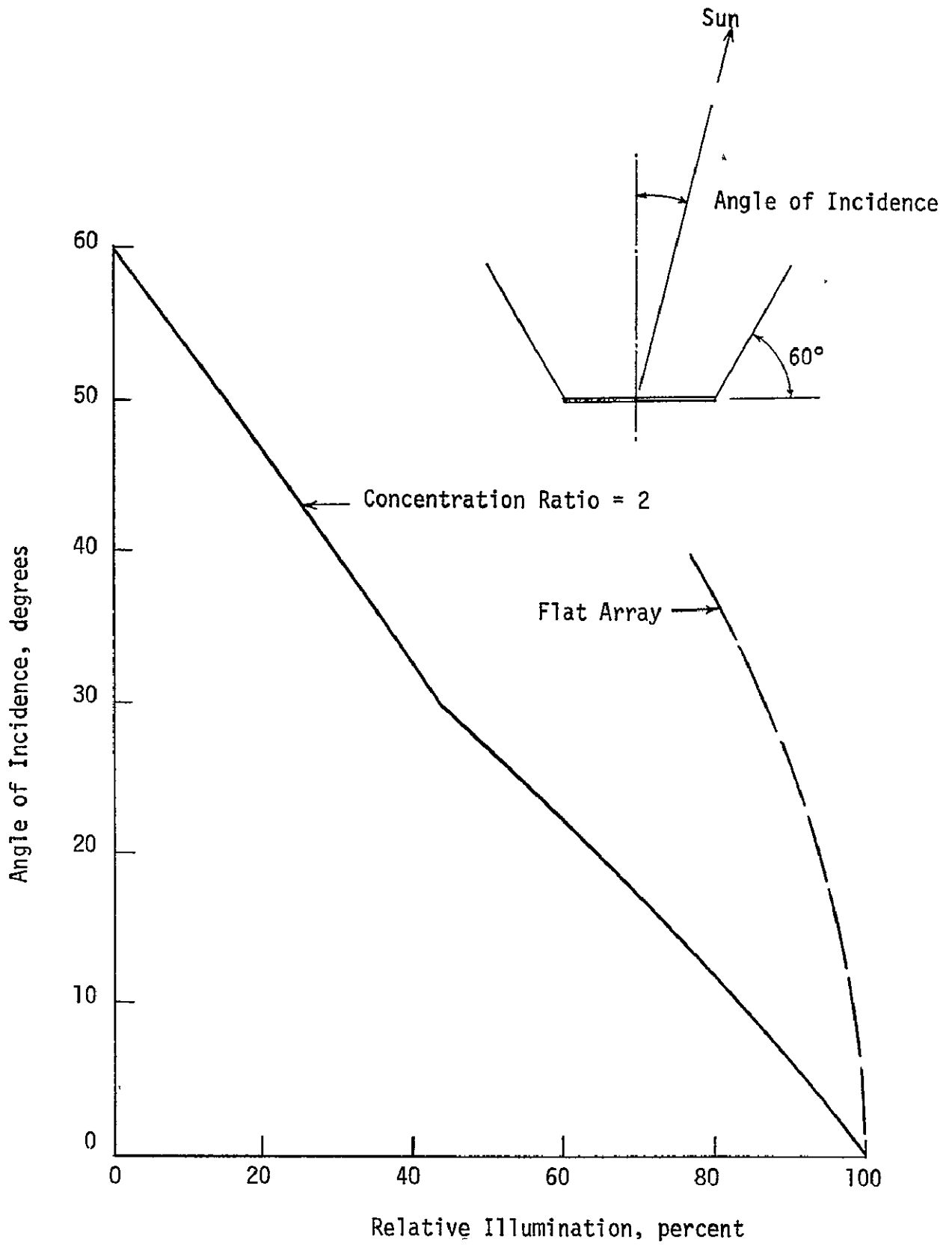
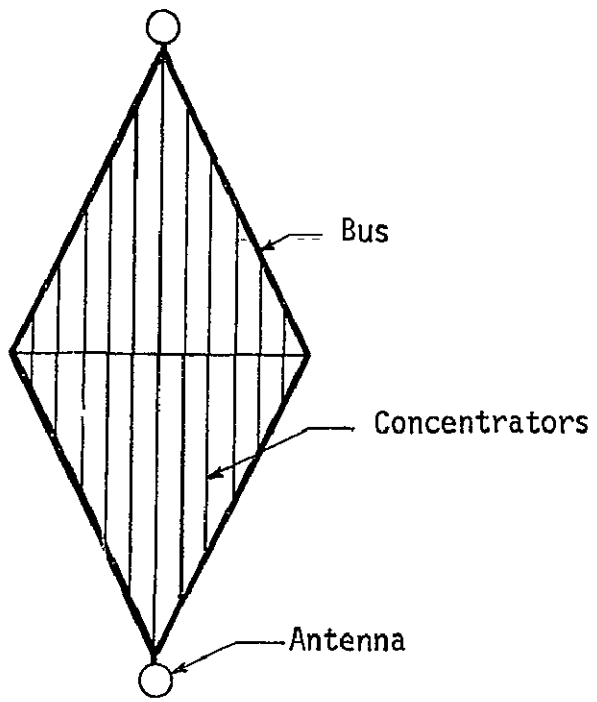
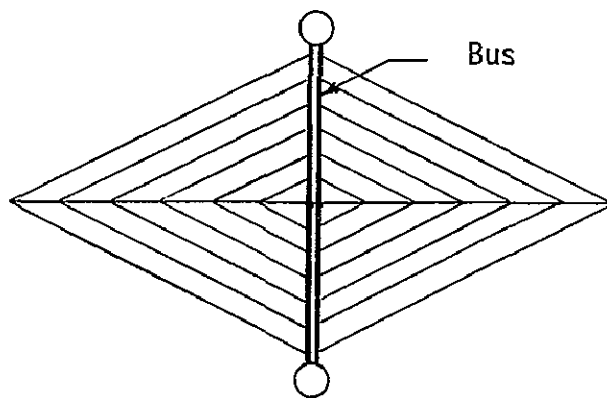


Figure IV-B-4-6. Illumination Loss with Trough Concentrators



POP Orientation



Solar Orientation

Figure IV-B-4-7. Concentrator and Bus Arrangements

(2) Truss Configuration

The preceding discussion of the column/cable configuration also applies, in general, to the truss. The major exception is that counterweights were not considered. The structural arrangement does not provide a natural attach point for counterweights, although such points could be provided at a modest weight penalty.

Propellant required to overcome short-period gravity gradient torque is shown in figure IV-B-4-8 as a function of the length/width ratio of the solar array. Propellant mass is given as a 30-year total to facilitate comparison with figure IV-B-4-3 which presents similar data for the column/cable configuration. It can be seen that propellant requirements are substantially higher for the truss configuration. High length/width ratios requires less propellant.

POP orientation is preferred for the truss as well as for the column/cable configuration. The logic is the same, although numerical values differ.

c. Sensing

The SPS presents a unique attitude sensing problem in that the axis to be held POP (nominally the Y axis) is not a geometrical axis but the axis of minimum moment of inertia. The relationship between these two axes cannot be precisely determined in advance and varies with time. Therefore, the geometrical axis will be used only as an initial approximation. After start-up, the control computer will monitor the RCS firing command history, infer from this history the actual position of the minimum-inertia axis relative to body axes, and make the necessary corrections to the thruster firing commands to maintain the actual minimum-inertia axis POP.

Star trackers together with the known orientation of the orbit plane (from ground tracking) provide a continuous attitude reference. Angular rates will be below the capability of rate gyros and will be computed as time rates of change of attitude.

X-axis orientation perpendicular to the solar vector will be detected by sun sensors. The criterion here is orientation of the body axis, not the principal axis of inertia, and the problem is straightforward.

Orbit parameters will be determined by ground tracking (optical and/or radar) both for greater accuracy and because orbit corrections must be commanded from the ground to insure coordination with other satellites, since all SPS will be in the same orbit.

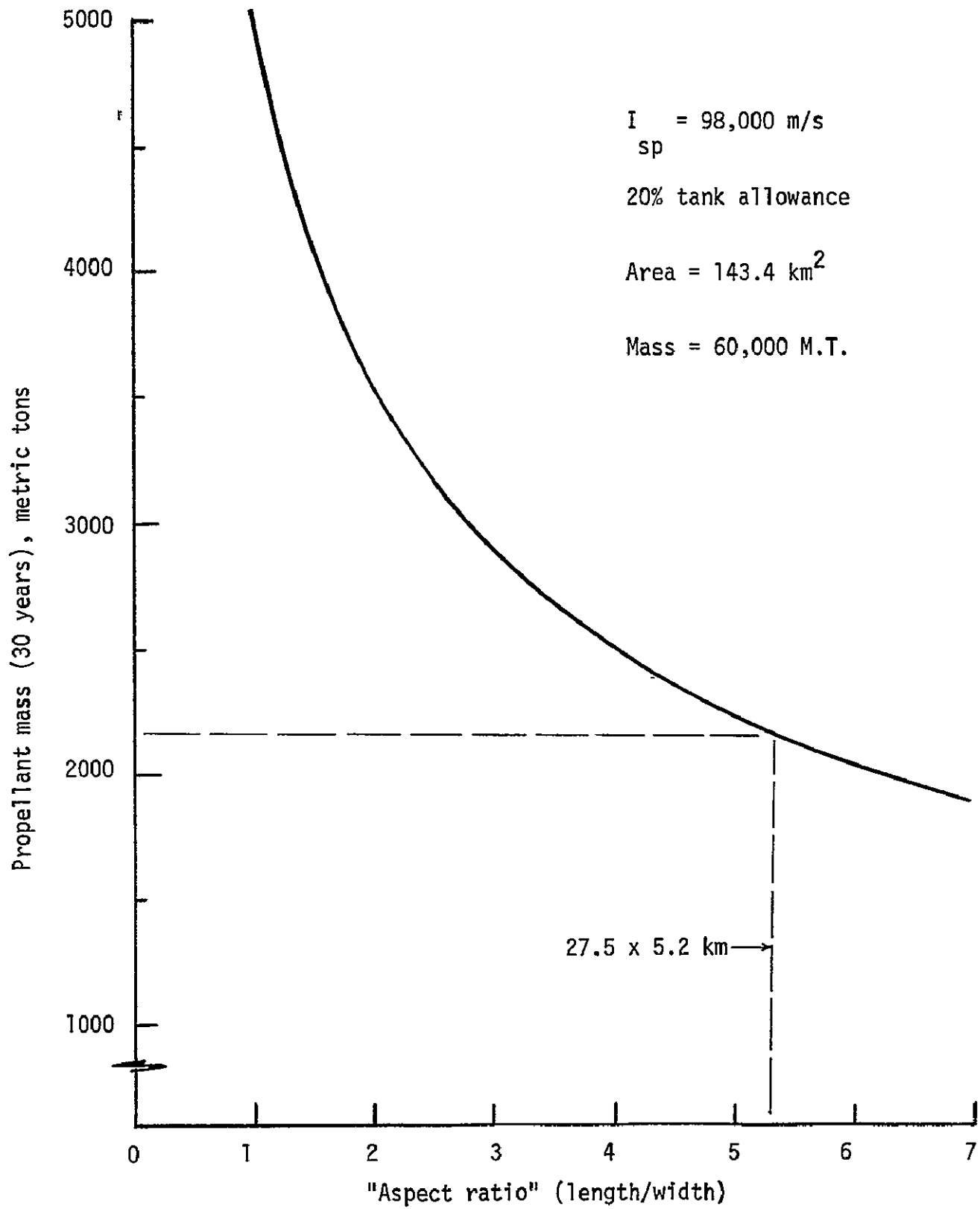


Figure IV-B-4-8. Gravity Gradient Propellant (Truss Configuration)

d. Reaction Control System

J. C. Hooper
Propulsion & Power Div.

The annual impulse requirements are summarized below for the column/cable configuration. It is assumed that inclination will be held at zero and mean longitude held constant, and that periodic eccentricity variations will not be counteracted. Mass is assumed to be 90×10^6 kg.

<u>Source</u>	<u>Annual Impulse, 10^6 N-s/yr</u>
Inclination buildup	4149
Longitude drift	468
Short-term gravity gradient (no counterweights)	3167
Long-term gravity gradient (Y-POP)	2052
Contingency (10%)	984
	<hr/>
	10820

Thrust level was set at 335 N at each of 16 locations (see figure IV-B-4-2) to provide adequate control authority. In-depth study of the requirements might reduce this figure substantially.

Several electric propulsion options were evaluated and are summarized in table IV-B-4-1. The candidate systems considered were electrostatic (ion) thrusters, magnetoplasmadynamic (MPD)-arc jet thrusters, thermal arc jet thrusters, and an O_2/H_2 chemical thruster system in which the propellants are produced electrolytically from water. For each of these systems, the required electrical power was assumed to be supplied by the satellite.

This group of systems is not, and is not intended to be, an inclusive list of all viable systems for performing the RCS functions for the power satellite. It is quite possible that a system not considered could be more desirable from an overall standpoint than any of those presented here. These systems do represent a range of electric propulsion options insofar as weight, performance, and power requirements are concerned. For the systems discussed, further study may indicate the desirability of operation at other than the maximum I_{sp} conditions (as assumed here), with an attendant reduction in power requirements and number of thrusters.

Table IV-B-4-1. Performance of Candidate Reaction Control Systems

	Ion (30 cm)	Ion (100 cm)	Arc Jet (MPD)	Arc Jet (Thermal)	O ₂ /H ₂ (Electrolysis)
Propellant	Argon	Argon	Argon	Ammonia	O ₂ /H ₂
Avg. Sp. Impulse, m/s (lb-s/lb)	49000 (5000)	196000 (20000)	98000 (10000)	14700 (1500)	3900 (400)
Thrust per Thruster, N	.085	3.76	111	111	334
Number of Thrusters	64000	1440	48	48	16
Specific Power, kW/N	39	122	68	18	4.2
Average Power, MW ¹	13	42	23	6.2	1.4
Annual Propellant ¹	221	55	110	736	2760
System Dry Weight ²	1905	2404	200	240	299
SPS Penalty (4.5 kg/kW)	60	188	105	28	6
1-year System Weight	2186	2647	415	1004	3065
30-year System Weight	8595	4242	3605	22348	83105

IV-B-4-15

1. Impulse = 10.82×10^9 N-s/yr
2. Includes thrusters, power processors and tanks; does not include radiators and wiring
3. All weights in metric tons

The 30 cm ion thruster system referred to in table IV-B-4-1 represents a relatively modest advance in current technology. The 100 cm ion thruster system represents an advanced system which is projected to be attainable in the time frame of the SPS. Compared to the 30 cm thrusters, the advanced ion thrusters have a much higher specific impulse and thrust, as well as a higher thrust to weight ratio. However, the higher projected power conditioned weights for the advanced thrusters result in a net increase in dry weight for the same installed thrust.

The MPD-arc jet is a thruster in the early stages of development that appears to have the potential (compared to ion thrusters) for higher thrust levels, higher thrust/weight ratios, and lower power conditioning requirements. Unfortunately, at this time, the I_{sp} , weights, and power requirements are considered highly speculative. The thermal arc jet is a relatively well-developed device; large arc jets have been used for materials testing and entry heating studies for years. Ammonia was chosen as the propellant, although hydrogen would give approximately twice the I_{sp} . It was felt that the penalties associated with the hydrogen storage and transfer (both from volumetric and temperature considerations) would greatly reduce if not eliminate the advantage associated with I_{sp} .

The final system listed is an electrolysis system, in which oxygen and hydrogen produced from water are combusted in a more-or-less conventional rocket engine. The primary advantage of this system over a conventional LO_2/LH_2 rocket engine system is the storage efficiency and handling ease of water compared to cryogenic oxygen and hydrogen.

The "system dry weight" in table IV-B-4-1 includes thrusters, power processing equipment, and propellant tankage (for one year's supply of propellant). System weight items that are not included are radiators required for heat rejection from the thrusters and electrical wiring to supply power. The "SPS penalty" weight is calculated as 4.5 kg/kW of average power required by the thrusters. The system weights represent the summation of the dry weight, SPS penalty, and the indicated number of years of propellant supply.

At a 6.4 percent duty cycle, a 30-year satellite life would require an average thruster life of 23 months. Of the systems discussed above, the ion thrusters have demonstrated 24-month lifetimes; experience with the other thrusters is considerably short of the requirement. Life predictions for an MPD thruster are difficult, but it may be in the same range as a thermal arc jet, which is to say in the range of 3 months. For the electrolysis system, a thruster life of some 6 months appears reasonable, with the electrolysis cells themselves having an essentially indefinite life with periodic refurbishment. Fortunately, the thrusters without sufficient life expectancy have a high thrust/weight ratio, so that either installed redundancy or periodic replacement seems feasible.

Of the systems discussed above, the MPD-arc jet system looks quite attractive; however, as mentioned above, this thruster is in such an early stage of development that the weight and performance values have considerable uncertainty. The conventional thermal arc jet system is also attractive, especially from the standpoint of inert weight. The electrolysis system has the advantage of drawing very little power, but has large resupply requirements. The ion systems have low resupply requirements but high inert weights and large power requirements.

The trade-offs among these systems are influenced by transportation costs, assembly schemes, and cost amortization as well as many other factors. For example, should impulse requirements drop significantly or installed thrust level increase, the ion systems would appear less attractive than under the current assumptions.

The MPD arc jet has been selected for the reference configuration primarily on the basis of low initial and total weights. The small number of thrusters should enhance reliability and is also a favorable consideration.

e. RCS Operation During Eclipse

L. E. Livingston
Spacecraft Design Div.

Eclipse by the earth for a maximum duration of 75 minutes (section IV-A-3) imposes a large energy storage requirement on the first three systems in table IV-B-4-1. Using an optimistic battery power density of 110 W-hr/kg, battery mass is 11400 kg per MW average power. On this basis, the MPD arc jet system at average power would require 261,000 kg of batteries. Since a 30-year life is very unlikely, periodic replacement would be necessary.

As an alternative, an O_2/H_2 (water electrolysis) system can be used during eclipse, eliminating the storage requirement for RCS electrical energy. Since the satellite is eclipsed only one percent of the time and half of the total estimated impulse requirement is for orbit corrections (which need not be performed during eclipse), the propellant required during eclipse is 1/200 of that given in table IV-B-4-1, or 14,000 kg per year. Furthermore, because the eclipses occur in two groups six months apart, only 7,000 kg maximum gaseous storage capacity is required. The electrolysis can be done continuously at a low rate to minimize electrolysis cell weight. The estimated dry weight of such a system is 34 M.T., with annual propellant requirements of 16 M.T., including tanks.

At the low angular velocities contemplated for the SPS (on the order of 0.25 deg/hr), delaying an attitude control pulse until after an eclipse would not seriously enlarge the deadband about the X and Z axes. If this is done, eclipse propellant can be reduced some 40 percent, to about 4200 kg per six months.

The electrolysis system could also be used, with added gas storage capacity, as a standby propulsion system if it should be necessary to maneuver the solar array away from the sun during maintenance periods to remove all voltages from the buses.

IV-B-5. Instrumentation, Control and Communications L. E. Livingston
Spacecraft Design Div.

A large quantity of subsystem status data will be required for automated control, onboard servicing and ground monitoring. This study has not gone to the depth necessary to produce sufficiently detailed subsystem definition for meaningful identification of instrumentation, control and communications requirements. However, present technology would be adequate for all foreseeable needs, and the weight impact on the SPS will be insignificant. Consequently, this subsystem has been deferred for later study.

IV-B-6. Maintenance Station

L. E. Livingston
Spacecraft Design Div.

Some maintenance of the SPS will be necessary from time to time. Propellant must be replenished periodically. Trouble-free thirty-year lifetimes for moving parts such as control moment gyros, antenna joints, star trackers, etc. are unrealistic. Comparatively reliable items such as solid state electronic components will experience random failures. Other problems, e.g., chafing of conductors, may be considered during design but frequently are fully resolved only with operational experience. The maintenance question has not been explored to any depth in this study, however, and the following represents a cursory consideration of the problem.

To minimize the payload of the maintenance spacecraft, as many facilities as possible should be incorporated into the SPS. These would include a normally unmanned, habitable control station, some repair and small spares storage facilities, and servicing and local transportation vehicles.

To facilitate troubleshooting, a central control station will provide status information on all subsystems. Insofar as feasible, all control equipment, computers, etc. will be located within this control station. The station will be connected to the habitation module.

A repair shop and airlock will be connected to the habitation module. It will provide bench repair facilities, storage for small spares, and berthing for servicing and local transport vehicles. These vehicles, as well as the habitation and shop modules, will be derivatives of those used in the construction phase to avoid duplicate development programs.

Many maintenance tasks, particularly those occurring on a more or less regular basis (e.g., propellant replenishment), can be planned for shirtsleeve operation from a maintenance vehicle with manipulators. Some electronic components can be located within the maintenance station. However, many repair operations will require dexterity not available from a manipulator; for these, extravehicular activity will be necessary. Most work of this type can be expected to require broad general capability but relatively little detailed subsystem knowledge. Thus, only part of the crew need be EVA-trained, and most of the subsystems experts can operate entirely in a shirtsleeve environment.

Based on the above, a minimum maintenance crew might consist of two pilot-astronauts, a maintenance chief, two general EVA technicians, two propulsion technicians, two microwave/electronic technicians and one guidance technician, or a total of ten crew members. A detailed analysis has not been performed, but it is possible that the desired degree of

specialization may not be achievable with a crew of this size. Since some maintenance will require at least a partial shutdown of the SPS, it also will be desirable to minimize the down time with a larger crew.

Assuming three work shifts and considering the size of the SPS, it would be possible to utilize almost any number of technicians. A practical limit may be established by the capacity of the personnel orbital transfer vehicle and the capacity of a construction habitation module.

SECTION IV.C.(1)

IV.C. MICROWAVE POWER TRANSMISSION SYSTEM

IV-C-1 ANTENNA ARRAY

a. RATIONALE

A SPS (Solar Power Satellite) in geosynchronous orbit collects and converts solar energy to DC electricity by either the photovoltaic process or by solar thermal converters. This electrical energy is transmitted back to the earth using a high power microwave transmission system. The microwave power transmission system consists of microwave generators, waveguides, a large planar phased array, a closed-loop phasing system, and a tracking system.

b. DEFINITION

The phased array antenna has a diameter of one kilometer, with a 10-dB Gaussian taper and a maximum power density at the center of 21 kW/m². The array consists of 7854 subarrays, each subarray being about 10 meters X 10 meters in area, and each subarray connected to its adjacent subarray by a flexible ground plane. Behind the waveguides of each subarray are mounted microwave generators which convert the high-voltage DC into microwave energy at S-band. The energy is then radiated into the slotted waveguides which transmit the RF electromagnetic energy in the form of a main lobe to an earth rectenna. The microwave generator may be a klystron or a crossed field amplifier (such as an amplitron) with the klystron generating 50 kW of RF power and the crossed field amplifier generating 5 kW of RF power. The waveguides are made of aluminum and, with the aid of phase control, will minimize the size of the sidelobes so that the efficiency of the antenna array will be as high as 90%.

c. OPERATING CHARACTERISTICS

The antenna array will perform its transmission function based upon a number of simultaneous actions. Each subarray will radiate through its slot apertures to create its own antenna pattern. The total number of subarrays will collectively transmit their beams to form a main lobe whose energy will be almost totally captured by the ground receiving antenna. The subarrays contain phasing circuits which provide phase front control for the propagated electromagnetic waves to accurately point the beam and focus the high power microwave beam in the presence of a non-homogeneous, time varying atmosphere and ionosphere, thermal deformation of the array waveguide and structure, and phase variation of transmission lines, converters, and phase shifters. There are two basic approaches to phase control: command and adaptive. The command makes field measurements at the rectenna and transmits this information by a telecommunications link to the transmitting array. The adaptive utilizes a reference beam sent from the receiving antenna location to the space transmitting antenna to enable phase measurements and corrections to be made at each subarray.

Numerous antenna types have been analyzed to accomplish the goal of high efficiency, low losses, reliable antenna pattern and low sidelobes. Conclusions are summarized below: (See Figure IV-C-1-1)

<u>TYPE ANTENNA</u>	<u>ADVANTAGES</u>	<u>DISADVANTAGES</u>
Parabolic Dishes	Lightweight Deployable	Low Efficiency Spillover Losses High Sidelobes
Pyramidal Horns	Lightweight	High Power Limited High Sidelobes Moderate Efficiency Susceptible to moding
Helix Radiators	High Efficiency (98%)	Dual Polarization at Receiver
Slotted Waveguides	High Efficiency (95%) Combines RF Distribution and Low Frequency Cut Off Reduces RFI	Minimal

Therefore, the slotted waveguide is recommended. The large size of the transmitting antenna dictates that it be split into many sub-arrays, or sections, so that errors due to mechanical distortion can be corrected.

In the study to determine the optimum size of the antenna array, the possibility of separating one large antenna into many small ones - all of which would equal the area of the large antenna - was explored. (The concept is known as the "cloud concept" in which the large antenna is split into many small antennas, each physically separate from the other and each antenna having its own solar collectors, its own distribution system and its own structural support). If the antenna could be split into many independent elements, the solar collectors could be smaller, the DC power distribution system less complex, and the transportation and manufacturing problems would be reduced. In order to determine the prospects of using this multiple antenna "cloud concept", a comparison was made with the single antenna approach.

- d. SINGLE ANTENNA VS. MULTIPLE ANTENNAS - "CLOUD CONCEPT"
(1) Array of Contiguous Subarrays (See Figure IV-C-1-2)

$$\text{Beamwidth} = \frac{2\lambda}{D}$$

Where D is array Diameter

$$\text{Peak of Beam} = \frac{\eta 4\pi A}{\lambda^2}$$

Where η is the aperture taper efficiency.

A is area of radiating antenna. For most aperture tapers 85-95 percent of radiated power is within the main beam.

In this configuration, the array does not exhibit high sidelobes. The antenna pattern is a result of the product of a subarray pattern and an array factor as shown in Figure IV-C-1-2. The array factor has high side-lobes (known as grating lobes) due to the wide spacing of the subarrays, but

these lobes are suppressed by the nulls of the subarray pattern.

(2) SAME SUBARRAYS SPREAD OUT ON REGULAR GRID (See Figure IV-C-1-3)

If the subarrays are spread out over a wider area, the beam-width of the array becomes more narrow, approximately equal to $2\lambda/D$, where D is the new, larger diameter. The gain of the beam remains $\eta 4\pi A/\lambda^2$ where A is the active area, i.e. the total subarray area. The transmitted power within the beam is reduced, since the peak of the beam is the same but the beam is narrower. This lost power is found to be radiated into the side-lobe region.

If the subarray spacing is regular (like a rectangular grid), the added sidelobe power will appear in discrete lobes, called grating lobes. The array factor grating lobes move inward because of the increased subarray spacing and, therefore, they move out from under the nulls of the subarray pattern. (Figure IV-C-1-3)

(3) SAME SUBARRAYS SPREAD OUT AT RANDOM (See Figure IV-C-1-4)

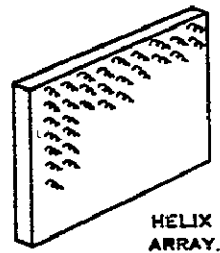
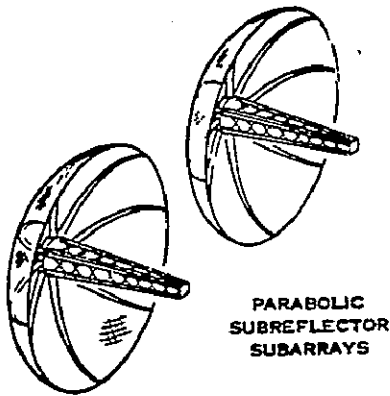
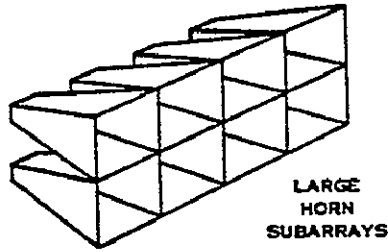
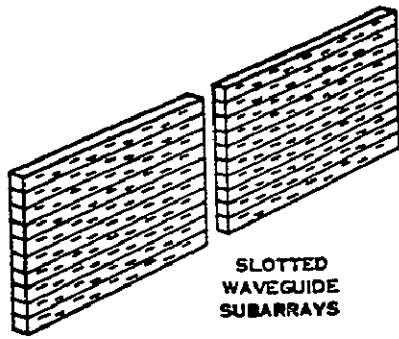
If the subarray spacings are randomized, the added power in the sidelobes will be spread out uniformly with noise-like peaks.

If the subarrays are spread out over an area twice as large as the subarray area, half of the power under the beam will be radiated into the sidelobes since this power is spread over a wide area, it cannot be effectively collected in a ground rectenna of fixed size.

When the subarray spacing is periodic, the power will occur in many lobes about the mainbeam and this too will be expensive to collect.

The effects of "splitting" a large antenna aperture can be seen in both the main beam and the sidelobes. In the case of an array of smaller antennas, each smaller antenna radiates over a larger area than does a large antenna. (The smaller the diameter, the broader the beam-width of the individual antenna). The energy in the sidelobes of an array increases as the spacing between antennas increases.

The conclusions reached are that "splitting" into many small antennas will increase sidelobe levels and will increase losses in the main beam so that antenna efficiency is prohibitively degraded.



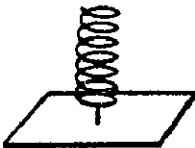

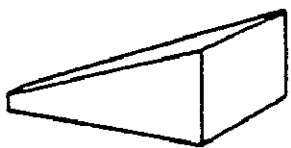
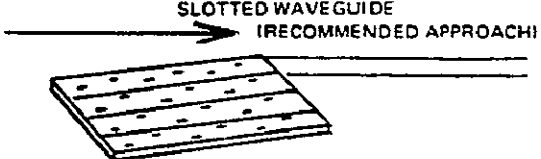
 <p>HELICAL RADIATORS</p> <p>ADVANTAGES</p> <ul style="list-style-type: none"> • HIGH EFFICIENCY (98%) <p>DISADVANTAGES</p> <ul style="list-style-type: none"> • DUAL POLARIZATION AT RXCV • REQUIRES RF DISTRIBUTION FROM CONVERTER 	 <p>UNFURLABLE GORE-TYPE PARABOLOIDS (MESH AND FLEX RINGS)</p> <p>ADVANTAGES</p> <ul style="list-style-type: none"> • EXTREMELY LIGHTWEIGHT • DEPLOYABLE <p>DISADVANTAGES</p> <ul style="list-style-type: none"> • SPILLOVER LOSSES • LOW EFFICIENCY (65%+) • HIGHER ARRAY SIDELOBES • FABRIC IS HIGH POWER LIMITED
 <p>PYRAMIDAL HORNS (MESH OR THIN METAL SIDES)</p> <p>ADVANTAGES</p> <ul style="list-style-type: none"> • LIGHTWEIGHT <p>DISADVANTAGES</p> <ul style="list-style-type: none"> • SUSCEPTIBLE TO MODING • HIGHER ARRAY SIDELOBES • MODERATE EFFICIENCY (90%) 	 <p>SLOTTED WAVEGUIDE (RECOMMENDED APPROACH)</p> <p>ADVANTAGES</p> <ul style="list-style-type: none"> • HIGH EFFICIENCY (99%) • COMBINES RF DISTRIBUTION AND ANTENNA • LOW FREQUENCY CUTOFF REDUCES RFI

Figure IV-C-1-1 Subarray Types

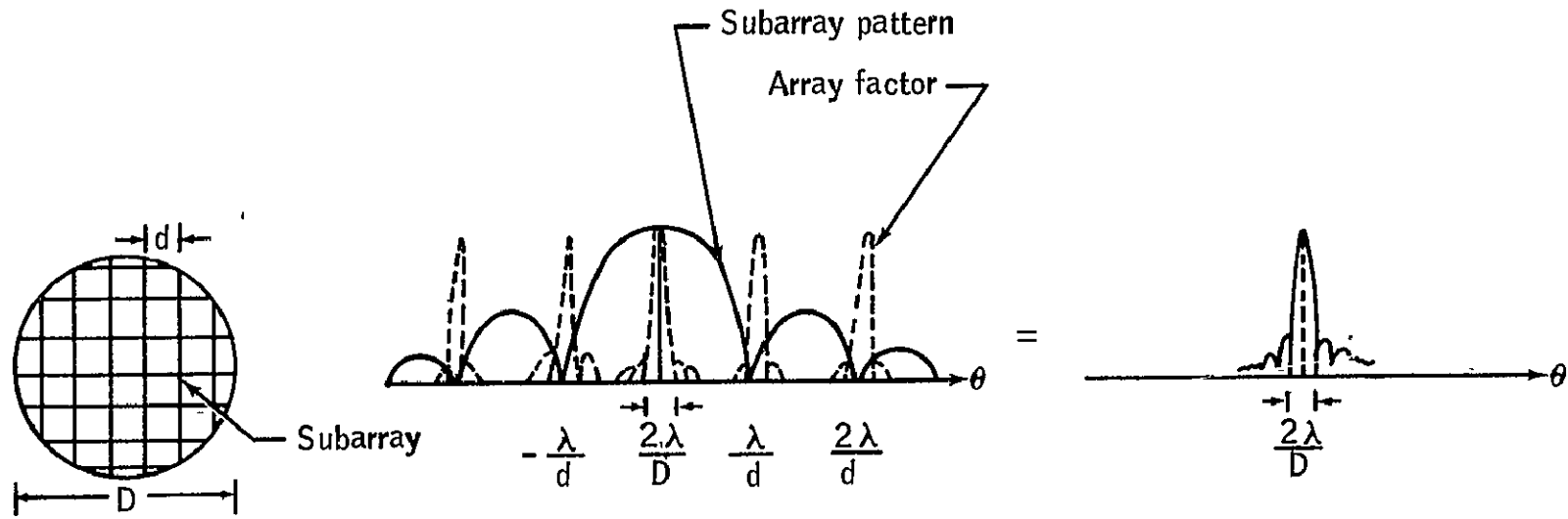


FIGURE IV-C-1-2 CONTIGUOUS, EQUAL-SIZE SUBARRAYS

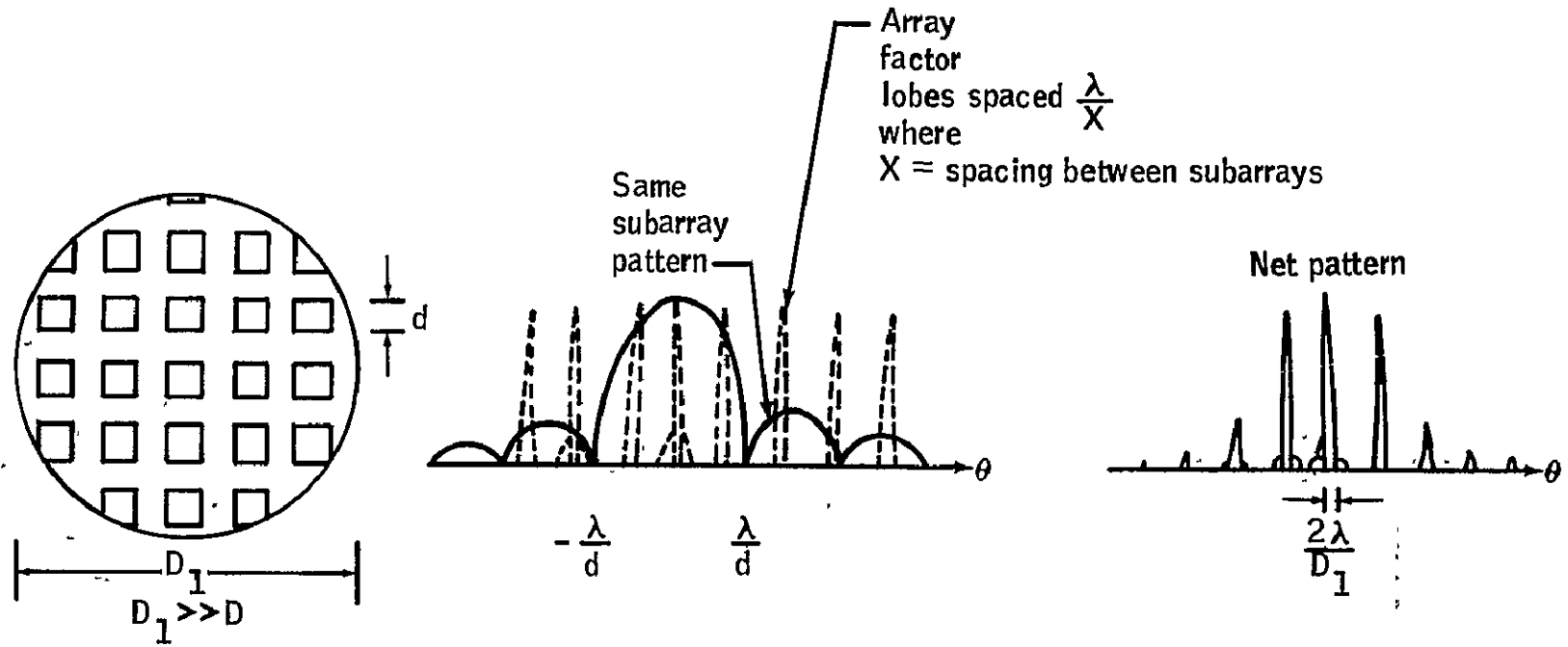


FIGURE IV-C-1-3 SAME SUBARRAYS SPREAD OUT ON REGULAR GRID

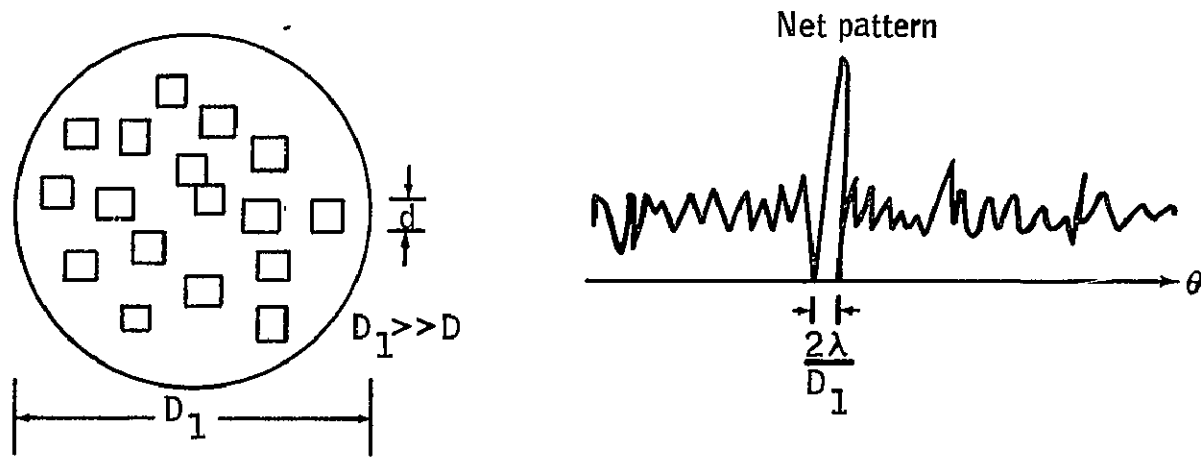


FIGURE IV-C-1-4 SAME SUBARRAYS SPREAD OUT ON NON-PERIODIC GRID

IV-C-2-a MICROWAVE GENERATORS

(1) RATIONALE

The primary candidates for DC to RF conversion are the amplitron and klystron. The microwave system, consisting of microwave generators, a large planar phased array antenna, and a ground antenna/rectifier combination must be capable of operating at high efficiencies over a 30-year lifetime with a low failure rate. Among the most important characteristics of the DC-RF converters are extremely high efficiencies and similarly high reliability punctuated by long life. In addition to the amplitron and the klystron, the traveling wavelube and solid state devices were investigated. Both the amplitron and klystron have exhibited a good record of operation in ground based systems and exhibit the best potential for the SPS.

(2) OPERATING CHARACTERISTICS

The amplitron possesses some characteristics, both physical and electrical, which appear very promising. Its weight for optimum efficiency of 88% is 2.27 kilograms. This includes the use of pyrolytic graphite for passive cooling of the 5 kilowatt tube. Because of the low power generated per amplifier, passive cooling will be possible.

The low weight and smaller dimensions of the amplitron allow for ease of handling and mounting on the waveguides. However, it also means that many more tubes will have to be assembled, tested, transported and mounted than the higher wattage klystron. Another desirable feature is that the amplitron will use a cold platinum cathode. Since hot cathodes wear out more quickly, the cold cathode should extend the length of life of an amplitron appreciably. Raytheon estimates that a 30 year longevity of operation of the amplitron is feasible.

The expected efficiency from the amplitron is somewhat higher (approximately 2% to 4%) than that to be achieved by the klystron. The power output of the amplitron is sensitive to changes in the input current. It is not markedly affected by voltage supply changes.

There are many apparent advantages in the choice for the klystron. After the manufacture of a klystron, it must be baked out. This is simply done by energizing a solenoid wound around the body of the klystron. On the other hand, the amplitron requires a separate facility to bake it out prior to full operation. Since this bakeout will be done in space, the facility to complete the amplitron production will be much more complex.

The klystron will operate to a higher temperature of 400°C because a solenoid coil is used to supply the magnetic fields. In the case of the amplitron, samarium-cobalt is the lightweight material to be used as magnets. It appears that there results a large drop in field intensity for a temperature change from 300°C to 350°C. Therefore, 300°C is the recommended upper limit for the amplitron.

The phase sensitivity of the klystron is a function of tube length, and thus of gain. A 50 kW 50 dB gain klystron will be close to 2000° long. (2 1/2 feet long) The phase sensitivity to beam voltage will be about -25°/kV. This means that as the beam voltage goes up one kilovolt, the electrons speed up and the phase length of the tube becomes shorter by 25 degrees. It further indicates that for close phase control, the beam voltage must be regulated. Moderate changes in beam voltage may,

of course, be accommodated by phase adjustments of the RF input drive, at the half watt level. The requirement for regulated beam voltage involves the cathode-body circuit, where power is relatively low.

Phase sensitivity for the amplatron, using constant current regulation, is $0.1^\circ/1\% \Delta V. = 0.1^\circ/\Delta 200 \text{ Volts}$. (Since the amplatron uses 20,000 volts on the anode, a 1% change equals 200 volts DC) Without this regulation, it would be $0.5^\circ/278 \text{ milliamperes change}$ or $3300^\circ/200 \text{ volts change}$. To regulate the phase, Raytheon proposes to control and regulate the voltage by varying the magnetic field. The output power is controlled by the applied DC voltage and the amplatron controls changes in this voltage by using a motor driven moveable pole piece, which varies the static magnetic field imposed on the tube. By changing the gap between the magnet poles, the magnetic field is changed. The pole gap is controlled by a DC brushless motor.

The klystron does not require a motor to control its magnetic field. It uses a fixed magnetic field.

In order to prevent breakdown in the amplatron due to arcing as a result of whisker growth on the tube elements, the DC arc will initiate a crowbar (circuitbreaker) which removes the DC voltage for 100 microseconds. The arcing which will arise in the klystron discharges internally and automatically to protect the tube.

Some of the tests which are contemplated for the microwave generators involve evaluating their performance in vacuum without the protection of envelopes. Under these conditions, their efficiencies must be determined, noise characteristics measured and heat transfer optimized. In the analysis of both crossed field amplifiers (amplitrons) and high-power linear-beam amplifiers (klystrons), most of the available data has originated from tests performed under earth atmospheric conditions. Exhaustive tests of these units in space are required.

The klystron has many desirable features as does the amplatron, therefore it is recommended that both klystrons and amplitrons be developed.

Some pertinent characteristics which are anticipated for the flight qualified microwave generators are listed in Table IV-C-2-a-1. Figures IV-C-2-a-1 and IV-C-2-a-2 are typical amplatron and klystron tube configurations which are being considered.

TABLE IV-C-2-a-1
SIGNIFICANT CHARACTERISTICS DC-RF CONVERTER SUMMARY

	<u>AMPLITRON</u>	<u>KLYSTRON</u>
DIMENSIONS	48 cms O.D. 16 cms LONG	75 cms O.D. 100 cms LONG
UPPER LIMIT OF TEMPERATURE	300°C	400°C
WEIGHT	5 POUNDS (2.27kg) FOR 5 kW TUBE	75 POUNDS (34.1kg) FOR 50 kW TUBE
TYPE OF TUNING	MECHANICAL TUNING BY MOTOR. MAGNETIC FIELD WILL BE TUNED AS PHASE SHIFTS.	FIXED
RF GAIN	7 dB	50 dB
RF INPUT DRIVE POWER	1250 WATTS	1 WATT
POWER OUTPUT PER TUBE	5000 WATTS	50,000 WATTS
EFFICIENCY	88%	86%
RF NOISE	MUCH HIGHER THEN KLYSTRON 70 dB/MHz DOWN. HARMONICS ARE 20 dB DOWN.	50 KHz FROM CARRIER 125 dB/KHz DOWN. HARMONICS ARE 40 dB DOWN

IV-C-2-a-3

TYPICAL

5 KW AMPLITRON ASSEMBLY

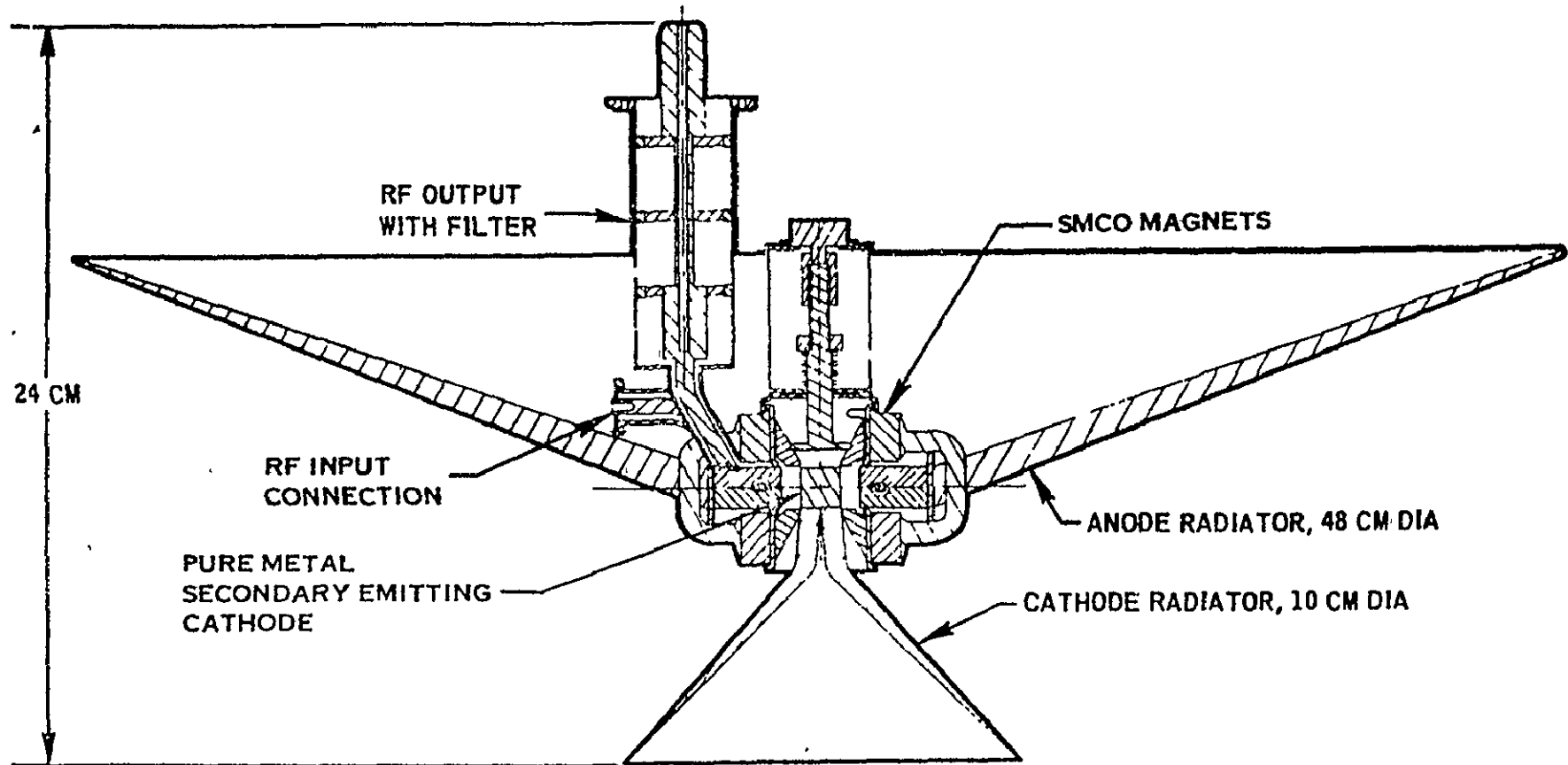


FIGURE IV C-2-a-1
IV-C-2-a-4

TYPICAL
50 KW KLYSTRON

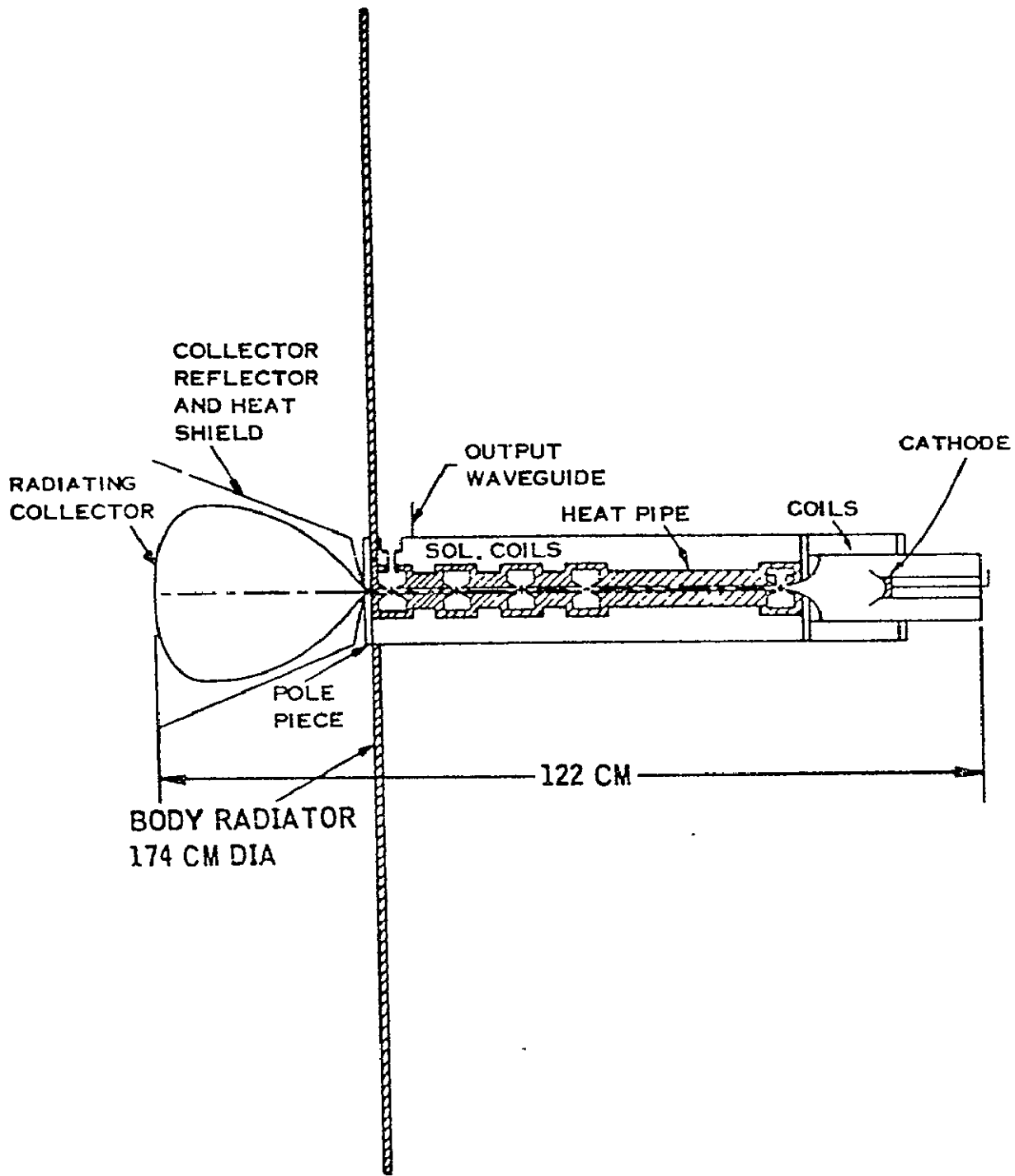


FIGURE IV C-2-a-2

IV-C-2-a-5

IV-C-2-b RADIO FREQUENCY INTERFERENCE

(1) RATIONALE

A solar power satellite (SPS) must be compatible with national and international users of the RF spectrum. The microwave generator, which will generate a high power main carrier frequency plus spurious noise near the carrier frequency and lower level harmonics, will be the main source of interference. Other sources of interference from the SPS will be power transfer equipment such as switches and slip rings, high voltage corona and high voltage arcs. Possible sources of susceptibility will be encountered in the monitoring and control links from the satellite power system to earth. These RF links will require sensitive receivers located near the high power DC to RF converters.

The frequency contemplated for use is 2450 MHz which has been allocated for industrial use. The DC to RF converters being considered for this application will require comprehensive test programs for the frequency spectrum emitted.

This section is the result of an evaluation of the RFI (radio frequency interference) considerations related to the design of an SPS. Interference to other users of the frequency spectrum (such as commercial radio, television, communications, navigation and radar equipments) may result from the operating frequency of the SPS as well as any spurious or harmonic frequencies it may generate. In the limited time available, this evaluation concentrated primarily on a review of existing documentation relevant to this problem. However, some limited laboratory testing was conducted to determine typical electromagnetic spectrum user equipment susceptibilities to such interference as the SPS would generate.

The transmission of solar energy to earth from orbital altitude by a microwave beam is a four-fold process: (1) conversion of prime source of energy into DC (direct current) power; (2) conversion of DC power into microwave power; (3) forming the microwave power into a narrow beam for transmission to the earth, and (4) collection and reconversion of microwave power into DC power. This evaluation of RFI considerations is concerned primarily with processes 2 and 3, since these may generate and radiate significant interference power which may affect other users of the electromagnetic frequency spectrum.

The SPS requirement for a converter that uses DC and converts this DC to high power microwave energy makes linear-beam tubes and crossed-field tubes theoretically acceptable for this operation. Some examples of linear beam tubes are klystrons and TWT's (traveling wave tubes). Examples of crossed-field tubes are magnetrons and amplitrons.

(2) DEFINITION

The linear-beam tubes exhibit better RFI characteristics than crossed-field tubes. In a typical linear-beam tube, spurious noise is down from the fundamental by -90 dB, while spurious noise is down only by -30 to -60 dB from the fundamental in a typical crossed-field tube. It was noted in an article from "Microwaves", entitled, "Controlling Interference in

Microwave Design", that the klystron amplifier is the "cleanest" tube at frequencies above and below the fundamental pass-band frequencies. The magnetron is rather noisy near the fundamental frequencies and frequently requires filtering. Amplitrons and magnetrons have the least second harmonic output, whereas the TWT's have the most. Magnetrons have particularly high third harmonic output levels. Klystrons and magnetrons generally work well into reflective filters, although absorptive filtering is recommended at megawatt pulsed or kilowatt cw (continuous wave) power levels.

If one considers the crossed-field devices (particularly the amplitron) because of parameters such as high efficiency and minimum weight as have nearly all present studies for proposed SPS designs, the following information should be noted. Most reentrant crossed-field amplifiers have cold cathodes and are started by applying RF drive. The RF drive power must be applied in time to permit the tube to start drawing current before the cathode voltage pulse overshoots the proper operating voltage. However, even when there is a drift region, the tube does not stop when RF drive is removed. The reentrant electrons still carry enough energy so that secondary emission from the cathode is maintained, and the tube will oscillate near a band edge or generate broadband noise until the cathode voltage pulse ends. From the above information, it is concluded that the amplitron generates broadband noise when RF drive is applied or removed until the tube stabilizes.

Figure IV-C-2-b-1 illustrates this unstable condition during application or removal of RF drive.

The amplitron and the klystron will require extensive testing to determine the exact noise characteristics for cw operation and to determine the degree of suppression or filtering that will be needed.

(3) ANTENNA CHARACTERISTICS AND RFI

The antenna being considered for forming the SPS microwave power beam directed toward the earth is a phased array, which makes use of the phase relationships among a number of individual radiating elements for combining the power from each element to form a main beam. The critical phase relationship between elements is a function of frequency as well as separation distance and the relationship of these parameters affects the main beam and sidelobes. For RFI considerations, the sidelobes at the operating frequency and off-frequency (spurious radiations and harmonics) are of interest. It should be noted that even with a clear channel assigned to the SPS, it is possible that interference may result to communications spectrum users due to the spurious responses of their individual equipments.

Unfortunately, no information on the off-frequency characteristics of phased array antennas could be located during the period of this study. This likely results from the past applications of this type antenna to radar systems, where off-frequency performance is not a primary consideration and is usually tolerated. Considerable tests will be necessary to develop this information for the SPS antenna application to allow evaluation of power station spurious and harmonic radiation effects on other users of the frequency spectrum.

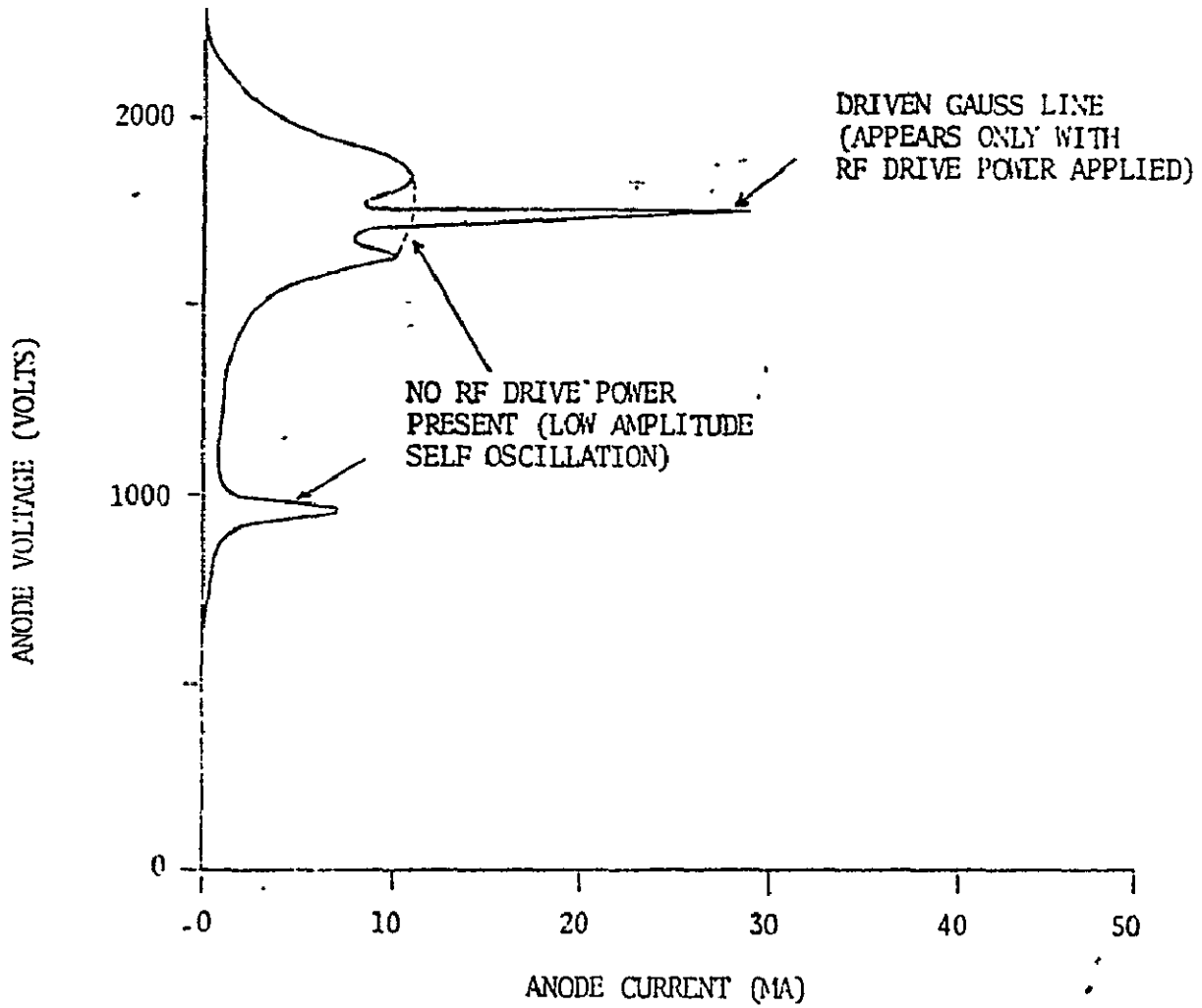


FIGURE IV C-2-b-1 VOLTAGE-CURRENT CHARACTERISTICS
 OF QKS 997A
 (CROSSED FIELD DEVICE)

Several reports which were reviewed assume that the primary radio frequency interference problem associated with the SPS is susceptibility to the fundamental operating frequency of the microwave transmission by other services users, due to side lobe radiation of the transmitting antenna. The validity of this assumption is dependent on the degree to which the output of the SPS can be filtered to remove unwanted spurious and harmonic frequencies. Given a transmitting antenna design, the structure and amplitude of the side lobes will vary with amplitude and phase errors on the transmitting aperture and the antenna side lobes are determined by the transmitting aperture distribution. In the case of a large antenna, additional contributing errors may be: flexing of the support structure, amplitude deviations in the outputs, and the possible failure of some of the microwave power generators.

(4) EARTH BASED CONSIDERATIONS

There is an acute lack of information on the RFI characteristics of cw high power amplifiers. Much testing is needed to measure the spurious output and harmonic output of several 5-10 kW cw power amplitrons or 50 kW klystrons. Measurements on several tubes are needed to determine a typical output spectrum since this spectrum will vary from tube to tube depending on the tolerances of the physical dimensions, the tube's operating voltages, and the vacuum in the tube. This testing, which could be performed in laboratories on earth, would determine if filtering is needed for the amplatron or klystron and what suppression engineering approaches should be examined. High power filter techniques need to be explored and tests need to be performed to determine the feasibility of implementing the techniques in hardware.

(5) CONCLUSIONS

The Solar Power Satellite as presently envisaged presents a possible radio frequency interference situation to other conventional service users of the electromagnetic spectrum. This will result from energy being radiated through the side lobes of the antenna at the operating frequency, as well as emission of spurious and harmonic frequencies. It is recommended that this problem continue to be studied. Extensive testing of DC to microwave power converters, high power filters and phased array antennas is necessary to fully evaluate methods of controlling interference. Finally, it would be desirable to perform interference tests on a pilot model of an SPS in low earth orbit to determine the total system effectiveness of interference control techniques applied to the elements comprising the SPS.

J. Kelley
L. Leopold
Tracking & Communications
Development Division

IV-C-3 SUBARRAY

The antenna array is made up of subarrays and each subarray contains elements which are the radiating portions of the antenna structure associated with the microwave generators. It is not necessary that each element be fabricated and assembled as a separate entity, but weight estimates in this report are based upon individual element design and assembly. The subarray reference configuration is a resonant slotted waveguide array where the guides are parallel fed by a "feedguide" which couples energy from the microwave generator into the slotted guides. The radiating surface is rectangular, deviating from a square to facilitate the buildup of multiple subarrays from identical elements for a given power density. The reference configuration maintains a constant output power level from the microwave generator and accomplishes power density variation by appropriate sizing of the element area.

a. RATIONALE

The function of the radiating elements is to couple RF power from the microwave generator into the radiated beam with a minimum power loss. This goal is approached by minimizing I^2R losses in the guides, maintaining a uniform amplitude and phase distribution at the radiating slots and providing a radiating surface that is essentially flat and perpendicular to the target line of sight.

The goal of uniform amplitude extends to the subarray level and, although amplitude taper is used for beam shaping, a controlled amplitude signal is required for the entire antenna. The net result of these prerequisites: controlled amplitude, minimum feed losses and minimum nonradiating area, leads to the selection of a slotted waveguide planar array (as has been the case for previous studies of the SPS system).

A resonant array, as opposed to a traveling wave array, can best fit these requirements, when coupled with the high power (50 kW), high gain (50dB) tube. The tubes can be excited in parallel using relatively low power levels of 2-3 watts and the entire power output fed to the radiating array. The resonant array couples all power, with the exception of I^2R losses, through the radiating slots into the RF beam and no power is dumped into a load (as would be the case for a traveling wave array).

b. SHAPE

Theoretically, the preferred geometry for the radiating surface of each element is a square since this shape minimizes the linear dimensions which in turn tend to reduce the surface error losses. The square configuration also minimizes the transmission line length in the guides, which also minimizes I^2R losses. However, neither of these effects is drastically changed by small variations from a square to a rectangular geometry. For example, the minimum transmission line length for a 1X4m rectangle is only 5/4 that for a 2X2m square element.

c. DEFINITION

There is a great deal of electromagnetic wave propagation art and analysis required in arriving at an effective slot array design. The design definition advanced here is a combination of textbook approximations, antenna experience and "rule-of-thumb" estimates. The objective was to obtain a configuration which would be adequate for weight estimation and the parameters determined in this study are suitable for this purpose.

The basic antenna element is depicted in Figure IV-C-3-1. The element components are: "The Input-Feed Guide" which distributes power from the tube to the radiating guides; the Back Face which contains slots for coupling power from the Feed Guide to the radiating guides and form the back wall for these guides; Vertical Walls which separate the radiating guides; Front Face which form the front wall of the radiating guide and contains the radiating slots; and End Walls which close out the ends of each guide.

The material chosen for all parts is aluminum which performs quite well electrically and which is both cheap and available as compared to the better electrical performers, copper and gold. The light weight and superior electrical characteristics of aluminum, lead to its choice over brass which is often used for waveguide applications on earth.

The proposed waveguide width is a nominal 10 cm (9.8 inside) for 2.45 GHz which leads to a slot spacing of 7.25 cm center to center. Errors in the location and length of these slots are very critical and tolerances will probably need to be held to a 0.001 in. or so with a surface accuracy of 0.1 in. in order to achieve a 95% element efficiency (worst case). However, these tolerances should be considered in conjunction with the various other loss factors for the antenna, i.e. phase control, pointing errors, surface distortions, generator phase and amplitude control, etc.

The reference configuration used for sizing and weight calculations may be a little conservative, however, caution should be taken not to remove weight from the antenna to the point where even more weight will be required in the total structure. Therefore, the antenna elements which lend themselves to structural support, feedguide and walls are sized at a thickness of 0.05 cm and the face sheets are carried at 0.025 cm.

d. OPERATING CHARACTERISTICS

The SPS antenna as conceived in this study is configured to operate as a large number of subarrays and elements (sub-subarray), each operating in parallel. The concept of parallel operation is important from the standpoint of controlling error buildup (correlation) and managing the attendant reduction in efficiency and sidelobe levels. All mechanical errors are translated into phase errors which are added to the electrical phase errors of the system.

Power density is accomplished by adjusting the size of the element to obtain an appropriate area while holding each generator at a constant power output level. This lends itself to a single tube design and allows the tube to operate at its maximum efficiency. However, if a

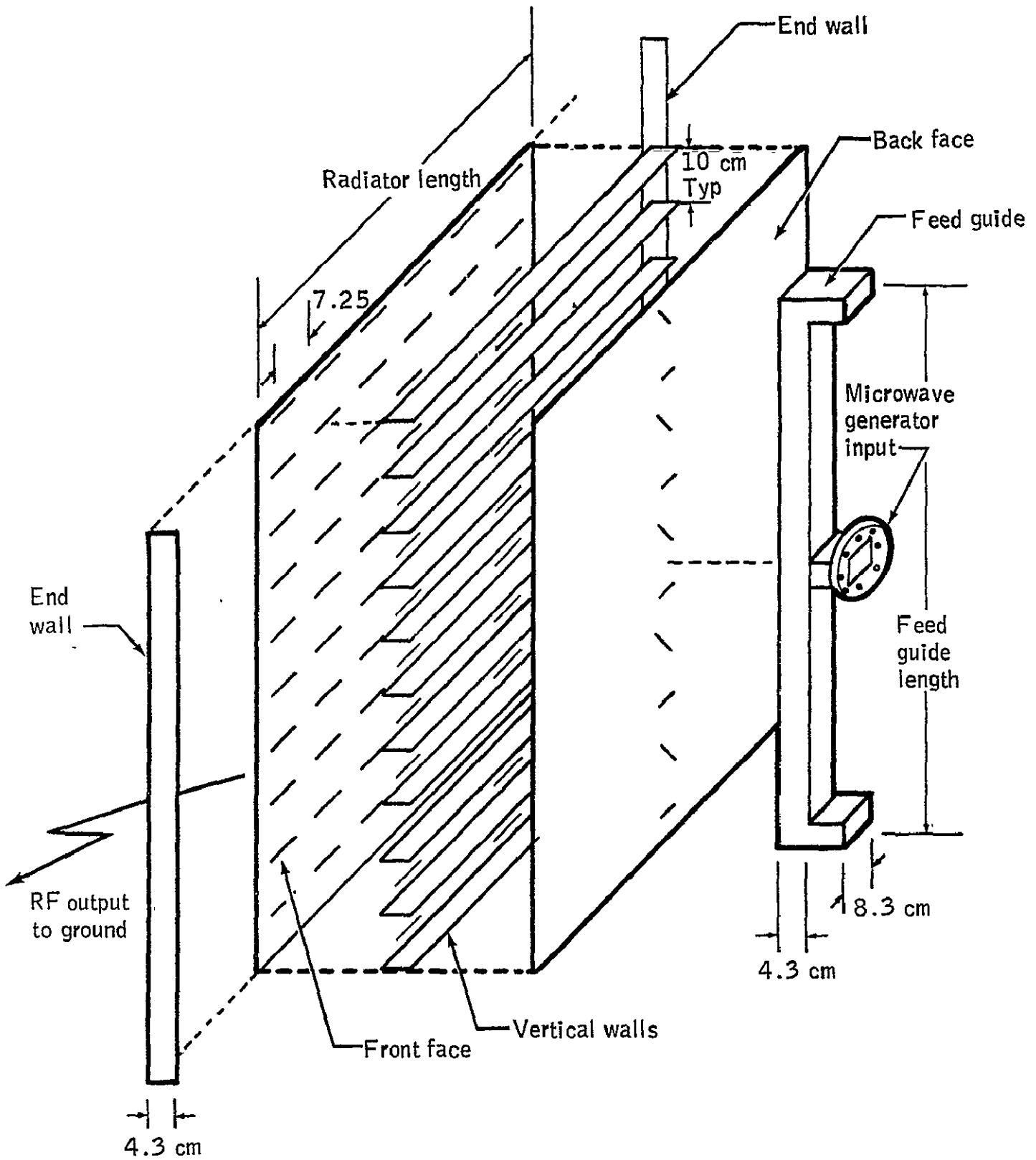


FIGURE IV-C-3-1 - Antenna element .

single antenna design is to be utilized for each subarray and a single subarray size is utilized through the antenna, element size and hence power density cannot be selected arbitrarily. Considerable leeway is available in selecting waveguide width, which then determines slot spacing; however, in attempting to obtain the maximum efficiency for a narrow bandwidth this width parameter becomes more stringent compared to the design of communication antennas.

The guide sizing and slot spacing in this study was primarily for the purpose of weight estimating and secondarily to provide some insight into manufacturing and assembly techniques. However, it has led to the conclusion that the antenna design should be investigated in detail analytically and experimentally to establish guide size and slot spacing for maximum efficiency. Then the exact subarray size and reasonable power density variation can be established.

In examining how the subarrays could be divided for power density requirements, consideration was given to the possibility of using common parts in elements of different areas. Only the feedguide and guidewalls are usable in this manner. Each change in radiating area requires different slot coupling factors and hence different slot locations. The walls are simply different lengths (measuring and cutting) which should not present too big a problem. This leaves only the feedguide as a multiple usage part.

The subarray size investigated was 100 m² (10m X 10m). Smaller subarrays tend to improve phase control and efficiency but increase cost, therefore, this is a reasonable place to work. Also, the cost vs weight tradeoff curve shows the 100 m² as the preferred size. The support structure design evolved toward a subarray side ratio of 0.866 to accommodate an equiangular triangular layout of mechanical pick up points. This could be accommodated with no apparent loss in efficiency when compared to a square subarray arrangement and there doesn't appear to be any change in weight. It is noted that the subarray layout was not reshaped for this configuration.

e. TECHNOLOGY STATUS

The technology base for designing and fabricating the proposed array elements is readily available. The following steps should be taken to achieve an antenna design capable of being assembled in space and approaching 95% (worst case) efficiency.

(1) Perform analysis, design and fabrication using current techniques to determine maximum achievable efficiency.

(2) Investigate compromise designs and determine efficiency loss incurred to reduce cost and/or facilitate on-orbit manufacturing and/or assembly.

f. WEIGHTS

The element sizing and power density levels used for weight estimates are given in Table IV-C-3-1. This is based upon a nominal guide width of 10 cm and no consideration is given to allowable radiator length in terms of integral slot spacings. A breakout of weight per part for a 20 kW/m² subarray is given in Table IV-C-3-2. As expected, the big weight factor is the face sheets.

The total weight was estimated in Table IV-C-3-3 from the JSC proposed 10 step power density profile (taper). To obtain the total weight for each specific power density area, the taper had to be reduced to 7 steps to produce a practical design for the sizing of the elements. This resulted in only 7 different sizes for the elements - one specific size for each power density area. Knowing the weight per element and the number of elements per subarray, the weight per subarray was calculated. The number of subarrays in each power density area was measured and final weights per power density area and per total antenna array were computed.

TABLE IV-C-3-1
SUBARRAY WEIGHT TABULATION

Constraints

50 kW Tube
10m X 10m Subarray
Uniform Element Design
each subarray

Power Density kW/m ²	Element Size Feed Guide X Radiator Length(m) Length(m)	Elements per Subarray	Weight per Subarray Kg
20	1 X 2.5	40	240
15	1 X 3.3	30	230
12.5	2 X 2	25	238
10	2 X 2.5	20	230
7.5	2 X 3.3	15	225
5	2 X 5	10	218
3	5 X 3.3	6	156

Required Component Designs

Face Sheets	7
Radiating Slots (Front Face)	4
Feed Slots (Back Face)	3
Feed Guide	3
Vertical Walls	4
End Walls	3

TABLE IV-C-3-2
TYPICAL ELEMENT WEIGHT TABULATION

Subarray Weight (Partial)

10m X 10m Subarray

20 kW/m² Power Density

50 kW Tube

Radiating Structure - 40 Elements	240 Kg
-----------------------------------	--------

Antenna Elements - 1m X 2.5m

Face Sheets - 0.010 in. Al	3.5 Kg
Vertical Walls - 0.020 in. Al	1.7
End Walls - 0.020 in. Al	0.1
Feed Guide - 0.020 in. Al	0.3
Input (flange 0.312 in. Al)	0.4
	6.0

TABLE IV-C-3-3
ANTENNA WEIGHT TABULATION

<u>Power Density kW/m²</u>	<u>Radius m</u>	<u>Area m²</u>	<u>Weight Kg/100m²</u>	<u>Total Weight Kg</u>
20.88	132.5	5.5 X 10 ⁴	240	1.32 X 10 ⁵
19.16			240	
16.97	295	21.9 X 10 ⁴	230	5.04 X 10 ⁵
14.88			230	
12.73			230	
10.55			230	
8.43	387.5	19.7 X 10 ⁴	225	4.43 X 10 ⁵
6.31			225	
4.13	455	17.9 X 10 ⁴	218	3.90 X 10 ⁵
2.59	500	13.5 X 10 ⁴	156	2.10 X 10 ⁵
				1.68 X 10 ⁶ Kg

IV-C-4 PHASING OF ANTENNA

a. RATIONALE

The antenna array must be coherently transponding and "central phasing" should be used on large, low mass arrays in order to transmit power from geosynchronous satellites to earth. An active retrodirective array is a self-phasing array which transmits a beam towards the source of an incident signal. All self-phasing transmitting arrays are based on the "phase conjugation" principle. Each subarray of the array is connected to a circuit which transforms the received phase $\omega t - \beta r$ into transmitted phase, $\omega t + \beta r$ (ω is the frequency of the incoming "pilot" signal, r is the distance from the pilot source to the subarray, and $\beta = \omega/v$ where v is the phase velocity in the intervening medium). Since $\omega t + \beta r$ is the phase of a wave traveling towards $r = 0$, the envelope of all the spherical waves radiated by each subarray is just the incident wave front reversed in direction.

b. DEFINITION

In order to efficiently transmit power from geosynchronous satellites using large phased array antenna systems, it is necessary to precisely control the phase of the radio frequency signal transmitted from each element in the array. To accomplish the required phasing precision, an array which is self-focusing is proposed. Such arrays are referred to as retrodirective in that the transmitted signal is directed toward a reference source or pilot signal transmitter at the rectenna. The pilot signal transmitter is located with the rectenna or ground receiving antenna and thus insures that the transmitted beam is properly phased for pointing in the desired direction. Figure IV-C-4-1 illustrates the basic concept of the retrodirective (adaptive phase control) array system.

c. OPERATING CHARACTERISTICS

Adaptive phase control is accomplished by the process of "phase conjugating" the received pilot signal. Each subarray of the transmitting antenna array is connected to a circuit which transforms the phase of the received pilot signal at that subarray ($\omega t - \beta r$), into a conjugated phase ($\omega t + \beta r + \theta_R$) for retransmission. ω is the frequency in radians per second of the RF (radio frequency) signal, t is time, r is the distance from the pilot transmitter to the receiving subarray, and β is a constant dependent on the transmission medium, and θ_R is a constant phase shift resulting from the reference system phase control. It should be noted the θ_R is the same for each subarray in the array system.

Since the retransmitted signal from each subarray has a phase which is exactly equal and opposite to the phase shift that results as it propagates back toward the pilot source (rectenna), then all subarray signals will be received at the rectenna with the same phase θ_R and the envelope of the spherical wave fronts will be normal to the rectenna.

Phase conjugating may be realized in several ways. A well-known technique employs heterodyning and is shown functionally in Figure IV-C-4-2. Other approaches include servoing phase shifting devices

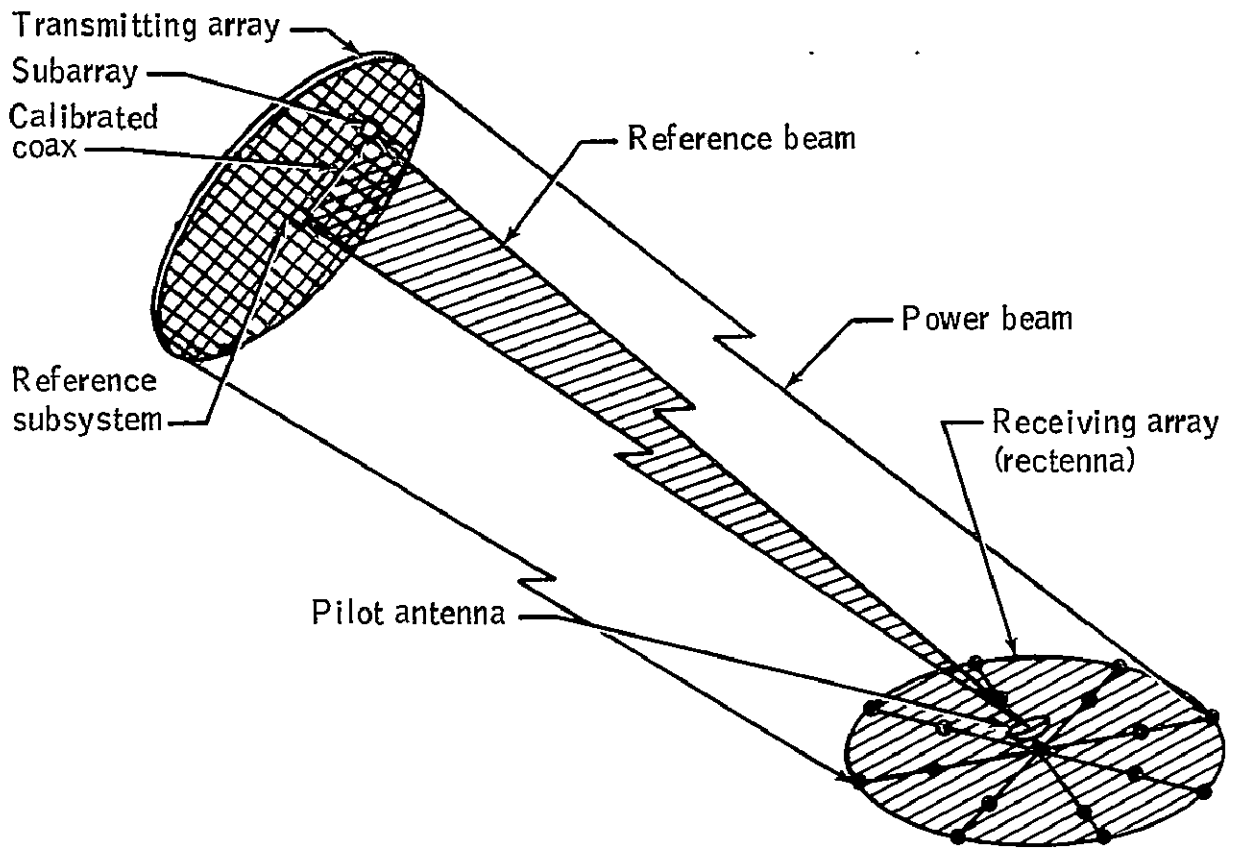


FIGURE IV-C-4-1 COMMAND AND ADAPTIVE PHASE FRONT CONTROL CONCEPTS

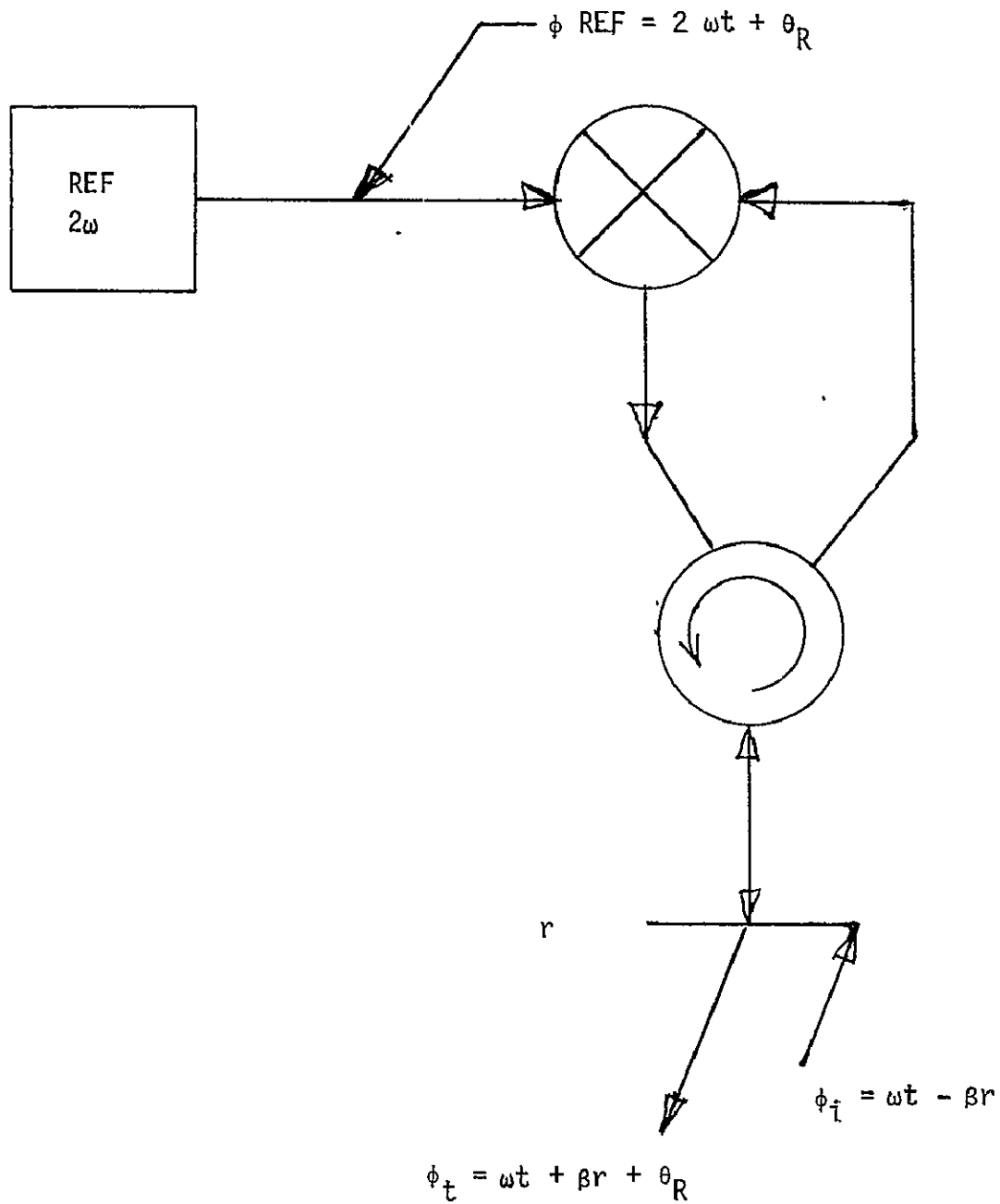


FIGURE IV-C-4-2 SIMPLE HETERODYNING PHASE CONJUGATING CIRCUIT

to bring the received signal phase into agreement with a reference phase, and then the transmitted signal is passed through the same phase shifter, and phase conjugation results.

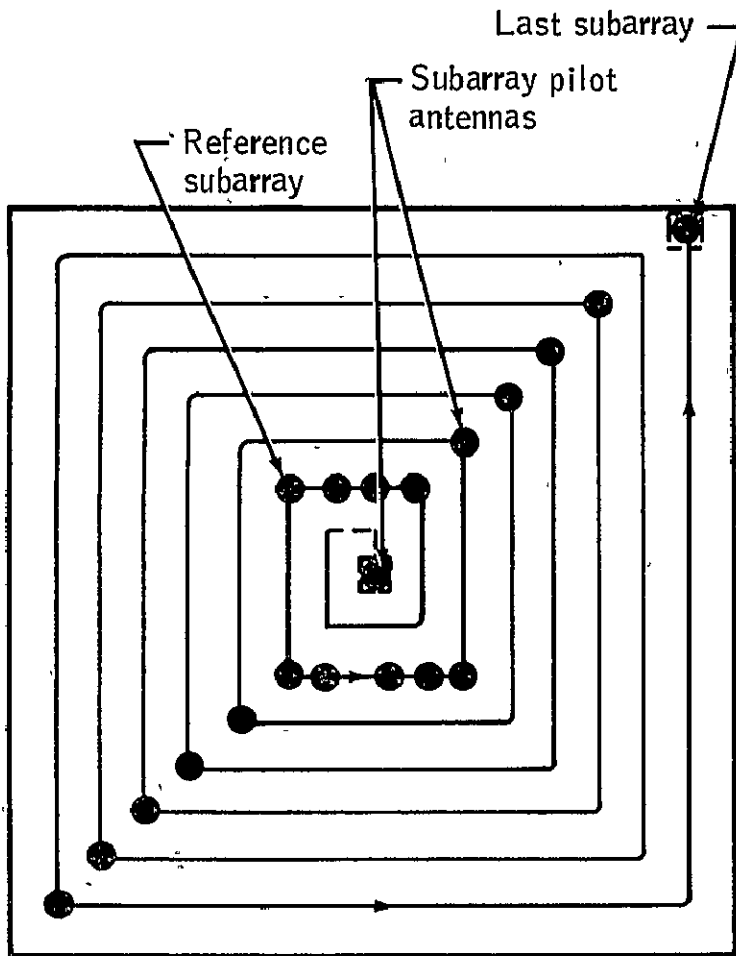
The heterodyning technique is recommended to be employed in the basis SPS (Solar Power Satellite) phase control system. The conjugation occurs by the process of heterodyning and sideband filtering. Referring to Figure IV-C-4-2, the incoming signal phase is $\theta_R = \omega t - \beta r$ where ω , t , β and r are as defined previously. The received signal is mixed (multiplied) by a reference signal of phase $\phi_{Ref} = 2 \omega t + \theta_R$. The signals resulting from the multiplication process include sum and difference terms whose phases are $(\omega t + \beta r + \theta_R)$ and $(3 \omega t - \beta r + \theta_R)$. By frequency selection (filtering), the signal with the desired phase (conjugated) for transmission can be obtained $\phi_t = \omega t + \beta r + \theta_R$. This process must be accomplished at each subarray, and the reference phase θ_R must be the same at each subarray. To accomplish the subarray phasing, a reference phase distribution system is required. Two approaches have been investigated. Both employ adaptive techniques.

The transmission line approach employs a central phase reference/control system and radio frequency transmission line distribution of the phase reference signal to each subarray. This system requires precise control of the phase shifts associated with each transmission line and if each subarray required an independent reference transmission line, cable weight would be extremely large. (A system for 1 km diameter circular transmitting antenna and 10m X 10m subarray has 7854 subarrays.)

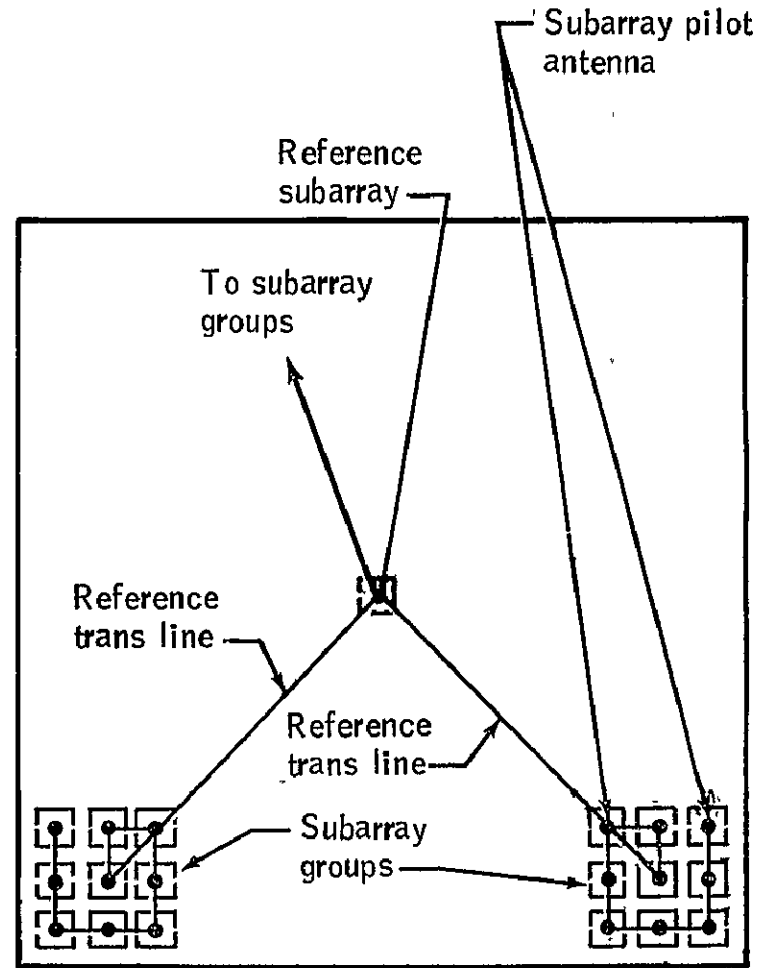
The subarray-to-subarray approach employs phase conjugating reference receivers at each subarray and distributes the initial reference phase from the first subarray to other subarrays, sequentially, until all subarrays are connected. This approach could result in extremely large phase error build-up at the subarrays furthest from the initial receiving subarray. As a result of these initial investigations, the proposed SPS phasing system is a combination of the two approaches studied. A central phase reference and distribution system will be employed, and the phase reference signal will be transmitted to groups of subarrays via RF cable. The subarray groups will then employ the subarray-to-subarray reference distribution scheme. This approach will reduce the amount of transmission cable required, and since only 8 or 10 subarrays will be connected in series, the phase error build-up will be insignificant. Figure IV-C-4-3 illustrates the totally sequential distribution system as well as the transmission line/subarray group sequential distribution systems discussed above.

Figure IV-C-4-4 shows the overall array approach proposed which utilizes the transmission line and subarray group sequential phase distribution system. The electronics required to accomplish the phase control/conjugating process is shown in the block diagram of Figure IV-C-4-5. The operation of the system is described below. At point 1, the received pilot signal phase θ_p at the central phase reference receiver is detected, and a locally generated reference signal is obtained by phase

IV-C-4-5



SEQUENTIAL (SUB-ARRAY TO SUB-ARRAY)
REFERENCE PHASE DISTRIBUTION



TRANSMISSION LINE AND SEQUENTIAL
REFERENCE PHASE DISTRIBUTION (HYBRID)

FIGURE IV-C-4-3 RETRODIRECTIONAL PHASING

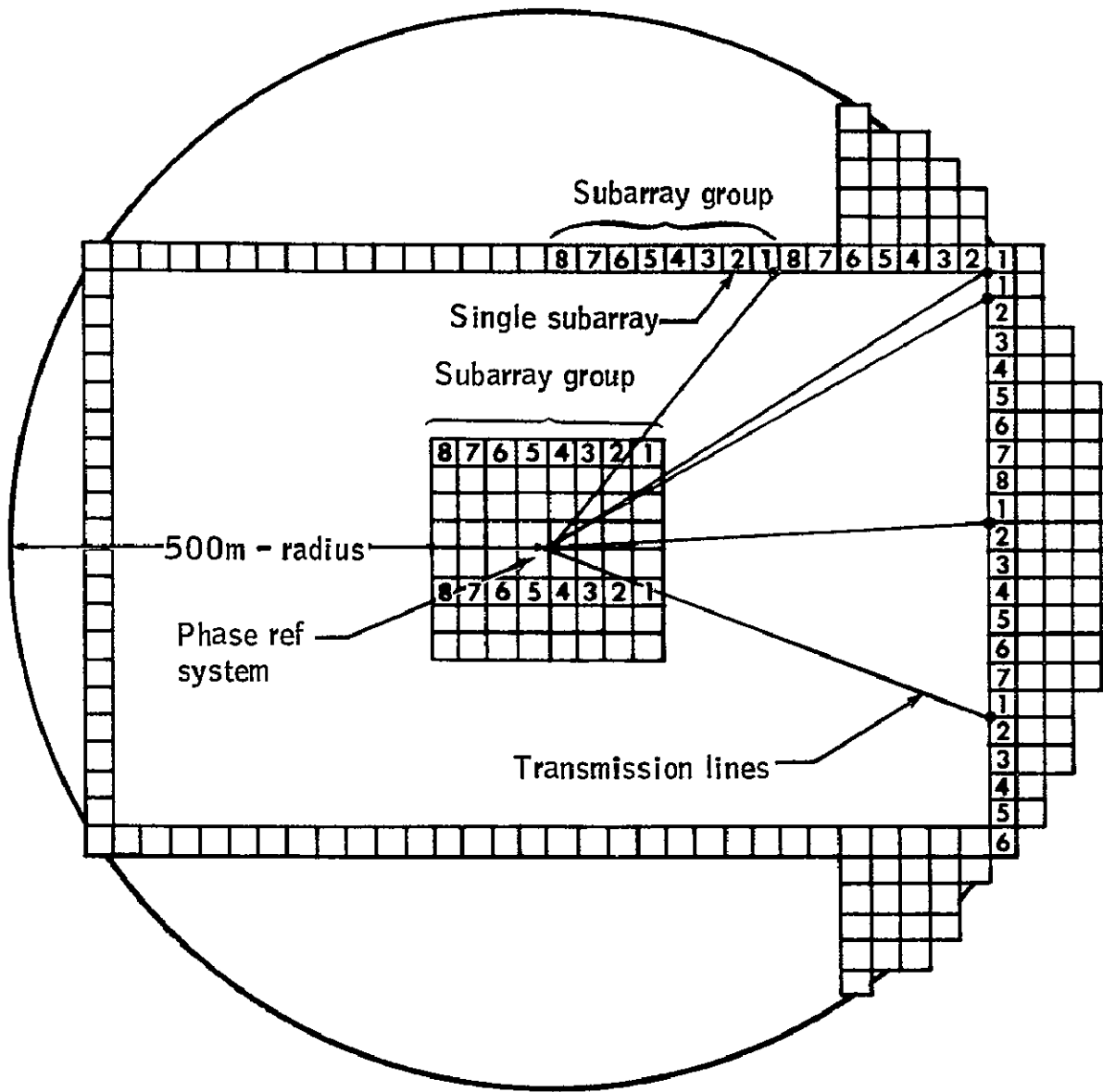
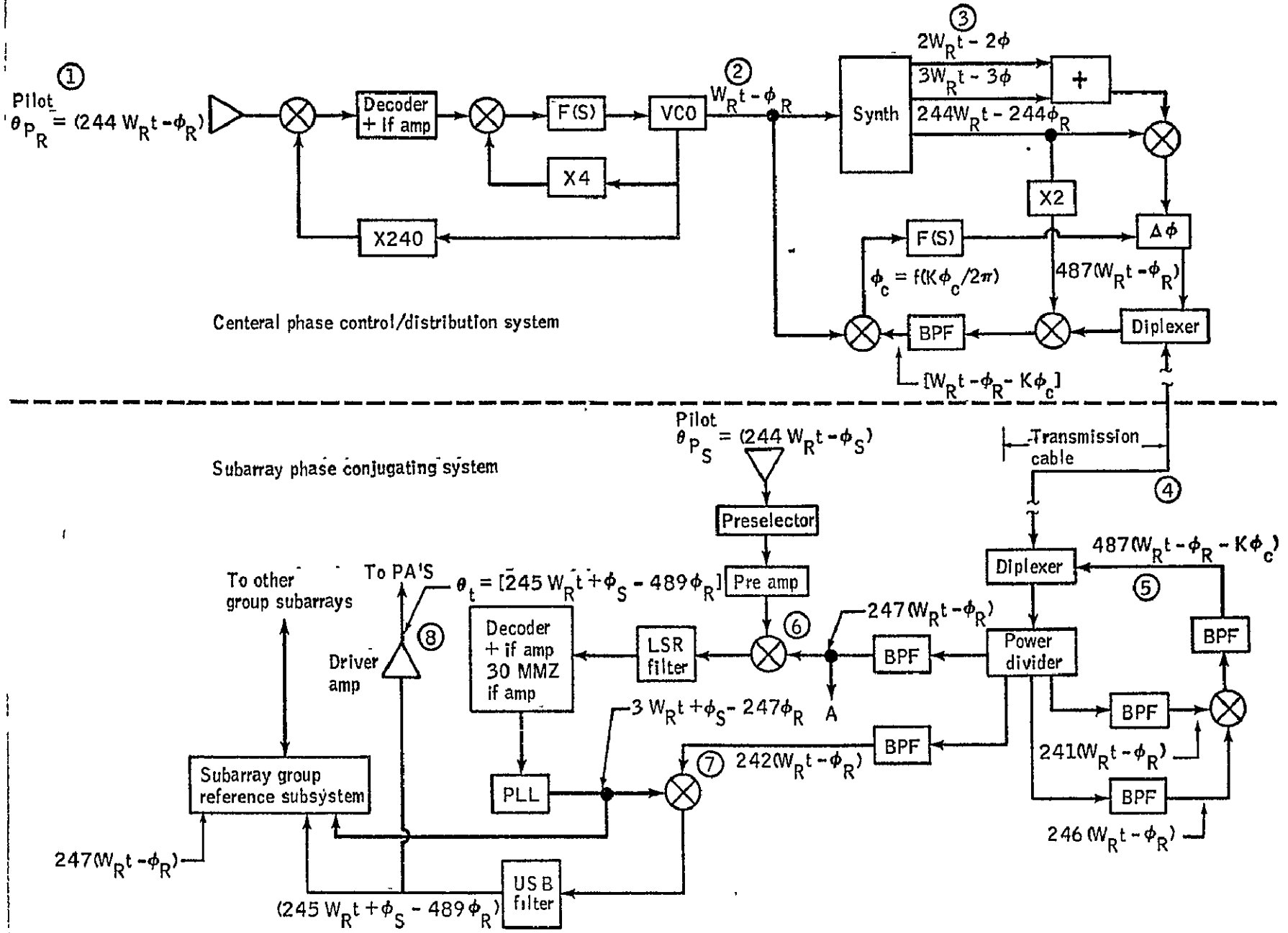


FIGURE IV-C-4-4 OVERALL ARRAY PHASING CONTROL CONCEPT 10X10 METER SUBARRAYS

ORIGINAL PAGE IS
OF POOR QUALITY

IV-C-4-7



lock techniques. This reference signal will then have a phase of $\omega_R t - \phi_R$ and occurs at point 2 on the diagram. In order to provide the necessary signals for phase conjugation and phase shift control of the transmission lines, the reference signal is coherently synthesized into several different frequencies, point 3 on the diagram. These signals are then transmitted via the distribution system to each subarray group, point 4. When the reference signals are received at the control subarray, the transmission phase control signals are recovered and transmitted back to the central phase control system for automatic adjustment of the transmission line time delay to maintain a constant phase shift at each subarray group. The phase control signals are formed by multiplying two of the phase reference terms and filtering the upper sideband signal. The control signal thus has a phase $487 (\omega_R t - \phi_R - K\phi_C)$ as seen at point 5 on the diagram. Figure IV-C-4-6 shows the frequency spectrum of the phase reference distribution signals, the received pilot signal, ω_p , transmitted power signal ω_t , and the phase control feedback signal ω_{FB} . The two reference signals used in the conjugating process are $242 \omega_R$ and $247 \omega_R$. These are filtered and used as reference signals for the two mixers (multipliers) shown at points 6 and 7, on Figure IV-C-4-5 respectively. At point 6, the $247 (\omega_R - \phi_R)$ phase reference signal is mixed with the pilot signal received at the particular subarray pilot receiver. This occurs at one of the subarrays in each subarray group, and the conjugation process is referenced to that pilot phase for all subarrays in that group. The lower sideband of the multiplication process is selected by filtering and the signal is locked to by a phase lock receiver. It should be noted here that the pilot signal is assumed to be modulated or coded to insure that other SPS systems will not interfere with the phase control process. This coding must be removed coherently and a clean unmodulated signal delivered to the power tubes. The cleaned-up signal is then mixed at point 7 with the $242 (\omega_R t - \phi_R)$ phase reference signal and the upper sideband of the multiplication terms is filtered. This signal is then the phase conjugated transmit signal desired with phase $245 \omega_R t + \phi_S - 489 \phi_R$. The signal is then amplified by the PA driver amp., (point 8) and transferred to the subarray transmitter via precisely controlled waveguide lengths. The properly phased "exciting power" must be distributed from the "electronics" on each subarray to the microwave generators. The path length between each tube and the electronics must be maintained constant and represent an integral number of wave lengths. Thin-walled aluminum waveguide is proposed for this function. The guide must be securely fixed to the subarray support structure and distortion of the guide should be minimized. Waveguide is selected over coax cable because of low RF losses.

A typical subarray layout is shown in Figure IV-C-4-7 for the center of the antenna. The total run of waveguide is 45m for a subarray weight of 18 kg.

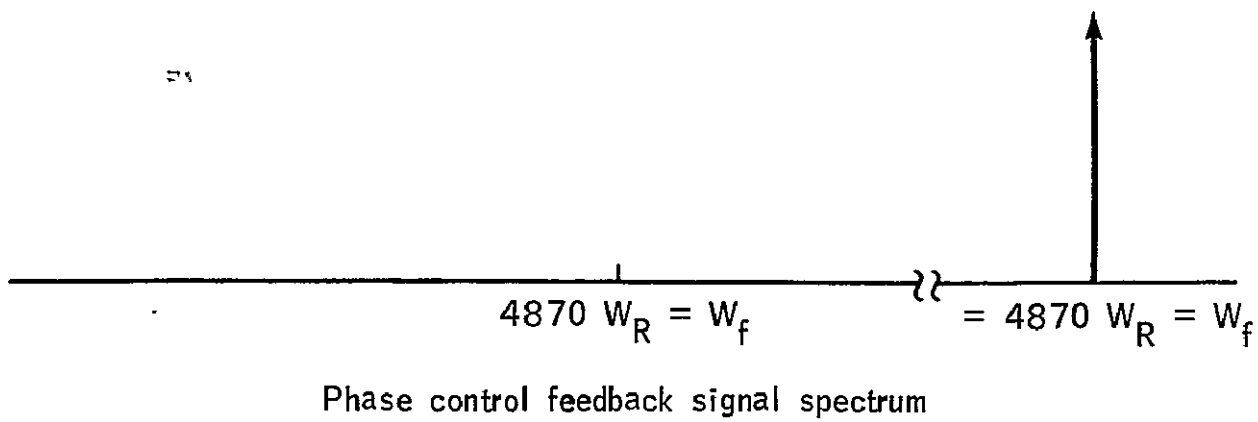
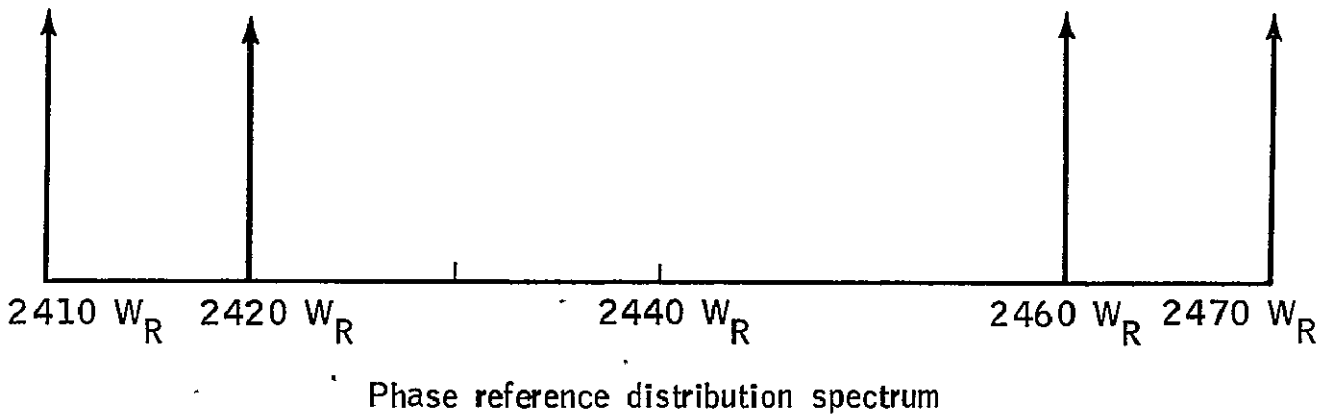
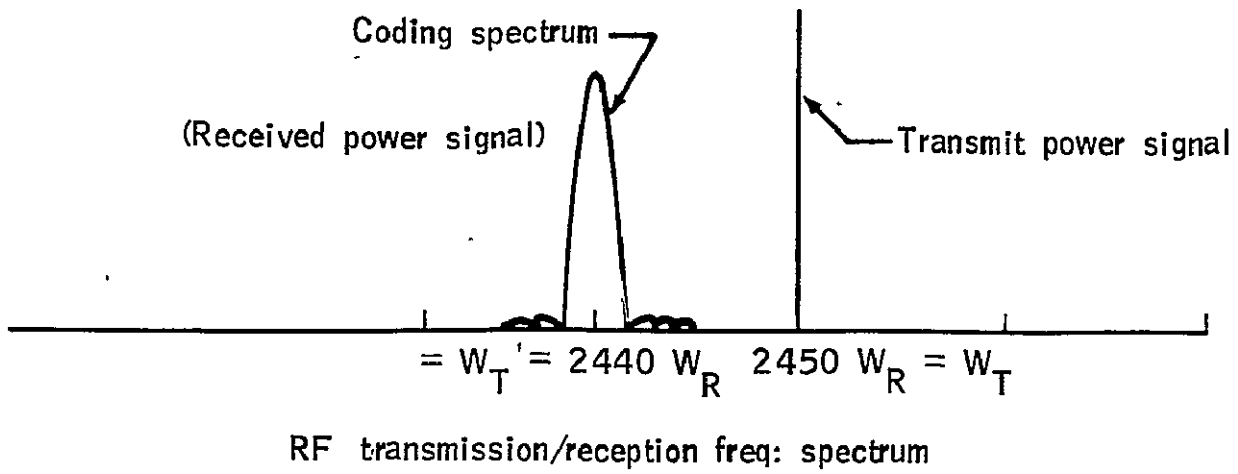


FIGURE IV-C-4-6 RF PHASE CONTROL/REFERENCE SIGNAL SPECTRA

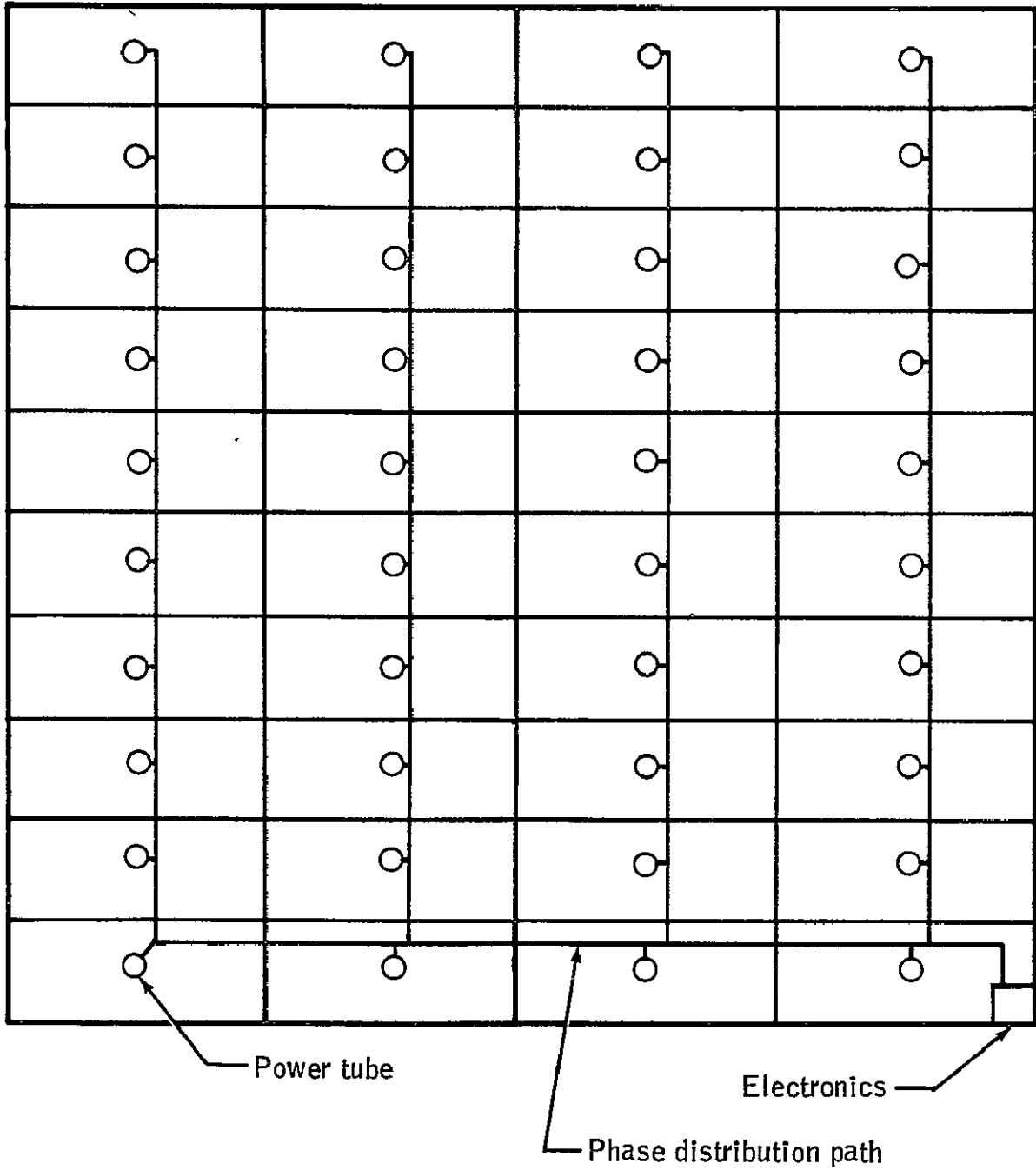


FIGURE IV-C-4-7 10 METER X 10 METER SUBARRAY LAYOUT 50 KW TUBE

Figure IV-C-4-8 illustrates an optical distribution technique under investigation. The system incorporates fiber optics transmission lines rather than RF cables for distribution of the phase reference RF signals. The techniques proposed have been determined to be feasible; however, space qualifiable fiber optic transmission lines are not presently available and a great deal of development will be required in this area. Because of the potential weight savings aspect of the fiber optics transmission lines, further investigation is recommended.

Additional recommendations include the investigation of the optimum phase distribution of the RF cables with respect to the reference phase. The subarray group size should be studied to reduce the number of RF transmission links and still limit the accumulated phase errors so that phase control is effective. The RF frequency spectrum should be investigated to establish a pilot reference signal. The goal would be to reduce transmitter interference problems, reduce the complexity of the phase electronics and reduce the weight of the electronics circuits.

Possibilities of major concern involve potential requirements of phase control for each klystron or each amplatron. The phase stability of the system components outside of the phase control system loop should be analyzed and tested. Electromagnetic and radio frequency interferences by the microwave power generators and the antenna array transmissions on the phase reference system need to be investigated.

The cost/weight estimates for the baselined phasing system is shown in Table IV-C-4-1.

Losses due to beam pointing error caused by designed frequency offset between the received pilot signal $244 \omega_R$ and the transmitted signal $245 \omega_R$ produces a pointing error in the transmitted beam. A received signal at a subarray at a distance L from the antenna reference receiver has a phase offset with respect to the reference signal of $\Delta\phi = \frac{2\pi L \sin \theta_r}{\lambda_r}$. (See Figure IV-C-4-9)

By definition, the transmitted signal will have the same phase offset which gives rise to a different phase front and hence a transmit angle θ_t different from θ_r .

$$\Delta\phi = \frac{2\pi L \sin \theta_T}{\lambda_T}$$

Since the phase offset $\Delta\phi$ is the same for transmit and receive:

$$\frac{2\pi L \sin \theta_T}{\lambda_T} = \frac{2\pi L \sin \theta_r}{\lambda_r}$$

$$\frac{\sin \theta_T}{\lambda_T} = \frac{\sin \theta_r}{\lambda_r} \quad \text{then} \quad \frac{\sin \theta_1}{\sin \theta_2} = \frac{\lambda_T}{\lambda_r}$$

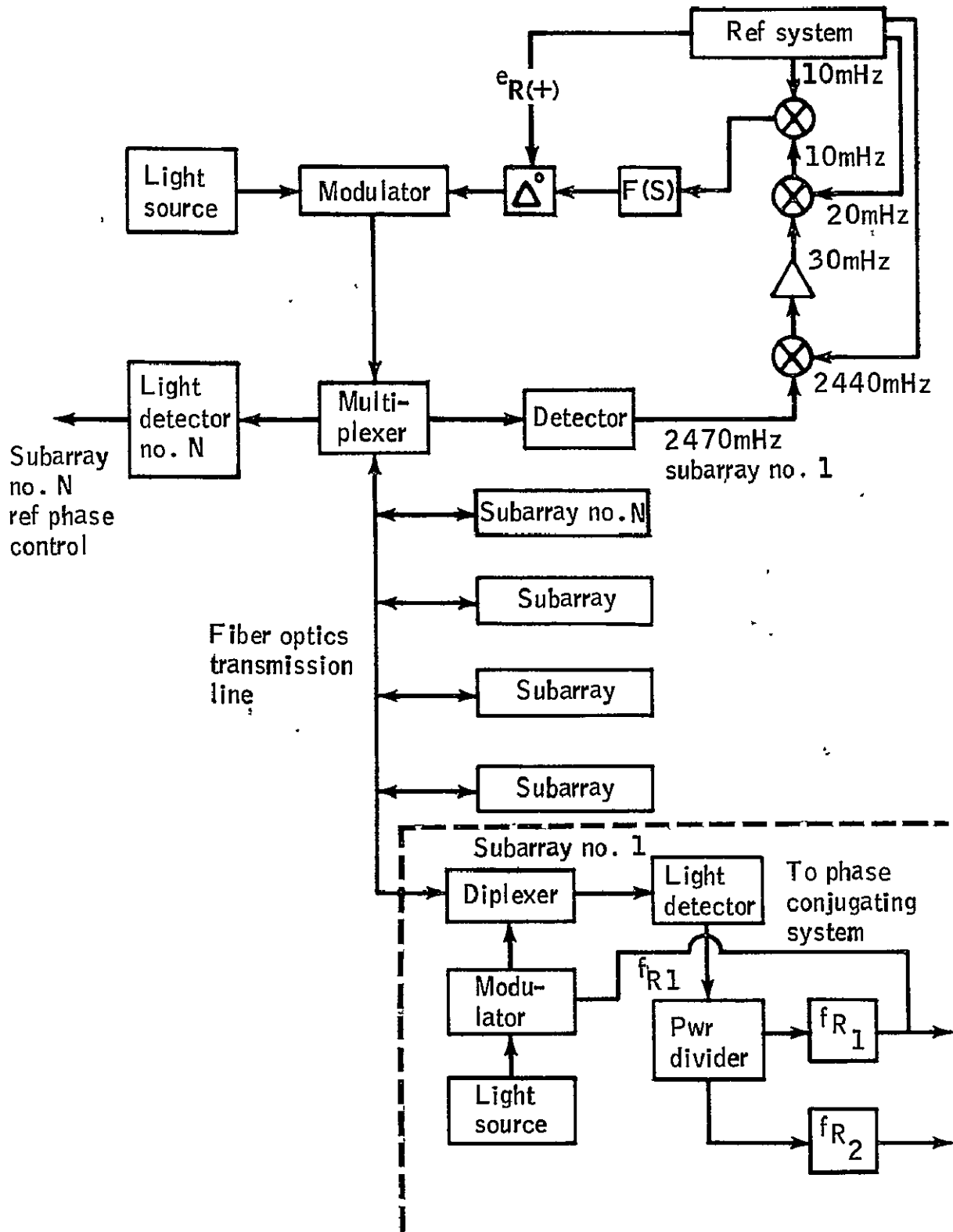


FIGURE IV-C-4-8 FIBER OPTICS DISTRIBUTION SYSTEM

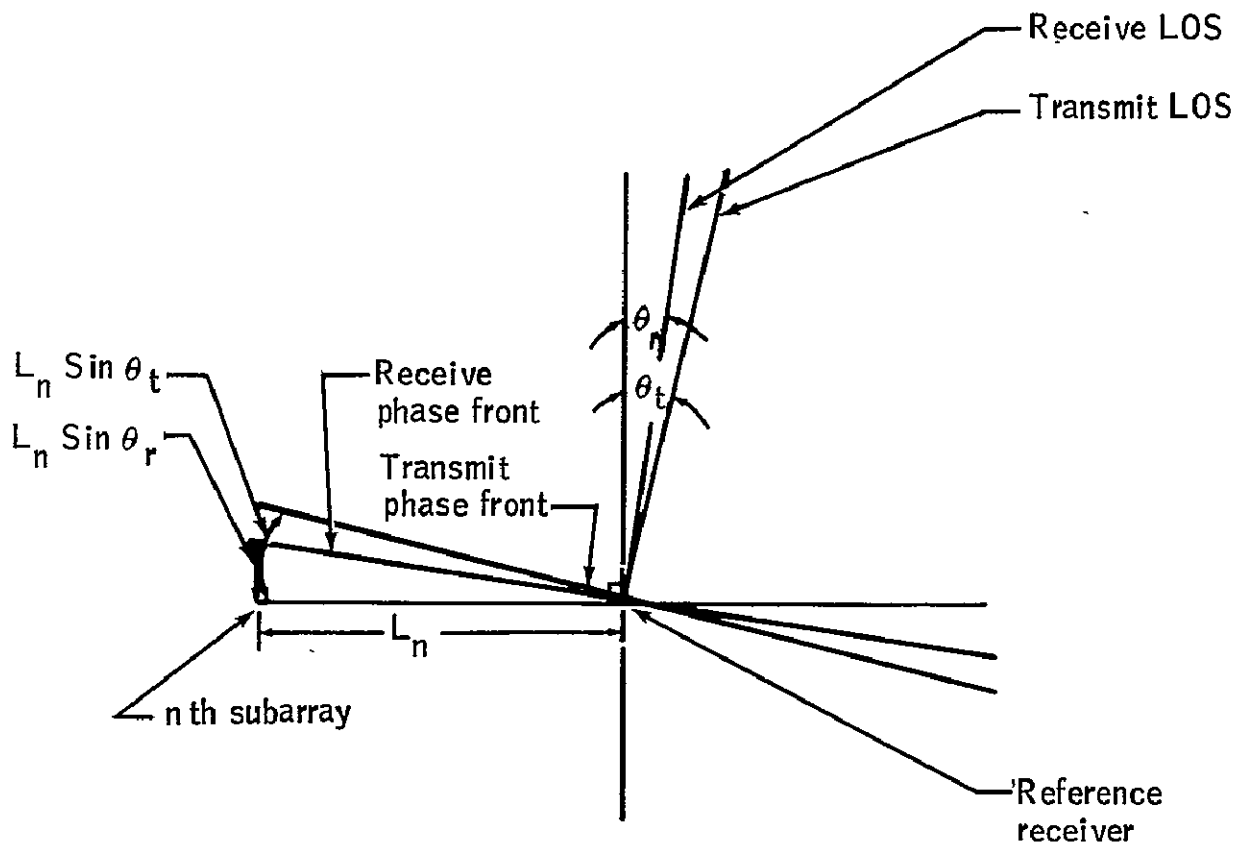


FIGURE IV-C-4-9 LOSSES DUE TO BEAM POINTING ERROR

For small angles (the antenna pointing error is limited to 1 arc min)
 $\sin \theta$ is approximately θ and

$$\lambda_T / \lambda_r = \frac{f_r}{f_T}$$

$$\frac{\theta_T}{\theta_r} = \frac{f_r}{f_T}$$

Where θ_r is the angle between the received electrical signal and the mechanical boresight.

Where θ_T is the angle between the transmitted electrical phase front signal and the mechanical boresight.

Where $\Delta\theta$ is the difference between the electrical boresight of the received signal and the electrical boresight of the transmitted signal.

The pointing error $\Delta\theta$ is

$$\Delta\theta = \theta_T - \theta_r$$

$$\frac{\Delta\theta}{\theta_r} = \frac{\theta_T}{\theta_r} - 1$$

$$\frac{\Delta\theta}{\theta_r} = \frac{f_r}{f_T} - 1$$

$$\frac{f_r}{f_T} = \frac{\Delta\theta}{\theta_r} + 1$$

Thus, the allowable frequency offset for the pilot signal is defined by the allowable pointing error:

$$\frac{f_r}{f_T} = 1 + \frac{\Delta\theta}{\theta_r}$$

For a frequency offset of 100 MHz:

$$\frac{2550}{2450} - 1 = \frac{\Delta\theta}{1} \text{ arc minute}$$

$$\Delta\theta = 1.04 - 1$$

$$\Delta\theta = .04 \text{ arc minute}$$

Since 1 arc minute = 10,500 meters on the ground

$$\Delta\theta = 420 \text{ meters}$$

The predicted noise states that we have to be 100 MHz away from the carrier frequency.

Based upon the maximum pointing error of 1 arc minute and the noise band of ± 50 MHz, the noise level at the phase receive frequency may be too high. This would require a pilot frequency of f_T (one-half the transmit frequency) or $2 f_T$ (double the transmit frequency) or an integral multiple of f_T to avoid $\frac{1}{2}$ the noise level generated at the carrier frequency and make for noise-free phase control.

TABLE IV-C-4-1

PHASING SYSTEM COST/WEIGHT SUMMARY
(10 X 10 METER SUBARRAYS)
TOTAL NUMBER OF SUBARRAYS 7854

I. CENTRAL PHASE REFERENCE AND CONTROL ELECTRONICS (WITH REDUNDANCY)

TOTAL WEIGHT -1000 POUNDS
TOTAL COST - 20 M

II. PHASING (CONTROL CONJUGATING) SYSTEM (WITH REDUNDANCY)

WEIGHT/SUBARRAY = 8 POUNDS
COST/SUBARRAY = \$50 K
TOTAL WEIGHT = 62,900 POUNDS
TOTAL COST = 471.2 M

III. CABLE TRANSMISSION SYSTEM (REF. PHASE DISTRIBUTION) (NO REDUNDANCY)

TOTAL WEIGHT = 323.6 K POUNDS (322,500 METERS OF CABLE)
TOTAL COST = \$1.6 M

IV. FIBER OPTICS TRANSMISSION SYSTEM (NO REDUNDANCY)

TOTAL WEIGHT = 75 K POUNDS (25,000 METERS OF OPTICAL TRANSMISSION LINE)
COST \$500 K (OPTICS ONLY)
\$20 M (LIGHT MODEMS)
TOTAL COST \$20.5 M

V. SYSTEM TOTAL WEIGHTS/COST

CABLE DISTRIBUTION
TOTAL WEIGHT - 387,500 POUNDS
TOTAL COST - 492.8 M

FIBER OPTICS DISTRIBUTION
TOTAL WEIGHT - 138,900 POUNDS
TOTAL COSTS - 511.7 M

IV-C-4-16

L. Leopold
L. Livingston
J. Seyl

IV-C-5 ANTENNA POINTING CONTROL

a. RATIONALE

Antenna pointing is required to point the SPS antenna to the ground rectenna to effect the maximum transfer of microwave energy from the solar power station to earth.

The first priority is to accomplish the initial acquisition of the beam of the spacecraft antenna. The second is that of maintaining the antenna beam so that the maximum power density remains at the center of the rectenna.

b. DEFINITION

The possible methods employed to perform the above are:

- (1) By utilizing the known orbital parameters of the satellite. (Guidance and Control System).
- (2) Obtain attitude of the spacecraft from star trackers on board. (Guidance and Control System).
- (3) Obtain pilot beam from rectenna to remove ambiguities of antenna pointing away from rectenna.
- (4) By utilizing phase control to supplement inaccuracies in precise pointing of the antenna.

c. OPERATING CHARACTERISTICS

The antenna pointing system operates in either an acquisition mode or a tracking mode. The acquisition mode is primarily required during start-up, when the antenna may not be oriented accurately enough for the tracking mode to function. The tracking mode operates while power is being transmitted and also operates during eclipses in order to minimize restart time.

In the acquisition mode, for initial start-up or after an extended period of down time, it must be assumed that the antenna is in an arbitrary attitude from which the phase control receivers cannot receive the pilot beam. However, the ephemeris of the orbit will be accurately known from ground tracking methods and SPS attitude can be determined from onboard star tracker and horizon scanner data. Thus, the required antenna gimbal angles can be computed for the known rectenna location on earth, and the antenna driven to the computed desired position. The accuracy of this position will probably be limited by structural alignment errors and flexibility. (No quantitative assessment of these errors has been made, but it should be possible to hold them well under one degree). If necessary, attitude sensors could be mounted directly on the antenna to reduce the errors, but this does not appear to be required.

The tracking mode utilizes the retrodirective phase ("pilot") beam as received at seven subarrays (see Figure IV-C-5-1). Primary pointing information is obtained from the four receivers at A and B, whose signals are fed to two phase comparators in pairs to determine pointing errors in azimuth (A) and elevation (B). To minimize distortion errors, the receivers are located symmetrically on the axes of the antenna. The separation distance "d" will be determined by the maximum height differential between subarrays (see Figure IV-C-5-2), since even the

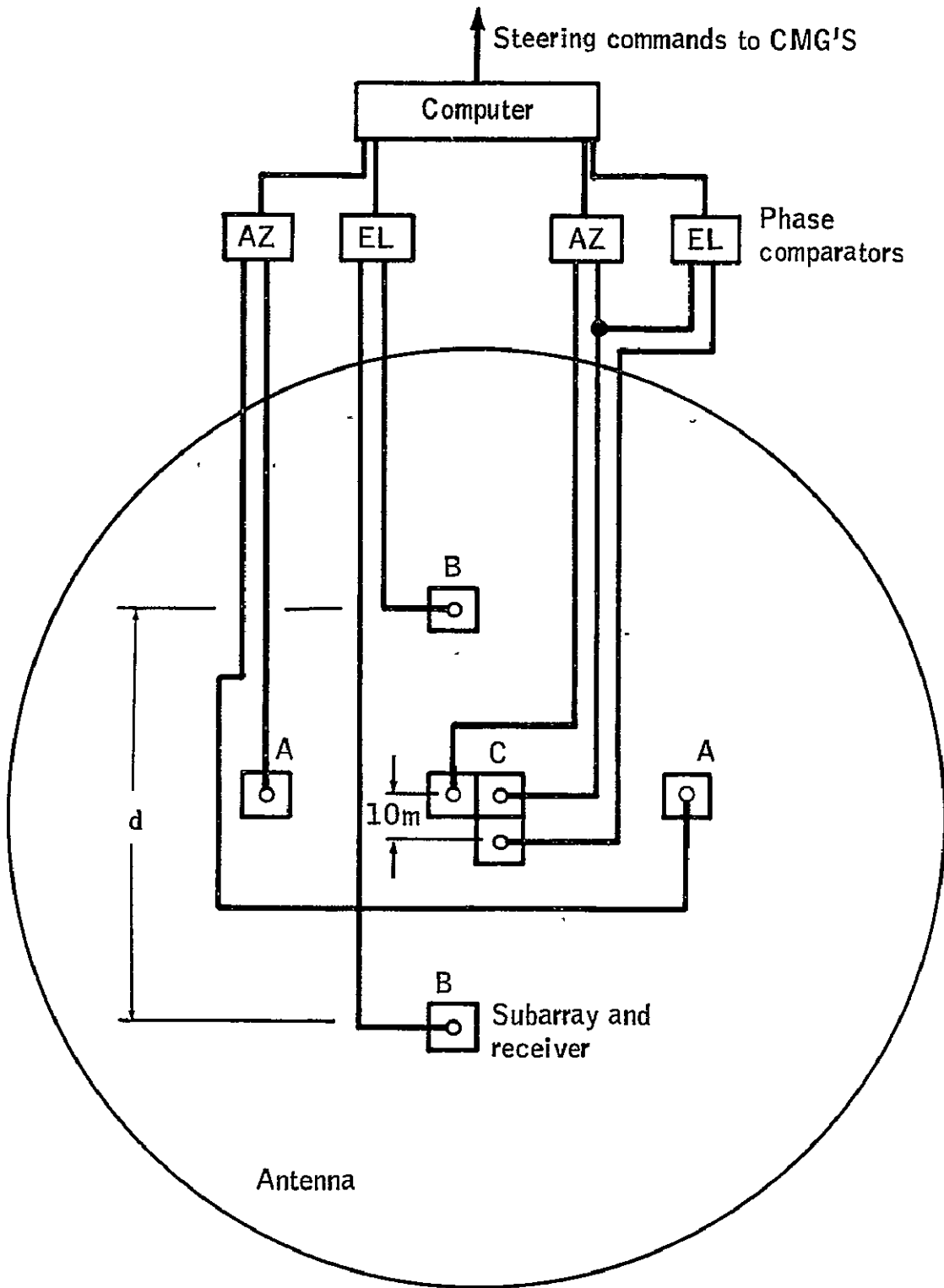


FIGURE IV-C-5-1 - DETERMINATION OF POINTING ERRORS

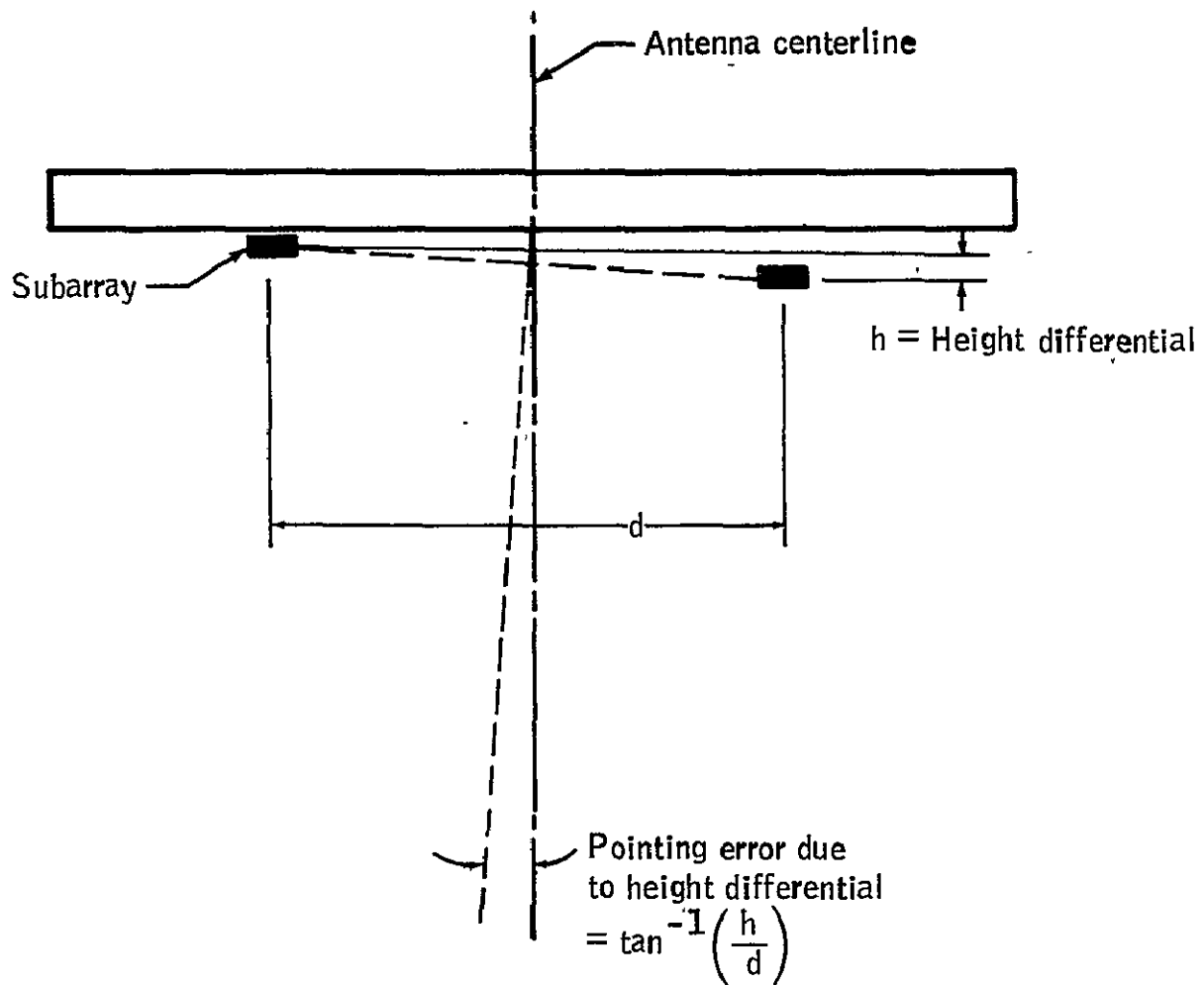


FIGURE IV-C-5-2 - DETERMINATION OF POINTING ERROR DUE TO HEIGHT DIFFERENTIAL

ten-meter separation between adjacent subarrays is sufficient for accuracies of 0.1 minute of arc (2.45 GHz pilot beam frequency and one degree phase error detection capability).

The receivers at C, in adjacent subarrays, are used to resolve phase ambiguities which could be troublesome at the larger separations between receivers A and B. These will be at or near the center of the antenna, so that three receivers, compared in two pairs, suffice. At 2.45 GHz, one wavelength is equivalent to 0.7° pointing error. Since the acquisition mode is expected to be at least this accurate, it should not be necessary to resort to additional frequencies for phase ambiguity resolution. If the pilot beam utilizes a lower frequency, the allowable acquisition error can be even greater.

Since existing receivers are used, the only weight associated with the system is the wiring from the receivers, the phase comparators and the computer. For reliability, several receivers and comparators at each location will be used, with their outputs averaged and out-of-tolerance data rejected.

Since the cost is minimal, it may be desirable to make the pointing system separate from the retrodirective phase control system.

IV-C-6 POWER DISTRIBUTION - J. PAWLOWSKI, AVIONICS SYSTEMS ENGINEERING DIVISION

The microwave antenna electrical power distribution system is designed to bring large quantities of electrical power from the rotary joint interface to the microwave generators. The sizing model used in this study calls for a 10 db 10-step truncated Gaussian taper with klystrons used as microwave generators. The klystrons require a 1.25 amp, 40K volt input, and are located in the subarrays which make up the antenna. Their density within a subarray is determined by the taper.

A block diagram of the electrical power distribution system is shown in Figure IV-C-6-1. Power is distributed from the rotary joint interface to switch gears which are located on the axis of the microwave antenna. Then power is distributed from the switch gears to a subarray distribution point from where it is distributed to individual klystrons located in the subarray.

IV-C-6-1 ASSUMPTIONS

A lateral power flow distribution system was selected since this method was demonstrated to result in less weight than the other methods investigated in "Microwave Power Transmission Studies" (NASA CR-134886, December 1975) which was prepared by Raytheon for Lewis Research Center (Contract NAS 3-17835). A representative lateral power flow distribution system is shown in Figure IV-C-6-2.

An operating temperature of 227°C was chosen because it was considered to be "worse case" according to the Raytheon report. Aluminum wire was selected as a conductor, and wire size was calculated from the formula

$$A = \frac{IpL}{\Delta E}$$

where:

- A = cross section area of the wire
- p = specific resistivity of aluminum at 227°C
- L = wire length
- I = current
- ΔE = maximum voltage drop per feeder assuming uniform loading along length

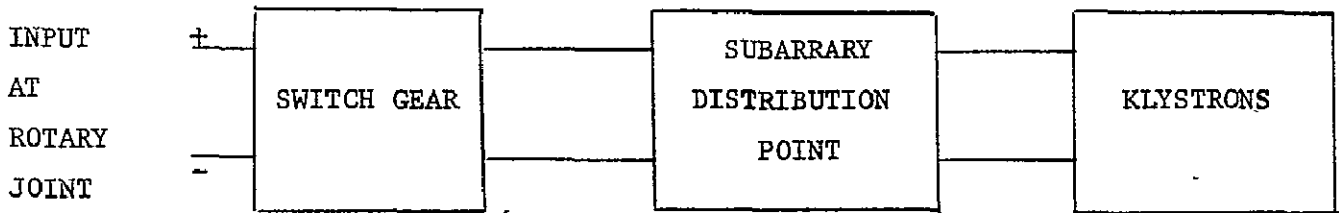


Figure IV-C-6-1 - Microwave Antenna Electrical Power Distribution System

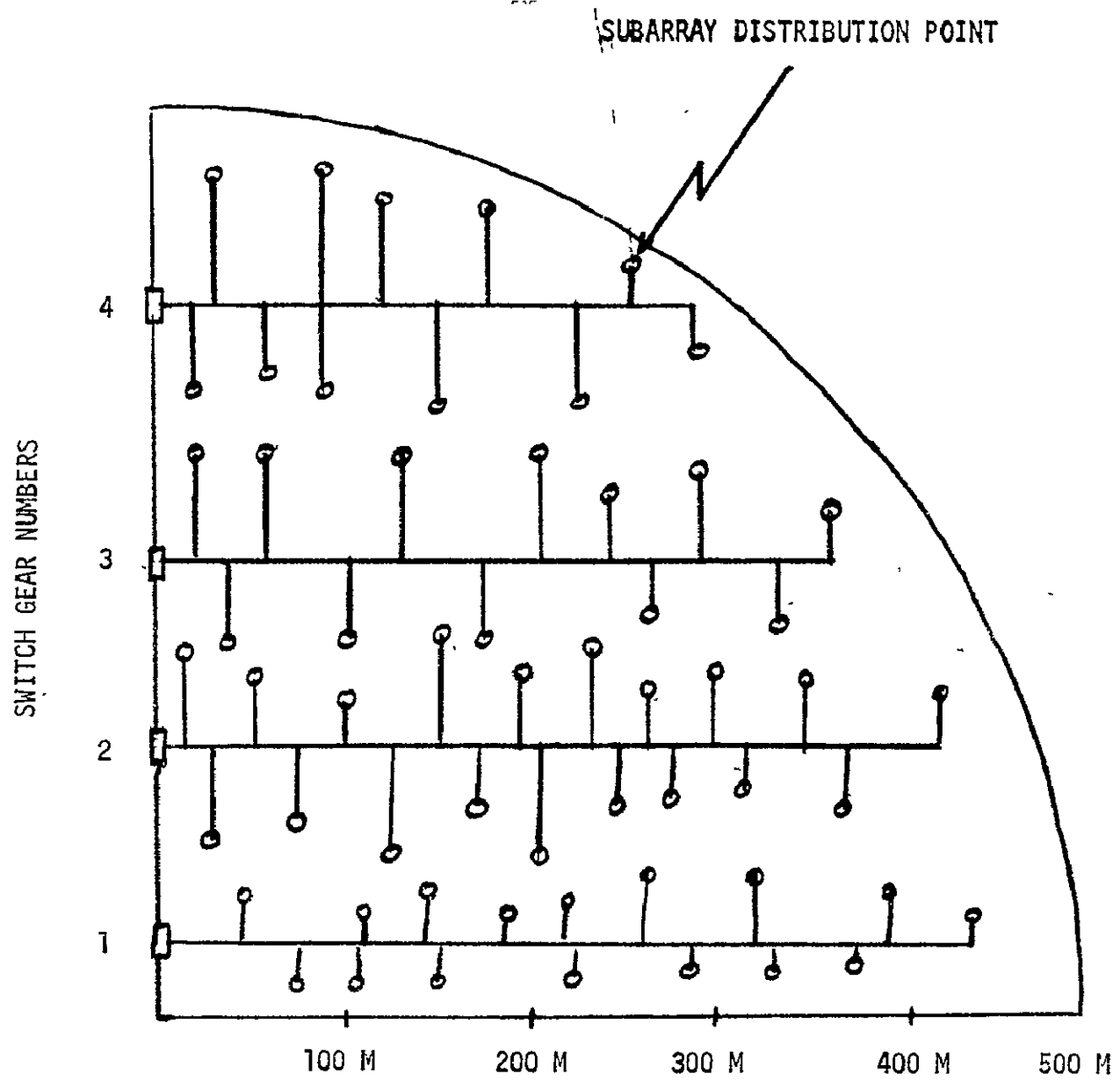


Figure IV-C-6-2 - Representative Lateral Power Flow Distribution System

IV-C-6-2 ROTARY JOINT TO SWITCH GEAR DISTRIBUTION

Power from the solar array is brought across the rotary joint interface where it is conducted by cables which run through the structure trusswork to switch gears located on the axis of the antenna. Figure IV-C-6-3 shows the relative locations of the switch gears and rotary joint along with the dimensions involved.

IV-C-6-3 SWITCH GEAR TO SUBARRAY DISTRIBUTION

Figure IV-C-6-4 shows one quadrant of the antenna with the switch gears located along one axis. The 10 areas determined by the 10-step 10 db taper are outlined. Power is conducted from each switch gear to a distribution point within a subarray or group of subarrays.

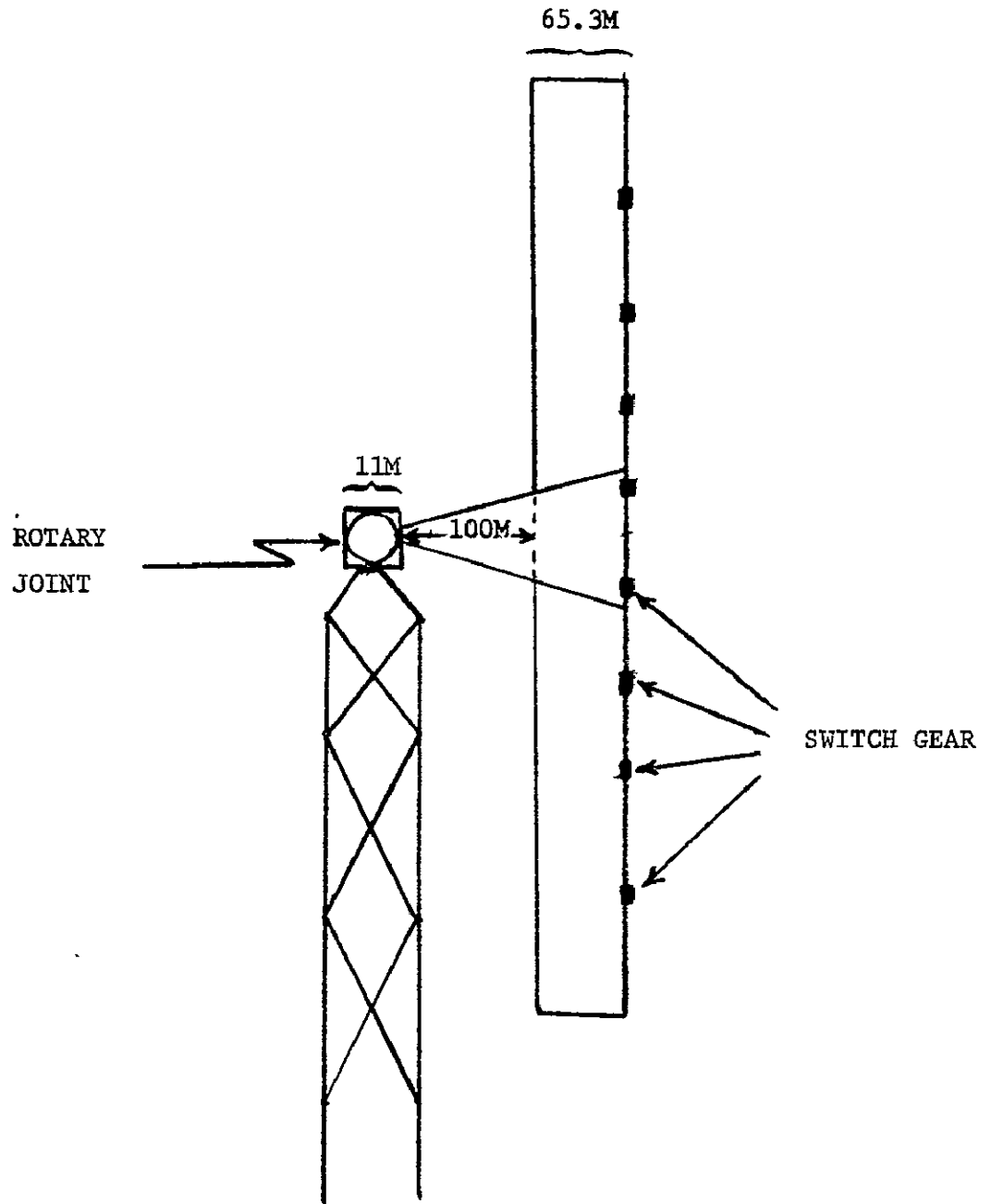
The total amount of current required by all the klystrons in one quadrant of the antenna was calculated to be 42,000 amperes. It was felt that four switch gear per quadrant was reasonable from both a complexity and a distributive point of view. This implies a current level of approximately 11,000 amperes per switch gear, which also seemed reasonable.

In addition to being a distribution point, it is felt that each switch gear will be a protective device and should be capable of being remotely controlled so that during initial power-up, or reinitialization following an eclipse, power could be brought up in a programmed sequence. The implementation of a control system for the switch gear is an area which must be investigated further.

IV-C-6-4 SUBARRAY DISTRIBUTION

The technique for distributing power throughout a subarray is shown in Figure IV-C-6-5a. Power is input at a distribution point from where it is distributed by feeders to each row of klystrons. Wire size for each feeder is determined by the number of klystrons it services since this determines the total current per row.

The 10 db, 10-step truncated Gaussian taper determines the number of klystrons per subarray. Those subarrays close to the center of the antenna have a greater klystron density than those close to the edge. In order to reduce the number of wires from each switch gear to the subarrays, the subarrays having the lowest klystron density (6-13) and therefore requiring the lowest current (8-16 amps) would be arranged in groups of fours and would be serviced by one distribution point. Those subarrays having a somewhat greater klystron density (17-25) would be paired and each pair would be serviced by one distribution point. Figures IV-C-6-5b and IV-C-6-5c depict this method.



3

Figure IV-C-6-3 - Antenna Support Structure

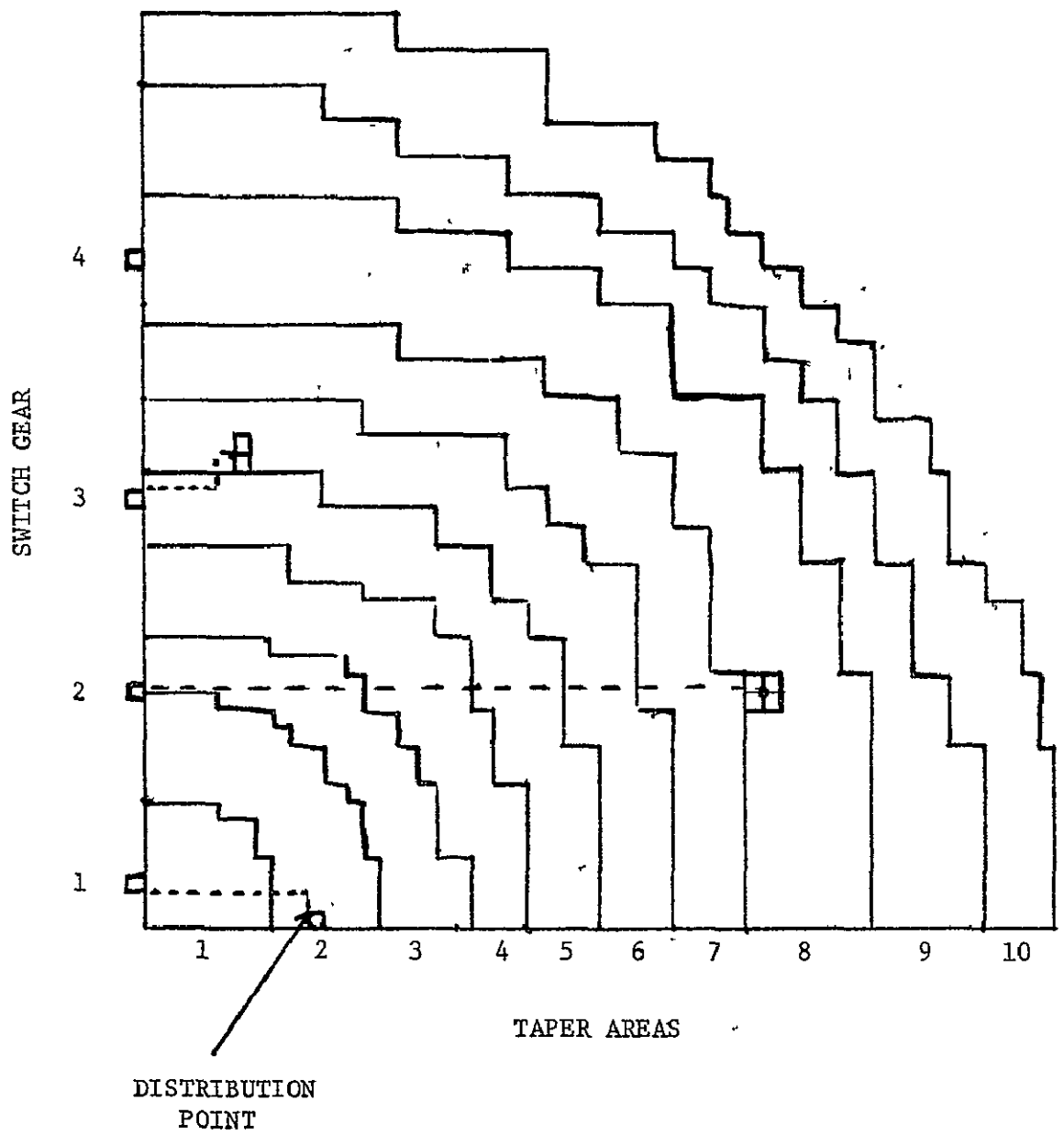


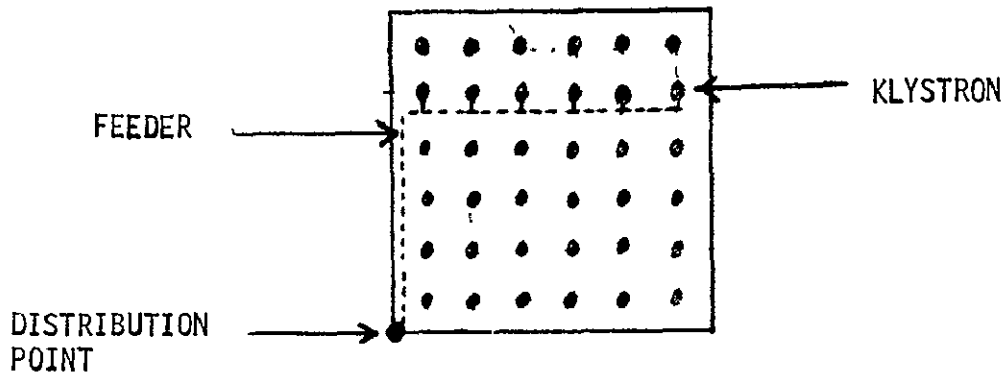
Figure IV-C-6-4 - Switch Gear to Subarray Distribution

Each subarray having a high klystron density (30-42) would be serviced by one distribution point (see Figure IV-C-6-5a). Table IV-C-6-1 shows the klystron density in each area of the antenna.

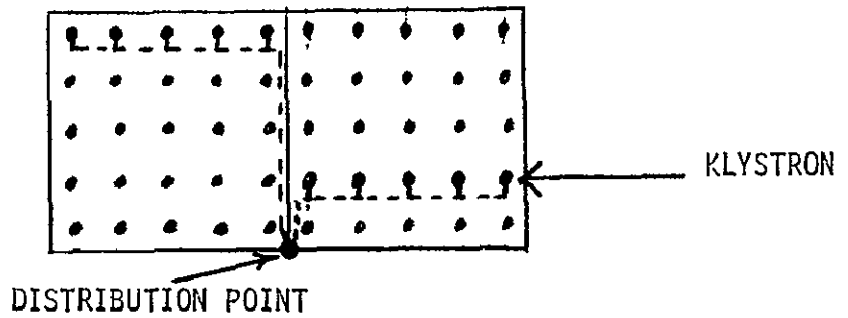
IV-C-6-5 POWER SYSTEM REGULATION

The klystrons require some magnitude of power supply regulation in order to function properly. On which side of the Solar Array/Microwave antenna interface the power supply regulation takes place should be the result of a tradeoff. Another tradeoff must be made on the merits of an extremely precise power supply regulator versus a klystron which will function properly over a large power range. The usual parameters of design complexity, cost, weight, and power consumption must be considered.

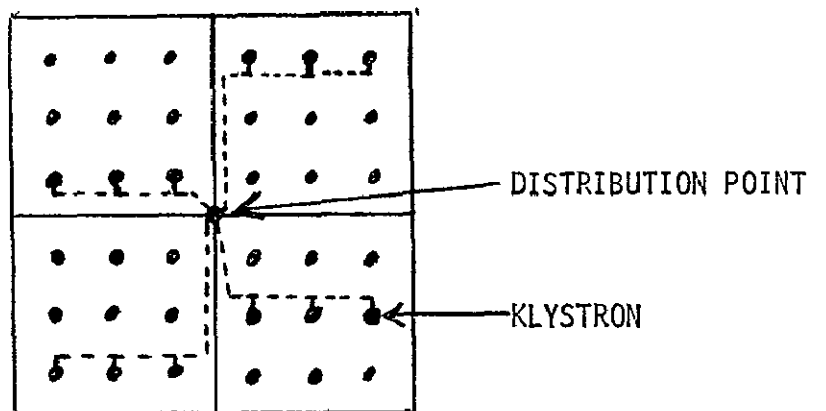
Assuming the power supply regulation takes place in the microwave antenna, then in order to avoid single point failures several power supply regulators must be used in the distribution circuit. It seems reasonable that the regulator should be included in the switch gear assemblies, so a failure of a power supply regulator would only affect 1/16th of the antenna electrical power.



a. One Subarray Per Distribution Point



b. Two Subarrays Per Distribution Point



c. Four Subarrays Per Distribution Point

Figure IV-C-6-5 - Subarray Distribution

TABLE IV-C-6-1 - KLYSTRON DENSITY

<u>AREA</u>	<u>RADII</u>	<u>KLYSTRONS/SUBARRAY</u>	<u>CURRENT/SUBARRAY</u>	<u>SUBARRAYS/DISTRIBUTION POINT</u>
1	0 - 75M	42	53 AMPS	1
2	75 - 132.5M	38	48 "	1
3	132.5 - 176.5M	34	43 "	1
4	176.5 - 215M	30	38 "	1
5	215 - 255M	25	31 "	2
6	255 - 295M	21	26 "	2
7	295 - 337.5M	17	21 "	2
8	337.5 - 387.5M	13	16 "	4
9	387.5 - 455M	8	10 "	4
10	455M - 500M	6	8 "	4

IV-C-6-6

IV-C-6-6 WEIGHT, COST, EFFICIENCY

An estimate of weight, cost, and power loss for the microwave antenna power distribution system is summarized in Table IV-C-6-2.

The conductor weights were calculated by determining the lengths then sizing the wire to give a minimal yet reasonable voltage drop.

The wire and switch gear cost and the switch gear weight were interpolated from the Raytheon report, "Microwave Power Transmission Studies" (NASA CR-134886).

The efficiency, E, of the power distribution system was calculated to be 98% using the formula

$$E = 1 - \frac{P_L}{\left(\frac{P_R}{E_T \cdot E_W} \right) + P_L}$$

where

P_L = total power loss of distribution system (151, 845 kw)

P_R = antenna radiated power (6.5×10^9 watts)

E_T = DC - RF conversion efficiency, (87%)

E_W = klystron to waveguide plus waveguide efficiency (98%)

IV-C-6-11

	WEIGHT	COST	POWER LOSS
SUBARRAY DISTRIBUTION	1,658 kg	\$ 3,648	7,127 KW
SWITCH GEAR TO SUBARRAY DISTRIBUTION	17,416 kg	\$38,315	65,859 KW
ROTARY JOINT TO SWITCH GEAR DISTRIBUTION	33,290 kg	\$73,238	65,859 KW
SWITCH GEAR (16)	31,000 kg	2848×10^3	13,000 KW
TOTAL	83,364 kg	2963×10^3	151,845 KW

TABLE IV-C-6-2 - WEIGHT, COST AND POWER LOSS ESTIMATES

IV-C-7. Structure

The microwave transmission antenna presents one of the most difficult tolerance problems in the SPS system. Although the precise targeting of the microwave beam is achieved through electronic phasing of the 7854 subarrays per antenna, each of the subarrays must maintain a relative mechanical pointing accuracy of 3.2 arc minutes to achieve the desired efficiency. As with the array, the antenna structure must have sufficient stiffness to maintain dynamic stability; in the case of the antenna, however, the control system is the design driver. Actually, the attitude control system selected for the microwave power transmission system is critical to attaining dynamic stability and, therefore, boresight alignment of the individual subarrays. The large size and mass and the planar character of this antenna system prohibit a natural frequency greater than the desired attitude correction frequency. The microwave power transmission system design requires a close integration (control system, structure, microwave radiator system and electronic phasing) to keep the dynamic motion of the antenna to a desirable form and level. In contrast to the array, the antenna undergoes a daily revolution with respect to the sun and, therefore, potential thermal strain becomes a significant design consideration. The most critical structural design requirements are: (1) minimization of the dynamic motion of the subarrays and maintenance of a maximum-time-average boresight alignment, (2) initial alignment of the subarrays with respect to the antenna boresight, and (3) accommodation of relative thermal strain occurring during an occultation.

Two previous transmission module designs by Raytheon Company/Grumman Aerospace Corporation (reference 1) and Martin Marietta Corporation (reference 2) used different structural configurations to support 18-meter by 18-meter subarrays. The Grumman design consists of a two "bed" approach. The first "bed" is a primary structure and furnishes overall stiffness. The second "bed" serves as secondary structure to join the subarrays to the prime structure. The Martin Marietta Corporation design is a single bed concept of cubical structure attuned to the subarrays. Although the latter approach offers a possible advantage in the repetitive nature of the assembly process, it is massive.

Figure IV-C-7-1 illustrates a potential design for the power transmission module prime structure. Four concentric polygons of 6, 12, 18 and 24 sides are held under hoop compression by radially joining cable tensile members. This places node points at radial distances of 125, 250, 375, and 500 meters, respectively, for the 1 kilometer diameter antenna. As illustrated, each circumferential compression (hoop) member is 130 meters long and consists of a rectangular frame 65 meters by 130 meters with cable cross bracing. The outer hoop members could have a decreased depth to minimize the effects of thermal strain associated with the daily solar cycle and yet retain sufficient stiffness. The radial symmetry of the prime structure affords a lower distortion due to the radial symmetry of the power generation, operating temperatures and radially varying loads.

Ninety-six planar truss secondary structural units are attached to the prime structure in a determinate manner at three points, each as illustrated in figure IV-C-7-1. Three points form a plane which will not introduce warping forces from contiguous structural units due to thermal distortion (as would occur during an eclipse). The planar secondary truss is made up of tetrahedrons which form triaxial patterns on the outer surfaces. As illustrated in figure IV-C-7-1,

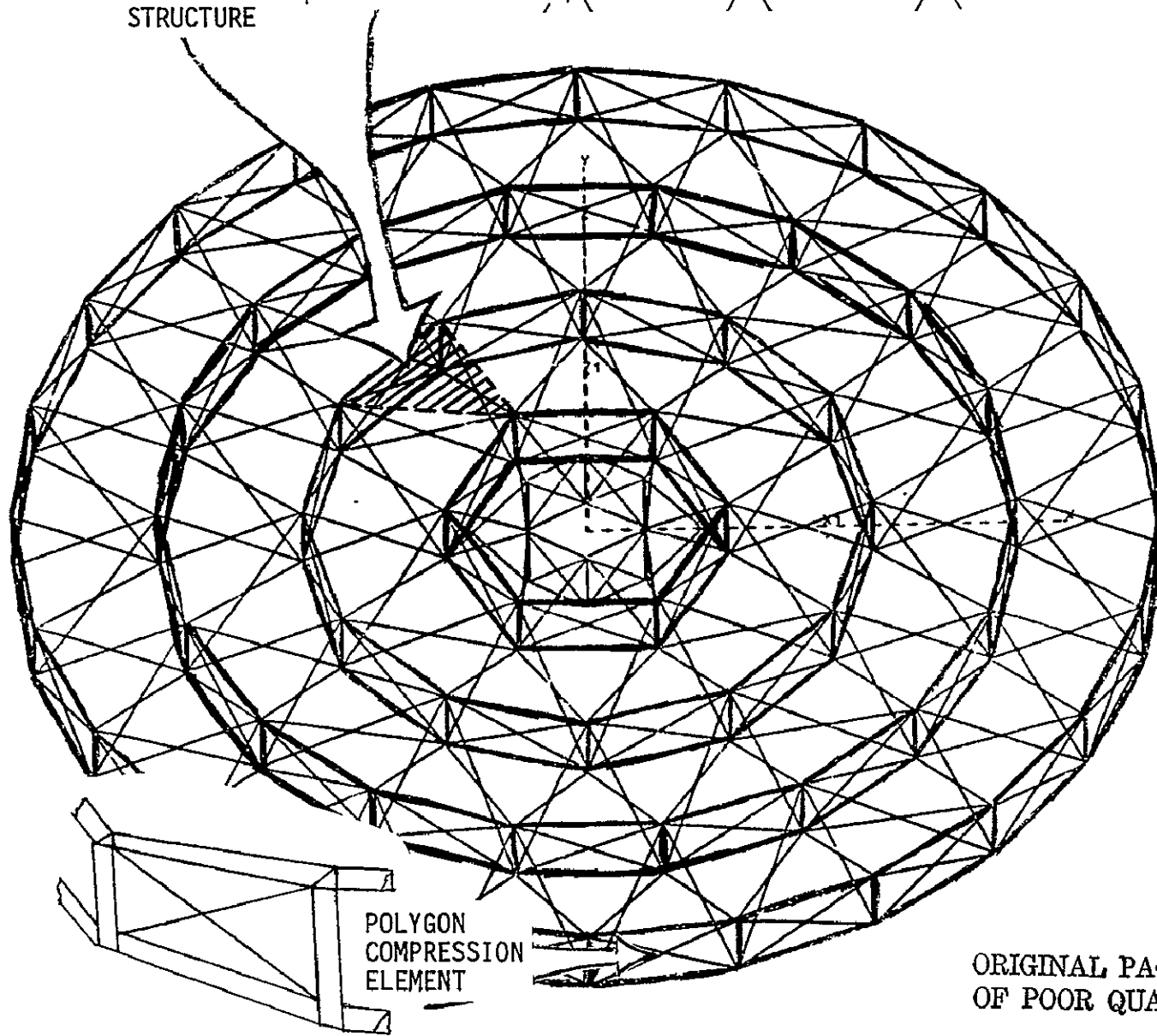
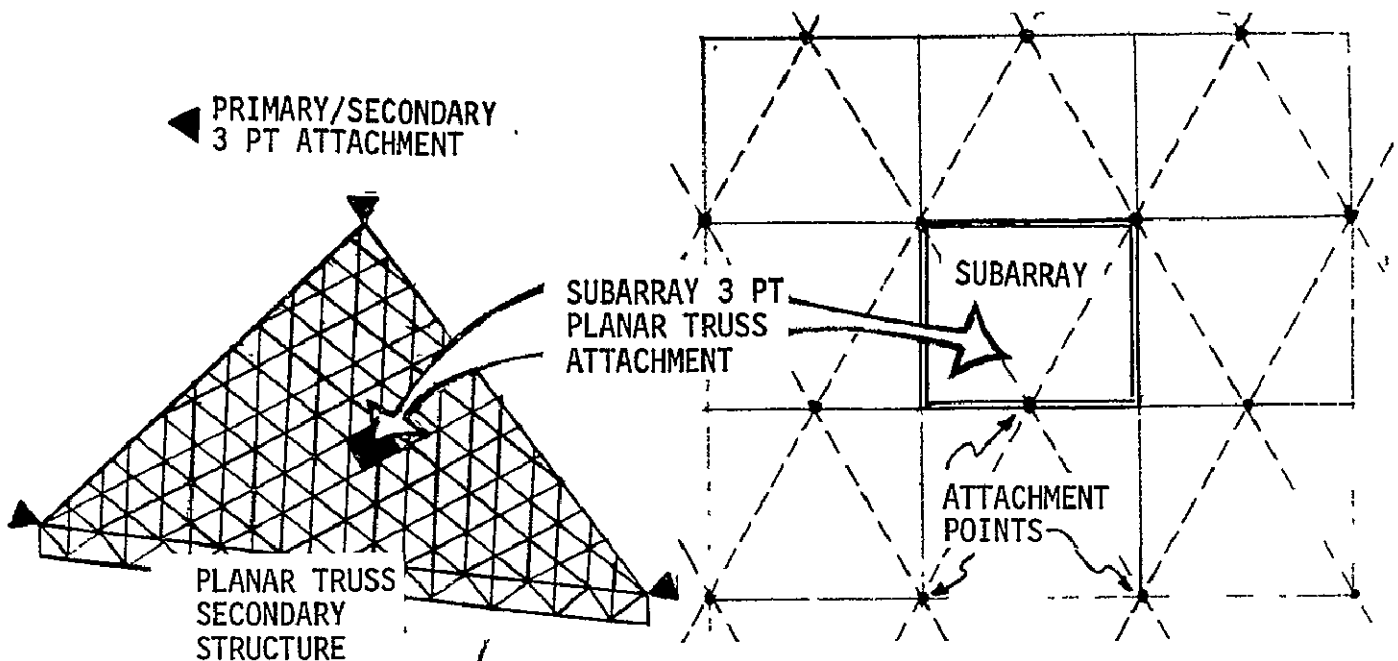


FIGURE IV-C-7-1 - TRANSMISSION MODULE (MICROWAVE ANTENNA STRUCTURE)

rectangular subarrays (9.31 meters by 10.75 meters, 100 meters²) are attached in a determinate manner to the triaxial grid points of the secondary truss. Two initial adjustments would be required to achieve boresight alignment of each subarray during the construction phase. Again, the three-point determinant support system could not transmit any flatness distortion.

The subarrays would also be an open structure which could utilize the rigidity of the waste heat thermal radiator associated with each microwave generator. Figure IV-C-7-2 illustrates a Klystron system set orthogonal to the beam to minimize the heat rejection path. Although the Klystron, wave guide, and thermal radiator would be a relatively rigid unit, the aluminum wave guides would have a significantly different thermal expansion coefficient than the pyrolytic graphite radiators or the graphite polyimide subarray structure. To accommodate the contraction associated with an eclipse, each wave guide unit would have to be structurally isolated from the surrounding units within the subarray. The aluminum wave guides could be dimpled in a random pattern to create an effective stiffness with a minimum distortion and loss.

A high-Young's modulus low thermal expansion graphite material would be used for the MPTS structure. Electrical conduction grade aluminum is required for electrical transmission. Different material requirements preclude efficient integration of the two systems.

The structural configuration shown in figure IV-C-7-3 was originally conceived for a large solar collector; however, it might be modified to serve as a structure for the transmission module. This configuration is composed of a single outer compression ring with a triaxial grid pattern of cable stretched over each "drum" surface and then tied together to form mirror symmetry paraboloids. For the solar collector, each triangular unit of one paraboloid surface would contain a flat reflector. Although this configuration would afford sufficient dynamic stability as a solar collector, the tension level required to provide sufficient stiffness for an antenna system is prohibitive.

The transmission module is a complex design task which requires relatively detailed study to achieve an efficient design. Of particular importance is the coupling of the structural requirements and the thermal environment. Figure IV-C-7-4 illustrates two detailed design approaches toward minimizing thermal distortion. The use of thermally opaque structural elements is an approach toward minimizing the thermal distortion which can arise in thin walled closed members. This allows the use of structurally efficient closed members but reduces the potentially significant thermal gradients ($\sim 100^\circ\text{K}$ across the diameter for a thin walled isolated aluminum cylinder normal to the solar flux). The use of structural material configuration to advantage is also illustrated by the thermally stable configuration shown in figure IV-C-7-4. Here the distance from point A to B is independent of the temperature level of this structural unit. Detailed design features such as these will be required for simple, low cost approaches to achieving the structural requirements.

a. References

1. Microwave Power Transmission System Studies, Fourth Engineering Review, Contract NAS 3-17835, Raytheon Company for Lewis Research Center, December 12, 1974.
2. Brodie, S. B., et al.: Orbital Assembly and Maintenance Study, NAS 9-14319, August 1975.

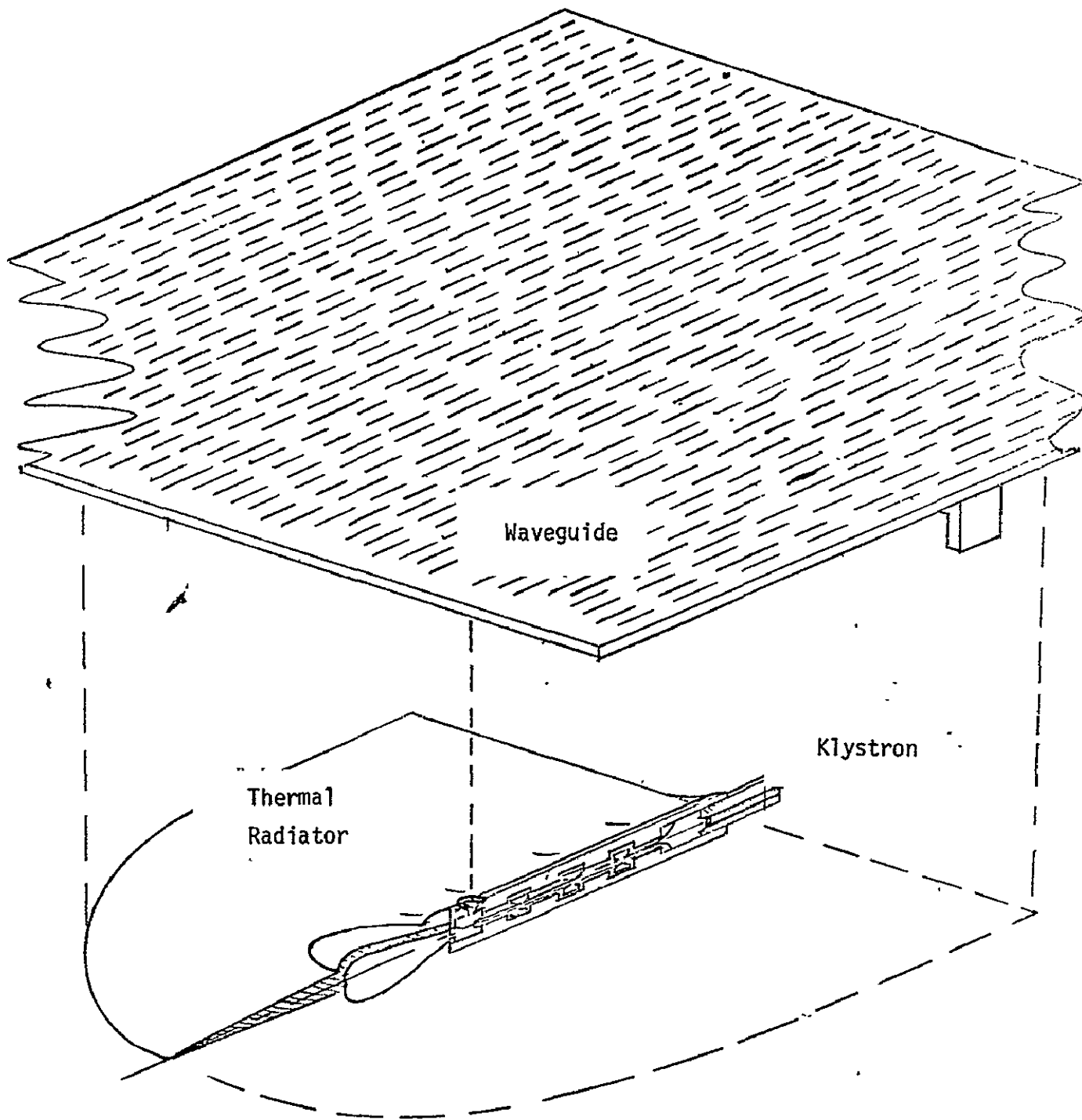


FIGURE IV-C-7-2

KLYSTRON/WAVEGUIDE/THERMAL RADIATOR UNIT

IV-C-7-4

IV-C-7-5

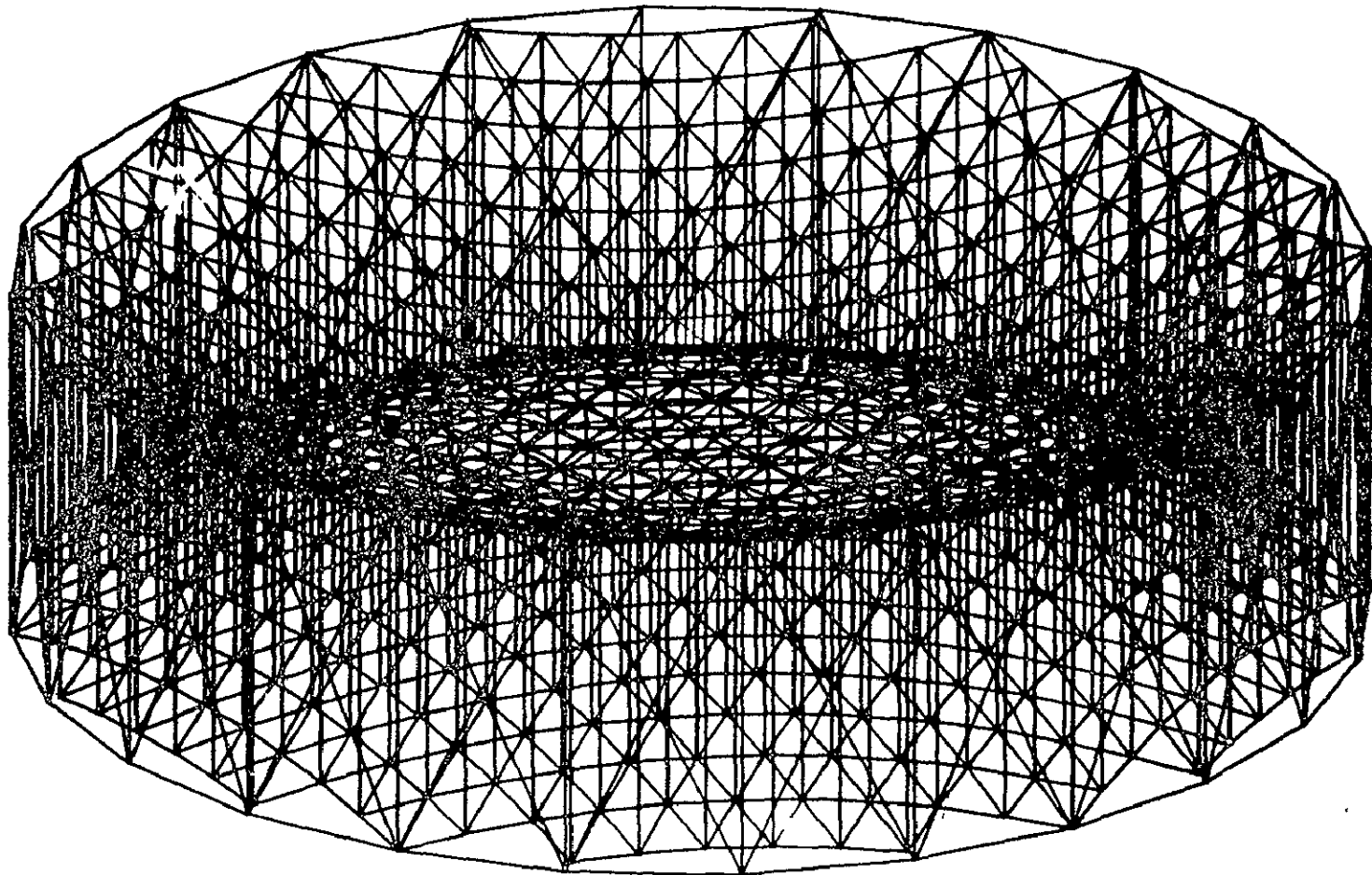
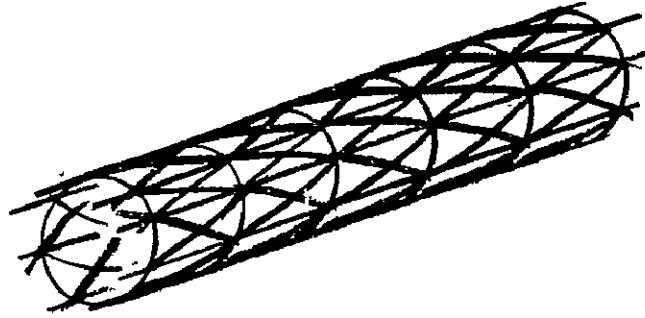
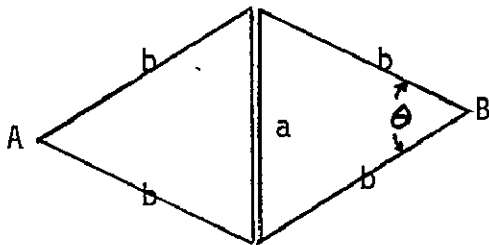


FIGURE IV-C-7-3
ALTERNATE MPTS STRUCTURE/
PARABOLIC SOLAR CONCENTRATOR

(1) Open Structural Elements to Relieve Thermal Gradients



(2) Thermally Stable Structural Configurations (Distance AB Independent of Temperature)



$$\frac{l \cdot a}{l \cdot b} \approx 2 \sqrt{\frac{\alpha_b}{\alpha_a}}$$

e.g. if a Aluminum
b Graphite
 $\theta = 31.6^\circ$

FIGURE IV-C-7-4 - THERMAL/STRUCTURAL CONFIGURATION/MATERIAL COUPLING

IV-C-8 ROTARY JOINT

J. C. Jones & J. D. Bradley
Spacecraft Design Division

A rotary joint or system of joints is required to point the antenna toward the rectenna on earth. Major functional requirements of the rotary joint may be summarized as follows:

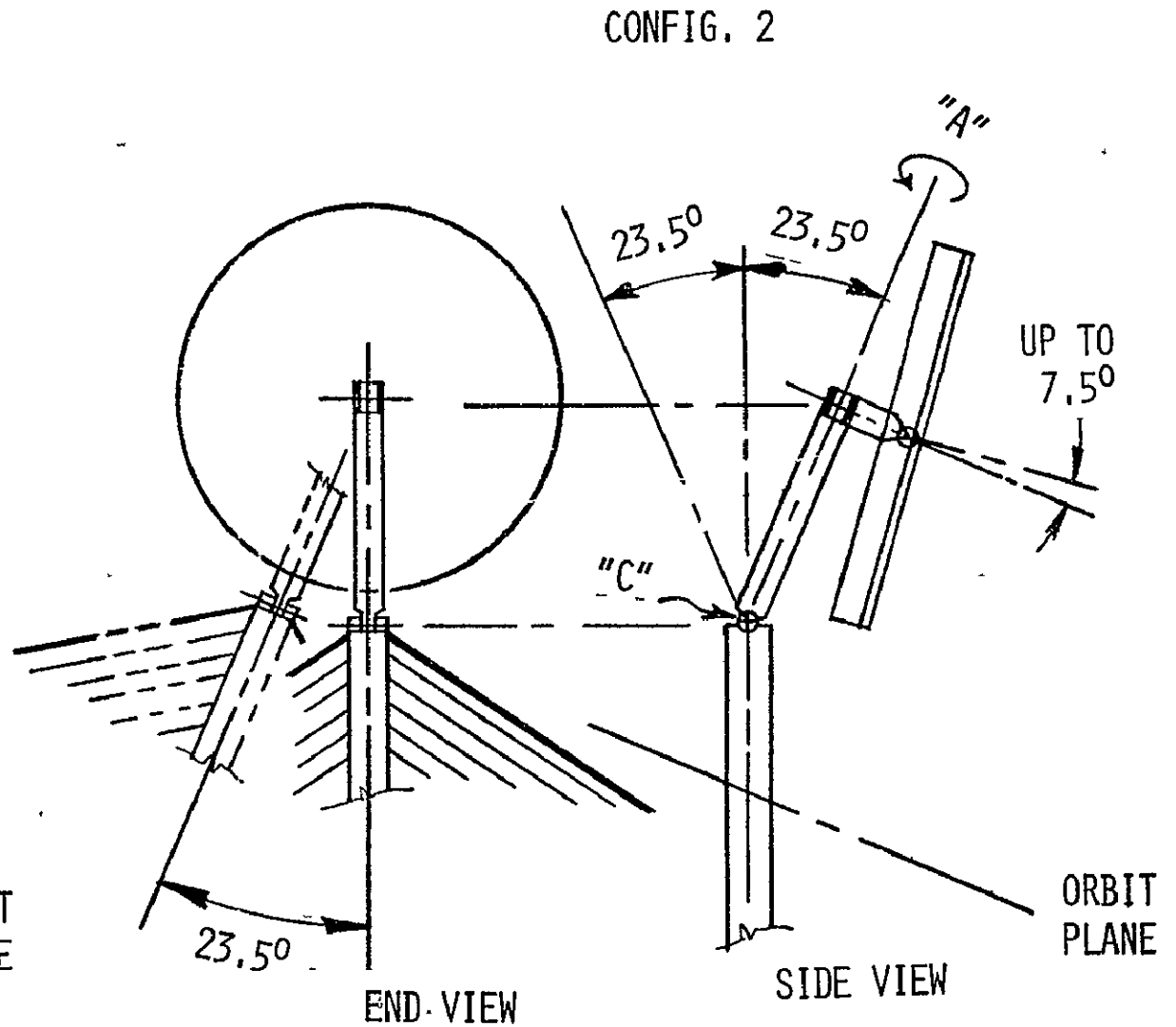
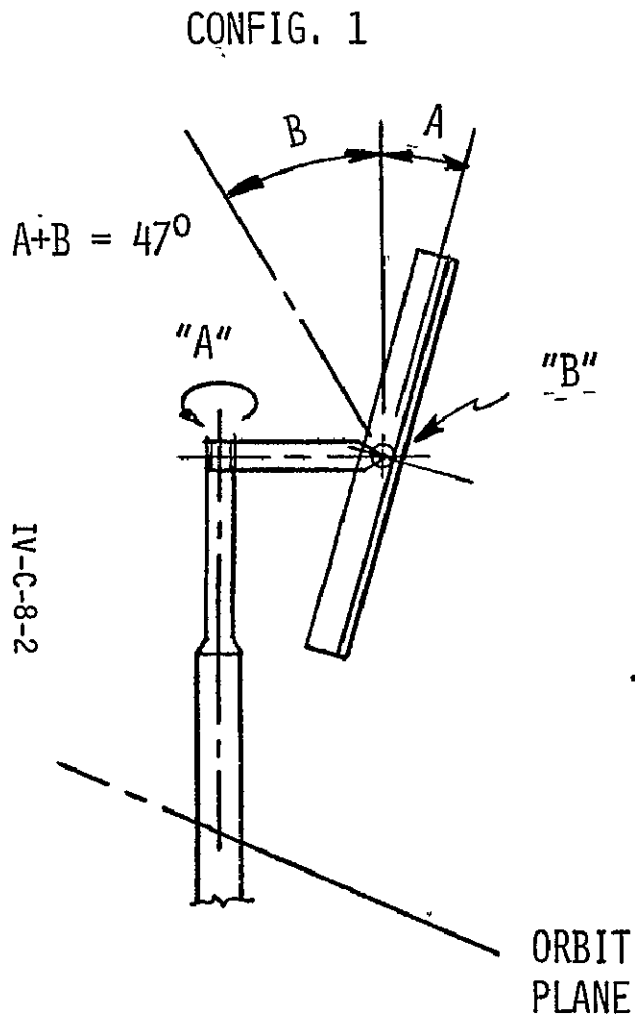
1. Provide structural connection between antenna and SPS while allowing proper angular motion.
2. Transfer electrical energy across rotating interface.
3. Contain a mechanical drive system to rotate the joint.

Two orthogonal axes are required for pointing the antenna. A third axis, on or parallel to the line of sight from the antenna to the rectenna is necessary in some configurations to maintain polarity of the antenna with respect to the rectenna on earth. However, this axis is not required for our reference configurations and orbits identified to date, assuming polarity differences of one or two degrees are tolerable. An additional axis is necessary for some arrangements to allow for positioning the outer axes so that the angular motion about those axes is, basically, uniform.

In this study several logical arrangements were identified, a general evaluation of each arrangement was made, and a configuration concept was selected. The selected joint configuration was evolved from consideration of numerous, overall "system" factors. The following paragraphs will attempt to explain those considerations.

Figure IV-C-8-1 illustrates two antenna mount configurations, both applicable to two antenna, solar oriented SPS configurations. It is a basic principle that the antenna must rotate approximately one revolution per day - relative to the SPS - about an axis (real or imaginary) parallel to the earth's polar axis. The arrangement shown as configuration 1 requires that the angular velocity about both axes vary cyclically twice each day. The antenna is also moved through large excursions relative to the solar array (almost 1/3 km normal to orbit plane, and .8 km parallel to orbit plane). The dynamics involved are judged to be intolerable. Configuration two improves the situation somewhat by adding an axis "C" which allows axis "A" to be positioned parallel to the earth's polar axis. Now, motion about axis A is, basically, uniform at 1 revolution per day. However, the mass center of the antenna is constantly being moved relative to the SPS, causing radical changes in the SPS inertia distribution. Also the attitude control of the SPS becomes involved with antenna pointing, requiring a change in attitude of 23.5° in a cyclic manner during each year.

Figure IV-C-8-2 shows three configurations which partially or completely eliminate the problems of the prior two configurations.



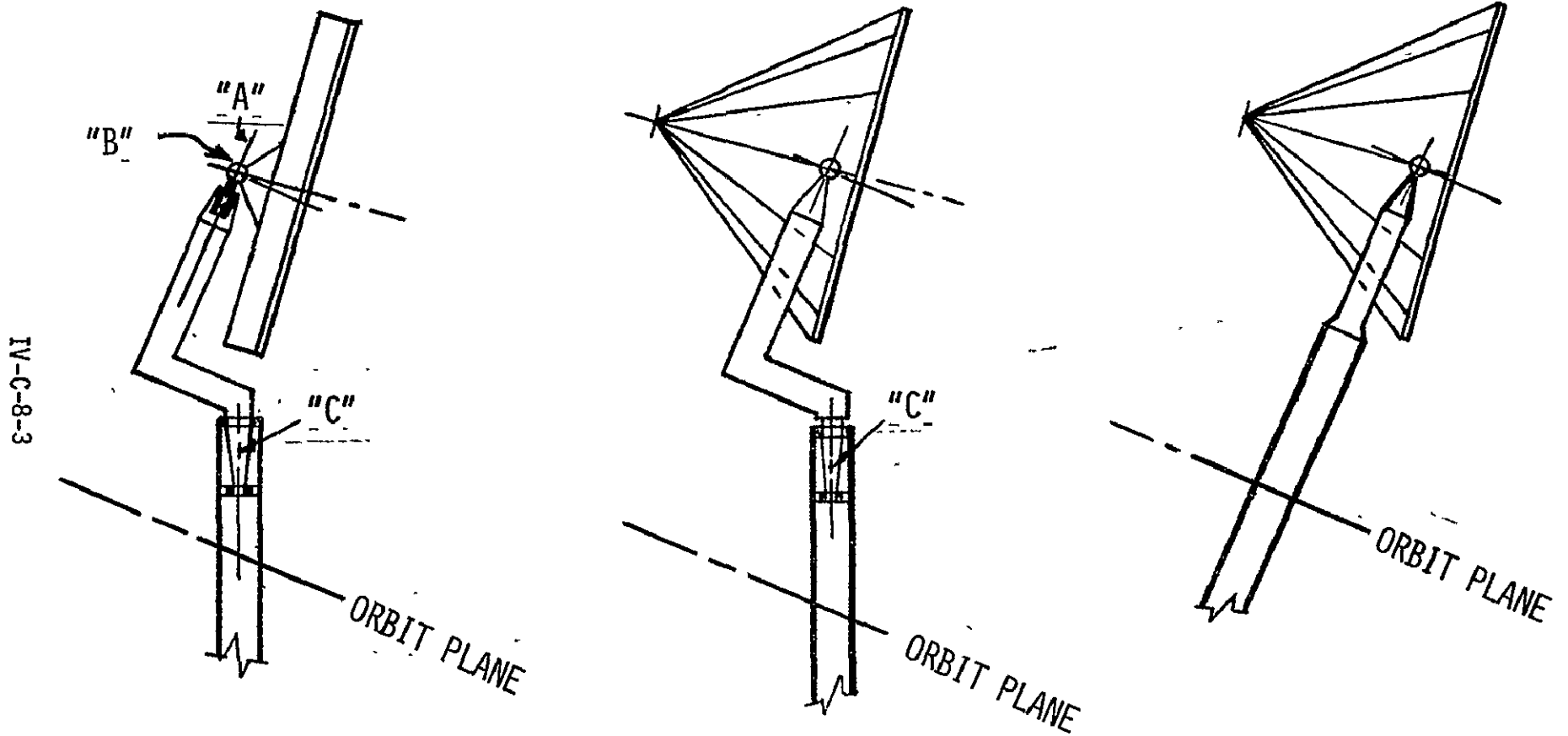
IV-C-8-2

FIG. IV-C-8-1 SPS ANTENNA CONCEPTS

CONFIG. 3

CONFIG. 4

CONFIG. 5



IV-C-8-3

FIG. IV-C-8-2 SPS ANTENNA CONCEPTS

Configuration 3 provides a "dog-leg" structure mounted to the solar array at axis C, which positions the mass center of the antenna more nearly on the primary axis of the SPS and positions axis A parallel to the earth's polar axis. Configuration 4 combines axes "A" and "B" into a ball-joint, and rearranges the antenna configuration from a disc to a cone having its mass center at the ball-joint. Configuration 5 is same as configuration 4 except that the solar array is oriented to be perpendicular to the orbit plane (P.O.P.), eliminating the requirement for axis "C". (Axis C was necessary to allow the array to be faced toward the sun while the dog-leg was positioned so that axis A was parallel to the earth's polar axis).

Figure IV-C-8-3 indicates antenna configuration 3 of the prior figure installed on the SPS, and shows the overall geometry and required basic rotation about the three axes. Figure IV-C-8-4 shows the nominal forces acting on the antenna support structure. These forces, resulting from orbital mechanics, are necessary to keep the antenna attached to the other parts of the SPS. It should be noted that the gravity gradient torque on the disc configuration antenna is on the order of 1000 N-m, when the antenna is pointed toward a rectenna at an earth location as indicated on the drawing.

There is also a dynamic unbalance due to the antenna's rotation about the axis normal to the orbit plane. This unbalance must be reacted by a torque applied to the antenna of about 200 N-m, as shown in the figure. Thus, about 1200 N-m of torque must be applied to the antenna to hold its attitude. The torques to correct antenna pointing errors would be applied in addition to the torque necessary to hold a fixed attitude. These forces and torques would appear to be relatively insignificant when considering the joint drive system. However, it is believed that a system to point the antenna by driving each joint mechanically, with torques acting on the antenna and reacting on the SPS structure, is not likely to provide the required pointing accuracy of about 1 arc minute. Figure IV-C-8-5 attempts to illustrate the problem and its possible solution.

If the antenna structure and the SPS structure were very rigid, such that the sketch on the left of the figure were representative of the situation, a direct drive at each joint could probably be designed to point the antenna within one arc minute. However, the SPS is more nearly like the middle sketch. A servomechanism operating under these conditions is not likely to achieve precise pointing of the antenna.

The solution is believed to be the concept on the right. Control moment gyros mounted on the antenna are used for attitude control torques input to the antenna, with the antenna being mounted through the "softest" possible mount to the SPS (low stiffness interconnection). The necessary rotary joint through which the electrical energy must pass would be driven by a servomechanism to track the antenna as its position and attitude

IV-C-8-5

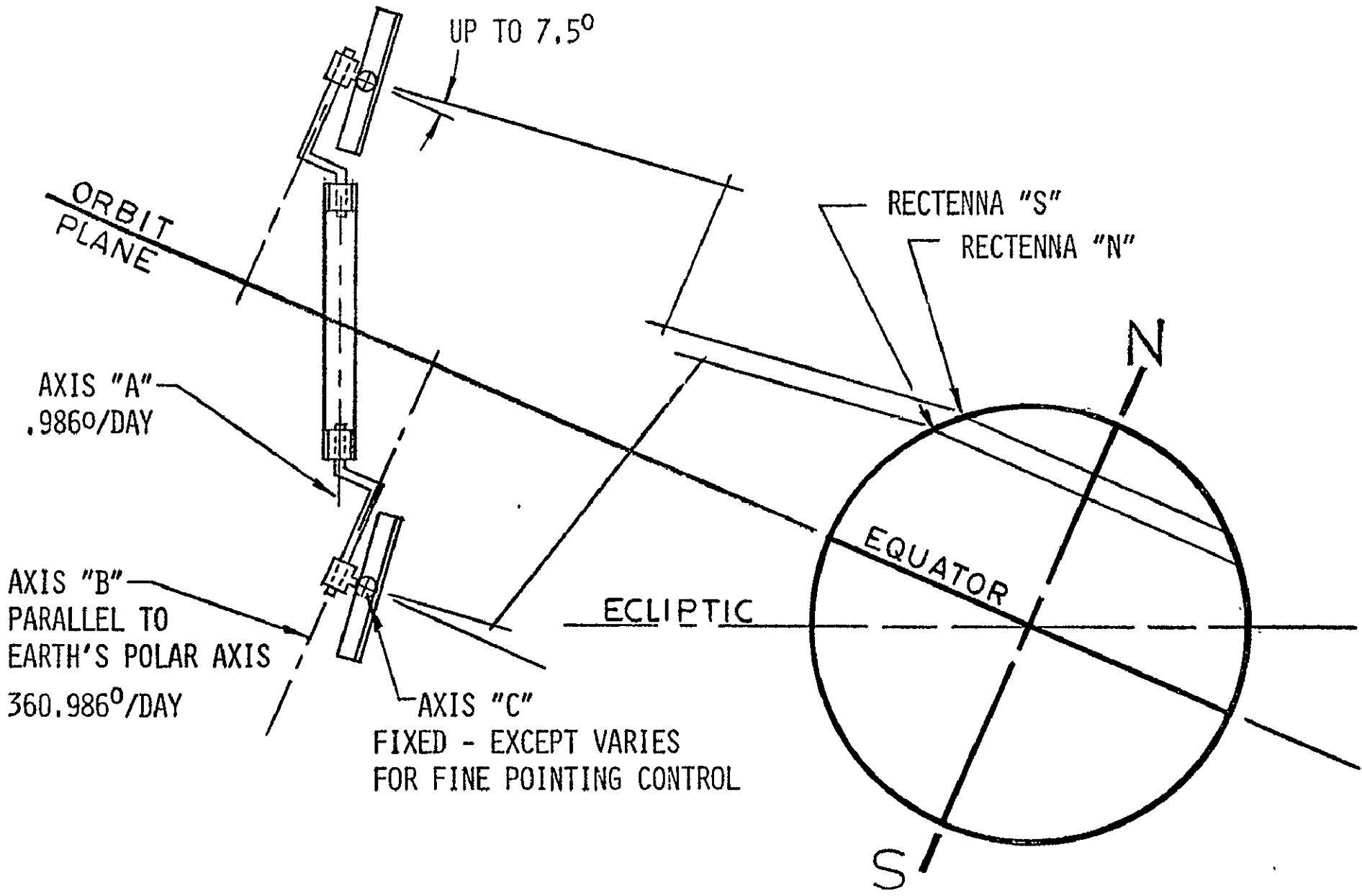
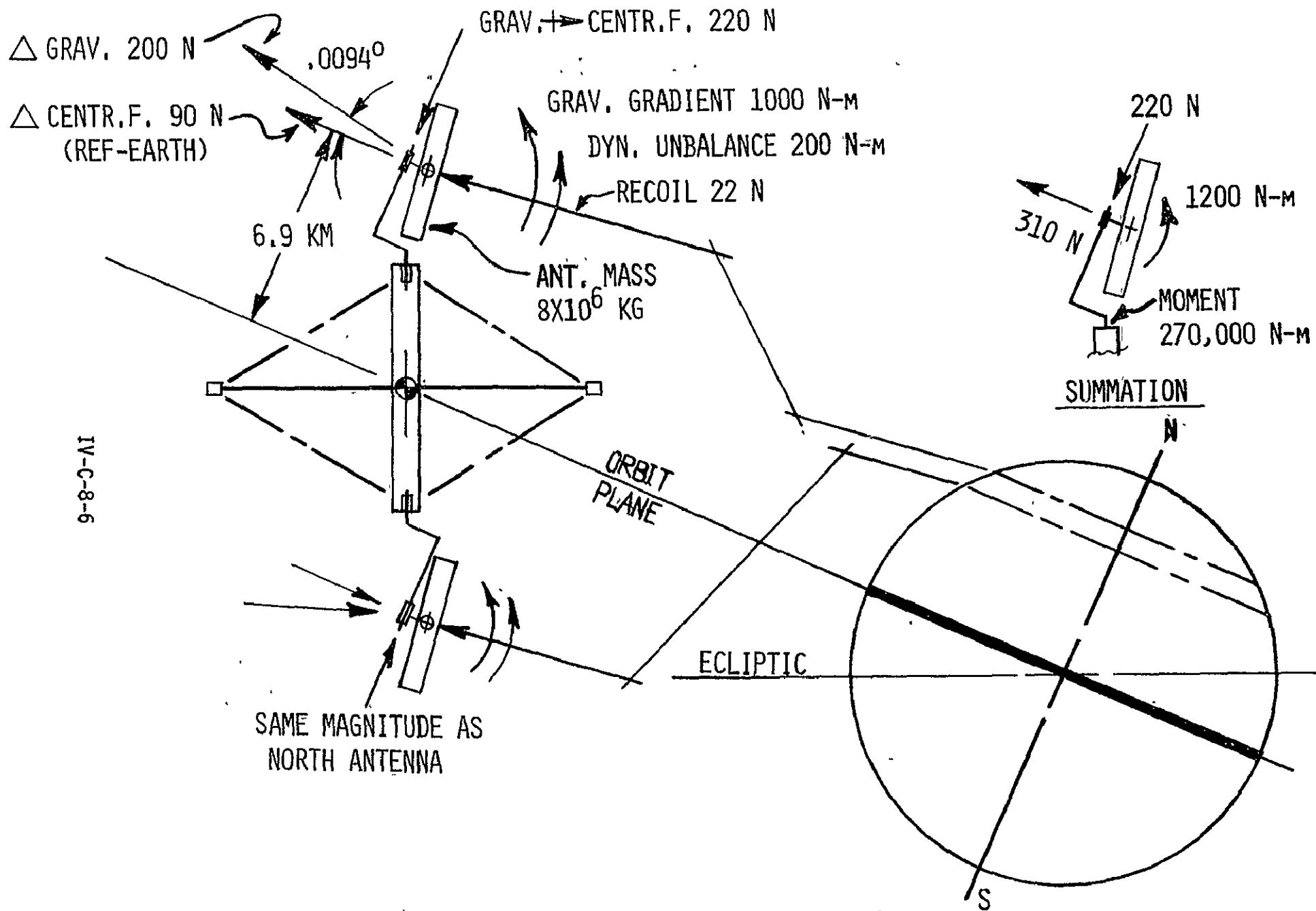


FIG. IV-C-8-3 ANTENNA AXES ARRANGEMENT CONCEPT



IV-C-8-6

FIGURE IV-C-8-4 FORCES ACTING ON ANTENNA

IV-C-8-7

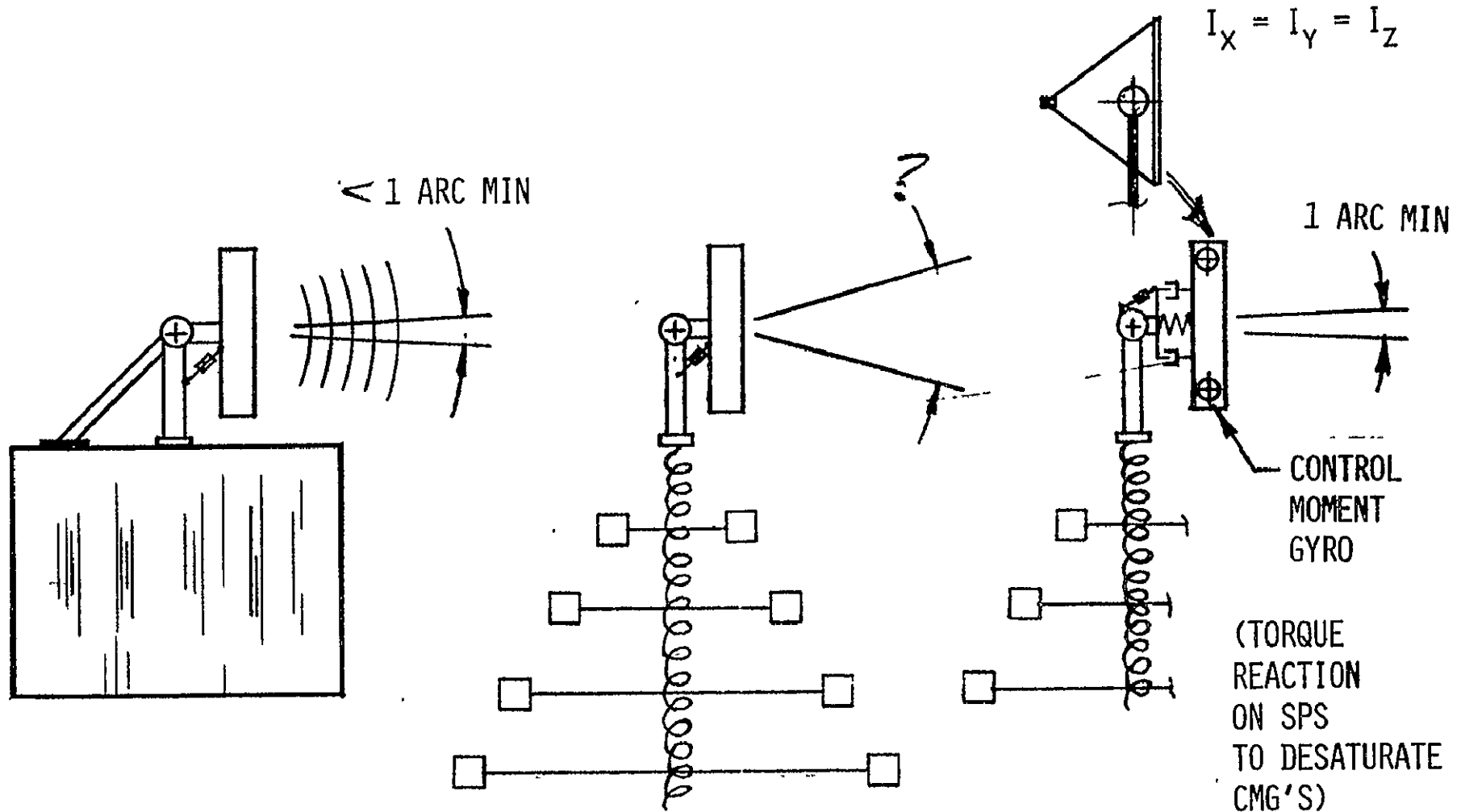


FIG. IV-C-8-5 SCHEMATIC-ANTENNA POINTING

changes with respect to the SPS. To eliminate the torque-input to the antenna from gravity gradient and dynamic unbalance, the antenna configuration is changed from a disc to a cone--the cone having the same mass moment of inertia about all axes.

Figure IV-C-8-6 shows the overall configuration of the antenna installed on either an SPS configuration that is solar oriented or one which is oriented perpendicular to the orbit plane (P.O.P.). The solar oriented configuration requires the dog-leg support and an additional rotary joint to allow the dog-leg support to be properly positioned with respect to earth as the solar array attitude changes to track the sun. A counterweight of approximately 1,000,000 kg is required to obtain equal inertia distribution for the antenna. The CMG's may be located at the counterweight position, reducing the requirement for "dead" weight. The ball joint is located at the antenna mass center. This is very important--so that the antenna has minimum externally applied torques. The major design problem is, now, the ball joint.

Figures IV-C-8-7 & 8 show the ball joint design for a dual antenna system (10 GW SPS) and Figure IV-C-8-10 shows a slightly different joint configuration for a single centrally located antenna system (5 GW SPS). The joint is a spherical ball approximately 7.6 meter diameter with an outer race that can rotate continuously about the axis of the ball connecting shaft and can oscillate up to 10° about any orthogonal axis, in the same manner as a conventional ball joint. The sliding contact surface between the ball and outer race provides the structural support (bearing) function and the transfer of electrical energy. The ball and connecting shaft (actually 2 concentric shafts), and the outer race are divided as indicated in the figure by insulation to provide the separate positive and negative electrical conduction paths. Electrical brushes provide the actual sliding/bearing contact between the ball and race. The brushes would be individually spring loaded to maintain proper contact pressure and to allow compliance with the probably-irregular-surface of the ball. It is estimated that about 5000 brushes, each having a 64.5 square centimeter contact area, would be used in both the positive and negative halves of the joint. The concept is to maintain the maximum possible contact area for transfer of electricity, considering the large size of the joint and the probable deviations from a perfectly spherical surface. Listed below are comments about some of the devices that were considered as possible candidates for transferring power across the rotary joint (*see reference at the bottom of the page for a discussion of these devices):

1. Power clutches - requires switching (interruption of current flow) which presents an arcing problem; concept requires development.

*Design Data Handbook for Flexible Solar Array Systems, Report No. LMSC-D159618, March 1973.

IV-C-8-9

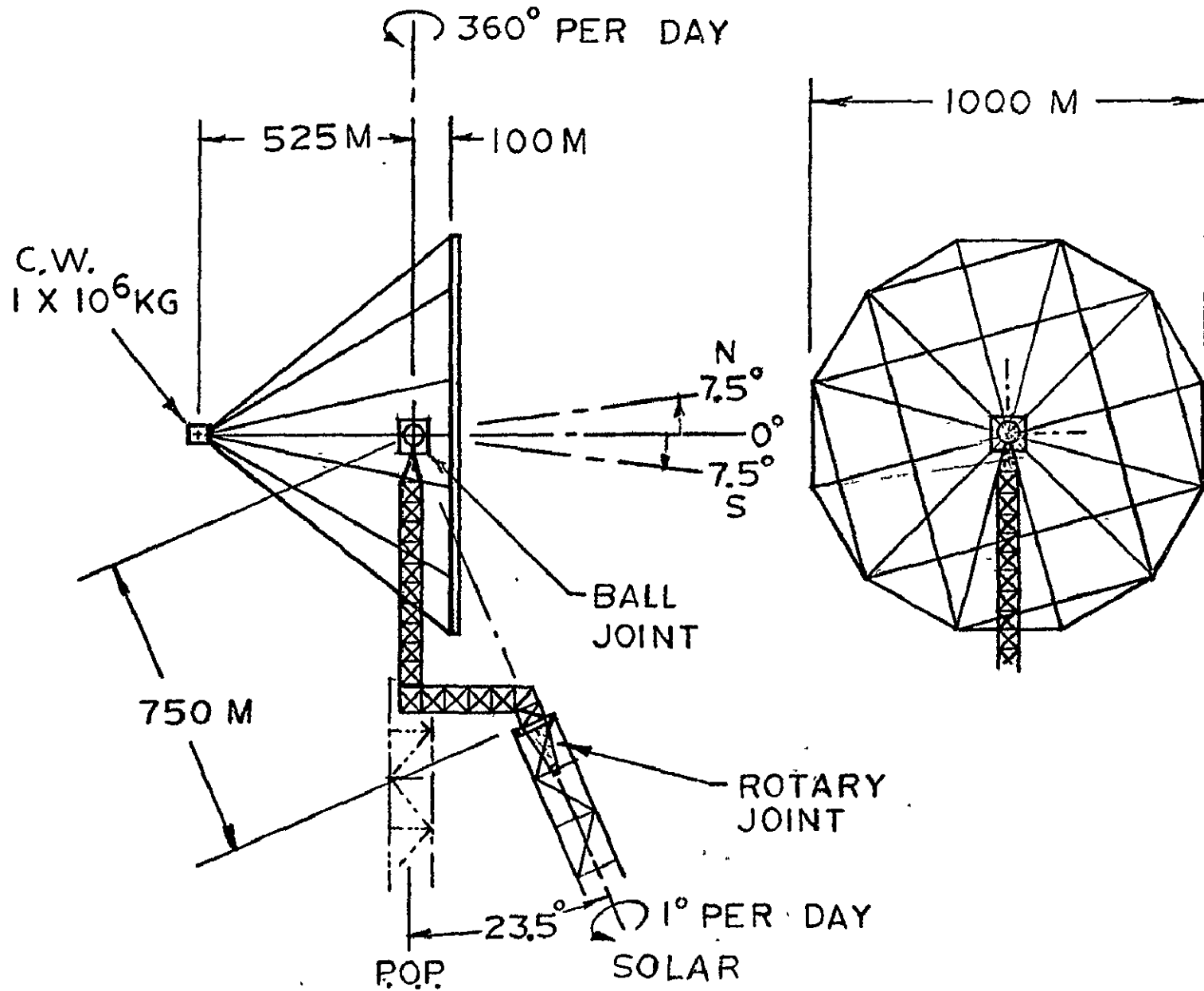


FIG. IV-C-8-6 SPS ANTENNA CONFIGURATION

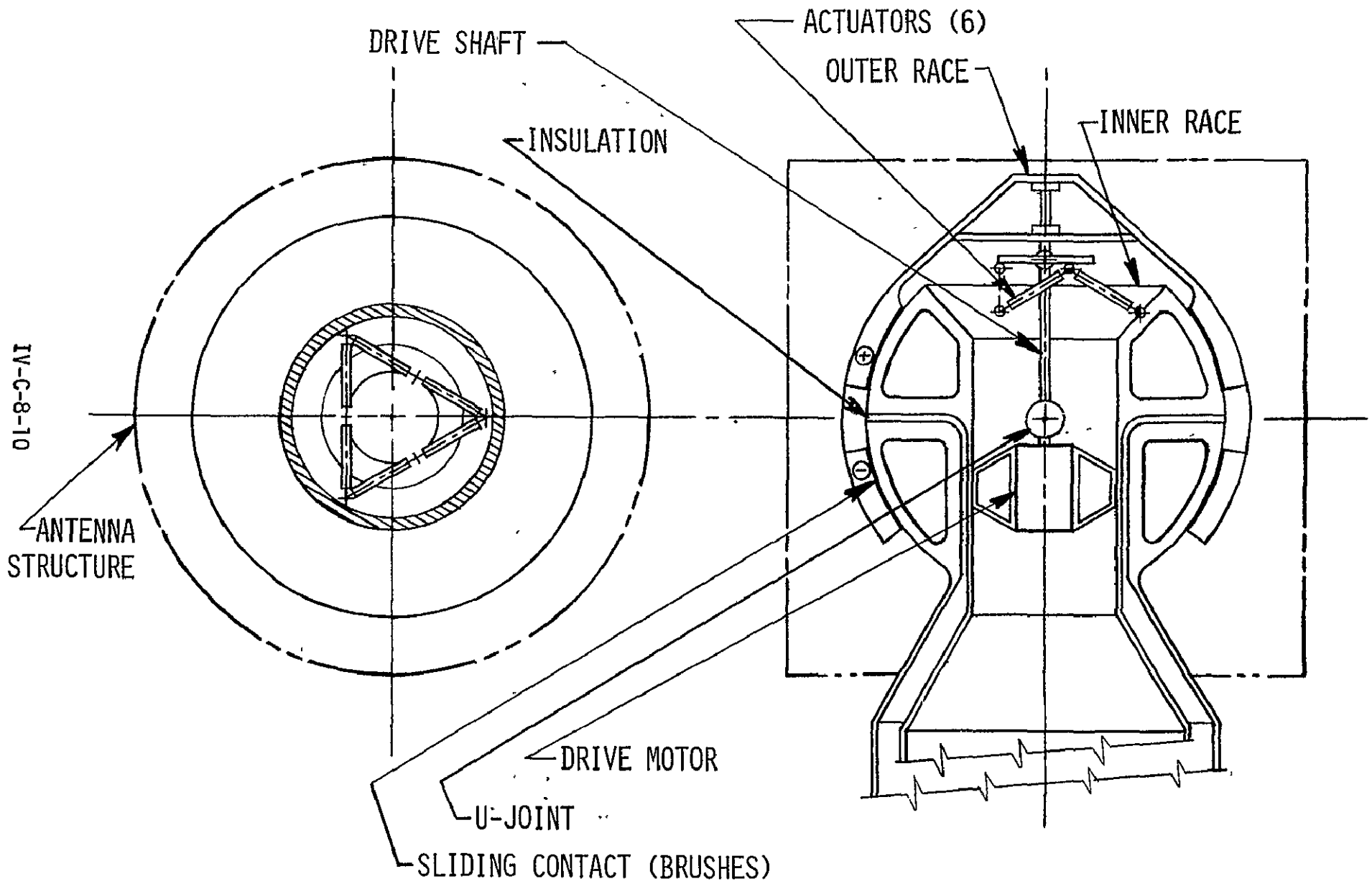


FIG. IV-C-8-7 BALL JOINT AND DRIVE CONCEPT

2. Flex cable - does not fit the joint design concept.

3. Rotary transformer - requires conversion from DC to AC and back to DC, these conversion losses add to the overall thermal problem and reduce the transformer efficiency; the transformer itself will produce high thermal loads (1% efficiency loss equals 100 megawatts of heat which must be rejected).

4. Rolling contacts - fatigue may be a problem; requires development.

In addition to the devices listed above slip rings were considered and selected as a best choice for the rotary ball joint because they are state-of-the-art, highly reliable and maintainable. The large surface area which is inherently available on the 7.6 meter diameter ball allows a large number of brushes to be used which results in a low current density (.78 amps/sq cm). It appears that the low current density and extremely low brush speed (approx. 1.5 cm per min.) will allow the slip ring and brush system to operate at a high efficiency.

The joint drive system includes the electric motor-gearbox (with adequate redundancy), a constant velocity universal joint and drive shaft as indicated on the drawing (Figure IV-C-8-7) to provide continuous rotation about the primary axis of the joint. Motion about an orthogonal axis (up to $\pm 10^\circ$) is obtained by 6 linear actuators arranged in a triangular pattern and mounted between the ball and a "table" that is bearing mounted to the outer race at the juncture of the drive shaft and outer race. The six actuators, by continuously changing their lengths, can position the ball in any attitude within the $\pm 10^\circ$ limit. If the ground receiving rectenna were located at 50° N. latitude on earth, for example, the antenna should be tilted up about 7.5° . In this case the 6 actuators would rotate the outer race of the ball joint 7.5° and, as the main drive shaft rotated the outer race at a rate of 360° per day, the 6 actuators would be driven to cause the outer race to "cone" through a total angle of 15° ($2 \times 7.5^\circ$) each day.

Figure IV-C-8-8 shows the soft suspension system connecting the antenna to the ball joint outer race. A cylindrical configuration outer structural shell is shown (though it may be of various configurations adaptable to the antenna structural arrangement) which connects to the antenna structure. This shell connects to the outer race of the ball joint through 6 suspension struts symmetrically arranged in a triangular pattern. These struts act as soft spring/dampers to allow small linear and angular excursions of the antenna with respect to the ball joint, while minimizing torque inputs to the antenna from the ball joint. The electric current is conducted from the ball joint outer race through literally thousands of small, stranded copper wires to busses at each end of the structural shell. These wires each are located along a radius vector from the center of the ball, and are installed so they are "slack". Small angular

and translational motions between the ball joint and antenna would meet a very minimal resistance from these wires. In conjunction with the copper conductors would be auxiliary tension cables or struts, again positioned radially to react translational movements but not rotation. These tension cables essentially "moor" the antenna structure to the outer race and provide a soft connection.

The total system then functions in a manner outlined as follows:

1. The CMG's control antenna pointing attitude in response to pointing error signals.
2. An attitude difference between the antenna and ball joint outer race is detected from position transducers within the 6 suspension struts.
3. The attitude difference signal is used as a basis to change the ball joint drive rate and/or the 6 angular position actuator rates, to cause the ball joint outer race to, in effect, track the antenna.

The ball joint drive system, then, functions only to overcome the friction in the joint and drive the joint to keep up with the antenna motion within a half-degree or so. The structure in the ball joint area is very stiff, and the friction is basically constant. Therefore, the difficulty in designing this servo-system is minimal. The nearly constant friction torque is considered to be a feature of the ball joint, which allows 3 axis freedom within a single bearing system, without any starting and stopping motion — with resulting static and dynamic friction coefficients — as would result in a discrete axis (gimbal) arrangement. The control system can allow the CMG's to be desaturated by feeding an angular impulse into the SPS through the joint drive and suspension system at a low rate over a long period of time, without significant complications from low spring rate SPS structure.

The overall size and weight of the ball joint is estimated to be well within the volume and payload weight capabilities of the Heavy Lift Launch Vehicle. Therefore, it would be completely manufactured on earth and at least two joints launched in the one launch vehicle.

A likely technical problem is heat rejection from the relatively compact configuration. Preliminary analysis indicates that the use of very low current densities (amps/square cm.) may reduce the electrical heating in the joint to a low enough rate so that radiation cooling is adequate. Heat pipes may be used to conduct heat from the outer race outward to larger area radiating surfaces. Cooling of the inner conducting tube of the 2 concentric tubes would be aided by not making the outer tube solid (i.e. provide holes in the outer tube to expose some of the inner tube surface).

IV-C-8-13

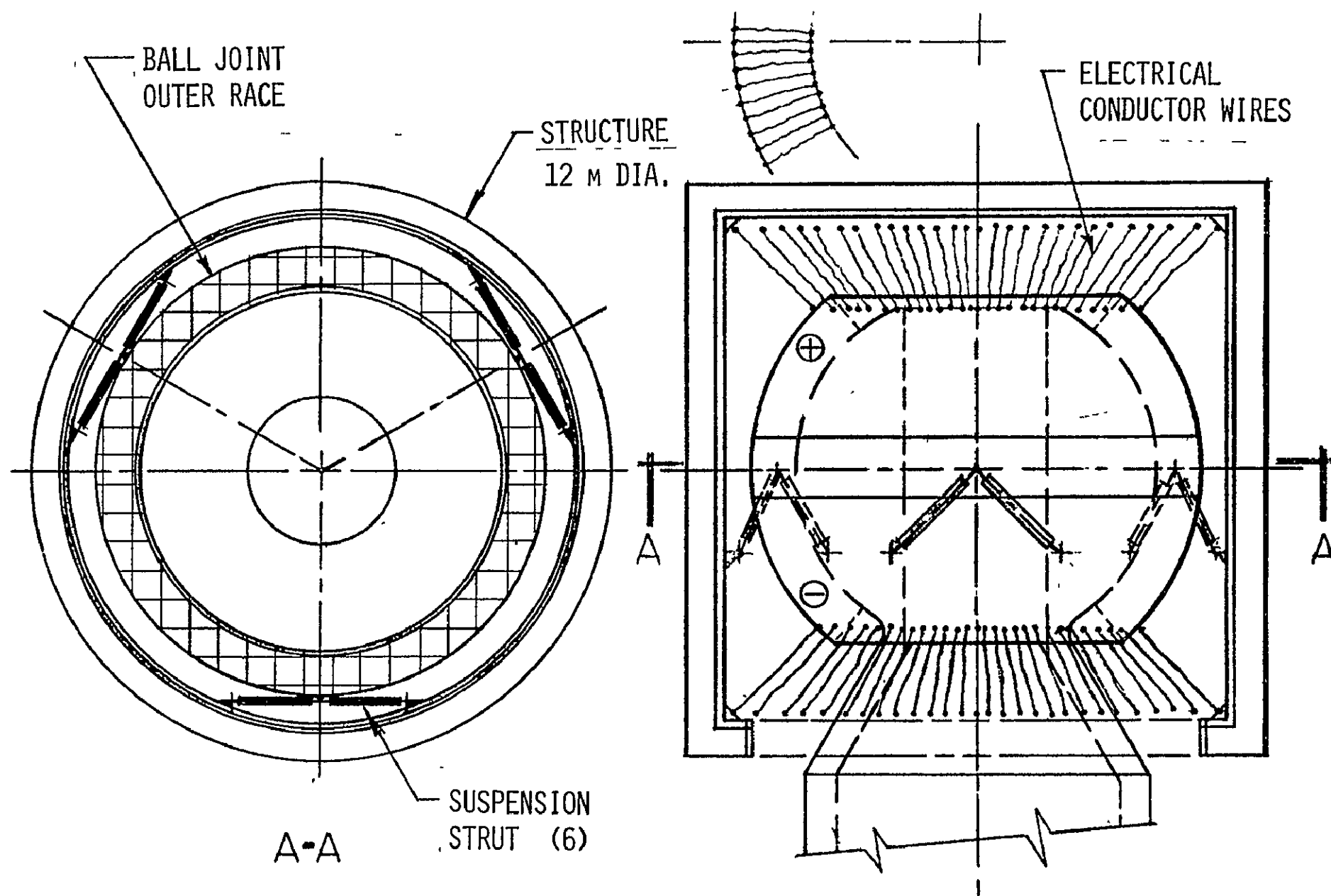


FIG. IV-C-8-8 ANTENNA SOFT SUSPENSION SYSTEM

Figure IV-C-8-9 shows some calculated values of current density and heat generated for a total current of 250,000 amps. The numbers indicate feasibility of achieving a satisfactory design.

Brush design and materials are considered to be development problems. Some candidate slip ring materials which should be considered are silver, copper, coin silver (90% silver, 10% copper) or a laminate of copper and coin silver.* An electrically conductive lubricant may be a valuable development item. Oils or grease lubricants should be avoided because of outgasing associated with vacuum operation.

In summary, it is believed that this concept for the antenna mount and pointing control has merit worthy of further design effort, and that this part of the SPS is not a high risk development item. It should also be noted that the ball joint concept can be applied to any SPS configuration identified to date. No significant design effort was applied to the antenna mount for an SPS which is oriented other than normal to the orbit plane (P.O.P.), because it is believed that the P.O.P orientation will prove to be superior from an overall system viewpoint.

*Design Data Handbook for Flexible Solar Array Systems, Report No. LMSC-D159618, March 1973.

IV-C-8-15

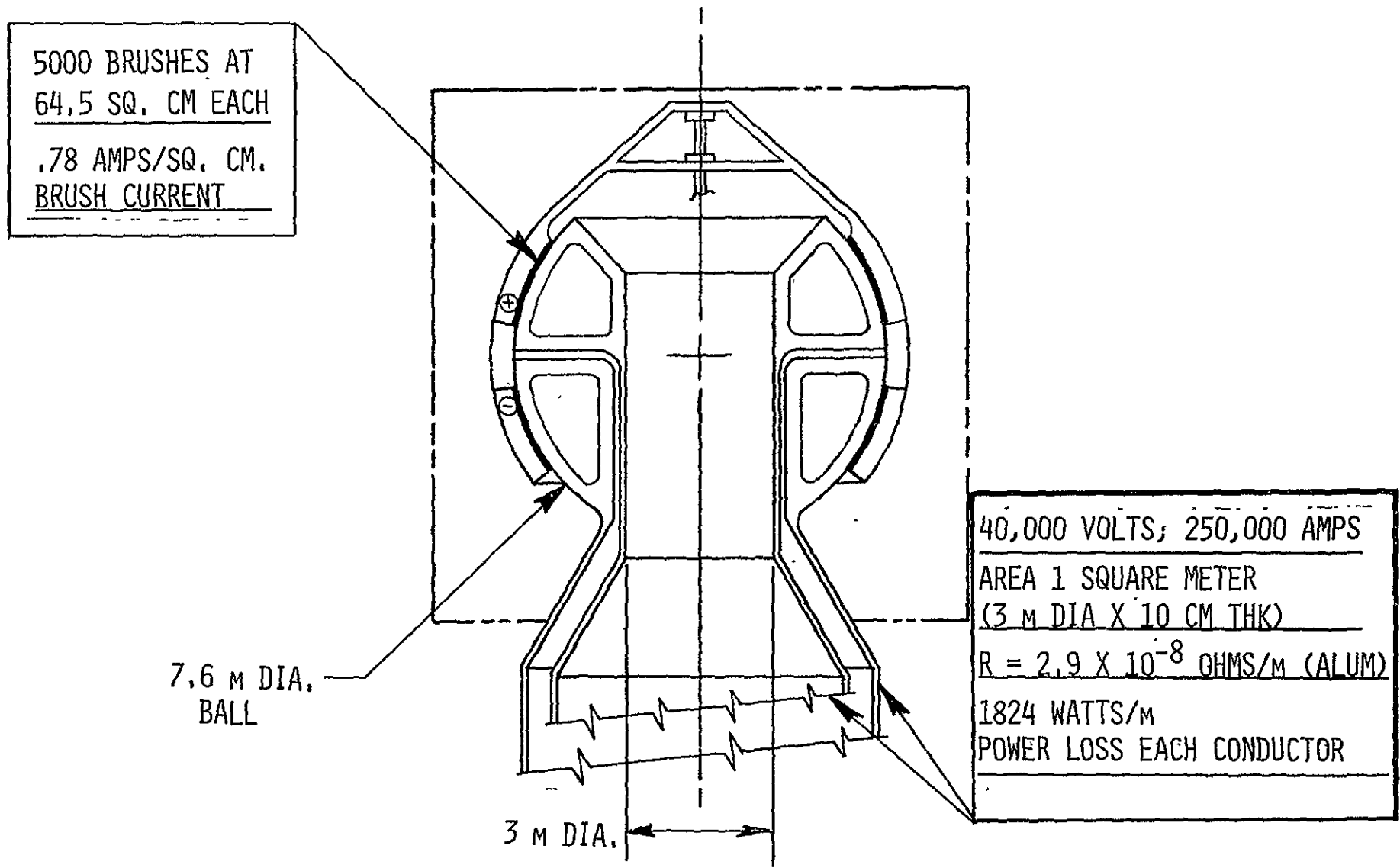


FIG. IV-C-8-9 BALL JOINT-POWER DISTRIBUTION

SUSPENSION
STRUT (6)

DRIVE MOTOR

ACTUATOR DRIVE RING

STRUCTURE
(12 M DIA.)

ACTUATORS (6)

IV-C-8-16

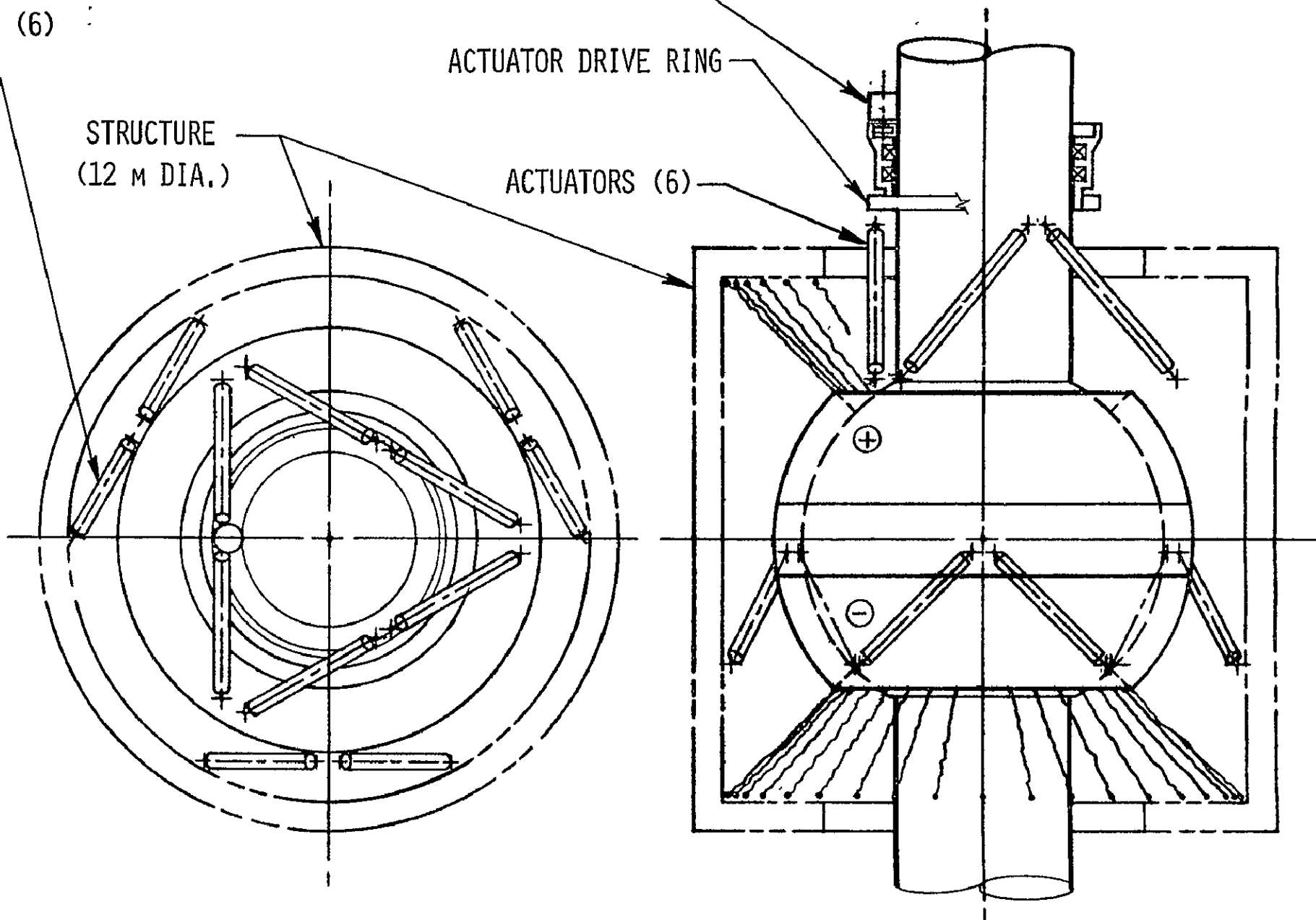


FIG. IV-C-8-10 BALL JOINT FOR SINGLE ANTENNA ARRANGEMENT

IV-C-9. Thermal Control

The thermal characteristics of the antenna have been investigated in some detail by the Raytheon Company and the Grumman Aerospace Corporation (reference 1). Current results tend to reinforce previous findings and support the contention that thermal control of the antenna can be achieved in a passive manner. However, the requirement for a very closely integrated design of the microwave generators, waveguide system, electronics, each level of structure, and materials all center around the thermal characteristics of the antenna. There are no apparent insurmountable thermal problems which cannot be solved through technology development programs and testing prior to SPS initiation. However, three significant thermal design considerations are apparent:

1. Rejection of waste heat.
2. Minimization of thermal distortions of the primary structure due to the daily solar orientation cycle.
3. Accommodation of thermal strain and elimination of excessive thermal stress occurring as a result of occultation by the earth.

The rejection of waste heat from the antenna requires thermal radiation from the rear of the antenna. Although operating temperatures could be reduced through high thermal emission from the waveguides, the waveguide configuration is a rather efficient thermal radiation shield. In addition, the waveguide efficiency requirement of high electrical conductivity on all exterior surfaces significantly limits the thermal emissivity obtainable. Fortunately, about half of the waste heat generated by a Klystron is produced at the anode, thereby affording a relatively simple path for thermal radiation rejection. The other half of the waste heat must be transmitted through radiation, conduction, or heat pipe to the radiator.

The representative thermal profile shown in figure IV-C-9-1 was obtained by assuming that 90 percent of the waste heat can be rejected out the back of the antenna with an additional 10 percent through the waveguides. The effect of antenna taper is to produce maximum temperatures at the center of the antenna. In addition, the operating temperature of the antenna is a strong function of the amount of waste heat. The operating temperature and variations in operating temperatures are potentially very important to the phasing electronics and phasing system as well as to the microwave generation and waveguide efficiencies, equipment lifetime and reliability.

The other major heat rejection problem is the rotary joint. Sufficient surface area must be provided to provide adequate thermal emission, and some means for transporting this heat to the exterior surface is required. To allow adequate heat flow and still maintain sufficient electrical insulation between the departing and returning current may require independent heat rejection systems. This problem has not been treated in depth; however, it does appear to be a potential area for heat pipe application.

If it is assumed that thermal distortion between an operating and non-operating antenna system can be accommodated through a calibrated alignment, then the thermal distortion problem is reduced to the effect of the daily solar orientation cycle. If a low thermal expansion coefficient material, such as a graphite composite, is utilized for all levels of structure, then thermal distortions are of significance only for the prime structure influence on the subarray orientation. The antenna tends to curl away from the sun with the maximum effect at the edges. The lower temperature regions are more strongly affected by the solar flux

IV-C-9-2

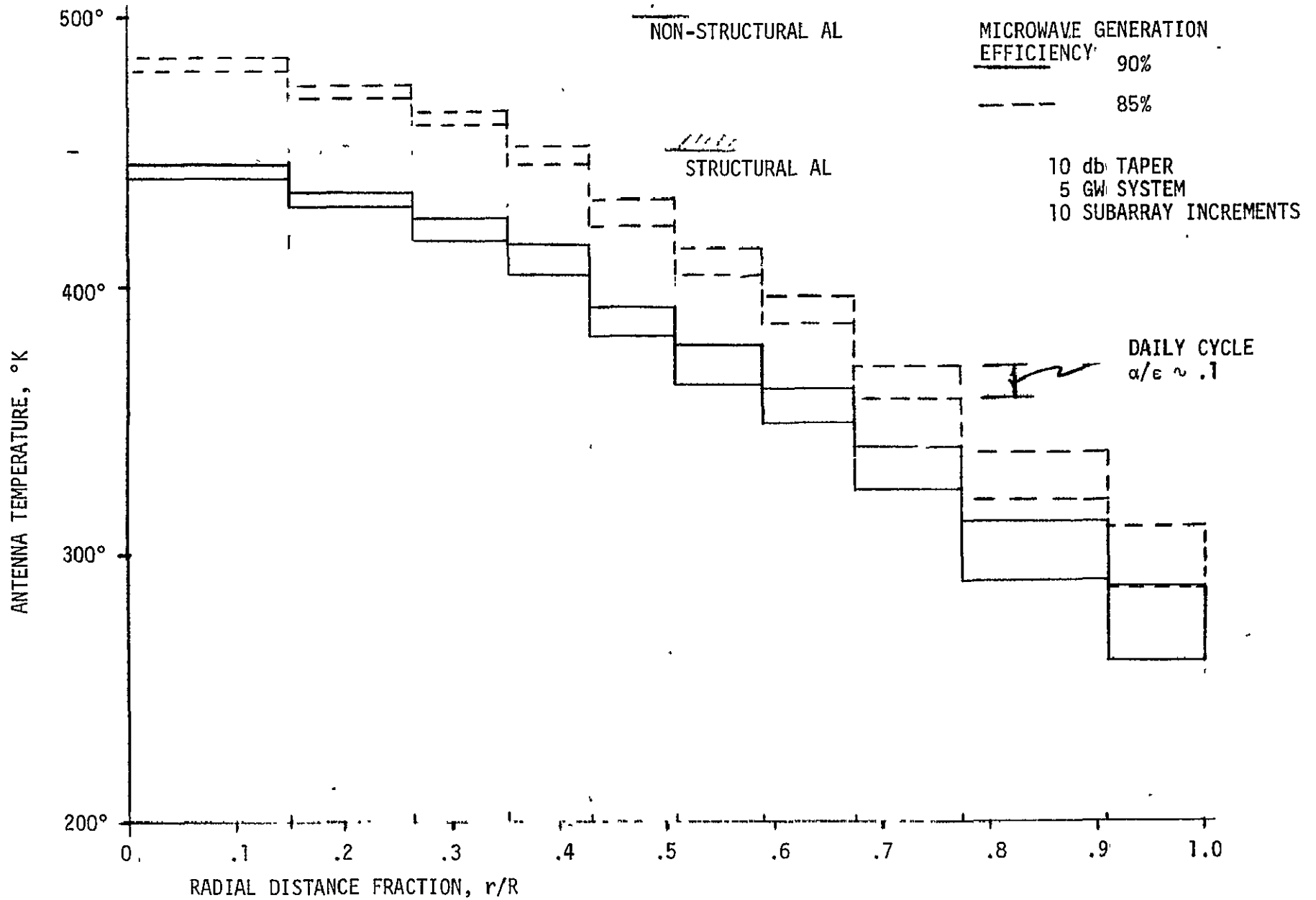


FIGURE IV-C(9)-1 - ANTENNA TEMPERATURE DISTRIBUTION

which cannot be reflected. There are two passive means for reducing this effect to within subarray structural alignment tolerance requirements (3 arc minutes on boresight). The first is to geometrically taper the antenna prime structure to be relatively thin at the outer edges. This is not inconsistent with structural load paths, stiffness requirements, and a reduction of gravity gradient torques. The second approach is to lower the emissivity of the surface and allow the waste heat to bring the operating temperatures at the large radii up to the levels at the center. There are many design advantages to operating the antenna at a uniform temperature; however, it must be emphasized that the temperature level would be established by waste heat generated at the peak power density center.

The third thermal consideration of significance to the antenna design is the relatively rapid and rather extreme temperature transients associated with eclipse by the earth. The characteristic time for the antenna to cool from operating temperatures is about twenty minutes. Since eclipse can last for up to 75 minutes, the potentially large changes in temperature (almost 500°K) impose a design requirement of thermal stress or strain. The major problem here is the disparity between necessarily low thermal expansion coefficient prime, secondary and subarray support structures and the high electrical conductivity waveguides which will have a significantly higher thermal expansion coefficient. A particular design solution would be to have the waveguides for each Klystron form a determinant structure relative to each Klystron. Thus, each Klystron and its waveguide will form a structural unit, as shown in figure IV-C-9-2, with the subarray structure supporting each Klystron unit individually. The waveguides for each unit, however, must not transmit loads from one waveguide to the next. If they did, the thermal stresses associated with occultation could be excessive.

The cost and weight estimates of thermal control for the transmission module are based on a conservative assumption that all exterior surface will require a thermal control coating. This is balanced by an assumption that if the production of space qualified thermal control coatings rises by several orders of magnitude the cost will drop from current values by at least one order of magnitude. Table IV-C-9-1 provides characteristics of three potential thermal control coatings. Although the metallized films are resistant to UV radiation, they are susceptible to charged particle degradation and have rather high spectral reflectance components. The white paints are fairly resistant to UV radiation; but they have significant limitations with respect to outgassing and an ability to be cleaned. Ideally coatings with little degradation from charged particles and with low (.08) solar absorptance need to be developed. Some progress along this line has been made with zinc orthotitanate pigments. Low α/ϵ , high electrical conductivity coatings have yet to be developed.

a. References

1. Microwave Power Transmission System Studies, Fourth Engineering Review, Contract NAS 3-17835, Raytheon Company for NASA Lewis Research Center, December 12, 1974.

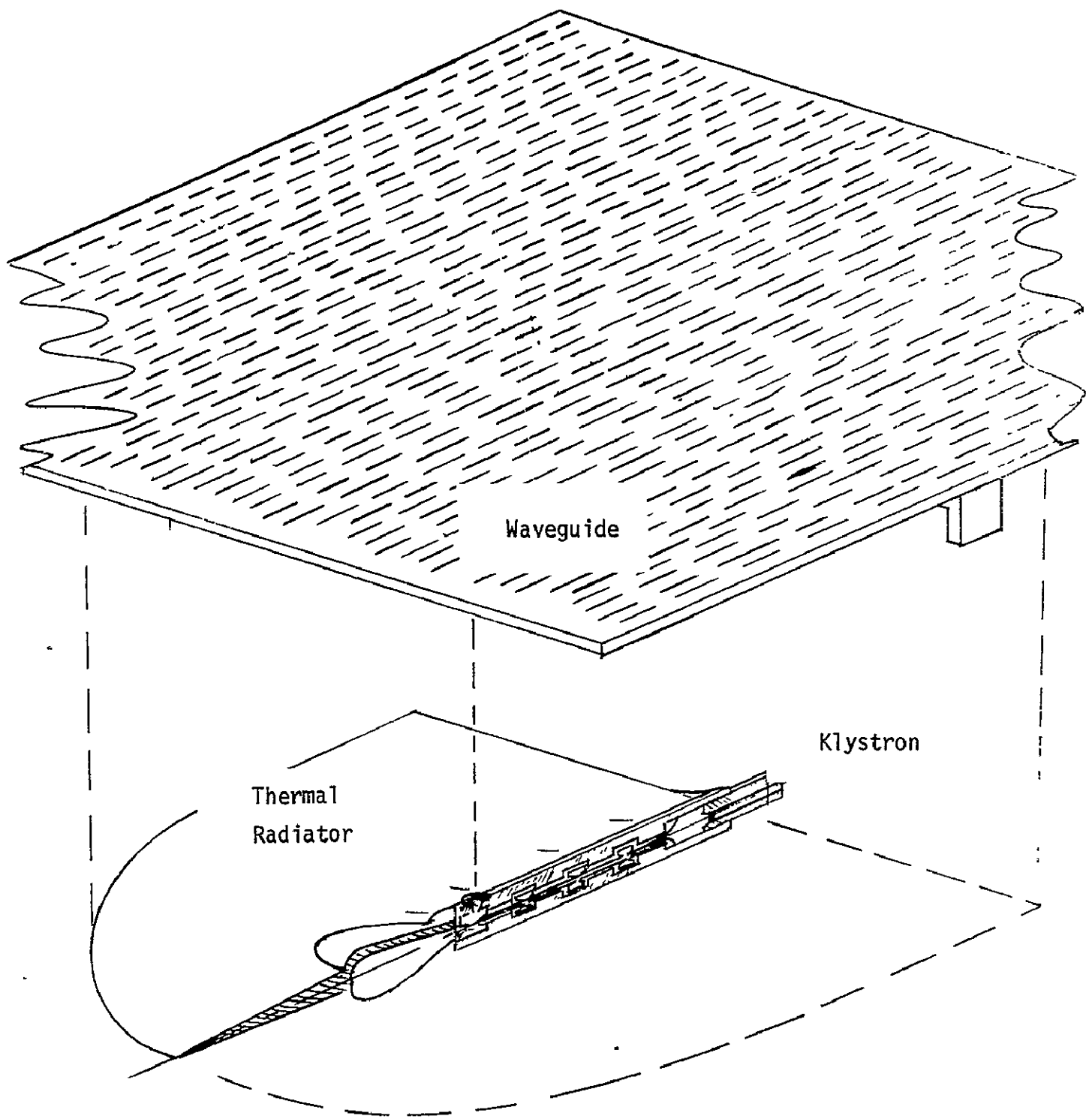


FIGURE IV-C-9-2

KLYSTRON/WAVEGUIDE/THERMAL RADIATOR UNIT

TABLE IV-C(9)-1

CURRENT THERMAL CONTROL COATING PARAMETERS

	CURRENT QUANTITY* COST/m ²	WEIGHT kg/m ²	OPTICAL PROPERTIES		U.V. STABILITY
			α_s	ϵ_{ir}	
METALIZED FILMS, E.G.					
SILVER TEFLON (@ 3 MILS)	\$183	.33	.08	.81	EXCELLENT** $\Delta\alpha_s \sim 0$
WHITE PAINT, E.G.					
S-13g (LO) (@ 10 MILS)	\$270	.43	.19	.92	VERY GOOD** $\Delta\alpha_s \sim .2$
GOLD (400 Å)	\$ 59	1.9×10^{-4}	.3	.03-.05	EXCELLENT

*INCLUDES COST OF OVERLAY AND ADHESIVE; DOES NOT INCLUDE APPLICATION

**2000-HOUR SOLAR EXPOSURE

IV. D. MICROWAVE RECEPTION AND CONVERSION SYSTEM

1. Rectenna

Rationale: The problem of collecting the microwave power from the SPS and then changing this to a useful form for transmission to the electric utility grid system has been the subject of much attention in the past several years. The concept which has developed is that of a receiving antenna combined directly with a rectifying element. This combination is known as a rectenna. This rectenna concept is essentially a one step process of collection of microwave power and rectifying this power into direct current all in one unit. This concept has been chosen over several others because it offers the potential of being the most efficient and most reliable as well as having the lowest production costs.

Some earlier concepts which have been investigated but have been rejected for various reasons are:

a. Microwave (MW) conversion into heat--the heat would be used to run a heat engine of some type which could then be used to generate the desired electrical current. The drawback to this concept is mechanical complications and low overall efficiency.

b. Microwave conversion to direct current (DC) (MW generator analogs) - concepts for use of traveling wave tube and Klystron analogs have been developed, but the early development of a magnetron analog led to the conclusion that the MW generator analogs were impractical.

c. Microwave conversion to direct current (diode rectifiers) - thermionic diodes reached a stage of early development, however, component reliability proved to be a serious problem, and the outlook for efficient rectification was not good.

Not until the introduction of the Gallium Arsenide Schottky barrier diode was there promise for an efficient, reliable device which could convert MW to DC. The next consideration in the rectenna concept is what is the best way to collect the microwave energy being transmitted from the SPS.

The question of collection of the microwave energy has also been investigated over the years and various antenna designs have been evaluated. The general desired requirements for such an antenna are:

- (1) Appropriate power handling capability.
- (2) High reliability.

- (3) Relatively nondirective aperture.
- (4) High absorption efficiency.
- (5) Passive radiation of waste heat.
- (6) Low radio frequency interference (RFI).
- (7) Capable of large aperture sizes.
- (8) Low mechanical tolerance requirements.
- (9) Low cost.

Of the several candidate antennas which have been chosen for analysis, each is required to interface with the RF/DC converter which shows the most promise, the diode rectifier. The diode may be used singly or in groups for each candidate antenna. If large numbers are grouped together then it will be necessary to provide for some type of auxiliary cooling.

There are four types of receiving antenna arrays which have been considered. The array of contiguous horns, as well as the array of contiguous reflectors and feed horns, both with the disadvantage that they cannot collect the impinging energy with as much efficiency as the other two approaches considered. The phased array of small elements with a common MW load can increase this efficiency by matching individual elements to the incident radiation, but this makes the phased array directive and the common MW load will require auxiliary cooling. The four approaches considered are shown in Figure IV-D-1-1. With the exception of the rectenna approach, all other approaches fail to meet the requirements in at least four ways.

Because of the above factors, the rectenna approach has been selected as the reference for continued analysis. It appears to be the most promising approach, and actual tests on some initial rectenna designs have gone far in proving the feasibility of this concept. In the latter part of 1975 JPL demonstrated the concept at their Goldstone Deep Space Facility in California. A level of 323 KW was transmitted at a frequency of 2.388 GHz and a 12 x 25-foot array of rectenna dipole/rectifier elements intercepted approximately 11.4 percent of the beam. Of the 36.8 KW intercepted, 30.4 KW of DC power was generated with an efficiency of conversion of 82.5 percent.

The power density at the rectenna elements of the above series of tests, however, was high compared to what can be expected at an operational SPS rectenna site, especially on the periphery. This low power density at the rectenna elements requires further investigations to determine how the output efficiency may be increased. This will be discussed more under the section on "Operating Characteristics" and "Technology Status, Criticality."

Antenna Requirements	Array of Contiguous Horns	Array of Contiguous Reflectors and Feed Horns	Phased Array of Small Elements With Common MW Load	Array of Small Elements with Independent MW Loads (Rectenna)
Appropriate power handling capability	yes	yes	yes	yes
High reliability	yes	yes	yes	yes
Relatively nondirective aperture	no	no	no	yes
High absorption efficiency	<70%	<70%	≈100%	≈100%
Passive radiation of waste heat	no	no	no	yes
Low radio frequency interference	yes	yes	yes	yes
Capable of large aperture sizes	yes	yes	yes	yes
Low mechanical tolerance requirements	no	no	no	yes
Low cost	no	no	no	yes

Figure IV-D-1-1.

COMPARISON OF ANTENNA APPROACHES FOR RECEPTION
OF SPACE-TO-EARTH POWER TRANSMISSIONS

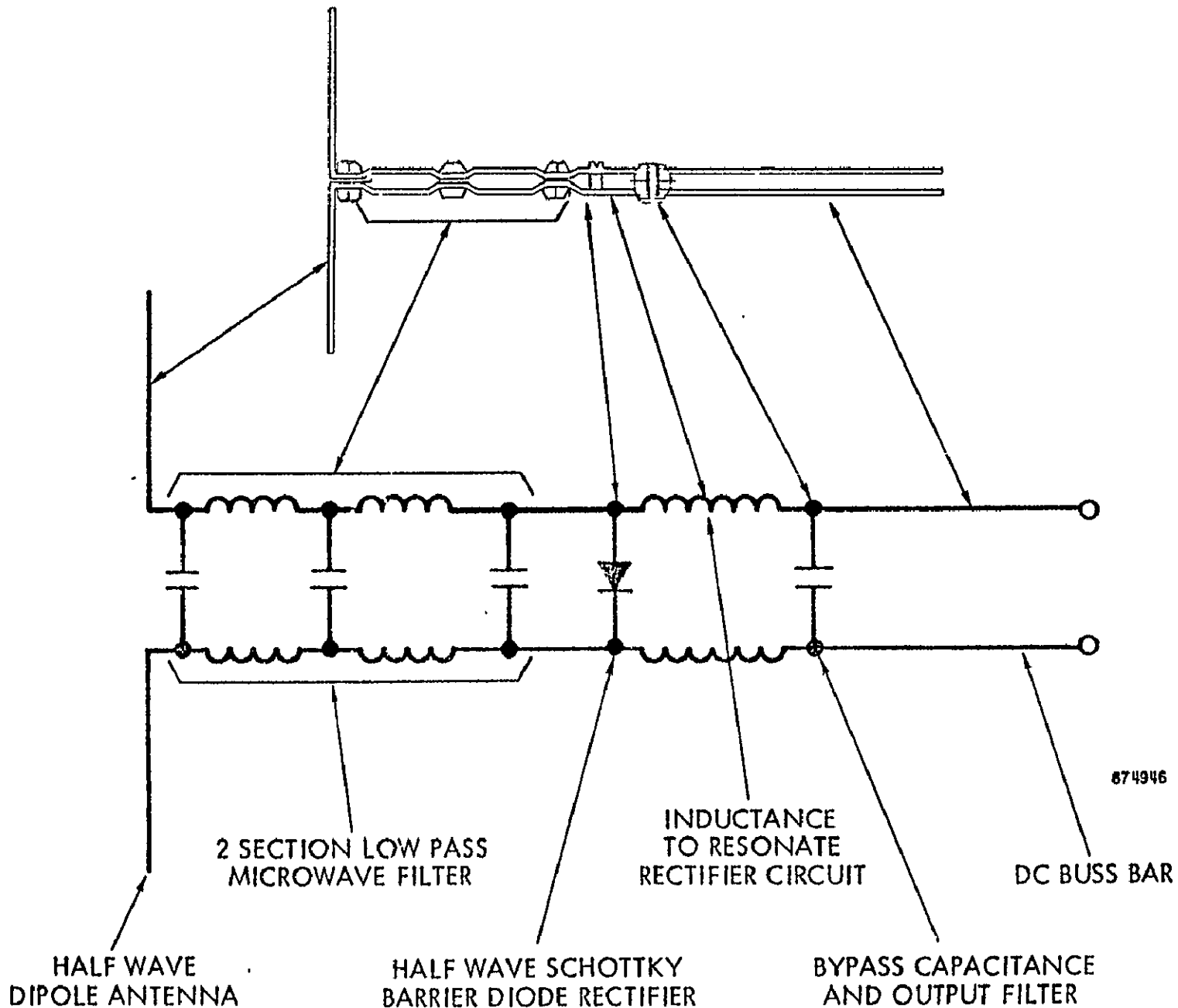
Definition: The use of the Schottky barrier diode, combined with a receiving dipole antenna led to the present concept of collection and rectification in one step--the ground rectenna. Each rectenna element is self-contained and collects and rectifies the microwave energy impinging upon it. These elements can be connected in series or parallel combinations to give an appropriate DC voltage output as the interface to the public utility power grid.

The present configuration of the rectenna element contains the following:

- a. A half-wave dipole antenna to collect the energy.
- b. A 2-section lowpass filter which serves as a harmonic filter to attenuate radiation of harmonic frequencies and as an energy storage device which feeds the rectifier circuit.
- c. Half-wave rectifier (Schottky barrier diode).
- d. Inductance resonator for rectifier output.
- e. Rectifier output filter.
- f. DC buss bar.

The mechanical drawing and simplified electrical schematic of the present rectenna element is shown in Figure IV-D-1-2. These elements are connected in parallel to collect the DC power and then summed in series to obtain the proper voltage level. The elements are mounted on a wire mesh which would be supported by a simple framework normal to the power beam phase front from the SPS. This mounting of the elements is shown in Figure IV-D-1-3. An overall view of the rectenna concept is shown in Figure IV-D-1-4.

IV-D-1-5



674946

FIGURE IV-D-1-2.
Simplified Electrical Schematic for the Rectenna Element

IV-D-1-6

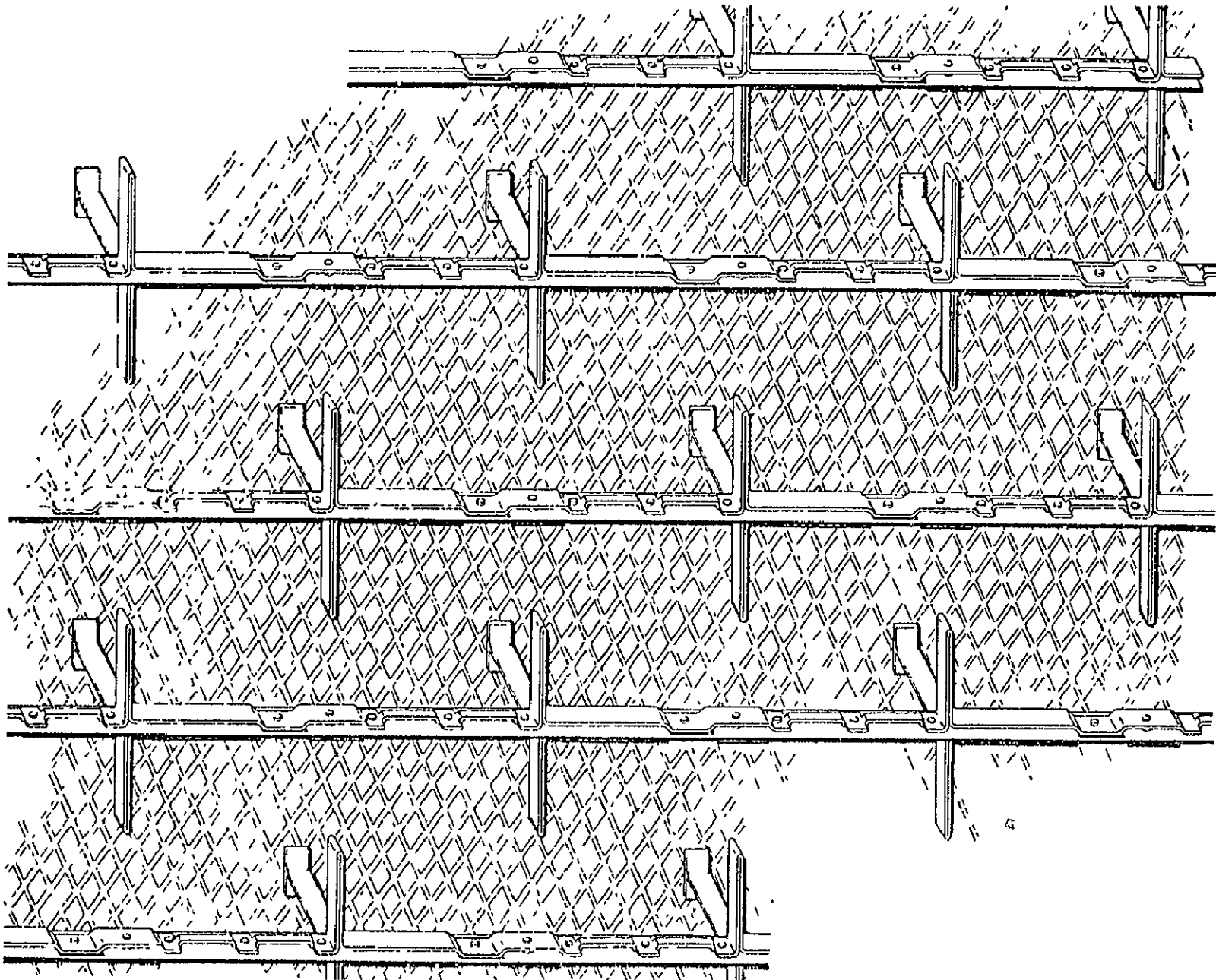


FIGURE IV-D-1-3.
RECTENNA ELEMENTS

SPACE SOLAR POWER STATION RECTENNA

IV-D-1-7

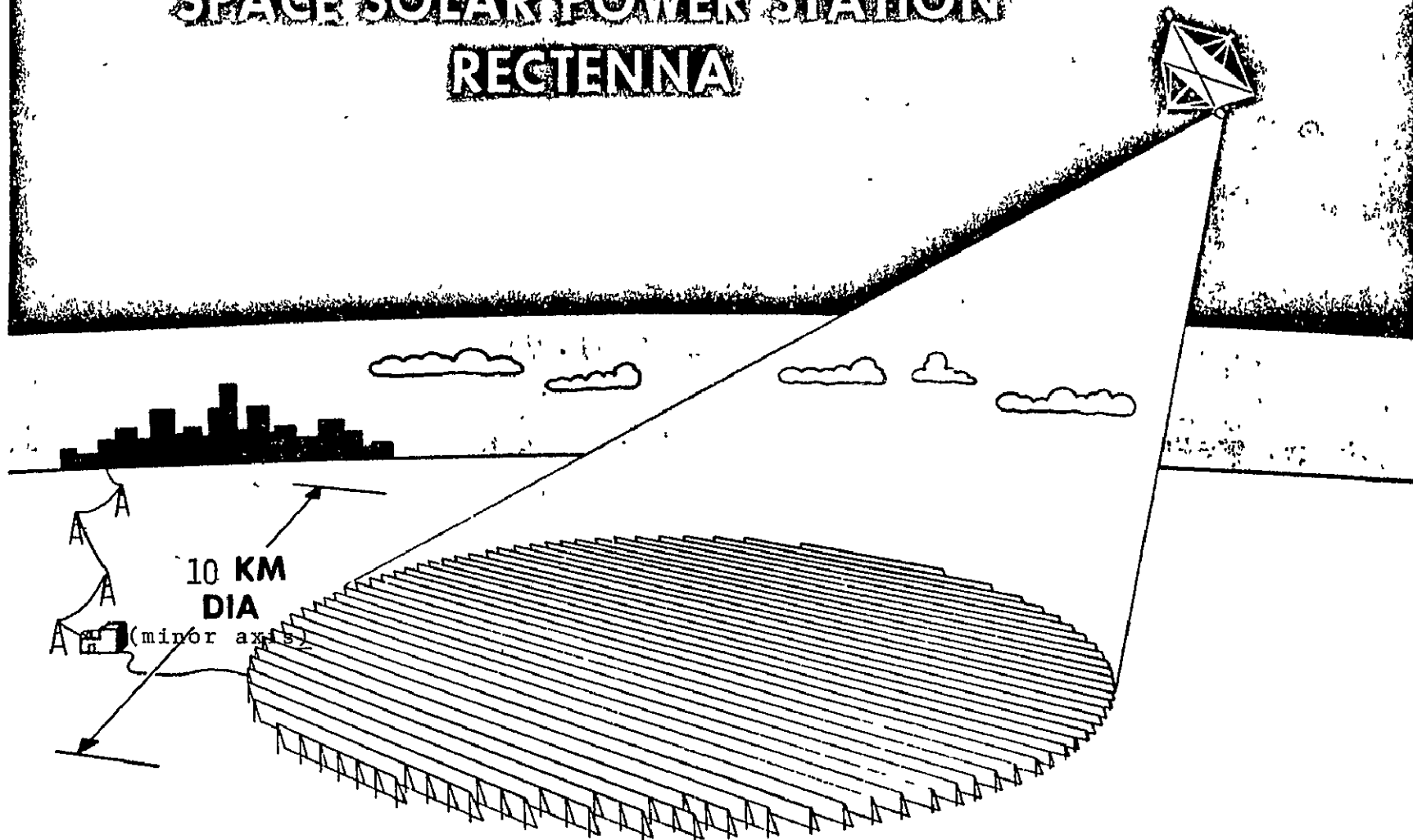


FIGURE IV-D-1-4.

Concept of microwave receiving station of a typical satellite power system.

Operating Characteristics: Based on system analysis data, the expected operating characteristics of the rectenna elements have been determined. The systems analysis data on which these calculations are based are as follows:

- a. $\lambda = 12$ cm wavelength of transmitted beam.
- b. $\sigma = 10^\circ$ phase error of transmitted beam.
- c. Amplitude error = +1 dB.
- d. Failure rate of Klystrons over 30-year period = 2 percent at any one time.
- e. 10 dB taper across transmitting antenna.
- f. Transmit antenna diameter = 1 km.
- g. Transmit antenna radiated power = 6.5 GW.

An overall MW collection efficiency of 87.5 percent can be realized if a rectenna is selected which has a 10 KM diameter on the minor axis. Thus a rectenna located on the equator at the same longitude as the SPS would be 10 KM round.

For a rectenna located in New Mexico (latitude $\approx 35^\circ\text{N}$) the rectenna would be approximately 10 KM on its minor axis and 13.2 KM on its major axis. For a rectenna located near the New York City area (latitude $\approx 42^\circ\text{N}$) the rectenna would be approximately 10 KM x 15 KM.

To determine the power density reaching various points on the rectenna, the above systems analysis data were used. In addition, the reference system efficiencies for atmospheric attenuation were also included. The power densities thus determined for boresight and at the 5 KM radius points are shown in Figure IV-D-1-5.

Taking these figures, it can be determined what the incident microwave power is for each rectenna element. The calculations are based on the center frequency of 2.45 GHz and the corresponding rectenna element cell area of 53 cm². These results are shown below:

Incident Microwave Power (Watts)			
	Minimum	Reference	Maximum
Element at rectenna center	1.14	1.12	1.07
Element at rectenna radius of 5 KM	0.047	0.046	0.044

The rectenna element efficiency can then be determined by referring to Figure IV-D-1-6. Thus the rectenna element at the center has an RF/DC conversion efficiency of approximately 82 percent. The rectenna element at the outer edge (radius = 5 KM) has an RF/DC conversion efficiency of

approximately 56 percent. It can be seen that only the rectenna elements at the center of the rectenna receive enough incident radiation to provide a relatively high DC/RF conversion efficiency. There are several ways to improve this condition.

a. The rectenna could be made larger to collect more incident radiation. This approach does not appear to be good because the power density levels drop off fairly rapidly for radii above 5 KM.

b. Investigate the use of an array of dipole antennas which would collect enough RF power to feed into a single diode--enough to operate on the high end of the diode efficiency curve.

c. Undertake development of a rectenna element with higher efficiencies at low power density levels.

Items b. and c., above should be studied further and will be discussed in somewhat more detail in the section on "Technology Status, Criticality."

POWER DENSITIES AT RECTENNA - mW/cm^2

	Minimum	Reference	Maximum
(Atmospheric attenuation)	0.98	0.96	0.92
Rectenna boresight	21.54	21.10	20.22
Rectenna radius of 5 KM	0.88	0.86	0.83

IV-D-1-10

FIGURE IV-D-1-5. Power Densities at Rectenna Center and Outer Edge

IV-D-1-11

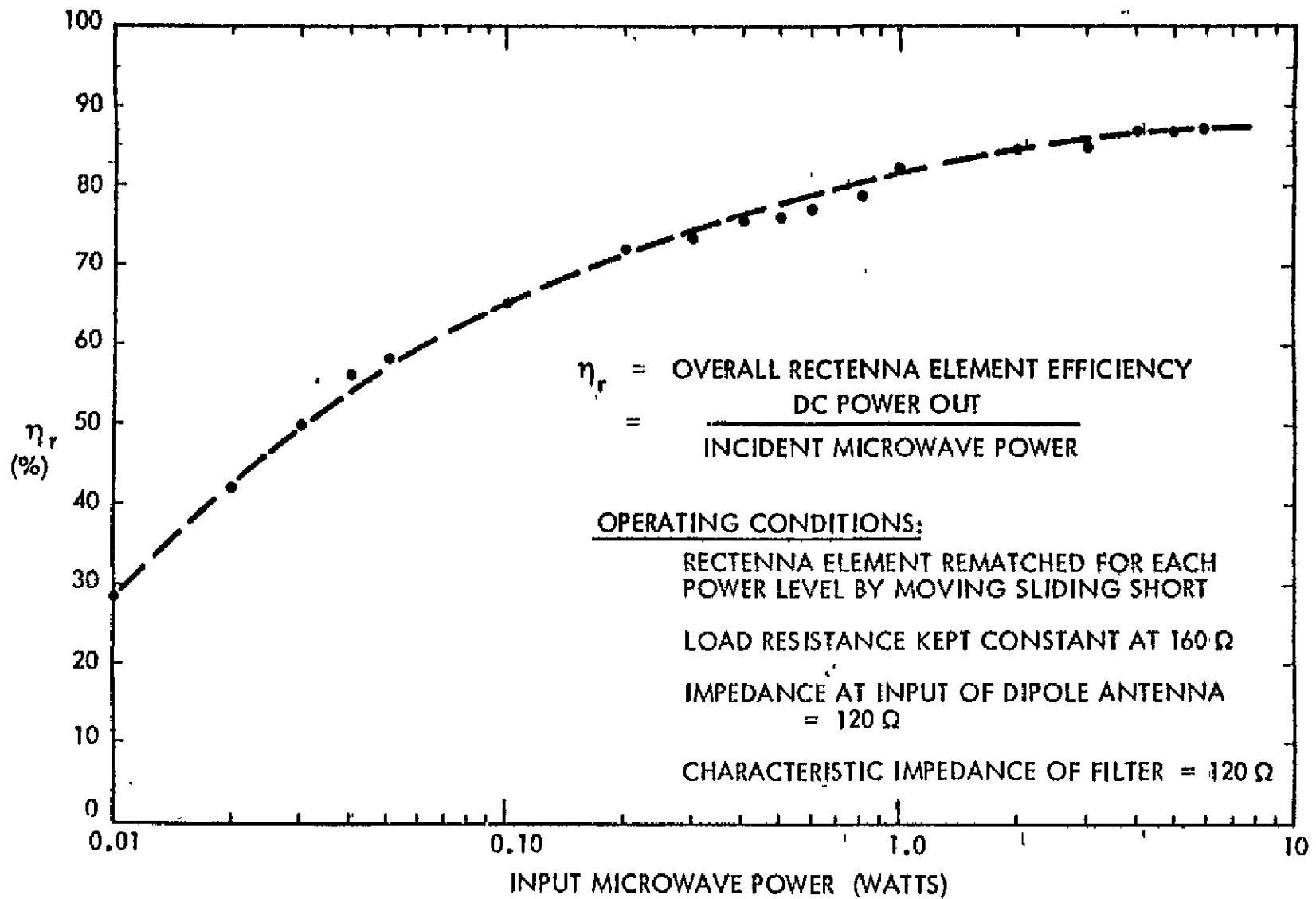


FIGURE IV-D-1-6.

Rectenna Element Efficiency as Function of Microwave Power Input

Unit Costs and/or Cost Methods or Inputs: Costs will only be estimated for the electronics portion of the rectenna in this section. That is, the one-half-wave dipole, filters, and rectifier circuit.

For a "typical" site in New Mexico, at a latitude of 35°N, the rectenna will be 10 KM x 13.2 KM, or 1.04×10^8 M². Based on a dipole/rectifier cell area of 53 cm² corresponding to 2.45 GHz, there will be approximately 190 elements/m². Assuming quantity production of diodes and rectenna elements in the billions (approximately 20 billion/rectenna) production costs could probably be brought down to approximately \$.03 per rectenna element. Therefore, the cost/m² is estimated to be \$5.70/m², or for the "typical" rectenna, approximately \$595M.

Technology Status, Criticality: There are several areas which require either further hardware development or further investigations.

a. One of the most critical is the development of a diode which will rectify with high efficiency at low levels of input. There are specific parameters which are involved in the development of this type of diode. These are:

- (1) A reduced junction area.
- (2) A change in junction materials.
- (3) Increase in circuit impedance of the rectenna element.

Present studies are being made under a NASA contract to investigate these parameters. These include reducing the diode chip area from 10^{-4} cm² to 0.125×10^{-4} cm², changing the junction material from Gallium Arsenide-Platinum to Gallium Arsenide-Wolfram to lower the barrier voltage, and changing the circuit impedance from 120 ohms to 480 ohms to increase the DC voltage for a given power out. On a scale from 1-5 (1 = low criticality, 5 = high criticality), the development criticality is about 3.

b. One of the big questions which the public will be interested in is the biological and ecological effects of large MW power densities reaching the Earth. At the present time there is not too much concern about short-term exposures to these power densities. The present military specification states a limit of 10 mW/cm² as the maximum level of continuous radiation to which humans may safely be exposed. Even the highest power density is only twice this amount at the very center of the rectenna and the power density drops off fairly rapidly from the center. Because of the concept of the wire mesh back-plane construction of the rectenna the levels underneath the rectenna will be considerably reduced.

Other studies on this subject suggest a much lower tolerance level for biological life. In a book by M. S. Tolgskaya and Z. V. Gordon, Pathological Effects of Radio Waves, the authors report microscopic changes

to nerve tissues in rabbits and rats subjected to power densities of 20 mW/cm² for 30 minutes. Another data point is that commercial microwave ovens typically leak RF at the door seals or window at densities of 1 to 20 mW/cm².

In summary, detailed investigations need to be conducted to insure complete understanding of biological and ecological effects for both short term and long-term exposures. On a scale from 1 to 5, the criticality is 5.

c. Ionospheric effects also require investigation; from the effects on the ionosphere of the MW beam, to the effects of the ionosphere on the phase front control system to be used on the SPS. The effects are presently believed to be small; however, other user effects will also have to be taken into consideration, such as earth-based long-haul communications and earth/space communications. Although the theoretical approaches to this problem are known, the resulting limits which may be imposed on the design of the SPS are not known. On a scale from 1 to 5, the criticality is estimated as between 3 and 4.

d. There may be some concern on the thermal heating effects of the atmosphere immediately above and adjacent to the rectenna site. With an overall RF/DC conversion efficiency of 85 percent, approximately 750 MW of heat will be continuously radiated from the rectenna. Whether this will have any adverse affect on the troposphere is not known at this time. It is not expected that this will be a difficult analytical assessment. On a scale of 1 to 5, the criticality is 2.

Test Plan: Three types of tests are envisioned for further understanding of the rectenna development problems.

a. One is associated with the acceptable power densities at the rectenna site with regard to biological and ecological effects. These tests appear to be comprehensive in scope if enough detailed data is to be obtained to evaluate the short-term and long-term effects on plant and animal life. These tests could be accomplished on the ground; however, the availability of equipment, duration of tests, and size of the test facility are driving factors in conduct and quantitative effectiveness of the tests.

b. Another type of test is that associated with determining optimum efficiency versus development costs of more efficient diodes for the low power density rectenna elements. These tests could be ground tests also. These should be closely coordinated with the present investigations into the high efficiency, low cost Schottky barrier diode.

c. The other type of test is that associated with testing microwave transmission concepts from space. Any tests associated with development of power amplifiers, RFI effects of the MW beam, transmitting antenna design, or phase control will require corresponding rectennas on the ground.

IV.-D-1-b. RECTENNA - STRUCTURAL SUPPORT AND GROUND PREPARATION

The support structure for the rectenna concept defined in Section IV.D.(1)a. has been preliminarily designed for the purpose of estimating the materials required and costing the rectenna structure. The preliminary design selected is a very simple structural concept and no attempt has been made to optimize the structure as to concept, weight or cost. The basic concept used is to divide the rectenna into a number of equal sections normal to the beam. Using a rationale that any point in the rectenna could require maintenance during the life of the rectenna, the spacing between sections was set at 6.4m to allow entrance of maintenance vehicles. This width corresponds to a Houston, Texas location which requires a 36° elevation from the horizontal. With a spacing of 6.4m, the face width of the sections is 15m. After selecting the section face width, a loads criteria was determined. Again, these loads are selected without optimization. With the location selected as the Houston area, ice and snow loads were determined to be negligible and wind loads were set at 100 mph for winter and 130 mph for fall. Because of the high wind load, the dead load of the dipoles and structure is negligible. Using some rationalization of the load, the selected load used to size the structure is 31.6 lb/ft² on the surface of the rectenna section.

Allowable stresses used for the structural design are based on ASCE recommendations for aluminum and AISC specifications for structural steel. The structure concept shown in Figure IV.D.(1).b-1 has been sized for the loads and allowable stresses discussed above. All members were sized using aluminum structural shapes and steel structural shapes. Concrete footings were placed at each support point as shown in Figure IV.D.(1) b.-1. The total weight for the concept is 0.62 million tons of aluminum or 1.38 million tons of steel and 1.289 million footings at 1.3 tons each.

The cost of structural materials, construction labor and site preparation, based on 1975 cost indexes, for the rectenna is \$125/kW for a 5 GW system using all aluminum structure and \$155/kW using all steel structure. Other studies have indicated a cost range for this purpose from \$100/kW to \$490/kW.

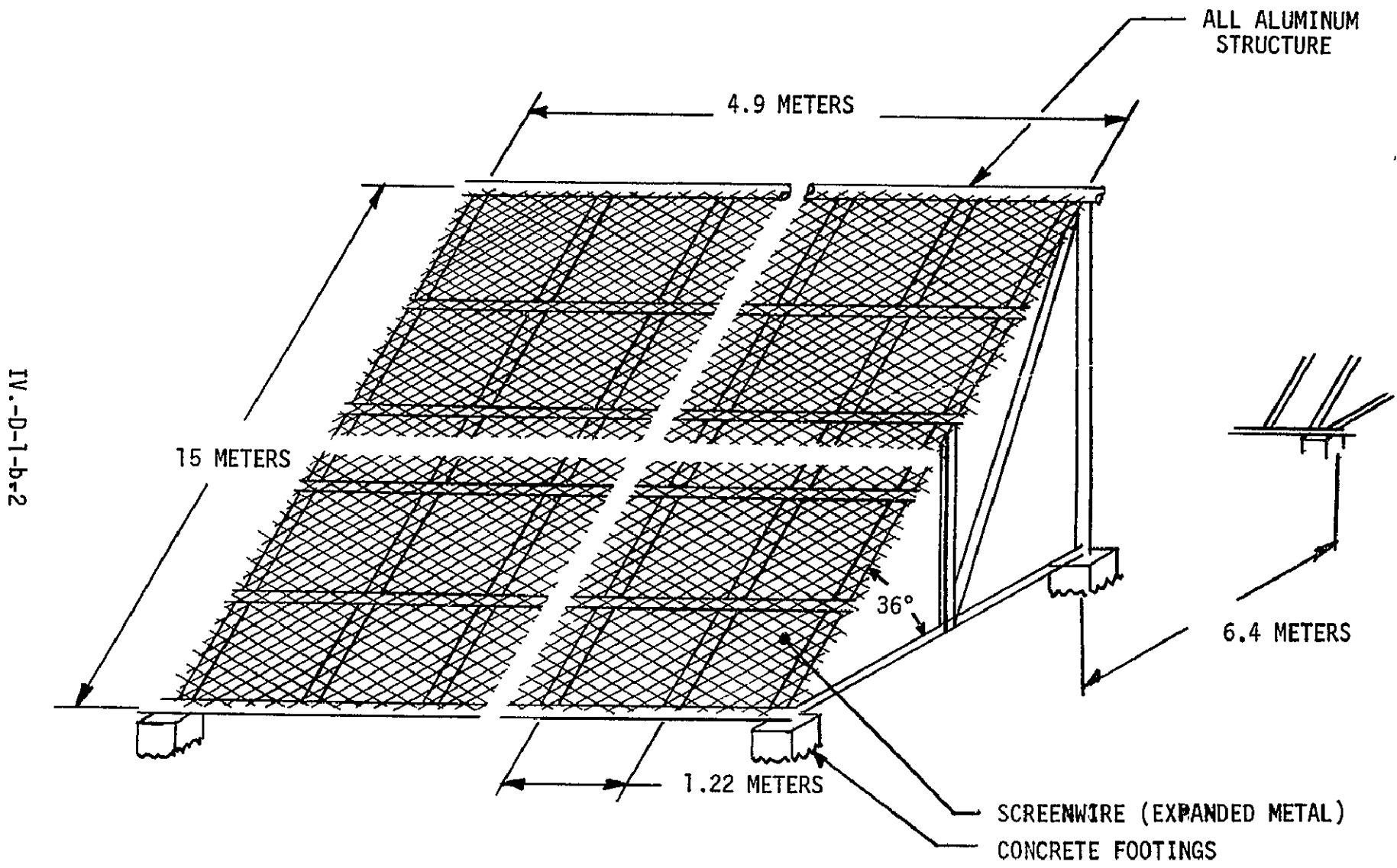


FIGURE IV.D.(1) b.-1

IV.D.2 GRID INTERFACE

Introduction

The grid interface system collects electrical energy in the form of direct current. Several billion rectenna subelements, transmit this power to DC-AC inverters and necessary safeguards and controls are provided for operation with the utility grid. In some instances it may be economically attractive to use high voltage DC power transmission. In this case power for AC loads would be provided by inverters located near the load center. A rectenna subelement consists of a half-wave dipole, diode rectifiers and filter. These subelements are positioned normal to the incoming microwave beam and are interconnected serially in strips. These strips and a reflecting screen are supported in a rigid attitude by a structure fixed to the earth. The overall rectenna shape is elliptical if located at any point on the earth other than the equator. For the location chosen in this study (40° N latitude) the rectenna has a major axis of 14.4 kilometers and a minor axis of 10 kilometers.

The length of series electrical interconnections of subelements is varied so that 1000 VDC is produced from each, independent of actual position within the rectenna. The power output (ampacity) of each will vary, however, with location. If the 1000 VDC is directly used as inverter input, many inverters would be incorporated to minimize conductor losses and cost. This configuration is the first option. In the second option, 250 KV DC is produced by connecting 250 of the 1000 volt circuits in series. This allows remote (centralized) inverter location because of greatly reduced power losses in high voltage transmission and fewer inverters for the same power output. The high voltage does create new insulation requirements and structural modification. The impact of both approaches is further discussed in the following paragraphs.

Grid Interface Requirements

In providing power to the grid, the interface system must control output voltage levels, phase, frequency and current demands. Present grid voltages range from 66 KV to 500 KV. Presently, inverters in the range of 1-50 MW provide output thermal voltages ranging from 13.8 KV to 69 KV at 60 Hz with an average efficiency of 96 percent. These inverters may be phase-locked to each other and the grid by using reactive power from the grid. The switching, regulation and control of rectenna power to the grid will be maintained at control center(s) located near the rectenna site. An illustrative representation of this interface is given in Figure IV-D-2-1.

The use of high voltage DC power transmission would involve different grid interface requirements from those discussed above. If a national DC grid system were established in the future, the compatibility of large power increments as provided by SPS would be enhanced. The method of producing the

high voltage DC for transmission may involve first conversion to AC so that the voltage may be stepped up to transmission levels using conventional transformers. The AC power would then be rectified to produce DC power. A more straight-forward approach would be to produce high voltage DC directly from the rectenna output. This possibility is discussed below under Design Option No. 2.

Design Option No. 1

In both options, low voltage subelements are series-connected to provide 1000 VDC outputs. In this option, low voltage feeders (1000 V) are paralleled to supply power to 500 inverters averaging 10 MW_e each.

The rectenna is made up of 1000 rows of rectenna elements as shown in Figure IV-D-2-2. The average length of these rows is 9 KM; with rectenna output of 5 GW_e, the average power per row is 5 MW_e. The insulation between structural support and subelements will be sufficient to maintain 1000 V dielectric strength so that branch circuit ampacity is the primary design consideration.

For the purpose of evaluating this option, a linear arrangement of variable size inverters has been assumed. The range of these is 1-50 MW_e so that for conductor requirements, one inverter serves four half-rows with a mean length of 4.5 KM. Each of the four 1000 V branch circuits would supply an average of 2.5 MW or 2,500 amperes. Although conductors could be tapered from the rectenna edge towards the inverter, the size of structural elements is sufficient. At a temperature rise in free air of 45°C, 3-inch standard aluminum pipe will conduct this current. The high voltage AC produced by the inverters would then be transmitted through suitable switchgear and transformers to the grid.

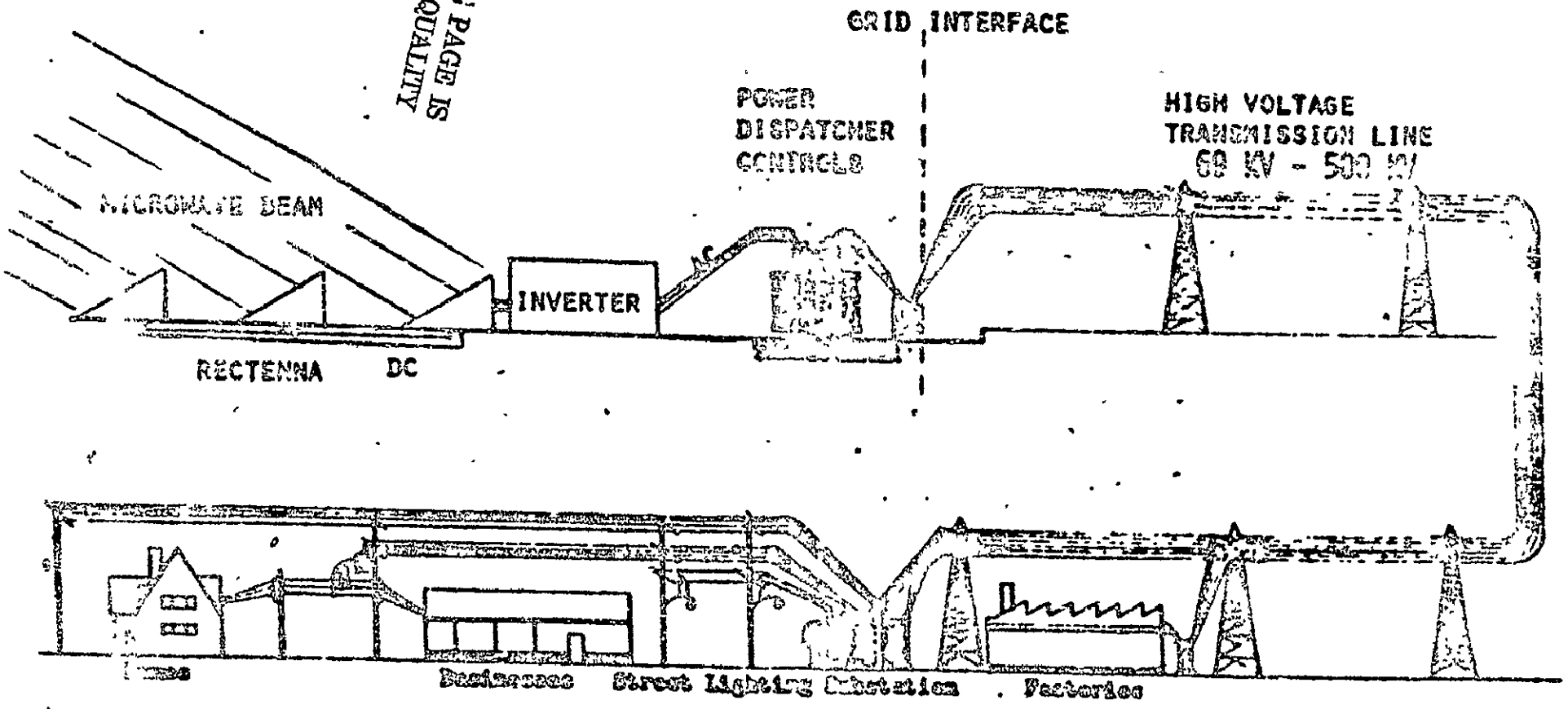
Design Option No. 2

This design option utilizes the same rectenna design as used in Option No. 1. However, the 1000 VDC terminals are connected in series to achieve a feeder output voltage of 250 KV DC. The subelements of this configuration are connected in parallel so that the ampacity of the 250 KV feeder is 2000 amperes. This provides for a feeder capacity of 500 megawatts. The structural support system may also be used as conductor material for completing the circuits in this design.

In order to produce this voltage and power, the feeders are connected radially from the center of the rectenna. The feeder voltage of 250 KV requires protection from faults to the ground. To achieve this protection, each 1000 volt terminal must be insulated from ground by the amount of voltage it is above the ground. A typical value of 2.5 CM/kilovolt for

IV-D-2-3

ORIGINAL PAGE IS
OF POOR QUALITY



ELECTRICAL POWER PROCESSING AND DISTRIBUTION SYSTEM

FIGURE IV-D-2-1

IV-D-2-4

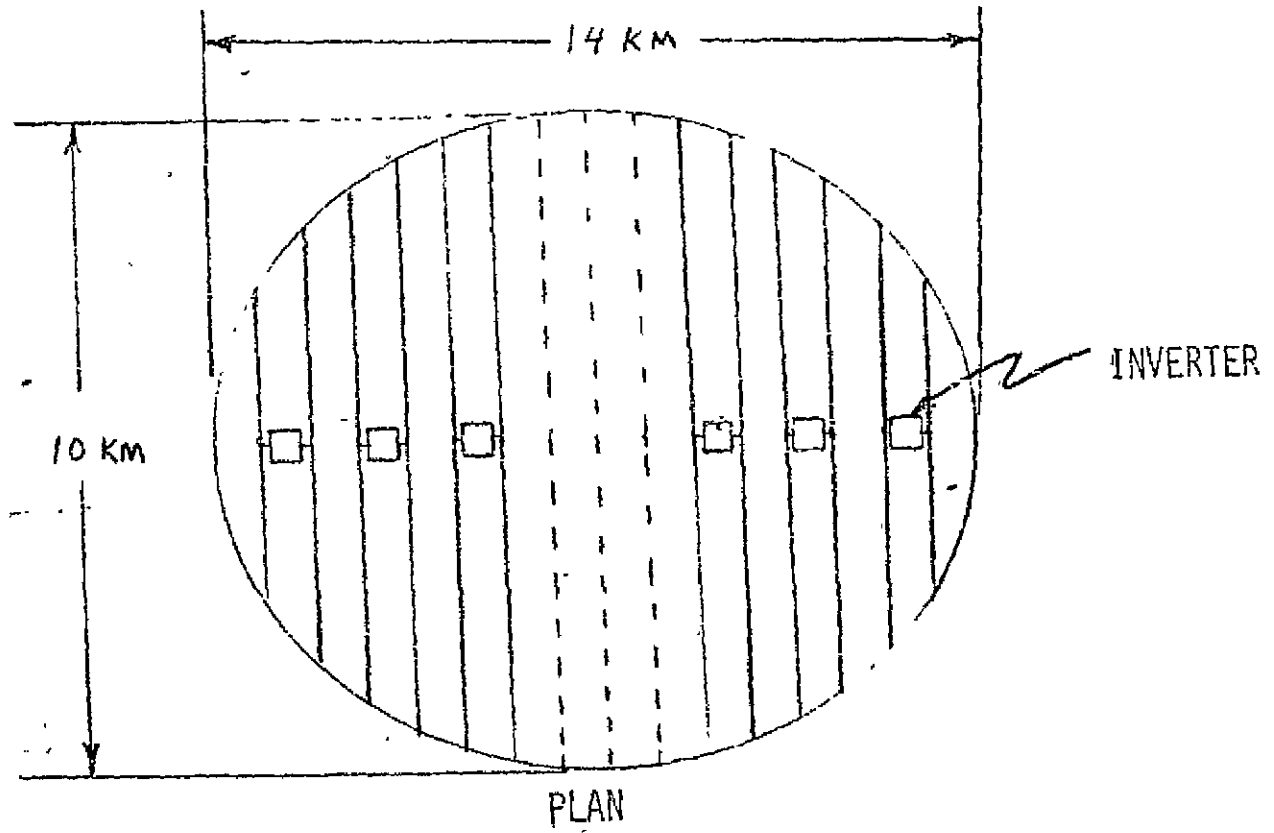


Figure IV-D-2-2 LOW VOLTAGE DC COLLECTION SYSTEM DEPICTING INVERTER LOCATIONS

ceramic insulators was used to determine the height of the rectenna elements. The elevation view given in Figure IV-D-2-3 shows the maximum height the structure has to be above the ground as well as the relative height of all rectenna elements to insure adequate fault protection to ground. Ten of these feeders are required to produce the total rectenna output of 5000 MW_e. The feeders are then routed to ten 500 megawatt inverters located at the edge of the rectenna.

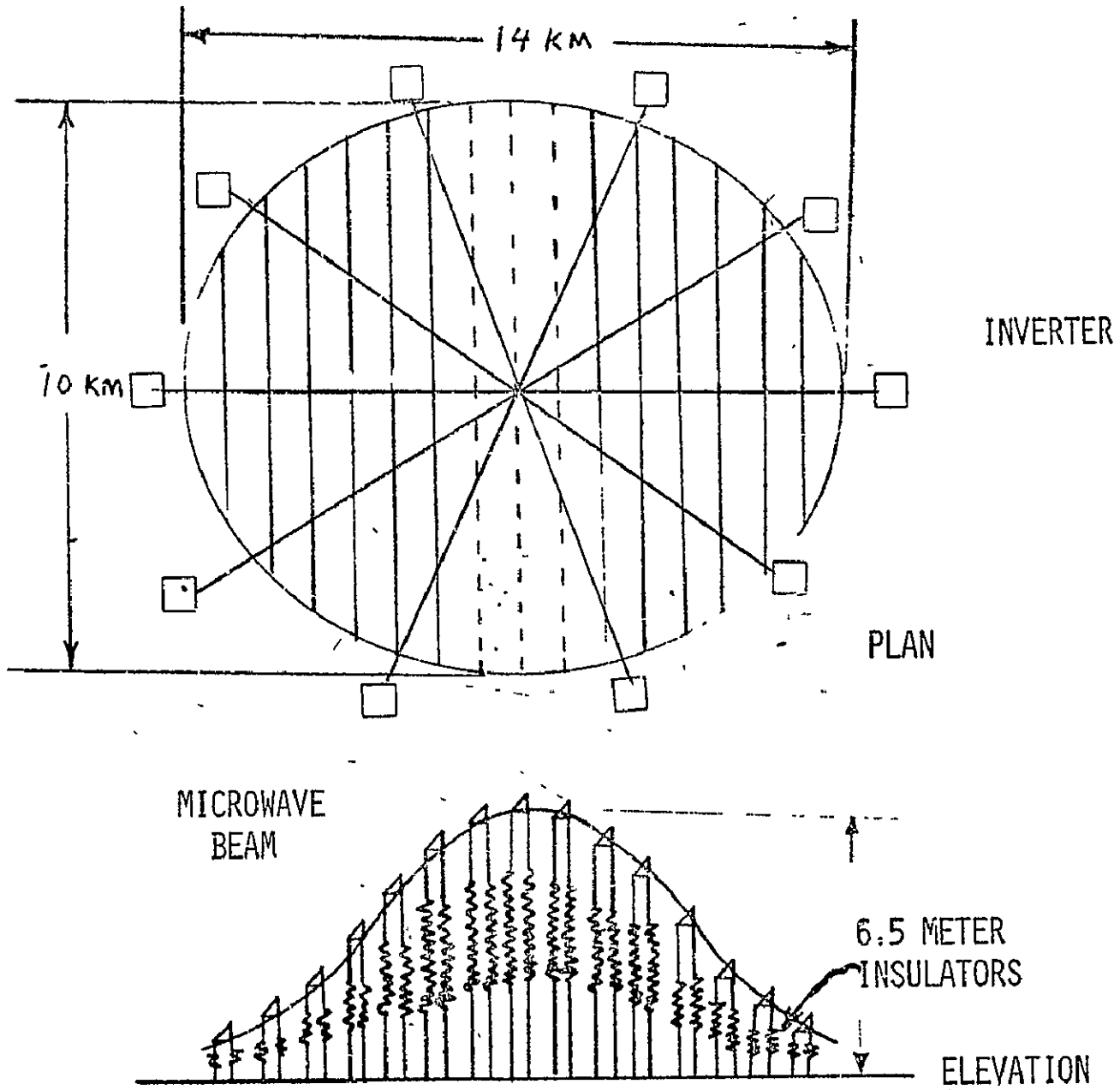
The inverters are made up of solid-state thyristors that operate at 250 KV, at an efficiency of 96 percent. These units use reactive power from the grid to gate the thyristors, which maintains synchronous operation with the grid. The output voltage may range between 66 KV and 500 KV. The costs for materials involved in the above option is given in Table IV-D-1. If the structure is to be used as the collection buss, the large costs associated with having many parallel conductors carrying high current (2500 amperes) is eliminated. In the LVDC configuration, the power is collected at inverters located along the major axis of the rectenna. The inverters change this power to high voltage AC. With the proper grid controls the inverter outputs are summed and transmitted along a high voltage transmission line also located along the major axis.

In the high voltage DC collection system, the 1000 VDC terminals are in series requiring much less conductor material. However, there is a requirement to insulate each 1000 VDC terminal from ground by the amount of voltage it exists above ground. This requires a support structure like the one shown in Figure IV-D-2-3. At present, there are no existing large-scale application for insulators that possess the structural characteristics required of this design. This is viewed as a new technology issue.

The 250 KVDC terminals are then routed to ten 500 megawatt inverters located at the edges of the rectenna through a radial network. If the inverters were required to be located remotely from the rectenna site, the HVDC could be transmitted more efficiently and at less cost than LVDC or high voltage AC. Cryogenic LVDC transmission may also be a viable option, in a case where the load density is unusually high.

In comparing the two options, the principal consideration is cost. The high voltage DC inverters are somewhat cheaper (\$30/KW HVDC; \$45/KW LVDC) than low voltage inverters. However, the efficiency of both is identical. The major cost uncertainty is in the insulators required by the high voltage system. In order to be competitive, the cost of these insulators must be on the order of \$15/KW for the entire rectenna, increasing the structural cost.

IV-D-2-6



RECTENNA STRUCTURAL SUPPORT AND INSULATORS FOR 250 KV DC COLLECTION SYSTEM

Figure IV-D-2-3

TABLE IV-D-2-1

RECTENNA HARDWARE COST
 (5000 MW_e - TOTAL POWER)

ITEM	QUANTITY	\$/KW	\$/LB.
Copper Conductors	-	-	.65
Transformers	-	1.07	-
Switchgear	-	.54	-
Inverter (Option 1)	500	45	-
Inverter (Option 2)	10	30	-
Insulators*	-	-	-
Grid Control Units	1	1.00	-

* New Technology Issue

Operational Considerations

The most efficient use of the electrical power from the SPS requires full grid utilization of the total power received at all times. Atmospheric conditions, pointing and phasing errors will cause the rectenna output to vary by several percent. The rectenna output is entirely governed by microwave power received. There is no "throttle" capability to allow even slight grid demand excesses without significant output voltage variations. To maximize the use of the power available, the system must be controlled so that it will operate with other generating plants on the grid. These plants must also maintain sufficient capacity for those periods when the SPS is shadowed. For typical grid operations, modularity in single generators rarely exceed 1.0 GW. This maximum size is closely tied to planned growth rates for conventional systems and it also allows for outage protection without maintaining excessive "spinning reserves." Accepting less than 5.0 gigawatts on the ground either by controls on the satellite or ground may be necessary, especially if the base load approaches 5.0 GW.

The loss of the SPS output at the equinoxes and during shadowing of other satellites creates somewhat extensive operational problems, possibly requiring "storage" and/or "load leveling" systems. These operational problems are being addressed by JSC through further review of the problem

IV-E. OPERATIONS

L. E. Livingston
Spacecraft Design Div.

Ideally, SPS power output would remain uniform at all times. In reality, however, there will be variations from several causes as illustrated in figure IV-E-1-1.

When the solar array is oriented perpendicular to the orbit plane, as has been found desirable from a weight standpoint (see section IV-B-4), the solar energy collected varies as the cosine of the sun's declination, producing the six-month cycle at the top of figure IV-E-1-1. Total variation is about 450 MW.

Orbit eccentricity will cause a cyclic fluctuation in satellite-to-rectenna distance. For an expected eccentricity of 0.04, this results in a daily power output variation of about 100 MW superimposed on the six-month variation.

Eclipses by the earth (see section IV-A-3) will cause total shutdowns daily around midnight for about six weeks in the spring and fall. Maximum duration is about 75 minutes. Eclipses by other SPS will cause shutdowns at about 6 a.m. and 6 p.m. for several days, also in the spring and fall, with a maximum duration of about 15 minutes.

Total shutdowns will also be required at times for maintenance. Duration is expected to be a few weeks, and frequency about once every five years.

The primary operational problems will arise from the eclipses. Starting and stopping a 5-GW standby generator system to fill these brief gaps will be difficult. At 0.5° spacing, as many as 38 SPS will be in the earth's shadow simultaneously. These will, in general, all be transmitting to rectennas in the same range of longitudes, and will tend to be the only SPS servicing these rectennas. Power sharing to spread the impact of these outages will therefore involve relatively long transmission distances for the shared power; this may limit the usefulness of power sharing to overcome this problem. A shifting, non-equatorial orbit that is never eclipsed has been examined and found to be impractical (see page IV-A-3-22). No entirely satisfactory solution to the eclipse problem is apparent, and further study is required. Maintenance shutdowns will be of much longer duration and less frequent, and should consequently present less of an operational problem.

The daily and six-month cyclic variations in power output can be eliminated if necessary. A circular orbit avoids the daily fluctuation, but at a cost in orbit maintenance propellant of some 200 M.T. per year ($I_{sp} = 10,000$ lb-s/lb). The six-month cycle can be eliminated by

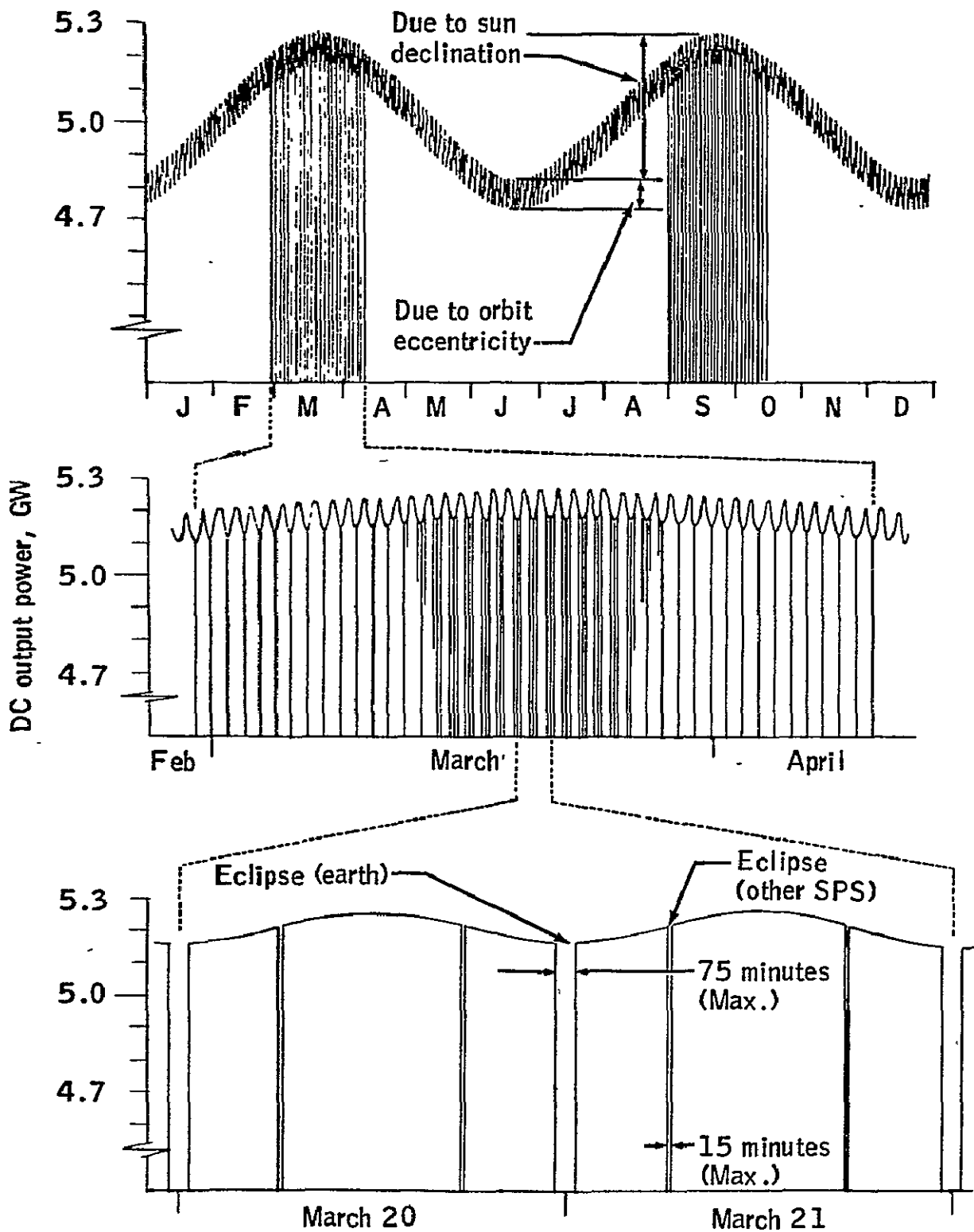


FIGURE IV-E-1-1- Variation in ground DC power output.

continuous solar orientation instead of POP. Additional reaction control propellant on the order of a few hundred tons per year would be required or, for the column/cable configuration, counterweights of some 7000 M.T. could be used (section IV-B-4). The system trade-offs relating to the power station have not taken into account any adverse impact of these fluctuations on the distribution grid. It is possible that inclusion of these considerations may alter the orbit and attitude recommended in this study, and further iterations of the trade-offs should be made.

For efficient utilization, the full output of the rectenna should be fed as a base load to the grid at all times. As a consequence, variations in output (from various causes) and fluctuations in demand must be compensated by ground-based generating plants on the grid, requiring an interactive control with these plants.

IV. F. UNIT COSTS

Table IV-F-1 shows a list of CER (cost estimating relationships) utilized for initial SPS costing. These CER's were produced using historically-derived CER's for similar space equipment. Because of the very high volume production rates required for items such as solar cells, Schottky diodes (rectenna elements), and microwave generators the CER's for these devices were substantially reduced below current values for space systems. An example of this expected cost reduction is illustrated in figure IV-F-1 for silicon solar cells. These cost reductions are projected by ERDA as a result of a major terrestrial photovoltaic R&D program currently in progress. ERDA's 1985 goal is to produce solar cells in quantities of 500 MW for \$500/KW peak. According to ERDA 48, Volume 2, a production capability of 50 GW(e) (equivalent to 2-12/ 10 GW SPS's) should be achieved by 2000 with a market price in the range of \$100 to \$300/KW. While recognizing that the weight requirements for solar cells to be used in space are different than for terrestrial use and \$100 to \$500 range appears reasonable and was used in the present study.

TABLE IV-F-1 - COST ESTIMATING RELATIONSHIPS (CER)

<u>CATEGORY</u>	<u>MIN</u>	<u>CER NOM</u>	<u>MAX</u>	<u>SOURCE/DERIVATION</u>
Solar Energy Collection System				
Solar Cell Blankets	\$100/kW	\$300/kW	\$500/kW	ERDA terrestrial photo- voltaic goals
Solar Concentrators	-	\$ 25/KW	-	\$0.70/m ²
Structure	-	\$ 7.00/KG	-	Space equipment
Power Distribution	-	\$ 4.00/KG	-	Space equipment
Other Systems	-	\$1000/KG	-	Electronic components; high reliability
IV-F-2 Microwave Power Transmission System				
Microwave Generator	-	\$2000/unit	-	Mgf. projection
Waveguides	-	\$ 70/KG	-	Design estimate
Structure	-	\$ 70/KG	-	Space equipment
Power Distribution	-	\$ 40/KG	-	Space equipment
Rotary Joints	-	\$ 100/KG	-	Design estimate
Phase Control	-	\$ 56/unit	-	Design estimate
Pointing Control	-	\$1500/KG	-	Electronic components
Other Systems	-	\$1000/KG	-	Electronic components high reliability
Microwave Reception and Conversion System				
Rectenna Array (Circuits) and Diode Assembly	\$6.00/m ²	\$8.00/m ²	\$8.00/m ²	Mfg. projection
Real Estate	-	\$0.15/m ²	-	\$ 650/acre
Site Preparation	-	\$0.40/m ²	-	\$1800/acre
Power Distribution & Control	-	\$2.50/m ²	-	\$ 45/KW
Support Structure	\$6/m ²	\$10/m ²	\$10/m ²	switchgear and inverters Design estimate

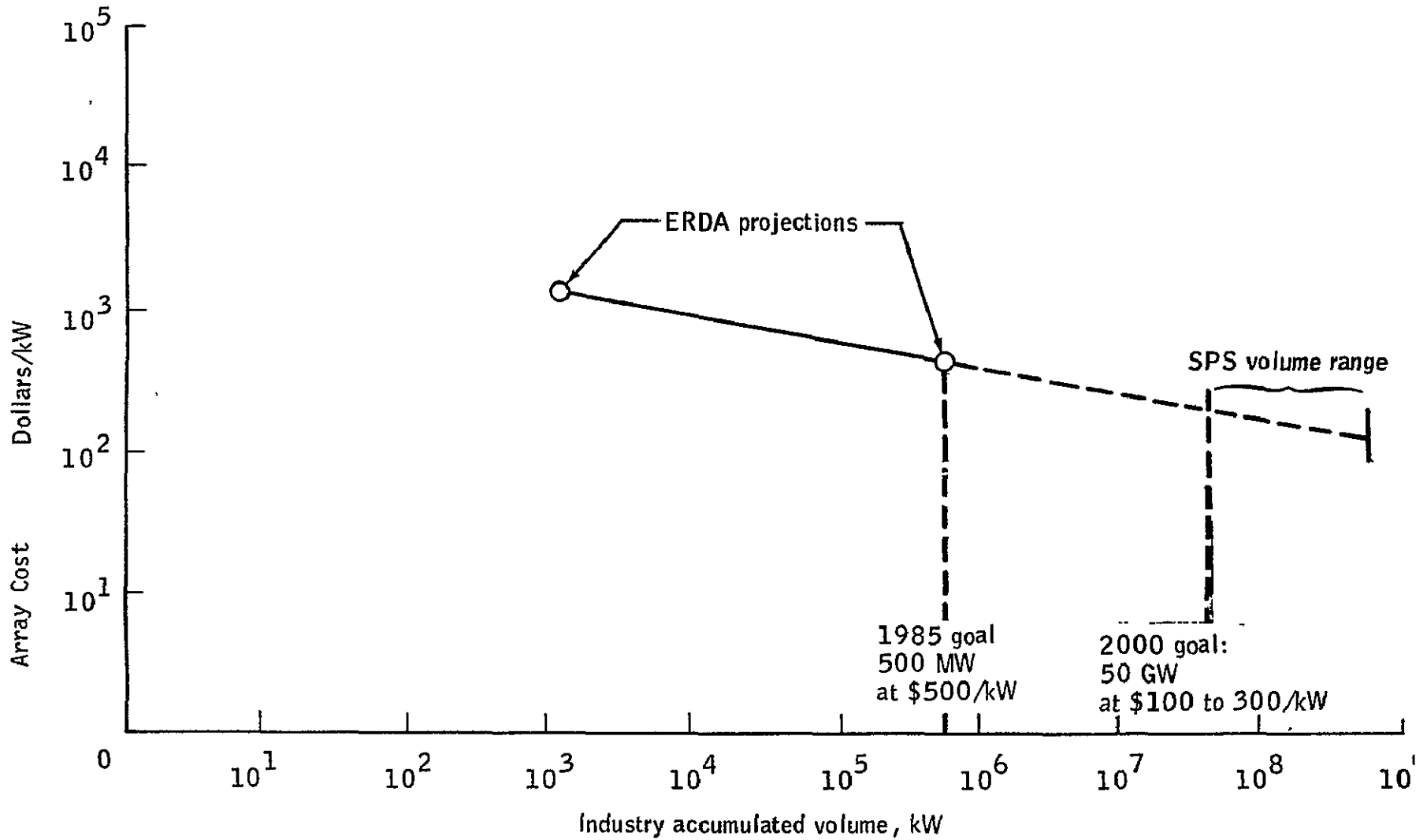


Figure IV-F-1- Photovoltaic array cost projection.

APPENDIX

Section IV

COMPARISON STUDY OF THERMAL ENGINE (BRAYTON CYCLE)
AND PHOTOVOLTAIC SPS DESIGN CONCEPTS

In an attempt to specifically identify differences and advantages between the Brayton cycle and photovoltaic methods of space-based solar energy conversion, an evaluation of existing conceptual designs was conducted and a comparability study was performed.

The SPS comparability study data was compiled from reports and presentation material provided by Boeing and ADL/Raytheon/GAEC teams. A listing of these documents is included as references. The primary difference between energy conversion concepts are provided in summary form in Table IV-APP-1 under level 2.0. More detailed comparisons on a subsystem and component basis are provided.

The primary thrust of the Raytheon studies is in the Microwave Power Transmission System (MPTS) which includes the transmitting antenna and ground-based rectenna for reception and rectification of the microwave power. Their concept incorporates solar cell energy conversion in the form of two large solar arrays with a centrally located power transmitting antenna (Figure IV-APP-1).

Boeing uses four large faceted concentrators to focus solar energy into cavity absorbers at the focal points. The heat thus provided drives Brayton cycle engine-generators to produce electricity (Figure IV-APP-2). The Boeing effort is primarily devoted to these systems. The MPTS is essentially the same as Raytheon's with variations required by higher output power levels.

Summary charts for both concepts are provided as Figures IV-APP-3 and IV-APP-4. These detail weight, efficiency, and power levels for subsystem elements as described in the reference documents and numbers as adjusted by JSC evaluators.

The solar cell conversion system is characterized by low operating efficiency and low weight. Relatively, the Brayton cycle system operates with twice the efficiency and 3.5 times the weight. For about the same station size, the Boeing system produces 10 GW on the ground, compared to 5 GW for Raytheon.

The primary adjustment made by JSC evaluations on the Raytheon system was an efficiency reduction from 13.3 to 10.4 for the solar array blankets. This

reduction was based on higher operating temperatures and thus lower cell efficiency. Any change in this number produces large weight and size variation in the overall station as demonstrated by the weight increase from 17.8 to 31.35×10^6 KG.

The Boeing transmitting antenna is about the same size as Raytheon's, but uses twice the number of amplifiers. Heat rejection capabilities of the tubes and surrounding structure are not sufficient to allow this, so that either a larger antenna or two antennas would be needed. Other JSC comments have been incorporated into the study in the evaluation column.

Performance degradation as a result of long term exposure to the radiation, material, and space vacuum environment may be a significant problem for both the photovoltaic and Brayton cycle systems. Performance degradation of silicon solar cells of the type proposed for the reference design SPS is discussed in Section IV-B-1-6 of this report. The ADL/Raytheon/GAEC concept allows six percent reduction in power output during the first 5 years of operation.

No discussion of continued reduction in output after five years was presented. Optimistic estimates would indicate a continued degradation of about one percent per year.

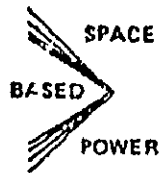
In the case of the Brayton cycle system, environmentally induced degradation occurs at both the solar concentrator and the waste heat radiator. Based on accelerated life tests of selected reflective materials subjected to proton flux, Boeing reports an approximate four percent per year reduction in concentrator reflectivity. The proposed means of repairing this condition is to utilize multilayer reflective material so that a degraded surface may be peeled off, thus exposing a new surface. Boeing estimates a 30 percent loss in radiator areas as a result of meteoroid impact. This is accommodated by oversizing the radiator initially. Loss of radiator area results in higher compressor inlet temperatures which, in turn, reduces overall cycle efficiency. Approximate analysis indicates that a 30 percent radiator area reduction would cause 27 percent per reduction in cycle efficiency or about 0.9 percent per year reduction in output power. This assumes that all other factors remain constant. Restoration of damaged radiator area may be accomplished by on-orbit repair or replacement of damaged sections.

In summary, environmentally induced performance degradation will occur in photovoltaic and closed Brayton cycle systems. Unless on-orbit repair can be accomplished, hardware replacement will be necessitated resulting in significant increased mass-to-orbit to maintain design power output.

Table IV-APP-2 provides a summary listing of advantages and disadvantages of the photovoltaic and Brayton cycle systems. This qualitative comparison is based primarily upon information found in the existing system design.

Table IV-APP-3 shows a summary of the cost comparisons. The JSC "adjusted" cost estimates were derived based on the orbital weight increases shown in Figure IV-APP-3 and IV-APP-4. Both increased hardware cost and the associated transportation costs are taken into account. Note in Table IV-APP-3 that the ADL/Raytheon/GAEC photovoltaic system was costed (reference 10) based on \$184/kg transportation cost, whereas the Boeing system used \$62/kg transportation cost. The JSC adjusted costs also use these transportation costs, but in addition, a transportation cost of \$55/kg is shown for both systems to provide comparable costs. No attempt was made to produce a JSC adjusted DDT&E cost for the two systems.

Figure IV-APP-1

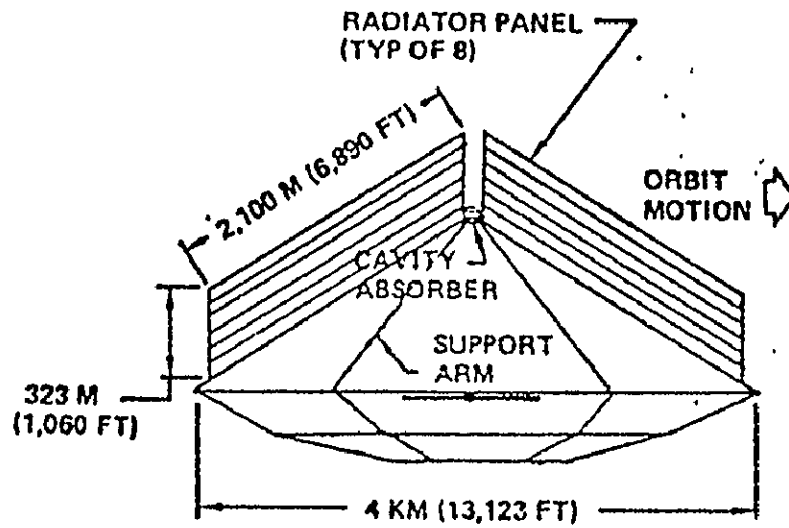


Solar Thermal Engine Powersat

GROUND OUTPUT: 10 000 MW
ORBITAL BUSBAR: 16 000 MW
TECHNOLOGY LEVEL: 1985 (1990 INTRODUCTION)
WEIGHT: 6.4×10^7 KG (140 MLBM)

BOEING

IV-APP-4



VIEW LOOKING NORTH TO SOUTH

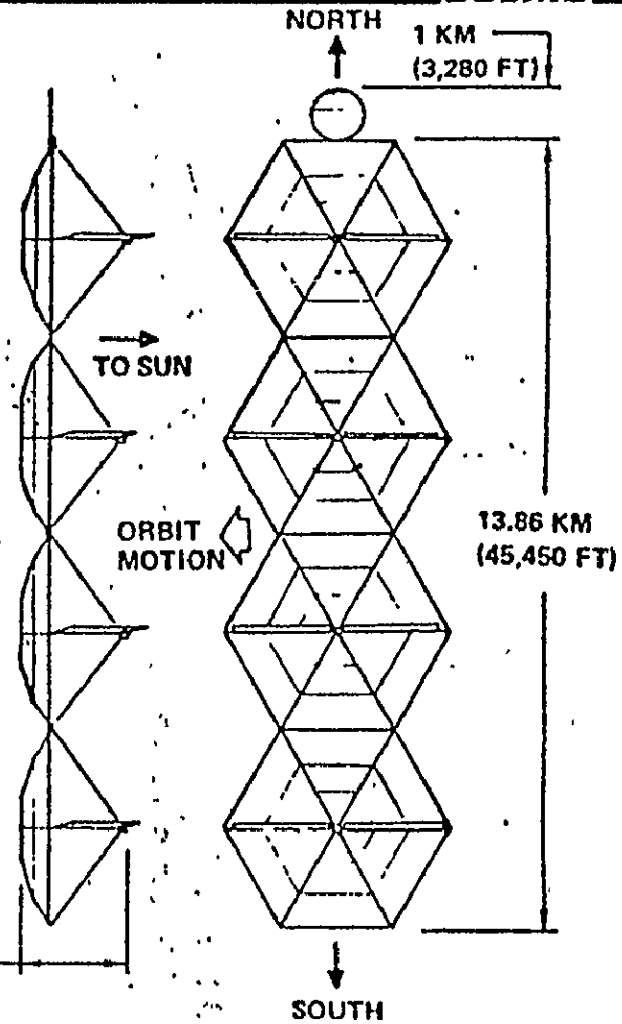
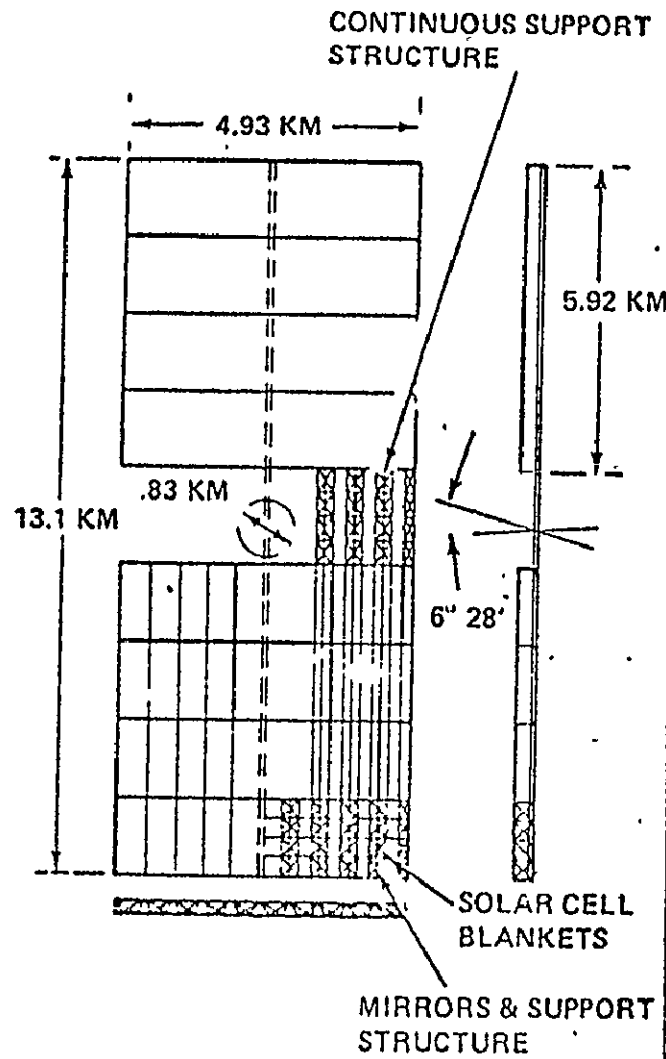


Figure IV-APP-2

17

SATELLITE SOLAR POWER STATION



IV-APP-5

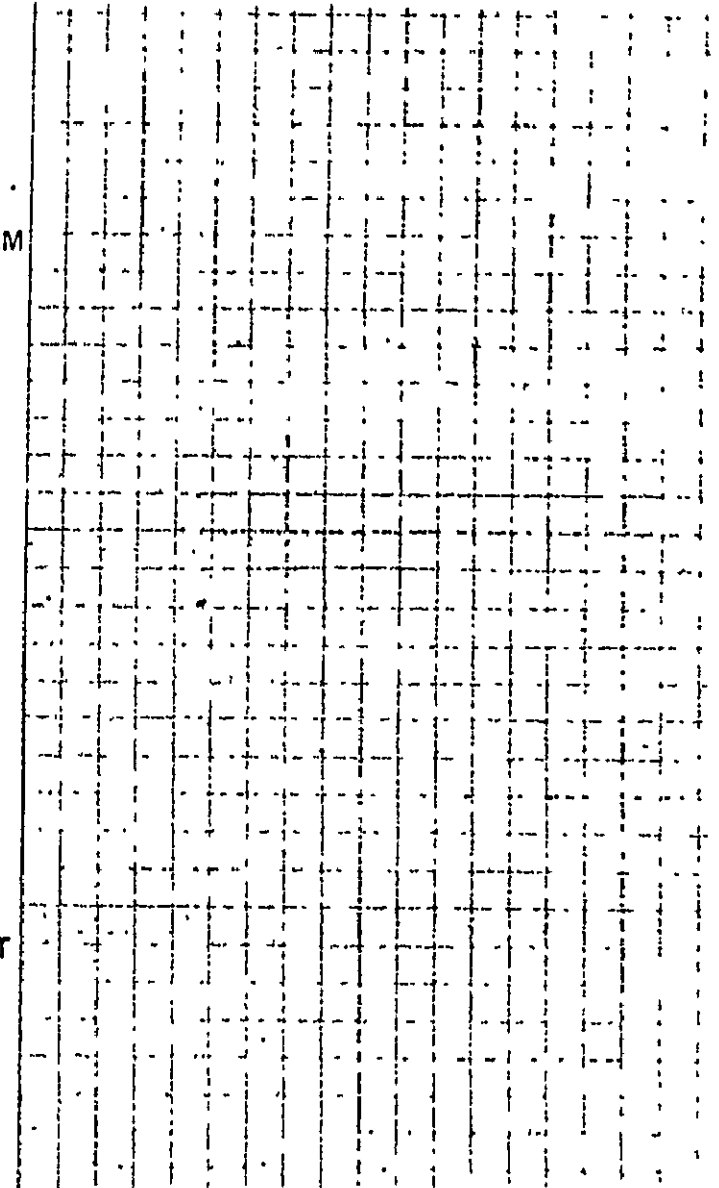


TABLE IV-APP-1

SPS COMPARABILITY STUDY

LEVEL 1.0 SATELLITE POWER SYSTEM (SPS) PROGRAM

LEVEL 2.0 MAJOR PROGRAM ELEMENTS (SUMMARY)

ELEMENT	ADL/RAYTHEON/GAEC (1)	BOEING (2)	EVALUATION
2.1 ORBITAL SYSTEM	<ul style="list-style-type: none"> o PHOTO VOLTAIC CONVERSION, CENTRALLY LOCATED MICROWAVE POWER TRANSMITTING ANTENNA. o RADIATED POWER = 6.7 GW o AREA = 59.4 KM² o SUPPORT FACILITIES NOT DISCUSSED o WEIGHT = 17.8 X 10⁶ KG 	<ul style="list-style-type: none"> o FACETED CONCENTRATOR POSITIONED TO DIRECT THE REFLECTED ENERGY TO A COMMON ABSORBER CAVITY WHICH DRIVES BRAYTON CYCLE GENERATORS WITH A SINGLE MICROWAVE TRANSMISSION ANTENNA. o RADIATED POWER = 12.99 GW o AREA = 56 KM² o SUPPORT FACILITIES NOT DISCUSSED o WEIGHT = 64.0 X 10⁶ KG 	<p>(2) LOWER WEIGHT, MORE ACCURATE CONCENTRATIONS ARE POSSIBLE BY INCREASING NUMBER OF FACETS.</p> <p>(2) FRESNEL-TYPE CONF. MAY BE SIMPLER IN SPACE - SAME CONTROL AS PARABOLIC REFLECTORS.</p> <p>(1) AREA AND WEIGHT TOO LOW</p>
2.2 TRANSPORTATION	<ul style="list-style-type: none"> o SHUTTLE BASELINED AS FREIGHT VEHICLE TO LEO AND TRANSFER TO GEO WITH SEPS. 	<ul style="list-style-type: none"> o THREE VEHICLES REQUIRED: SPACE SHUTTLE, SPACE FREIGHTER, AND ORBIT TRANSFER VEHICLE. 	
2.3 MISSION OPERATION	<ul style="list-style-type: none"> o ASSEMBLY IN LEO o 156 MEN, TOTAL Q&M = \$96M/FIRST YEAR. 	<ul style="list-style-type: none"> o ASSEMBLY IN LEO o NOT DISCUSSED 	<p>(1) PARTIAL ASSEMBLY ONLY IN LEO</p>
2.4 GROUND POWER GRID INTERCONNECT	<ul style="list-style-type: none"> o 5 GW_e DELIVERED TO GRID. o RECTENNA SIZE IS 10.3 X 13.4 KM 	<ul style="list-style-type: none"> o 10 GW_e DELIVERED TO GRID. o RECTENNA SIZE NOT DESCRIBED. 	
2.5 PROGRAMMATIC FACTORS	<ul style="list-style-type: none"> o I.O.C. IS 16 YEARS FROM START OF GROUND TEST PROGRAM. 	<ul style="list-style-type: none"> o I.O.C. IS 16 YEARS FROM START OF PROGRAM. 	

IV-APP-6

TABLE IV-APP-1 (Cont'd)

LEVEL 2.1 ORBITAL SYSTEMS

LEVEL 3.0 SUBSYSTEMS AND SUPPORT FACILITIES

IV-APP-7

ELEMENT	ADL/RAYTHEON/GAEC (1)	BOEING (2)	EVALUATION
<p>3.1 POWER GENERATION SUBSYSTEM</p>	<ul style="list-style-type: none"> o TWO PHOTOVOLTAIC BLANKET STRUCTURES EACH 5.0 X 5.2 KM AND 250 M THICK (MAX.) o POWER OUTPUT OF APPROX. 4.6 GW_e/PHOTOVOLTAIC BLANKET. o USES SILICON PHOTOVOLTAIC ARRAYS o SOLAR ARRAY EFFICIENCY = 11.3% o COST IS 1023 \$/KW o PGS WEIGHT = 11.8 X 10⁶ KG 	<ul style="list-style-type: none"> o FOUR POWER PRODUCTION MODULES CONSISTING OF HEXAGON-SHAPED CONCENTRATORS 4 KM ON MAJOR AXIS. CAVITY ABSORBER AT FOCAL DISTANCE OF 1.75 KM. o MOUNTED ON EACH ABSORBER ARE 12 CLOSED BRAYTON CYCLE TURBO-MACHINE SETS. EACH SET HAS OUTPUT OF 300 MW_e. o POWER OUTPUT = 14.4 GW_e o PGS WEIGHT = 13.6 X 10⁶ KG/POWER PRODUCTION MODULE. 	<p>(1) TWO BLANKETS ALLOW MIN. DISTANCE FOR TRANSMISSION LINES TO ANTENNA.</p> <p>EQUAL MASS MOVEMENT OF INERTIA RECOMMENDED THRU STEPPED CONFIGURATION.</p> <p>(2) 300 MW_e IS CONSISTANT WITH HLLV CAPACITY.</p>
<p>3.2 TRANSMITTING ANTENNA</p>	<ul style="list-style-type: none"> o 0.91 KM DIA., 40M THICK CIRCULAR, PLANNER, ACTIVE PHASED ARRAY. o 65 X 10⁴ M² AREA o 5 db BEAM TAPER o 78% EFFICIENCY OVERALL o COST IS 500 \$/KW o POWER OUTPUT ABOUT 6.7 GW o WEIGHT = 6.02 X 10⁶ -KG 	<ul style="list-style-type: none"> o THEY BASICALLY PROPOSE USE OF RAYTHEON 1 KM DIA., AMPLITRON DESIGN. o 65 X 10⁴ M² AREA o 85% OVERALL EFFICIENCY o POWER OUTPUT ABOUT 12.99 GW o WEIGHT = 11.03 X 10⁶ KG 	<p>(1) .91 KM TOO SMALL, 10 db IS USED FOR JSC SYSTEM.</p> <p>(2) NOT BIG ENOUGH TO RADIATE HEAT.</p>

TABLE IV-APP-1 (Cont'd)

LEVEL 2.1 ORBITAL SYSTEMS

LEVEL 3.0 SUBSYSTEMS AND SUPPORT FACILITIES

IV-APP-8

ELEMENT	ADL/RAYTHEON /GAEC (1)	BOEING (2)	EVALUATION
3.3 ATTITUDE CONTROL AND STABILIZATION	<ul style="list-style-type: none"> o TRANSMITTING ANTENNA ATTITUDE CONTROL BY ROTARY JOINT WITH TWO AXES OF ROTATION. o SSPS CONTROL IS REACTION JETS WITH ARGON PROPELLENT PREFERRED (15-50 X 10³ KG/YEAR); OVERALL POINTING ACCURACY IS 1° TO THE SUN. 	<ul style="list-style-type: none"> o TRANSMITTING ANTENNA - NOT DESCRIBED. o FACET CONTROL ± 5°, SERVO ACTUATORS - HUB MOUNTED- SENSOR CONTROLLED FROM CENTRAL CAVITY. 	<p>(2) REACTION JETS SHOULD BE USED ONLY AS BACKUP.</p> <p>MAG. LOOP CONTROL AND GRAV. GRAD. PRIMARY.</p>
3.4 MAJOR STRUCTURES	<ul style="list-style-type: none"> o TRANSMITTING ANTENNA HAS RECTANGULAR GRID STRUCTURAL LAYERS USING TRIANGULAR GIRDERS MADE OF GRAPHITE EPOXY WITH THERMAL COATING; PRIMARY STRUCTURAL GRID IS 108 X 108 X 35 M AND SECONDARY GRID IS 18 X 18 X 5 M; TOTAL WEIGHT IS 0.14 X 10⁶ KG. o POWER GENERATION STRUCTURE DESIGN IS NOT DISCUSSED; WEIGHT IS 2.14 X 10⁶ KG. 	<ul style="list-style-type: none"> o TRANSMITTING ANTENNA WEIGHT 0.76 X 10⁶ KG (INCLUDE R. JOINT). o RECTANGULAR, FOLD-OUT BEAM STRUCTURE-ALUMINUM - CAVITY SUPPORT ABOVE CONCENTRATORS. o CONCENTRATOR STRUCTURE FORMED ON ORBIT OF FLAT STOCK ALUMINUM ON ROLLS. o CONCENTRATOR REFLECTIVE SURFACE OF ALUMINIZED KAPTON. o CONCENTRATOR MASS IS .29 KG/M² o 25 M DIA BY 25 M LENGTH MAXIMUM LEO PAYLOAD SIZE. 	

TABLE IV-APP-1 (Cont'd)

LEVEL 2.1 ORBITAL SYSTEMS

LEVEL 3.0 SUBSYSTEMS AND SUPPORT FACILITIES

ELEMENT	ADL/RAYTHEON/GAEC	BOEING	EVALUATION
3.5 SUPPORT FACILITIES	<ul style="list-style-type: none"> o SSPS ASSEMBLY; CREW SUPPORT AND COMMUNICATIONS MODULE, 2 REQUIRED; REMOTE CONTROL MANIPULATOR MODULE 91 REQUIRED; MANUFACTURING MODULE, 4 REQUIRED. o 6-12 MAN ON-ORBIT CREW 	<ul style="list-style-type: none"> o FOR SPS MAN./ASSY. 100 MAN CREW AND HOUSING; NO DETAIL DISCUSSION. 	

IV-APP-9

TABLE IV-APP-1 (Cont'd)

LEVEL 2.1 ORBITAL SYSTEMS

LEVEL 3.1 POWER GENERATION SUBSYSTEM

LEVEL 4.0 MAJOR COMPONENTS

ELEMENT	ADL/RAYTHEON/GAEC (1)	BOEING (2)	EVALUATION
IV-APP-10 4.1 SOLAR ENERGY COLLECTION	<ul style="list-style-type: none"> o SOLAR CELL BLANKETS o 14% CELL EFFICIENCY o 2 TO 1 CONCENTRATION RATIO o AREA IS 51.48 KM² o CELL AND CONCEN. WEIGHT IS 8.67 X 10⁶ KG 	<ul style="list-style-type: none"> o FACETED MIRROR REFLECTORS o 74% EFFICIENT REFLECTORS o CONCENTRATION RATIO 3600 TO 1 o ABSORBER CAVITY 89% EFFICIENT o CONCENTRATOR UNIT WEIGHT = 0.29 KG/M² o TOTAL WEIGHT NOT GIVEN 	(1) CELL EFFICIENCY LOWER DUE TO HIGHER OPERATING TEMP. - 10.96%
4.2 POWER CONVERSION	o N/A	<ul style="list-style-type: none"> o BRAYTON CYCLE THERMAL ENGINE o 35% EFFICIENT o ELECTRICAL GENERATOR 98% EFFICIENT o 400-600 Hz OUTPUT o 60 KV 	
4.3 POWER COLLECTION AND DISTRIBUTION	<ul style="list-style-type: none"> o 92% EFFICIENCY o 20 KV o 0.99 X 10⁶ KG WEIGHT o COLLECTION AND DISTRIBUTION SYSTEM USES STRUCTURAL MEMBERS o I²R LOSSES, ALTHOUGH GREATER, ARE NOT DISCUSSED 	<ul style="list-style-type: none"> o EFFICIENCY 99.5% o 382 KV AC o .17 KG/KW, 2.67 X 10⁶ KG o STRUCTURAL ELEMENTS (TRIANGULAR TRUSS MEMBERS) USED FOR ELECTRICAL POWER CONDUCTION TO ROTARY JOINT o I²R LOSSES DETERMINE STRUCTURAL MEMBER SIZE RATHER THAN MECHANICAL LOADS. 	(1) 92% SHOULD BE 85-93% (2) 99.5% TOO HIGH

TABLE IV-APP-1 (Cont'd)

LEVEL 2.1 ORBITAL SYSTEMS

LEVEL 3.1 POWER GENERATION SUBSYSTEM

LEVEL 4.0 MAJOR COMPONENTS

ELEMENT	ADL/RAYTHEON/GAEC (1)	BOEING (2)	EVALUATION
4.4 THERMAL CONTROL	o N/A -	<ul style="list-style-type: none"> o TWO HELIUM RADIATOR SYSTEMS (535°K) PER POWER GENERATION MODULE (AREA = 6.8×10^5 M² EACH). o SIX SEPARATE RADIATORS PER RADIATOR SYSTEM (1 PER TURBO MACHINE SET). o TOTAL SSPS RADIATOR AREA = 10.9×10^6 M² (TOTAL BOTH SIDES) o TOTAL SSPS RADIATOR WEIGHT = 39×10^6 KG o TARGET DEGRADATION IS 30% IN 30 YEARS (WITH SOME REPAIR) 	<p>(1) THERMAL CONTROL COATINGS ARE INTEGRAL PART OF CELL BLANKET AND REFLECTOR DESIGN.</p> <p>(2) LATEST BOEING CONCEPT IS NAK LOOP.</p> <p>(2) FOR HELIUM SYSTEM, MIXTURE IS PREFERRED. (HE AND ARGON)</p>

IV-APP-11

TABLE IV-APP-1 (Cont'd)

LEVEL 2.1 ORBITAL SYSTEMS
 LEVEL 3.2 TRANSMITTING ANTENNA
 LEVEL 4.0 MAJOR COMPONENTS

ELEMENT	ADL/RAYTHEON/GAEC (1)	BOEING (2)	EVALUATION
IV-APP-12 4.1 DC-RF CONVERSION	<ul style="list-style-type: none"> o AMPLITRONS USED AS BASELINE. o OPERATION FREQ. 2.45 GHz o 0.33 KG/KW, 18 \$/KW o 85% OPERATING EFFICIENCY o 20 KV DC INPUT o 5 KW OUTPUT/TUBE o APPROX. 1.5×10^6 TUBES o PASSIVE COOLING OF AMPLITRONS o 2.4×10^6 KG AMPLITRON WT. 	<ul style="list-style-type: none"> o AMPLITRONS USED AS BASELINE. o OPERATION FREQ. 2.45 GHz o 88% OPERATING EFFICIENCY o 25 KV DC INPUT o APPROX. 3.0×10^6 TUBES o 4.68×10^6 KG AMPLITRON WT. 	
4.2 WAVEGUIDES	<ul style="list-style-type: none"> o 0.5 MM WALL THICKNESS o 95% EFFICIENCY o WEIGHT IS 2.5×10^6 KG 	<ul style="list-style-type: none"> o 0.5 MM WALL THICKNESS o 95% EFFICIENCY o WEIGHT IS 2.5×10^6 KG 	(1), (2) WEIGHT TOO LOW SHOULD BE 3.2×10^6 KG
4.3 POWER DISTRIBUTION	<ul style="list-style-type: none"> o LATERAL POWER FLOW, RECYCLING SWITCH GEAR. o 96% EFFICIENCY o COST IS $\\$91.6 \times 10^6$ o WEIGHT = $.511 \times 10^6$ KG 	<ul style="list-style-type: none"> o NOT DISCUSSED o WEIGHT = 1.04×10^6 KG 	
4.4 ROTARY JOINT	<ul style="list-style-type: none"> o DRIVEN BY DC MOTORS, GEARS, ETC. o 360° AZIMUTH ROTATION o $\pm 6^\circ$ ELEVATION ROTATION o ACCURACY = ONE ARC. MIN. o WEIGHT = 57×10^3 KG. 	<ul style="list-style-type: none"> o ROTARY TRANSFORMER ASSY, 20M IN DIA-STEPDOWN 382 KV to 20 KV. 0.15 KG/KW - EFF. = 99%. 	(1) ONE ARC MINUTE NOT ACCURATE ENOUGH.

TABLE IV-APP-1 (Cont'd)

LEVEL 2.2 TRANSPORTATION SYSTEMS

LEVEL 3.0 VEHICLES AND FACILITIES

ELEMENT	ADL/RAYTHEON /GAEC (1)	BOEING (2)	EVALUATION
3.1 LAUNCH SITE	o JFK SPACE CENTER	o JFK SPACE CENTER	
3.2 GROUND TRANSPORTATION	o NOT DESCRIBED	o NOT DESCRIBED	
3.3 PRIMARY LAUNCH VEHICLE	o SHUTTLE BASELINED o 15 SHUTTLE VEHICLES REQUIRED	o VERTICAL TAKE-OFF/VERTICAL LAND SINGLE STAGE TO ORBIT FREIGHTER 2.5 X 10 ⁵ KG PAYLOAD. 50 \$/KG TARGET COST.	
3.4 LOGISTICS VEHICLE	o SHUTTLE TO LEO o TUG TO GEO	o SHUTTLE TO LEO o GEO NOT DESCRIBED	
3.5 ORBIT TRANSFER	o SEPS (SOLAR ELECTRIC PROPULSION SYSTEMS) o ARGON ELECTRICAL ROCKETS SELF-POWERED BY PARTIALLY DEPLOYED SOLAR BLANKET.	o ARGON ELECTRICAL ROCKETS SELF-POWERED AND LO ₂ /LH ₂ ROCKET FOR SOLAR OCCULTATIONS	

IV-APP-13

TABLE IV-APP-1 (Cont'd)

LEVEL 2.3 MISSION OPERATIONS

LEVEL 3.0 OPERATION PHASE

IV-APP-14

ELEMENT	ADL/RAYTHEON/GAEC (1)	BOEING (2)	EVALUATION
3.1 PRIMARY ASSEMBLY	<ul style="list-style-type: none"> o ASSEMBLE AT 190 N.M. IN 2 YEARS. o 501 SHUTTLE FLIGHTS (0.7 FLIGHTS/DAY). o ON-ORBIT FABRICATION OF STRUCTURE. o REMOTE - CONTROLLED ASSEMBLY USING MANIPULATOR MODULES. 	<ul style="list-style-type: none"> o ASSEMBLE IN 1 YEAR IN LEO. o 720 FLIGHTS OF FREIGHT VEHICLE. o CREW OF 100 MEN ON-ORBIT. 	<p>(1) FULLY LOADED SHUTTLE NOT COMPATIBLE WITH FIGURES.</p>
3.2 ORBIT TRANSFER	<ul style="list-style-type: none"> o USES SELF-POWERED SOLAR ELECTRIC PROPULSION UNIT o 1 YEAR TRANSFER TIME o 120 DAYS IN VAN ALLEN BELT o SOLAR PROPULSION ARRAY WILL BE DEGRADED BY 40%. 	<ul style="list-style-type: none"> o USES SELF-POWERED SOLAR ELECTRIC PROPULSION VEHICLE o 7 VEHICLES PER POWER PRODUCTION MODULE FOR TRANSFER (1/4 SSPS). o VEHICLES RETURN TO LEO FOR NEXT MODULE. 	
3.3 MAINTENANCE	<ul style="list-style-type: none"> o 156 MEN/YEAR (FIRST YEAR) o FIRST YEAR O&M IS \$19.25/KW. o TWO SHUTTLE FLIGHTS/YEAR o O&M 30 YEAR AVERAGE IS \$9.13/KW. 	<ul style="list-style-type: none"> o NOT DESCRIBED 	

TABLE IV-APP-1 (Cont'd)

LEVEL 2.4 GROUND POWER GRID INTERCONNECT

LEVEL 3.0 RECEIVING STATION AND POWER GRID INTERFACE

ELEMENT	ADL/RAYTHEON/GAEC (1)	BOEING (2)	EVALUATION
3.1 RECTENNA IV-APP-15	<ul style="list-style-type: none"> o AN ARRAY OF SOLID STATE DIODE RECTIFIER ELEMENTS EACH COMBINED WITH INDIVIDUAL DIPOLE ANTENNA AND SUITABLE FILTER. o ELLIPTICAL SHAPED 10.3 X 13.4 KM o \$14.75/M² TOTAL GROUND SYSTEM COST o PEAK POWER DENSITY 27 MW/CM² o TOTAL RECTENNA AREA 108 KM² o RECTENNA EFFICIENCY = 90% o TOTAL UNIT COST = 320 \$/KW 	<ul style="list-style-type: none"> o NOT DESCRIBED IN DETAIL REF. W. C. BROWN (RAYTHEON DESIGN). 	(1) COST IS LOW (14.75) SHOULD BE \$26.50/M ²
3.2 GRID INTERFACE	<ul style="list-style-type: none"> o 1,000 VDC RECTENNA OUTPUT VOLTAGE 5,000 DC-AC INVERTERS WITH 66 KV OUTPUT, 3 Ø, 60 Hz o TRANSMISSION, COLLECTION AND INVERSION TOTAL EFFICIENCY = 85%. o COST = \$45/KW. 	<ul style="list-style-type: none"> o NOT DESCRIBED 	

TABLE IV-APP-1 (Cont'd)

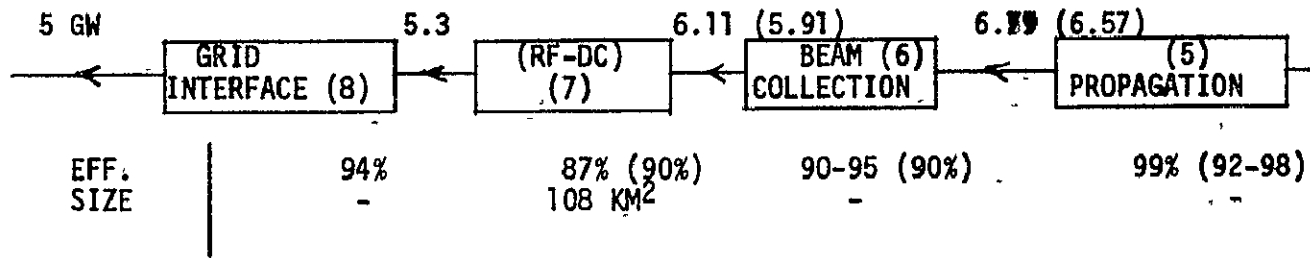
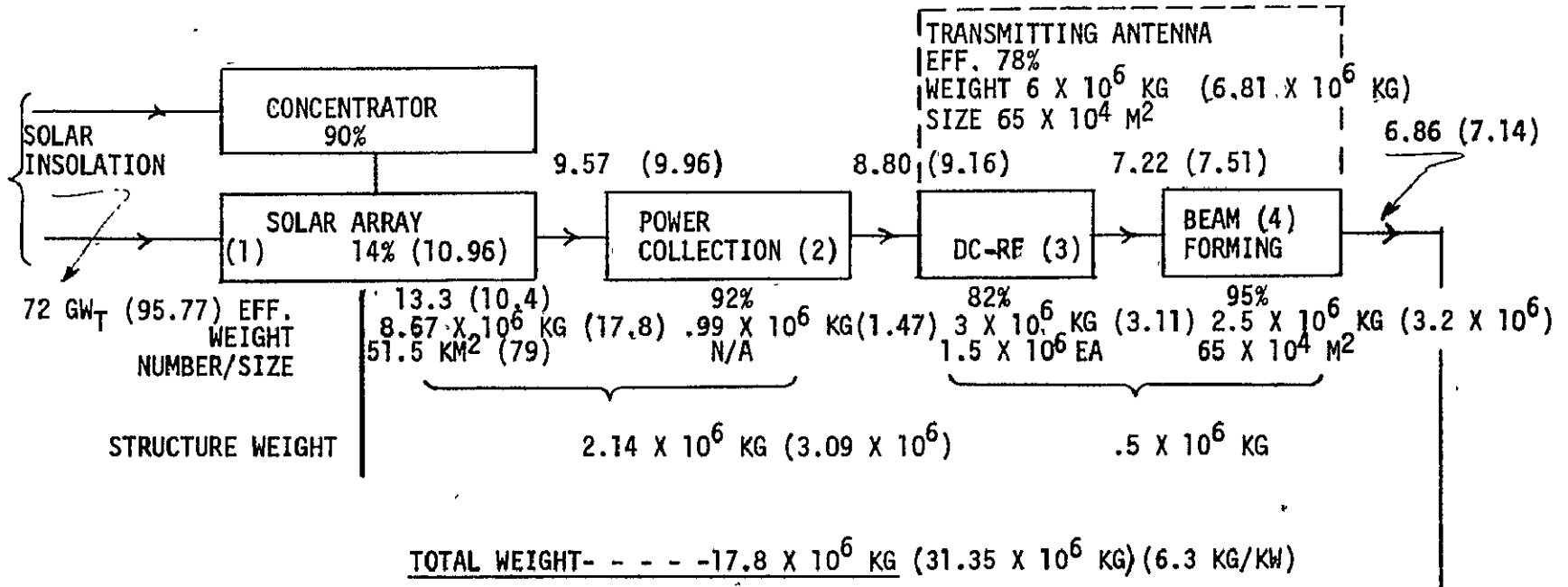
LEVEL 2.5 PROGRAMMATIC FACTORS

LEVEL 3.0 PROGRAM ELEMENTS

ELEMENT	ADL/RAYTHEON/GAEC	BOEING	EVALUATION
3.1 PROGRAM SCHEDULES	<ul style="list-style-type: none"> o I.O.C. = 16 YEARS FROM START OF GROUND TEST PROGRAM o ASSEMBLY TIME = 2 YEARS 	<ul style="list-style-type: none"> o I.O.C. = 16 YEARS FROM START OF PROGRAM o ASSEMBLY TIME = 1 YEAR 	
3.2 COSTS	<ul style="list-style-type: none"> o 45 MILLS/KW HOUR FOR 80% PLANT FACTOR AND 15% ANNUAL RATE OF RETURN. 26.7 MILLS/KWH (ECON) o TOTAL UNIT COST = 1500 \$/KW o TOTAL COST = \$7.6 BILLION o ORBITAL SYSTEM COST = \$6.0 BILLION o GROUND SYSTEM COST = \$1.6 BILLION o TRANSPORTATION COST = \$184/KG o MAINTENANCE AND OPERATION COST = \$96M/FIRST YEAR o DDT&E COST = \$43.9 BILLION 	<ul style="list-style-type: none"> o 25 MILLS/KW HOUR TARGET o TOTAL UNIT COST USING TARGET = 1300 \$/KW o TOTAL COST = \$13 BILLION TARGET INCLUDING RECTENNA o ORBITAL SYSTEM COST = \$11.8 BILLION o GROUND SYSTEM COST = \$1.2 BILLION o TRANSPORTATION COST = \$61.6/KG o MAINTENANCE AND OPERATIONS COST NOT DISCUSSED o DDT&E COST = \$60 BILLION 	
3.3 ECONOMIC FACTORS	<ul style="list-style-type: none"> o ORBITAL SYSTEM LIFE = 30 YEARS 	<ul style="list-style-type: none"> o ORBITAL SYSTEM LIFE = 30 YEARS 	

IV-APP-16

FIGURE IV-APP-3



OVERALL EFFICIENCY

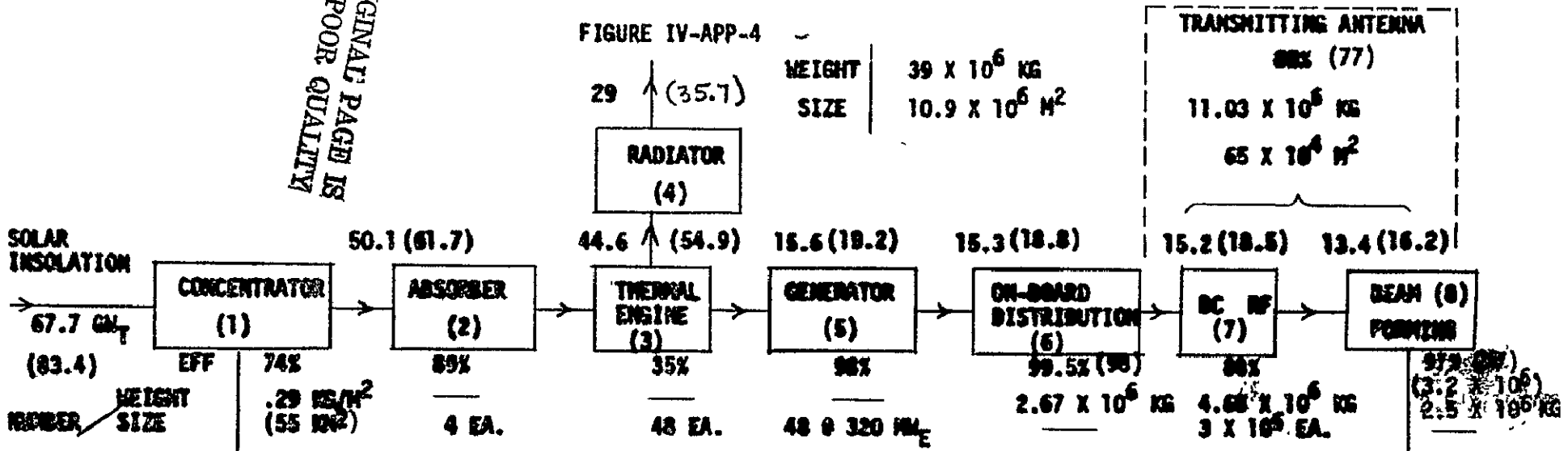
ADL/RAYTHEON/GAEC - 6.9%
 JSC - 5.2%

ADL/RAYTHEON/GAEC

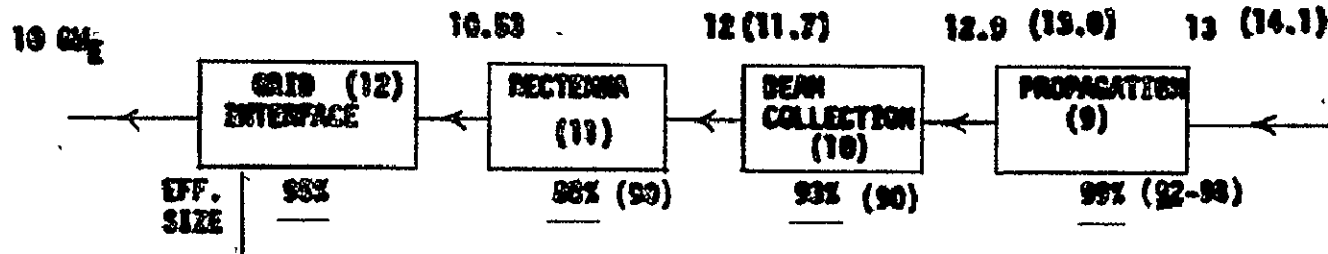
IV-APP-17

ORIGINAL PAGE IS OF POOR QUALITY

FIGURE IV-APP-4



TOTAL WEIGHT - - 64 x 10⁶ KG (70.8 x 10⁶) - (7.08 KG/CM²)



OVERALL EFFICIENCY

DSRMS - 14.83
JSC - 12.18

DSRMS SSPS

IV-APP-18

Table IV-APP-2

POWER CONVERSION SYSTEMS COMPARISONS

SOLAR PHOTOVOLTAIC CONVERSION		SOLAR THERMAL CONVERSION (BRAYTON CYCLE)	
ADVANTAGES	DISADVANTAGES	ADVANTAGES	DISADVANTAGES
1. Static conversion (no moving parts) provides long life and good reliability.	1. Degradation of output with time - amount uncertain.	1. Component technology understood; no breakthrough required.	1. No space experience with large, light weight focusing collectors and cavity absorbers (degradation).
2. Direct conversion of solar radiation to electricity provides design simplicity and improved reliability.	2. Major weight reductions required (factor of 2-4).	2. Ground tests of Brayton conversion system straight-forward, except for life tests.	2. Active cooling system (radiators) required.
3. Modularity provides flexibility in assembly and repair/replacement.	3. High voltage DC switching difficult.	3. AC power generation in large blocks - minimize conductor weight.	3. Pointing to sun critical? imposes attitude control penalties
4. Passive thermal control, no radiator.	4. Attitude control propellant high due to high moment of inertia (large areas/dimensions).	4. High conversion efficiency (35-40%) provides reduced solar collector area.	4. Leakage of working fluids and cooling imposes maintenance/design problems.

IV-APP-19

Table IV- APP-2, (Cont'd)

IV-APP-20

SOLAR PHOTOVOLTAIC CONVERSION		SOLAR THERMAL CONVERSION (BRAYTON CYCLE)	
ADVANTAGES	DISADVANTAGES	ADVANTAGES	DISADVANTAGES
5. Pointing (to sun) requirement less stringent.	5. High voltage DC power transmission imposes design complexities to minimize weight.	5. Potential long life, low maintenance with gas bearings; no wear out mode identified. Non-corrosive working fluid.	5. Coupling of ground-based and aerospace turbomachinery technology, required but not demonstrated
6. DC output compatible with DC-RF converters	6. Ground test difficult (large, light weight structures).	6.	6. High temperature (1800-2000°F) materials required for high efficiency (38-40%) conversion systems - technology development
7. Much experience with silicon solar cell space power systems; history of continued improvements.	7. Maximum Theoretical efficiency - 22% for silicon cells.	7.	7.

Table IV-APP-3 SPS CONCEPTS - COST COMPARISONS

	PHOTOVOLTAIC - 5 GW		BRAYTON CYCLE - 10 GW	
	ADL/RAYTHEON/GAEC	JSC ADJUSTED	BOEING	JSC ADJUSTED
<u>CAPITAL COST</u>				
o UNIT, \$BILLION (AS REPORTED)	7.6 ⁽³⁾	12.3 ⁽³⁾	13.0 ⁽⁴⁾	15.6 ⁽⁴⁾
o UNIT, SPACE & GROUND HARDWARE & ASSEMBLY (NO TRANSPORTATION), \$ BILLION	4.2	7.3	9.1	10.8
o \$/KW AT RECTENNA (AS REPORTED)	1500 ⁽³⁾	2460 ⁽³⁾	1300 ⁽⁴⁾	1560 ⁽⁴⁾
o \$/KW AT \$140/KG TRANSPORTATION COST	1360	2140	1810	2170
<u>POWER PRODUCTION COST, MILLS/KWH</u>				
o AS REPORTED	26.7 ⁽¹⁾	47 ⁽⁵⁾	25 ⁽²⁾	30 ⁽⁵⁾
o AT \$140/KG TRANSPORTATION COST	24.2 ⁽¹⁾	41 ⁽⁵⁾	35 ⁽²⁾	42 ⁽⁵⁾
<u>DDT&E COST, \$BILLION</u>	43.9	NO ESTIMATE	60	NO ESTIMATE

NOTES:

- (1) ANNUAL COST = 15.4% INCLUDING MAINTENANCE
- (2) 95% PLANT FACTOR; 8% RATE OF RETURN; 30 YEARS
- (3) \$184/KG TRANSPORTATION COST
- (4) \$62/KG TRANSPORTATION COST
- (5) 90% PLANT FACTOR; 15% RATE OF RETURN; 30 YEARS - NO OPS/MAINTENANCE INCLUDED

CONCLUSIONS

Based on the preceding analysis and discussion, the following conclusions are submitted:

(1) Existing SPS designs produced by ADL/Raytheon/GAEC and The Boeing Company utilize photovoltaic and Brayton cycle conversion systems, respectively. The design of both systems is predicated upon technology improvements to achieve the long life, high efficiency requirements. Therefore, from a technology status standpoint, no significant differences are noted between the system systems.

(2) Based on the cost factors reported by the two designers and a "normalized" transportation cost of \$140/KG to GEO, the capital costs of the two systems on a per KW basis are about the same.

REFERENCES

1. Space-Based Power Conversion and Power Relay Systems, Executive Summary, Second Performance Review Briefing, Boeing Aerospace Company, NASA 8-31268.
2. Space-Based Power Conversion and Power Relay Systems, Executive Summary, First Performance Review Briefings, Boeing Aerospace Company, NASA 8-31628.
3. Powersat, A Solar Power Satellite - Boeing Aerospace Company - Potential for Space-Based Solar Power, October 15, 1975, John Winch.
4. Microwave Power Transmission System Studies, Raytheon Company, NASA CR-134886, ER75-4368.
5. International Astronautical Federation, XXVith Congress, September 1975, The Satellite Solar Power Station - Dr. Peter E. Glaser, Authur D. Little, Inc.
6. Space-Based Solar Power Conversion and Delivery System Study, ECON, Inc., January 8, 1976.

V. SPS CONSTRUCTION AND MAINTENANCE SYSTEM

A. System Requirements and Analysis

L. Jenkins
Spacecraft Design Div.

1. Summary

Study of SPS construction concentrated exclusively on the photovoltaic configurations, however, construction of thermal conversion configurations appears to be analogous. The large size and low density of an SPS and the advantages of designing for operational loads rather than launch loads dictate an orbital fabrication and assembly approach to construction of the SPS. The complex elements or components such as antenna rotary joints and control system modules can be manufactured on the ground for assembly into the overall system. Other components such as the microwave generators, solar cell blankets, concentrator sheets and power distribution harnesses are amenable to dense packaging for launch and deployment in orbit.

SPS structure is a low density in its final configuration when designed for orbital loading conditions. The packing density of fold-deploy systems is much too low for efficient operation of the transportation system. In addition, structural joint design and launch loading conditions have an adverse effect on structural weight. An alternative is to manufacture the structure in orbit. Automatic machines generate structural elements from preprocessed stock. Combinations of the machines are utilized to build trusses for the primary structure.

Another candidate for orbital manufacture is the antenna subarray. The waveguides of the phased array must be built to very precise geometry, yet the finished product has very low density. By fabricating the subarrays in orbit, problems with launch loading and low density packaging can be avoided.

The large size of the SPS requires a high degree of automation to achieve the necessary construction rates. The construction crew can be best utilized in servicing and maintaining automated equipment, evaluating the operation and output, and performing contingency operations. The construction and support crew operate a construction base consisting of construction and manufacturing facilities, orbital construction and support equipment, logistic facilities, integration management facilities, and crew habitation facilities.

The configuration and sequence of construction will generally define the requirements for the construction base. The structural concept may be modified from an optimum design in order to simplify construction. Requirements for orientation of the concentrator arrays in the perpendicular to orbit plane (POP) configuration is an example of configuration influence on construction procedures. From the construction

standpoint, construction in GEO has a number of advantages, however, transportation considerations utilizing high I_{sp} systems may reduce overall costs. Additional study of critical parameters is required in order to select the construction location.

2. Construction Approach Guidelines and Criteria

The following guidelines and criteria were used in development of the construction approaches and concepts:

- a. Simple repetitive elements or components will be fabricated in geosynchronous orbit by automated machines.
- b. Complex elements or components will be manufactured in modules on the ground for assembly into the SPS in LEO.
- c. Personnel will be used primarily in monitoring and inspection functions from a shirtsleeve environment.
- d. EVA capability will be provided for unique nonrepetitive tasks or for contingency operations.
- e. "Bootstrap" locomotion is the prime mode around the launch site. Free-flyers are too great a penalty for common usage.

3. Construction Steps

The major steps in establishing a photovoltaic station without reference to sequence or phasing are as follows:

- a. Establish construction base.
- b. Assemble and checkout orbital construction equipment.
- c. Fabricate the solar array primary structure.
- d. Attach control system modules.
- e. Fabricate solar array secondary structure.
- f. Install solar cell blankets.
- g. Install concentrator sheets.
- h. Install power distribution system.
- i. Attach antenna gimbal and slip ring assembly.
- j. Install antenna drive system.

- k. Fabricate antenna primary structure.
- l. Fabricate antenna secondary structure.
- m. Install antenna subarrays.
- n. Install antenna power distribution system.
- o. Install antenna phasing system.
- p. Align antenna.
- q. Checkout system operation.

The sequence or phasing of construction steps depends on the configuration of SPS subsystems and the construction approach. Such items as whether the structure is functional when partially completed; whether the configuration is solar oriented or "POP"; orientation during construction; and relationship of the antenna to the solar array during buildup are other significant factors.

4. Types of Construction Processes

There are numerous processes or operations that will be necessary in the construction of the SPS. Many are somewhat independent of the construction approach or detail subsystem configuration. The following list provides a reference to the types of processes or operations that must be blended into an overall construction approach:

- a. Form long structural members.
- b. Stiffen structural members.
- c. Join cross members to long members.
- d. Join assembled structural members into larger truss assembly.
- e. Attach active elements or modules to structure.
- f. Align active elements or modules.
- g. Join current carrying elements of power distribution network.
- h. Checkout circuits.
- i. Apply thermal control coatings or finish.
- j. Deploy preassembled elements such as structural members, solar cell blankets or antenna subarrays.

- k. Provide stock control and delivery of materials, sub-assemblies, and modules.
- l. Attach and remove temporary supports or handling members.
- m. Checkout and troubleshoot active subsystems.
- n. Inspect completed operations.

Each of these processes may be expanded into additional detail when subsystem configurations are firm and if a particular process is expected to be a driver in defining a construction approach.

Appendix V-A-1 describes some construction related contractor studies. Appendix V-A-2 discusses joining processes for SPS construction.

5. Construction Options

a. Fabrication Locations - The principal option in construction location is between LEO (Low Earth Orbit) and GEO (Geosynchronous Earth Orbit) since the SPS is a little large for a single launch. Table V-A-5-1 summarizes the important parameters in the comparison and indicates the effect of each. One of the major considerations for LEO construction is the potential use of the solar array as a power source for a high I_{sp} propulsion system. Significant problems with this approach may offset the energy efficiencies. The exposed solar cells will be degraded by radiation from the Van Allen Belts. Offsetting gravity gradient torques to maintain orientation toward the sun combined with thrust loads will affect the array structural design. Orientation to reduce drag will be an important consideration. The long transit time associated with low thrust levels results in an additional capital investment period for interest charges.

On the other hand, logistics and support will be simpler and cheaper in LEO. Lead time for delivery of components is shorter than to GEO particularly if the OTV is ion propelled. The launch penalty to place construction equipment in orbit is much greater to GEO, but if a large number of stations are built, the impact is much smaller for each station.

Another important difference in construction in LEO is the continual sunlight-darkness cycle. The construction facility will need the capability to store power and provide lighting to maintain continuous operations. Also, the changing thermal gradients may cause problems in aligning the station to required geometry during construction.

Table V-A-5-1. Orbit Height Trade Parameters

<u>PARAMETER</u>	<u>CONSTRUCTION IN LEO EFFECT</u>	<u>CONSTRUCTION IN GEO EFFECT</u>
DRAG	ORIENT TO STREAMLINE	NEGLECTIBLE
RADIATION BELT	DEGRADES INSTALLED SOLAR CELLS REDUCES CREW EXPOSURE LEVELS	INCREASED CREW EXPOSURE LEVELS
ORBIT-TO-ORBIT TRANSIT TIME	ADDS SERIAL TIME TO BUILDUP AND OPERATION OF SPS	COMPATIBLE WITH CONTINUOUS FLOW OF MATERIAL
ASSEMBLED TRANSIT LOADS	EXPECTED TO BE GREATEST LOADS APPLIED	NOT APPLICABLE LOWER GRAVITY GRADIENT LOADS
LIFE SUPPORT	REDUCED PENALTY FOR LOGISTICS	GREATER PENALTY FOR LOGISTICS
LOGISTICS	REDUCED LEAD TIME FOR DELIVERY OF COMPONENTS	LONG TRANSIT TIME ON COMPONENTS
PERFORMANCE CONSIDERATIONS	MAY USE ARRAY AS POWER SOURCE (ORIENTATION LOADS WILL REDUCE EFFICIENCY) GANG TUGS TO MOVE LARGE WEIGHTS	PENALTY FOR CONSTRUCTION EQUIPMENT (MINIMIZED IMPACT FOR LARGE NUMBER OF STATIONS)
LAUNCH PHASING	IMPORTANT FOR LEO	IMPORTANT FOR TUG RENDEZVOUS
DAY-NIGHT CYCLE	POWER STORAGE LIGHTING THERMAL TRANSIENTS	NOT APPLICABLE

V-A-5

The best orbit for construction of the station is too dependent on a number of parameters to reach a distinct conclusion. Additional study, particularly of performance penalties will be necessary.

b. Degree of Automation - A second construction option is the degree of automation of the construction operations. Total automation with control from the ground does not appear to be a viable choice because of the complexity of the system and the size of the operation. High degree of manual involvement is not acceptable because of the number of personnel which would be required and the highly repetitive nature of the tasks. Automation with orbital control and monitoring can be expected to provide the greatest overall system benefits. With automatic equipment to perform the great number of repetitive construction operations, a minimum number of men can control the operation and provide intelligent decision making capability for off nominal or contingency situations.

c. Manufacture-Assemble-Deployment - The construction approach will include some of each of the options of onsite manufacture, assembly of prefabricated components and deployment of a pre-packaged modules. It is expected that on site manufacturing of structure will predominate because of the advantages of transporting pre-processed bulk materials. The material packing density for raw stock is greater and less sensitive to boost loads. On site manufacturing drives the configuration of the SPS toward a regular geometry with simple repetitive operations. Orbiting manufacture of structure stimulated the concept of a continuous structural truss fabrication machine which was termed a "beam building machine." Figure V-A-5-1 illustrates a concept developed at JSC for an experiment on the Space Shuttle. Appendix V-A-5-3 provides additional information on the approach. Several contractors are working on similar "beam building machines" concepts which provides confidence that the construction approach is sound.

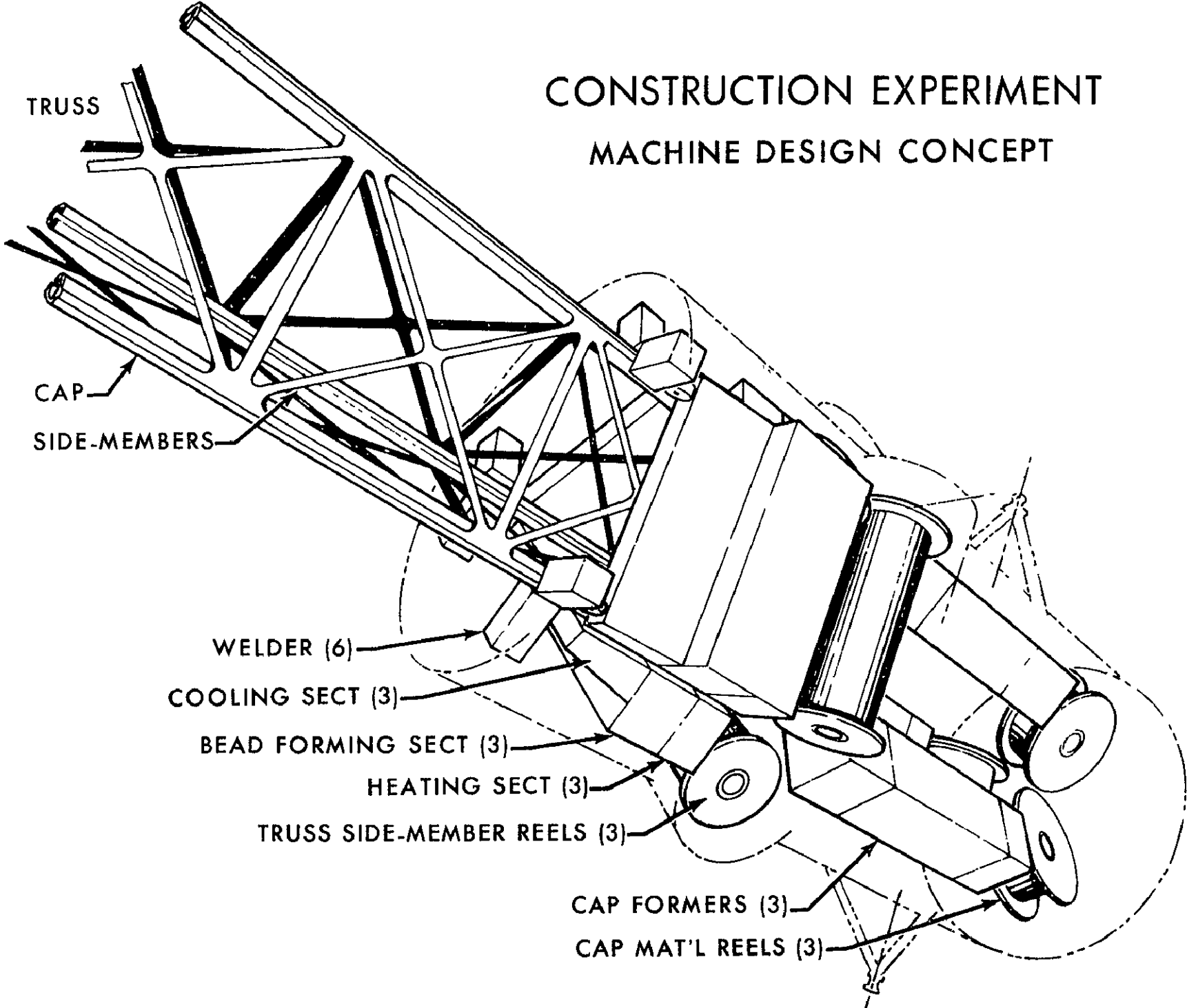
d. Locomotion Around the Construction Site - Classically movement in space from one point to another is illustrated as a free-flyer. Assessment of the free-flying mode for construction of the SPS indicates that a mode where the transient vehicle remains attached to the construction base or SPS is a better choice. Table IV.A.4.d-1 summarizes the comparison.

6. Construction Concepts

Within the guideline of automated construction, the SPS structural configuration has a great influence on the construction concept. Construction approaches for the column/cable and the truss configuration in GEO were evaluated in greater detail than the modular buildup of the truss in LEO.

C.S.

CONSTRUCTION EXPERIMENT MACHINE DESIGN CONCEPT



V-A-7

Figure V-A-5-1

Table IV.A.4.d-1. Free-Flyer vs. SPS Attached Locomotion

- FREE FLYER

- MOVEMENT NOT RESTRICTED IF CLEARANCE AVAILABLE
- ORBITAL MECHANICS A FACTOR IN LONG TRANSITS
- FORCE APPLICATION LIMITED TO THE REACTION THRUST CAPABILITY
- COMPLEX REACTION CONTROL SYSTEM MUST STABILIZE THE FLYER, PROPELL THE FLYER, AND STOP AND START IT
- REACTION JETS MAY CONTAMINATE SPS SUBSYSTEMS OR RESULT IN DAMAGE FROM JET IMPINGEMENT

- ATTACHED LOCOMOTION

- VERY LITTLE OR NO PROPELLANT REQUIRED FOR MANEUVERS
- ORIENTATION REFERENCED TO SPS
- TETHERED TO SPS
- FORCE APPLICATION LIMITED ONLY BY STRUCTURE TO WHICH ATTACHED

a. Column/Cable Configuration - The construction approach for the column/cable configuration considered a dispersed construction base as illustrated in figure V-A-6-1. Construction begins at the intersection of the six columns. The construction facilities are set up to move out from the center of the SPS array as the trusses forming, the columns are manufactured. Operating from the construction facilities, packages of solar cell blankets and concentrators are prepared for deployment, installed along the column and attached to the tension cables at the periphery of the array. Power distribution cable hookups are also made at this point. As the columns continue to grow, the blankets and concentrators are deployed as shown in figure V-A-6-2. Figure V-A-6-3 illustrates an interim array position with the array partially constructed. One of the principal concerns with the column/cable construction is the maintenance of tension in the cables which provide the structural integrity and alignment. Tension adjustments will also be necessary to align to the final geometry.

An example of the construction sequence for the column/cable is shown in figure V-A-6-4. The sequence was developed using the following ground rules:

- The construction base (construction facilities, logistics facility, habitat and orbital construction support equipment) were primarily assembled in LEO, checked out, then transported to GEO.
- Several SPS's had been completed so the steep part of the learning curve was past and the construction base is available, operational, and sized to meet the required rate of construction.
- Construction time of one year.
- Antenna subarrays fabricated in LEO and transported in GEO for installation on antenna structure.
- SPS configuration is 10 GW, POP oriented, column/cable structure.

In order to estimate the number and type of machines needed for construction, construction analysis sheets were prepared. Tables V-A-6-1 thru V-A-6-4 are examples for the column/cable buildup for the construction steps outlined in figure V-A-6-4. A summary of the amount of construction equipment is given in table V-A-6-5.

Construction on the antenna originates from a construction facility attached to two of the column construction facilities. A description of the antenna construction concept is provided after the discussion of the truss configuration buildup.

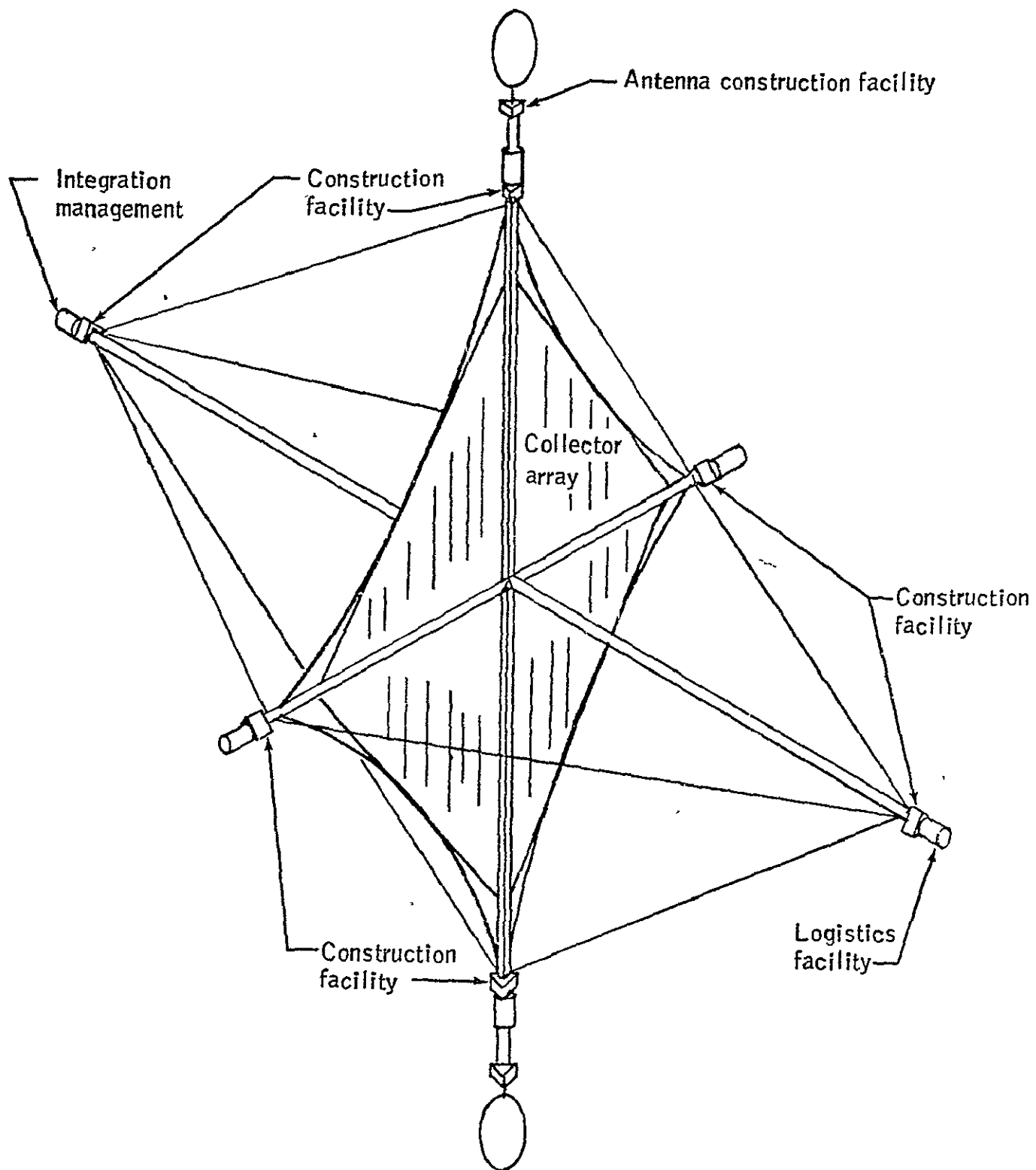


Figure V-A-6-1 - Construction base concept for column/cable configuration.

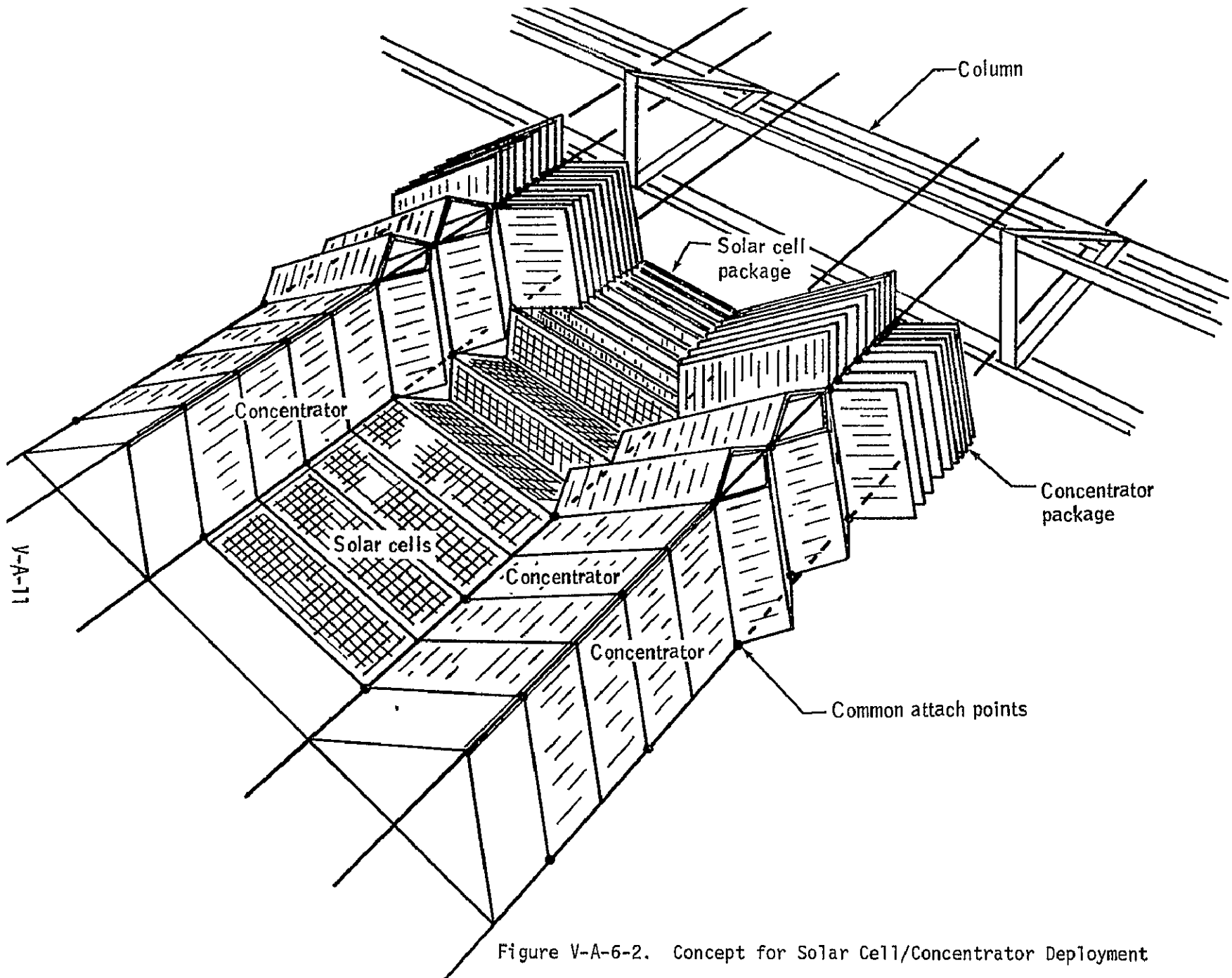


Figure V-A-6-2. Concept for Solar Cell/Concentrator Deployment

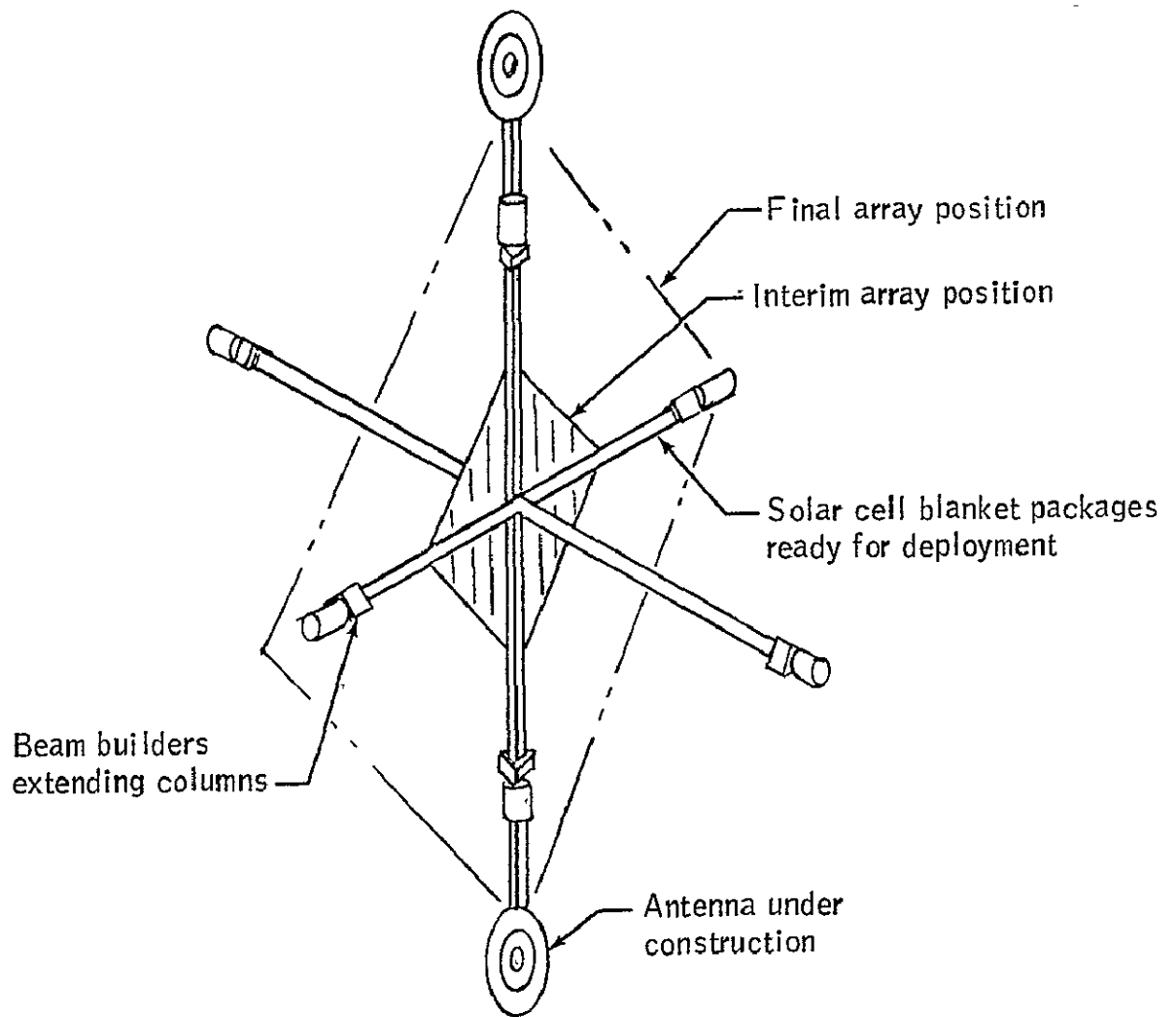
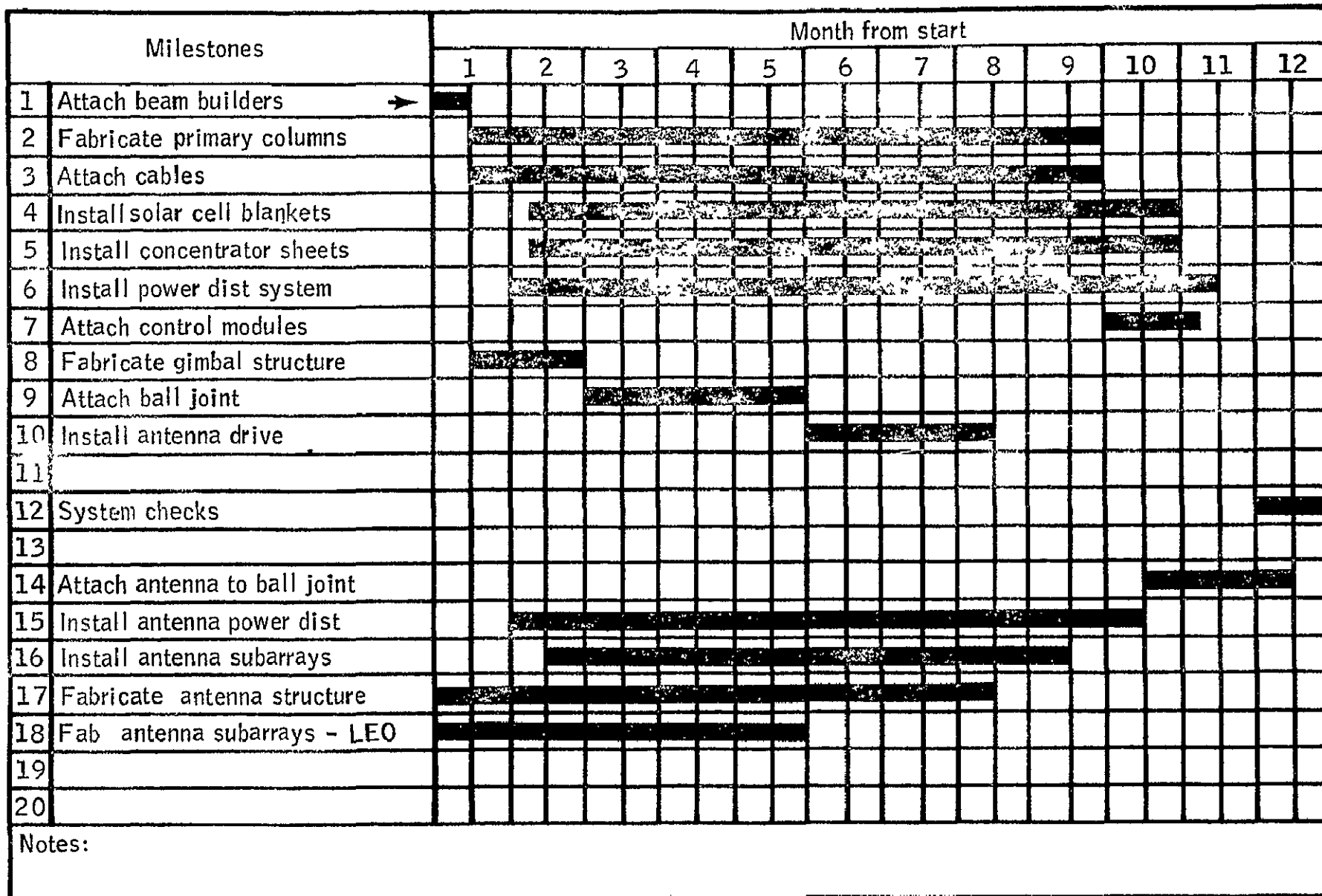


Figure V-A-6-3. Column/Cable Configuration Partially Constructed

V-A-13



ORIGINAL PAGE IS
OF POOR QUALITY

Figure V-A-6-4. - Typical SPS construction sequence-column/cable (POP)

TABLE V-A-6-1 SPS CONSTRUCTION ANALYSIS
COLUMN/CABLE POP

CONSTRUCTION STEP	CONSTRUCTION TECHNIQUE	CONSTRUCTION RATE = 1 PER YEAR		
		OC/SE REQUIRED	LOGISTICS REQUIREMENTS	PERSONNEL REQUIREMENTS
Build Prime Structure	<ul style="list-style-type: none"> o Fabricate truss o Fabricate and install joints o Compression check o Assemble in column o Install guy cables o Adjust for configuration under assembly environment (e.g., loads, temperatures) 	<ul style="list-style-type: none"> 1) Fabricators 30 2) " 30 3) Compression guage (test of) (6) 4) Manipulators (12) 5) Cable rigging equipment (12) 6) Alignment sensing system of feedback (6) 	<p>266000 kg at start of construction</p> <p>Max Fab Rate 0.3 m/min</p>	<p>4 per column X6 = 24</p>

V-A-14

TABLE V-A-6-2 SPS CONSTRUCTION ANALYSIS
COLUMN/CABLE (POP)

CONSTRUCTION STEP	CONSTRUCTION TECHNIQUE	CONSTRUCTION RATE 1 PER YEAR		
		OC/SE REQUIRED	LOGISTICS REQUIREMENTS	PERSONNEL REQUIREMENTS per shift
DEPLOY SOLAR CELL BLANKETS AND CONCENTRATOR SHEETS.	PACKAGED FOLDED BLANKETS WITH EDGE CABLES ARE DEPLOYED FROM MAIN COLUMNS. DEPLOYMENT CONTROLLED BY ATTACHING TO CABLES BETWEEN COLUMNS. SETUP FOR PACK FROM STAGING ON THE BEAM BUILDER MODULE.	<ol style="list-style-type: none"> 1. STAGING AND RMS TO INSTALL PACKAGES CONNECT TO POWER DIST. (4). 2. BLANKET TO CONC. ATTACHMENT MECHANISMS (1040) 3. TROLLEY MOUNTED MANNED SPIDER FOR MONITORING DEPLOYMENT AND INSPECTION (8). 	<p>1800 PACKAGES 10M x 10M x 8M</p> <p>INSTALL ~ 8 PER DAY</p>	24

V-A-15

TABLE V-A-6-3 SPS CONSTRUCTION ANALYSIS
COLUMN/CABLE (POP)

CONSTRUCTION STEP	CONSTRUCTION TECHNIQUE	CONSTRUCTION RATE 1 PER YEAR		
		OC/SE REQUIRED	LOGISTICS REQUIREMENTS	PERSONNEL REQUIREMENTS PER SITE
INSTALL POWER DISTRIBUTION.	MAIN BUSS DEPLOYED FROM STAGING ON BEAM BUILDER MODULE. HOOKUP TO SOLAR CELLS WHEN BLANKET PACKAGE IS PREPARED FOR DEPLOYMENT.	1. STAGING AND RMS TO CONNECT POWER DIST. TO SOLAR ARRAY (4). 2. CABLE CONNECT DEVICES (4). 3. CABLE DEPLOY REELS (4). 4. CONTINUITY CHECKERS (4).	POWER DISTRIBUTION CABLE ASSEMBLY (4)	1. } 2. } 4 3. } 4. }

V-A-16

TABLE V-A-6-4 SPS CONSTRUCTION ANALYSIS
COLUMN/CABLE (POP)

CONSTRUCTION STEP	CONSTRUCTION TECHNIQUE	CONSTRUCTION RATE 1 PER YEAR		
		OC/SE REQUIRED	LOGISTICS REQUIREMENTS	PERSONNEL REQUIREMENTS
INSTALL CONTROL MODULES.	DOCK PREFABRICATED MODULE WITH HANDLING EQUIPMENT ON BEAM BUILDER MODULE. POSITION AND ATTACH TO SPS PRIMARY STRUCTURE. MAKE CABLE CONNECTIONS AND CHECK OUT SYSTEM.	<ol style="list-style-type: none"> 1. HANDLING EQUIPMENT. 2. TROLLEY MOUNTED MANNED SPIDER (4 COMMON USE). 3. CHECKOUT EQUIPMENT. 	FOUR MODULES ~ 100 MT EACH	WITHIN PRODUCTION CREW REQUIREMENTS.

V-A-17

Table V-A-6-5. Orbital Construction Equipment Requirements

<u>SECS</u>	<u>COLUMN/CABLE</u>	<u>TRUSS</u>
BEAM BUILDING MACHINES	30	61
CABLE RIGGING DEVICES	8	0
SOLAR CELL BLANKET PACKAGE INSTALLERS	4	4
REFLECTOR PACKAGE INSTALLERS	4	8
POWER DISTRIBUTION HARNESS INSTALLERS	4	4
MOBILE MANNED MANIPULATORS	8	5
FACILITY MANNED MANIPULATORS	12	2
<u>MPTS</u> (TWO ANTENNAS)		
SUBARRAY MANUFACTURING (TWO PER HOUR)	8	8
BEAM BUILDING MACHINES		
SUBARRAY SUPPORT STRUCTURE	18	18
PRIMARY STRUCTURE	8	8
CABLE RIGGING DEVICES	12	12
POWER DISTRIBUTION HARNESS INSTALLERS	4	4
SUBARRAY INSTALLERS	4	4

V-A-18

b. Truss Configuration - The truss configuration was conceived as an aid to construction. With the regular geometry of the truss configuration, a construction base concept as illustrated in figure V-A-6-5 is possible. A large space frame, the entire width of the collector array, supports the equipment necessary for completion of the array. A central facility receives and distributes materials for construction. Primary structural trusses are manufactured by automatic machines. Before the array leaves structural support of the construction base, concentrators and solar cell blankets are deployed from their shipment packages. Power distribution cables are installed and checked. The entire process is set up to proceed at a uniform rate such that the array is extruded from the construction base. To preclude stopping the process, in the event of a breakdown, individual machines must be designed to slip relative to the base then make up time when repaired.

A construction sequence for the truss configuration is shown in figure V-A-6-6. The equipment to construct the array appears in table V-A-6-5.

c. MPTS - Antenna construction parallels construction of the collector array. One antenna construction facility is attached to the construction base, the other is a separate facility attached to the end of the collector array where construction begins.

The antenna construction sequence outlined in figure V-A-6-6 begins with fabrication of the support structure and installation of the ball joint and drive mechanism. Then buildup of the primary structure shown in figure V-A-6-7 can take place. The construction concept envisions the concentric installation of the secondary structural units which are used as construction staging for assembly of the primary structure rings. When each ring is in place, the cables to the next inner ring are tensioned to rigidize the structure. The next band of secondary structure is constructed followed by next outer ring until the structure is complete. Subarray installation immediately follows the structural buildup of each ring to take advantage of the position of the construction facility. Tables V-A-6-6 and V-A-6-7 evaluate equipment requirements which are summarized in table V-A-6-5.

The antenna subarrays are a prime candidate for manufacture in an orbiting facility. The waveguides should be very light weight which would result in a low density packaging if made on earth and transported to orbit. The microwave generator is a high density item which would be a design penalty to a earth launched subarray. By setting up an orbiting manufacturing facility, probably in LEO, a lightweight precision design appears achievable.

d. Modular Truss Configurations in LEO - A third construction option which was considered in less detail is the manufacture of sections of the collector array in LEO. A portion of the solar cell

V-A-20

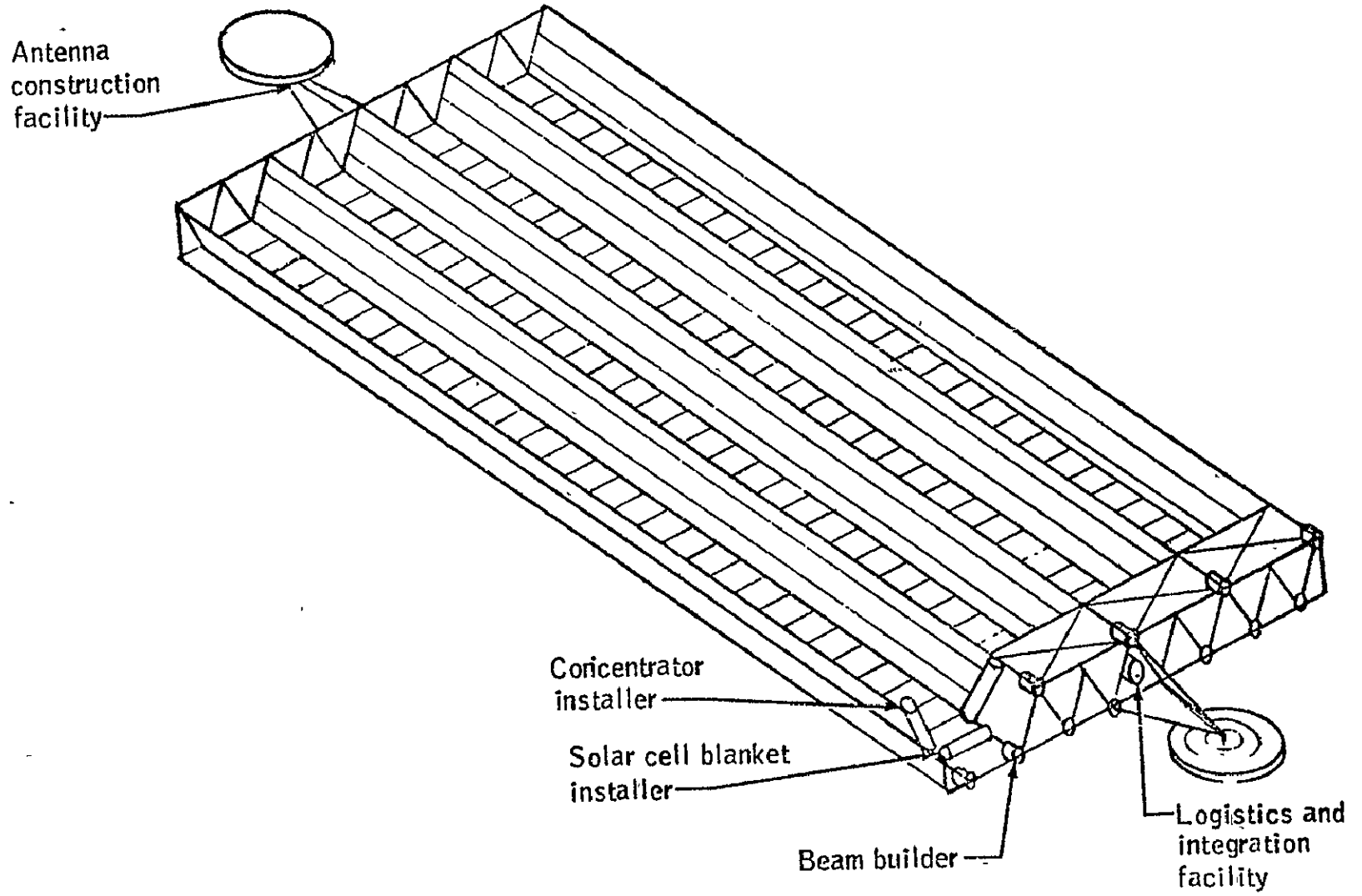
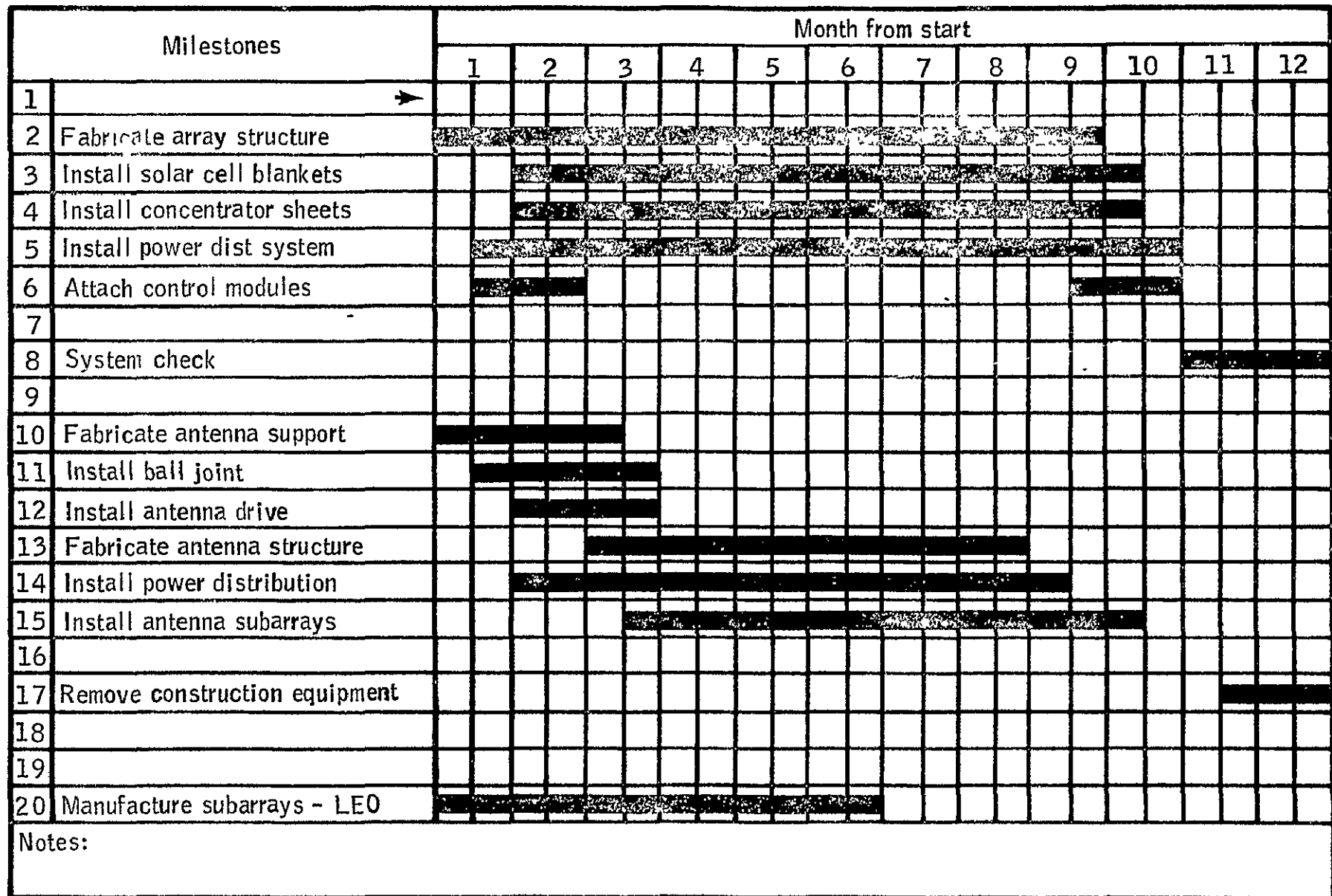


Figure V-A-6-5

- Construction base concept for truss configuration.

Y-A-21



ORIGINAL PAGE IS
OF POOR QUALITY

Figure V-A-6-6. - Typical SPS construction Sequence-Truss configuration.

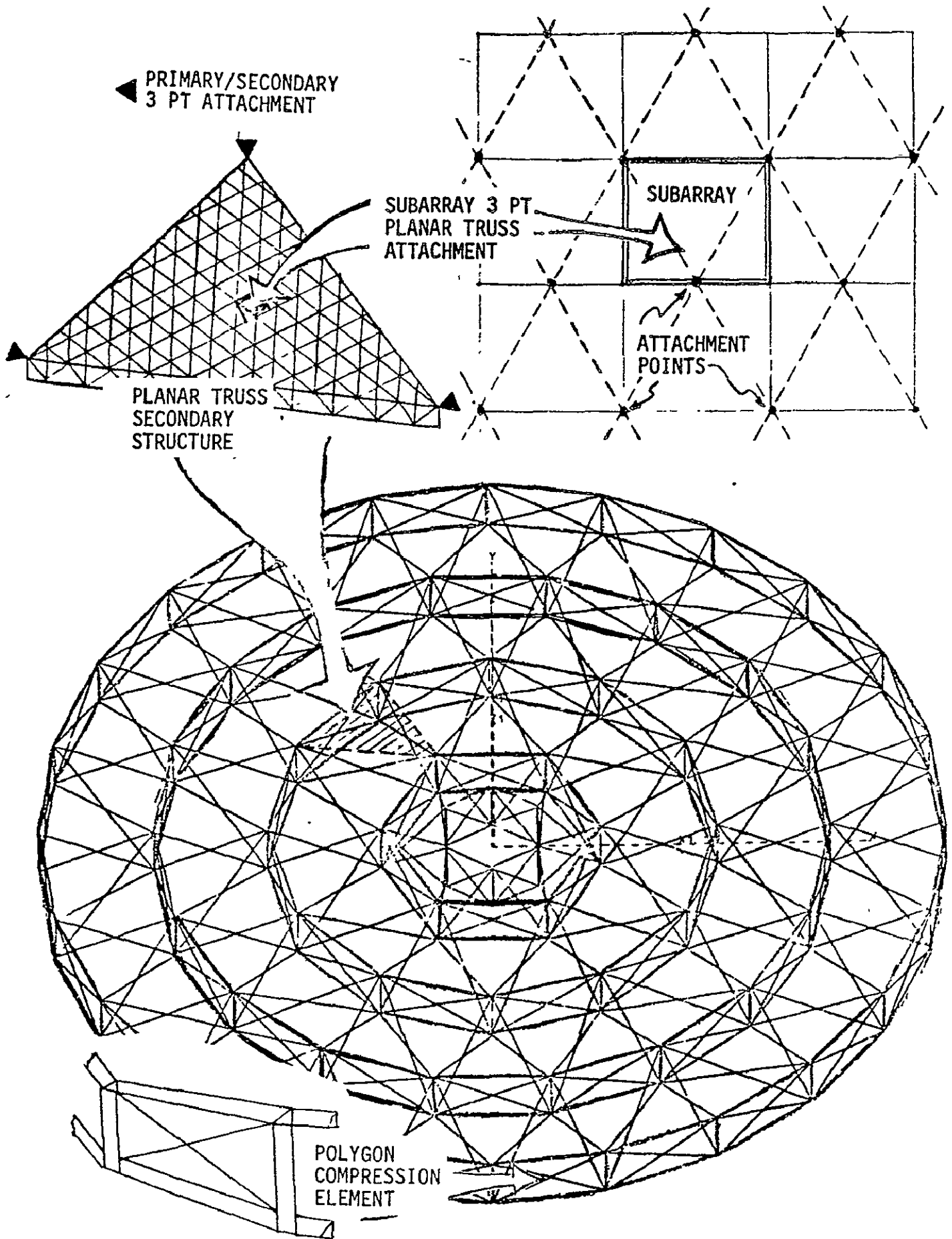


Figure V-A-6-7. MPTS Antenna Structure

TABLE V-A-6-6

SPS CONSTRUCTION ANALYSIS
ANTENNA

CONSTRUCTION STEP	CONSTRUCTION TECHNIQUE	CONSTRUCTION RATE 1 PER YEAR		
		OC/SE REQUIRED	LOGISTICS REQUIREMENTS	PERSONNEL REQUIREMENTS
Manufacture parts	Fabricated-in-space thermo-plastic graphite truss elements and joints.	Manufactured-in-space fabrication machine.		
Assembly of (1) into hoop compression elements.	Manufacture-in-space machine fabricated.	Ultrasonic welder.	120-130mm long trusses. 60-65m long trusses.	
Manufacture parts.	Fabricated-in-space thermo-plastic graphite machine producing joint articulators and cable connectors.	Manufactured-in-space fabrication machine.	200000 kg of graphite tape.	16 per shift
Assembly of axially loaded "hoop" member.	Member by member joining of articulators (3) and trusses (2) to cradle supports.	Manipulator ultrasonic welder.	120-130mm long trusses. 60-65 long trusses.	
String Cable.		Manipulator.	60335 meters of Kevlar cable.	

TABLE V-A-6-7 SPS CONSTRUCTION ANALYSIS
ANTENNA

CONSTRUCTION STEP	CONSTRUCTION TECHNIQUE	CONSTRUCTION RATE 1 PER YEAR		
		OC/SE REQUIRED	LOGISTICS REQUIREMENTS	PERSONNEL REQUIREMENTS PER SHIFT
INSTALL ANTENNA SUBARRAYS	PREFABRICATED SUBARRAYS ATTACHED TO SUPPORT STRUCTURE AT THREE POINTS. HANDLING, POSITIONING, AND ATTACHMENT DONE BY MOBILE ASSEMBLER.	<p>1. MOBILE ASSEMBLER WITH RACK FOR HANDLING SUBARRAYS. TWO RMS, DEVICES FOR SUPPORTING ASSEMBLER ON SUBSTRUCTURE (2).</p> <p>2. LOGISTICS VEHICLE TO DELIVER SUBARRAYS TO ASSEMBLER.</p>	1. 20-9.31 x 10.75M SUBARRAYS PER DAY EACH MACHINE.	<p>1. 6</p> <p>2. 2</p>

V-A-24

blanket would be exposed to the sun to provide electrical energy to a high performance propulsion system which would propel the module to GEO. In GEO, the modules would be assembled into the final configuration. Detailed trades are needed of the considerations which may offset the expected OTV savings. Such considerations are degradation of deployed cells, docking of large masses, and fiscal effects of tying up capital for the relatively long transit time.

7. Configuration Comparison

Review of the construction concepts for the column/cable and truss configurations provides some considerations for future study. The discrete sites where specific activity takes place are fewer for the column/cable than for the truss. However, the level of activity for the column/cable is expected to be greater at each site. The activity at truss construction locations appears more passive and amenable to remote monitoring to permit reduction in crew size. The truss configuration may be capable of more rapid construction after the initial setup because there would be less alignment and adjustment of the structure and the construction facility is centralized.

Orientation of the configuration during construction may be important to keep sunlight on the solar cells from generating voltage which could be hazardous to operations. Gravity gradients will orient the SPS with the two antennas on a line through the center of the earth and with the array in the orbit plane. The solar cells can be shaded by rotating the array when the sun reaches the equinox. This may be preferred to maintaining an unnatural orientation with resultant large propellant penalties.

APPENDIX V-A-1

CONSTRUCTION STUDIES

H. G. Patterson
Future Programs Office

1.0 CONTRACTOR STUDIES

This section will cover the following completed studies.

1.1 Orbital Assembly and Maintenance Study (Reference 1)

The Martin Marietta Aerospace Corporation, under contract to NASA-JSC, has derived a concept to construct the support structure for the microwave power transmission system portion of the solar power station using STS elements (Figure 1). The support structure is one kilometer in diameter and consists of 2520 60-foot cubes with a total weight of approximately two million pounds. The material used for the structure is coated steel.

The first phase in the total construction process is to assemble the middle 60-foot cube. The first Shuttle flight contains the basic core structure with folding alignment and support member, 12 beam members with cross braces, and two sets of mobile assemblers and beam holders. The center core is extracted from the cargo bay, positioned and docked on the Shuttle docking module with the RMS. The alignment beams are unfolded from beside the core structure and the tension rods are positioned. A rotary docking interface is required at the docking port since the RMS cannot reach completely around the core structure. The remainder of the beams are extracted from the cargo bay, placed in the correct position and alignment, and then welded in place, one at a time. The two sets of mobile assemblers and mobile beam package holders are placed on either side of the cube.

The second Shuttle flight contains two beam packages. These are nonstandard in that they are split longitudinally so that a package can be placed on each side of the cube. The beam packages are 60 foot long and fill the cargo bay. Thirty-eight more cubes are constructed using the assemblers. When this structure is completed, the assembly equipment is stowed and the structure is readied for boost.

The 39 cube structure is readied for boost by docking two Tugs and two SEPS. This assembly is then boosted to intermediate orbit with two Tugs. The Tugs will return and the SEPS will boost the assembly to

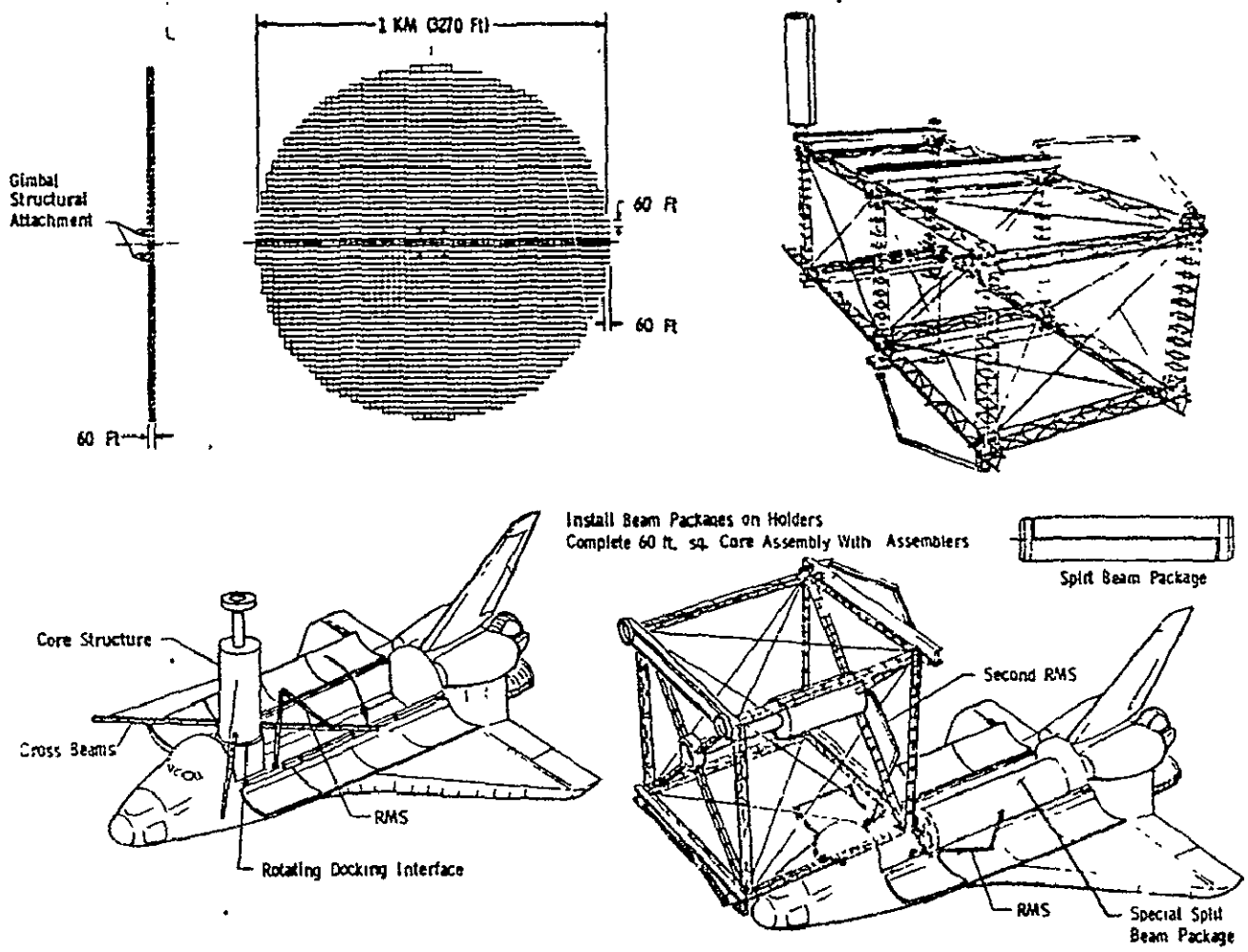


Figure 1. - Martin Marietta Corporation SPS Antenna Support Structure

ORIGINAL PAGE IS
OF POOR QUALITY

geosynchronous Earth orbit. Once the structure is in GEO additional beam packages are transported and docked to the structure as required. The assemblers proceed to build outward from the center until the total 2520 cube support structure is complete.

1.2 Microwave Power Transmission System Studies (Reference 2)

The Raytheon/Grumman Aerospace Companies, under contract to NASA-Lewis, has also derived a concept for the construction of the support structure for the microwave power station (Figure 2). The concept contains 69 structural modules which are 350 ft. square by 120 ft. deep. The total assembly measures 1 Km (3,270 ft.) in diameter and 120 ft. deep, excluding the gimbal mounting structure. Detailed space assembly techniques were not the prime consideration during the design of this structure.

Figure 3 shows a detailed view of one of the Raytheon/Grumman 350 x 120 ft. structural elements which make up the 1 Km microwave antenna. The base structure is composed of 36 modules approximately 59 ft. square by 16 ft. deep. Each of these 36 module elements is ringed by a 115 ft. wall composed of cable supported beams.

Figure 4 shows a cross section detail of a segment of the Raytheon/Grumman microwave antenna structure. This design uses four basic beam sizes: 18 m (59 ft.) x 3 m (9 ft.); 35 m (115 ft.) x 3 m (9 ft.); 18 m (59 ft.) x 1 m (3 ft.); and 5 m (15 ft.) x 1 m (3 ft.). Each of the beam segment junctions are supported by tension cables that must be emplaced after the beams are assembled. This drawing shows both the support structure and waveguide array.

1.3 Design Differences

The key antenna design differences between the Raytheon/Grumman and the Martin Marietta concepts are shown in Table I. The MMC has a study groundrule that all structural components be compatible with the Shuttle cargo bay while GAC assumed that the beams are assembled in space.

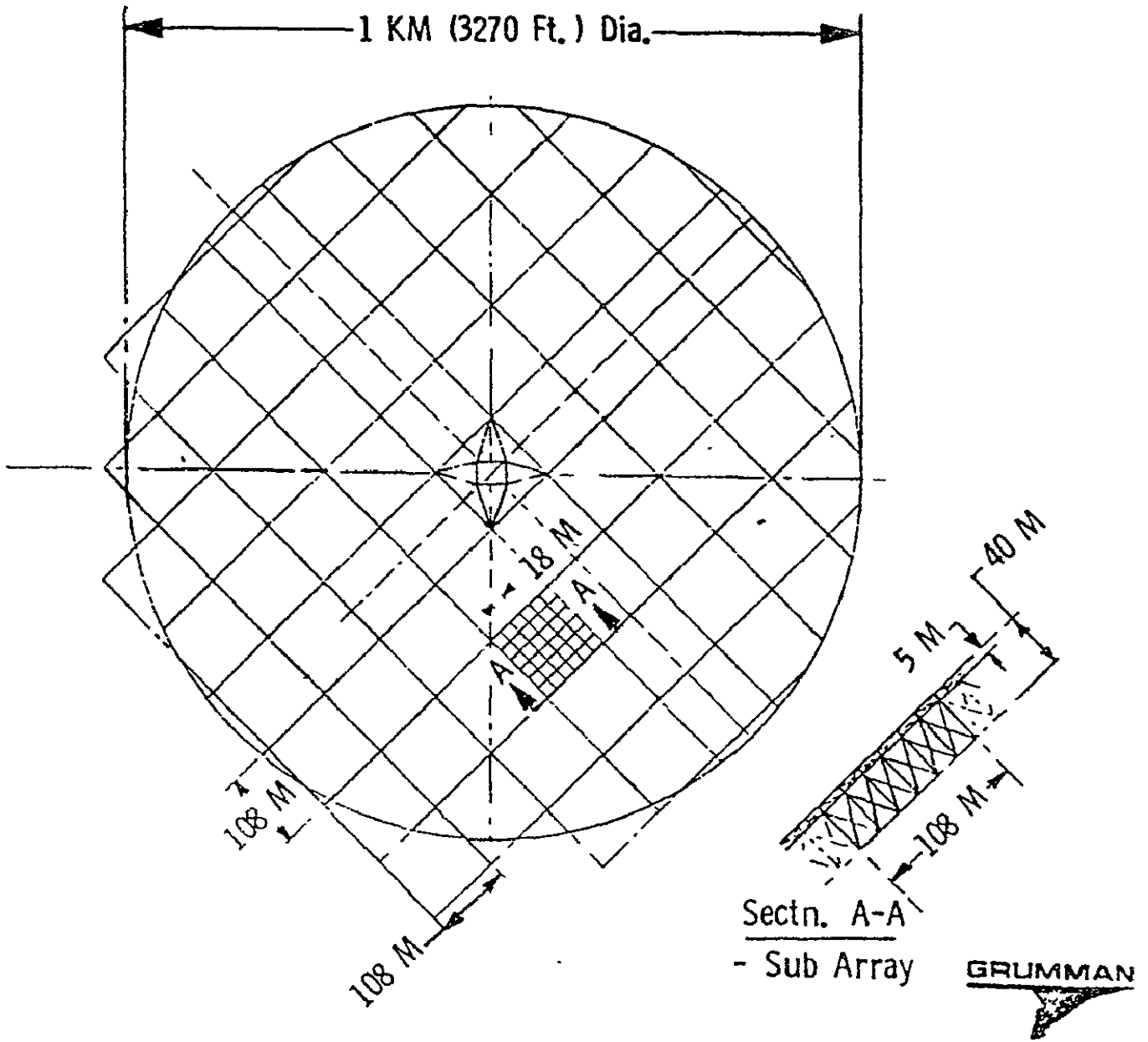


Figure 2. - Grumman Aerospace Company SPS Antenna Support Structure

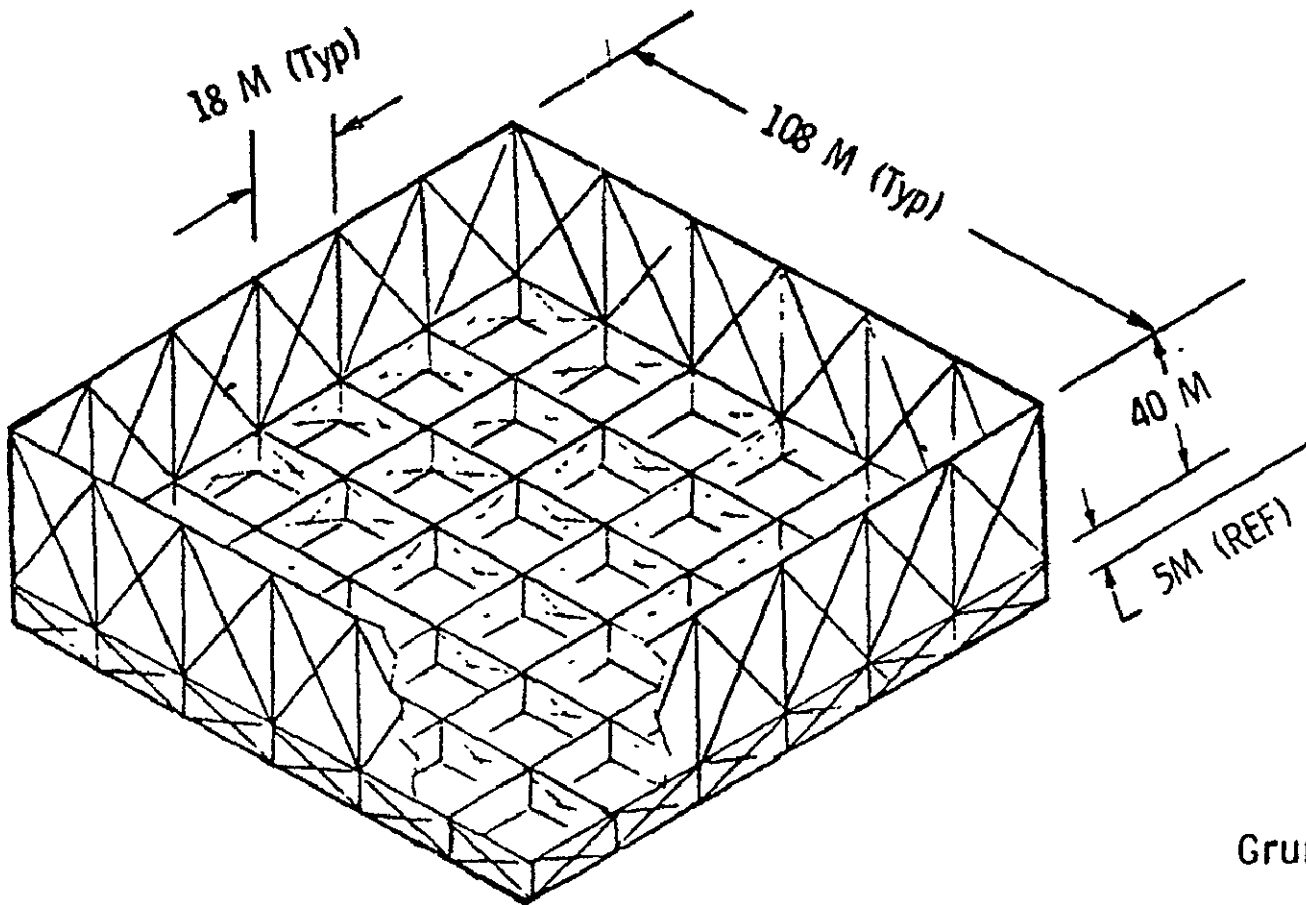


Figure 3. - Raytheon/Grumman Typical Antenna Construction Technique

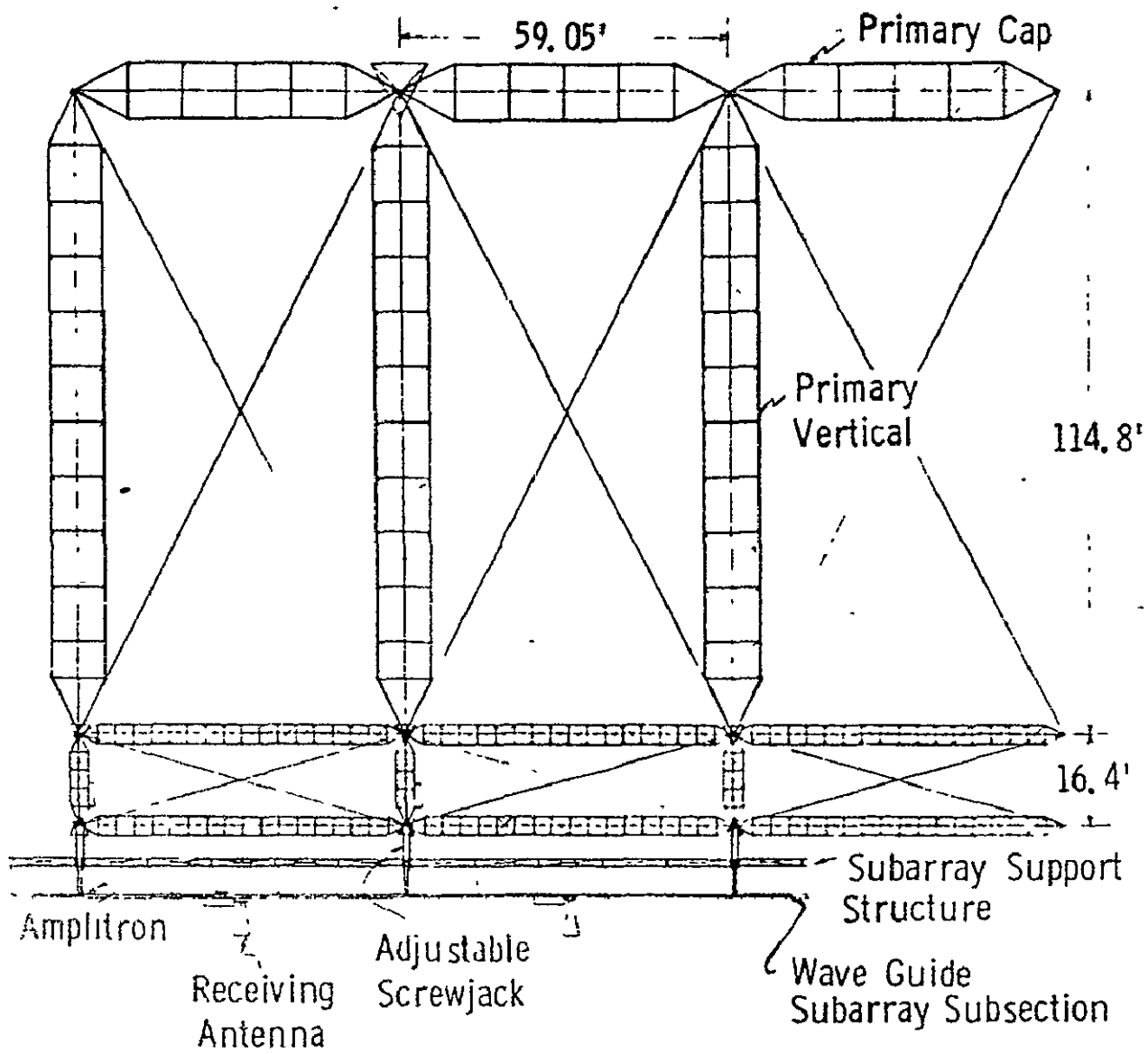


Figure 4. - Raytheon/Grumman Antenna Cross Section

ORIGINAL PAGE IS
OF POOR QUALITY

APP-V-A-1-6

Table I. - Key Antenna Design Differences

<u>Item</u>	<u>Raytheon/Grumman</u>	<u>Martin Marietta</u>
Support Structure	Two Tier	One Tier
Support Structure Depth	131.2 ft.	60 ft.
Support Structure Weight	1.1M lbs.	2.0M lbs.
Beam Sizes	(4) 114.8 ft. x 9 ft. max 16.4 ft. x 3 ft. min	(1) 56.2 ft. x 30 in.
Adjustment for Structural Tolerance	None	Adjustable beam intersections
Compatibility with Shuttle	Beams must be assembled in space	All beams less than 60 ft. long and collapsible

REFERENCES:

1. Final Report MCR-75-319 - Orbital Assembly and Maintenance Study, NAS 9-14319, Martin Marietta Corporation, Denver, Colorado, August 1975.
2. Final Report NASA CR-134886-ER75-4368 - Microwave Power Transmission System Studies, NAS 3-17835, Raytheon Company, Sudbury, Mass., December 1975.

APPENDIX V-A-2

CONSIDERATION OF JOINING PROCESSES FOR SPS CONSTRUCTION

J. D. Medlock
Structures & Mechanics Division

Introduction

Joining processes suitable for use during in-space construction of the Satellite Power System (SPS) are highly dictated by the type of materials being joined. The following candidate materials are being considered for use, and will require reliable processes for joining them to each other and to other materials.

1. Graphite composites (epoxy, polysulfone, polyimide, etc. matrices)
2. Aluminum alloys
3. Beryllium/aluminum composites
4. Polyimide (Kapton) and polyester (Mylar) films
5. Polyamide (Kevlar 49) cables
6. Thermal control coated materials
7. Electrical conductive systems

Although there are many joining processes adequate for use on these materials in a terrestrial environment, the application of joining processes in the space environment requires additional consideration. The effects of vacuum, temperature extremes, radiation, and zero gravity fabrication difficulty must be fully investigated. The fact that electrical power is readily available to provide energy requirements for the joining process tend to favor electrically powered joining techniques.

The following sections discuss candidate joining requirements and methods for joining materials proposed in the SPS construction.

Joining Requirements

The major structural joining requirements for the SPS reference configurations involve graphite composite materials. The graphite/binder matrix material in "green" tape form, may be heated (activated), shaped, and cured in a continuous process to produce structural beams. Because of the high volume of structure required in a relatively short time, automatic equipment for high-speed wrap and joining fabrication of the structure is presently visualized as a necessity, although manual operations for equipment maintenance, specialized repair, alignment, etc., will probably also be required. The maximum anticipated exposure temperature (500°K on the antenna structure) indicates that the fabrication/joining of the graphite composite can be accomplished with epoxy

or thermoplastic resin matrices and adhesives. For higher temperature requirements, high temperature resistant resins (i.e., polyimide) will be required which could result in more complex, heavier, and higher temperature resistant fabrication and forming equipment.

The joining of the nonstructural elements of the SPS comprise the majority of the fabrication requirements on the SPS. Attachment of the solar reflectors (aluminized polyester or polyimide films) to each other and to attachment structural interfaces presents some problems. Heat joining of polyimides films (Kapton) which do not exhibit melting or softening properties, require an intermediate film or coating such as FEP fluorocarbon (Teflon) which does "soften" sufficiently to facilitate bonding.

The only significant metal joining requirement on the SPS is the antenna waveguides which are fabricated from aluminum alloy. The waveguides must be accurately fabricated into rectangular tubular sections, requiring full length continuous seam joints in each element. Welding these joints using resistance or ultrasonic welding techniques are two potential fabrication methods for accomplishing this task.

In reviewing joining processes for use in the space environment, past studies have been concentrated on metals joining. In 1966, Hughes Aircraft conducted a study on "Space Environment Fabrication and Repair Technique" (Contract NAS 9-4546), and Hamilton Standard developed a "Hand-held Electron Beam Welding Gun" (Contract NAS 9-4501) under contract to NASA-JSC. In 1968, Westinghouse produced a battery powered electron beam welder under contract to NASA-MSFC which was subsequently evaluated and tested in orbit during a Skylab mission. In 1969, Battelle conducted a study on "Feasibility of Resistance Welding in Hard Vacuum" (Contract NAS 8-21196) with NASA-MSFC. The results of these studies concluded that resistance welding and electron beam welding were both viable candidates for the joining of a variety of metals in the space environment.

In contrast, there has been very little work done in developing joining techniques for non-metal materials for in-space fabrication until recently. Recent advancements in composites for structural use for aerospace/aircraft programs reveal that the high strength, low density, composites definitely promise advantages for in-space structures that metals cannot meet. "Tailoring" of graphite composites to produce "almost" zero coefficient of thermal expansion, for example, is one prime requirement which is desirable if large continuous space structures are to endure the thermal cyclic extremes experienced in space.

In summary, methods for joining metals in the environment of space are well advanced when compared to non-metals. However, the apparent advantages of non-metals such as graphite composites, require that suitable joining techniques be developed to allow the efficient fabrication of non-metals for space structures.

Nonmetallic Joining Processes

Since the joining requirements for the SPS primarily involve nonmetallic materials, processes for the joining of non-metals (or plastics) generally fall into four common categories: hot gas welding, friction welding, heated tool welding (contact welding), and ultrasonic welding. Of these four categories; only contact welding and ultrasonic welding appear feasible for application to SPS construction.

Heated tool welding is essentially a process which could be used to activate "green" tape graphite composite during layup fabrication. The joint is held at activation temperature under slight pressure (with forming rollers or dies, for example), and cooled to maintain the shape and provide the desired joint. Although heated tool welding can possibly be used for activating thermosetting materials (e.g., most epoxies and polyimides), its primary use has been in the joining of thermoplastic materials (e.g., polysulfones) for commercial uses. The heated tool welding is highly successful for joining thin flexible sheets or films (e.g., polyamides).

Ultrasonic welding is a fairly new method used for joining plastic parts, and is particularly useful for joining thermoplastic materials. This technique is a thermal bonding method that welds parts with frictional heat generated in the joint by mechanical vibrations at ultrasonic frequency. Typical commercial ultrasonic welding systems for plastics converts 60 Hz electrical energy into 20,000 Hz mechanical energy. Welding between joints is very rapid (fractions of a second), and therefore does not degrade the strength of material adjacent to the weld. Joint design is very critical in bringing the material to melting temperature by optimizing the vibratory energy. One of the many advantages of ultrasonic welding is that completely automatic joining systems can be utilized. A particular advantage for ultrasonic welding on SPS is that metals as well as nonmetals, can be joined efficiently with the process.

Metallic Joining Processes

As presently conceived, the SPS reference configurations contain a minimum of metallic materials, primarily aluminum alloy for the antenna waveguides. Candidate joining processes for joining aluminum include resistance welding, ultrasonic welding, and perhaps electron beam welding.

As previously mentioned, much work has been devoted in the past to developing electron beam welding techniques and equipment for in-space fabrication. One major advantage for using electron beam welding is that the process requires a vacuum environment (such as encountered in space) for its operation. The major disadvantage (for SPS application)

of the process is that it does not adapt to joining nonmetallic parts, which comprise the major portion of the SPS components. Electron beam welding is a process which produces heat with a concentrated beam of high velocity electrons impinging on the surfaces to be joined. The rate of energy input to the work piece being joined is generally expressed by the following relation (Ref. Welding Handbook):

$$\text{Energy Input} = \text{Joules/Cm} = 0.394 \frac{VI}{S}$$

where: V = beam accelerating potential (volts)
I = beam current (amperes)
S = welding speed (cm/second)

Typical power requirements for electron beam welding 0.127 cm. thick aluminum alloy are 27,000 volts, 21 milliamperes, 3 cm/second, resulting in a power requirement of 0.19 kilojoules per linear cm. of weld. Electron beam welding has been used for welding fairly thin aluminum foils (≈ 0.02 mm.), but for all practicability considering the high volatilization of aluminum and precise electronic welding controls required, a lower limit of thickness for aluminum material is approximately 0.25 mm. Aluminum alloy thicker than 12.0 cm. has been successfully welded for terrestrial applications. One item requiring additional development before electron beam welding can be utilized for SPS construction is a flight type power supply for converting the available solar energy into high voltage welding energy for continuous operation and control of the space environment. In summary, electron beam welding does not appear to be a serious contender for SPS fabrication because of the limited amount of metallic materials requiring joint construction.

Resistance welding is another candidate method for joining metallic materials on SPS. Like electron beam welding, resistance welding is not adaptable to joining of the nonmetallic materials which comprise the major portion of the SPS. Spot, roll-spot, seam, and projection welding are the group of specific processes which fall under the heading of resistance welding. Resistance welding is essentially a joining process where the required heat at the joint is generated by the resistance offered through the work parts to the relatively short-time flow of low-voltage, high-density electric current. Force is always applied before, during, and after current application to insure electrical continuity and to forge the heated parts together. For SPS application (aluminum waveguides), the seam weld process, where a continuous weld is made consisting of a single weld bead or a series of overlapping spot welds, would probably be used. Regarding energy requirements for resistance welding, the majority of terrestrial welding equipment uses alternating 60 Hz current, with a voltage between 1.0 to 25.0, and a current of 1000 to 100,000 amperes. The heat generated in the work being welded (and in the weld electrodes) is expressed by (Ref. Welding Handbook):

$$H = I^2 RT$$

Where: H = total heat energy (watt-sec)
 I = current (amperes)
 R = contact resistance sum (ohms)
 T = time of current application (seconds)

Typical weld parameters for producing a continuous seam weld in 0.54 mm. thick aluminum alloy sheet lap joints are 24,000 amperes current, 8 spot welds per cm., 20 milliseconds time per weld, 245 kilograms weld force, producing a continuous weld at 1.7 cm per second. One big problem with resistance welding resulting from the required high weld currents is to provide sufficient cooling to the weld electrodes; this problem requires additional study before adapting resistance welding equipment to the space environment for SPS construction tasks.

Ultrasonic welding is another promising candidate for joining metallic materials on SPS. In fact, since nonmetallic materials (such as graphite composites with thermoplastic matrices) can also be joined using ultrasonic weld techniques, the possibility of having a single joining process applicable to all materials on SPS is extremely attractive. As defined previously, ultrasonic welding occurs by applying high frequency vibratory energy to the joint while the joint is under moderate low static force. Although the precise mechanism by which ultrasonic welds are produced has not been completely established, it is theorized that very local slip between the workpieces to be joined expell foreign matter, permitting intimate metal to metal contact and joining at temperatures below the normal melting point of the material. The delivered vibratory energy degrades to moderate heat energy which must be absorbed by the workpiece, but apparently the heat plays no significant role in the joining process. The power required to spot weld two metal sheets together is generally given as (Ref.: Welding Handbook):

$$E = KH^{3/2}t^{3/2}$$

where: E = electrical energy (joules)
 K = constant (600 for ceramic transducer system)
 H = Vickers microindentation hardness number of material
 t = thickness of sheet (cm)

For a 0.051 cm. thick aluminum alloy having a Vickers hardness of 40, approximately 110 joules of electrical energy is required to produce one spot weld by ultrasonic welding techniques. Continuous seam welds are produced by overlapping spot welds for the length of weld required.

Summary of Candidate Joining Processes

A review of various candidate joining processes for use on SPS construction indicate the following:

1. The availability of electrical power favors the use of electrically actuated joining processes.

2. The primary joining requirements apply to non-metallic materials; the only major metal joining requirement is the aluminum alloy antenna waveguides.

3. Ultrasonic welding, which can be used on both metals and non-metals, represents the best candidate for development for the SPS construction tasks.

APPENDIX V-A-3

PROPOSED CONSTRUCTION EXPERIMENT FOR SHUTTLE ORBIT FLIGHT

J. C. Jones
Spacecraft Design Division

One of the key concepts to construction of the SPS is the manufacture of continuous structural elements in space. JSC has studied this approach and developed concepts for machines capable of manufacturing lightweight structural elements. These data are summarized in the following charts.

OBJECTIVES - CONSTRUCTION EXPERIMENT

SPACECRAFT DESIGN DIVISION - EW

A. J. LOUVIERE 6/28/76



JOHNSON SPACE CENTER

ENGINEERING

- INITIATE DEVELOPMENT OF AUTOMATED FABRICATION OF VERY LARGE, VERY LOW DENSITY STRUCTURE FOR FUTURE SPACE SYSTEMS
 - FABRICATE A STRUCTURAL TRUSS, FROM ALUMINUM OR COMPOSITE MATERIAL, 0.2 TO 1.0 KILOMETER IN LENGTH
 - PERFORM ENGINEERING TESTS WHICH INCLUDE:
 - STRUCTURAL LOADING
 - STRUCTURAL DYNAMICS
 - THERMAL EFFECTS
 - DETERMINE EFFECTS OF FABRICATION RATES
 - DETERMINE STABILITY AND HANDLING CHARACTERISTICS AND TECHNIQUES

POSSIBLE ADDITIONAL

- USE THE STRUCTURE FOR LARGE ANTENNA (GIANT SYNTHETIC APERTURE RADAR, ETC.)
- ATTACH PROPULSION PACKS TO INVESTIGATE ATTITUDE CONTROL TECHNIQUES FOR LARGE SEMI-RIGID STRUCTURE

AUTOMATED FABRICATION OF STRUCTURE IN SPACE
PURPOSE

SPACECRAFT DESIGN DIVISION - EW

A. J. LOUVIERE 6-28-76



JOHNSON SPACE CENTER

- STRUCTURE OF PROJECTED FUTURE SPACE SYSTEMS (LARGE ANTENNAS, SOLAR POWER STATION, ETC.) IS CHARACTERIZED BY:
 - LARGE SIZE
 - LOW WEIGHT IN RELATION TO SIZE
 - REPETITIVE STRUCTURAL CONFIGURATION
- MANUFACTURE IN SPACE INSTEAD OF ON EARTH
 - REQUIRES MUCH SMALLER LAUNCH VEHICLE PAYLOAD VOLUME
 - ELIMINATES EFFECT OF LAUNCH LOADS ON STRUCTURAL WEIGHT
 - ELIMINATES FOLDING MECHANISMS & DEPLOYMENT DYNAMICS PROBLEMS
 - ELIMINATES ALL OR PART OF PROBLEM OF HANDLING AND JOINING LARGE SUB-ASSEMBLIES IN SPACE
 - IS PROBABLY ONLY FEASIBLE APPROACH FOR SYSTEMS OF KILOMETER SIZE
- AUTOMATION IS NECESSARY TO REDUCE TIME/COST TO ACCEPTABLE LEVELS

APP-V-A-3-2

ORIGINAL PAGE IS
OF POOR QUALITY

APP-V-A-3-3

DATA BASE FOR FUTURE PROGRAMS

SPACECRAFT DESIGN DIVISION - EW

A, J, LOUVIERE 6/28/76



JOHNSON SPACE CENTER

- INITIAL DATA AND TECHNIQUES WILL SERVE AS BASIS FOR FUTURE PROJECTS AND PROGRAMS
 - OPERATIONAL SHUTTLE SORTIE MISSIONS - FABRICATION OF LARGE, UNPRESSURIZED STRUCTURE
 - SPACE STATION - BASIS FOR DESIGN OF CONSTRUCTION FACILITY EQUIPMENT
 - SOLAR POWER STATION - BASIS FOR DESIGN OF LIGHTWEIGHT STRUCTURE, TRUSS CONFIGURATIONS, AND HANDLING TECHNIQUES FOR ASSEMBLY
- CONSTRUCTION EXPERIMENT WILL PROVIDE CAPABILITY AND TECHNOLOGY BASE AS A COMPLEMENT TO PREVIOUS REPAIR EXPERIENCES.

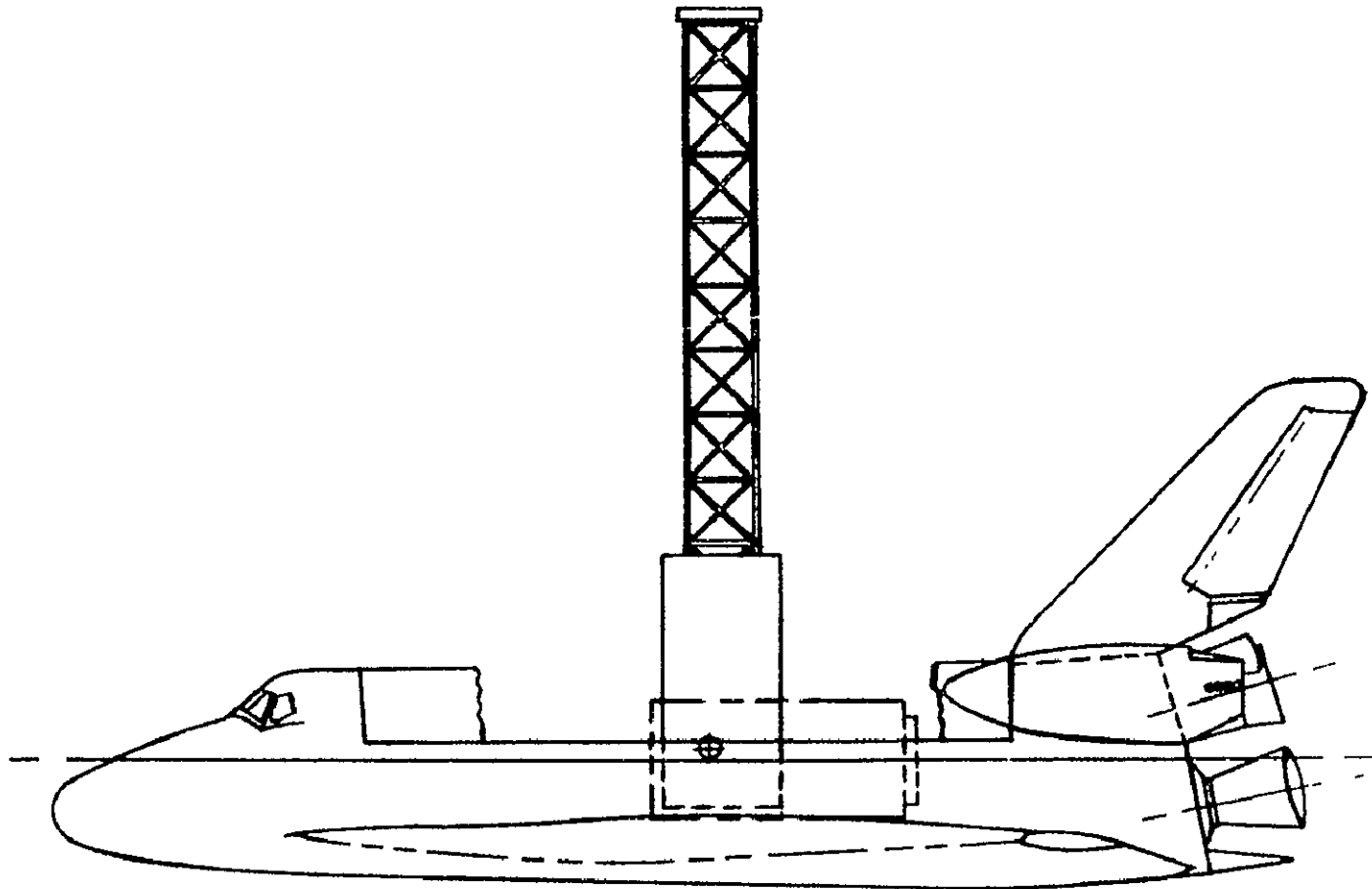
CONSTRUCTION EXPERIMENT - IN OPERATION

SPACECRAFT DESIGN DIVISION - EW

JAMES C. JONES 6-28-76



JOHNSON SPACE CENTER



APP-V-A-3-4

TRUSS STRUCTURE - REPRESENTATIVE CONFIGURATIONS

SPACECRAFT DESIGN DIVISION - EW

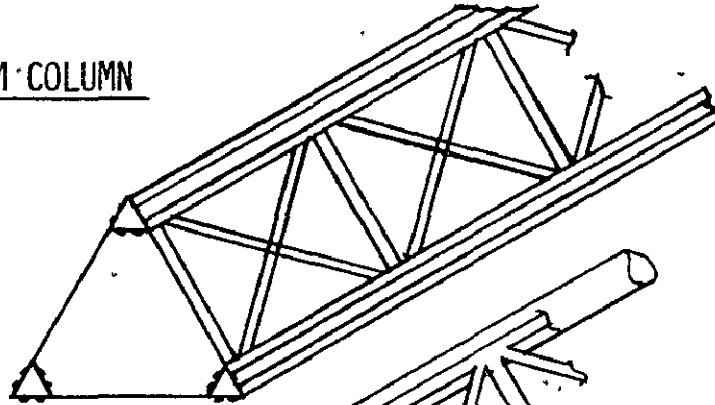
JAMES C. JONES 6-28-76



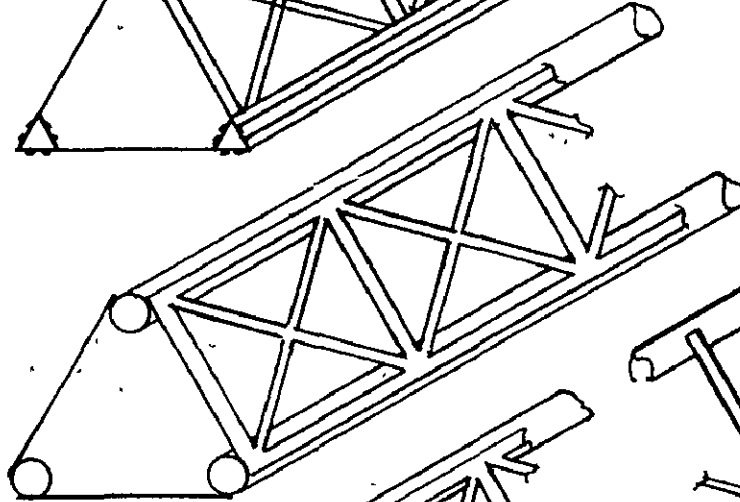
JOHNSON SPACE CENTER

COLUMN/BEAM COLUMN

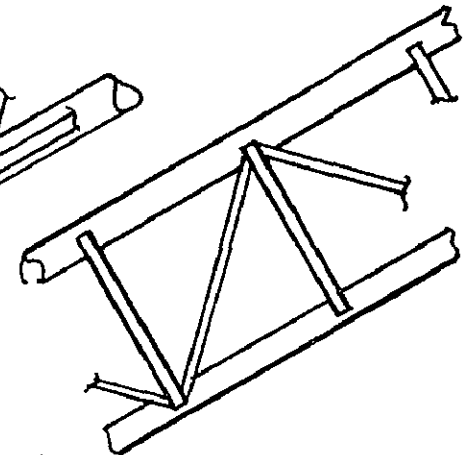
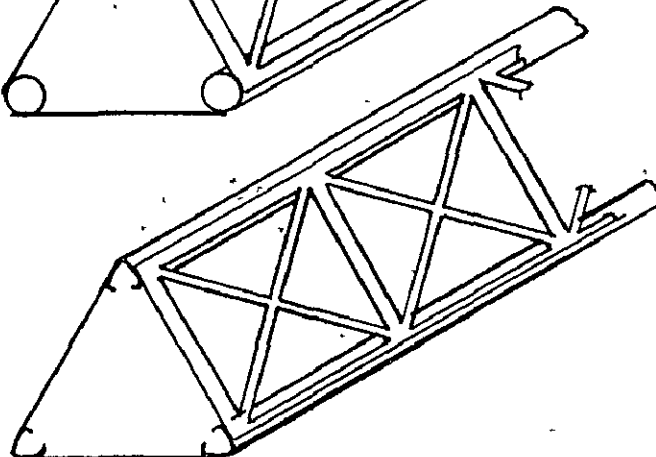
- BEADED TRIANGULAR CORNER TRUSS



- UNSTIFFENED TUBE CORNER TRUSS



- OPEN TRIANGULAR HAT CORNER TRUSS



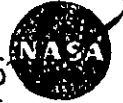
ALTERNATE
COMPRESSION
DIAGONALS

APP-V-A-3-5

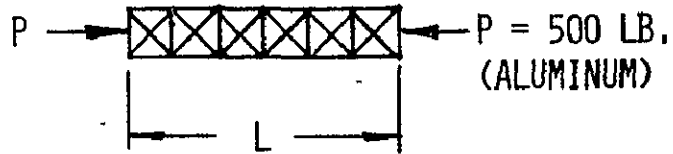
TRUSS STRUCTURE - REPRESENTATIVE WEIGHT

SPACECRAFT DESIGN DIVISION - EW

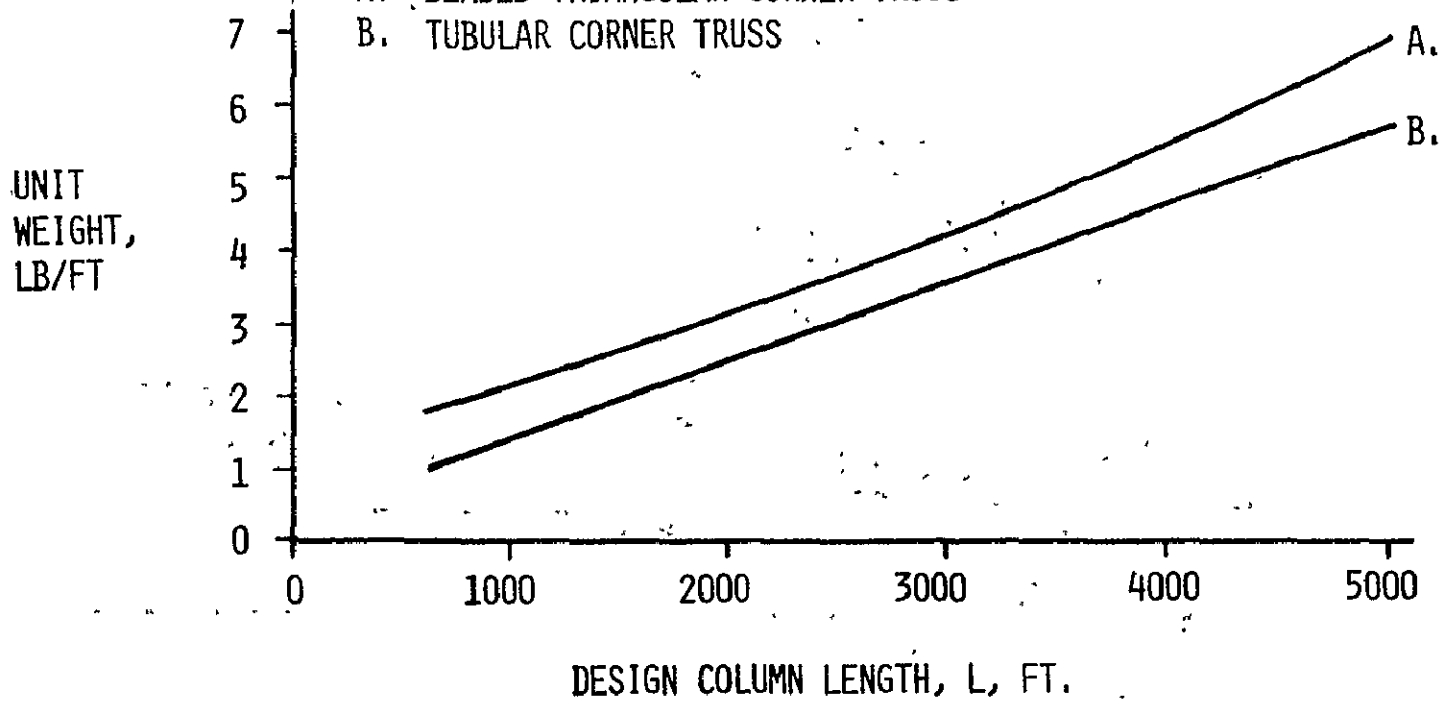
JAMES C. JONES 6-28-76



JOHNSON SPACE CENTER



- A. BEADED TRIANGULAR CORNER TRUSS
- B. TUBULAR CORNER TRUSS



APP-V-A-3-6

POTENTIAL OF COMPOSITES FOR
REDUCTION OF WEIGHT AND THERMAL DISTORTION

SPACECRAFT DESIGN DIVISION - EW

JAMES C. JONES 6-28-76



JOHNSON SPACE CENTER

- o WEIGHT PER FOOT DEPENDS ON " $\rho/E^{2/3}$ "
- o THERMAL DISTORTION DEPENDS ON " α "

MATERIAL	$\rho/E^{2/3} \times 10^6$	$\alpha \times 10^6$
ALUMINUM	2.1	12.6
GRAPHITE - POLYSULFONE (QUASI-ISOTROPIC)	1.1	~ 0
GRAPHITE - POLYSULFONE (UNIDIRECTIONAL)	.7	~ 0

SUPPLY/COST SITUATION FOR COMPOSITES

- AMPLE SUPPLY OF MATERIAL
- REASONABLE COST

APP-V-A-3-7

CONTINUOUS COMMERCIAL PRODUCTION PROCESSES
(POTENTIALLY APPLICABLE)

SPACECRAFT DESIGN DIVISION - EW

JAMES C. JONES 6-28-76



JOHNSON SPACE CENTER

PRODUCT

CANS, DUCTING, TUBING, SHAPES

AUTOMOBILES, ELECTRONICS,
AIRCRAFT, ETC.

FIBERGLASS & PLASTICS

PAPER

TEXTILES

PRODUCTION PROCESS

ROLL FORMING, SPIRAL TUBE FORMING,
SEAM JOINTS

AUTOMATED PARTS HANDLING
AUTOMATED ASSEMBLY
BONDING
BRAZING, WELDING
RIVETING, BOLTING

FILAMENT WINDING
EXTRUSION
PULTRUSION

STRIP WINDING
CORRUGATION

WEAVING, BRAIDING, SEWING

APP-V-A-3-8

ROLL FORMING

SPACECRAFT DESIGN DIVISION - EW

JAMES C. JONES 6-28-76



JOHNSON SPACE CENTER

- PROCESS OF CONTINUOUSLY SHAPING, USING ROLLERS, WITHOUT HEAT, DUCTILE MATERIAL



- SHEET OR STRIP
- SERIES OF FORMING ROLLS (MULTIPLE PASSES)
- VELOCITY UP TO 200 FPM
- HIGH QUALITY, CLOSE TOLERANCE
- THICKNESS .005" - .750"
- HOT ROLL THERMOPLASTIC

ROLL FORMING

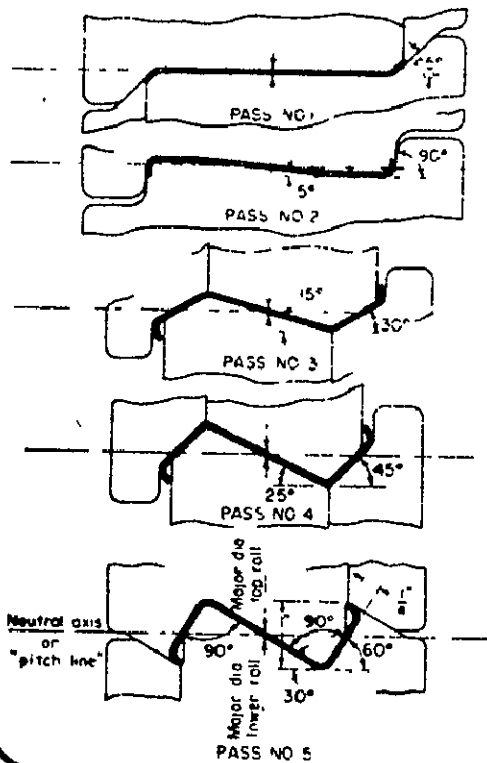
SPACECRAFT DESIGN DIVISION - EW

JAMES C. JONES 6-28-76

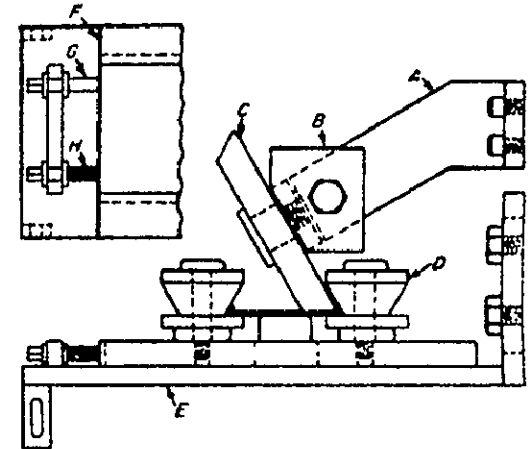


JOHNSON SPACE CENTER

SOME DETAILS ON ROLL FORMING



A ZEE SECTION PIECE IS SHOWN BEING FORMED IN STAGES, PASSING THROUGH 5 PAIRS OF SHAPED ROLLERS IN SEQUENCE.



A TYPICAL ROLLER SET-UP ON A PRODUCTION MACHINE

APP-V-A-3-10

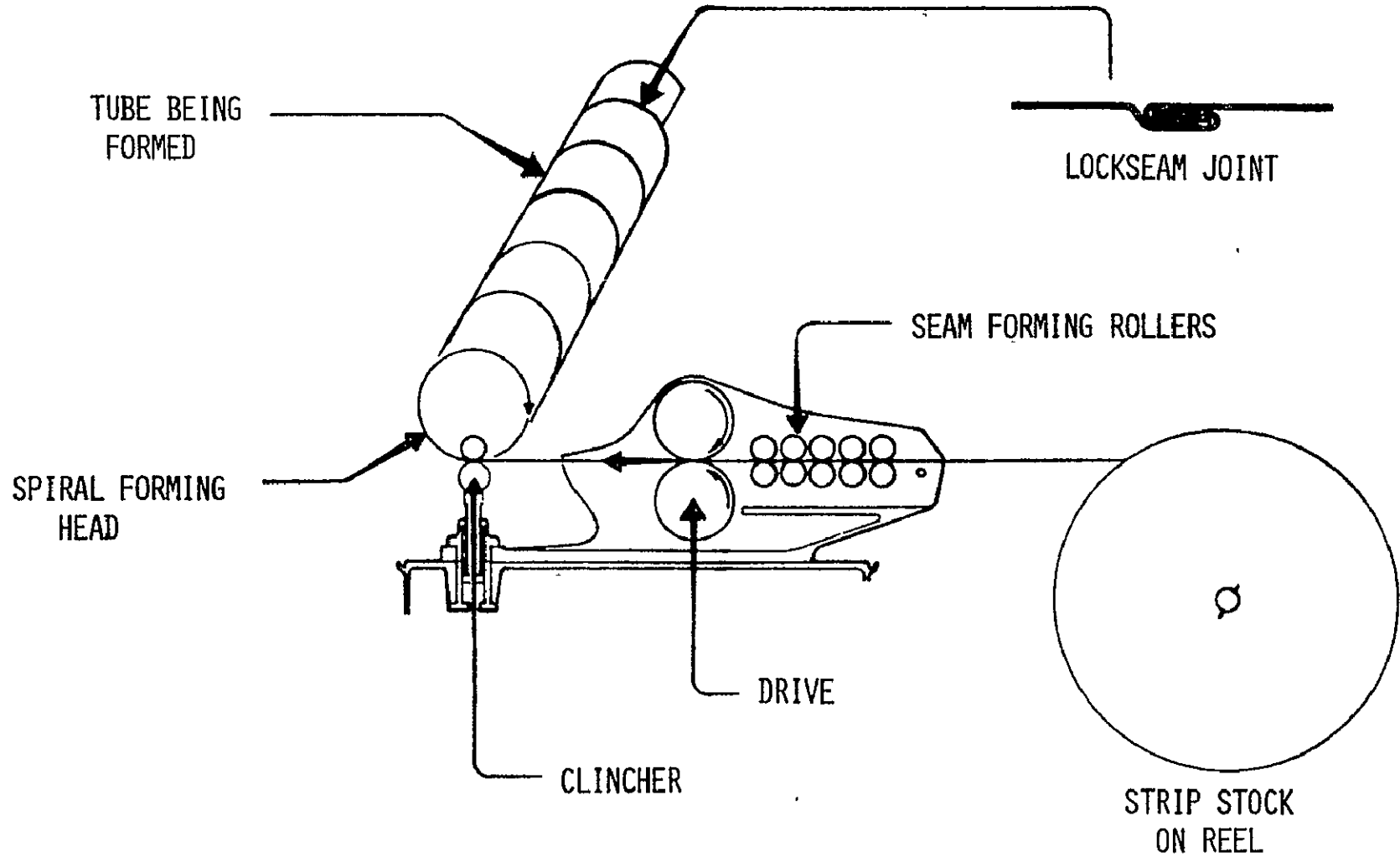
SPIRAL TUBEFORMING MACHINE

SPACECRAFT DESIGN DIVISION - EW

JAMES C. JONES 6-28-76



JOHNSON SPACE CENTER



APP-V-A-3-11

FORMING COMPOSITES

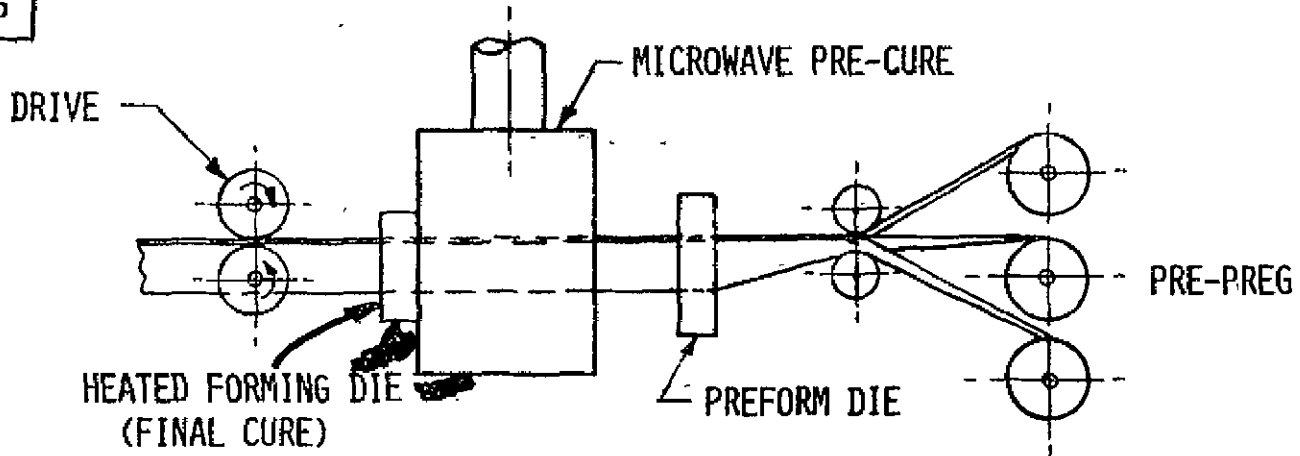
SPACECRAFT DESIGN DIVISION - EW

JAMES C. JONES 6-28-76

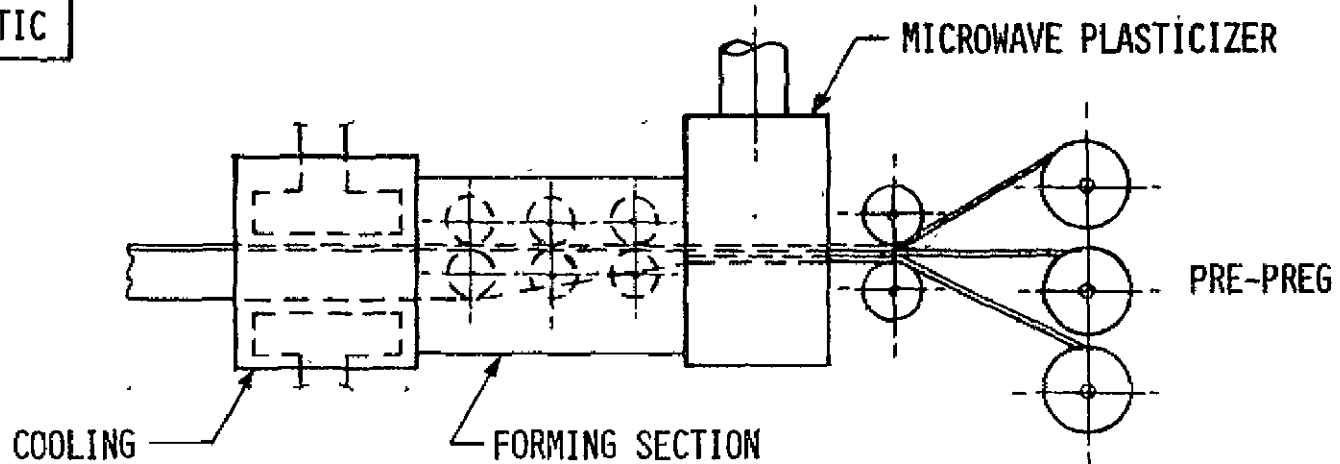


JOHNSON SPACE CENTER

THERMOSETTING



THERMOPLASTIC



APP-V-A-3-12

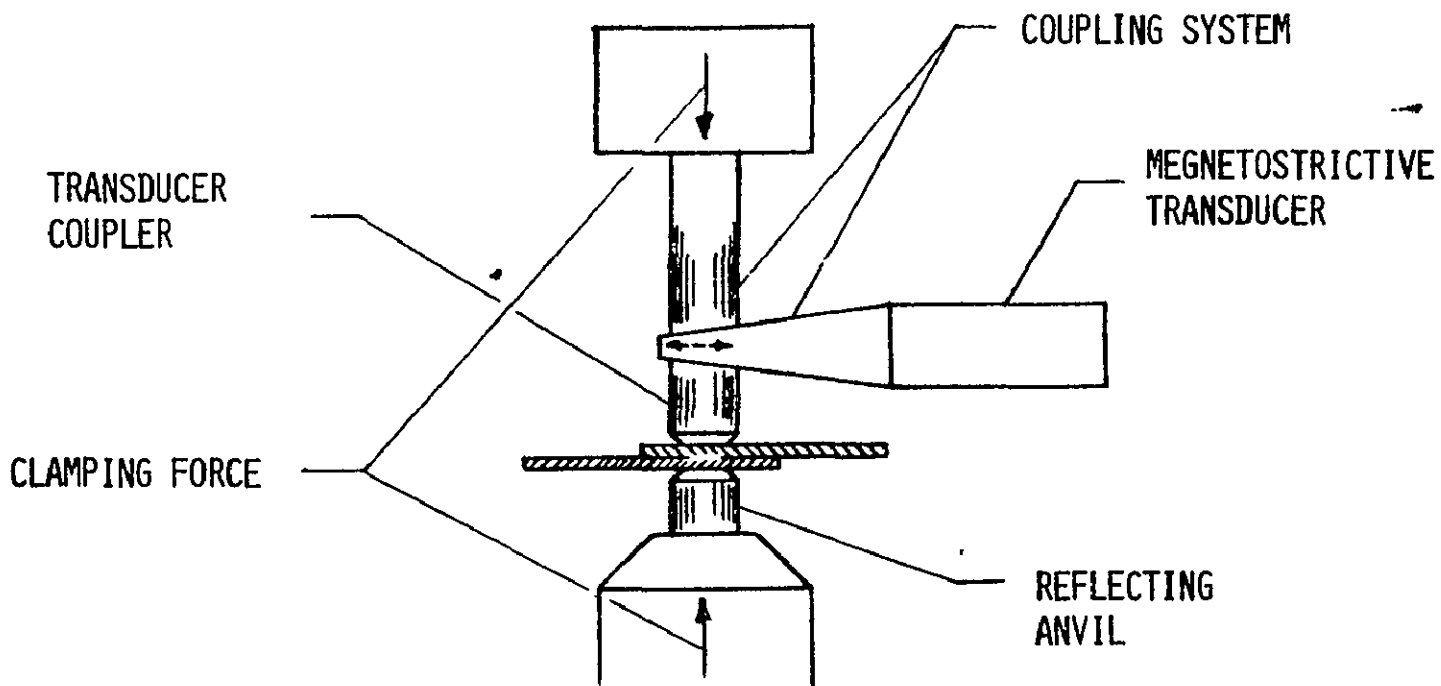
BASIC ULTRASONIC SPOT WELD
EQUIPMENT

SPACECRAFT DESIGN DIVISION - EW

JAMES C. JONES 6-28-76



JOHNSON SPACE CENTER



APP-J-A-3-13

ULTRASONIC WELD
INFORMATION

SPACECRAFT DESIGN DIVISION - EW

JAMES C. JONES 6-28-76



JOHNSON SPACE CENTER

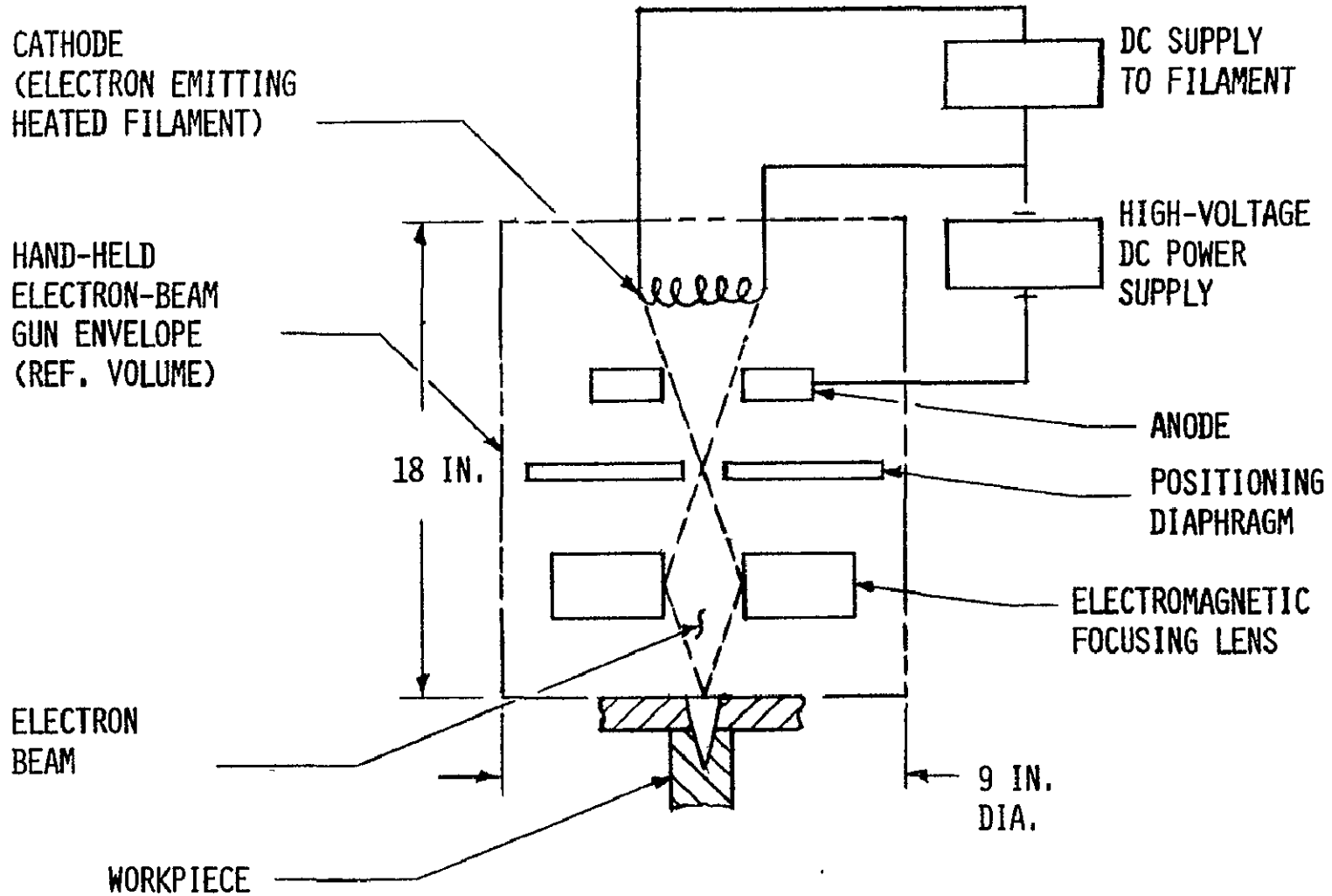
- A. PRINCIPAL OF OPERATION
 - 1. VIBRATES AT ULTRASONIC FREQUENCY WHILE UNDER PRESSURE
- B. TYPES OF WELDS THAT CAN BE MADE
 - 1. SPOT
 - 2. SEAM
 - 3. BUTT
- C. MATERIALS THAT MAY BE JOINED
 - 1. ALUMINUM
 - 2. COPPER
 - 3. CARBON STEEL (PROBLEMS WITH ALLOY STEELS)
 - 4. PLASTICS AND SOME DISSIMILAR METALS
- D. MATERIAL THICKNESS THAT MAY BE WELDED - .005 (FOIL) TO .093 IN.
- E. CONTROL REQUIREMENTS
 - 1. CLAMPING FORCE ON MATERIALS PER SPOT - 250 TO 1500 LBS.
 - 2. OPERATION POWER PER SPOT - 500 TO 800 WATTS (PULSE)
 - 3. WELDING TIME - .005 TO 2 SECONDS
- F. ADVANTAGES
 - 1. NO MARKED HEAT EFFECTS OR OUT-GASSING
 - 2. NO NEED FOR FLUXES OR SHIELDING GASSES

BASIC ELECTRON BEAM
WELD SYSTEM

SPACECRAFT DESIGN DIVISION - EW
JAMES C. JONES 6-28-76



JOHNSON SPACE CENTER



APP-V-A-3-15

ELECTRON BEAM WELD
INFORMATION

SPACECRAFT DESIGN DIVISION - EW

JAMES C. JONES 6-28-76



JOHNSON SPACE CENTER

A. TYPES OF WELDS THAT CAN BE MADE

1. SPOT
2. BUTT
3. FILLET
4. EDGE

B. SOME MATERIALS THAT MAY BE WELDED

1. ALUMINUM
2. MAGNESIUM
3. STEEL
4. SOME DISSIMILAR MATERIALS AND NON-METALS

C. POWER REQUIREMENTS

1. VOLTAGE OF 10 TO 150 KILOVOLTS
2. CURRENT OF 2 TO 20 MILLIAMPERES

D. ADVANTAGES

1. DEEP PENETRATION WITH MINIMUM DISTORTION
2. SHORT WELDING TIME WITH PRECISE HEAT CONTROL
3. WELD IN VACUUM ENVIRONMENT

E. DISADVANTAGES

1. REQUIRES PRECISE JOINT FIT FOR NARROW BEAM WELD
2. CREATES X-RAY RADIATION

THE ADHESIVE BONDING OF METALS
ADVANTAGES AND DISADVANTAGES

SPACECRAFT DESIGN DIVISION - EW

JAMES C. JONES 6-28-76



JOHNSON SPACE CENTER

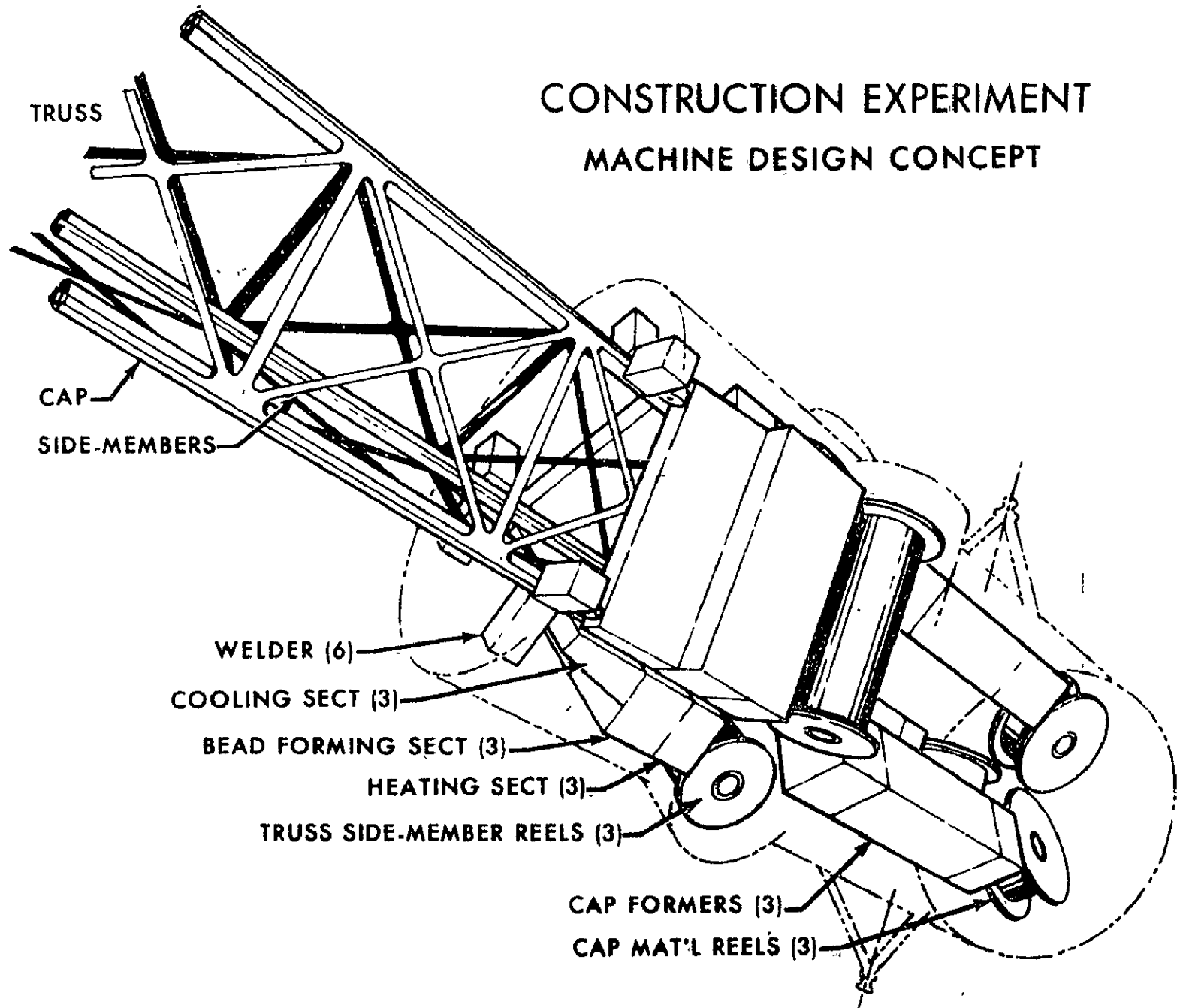
A. ADVANTAGES

1. FASTENS THE ENTIRE BONDING SURFACE WHICH ELIMINATES ANY LOCALIZED STRESSES.
2. FACILITATES CLOSE CONTROL OF WEIGHT DISTRIBUTION.
3. METALS WITH DIFFERENT COEFFICIENTS OF EXPANSION CAN BE BONDED WITH LOW MODULUS ADHESIVES.

B. DISADVANTAGES

1. THE DEGREE OF BONDING CANNOT BE DETERMINED.
2. CLEAN SURFACE IS ESSENTIAL FOR AN EFFECTIVE BOND.
3. HOLDING FIXTURES, PRESSES, AND OVENS ARE NECESSARY FOR MOST ADHESIVE BONDING.
4. MOST BONDING REQUIRES AT LEAST ONE HOUR OF CURING TIME.
5. HIGHER CURING TEMPERATURE GIVES HIGH TEMPERATURE RESISTANCE.

CONSTRUCTION EXPERIMENT MACHINE DESIGN CONCEPT



APP-V-A-3-18

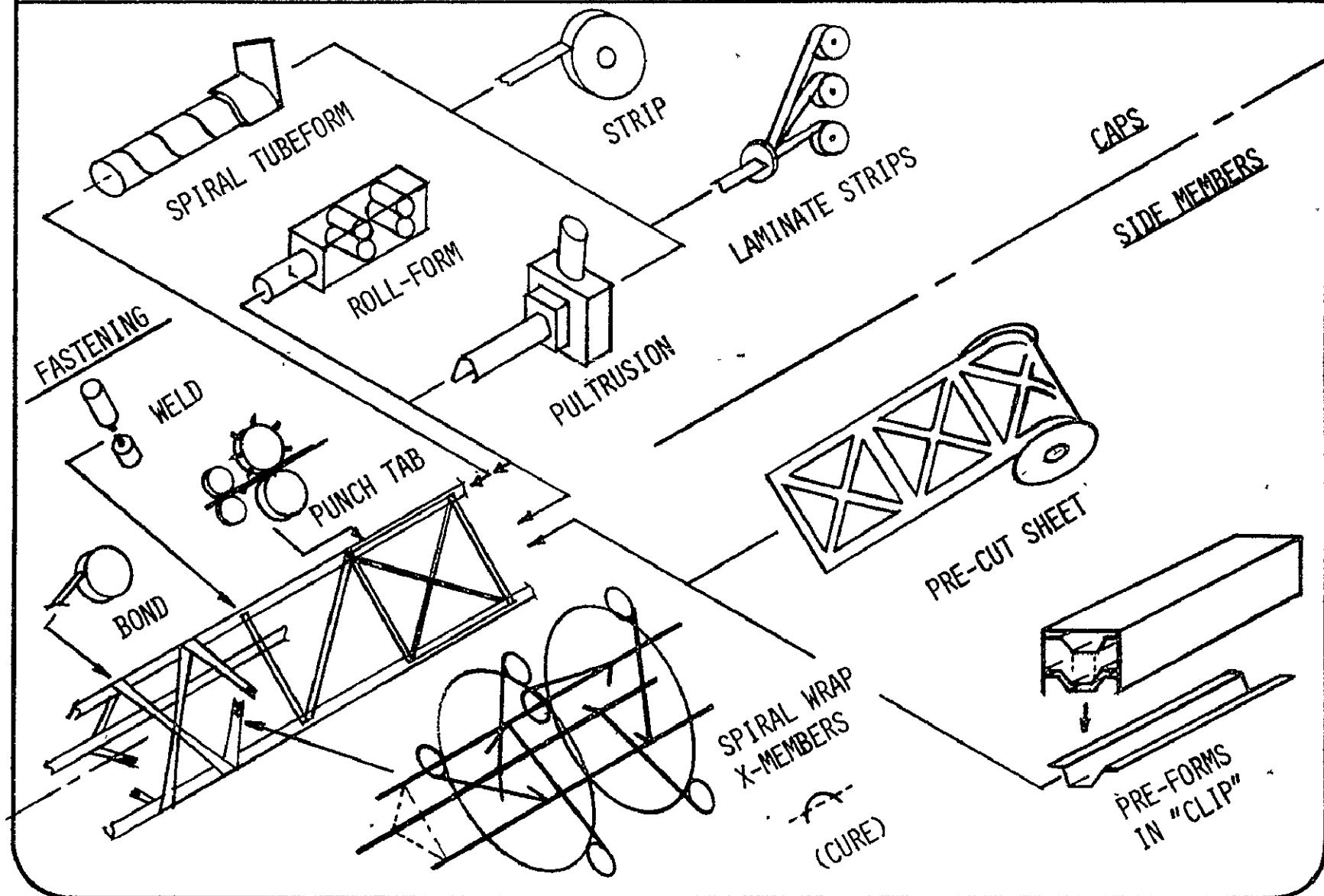
MACHINE DESIGN - PROCESS OPTIONS

SPACECRAFT DESIGN DIVISION - EW

JAMES C. JONES 6-28-76



JOHNSON SPACE CENTER



APPJ-A-3-19

CONSTRUCTION EXPERIMENT
DESIGN & INTEGRATION CONSIDERATIONS

SPACECRAFT DESIGN DIVISION - EW

JAMES C. JONES, 6-28-76



JOHNSON SPACE CENTER

MACHINE DESIGN:

GENERAL

- BUILDING TRUSS AT VELOCITY OF 0.5 IN./SEC. REQUIRES 24 HOURS TO BUILD 1 KM
- POWER REQUIRED PROBABLY LESS THAN 3 KW
- EXTEND TRUSS ALONG LOCAL VERTICAL (ATTITUDE CONTROL AND DYNAMICS PROBLEMS)
- MACHINE MUST BE DESIGNED TO APPROACH AEROSPACE STRUCTURAL EFFICIENCY (WEIGHT PROBLEM)

WEIGHTS

- MACHINE - - - - -	15,000 TO 30,000 LBS	OFT "BOGEY" WT. 22,000 LBS.
- TRUSS - - - - -	4,000 TO 7,500 LBS.	7,500 LBS.
- INSTRUMENT PKG - - - - -	<500 LBS.	500 LBS
		<hr/>
		30,000 LBS.

INTEGRATION WITH ORBITER

- 4 MAN CREW , WITH EVA CAPABILITY (FOR SAFETY ONLY)
- PAYLOAD WT. OF 30,000 LBS. (22,000 LBS. NORMAL ENTRY)
- 2 DAYS EXP. TIME, Z-LV ATTITUDE
- 3 KW ELECTRICAL POWER TO EXPERIMENT

APP-V-A-3-20

CONSTRUCTION EXPERIMENT - INSTL. IN ORBITER

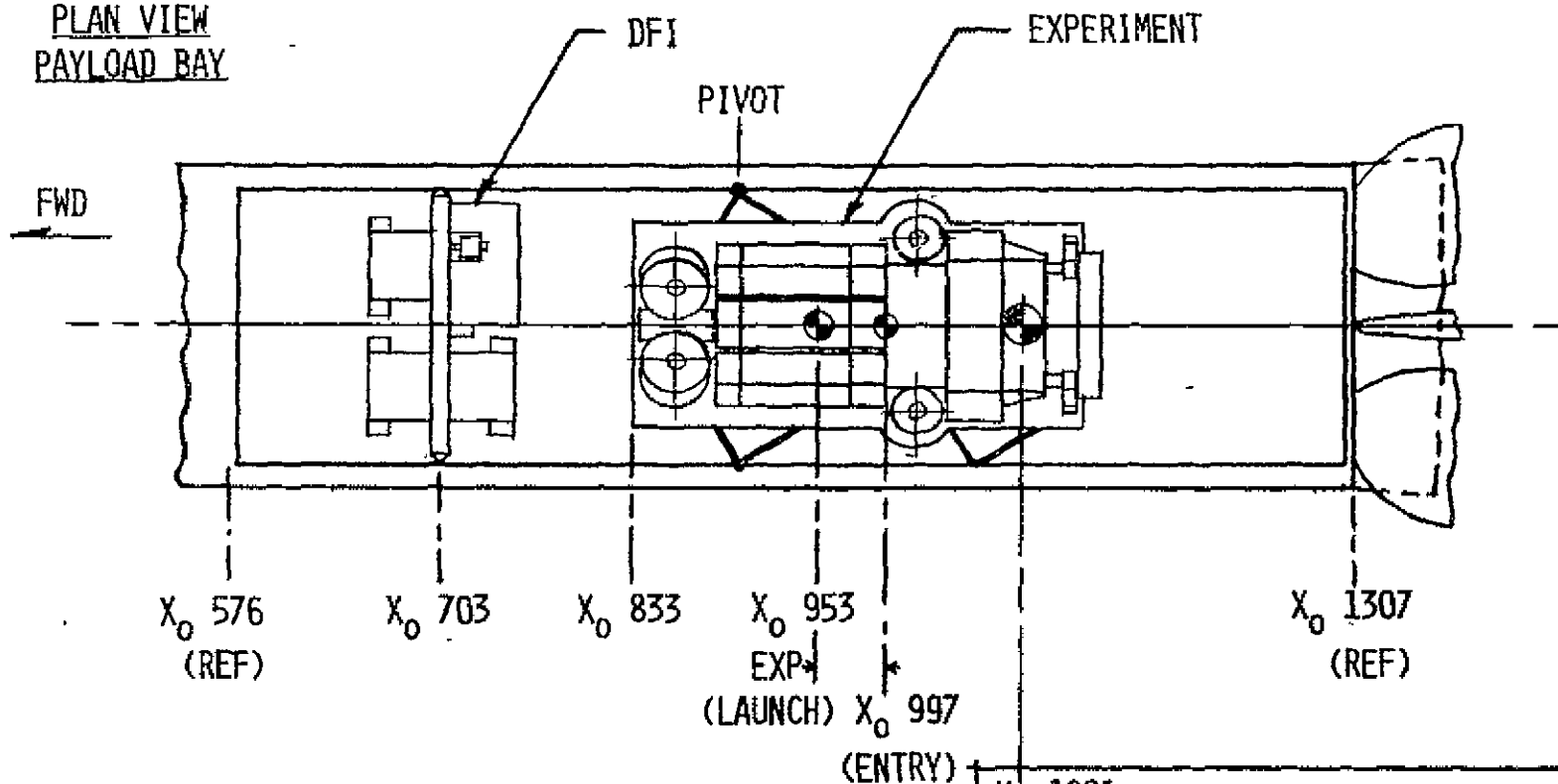
SPACECRAFT DESIGN DIVISION - EW

JAMES C. JONES 6-28-76



JOHNSON SPACE CENTER

PLAN VIEW
PAYLOAD BAY



X_0 1091

ORBITER ENTRY CG - 66.1% BODY LENGTH
(ALLOWABLE RANGE 65-67.5%)

APP-V-A-3-21

Construction base design is sensitive to the operational concept for its intended use in support of large structure manufacturing and design in a hostile environment. Crew size and associated support is a major driver in sizing the construction base. The early construction base located in LEO will most likely be a "pilot station" and therefore limited in crew size compared with the full size base located in GEO because of cost, functions, and operations considerations.

Base design requirements will be influenced by system safety analysis with respect to manufacturing and construction operations. Specific operations requiring analysis such as assembly operations, docking of transport vehicles, propellant transfer, maintenance operations, crew rescue, and radiation environment monitoring and emergency operations all contribute to design requirements.

The physical configuration of the SPS will also be a determining factor in construction base design. Considerations such as whether a portion of the construction base is free-flying or entirely attached to the SPS structure, the degree of subsystem support provided by each element of the base for the fabrication process, and the physical proximity of each element with respect to each other and the SPS structure must be considered.

Five major elements of the LEO and GEO orbital construction base are defined as follows:

1. Construction and Manufacturing Facilities
2. Orbital Construction and Support Equipment
3. Logistics Facility
4. Integration Management Facility
5. Crew Habitation Facilities

Each element contains equipment that is used to perform certain functions and tasks commensurate with the required step-by-step SPS sequential construction operations. Tables V-B-1 through V-B-7 list the functional elements, associated equipment, capability, and major systems needed for a LEO and GEO construction base. The five major elements, as listed above, are needed for both LEO and GEO construction bases. The major differences between the LEO and GEO construction and manufacturing facilities are due to the nature of the functions and tasks required for construction in the respective orbits. However, commonality of construction equipment should be used wherever possible in LEO and GEO for cost effectiveness and keeping crew training and man-machine interfaces within acceptable levels.

TABLE V-B-1 SPS FUNCTIONAL SUPPORT EQUIPMENT IDENTIFICATION
LEO CONSTRUCTION BASE

FUNCTIONAL ELEMENT	EQUIPMENT	CAPABILITY		SYSTEMS
		FUNCTION	TASKS/USE	
Construction and Manufacturing Facilities.	Antenna subarray manufacturing/construction and checkout.	Provides a shirtsleeve environment for crew during fabrication of antenna subarrays.	Construct and assemble solar concentrators and solar cell blankets. Assemble power distribution system. Package subarrays for transfer from LEO to GEO via COTV.	Required mechanical systems for assembly of concentrators, solar cell blankets, and electrical power distribution system.
	Antenna gimbal and ball joint assembly.	Provides capability for antenna and ball joint assembly.	Receive, align, assemble antenna gimbal and ball joint.	Required mechanical systems for assembly of components via crew monitoring.
	Central hub assembly.	Capability to assemble GEO work platform in LEO.	Assemble prefabricated parts. Erect folded structure. Grow structure members and assemble. Attach docking mechanisms.	LEO transportation system (Shuttle). HLLV. Manipulators. EVA Module.

ORIGINAL PAGE IS
OF POOR QUALITY

TABLE V-B-2 SPS FUNCTIONAL SUPPORT EQUIPMENT IDENTIFICATION
GEO CONSTRUCTION BASE

FUNCTIONAL ELEMENT	EQUIPMENT	CAPABILITY		SYSTEMS
		FUNCTION	TASKS/USE	
Construction and Manufacturing Facilities.	Primary structure manufacturing and construction.	Provides for direct fabrication of complex beam structures.	Crew monitoring and override capability of automatic operations. Materials loading. Welding. Cutting. Bolting. Assembly. Alignment. Rigging. Sequencing. Positioning.	Reel feed system. Heat source. Energy pack. Mandrel. Telemetry. Communications. ECLS, EVA. Lighting. Attitude control system. Docking ports. Automatic machinery. Inter-transit port.
	Antenna secondary structure manufacturing and construction.	Provides capability for manufacturing and assembly of antenna structure.	Same as above except tasks are for antenna construction.	Systems similar to above.
	Phasing network.	Provides for installation of phase control and waveguides.	Assemble phase control electronics and waveguides.	Mechanical systems for waveguide and phase control.

V-B-3

TABLE V-B-3 SPS FUNCTIONAL SUPPORT EQUIPMENT IDENTIFICATION

GEO CONSTRUCTION BASE

FUNCTIONAL ELEMENT	EQUIPMENT	CAPABILITY		SYSTEM
		FUNCTION	TASKS/USE	
Construction and Manufacturing Facilities (Continued).	Subarray to antenna structure attachment.	Provides method of positioning and attachment of subarrays to antenna structure.	Subarray unstow. Alignment. Attachment to antenna structure. Subarray replacement.	Automatic systems with crew monitoring and override capability.
	Cable positioning.	Provides capability of attachment of cables to primary structure.	Cable laying. Attachment. Torqueing. Cutting. Alignment.	Automatic systems with crew monitoring and override capability.
Logistics Facility.	Materials supply storage module.	Provides "warehouse" storage for logistics supplies, construction materials, fuels, spare parts inventory, and maintenance tools.	Construction materials and logistics receiving, storage, and distribution. Spare parts inventory. Fuel tankage storage. Construction equipment storage and checkout.	Rapid materials distribution system. Computer inventory. Safety/quality assurance. Specialized storage. Trolley vehicles. Emergency warning system.

V-B-4

TABLE V-B-4 SPS FUNCTIONAL SUPPORT EQUIPMENT IDENTIFICATION
GEO CONSTRUCTION BASE

FUNCTIONAL ELEMENT	EQUIPMENT	CAPABILITY		SYSTEMS
		FUNCTION	TASKS/USE	
Logistics Facility (Continued).	Docking port module.	Used as a loading/unloading "platform" for arriving and departing LEO-GEO vehicles.	Accommodates transit vehicles for docking and undocking operations. Payload transfer to storage module. Staging area for on call rescue vehicles.	Standardized docking ports/systems. Loads attenuation. Emergency release. Automatic control. Target alignment system.
	Docking/servicing maintenance module.	Provide vehicle and construction equipment docking, servicing, refurbishment, and maintenance services.	Maintenance and repair/refurbishment of LEO-GEO engines. Vehicle systems. GEO electronic sub-modules. Remote control manipulators. Fueling operations.	Electrical power. ECLS, EVA. Docking mechanisms. Electronic systems. Fueling systems. Maintenance systems. Payload handling and transfer.
	Transit system (attached trolley).	Provides transportation for personnel and materials.	Transport personnel and materials from habitat to work site and element to element within construction base. Emergency rescue.	Cable and track system. Electrical power. Communications. ECLS. Emergency escape. Lighting system. Vehicle control.

V-B-5

TABLE V-B-5 SPS FUNCTIONAL SUPPORT EQUIPMENT IDENTIFICATION
GEO CONSTRUCTION BASE

FUNCTIONAL ELEMENT	EQUIPMENT	CAPABILITY		SYSTEMS
		FUNCTION	TASKS/USE	
Crew Habitation Facilities. (Required at major work stations.)	Habitation modules.	Provides for shirt-sleeve environment for personnel and crew quarters for eating, sleeping, personal hygiene, medical, exercise, and off-duty relaxation.	Habitat systems ops. Housekeeping. Food preparation and cleanup. Equipment storage. Logistics. Resupply. Medical operations. EVA/IVA.	Air revitalization. Water management. Waste management. Personal hygiene. Galley. Lighting. Emergency. Audio Intercom, TV. Food storage. Radiation shelter.
	Subsystems module.	Contains subsystems for support and operation of habitat.	Maintenance and repair. CCTV. Consumables mgmt. Docking control. Communications mgmt. Activity scheduling.	Electrical power. Environmental control Life support. Data management. Communications. Stabilization/attitude control. Caution and warning.
	Power module.	Generates electrical power to operate habitat subsystems.	Convert solar energy into electrical energy. Provide system redundancy or backup power.	Solar collectors. Inverters. Switching control. Distribution bus.

V-B-6

TABLE V-B-6 SPS FUNCTIONAL SUPPORT EQUIPMENT IDENTIFICATION
GEO CONSTRUCTION BASE

FUNCTIONAL ELEMENT	EQUIPMENT	CAPABILITY		SYSTEMS
		FUNCTION	TASKS/USE	
Orbital Construction and Support Equipment (OCSE).	Antenna laser alignment.	Provides for dynamic alignment "flatness" of subarrays.	Operate laser. Activate sensors. Optical sighting.	Screw jacks. Rotating laser beams. Receiver sensors. Amplifier package. Electrical power.
	EVA module.	Provides free-flight capability for EVA crewmen and airlock capability.	Contingency operations. Rescue. Protects crewman from hostile space environment.	Manned maneuvering unit. Recharge system. Pressure suits. Tethers. Attitude/stabilization. Communications. Propulsion. Airlock.
	Manned remote controlled manipulators.	Provides shirtsleeve environment for remote controlled operations.	Man/machine interface. Grappling. Positioning. Locating. Alignment. Assembly.	Electrical power. ECLS. Manipulator controls. Communications. Grappling fixtures. Lighting system. Attachment and translation. Alignment targets. Docking system.

V-B-7

TABLE V-B-7 SPS FUNCTIONAL SUPPORT EQUIPMENT IDENTIFICATION
GEO CONSTRUCTION BASE

FUNCTIONAL ELEMENT	EQUIPMENT	CAPABILITY		SYSTEMS
		FUNCTION	TASKS/USE	
Integration Management Facility.	Communications network.	Provides voice, TV, TLM, and hardcopy for construction base elements and interface with other satellites, transportation system, and major ground facilities network.	Management of voice, TV, and intercom. Switching network. Maintenance scheduling. Logistics scheduling. Overall operations management.	Ground communication stations-STDN. TDRS's. Transportation com. Industrial stations.
	Information management.	Provides for overall construction base element data base, computer processing, and display of needed data.	Maintain data base, data processing, evaluation, and distribution. Data display generation. C.G. and weight mgmt. Solar flare monitoring and warning.	Computers-processors. Electrical power. Data bus. Input/output. Bus control. Display/control. Software.
	Mission and operation control.	Provides for centralized operations mgmt. of construction base activities and resources.	Mission logistics. Construction operation. Transportation and docking control. Activity scheduling. Consumables mgmt. Safety operations. Statusing. C.G. and weight distri. Laser alignment. Visual and telescopic.	Display/control console. Communications. Electrical power. Processors/IO. Data bus. Software.

V-B-8

V-B-1 Construction and Manufacturing Facilities

The Construction and Manufacturing Facilities provide the capability for direct construction operations. The crew monitors automated manufacturing and construction functions; however, the systems will be designed to provide a crew override capability in the event of systems malfunction.

The facilities consist of machines for fabricating the structural elements of the SPS collector system. Preprocessed stock is supplied to the machines and processed into structural truss members. These trusses, in turn, are then connected to form the larger trusses of the SPS primary structure. Cable rigging devices are also operated from the facility. Packages of solar cell blankets and collectors are positioned by equipment in the facility for deployment. The construction facilities also provide a means for connection and deployment of power distribution cabling.

Two construction facilities are used for antenna construction. Machines for structural fabrication and assembly will build the primary antenna structure and subarray support structure. Other machines will install antenna subarrays.

A portion of the construction facilities will contain a pressurized shirtsleeve environment which will be used for manufacture of the subarrays. This is conceived as an assembly line type of operation. Antenna subarray manufacture could be done in LEO, packaged and transferred to GEO via orbital transfer vehicles. This would reduce personnel logistics requirements for the GEO base.

V-B-2 Orbital Construction and Support Equipment

This is the equipment required to monitor the machines in the construction base, to service them, to inspect subsystem installation and to perform contingency operations. Manned remote controlled manipulators will provide a shirtsleeve environment for man-machine operations. Manipulators will be used for grappling, positioning, alignment, holding, and assembly of structural components. Conceptually there would be facility manipulators attached to the construction facilities and mobile manipulators with a capability for moving along the SPS structure.

EVA capability will be provided by an EVA module which houses all of the associated EVA equipment hardware, its checkout facility, recharge, stowage and donning facilities, and an airlock to gain access to the vacuum environment. Each module will support two to four men and their associated hardware to provide EVA capability on quick notice (24 hr/day). EVA will be used for contingency operation, rescue, and for equipment malfunction retrieval.

V-B-3 Logistics Facility

The Logistic Facility consists of a Materials Supply Storage Module, Docking Port Module, Docking/Service and Maintenance Module, and attached Transit System. The Logistic Facility's principal function is a "warehouse" in orbit to provide the capability for receiving, storage, and distribution of supplies, construction materials, fuels, spare parts, and maintenance tools. An efficient storage and distribution management capability will be needed in the Materials Supply Storage Module due to the magnitude of materials traffic.

The logistics of personnel and construction materials as they are required in different manufacturing facilities and locations about the SPS will require a sophisticated transit system. This transit system could be powered by rechargeable batteries or fuel cells.

The transport of personnel and materials about the column/cable configuration can be accomplished by three types of vehicles:

a. Personnel carriers - Sized to carry 25 people seated, 50 for emergency conditions. Each contains oxygen, water, and food for 50 people. The carriers could serve as a safe haven for protection in emergencies due to pressure loss in habitation modules.

b. Cargo carriers - Pallets which attach together forming a small train to transport containerized or packaged cargo.

c. Propulsion unit - To propel items a and b above and can be manned, unmanned, or computer controlled similar to the railroad system. (The propulsion units may be ganged together for large loads.)

A Docking Port Module will be an integral part of the Logistics Facility and will be used for loading/unloading and servicing arriving and departing orbital transfer vehicles. Payloads (materials and personnel) will be transferred from the Docking Port Module via the attached transit system to other elements of the construction base. The Docking Port Module will also serve as a staging area for on-call crew rescue orbital transfer vehicles.

Maintenance, repair, refurbishment, and servicing for construction equipment and vehicle systems will be done in the docking/servicing maintenance module. Fuel storage and fuel transfer operations will also be provided by this module.

V-B-4 Integration Management Facility

Because of the number of daily arriving and departing Orbital Transfer Vehicles, the displacement of construction base elements, timing of sequence of construction operations, and communications between

construction base elements, transportation vehicles, and ground, an "air traffic control center" will be needed to integrate all operations in orbit. This facility will provide a communications capability (voice, TV, TLM, etc.) to construction base elements, other satellites, transportation systems, and major ground facilities network. Activities such as maintenance scheduling, logistics scheduling, switching control, communications management, and solar flare caution and warning will be done in this facility.

A computer processing system will be needed to maintain a data base, data base processing, evaluation, and distribution. Center of gravity and weight management will be required for construction elements during construction buildup.

Centralization for overall mission and operations control for the construction base and its interfaces is a key element in the organization of the base. Mission and operation control will include activities such as transportation and docking control, construction activity scheduling, consumables management, safety operations, laser alignment, and mission logistics.

V-B-5 Crew Habitation Facilities

Crew Habitation Facilities consist of a number of types of equipment--the habitation module, subsystems module, and power module. The habitation modules will provide a shirtsleeve earth type environment for personnel at the eight major worksites. Eating, sleeping, and personnel hygiene functions will be done in these modules. Because of the large numbers of personnel required (200-800) for the GEO construction base, habitation modules will be needed for cafeteria, hospital, exercise, and off-duty relaxation type functions. Airlocks will also be needed for EVA/IVA operations.

The subsystem modules will contain the necessary subsystems for support and operation of the Construction Base. The power module is attached to or an integral part of the subsystem module. This module will provide electrical power to operate the required subsystems. Systems redundancy or backup power will be needed for reliability and safety reasons.

V-B-6 Construction Base Configuration Evaluation

The unique geometric configuration of the SPS column/cable influences the required relative grouping and location of Construction Base elements with respect to systems design, operation, and interface with other orbital elements. Therefore, a subjective comparison was made of five configuration alternatives (Figures V-B-6-1 through V-B-6-3) in an attempt to determine an optimum configuration with regard to established construction steps and techniques. A configuration evaluation

for the SPS truss configuration was not made since the geometry of the truss offers the capability of centralizing construction base elements.

Table V-B-6 shows the results of the column/cable comparison. Weighted values were assigned to 14 evaluation criteria. The criteria were given a weight value with respect to their importance for the configuration alternatives. A narrative description of each criteria is given below under the heading "Configuration Evaluation Criteria". Each evaluation criteria is given a rating of 1 through 5 for each configuration. The highest value is considered the "best" and the lowest value considered "poor". The total rating for each criteria is obtained by multiplying the weight value by the assigned rating number.

Configuration Evaluation Criteria

1. Facility Operations. Pre and Post SPS Construction

This item encompasses the level of overall efficient operation of the construction base, including interfaces with other orbital elements and transportation systems. Also, the degree of complexity of pre and post SPS construction with regard to construction base component buildup and subsequent base transfer to begin construction of other SPS satellites.

2. Traffic Pattern

This area includes the design for internal (attached to the SPS) traffic pattern as well as the external (detached) traffic pattern for moving personnel and materials within the SPS and to and from the ground.

3. Man-Machine Accessibility to SPS Elements

This item includes the ability of construction crews to have access to various SPS construction components during the buildup sequence. The access includes manned manipulator operations to SPS components and EVA/IVA for contingency situations such as equipment failure, maintenance and repair operations, and crew rescue.

4. Communications

This area pertains to communications, such as voice, TV, TLM, and intercom between construction base elements, transportation systems, orbital communications satellites, and the ground. The degree of base centralization vs. decentralization is also included.

5. Logistics

This item addresses the ease and/or capability to supply and maintain the construction base elements with construction materials, spare parts, and also to rotate large crews on a regular basis.

TABLE V-B-6 COLUMN/CABLE
GEO CONSTRUCTION BASE CONFIGURATION ALTERNATIVES

ITEM NO.	EVALUATION CRITERIA	WEIGHT	CONFIGURATION ALTERNATIVES									
			A		B		C		D		E	
			RAT- ING	TOTAL	RAT- ING	TOTAL	RAT- ING	TOTAL	RAT- ING	TOTAL	RAT- ING	TOTAL
1	FACILITY OPERATIONS. PRE AND POST SPS CONSTRUCTION	30	3	90	2	60	4	120	4	120	5	150
2	TRAFFIC PATTERN	28	1	28	1	28	3	84	4	112	5	140
3	MAN/MACHINE ACCESSIBILITY TO SPS ELEMENTS	26	3	78	3	78	3	78	3	78	3	78
4	COMMUNICATIONS	24	3	72	2	48	2	48	4	96	4	96
5	LOGISTICS	22	1	22	1	22	2	44	3	66	4	88
6	CREW SUPPORT CAPABILITY	20	3	60	3	60	2	40	5	100	5	100
7	TRANSPORTATION BETWEEN ELEMENTS	18	1	18	1	18	2	36	4	72	4	72
8	INFREQUENT DOCKING/UNDOCKING	16	1	16	1	16	2	32	3	48	4	64
9	CENTRAL CONTROL FOR SUBSYSTEMS	14	3	42	2	28	2	28	4	56	4	56
10	LESS DUPLICATION OF SYSTEMS AND MODULES	12	4	48	2	24	1	12	4	48	4	48
11	LOCATION FOR MAINTENANCE AND REPAIR OF SYSTEMS	10	4	40	4	40	5	50	5	50	5	50
12	ORBITAL EFFICIENCY	8	2	16	2	16	3	24	3	24	5	40
13	FACILITY INGRESS/EGRESS	6	1	6	1	6	4	24	3	18	4	24
14	LOCATION RELATIVE TO GROWTH FACILITIES	4	3	12	3	12	3	12	3	12	5	20
(HIGHEST VALUES ARE BEST)		TOTAL		548		456		632		900		1026

V-B-13

6. Crew Support Capability

This item includes crew support with regard to routine crew supplies, emergency resupply, and crew subsystem support for centralized vs. dispersed crew locations.

7. Transportation Between Elements

This area concerns the need and frequency of internal and external transportation between construction base elements due to SPS configuration complexity.

8. Infrequent Docking/Undocking

This item addresses the level of docking/undocking required during the SPS construction phase.

9. Central Control for Subsystems

This item concerns centralized vs. decentralized control for subsystem operation during SPS construction.

10. Less Duplication of Systems and Modules

This item concerns the level of systems and module duplication which should be kept to a minimum without compromising system efficiency.

11. Location for Maintenance and Repair of Systems

This item concerns location of maintenance and repair facilities during SPS construction and subsequent location during SPS operational phase.

12. Orbital Efficiency

This item concerns the initial and final locations of the entire construction base elements during the construction phases such that the overall control of the SPS can be enhanced with regard to reducing gravity gradient torques and attitude control propellant use.

13. Facility Ingress/Egress

This area relates to the ease or capability available for the crew to ingress/egress construction base elements such as emergency escape routes, EVA route, and facility to transportation system route.

14. Location Relative to Growth Facilities

This item regards the initial buildup configuration and facility add-on capability.

Construction and Manufacturing Facilities (CF)

Logistics Facility (LF).

Crew Habitation Facilities -(H) - Includes Subsystem and Power Modules

Orbital Construction and Support Equipment (OCSE)

Integration Management Facility (IMF)

<u>Configuration</u>		<u>Facility Grouping</u>
A	(H + IMF) Free-Flyer	(CF + LF + OCSE + H) Attached to SPS
B	H Free-Flyer	(CF + LF + OCSE + IMF + H) Attached to SPS
C	(H + IMF + CF + LF + OCSE) 6 attached to SPS - primary structure 2 attached to SPS - antenna structure	
D	(H + IMF + LF) 1 attached to SPS	(CF + OCSE + H) 6 - primary structure 2 - antenna structure
E	(H + IMF + LF) 2 attached to SPS	(CF + OCSE + H) 6 - primary structure 2 - antenna structure

Configuration A

Configuration B - same as Configuration A except
IMF located with each attached element

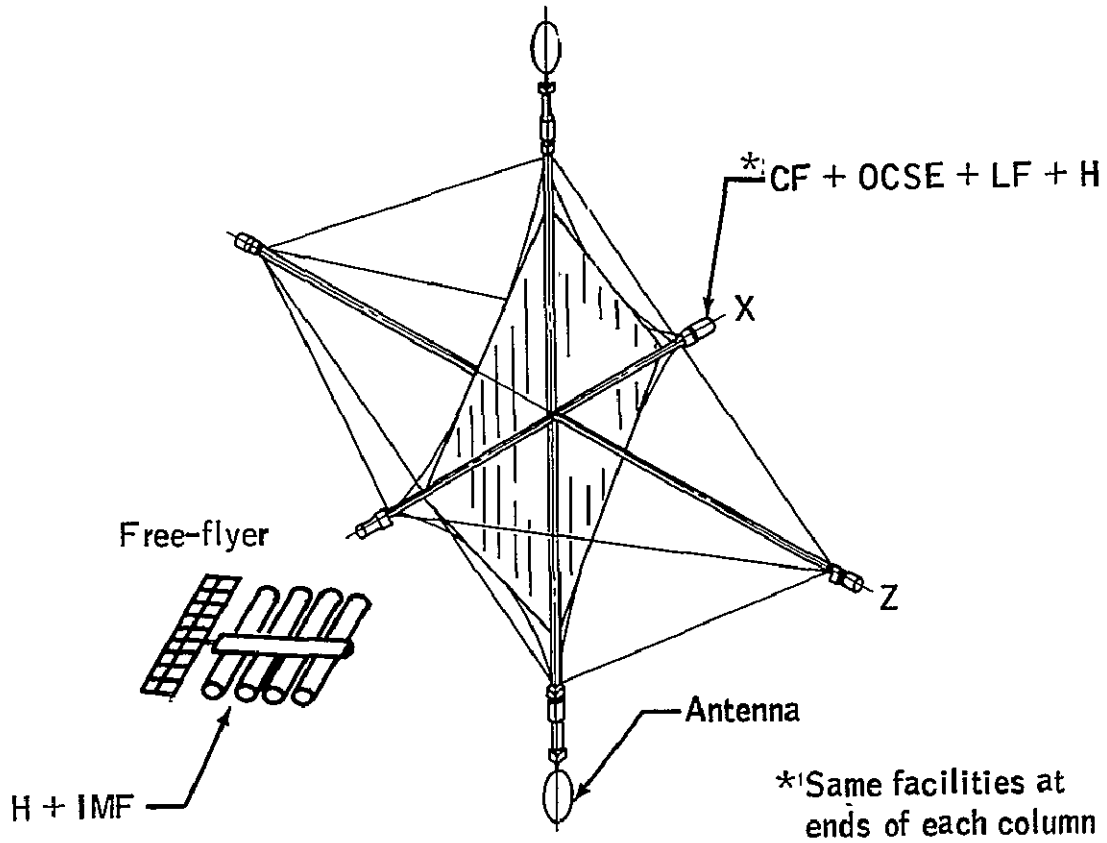


Figure V-B-6-1.-Alternatives to construction base approach for column/cable SPS.

Configuration C

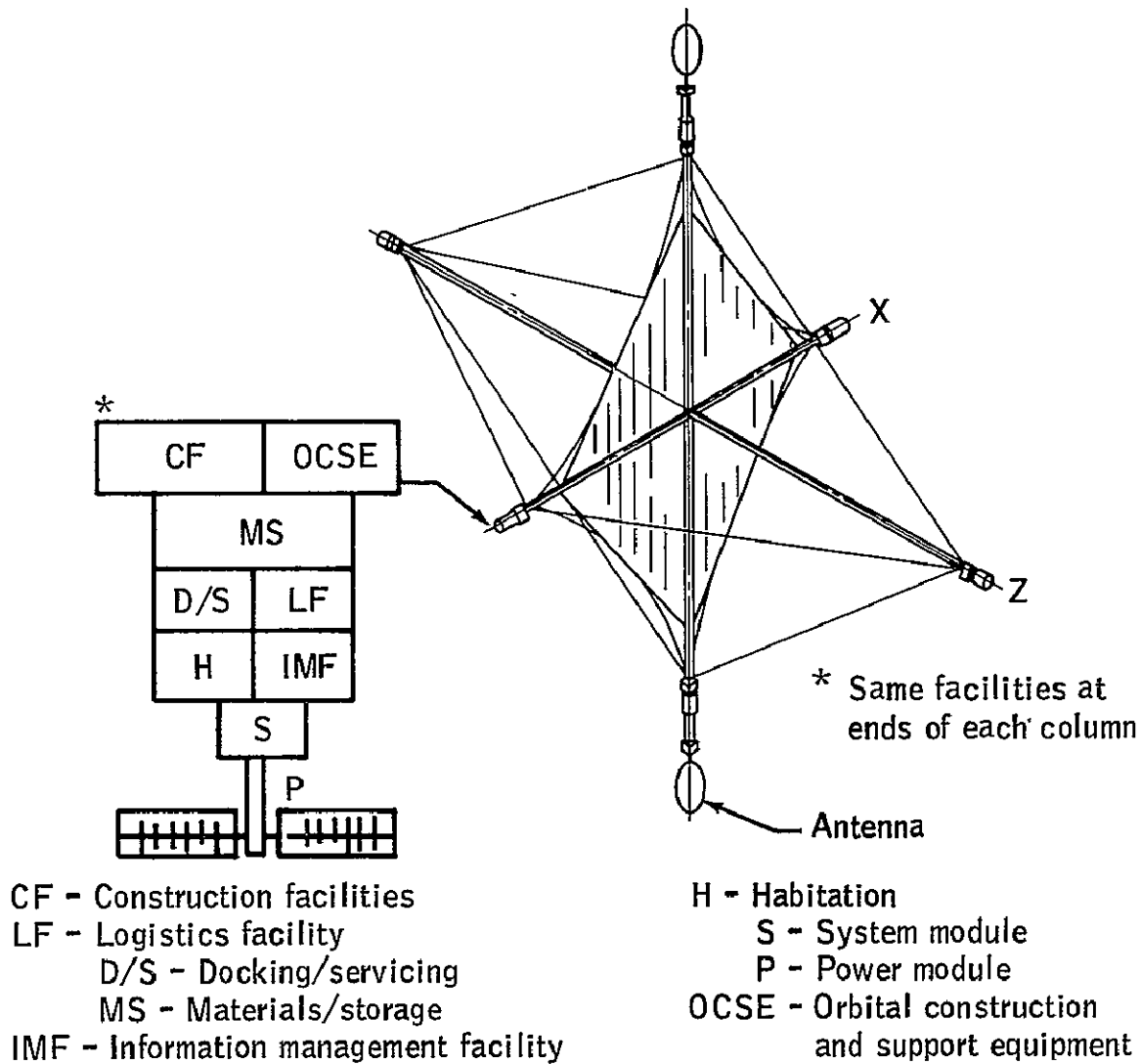
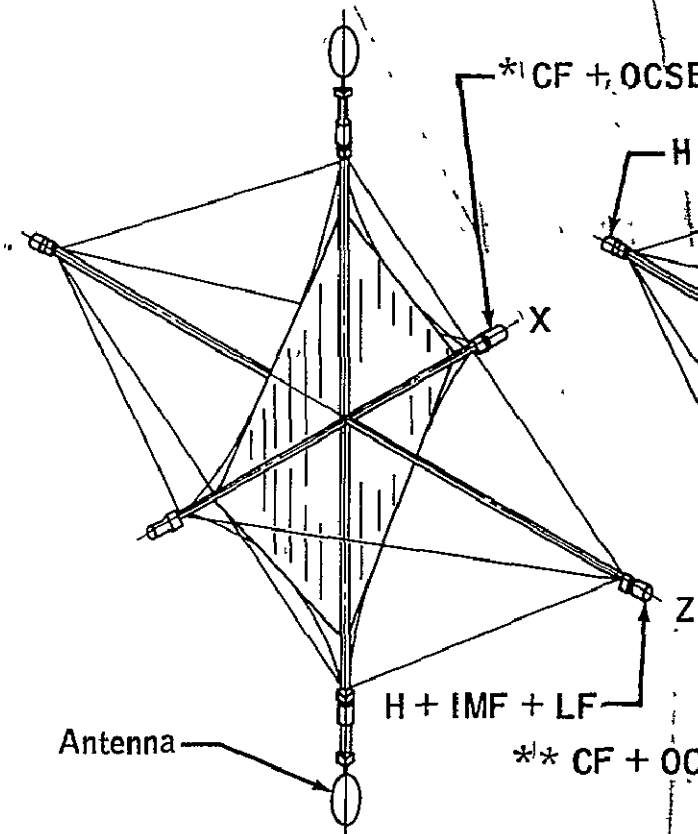


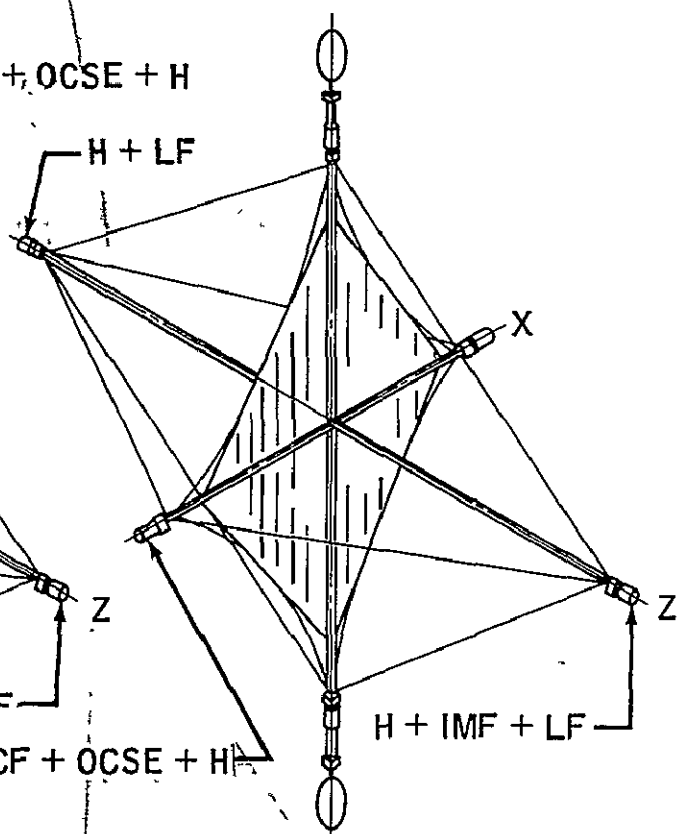
Figure V-B-6-2.-Alternatives to construction base approach for column/cable SPS.

Configuration D.



* Same facilities at 4 other locations

Configuration E



** Same facilities at 3 other locations

Figure V-B-6-3.-Alternatives to construction base approach for column/cable SPS.

1. Construction Base Organization and Staffing

The preceding section has outlined the methods used to evaluate several candidate configurations of support and habitability facilities that might be employed during the SPS construction phase. For the configuration selected as the most advantageous (Configuration E - figure V-B-6-3), this section will propose a candidate staffing plan and offer an initial method of employing the proposed cadre of personnel by developing the logic leading toward a work/rest cycle for the construction crews.

Assumptions: Certain assumptions are necessary to create a sufficiently stable base from which to make conjectures about the type of organization and quantity of personnel necessary to perform the on-orbit portion of the SPS construction task. The following assumptions were made to satisfy this requirement:

- Each construction base in GEO will have an autonomous organization unto itself.
- All modules needed to construct a base will be resident and attached to the base itself.
- Nominal construction activity will continue on a three-shift, 24 hr/day basis.
- The staffing plan is applicable to either the column/cable or the truss configuration from an organizational viewpoint and separate crew sizes are provided for each configuration.
- Crew staytime on-orbit is limited to 180 days.
- Sufficient personnel are required to staff four shifts for practically all positions so that off-duty time and contingency operations can be programmed into the schedule.
- Staffing buildup and trailoff are anticipated at the beginning and termination of the construction phase. There will not be a constant population at the site throughout the construction phase.
- Construction crews live at or in close proximity to their worksite.
- Considerable cross training will be required to minimize the on-orbit crew size.
- The staffing plans presented account for major automation in the construction process. Less automation could result in population increases of four or more times those proposed.

Base Organization: A contracted study conducted by Grumman Aerospace Corporation for JSC in 1971 (NAS 9-10951) evaluated numerous command structures for space stations and concluded that different organizations were appropriate for different operational situations. One of the suggested command structures, the line item concept (figure V-C-1), seems very appropriate for application to the SPS construction base. The line item is defined as a three-level command team structure consisting of a first level command, a second level of managers (the major functional element leaders) and a third intermediate level of assistants providing a direct line of communication between the managers and the working level personnel (first line supervisors and team members).

Command Function

The station director has the on-orbit responsibility for the entire project. His managers, acting on the authority delegated to them, carry out his decisions and direct activities within their cognizant areas.

Staff Function

The deputy is the second in command and as the leader of the staff function is responsible for providing the director with detailed information, advice and expertise.

Manager Function

These second level major functional element leaders have the authority and responsibility for implementation and completion of tasks in specific areas; i.e., construction/manufacturing, operations and support. They provide indepth problem solving ability to their subordinates.

Assistant Leader Functions

These third level intermediate management level positions narrow the responsibilities to a specific area and exercise technical control over the workmanship in their particular discipline through working firstline supervisory team members.

Communications

The station director communicates directly to his command team; i.e., deputy/staff and the three managers. Managers communicate with one another and their subordinate assistants but report such communications to the director, primarily to keep him informed of progress and so he can resolve conflicts as they occur. The assistants communicate directly with their third level leaders and subordinate first line supervisors and supporting personnel. The leader/follower relationships are

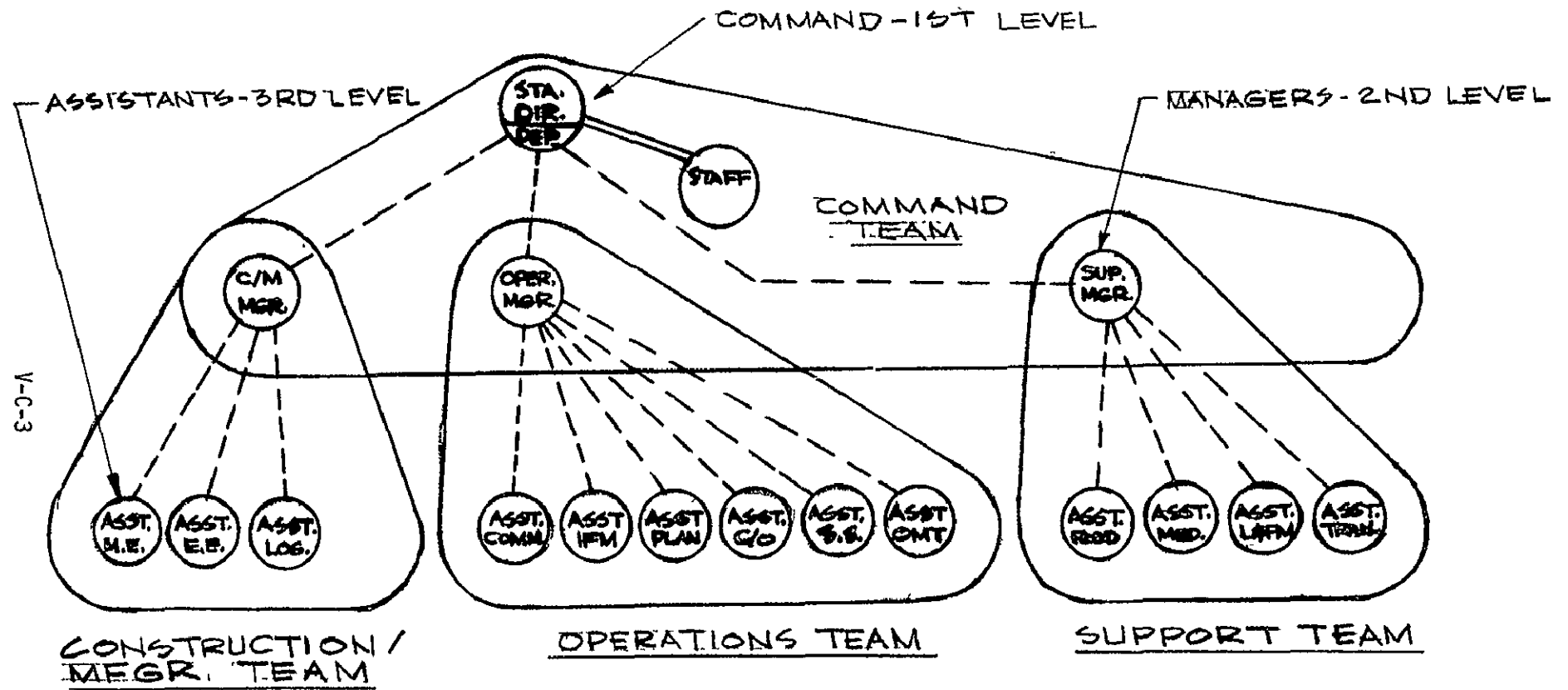


Figure V-C-1. Recommended Command Structure-Line Item Concept

likely to remain relatively stable due to the high degree of task specialization in this command structure. Crew interface can be handled directly at the intermediate leader level (assistants) and the director is brought into the loop in a dynamic way when a decision is required. Managers provide the director with periodic status reports so that when a decision is required, his information is valid and up to date.

The SPS construction project will be the most ambitious undertaking in space to be attempted. As such, multiple difficulties and new approaches, some not even conceived yet, will complicate the project's progress. Accordingly, sufficient personnel and organizational authority must be present on orbit to deal not only with the routine daily chores of construction and crew support, but to also handle the on-the-spot decisions necessary to solve realtime problems and keep the effort moving. Table V-C-1 shows a proposed organization for the GEO construction base. The accompanying staffing rationale is intended to give a preliminary assessment of management and personnel needs to staff a single SPS construction project. As shown, the organization assumes a fully functioning project following whatever buildup period that may be necessary to achieve full staffing.

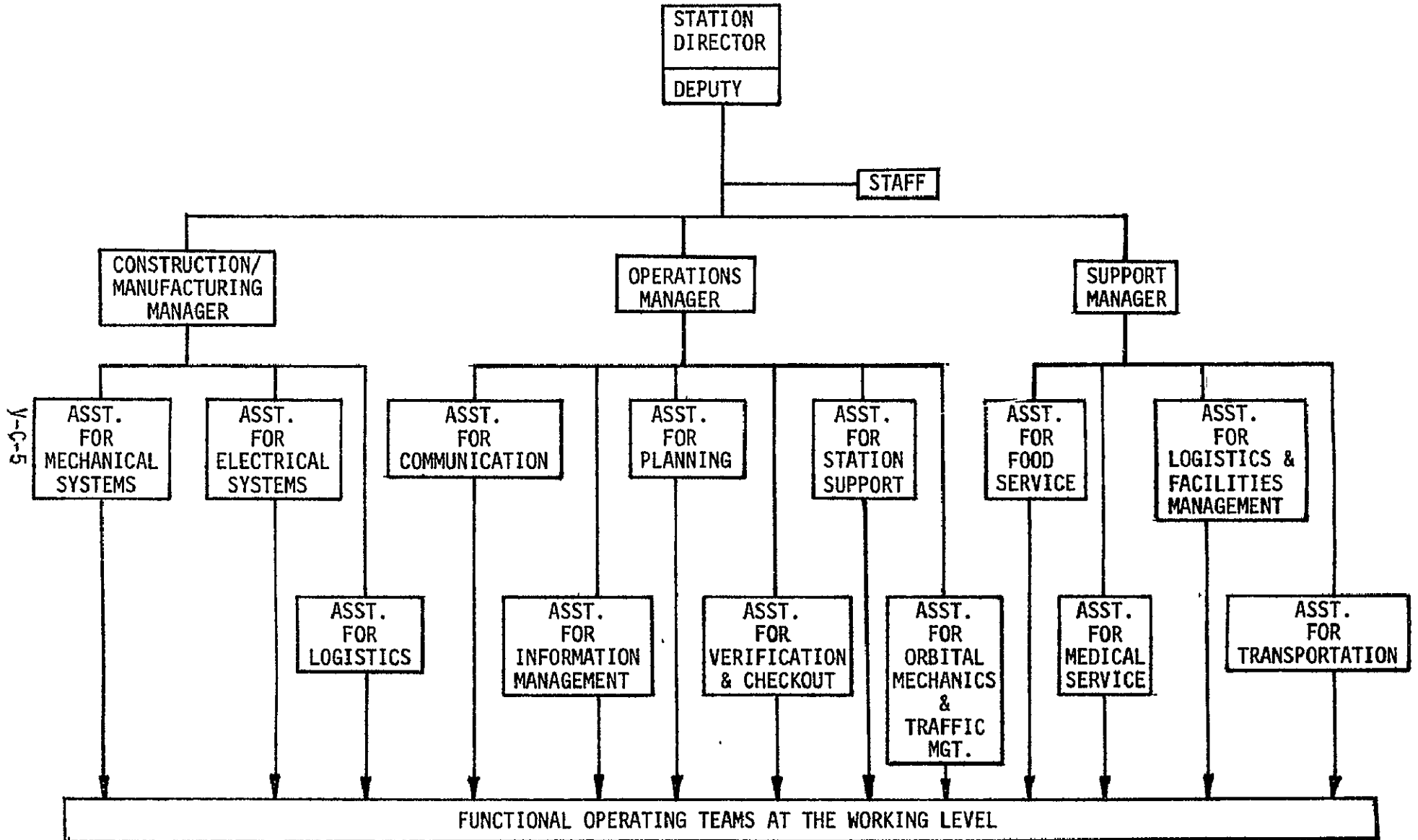
Each organizational element is explained in sufficient detail to enable the reader to understand the rationale behind the position and to have some appreciation for the staffing necessary to support the function (see Appendix V-C-1).

Construction Facility Work Schedule: Each construction facility will provide permanent living quarters for assigned workers in addition to providing the operator's and observer's stations for operating and monitoring the manufacturing and construction equipment. The living quarters will house four teams. The teams will work on an eight-day rotation consisting of six consecutive work days followed by a day of housekeeping activity and an off-duty day. The housekeeping day will insure that the living quarters will be subjected to a clean sweepdown and routine preventative maintenance tasks every other day. The off-duty day can be spent in the living quarters at the construction worksite or at the recreation facility in one of the major modules at one end or the other of the major non-array column.

The scheme of living at the construction worksite will greatly reduce the quantity and frequency of personnel transportation trips between centrally located living quarters and the worksites.

The timeline shown below will be repeated on a 8-day cycle throughout a proposed six month on-orbit stay time.

Table V-C-1. GEO Construction Base Organization



	DAYS															
	1	2	3	4	5	6	7	8	9	10	11	12	13	14	15	16
Crew 1	W	W	W	W	W	W	HK	OD	W	W	W	W	W	W	HK	OD
Crew 2	W	W	W	W	HK	OD	W	W	W	W	W	W	HK	OD	W	W
Crew 3	W	W	HK	OD	W	W	W	W	W	W	HK	OD	W	W	W	W
Crew 4	HK	OD	W	W	W	W	W	W	HK	OD	W	W	W	W	W	W

W - Work Day
 HK - Housekeeping Day
 OD - Off Duty Day

Operational Logic: An operational schematic for a construction base (column/cable) is shown in figure V-C-2 where the materials are delivered from LEO to GEO to the logistics facility and eventually transported to the worksites in order to perform the construction functions.

Construction Sequence: Figures V-C-3 and V-C-4 show the comparison of the column/cable and truss SPS configurations construction sequence over a 12-month work period including the major milestones of structure fabrication, solar cell blankets and concentrator sheets, and antenna construction. From the operational schematic and construction sequence are developed the numbers of machines, the number of operations, and the personnel requirements.

Equipment Requirements: Table V-C-2 tabulates the construction equipment requirements comparing the column/cable and truss configurations. The truss configuration requires twice as many beam building machines but less manned manipulators with all other equipment requirements quite similar.

Manpower Requirements: A very preliminary assessment of manpower needed to staff this organization indicated that approximately 150 persons were needed to man the construction, operations, and manufacturing portions of the job. Manpower requirements to staff the support area pushed the total on-orbit population to an estimated 228 persons as reflected in table V-C-3. Continuing refinements were made to the organizational and staffing requirements as more definitive information was developed with respect to configuration and construction techniques.

V-C-7

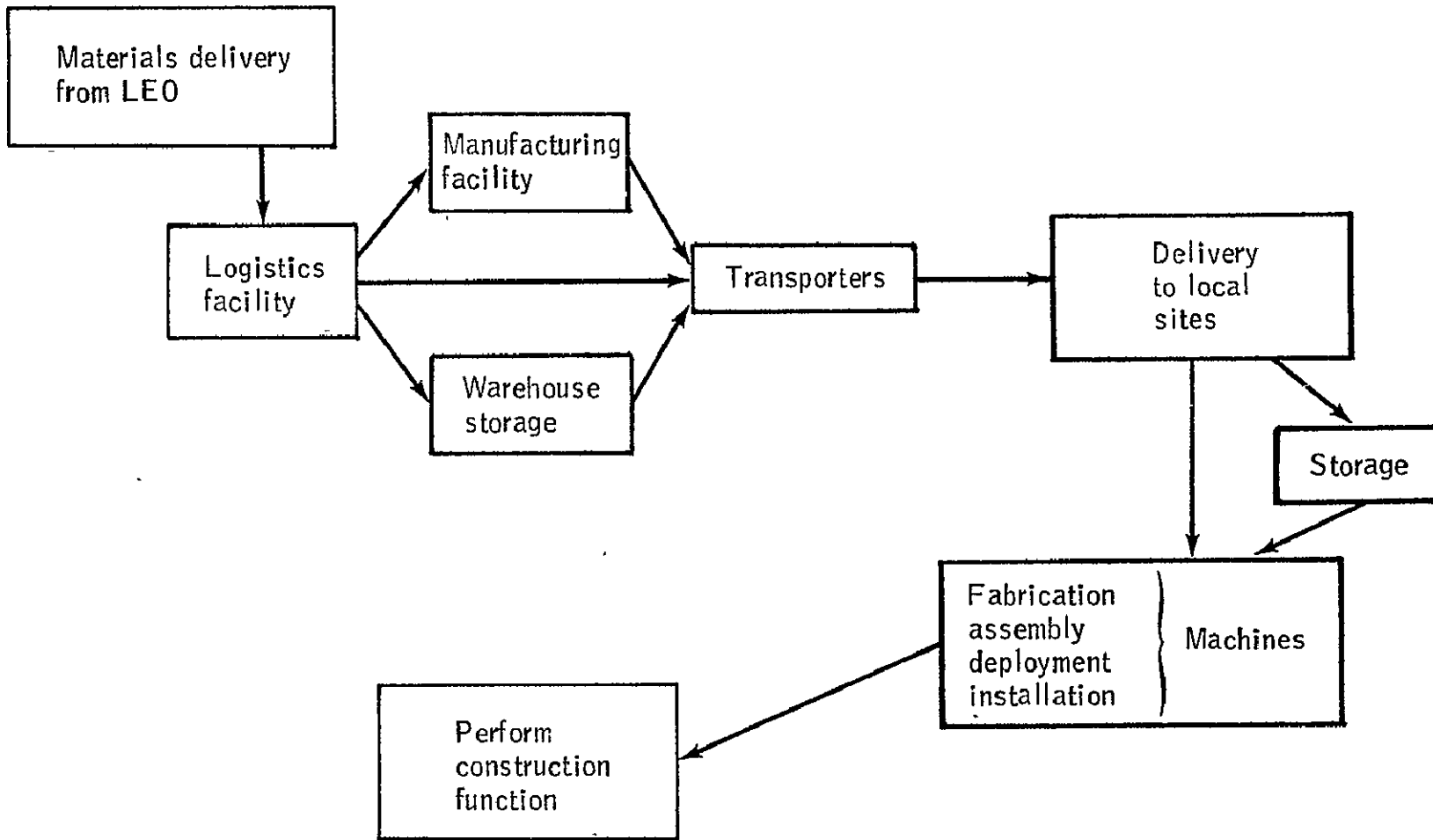


Figure V-C-2. - Operational schematic of construction base (column-cable).

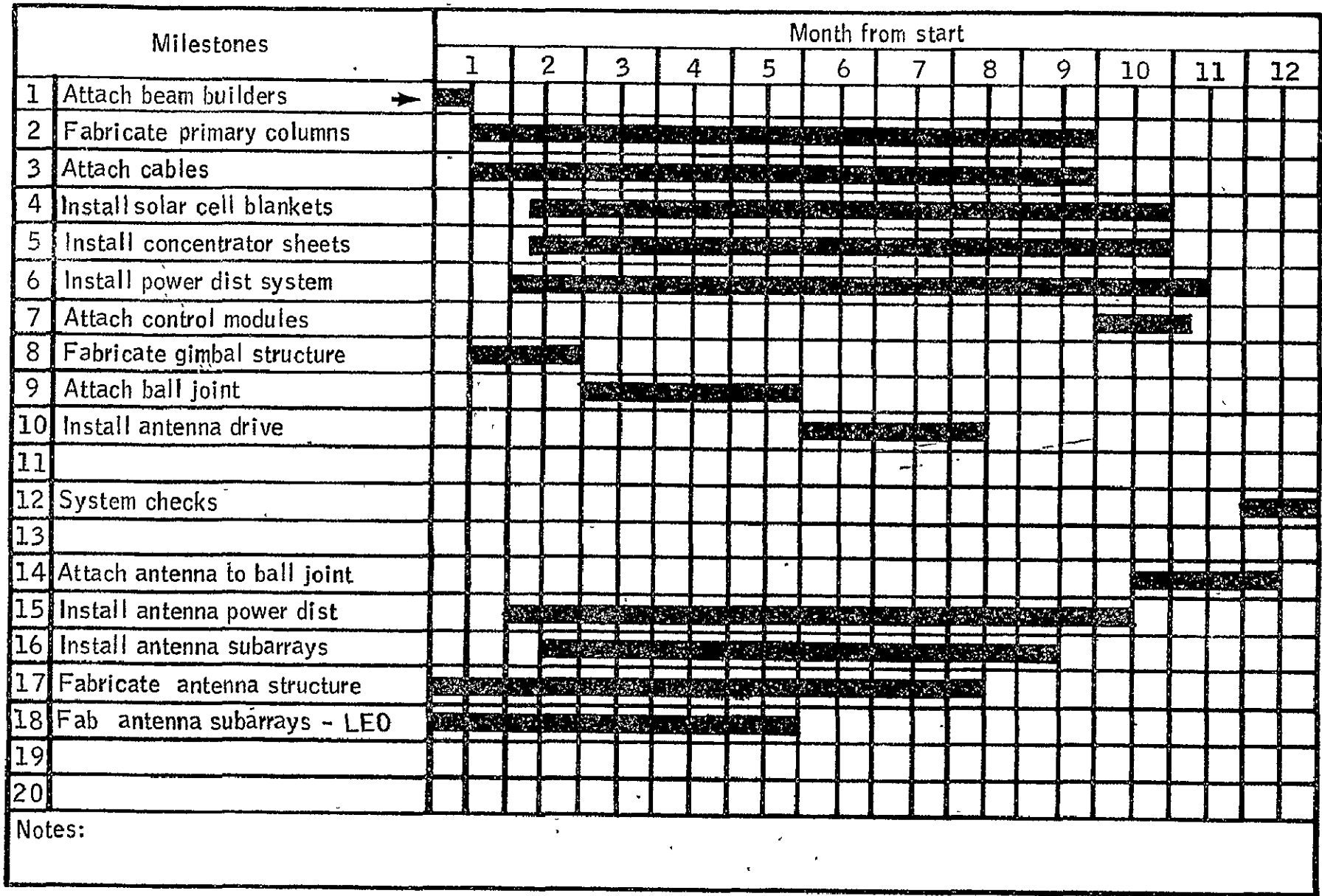


Figure V-C-3. Typical SPS Construction Sequence-Column/Cable (POP)

V-C-9

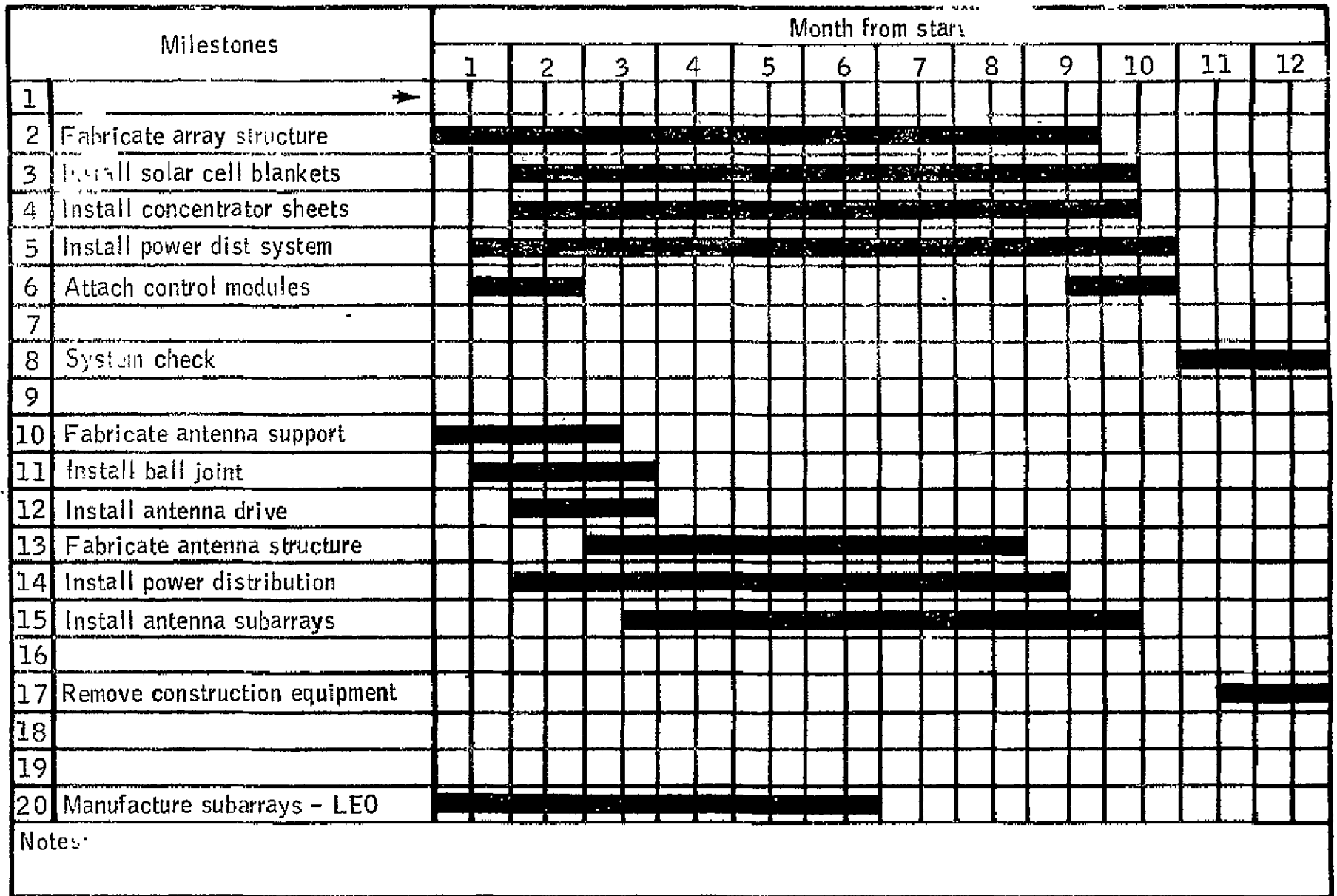


Figure V-C-4. Typical SPS Construction Sequence - Truss Configuration

Table V-C-2. Orbital Construction Equipment Requirements

<u>SECS</u>	<u>COLUMN/CABLE</u>	<u>TRUSS</u>
BEAM BUILDING MACHINES	30	61
CABLE RIGGING DEVICES	8	0
SOLAR CELL BLANKET PACKAGE INSTALLERS	4	4
REFLECTOR PACKAGE INSTALLERS	4	8
POWER DISTRIBUTION HARNESS INSTALLERS	4	4
MOBILE MANNED MANIPULATORS	8	5
FACILITY MANNED MANIPULATORS	12	2
<u>MPTS</u> (TWO ANTENNAS)		
SUBARRAY MANUFACTURING (TWO PER HOUR)	8	8
BEAM BUILDING MACHINES		
SUBARRAY SUPPORT STRUCTURE	18	18
PRIMARY STRUCTURE	8	8
CABLE RIGGING DEVICES	12	12
POWER DISTRIBUTION HARNESS INSTALLERS	4	4
SUBARRAY INSTALLERS	4	4

V-C-10

Table V-C-3. Crew Composition for GEO SPS

<u>POSITION</u> (See organization chart)	<u>PERSONNEL</u>
o Station Director, Deputy, Staff	10
o Organizational Heads	16
o Construction Crews	80
Column/Array Crew	- 4
Crews per Site	- 4
Total Sites	- 4
	<hr style="width: 50px; margin-left: auto; margin-right: 0;"/> 64
Column Only Crew	- 2
Crews per Site	- 4
Total Sites	- 2
	<hr style="width: 50px; margin-left: auto; margin-right: 0;"/> 16
o Control Center Teams	40
Members per Team	- 10
Total Teams	- 4
	<hr style="width: 50px; margin-left: auto; margin-right: 0;"/> 40
o Logistics and Facilities Management	28
Members per Team	- 7
Total Teams	- 4
	<hr style="width: 50px; margin-left: auto; margin-right: 0;"/> 28

Table V-C-3. Crew Composition for GEO SPS - Concluded

<u>POSITION</u> (See organization Chart)		<u>PERSONNEL</u>
o Transportation Services		20
Members per Team	- 5	
Total Teams	- 4	
	<u>20</u>	
o Food Services		24
Members per Team	- 3	
Total Teams	- 8	
	<u>24</u>	
o Medical Services		10
Total Personnel	- 10	
		<u>228</u>
	TOTAL ESTIMATED PERMANENT POPULATION	

Table V-C-4 provides an estimate of the personnel requirements for the column/cable configuration construction and support. A typical peak staffing estimate for the truss configuration is provided by table V-C-5. Table V-C-6 shows a typical staffing for manufacture of antenna subarrays in LEO. Table V-C-7 provides an estimate of the personnel requirements for the truss configuration construction and support. The estimated range of personnel requirements is 250 to 800 for the column/cable and 200 to 750 for the truss configuration.

The functional distribution of facilities and tasks for the SPS reference configuration (column/cable) is shown in figure V-C-5. The integration management facility houses construction workers and other permanent residents, management offices, control center, R and R facility, and the medical facility. The logistics facility houses construction workers and other permanent residents, shop, warehouse, motor pool, laundry, and personal equipment supply.

Table V-C-4. Column/Cable Configuration Typical Man Loading

V-C-14

		ESTIMATED MAN LOADING PER MONTH (CONSTRUCTION PERSONNEL)											
TASKS		1	2	3	4	5	6	7	8	9	10	11	12
1	ATTACH BEAM BUILDERS TO HUB	48											
2	BUILD PRIMARY STRUCTURE		48	48	48	48	48	48	48	48			
3	RIG CABLES		24	24	24	24	24	24	24	24			
4	INSTALL SOLAR BLANKETS			48	48	48	48	48	48	48	48		
5	INSTALL REFLECTORS				48	48	48	48	48	48	48	48	
6	INSTALL POWER DISTRIBUTION SYSTEM				16	16	16	16	16	16	16	16	16
7	BUILD ANTENNA SUB STRUCTURE		16	16	16	16	16	16	16	16	16		
8	BUILD ANTENNA PRIMARY STRUCTURE			16	16	16	16	16	16	16			
9	INSTALL SUBARRAYS				16	16	16	16	16	16	16		
10	SYSTEMS CHECKS											8	8
	SUB TOTAL:	48	88	152	232	232	232	232	232	232	144	72	8

		(SUPPORT FUNCTION PERSONNEL)											
SUPPORT FUNCTIONS		1	2	3	4	5	6	7	8	9	10	11	12
1	MANAGEMENT	10	20	20	20	20	20	20	20	20	20	20	10
2	FOOD SERVICE	32	36	44	48	48	48	48	48	48	48	32	28
3	CONTROL CENTER	40	40	40	40	40	40	40	40	40	40	40	30
4	WAREHOUSE	40	40	40	40	40	40	40	40	40	40	40	30
5	MOTOR POOL	30	40	40	40	40	40	40	40	40	40	40	30
6	MEDICS	10	10	10	10	10	10	10	10	10	10	10	10
7	OTHER SUPPORT	36	44	44	44	44	44	44	44	44	44	44	36
	SUB TOTAL:	198	230	238	242	242	242	242	242	242	242	226	174
	GRAND TOTAL:	246	318	390	474	474	474	474	474	474	386	298	182

ORIGINAL PAGE IS
OF POOR QUALITY

Table V-C-5. Truss Configuration Typical Peak Staffing (GEO)

<u>FUNCTION</u>	<u>PERSONNEL PER SHIFT</u>	<u>TOTAL</u>
<u>CONSTRUCTION</u>		
BEAM BUILDERS	39	156
SOLAR CELL BLANKET INSTALLERS	8	32
CONCENTRATOR SHEET INSTALLERS	16	64
MOBILE MANIPULATORS	4	16
FACILITY MANIPULATORS	10	40
ANTENNA PRIMARY STRUCTURE	4	16
ANTENNA SUPPORT STRUCTURE	4	16
ANTENNA HARNESS & ARRAY INSTALLERS	4	16
	SUB TOTAL	<u>356</u>
SUPPORT		
MANAGEMENT	--	20
CONTROL CENTER	10	40
WAREHOUSE	10	40
MOTOR POOL	10	40
MEDICS	--	10
OTHER SUPPORT	10	40
FOOD SERVICE	7	28
	SUB TOTAL	<u>218</u>
PEAK ACTIVITY POPULATION		574

V-C-15

Table V-C-6. Typical Peak Staffing (LEO) Antenna Subarray Fabrication

<u>FUNCTION</u>	<u>PERSONNEL PER SHIFT</u>	<u>TOTAL</u>
MFG SUB ARRAYS	16	64
WAREHOUSE	4	16
MANAGEMENT	--	3
MEDICS	--	4
CONTROL CENTER	3	12
OTHER SUPPORT	4	16
FOOD SERVICE	2	8
	TOTAL -	<u>123</u>

V-C-16

Table V-C-7. Truss Configuration Typical Man Loading

		ESTIMATED MAN LOADING PER MONTH TRUSS CONFIGURATION (GEO)												
<u>CONSTRUCTION FUNCTIONS</u>		MONTHS	<u>1</u>	<u>2</u>	<u>3</u>	<u>4</u>	<u>5</u>	<u>6</u>	<u>7</u>	<u>8</u>	<u>9</u>	<u>10</u>	<u>11</u>	<u>12</u>
1	BEAM BUILDERS		78	117	156	156	156	156	156	156	156			
2	SOLAR CELL BLANKET INSTALLERS		8	32	32	32	32	32	32	32	32	32		
3	CONCENTRATOR SHEET INSTALLERS		12	61	64	64	64	64	64	64	64	64	64	
4	MOBILE MANIPULATORS		12	16	16	16	16	16	16	16	16	12		
5	FACILITY MANIPULATORS		20	40	40	40	40	40	40	40	40	20		
6	ANTENNA PRIMARY STRUCTURE			16	16	16	16	16	16	16	16	16		
7	ANTENNA SUPPORT STRUCTURE			16	16	16	16	16	16	16	16	16		
8	ANTENNA HARNESS AND ARRAY INSTALL.			16	16	16	16	16	16	16	16	16		
9	SYSTEM CHECKS												10	10
	SUB TOTAL		130	269	356	356	356	356	356	356	356	176	74	10
<u>SUPPORT FUNCTIONS</u>														
1	MANAGEMENT		10	20	20	20	20	20	20	20	20	20	15	10
2	CONTROL CENTER		40	40	40	40	40	40	40	40	40	40	35	30
3	WAREHOUSE		40	40	40	40	40	40	40	40	40	40	35	30
4	MOTOR POOL		30	40	40	40	40	40	40	40	40	40	35	30
5	MEDICS		10	10	10	10	10	10	10	10	10	10	10	10
6	FOOD SERVICE		18	20	28	28	28	28	28	28	28	20	15	10
7	OTHER SUPPORT (Laundry, R&R Facility, Shop, Equipment Issue).		32	40	40	40	40	40	40	40	40	36	32	28
	SUB TOTAL		180	210	218	218	218	218	218	218	218	206	177	148
	GRAND TOTAL		310	479	574	574	574	574	574	574	574	382	251	158

V-C-17

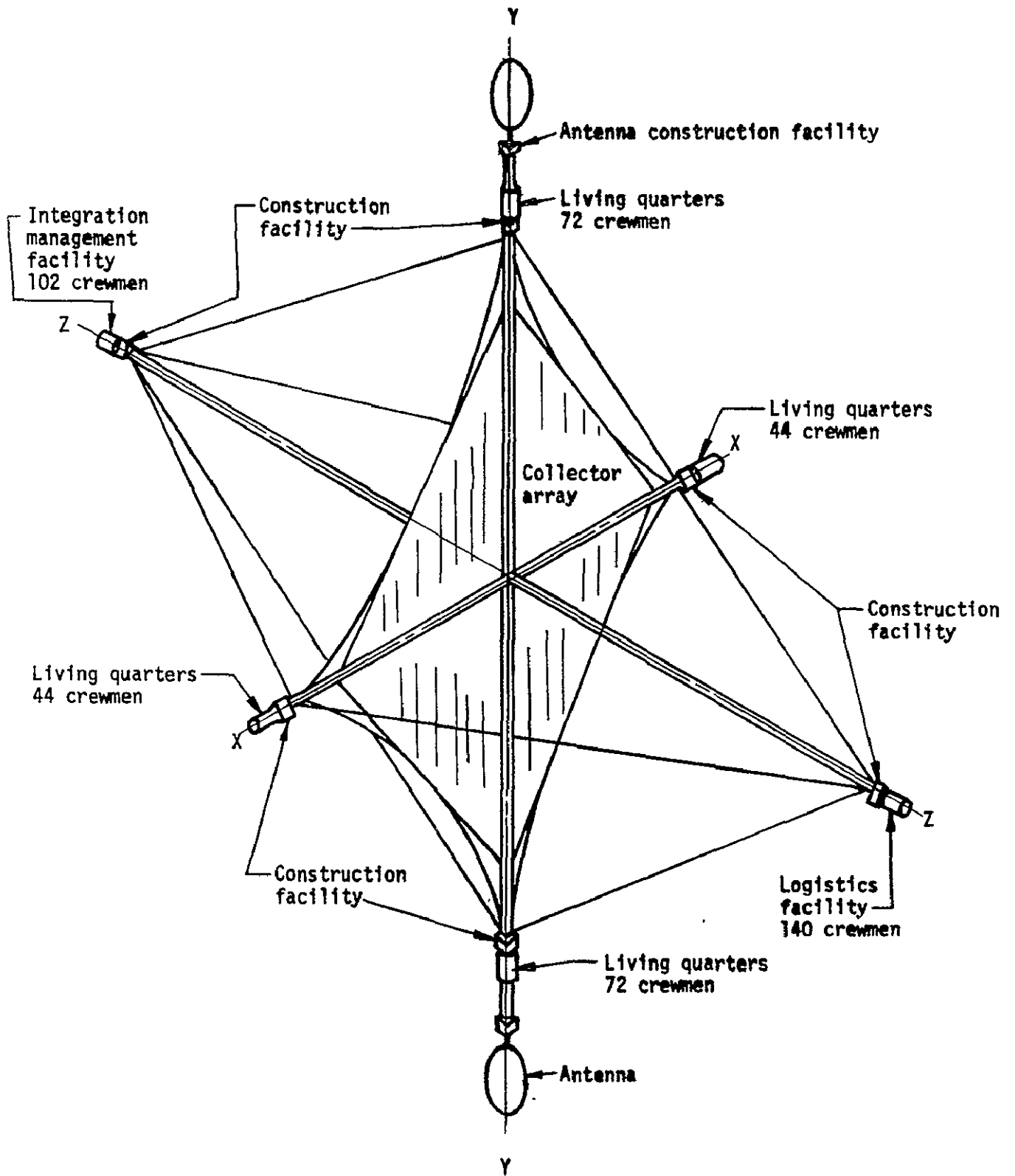


Figure V-C-5. SPS Reference Configuration-Functional Distribution of Facilities and Tasks

V. C. 2. Space Environment Impact on Long-Term Manned Operations

J. V. Bailey
Medical Research & Operations Div.

Earth orbital operations entail exposure of personnel to essentially continuous radiation fields ranging in intensity from almost negligible to very intense with the possibility of serious injury in a very short time. The actual radiation exposure rates to be experienced are dependent upon altitude and inclination of orbits, effectiveness of the space vehicle or suit for shielding the astronaut, and occurrence of natural events that modify the trapped radiation environment.

The radiation protective guides (limits) adopted for space-flight exposure are five or more times the current occupational radiation protection guides. The scientific basis for these space exposure limits is a large body of radiobiological data on radiation exposure of a variety of animal types extending over 50 years. However, the available human exposure data covers a time span of a little more than 20 years. In about half again as long, NASA will be flying significant numbers of people for up to a year at a time in a chronic radiation exposure situation that has no parallel in past applications of radiation technology. With the advice of the Radiobiological Advisory Panel, Space Science Board, National Academy of Sciences, NASA has established radiation protection guides (exposure limits) for the design of space programs such as the Space Station or the Solar Power Satellite Systems. Reference table V-C-8, these design limits were proposed with conditions as follows:

"They are proposed on the assumptions that (a) they are to be used only for current space-mission and vehicle-design studies; (b) space missions of the next 10 to 20 years will will high-risk operations, and the radiation hazard should be considered realistically and in perspective with other inherent risks; (c) they will be subject to review and revision as additional pertinent information becomes available and before application to actual operations; (d) an active career in earth-orbital operations can be terminated at the end of any specific mission; (e) the number of people involved will be small and most will be in the older-than-30 age group; (f) participants will be highly motivated volunteers well informed about the nature and extent of the radiation risk; and (g) the agencies concerned appreciate the desirability of keeping exposure as low as practicable by appropriate engineering and operational considerations."

There is a complicating factor in the radiation environment at geosynchronous altitudes, the galactic cosmic rays. Referred to as HZE particles (for high atomic number, high energy), the galactic cosmic rays are

Table V-C-8. Design Exposure Limits and Exposure Accumulation Rate Constraints

<u>Constraint</u>	<u>Primary Reference Risk (rem at 5 cm)</u>	<u>Bone Marrow (rem at 5 cm)</u>	<u>Skin (rem at 0.1 mm)</u>	<u>Ocular Lens (rem at 3 mm)</u>
1-year average daily rate		0.2	0.6	0.3
30-day maximum		25	75	37
Quarterly maximum ^a		35	105	52
Yearly maximum		75	225	112
Career limit	400	400	1200	600

^aMay be allowed for two consecutive quarters followed by six months of restriction from further exposure to maintain yearly limit.

capable of intense energy deposition over a very small volume of tissue; killing or damaging any cell that they transverse along a cylinder of tissue of very small diameter (microbeam). The quantification of the effects of exposure to the HZE particles is the subject of extensive debate among the radiobiologists involved in NASA's research programs. Conventional dosimetric concepts (as represented by the units of dose in the preceding table) are difficult to apply. The current trend of thinking holds that new concepts of radiation dose expression will be necessary for "bookkeeping" on this component of the total space radiation exposure problem. Recommendations are currently being formulated as to objectives for NASA's radiobiology research and they are expected to focus upon the HZE particles as uniquely NASA's problem and as a potentially serious source of radiation exposure.

The key to assessing radiation hazards to personnel involved in such programs as the SPS is, of course, the accuracy of the models of the ambient space radiation environment. Currently the environment is well known qualitatively and the mathematical models describing it are adequate for determining the relative level of hazard. The model describing the geosynchronous electron environment, designated AE3, was stated to be reliable to about a factor of 2, at the time of its publication. Recent data from ATS-6 differ from the model AE3 by an order of magnitude in terms of calculated tissue absorbed dose. Thus, significant improvement in the environmental models in terms of absolute numbers of particles and their energy distribution, magnitude of cyclic variations and the periodicity of the variations and the potential for transient shifts must be accomplished before major design efforts are started, particularly for facilities in geosynchronous orbit.

The space radiation environment will be a major driver on design of manned facilities and vehicles. Design to current radiation exposure standards will require increase in shielding effectiveness for long-term orbital facilities by factors of 2 to 5 over current design practices. LEO to GEO transfer for crews and radiation sensitive cargo will require high specific impulse vehicles with shielding effectiveness comparable to the Apollo CM. The radiation environment presents no impediment to further design and development; however, two areas require attention: (1) better quantitation of the environment and resultant radiation exposure liability, and (2) quantitation of the level of risk and the nature of the injury from long-term exposures to the galactic cosmic rays (HZE particles). Research on the latter is currently underway.

In the area of microwave radiation and the hazards of exposures, the research has been "shot gunned" and it is difficult to collate the results into a coherent evaluation. Another shortcoming of all the research is the dosimetry technique since it is extremely difficult to make meaningful measurement of an RF energy field without distorting that field, particularly measurements of energy deposition into biological tissue.

The following summary of the Proceedings of the International Symposium on the Biological Hazards of Microwave Radiation, held in Warsaw, Poland, October 15-18, 1973 represents the status of this field of research. The subjects of the reports given at this symposium fall generally into four categories: (1) the gross effects of acute exposure of experimental animals to microwaves; (2) the more subtle effects of less severe and of chronic, low-level exposures to both experimental animals and occupationally exposed humans; (3) the electrical properties of biological systems, and possible modes of interaction of microwaves with cells and biological molecules; and (4) the problems and proposed methods of quantifying exposure and absorbed dose. This summary sets forth significant points from each of these categories.

A number of studies of the microwave lethal dose for small animals were referenced. A wide range of parameters were used in these studies: wavelengths in the range of millimeters to decimeters, power densities up to 300 mW/cm², and both pulsed and continuous waves. It was reported that the most rapid deaths were produced using continuous "10 cm waves" of high power density with most of the work apparently being done at 10.7 and 12.2 cm wavelengths. It was also noted that, in addition to the direct heating effect of the microwaves, "there is evidently also a direct effect of microwaves on thermoregulatory centers."

With regard to less severe microwave exposures, there was much debate as to whether or not certain effects were cumulative, delayed, and/or non-thermal. Results indicate an apparent threshold power density for cataractogenesis in animals, but there are indications that other effects, (e.g., disturbances in brain metabolism and central-nervous-system functions) may be cumulative in nature. One report asserted that "thermal stimulation of peripheral nerves can produce the neurophysiological and behavioral changes that have been observed"; however, others reported observations which seem to contraindicate this stance. Epidemiological studies conducted on microwave workers in the Soviet Union and Czechoslovakia found not only an increase in certain subjective and objective disorders, but defined "microwave sickness" as a nosological entity; similar studies in Czechoslovakia and Poland found no "statistically significant" increase in disorders. A variety of experiments were described with wide variation in parameters and dosimetry. It was stressed, however, that no serious cardiovascular disorders attributable to microwaves had ever been found, and that "microwave sickness" was generally not found to be a serious disorder. A number of methods and instruments have been used for measuring field strength and absorbed dose. All had shortcomings, usually serious. At the time of this conference, the lack of accurate, noninterfering dosimetry remained a serious problem.

There are two miscellaneous points which seem deserving of mention. The first is that the recommended maximum power density (based mainly upon the risk of thermal cataractogenesis) for occupational exposure

in the United States is one thousand times as large as the similar standard (based on nonthermal effects) in the Soviet Union. The second, that since the feathers of migratory birds are thought to function as antennae, large concentrations of electromagnetic power, such as are envisioned for Satellite Power Station, might serve to disorient and to disrupt the migratory patterns of these birds, in addition to other possible side effects.

Potential impacts of the solar ultraviolet radiation upon manned operation under long-term exposure situations are under investigation. At the present time there do not seem to be any problems to arise from the UV since protective measures to be used against the trapped radiation environment would automatically ameliorate the UV problem.

APPENDIX V-C-1

SPS ORBITAL CONSTRUCTION ORGANIZATION

Station Director - A single manager on-orbit responsible for the entire project (for any one SPS).

Deputy and Staff - A second in command who can function as the director when needed and who actively directs the efforts of the support staff. This staff will consist of no more than ten persons and will handle the routine daily administrative chores necessary to keep a space colony of 250-800 personnel properly outfitted, fed, located, functioning, etc. Even though substantial ground support is anticipated, there will still be needs that can best be met on site, and this group will be needed to provide that support.

The second line or level of management will be the major functional element leaders, responsible for overall planning and management of the project in some specific area. Three such managers are proposed, one for construction/manufacturing, one for operations, and one for support.

Construction/Manufacturing Manager - This position calls for a general overseer of all phases of the construction and manufacturing processes that take place on orbit. The job will demand a thorough knowledge of the methods employed, the functioning of the hardware, the integration of subordinate subsystems into a functioning whole, and the day to day scheduling needs necessary to support major milestones.

Operations Manager - This position will essentially establish a control center on orbit. The position will call for a person well versed in operations and the nominal and off-nominal aspects of running a large manned facility. Such a position will be required in addition to a comparable position on the ground due to the need to maintain on-site monitoring and control of the entire facility and its personnel, independent of depending on up and down link communications with the ground.

Support Manager - With the major emphasis being placed on getting the SPS built, and an almost equal status being given to the needs for maintaining in-site cognizance over that progress, there logically appears to be a need to establish a position to maintain control of all the ancillary support needed to keep the entire project functioning. Caring for the needs of the personnel and their supportive habitats will be another major area of endeavor and will require an overseer just as the construction and operations areas.

Supporting these major organizational key positions leads to establishing a line of direct communication between the major managers and the working troops. At this intermediate level of management, the positions can be defined to narrow the responsibilities to a specific area, thus allowing more expert attention to be brought to bear on a smaller segment of the overall effort. These positions are defined below.

Assistant for Mechanical Systems - This position will allow a single point of focus through which all the activity can be coordinated that has to do with the mechanical aspects of the construction project. This would include the basic structure (beams, cables, etc.), the RCS for orbital attitude control, and the mechanical portions of the array and antenna.

Assistant for Electrical Systems - This position is identical to that defined above for mechanical systems except that the area of responsibility is for electrical systems.

Assistant for Logistics - This position was defined to establish a single focal point for the task of determining what construction supplies, tools, and support hardware were needed, when, where, and why. The position will call for detailed knowledge of schedule, activity, delivery, storage, etc. of all hardware needed by the construction teams to accomplish their jobs.

Assistant for Communications - Communicating between the various groups accomplishing the integrated construction task will probably be one of the major interfaces at the site. A position was established on the control center team to serve as a focal point for communications, both within the station and to the ground.

Assistant for Information Management - This position is defined as the computer interface position necessary to handle all the information flow and status summaries necessary to keep up with the progress of the construction job and the overall health and well being of the station.

Assistant for Planning - This position is envisioned as a flight planning type position responsible for keeping a coordinated flow of activity running smoothly throughout the station.

Assistant for Station Support - This position is somewhat analogous to a base civil engineer; responsible for monitoring all the subsystem functions that keep the station running. Problem identification, trouble shooting initiation, and maintenance requests would originate with this position.

Assistant for Orbital Mechanics and Traffic Management - This position will have responsibility for determining orbital mechanics effect on the station during all phases of buildup and determining corrective action, if necessary. Mass properties will be tracked through this position. The position will also serve as a control tower for the vehicles coming and going from the station as well as for local free flyer traffic.

Assistant for Verification and Checkout - This position will serve as the focal point for determining the health and functional performance of the array as it is being constructed. Continual monitoring of the functional interfaces and their operational status will provide immediate assessment at any time of the progress being made toward fully operational capability.

Assistant for Food Service - This position will be responsible for seeing to the feeding of the entire population of the station.

Assistant for Medical Services - This position seems necessary in view of the size of the population. Emergency and routine medical services will need to be provided for on orbit personnel.

Assistant for Logistics and Facility Management - This position is intended to act as the action arm for the operations position that identifies station problems in need of attention. Maintenance personnel would be members of this unit. Also, the position includes the actual management of the living facilities, something like a hotel manager. Issuance of personal equipment, clothing, linen, etc. would be a function of this position as would be the cleaning and maintenance of these items. Tracking logistic needs to determine use rates, resupply requirements, and disposal needs are also responsibilities assigned to this position.

Assistant for Transportation - The need for frequent transport of both personnel and equipment led to the creation of a position similar to a motor pool operation, complete with drivers, handlers, and dispatchers.

Below these intermediate managers in the organization come the first line supervisors and their team members. It is assumed that first line supervisors will be working members of the team, but will have the additional responsibility of acting as foremen while functioning as an integral member of the team.

VI. SPACE TRANSPORTATION SYSTEM

A. SYSTEM REQUIREMENTS (E. M. Crum, Future Programs Office)

1. Background and Related Work

The magnitude of the SPS program will require a dedicated, optimized transportation system to transfer men and cargo from Earth to the SPS position in geosynchronous space and, in the case of men and a small portion of the cargo, return them to Earth. The system will include growth versions of the Shuttle to transport men, Heavy Lift Launch Vehicles (HLLV) for cargo to low Earth orbit (LEO), and orbital transfer vehicles (OTV) to transfer men and cargo to geosynchronous orbit (GEO).

Several investigations and contracted studies, although independent of the SPS, have contributed to the understanding and data base available for the HLLV elements of the transportation system. These studies include the forecast analyses done for the space transportation system section of the agency "Outlook for Space" study (NASA SP-386, January 1976) in which transportation costs of \$20 per pound (\$44/kg) payload to low Earth orbit were predicted and the Systems Concepts for STS Derived Heavy Lift Launch Vehicles study (NAS 9-14710) that investigated alternative design concepts and made similar cost predictions. The Shuttle Growth Study (Booster and External Tank Options (NAS 8-32015) which was contracted to Rockwell International in June 1976 will provide indications of what performance increases and cost reductions may be expected for the transportation of crews and high priority cargos to LEO.

The orbital transfer vehicle has not been studied to the same extent but propulsion studies beginning with those for the shuttle tug have given some insight into the possible contributions of various propellants, nuclear engines and staging schemes while the MSFC Solar Electric Propulsion Studies provide a starting point for the consideration of low thrust, high specific impulse systems.

2. Requirements

The requirements placed on elements of the transportation system are in general known well enough to define and evaluate conceptual designs. The primary uncertainty at this time is whether or not the payload will provide power to the OTV on the trip from LEO to GEO. This hinges, in part, on whether the SPS is to be assembled, or partly assembled at a LEO staging point and then transported to GEO with the capability of providing power to the OTV enroute, or whether it is to be assembled, and, perhaps, manufactured at GEO with no capability to provide power during the LEO to GEO transfer. The truss type SPS is amenable to either assembly option while the column/cable configuration is considered for GEO assembly only.

The decision concerning LEO versus GEO assembly will be determined by overall system costs and will not be made in the near future.

Since the features and characteristics of the OTV's that result from each option will be a significant factor in the systems evaluation it will be necessary to develop a cargo OTV (COTV) for each assembly option to a sufficient level of detail to permit a comparative evaluation.

Preliminary ground rules, mission requirements, and performance requirements were generated to provide an initial transportation system baseline and to assist in coordinating requirements and capabilities. Since a prototype requirements document was desired, the level of detail in some cases goes beyond the current requirements for design concepts and beyond the present need or capability to quantify. General ground rules, applicable to all transportation system elements are:

a. The SPS transportation system elements, with the exception of the Shuttle, are dedicated and optimized for the installation, operation, and maintenance of the SPS.

b. The SPS transportation system will be designed for minimum total program cost.

c. Energy requirements will be minimized consistent with minimum cost.

d. Environmental impact will be minimized and, so far as possible, protective measures needed will be factored into cost analyses.

e. The use of critical materials will be minimized consistent with cost, energy and environmental impact requirements.

Ground rules and requirements developed for each type of vehicle are:

2.1 Heavy Lift Launch Vehicle (HLLV)

Ground Rules

a. The HLLV may impose up to 4g's on the payload during delivery to the staging orbit.

b. The maximum temperature within the HLLV payload bay shall be 200^oF or less.

c. The acoustic and structural dynamic loading on HLLV payloads shall be equal to or better than the Shuttle orbiter payload bay requirements.

d. The HLLV launch reliability shall be 0.97 or better.

e. The HLLV will provide no services to the payload and shall require no services from the payload.

.. The HLLV fleet will have a launch rate capability margin of 50% beyond the average annual rate requirement. (The average will include operational LEO needs and OTV propellant losses, if any.)

Mission Requirements

a. Launch Site - The HLLV shall be launched from the Eastern Launch Site at KSC, or from a launch site location on a U.S. possession at a lower latitude, to be determined by launch project economics and environmental considerations.

b. HLLV Capability - The HLLV shall be capable of transporting, unmanned, SPS components and related cargo from the launch site to the low Earth orbit staging point as required to install up to seven Solar Power Stations per year. No return cargo capability shall be provided by the HLLV.

c. Orbital Parameters - The HLLV mission shall originate at the launch site, latitude TBD, and terminate at the low Earth orbit staging point in a 500 km circular orbit with an inclination consequent to a due east launch from the selected launch site.

d. Mission Duration - The HLLV mission will extend from launch to recovery at the launch site and shall include unloading of the cargo at the low Earth orbit destination and the recovery operations of the HLLV.

e. Launch Window Constraints - Launch window constraints shall not preclude the launch rate necessary to establish up to seven SPS units per year.

f. Intact Abort - No intact abort capability will be provided by the HLLV for the payloads except as required by range safety considerations. Safe return of the launch vehicle elements shall require either nominal mission completion through cargo delivery or jettison of the cargo.

Performance Requirements

a. Payload Requirements - The HLLV shall be capable of transporting from the launch site to the low Earth orbit assembly point a payload of at least 450 to 900 tons mass, 48 to 80 kg/m³ density, and dimensions of 12 x 10 x 10 m, which is the largest and/or heaviest irreducible component of the SPS. The payload diameter shall be not less than 12m and no greater than 30m in diameter.

b. Guidance and Navigation Accuracies - The HLLV shall be capable of guidance and navigation accuracy consistent with placing its payload at the assembly point and the recovery operation. The OMS

package will provide rendezvous capability to the assembly point within + TBD NM altitude, + TBD^o inclination and + TBD^o longitude within TBD hours of insertion. The HLLV will insert the payload into a 80 km x 500 km orbit with an inclination equal to the launch site latitude. The OMS package on the payload will circularize at 500 km x 500 km.

2.2 Cargo Orbital Transfer Vehicle (COTV)¹

Ground Rules

- a. The COTV may impose up to .001g's on the payload in transferring a deployed or partially deployed or assembled SPS to geostationary orbit
- b. The COTV payloads may be suitable for either single point or multi-point application or thrust loads during orbital transfer.
- c. Degradation of exposed solar cells during transfer through the Van Allen belt is acceptable, and overall system cost optimization will determine the acceptable level of degradation.
- d. A power output of 4 GW from the 1b payload will be considered available as an upper limit (for dependent OTV's).
- e. The COTV will provide no services to the payload.
- f. The COTV mission reliability shall be 0.97 or better.
- g. Only gaseous propellants will be considered for possible COTV use.
- h. Reuse of the COTV will be based solely on economics.

Mission Requirements

- a. Launch Site - OTV's shall be launched from and return to the vicinity of the low Earth orbit staging point.
- b. Cargo OTV Capability - COTV's shall be capable of transporting, unmanned, SPS components and related cargo from the low Earth orbit launch position to the geostationary position as required to install up to seven SPS systems per year. The return capability to the staging point is (TBD).

¹The requirements for COTV's will later be developed separately for COTV's suitable for stations assembled or partly assembled in LEO (COTV_L) and those suitable for the GEO assembly option (COTV_G).

c. Orbital Parameters - COTV missions shall be between the low Earth orbit staging point (positions TBD) and the geostationary orbit longitudes of the power stations (positions TBD).

d. Trip Time - COTV trip time shall be a maximum of 180 days and a minimum as required by an acceleration of 0.001g's (approx. seven days).

Performance Requirements

a. Payload Requirements - The COTV shall be capable of transporting from the low Earth orbit staging point to the geostationary location a SPS payload weighing (TBD) tons. For dependent systems, the payload shall provide up to 4 GW of electrical power at (TBD) volts while illuminated by the sun. The time of flight and trajectory for a photovoltaic system shall be consistent with a solar cell degradation of not more than (TBD) % of the total array. The payload will be solar oriented for dependent vehicles and there will be no payload attitude constraint for passive payloads.

b. Guidance and Navigation Accuracies - The COTV shall be capable of guidance and navigation accuracy consistent with placing its payload at the geostationary point within (TBD).

c. Orbital Maneuvering Capability - The COTV shall have the capability of providing an unscheduled longitude shift of TBD degrees within TBD days and an inclination change of TBD degrees within TBD days after arrival at the initial targeted destination.

d. Structural Requirements - The COTV structure shall be compatible with the launch loads associated with the HLLV and/or Shuttle

e. Energy Requirements - The COTV shall provide any energy required above that supplied by the payload to meet the flight duration and trajectory requirements.

2.3 Personnel and High Priority Cargo Launch Vehicle (PLV)

Ground Rules

a. The Personnel and High Priority Cargo Launch Vehicle (PLV) shall be derived from the STS, in so far as feasible.

Mission Requirements

a. Launch Site - The PLV launch site shall be the same latitude as that for the HLLV.

b. Abort Capability - Full abort capability, including pad abort, shall be provided.

c. Nominal Stay Time - The nominal passenger stay time in the PLV shall be six hours from initiation of loading until completion of passenger transfer for a 5-hour maximum mission flight time, for both ascent and return missions.

d. Emergency Stay Time - Means shall be provided for emergency passenger stay time in the PLV of 24 hours.

e. Passive Docking - The PLV shall be capable of passive docking in LEO for up to 24 hours.

Performance Requirements

a. Passenger Capacity - The PLV shall be capable of transporting 50 to 100 passengers to the low Earth orbit staging point.

b. Cargo Capability - The PLV shall have a discretionary cargo capability of TBD pounds and TBD cubic feet in addition to the passenger load up, and TBD pounds and TBD cubic feet in addition to the passenger load down.

c. Rendezvous Capability - as per Shuttle.

d. Cross Range Capability - The PLV shall have a cross range capability requirement sufficient for once around abort only.

2.4 Personnel Orbit Transfer Vehicle (POTV)

Ground Rules

a. The Personnel OTV shall be a new vehicle, optimized for Satellite Solar Power Station service. However, if the cargo OTV is such that it can meet the personnel transfer time requirements it may be utilized to the extent possible for the POTV.

Mission Requirements

a. Launch Site - The POTV will be either space or Earth launch site based to be determined by project economics.

b. Abort Capability - Rescue or abort capability will be provided.

c. Nominal Stay Time - The nominal passenger stay time in the vehicle will be less than 18 hours.

d. Emergency Stay Time - Means shall be provided for emergency passenger stay time in the vehicle for up to 36 hours.

e. Passive Docking - The POTV shall be capable of passive docking at the geostationary station for 90 days.

f. Propellant Loading - Propellant loading at the geostationary station, using propellant previously delivered by cargo OTV, shall be considered.

Performance Requirements

a. Payload Requirements - The POTV shall be capable of transporting a crew of three and (TBD) passengers and/or high priority cargo of TBD kgs and TBD m³ from the low Earth orbit staging point to the geostationary location and return to the low Earth orbit point of origin or to the launch site. External payload mounting provisions for maximum capability deployed payload weight.

b. Guidance and Navigation Accuracies - The POTV shall be capable of guidance and navigation accuracy consistent with placing its payload at the geostationary location within limits (TBD). The return to low Earth orbit option accuracy shall be (TBD). The POTV return to launch site option accuracy shall be (TBD). Rendezvous capability shall be per MSFC tug (cryo) specifications.

c. The nominal transfer time shall be not greater than 12 hours.

d. Structural Requirements - The POTV structure shall be compatible with the launch loads associated with the HLLV and/or Shuttle and reentry loads associated with the return to launch site option.

e. Habitability Requirements - The POTV shall provide a habitable crew compartment and provisions for a transfer time of 12 hours and a contingency time of up to 36 hours. The nominal stay time shall be less than 18 hours.

f. OMS Capability - The POTV shall provide OMS capability at GEO of 500 ft/sec beyond primary maneuver and nominal rendezvous requirements.

3. Options

3.1 Heavy Lift Launch Vehicle (HLLV)

Eleven configurations were identified as candidates to serve the HLLV purpose. A number of these were two-staged winged vehicles utilizing hydrogen/oxygen propellants for the upper stage and either hydrogen/oxygen or hydrocarbon/oxygen propellants for a boost vehicle.

Other candidates were two-stage ballistic entry vehicles of four types and a final candidate HLLV was devised to achieve the capability of providing alternative launch service for cargo or a personnel carrying vehicle derived from the Space Shuttle Orbiter. There has not been any attempt as yet to define the optimum size size of the launch vehicle nor at this moment can significant differences be detected between their potential cost effectiveness. As the configuration definition evolves and additional cost data becomes available, the candidate vehicles may be narrowed to a baseline configuration. Reduction to a single baseline vehicle is not considered appropriate until the cost data is available and requirements more thoroughly understood consequent to the satellite design activity.

3.2 Personnel and High Priority Cargo Launch Vehicle (PLV)

The assumption is made that man rating of the HLLV will constitute an incremental cost upon its development and operation. For this reason and for the operational flexibility provided, an entirely separate launch vehicle is presumed required to serve the needs of the satellite power station program. This vehicle will be utilized to transport all personnel to low Earth orbit and can in addition fulfill high priority delivery functions of a modest scale. Although a new vehicle such as a single-stage-to-orbit (SSTO) may be developed to fulfill this need, the justification for embarking upon the development program of a "clean sheet" design is not immediately evident. Consequently, the approach taken in this study is to modify the current Shuttle vehicle to fulfill these needs. Studies have indicated that the baseline Shuttle system can be improved in both payload capability and operating cost by replacement of the solid rocket booster with a new booster utilizing liquid oxygen and kerosene propellants. Such a booster can be provided using the F-1 engines from the Saturn V first stage. If available for heavy lift vehicle use, a new, more efficient, hydrocarbon/oxygen engine can be advantageously employed. The payload capability assumed for sizing this new booster is 100,000 pounds to the mission one requirements of the current baseline Shuttle. A more important parameter than payload weight for this vehicles application to satellite power program needs may be its ability to carry a number of personnel on each flight. Brief studies have been performed which indicate that, given the maturity of operation to be provided by the baseline shuttle operation, modifications to the Shuttle Orbiter may be accomplished to enable transportation to low Earth orbit of 50 to 80 persons per flight. These modifications can be incorporated in orbiter vehicles taken from the operational fleet should that prove to be financially advantageous.

3.3 Cargo Orbital Transfer Vehicle (COTV)

The characteristics of the cargo OTV will be largely shaped by the choice of satellite power station construction location. If the low Earth orbit may be employed for assembly of power producing payload elements, their power output may be utilized for electric thrusters to

drive the cargo OTV, removing the necessity of returning this power source to low Earth orbit for reuse and effecting great economies in the overall operation. If, however, bulk cargo and supplies must be delivered to geosynchronous orbit for construction at that location, then an orbit transfer vehicle capable of supplying its own energy for the transfer is necessary. Conventional oxygen/hydrogen chemical propulsion is a candidate for this latter function. The scale of the operation will justify the employment of the highest technology chemical propulsion systems can offer and vehicle arrangements offering the maximum degree of efficiency by use of such stratagems as staging and expending inexpensive components. One candidate system to fulfill this need is a 2-1/2 stage oxygen/hydrogen vehicle. This vehicle is sized to fulfill the requirements of 225 ton payload transferred each trip from low Earth orbit to geosynchronous orbit with dimensions of the payload of 12 m dia. by 12 m in length. The 2-1/2 stage vehicle consists of a lower stage, carrying the greater portion of the propellants, which performs an insertion burn to a near-geosynchronous altitude apogee elliptical orbit. The second stage with the payload separates from the first stage and performs the remainder of the altitude increase to geosynchronous orbit, the circularization burn in geosynchronous orbit and any necessary plane change. The payload and the propellant tanks used by the second stage for its placement burns are separated in geosynchronous orbit and the second stage returned under its own power to low Earth orbit for refueling and reuse. The first stage had earlier performed a circularization burn at the low Earth orbit altitude for rendezvous with the operational support space station in low Earth orbit. The rationale for expending the tanks of the second stage is that the cost of placing the propellants in low orbit which are necessary to achieve the return of the tanks to low Earth orbit exceed the price of replacing them for each mission. This hypothesis may be valid or invalid, depending upon the relative cost of the launch service and fabrication of the propellant tanks which is yet to be determined.

3.4 Personnel Orbit Transfer Vehicle

Due to the much smaller payload requirements for transporting personnel, even relatively large numbers of 200 to 500 persons per year, it is assumed that the personnel orbit transfer vehicle is a special purpose device optimized for that function. For an independent chemical propulsion cargo OTV, it may be possible to delete this development and fly the passenger-carrying module as a part of the large chemical OTV outbound cargo. This program cost saving may be assumed whenever the geosynchronous orbit construction location and chemical cargo orbit transfer vehicles are considered. In all other cases, the dedicated personnel orbit transfer vehicle will be required due to the very slow trip made by low thrust cargo OTV's through the Van Allen belt. Information generated by the Future Space Transportation Systems Analysis Study, previous JSC in-house work, and the extensive space tug studies conducted by both NASA and the USAF over the past five years have resulted in a wealth of background information of one candidate concept to achieve this purpose. This concept deploys from the Shuttle operational altitude to

geosynchronous orbit, and return to that orbit for subsequent rendezvous with an orbiting craft or support facility for refueling and reuse. An alternative mission sequence for performing personnel interchange between low Earth orbit and geosynchronous operating locale would be to employ chemical propulsion for the outbound journey and make use of the Earth's atmosphere for braking for the return journey. This operating mode has been suggested by studies performed at the MSFC. The concept, known as "AMOOS" (Atmospheric Maneuvering Orbit to Orbit Stage), employs multiple passes through the Earth's atmosphere to acquire low Earth orbit. Significant savings in propellant quantity are thus achieved and translate into additional payload fraction of the outbound ignition weight of the vehicle. The potential improvement is reduced by the weight of the necessary retrobraking and thermal protection devices to provide the deceleration in a reasonable number of passes. An extension and perhaps improvement to this concept is to employ the Earth's atmosphere for braking with the target being atmospheric flight return directly to Earth. In this mission mode, the deorbit burn from geosynchronous altitude is reduced to a minimum, and a direct single pass entry established for return to a desired location on the surface of the Earth. Either winged or ballistic entry bodies may be employed for this purpose. This mission mode enjoys an increase in payload fraction of the initial mass in low orbit and, in addition, offers the operational advantage of returning the crew and passengers directly to a desired location on Earth rather than requiring the intermediate stop in low Earth orbit and solution of the rendezvous problem. This mission possibility has not yet been subjected to analysis and requires study in the months to come in order to quantify the benefits. For the purpose of the present JSC in-house SPS study, the conservative choice is made to employ conventional chemical rocketry with return of the vehicle and crew to low Earth orbit. Single stage, 1-1/2 stage (outbound propellant tanks left in geosynchronous orbit), 2 stage, and 2-1/2 stage configurations are all candidates for this mission. Additionally, for those cases where economic (electric propulsion) cargo transportation is possible, significant advantages accrue to the orbit transfer vehicle for personnel by storing propellants for the return journey in geosynchronous orbit, having previously been delivered there by the more economic cargo OTV. All of these candidates deserve scrutiny to support the orbit transfer of personnel and occasional high priority freight.

4. Systems Requirements Analysis

The Satellite Power Station Program poses a set of space transportation systems requirements which are unprecedented in scale and in the press for economy of operation. The Space Shuttle will serve the purpose of providing orbital test of satellite power station technology and components in the 1980 time frame, of providing the operational and facility structure on which the satellite power station transportation system may be based, and in providing the basis for evolutionary development of an effective personnel and priority vehicle to be used in the

mainline operational power satellite program. The Space Shuttle is designed to operate only to low Earth orbit, i.e., 500 km circular orbit altitude and below. Consequently, the transportation of personnel and material to the geosynchronous orbit will require the development of new systems. Earlier NASA plans called for development of a vehicle called the Space Tug. This vehicle was designed for unmanned deployment and retrieval of payloads from geosynchronous orbit based from the Shuttle orbit of approximately 200 kilometers. The Space Tug, as envisioned in these earlier studies, is not adequate to fulfill the needs of a Satellite Power Station Program, hence new systems must be defined to fulfill these far larger requirements.

The mass of material necessary to be placed in low Earth orbit for the Power Satellite Program includes the mass of the satellite itself, the necessary equipment and material to perform the construction process, the structures and systems for housing the personnel to be involved in the construction activity and the orbital transfer systems and the propellants for them necessary to transfer the power satellite and supportive elements from low orbit to geosynchronous orbit. Perhaps the most important two drivers upon the launch system are the specific mass of the power satellite (KG/KW) and the propellant needs of the orbit transfer vehicle. The term "orbit burden factor" will be utilized to describe the low Earth orbit payload requirements, in excess of those required for placement of the satellite elements themselves. The "orbit burden factor" is defined as the ratio of those masses necessary to provide the orbit transfer function and to support the construction and operation activities associated with the satellite power station program to the mass of the satellite itself.

Conventional chemical propulsion, if utilized for transfer of all of the necessary mass to geosynchronous orbit, will require that propellants be supplied to low Earth orbit in amounts of twice or more the mass of the satellite materials and parts to be transported. This obviously constitutes a heavy burden upon the launch vehicle fleet and results in increased costs for the transportation. Consequently, it is of interest to examine more efficient propulsive schemes than conventional chemical rocketry. Electric propulsion devices of several forms have been defined and, in a few instances, reduced to practice. These devices offer significant improvement in specific impulse levels achievable and hence significant reduction of the "orbit burden factor" associated with supplying their propellants to low Earth orbit. The electric propulsion devices require, however, that electrical energy be supplied, in addition to a working fluid, in order to produce the impulse necessary to effect the transfer. Electrical power may be produced by an independent power supply that is an integral part of the transfer system itself or may, in the case of low Earth orbit construction, be fulfilled by drawing power from the satellite power station module being transported. This latter possibility may result in a more efficient and more cost effective orbit transfer system. It now appears the more effective choice is to utilize expendable rather than reusable propulsive devices if payload-supplied power can be made available. System requirements for low Earth orbit

and geosynchronous Earth orbit construction will differ to respond to the differing needs of a program performing the construction. Low Earth orbit construction offers the potential for employment of the payload to produce electrical power, as differentiated from the more severe transportation requirements posed by deferring assembly of the power satellite modules until they are transported to geosynchronous orbit. In this latter case, an independent power source such as a nuclear reactor or solar collector must be supplied for any electric propulsion type OTV, or a conventional chemical propulsion system used.

Alternative types of OTV's corresponding to LEO and to GEO assembly choices, will have to be analyzed and defined for comparative evaluation until the assembly location choice and payload power availability for orbital transfer determination is made.

VI-B HEAVY LIFT LAUNCH VEHICLE (HLLV)

(E. M. Crum, Future Programs Office and D. Webb, Resources Management Office)

B-1 SUMMARY

The HLLV is responsible for transporting all SPS freight, except crews and high priority cargo, from Earth to LEO. The launch site is assumed to be KSC and payloads are launched into approximately 500x100 km, 28.5° inclination insertion orbits. Payload circularization and rendezvous propulsion is provided by an orbital maneuvering system (OMS) to decrease launch velocity requirements and facilitate recovery. This imposes a weight penalty of approximately 3% on the payload for the OMS, including propellant, and requires a subsequent return to Earth of at least the OMS engines and avionics by Shuttle or the Personnel and Priority Cargo Launch Vehicle (PLV). The cost of OMS recovery has not been investigated further in this study. The ground rules and requirements developed for the HLLV may be found in the previous section.

The key figure of merit for the HLLV is the cost per pound of payload to LEO. Minimizing this cost requires attaining as much reusability as possible with as little refurbishment and parts replacement as can be achieved. Reuse goals of 300 and 500 flights were confirmed to be attainable from a structural design (fracture mechanics) standpoint and are suggested as the range for launch vehicle replacement calculations and costing purposes.

A 1995 level of technology is assumed, although no particularly large or vital technical advances appear to be mandatory. Hydrocarbon fuel density improvement over hydrogen allows enough decrease in structure with related cost advantages to outweigh the higher specific impulse of hydrogen fueled engines. Engines considered were:

<u>Engine</u>	<u>Fuel</u>	<u>Oxidizer</u>	<u>Specific Impulse</u>		<u>Vac. Thrust/Dry Wt</u>
			<u>S. L.</u>	<u>Vac.</u>	
F-1 ($\epsilon = 10$) ²	RP-1	O ₂	262	288.4	93
SSME ¹	H ₂	O ₂	363.2	455.2	74
New RP-1 ¹	RP-1	O ₂	313	344	90
New RP-1 ²	RP-1	O ₂	280.2	312.8	107
New propane ²	C ₃ H ₈	O ₂	302.8	337.5	100
Growth SSME ¹	H ₂	O ₂	--	466	75

¹Staged combustion.

²Gas generator.

Numerous configurations were considered as candidate HLLV's including concepts developed by contractors. Three JSC design teams investigated the following candidate concepts and variations:

<u>Candidates</u>	<u>1st Stage</u>	<u>2nd Stage</u>	<u>Payload Metric Tons</u>
Modified SSTO (H ₂ Drop Tank)	O ₂ /H ₂	--	100-175
2 Stage Winged	O ₂ /H ₂	O ₂ /H ₂	450
	O ₂ /RP-1	O ₂ /H ₂	450
	O ₂ /Propane	O ₂ /H ₂	450
2 Stage Ballistic	O ₂ /RP-1	O ₂ /H ₂	450
	O ₂ /Propane	O ₂ /H ₂	450
	O ₂ /RP-1	O ₂ /H ₂	900
	O ₂ /Propane	O ₂ /H ₂	900

These systems represent the range of launch vehicle concepts suggested by the Technology Forecast Section of the Outlook for Space Report and by NASA and industry experts. Particular omissions, such as mixed ballistic and winged systems and the very large (450 ton payload) single stage to orbit (SSTO) vehicles were considered in a study contracted to Boeing (NAS 9-14710). Study analyses conducted to date did not identify the mixed systems as leading candidates, although the large SSTO was considered a close competitor to the two-stage ballistic vehicle.

The DDT&E costs developed for the HLLV concepts include the non-recurring costs associated with the design, development, test and evaluation of the vehicle. The TFU costs include the recurring costs associated with the production of the first article in a hardware production program. No learning has been assumed as a part of the TFU cost. The estimating was done by using parametric cost estimating relationships (CER's) in which, for most subsystems, weight is the independent variable. In general, the data base used to develop these CER's included the following programs: Shuttle, SIVB, SIC, SII, Centaur, and various airplanes, with emphasis on the C5A. The data from these programs was collected, analyzed, formatted to a common work breakdown structure, normalized, and converted to a constant year dollar base. The adjusted data was then analyzed and regressed statistically. These statistical regressions, CER's, were then used to estimate the various elements of the vehicle. The sum of the elements gives the total TFU and DDT&E costs for each vehicle. In the cases where Shuttle hardware was used as is, the TFU cost was taken directly from Shuttle data and was not estimated by using the above approach. The DDT&E costs for this Shuttle hardware were estimated at a

fraction of the cost for a completely new development. The management and support types of CER's relied heavily on Shuttle data.

The Operations Costs for a flight were developed from Shuttle data and from expected improvements in operations capability by the 1995 time frame. The cost for the refurbishment of the vehicle per flight was reduced from the Shuttle's 3% TFU to less than 1% TFU. The cost of personnel per flight was reduced to about one-half that of Shuttle. Recovery operations costs were based on an Apollo size crew and fuel costs were based on today's prices.

The three following sections are the reports of the individual design teams.

VI-B-2 MODIFIED SINGLE STAGE TO ORBIT HEAVY LIFT LAUNCH VEHICLE

JACK FUNK
MISSION PLANNING AND ANALYSIS DIVISION

I. GENERAL DESCRIPTION

The single stage to orbit (SSTO) heavy lift launch vehicle configuration is shown in figure VI-B-2-1. The vehicle consists of a lifting body entry vehicle which contains the liquid oxygen propellant tank, main propulsion systems, guidance system and other support systems, and an external expendable liquid hydrogen fuel tank. The vehicle is operated single stage to orbit, that is, the hydrogen tank is carried all the way to orbit where it is staged for disposal with a technique similar to the disposal of the shuttle external propellant tank. Launches from KSC would use a disposal area in the Indian Ocean, the same as the shuttle. The entry vehicle and payload proceed to 185 KM (100 n.mi.) circular orbit using the on-orbit maneuvering system. The payload is separated and the heavy lift launch vehicle returns to the launch site for a horizontal landing.

After separation the payload completes the orbit phase of the mission using an on-orbit maneuvering system.

The heavy lift launch vehicle does not have a payload bay for launch and return of the payload. All payloads are carried external-piggy back. Manned payloads and payloads returned from orbit are carried in a modified shuttle orbiter. Since the shuttle orbiter no longer requires a main propulsion system, it can be modified to increase its payload, improve its landing characteristics, and safety of operation.

Cargo for construction of the Solar Power Satellite Systems (SPS) is carried to orbit in a reusable cargo glider. Figure VI-B-2-2 shows the launch configuration with the cargo glider. The cargo glider is a light weight entry vehicle with a monocoque fuselage to carry cargo, light weight wings for entry and landing, an orbit maneuvering system, attitude control and guidance. The glider is unmanned and has no return payload capacity.

Although the heavy lift launch vehicle is primarily being sized to support the Solar Power Satellites (SPS), this particular configuration is general purpose and can support all future space missions. This flexibility is obtained by carrying the modified orbiter as a payload. Since the vehicle is single stage to orbit, it also can operate from a variety of launch sites using the suborbital staging technique developed for disposal of the shuttle external tank. Suitable water disposal areas are available from many launch site locations.

II. VEHICLE SIZING ANALYSIS

The basic considerations in the sizing analysis are the weight of payloads to be carried, the systems and structure weight scaling factors

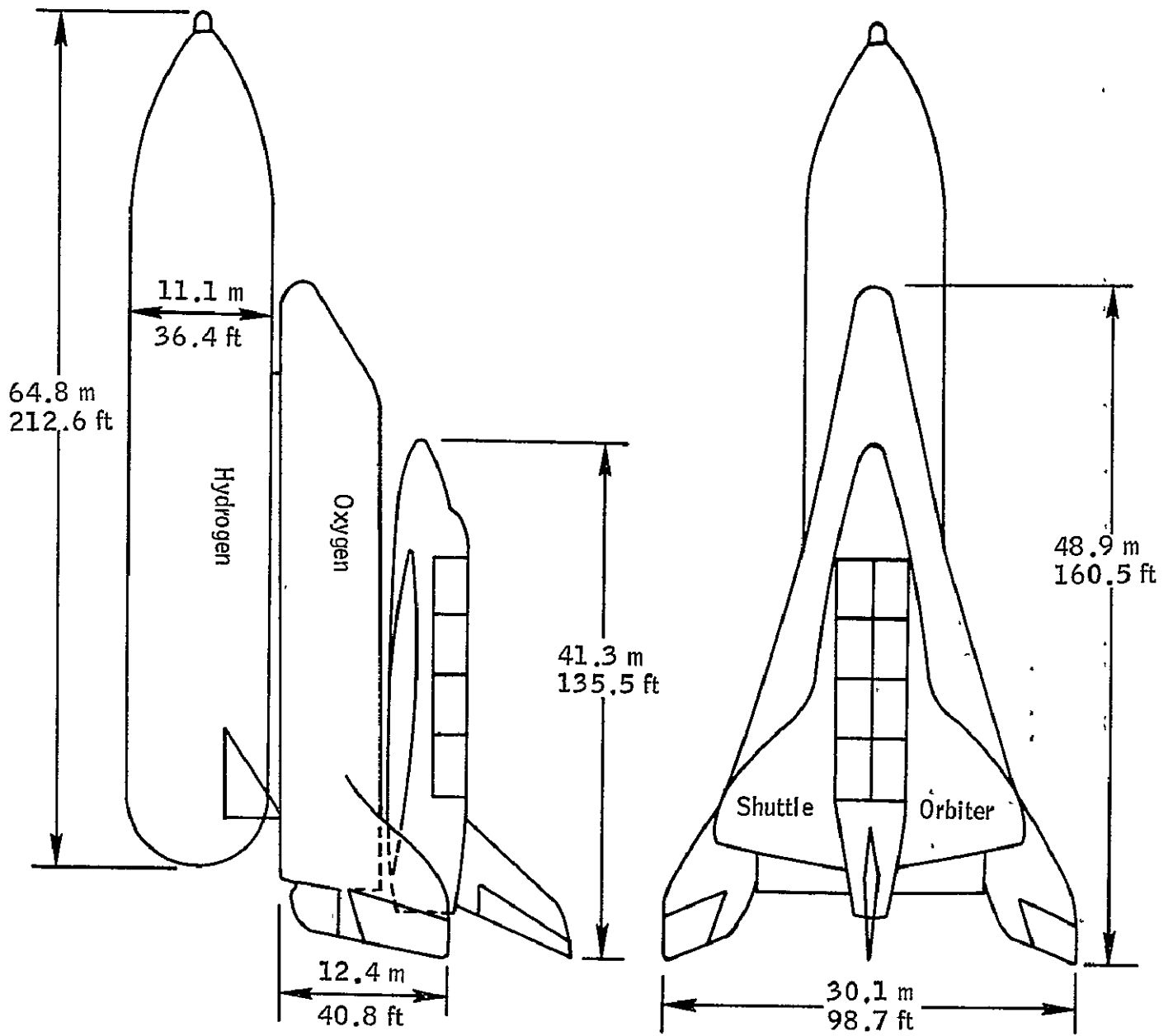


Figure VI-B-2-1.- Single stage to orbit heavy lift launch vehicle with shuttle orbiter payload.

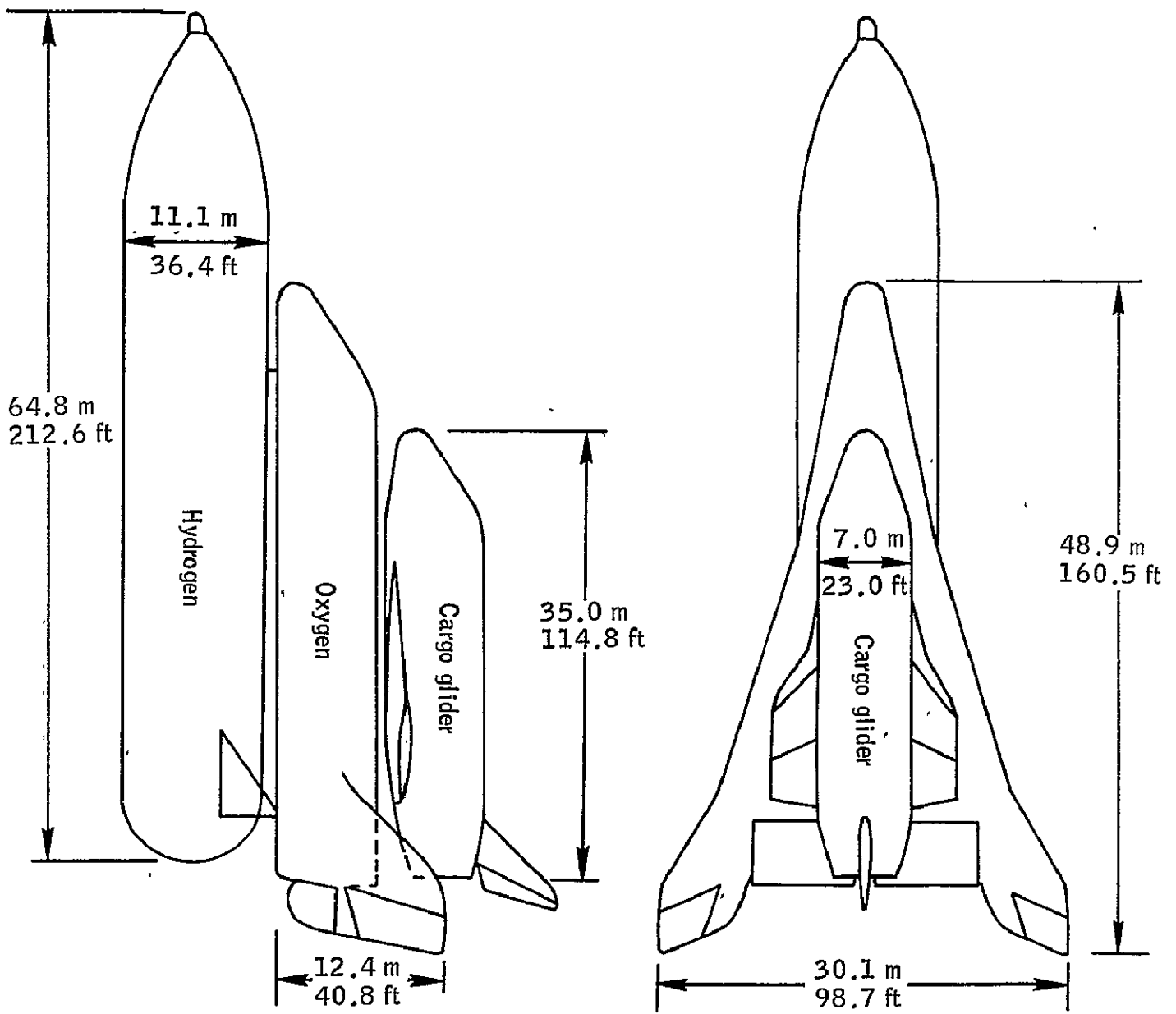


Figure VI-B-2-2. - Single stage to orbit heavy lift launch vehicle with cargo glider payload.

for current and future technology projections, and the number and size of the main propulsion rocket engines. The payload chosen to size the heavy lift launch vehicle is the modified orbiter with 45,000 Kg (100,000 pounds) payload. The gross weight of this payload is about 129,000 Kg (283,800 pounds) (see table VI-B-2-9).

The weight scaling factors used for structure and system weight estimates are based on current technology. Where applicable the weight scaling factors were based on shuttle technology. Scaling factors obtained from several studies and the shuttle project weight statements are shown in table VI-B-2-1. In each category the first scale factor listed is the one used.

The sizing studies were carried out using the current shuttle SSME's as the main propulsion unit and with an uprate version of the shuttle SSME's. The uprated version consisted of increasing the chamber pressure from 3,000 to 4,000 psi. The characteristics of the current and uprated engines are shown in table VI-B-2-2. The data for the uprated engine were supplied by the JSC Propulsion and Power Division.

The launch simulation used in the sizing analysis consisted of two dimensional integrated trajectories with a gravity turn (zero angle of attack) to 30,480 meters (100,000 feet) altitude and optimum steering above 30,480 meters (100,000 feet) altitude. The thrust to weight at lift off was constant at 1.25. Launches were due east at 28.5 degrees latitude to 111.1 KM (60 n.mi.) altitude above the equatorial radius. The external fuel tank was staged at 7,823 meters/seconds (25,665 feet/seconds) and a flight path angle of 0.5 degrees. These staging conditions result in a tank impact in the Indian Ocean if launch is from KSC. The orbit maneuvering propellant requirements for circularization in 185 KM (100 n.mi.) orbit and deorbit was calculated for a specific impulse of 313. The 1962 standard atmosphere was used for drag calculations.

The drag coefficient as a function of Mach number is given in table VI-B-2-3 for the lifting body and the external tank. The forebody drag coefficient is given for the lifting body and this is combined with the power on base pressure to obtain the total drag. The drag coefficient for the external tank is power off total drag. It was assumed that there is no power on effect on the base of either the external tanks or payload.

The drag calculations are based on a reference platform area for the lifting body of 453.2 square meters (4,878 feet squared) and is varied according to the square of the scale. The vehicle scale is determined by the LOX volume and the system volume requirements given in table VI-B-2-4. The lifting body scale factor is the cube root of the ratio of the total volume to the reference volume of 2,738.2 cubic meters (96,700 cubic feet).

TABLE VI-B-2-1
WEIGHT SCALING FACTORS

<u>Item</u>	<u>Scale Factor</u>	<u>Reference</u>
Tail Surface (% Dry Wt.)	6.13 1.89 2.59	Lockheed 1½ Stage Study Shuttle Orbiter Martin-Langley STO Study
Body LOX Tank (lb/ft ³)	1.034 0.803 0.473*	Shuttle ET LOX Tank Increased Safety Factor to 1.8 Shuttle LOX ET Martin Langley STO Study
Thrust Structure (% Thrust)	0.3943 0.249	Lockheed 1½ Stage Study Shuttle Orbiter
Heat Shield (% Dry Wt.)	11.9 12.13 19.5	Shuttle Orbiter Lockheed 1½ Stage Study Martin-Langley STO Study
Landing and Aus. Systems (% Dry Wt.)	3.5 3.38 4.07 5.50	Shuttle Orbiter Geal Only Lockheed 1½ Stage Study Martin-Langley STO Study
Surface Controls (% Dry St.)	1.25 1.82 1.30	Lockheed 1½ Stage Study Shuttle Orbiter Martin-Langley STO Study
Margin (% Dry Wt.)	10.0%	
External Hydrogen Tank (lbs/ft ³)	.7739	Shuttle ET
Gasses and Unusable Propellant	.1806	Shuttle ET
Propulsion Main - Shuttle SSME weight statement, see table.		
Propulsion OMS RCS Prime Power Electrical Conversion and Distribution Hydraulic Conversion and Distribution Avonics		Fixed weights from shuttle orbiter weight statement. Avonics reduced by ½ to reflect reduced redundancy and on-orbit requirements.

*Includes payload bay and crew compartments. Average of both hydroben and LOX tanks and thrust structure-

TABLE VI-B-2-2

MAIN PROPULSION SYSTEM WEIGHT AND
PERFORMANCE DATA BASED ON SSME

Expansion Ratio	Vacuum Specific Impulse (Sec)	Vacuum Thrust (Lbs)	Mixture Ratio	Weight* (Lbs)	Ae/Fv (In ² /Lbs)
77.5	455.3	512,300	.6.0	8,779	0.01261
60.0	451.2	507,687	6.0	8,513	0.009858
50.0	448.3	504,424	6.0	8,347	0.008265
40.0	444.4	500,035	6.0	8,153	0.006672
Up-rated SSME					
40.0	442.0	626,596	6.0	8,460	0.005324

*Weight without gimble system. Gimble system 600 lbs. per engine.

TABLE VI-B-2-3

LAUNCH VEHICLE DRAG CHARACTERISTICS

Lifting Body		External Tank	Lifting Body Power on Base Pressure	
M	C_{AF}	C_A	ALT(ft)	PSI
0.0	.055	.409	0	-0.8
0.6	.055	.409	4000	-1.2
0.7	.056	.430	8000	-1.5
0.8	.063	.454	13000	-1.5
0.9	.080	.475	20000	-1.2
1.0	.111	.663	27500	-0.8
1.1	.134	.774	37000	0
1.2	.147	.819	43500	0.4
1.4	.155	.850	54500	0.8
1.6	.157	.846	70000	1.10
1.8	.153	.808	80000	1.15
2.0	.148	.772	90000	1.15
2.4	.140	.707	100000	1.11
3.0	.130	.608	120000	1.05
4.0	.122	.500	140000	1.00
5.0	.117	.464	160000	1.00
25.0	.117	.464	500000	1.00

In a similar manner the external hydrogen tank drag is based on the shuttle external tank shape scaled to contain the required volume of liquid hydrogen. The reference area for the external tank is 55.56 square meters (598 square feet) and the reference volume is 2,220.9 cubic meters (78,431 cubic feet).

The power on base force was calculated from the power on base pressure using the total area of the base of the lifting body minus the area of the engine bells. As engines were turned off, the force was reduced by the percentage of engines not operating. The power on based pressure data given in table VI-B-2-4 were obtained from the shuttle phase B study reports.

An analysis was made to determine the best expansion ratio for the SSME. Simulations were run using 15 SSME's for expansion ratios of 77.5, 60, 50, and 40. Payload as a function of expansion ratio is shown in figure VI-B-2-3. It is observed that the lower expansion ratio results in the largest payload. The increased thrust at sea level from the lower expansion ratio results in more propellant being lifted off the launch pad. The added propellant increases the payload more than the loss in specific impulse as the lower expansion ratio decreases the payload. This is an important result since the size of the lifting body is limited by the number of engines that can be fitted on the base, the volume of the lifting body increases as the cube of the scale, whereas, the base area increases only as the square and therefore, for each type engine, there is a maximum vehicle size. The smaller expansion ratios result in a higher thrust density and a larger maximum size.

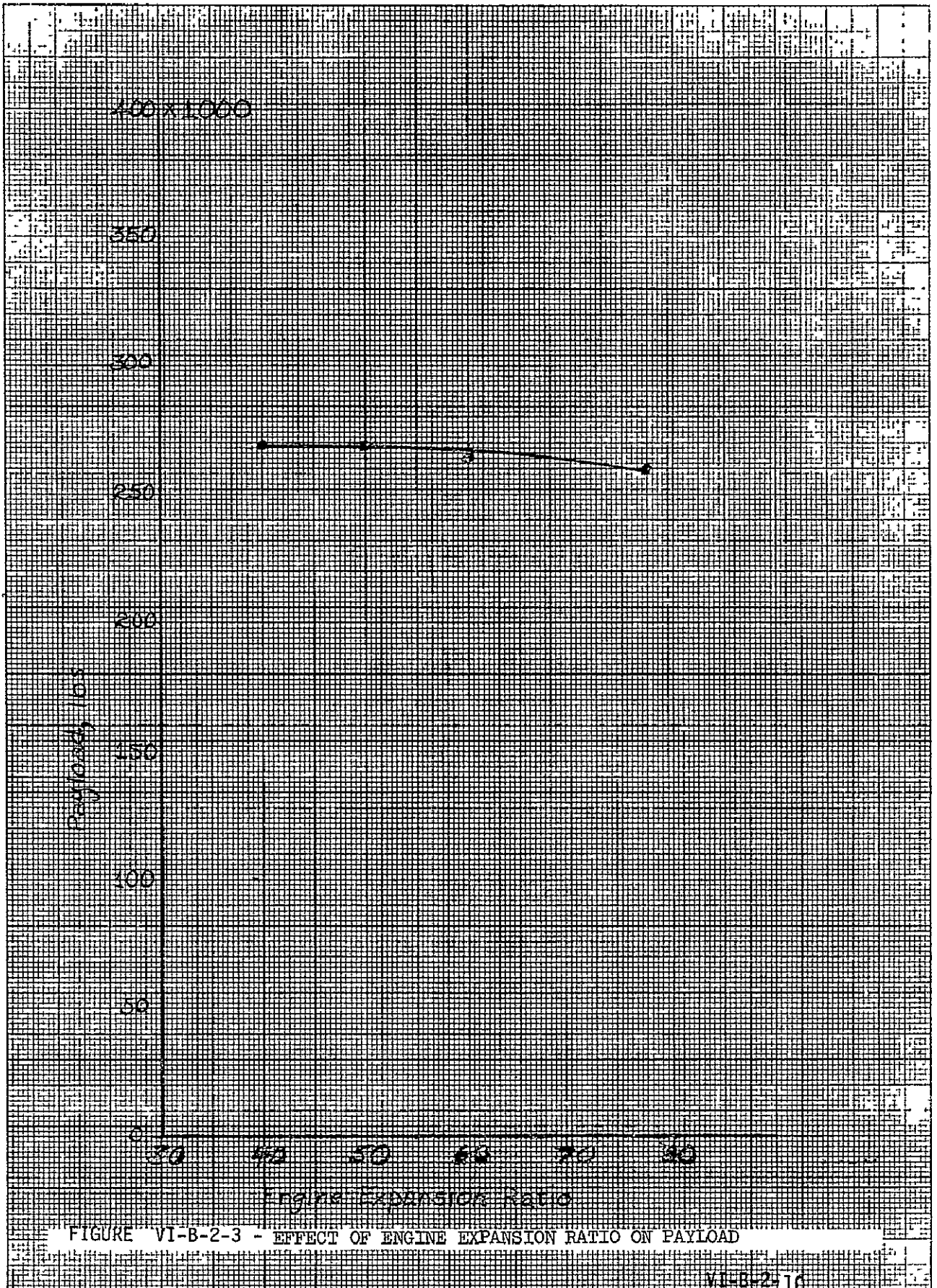
Payload as a function of the number of main engines for 40.1 expansion ratio is shown in figure VI-B-2-4 for both the SSME and the uprated SSME. As should be expected, the payload is linearly related to the number of main propulsion engines.

III. VEHICLE SIZE

The baseline heavy lift launch vehicle was sized to carry the modified orbiter glider with 45,000 Kg (100,000 pounds) payload in the payload bay. The gross weight of the modified orbiter from table VI-B-2-8 is 129,000 Kg (283,800 pounds). From figure VI-B-2-4 it is seen that the heavy lift launch vehicle required 19 standard SSME's or 15 uprated SSME's to lift the modified orbiter into orbit. Since it may not be possible to mount 19 standard engines on the base, the baseline launch vehicle has 15 uprated SSME's and can carry a 324,000 pound payload into 100 n.mi. circular orbit. A typical launch trajectory for the 15 engine vehicle is shown in table VI-B-2-5. A weight summary for the baseline vehicle is given at the bottom of table VI-B-2-5.

TABLE VI-B-2-4
VOLUME REQUIREMENTS

	Fraction of Total
Air Frame Structure, Tank Walk and TPS	.09867
Wheel Wells	.01865
Equipment and ACS	.01025
Prop Liner and Tank Support	.01393
Thrust Structure	.04734
Main Engines and OMS Engines	.06045
Base Between Engines	.04908
Lower Flap	.01363
Fin Rudder and Aux Surface	.04436
Flap Stowage	.04375
LOX Tankage	.59989
Total	1.0000



ORIGINAL PAGE IS
OF POOR QUALITY

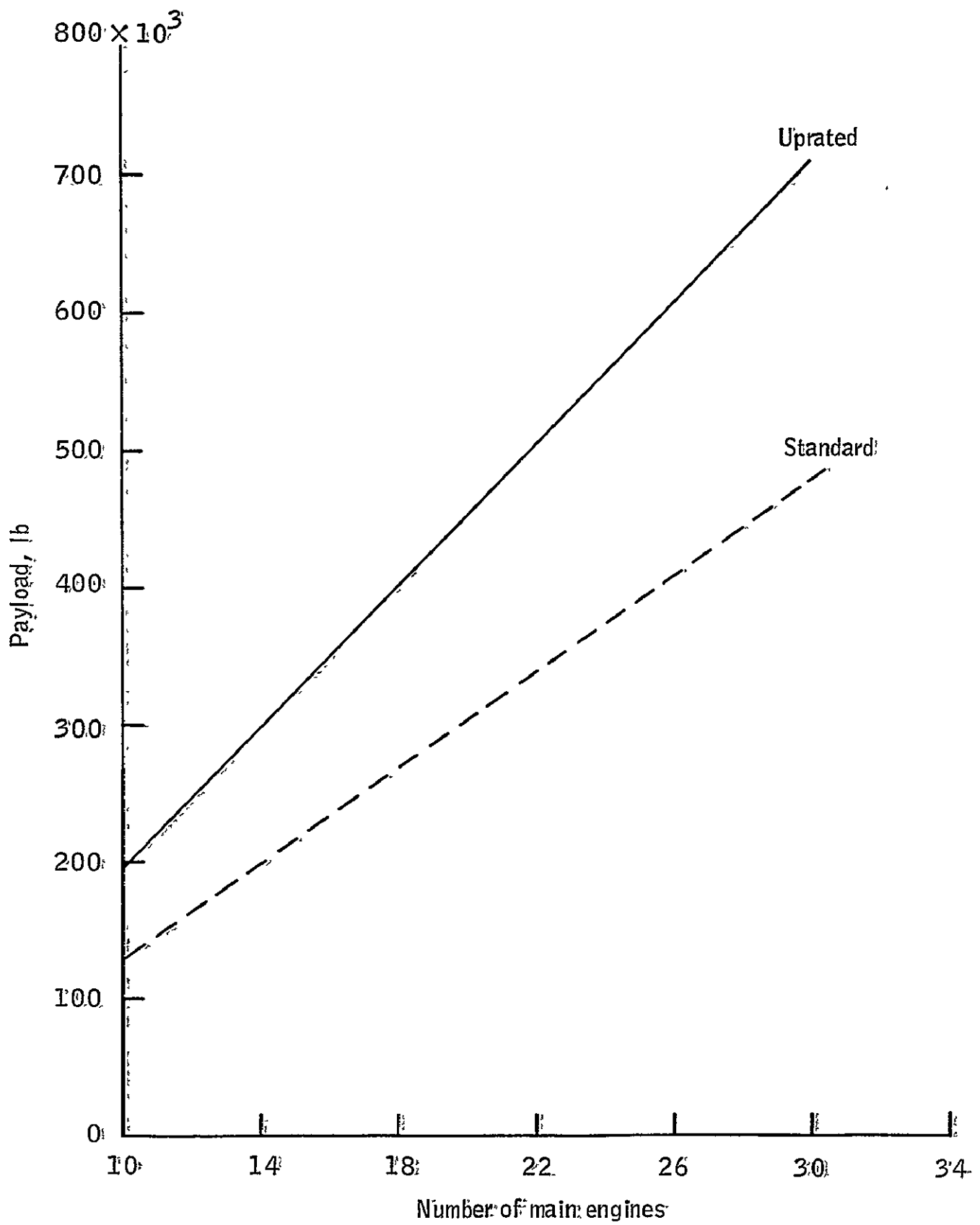


Figure VI-B-2-4.- Payload as function of number of main engines, 40:1 expansion ratio.

TABLE VI-B-2-5

SINGLE STAGE TO ORBIT HEAVY LIFT LAUNCH VEHICLE LAUNCH
TRAJECTORY PARAMETERS AND WEIGHT SUMMARY

#INPUT GAMI=89.950, NEAI=15, NEBI=0, NECI=0, VSTAGE=26000, #END											
GLOW = 6930682		T/W = 1.25		INC = 28.5		AZI = 0					
TIME	ALT	VEL	GAMA	TANG	WEIGHT	TWR	NE	DPAG	BP		
0.0	0.	0.	0.	0.	6930682	1.250	15	-440994.	1.		
10.0	403.	82.	0.	0.	6718036.	1.250	15	1488806.	1.		
20.0	1674.	175.	0.	0.	6505391.	1.338	15	1976698.	-1.		
30.0	3940.	281.	0.	0.	6292745.	1.338	15	2855933.	-1.		
40.0	7224.	400.	1.	0.	6080100.	1.454	15	4014888.	-1.		
50.0	11348.	535.	1.	0.	5867455.	1.554	15	5985337.	-1.		
60.0	17930.	692.	1.	0.	5654810.	1.554	15	5985337.	-1.		
70.0	27535.	878.	1.	0.	5442165.	1.678	15	6951884.	-1.		
80.0	34163.	1089.	1.	0.	5229520.	1.763	15	1111792.	-1.		
90.0	44106.	1336.	1.	0.	5016875.	1.951	15	1073017.	-1.		
100.0	54998.	1646.	1.	0.	4804230.	1.951	15	8931178.	-1.		
110.0	66486.	2032.	1.	0.	4591585.	1.951	15	6773115.	-1.		
120.0	78302.	2490.	1.	0.	4378940.	1.441	15	4773309.	-1.		
130.0	90089.	3035.	1.	0.	4166295.	1.951	15	3241449.	-1.		
139.0	100295.	3585.	1.	0.	3953650.	1.951	15	2660028.	-1.		
CHANGE TO INERTIAL											
139.0	100295.	4885.	210.	13.0	3974908.	1.363	15	2368003.	1.		
140.0	101403.	4960.	208.	13.0	3953643.	1.363	15	1956881.	1.		
150.0	113130.	5735.	174.	12.4	3740998.	1.111	15	1400995.	1.		
175.0	146653.	7887.	86.	10.4	3270938.	1.073	15	-189999.	1.		
200.0	183339.	10205.	39.	8.5	2724444.	1.133	15	-779999.	1.		
225.0	220997.	12504.	15.	6.9	2231344.	1.111	15	-294170.	1.		
250.0	257723.	14779.	5.	5.4	1969960.	1.073	15	-104072.	1.		
275.0	294900.	17075.	1.	4.1	1679901.	1.073	15	-284444.	1.		
300.0	318557.	19305.	0.	3.0	1431667.	1.073	15	-657220.	1.		
325.0	340889.	21530.	0.	2.0	1214693.	1.073	15	-549777.	1.		
350.0	356599.	23767.	0.	1.2	1047488.	1.073	15	-550534.	1.		
372.7	364594.	25666.	0.	0.6	917778.	1.073	15	-440542.	1.		
VC	28750.	SPET	1.353	SF	1.073						
APOGEE ALTITUDE 481401.		PERIGEE ALTITUDE 88626.									
DV1	81.	APOGEE ALTITUDE 607885.		PERIGEE ALTITUDE 230373.							
DV2	259.	CIRCULAR ORBIT 100 NMI		DEORBIT VELOCITY 250.							
SINGLE STAGE TO ORBIT HEAVY LIFT-LIFTING BODY STUDY											
PALOAD 324017.											
TAIL STRUCTURE	23622.	PRIME POWER	2895.								
BODY STRUCTURE	108891.	ELECTRICAL CONV&DIST	6915.								
HEAT SHIELD	45864.	HYDRAULIC CONV&DIST	1840.								
LANDING AND AUX SYST	13430.	SURFACE CONTROLS	4797.								
PROPULSION-MAIN	129900.	AVONICS	2500.								
PROPULSION-OMS&PCS	5000.	MARGIN	38373.								
INERT WEIGHT 383727.											
RESIDUAL UNUSABLE FL	15287.	PROPELLANT OMS	27978.								
RESERVE FLUIDS	0.	PROPELLANT PCS	5000.								
INFLIGHT LOSSES	0.	FLIGHT PERFORM RES	4992.								
ORBIT HYDROGEN TANK	151974.	HYDROGEN FUEL	858986.								
PP-1 TANK	0.	PP-1	0.								
LOX TANK	74732.	OXYGEN	5153915.								
INPUT											

ORIGINAL PAGE IS
OF POOR QUALITY

The plan form of the lifting body is scaled from the Lockheed 1 1/2 stage shuttle phase B study since this shape has a large amount of aerodynamic stability and entry data available. The volumetric requirements of the various systems are given in table VI-B-2-4. From this table it is seen that 60% of the volume is LOX. The GLOW of the 15 engine vehicle is 3,150.3 MT (6,930,682 pounds) of which 2,350 MT (5,170,064 pounds) is LOX. The LOX tank volume requires 2,053.3 cubic meters (72,511 cubic feet). The air frame volume, therefore, is 3,422.1 cubic meters (120,852 cubic feet). This is a 25 percent increase in volume over the phase B shuttle studies of the lifting body. Since the dimensions scale is the cube root of the volume, the scale factor is 1.074. A three view drawing is shown in figure VI-B-2-5.

IV. MODIFIED ORBITER

The shuttle orbiter carried as a payload on the SSTO heavy lift launch vehicle does not require a main propulsion system. The orbiter, therefore, can be modified to reduce its weight and improve its aerodynamic characteristics. The main propulsion system and thrust structure can be removed. A tail section is added behind the payload bay to reduce base drag. The aft Reaction Control System and Orbit Maneuvering System systems are moved from the side into the tail section, and to provide an off the pad abort capability, one SSME with an expansion ratio of 9 mounted in the back of the tail section. This engine will provide 500,000 pounds of thrust which will lift the orbiter and its payload off the pad with an acceleration of 2g.

Since the pad abort SSME requires LOX hydrogen as a propellant, the orbit maneuvering system is changed to use LOX/LH2 as a propellant and two RL10 engines are mounted, one each above and below the abort engine for on-orbit maneuvering. The propellant tanks are mounted in the tail section and are used to fuel either the on-orbit maneuver or the abort engine. The AFT RCS tanks are also mounted in the tail section.

The weights for the combined orbit maneuvering and abort system are shown in table VI-B-2-6.

An analysis of the inert weight and center of gravity location of the modified shuttle is shown in table VI-B-2-7. Platform and side elevation of the modified orbiter showing the location of the orbit maneuvering system, pad abort engine, and propellant tank is shown in figure VI-B-2-6. The modified orbiter weight summary is shown in table VI-B-2-8.

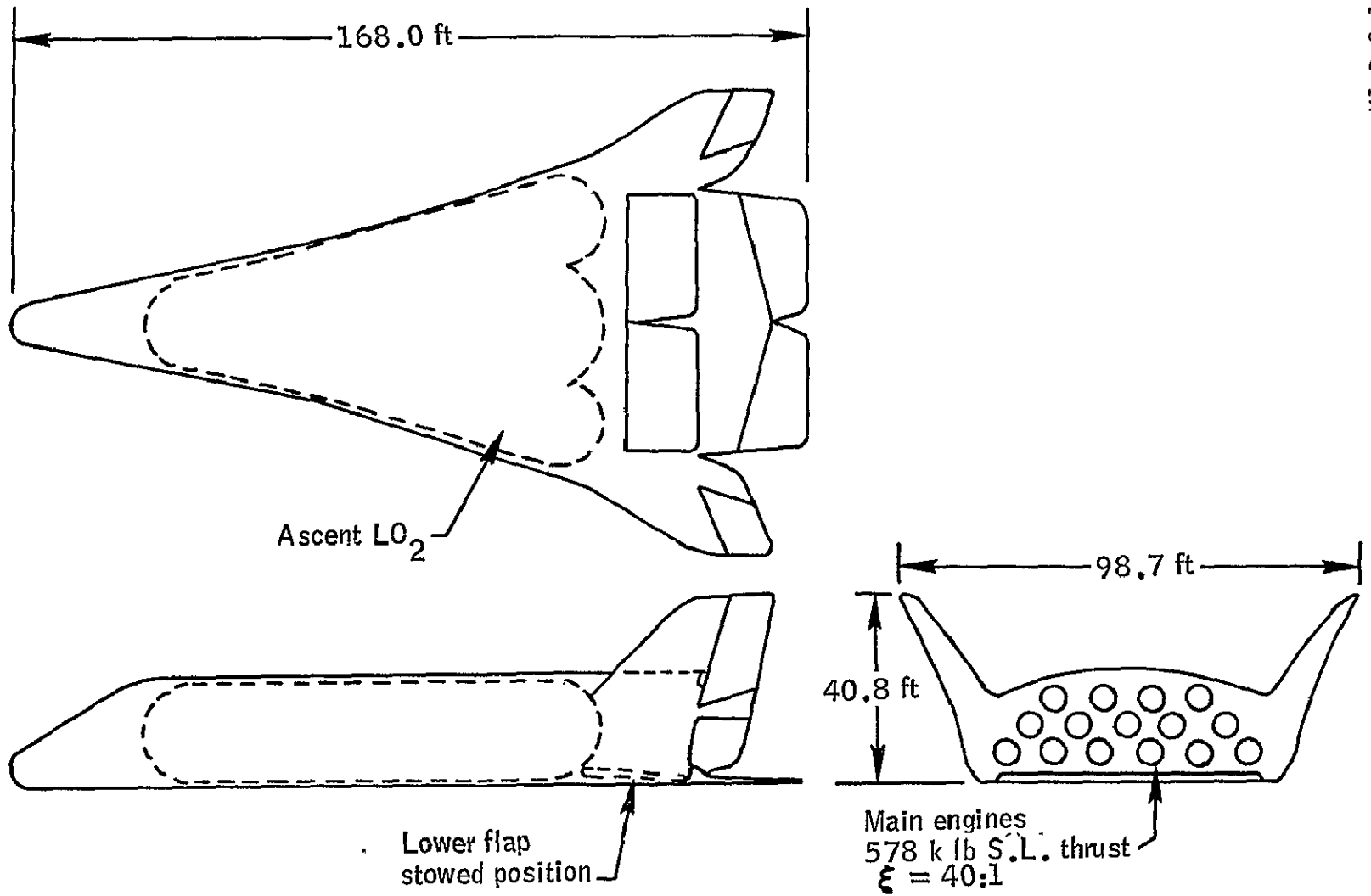


Figure VI-B-2-5.- Heavy lift launch vehicle - entry configuration.

TABLE VI-B-2-6
 COMBINED ORBIT MANEUVERING AND ABORT SYSTEM

Propellant Capacity (lb)	36,000
Tank Volume (ft ³)	1,635
Tank, Feed and Pressurization Weight (lb)	4,024
OMS Engine Weight 2 Engines	720
Abort Engine Weight (lbs)	8,000
Thrust Structure (lbs)	2,000
OMS Engine Volume Specific Impulse (sec)	444
OMS Engine Thrust, Lach (lbs)	15,000
Abort Engine Sea Level Specific Impulse (sec)	400
Abort Engine Sea Level Thrust (lbs)	500,000

TABLE VI-B-2-7

MODIFIED ORBITER GLIDER WEIGHT AND CENTER OF GRAVITY

	Weight (lbs)	X-GG (in)
Shuttle Orbiter	151,428	1118.7
1. Remove Main Propulsion	-28137	1466.4
2. Remove Thrust Structure	-3831	1423.6
3. Remove OMS System	-29042	1458.0
4. Remove OMS/RCS Pod	-2293	1457.2
5. Remove OMS Pod TPS	- 600	1460.0
6. Add 20 Ft Tail Section	+5000	1543.0
7. Add Tail Section TPS	+1500	1543.0
8. Add Abort Engine	+8000	1610.0
9. Add Thrust Structure	+2000	1580.0
10. Add OMS Engines	+ 720	1610.0
11. Add OMS Tank and System	+4024	1520.0
12. Move Aft RCS	-1399	1449.8
	+1399	1629.8
Total	134,907	1095.8

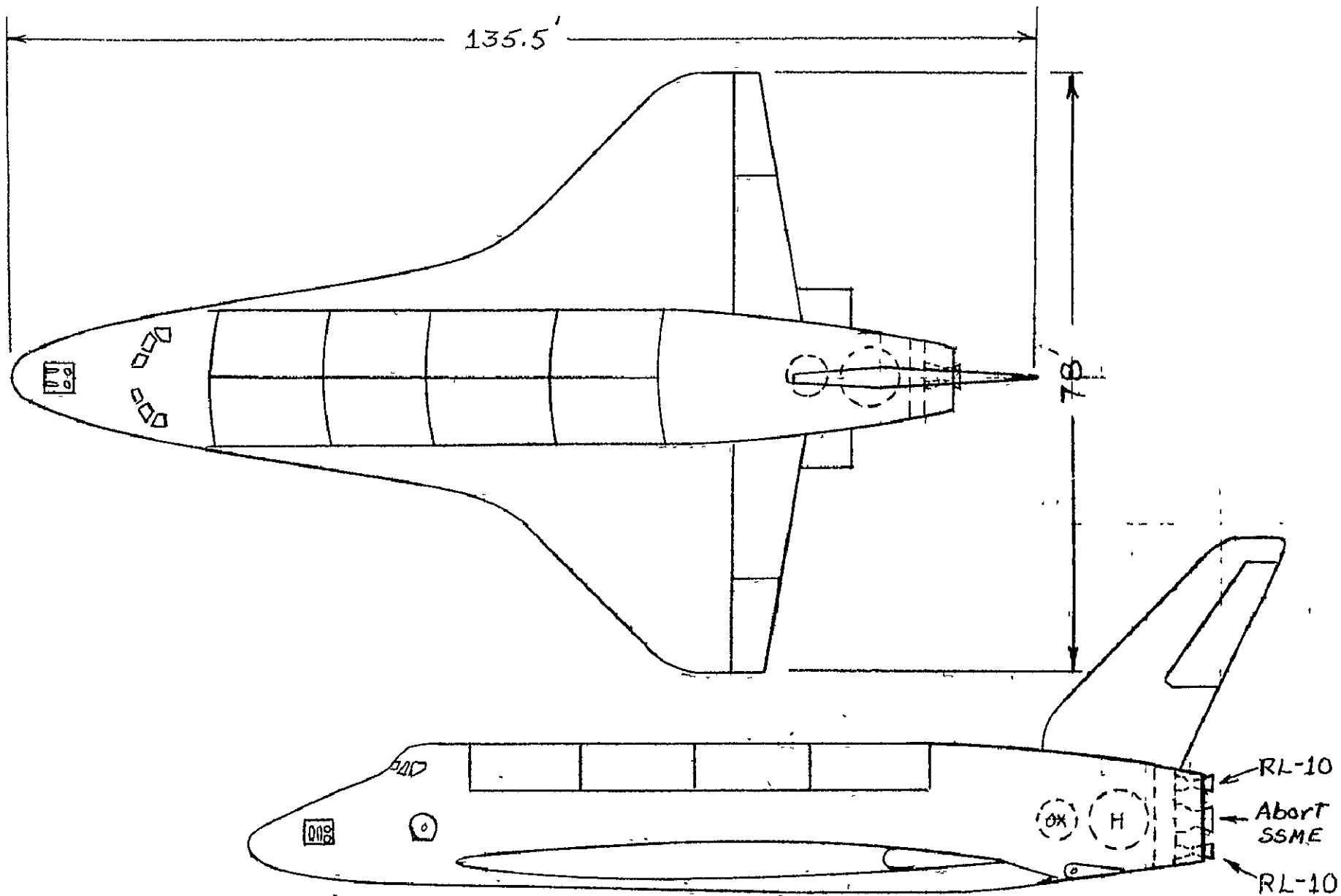


FIGURE VI-B-2-6 - MODIFIED SHUTTLE ORBITER

TABLE VI-B-2-8
MODIFIED ORBITER WEIGHT SUMMARY

Inert Weight	134,907
Personnel	2,644
Payload Accommodations	450
Payload Up	100,000
Residual and Unusable Fluids	1,503
Reserve Fluids	1,469
Propellant OMS	36,000
Propellant RCS	5,278
Total	282,251

V. MAXIMUM VEHICLE SIZE

Preliminary layouts were made of the base area of the lifting body for various vehicle size to determine the maximum size. The engine units were mounted 96 inches on centers. The power head diameter is 65 inches. The required dimensional scale to contain the LOX propellant is shown in figure VI-B-2-7 as a function of the number of main engines.

Layouts of the base area are shown in figure VI-B-2-8 for 21 and 28 uprated SSME's. The maximum size for 96 inches on center mounting of the SSME's appears to be about 28 units. This results in a heavy lift launch vehicle with a GLOW just under 5,900,000 Kg (13,000,000 pounds) and a payload of 294,000 kg (647,000 pounds) to 185 KM (100 n.mi.) circular orbit.

VI. CONCLUDING REMARKS

The lifting body launch vehicle with external hydrogen tank provides a single stage to orbit heavy lift launch capability which can be constructed with current technology. Additional payload gains can be achieved within current technology by the use of pressurized tank structure on the launch pad. Studies by Martin Marietta and co-sponsored by Langley Research Center (Contract NAS1-13916) indicate that the external tank weights can be reduced as much as 50 percent by the use of membrane tanks. This results in 34,000 to 63,000 Kg (75,000 to 140,000 pounds) gain in payload depending on the HLV size.

Single stage to orbit has the advantage of being operationally simple when compared to a two stage and ballistic launch vehicle. It eliminates the staging operation on launch and the in flight start of the main engines. The horizontal landing on a runway is a much simpler recovery technique than ballistic landing on either land or water. Sea recovery of large boost vehicles can not be considered state-of-the-art, whereas, horizontal landing on a runway is a proven technique. Any cost comparison between this configuration and the two stage ballistic should include RDT&E for development of sea recovery and an estimate of the capital investment in ship, docking facilities, handling facilities, and other support requirements for the sea recovery.

The expendable external tank probably increases the cost per flight. However, this depends on the cost of manufacturing the tank. There are several advantages of the external tank. Hydrogen leaks are less likely to cause explosions with the external tank, and hydrogen leaks were a major problem with the Saturn Launch Vehicle. The

ORIGINAL PAGE IS
OF POOR QUALITY

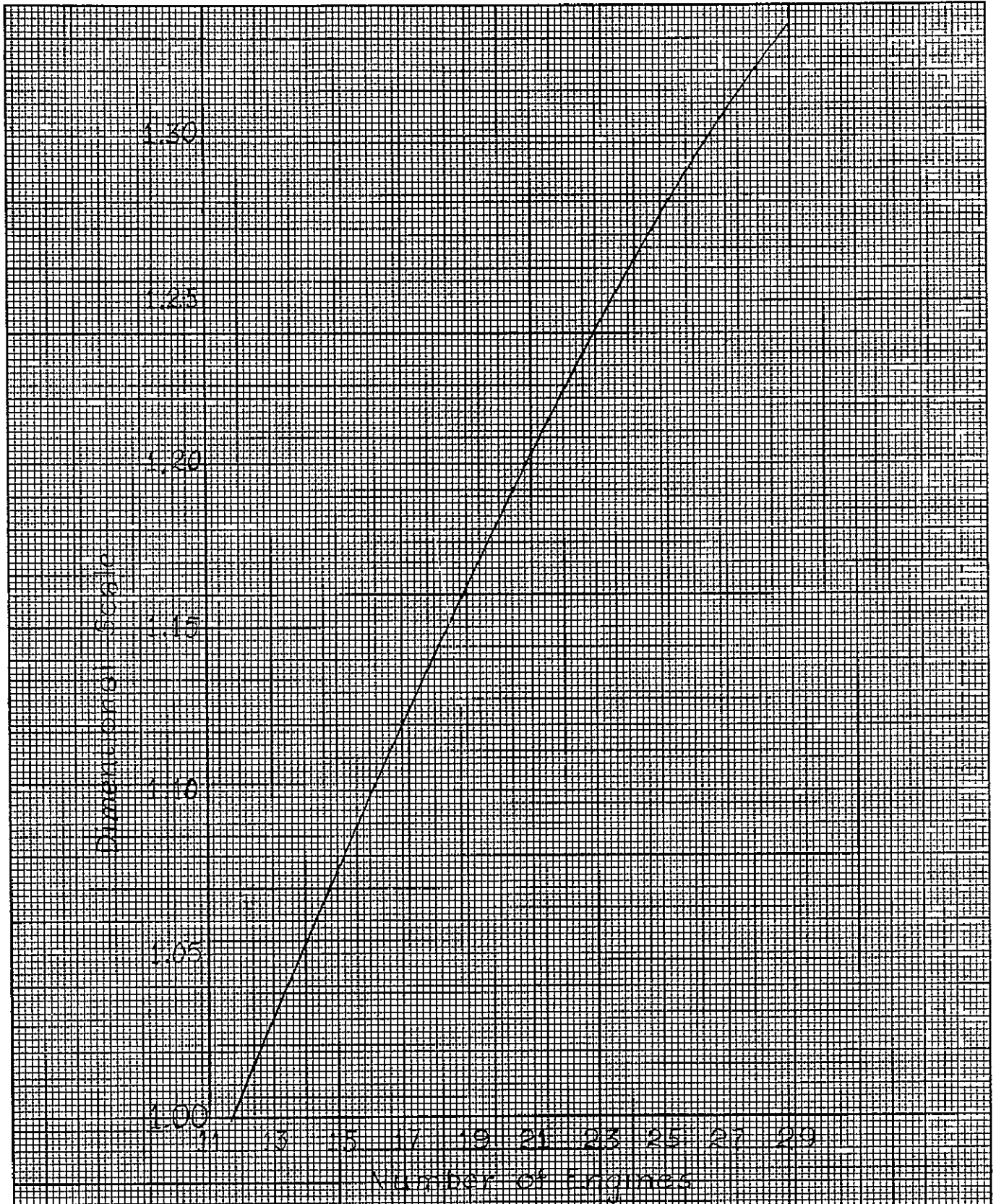
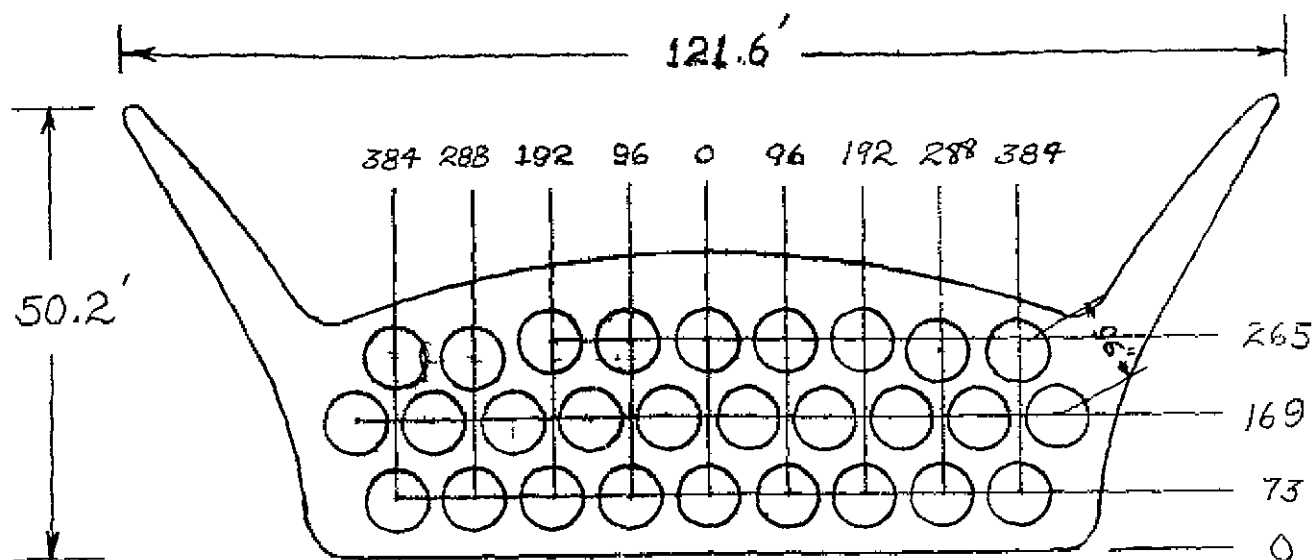
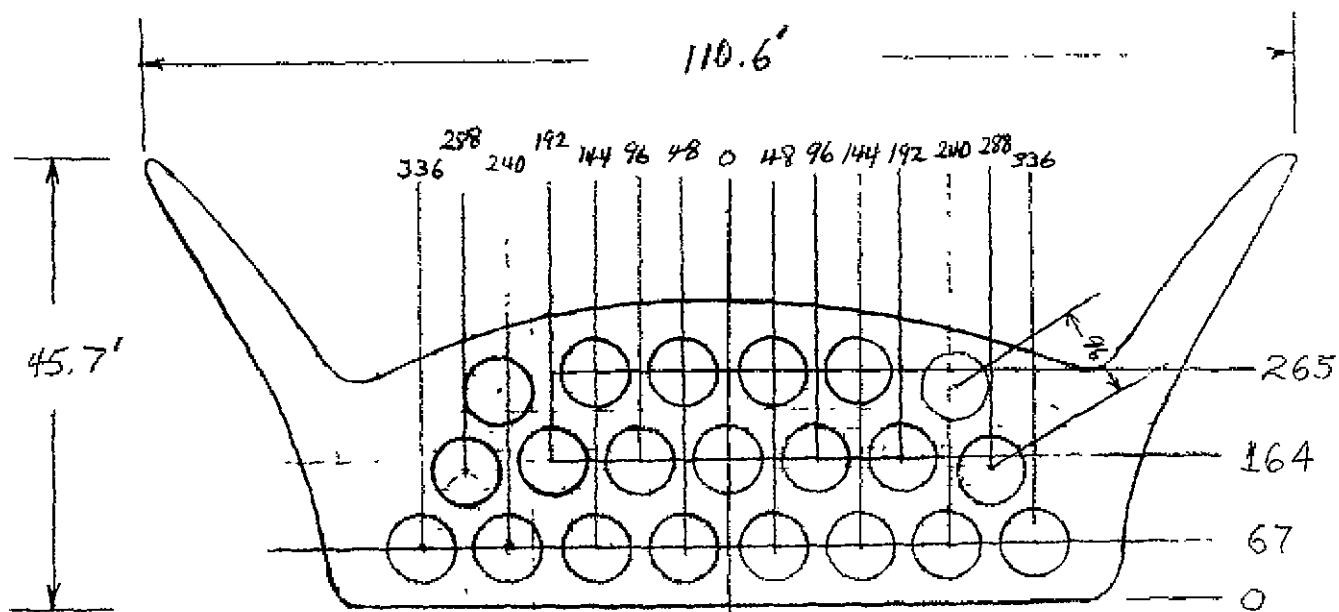


FIGURE VI-B-2-7 - VEHICLE SCALE FACTOR



Scale = 1.322
28 Engines



Scale = 1.202
21 Engines

FIGURE VI-B-2-8 - PRELIMINARY BASE AREA ENGINE LAYOUTS

physical size of the reusable vehicle is considerably reduced and this results in a smaller investment in support facilities. There is a possibility that the aluminum tank can be used as a source of raw aluminum for manufacture of structures in orbit for the solar power system. This would increase the effective payload in orbit by about 25 percent.

The single stage to orbit heavy lift launch vehicle has a high degree of mission flexibility. Designed for a capacity of 150 metric tons, or greater, it can carry, in addition to HLV payloads, the shuttle orbiter. Therefore, it can support all currently planned space missions and missions too heavy or too bulky for the current shuttle, such as space stations and high energy interplanetary missions. The 150 MT vehicle could support all space missions including the SPS pilot plant. The operational phase of the SPS would probably require a larger capacity. Vehicles with a capacity greater than 350 MT would require some technology developments such as a reduction in engine spacing, a change in the aerodynamic shape, or solid rocket thrust augmentation.

Robert B. Bristow
Engineering Analysis Division

SUMMARY

The purpose of this study was to define a heavy lift launch vehicle for the solar power satellite system. Each solar power satellite has been estimated to weigh nearly 91,000 metric tons (200,000,000 pounds) in geosynchronous earth orbit, and would thus require the launch vehicle fleet to deliver close to 227,000 metric tons (500,000,000 pounds) to a low earth assembly orbit for each power satellite.

The mission profile used in sizing the launch vehicles was an unmanned launch from the Kennedy Space Center to an elliptical earth orbit. The launch vehicle injected the payload into a 92.5 x 500 kilometer (50 x 270 nautical mile) orbit; the orbit injection point was near the 92.6 kilometer (50 nautical mile) perigee. After injection the payload was separated from the launch vehicle's second stage. The payload was then placed into a circular orbit at the 500 kilometer (270 nautical mile) apogee by a propulsive system in the payload. Payload at 500 kilometer (270 nautical mile) circular was 453.59 metric tons (1,000,000 pounds). The second stage of the launch vehicle would reenter the earth's atmosphere at an altitude of 121,920 meters (400,000 feet after one orbit. The mission profile required each spent stage of the launch vehicle to be returned to the launch site for reuse.

Candidate concepts for the launch vehicle were sized based on a predicted technology level expected in 1995. In addition, 20 percent of the vehicle's booster stage dry weight was established for growth allowance. The configurations investigated were two stage launch vehicles; the propulsion sequence was a series burn. Recovery systems were defined and sized for each stage. The systems studied were: (1) winged, powered flyback; and (2) winged, nonpowered glideback systems.

A 3 degree-of-freedom launch trajectory program was used to simulate vehicle flight for each of the configurations studied. The analysis program optimized the launch vehicle tilt profile and exo-atmospheric portion of the flight. A parametric study was made of stage mass fractions, wing configuration, and booster fuel. The launch vehicles considered were sized for payloads of 453.59 metric tons (1,000,000 pounds).

The launch vehicle defined in this study was a two stage, series burn, winged vehicle, with a payload capability to the target orbit of 453.59 metric tons (1,000,000 pounds). Vehicle gross lift off weight was 13,738 metric tons (30,286,651 pounds) and the thrust to weight ratio at lift off was 1.3. The booster stage was a heat sink powered flyback stage that required 20 LOX/C₃H₈ high chamber pressure engines for boost, and

airbreathing engines for flyback to the launch site. Landing speed for both the booster and the upper stage was 92.6 meters per second (180 knots). The second stage of the baseline vehicle was powered by seven Space Shuttle main engines, and its wings were sized to permit unpowered atmospheric glide back to the launch site after one orbit. Main propulsion systems for both stages were updated in performance characteristics to that considered feasible in the 1995 time frame.

From an assumed launch site at a latitude of 7 degrees the payload capability of the vehicle was determined; a simulated due east launch was flown to the target orbit. The payload was 466.75 metric tons (1,029,006 pounds).

ANALYSIS

In an effort to formulate a directed study to investigate viable candidate launch vehicles for the SPSS program, several concepts have been studied. The EDIN Design Center under the direction of Mr. R. Abel, Engineering Analysis Division/EX42, undertook a study to size one of these concepts: two-stage winged reusable HLLV's.

For the initial investigation, six candidate vehicles were sized for a range of stage mass fractions typical of winged launch vehicles. The payload for these vehicles was chosen as 226.795 metric tons (500,000 pounds), and the payload was delivered to a 92.6 x 500 kilometer (50 x 270 nautical mile) elliptical orbit.

Two booster engines were used in this study:

1. High chamber pressure, staged combustion cycle engines using LOX/RP-1 propellant, and
2. High chamber pressure, staged combustion cycle engines using LOX/LH2 propellant.

Performance characteristics of these booster stage engines, provided by Mr. M. Lausten of the Power and Propulsion Division, are given in Table 1. The data represent the performance characteristics expected achievable for these engine types by 1995. The mass fractions used in this preliminary sizing are given in Table 2 which shows a matrix of the six vehicles initially investigated. The upper stages of all the vehicles used updated Space Shuttle Main Engines (SSME's). The performance characteristics of these engines were also estimated for the 1995 time period, and their specifications are included in Table 1.

Three degree of freedom trajectory computer programs were used to simulate launch vehicle flight and performance. The trajectories were optimized for initial tilt rate and exo-atmospheric pitch profile. Weight estimating routines (WER's) were used to determine subsystem weights and resulting stage mass fractions. The WER's were developed and equation coefficients chosen to provide system weights expected to be achieved in the target 1995 time frame. Subsequent to the initial sizing of the 226.795 metric tons (500,000 pounds) payload class vehicles, ground rules were established which pointed the study toward developing launch vehicles capable of injecting greater payloads into the required orbit. Consequently, the candidate vehicles were sized for payloads of 453.59 metric tons (1,000,000 pounds). The groundrules for this study are given in table 3; evaluation criteria used for baseline selection are listed in Table 4.

A propulsion system was sized to circularize the payload at 500 kilometers (270 nautical miles). A vacuum specific impulse of 2942 newtons - second per kilogram (300 seconds) and a mass fraction of 0.8 was assumed for this system. The velocity change required at apogee for this maneuver

ENGINE PERFORMANCE CHARACTERISTICS

~ 1995 TECHNOLOGY

PROPELLANT (OX/FUEL)	BOOSTER STAGE		UPPER STAGE
	LOX/LH ₂	LOX/RP*1	LOX/LH ₂
CHAMBER PRESSURE, $\frac{N.}{M^2} \times 10^6$ (PSIA)	27.579 (4000)	27.579 (4000)	27.579 (4000)
SEA LEVEL SPECIFIC IMPULSE, $\frac{N.-SEC.}{KG.}$ (SEC.)	3994.2 (407.3)	3037.9 (309.8)	—————
VACUUM SPECIFIC IMPULSE, $\frac{N.-SEC.}{KG.}$ (SEC.)	4334.5 (442)	3373.5 (344)	4569.9 (466)
OX/F RATIO	6:1	2.6 : 1	6 : 1
EXPANSION RATIO	40 : 1	50 : 1	200 : 1
VACUUM THRUST, NEWTONS (POUNDS)	8,596,384 (1,932,544)	8,496,500 (1,910,089)	4,230,000 (950,000)

TABLE VI-B-3-1

VI-B-3-4

VI-B-3-5

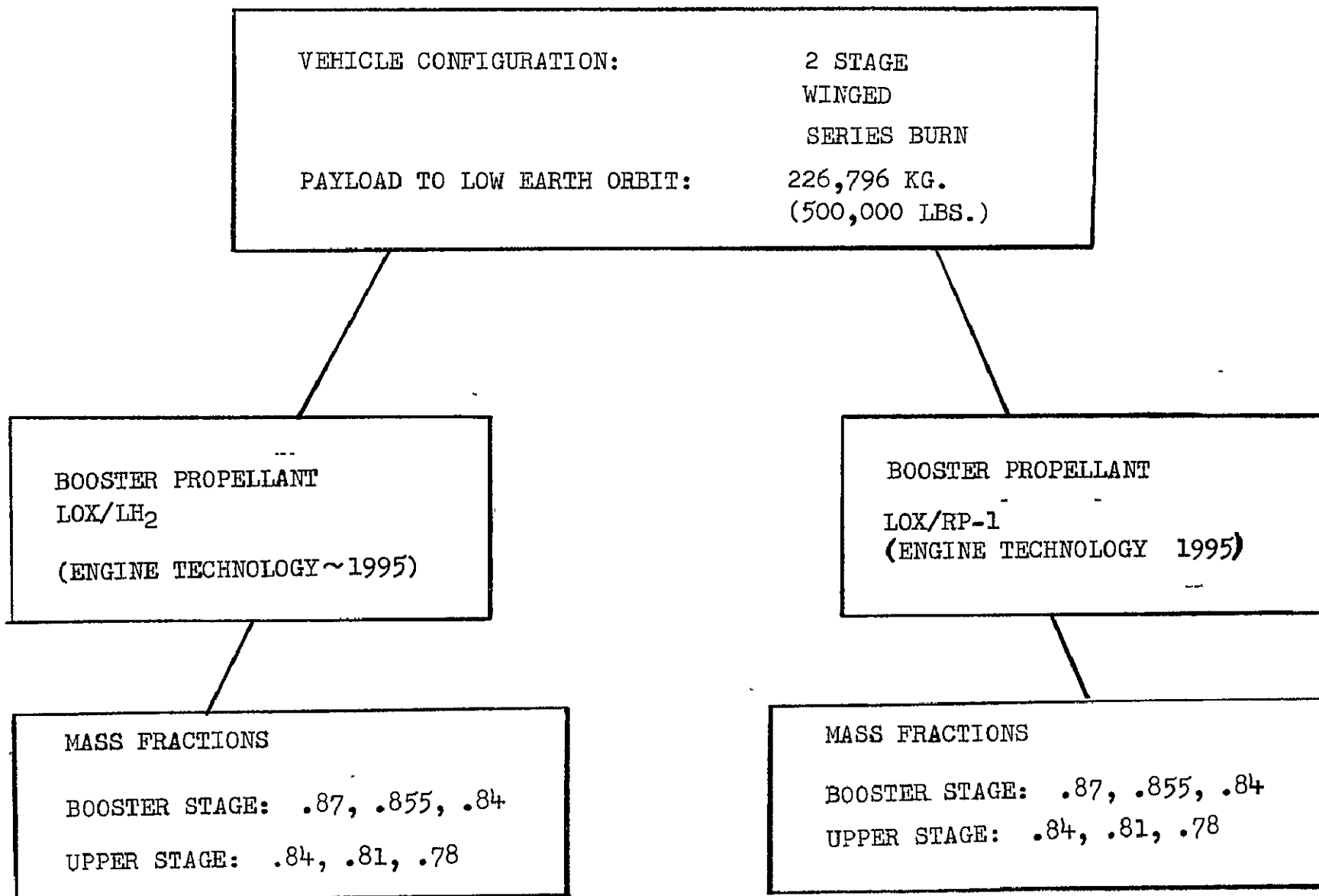


TABLE VI-B-3-2

HLLV GROUND RULES

- PAYLOAD SHROUD DIAMETER 12-34 METERS (40-100 FT.)
- PAYLOAD DENSITY 56-80 KG./M³ (3.5-5 LBS./FT.³)
- PAYLOAD 453-907 M.TONS (1-2 X 10⁶LBS.)
- NO PAYLOAD RETURN
- MAXIMUM ACCELERATION 4 G's
- MAXIMUM PAYLOAD BAY TEMPERATURE 93°C. (200° F.)
- UNMANNED LAUNCH
- RANGE SAFETY IS THE ONLY ABORT CONSIDERATION
- REQUIRED LAUNCH RELIABILITY = 0.97
- LAUNCH SITE RECOVERY OF SPENT STAGES
- PAYLOAD ORBIT : 500 KM. (270 N.M.)
- ORBIT INCLINATION EQUAL TO LAUNCH SITE LATITUDE
- RENDEZVOUS, DOCKING DELTA V IS IN THE PAYLOAD
- NO PAYLOAD ⇒ LAUNCH VEHICLE SERVICES REQUIRED
- LAUNCH RATE CAPABILITY WILL BE 50% GREATER THAN THE
AVERAGE OF THE ANNUAL LAUNCH RATE

TABLE VI-B-3-3

VI-B-3-6

LAUNCH VEHICLE
EVALUATION CRITERIA

- * PERFORMANCE
- * COST
- * TECHNOLOGICAL RISK / RELIABILITY
- * PROGRAM IMPACT
- * VERSATILITY
- * ENVIRONMENTAL FACTORS
- * OPERATIONS COMPLEXITY

TABLE VI-B-3-4

was 117.35 meters per second (385 feet per second). The shroud for the payload was considered to be included in the 453.59 metric tons (1,000,000 pounds) of the payload.

The initial concept for the winged vehicle consisted of a heat sink straight wing booster and a delta winged second stage. The booster would be flown back to the launch site; air breathing engines (ABE's) of 222,411 newtons (50,000 pounds) thrust were used in the flyback simulation. The upper stage did not use ABE's but was designed to reenter the earth's sensible atmosphere after one orbit and glide back to the launch site. This first sizing effort resulted in a launch vehicle using LOX/RP-1 booster engines and weighed over 32 million pounds at lift off. Mr. W. Taub of the Spacecraft Design Division provided layout support for the transportation system sizing effort, and several of his drawings of this initial vehicle are included. Figure 1 shows views of the booster stage, and incorporates some unique-concepts. The ABE's are shown stored in the nose cone of the booster stage, deployable for powered flyback. Landing gear stowage areas are given and an engine packaging scheme is shown. Figure 2 gives similar views of the delta winged upper stage. The stages are shown in a stacked launch configuration in Figure 3. A conceptual "piggy-back" launch configuration is provided in Figure 4, and Figure 5 shows a launch arrangement for a parallel burn lift off. No trajectories were flown for the parallel burn operations mode, but the illustration shows the height of the lift off configuration could be considerably reduced. A further reduction in launch configuration height is shown in figure 6 which shows the payload in two modules; one mounted on each wing of the upper stage. Such diverse conceptual designs as these by Mr. Taub are an integral part of the definition of a viable launch vehicle. Figure 7, using the parallel burn launch configuration, provides an illustration of the HLLV winged launch vehicle mission profile.

After several simulations certain parameters were selected and held constant in order to equitably evaluate both the LOX/RP-1 and the LOX/LH2 flying booster concepts. The booster wing loading was established at 5267 newtons per square meter (110 pounds per square foot) of wing area, the leading edge sweep was selected as 10 degrees, and a landing speed of 92.6 meters per second (180 knots) was chosen. The thrust to weight ratio at lift-off was 1.3 for all cases; the initial thrust to weight ratio of the upper stage was 0.97. Subsequent iterations also led to the selection of a straight wing for the upper stage with the same loading; its leading edge sweep was also 10 degrees. Trajectory constraints for all simulations were:(1) 4 g maximum acceleration during ascent, and (2) maximum dynamic pressure of 31.122 newtons per square meter (650 pounds per square foot).

The LOX/RP-1 vehicle was sized to a gross lift off weight (GLOW) of 13,359 metric tons (29,451,478 pounds). This weight includes an allowance for growth in the booster stage, which was fixed at twenty percent of the booster dry weight. A weight and performance summary for this vehicle is given in Table 5; the trajectory time histories are presented in

ORIGINAL PAGE IS
OF POOR QUALITY

VI-B-3-9

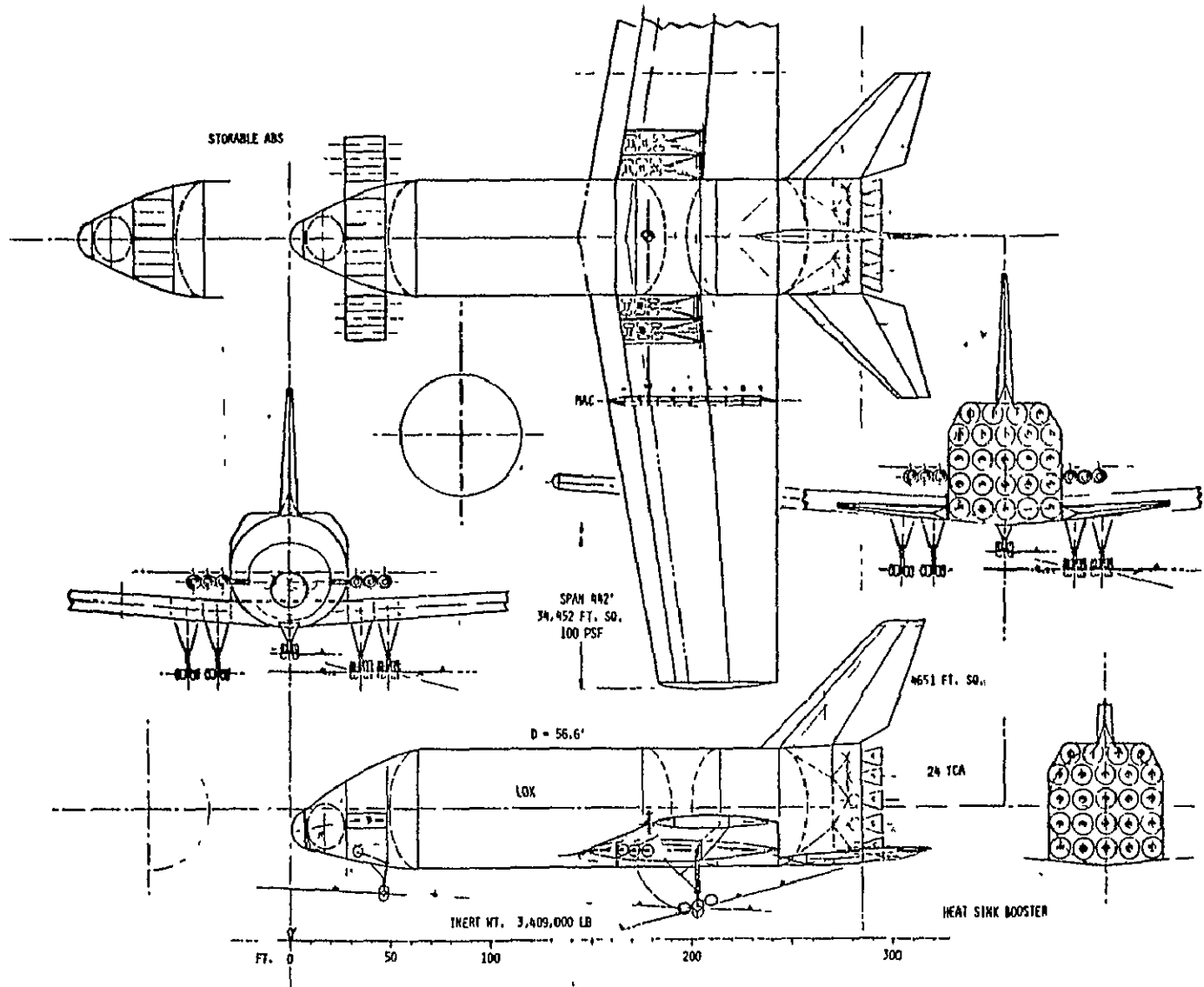


FIGURE VI-B-3-1

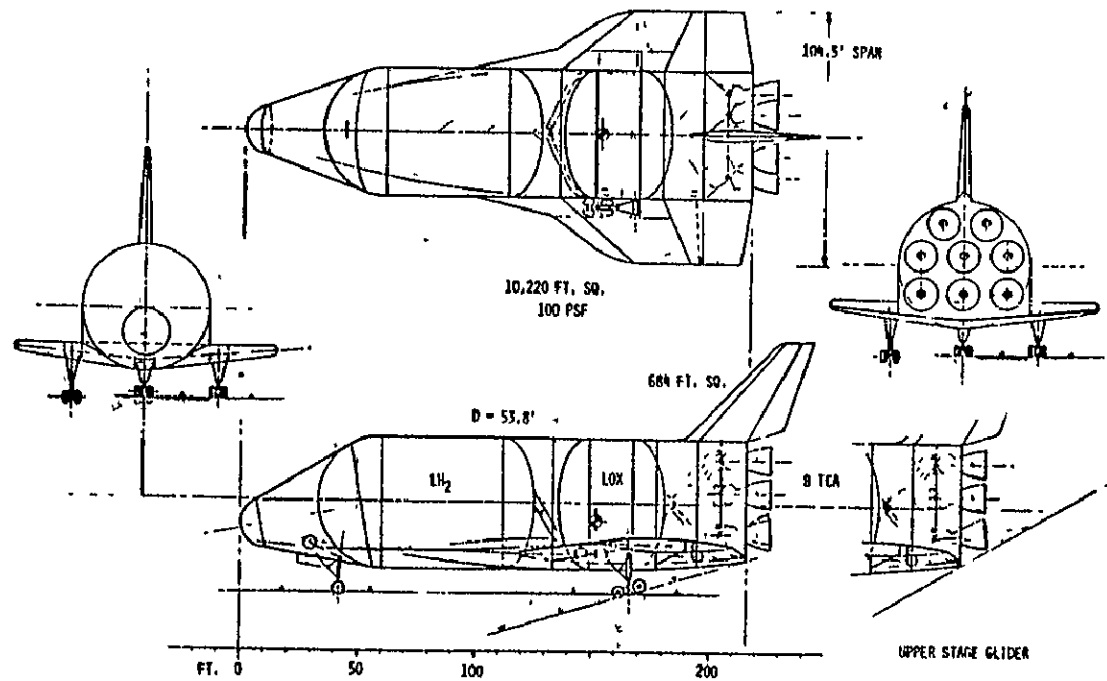


FIGURE VI-B-3-2

ORIGINAL PAGE IS
OF POOR QUALITY

VI-B-3-11

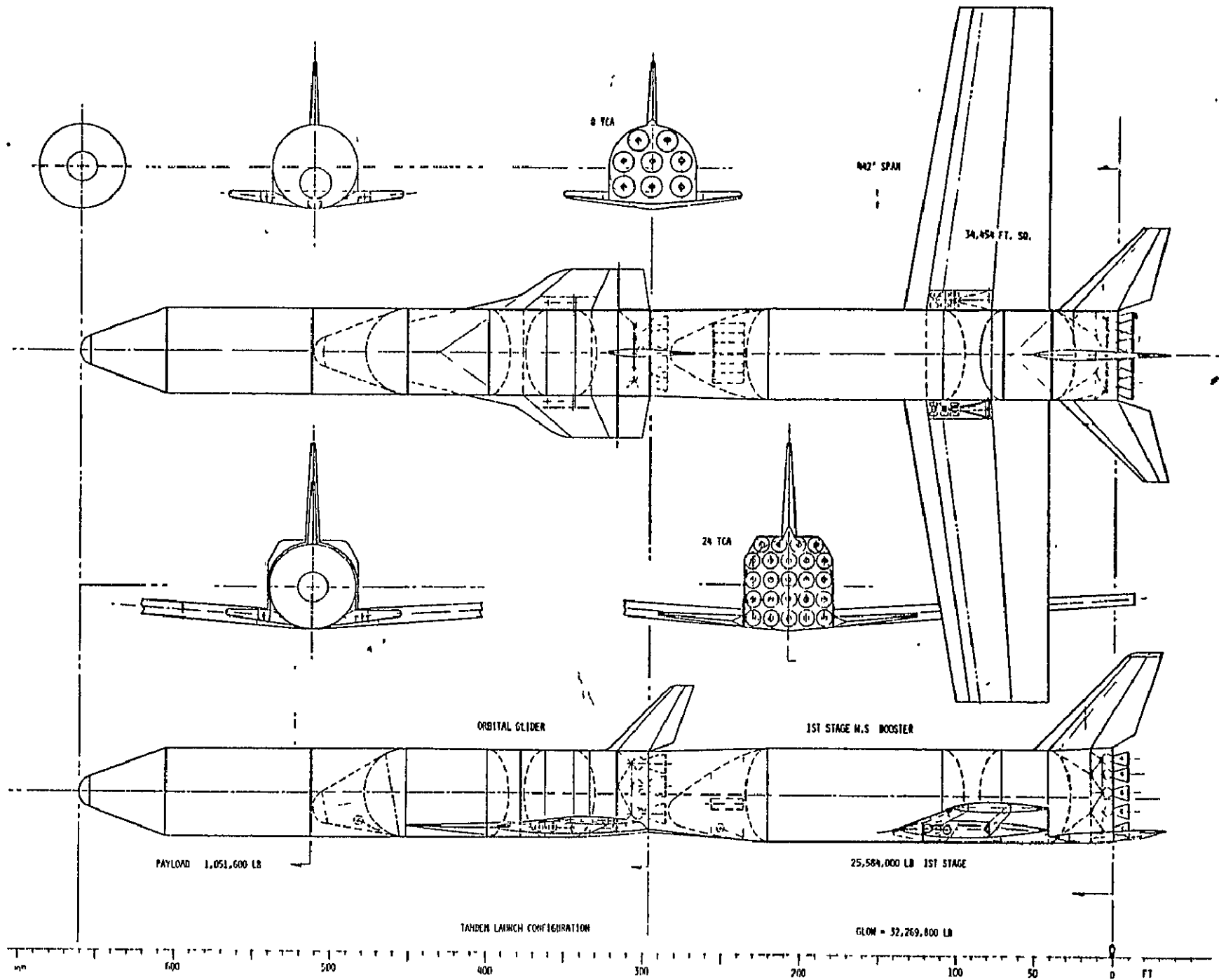


FIGURE VI-B-3-3

VI-B-3-12

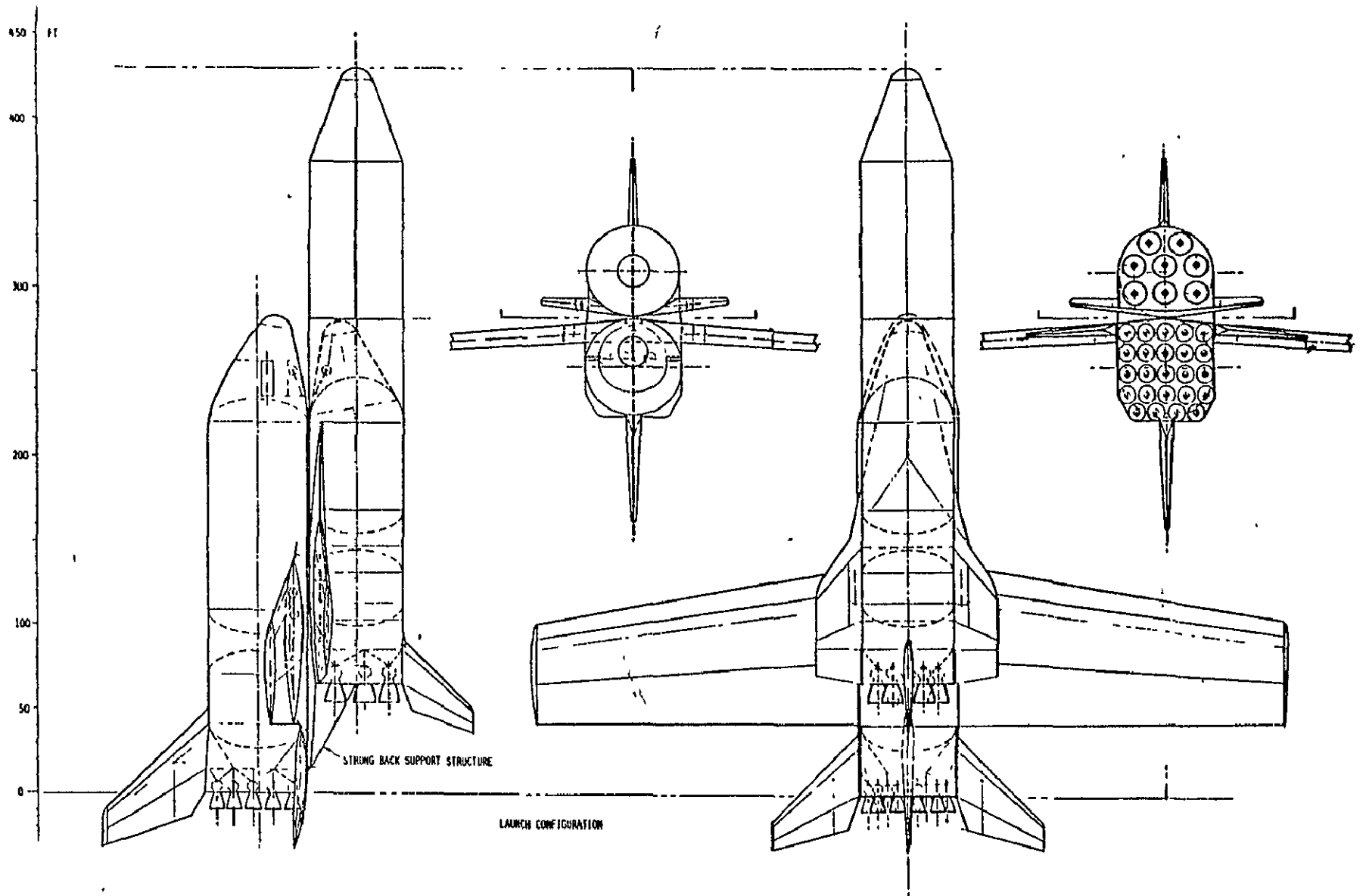


FIGURE VI-B-3-4

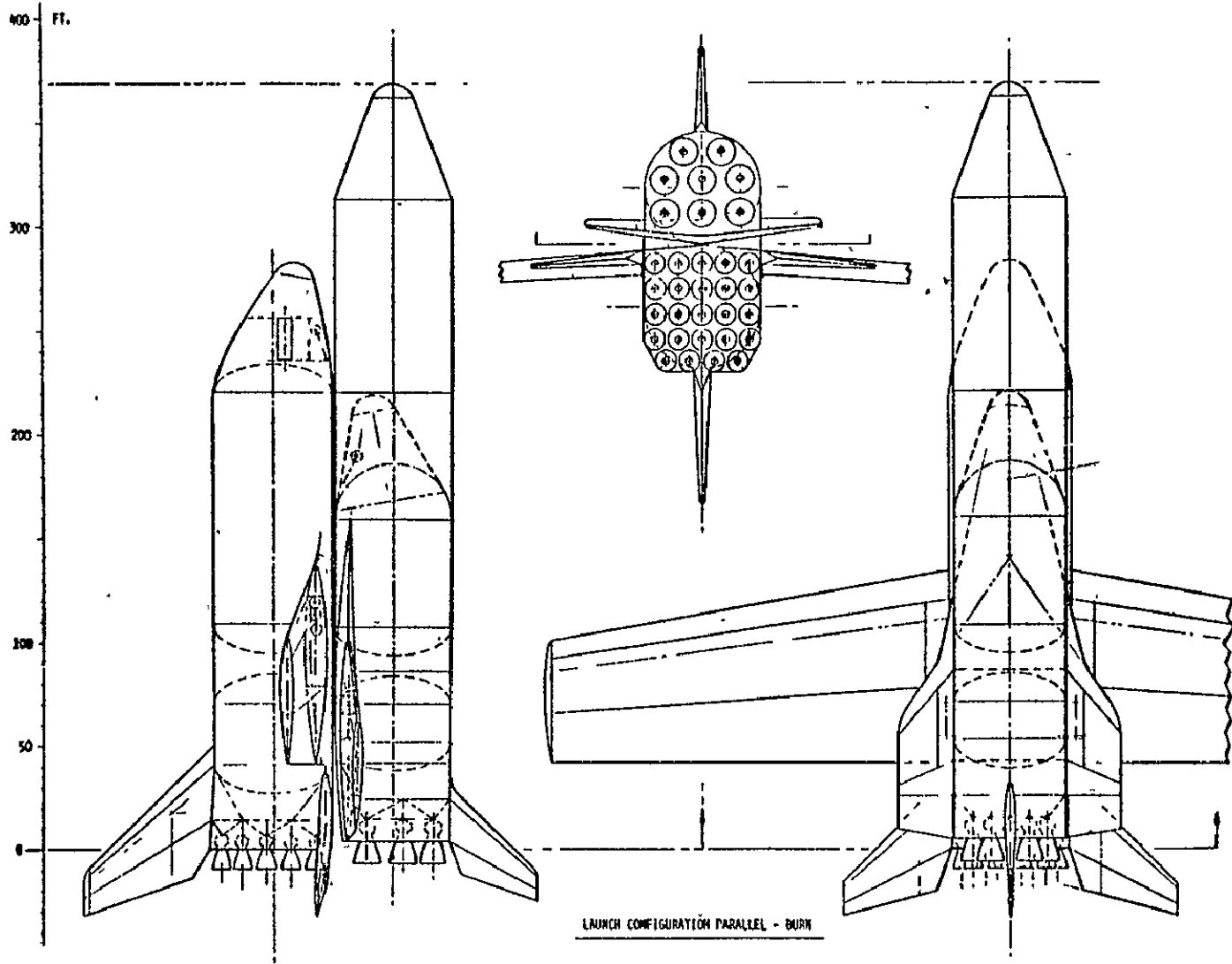


FIGURE VI-B-3-5

VI-B-3-14

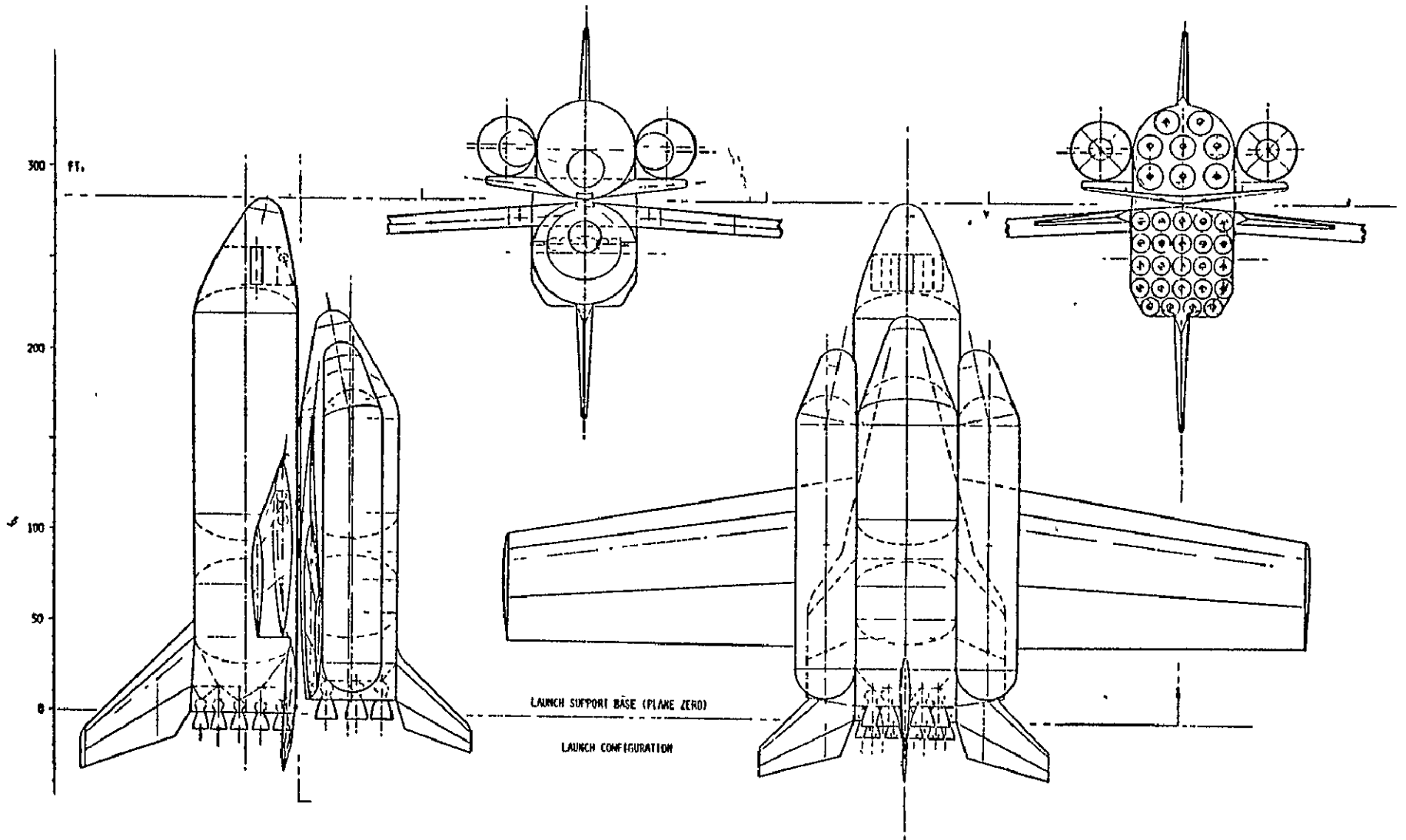


FIGURE VI-B-3-6

ORIGINAL PAGE IS
OF POOR QUALITY

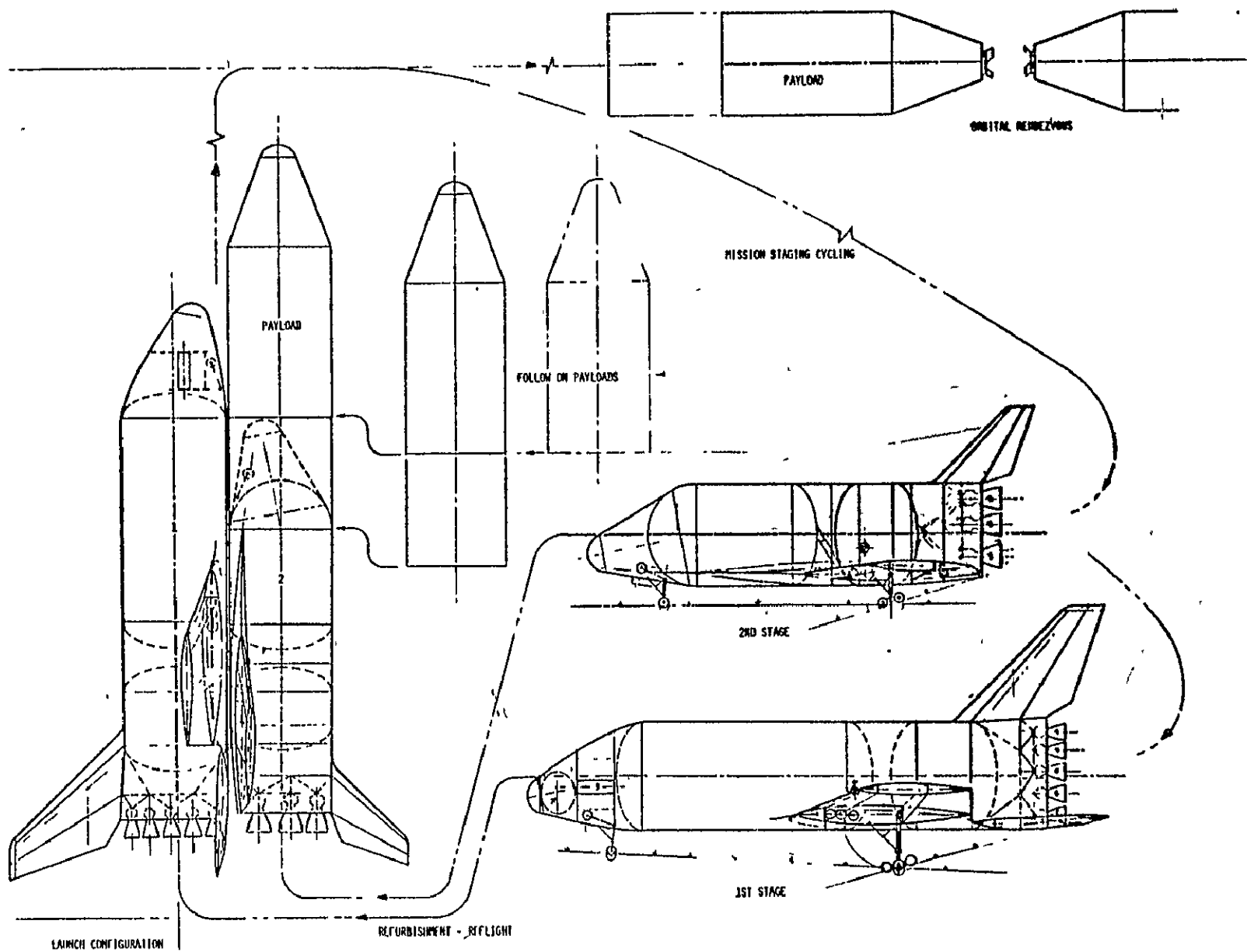


FIGURE VI-B-3-7

LOX / RP-1 BOOSTER VEHICLE

WEIGHT SUMMARY, METRIC TONS (POUNDS)

PAYLOAD		477.17	(1,051,980)
STAGE 1 LIFT OFF		10,611.7	(23,394,872)
INERT	1,330.9	(2,934,240)	
PROPELLANT	9,280.8	(20,460,632)	
STAGE 2 LIFT OFF		2,270.1	(5,004,627)
INERT	431.6	(951,526)	
PROPELLANT	1,838.5	(4,053,101)	
GROSS LIFT OFF WEIGHT		13,359.0	(29,451,478)

PERFORMANCE SUMMARY

	STAGE 1	STAGE 2
IDEAL VELOCITY, MPS (FPS)	3,776.2 (12,839.1)	5,055.4 (16,586.1)
THRUST/WEIGHT	1.3	0.97
NUMBER ENGINES	22.	7.
MASS FRACTION	0.8746	0.81
BURN TIME, SEC.	168 .18	287 .0
PAYLOAD, M. TONS (LBS.)	2,747.2 (6,056,607)	477.17 (1,051,980)
STAGING: ALTITUDE, M. (FT.)		58,389 (191,566)
VELOCITY, MPS (FPS)		2,695 (8,842.7)
FLIGHT PATH, DEG.		12.593

TABLE VI-B-3-5

Figures 8 through 11. Figure 11 shows a time history of booster stage ballistic entry; the resulting total heat and heat rates were used to provide inputs to the sizing program for sizing aerosurfaces.

The GLOW of the LOX/LH2 vehicle was 11,054 metric tons (24,370,200 pounds). Since the performance characteristics of the booster engines were closer to those of the upper stage than were the LOX/RP-1 booster engines, the ideal velocity for the stages was about equal. The LOX/LH2 booster staging point was about 12,000 meters (41,000 feet) higher and the velocity about 230 meters per second (750 feet per second) greater than that of the LOX/RP-1 booster.

A weight and performance summary for the LOX/LH2 vehicle is presented in Table 6, and the trajectory time histories for this vehicle are given in Figures 12 through 15. Figure 15 shows the resulting ballistic entry heating of the booster stage.

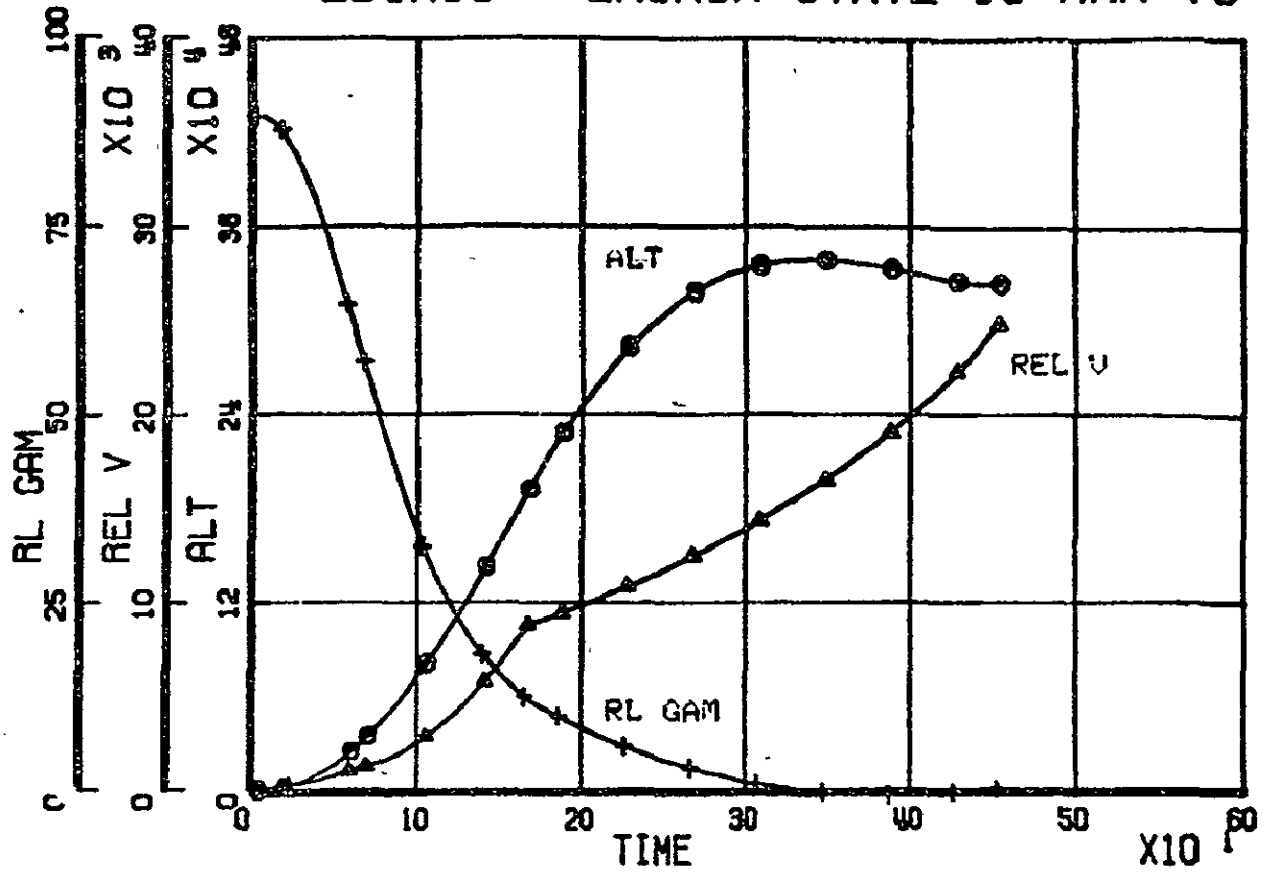
After these vehicles had been sized, a LOX/C3H8 (propane) engine was proposed for the boost stage of an HLLV. Engine performance characteristics of this gas generator cycle engine are given in Table 7. Sizing studies and trajectory analysis defined the propane vehicle; its GLOW was 13,737.8 metric tons (30,286,651 pounds). As with the other vehicles, a growth allowance of twenty percent dry weight was maintained. A weight and performance summary of this vehicle is shown in Table 8 and trajectory time histories are given in Figures 16 through 19. The heat and heat ratings from the booster stage ballistic trajectory are shown in Figure 19.

Table 9 lists the inert weight of each of the three candidate launch vehicles, and gives a brief summary of the geometric characteristics of each. Although the GLOW of the LOX/LH2 vehicle is about 2300 - 2800 metric tons (5-6 million pounds) less than the LOX/RP-1 or the LOX/C3H8 vehicles it is also by far the largest vehicle. The LOX/RP-1 and the LOX/C3H8 vehicles, however, are quite similar in both size and weight. Each of the candidate vehicles could meet the performance requirements of the SPSS.

Ms. D. Webb of the Management Resources Office provided support to the HLLV sizing study by costing the candidate vehicles. Detailed cost statements are given in Tables 10 (LOX/LH2 vehicles), 11 (LOX/RP-1 vehicle), and 12 (LOX/C3H8 vehicle). A summary of the costs of these vehicles is presented in Table 13.

Final evaluation of the winged two stage concept resulted in the selection of the LOX/C3H8 booster engines. A detailed weight statement for this vehicle is given in Tables 14, 15 (booster stage) 16, 17 (upper stage) and a geometry summary is shown in Tables 18 (booster stage) and 19 (upper stage). A reference trajectory is listed in Appendix A.

EDIN06 LAUNCH STATE 18 MAR 76



EDIN06 PROPULSION DATA MAR 76

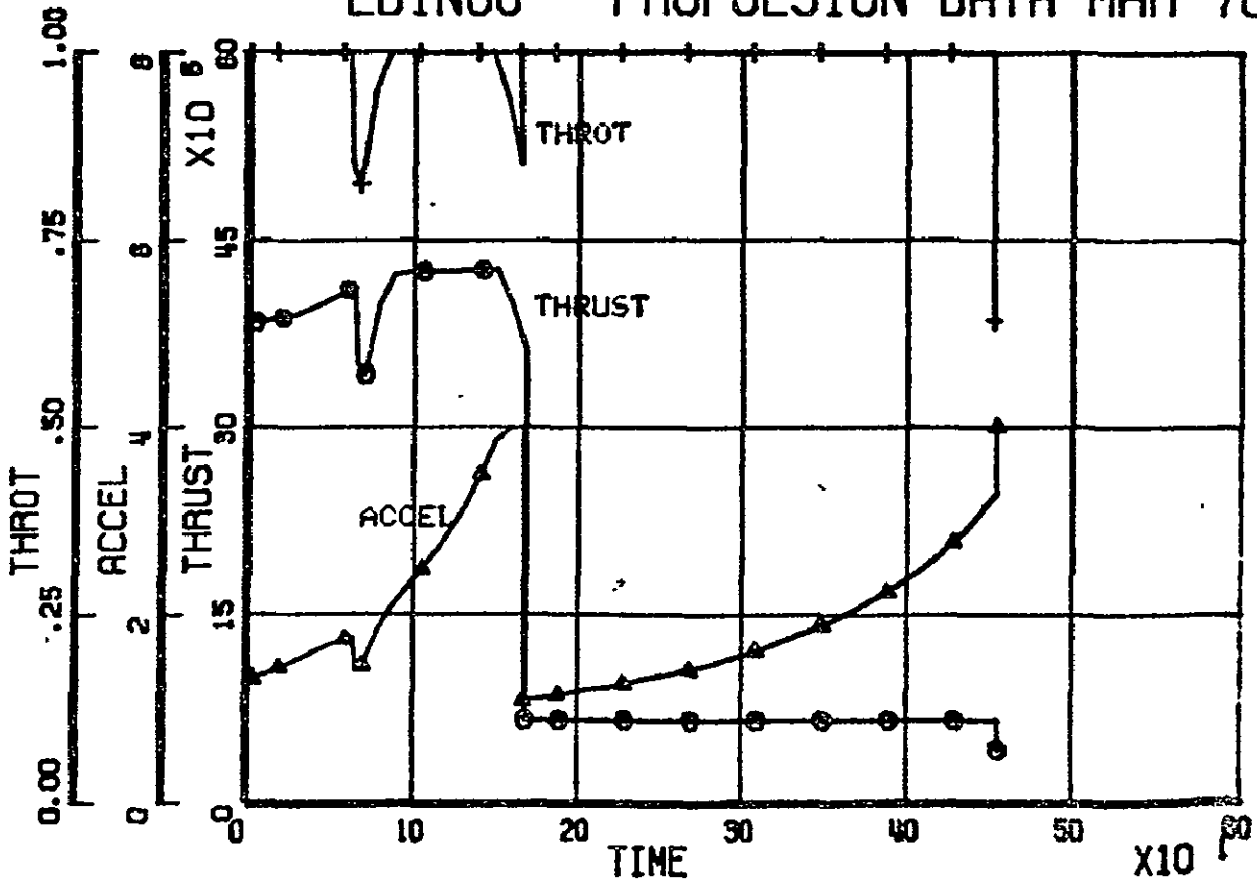
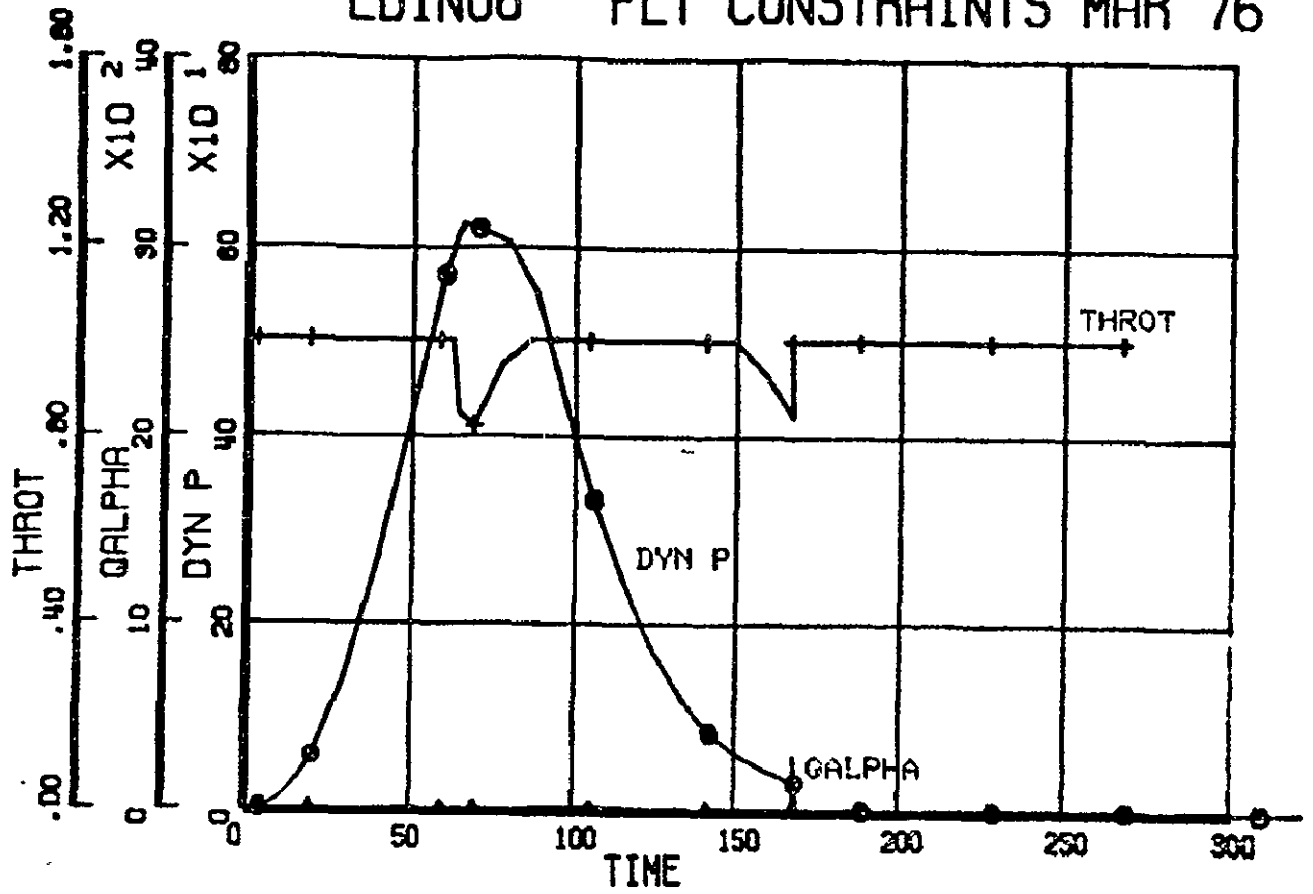


FIGURE VI-B-3-8
VI-B-3-18

EDIN06 FLT CONSTRAINTS MAR 76



EDIN06 FLIGHT ATTITUDE MAR 76

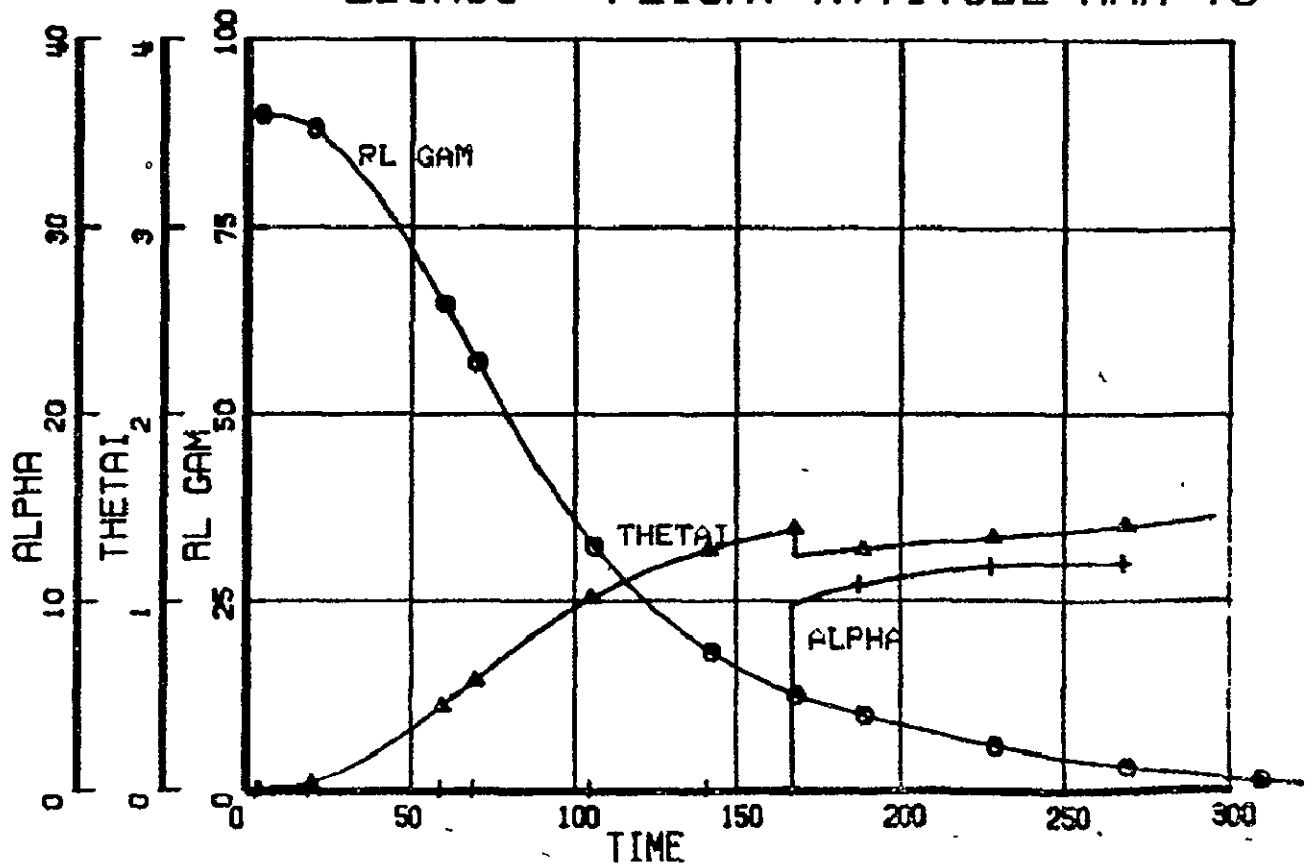


FIGURE VI-B-3-9

EDIN06 H-V PROFILE 18 MAR 76

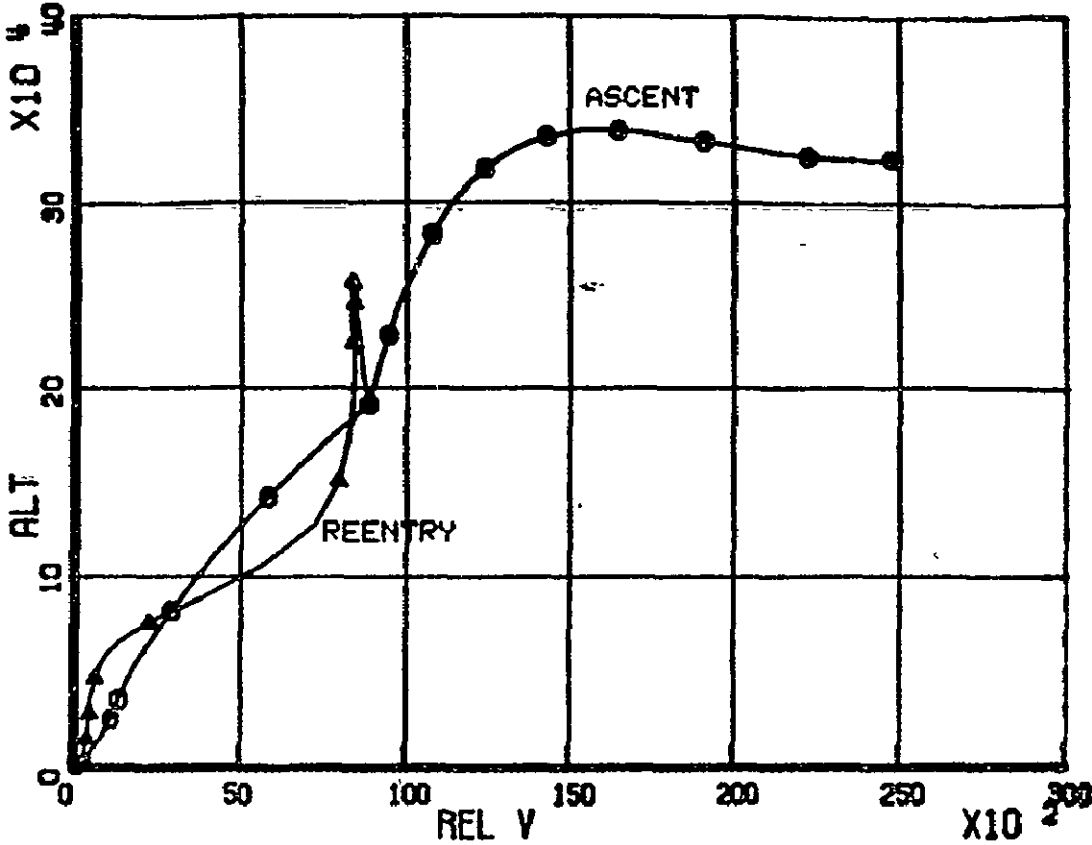
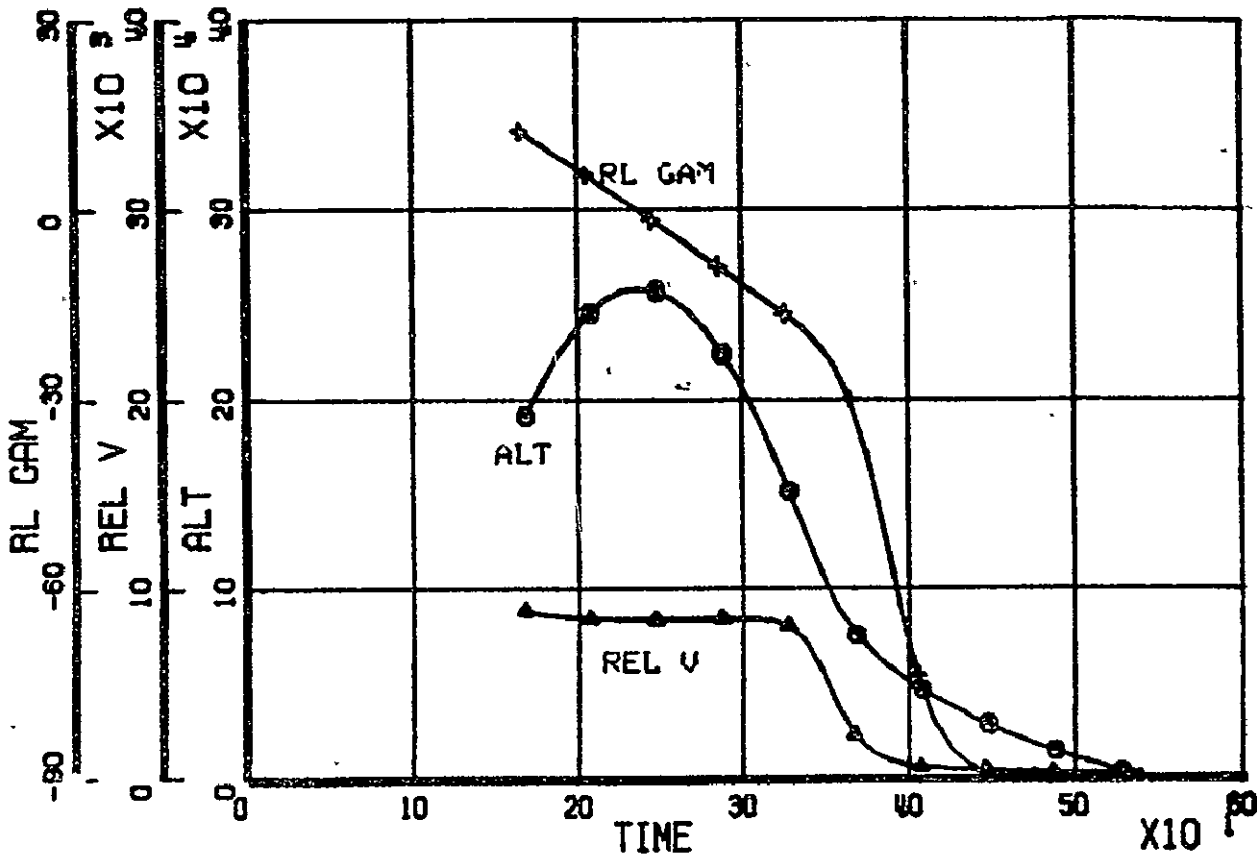


FIGURE VI-B-3-10

VI-B-3-20

EDIN06 STG 1 REENTRY STATE MAR 76



EDIN06 REENTRY HEATING MAR 76

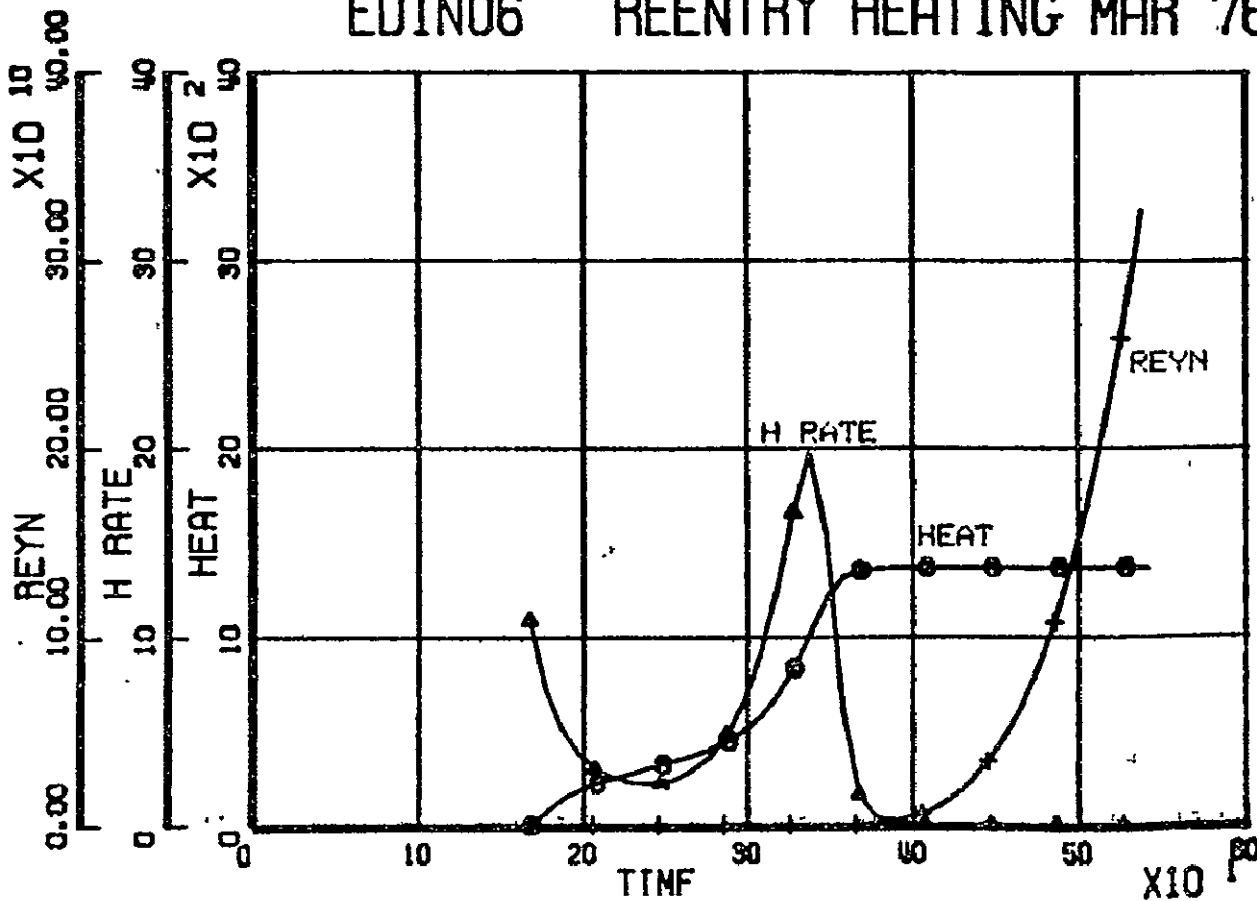


FIGURE VI-B-3-11
VI-B-3-21

LOX / LH₂ BOOSTER VEHICLE

WEIGHT SUMMARY, METRIC TONS (POUNDS)

PAYLOAD		477.14 (1,051,906)
STAGE 1 LIFT OFF		8,638.40 (19,044,435)
INERT	1,602.9 (3,533,681)	
PROPELLANT	7,035.6 (15,510,754)	
STAGE 2 LIFT OFF		1,938.60 (4,273,860)
INERT	368.5 (812,392)	
PROPELLANT	1,570.1 (3,461,468)	
GROSS LIFT OFF WEIGHT		11,054.10 (24,370,200)

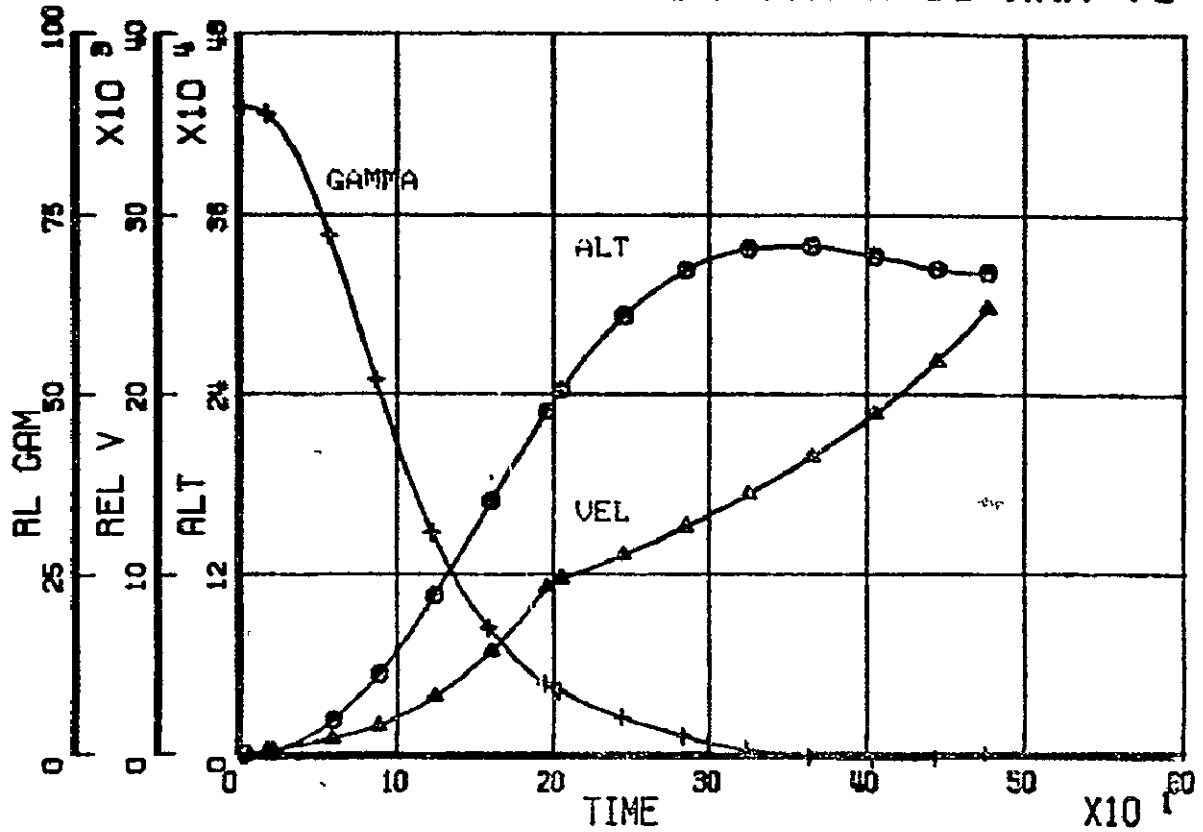
PERFORMANCE SUMMARY

	STAGE 1	STAGE 2
IDEAL VELOCITY MPS (FPS)	4,316.2 (14,163.2)	4,796.9 (15,737.8)
THRUST/WEIGHT	1.3	0.97
NUMBER ENGINES	18.	6.
MASS FRACTION	0.8145	0.81
BURN TIME, SEC.	199.4	278.74
PAYLOAD, M. TONS (LBS.)	2,415.7 (5,325,765)	477.14 (1,051,906)
STAGING:	ALTITUDE, M. (FT.)	70,382 (232,390)
	VELOCITY, MPS (FPS)	2,925 (9,596.5)
	FLIGHT PATH ANGLE, DEG.	9.494

TABLE VI-B-3-6

LH₂

EDIN06 LAUNCH STATE 19 MAR 76



EDIN06 PROPULSION DATA MAR 76

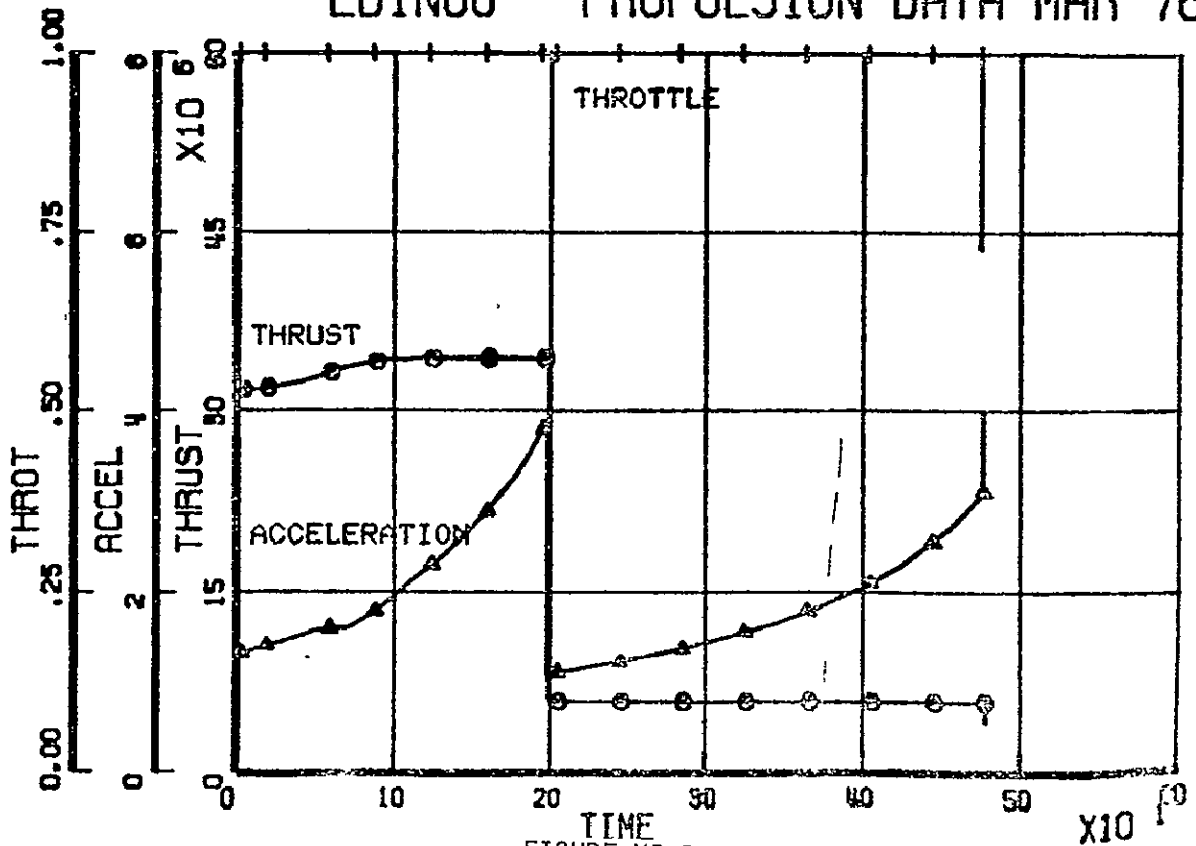
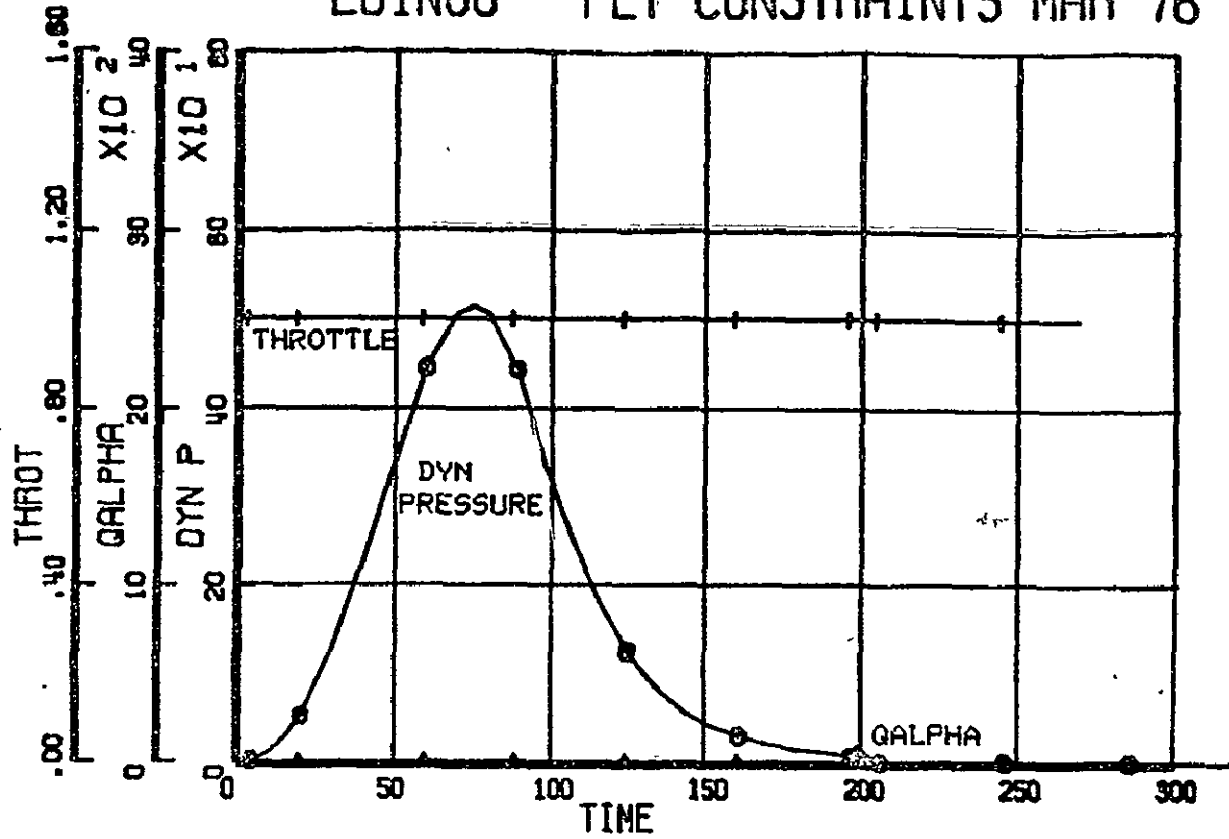
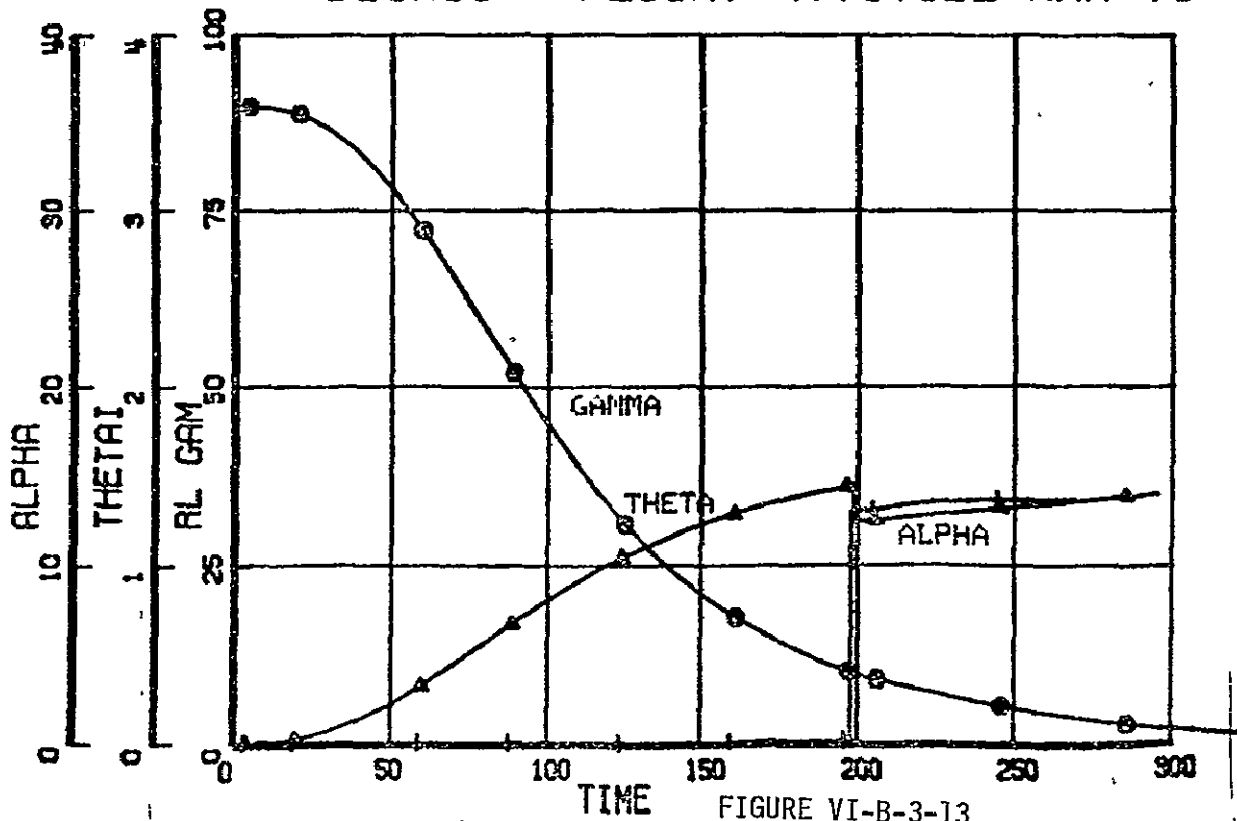


FIGURE VI-B-3-12
VT-R-3-23

EDIN06 FLT CONSTRAINTS MAR 76



EDIN06 FLIGHT ATTITUDE MAR 76



EDIN06 STG 1 REENTRY STATE MAR 76

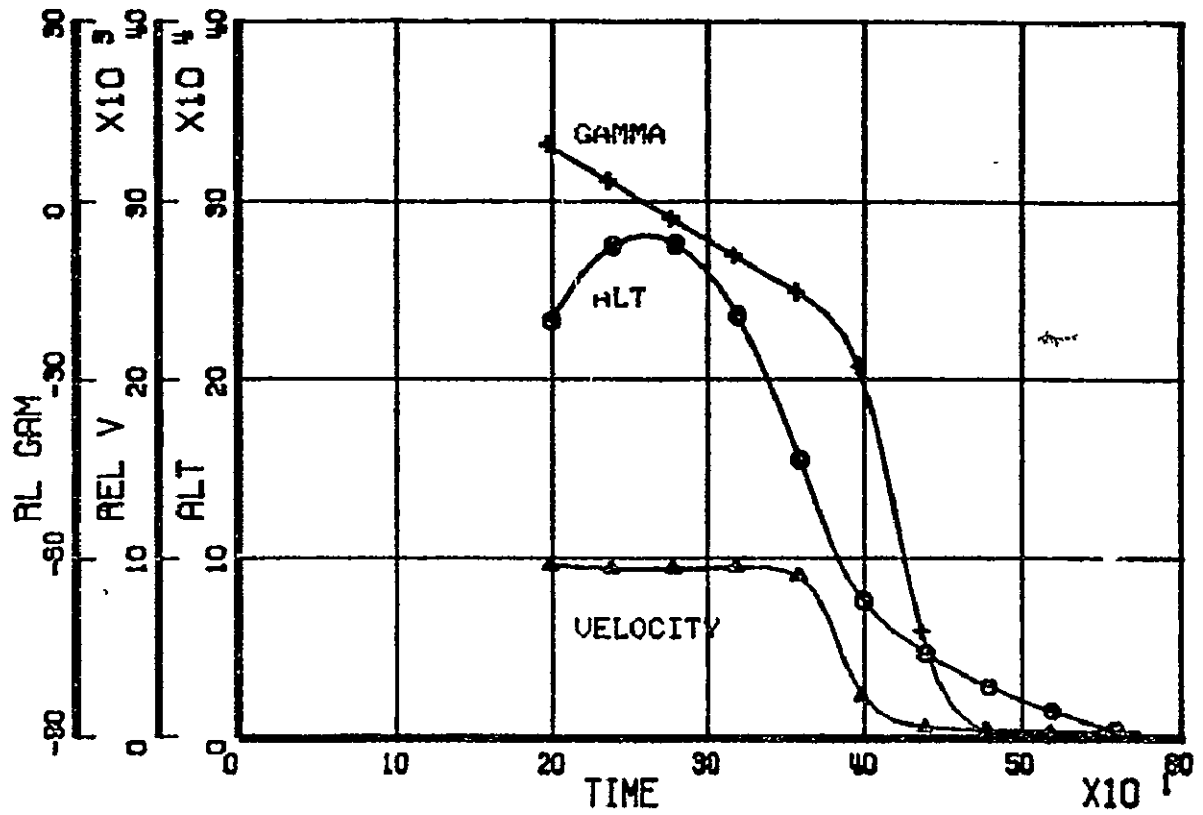
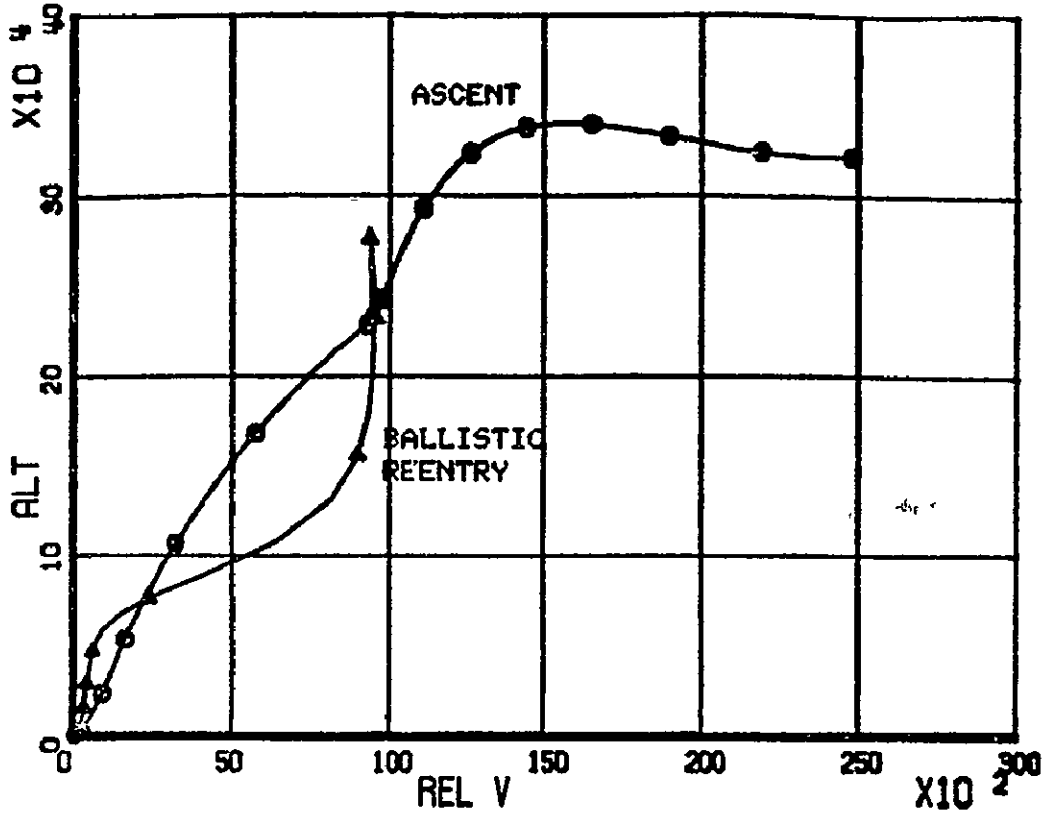
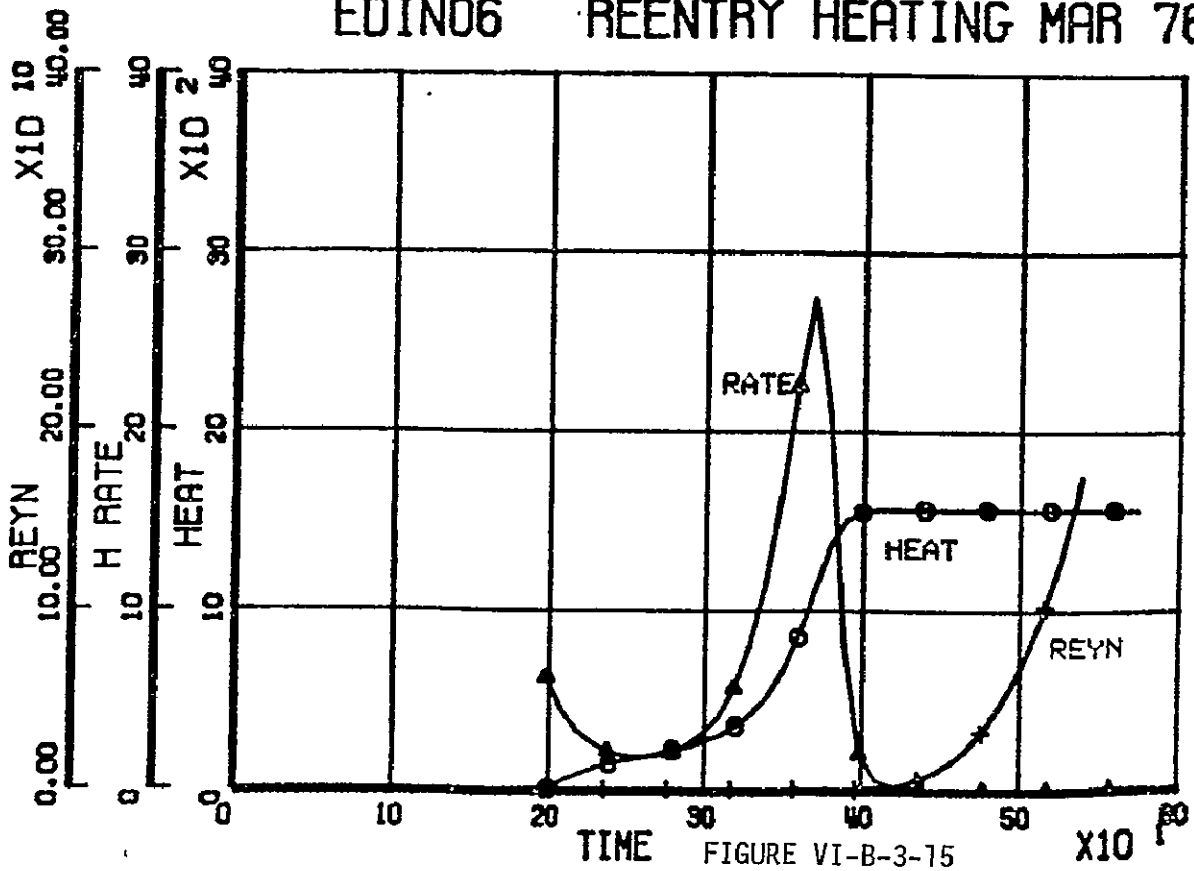


FIGURE VI-B-3-14

EDIN06 H-V PROFILE 19 MAR 76



EDIN06 REENTRY HEATING MAR 76



PROPANE ENGINE PERFORMANCE

CHARACTERISTICS

~ 1995 TECHNOLOGY

APPLICATION:	BOOSTER STAGE
PROPELLANT (OX/FUEL)	LOX / C ₃ H ₈
CHAMBER PRESSURE, $\frac{lbf}{in^2} \times 10^6$ (PSIA)	20.684 (3000)
SEA LEVEL SPECIFIC IMPULSE, $\frac{N.-SEC.}{KG.}$ (SEC.)	2,956.62 (301.49)
VACUUM SPECIFIC IMPULSE, $\frac{N.-SEC.}{KG.}$ (SEC.)	3,309.7 (337.5)
OX/FUEL RATIO	2.68 : 1
EXPANSION RATIO	40 : 1
VACUUM THRUST, NEWTONS (LBS.)	9,798,636. (2,202,821.)

TABLE VI-B-3-7
VI-B-3-27

LOX / C₃H₈ BOOSTER VEHICLE

WEIGHT SUMMARY, METRIC TONS (POUNDS)

PAYLOAD		477.	(1,050,456)
STAGE 1 LIFT OFF		10,927.	(24,090,128)
INERT	1,346.7	(2,968,857)	
PROPELLANT	9,580.4	(21,121,271)	
STAGE 2 LIFT OFF		2,334.2	(5,146,067)
INERT	443.7	(978,299)	
PROPELLANT	1,890.6	(4,167,768)	
GROSS LIFT OFF WEIGHT		13,737.8	(30,286,651)

PERFORMANCE SUMMARY

	STAGE 1	STAGE 2
IDEAL VELOCITY, MPS (FPS)	3,847.4 (12,662.6)	5,102.6 (16,740.7)
THRUST/WEIGHT	1.3	0.97
NUMBER ENGINES	20.	7.
MASS FRACTIONS	0.8768	0.81
BURN TIME, SEC.	165.09	288.46
PAYLOAD, M. TONS (LBS.)	2,810.7 (6,196,524)	477. (1,050,456)

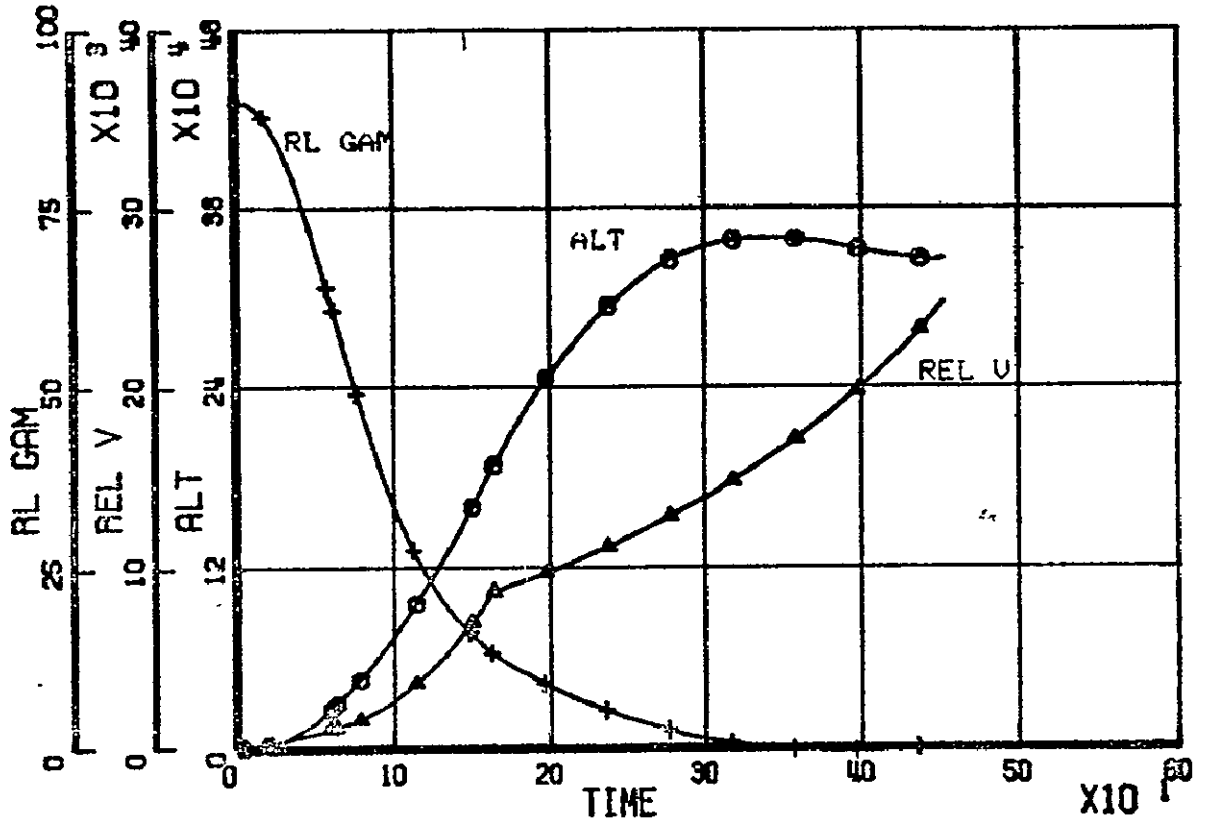
STAGING:	ALTITUDE, M. (FT.)	57,197. (187,655)
	VELOCITY, MPS (FPS)	2,653. (8,704.2)
	FLIGHT PATH ANGLE, DEG.	13.097

TABLE VI-B-3-8

VI-B-3-28

C₃ H₈

EDIN06 LAUNCH STATE 19 MAR 76



EDIN06 PROPULSION DATA MAR 76

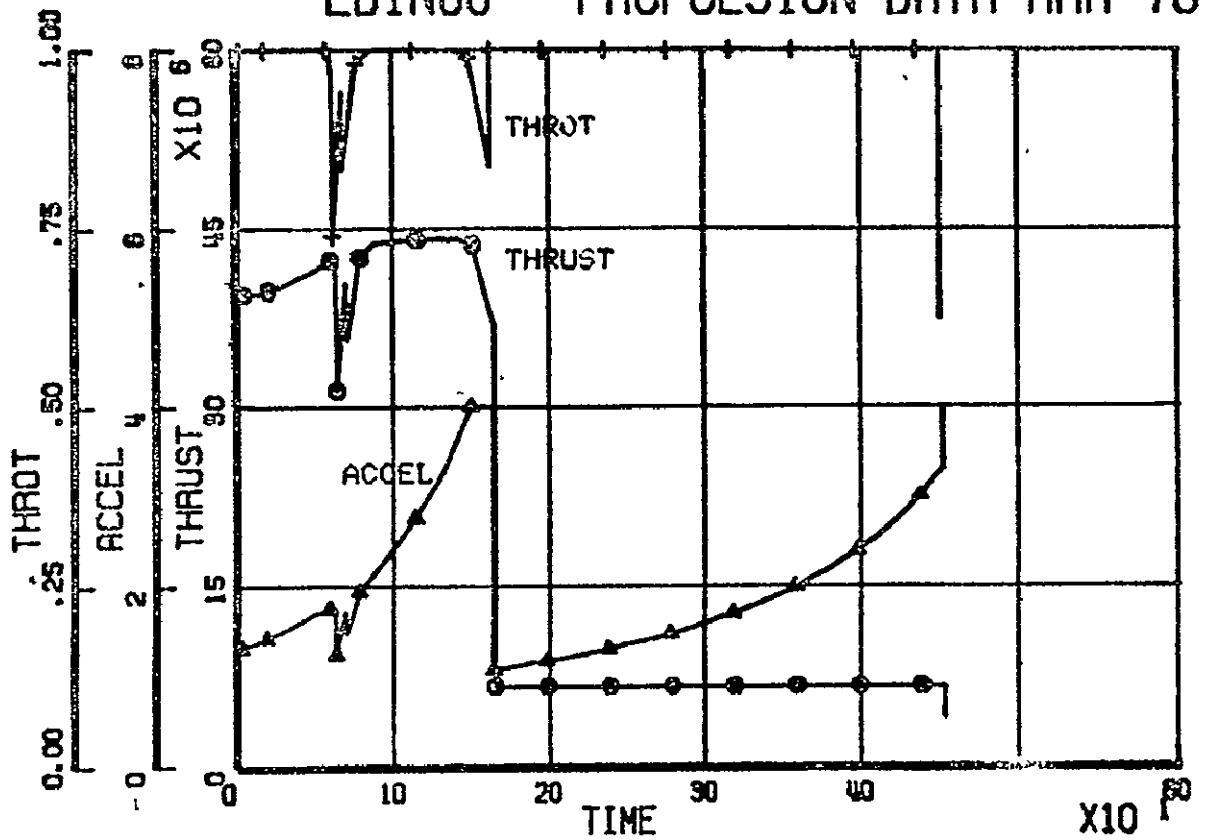
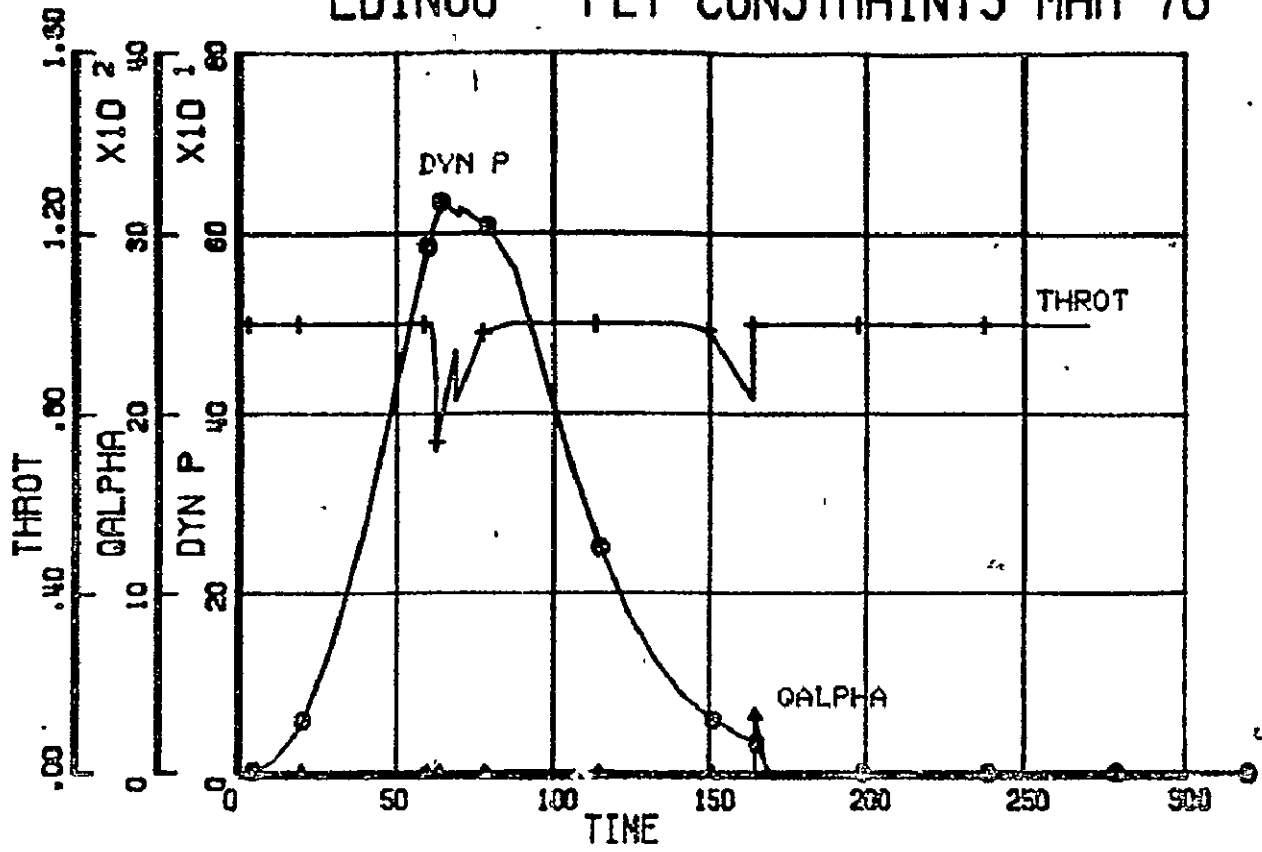


FIGURE VI-B-3-16

VI-B-3-29

EDIN06 FLT CONSTRAINTS MAR 76



EDIN06 FLIGHT ATTITUDE MAR 76

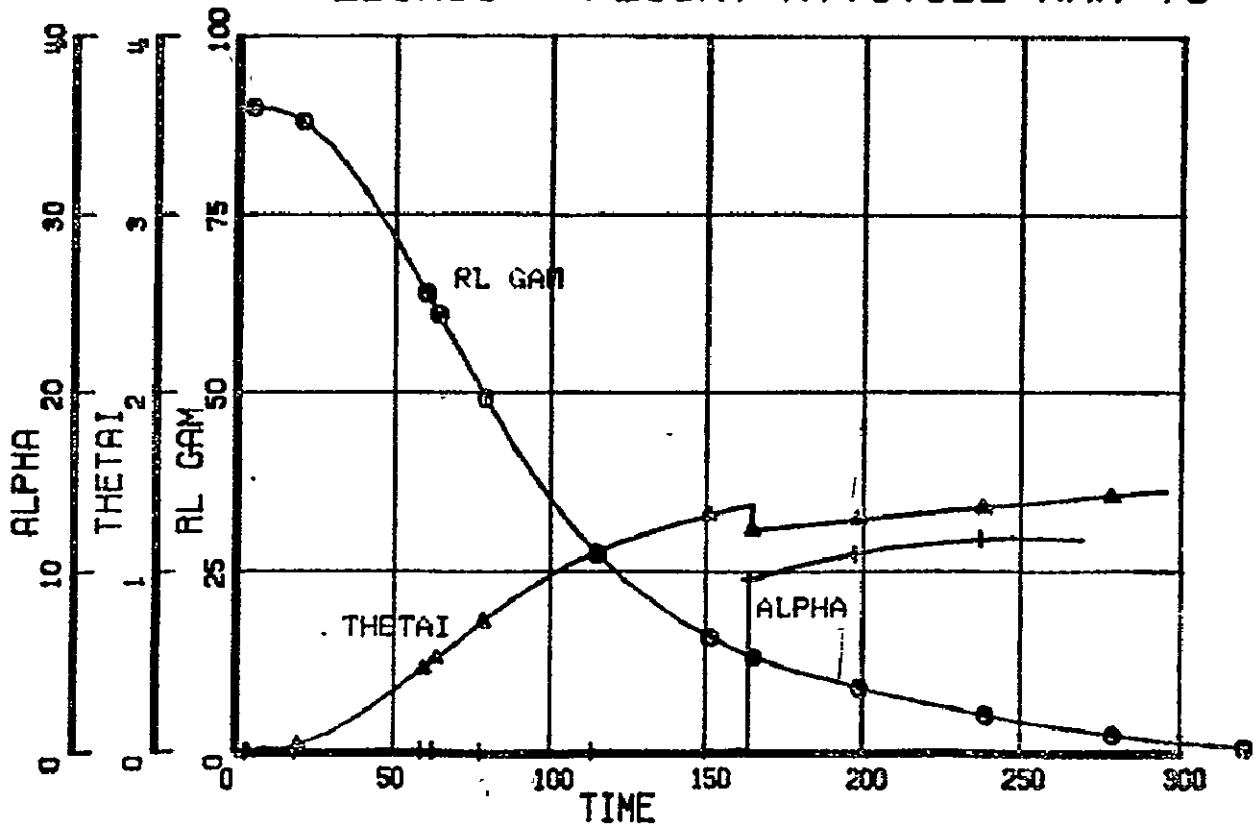


FIGURE VI-B-3-17

EDIN06 | H-V PROFILE 19 MAR 76

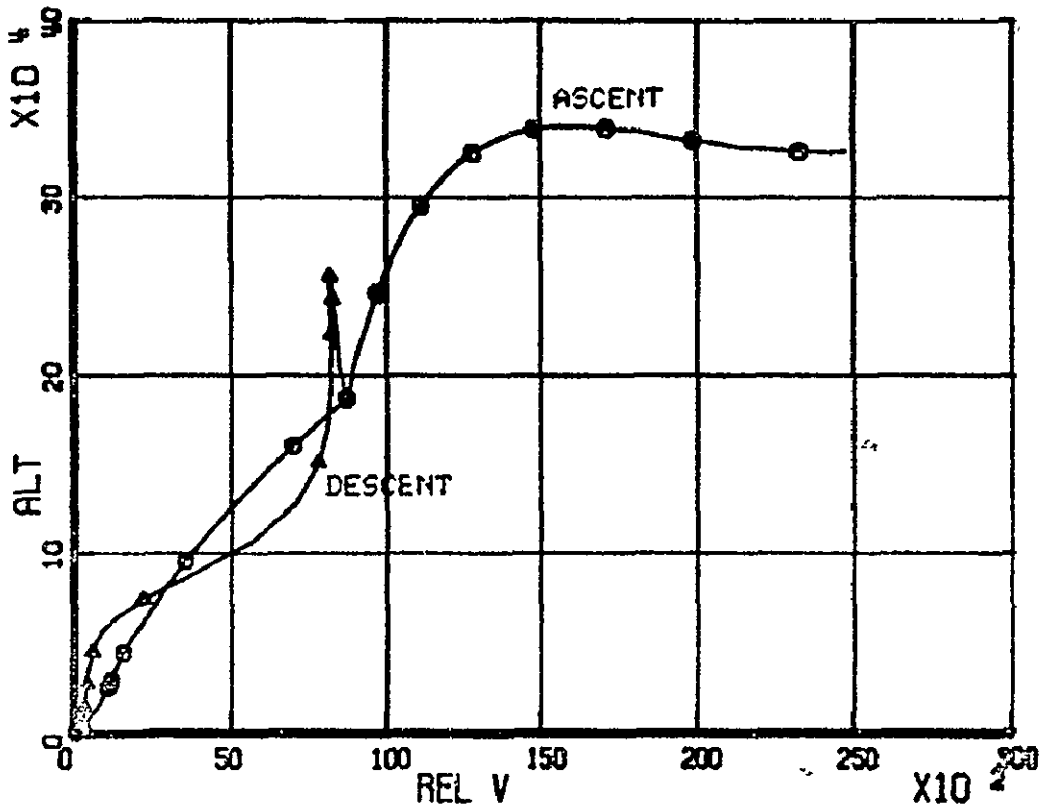
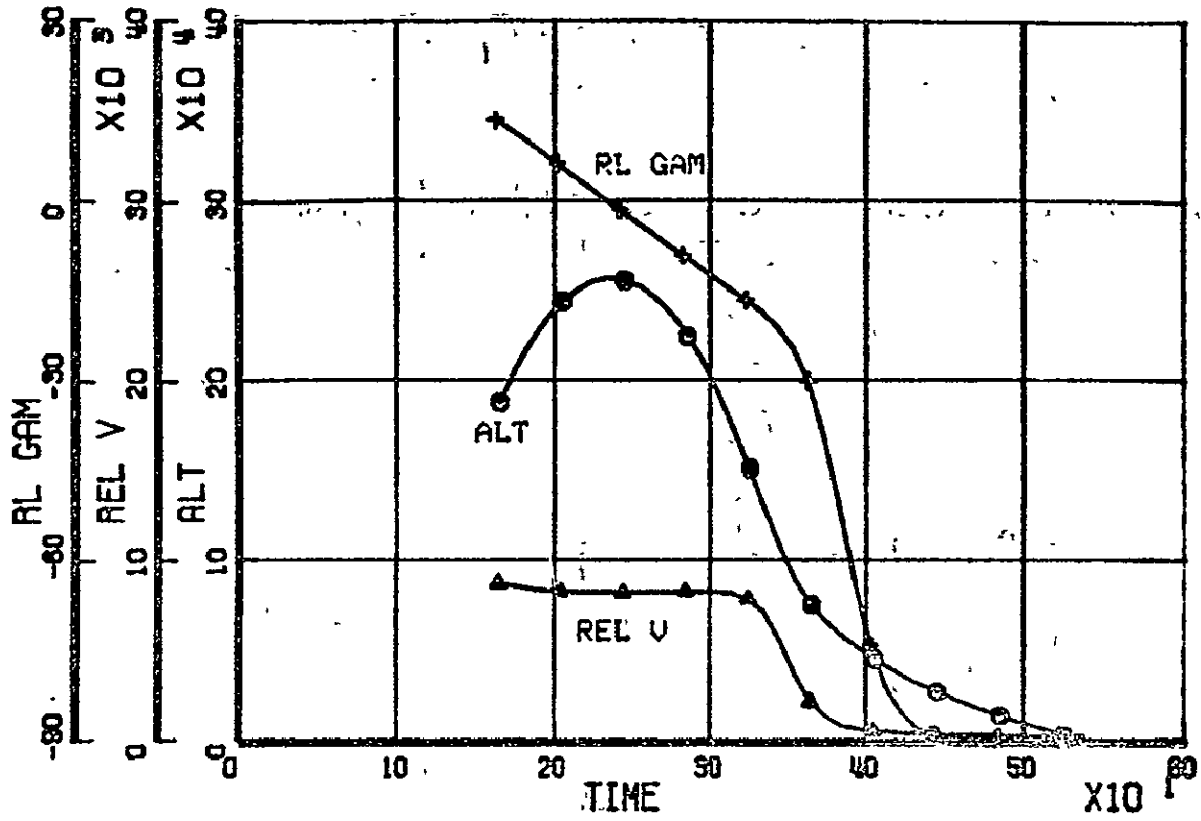


FIGURE VI-B-3-18

EDIN06 STG 1 REENTRY STATE MAR 76



EDIN06 REENTRY HEATING MAR 76

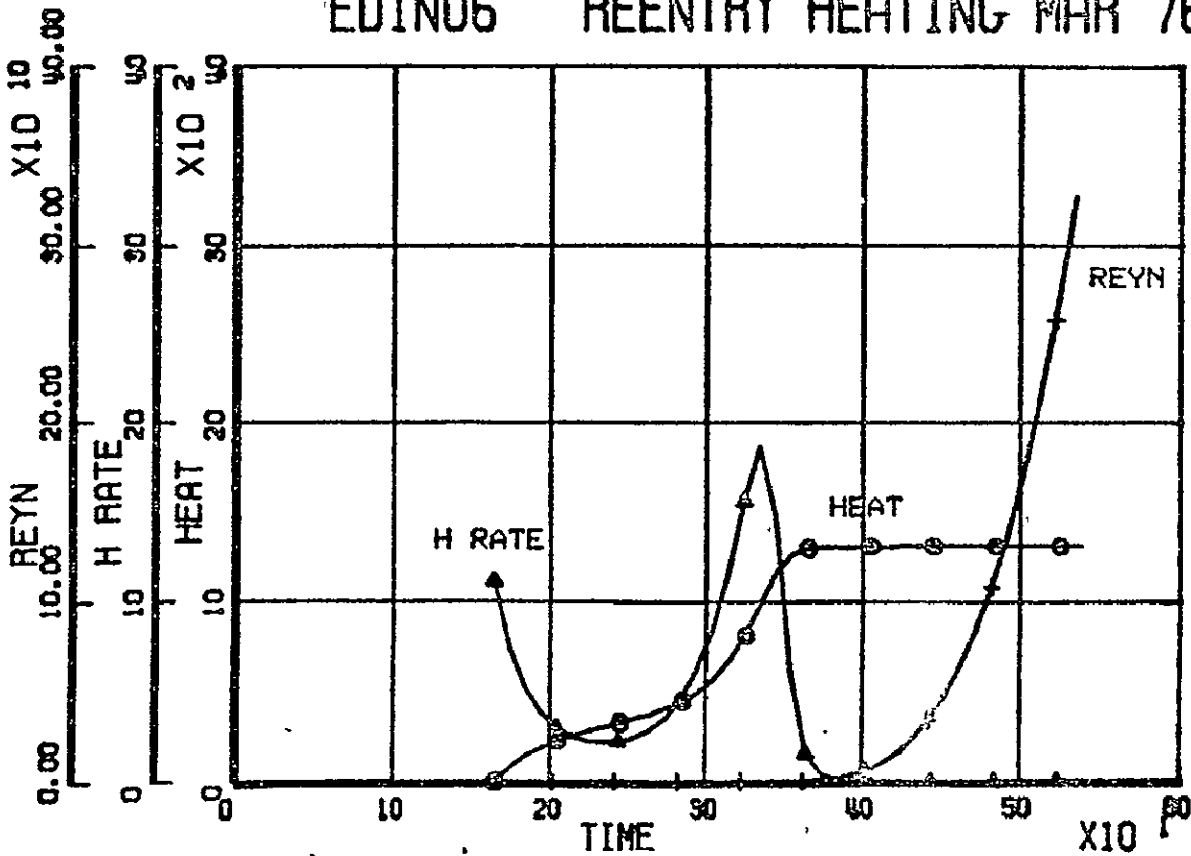


FIGURE VI-B-3-19
VI-B-3-32

HLLV GEOMETRIC SUMMARY

STAGE 1	LOX/LH ₂	LOX/RP-1	C ₃ H ₈
INERT WT.	3.53 M.LBS.	2.93 M.LBS.	2.97 M.LBS.
ENGINES	18	22	20
LENGTH	344 FT.	278 FT.	285 FT.
DIAMETER	69 FT.	56 FT.	57 FT.
WING SPAN	393 FT.	357 FT.	360 FT.
STAGE 2			
INERT WT.	812 K.LBS.	952 K.LBS.	927 K.LBS.
ENGINES	6	7	7
LENGTH	200 FT.	208 FT.	210 FT.
DIAMETER	50 FT.	52 FT.	53 FT.
WING SPAN	198 FT.	215 FT.	218 FT.

TABLE VI-B-3-9
VI-B-3-33

LOX/LH₂ COST ESTIMATE
(M OF 76 \$)

	<u>TFU</u>	<u>DDT&E</u>
LOX/LH ₂ Vehicle	<u>1016</u>	<u>11510</u>
Program Management	0	260
SE&I	0	490
System Support	0	950
Stage 1	<u>761</u>	<u>6730</u>
Project Management	0	200
SE&I	0	310
Hardware	<u>761</u>	<u>6220</u>
Structures	294	3120
TPS	2	30
Launch & Recovery	20	80
Propulsion	253	1560
Orient., Control, & Sep.	36	300
Avionics	35	710
Power Systems	16	140
Inst., Ass., & C.O.	105	160
Major Ground Test	0	120
Stage 2	<u>255</u>	<u>3080</u>
Project Management	0	120
SE&I	0	140
Hardware	<u>255</u>	<u>2820</u>
Structures	116	1140
TPS	1	10
Launch & Recovery	6	20
Propulsion	45	810
Orient., Control, & Sep.	15	130
Avionics	30	560
Power Systems	7	60
Inst., Ass., & C.O.	35	50
Major Ground Test	0	40

TABLE VI-B-3-10

LOX/RP1 COST ESTIMATE
(M OF 76 \$)

	<u>TFU</u>	<u>DDT&E</u>
LOX/RP1 Vehicle	<u>984</u>	<u>10730</u>
Program Management	0	250
SE&I	0	460
System Support	0	880
Stage 1	<u>701</u>	<u>5820</u>
Project Management	0	180
SE&I	0	270
Hardware	<u>701</u>	<u>5370</u>
Structures	<u>216</u>	<u>2450</u>
TPS	1	10
Launch & Recovery	18	70
Propulsion	281	1460
Orient., Control, & Sep.	39	330
Avionics	33	660
Power Systems	16	140
Inst., Ass., & C.O.	97	140
Major Ground Test	0	110
Stage 2	<u>283</u>	<u>3320</u>
Project Management	0	120
SE&I	0	150
Hardware	<u>283</u>	<u>3050</u>
Structures	<u>132</u>	<u>1310</u>
TPS	1	10
Launch & Recovery	7	30
Propulsion	51	820
Orient., Control, & Sep.	15	130
Avionics	30	570
Power Systems	8	80
Inst., Ass., & C.O.	39	60
Major Ground Test	0	40

ORIGINAL PAGE IS
OF POOR QUALITY

TABLE VI-B-3-11

VI-B-3-35

LOX/C₃H₈ COST ESTIMATE
(M OF 76`\$)

	<u>TFU</u>	<u>DDT&E</u>
LOX/C ₃ H ₈ Vehicle	<u>911</u>	<u>10520</u>
Program Management	0	240
SE&I	0	450
System Support	0	860
Stage 1	<u>621</u>	<u>5600</u>
Project Management	0	170
SE&I	0	260
Hardware	<u>621</u>	<u>5170</u>
Structures	<u>222</u>	<u>2470</u>
TPS	1	20
Launch & Recovery	18	70
Propulsion	204	1200
Orient., Control, & Sep.	40	340
Avionics	33	660
Power Systems	18	180
Inst., Ass., & C.O.	85	130
Major Ground Test	0	100
Stage 2	<u>290</u>	<u>3370</u>
Project Management	0	130
SE&I	0	150
Hardware	<u>290</u>	<u>3090</u>
Structures	<u>136</u>	<u>1350</u>
TPS	1	10
Launch & Recovery	7	30
Propulsion	52	820
Orient., Control, & Sep.	16	130
Avionics	30	570
Power Systems	8	80
Inst., Ass., & C.O.	40	60
Major Ground Test	0	40

TABLE VI-B-3-12

COST SUMMARY
(M OF 76 \$)

VEHICLE	TFU	DDT&E
LOX/C ₃ H ₈	911	10,520
LOX/RP1	984	10,730
LOX/LH ₂	1,016	11,510

TABLE VI-B-3-13

STAGE 1 WEIGHT STATEMENT:

AERODYNAMIC SURFACES		501882.
WING	434288.	
HEAT SHIELD PENALTY (WING)	0.	
VERTICAL TAIL	17203.	
HORIZONTAL STABILIZER	17869.	
HEAT SHIELD PENALTY (STAB)	38521.	
BODY STRUCTURE		551991.
INTEGRAL LOX TANK	134073.	
HEAT SHIELD PENALTY (LOX)	0.	
INTEGRAL FUEL TANK	70528.	
HEAT SHIELD PENALTY (FL)	0.	
THROAT STRUCTURE	169432.	
INTERTANK STRUCTURE	114927.	
NOSE STRUCTURE	18634.	
INTERSTAGE STRUCTURE	36240.	
SECONDARY STRUCTURE	8158.	
INDUCED ENVIRONMENTAL PROTECTION		5833.
TANK INSULATION	5833.	
MISCELLANEOUS	0.	
LAUNCH AND RECOVERY SYSTEM		128600.
LAUNCH GEAR	7227.	
LANDING GEAR	121373.	
PROPULSION		758593.
MAIN ENGINE	440565.	
AIRBREATHING ENGINE	82235.	
AIRBREATHING TANKAGE	40822.	
PROPELLANT FEED SYSTEM	133130.	
MAIN ENGINE MOUNTS	4406.	
PRESSURIZATION SYSTEM	44691.	
HEAT SHIELD	12745.	
ORIENTATION, CONTROL & SEPARATION		110275.
MAIN ENGINE GIMBAL SYSTEM	79078.	
ACC	12004.	
ACC TANKAGE	2204.	
AERODYNAMIC CONTROL	12667.	
SEPARATION SYSTEM	4321.	
AVIONICS		5625.
ELECTRICAL POWER SYSTEM		3253.
HYDRAULIC & PNEUMATIC SYSTEM		29698.
<hr/>		
DRY WEIGHT		2095750.
DESIGN RESERVE		419150.
EMPTY WEIGHT		2514900.

ORIGINAL PAGE IS
OF POOR QUALITY

TABLE VI-B-3-14

VI-B-3-38

MAIN PROPELLANT:		21121271.
OXIDIZER	15381795.	
FUEL	5739476.	
RESIDUAL PROPELLANT:		148983.
TRAPPED GASES	5138.	
TRAPPED OXIDIZER	50197.	
TRAPPED FUEL	34437.	
TRAPPED ENGINE PROPELLANT	59212.	
RESERVE PROPELLANT:		0.
OXIDIZER	0.	
FUEL	0.	
INFLIGHT LOSES:		51883.
OXIDIZER	41838.	
FUEL	10044.	
AUXILIARY PROPELLANT:		253093.
ACC PROPELLANT	12963.	
AIRBREATHING ENGINE FUEL	240129.	
<hr/>		
BOOSTER LIFTOFF WEIGHT		24090128.
<hr/>		
MASS FRACTION		.877
<hr/>		
BOOSTER WEIGHT AT STAGING		2880735.
<hr/>		
ENTRY WEIGHT (ATMOSPHERIC INTERFACE)		2809856.
<hr/>		
BOOSTER LANDING WEIGHT		2513086.
<hr/>		

SYSTEM AND SUBSYSTEM WEIGHT PERCENTAGES: (%)

AERODYNAMIC SURFACE	2.0834	
BODY STRUCTURE	2.2914	
ENVIRONMENTAL PROTECTION	.0242	
LAUNCH AND RECOVERY	.5338	
PROPULSION	3.1490	
ORIENTATION CONTROL/SEPARATION	.4578	
AVIONICS	.0233	
ELECTRICAL POWER SYSTEM	.0135	
HYDRAULIC & PNEUMATIC SYSTEM	.1233	
DRY WEIGHT		8.6996
DESIGN RESERVE	1.7399	
EMPTY WEIGHT		10.4395
MAIN PROPELLANT:	87.6760	
TRAPPED PROPELLANT:	.6184	
RESERVE PROPELLANT:	.0000	
INFLIGHT LOSSES:	.2154	
AUXILIARY PROPELLANT:	1.0506	

ORIGINAL PAGE IS
OF POOR QUALITY

STAGE 2 WEIGHT STATEMENT:

<p> REPODYNAMIC SURFACE: WING VERTICAL TAIL HORIZONTAL STABILIZER </p>	<p> 340862. 5612. 2803. </p>	<p> 349277. </p>
<p> BODY STRUCTURE INTEGRAL LOX TANK INTEGRAL FUEL TANK THRUST STRUCTURE INTERTANK STRUCTURE NOSE STRUCTURE INTERSTAGE STRUCTURE SECONDARY STRUCTURE </p>	<p> 31467. 66146. 19507. 50447. 14460. 16444. 2977. </p>	<p> 201448. </p>
<p> INDUCED ENVIRONMENTAL PROTECTION TANK INSULATION MISCELLANEOUS </p>	<p> 3856. 0. </p>	<p> 3856. </p>
<p> LAUNCH AND RECOVERY SYSTEM LAUNCH GEAR LANDING GEAR </p>	<p> 1859. 34495. </p>	<p> 36354. </p>
<p> PROPULSION MAIN ENGINE: AIRBREATHING ENGINE: AIRBREATHING TANKAGE PROPELLANT FEED SYSTEM MAIN ENGINE MOUNT: PREOCCUPATION SYSTEM HEAT SHIELD </p>	<p> 89773. 0. 0. 12001. 673. 24869. 11046. </p>	<p> 136361. </p>
<p> ORIENTATION, CONTROL & SEPARATION MAIN ENGINE GIMBAL SYSTEM ACS ACS TANKAGE AERODYNAMIC CONTROLS SEPARATION SYSTEM </p>	<p> 12351. 11415. 1532. 5632. 3004. </p>	<p> 33933. </p>
<p> AVIONICS ELECTRICAL POWER SYSTEM HYDRAULIC & PNEUMATIC SYSTEM </p>	<p> </p>	<p> 5012. 2994. 9702. </p>
<p> DRY WEIGHT DESIGN RESERVE EMPTY WEIGHT </p>	<p> </p>	<p> 780937. 98500. 879437. </p>
<p> PAYLOAD </p>	<p> </p>	<p> 1051923. </p>

TABLE VI-B-3-16

MAIN PROPELLANT:		4166302.
OXIDIZER	3571116.	
FUEL	595186.	
RESIDUAL PROPELLANT:		28523.
TRAPPED GAGES	2823.	
TRAPPED OXIDIZER	8042.	
TRAPPED FUEL	5593.	
TRAPPED ENGINE PROPELLANT	12065.	
RESERVE PROPELLANT:		49996.
OXIDIZER	42853.	
FUEL	7142.	
INFLIGHT LOSES:		11332.
OXIDIZER	9713.	
FUEL	1619.	
AUXILIARY PROPELLANTS:		9011.
ACC PROPELLANT	9011.	
AIRBREATHING ENGINE FUEL	0.	

STAGE LIFTOFF WEIGHT MINUS PAYLOAD 5144601.

STAGE LIFTOFF WEIGHT WITH PAYLOAD 6196524.

MASS FRACTION (BASED ON INERT WEIGHT) .810

WEIGHT AT INJECTION (INCL PAYLOAD) 2002446.

ENTRY WEIGHT (ATMOSPHERIC INTERFACE) 930348.

STAGE LANDING WEIGHT 918582.

SYSTEM AND SUBSYSTEM WEIGHT PERCENTAGE: (%)

AERODYNAMIC SURFACES	6.7892	
BODY STRUCTURE	3.9157	
ENVIRONMENTAL PROTECTION	.0750	
LAUNCH AND RECOVERY	.7066	
PROPULSION	2.6894	
ORIENTATION CONTROL: SEPARATION	.6596	
AVIONICS	.0974	
ELECTRICAL POWER SYSTEM	.0582	
HYDRAULIC & PNEUMATIC SYSTEM	.1886	
DRY WEIGHT		15.1797
DESIGN RESERVE	1.9146	
EMPTY WEIGHT		17.0944
MAIN PROPELLANT:	80.9340	
TRAPPED PROPELLANT:	.5544	
RESERVE PROPELLANT:	.9718	
INFLIGHT LOSSES:	.2203	
AUXILIARY PROPELLANT:	.1752	

ORIGINAL PAGE IS
OF POOR QUALITY

TABLE VI-B-3-17

STAGE 1 GEOMETRIC CHARACTERISTICS:

FUSELAGE:		
TOTAL LENGTH (FT)		282.7
STAGE DIAMETER (FT)		56.5
LENGTH DIAMETER RATIO		5.00
AFT CHIPT LENGTH (FT)	40.0	
INTERTANK SPACING (FT)	10.0	
NOSE LENGTH (FT)	50.0	
LOD: TANK LENGTH (FT)	110.4	
FUEL TANK LENGTH (FT)	72.3	
TOTAL TANK VOLUME INCL ULLAGE		351687.
LOD: TANK VOLUME	223454.	
FUEL TANK VOLUME	128233.	
WING:		
WING AREA (SQ FT)		22846.3
WING LOADING (LBS SQ FT)		110.0
WING SPAN (FT)		360.0
STRUCTURAL WING SPAN (FT)		361.3
ROOT CHORD (FT)		79.3
THEORETICAL ROOT THICKNESS (FT)		9.5
TIP CHORD (FT)		47.6
TAPER RATIO		.600
ASPECT RATIO		5.7
SWEEP OF FILLET (DEG)		30.0
LEADING EDGE SWEEP (DEG)		10.0
TRAILING EDGE SWEEP (DEG)		.0
SPANWISE DISTANCE		.0
DV1		9.0
DV2		171.0
CF		5.2
C1		82.9
C2		77.8
C3		1.6
C4		.0
C5		2.6
C6		.8
C7		3.9
C8		1.2
LAM C 2:1		.3
LAM C-2:2		.1
COE LAM C 1		.9608
COE LAM C 2		.9961
COE LAM 2 EFF		8.5371
CLA TRUE		.02
CLA REF		.06
VERTICAL TAIL:		
VERTICAL TAIL AREA (SQ FT)		3084.3
HORIZONTAL STABILIZER:		
HORIZONTAL STABILIZER AREA (SQ FT)		4112.3

TABLE VI-B-3-18

VI-B-3-42

STAGE 2 GEOMETRIC CHARACTERISTICS:

FUSELAGE:

TOTAL LENGTH (FT)		209.8
STAGE DIAMETER (FT)		52.6
LENGTH DIAMETER RATIO		4.00
AFT CHIPT LENGTH (FT)	30.0	
PAYLOAD CHORD (FT)		97.0
PAYLOAD DENSITY (LB/CU FT)	5.0	
INTERTANK SPACING (FT)	10.0	
NOSE LENGTH (FT)	40.0	
LOD: TANK LENGTH (FT)	43.8	
FUEL TANK LENGTH (FT)	85.9	
TOTAL TANK VOLUME		196242.
LOD: TANK VOLUME	52445.	
FUEL TANK VOLUME	143797.	

WING:

WING AREA (SQ FT)		8350.7
WING LOADING (LB/SQ FT)		110.0
WING SPAN (FT)		217.6
STRUCTURAL WING SPAN		218.5
ROOT CHORD (FT)		48.0
THEORETICAL ROOT THICKNESS		3.8
TIP CHORD (FT)		28.6
TAPEF RATIO		.600
ASPECT RATIO		5.7
SWEEP OF FILLET (DEG)		30.0
LEADING EDGE SWEEP (DEG)		10.0
TRAILING EDGE SWEEP (DEG)		.0
SPANWISE DISTANCE		.0
DY1		5.4
DY2		103.4
CF		3.1
C1		50.1
C2		47.0
C3		1.0
C4		.0
C5		1.6
C6		.5
C7		2.4
C8		.7
LAM C 2:1		.3
LAM C 2:2		.1
COD LAM C 1		.9608
COD LAM C 2		.9961
COD LAM 2 EFF		8.5371
CLA TRUE		.08
CLA PEF		.08
VERTICAL TAIL:		
VERTICAL TAIL AREA (SQ FT)		1127.2
HORIZONTAL STABILIZER:		
HORIZONTAL STABILIZER AREA (SQ FT)		1503.1

Figures 20 through 23 show conceptual drawings of a 1,000,000 pound payload class heavy lift launch vehicle. Figure 20 gives views of the booster stage and the packaging of its 20 engines. In this figure the ABE's are shown mounted on a canard with moveable inlet closures for ascent heat protection. Figure 21 gives illustrations of the straight wing upper stage and its 7 ascent boost engines. Canards are also shown for this stage. A view showing this vehicle in a parallel burn configuration is given in Figure 22. Figure 23 gives an illustration of an HLLV in a stacked, series burn configuration.

ORIGINAL PAGE IS
OF POOR QUALITY

VI-B-3-45

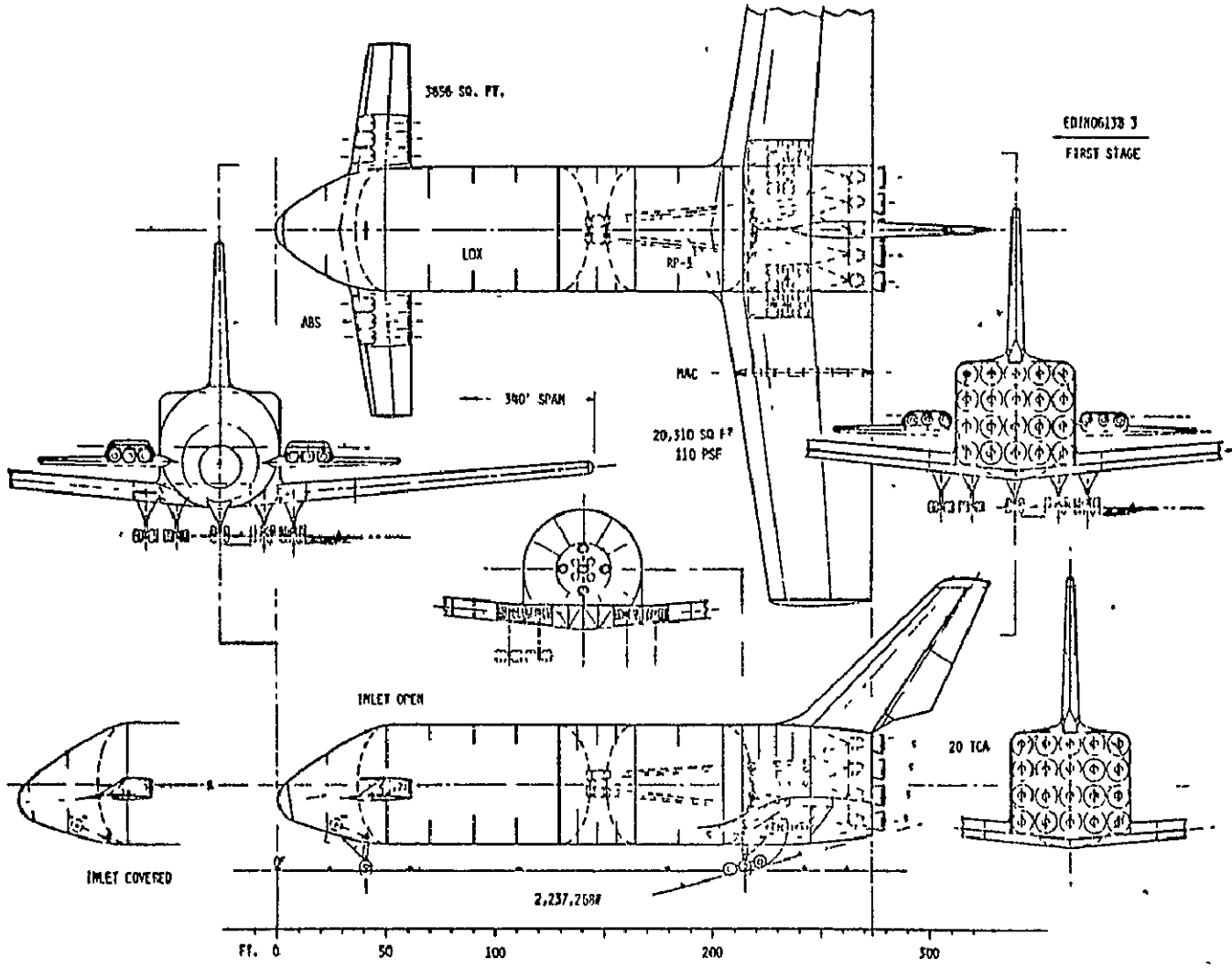


FIGURE VI-B-3-20

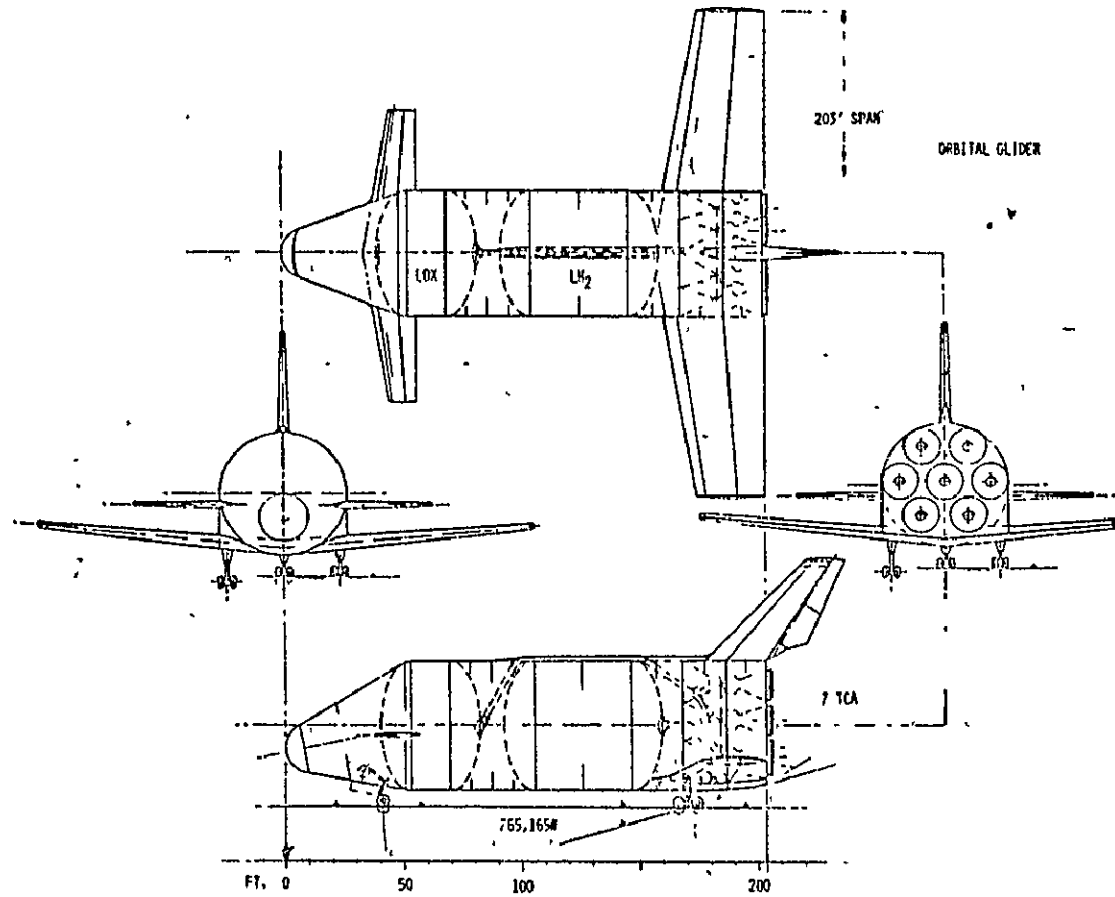


FIGURE VI-B-3-21

ORIGINAL PAGE IS
OF POOR QUALITY

VI-B-3-47

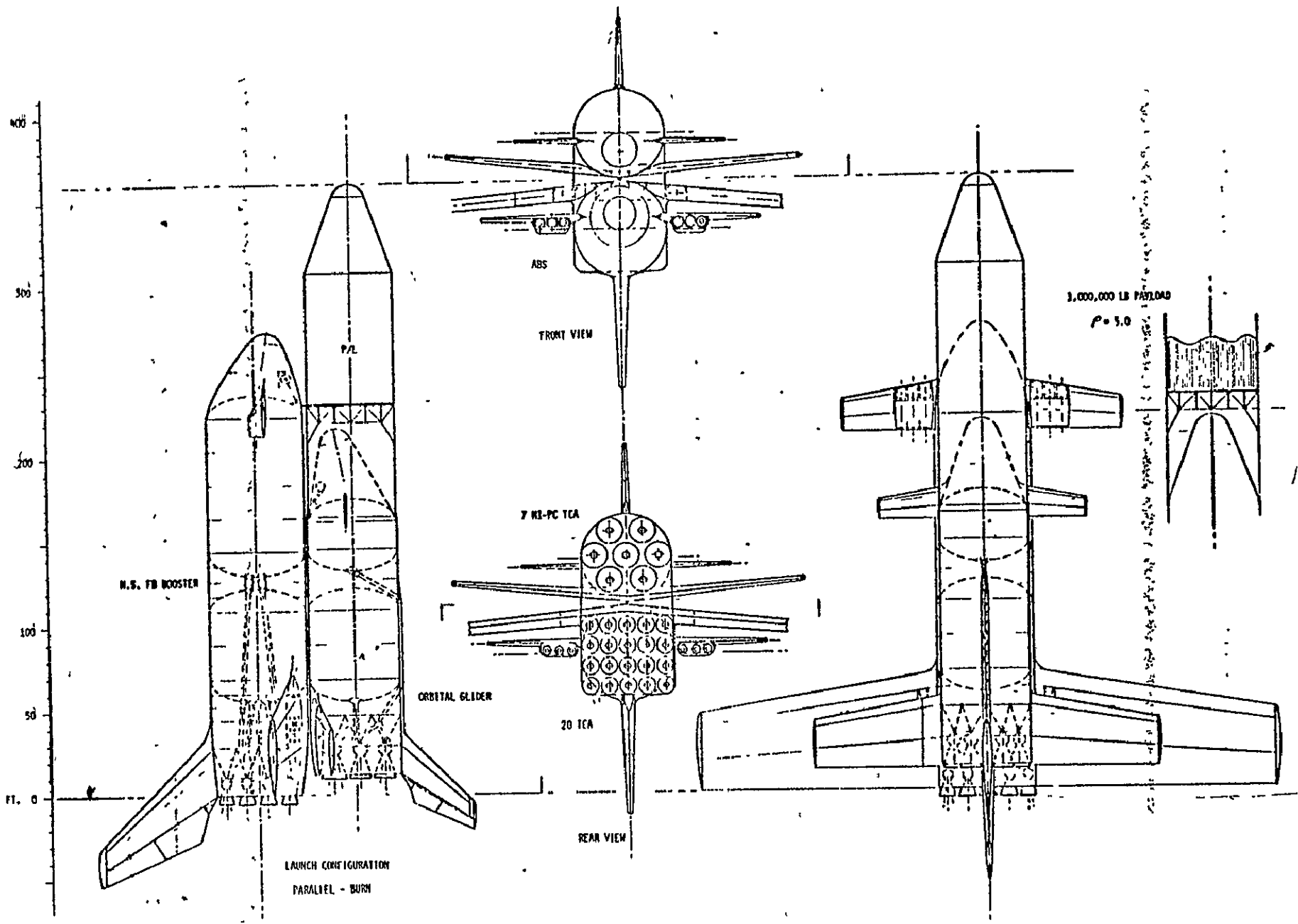


FIGURE VI-B-3-22

VI-B-3-48

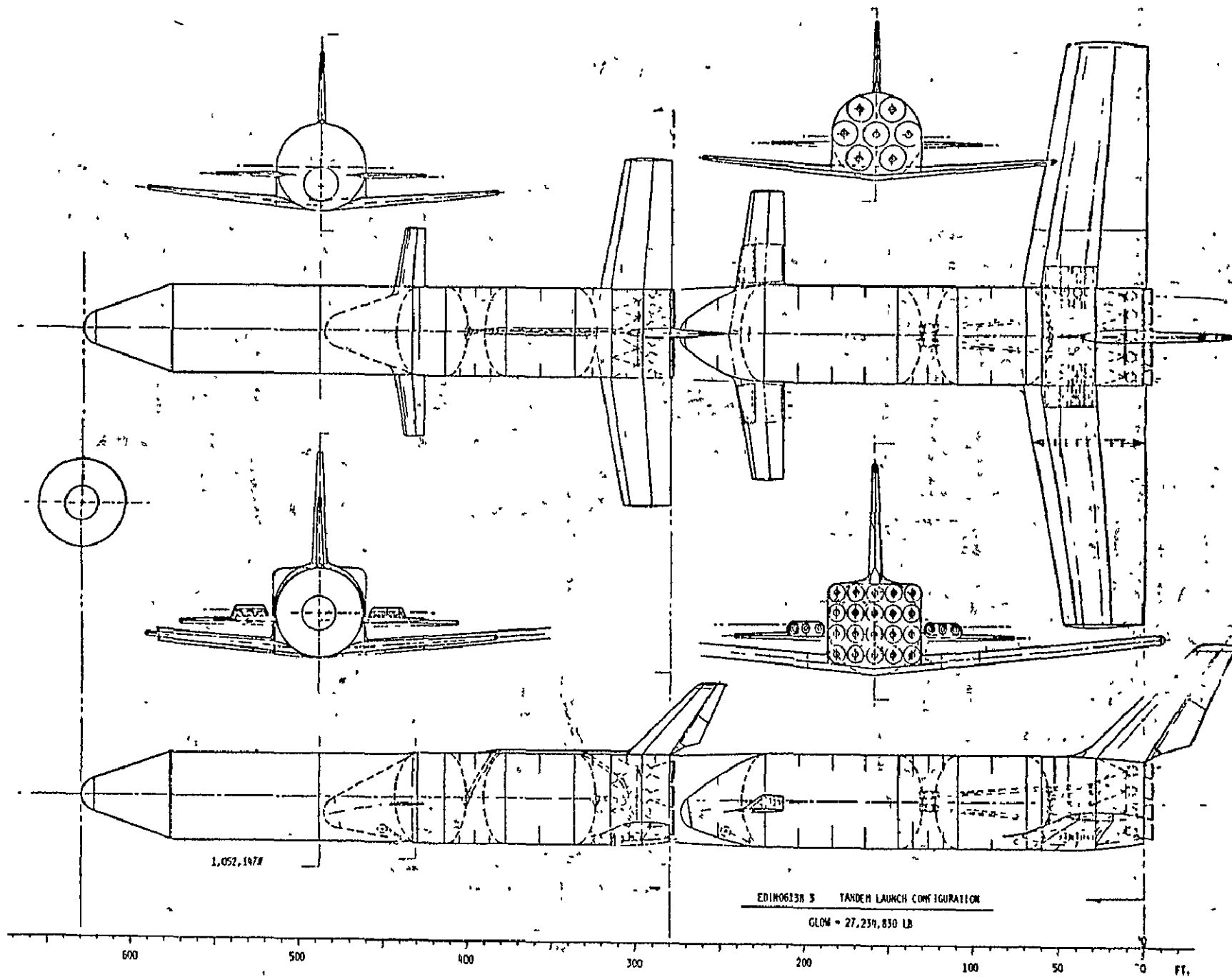


FIGURE VI-B-3-23

RESULTS

The study results indicate that the two stage winged vehicle featuring LOX/C3H8 booster engines and LOX/LH2 upper stage engines would meet the basic requirements of the SPSS launch vehicle. Detailed weight statements of this vehicle are presented in Tables 14 through 17. Geometric description of the baseline vehicle is given in Tables 18 and 19; drawings giving typical HLLV sizes and configurations are shown in Figures 20 through 23. A chart showing a brief weight and performance summary of the baseline vehicle is given in Table 5. A complete trajectory is given in Appendix A.

Although the study indicated the development of launch vehicles to meet the SPSS requirements is feasible, further study is recommended in the areas of vehicle configuration analysis, tank weights, loads and stress analyses, thermal analysis, and control capabilities.

APPENDIX A

C₃H₈

PAGE 1

EDIN TPAJ. REPORT
STATE HISTORY

TIME	WEIGHT	THRUST	LD FAC	LIFT	DRAG	D'Y N P	HEAT	HT FT
LIFT-OFF								
.0	20286652.	39355913.	1.30	0.	0.	.0	0.	0.
4.0	29764501.	39368751.	1.32	0.	3238.	1.8	0.	0.
BEGIN TILT								
6.0	29503426.	39385269.	1.33	160.	7583.	4.3	0.	0.
10.0	28981276.	39439390.	1.36	3627.	22757.	12.7	0.	0.
END TILT								
16.0	28198050.	39575397.	1.40	6194.	64910.	35.7	0.	0.
20.0	27675900.	39703728.	1.43	8.	108365.	58.8	0.	0.
30.0	26370525.	40154789.	1.51	268.	295761.	147.0	0.	0.
40.0	25065149.	40768836.	1.60	1255.	633244.	276.9	0.	0.
50.0	23759774.	41486922.	1.70	3448.	1185650.	434.6	0.	0.
60.0	22454398.	42223425.	1.75	7000.	2988578.	585.3	0.	0.
THROTTLE BND								
62.0	22192910.	42364474.	1.75	8091.	3631106.	609.3	0.	1.
O MAXIMUM								
63.0	22067821.	40947263.	1.69	8476.	3698197.	617.4	0.	1.
O MAXIMUM								
63.8	21967738.	37249417.	1.52	8788.	3750462.	623.5	0.	1.
O MAXIMUM								
64.0	21930293.	31343621.	1.26	8925.	3818130.	633.4	0.	1.
O MAXIMUM								
70.0	21285038.	40301518.	1.72	10912.	3784330.	619.1	0.	1.
70.0	21281339.	39978865.	1.70	10925.	3784499.	619.2	0.	1.
O MAXIMUM								
70.3	21234043.	35636263.	1.50	11118.	3817538.	626.3	0.	1.
79.0	20227890.	42497479.	1.93	14213.	3507990.	606.6	0.	1.
88.0	19061952.	43637929.	2.13	16516.	2978588.	556.5	0.	2.
97.0	17887114.	43829906.	2.33	17063.	2222939.	443.4	0.	2.
106.0	16712276.	43937027.	2.54	16959.	1569447.	339.6	0.	3.
115.0	15537438.	43994751.	2.76	15899.	1092209.	251.3	0.	4.
124.0	14362600.	44025087.	3.01	13951.	727685.	178.5	0.	5.
133.0	13187762.	44040687.	3.30	11662.	476792.	124.1	0.	7.
142.0	12012924.	44048667.	3.64	9431.	315000.	85.8	0.	8.
151.0	10838758.	43570255.	4.00	7549.	215225.	60.0	0.	9.

ORIGINAL PAGE IS
OF POOR QUALITY

PRECEDING PAGE BLANK NOT FILMED

EDIN TPAJ. REPORT
STATE HISTORY

TIME	WEIGHT	THPUST	LD FAC	LIFT	DRAG	D'YN P	HEAT	HT FT
160.0	9737482.	39102552.	4.00	6074.	152625.	42.6	0.	11.
165.1	9165381.	36784228.	4.00	5228.	122706.	34.2	0.	11.
THPUST EVENT								
165.1	6196524.	6732122.	1.08	1911.	44851.	34.2	0.	11.
BEGIN MIN-H								
165.1	6196524.	6732963.	1.08	1911.	44851.	34.2	0.	11.
169.0	6140034.	6732963.	1.10	0.	0.	.0	0.	12.
179.0	5995549.	6732963.	1.12	0.	0.	.0	0.	11.
189.0	5851065.	6732963.	1.15	0.	0.	.0	0.	9.
199.0	5706581.	6732963.	1.18	0.	0.	.0	0.	7.5
209.0	5562097.	6732963.	1.21	0.	0.	.0	0.	5.
219.0	5417613.	6732963.	1.24	0.	0.	.0	0.	4.
229.0	5273129.	6732963.	1.28	0.	0.	.0	0.	3.
239.0	5128644.	6732963.	1.31	0.	0.	.0	0.	3.
249.0	4984160.	6732963.	1.35	0.	0.	.0	0.	2.
259.0	4839676.	6732963.	1.39	0.	0.	.0	0.	2.
269.0	4695192.	6732963.	1.43	0.	0.	.0	0.	2.
279.0	4550708.	6732963.	1.48	0.	0.	.0	0.	2.
289.0	4406223.	6732963.	1.53	0.	0.	.0	0.	2.
299.0	4261739.	6732963.	1.58	0.	0.	.0	0.	2.
309.0	4117255.	6732963.	1.64	0.	0.	.0	0.	2.
319.0	3972771.	6732963.	1.69	0.	0.	.0	0.	2.
329.0	3828287.	6732963.	1.76	0.	0.	.0	0.	2.
339.0	3683803.	6732963.	1.83	0.	0.	.0	0.	2.
349.0	3539319.	6732963.	1.90	0.	0.	.0	0.	2.
359.0	3394834.	6732963.	1.98	0.	0.	.0	0.	2.
369.0	3250350.	6732963.	2.07	0.	0.	.0	0.	3.
379.0	3105866.	6732963.	2.17	0.	0.	.0	0.	3.
389.0	2961382.	6732963.	2.27	0.	0.	.0	0.	4.
399.0	2816898.	6732963.	2.39	0.	0.	.0	0.	4.
409.0	2672413.	6732963.	2.52	0.	0.	.0	0.	5.
419.0	2527929.	6732963.	2.66	0.	0.	.0	0.	6.
429.0	2383445.	6732963.	2.82	0.	0.	.0	0.	7.
439.0	2238961.	6732963.	3.01	0.	0.	.0	0.	9.
449.0	2094477.	6732963.	3.21	0.	0.	.0	0.	9.
INJECTION								
453.5	2028756.	6732963.	3.32	0.	0.	.0	0.	9.

EDIN TRAJ. REPORT
STATE HISTORY

TIME	REL VEL	PL FPA	ALT	RANGE	REL AZ	GC LAT	LONG	TRANGE
LIFT-OFF								
.0	.0	.06	-1.	10.56	19.69	28.37	-80.56	10.
4.0	40.1	89.84	78.	10.	-5.12	28.37	-80.56	10.
BEGIN TILT								
6.0	61.3	89.84	180.	10.	-7.54	28.37	-80.56	10.
10.0	106.1	89.74	513.	10.	51.97	28.37	-80.56	10.
END TILT								
16.0	179.6	88.86	1366.	10.	81.93	28.37	-80.56	10.
20.0	233.3	87.92	2190.	10.	85.63	28.37	-80.56	10.
30.0	385.7	84.10	5254.	10.	88.54	28.37	-80.56	11.
40.0	568.7	78.42	9940.	10.	89.34	28.37	-80.56	13.
50.0	789.0	71.49	16456.	10.	89.67	28.37	-80.56	10.
60.0	1047.5	63.99	24913.	10.	89.84	28.37	-80.55	11
THRUSTLE BND								
62.0	1102.7	62.47	26833.	10.	89.87	28.37	-80.54	12.
0 MAXIMUM								
63.0	1128.1	61.70	27818.	10.	89.88	28.37	-80.54	12.
0 MAXIMUM								
63.8	1148.7	61.09	28618.	10.	89.89	28.37	-80.54	13.
0 MAXIMUM								
64.0	1161.0	60.96	28784.	10.	89.89	28.37	-80.54	13.
0 MAXIMUM								
70.0	1277.1	56.29	34998.	10.	89.96	28.37	-80.53	15.
70.0	1278.0	56.27	35030.	10.	89.96	28.37	-80.53	15.
0 MAXIMUM								
70.3	1292.3	56.04	35333.	10.	89.97	28.37	-80.53	15.
79.0	1537.2	49.20	45021.	10.	90.05	28.37	-80.50	21.
88.0	1918.9	42.61	56099.	11.	90.12	28.37	-80.47	31.
97.0	2380.7	36.78	68369.	12.	90.19	28.37	-80.42	46.
106.0	2922.7	31.74	81712.	14.	90.27	28.37	-80.36	65.
115.0	3547.6	27.43	95996.	18.	90.34	28.37	-80.28	89.
124.0	4259.6	23.77	111087.	22.	90.43	28.37	-80.19	118.
133.0	5065.3	20.68	126870.	28.	90.52	28.37	-80.07	154.
142.0	5974.7	18.06	143258.	35.	90.62	28.37	-79.92	197.
151.0	7001.6	15.86	160205.	44.	90.73	28.37	-79.75	250.

EDIN TPAJ. REPORT
STATE HISTORY

TIME	PEL	VEL	PL	FPA	ALT	RANGE	PEL	AZ	GC	LAT	LONG	TRANGE
160.0	8086.8	14.01	177649.	55.	90.86	28.36	-79.55	310.				
165.1	8704.2	13.10	187655.	61.	90.94	28.36	-79.42	347.				
THRUIT EVENT												
165.1	8704.2	13.10	187655.	61.	90.94	28.36	-79.42	347.				
BEGIN MIN-H												
165.1	8704.2	13.10	187655.	61.	90.94	28.36	-79.42	347.				
169.0	8812.8	12.55	195253.	67.	91.01	28.36	-79.32	356.				
179.0	9101.1	11.23	213682.	81.	91.18	28.36	-79.04	380.				
189.0	9404.3	9.99	230689.	96.	91.35	28.35	-78.76	405.				
199.0	9722.5	8.84	246303.	111.	91.53	28.34	-78.47	430.				
209.0	10055.8	7.77	260557.	127.	91.71	28.34	-78.17	455.				
219.0	10404.1	6.78	273481.	143.	91.90	28.33	-77.86	482.				
229.0	10767.7	5.87	285111.	160.	92.09	28.32	-77.54	509.				
239.0	11146.7	5.03	295484.	178.	92.28	28.31	-77.20	537.				
249.0	11541.6	4.26	304636.	196.	92.48	28.29	-76.86	567.				
259.0	11952.6	3.56	312610.	215.	92.69	28.28	-76.50	597.				
269.0	12380.3	2.92	319449.	235.	92.90	28.26	-76.13	628.				
279.0	12825.2	2.34	325200.	255.	93.12	28.25	-75.74	661.				
289.0	13287.9	1.83	329913.	276.	93.34	28.23	-75.34	696.				
299.0	13769.3	1.36	333641.	298.	93.57	28.20	-74.93	732.				
309.0	14270.1	.96	336442.	321.	93.80	28.18	-74.50	770.				
319.0	14791.5	.60	338378.	344.	94.04	28.15	-74.06	810.				
329.0	15334.5	.30	339518.	369.	94.29	28.12	-73.60	854.				
339.0	15900.6	.04	339932.	394.	94.55	28.09	-73.12	901.				
349.0	16491.1	-.17	339702.	420.	94.81	28.06	-72.63	951.				
359.0	17107.9	-.33	338913.	447.	95.08	28.02	-72.12	1007.				
369.0	17753.0	-.45	337659.	475.	95.36	27.97	-71.59	1069.				
379.0	18428.6	-.53	336043.	505.	95.64	27.93	-71.04	1141.				
389.0	19137.4	-.57	334179.	535.	95.94	27.88	-70.47	1224.				
399.0	19882.5	-.56	332190.	567.	96.24	27.82	-69.88	1326.				
409.0	20667.5	-.51	330216.	599.	96.56	27.76	-69.26	1456.				
419.0	21496.5	-.43	328407.	634.	96.88	27.69	-68.63	1636.				
429.0	22374.6	-.30	326933.	669.	97.21	27.62	-67.96	1920.				
439.0	23307.7	-.13	325983.	706.	97.56	27.54	-67.27	2522.				
449.0	24303.0	.08	325770.	745.	97.91	27.45	-66.56	2522.				
INJECTION												
453.5	24778.7	.18	325981.	763.	98.08	27.41	-66.22	2522.				

EDIN TRAJ. REPORT
STATE HISTORY

TIME	MACH	ALPHA	BANK	VELI	FPAI	AZI
LIFT-OFF						
.0	.000	.00	90.00	1341.6	.00	90.00
4.0	.035	.00	90.00	1342.2	1.71	90.00
BEGIN TILT						
6.0	.054	.02	-1.14	1343.0	2.62	89.99
10.0	.093	.16	-.13	1346.2	4.52	89.99
END TILT						
16.0	.159	.10	-.09	1357.2	7.60	89.98
20.0	.207	.00	90.00	1370.2	9.80	89.97
30.0	.345	.00	90.00	1433.9	15.52	89.96
40.0	.516	.00	90.00	1559.3	20.93	89.95
50.0	.731	.00	90.00	1760.1	25.16	89.95
60.0	1.005	.01	90.00	2033.7	27.58	89.96
THRUSTLE BND						
62.0	1.067	.01	90.00	2095.2	27.82	89.96
O MAXIMUM						
63.0	1.096	.01	90.00	2124.6	27.87	89.97
O MAXIMUM						
63.8	1.121	.01	90.00	2148.6	27.91	89.97
O MAXIMUM						
64.0	1.134	.01	90.00	2160.4	28.02	89.97
O MAXIMUM						
70.0	1.285	.01	90.00	2311.3	27.36	89.99
70.0	1.286	.01	90.00	2312.3	27.36	89.99
O MAXIMUM						
70.3	1.303	.01	90.00	2327.3	27.42	89.99
79.0	1.615	.01	90.00	2621.4	26.35	90.02
88.0	2.048	.01	90.00	3048.2	25.22	90.06
97.0	2.483	.02	90.00	3551.5	23.66	90.11
106.0	2.985	.02	90.00	4129.4	21.86	90.17
115.0	3.563	.03	90.00	4784.3	19.97	90.24
124.0	4.183	.03	90.00	5520.7	18.12	90.32
133.0	4.853	.04	90.00	6346.0	16.37	90.40
142.0	5.590	.05	90.00	7271.0	14.76	90.50
151.0	6.457	.06	90.00	8310.4	13.31	90.61

EDIN TRAJ. REPORT
STATE HISTORY

TIME	MACH	ALPHA	BANK	VELI	FPAI	AZI
160.0	7.585	.06	90.00	9405.2	12.02	90.74
165.1	8.286	.07	90.00	10027.3	11.34	90.81

THRUIT EVENT

165.1	8.286	.07	90.00	10027.3	11.34	90.81
-------	-------	-----	-------	---------	-------	-------

BEGIN MIN-H

165.1	8.286	9.52	90.00	10027.3	11.34	90.81
169.0	.000	9.74	90.00	10138.9	10.89	90.87
179.0	.000	10.25	90.00	10433.8	9.78	91.02
189.0	.000	10.66	90.00	10742.7	8.73	91.18
199.0	.000	11.00	90.00	11065.7	7.76	91.34
209.0	.000	11.28	90.00	11403.0	6.85	91.50
219.0	.000	11.51	90.00	11754.7	6.00	91.67
229.0	.000	11.68	90.00	12121.1	5.21	91.85
239.0	.000	11.80	90.00	12502.5	4.48	92.03
249.0	.000	11.86	90.00	12899.2	3.81	92.22
259.0	.000	11.88	90.00	13311.8	3.19	92.41
269.0	.000	11.85	90.00	13740.6	2.63	92.61
279.0	.000	11.77	90.00	14186.4	2.12	92.82
289.0	.000	11.66	90.00	14649.9	1.66	93.03
299.0	.000	11.50	90.00	15131.7	1.24	93.24
309.0	.000	11.31	90.00	15632.9	.87	93.47
319.0	.000	11.08	90.00	16154.5	.55	93.70
329.0	.000	10.81	90.00	16697.6	.27	93.94
339.0	.000	10.51	90.00	17263.7	.04	94.19
349.0	.000	10.18	90.00	17854.2	-.16	94.44
359.0	.000	9.82	90.00	18470.9	-.31	94.70
369.0	.000	9.43	90.00	19115.8	-.42	94.97
379.0	.000	9.02	90.00	19791.3	-.50	95.25
389.0	.000	8.58	90.00	20499.9	-.53	95.54
399.0	.000	8.12	90.00	21244.9	-.52	95.84
409.0	.000	7.64	90.00	22029.7	-.48	96.15
419.0	.000	7.13	90.00	22858.5	-.40	96.47
429.0	.000	6.61	90.00	23736.5	-.28	96.80
439.0	.000	6.06	90.00	24669.6	-.12	97.14
449.0	.000	5.51	90.00	25664.8	.07	97.49

INJECTION

453.5	.000	5.25	90.00	26140.5	.17	97.65
-------	------	------	-------	---------	-----	-------

PROPANE BOOSTER TURN AROUND

LIFTING TRAJECTORY

EDIN TRAJ. REPORT
STATE HISTORY

TIME	WEIGHT	THRUST	LD FAC	LIFT	DRAG	D/W P	HEAT	HT	PT
165.1	2968857.	0.	.26	421417.	662227.	18.8	0.	8.	
175.0	2968857.	0.	.12	197920.	311018.	8.8	67.	5.	
185.0	2968857.	0.	.06	98113.	154178.	4.4	112.	4.	
195.0	2968857.	0.	.03	52614.	82679.	2.3	145.	3.	
205.0	2968857.	0.	.02	31161.	48967.	1.4	168.	2.	
215.0	2968857.	0.	.01	20757.	32618.	.9	187.	2.	
225.0	2968857.	0.	.01	15531.	24406.	.7	202.	1.	
235.0	2968857.	0.	.01	13355.	20986.	.6	216.	1.	
245.0	2968857.	0.	.01	13378.	21023.	.6	229.	1.	
255.0	2968857.	0.	.01	15611.	24532.	.7	243.	1.	
265.0	2968857.	0.	.01	20903.	32848.	.9	259.	2.	
275.0	2968857.	0.	.02	31423.	49379.	1.4	277.	2.	
285.0	2968857.	0.	.03	53012.	83305.	2.4	301.	3.	
295.0	2968857.	0.	.06	98375.	154589.	4.4	333.	4.	
305.0	2968857.	0.	.12	195904.	307849.	8.7	378.	5.	
315.0	2968857.	0.	.26	408227.	641499.	18.2	442.	8.	
O TRIGGER									
320.6	2968857.	0.	.39	624881.	981955.	27.9	490.	10.	
325.0	2968857.	0.	.52	935991.	1213743.	38.9	535.	11.	
334.0	2968857.	0.	1.03	1860742.	2412635.	77.3	654.	15.	
343.0	2968857.	0.	2.08	3773434.	4892294.	156.8	816.	20.	
352.0	2968857.	0.	3.69	6812082.	8572898.	284.0	1016.	23.	
361.0	2968857.	0.	4.77	9194862.	10759492.	387.8	1219.	21.	
370.0	2968857.	0.	4.79	9624631.	10453471.	411.1	1381.	15.	
379.0	2968857.	0.	4.50	9241359.	9632390.	394.0	1492.	10.	
388.0	2968857.	0.	4.03	8400674.	8512157.	352.3	1563.	6.	
397.0	2968857.	0.	3.38	7270493.	6912885.	303.9	1606.	4.	
406.0	2968857.	0.	2.77	6238645.	5350673.	267.6	1632.	2.	
415.0	2968857.	0.	2.39	5646013.	4294754.	250.2	1649.	2.	
424.0	2968857.	0.	2.26	5502299.	3821524.	246.6	1661.	1.	
433.0	2968857.	0.	2.25	5576285.	3675786.	248.9	1670.	1.	
442.0	2968857.	0.	2.25	5672416.	3547018.	253.6	1676.	1.	
451.0	2968857.	0.	2.19	5525414.	3449035.	256.2	1681.	0.	
RZ TRIGGER									
459.4	2968857.	0.	2.07	5182648.	3281525.	253.4	1684.	0.	
460.0	2968857.	0.	2.06	5175415.	3276819.	253.1	1684.	0.	
469.0	2968857.	0.	1.78	4459050.	2823252.	218.0	1686.	0.	
478.0	2968857.	0.	1.35	3385475.	2143517.	165.5	1688.	0.	
487.0	2968857.	0.	1.04	2598524.	1645258.	127.1	1689.	0.	
496.0	2968857.	0.	.88	2217920.	1404278.	108.4	1689.	0.	
505.0	2968857.	0.	.86	2163571.	1369867.	105.8	1690.	0.	
514.0	2968857.	0.	.92	2298517.	1455309.	112.4	1690.	0.	

ORIGINAL PAGE IS
OF POOR QUALITY

EDIN TRAJ. REPORT
STATE HISTORY

TIME	WEIGHT	THRUST	LD	FAC	LIFT	DFAG	DYN F	HEAT	HT FT.
523.0	2968857.	0.	.99	2480529.	1570550.	121.3	1691.	0.	
532.0	2968857.	0.	1.04	2605119.	1649434.	127.4	1691.	0.	
541.0	2968857.	0.	1.05	2641957.	1672758.	129.2	1691.	0.	
550.0	2968857.	0.	1.04	2618665.	1658010.	128.0	1692.	0.	
559.0	2968857.	0.	1.03	2579023.	1632911.	126.1	1692.	0.	
568.0	2968857.	0.	1.02	2551710.	1615618.	124.8	1693.	0.	
577.0	2968857.	0.	1.01	2543005.	1610106.	124.3	1693.	0.	
586.0	2968857.	0.	1.01	2545542.	1611713.	124.5	1693.	0.	
595.0	2968857.	0.	1.02	2549873.	1614455.	124.7	1693.	0.	
604.0	2968857.	0.	1.02	2551143.	1615259.	124.7	1694.	0.	
613.0	2968857.	0.	1.02	2549361.	1614131.	124.7	1694.	0.	
MIN. ALT.									
616.5	2968857.	0.	1.02	2548234.	1613417.	124.6	1694.	0.	

EDIN TRAJ. REPORT
STATE HISTORY

TIME	REL VEL	RL FPA	ALT	PANGE	REL AZ	GC LAT	LONG	TRANGE
165.1	8703.2	13.09	203545.	58.	90.94	28.36	280.52	58.
175.0	8586.9	11.58	221847.	71.	91.10	28.36	280.77	71.
185.0	8504.1	9.92	237792.	85.	91.27	28.35	281.03	85.
195.0	8442.4	8.17	251114.	99.	91.44	28.35	281.29	99.
205.0	8395.8	6.39	261781.	112.	91.60	28.34	281.55	112.
215.0	8361.5	4.57	269779.	126.	91.77	28.33	281.80	126.
225.0	8338.5	2.74	275099.	139.	91.93	28.33	282.06	139.
235.0	8326.2	.90	277740.	153.	92.09	28.32	282.32	153.
245.0	8324.1	-.94	277699.	166.	92.26	28.31	282.57	166.
255.0	8331.9	-2.79	274979.	179.	92.42	28.30	282.83	179.
265.0	8349.0	-4.62	269580.	193.	92.58	28.29	283.08	193.
275.0	8374.9	-6.44	261509.	206.	92.75	28.28	283.34	206.
285.0	8408.0	-8.23	250779.	220.	92.91	28.27	283.59	220.
295.0	8445.3	-9.99	237419.	233.	93.08	28.26	283.85	233.
305.0	8480.4	-11.67	221491.	247.	93.24	28.24	284.10	247.
315.0	8499.3	-13.24	203139.	260.	93.40	28.23	284.36	260.
O TPIGGER								
320.6	8492.4	-14.03	191824.	268.	93.49	28.22	284.50	268.
325.0	8477.2	-14.54	182689.	274.	93.56	28.22	284.61	274.
334.0	8380.3	-15.25	163087.	286.	93.71	28.21	284.84	286.
343.0	8113.0	-15.06	143486.	298.	93.85	28.19	285.06	298.
352.0	7525.4	-13.10	126049.	309.	94.20	28.18	285.27	309.
361.0	6616.7	-9.69	113380.	319.	97.70	28.16	285.46	319.
370.0	5615.1	-8.33	105017.	328.	105.65	28.13	285.63	328.
379.0	4677.4	-8.64	98165.	335.	115.82	28.09	285.76	335.
388.0	3832.0	-9.29	92188.	341.	127.33	28.04	285.86	341.
397.0	3129.3	-10.57	86794.	345.	139.78	27.98	285.93	345.
406.0	2588.7	-12.71	81619.	347.	152.89	27.92	285.97	347.
415.0	2194.3	-15.75	76337.	349.	166.73	27.87	285.99	349.
424.0	1889.9	-19.46	70773.	350.	182.18	27.82	286.00	350.
433.0	1630.3	-23.59	64952.	350.	200.51	27.78	286.99	350.
442.0	1403.4	-28.00	59011.	349.	222.84	27.76	286.97	349.
451.0	1205.8	-32.69	53094.	348.	249.96	27.74	286.95	348.
AC TPIGGER								
459.4	1052.8	-37.50	47641.	346.	279.43	27.74	286.92	346.
460.0	1043.7	-36.56	47285.	346.	279.43	27.74	286.92	346.
469.0	883.1	-23.17	42996.	345.	279.43	27.74	286.90	345.
478.0	733.9	-15.55	40652.	344.	279.43	27.74	286.88	344.
487.0	624.0	-14.85	39115.	343.	279.42	27.75	286.86	343.
496.0	560.2	-19.22	37595.	342.	279.41	27.75	286.94	342.
505.0	534.9	-25.07	35748.	341.	279.40	27.75	286.83	341.
514.0	530.4	-29.34	33547.	341.	279.38	27.75	286.82	341.

EDIN TRAJ. REPORT
STATE HISTORY

TIME	VEL	PL	FPA	ALT	PANSE	VEL	AZ	GC	LAT	LONG	TRANGE
523.0	528.5	-31.06		31136.	340.	279.37		27.75	285.80		340.
532.0	519.9	-30.92		28698.	339.	279.35		27.76	285.79		339.
541.0	503.8	-30.07		26359.	339.	279.34		27.76	285.78		339.
550.0	484.0	-29.40		24157.	338.	279.32		27.76	285.77		338.
559.0	464.5	-29.24		22072.	338.	279.30		27.76	285.76		338.
568.0	447.5	-29.49		20064.	337.	279.27		27.76	285.75		337.
577.0	433.1	-29.86		18104.	336.	279.25		27.76	285.73		336.
586.0	420.4	-30.17		16184.	336.	279.22		27.77	285.72		336.
595.0	408.5	-30.34		14306.	335.	279.19		27.77	285.71		335.
604.0	397.1	-30.44		12474.	335.	279.16		27.77	285.71		335.
613.0	386.0	-30.52		10687.	334.	279.13		27.77	285.70		334.
MIN. ALT.											
616.5	381.8	-30.56		10000.	334.	279.12		27.77	285.69		334.

EDIN TPAJ, REPORT
STATE HISTORY

TIME	MACH	ALPHA	BANK	VELI	GAMI	AZI
165.1	8.524	50.00	.00	10027.3	11.34	90.81
175.0	8.724	50.00	.00	9918.2	10.01	90.95
185.0	8.927	50.00	.00	9843.5	-8.56	91.09
195.0	9.110	50.00	.00	9788.2	7.04	91.24
205.0	9.268	50.00	.00	9746.9	5.50	91.38
215.0	9.400	50.00	.00	9716.7	3.93	91.52
225.0	9.433	50.00	.00	9696.4	2.36	91.66
235.0	9.419	50.00	.00	9685.4	.77	91.80
245.0	9.416	50.00	.00	9683.2	-.81	91.94
255.0	9.425	50.00	.00	9689.6	-2.40	92.08
265.0	9.382	50.00	.00	9704.0	-3.97	92.22
275.0	9.239	50.00	.00	9725.8	-5.54	92.36
285.0	9.066	50.00	.00	9753.5	-7.09	92.50
295.0	8.859	50.00	.00	9784.2	-8.61	92.64
305.0	8.609	50.00	.00	9811.8	-10.07	92.78
315.0	8.318	50.00	.00	9822.6	-11.43	92.92
O TRIGGER						
320.6	8.141	50.00	.00	9811.2	-12.11	93.00
325.0	8.008	50.00	.00	9792.8	-12.56	93.06
334.0	7.740	50.00	.00	9691.0	-13.15	93.18
343.0	7.588	50.00	.00	9423.6	-12.93	93.28
352.0	7.219	49.00	15.00	8844.7	-11.12	93.55
361.0	6.475	46.75	48.75	7942.2	-8.06	96.38
370.0	5.565	44.67	75.00	6914.8	-6.76	102.61
379.0	4.683	43.21	75.00	5912.3	-6.83	110.07
388.0	3.870	41.74	75.00	4964.0	-7.16	117.75
397.0	3.178	40.27	75.00	4122.3	-8.01	125.13
406.0	2.645	38.80	75.00	3412.3	-9.61	131.93
415.0	2.258	37.34	75.00	2820.8	-12.19	138.21
424.0	1.963	35.87	75.00	2284.5	-16.00	144.18
433.0	1.711	34.40	75.00	1752.8	-21.85	149.36
442.0	1.489	32.93	75.00	1233.1	-32.30	150.69
451.0	1.287	31.47	75.00	839.4	-50.88	131.07
AC TRIGGER						
459.4	1.115	30.09	75.00	842.1	-49.57	75.47
466.0	1.104	30.09	.00	825.7	-48.85	75.34
469.0	.921	30.09	.00	665.2	-31.49	76.43
478.0	.759	30.09	.00	693.3	-16.48	79.96
497.0	.641	30.09	.00	779.9	-11.82	82.56
496.0	.571	30.09	.00	854.6	-12.46	84.04
505.0	.541	30.09	.00	906.1	-14.49	84.82
514.0	.530	30.09	.00	935.4	-16.13	85.18

ORIGINAL PAGE IS
OF POOR QUALITY

EDIN TRAJ. REPORT
STATE HISTORY

TIME	MACH	ALPHA	BANK	VELI	GAMI	AZI
525.0	.522	30.09	.00	947.8	-16.72	85.34
532.0	.507	30.09	.00	952.2	-16.29	85.45
541.0	.486	30.09	.00	957.4	-15.29	85.60
550.0	.463	30.09	.00	966.9	-14.22	85.82
559.0	.440	30.09	.00	979.6	-13.39	86.06
566.0	.420	30.09	.00	992.9	-12.92	86.28
577.0	.404	30.09	.00	1005.0	-12.39	86.47
586.0	.389	30.09	.00	1015.4	-12.01	86.64
595.0	.376	30.09	.00	1024.7	-11.62	86.78
604.0	.363	30.09	.00	1033.3	-11.23	86.92
613.0	.351	30.09	.00	1041.6	-10.85	87.04

MIN. ALT.						
616.5	.347	30.09	.00	1044.7	-10.71	87.09

BASELINE TRAJECTORY FROM
LAUNCH SITE AT 7° LATITUDE



LAT 7°

PAGE 1

EDIN TRAJ. REPORT
STATE HISTORY

TIME	WEIGHT	THRUST	LD FAC	LIFT	DRAG	DYN P	HEAT	HT FT
LIFT-OFF								
.0	30286652.	39355913.	1.30	0.	0.	.0	0.	0.
4.0	29764501.	39363833.	1.32	0.	3262.	1.9	0.	0.
BEGIN TILT								
6.0	29503426.	39385391.	1.33	186.	7637.	4.3	0.	0.
10.0	28981276.	39439592.	1.36	3998.	22914.	12.8	0.	0.
END TILT								
16.0	28198050.	39576066.	1.40	5554.	65332.	35.9	0.	0.
20.0	27675900.	39704805.	1.43	43.	109041.	59.2	0.	0.
30.0	26370525.	40156948.	1.51	144.	297595.	147.8	0.	0.
40.0	25065149.	40772155.	1.60	420.	637182.	278.2	0.	0.
50.0	23759774.	41490768.	1.70	990.	1192986.	436.6	0.	0.
60.0	22454398.	42226890.	1.75	1907.	3033933.	587.8	0.	0.
THROTTLE END								
62.0	22190381.	42367764.	1.74	2187.	3656502.	613.1	0.	1.
Q MAXIMUM								
63.0	22066262.	38923215.	1.60	2284.	3720612.	620.7	0.	1.
Q MAXIMUM								
63.4	22010642.	34753437.	1.41	2330.	3771954.	627.6	0.	1.
70.0	21285969.	34572190.	1.45	2899.	3790797.	620.4	0.	1.
79.0	20241991.	39562673.	1.78	3729.	3506029.	606.0	0.	1.
88.0	19076579.	43635334.	2.13	4324.	2994874.	559.5	0.	2.
97.0	17901741.	43827223.	2.32	4471.	2250796.	449.1	0.	2.
106.0	16726903.	43934777.	2.53	4457.	1600933.	346.5	0.	3.
115.0	15552065.	43993037.	2.76	4204.	1124707.	259.0	0.	4.
124.0	14377228.	44023881.	3.01	3719.	757340.	185.9	0.	6.
133.0	13202390.	44039874.	3.30	3140.	502016.	130.8	0.	7.
142.0	12027552.	44048139.	3.63	2568.	335896.	91.6	0.	8.
151.0	10853198.	43645354.	4.00	2080.	232565.	64.8	0.	10.
160.0	9750060.	39167505.	4.00	1696.	167267.	46.6	0.	11.
165.2	9165381.	36797155.	4.00	1474.	135633.	37.8	0.	12.
THRUST EVENT								
165.2	6196524.	6732031.	1.08	539.	49576.	37.8	0.	12.
BEGIN MIN-H								
165.2	6196524.	6732963.	1.08	539.	49576.	37.8	0.	12.
169.0	6141574.	6732963.	1.10	0.	0.	.0	0.	12.

ORIGINAL PAGE IS
OF POOR QUALITY

EDIN TRAJ. REPORT
STATE HISTORY

TIME	WEIGHT	THRUST	LD FAC	LIFT	DRAG	DYN P	HEAT	HT FT
179.0	5997090.	6732963.	1.12	0.	0.	.0	0.	12.
189.0	5852606.	6732963.	1.15	0.	0.	.0	0.	9.
199.0	5708122.	6732963.	1.18	0.	0.	.0	0.	7.
209.0	5563637.	6732963.	1.21	0.	0.	.0	0.	6.
219.0	5419153.	6732963.	1.24	0.	0.	.0	0.	5.
229.0	5274669.	6732963.	1.28	0.	0.	.0	0.	4.
239.0	5130185.	6732963.	1.31	0.	0.	.0	0.	3.
249.0	4985701.	6732963.	1.35	0.	0.	.0	0.	3.
259.0	4841217.	6732963.	1.39	0.	0.	.0	0.	2.
269.0	4696732.	6732963.	1.43	0.	0.	.0	0.	2.
279.0	4552248.	6732963.	1.48	0.	0.	.0	0.	2.
289.0	4407764.	6732963.	1.53	0.	0.	.0	0.	2.
299.0	4263280.	6732963.	1.58	0.	0.	.0	0.	2.
309.0	4118796.	6732963.	1.63	0.	0.	.0	0.	2.
319.0	3974311.	6732963.	1.69	0.	0.	.0	0.	2.
329.0	3829827.	6732963.	1.76	0.	0.	.0	0.	2.
339.0	3685343.	6732963.	1.83	0.	0.	.0	0.	3.
349.0	3540859.	6732963.	1.90	0.	0.	.0	0.	3.
359.0	3396375.	6732963.	1.98	0.	0.	.0	0.	3.
369.0	3251891.	6732963.	2.07	0.	0.	.0	0.	4.
379.0	3107406.	6732963.	2.17	0.	0.	.0	0.	5.
389.0	2962922.	6732963.	2.27	0.	0.	.0	0.	5.
399.0	2818438.	6732963.	2.39	0.	0.	.0	0.	7.
409.0	2673954.	6732963.	2.52	0.	0.	.0	0.	8.
419.0	2529470.	6732963.	2.66	0.	0.	.0	0.	9.
429.0	2384986.	6732963.	2.82	0.	0.	.0	0.	11.
439.0	2240501.	6732963.	3.01	0.	0.	.0	0.	13.
449.0	2096017.	6732963.	3.21	0.	0.	.0	0.	13.
INJECTION								
451.5	2059211.	6732963.	3.27	0.	0.	.0	0.	13.

EDIN TRAJ. REPORT
STATE HISTORY

TIME	REL VEL	PL FPA	ALT	RANGE	REL AZ	GC LAT	LONG	TRANGE
LIFT-OFF								
.0	.0	.02	-1.	3.5283.27	6.95	-80.56	3.	
4.0	40.2	89.95	79.	3. -19.55	6.95	-80.56	3.	
BEGIN TILT								
6.0	61.5	89.95	180.	3. -27.70	6.95	-80.56	3.	
10.0	106.4	89.79	515.	3. 77.27	6.95	-80.56	3.	
END TILT								
16.0	180.2	89.84	1370.	3. 87.75	6.95	-80.56	3.	
20.0	234.0	87.87	2197.	3. 88.78	6.95	-80.56	3.	
30.0	386.8	83.98	5270.	3. 89.59	6.95	-80.56	3.	
40.0	570.3	78.24	9967.	3. 89.81	6.95	-80.56	3.	
50.0	791.2	71.24	16494.	3. 89.90	6.95	-80.56	4.	
60.0	1050.5	63.69	24959.	3. 89.95	6.95	-80.55	8.	
THRUSTLE BND								
62.0	1106.9	62.16	26879.	3. 89.96	6.95	-80.54	9.	
Q MAXIMUM								
63.0	1132.0	61.39	27865.	3. 89.96	6.95	-80.54	9.	
Q MAXIMUM								
63.4	1145.5	61.10	28247.	3. 89.96	6.95	-80.54	9.	
70.0	1279.8	55.92	35054.	3. 89.98	6.95	-80.53	13.	
79.0	1535.5	48.81	44989.	4. 90.01	6.95	-80.51	20.	
88.0	1918.0	42.17	55979.	6. 90.03	6.95	-80.48	31.	
97.0	2380.8	36.32	68129.	8. 90.04	6.95	-80.44	47.	
106.0	2923.8	31.27	81315.	11. 90.06	6.95	-80.38	66.	
115.0	3549.6	26.96	95396.	15. 90.08	6.95	-80.31	91.	
124.0	4262.4	23.30	110233.	20. 90.10	6.95	-80.23	120.	
133.0	5068.8	20.21	125705.	27. 90.12	6.95	-80.12	156.	
142.0	5978.8	17.60	141722.	34. 90.15	6.95	-79.99	200.	
151.0	7006.5	15.40	158230.	43. 90.18	6.95	-79.84	252.	
160.0	8093.8	13.58	175167.	54. 90.21	6.95	-79.66	312.	
165.2	8725.4	12.63	185060.	61. 90.22	6.95	-79.54	350.	
THRUST EVENT								
165.2	8725.4	12.63	185060.	61. 90.22	6.95	-79.54	350.	
BEGIN MIN-H								
165.2	8725.4	12.63	185060.	61. 90.22	6.95	-79.54	350.	
169.0	8832.0	12.11	192211.	66. 90.24	6.95	-79.45	359.	

ORIGINAL PAGE IS
OF POOR QUALITY

EDIN TRAJ. REPORT
STATE HISTORY

TIME	REL VEL	PL FPA	ALT	RANGE	REL AZ	GC LAT	LONG	TRANGE
179.0	9122.6	10.79	210011.	81.	90.28	6.95	-79.21	382.
189.0	9428.2	9.56	226379.	95.	90.32	6.95	-78.96	407.
199.0	9748.6	8.42	241348.	111.	90.36	6.95	-78.71	432.
209.0	10084.0	7.37	254949.	127.	90.40	6.95	-78.44	457.
219.0	10434.4	6.39	267217.	143.	90.45	6.94	-78.16	484.
229.0	10799.9	5.49	278188.	160.	90.49	6.94	-77.87	511.
239.0	11180.8	4.67	287900.	178.	90.54	6.94	-77.57	539.
249.0	11577.4	3.91	296392.	197.	90.58	6.94	-77.27	568.
259.0	11990.1	3.23	303710.	216.	90.63	6.93	-76.96	598.
269.0	12419.3	2.60	309897.	235.	90.68	6.93	-76.64	629.
279.0	12865.5	2.04	315004.	256.	90.73	6.92	-76.32	662.
289.0	13329.5	1.54	319083.	277.	90.78	6.92	-75.99	696.
299.0	13812.0	1.10	322191.	299.	90.83	6.91	-75.65	732.
309.0	14313.9	.71	324387.	322.	90.89	6.91	-75.31	770.
319.0	14836.1	.37	325739.	345.	90.95	6.90	-74.97	811.
329.0	15379.8	.08	326317.	370.	91.00	6.90	-74.63	854.
339.0	15946.4	-.16	326197.	395.	91.06	6.89	-74.29	901.
349.0	16537.4	-.35	325464.	421.	91.12	6.88	-73.94	952.
359.0	17154.5	-.50	324207.	448.	91.18	6.87	-73.60	1008.
369.0	17799.6	-.60	322527.	477.	91.25	6.86	-73.25	1071.
379.0	18475.2	-.65	320532.	506.	91.31	6.85	-72.90	1144.
389.0	19183.8	-.67	318341.	537.	91.38	6.84	-72.55	1229.
399.0	19928.4	-.64	316085.	568.	91.45	6.82	-72.20	1334.
409.0	20712.8	-.58	313909.	601.	91.53	6.81	-71.84	1470.
419.0	21541.0	-.47	311972.	635.	91.60	6.79	-71.49	1663.
429.0	22418.1	-.32	310452.	671.	91.68	6.78	-71.13	1980.
439.0	23350.1	-.13	309550.	708.	91.76	6.76	-70.78	2330.
449.0	24344.0	.10	309488.	746.	91.84	6.74	-70.44	2730.
INJECTION								
451.5	24608.1	.17	309635.	757.	91.86	6.73	-67.87	2730.

1
EDIN TRAJ. REPORT
STATE HISTORY

TIME	MACH	ALPHA	BANK	VELI	FPAI	AZI
LIFT-OFF						
.0	.000	.00	90.00	1514.6	.00	90.00
4.0	.035	.00	90.00	1515.2	1.52	90.00
BEGIN TILT						
6.0	.054	.02	.99	1515.9	2.32	90.00
10.0	.094	.18	.13	1518.8	4.02	90.00
END TILT						
16.0	.159	.09	.26	1529.0	6.77	89.99
20.0	.207	.00	90.00	1541.3	8.73	89.99
30.0	.346	.00	90.00	1602.4	13.89	89.99
40.0	.517	.00	90.00	1724.5	18.89	89.99
50.0	.733	.00	90.00	1922.3	22.94	89.99
60.0	1.008	.00	90.00	2194.4	25.41	89.99
THRUSTLE BND						
62.0	1.071	.00	90.00	2256.8	25.70	89.99
Q MAXIMUM						
63.0	1.100	.00	90.00	2285.9	25.77	89.99
Q MAXIMUM						
63.4	1.116	.00	90.00	2300.4	25.84	89.99
70.0	1.288	.00	90.00	2473.0	25.38	89.99
79.0	1.613	.00	90.00	2780.6	24.55	90.00
88.0	2.047	.00	90.00	3209.8	23.65	90.01
97.0	2.484	.00	90.00	3715.8	22.30	90.02
106.0	2.988	.01	90.00	4296.6	20.68	90.04
115.0	3.568	.01	90.00	4954.1	18.95	90.05
124.0	4.191	.01	90.00	5692.8	17.23	90.07
133.0	4.865	.01	90.00	6520.1	15.58	90.09
142.0	5.605	.01	90.00	7446.7	14.05	90.12
151.0	6.467	.01	90.00	8487.5	12.67	90.14
160.0	7.567	.02	90.00	9585.2	11.42	90.17
165.2	8.272	.02	90.00	10221.9	10.76	90.19
THRUST EVENT						
165.2	8.272	.02	90.00	10221.9	10.76	90.19
BEGIN MIN-H						
165.2	8.272	9.62	90.00	10221.9	10.76	90.19
169.0	.000	9.82	90.00	10331.5	10.33	90.20

EDIN TRAJ. REPORT
STATE HISTORY

TIME	MACH	ALPHA	BANK	VELI	FPRI	AZI
179.0	.000	10.28	90.00	10629.2	9.25	90.24
189.0	.000	10.68	90.00	10940.9	8.23	90.27
199.0	.000	11.02	90.00	11266.4	7.28	90.31
209.0	.000	11.31	90.00	11606.1	6.40	90.35
219.0	.000	11.53	90.00	11960.0	5.57	90.39
229.0	.000	11.71	90.00	12328.5	4.81	90.43
239.0	.000	11.83	90.00	12711.8	4.10	90.47
249.0	.000	11.90	90.00	13110.3	3.45	90.52
259.0	.000	11.92	90.00	13524.5	2.86	90.56
269.0	.000	11.90	90.00	13954.9	2.32	90.61
279.0	.000	11.84	90.00	14402.1	1.82	90.65
289.0	.000	11.73	90.00	14866.7	1.38	90.70
299.0	.000	11.59	90.00	15349.7	.99	90.75
309.0	.000	11.40	90.00	15851.8	.64	90.80
319.0	.000	11.19	90.00	16374.2	.33	90.86
329.0	.000	10.93	90.00	16918.0	.07	90.91
339.0	.000	10.65	90.00	17484.6	-.14	90.97
349.0	.000	10.33	90.00	18075.5	-.32	91.03
359.0	.000	9.99	90.00	18692.5	-.45	91.09
369.0	.000	9.62	90.00	19337.5	-.55	91.15
379.0	.000	9.22	90.00	20012.9	-.60	91.21
389.0	.000	8.80	90.00	20721.3	-.62	91.28
399.0	.000	8.35	90.00	21465.8	-.60	91.35
409.0	.000	7.88	90.00	22250.0	-.54	91.42
419.0	.000	7.39	90.00	23078.1	-.44	91.49
429.0	.000	6.88	90.00	23955.2	-.30	91.57
439.0	.000	6.36	90.00	24887.1	-.12	91.65
449.0	.000	5.81	90.00	25880.9	.10	91.73
INJECTION						
451.5	.000	5.67	90.00	26145.1	.16	91.75

G. Launey and W. Richards
Engineering Analysis Division

The Launch Analysis Section of the Engineering Analysis Division has initiated a study to determine the requirements for a two stage reusable ballistic entry launch vehicle to deliver the SPS into a 50 x 270 nautical mile (92.6 x 500 KM) insertion orbit. The vehicles were sized to deliver one and two million pound payloads into the insertion orbit when launched due east from ETR (Eastern Test Range). The performance capability of these vehicles was then determined when launched due east from a launch site latitude of 7 degrees.

All trajectories for this analysis were computed using a 3 degree-of-freedom trajectory program integrating the equations of motion of a particle moving over a rotating oblate spheroid planet under the influence of gravity, thrust, and aerodynamic forces. During first stage flight, the vehicle flew a vertical rise for 16 seconds and then pitched over a constant inertial pitch rate for 10 seconds. The vehicle then flew a gravity turn trajectory to staging. A 4 second coast period was allowed for stage separation. During second stage flight the vehicle was flown using a near optimum linear-tangent steering law to injection. The second stage flight used an exoatmospheric simulation.

All vehicle stages were sized using a set of weight scaling equations. The coefficients for these weight scaling equations were derived from Saturn V weight and geometry data obtained from Mr. W. Heineman of the Spacecraft Design Division. The S-IC stage weight and geometry data was used to generate weight scaling coefficients for body structure and miscellaneous item weights for the booster stages. The S-II stage data was used for the second stage body structure and miscellaneous item weights. The entry thermal protection and recovery system weight coefficients for both stages were obtained from Sigma Corporation. The rocket engine propulsion system weight scaling and performance data was obtained from Mr. M. F. Lausten of the Propulsion and Power Division. Saturn V aerodynamic data was used for all configurations. The reference areas used in conjunction with the aerodynamic data were calculated based on the cross sectional area of the base diameter of the vehicles investigated in this analysis.

The stage propellant tanks and skirts are constructed of the same aluminum alloy used on the Saturn V S-IC and S-II stages. The exposed surfaces of these tanks and skirts are coated with a super Koropon primer film to protect the aluminum material from salt water as recommended by Mr. Don Medlock of Structures and Mechanics Division.

The recovery system includes a parachute/retrorocket combination used to decelerate the stages to a terminal velocity of 150 fps (45.7 MPS)

In this analysis the retrorockets were used to terminate the final velocity of 150 fps (45.7 mps).

The vehicles investigated all used a LOX/LH₂ propellant second stage with high chamber pressure (Pc = 4000 psia) staged combustion cycle engines. Two booster classes were used. The first class used LOX/RP-1 propellant with high chamber pressure (Pc = 4000 psia) staged combustion cycle engines. The second booster class had LOX/propane for propellant and used lower chamber pressure (Pc = 3000 psia) gas generator cycle engines.

The groundrules used for sizing the vehicles are summarized in figure VI-B-4-1. In addition to a 20 percent contingency that was added to the vehicle stage dry weights for uncertainty and vehicle weight growth, a 20 percent increase was added to the tank weights for slapdown loads and reusability considerations. The dry weight contingency on the booster stages was assumed to include the preignition and thrust buildup propellant of the second stages.

Aerodynamic and propulsive data bases are presented in figures VI-B-4-2 through VI-B-4-4 respectively. Figures VI-B-4-5 through 22 present the major and detailed weight breakdowns for the launch system. Figure VI-B-4-23 outlines the payload changes expected for vehicles launched from 28.5 degrees and 7 degrees. Figure VI-B-4-24 outlines proposed future work for the SPS system.

Questions concerning the results herein should be addressed to Mr. Gerald Launey and Mr. William Richards at extension 6258.

- REUSABLE BALLISTIC ENTRY STAGES
- SATURN V (S-IC AND SII) WEIGHT AND GEOMETRY TECHNOLOGY OBTAINED FROM W. HEINEMAN OF EW USED FOR STRUCTURE AND MISCELLANEOUS WEIGHT SCALING
- 20 PCT PROPELLANT TANK "BEEF UP" FOR WATER IMPACT AND REUSABILITY
- 20 PCT DRY WEIGHT CONTINGENCY ADDED ON BOTH STAGES
- PROPULSION SYSTEM WEIGHTS AND PERFORMANCE DATA FROM EP FOR ADVANCED ENGINES
- LOX/RP-1 AND LOX/C₃H₈ PROPELLANT FOR BOOSTER STAGES
- LOX/LH₂ PROPELLANT IN SECOND STAGE
- 950 PSF MAX Q CONSTRAINT (WHERE REQUIRED)
- 4 g MAXIMUM ACCELERATION LIMIT
- 1 AND 2 MILLION LB PAYLOAD VEHICLES (INCLUDING SHROUD)
- 50 FT PAYLOAD SHROUD DIAMETER
- DUE EAST LAUNCH FROM ETR INTO A 50 X 270 N.MI. INSERTION ORBIT
- ON-ORBIT AND RETRO PROPULSION SYSTEM AND PROPELLANT INCLUDED IN PAYLOAD
- BOOSTER F/W = 1.4; SECOND STAGE F/W = 1.1
- SATURN V LAUNCH VEHICLE AERODYNAMIC DATA
- FPR PROPELLANT CALCULATED BASED ON RESERVING 0.75% OF TOTAL IDEAL VELOCITY

FIGURE VI-B-4-1.- PRELIMINARY HLLV SIZING GROUND RULES

VI-B-4-4

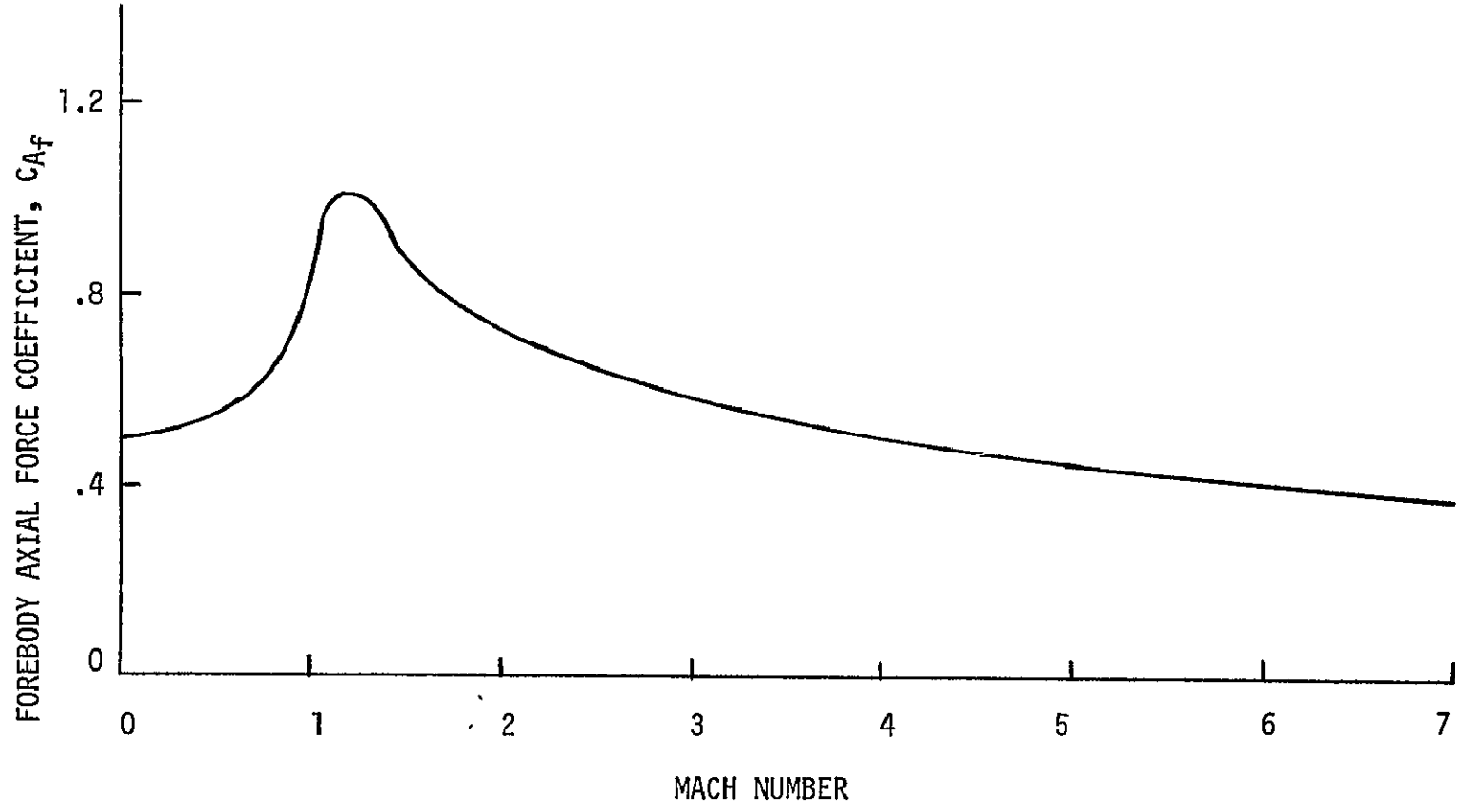


FIGURE VI-B-4-2.- FOREBODY AXIAL FORCE COEFFICIENT VERSUS MACH NUMBER

VI-B-4-5

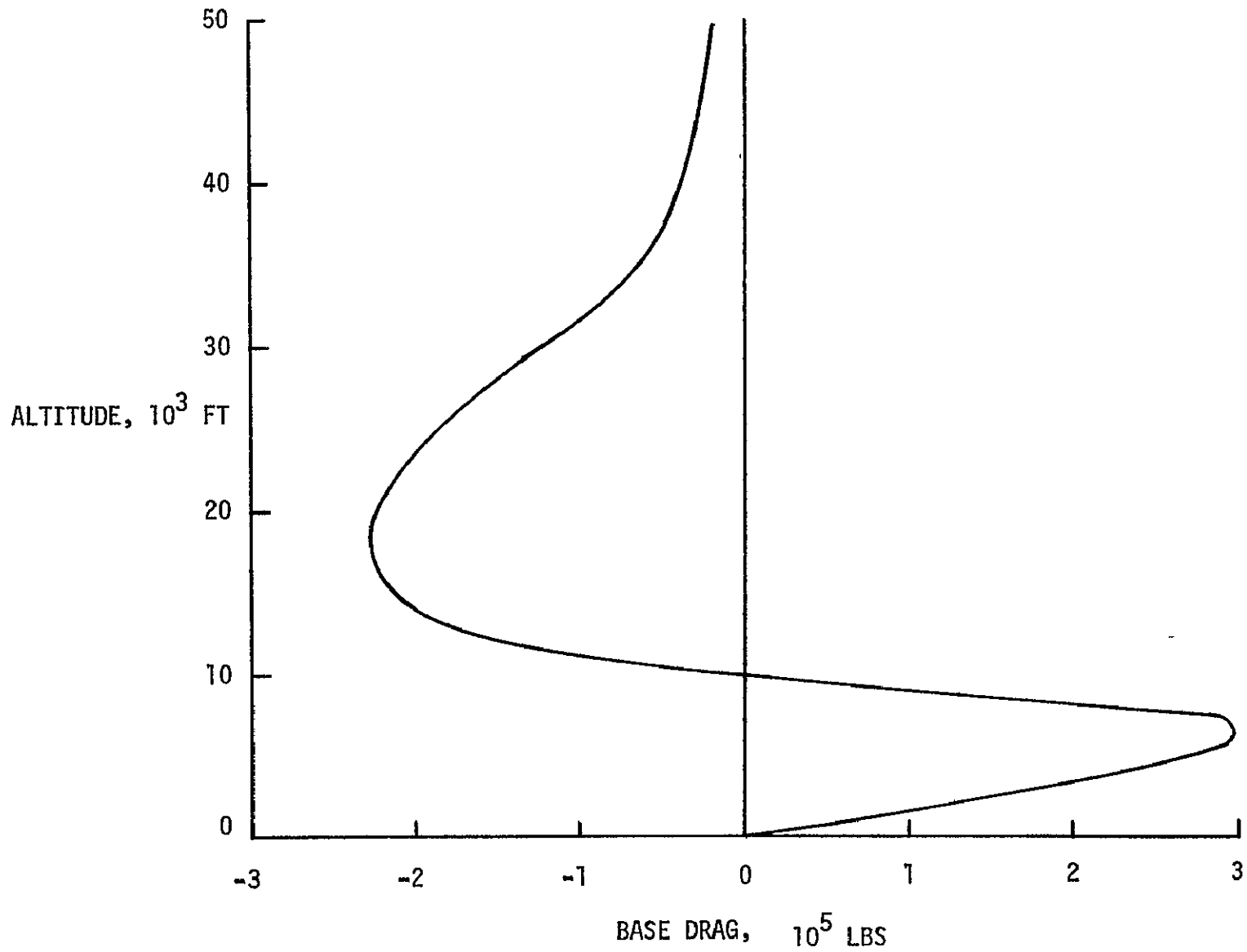


FIGURE VI-B-4-3.- ALTITUDE VERSUS BASE DRAG

VI-B-4-6

PARAMETER	STAGE I	STAGE I	STAGE II
PROPELLANT	LOX/RP-1	LOX/C ₃ H ₈	LOX/LH ₂
MIXTURE RATIO (O/F)	2.60	2.68	6.0
CHAMBER PRESSURE (P _c), PSIA	4,000	3,000	4,000
ENGINE OPERATION CYCLE	STAGED COMBUSTION	GAS GENERATOR	STAGED COMBUSTION
EXPANSION RATIO (ϵ), A _e /A _t	50	40	200
VACUUM SPECIFIC IMPULSE (I _v), SEC	344.0	337.5	466.0
SEA LEVEL SPECIFIC IMPULSE (I _s), SEC	309.78	301.49	--
FUEL DENSITY (ρ_f), LBS/CU FT	50.45	46.5	4.42
OXIDIZER DENSITY (ρ_o), LBS/CU FT	71.38	71.38	71.38
FUEL STORAGE TEMP., DEG F	AMBIENT	-297	-420
OXIDIZER STORAGE TEMP., DEG F	-297	-297	-297

FIGURE VI-B-4-4.- ROCKET ENGINE PROPULSION SYSTEM PARAMETERS

VI-B-4-7

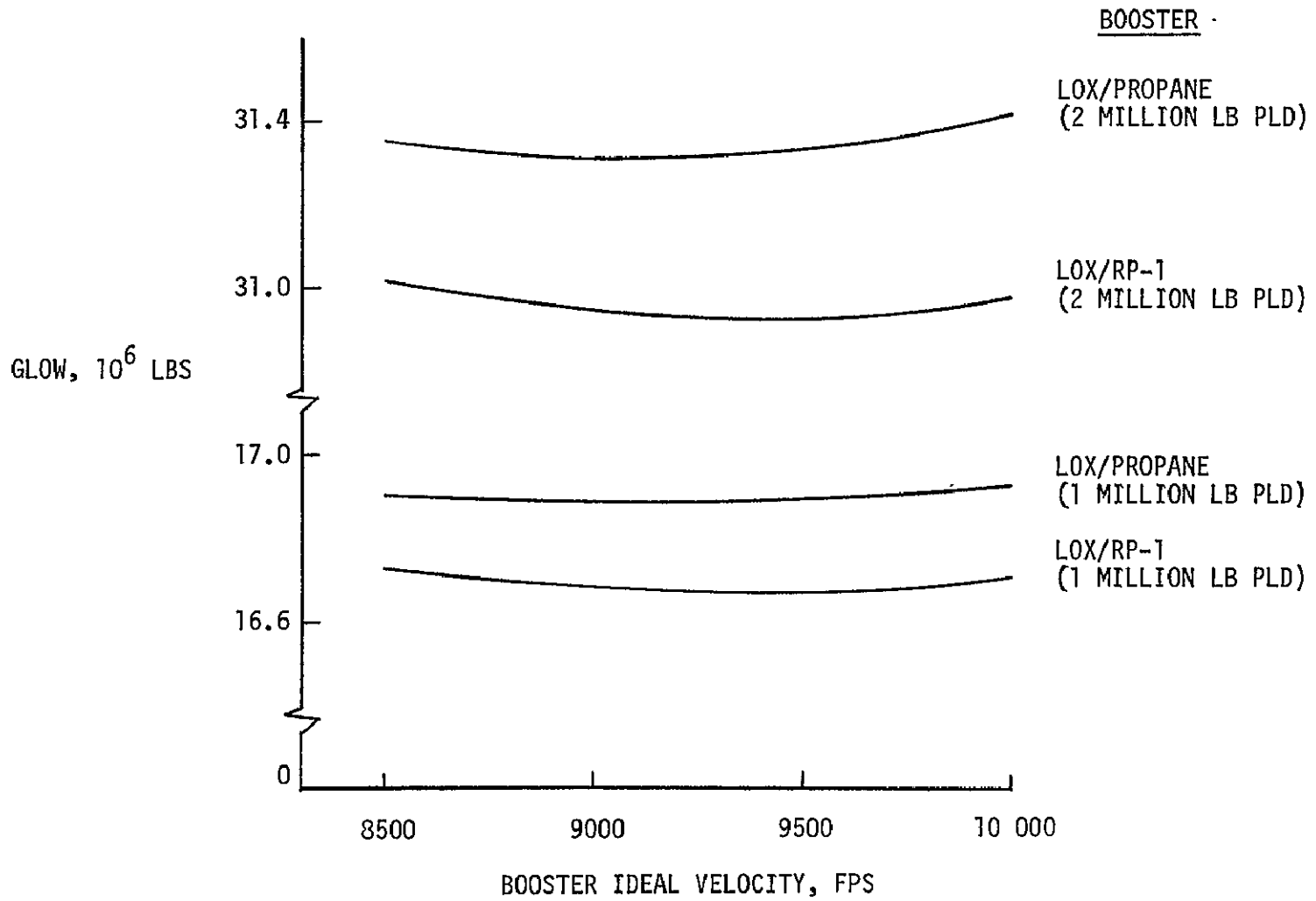


FIGURE VI-B-4-5.- GLOW VERSUS BOOSTER IDEAL VELOCITY

VI-B-4-8

(LOX/RP-1 BOOSTER) (LOX/LH ₂ SECOND STAGE)	1 MILLION LB PAYLOAD		2 MILLION LB PAYLOAD	
	POUNDS	METRIC TONS	POUNDS	METRIC TONS
GLOW (T/W = 1.4)	16,681,400	7,565.2	30,937,400	14,030.6
BLOW	(10,895,100)	(4,941.1)	(20,121,200)	(9,125.3)
MAINSTAGE PROPELLANT	9,793,200	4,441.4	18,160,100	8,235.9
INERT WEIGHT (LESS CONT.)	949,400	430.6	1,691,900	767.3
DRY WEIGHT CONTINGENCY	152,500*	69.1	269,200*	122.1
STAGE MASS FRACTION	0.90222		0.90595	
SSLOW (T/W = 1.1)	(4,786,300)	(2,170.7)	(8,816,200)	(3,998.3)
MAINSTAGE PROPELLANT	4,271,900	1,937.4	7,935,200	3,598.7
INERT WEIGHT (LESS CONT.)	439,700	199.4	754,800	342.3
DRY WEIGHT CONTINGENCY	74,700	33.9	126,200	57.3
STAGE MASS FRACTION	0.89255		0.90008	
PAYLOAD	1,000,000	453.5	2,000,000	907.0
BOOSTER IDEAL VELOCITY (FPS)	9,500		9,500	
MAX DYNAMIC PRESSURE (PSF)	810		892	
MAX DYNAMIC PRESSURE TIME (SEC)	70		70	
*INCLUDES SECOND STAGE PRE-IGNITION AND THRUST BUILDUP PROPELLANT				

FIGURE VI-B-4-6.- REUSABLE TWO STAGE BALLISTIC ENTRY LAUNCH VEHICLE SUMMARY WEIGHT BREAKDOWNS

VI-B-4-9

(LOX/C ₃ H ₈ BOOSTER) (LOX/LH ₂ SECOND STAGE)	1 MILLION LB PAYLOAD		2 MILLION LB PAYLOAD	
	POUNDS	METRIC TONS	POUNDS	METRIC TONS
GLOW (T/W = 1.4)	16,888,600	7659.2	31,317,900	14,203.1
BLOW	(10,794,600)	(4895.5)	(19,939,700)	(9,042.9)
MAINSTAGE PROPELLANT	9,724,500	4410.2	18,031,300	8,177.5
INERT WEIGHT (LESS CONT.)	921,300	417.8	1,645,100	746.0
DRY WEIGHT CONTINGENCY	148,800*	67.5	263,300*	119.4
STAGE MASS FRACTION	0.90444		0.90792	
SSLOW (T/W = 1.1)	(5,094,000)	(2310.2)	(9,378,200)	(4,253.2)
MAINSTAGE PROPELLANT	4,553,900	2065.3	8,450,000	3,832.2
INERT WEIGHT (LESS CONT.)	461,900	209.5	795,500	360.8
DRY WEIGHT CONTINGENCY	78,200	35.4	132,700	60.2
STAGE MASS FRACTION	0.89397		0.90103	
PAYLOAD	(1,000,000)	453.5	(2,000,000)	907.0
BOOSTER IDEAL VELOCITY (FPS)	9,000		9,000	
MAX DYNAMIC PRESSURE (PSF)	824		921	
MAX DYNAMIC PRESSURE TIME (SEC)	70		70	

*INCLUDES SECOND STAGE PRE-IGNITION AND THRUST
BUILDUP PROPELLANT

FIGURE VI-B-4-7.- REUSABLE TWO STAGE BALLISTIC ENTRY LAUNCH VEHICLE SUMMARY WEIGHT BREAKDOWNS

VI-B-4-10

LOX/RP-1 BOOSTER LOX/LH ₂ SECOND STAGE	1 MILLION LB PAYLOAD		2 MILLION LB PAYLOAD	
	STAGE I	STAGE II	STAGE I	STAGE II
NUMBER OF ENGINES	12	6	24	12
VACUUM THRUST/ENGINE (LBS)	2,161,110	1,060,810	2,004,010	991,480
VACUUM ISP (SEC)	344.0	466.0	344.0	466.0
S.L. THRUST/ENGINE (LBS)	1,946,160	--	1,804,680	--
S.L. ISP (SEC)	309.78	--	309.78	--
EXIT AREA/ENGINE (SQ. IN.)	14,572	26,785	13,513	25,035
ENGINE WEIGHT (LBS)	24,012	14,144	22,267	13,220

FIGURE VI-B-4-8.- ROCKET ENGINE DATA FOR LOX/RP-1 BOOSTER VEHICLES

VI-B-4-11

LOX/C ₃ H ₈ BOOSTER LOX/LH ₂ SECOND STAGE	1 MILLION LB PAYLOAD		2 MILLION LB PAYLOAD	
	STAGE I	STAGE II	STAGE I	STAGE II
NUMBER OF ENGINES	12	6	24	12
VACUUM THRUST/ENGINES (LBS)	2,205,660	1,117,230	2,045,070	1,042,995
VACUUM ISP (SEC)	337.5	466.	337.5	466
S.L. THRUST/ENGINES (LBS)	1,970,330	-	1,826,875	-
S.L. ISP (SEC)	301.49	-	301.49	-
EXIT AREA/ENGINE(SQ. IN.)	15,954	28,210	14,792	26,336
ENGINE WEIGHT (LBS)	22,057	14,896	20,451	13,907

FIGURE VI-B-4-9.- ROCKET ENGINE DATA FOR LOX/PROPANE BOOSTER VEHICLES

VI-B-4-12

	LOX/RP-1		LOX/C ₃ H ₈	
	1 MILLION	2 MILLION	1 MILLION	2 MILLION
IDEAL STAGING VELOCITY (FPS)	9,500	9,500	9,000	9,000
STAGING FLIGHT PATH ANGLE (DEG)	20.18	18.75	22.93	20.27
STAGING VELOCITY (FPS)	6,023	6,261	5,579	5,839
ALTITUDE (FT)	142,345	142,648	135,496	133,208
STAGING DYNAMIC PRESSURE (PSF)	90.6	96.7	103.7	125.2
STAGING RANGE(N.MI.)	33.05	35.53	28.45	31.20
STAGING ACCELERATION (g's)	3.75	3.75	3.67	3.68
BOOSTER BURN TIME (SEC)	129.90	129.89	124.00	123.99
BOOSTER VACUUM IMPACT RANGE (N.MI.)	206	214	187	193
MAXIMUM DYNAMIC PRESSURE (PSF)	810	892	824	921
INJECTION ACCELERATION (g's)	4.0	4.0	4.0	4.0
APOGEE ALTITUDE (N.MI.)*		270.0		
PERIGEE ALTITUDE (N.MI.)*		50.0		
INJECTION ALTITUDE (N.MI.)*		50.5		

*ABOVE EQUATORIAL RADIUS

FIGURE VI-B-4-10.- LAUNCH VEHICLE TRAJECTORY PARAMETER SUMMARY

FIGURE VI-B-4-11.- LOX/RP-1 BOOSTER VEHICLE
(1 MILLION LB PAYLOAD)

* * * * * LIQUID ROCKET BOOSTER WEIGHT STATEMENT * * * * *

BODY STRUCTURE		331633.	
FWD SKIRT	42590.		
LOX TANK	45674.		
FUEL TANK	52582.		
THRUST STRUCTURE	142722.		
BASE SKIRT	18660.		
THERMAL PROTECTION		45227.	
ENTRY HEAT SHIELD	21942.		
FLAME SHIELD	19433.		
INTER-TANK INSULATION	3656.		
BODY ENTRY COVER PANELS	209.		
ELECTRICAL POWER SYSTEM		1230.	
INSTRUMENTATION		4428.	
PROPULSION		335808.	
URK ENGINES	266148.		
CONTROL SYSTEM	36625.		
FUEL SYSTEM	0.		
OXIDIZER SYSTEM	10835.		
MISCELLANEOUS ITEMS		1166.	
SEPARATION AND RECOVERY		43374.	
SEPARATION SYSTEM	4666.		
PARACHUTES	21399.		
FLUTATION SYSTEM	387.		
RECOVERY AIDS	384.		
FITTING AND SUPPORTS	737.		
RETRONUTERS	15803.		
CONTINGENCY		152574.*	
STAGE DRY WEIGHT			762808.
RESIDUAL AND RESERVE PROP		186529.	
FUEL DRAIN	11461.		
LOX TANK VAPORS	15062.		
FUEL TANK VAPORS AND/OR GASES	1024.		
TRAPPED FROST	3351.		
TRAPPED FUEL (TANK)	46573.		
TRAPPED LOX (TANK)	74460.		
TRAPPED PROPELLANT (ENGINES)	34578.		
STAGE INERT WEIGHT			1101971.
MAINSTAGE PROPELLANT		9793159.	
BOOSTER LIFTOFF WEIGHT			10695130.
TOTAL LOX WEIGHT		7436518.**	
TOTAL FUEL WEIGHT		2846143.**	

*INCLUDES 40,500 LBS SECOND STAGE PRE-IGNITION AND THRUST BUILDUP PROPELLANT

**INCLUDES BOOSTER PRE-IGNITION AND THRUST PROPELLANT

FIGURE VI-B-4-12.- LOX/RP-1 BOOSTER VEHICLE
(1 MILLION LB PAYLOAD)

LAUNCH VEHICLE SECOND STAGE WEIGHT STATEMENT

BODY STRUCTURE		232724.	
END SKIRT	11929.		
FUEL TANK	111957.		
LOX TANK	40793.		
THRUST STRUCTURE	36490.		
AFI SKIRT	23192.		
BASE SKIRT	6368.		
AERODYNAMIC FAIRINGS		400.	
THERMAL PROTECTION		21053.	
ENTRY HEAT SHIELD	16559.		
FLAME SHIELD	1667.		
INTER-TANK INSULATION	2013.		
BODY ENTRY COVER PANELS	214.		
ELECTRICAL POWER SYSTEM		729.	
INSTRUMENTATION		3915.	
PROPULSION		93103.	
DRY ENGINES	64064.		
CONTROL SYSTEM	7490.		
FUEL SYSTEM	749.		
VALVE SYSTEM	0.		
MISCELLANEOUS ITEMS		1252.	
SEPARATION AND RECOVERY		19211.	
SEPARATION SYSTEM	163.		
PARACHUTES	10519.		
FLUTATION SYSTEM	190.		
RECOVERY AIDS	186.		
FITTING AND SUPPORTS	362.		
RETRU HOULRS	7768.		
CONTINGENCY		74578.	
STAGE DRY WEIGHT			376692.
RESIDUAL AND RESERVE PROP		60007.	
FUEL BIAS	7645.		
LOX TANK VAPORS	22767.		
FUEL TANK VAPORS AND/OR GASES	5923.		
TRAPPED FUEL (TANK)	11040.		
TRAPPED LOX (TANK)	12643.		
TRAPPED PROPELLANT (ENGINES)	6769.		
STAGE INERT WEIGHT			614278.
MAINSTAGE PROPELLANT		4271945.	
FLIGHT PERFORMANCE RESERVES	22588.		
IMPULSIVE PROPELLANT	4249357.		
UPPER STAGE LIFTOFF WEIGHT			4706223.
TOTAL FUEL WEIGHT		637885.*	
TOTAL LOX WEIGHT		3741370.*	

*INCLUDES PRE-IGNITION AND THRUST BUILDUP PROPELLANT

FIGURE VI-B-4-13.- LOX/RP-1 BOOSTER VEHICLE
(1 MILLION LB PAYLOAD)

* * * * *
* * * * * LIQUID ROCKET BOOSTER GEOMETRY SUMMARY * * * * *
* * * * *

LOX TANK VOLUME	107187.
FULL TANK VOLUME	58160.
AFT DIAMETER	70.00
FWD DIAMETER	60.00
TOTAL STAGE LENGTH	115.45
BASE SKIRT LENGTH	20.00
AFT SKIRT LENGTH	32.40
FUEL TANK AFT BKD LENGTH	22.96
FUEL TANK BARREL LENGTH	17.53
FUEL TANK FWD BKD LENGTH	.00
INTER-TANK CLEARANCE	.00
LOX TANK AFT BKD LENGTH	22.96
LOX TANK BARREL LENGTH	22.55
LOX TANK FWD BKD LENGTH	22.98
FWD SKIRT LENGTH	22.95
INTERSTAGE LENGTH	.00
INTERSTAGE AFT DIAMETER	60.00
INTERSTAGE FWD DIAMETER	50.00

* * * * *
* * * * * LAUNCH VEHICLE SECOND STAGE GEOMETRY SUMMARY * * * * *
* * * * *

FUEL TANK VOLUME	147400.
LOX TANK VOLUME	53707.
AFT DIAMETER	60.00
FWD DIAMETER	50.00
TOTAL STAGE LENGTH	140.54
BASE SKIRT LENGTH	15.00
AFT SKIRT LENGTH	29.70
LOX TANK AFT BKD LENGTH	19.45
LOX TANK BARREL LENGTH	14.35
LOX TANK FWD BKD LENGTH	19.45
INTER-TANK CLEARANCE	.00
FUEL TANK AFT BKD LENGTH	.00
FUEL TANK BARREL LENGTH	62.04
FUEL TANK FWD BKD LENGTH	19.45
FWD SKIRT LENGTH	19.45
INTERSTAGE LENGTH	.00
INTERSTAGE AFT DIAMETER	50.00
INTERSTAGE FWD DIAMETER	40.00

ORIGINAL PAGE IS
OF POOR QUALITY

FIGURE VI-B-4-14.-LOX/RP-1 BOOSTER VEHICLE
(2 MILLION LB PAYLOAD)

LIQUID ROCKET BOOSTER WEIGHT STATEMENT

BODY STRUCTURE		562271.	
FWD SKIRT	22543.		
LOX TANK	177416.		
FUEL TANK	97508.		
THRUST STRUCTURE	264644.		
BASE SKIRT	18060.		
THERMAL PROTECTION		45300.	
ENTRY HEAT SHIELD	21942.		
FLAME SHIELD	19433.		
INTER-TANK INSULATION	3050.		
BODY ENTRY COVER PANELS	283.		
ELECTRICAL POWER SYSTEM		1016.	
INSTRUMENTATION		4420.	
PROPULSION		639961.	
DRY ENGINES	534402.		
CONTROL SYSTEM	60297.		
FUEL SYSTEM	0.		
GAUZE SYSTEM	37262.		
MISCELLANEOUS ITEMS		1264.	
SEPERATION AND RECOVERY		73144.	
SEPERATION SYSTEM	4666.		
PARACHUTES	37057.		
FLUTATION SYSTEM	685.		
RECOVERY AIDS	670.		
FITTING AND SUPPORTS	1303.		
RETRONUTERS	27950.		
CONTINGENCY		265190.*	
STAGE DRY WEIGHT			1345971.
RESIDUAL AND RESERVE PROP		345900.	
FUEL BIAS	21252.		
LOX TANK VAPORS	2731.		
FUEL TANK VAPORS AND/OR GASES	1699.		
TRAPPED FROST	6210.		
TRAPPED FUEL (TANK)	66364.		
TRAPPED LOX (TANK)	138114.		
TRAPPED PROPELLANT (ENGINES)	64120.		
STAGE INERT WEIGHT			1961092.
MAINSTAGE PROPELLANT		18160119.	
BOOSTER LIFTOFF WEIGHT			20121211.
TOTAL LOX WEIGHT		13790100.**	
TOTAL FUEL WEIGHT		5277010.**	

*INCLUDES 75,700 LBS SECOND STAGE PRE-IGNITION AND THRUST BUILDUP PROPELLANT

**INCLUDES BOOSTER PRE-IGNITION AND THRUST BUILDUP PROPELLANT

FIGURE VI-B-4-15.- LOX/RP-1 BOOSTER VEHICLE
(2 MILLION LB PAYLOAD)

* * * * * LAUNCH VEHICLE SECOND STAGE WEIGHT STATEMENT * * * * *			
BOUY STRUCTURE			395448.
FWO SKIRT	11929.		
FUEL TANK	207969.		
LOX TANK	75780.		
THRUST STRUCTURE	68210.		
AFT SKIRT	23192.		
BASL SKIRT	8368.		
AERODYNAMIC FAIRINGS		900.	
THERMAL PROTECTION		21167.	
ENTRY HEAT SHIELD	10559.		
FLAME SHIELD	1667.		
INTER-TANK INSULATION	2613.		
BOUY ENTRY COVER PANELS	328.		
ELECTRICAL POWER SYSTEM		729.	
INSTRUMENTATION		3915.	
PROPULSION		174841.	
DRY ENGINES	158037.		
CONTROL SYSTEM	14001.		
FUEL SYSTEM	2203.		
OXIDIZER SYSTEM	0.		
MISCELLANEOUS ITEMS		1252.	
SEPERATION AND RECOVERY		32308.	
SEPERATION SYSTEM	183.		
PARACHUTES	17793.		
FLotation SYSTEM	322.		
RECOVERY AIDS	318.		
FITTING AND SUPPORTS	613.		
RETRU MOTERS	13140.		
CONTINGENCY		120124.	
STAGE DRY WEIGHT			630020.
RESIDUAL AND RESERVE PROP		124182.	
FUEL DRAIN	14200.		
LOX TANK VAPORS	42293.		
FUEL TANK VAPORS AND/OR GASES	11002.		
TRAPPED FUEL (TANK)	20508.		
TRAPPED LOX (TANK)	23487.		
TRAPPED PROPELLANT (ENGINES)	12091.		
STAGE INERT WEIGHT			880927.
MAINSTAGE PROPELLANT		7935246.	
FLIGHT PERFORMANCE RESERVES	42567.		
IMPULSIVE PROPELLANT	7892659.		
UPPER STAGE LIFTOFF WEIGHT			8816173.
TOTAL FUEL WEIGHT		1184924.*	
TOTAL LOX WEIGHT		6950216.*	

*INCLUDES PRE-IGNITION AND THRUST BUILDUP PROPELLANT

ORIGINAL PAGE IS
OF POOR QUALITY

FIGURE VI-B-4-16.- LOX/RP-1 BOOSTER VEHICLE
(2 MILLION LB PAYLOAD)

* * * * *
* LIQUID ROCKET BOOSTER GEOMETRY SUMMARY * * * * *
* * * * *

LOX TANK VOLUME		198765.
FUEL TANK VOLUME		107850.
AFT DIAMETER		70.00
FWD DIAMETER		60.00
TOTAL STAGE LENGTH		158.03
BASE SKIRT LENGTH	20.00	
AFT SKIRT LENGTH	32.40	
FUEL TANK AFT BKD LENGTH	22.98	
FUEL TANK BARREL LENGTH	32.50	
FUEL TANK FWD BKD LENGTH	.00	
INTER-TANK CLEARANCE	.00	
LOX TANK AFT BKD LENGTH	22.98	
LOX TANK BARREL LENGTH	50.15	
LOX TANK FWD BKD LENGTH	22.98	
FWD SKIRT LENGTH	22.98	
INTERSTAGE LENGTH	.00	
INTERSTAGE AFT DIAMETER	60.00	
INTERSTAGE FWD DIAMETER	50.00	

* * * * *
* LAUNCH VEHICLE SECOND STAGE GEOMETRY SUMMARY * * * * *
* * * * *

FULL TANK VOLUME		273807.
LOX TANK VOLUME		99770.
AFT DIAMETER		60.00
FWD DIAMETER		50.00
TOTAL STAGE LENGTH		213.13
BASE SKIRT LENGTH	15.00	
AFT SKIRT LENGTH	29.70	
LOX TANK AFT BKD LENGTH	19.45	
LOX TANK BARREL LENGTH	33.74	
LOX TANK FWD BKD LENGTH	19.45	
INTER-TANK CLEARANCE	.00	
FUEL TANK AFT BKD LENGTH	.00	
FUEL TANK BARREL LENGTH	115.25	
FUEL TANK FWD BKD LENGTH	19.45	
FWD SKIRT LENGTH	19.45	
INTERSTAGE LENGTH	.00	
INTERSTAGE AFT DIAMETER	50.00	
INTERSTAGE FWD DIAMETER	40.00	

FIGURE VI-B-4-17.- LOX/C₃H₈ BOOSTER VEHICLE
(1 MILLION LB PAYLOAD)

LIQUID ROCKET BOOSTER WEIGHT STATEMENT

BODY STRUCTURE		338708.
FWD SKIRT	22593.	
LOX TANK	95786.	
FUEL TANK	56605.	
THRUST STRUCTURE	145664.	
BASE SKIRT	18060.	
THERMAL PROTECTION		41581.
ENTRY HEAT SHIELD	21942.	
FLAME SHIELD	19433.	
INTER-TANK INSULATION	0.	
BODY ENTRY COVER PANELS	206.	
ELECTRICAL POWER SYSTEM		1243.
INSTRUMENTATION		4428.
PROPULSION		314498.
DRY ENGINES	264679.	
CONTROL SYSTEM	37584.	
FUEL SYSTEM	0.	
OXIDIZER SYSTEM	12235.	
MISCELLANEOUS ITEMS		1170.
SEPERATION AND RECOVERY		42413.
SEPERATION SYSTEM	4666.	
PARACHUTES	20868.	
FLOTATION SYSTEM	377.	
RECOVERY AIDS	373.	
FITTING AND SUPPORTS	718.	
RETRO MOTORS	15410.	
CONTINGENCY		148808.*
STAGE DRY WEIGHT		744041.
RESIDUAL AND RESERVE PROP		177210.
FUEL BIAS	11380.	
LOX TANK VAPORS	15080.	
FUEL TANK VAPORS AND/OR GASES	1103.	
TRAPPED FROST	3355.	
TRAPPED FUEL (TANK)	45257.	
TRAPPED LOX (TANK)	74567.	
TRAPPED PROPELLANT (ENGINES)	26468.	
STAGE INERT WEIGHT		1070059.
MAINSTAGE PROPELLANT		9724497.
BOOSTER LIFTOFF WEIGHT		10794556.
TOTAL LOX WEIGHT		7445195.**
TOTAL FUEL WEIGHT		2765738.**

*INCLUDES 42,600 LBS SECOND STAGE PRE-IGNITION AND THRUST BUILDUP PROPELLANT

**INCLUDES BOOSTER PRE-IGNITION AND THRUST BUILDUP PROPELLANT

FIGURE VI-B-4-18.- LOX/C₃H₈ BOOSTER VEHICLE
(1 MILLION LB PAYLOAD)

LAUNCH VEHICLE SECOND STAGE WEIGHT STATEMENT		
BODY STRUCTURE		244739.
FWD SKIRT	11929.	
FUEL TANK	119339.	
LOX TANK	43479.	
THRUST STRUCTURE	38431.	
AFT SKIRT	23192.	
BASE SKIRT	8368.	
AERODYNAMIC FAIRINGS		900.
THERMAL PROTECTION		21062.
ENTRY HEAT SHIELD	16559.	
FLAME SHIELD	1667.	
INTER-TANK INSULATION	2613.	
BODY ENTRY COVER PANELS	223.	
ELECTRICAL POWER SYSTEM		729.
INSTRUMENTATION		3915.
PROPULSION		98090.
DRY ENGINES	89378.	
CONTROL SYSTEM	7889.	
FUEL SYSTEM	823.	
OXIDIZER SYSTEM	0.	
MISCELLANEOUS ITEMS		1252.
SEPERATION AND RECOVERY		20126.
SEPERATION SYSTEM	183.	
PARACHUTES	11025.	
FLOTATION SYSTEM	199.	
RECOVERY AIDS	197.	
FITTING AND SUPPORTS	380.	
RETRO MOTORS	8142.	
CONTINGENCY		78163.
STAGE DRY WEIGHT		390813.
RESIDUAL AND RESERVE PROP		71124.
FUEL BIAS	8149.	
LOX TANK VAPORS	24266.	
FUEL TANK VAPORS AND/OR GASES	6313.	
TRAPPED FUEL (TANK)	11768.	
TRAPPED LOX (TANK)	13476.	
TRAPPED PROPELLANT (ENGINES)	7150.	
STAGE INERT WEIGHT		540099.
MAINSTAGE PROPELLANT		4553915.
FLIGHT PERFORMANCE RESERVES	22991.	
IMPULSIVE PROPELLANT	4530924.	
UPPER STAGE LIFTOFF WEIGHT		5094014.
TOTAL FUEL WEIGHT		679949.*
TOTAL LOX WEIGHT		3987746.*

*INCLUDES PRE-IGNITION AND THRUST BUILDUP PROPELLANT

FIGURE VI-B-4-19.- LOX/C₃H₈ BOOSTER VEHICLE
(1 MILLION LB PAYLOAD)

LIQUID ROCKET BOOSTER GEOMETRY SUMMARY

LOX TANK VOLUME 107312.
FUEL TANK VOLUME 62609.

AFT DIAMETER 70.00
FWD DIAMETER 60.00
TOTAL STAGE LENGTH 116.83
BASE SKIRT LENGTH 20.00
AFT SKIRT LENGTH 32.40
FUEL TANK AFT BKD LENGTH 22.98
FUEL TANK BARREL LENGTH 18.87
FUEL TANK FWD BKD LENGTH .00
INTERTANK CLEARANCE .00
LOX TANK AFT BKD LENGTH 22.98
LOX TANK BARREL LENGTH 22.59
LOX TANK FWD BKD LENGTH 22.98
FWD SKIRT LENGTH 22.98
INTERSTAGE LENGTH .00
INTERSTAGE AFT DIAMETER 60.00
INTERSTAGE FWD DIAMETER 50.00

LAUNCH VEHICLE SECOND STAGE GEOMETRY SUMMARY

FUEL TANK VOLUME 157120.
LOX TANK VOLUME 57244.

AFT DIAMETER 60.00
FWD DIAMETER 50.00
TOTAL STAGE LENGTH 146.11
BASE SKIRT LENGTH 15.00
AFT SKIRT LENGTH 29.70
LOX TANK AFT BKD LENGTH 19.45
LOX TANK BARREL LENGTH 15.84
LOX TANK FWD BKD LENGTH 19.45
INTERTANK CLEARANCE .00
FUEL TANK AFT BKD LENGTH .00
FUEL TANK BARREL LENGTH 66.13
FUEL TANK FWD BKD LENGTH 19.45
FWD SKIRT LENGTH 19.45
INTERSTAGE LENGTH .00
INTERSTAGE AFT DIAMETER 50.00
INTERSTAGE FWD DIAMETER 40.00

FIGURE VI-B-4-20.- LOX/C₃H₈ BOOSTER VEHICLE
(2 MILLION LB PAYLOAD)

LIQUID ROCKET BOOSTER WEIGHT STATEMENT

BODY STRUCTURE		593336.
FWD SKIRT	22593.	
LOX TANK	177608.	
FUEL TANK	104957.	
THRUST STRUCTURE	270118.	
BASE SKIRT	18060.	
THERMAL PROTECTION		41663.
ENTRY HEAT SHIELD	21942.	
FLAME SHIELD	19433.	
INTER-TANK INSULATION	0.	
BODY ENTRY COVER PANELS	287.	
ELECTRICAL POWER SYSTEM		1639.
INSTRUMENTATION		4428.
PROPULSION		602581.
DRY ENGINES	490817.	
CONTROL SYSTEM	69696.	
FUEL SYSTEM	0.	
OXIDIZER SYSTEM	42068.	
MISCELLANEOUS ITEMS		1269.
SEPERATION AND RECOVERY		71641.
SEPERATION SYSTEM	4666.	
PARACHUTES	37026.	
FLOTATION SYSTEM	670.	
RECOVERY AIDS	661.	
FITTING AND SUPPORTS	1275.	
RETRO MOTORS	27343.	
CONTINGENCY		263311.*
STAGE DRY WEIGHT		1316557.
RESIDUAL AND RESERVE PROP		328591.
FUEL BIAS	21101.	
LOX TANK VAPORS	27962.	
FUEL TANK VAPORS AND/OR GASES	2045.	
TRAPPED FROST	6220.	
TRAPPED FUEL (TANK)	83917.	
TRAPPED LOX (TANK)	138264.	
TRAPPED PROPELLANT (ENGINES)	49082.	
STAGE INERT WEIGHT		1908459.
MAINSTAGE PROPELLANT		18031280.
BOOSTER LIFTOFF WEIGHT		19939739.
TOTAL LOX WEIGHT		13805019.**
TOTAL FUEL WEIGHT		5128277.**

*INCLUDES 79,600 LBS SECOND STAGE PRE-IGNITION AND THRUST BUILDUP PROPELLANT

**INCLUDES BOOSTER PRE-IGNITION AND THRUST BUILDUP PROPELLANT

FIGURE VI-B-4-21.- LOX/C₃H₈ BOOSTER VEHICLE
(2 MILLION LB PAYLOAD)

* * * * * LAUNCH VEHICLE SECOND STAGE WEIGHT STATEMENT * * * * *		
BODY STRUCTURE		417372.
FWD SKIRT	11929.	
FUEL TANK	221445.	
LOX TANK	80683.	
THRUST STRUCTURE	71754.	
AFT SKIRT	23192.	
BASE SKIRT	8368.	
AERODYNAMIC FAIRINGS		900.
THERMAL PROTECTION		21183.
ENTRY HEAT SHIELD	16559.	
FLAME SHIELD	1667.	
INTER-TANK INSULATION	2613.	
BODY ENTRY COVER PANELS	344.	
ELECTRICAL POWER SYSTEM		729.
INSTRUMENTATION		3915.
PROPULSION		184043.
DRY ENGINES	166879.	
CONTROL SYSTEM	14729.	
FUEL SYSTEM	2435.	
OXIDIZER SYSTEM	0.	
MISCELLANEOUS ITEMS		1252.
SEPERATION AND RECOVERY		34044.
SEPERATION SYSTEM	183.	
PARACHUTES	18719.	
FLOTATION SYSTEM	339.	
RECOVERY AIDS	334.	
FITTING AND SUPPORTS	644.	
RETRO MOTORS	13824.	
CONTINGENCY		132688.
STAGE DRY WEIGHT		663438.
RESIDUAL AND RESERVE PROP		132061.
FUEL BIAS	15122.	
LOX TANK VAPORS	45030.	
FUEL TANK VAPORS AND/OR GASES	11715.	
TRAPPED FUEL (TANK)	21837.	
TRAPPED LOX (TANK)	25007.	
TRAPPED PROPELLANT (ENGINES)	13350.	
STAGE INERT WEIGHT		928167.
MAINSTAGE PROPELLANT		8449953.
FLIGHT PERFORMANCE RESERVES	43308.	
IMPULSIVE PROPELLANT	8406645.	
UPPER STAGE LIFTOFF WEIGHT		9376140.
TOTAL FUEL WEIGHT		1261708.*
TOTAL LOX WEIGHT		7399951.*

ORIGINAL PAGE IS
OF POOR QUALITY

*INCLUDES PRE-IGNITION AND THRUST BUILDUP PROPELLANT

FIGURE VI-B-4-22.-LOX/C₃H₈ BOOSTER VEHICLE
(2 MILLION LB PAYLOAD)

LIQUID ROCKET BOOSTER GEOMETRY SUMMARY

LOX TANK VOLUME	198979.
FUEL TANK VOLUME	116090.
AFT DIAMETER	70.00
FWD DIAMETER	60.00
TOTAL STAGE LENGTH	160.57
BASE SKIRT LENGTH	20.00
AFT SKIRT LENGTH	32.40
FUEL TANK AFT BKD LENGTH	22.98
FUEL TANK BARREL LENGTH	34.98
FUEL TANK FWD BKD LENGTH	.00
INTERTANK CLEARANCE	.00
LOX TANK AFT BKD LENGTH	22.98
LOX TANK BARREL LENGTH	50.21
LOX TANK FWD BKD LENGTH	22.98
FWD SKIRT LENGTH	22.98
INTERSTAGE LENGTH	.00
INTERSTAGE AFT DIAMETER	60.00
INTERSTAGE FWD DIAMETER	50.00

LAUNCH VEHICLE SECOND STAGE GEOMETRY SUMMARY

FUEL TANK VOLUME	291550.
LOX TANK VOLUME	106226.
AFT DIAMETER	60.00
FWD DIAMETER	50.00
TOTAL STAGE LENGTH	223.31
BASE SKIRT LENGTH	15.00
AFT SKIRT LENGTH	29.70
LOX TANK AFT BKD LENGTH	19.45
LOX TANK BARREL LENGTH	36.46
LOX TANK FWD BKD LENGTH	19.45
INTERTANK CLEARANCE	.00
FUEL TANK AFT BKD LENGTH	.00
FUEL TANK BARREL LENGTH	122.72
FUEL TANK FWD BKD LENGTH	19.45
FWD SKIRT LENGTH	19.45
INTERSTAGE LENGTH	.00
INTERSTAGE AFT DIAMETER	50.00
INTERSTAGE FWD DIAMETER	40.00

VI-B-4-25

VEHICLE BOOSTER PROPELLANT	ETR PAYLOAD (LBS)	±7 DEG LATITUDE LAUNCH SITE PAYLOAD (LBS)	PAYLOAD INCREASE (LBS)
LOX/RP-1	1,000,000	1,027,600	27,600
LOX/RP-1	2,000,000	2,052,800	52,800
LOX/PROPANE	1,000,000	1,028,600	28,600
LOX/PROPANE	2,000,000	2,053,700	53,700

FIGURE VI-B-4-23.- LAUNCH VEHICLE PERFORMANCE FROM ±7 DEGREE LAUNCH SITE LATITUDE

- PAYLOAD SHROUD MAY BE EXCLUDED FROM PAYLOAD WEIGHT
- REVISE WEIGHT SCALING TECHNOLOGY AND GEOMETRY AS REQUIRED
- INVESTIGATE AERODYNAMIC DATA EFFECTS ON VEHICLE REQUIREMENTS AND PERFORMANCE
- INVESTIGATE THE EFFECTS OF LEAVING THE SECOND STAGE HYDROGEN TANK IN ORBIT TO REDUCE ENTRY THERMAL PROTECTION AND RECOVERY SYSTEM REQUIREMENTS
- INVESTIGATE LOX/LH₂ BOOSTERS

FIGURE VI-B-4-24.- FUTURE ANALYSIS

VI-C PERSONNEL AND PRIORITY CARGO LAUNCH VEHICLE (PLV)
(C. Mac Jones, Future Programs Office)

GENERAL

The PLV will be utilized to transport all personnel to low Earth orbit (LEO) and in addition can fulfill high priority delivery functions of a modest scale. The approach taken in this study is to modify the current Space Shuttle vehicle to fulfill these requirements. In-house IR&D studies by the Boeing Aerospace Company and Rockwell International Corporation have indicated that the baseline Shuttle system can be improved in both payload capability and operating cost by replacement of the two solid rocket boosters (SRB) with a new booster utilizing liquid oxygen and hydrocarbon propellants. Such a booster, herein called the "Liquid Replacement Booster" (LRB), could be developed using the F-1 engines from the Saturn V first stage. If available for heavy lift vehicle use, a new more efficient oxygen/hydrocarbon engine can be advantageously employed to increase the payload capability of this growth Shuttle or enable a decrease in propellant requirements. Briefly, the LRB is a 10M (33 ft.) diameter stage with integral propellant and mounted beneath the Shuttle external tank (ET). The stage is recoverable down-range following a parachute water landing.

The following vehicle sizing results presented are a product of the EDIN Computer Design Center effort on Alternate Shuttle configurations. The EDIN computer graphic depiction of the Shuttle/ET/LRB mission sequence is presented on Figures VI-C-1 (a)-(d).

ASSUMPTIONS AND GUIDELINES

The design points for the study are under the groundrules for Shuttle Reference Mission 1 (due east launch from the Eastern Test Range to 50x100 NM orbit), modified to achieve a payload of 45 metric tons (100,000 pounds). Resultant payload to the proposed SPS LEO operational altitude of 500 km circular will be approximately 36 metric tons. The launch trajectory is constrained to pass through both the RTLS/AOA and MECO points of the Shuttle Reference Mission 1. The initial tilt rate and exo-atmospheric pitch profile are optimized to obtain the trajectory for maximum payload or minimum gross lift-off weight (GLOW) in each study case. The trajectories employ a gravity turn from end of tilt to booster engine cut-off (BECO) and are constrained to prohibit dynamic pressure in excess of 650 psf and longitudinal acceleration in excess of 3.0g by engine throttling and/or shutdown. The LRB and ET are sized to satisfy performance requirements with minimum GLOW.

The LRB is sized according to weight estimating relationships based on Saturn technology. ET sizing is accomplished by employing a fixed mass fraction to distribute ET component weights in accordance with the Shuttle ET weight statement. The Orbiter is modified to include

the additional structural weight necessary to accommodate the increased up payload.

REFERENCE CONFIGURATION DESCRIPTION (LRB W/4 F-1)

Both series burn and parallel burn Shuttle/LRB configurations utilizing 4 and 3 F-1's, respectively, were studied by the EDIN design sizing simulations. The series burn mode configuration designated EDIN0505 achieved minimum GLOW in the design cases simulated and thus was selected as the PLV reference configuration. Launch vehicle configuration, weights summary, and comparison of this design point to the Baseline Shuttle are presented on Figure VI-C-2. A mission parameter summary by event is presented on Figure VI-C-3 with the mission altitude versus velocity profile.

In minimizing the GLOW for the reference configuration, the ET was resized for a usable propellant loading of 1325 metric tons (2.920M pounds) at an average specific impulse of 281.93 seconds versus the baseline Shuttle two SRB combined propellant loading of 1007 metric tons (2.221M pounds) at an average specific impulse of 262.2 seconds. Preliminary cost estimated breakouts are given in Table VI-C-1 as provided by Ms. Debbie Webb of the Resources Management Office. DDT&E is estimated at \$510M with \$460M attributed to the LRB; TFU is estimated at \$376M with \$73M attributed to the LRB and \$300M for an Orbiter unit buy.

ALTERNATE REFERENCE CONFIGURATION DESCRIPTION (LRB W/3 O₂ PROPANE ENGINES)

An alternate series burn PLV design point utilized 3 new O₂/propane "paper" engines in the LRB instead of the 4 F-1's as in the previous reference configuration and was designated EDIN0511. The O₂/propane engine characteristics, as provided by Mr. Merle Lausten of the Propulsion and Power Division, are compared to the F-1 in Table VI-C-2. The EDIN0511 weights summary is compared to the EDIN0505 design point in Table VI-C-3. Both ET and LRB main propellant tankage is seen to be reduced with a reduction in GLOW from 2193 metric tons (EDIN0505) to 1779 metric tons (EDIN0511). A mission parameter summary by event is presented on Figure VI-C-4 with mission altitude versus velocity profile. Preliminary cost estimate breakouts are given in Table VI-C-4, again provided by Ms. Webb. DDT&E is estimated at \$1140 with \$1090M attributed to the LRB. Approximately \$500M of the \$1090M is estimated for the development of the "new" O₂/propane booster engine, which may be available from the HLLV program. TFU is estimated at \$367M with \$64M attributed to the LRB and \$300M for an Orbiter unit buy.

ORBITER PASSENGER TRANSPORT

Concepts for a modified Orbiter for passenger transport have been devised by Rockwell International Corporation in an in-house effort and provided for inclusion in this report. The concepts vary in passenger capability from 80 to 68 to 50. The 80-passenger configuration has only

two loading and unloading doors. A four-door configuration can hold 68 passengers within the baseline cargo bay length (Figure VI-C-5). The passenger module length must be increased 6 feet to carry 80 passengers in the four-door configuration. An OMS kit is required by the baseline Space Shuttle to reach the 500 km altitude and takes 9 feet of the aft part of the cargo bay for installation. With the OMS kit installed a 50-passenger module in a four-door configuration can be carried in the baseline cargo bay.

Preliminary cost estimates of the 80 passenger, 2-door passenger transport kit were given as \$220M including DDT&E plus two kit sets. Weight estimates for loaded passenger kits range from 26 metric tons to 28 metric tons for 50 to 80 passengers loaded, respectively.

CONCLUDING REMARKS

Additional study is required on both upgraded Space Shuttle configurations and passenger transport concepts to support follow-on SPS studies. Two Headquarters Advanced Programs Office funded studies on Shuttle Growth (one, on booster and external tank options, awarded by Marshall Space Flight Center to Rockwell International in May 1976, and the other, on orbiter modifications, expected to be contracted by JSC at a later date), should provide more developed point designs.

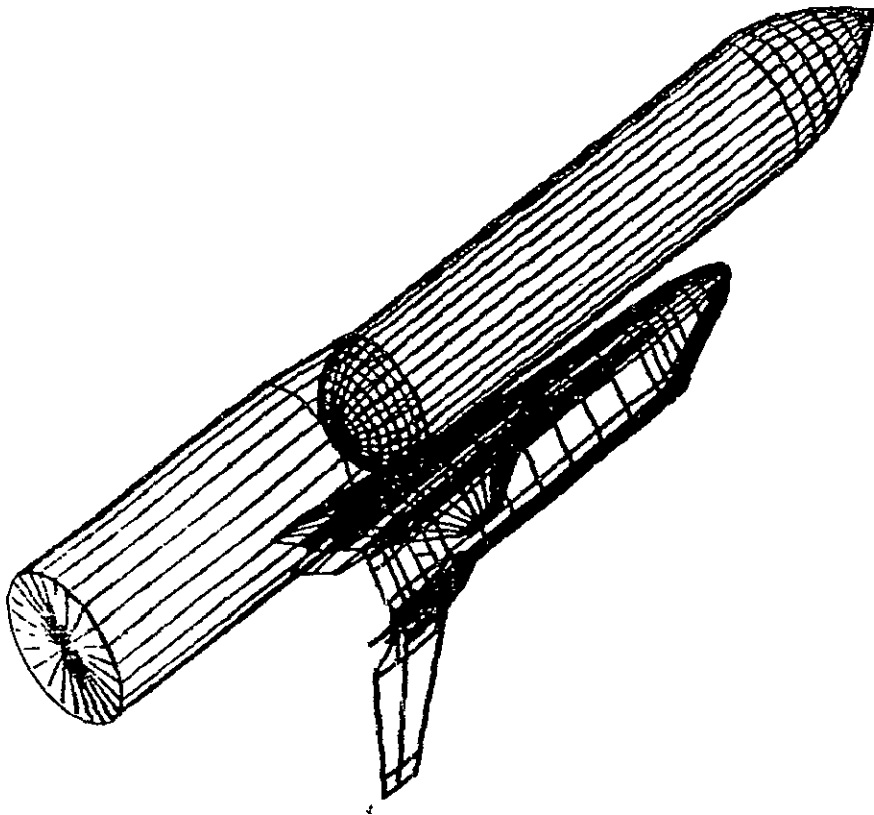


Figure VI-C-1(a). Mission sequence before BECO

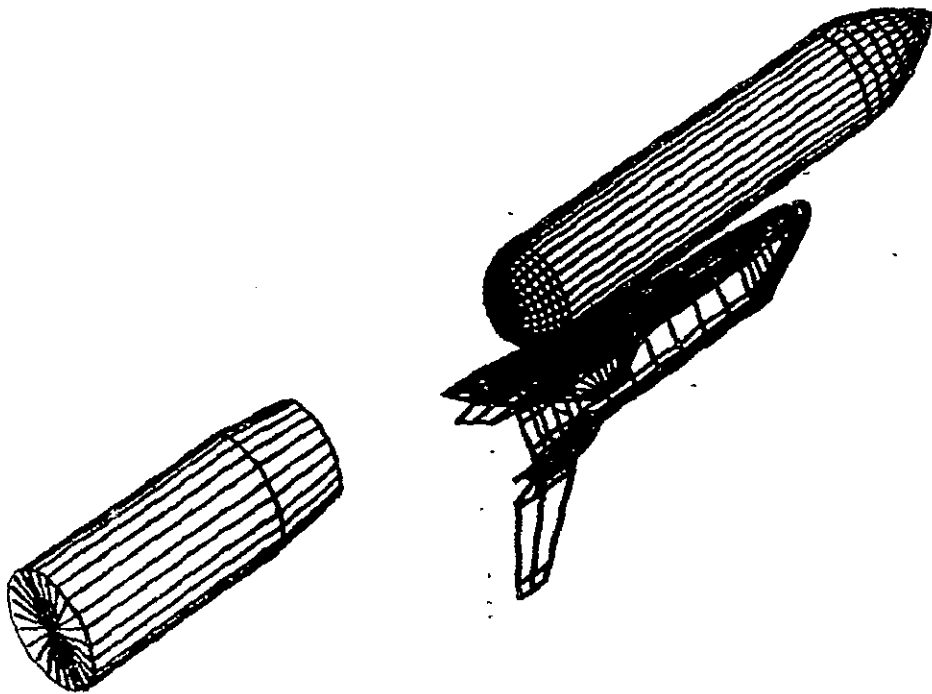


Figure VI-C-1(b). Mission sequence post-BECO

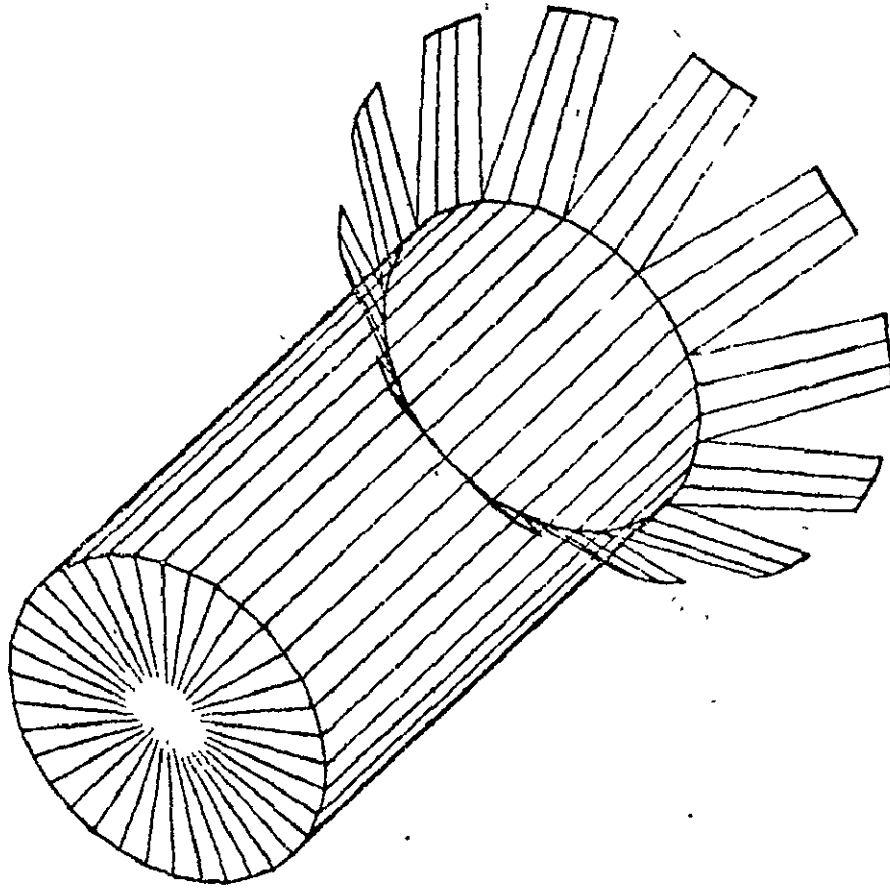


Figure VI-C-1(c). Mission sequence LRB reentry

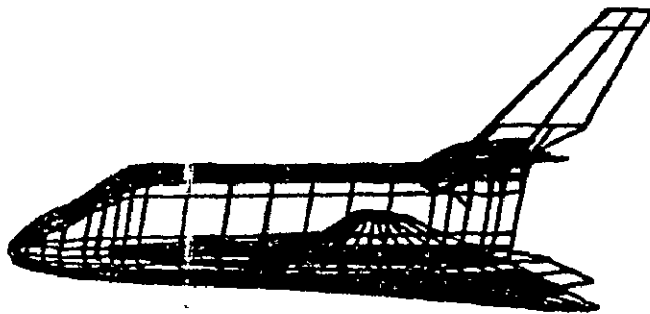
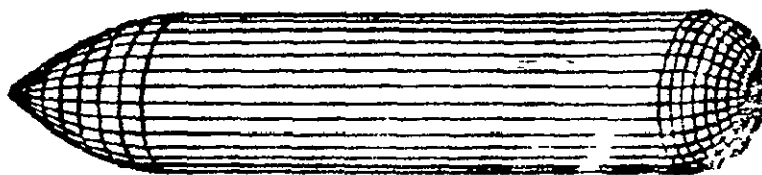
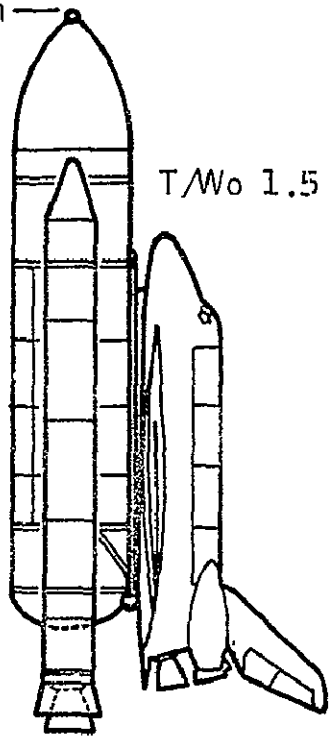


Figure VI-C-1(d). Mission sequence post-MECO



Transport to LEO
500 km circ, 28-1/2°

Parallel burn glow 2032 tons
56.1m

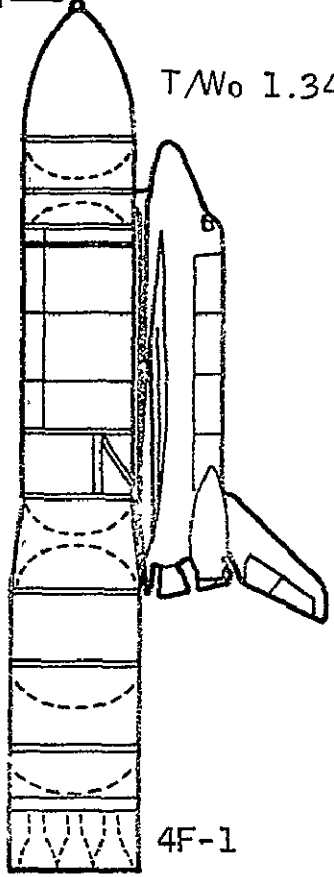


Baseline Shuttle

29.5 tons payload (ETR)
≈\$15M/ft

Series burn glow |2193 tons
69.2m

T/Wo 1.34



EDIN0505 Growth Shuttle

≈36 tons payload (ETR)
≈\$10M/ft

Payload, tons	36 (internal orbiter)
Payload, passengers	40 to 50
Orbiter, inert, tons	85
External tank, inert, tons	33
External tank, propellant, tons	567
Liquid rocket booster, inert, tons	138
Liquid rocket booster, propellant, tons	1325
Gross lift-off weight, tons	2193
Number of engines, (F-1's)	4
Staging altitude (booster) km	45.54
Staging velocity, km/sec	1.40

Figure VI-C-2. Personnel and Priority Cargo Launch Vehicle (PLV)
Reference Configuration - EDIN0505

MISSION SUMMARY

PARAMETER	EVENT 1	EVENT 2	EVENT 3	EVENT 4	EVENT 5
TIME (SEC)	62.50	140.2	283.8	536.0	490.0
ALTITUDE (K FT)	30.75	149.4	348.6	394.5	0
REL VELOCITY (100 FPS)	12.2	45.8	81.4	243.0	2.15
REL GAMMA (DEG)	66.6	24.4	8.27	.527	-89.8
WEIGHT (K LBS)	4795.2	3285.1	1611.5	1126.9	264.9
WEIGHT DROP (K LBS)	0	264.9	0	73.08	0
THROW WEIGHT (K LBS)	3285.1	1611.5	1126.9	287.62	0
CUM VIDEAL (100 FPS)		85.10		304.3	0
DOWNRANGE (NMI)	1.38	28.97	187.7	865.3	136.0

EVENT 1 ONE F-1 ENGINE SHUTDOWN
 EVENT 2 BECD/SEPARATION
 EVENT 3 PTL5/ADA CONSTRAINT
 EVENT 4 MECO/INJECTION
 EVENT 5 LFB TOUCHDOWN

EDIN0505 H-V PROFILE

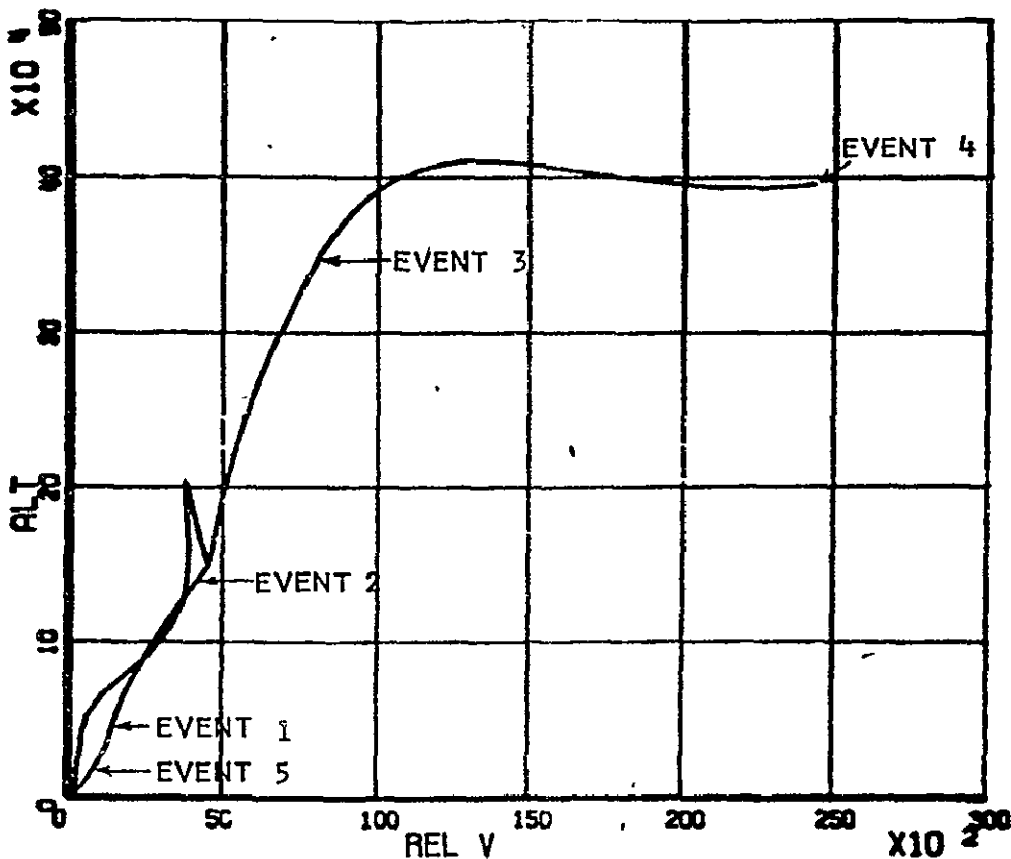


Figure VI-C-3. Mission Events - EDIN0505

	(M of 76 \$)	
	<u>TFU</u>	<u>DDT&E</u>
Personnel Launch Vehicle	<u>376</u>	<u>510</u>
Liquid Replacement Booster	<u>73</u>	<u>460</u>
Program Management	0	30
SE&I	0	20
System Support	0	60
Hardware	<u>73</u>	<u>350</u>
Structures	23	130
TPS	7	10
Separation & Recovery	5	40
Propulsion	33	130
Instrumentation	1	10
Power Systems	1	10
Inst., Ass., & C. O.	9	10
Major Ground Test	0	10
Orbiter	<u>300</u>	<u>0</u>
External Tank	<u>3</u>	<u>50</u>

Table VI-C-1. Preliminary Cost Estimates
 PLV Reference Configuration
 EDIN0505 (LRB W/4 F-1)

	F-1 (O ₂ /RP-1)	"New" Engine (O ₂ /Propane)
Thrust (SL), lbs	1,606,789	2,000,000
Thrust (VAC), lbs	1,748,060	2,168,800
Throttle	1.00	1.00 to .75
Isp (SL), Sec	266.01	306.40
Isp (VAC), Sec	289.40	332.30
Flowrate, lb/sec	6040.3	6527.5
Exit Area, sq ft	66.763	76.718
Expansion Ratio	10:1	30:1
Mixture Ratio	2.27:1	2.68:1
Engine Wt Dry, lbs	19,038	22,000

Table VI-C-2. Comparison of Engine Characteristics
F-1 Vs. "New" O₂/Propane Engine

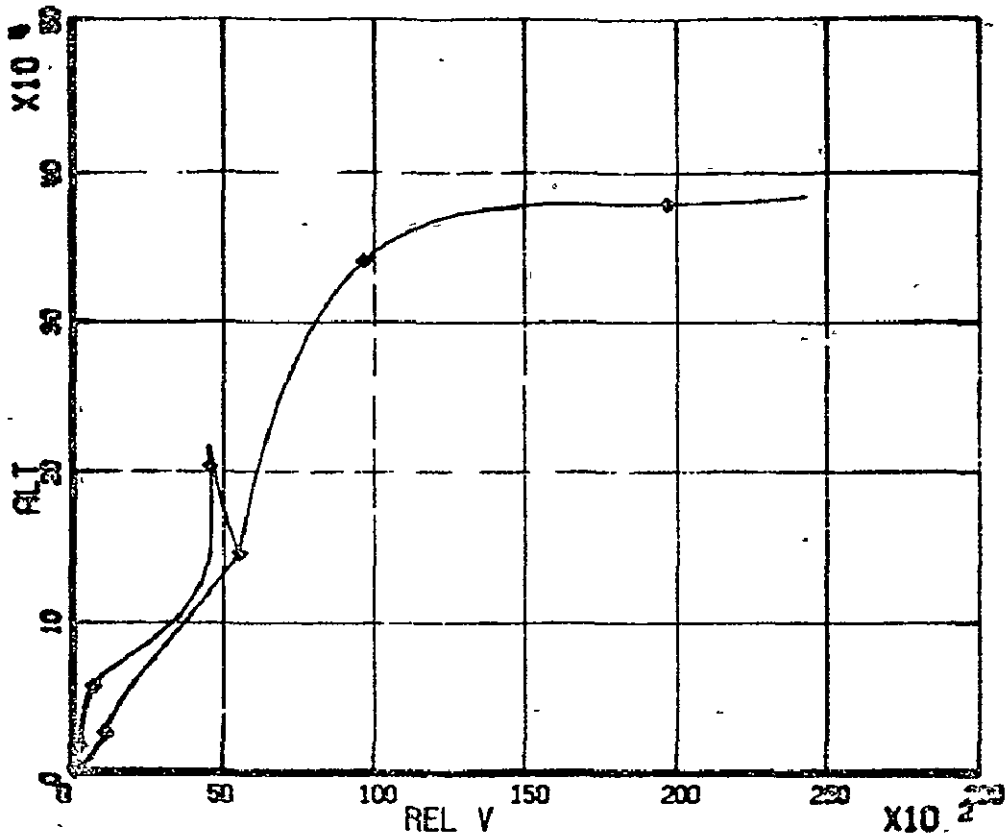
Configuration No.	EDIN0505	EDIN0511
Burn Mode	Series	Series
LRB	Resized	Resized
ET	Resized	Resized
LRB Engines	4 F-1	3 O ₂ /Propane
PL (Ref. Mission 1)	45 MT	45 MT
GLOW	2193	1779
ET Propellant	567	471
ET Inert	33	28
LRB Propellant	1325	1029
LRB Inert	138	121
Orbiter Inert	85	85

Table VI-C-3. Design Point Comparison
EDIN0505 Vs. EDIN0511

VI-C-9'

CONFIDENTIAL

EDIN0511 H-V PROFILE 21 MAY 76



MISSION SUMMARY: MAY 21, 1976

PARAMETER	EVENT 1	EVENT 2	EVENT 3
TIME (SEC)	124.5	465.7	891.6
ALTITUDE (FT)	145.3	393.7	0.
REL VELOCITY (100 FPS)	55.4	242.9	215.0
REL GAMMA (DEG)	23.3	.550	-89.8
WEIGHT (LBS)	3921.5	1337.5	266.2
WEIGHT DROP (LBS)	255.2	51.21	0
THROW WEIGHT (LBS)	1357.5	233.20	0
CUM VIDEAL (100 FPS)	90.00	232.0	0
DOWNRANGE (NMI)	30.81	717.0	154.2

EVENT 1 BSCD DEPARATION EVENT 3 LPB TOUCHDOWN
 EVENT 2 MED-INJECTION

Figure VI-C-4. Mission events - EDIN0511

ORIGINAL PAGE IS
OF POOR QUALITY

	(M of 76 \$)	
	<u>TFU</u>	<u>DDT&E</u>
Personnel Launch Vehicle	<u>367</u>	<u>1140</u>
Liquid Replacement Booster	<u>64</u>	<u>1090</u>
Program Management	0	60
SE&I	0	40
System Support	0	130
Hardware	<u>64</u>	<u>860</u>
Structures	20	120
TPS	1	10
Separation & Recovery	5	40
Propulsion	30	650
Instrumentation	1	10
Power Systems	1	10
Inst., Ass., & C. O.	6	10
Major Ground Test	0	10
Orbiter	<u>300</u>	<u>0</u>
External Tank	<u>3</u>	<u>50</u>

Table VI-C-4. Preliminary Cost Estimates
 Alternate PLV Reference Configuration
 EDIN0511 (LRB W/3 O₂/Propane Engines)

VI-D CARGO ORBIT TRANSFER VEHICLE
(John C. Hooper, Primary Propulsion Branch, EP2)

1.0 LOW THRUST CARGO OTV

1.1 GROUND RULES AND ASSUMPTIONS

The low-thrust cargo OTV (COTV) is used to transport either the entire SPS as a unit or major subassemblies of the SPS from the construction site in low earth orbit (LEO) to geosynchronous orbit (GSO). In either case, the satellite is assumed to be capable of providing power to the COTV during the transfer. Any satellite penalties resulting from this mode of operation were not assessed (a summary of these ground rules is included as figure VI-D-1-1). A payload mass of 42 million pounds was selected as representative of half of a 5 GW (ground power) station; it was assumed that the payload would be capable of supplying a maximum of 4 GW to the COTV during transit.

Structural considerations were assumed to limit the maximum vehicle acceleration to 10^{-3} g; the minimum acceleration was assumed to be limited by economic considerations relating to trip time and an arbitrary value of 5×10^{-3} g (corresponding to 180 day transit time) was selected. The attitude control system of the satellite is assumed to be capable of performing satellite orientation that cannot be accomplished by gimbaling of the COTV main engines.

ORBIT TRANSFER GROUND RULES
FOR
JSC SOLAR POWER SATELLITE STUDY

- MAX T/W = 10^{-3} G (END OF BURN)
- PAYLOAD MASS = 42×10^6 LB (HALF OF 5 GW STATION)
- MAX POWER AVAILABLE = 4 GW PER 42 MLB
- MAX TRIP TIME = 180 DAYS (T/W $\approx 5 \times 10^{-5}$)

VI-D-1-2

FIGURE VI-D-1-1.

1.2 CHEMICAL STAGE

1.2.1 PARAMETRIC DATA

The low-thrust chemical stage uses O_2/H_2 propellants. The propellant selection was based on considerations of cost, availability, technology base, and environmental effects of exhaust gases.

Stage weight trends for the chemical stage were developed using a computerized vehicle synthesis program known as SWOP (Stage Weight Optimization Program). The model used was one developed for a LO_2/LH_2 space tug several years ago during the course of the JSC in-house Space Tug Study. The results from this model are shown in figure VI-D-1-2 as stage mass fraction (impulse propellant/stage weight) versus impulse propellant mass. Also indicated on figure VI-D-1-2 are data points representing point designs of LO_2/LH_2 COTV's done by the Boeing Company for the FSTSA study. All these data points are for a system with a relatively high T/W in the range of 0.2 and a mission duration of approximately 5 days. Some cursory hand calculations indicated that the reduced T/W requirement would reduce main propulsion system weight so that the stage mass fraction would be .01-.02 higher; however, the longer mission duration will require additional insulation and power, and will result in increased boiloff losses so that, as an initial approximation, the same curve was used for sizing studies for both the high and low thrust chemical stages.

Performance values for the O_2/H_2 propellant combination are well-known and documented; using an expander cycle engine of 25,000 lbf thrust at a chamber pressure of 600 psia and an area ratio of 400:1, the expected nominal Isp is 460 seconds.

Figure VI-D-1-3 illustrates the payload capability of a chemical stage operating in an expendable mode. The ratio of propellant weight to payload weight (WP/WPL) is shown as a function of the stage mass fraction. The two curves shown for a T/W of 10^{-3} are applicable to this vehicle. The shaded band of each curve illustrates the effect of an Isp variation from 450 to 470 seconds. The ΔV of 19,000 ft/sec corresponds to a KSC launch, while the 15,000 ft/sec ΔV is the orbit transfer requirement if an equatorial launch site is used. From figure VI-D-1-3, it is seen that, at a mass fraction of .93 and an Isp of 460, launching from KSC results in a ratio of propellant weight to payload weight of 3.3; from an equatorial launch site, the value of WP/WPL is approximately 2. Thus, the choice of launch site is seen to be extremely important for a low Isp COTV such as the O_2/H_2 stage.

The effects of staging are illustrated by figure VI-D-1-4. The upper and lower sets of curves are for the KSC and equatorial launch sites respectively, as discussed above. The "single stage" curves are reproduced from figure VI-D-1-3 for comparison. The two-stage curves illustrate the performance of two equally-sized stages. With this ground rule, the ΔV of first stage is approximately 6500 ft/sec for the KSC launch case and 5500 ft/sec for the equatorial launch case.

VI-D-1-4

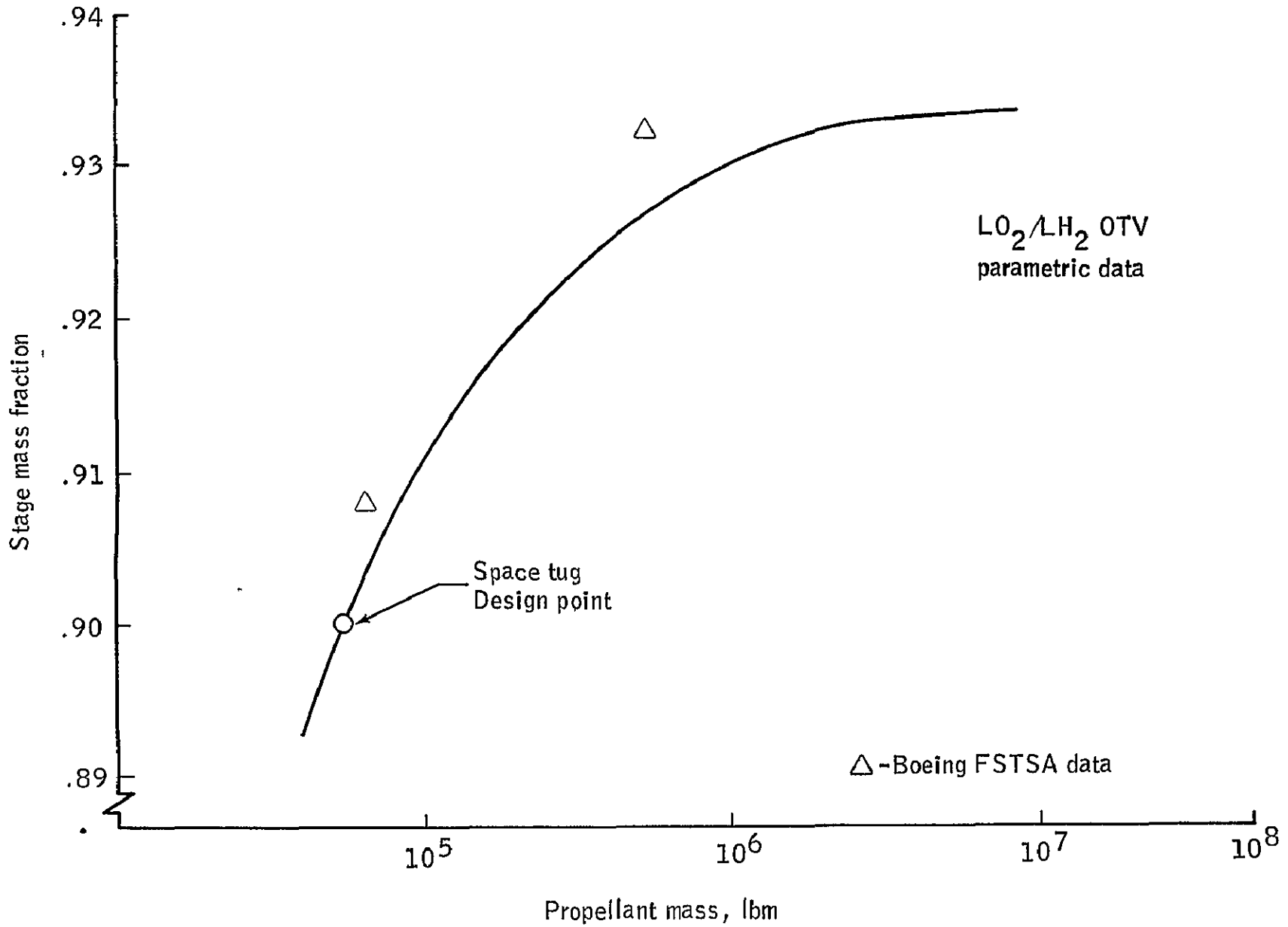


FIGURE VI-D-1-2. - LO₂/LH₂ OTV parametric data.

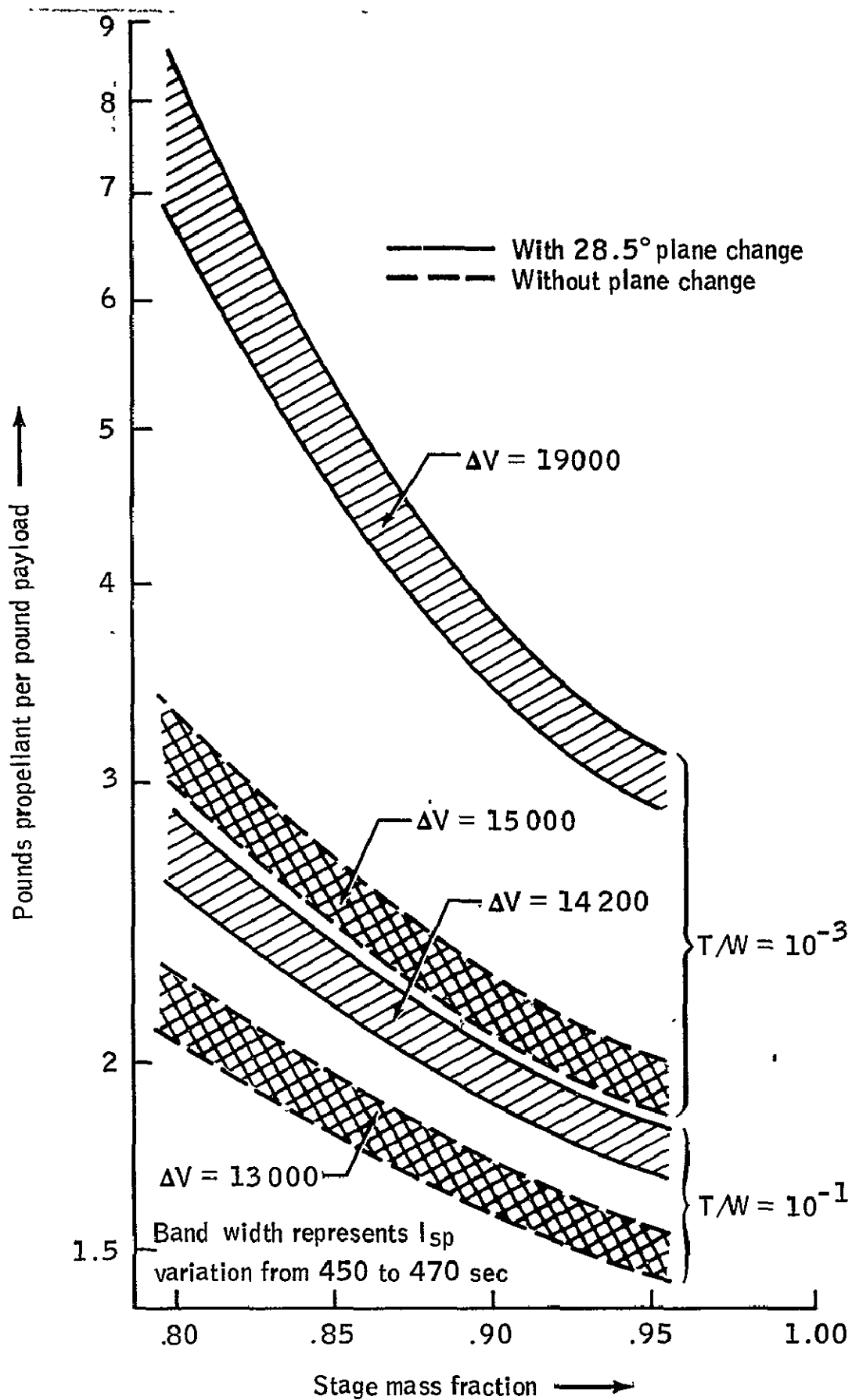


FIGURE VI-D-1-3. - Orbit transfer LO_2/LH_2 OTV.

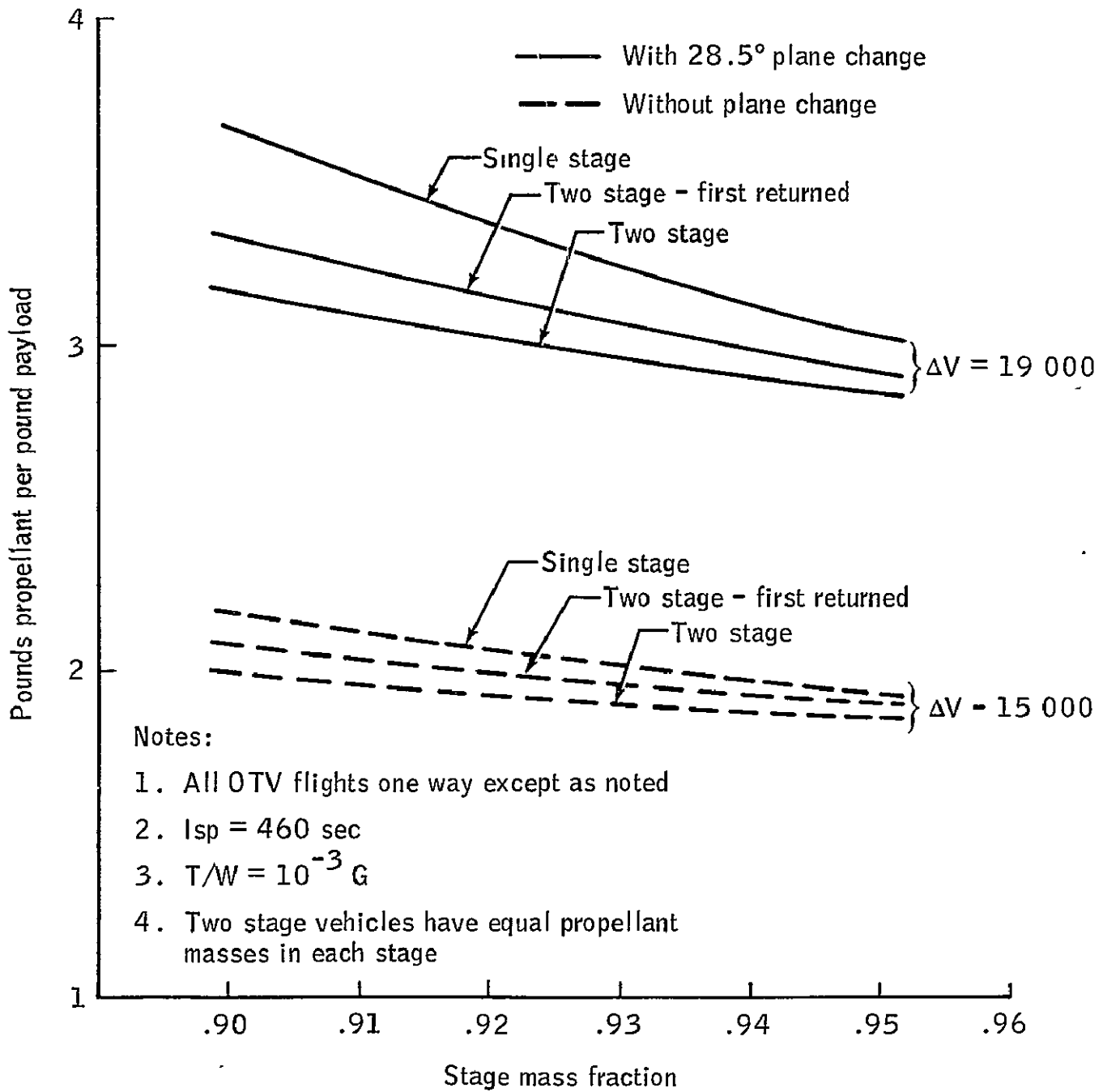


FIGURE VI-D-1-4. - LO_2/LH_2 OTV staging effects.

The mass fraction penalties for staging should be small for the propellant quantities involved; using a constant mass fraction, for the KSC launch going to a two-stage vehicle would reduce the propellant requirement from 3.25 to 2.96 pounds per pound of payload, an eleven percent reduction. If it were deemed desirable to return the first stage to low earth orbit for reuse, the ΔV for the first stage becomes approximately 6200 fps and the ratio of propellant to payload becomes 3.06 for the KSC launch case. For the equatorial launch case, return of the first stage degrades the two-stage propellant payload ratio from ~ 1.90 to 1.97 pounds per pound.

The considerations discussed above show a strong incentive for the utilization of an equatorial launch site for a LO_2/LH_2 COTV; the 4000 fps reduction in ΔV resulting from the elimination of a 28.5 plane change gives a propellant savings of some 40 percent for a single stage vehicle; from that point, a two-stage system would result in an additional 6 percent reduction.

1.2.2 OPERATIONAL CONSIDERATIONS

The various system weight characteristics, engine performance values, and staging options discussed above result in a range of the ratio of propellant/payload mass of from 1.9 to 3.3 pounds per pound. For the representative payload mass of 42 million pounds, this gives a LEO propellant requirement of from 80 to 140 million pounds for a LO_2/LH_2 COTV. Since this mass will obviously require multiple launches to emplace in LEO, the propellants will have to be stored in LEO for some time prior to their use.

Assuming an HLLV payload capacity of 10^6 lbm, and making allowances for tankage, fairings, insulation, and other structure, to transfer the required propellant load to LEO will require some 90 to 160 HLLV launches, or 7 to 11 weeks at a two-a-day launch rate. Obviously propellant loading would only be initiated when everything was in readiness for the orbit transfer, but even so, a significant propellant storage problem will exist. Since the LH_2 tank presents the most severe storage problem, the loading sequence would involve putting up the LO_2 tanks first. Although this mode is definitely preferable to the inverse procedure of launching the LH_2 first, it does impose a long duration LEO storage requirement on the LO_2 .

Two basic approaches seem to be applicable to this problem; one would be to use a very low heat leak propellant tank to minimize the boiloff experienced during the LEO "hold" time while propellants are being accumulated; the other approach would launch a relatively high heat leak tank (optimized for the transit time from LEO to GSO) as well as a liquification plant to re-liquify the boiloff gases and return them to the propellant tank. It was found that a middle of the road approach was most favorable; a tank with sufficient thermal performance to limit the boiloff losses to a manageable level while not imposing an undue weight penalty on the stage appears feasible.

Another justification of this selection is found in the independent nature of the chemical COTV. The primary incentive for utilization of the chemical COTV would be to avoid the penalties associated with tapping the satellite power; yet operation of the liquification plant would require external power, largely negating the justification for choosing the chemical COTV.

1.2.3 REPRESENTATIVE CONFIGURATION

The representative LO_2/LH_2 COTV was derived using the following constraints and assumptions:

- KSC site for launch into LEO
- two-per-day HLLV flights each carrying 1 million pounds payload for tanking propellant
- earth-launch propellant tank is plugged into a structural and feed system array that becomes the "stage" (no propellant transfer)

The general requirements for a LO_2/LH_2 COTV engine are primarily long life (1000 hrs), simplicity (minimum active controls), and high specific impulse. An expander cycle (like the RL-10) was selected because of its high performance combined with relatively low chamber pressures (600 - 800 psia) and corresponding pump speeds. The low temperature heated hydrogen turbine provides for long life and active controls are minimized by using a single shaft for the pumps and turbine. A thrust level of 25,000 lb_f was selected to provide maximum pump and turbine efficiencies at low speeds and minimize kinetic losses that occur at lower thrust levels. Engine weight is not nearly as important as performance so a very high nozzle area ratio was selected. The only technical issues are associated with the turbo-machinery. Low speed/heavy weight pumps will utilize advances in technology. The proposed engine characteristics are given in table VI-D-1-1.

Tank-mounted zero NPSH electric driven boost pumps supply propellant to the engine. The concept envisioned for assembling the stage is illustrated in figure VI-D-1-5. The tanks employ series feed through connections made while the stage is being assembled.

No reaction control capability is provided by the COTV; a greater than normal gimbal range will probably be required, but the attitude control system of the satellite is assumed to be capable of performing any orientation that cannot be done by differential gimbaling of the COTV main engines.

A weight statement for the O_2/H_2 COTV is included as table VI-D-1-2.

The numbers provided must be regarded as highly preliminary since the COTV concept is somewhat unconventional and a large number of assumptions are required in order to calculate any weights.

1.2.4 TECHNOLOGY ISSUES

Technology issues are not a significant problem with this COTV concept. The size of the stage, its manner of construction and operation, and its economic viability will inevitably give rise to a large number

TABLE VI-D-1-1. LO₂/LH₂ ENGINE CHARACTERISTICS

DESCRIPTION	EXPANDER CYCLE WITH SINGLE SHAFT TPA
THRUST	25000 lbf
CHAMBER PRESSURE	600 psia
MIXTURE RATIO	6:1
Isp	460 SEC
AREA RATIO	400:1
WEIGHT	675 lbm
LENGTH	150"
EXIT DIAMETER	106"

VI-D-1-9

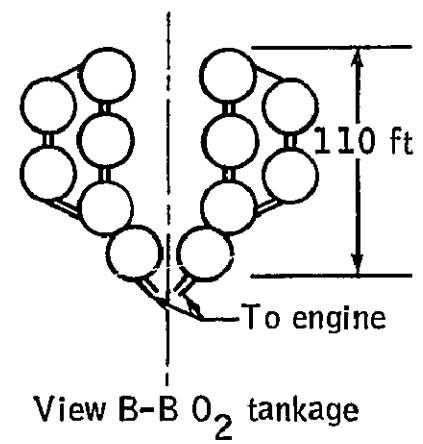
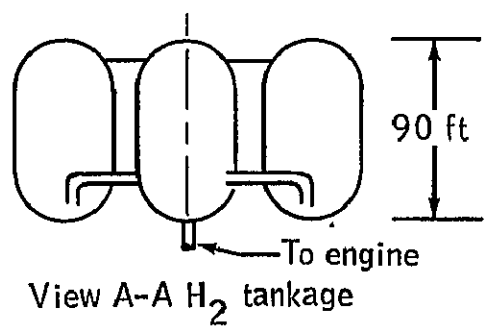
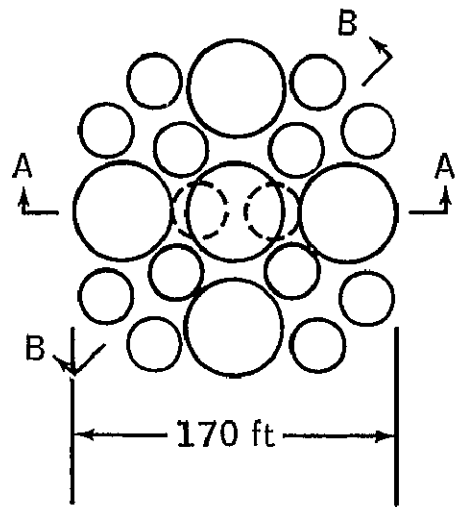


Figure VI-D-1-5. - O₂H₂ OTV tankage arrangement.

VI-D-1-10

TABLE VI-D-1-2. O₂/H₂ OTV WEIGHT STATEMENT

VI-D-1-11

PROPELLANT STORAGE & FEED SYSTEM	MLB
OXIDIZER TANKS	1.092
FUEL TANKS	1.740
FEED SYSTEM)	
PRESSURIZATION SYSTEM)	
THRUST STRUCTURE)	1.718
ATTACH STRUCTURE)	
ENGINES	.006
MISC. (20%)	.911
TOTAL DRY WEIGHT	5.467
PROPELLANT	
IMPULSE PROPELLANT	134.
LEO BOILOFF	.989
PRESSURANT	.383
RESIDUAL	2.680
OUTAGE	.191
TOTAL PROPELLANT WEIGHT	138.243

of technical problems, but aside from the issues of component and system lifetime found throughout the SPS, no major advances in technology are required.

1.3 ELECTRICALLY-POWERED COTV (LOW Isp)

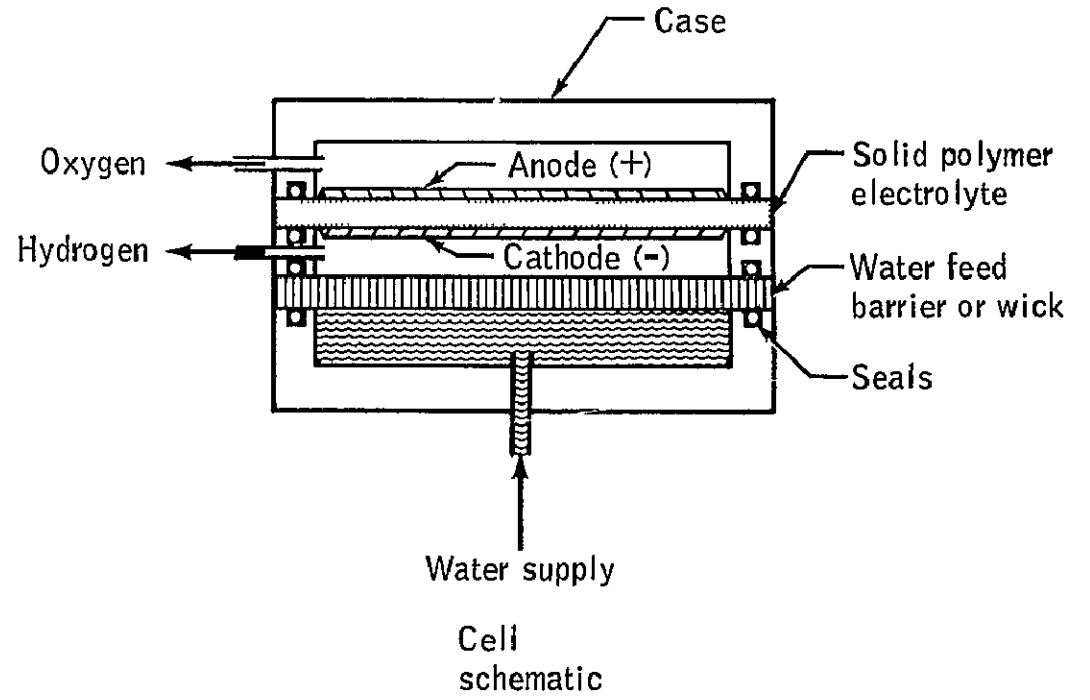
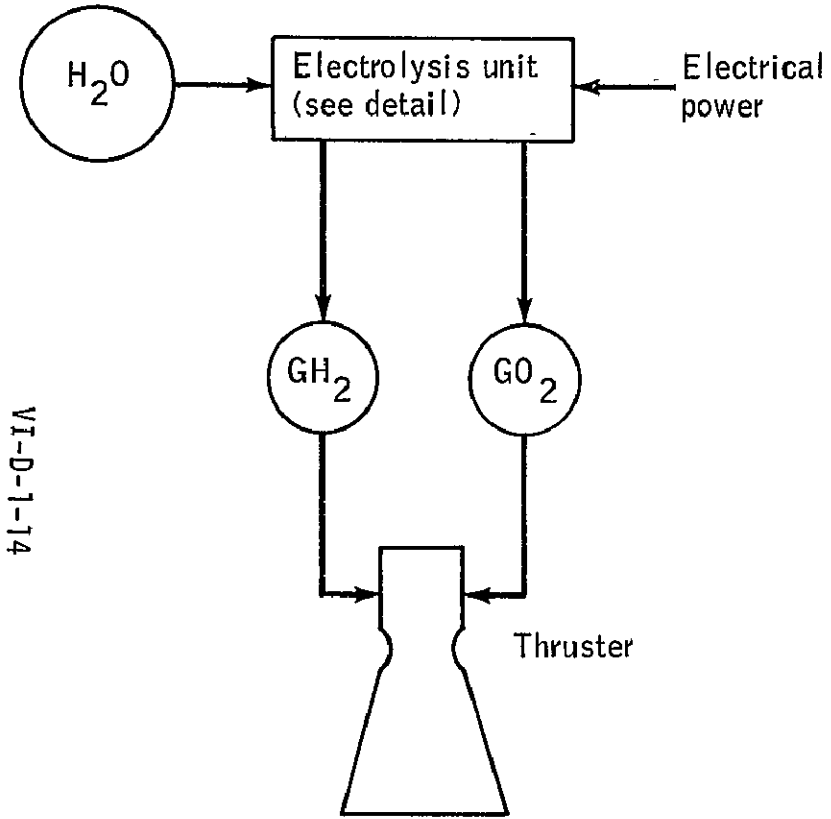
The electrically-powered stages take advantage of the satellite's assumed capability to supply power during transit; by doing so, the COTV avoids the penalty of providing its own power generation equipment. Although an electrical COTV with an independent power supply is technically feasible, the incentive for exploitation of the satellite's capability (for power levels as high as these systems require) was felt to be irresistible.

In contrast to the chemical stage, where a final T/W of 10^{-3} was selected, the electrical stages were sized using a final T/W of 10^{-4} where possible. The effect of this is to change the trip time from 15 days (for the chemical stage) to about two months.

The types of electric thrust systems covered are electrochemical, resistojet, and arcjet systems. The electrochemical concept is a hybrid electrical/chemical system; it utilizes an electrolysis unit to produce gaseous O_2 and H_2 from water. These propellants are then burned in a more-or-less conventional rocket engine. A resistojet thruster operates by transferring heat from an electrically-heated element to the propellant, which is then expanded in a nozzle. For this study, only H_2 was considered for use in the resistojet. The thermal arcjet thruster operates on the same basic principle as a resistojet, but is capable of much higher temperature operation because, instead of a metallic heating element, an electrical arc is used as the heat source. To gain some insight into the effects of density and Isp, ammonia (NH_3) and H_2 propellants were considered for the arcjet.

1.3.1 CONCEPT DESCRIPTIONS

A schematic of an electrochemical propulsion system is shown in figure VI-D-1-6. It consists of the electrolysis unit, gaseous propellant accumulators, and the pressure-fed gas/gas thrusters. The potential advantages of an electrolysis thruster system over a conventional LO_2/LH_2 rocket engine lie in the cost, handling, storage, and transport of water rather than LO_2 and LH_2 . The disadvantages include dependence of external power (from the SPS), high thruster assembly weights at high power levels, and lower Isp (due to operation at the stoichiometric mixture ratio of 8:1). When an attempt was made to size a system for a 60-day trip time, the system weights were very high; by bringing the thrust level down a more reasonable weight was attained. Operation at the stoichiometric mixture ratio results in a small rise in combustion temperature (less than $200^\circ F$) and a 4 percent decrease in Isp. Details on the electrochemical system are shown in table VI-D-1-3. In the numbers shown, electrothermal pumping was used to raise the pressure of propellants and the engines are pressure-fed. Further work on this system could show that it would be more desirable from a weight standpoint to operate the electrolysis unit at a low pressure and utilize electric-powered compressors to raise the pressure of the propellants.



VI-D-1-14

Figure VI-D-1-6. - Electrochemical propulsion system schematic.

TABLE VI-D-1-3. ELECTROCHEMICAL PROPULSION SYSTEM CHARACTERISTICS

ELECTROLYSIS UNIT

CURRENT	24,000 AMPS
VOLTAGE	8,000 VOLTS
CELL SIZE	12 FT ² /CELL, 1/4" THICK
GAS OUTLET CONDITIONS	600 PSIA, 300°F
WEIGHT (WITH RADIATOR)	1510,000 LBM

THRUSTER

DESCRIPTION	PRESSURE FED REGEN COOLED
THRUST	2,000 LB _f
CHAMBER PRESSURE	300 PSIA
MIXTURE RATIO	8:1
ISP	440 SEC.
AREA RATIO	200:1
WEIGHT	100 lbm
LENGTH	64"
EXIT DIAMETER	28.6"

VI-D-1-15

A resistojet thruster schematic is shown in figure VI-D-1-7. The resistojet is a simple, relatively low performance electrical thruster that has had much development work and has some flight experience. The factors limiting the performance of a resistojet are the propellant molecular weight and the propellant temperature as indicated from the relation

$$I_{sp} \propto \sqrt{T/M}$$

where

T = gas temperature
M = molecular weight

Since the maximum temperature is restricted by material limits of the heating element, low molecular weight is important for high I_{sp} . This leads to the use of hydrogen for a resistojet, in spite of its disadvantages of low liquid density and low boiling point. Predicted values for delivered I_{sp} as a function of gas temperature for a hydrogen resistojet is shown in figure VI-D-1-8. For the thruster characteristics shown in table VI-D-1-4, an I_{sp} of 1000 seconds is thought to be attainable within the life constraints of a two-month trip time.

Although the performance of an arcjet thruster is governed by the same relation as given above for the resistojet, the heat source is an electrical arc rather than a metallic heating element (see schematic, figure VI-D-1-9). This allows much higher temperature operation and thus higher performance. A considerable amount of experience exists with arcjets as plasma sources for materials testing, and a good deal of effort has been put into arcjet thrusters for space applications. Arcjet thruster characteristics are shown in table VI-D-1-5 which result in predicted performance values of 1500 seconds for NH_3 and 3000 seconds for H_2 .

1.3.2 PARAMETRIC DATA

Figure VI-D-1-10 and VI-D-1-11 illustrate the trends of WP/WPL for the electric COTV options considered for KSC and equatorial launches. The effect of high I_{sp} systems on reducing both the effect of stage mass fraction and the plane change penalty for a KSC launch is notable. At a ΔV of 19,000 ft/sec, the electrochemical stage has a ratio of WP/WPL in the range of 3 to 4, approximately the same as a conventional chemical stage and considerably higher than the other electric options. For the resistojet, WP/WPL ranges from 1 to 1.8, for the NH_3 arcjet, .6 to 1.0, and for the H_2 arcjet .23 to .4 (all values based on 19,000 ft/sec ΔV).

At the performance levels of these stages (except for the electrochemical system) staging would probably not be an attractive option. For example, if a two-stage resistojet COTV could attain the same mass fraction as a single-stage system, the reduction in propellant required would be approximately 10 percent.

1.3.3 OPERATIONAL CONSIDERATIONS

All of the COTV's considered here have a propellant requirement considerably in excess of the assumed capability of the HLLV; multiple HLLV flights will be required to emplace the COTV propellant in LEO.

VI-D-1-17

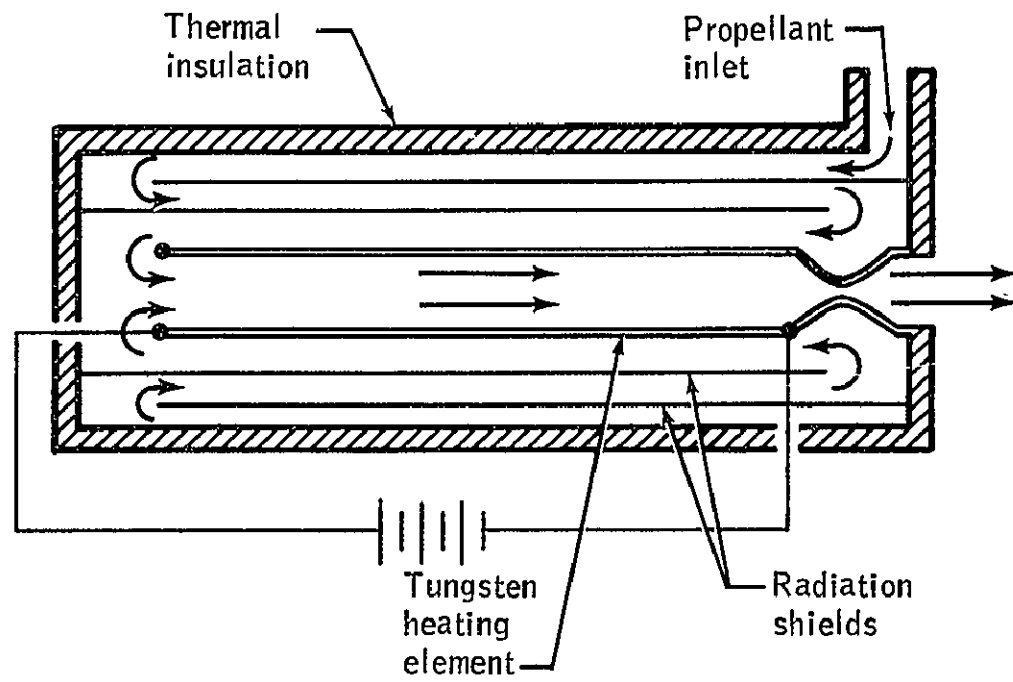


Figure VI-D-1-7. - Resistojet thruster schematic.

81-1-0-1A

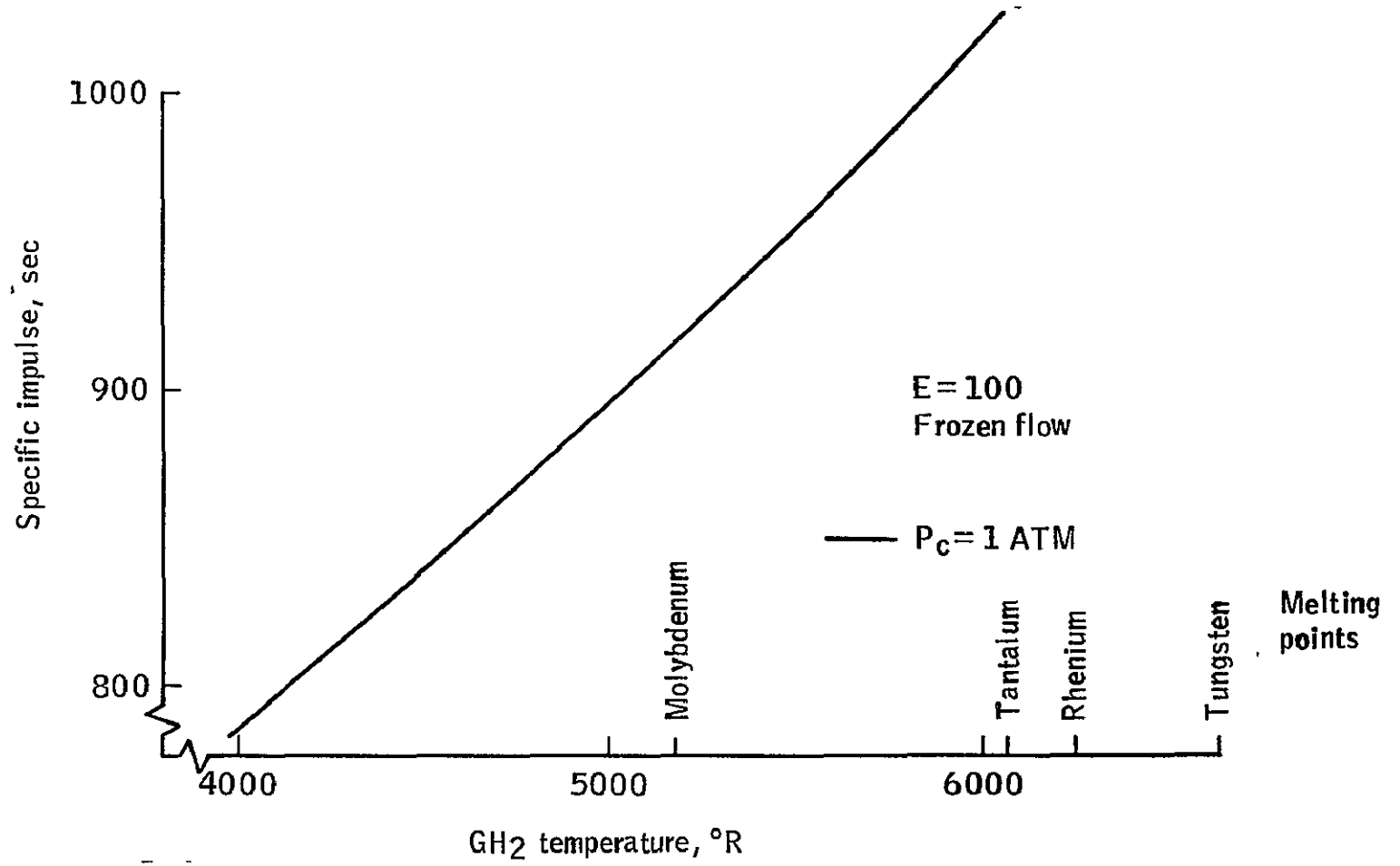


FIGURE VI-D-1-8.- Resistojet performance prediction.

TABLE VI-D-1-4. RESISTOJET THRUSTER CHARACTERISTICS

DESCRIPTION	PRESSURE-FED, GH_2 , CONVECTIVELY HEATED BY RESISTANCE HEATER
THRUST	1,000 lbf
CHAMBER PRESSURE	14.7 psia
ISP	1,000 sec.
AREA RATIO	100
INPUT POWER	35 MW
INPUT VOLTAGE	1,000 V. (DC or AC)
THERMAL EFFICIENCY	98
OVERALL EFFICIENCY	65
WEIGHT	1,000 lbm
LENGTH	12'
EXIT DIAMETER	6'

VI-D-1-19

ORIGINAL PAGE IS
OF POOR QUALITY

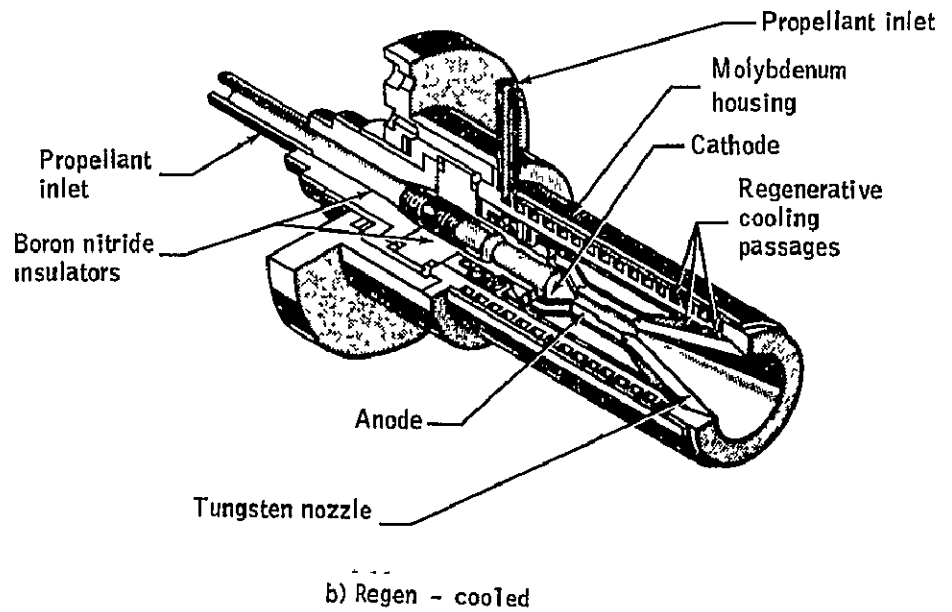
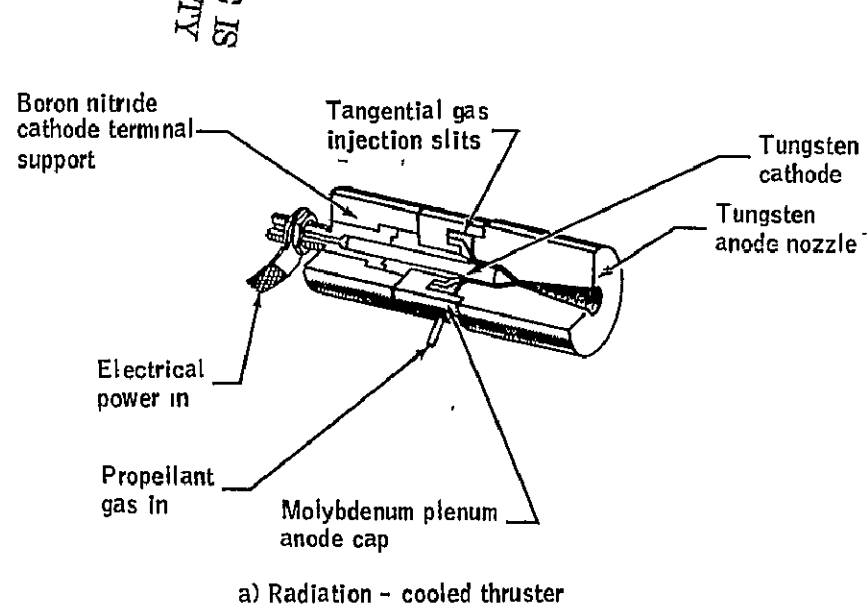


Figure VI-D-1-9. - Arc jet thruster schematics

TABLE VI-D-1-5. ARC JET THRUSTER CHARACTERISTICS

DESCRIPTION	PRESSURE-FED, GAS HEATED BY ELECTRIC ARC	
	NH ₃	H ₂
PROPELLANT	NH ₃	H ₂
THRUST	50 lb _f	50 lb _f
CHAMBER PRESSURE	1 ATM	1 ATM
ISP	1,500 SEC	3,000 SEC
INPUT POWER	4 MW	6.5 MW
VOLTAGE (DC)	100	200
THERMAL EFFICIENCY	80	90
OVERALL EFFICIENCY	40	50
WEIGHT	5,000	5,000

VI-D-1-21

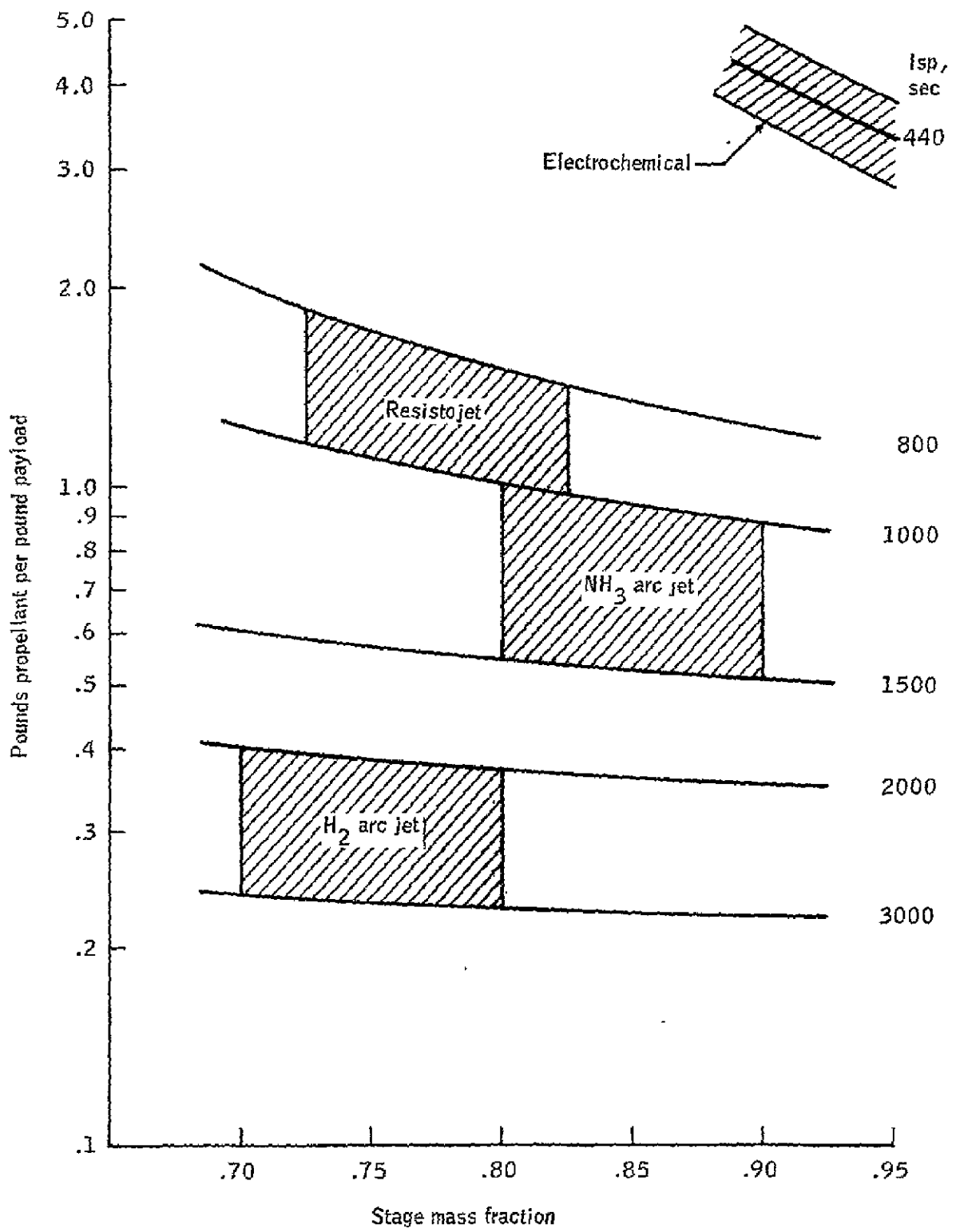


FIGURE VI-D-1-10. Electric OTV parametrics, $\Delta V = 19\ 000$ (KSC launch).

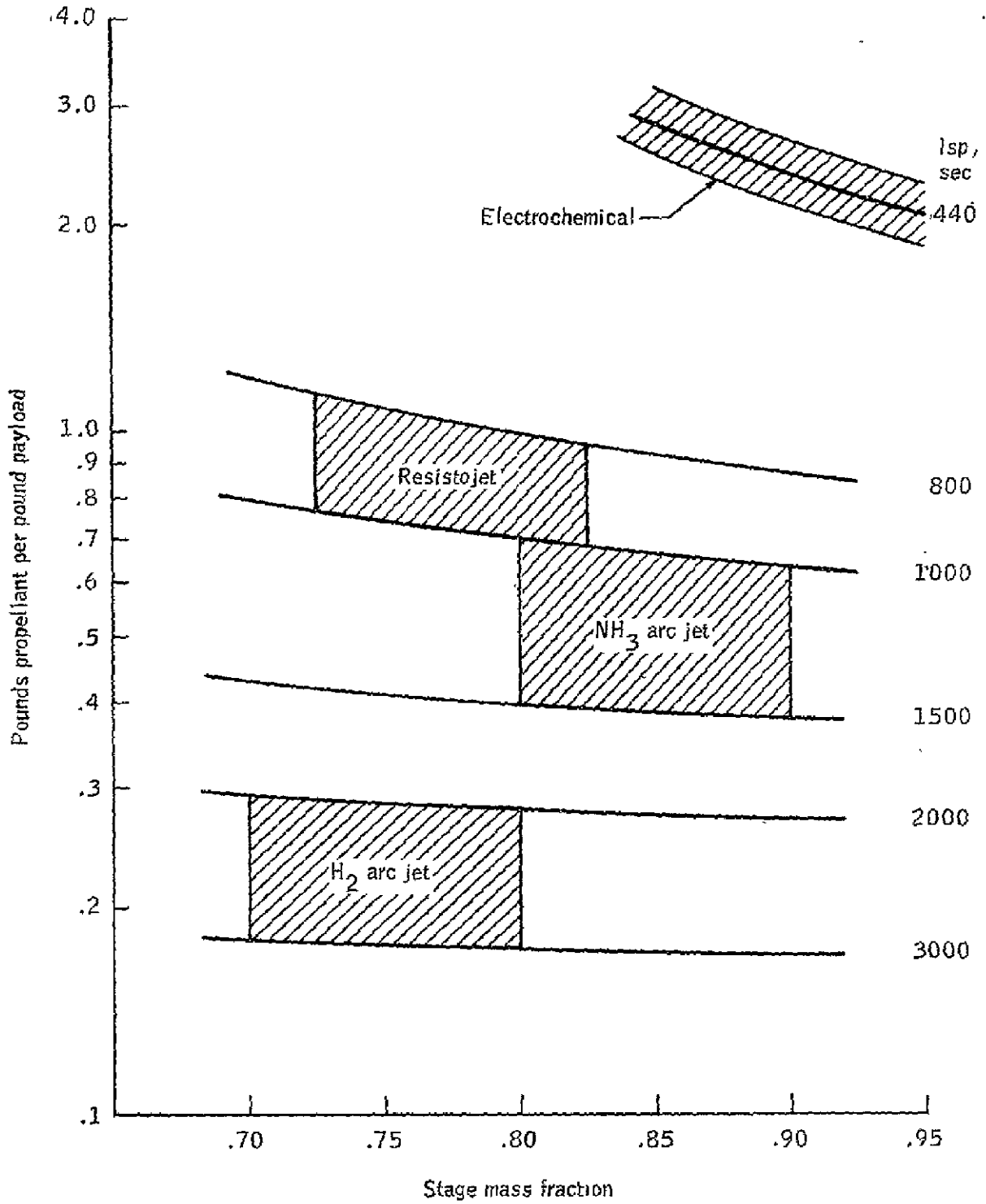


FIGURE VI-D-1-11. - Electric OTV parametrics, $\Delta V = 15\ 000$ (equatorial launch).

The line of reasoning followed for the chemical stage which led to the selection of a stage consisting of clustered propellant tanks, each of which comprises an HLLV payload, is also applicable to the electric stages.

An additional consideration for the dependent electric COTV's is that the satellite must be configured and oriented such that sufficient power is available from the satellite to maintain the required thrust. This requirement could result in impacts to the SPS arrays, RCS, and structures that have not been assessed.

These COTV options also have a problem with respect to occultation by the earth while in LEO. Preliminary estimates are that, until the orbit altitude reaches some 400 nmi, occultation will occur during each orbit. Although the ΔV budgets and trip time relations used were developed on the basis of no primary propulsion during occultation, some darkside thrust capability would seem desirable if not necessary.

Without resorting to electrical energy storage, three options are available: (1) use of an independent power source up to the altitude where occultation is not a problem; (2) use of auxiliary chemical engines on the electric COTV for darkside thrusting; or (3) operation of the electric thrust systems in some type of tailoff mode.

As an example of the first option, figure VI-D-1-12 presents a plot of the total weight of a two-stage hybrid COTV (using a chemical first stage and an arcjet second stage) as a function of the first stage ΔV . At 7200 ft/sec, the total weight is found to be approximately 83 MLB, or some 27 MLB more than using a single-stage arcjet neglecting the occultation problem. Option (2) was favored by Boeing in their look at the SPS transportation problem in the FSTSA study. They estimated a required ΔV of 790 ft/sec, resulting in a propellant requirement of 3.24 MLB of O_2/H_2 propellants.

The third option envisions using the inherent capability of the thruster itself in some type of tailoff mode. For the electrochemical system, a simple oversizing of the gaseous propellant accumulators would allow darkside thrusting with a moderate weight penalty and little or no performance degradation. For the arcjet thrusters, tailoff mode operation (with electrical power off) has been investigated. Figure VI-D-1-13 illustrates the type of performance that can be obtained; even after several thousand seconds, the thrust and Isp are considerably higher than cold-flow values. Assuming an effective Isp of 15 percent of nominal, the propellant penalty for operating in this mode would be on the order of 3.5 MLB.

The resistojet probably does not have as good a tailoff performance characteristics as an arcjet; the performance would essentially be at cold-flow levels.

1.3.3 SYSTEM COMPARISONS

The electric COTV concepts are compared in table VI-D-1-6. The thrust level was determined by arbitrarily setting the initial T/W to 10^{-4} g, except for the electrolysis stage, where the initial T/W was reduced to 5×10^{-5} g to avoid excessive weights of the

VI-D-1-25

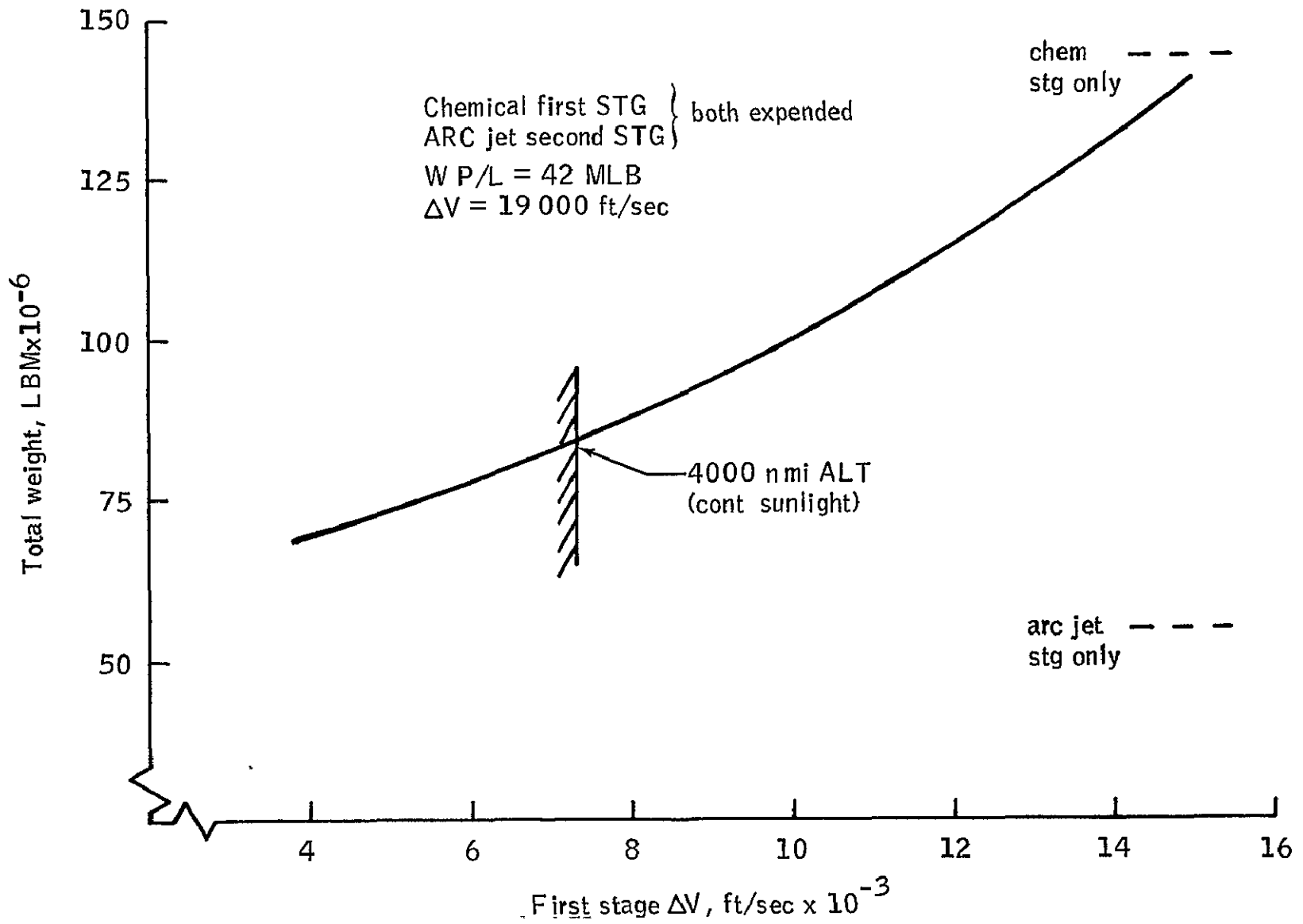


FIGURE VI-D-1-12.- 2-stage hybrid OVT.

ORIGINAL PAGE IS
OF POOR QUALITY

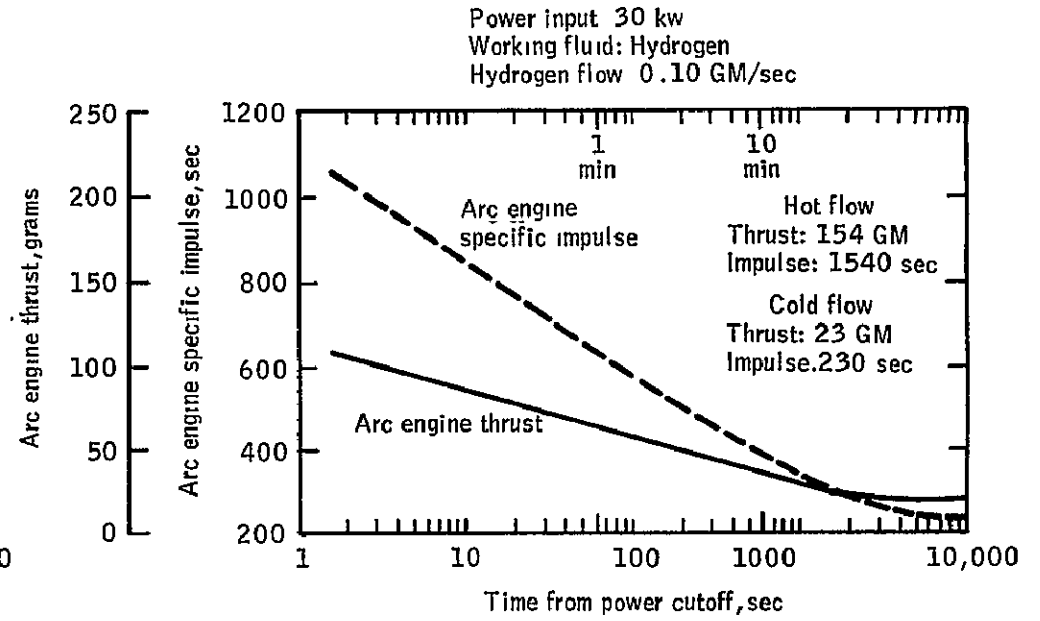
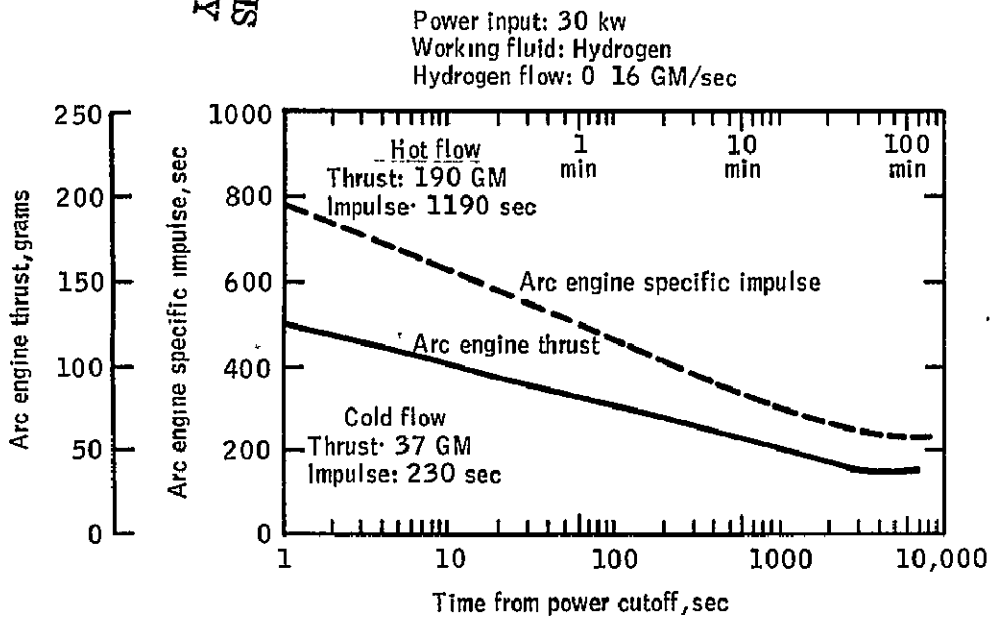


Figure VI-D-1-13. - Arc engine thrust and specific impulse vs time from power shut-off for a low hydrogen flow rate

TABLE VI-D-1-6.

ELECTRIC OTV CONCEPT COMPARISON

		ELECTRO CHEMICAL		RESISTO- JET		ARC JET		ARC JET
PROPELLANT		H ₂ O	-	H ₂		NH ₃		H ₂
Isp (SEC)		440		1,000		1,500		3,000
THRUST (LBF)		10K		11K		6.7K		5.6K
BURNOUT T/W (G)		1.9×10^{-4}		1.9×10^{-4}		1.5×10^{-4}		1.2×10^{-4}
TRIP TIME (DAYS)		98		55		57		61
POWER REQUIRED (GW)		0.20		0.38		0.54		0.73
POWER REQUIRED (% OF CAP.)		5		9.5		13.5		18.3
WEIGHTS (MLB)								
THRUSTERS		.01		.01		.67		.56
POWER COND.		1.52		.08		.11		.15
PROP TANKS		3.55		10.38		.93		2.27
STRUCTURE		3.41		1.67		.69		.41
OTHER		1.70		2.43		.48		.68
TOTAL DRY WEIGHT		10.19		14.57		2.88		4.07
UNUSABLE PROP.		1.68		1.12		.37		.24
TOTAL INERT WEIGHT		11.87		15.69		3.25		4.31
IMPULSE PROP		150.8		46.2		21.84		10.08
TOTAL STAGE WEIGHT		162.67		61.89		25.09		14.39
PAYLOAD		42		42		42		42
TOTAL LEO WEIGHT		204.7		103.9		67.1		56.4

VI-D-1-27

electrolysis unit. The variation in trip time among the other concepts is merely the result of weight variations and is not significant. Since none of these concepts uses over 20 percent of the available satellite power, shorter trip times are possible for each, with weight penalties dependent on each concept. Figure VI-D-1-14 illustrates the trend of trip time with power requirements.

For the numbers presented in table VI-D-1-6, the same caveat as expressed for the chemical stage applies: these values must be regarded as highly preliminary and subject to large changes as the ground rules and assumptions change. Three major assumptions for these dependent electric COTV concepts that do influence the COTV sizing are as follows:

- no satellite penalty for supplying power to COTV
- satellite performs own altitude control
- no allowance made for occultation thrusting

1.3.4 TECHNOLOGY ISSUES

Except for the issue common to all dependent electric COTV's of power distribution from the satellite, there do not appear to be any significant technology issues for the electrolysis concept. It shares, with the chemical as well as the other electric stages, the problem of size, construction, operation, and economic viability discussed earlier.

The resistojet is a simple electric thruster with demonstrated high reliability. The major technology issue associated with the resistojet is the unknown impacts of the several order-of-magnitude scale-up from existing thrusters to the size required for the COTV.

A similar uncertainty regarding scale-up exists for the arcjet thruster, together with concerns regarding the weight and cost of a thruster some 20 to 50 times larger than the largest existing thruster. Electrode erosion has been a life-limiting factor for arcjet, and the attempt to build high performance, lightweight, long-life thrusters will be a significant technology challenge.

62-1-0-1A

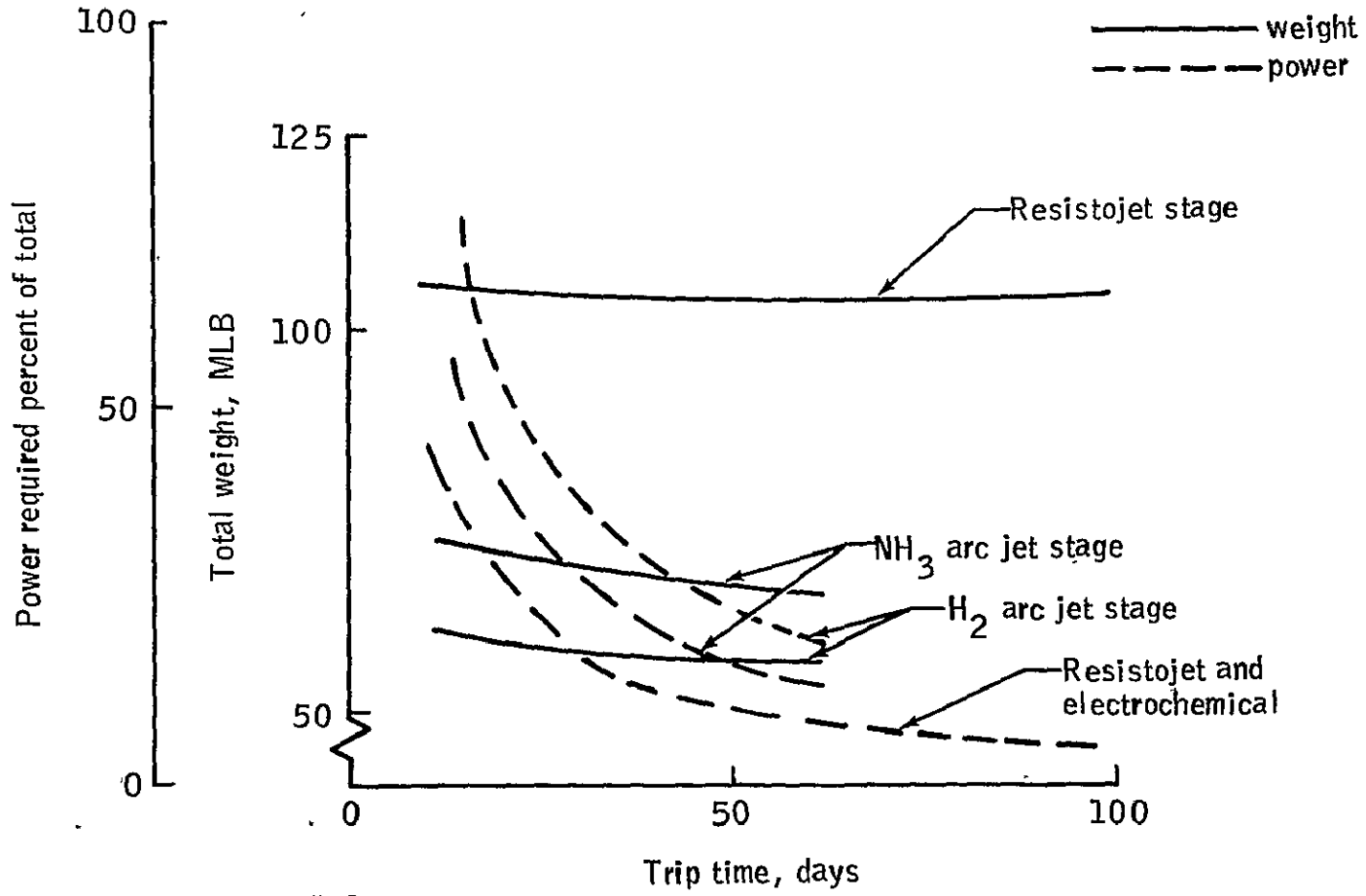


FIGURE VI-D-1-14.- Electric OTV effect of trip time on weight and power.

1.4 ELECTRICALLY - POWERED COTV - HIGH SPECIFIC IMPULSE (W. F. Perlich, Future Programs Office)

1.4.1 GENERAL

Electrically powered propulsion systems of the previous section all derive their thrust by thermal propellant heating in a pressure chamber and normal exhaust via an engine nozzle. Maximum specific impulse values between 440 and 3000 seconds are predicted.

This section investigates thruster concepts in which the propellant is ionized and electrostatically or electromagnetically accelerated to very high exhaust velocities. With argon as a propellant, maximum specific impulses of 5,000 to 20,000 seconds appear to be attainable.

Two specific designs falling within this context are selected as representative and most appropriate for COTV/SPS functions: a relatively straightforward ion design and a combined magnetoplasma-dynamic-arcjet (MPD-arcjet) design with external magnetic coil for arc control and stability. Both independent operation and operation dependent upon SPS electrical power is considered.

1.4.2 THRUSTERS

1.4.2.1 PROPELLANT SELECTION

Mercury and cesium have been almost exclusively selected as a propellant for early engine development because of easy ionization, high density/efficient storage, and compatibility with electrical thruster design considerations. They are not acceptable for the SPS orbit transfer function, however, because of scarcity, high cost, and for mercury, a serious environmental compatibility question. Therefore, argon has been selected as the propellant for both ion and MPD-arcjet thrusters since it is cheap and abundant, possesses good density/storage and performance qualities, is nonpolluting, and unlike hydrogen and helium, possesses excellent frozen flow efficiencies as shown in Figure VI-D-1-15. Its major disadvantage, cryogenic handling and storage, is not considered an overriding issue.

1.4.2.2 ION CHARACTERISTICS

The ion/argon thruster design is based on previous extensive electrical propulsion R&D activities, including the Lewis Research Center (LeRC) development of their 30 centimeter mercury bombardment ion thruster and propulsion system. The magnitude of the effort required for extrapolation of the LeRC design to a larger size (30 to 150 centimeters) and argon propellant is uncertain but is generally considered to be entirely feasible.

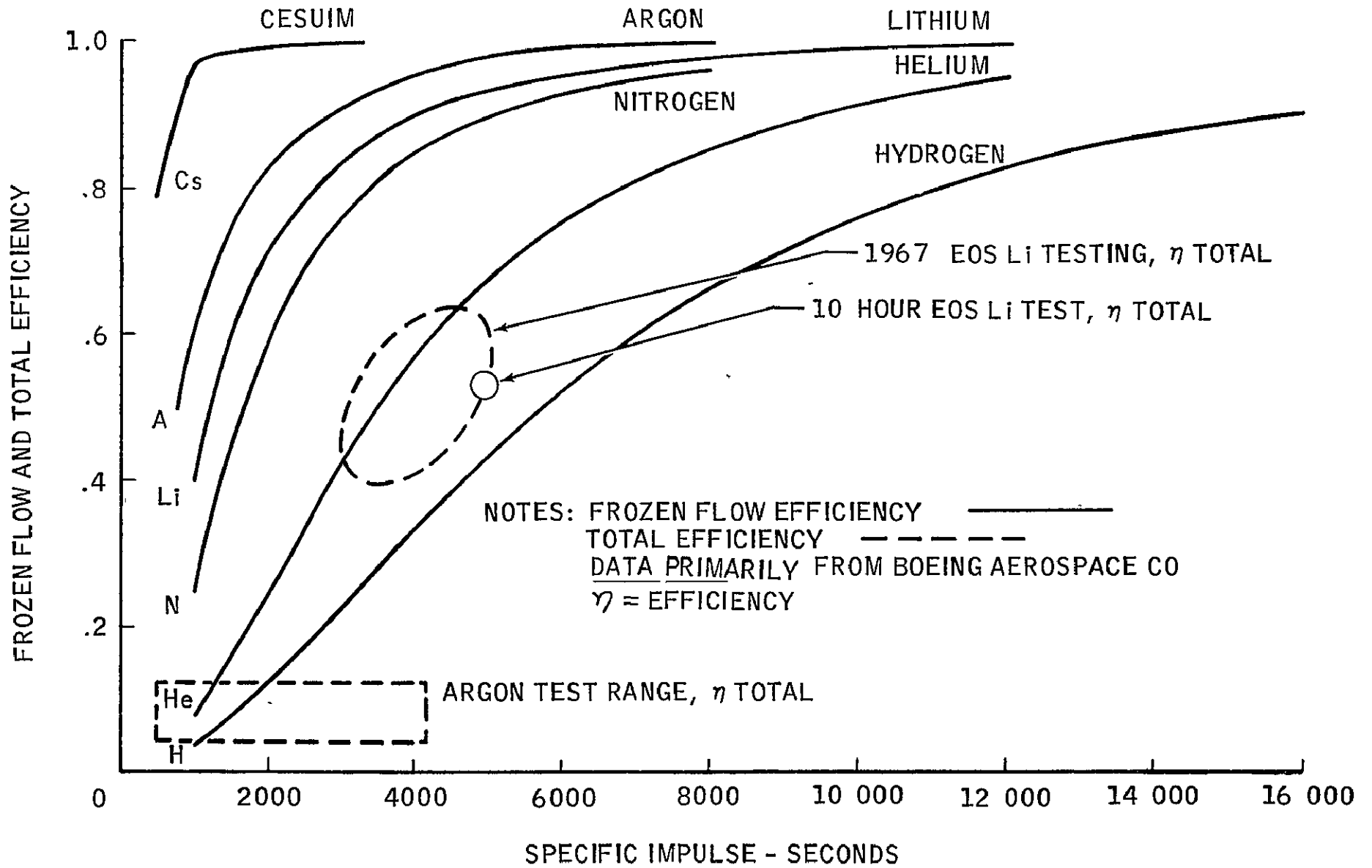


FIGURE VI-D-1-15. - THEORETICAL FROZEN FLOW AND TOTAL TEST EFFICIENCIES.

Table VI-D-1-7 shows predicted characteristics for two sizes of argon thrusters, with the 30 centimeter size described at the lower end, and the 100 centimeter size at the higher end of the specific impulse range. This range of about 7,500 to 20,000 seconds is limited on the low end by a rapid loss of efficiency and at the high end by high voltage constraints. Within the range, however, the designer has full flexibility of specific impulse selection by proper choice of design and operating parameters. Particularly important characteristics, inherent in electrostatic acceleration thrust devices and which significantly impact the selection and application of the ion thruster, include the following:

- o Low thrust level, an inherent current density limitation due to the exhaust space charge, dictates large numbers of heavy thrusters to achieve an adequate total propulsive force for transfer times of 6 months or less.

- o Low thrust to weight ratio due to complex hardware and the low thrust level.

- o Extremely high exhaust velocity (or specific impulse), limited primarily by accelerating voltage breakdown levels, allows a tremendous reduction in total propellant mass.

- o High input power to thrust ratio, a penalty of achieving high specific impulse, dictates a correspondingly large electrical power source.

- o High overall efficiency reduces waste heat/thermal control problems.

- o Requirement for very stable, multilevel voltages dictates expensive, complex, heavy power conditioning.

Although little doubt exists as to the basic feasibility of developing an ion/argon engine, available data is insufficient to define exact characteristics within the ranges shown in Table VI-D-1-7. A best estimate at this time, however, indicates a multiple cathode device of at least 100 centimeter size and a specific impulse of about 10,000 seconds. This value is well above the efficiency roll-off point and yet does not seriously push into extremely high exhaust velocity ranges. Based on the mercury engine, a 24 month operating life is probably realistic.

1.4.2.3 MPD-ARCJET CHARACTERISTICS

At the present time, MPD type thrusters are receiving limited United States research attention, primarily by Princeton University, but have received little attention since the late 1960's when emphasis

TABLE VI-D-1-7. POTENTIAL THRUSTER CHARACTERISTICS

<u>ITEM</u>	<u>MPD</u>	<u>30 CM</u>	<u>ION</u>	<u>100 CM</u>
Propellant	Argon	Argon		Argon
Specific Impulse (Sec)	2K-10K(2)	5K-20K(1)		5K-20K(2)
Thrust (lbf)	50	0.02		0.85
Input Power (kWe)	1.6K-16K	3.3		459
Voltage (DC Volts)	300	600		10K
Thrust/Weight	0.01 to 0.1	3.8×10^{-4}		2.5×10^{-4}
Input Power/Thrust (kWe/lbf)	300	175		543
Overall Efficiency (%)	45-70	65		85
Continuous Operating Life (Months)	3-24	24		24
Recurring Cost (\$K)	TBD	7.5-24		13-65

(1) The following characteristics relate to low specific impulse value.

(2) The following characteristics relate to high specific impulse value.

increasingly focused on electrostatic devices which are more suitable than MPD devices for the very high energy planetary missions. In addition, basic MPD theory is not well understood, and important anomalies within test results remain essentially unresolved. Consequently, MPD thruster and propulsion system characteristics and programmatic factors cannot be confidently predicted.

The proposed thruster, which ionizes argon propellant by means of an electric arc, accelerates the plasma both by MPD action and by the thermal energy generated in the plasma by the arc. Thus, the dual operation, MPD-arcjet thruster is designed to optimize total combined performance from both accelerating forces.

Figure VI-D-1-15 indicates very poor overall efficiencies resulting during the very limited past laboratory testing of argon as a propellant. Note, however, that 1967 Electro-Optical Systems Company (EOS) lithium propellant tests resulted in much improved performance and that theoretical frozen flow losses (a major determinate of total efficiency) for argon are actually less than for lithium. These factors have generated considerable agency and industry optimism that argon performance can be improved to acceptable levels with additional laboratory research.

Table VI-D-1-7 shows predicted MPD-arcjet characteristics, with a range of performance uncertainties just discussed. As with the ion thruster, the designer has full flexibility to adjust the operating specific impulse within the full design range.

Important factors, inherent in MPD-arcjet thrust devices, which significantly impact selection for the COTV function, include the following:

- o Moderate thrust levels and thrust to weight ratios.
- o Possibly high specific impulse.
- o Simple thruster hardware with nominal amounts of power conditioning.
- o Uncertain overall efficiency and corresponding thermal control considerations.
- o Uncertain operating life without refurbishment.
- o Definite requirement for additional, laboratory hardware research and state-of-the-art advancement.

In summary, the MPD-arcjet thruster holds promise of being the optimum selection for the COTV propulsion function; however, even its basic feasibility cannot be determined without additional laboratory research.

1.4.3 PROPULSION SYSTEMS

Since detailed, firm MPD or ion/argon thruster data is not available, comprehensive and accurate system design is not possible at this time. Assessment and integration of various contractor and NASA (including JSC) studies, estimates, and considerations, however, results in the system descriptions of this section.

1.4.3.1 INDEPENDENT COTV

The most promising application of high performance electrical thrusters to the independent COTV consists of the nuclear reactor-electrical thruster combination (or nuclear-electric COTV). Major advantages of this approach, as compared to propulsion systems utilizing SPS electrical power, include avoidance of Van Allen belt radiation damage to the payload's solar energy collector, elimination of primary power loss during Earth occultation, and availability of the COTV for a wide variety of cargo and payload transport in addition to the specialized function of SPS orbit transfer.

THRUSTER SELECTION

Since the self contained power source is limited in capacity, extremely high specific impulse thrusters with their correspondingly high input power demands tend to be ruled out. Thus, the simple, low specific mass, MPD-arcjet thruster with moderate power conditioning requirements is chosen over the complex, high specific mass ion engine and extensive, heavy power conditioning unit.

REPRESENTATIVE SYSTEM

A representative, independent COTV system consists of MPD-arcjet thrusters, argon propellant, a high temperature/fast spectrum reactor cooled by heat pipes (a JPL design), and either a thermionic or Brayton cycle turbo generator energy converter. Mass properties of the COTV presented in Tables VI-D-1-8 and VI-D-1-9 were derived from data generated in Boeing's "Future Space Transportation Systems Analysis Study" and were based on the following mission and hardware assumptions:

- o Payload is 500,000 lb (226.76 metric tons)
- o Representative mission: 92 day low Earth orbit (LEO) to geosynchronous Earth orbit (GEO) payload transfer; 29 day COTV return to LEO.
- o Maximum mission: 120 day LEO to GEO payload transfer; 416 day COTV disposal to solar system escape (SSE).
- o LEO to GEO $\Delta v = 19,685$ fps for orbit transfer, 28.5° plane change, 1.9% thrust vector loss, and 2% reserve. GEO to SSE $\Delta v = 64,800$ fps for trajectory, 2% thrust vector loss, and 2% reserve.

TABLE VI-D-1-8. NUCLEAR-ELECTRIC COTV MASS

<u>Subsystem</u>	<u>KG</u>	<u>LB</u>
STRUCTURE	(3,640)	(8,026)
PROPULSION	(6,700)	(14,774)
Main Thrusters	400	882
Main Tanks/Plumbing	4,800	10,584
Aux. Thrusters	330	728
Aux. Tanks/Plumbing	1,170	2,580
AVIONICS	(260)	(573)
ELECTRICAL POWER	(85,060)	(187,557)
Reactor/Reflector	19,960	44,012
Heat Exch./Prim. Loop	5,200	11,466
Turbogen/Recuperator	19,600	43,218
Outer Gamma Shield	14,500	31,973
Power Processor	12,000	26,460
Radiator/Cooling Loops	11,500	25,357
Power Distribution	400	882
Aux. Power	1,900	4,189
THERMAL CONTROL	(2,220)	(4,895)
CONTINGENCY (APPROX. 15%)	<u>(14,430)</u>	<u>(31,818)</u>
TOTAL DRY MASS	(112,310)	(247,643)
Unused Propellant	(7,350)	(16,207)
Elect. Power Reactants	<u>(364)</u>	<u>(803)</u>
TOTAL PROPULSION VEHICLE	(120,024)	(264,653)

TABLE VI-D-1-9. NUCLEAR-ELECTRIC COTV EXPENDABLES

MISSION: Payload LEO to GEO & COTV Return to LEO

o UP Trip $\Delta v = 19,680$ fps		
Main Propellant	105,857 KG	(233,414 LB)
Aux. Propellant	<u>2,604 KG</u>	<u>(5,742 LB)</u>
Total Up Propellant	108,461 KG	(239,156 LB)
o DOWN Trip $\Delta v = 19,680$ fps		
Main propellant	33,288 KG	(73,399 LB)
Aux. Propellant	<u>819 KG</u>	<u>(1,806 LB)</u>
Total Down Propellant	34,107 KG	(75,205 LB)
o TOTAL EXPENDABLES	142,568 KG	(314,361 LB)

MISSION: Payload LEO to GEO & COTV Disposal to Solar System Escape (SSE)

o LEO to GEO $\Delta v = 19,680$ fps		
Main Propellant	139,256 KG	(307,060 LB)
Aux. Propellant	<u>3,426 KG</u>	<u>(7,554 LB)</u>
Total LEO-GEO	142,682 KG	(314,614 LB)
o GEO to SSE $\Delta v = 64,800$ fps		
Main Propellant	150,467 KG	(331,780 LB)
Aux. Propellant	<u>3,701 KG</u>	<u>(8,162 LB)</u>
Total GEO to SSE	154,168 KG	(339,942 LB)
o TOTAL EXPENDABLES	296,850 KG	(654,556 LB)

- o MPD-arcjet thruster specific impulse = 2500 sec, efficiency = 45%, and specific power = 10 KWj/KG (or thrust/weight about 0.08).

- o Single ended Brayton cycle turbogenerator energy converter system, arbitrarily selected because of its better definition.

- o Total thrust power = 4.0 MWj._____

It is noted that recent Boeing study indicates that total spacecraft mass is nearly identical for either the thermionic or Brayton converter design. Thus, total COTV hardware and propellant mass figures are representative of either design. Additionally, final disposal of the COTV's nuclear reactor to solar system escape (SSE) is costly in COTV propellant tank weight; alternate disposal techniques, such as solar orbit or even storage in orbit with subsequent disassembly and selective component return to Earth, may prove to be a better choice. Finally, the selection of 2500 sec specific impulse is thought to be conservative and based on the uncertainties of thruster performance. Recent Boeing studies indicate that a figure of about 5000 sec, if attainable, is closer to optimum.

In summary, a round trip nuclear-electric tug for 3 month LEO-GEO transfer of a 500,000 lb. payload has a total vehicle and propellant mass about equal to the payload mass. Due to the need for Earth biosphere protection, disposal of the tug's radioactive components after useful life appears to be a serious problem.

OPERATIONS

The nuclear-electric tug is operationally expensive, both because of the 120 day round trip transfer time required for the basic mission and due to the long operational period associated with final disposal of the vehicle at the end of its service life. For its basic, orbit transfer mission, SPS operational capabilities, including ground tracking, communication, monitor, and control, would be used. The major tradeoff is between long operating time versus COTV/propellant life, size, mass, and cost. The 90 day up trip time is considered about a minimum commensurate with reasonable vehicle design. A major unique requirement for the nuclear-electric COTV consists of long term, separate, deep space operational support for vehicle disposal to solar system escape or to solar orbit. This assumes that vehicle disassembly and recovery of the reactor for alternate, radioactive waste disposal does not prove to be feasible, and requires that a significant portion of the system life must be reserved for the disposal mission.

COSTS

A comprehensive cost analysis, including all nonrecurring as well as recurring programmatic costs, has not been made of the nuclear-electric COTV. JPL has made a rough, recurring cost estimate of \$50M

per MWe of thruster input power for a generally similar thermionic converter vehicle with the following characteristics:

- o Payload: 500,000 lb. (226,757 KG)
- o Tug lifetime: 97.2 months
- o LEO to GEO transfer time with payload: 123 days minimum
- o Specific impulse: 2040 sec.
- o MPD thruster efficiency = 50%

Extrapolating from this data, the tug of this section is estimated to have a recurring, hardware cost of \$400M and a cost per flight (excluding refurbishment and assuming 20 months of useful, Earth orbit transfer lifetime) of \$400M/5 trips or \$80M/flight.

1.4.3.2 MPD-ARCJET DEPENDENT COTV

Recent studies within industry and NASA suggest that the MPD-arcjet design becomes a leading contender for the low thrust COTV application if the upper range of MPD thruster efficiency, jet velocity, and operational life can be achieved. Boeing FSTSA studies have defined the system presented in this section. This system, considered broadly representative of the more optimistic MPD designs, derives its basic electrical power from an external source, and is based on assumptions shown in Table VI-D-1-10. Important factors leading to this design include the following:

EFFICIENCY

Predictions of attainable MPD-arcjet thruster efficiencies vary from 10% in the earlier literature to current estimates up to 80%. The resulting MPD system assessment for the COTV function thus ranges from worthless to possibly the best of all choices. JPL assumes a constant efficiency of between 40 to 50%, whereas Boeing considers the efficiency variable with jet velocity, from about 35% to 70%. The MPD-arcjet COTV of this section incorporates the latter assumption and thus may achieve an improved thruster compared to the JPL concept and a reduction in required SPS power at any particular specific impulse design point.

SPECIFIC IMPULSE

Early estimates of the optimum specific impulse (or jet velocity) for MPD-arcjet thruster operation in the dependent COTV mode were in the 2000 to 2500 second range. Based on the assumptions of Table VI-D-1-10 and the factors of this section, however, an optimum specific impulse of between 6100 and 8200 seconds (60 and 80 KM/sec) is indicated. This is presented in Table VI-D-1-11 and Figure VI-D-1-16. Note that for the constant efficiency thruster assumption, a much lower specific impulse and jet velocity of about 4100 seconds and 40 KM/second, respectively, is indicated.

TABLE VI-D-1-10. VARIABLE EFFICIENCY MPD-ARCJET SYSTEM ASSUMPTIONS

JET VELOCITY - 20 KM/SEC TO 80 KM/SEC

SPECIFIC IMPULSE - 2040 SEC to 8160 SEC

EFFICIENCY INCLUDING PROCESSING - 34% TO 70%

THRUSTER MASS MODEL - 10^6 KG PER KG/SEC MASS FLOW

THRUSTER COST MODEL - \$500/KG

PROCESSOR MASS MODEL - 1 KG/KWe

PROCESSOR COST MODEL - \$100/KWe

SPS MASS MODEL - 20,000 METRIC TONS (44M LB)

SPS ON-BOARD POWER - 4 GW

SPS GROUND POWER - 2.5 GW

SPS COST - \$2 BILLION

TABLE VI-D-1-11. POWER SATELLITE ORBIT TRANSFER COST

	<u>Ion</u>		<u>MPD</u> <u>Variable Efficiency</u>		
Efficiency of Elec. Thrust System	57	34	58	66	70
Jet Velocity, M/Sec	50,000	20,000	40,000	60,000	80,000
Specific Impulse (Sec)	5,100	2,040	4,080	6,120	8,160
Thurster Mass (Metric Tons)	2,330	1,460	640	420	320
Thurster Cost @ \$500,000/Ton (\$M)	1,165	730	320	210	160
PPU Power (MW)	1,536	823	881	1,110	1,400
PPU Cost @ \$100,000/MW _E (\$M)	154 ⁽¹⁾	82	88	111	140
Propellant Mass (Metric Tons)	3,630	7,550	3,310	2,200	1,650
Propellant Cost @ \$350/Ton (\$M)	1.37	2.6	1.2	.8	.6
Chem. Tug Mass (Metric Tons)	4,290	3,800	3,160	3,020	2,980
Chem. Tug Cost @\$9000/Ton/Mission (\$M)	38.6	34.2	28.4	27.2	26.8
Total Mass (Inc. Satellite Module @ 20,000, Tons)	37,930	33,630	27,990	26,750	26,350
Lift Cost @ \$45,000/Ton (\$M)	1,707	1,513	1,260	1,204	1,186
Total Cost for Transportation, Millions	3,066	2,362	1,698	1,553	1,513
Direct Transport Cost (\$/Ton)	153,300	118,000	84,900	77,600	75,700
% Module Power Used	38%	21%	22%	28%	35%
Degradation Factor ⁽²⁾	.886	.937	.934	.916	.895
Resulting Available Ground Output M _{W_e}	2,215	2,342	2,335	2,290	2,238
Assumed Satellite Module Cost, Millions	2,000	2,000	2,000	2,000	2,000
Total Cost Including Satellite, Millions	5,066	4,362	3,698	3,553	3,513
Total Cost \$/KW _E Ground Output	2,287	1,863	1,584	1,551	1,570

(1) \$100,000/MW_E is very optimistic for ion engine power processing.

(2) Assumes 30% of power used is lost due to Van Allen radiation.

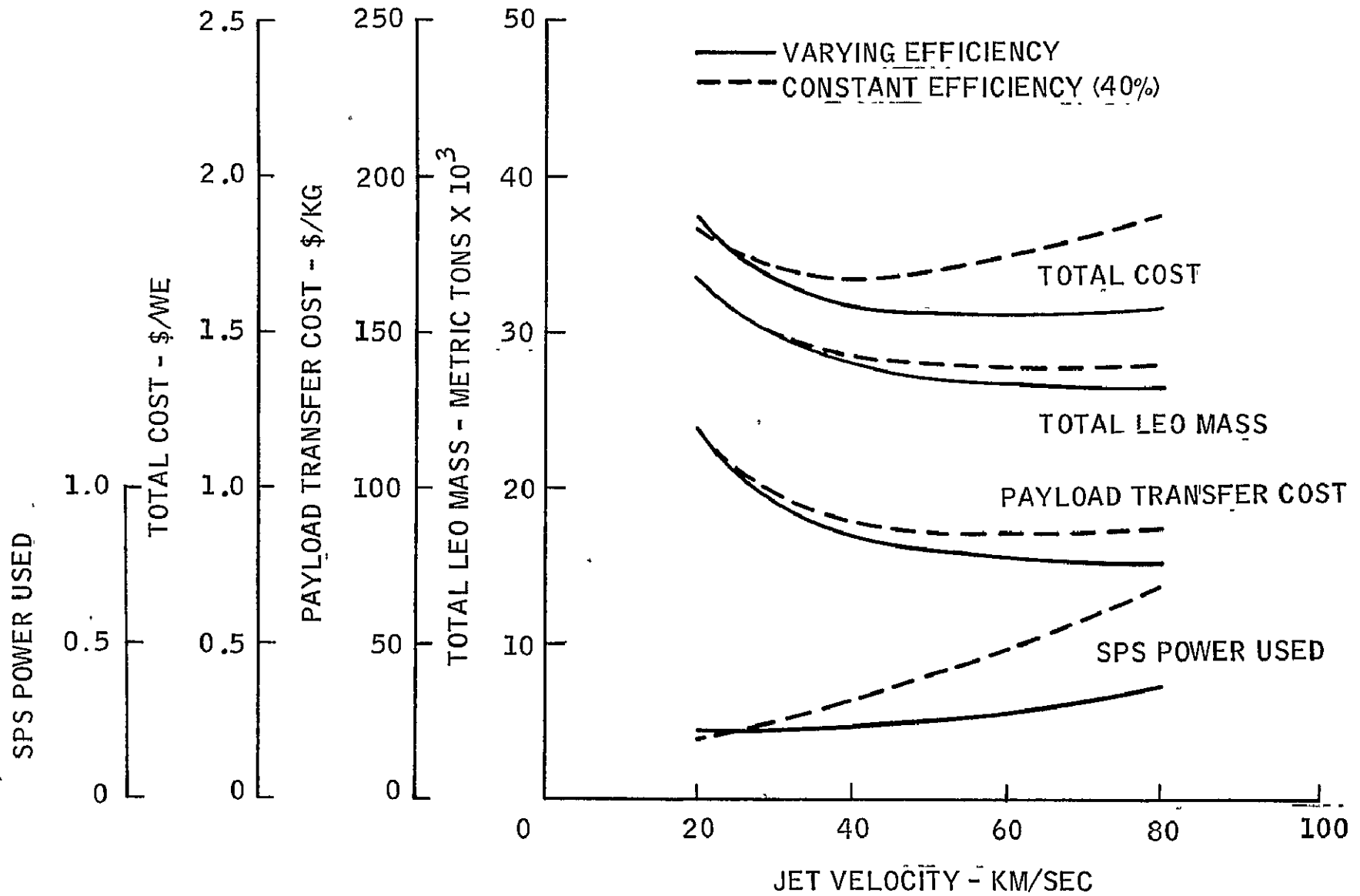


FIGURE VI-D-1-16. MPD-ARCJET COTV CHARACTERISTICS.

INPUT POWER

Figure VI-D-1-16 shows that electrical power demand on the SPS is roughly equal at about 35% of total capacity for the variable efficiency MPD-arcjet thruster operating within its optimum range at about 80 KM/sec. Input power is an important consideration since it defines the amount of SPS solar energy collector which must be exposed to Van Allen Belt radiation damage. This factor, in conjunction with orbit transfer time (or time in the radiation belt) determines total SPS generating capacity loss. Assuming that 30% of the power used for propulsion is lost due to radiation damage, the total station power loss is 10.5%.

OCCULTATION AND TRANSFER TIME

Loss of sunlight due to occultation by the Earth results in the periodic loss of SPS electrical power and attitude control. An early, generally proposed solution to the problem consisted of providing a chemical thrust system for attitude control and propulsion during occultation periods. This results, however, in many periodic start-up/run/shutdown operating cycles of both the SPS and the COTV chemical and electrical propulsion systems. Boeing proposes a different approach that first chemically transfers the SPS to an intermediate, continuous sunlight orbit and then electrically completes the GEO transfer in a continuous operation. This requires a careful combination of departure window, switchover orbit altitude and inclination, and transfer time limitation to stay in sunlight throughout the ascent. Although a switchover orbit inclination of about 55 degrees allows continuous electrical operation from the 270 NM SPS assembly orbit, Boeing proposes and utilizes a 10 day window, 1500 KM (810 NM) altitude, and 34 degree switchover orbit, and 60 day (maximum is 62 days) GEO transfer time as the optimum combination of factors.

OPERATING LIFE

Although not considered by Boeing in their recent studies, MPD thruster life predictions are perhaps the most speculative of all factors, with estimates ranging from a JSC in-house estimate of 3 months to JPL's recent assumption of 70,000 hours (about 97 months). The former fits comfortably within a single SPS transfer mission with expendable thrusters and the latter suggests the possibility of further engine utilization at GEO for SPS attitude control after the orbit transfer operation. The longer lifetimes appear to be questionable and a nominal value of 7 or 8 months (about 5,000 and 5,800 hours, respectively) within a total range of 2 to 24 months is suggested for current study purposes.

ACCELERATION

Electrical propulsion acceleration of the "reference" system varies from 10^{-4} g at start of thrust to 1.25×10^{-4} g at thrust termination.

REPRESENTATIVE SYSTEM

An exhaustive and accurate design of the MPD-arcjet COTV appears beyond our grasp at this time due to uncertainty in thruster performance

and mass characteristics. The data of Table VI-D-1-9, based on the assumptions of Table VI-D-1-10 are therefore considered as representative as is available at this time. The mass breakdown is as follows:

Electrical Thrusters	420,000 KG
PPU, structure, other	1,110,000 KG
Chemical tug, dry*	<u>181,200 KG</u>
Total dry COTV	1,711,200 KG
*Assumes 0.94 mass fraction	
Argon (5,730 M/S Δv)	2,200,000 KG
LOX/LH ₂ (500 M/S Δv)	<u>2,838,800 KG</u>
Gross Mass	6,750,000 KG

Total vehicle and payload mass characteristics as a function of switchover altitude are shown in Figure VI-D-1-17.

OPERATIONS

The COTV is not reused after SPS orbital transfer. Consequently, COTV operations are limited to standard launch to LEO, installation of COTV modules on the SPS structure, and the LEO to GEO transfer flight. During the transfer mission, the COTV operates integrally with the SPS and depends primarily upon SPS ground support capacities and facilities, supplemented as required for specialized COTV functions.

COSTS

Recurring cost estimates are shown in Table VI-D-1-11 and summarized on Figure VI-D-1-16. R&D costs to achieve a satisfactory and dependable thruster are unknown but are expected to be relatively high.

1.4.3.3 ION DEPENDENT COTV

Assuming the more optimistic MPD thruster performance predictions of Table VI-D-1-7, ion/argon propulsion systems appear to be less desirable than MPD/argon systems for the SPS dependent orbit transfer operation. This may be seen by comparing Boeing's ion/argon system of Table VI-D-1-11 and Figure VI-D-1-18 with their MPD systems. Note, however, that Boeing assumes a relatively pessimistic ion system with a specific impulse of only 5,100 seconds, an efficiency of only 57%, and power processing hardware five times heavier than for the MPD system. Relatively small shifts in either ion or MPD assumptions can have a significant impact on the relative merits of these systems.

The ion system, based on extrapolation of actual hardware experience and a much better theoretical understanding, generates a considerably higher confidence level in ultimate feasibility, design

FIGURE VI-D-1-17. MPD COTV SYSTEM CHARACTERISTICS

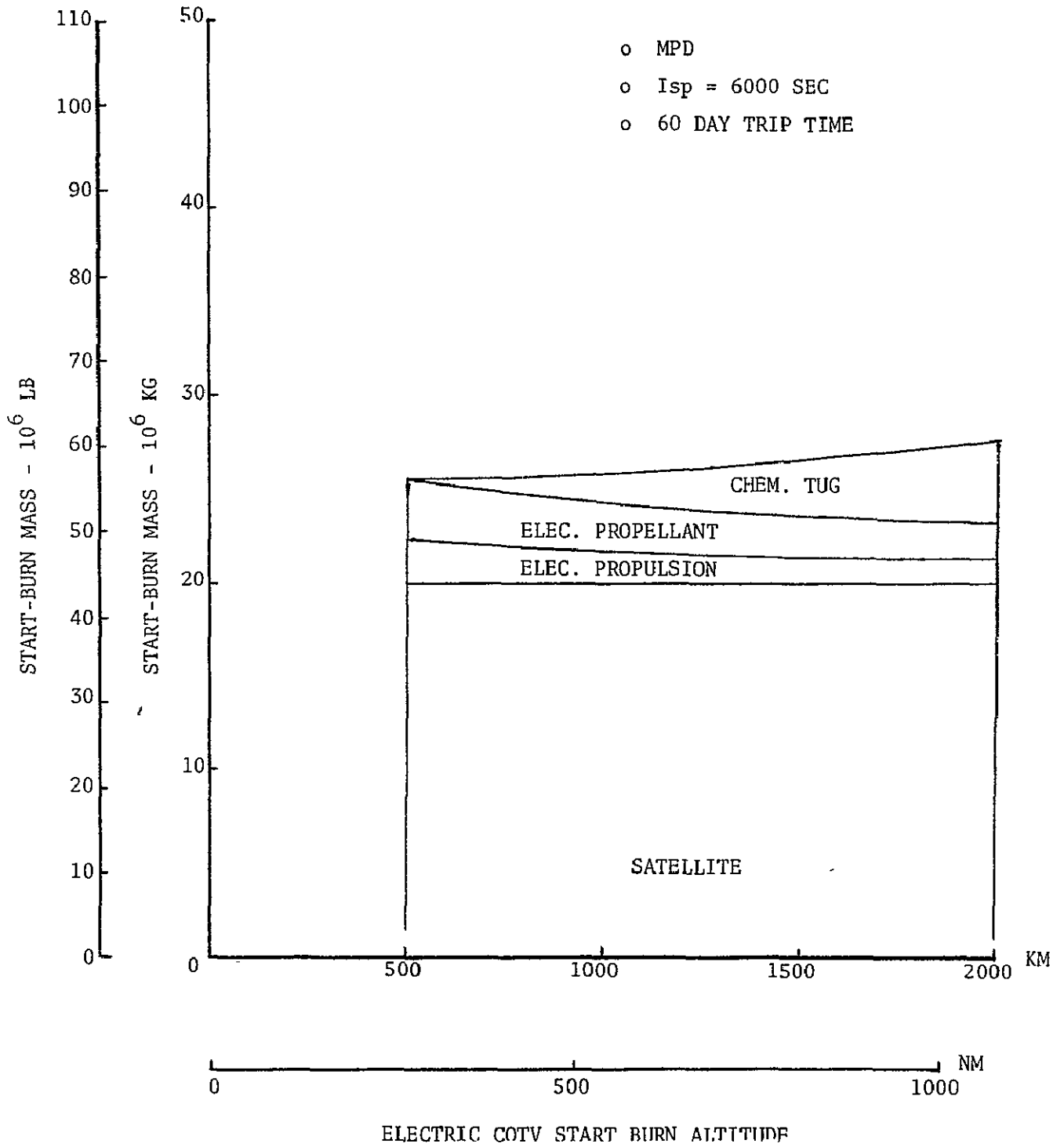
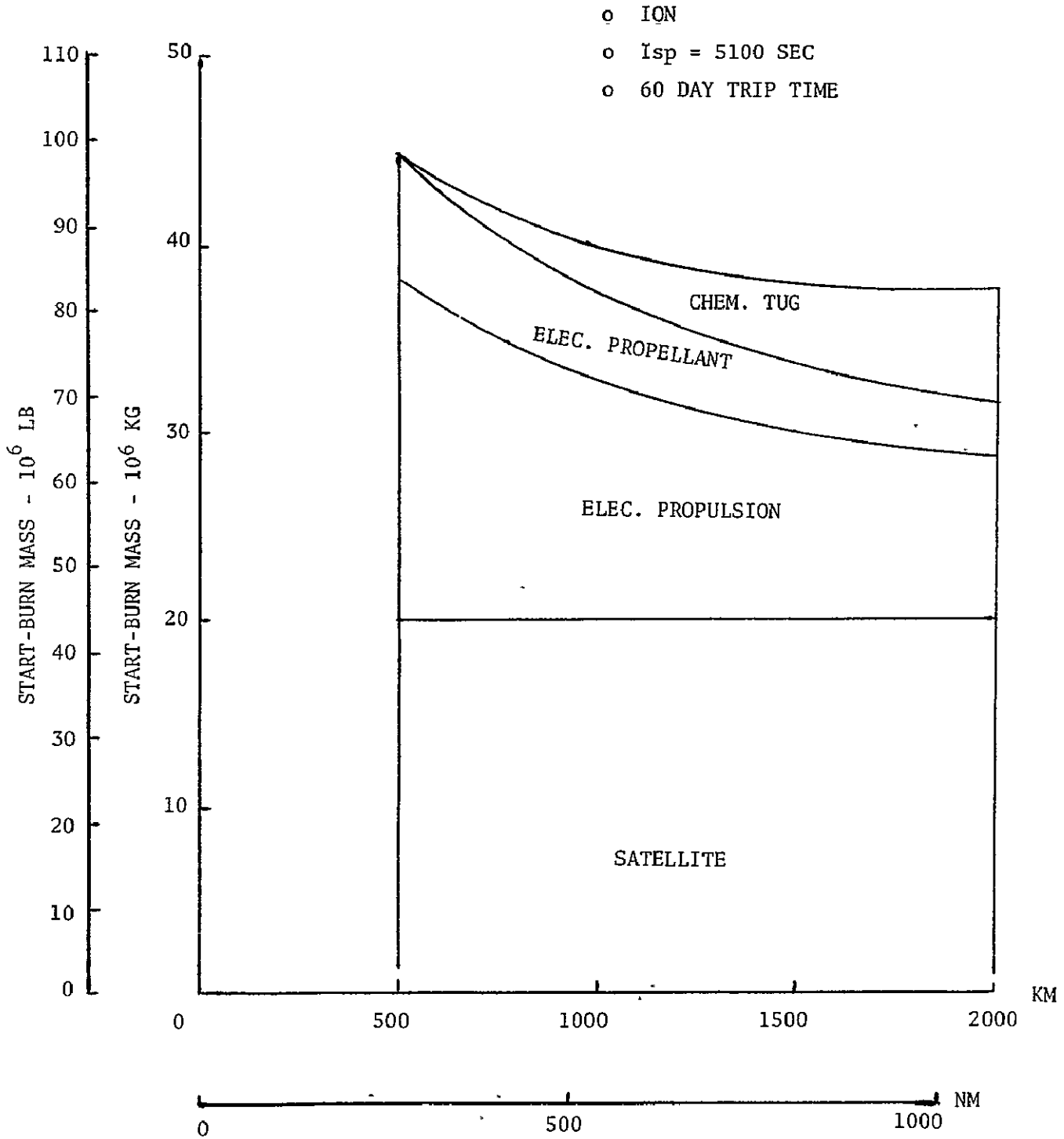


FIGURE VI-D-18. ION COTV SYSTEM CHARACTERISTICS



ELECTRIC COTV START BURN ALTITUDE

adaptation, and performance achievement. In addition, it presents the possibility of utilizing the highest jet velocities (specific impulses) of any system and may provide a much longer operating life. Therefore, it is suggested that additional study is needed before the ion/argon device is discarded as a dependent SPS propulsion system. Specific issues recommended for consideration are given in the next section, Technology Issues.

1.4.4 TECHNOLOGY ISSUES

The following issues must be resolved before a high performance electric propulsion system concept can be selected and operational hardware development initiated.

1.4.4.1 MPD THRUSTER BASIC FEASIBILITY

Resolution of the basic feasibility and gross performance of the MPD thruster requires laboratory research including development, test, and operation of a variety of laboratory thruster hardware configurations. Detailed definition and establishment of a suitable research program is indicated as a next step if the MPD device is to receive additional consideration for use in the SPS orbital transfer operation.

1.4.4.2 ION PROPULSION SYSTEM OPTIMIZATION

As discussed in section 1.4.3.3, selection of ion thrusters for the SPS orbit transfer function is dependent not so much upon basic thruster feasibility as upon thruster system performance and cost optimization and upon SPS design in enhancement of the thruster system. The following considerations are particularly significant:

- o Ion thruster and SPS power source design to minimize power conditioning requirements and hardware complexity, weight, and cost.
- o Applicability and achievement of very high jet velocities.
- o Increased engine thrust level and thrust to weight ratio.
- o Validation of expected efficiencies, shown as up to 85% for the 100 cm size thrusters in Table VI-D-1-7.
- o Define expected engine life and refurbishment requirements.

This effort is expected to be a study by knowledgeable personnel and supported by a limited amount of laboratory testing.

1.4.4.3 MPD PROPULSION SYSTEM OPTIMIZATION

After demonstration of MPD thruster basic feasibility as described in section 1.4.4.1, a system optimization can be accomplished. This will be based upon the findings of the basic research laboratory testing.

2.0 HIGH-THRUST COTV

(John C. Hooper, Primary Propulsion Branch, EP2)

2.1 GROUND RULES & ASSUMPTIONS

The high-thrust COTV is used to transport material for construction of the SPS from a LEO staging orbit to GSO. The high-thrust COTV is able to operate at a high T/W (greater than 0.1) since the payload is packaged in such a manner that it can withstand such loads. Because of the nature of the payload, it is not capable of supplying power to the COTV and the dependent power option considered for the low-thrust COTV does not exist for the high-thrust case. An HLLV payload capability of 10^6 lbm to a LEO staging point where the payload/COTV rendezvous could take place and where COTV propellant tanking could occur for a reusable COTV was assumed.

2.2 CHEMICAL STAGE
2.2.1 PARAMETRIC DATA

The high-thrust chemical COTV uses O_2/H_2 propellants. Stage weight trends for these vehicles were based on the SWOP results referenced earlier (see figure VI-D-1-2) and on sizing data provided by Boeing for the FSTSA study.

The engine size required is approximately that of the SSME; therefore, SSME derivative characteristics were used as shown in table VI-D-2-1.

Staging options considered included a single-stage expendable vehicle, and one-and-two-stage reusable vehicles. Figure VI-D-2-1 illustrates the ratio of propellant mass to payload mass for these staging modes. The curves in figure VI-D-2-1 were generated for an orbit transfer ΔV consistent with launch of the HLLV from KSC. Figure VI-D-1-3 illustrates the effect of an equatorial launch versus the KSC launch for the single-stage expendable case. Figure VI-D-1-3 also illustrates the relatively dramatic reduction in ΔV for the high T/W orbit transfer.

At a constant stage mass fraction of 0.93, the ratio of W_p/W_{p1} is 1.83 for the single-stage expendable, 2.16 for the two-stage reusable, and 2.86 for the single-stage reusable vehicle. Thus for a one million pound payload, the additional propellant required for return of the stage is 330,000 lbm for the two-stage and 1.03×10^6 for the single-stage. The boost cost alone for this propellant is \$6.6M for the two-stage or \$20.6M for the single stage (\$20/lb HLLV cost). To this must be added the propellant cost, the additional operations cost for stage retrieval and turnaround, and the additional costs for long-life reusable components.

Other options are possible, including stage-and-a-half configuration in which most of the outbound propellant is carried in expendable drop tanks left at GSO; another option is to utilize ballistic entry and recovery for certain items such as the main engine and some avionics gear. These schemes for limited or partial reusability should be investigated to determine their economic viability. For the purpose of this study, an expendable single-stage vehicle will be used.

2.2.2 OPERATIONAL CONSIDERATIONS

The basic consideration involved is whether the payload and its COTV are launched as a single HLLV payload or whether a LEO assembly is used to mate the payload and its propulsion unit following multiple HLLV launches.

For the former case, a total HLLV payload of 10^6 lbm would result in a payload delivered to GSO of approximately 330,000 lbm. Should it be required to transport an unitary payload exceeding that mass, multiple launches and LEO assembly would be required. The latter case, which admits to the requirement of LEO assembly of multiple HLLV payloads, seems to be the more conservative and flexible assumption.

TABLE VI-D-2-1. HIGH-THRUST O_2/H_2 OTV ENGINE CHARACTERISTICS

DESCRIPTION	STAGED COMBUSTION CYCLE WITH LH_2 REGEN COOLING
THRUST	500K lbf
CHAMBER PRESSURE	4,000 psia
MIXTURE RATIO	6:1
Isp	466 SEC
AREA RATIO	200:1
WEIGHT	6,700 lbm

VI-D-2-3

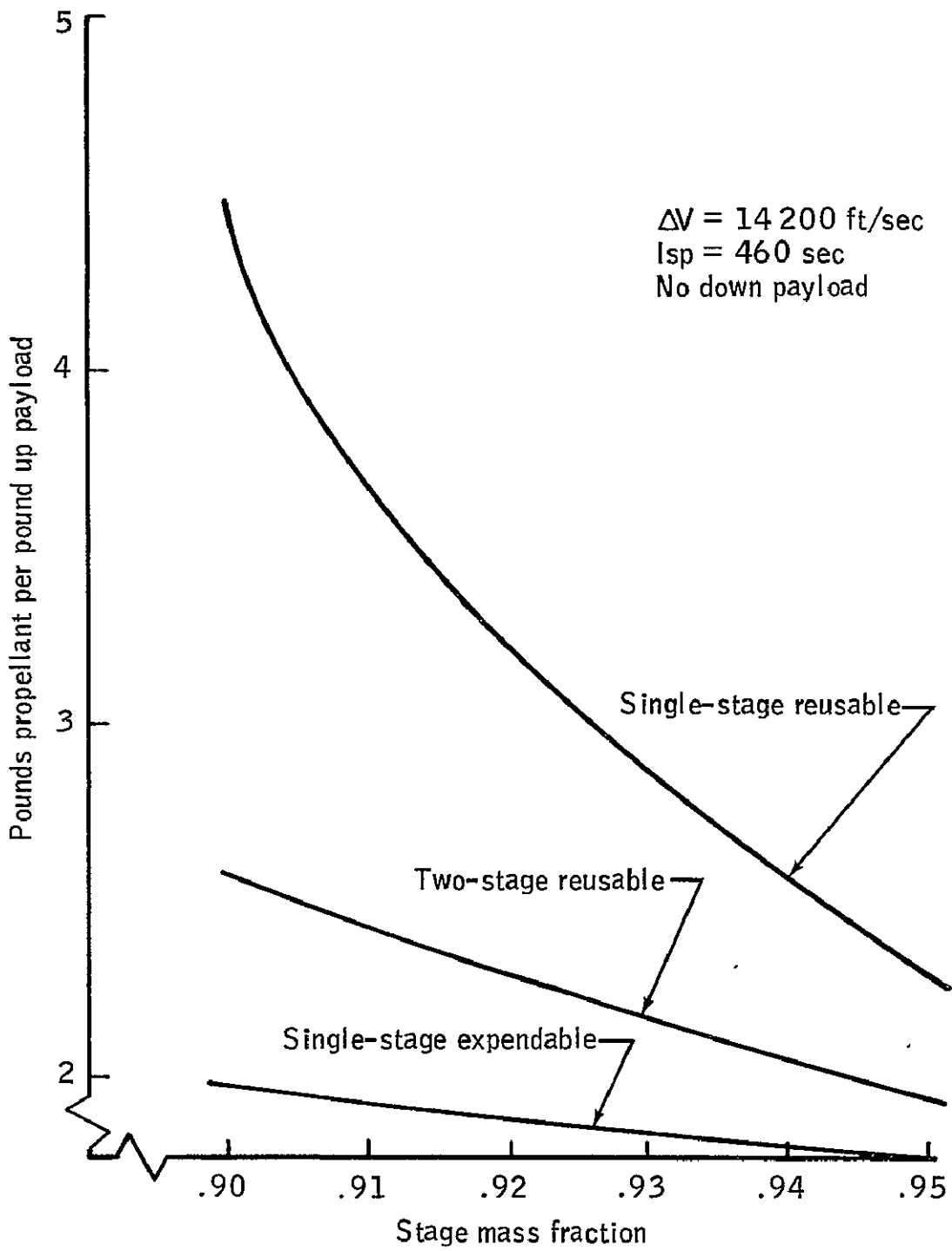


Figure VI-D-2-1. - High-thrust O_2/H_2 OTV

2.2.3 REPRESENTATIVE CONFIGURATION

The representative configuration for a high-thrust O_2/H_2 CTOV is illustrated in figure VI-D-2-2. It is an expendable single-stage vehicle capable of transporting a one million pound payload from LEO to GSO. The stage requires two launches to emplace in LEO; one launch for a complete stage with an undersized LOX tank, the second launch for the remainder of the LOX in its own tank which is plugged into the stage without a propellant transfer requirement.

A weight statement for this stage is given in table VI-D-2-2.

2.2.4 TECHNOLOGY ISSUES

There are no significant technology issues associated with this concept.

2.2.5 COTV_G REFERENCE CONFIGURATION - 2-1/2 STAGE O_2/H_2

A parametric vehicle sizing exercise was performed to determine vehicle ignition weights for various LEO reusable COTV_G (subscript "G" denoting SPS construction at GEO) staging options including single stage, 2-stage, 1-1/2 stage, and 2-1/2 stage. The latter two options involve expending the outbound propellant tanks at GEO and returning the "core" to LEO for reuse. Parametric stage mass fraction data utilized were derived from the Boeing FSTSA study and included a 15% dry weight contingency. Results are plotted on Figure VI-D-2-3 and indicate that the 2-1/2 stage option achieves minimum ignition weight and therefore would require less HLLV Earth launch support.

On this basis, the 2-1/2 stage has been selected as the reference configuration for the space transportation scenario analysis in Section VI-F and the program model analysis in Section VII. The resulting point design "nominal" configuration and data are presented on Figure VI-D-2-4. The stage 2 drop tanks and stage 1 main propellant tanks are identical in size. Using an RL-10 Cat. IV O_2/H_2 engine as baseline, 8 and 11 engines are required for stage 2 and stage 1, respectively, to provide the .1 G acceleration during main propulsion operations.

The 2-1/2 stage payload delivery mission is performed similarly to the 2-stage except that the stage 2 outbound propellant tanks are "expended" at GEO. The empty drop tanks may be left with the SPS as parasitic weight without penalty, or perhaps even utilized in the SPS construction at GEO. During the mission, stage 1 provides approximately 1600 meters/sec of the required 4330 meters/sec one way delta velocity. Stage 1 returns itself to the LEO OTV operations depot for reuse. Stage 2 completes the transfer to GEO with its drop tank propellant. After docking with the GEO SPS construction facility and offloading payload, the stage 2 core returns itself to LEO for reuse.

In the case of this high-thrust COTV_G and resultant low trip time to GEO (less than 1 day), it may be possible to delete the development of a POTV_G and fly the passenger carrying module as part of the large COTV_G outbound cargo. This program deletion, and possible cost saving may be addressed in subsequent studies should the GEO construction location and high-thrust chemical COTV be selected.

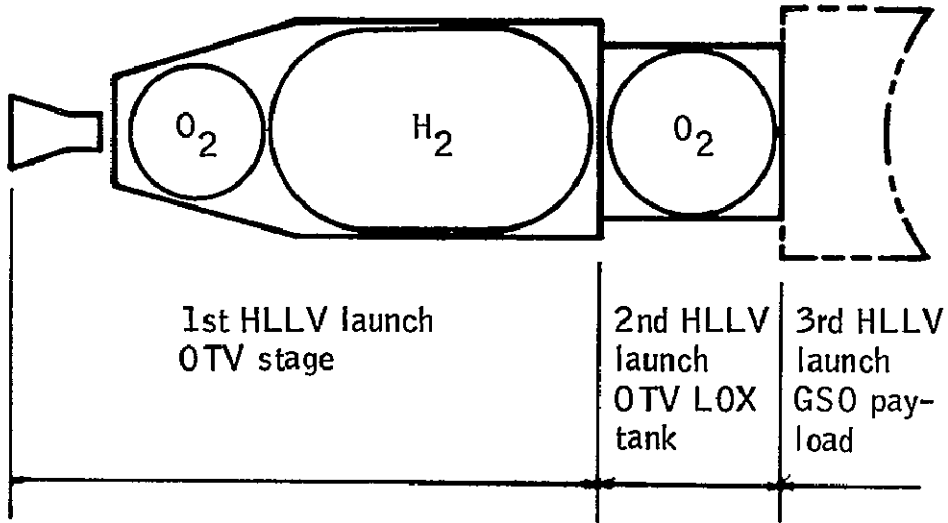


Figure VI-D-2-2. High-thrust O_2/H_2 OTV configuration

TABLE VI-D-2-2. HIGH-THRUST O₂/H₂ OTV WEIGHT STATEMENT

STAGE STRUCTURE	13,900
LH ₂ TANK & INSULATION	17,200
LO ₂ SUMP TANK	4,600
LO ₂ STORAGE TANK	11,900
MAIN ENGINE	6,700
OTHER PROPULSION (FEED SYSTEM, PRESSURIZATION, RCS)	35,000
MISC. SYSTEMS	6,500
! 20% CONT	<u>19,160</u>
DRY WEIGHT	<u>114,960</u>
PROPELLANT	1,885,000
IMPULSE PROPELLANT	1,830,000
BOILOFF	11,900
PRESSURANT	3,940
RESIDUAL	36,600
OUTAGE	2,600
TOTAL WEIGHT	2,000,000

VI-D-2-7

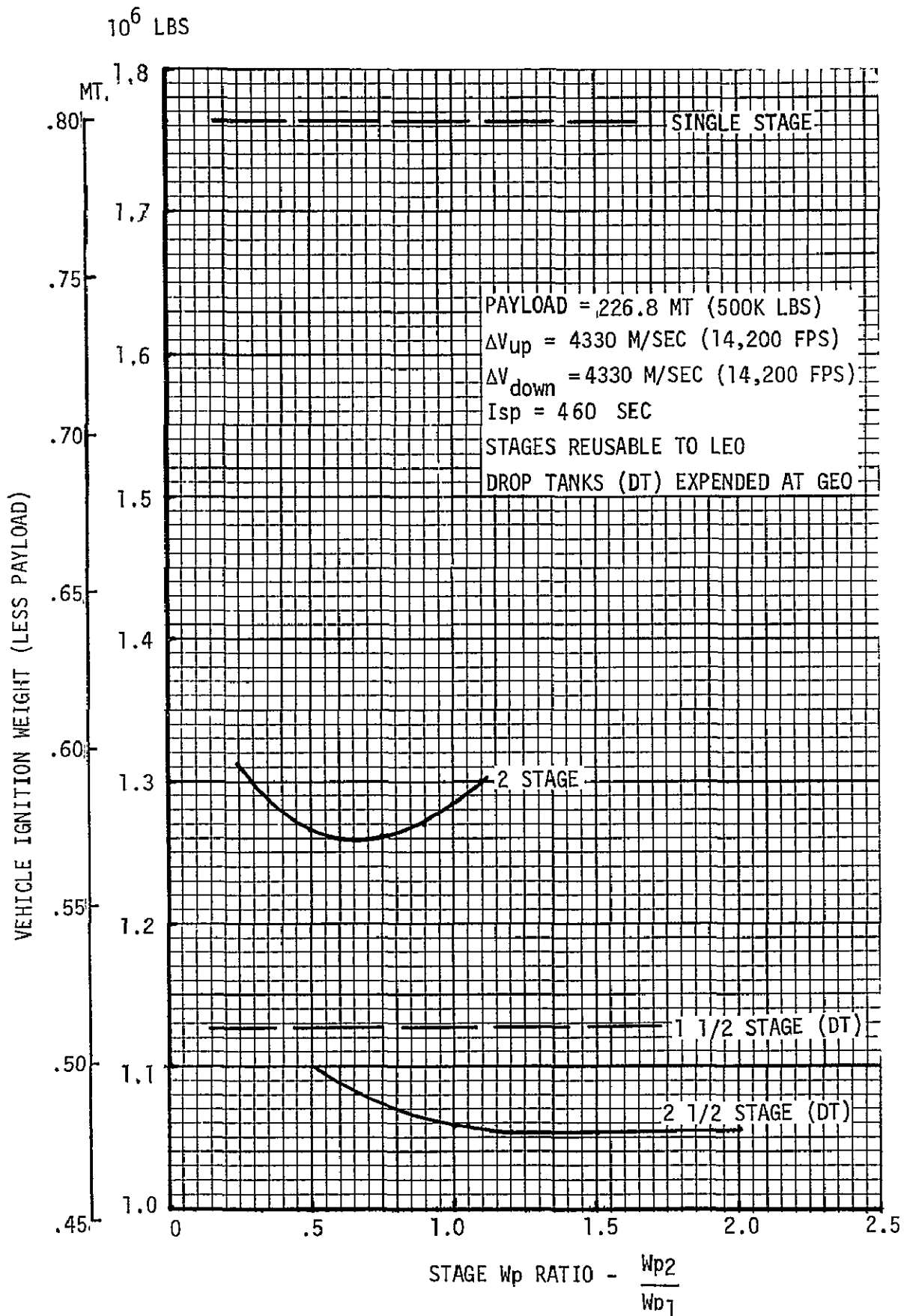
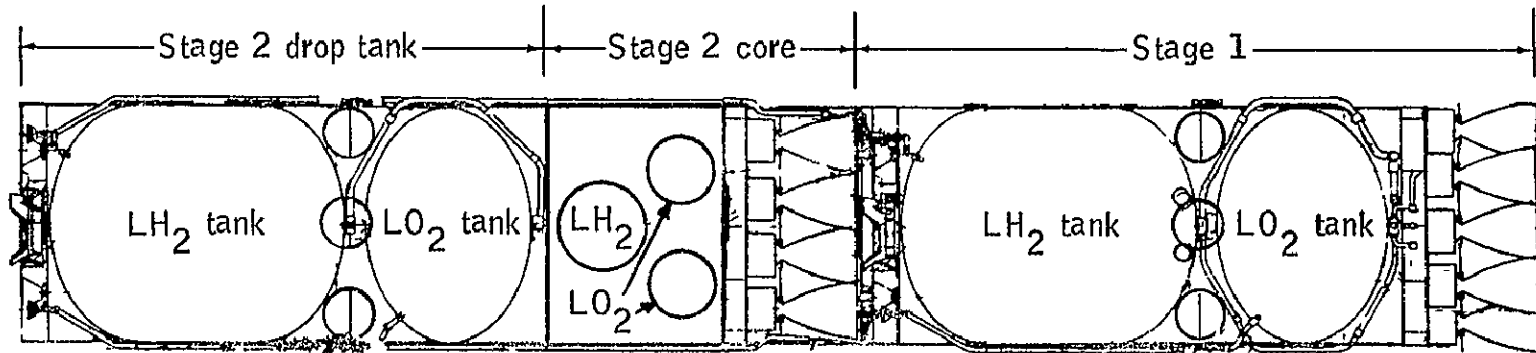


Figure VI-D-2-3.-COTV_G staging option comparison
Payload delivery to GEO



2-1/2 stage LO₂/LH₂
 Life: 30 missions
 Payload: 250 tons
 ≈\$10M/ft

Length: 48M
 Diam: 8.4M
 Total weight: 510 tons
 Propellant weight: 475 tons

Figure VI-D-2-4. Cargo orbital transfer vehicle (COTV_G) characteristics

2.2 NUCLEAR STAGE

2.3.1 PARAMETRIC DATA

The high-thrust nuclear COTV considered here is a NERVA-engined vehicle. The primary data source for this stage was the Boeing FSTSA study results. Figure VI-D-2-5 presents the payload capability of this stage as a function of stage mass fraction and engine Isp. The characteristics of this stage appear to place it in the knee of the W_p/W_{p1} curves when operated in a reusable mode where small changes in engine Isp or stage mass fraction result in a large effect on capability. It is doubtful that the cost of the nuclear power plant could be reduced to the point where operation of this stage in an expendable mode would be attractive, but for the expendable mode, a W_p/W_{p1} of 1 to 1.3 would be expected for the reusable case. Boeing's values give a stage mass fraction of .75 at an impulse propellant mass of 220,000 lbm; at the predicted effective delivered Isp of 768 seconds, approximately 2.7 lbm of propellant are required per pound of payload. Thus the stage could deliver a payload of 81,500 lbm to GSO and return itself to LEO. However, operation in a reusable mode would require greater engine life than has been possible to date. It is possible that new materials or techniques could increase engine life. But if engine life requirements forced a reduction in operating temperature, the effect of lower Isp on the payload capability could be disastrous.

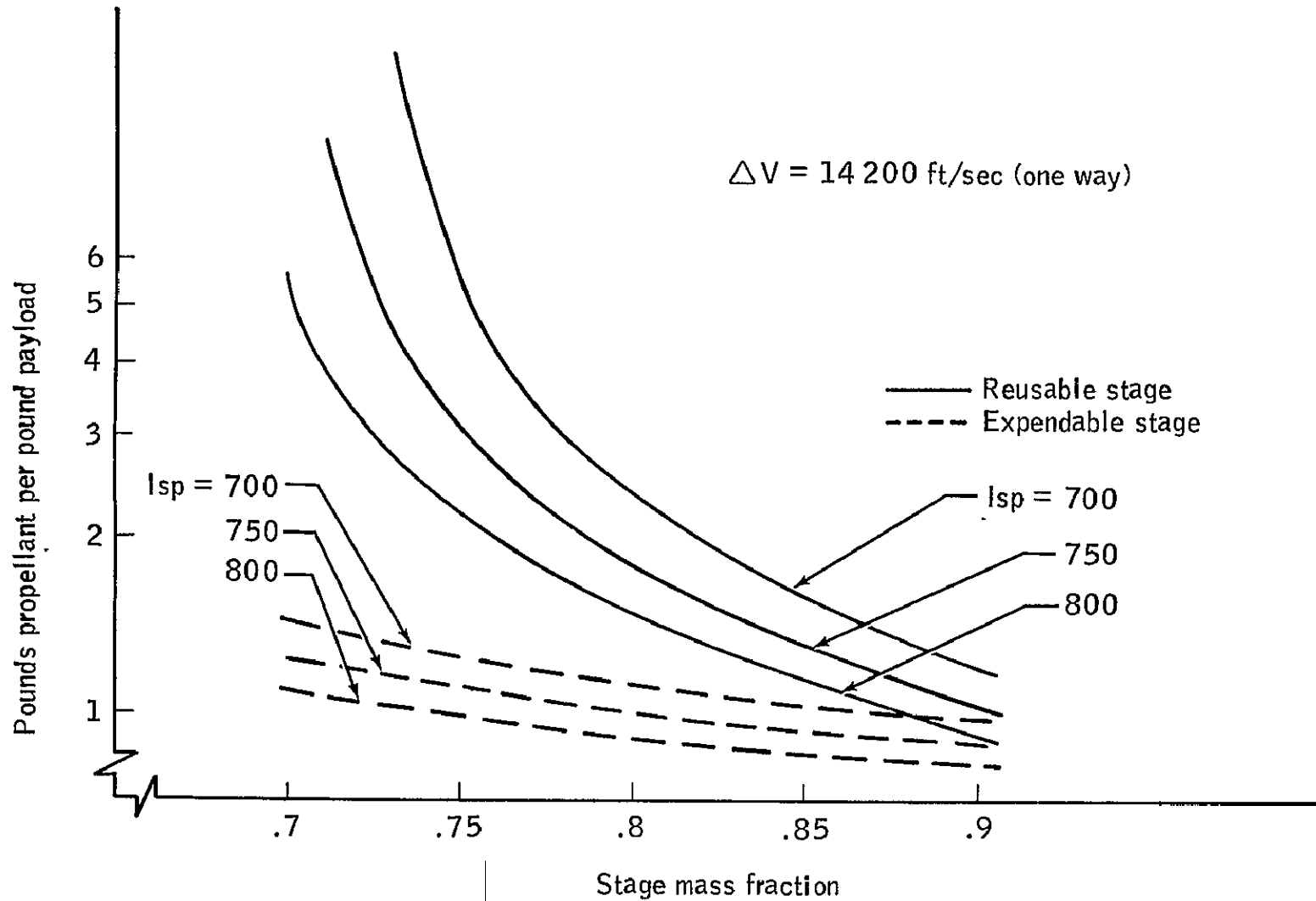


Figure VI-D-2-5. - Nerva OTV parametrics

VI-D-2-11

3.0 ORBITAL TRANSFER MECHANICS (G. Babb, Advanced Mission Design Branch (FM5))

3.1 LOW THRUST ORBITAL OPERATIONS--INTRODUCTION

Previous sections indicated that the COTV may be required to utilize thrust/weight levels of 10^{-3} and below for orbital transfer maneuvers. This is substantially below the accelerations currently considered normal for Earth orbit operations.

Orbital operational experience to date has been with thrust levels high enough so that orbital maneuvers could be considered as a perturbation of the impulsive transfer case.

At the low thrust levels of the COTV, however, orbital transfers take on an entirely different character. Thrusting now takes place during virtually the entire transfer time and the flight path becomes a tightly coiled spiral connecting the initial and final orbits (Figure VI-D-3-1). At $T/W = .001$, for instance the transfer from low parking orbit (250 NM) to a geosynchronous orbit (no plane change) takes 33 revolutions of the spacecraft over 5.5 days under continuous thrusting.

The delta V requirements, flight times, and guidance and navigation requirements are all different from the more usual high thrust cases.

3.1.1 DEFINITION OF LOW THRUST

The impact of lower thrust levels on delta V requirements and basic operational techniques becomes significant when the thrusting phase becomes equal to or greater than an orbital period.

For delta V level on the order of escape, it can be shown that in general the operation is approximately impulsive, that is high thrust, so long as the thrust levels are on the order of the accelerations of the primary (central) body at that point (that is the local g values). When the thrust levels become several orders of magnitude less than this (local g value), the system exhibits all the characteristics of the low thrust systems. Starting in low Earth orbit going to geosynchronous orbit, thrust levels of 10^{-2} and 10^{-3} g and below are low thrust in character, that is it requires a number of orbital periods and a number of orbital circuits during the thrust phase. Thrust levels of .1 to 1g and above are high thrust in nature. Between .1g and .01g is a transition region. For thrust levels in this region, operational techniques such as multiple orbit injection (thrusting near perigee on successive orbits) are effective in minimizing the so-called "gravity losses" of low thrust operations. For thrust levels below .01g these techniques lose effectiveness within reasonable time limits.

The two thrust modes, high thrust and low thrust, do approach each other in character as the delta V being imposed approaches zero.

3.2 EFFECTS OF T/W ON DELTA V AND TRIP TIMES

For a low thrust case with a constantly thrusting spiral flight path, the delta V, from energy considerations, turns out to be the absolute value of the difference in circular orbit velocity between the beginning circular orbit and the final circular orbit. This is independent of the thrust level so long as it is down in the very low thrust region. Thus, the delta V required for geosynchronous transfer with a 10^{-3} thrust level is the same as it is with a 10^{-4} or 10^{-5} or 10^{-6} g thrust level.

Trip times, however, are inversely proportional to the thrust. Trip time can be approximated by delta V divided by the acceleration (T/W). This gives the thrusting time which is very close to the total flight time. As the thrust level decreases and flight time increases this approximation becomes more and more accurate. Toward the end of the transfer there is often a short coasting phase but this is never more than a few hours from Earth orbit operations. A plot of altitude reached vs delta V and/or flight time is given in Figure VI-D-3-2.

Delta V for a geosynchronous transfer from a 250 NM initial parking orbit with zero plane change is 15,000 fps. Trip time for a vehicle with .001 T/W, which is probably an upper limit for moving a large station, is approximately 5 1/2 days. As a comparison the same transfer with a high (impulsive thrust level requires a delta V of 12,700 fps and a transfer time approx. .25 days (see Table VI-D-3-1).

3.3 GUIDANCE AND NAVIGATION (G&N) REQUIREMENTS

Guidance and navigation requirements can be greatly simplified by going to very low thrust operations. Things happen so slowly that real time calculations and tracking can be carried out on the ground during the thrusting operation. A simple efficient guidance is by thrusting horizontally to the ground in the plane of the orbit. While the most optimum thrust is along the velocity vector, for low thrust the velocity vector stays very horizontal and the efficiency losses of a horizontal thrust are entirely negligible. The advantage of horizontal thrust is in simplicity of implementation. The pointing accuracies required are very low (5 to 10 degs) during everything but the very final orbit corrections. Navigation would be by tracking and computer calculations on the ground. Time elements are so slow, with flight times of at least on the order of a week, that integrations on the ground can be very easily carried out even on something as unsophisticated as a small desk computer. Guidance would then simply be by transmitting an enable/disable command to the thrusters.

3.4 THE IMPACT OF LAUNCH SITE ON ORBITAL OPERATIONS

The launch site should, if at all possible, be selected in plane with the final destination orbit. This greatly simplifies operations and at the same time considerably decreases delta V requirements. Having the launch site at the latitude of KSC when the final orbit is equatorial requires a 28.5° plane change during the orbit transfer. Making this plane change requires an additional delta V of at least 4000 fps over the simple in-plane transfer. This is the additional delta V quoted in the literature. It requires out-of-plane thrusting during each orbit of the entire flight. Another option is an in-plane transfer to geosynchronous altitude with the plane change being made at that point. This requires 5,000 fps delta V for the plane change but the operations are simplified somewhat.

Trip times are increased by more than just the extra delta V that must be input to the system. Even with lateral thrust applied during the climb to altitude much of the plane change remains to be made after synchronous altitude is reached. Delta V for this plane change can only be applied close to the nodes of the two orbits. This means thrusting is occurring only 1/3 to 1/5 of the time. The net result is that the 28.5° plane change could more than double total flight time for the low thrust transit.

G&N would be significantly complicated by the introduction of a large plane change, requiring three dimensional operation rather than two dimensional.

All of this is eliminated by a launch site in plane with the final orbit. There are also other advantages to low inclination launch sites such as; multiple launch opportunities, somewhat increased launch vehicle payload, and multiple rescue opportunities. These factors are discussed elsewhere.

3.5 OCCULTATION EFFECTS AND IMPACT ON SELF-ELECTRIC POWERED VEHICLE

Because the transfer starts from a low Earth orbit at a (relatively) low inclination, the vehicle spends a portion of each of at least the low altitude orbits in the Earth shadow (night). This occultation of the sun every few hours creates a special problem for the self-powered electric vehicles. For these cases at least part of the SSPS is generating power for use by the thrusters. Thus, the entry into Earth's shadow and reemergency into sunlight represents a shut-down and start-up of a gigawatt level power system with the attendant mechanical and thermal shocks. There is also the problem of attitude control loss during occultation. The severity of this problem is not yet established.

If the transfer plane contains the earth-sun line, shadow passage would occur during every orbit all the way out to geosynchronous

altitude. The total time in shadow during such a passage would be approx. 20% of the flight time. In practice the time in shadow would always be considerably less than this.

Time in shadow could be minimized by proper selection of the initial orbit inclination and orientation (nodal position), considering such factors as thrust levels (flight time), nodal regression rates, and solar position at start of flight (time of year). This time cannot however, be eliminated altogether for the entire flight.

3.6 HIGH-THRUST ORBITAL MECHANICS IN COMPARISON TO LOW THRUST

For those phases of construction and repair that require manned operations at geosynchronous orbit, a high thrust system will be required. Low thrust will not be desirable because of long duration flight times which take place in a hostile environment (the radiation belt).

Undoubtedly a more conventional level thrust system will be used. Delta V for transfer from 250 NM. LEO to synchronous orbit in-plane is approx. 12,700 fps. Requiring a 28.5° plane change increases this to 13,800 fps. With a high thrust system the plane change is not as costly in delta V as with the lower thrust. However, because of the lower Isp normally associated with higher thrust systems (i.e., <1000 sec), coupled with the fact that the manned operation generally requires a round trip, the added propellant weight due to this plane change is often considerably greater than with the low thrust system.

TABLE VI-D-3-1

GEOSYNCHRONOUS TRANSFER PARAMETERS

Orbit Characteristics

Low Earth Orbit (LEO)

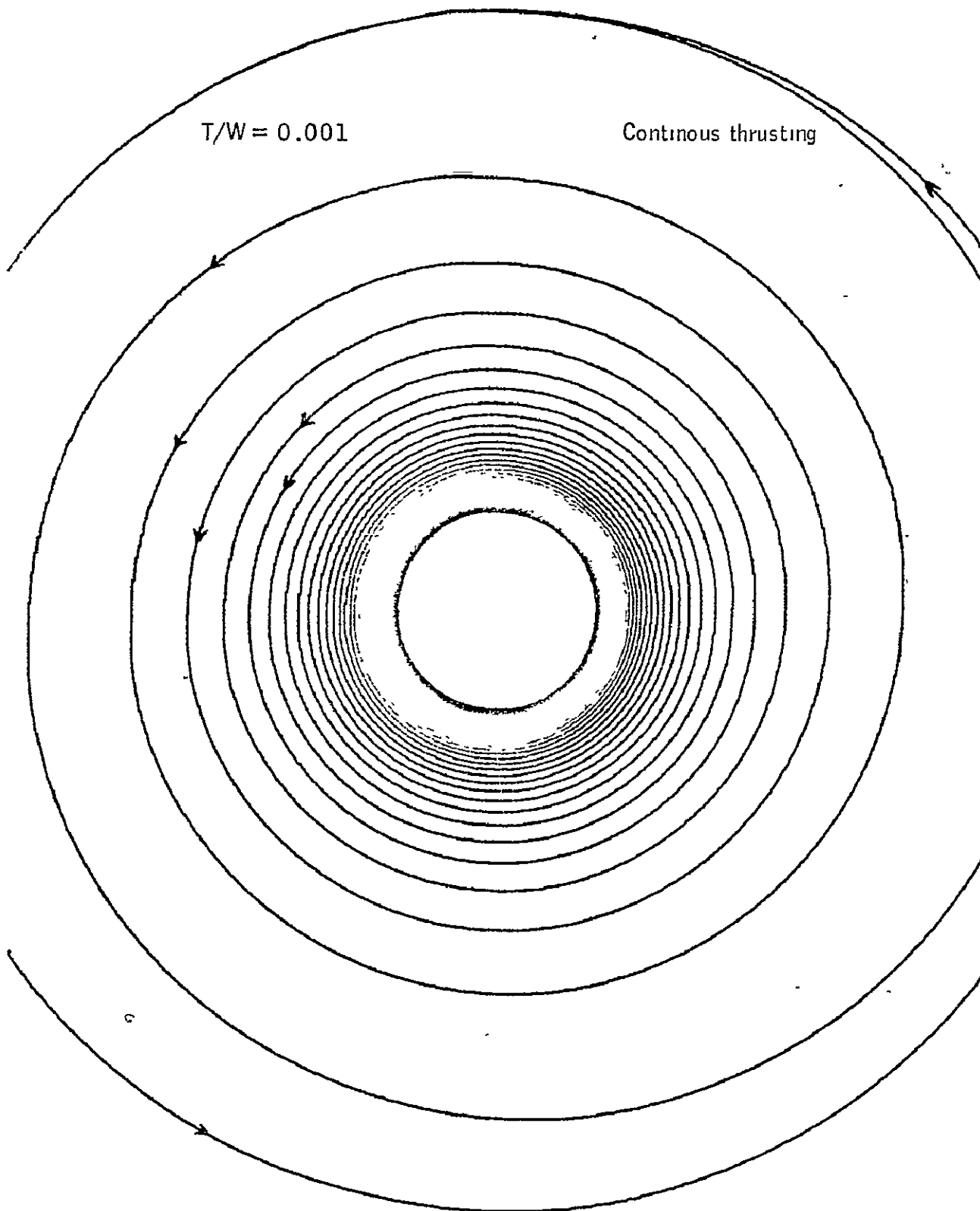
$h = 250$ n.mi.; Circular Velocity = 25,043 fps; Period = 1.56 hr

Geo Synchronous Orbit

$h = 19,323$ n.mi.; Circular Velocity = 10,087 fps; Period = 23.93 hr
(1 sidereal day)

Transfer Characteristics
LEO to Geosync

	High Thrust	Low Thrust
Zero Plane Change		
Transfer ΔV	12,700 fps	15,000 fps
Flight time	$\frac{1}{4}$ day	5.5 day; $T/W=10^{-3}$ 55 day; $T/W=10^{-4}$ 550 day; $T/W=10^{-5}$
28.5° Plane Change		
Transfer ΔV	13,800 fps	19,000 fps
Flight time	$\frac{1}{4}$ day	> 6.8 day; $T/W=10^{-3}$ > 68 day; $T/W=10^{-4}$ > 680 day; $T/W=10^{-5}$
21° Plane Change		
Transfer ΔV	13,300 fps	17,700 dps
Flight time	$\frac{1}{4}$ day	> 6.4 day; $T/W=10^{-3}$ > 64 day; $T/W=10^{-4}$ > 640 day; $T/W=10^{-5}$



Flight time = 5.4 days
Starting altitude = 250 n. mi.

$\Delta V = 15\ 000$ fps

Figure VI-D-3-1 .- Low thrust trajectory to synchronous orbit.
VI-D-3-6

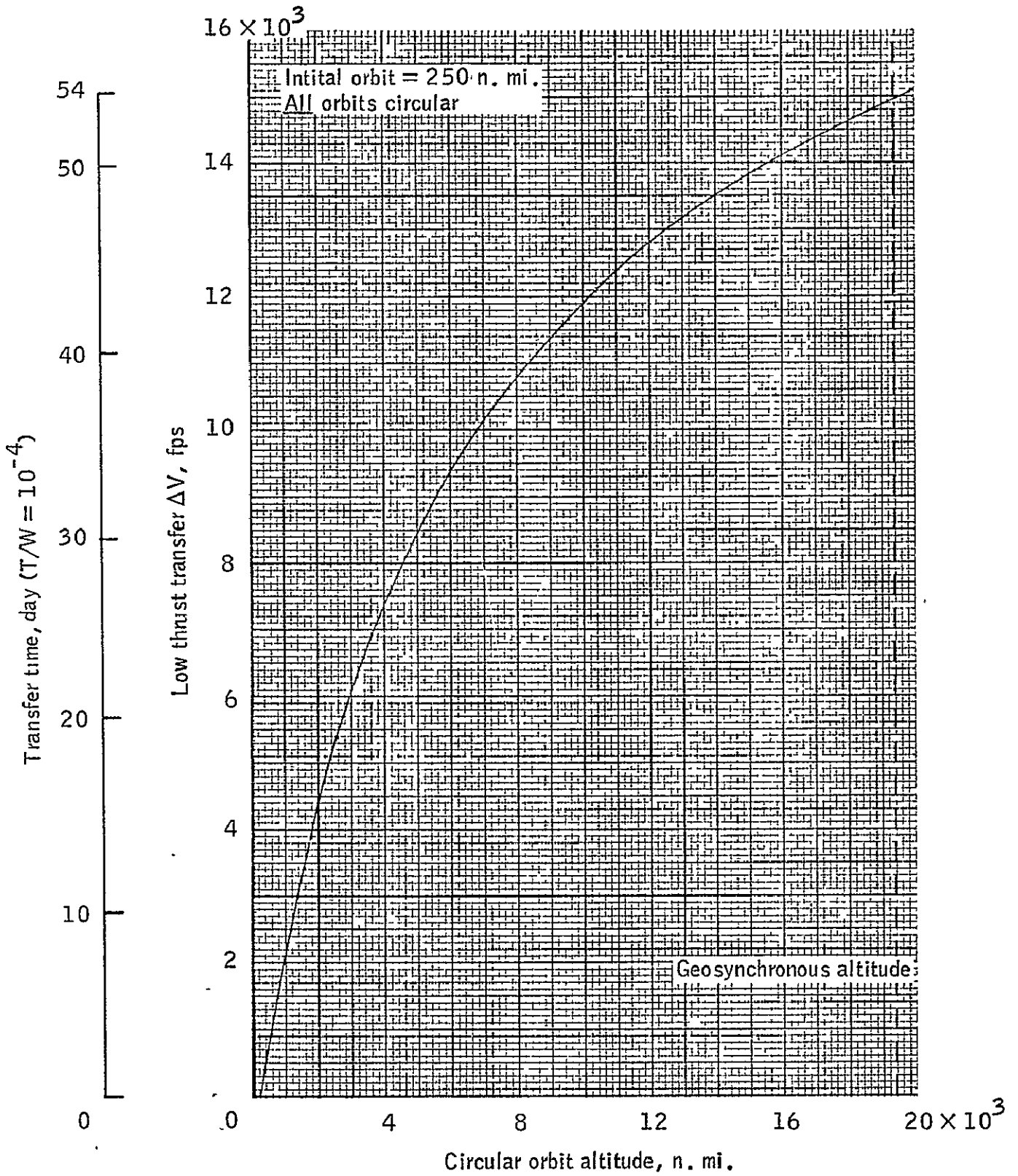


Figure VI-D-3-2 .- Low thrust transfer ΔV to high Earth orbits.
VI-D-3-7

VI-E PERSONNEL ORBITAL TRANSFER VEHICLE (POTV)
(C. Mac Jones, Future Programs Office)

GROUND RULES AND ASSUMPTIONS

Due to the much smaller payload requirements for transporting personnel and high priority equipment than SPS construction cargo to GEO, it is assumed that the POTV is a special purpose device optimized for that function. For the independent chemical propulsion cargo OTV (COTV_G) used in the GEO construction of the SPS, it may be possible to delete the development of a POTV and fly the passenger carrying module as part of the large COTV_G outbound cargo. This program deletion and possible cost saving may be addressed in subsequent studies should the GEO construction location and chemical cargo orbit transfer vehicles be selected. In particular for the low Earth orbit (LEO) SPS construction, a dedicated personnel orbital transfer vehicle (POTV_L) will be required.

For the purpose of the JSC in-house SPS study, the conservative choice is made to employ conventional chemical rocketry with return of the vehicle and crew to low Earth orbit. Information generated by the Future Space Transportation Systems Analysis Study (NAS 9-14323), previous JSC in-house work, and the extensive Space Tug studies conducted by both NASA and the USAF over the past 5 years are utilized as reference material. The POTV concept deploys from LEO operational altitudes (200 to 500 km) to GEO, and returns all-propulsively to LEO for subsequent rendezvous with an orbiting craft or support facility for refueling and reuse. Other crew return concepts deserve recognition and study such as aeromaneuvering and aerobraking, and winged and ballistic entry modes but are not treated in this study.

Single stage, 1 1/2 stage (outbound propellant tanks expended), and common stage configurations are all candidates for the POTV mission. Additionally, for those cases where economic cargo transportation is possible, significant advantages accrue to the POTV by having its return propellants delivered by the more economic COTV and stored in GEO.

TECHNOLOGY BASE

The following POTV technology definitions and selections have been developed as compatible with an assumed 1980 + technology base. (excerpted from the Boeing FSTSA Study.)

Structures:

- o Graphite-plastic matrix composites are assumed for unpressurized main structures.

- o Aluminum is assumed for main propellant tanks with integral stiffening as required.

- o Elevated temperature materials are assumed where normal working temperatures for aluminum or composites are exceeded.

- o High temperatures and associated environments are limited to known capabilities of known engineering materials.

Avionics:

- o LSI circuit chip technology is assumed available for data processing hardware; data bus techniques are assumed to minimize wire mass.

- o Communications and GN&C systems assumed Shuttle and full-capability tug technology levels. Laser radar is assumed available for rendezvous as required.

Electric Power:

- o Fuel cells and batteries are assumed for electric power.

Main Propulsion:

- o The P&WA design RL-10 Category IV engine is assumed as the baseline engine. Stage thrust-to-weight calculations will determine appropriate numbers of engines per stage.

- o RL-10 Category IV characteristics assumed are as follows:

Thrust:	15,000 lb.
Chamber Pressure:	915 psia
Area Ratio:	401
Isp:	462 sec at 6.0 MR
Operation:	Full thrust (saturated propellants) Maneuver thrust (saturated propellants)
Conditioning:	Tank head idle
Weight:	424 lb.
Fuel:	O ₂ /H ₂

Auxiliary Propulsion:

- o The use of a hydrazine monopropellant system is baselined. Storable bipropellant and advanced O₂/H₂ auxiliary propellant technologies are assumed available as needed.

Thermal and Meteoroid Protection:

- o Multilayer metallized plastic film insulation (MLI) is assumed for thermal protection of all main propellant tanks. A metal skin, non-structural for vehicles with integral tanks, is assumed external to the

MLI and is to be thick enough so that, in conjunction with the MLI, it provides sufficient meteoroid protection.

Docking:

- o The international docking system (ASTP) type is assumed for POTV stage to payload module docking.

- o POTV stage-to-stage docking system design is assumed as a multiple probe/drogue system with latching at stage O.D.

MISSION DEFINITIONS

The POTV LEO to GEO mission is assumed to be initiated at the LEO orbit transfer operation base or early in the program, the Shuttle at LEO operational altitudes (200 to 500 km). Modular POTV elements are docked together and propellants tanks topped off. A two-burn injection places the POTV and payload on the final synchronous transfer ellipse with a trip time of 8 to 9 hours. At apogee the circularization maneuver is performed and rendezvous accomplished with the GEO site. GEO orbital stay for a typical mission is between 2 and 7 days. Orbital stay time can be extended for GEO refueling applications. Return to the LEO base is all-propulsive. Mission delta-velocity budgets for the main propulsion system are tabulated for the common stage POTV in Tables VI-E-1, VI-E-2, and VI-E-3 for these modes: GEO satellite maintenance sortie, GEO crew rotation/resupply (both stages refueled at LEO), and GEO crew rotation/resupply (stage 1 refueled at LEO, stage 2 refueled at GEO). Servicing/refurbishment is accomplished at LEO, and refueling is done by artificial gravity from orbital storage tanks (in the operational phase).

POTV PAYLOADS

Three different payloads have been characterized for POTV: crew rotation passenger module, station resupply module, and crew module for a geosynchronous sortie (optional).

Geosynchronous Sortie Crew Module - Possibly the first payload to fly with the POTV would be the crew module required for a manned geosynchronous sortie. A reference mission may consist of a 4 man crew performing 1 week of satellite maintenance operations, visiting four satellites with transfers up to 15° longitude between each satellite visit. Additionally, sortie GEO missions may be required during the SPS test program. A crew module concept from the Boeing FSTSA study is shown on Figure VI-E-1 and its associated weight estimate presented in Table VI-E-4. DDT&E and TFU costs of the crew module have been estimated at \$365M and \$34M, respectively.

Crew Rotation Passenger Module - For the operational program phase, crew rotation is expected to occur at least every 6 months in

TABLE VI-E-1

Main Propulsion Delta-Velocity Budget
Common Stage POTV* for GEO Satellite Maintenance Sortie

	<u>Mission Delta-V (FPS)</u>	<u>Stage 1 Delta-V (FPS)</u>	<u>Stage 2 Delta-V (FPS)</u>
LEO parking orbit (270x270 NM, 28.5°)			
1. LEO first injection burn	4270	4270	--
2. LEO second injection burn	3588	2730	858
Injection and circularization burns gravity losses	190	--	190
3. GEO circularization burn (12,323x19,323 NM, 0°)	5804	--	5804
4. GEO rendezvous and docking, Sat. 1	131	--	131
5. 45° longitude shift, rendezvous and docking, Sats, 2, 3, & 4	1278	--	1278
6. GEO deorbit burn (270x19,323 NM, 26.3°)	5804	--	5804
7. LEO circularization burn (270x270 NM, 28.5°)	7858	7000	7858
Deorbit and circularization burns gravity losses	50	50	50
8. LEO rendezvous and docking	131	131	131
9. Flight performance reserves (2% total Delta-V)	<u>582</u>	<u>284</u>	<u>442</u>
TOTAL DELTA-VELOCITY (FPS)	29,686	14,465	22,546
(Meters/Sec)	9,048	4,409	6,872

* Both stages refueled at LEO.

TABLE VI-E-2

Main Propulsion Delta-Velocity Budget
Common Stage POTV*for GEO Crew Rotation/Resupply

	<u>Mission Delta-V (FPS)</u>	<u>Stage 1 Delta-V (FPS)</u>	<u>Stage 2 Delta-V (FPS)</u>
LEO parking orbit (270x270 NM, 28.5°)			
1. LEO first injection burn	4270	4270	--
2. LEO second injection burn	3588	1730	1858
Injection & circularization burns gravity losses	190	--	190
3. GEO circularization burn (19,323x19,323 NM, 0°)	5804	--	5804
4. GEO rendezvous and docking	131	--	131
5. GEO deorbit burn (270x19,323 NM, 26.3°)	5804	--	5804
6. LEO circularization burn (270x270 NM, 28.5°)	7858	6000	7858
Deorbit and circularization burns gravity losses	50	50	50
7. LEO rendezvous and docking	131	131	131
8. Flight performance reserves (2% total Delta-V)	<u>557</u>	<u>244</u>	<u>437</u>
TOTAL DELTA-VELOCITY (FPS)	28,383	12,425	22,263
(Meters/Sec)	8,651	3,787	6,786

* Both stages refueled at LEO.

TABLE VI-E-3

Main Propulsion Delta-Velocity Budget
Common Stage POTV* for GEO Crew Rotation/Resupply

<u>Mission Event</u>	<u>Mission Delta-V (FPS)</u>	<u>Stage 1 Delta-V (FPS)</u>	<u>Stage 1 Delta-V (FPS)</u>
LEO parking orbit (270x270 NM, 28.5°)			
1. LEO first injection burn	4270	4270	--
2. LEO second injection burn	3588	1130	2458
Injection and circularization burns gravity losses	190	--	190
3. GEO circularization burn (19,323x19,323 NM, 0°)	5804	--	5804
4. GEO rendezvous and docking	131	--	131
5. LEO circularization burn (270x270 NM, 28.5°)	5400	5400	--
Deorbit and circularization burns gravity losses	35	35	--
6. LEO rendezvous and docking	131	131	--
7. Flight performance reserves (2% total Delta-V)	391	219	172
TOTAL DELTA-VELOCITY (FPS)	19,940	11,185	8,755
(Meters/Sec)	6,078	3,409	2,669

* Stage 1 refueled at LEO, Stage 2 refueled at GEO.

VI-E-7

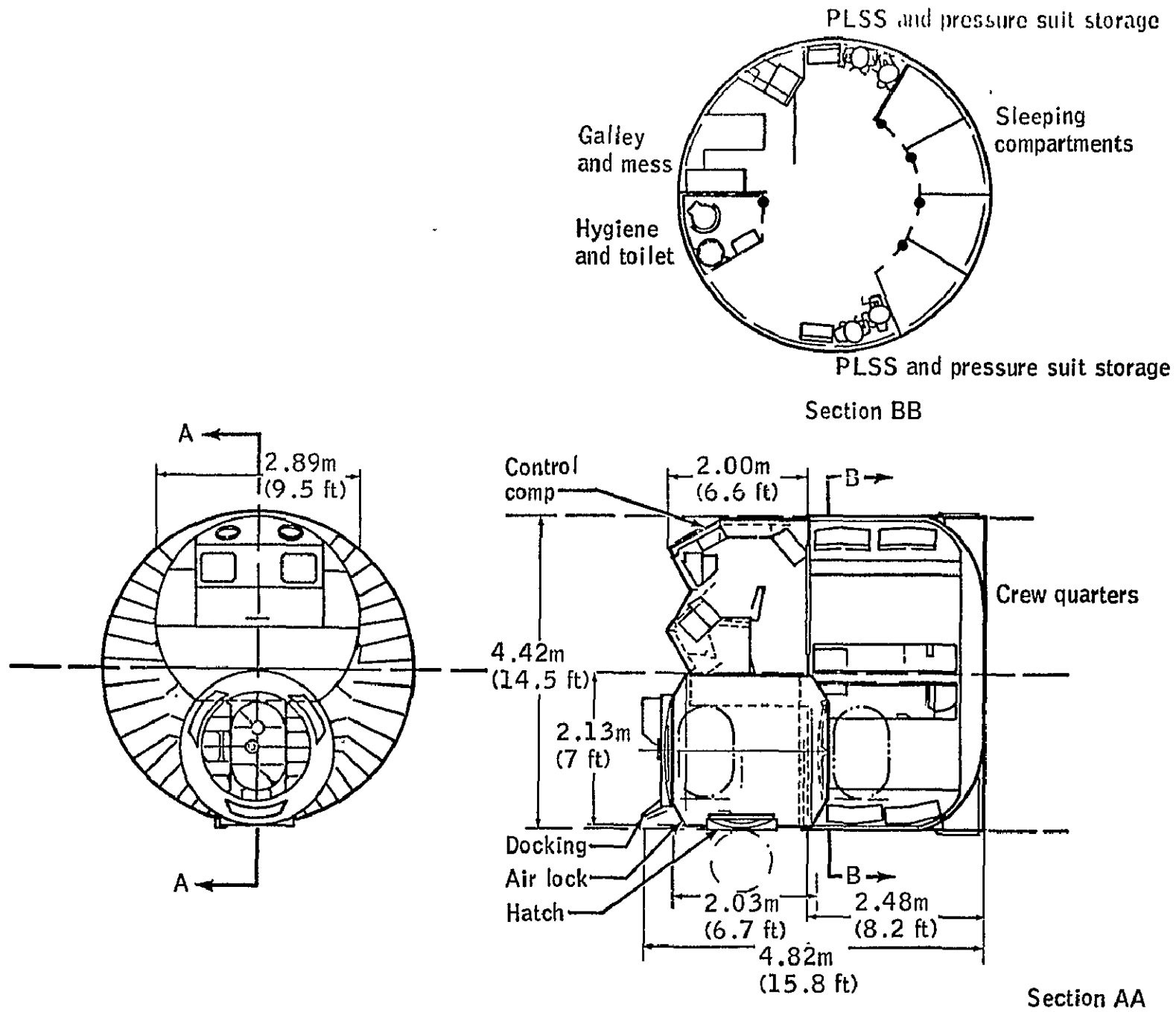


Figure VI-E-1. Crew module concept

TABLE VI-E-4

CREW MODULE
PRELIMINARY WEIGHT STATEMENT

Primary Structure ⁽¹⁾	1248 kg	4 Crew + 1 Day Reserves	676 kg
Secondary Structure ⁽²⁾	771	Consumables ⁽³⁾	408
Airlock	236	Manned Maneuvering Units ⁽²⁾	<u>181</u>
Mission Support Module	<u>272</u>	Total Variables	1265
Total Structure	2527		
Crew Accommodations	181		
Environmental Control	290	Total CM Wt	5949 kg
Elect. Power & Distribution	386	Repair Parts	907 kg
Avionics & Console	363		
25% Wt. Growth Contingency	<u>937</u>	Total Payload to GEO	6856 kg (15,116 lbs)
Total Dry Weight	4684	Return Payload to LEO	5582 kg (12,315 lbs)

(1) Control Compt 12.18 M³ (430 ft³)

Crew Quarters 33.81 M³ (1194 ft³)

(2) Hatches, Windows, Docking, Arms

(3) 9-Day Mission, 10 Airlocks

order not to exceed the allowable radiation dose. A crew rotation passenger module is required for the Earth to LEO and LEO to GEO transfer. The passenger module shown on Figure VI-E-2 first flies in the Shuttle payload bay and then is deployed and docked to the POTV at the LEO operations base. Adequate structural weight allowance is provided for the necessary shielding for safe passage through the Van Allen Belt. Crew size requirements for GEO operations have not been focused sufficiently to allow final passenger size accommodation selection or optimization of rotation timelines and POTV mission costs. For cost estimating purposes, a 75-man module has been selected with a total loaded weight of 19 metric tons. DDT&E and TFU costs of this crew rotation passenger module have been estimated at \$120M and \$6M, respectively.

Resupply Module - The third payload characterized for the POTV is the resupply module. Resupply has been defined as replenishment of the GEO station consumables, supplies, and equipment necessary for 180 days. For purposes of sizing, a 25 man/180 day resupply has been selected. The corresponding conceptual resupply module is shown on Figure VI-E-3. It will house the 29 metric tons of resupply items in a 6 metric tons empty weight module at 128 kg/m³ assumed payload density.

All three of the above modules are sized to be compatible with the Shuttle payload bay as are the POTV module elements.

POTV PARAMETRIC STAGE SIZING

A parametric sizing study was performed to determine vehicle ignition weights for various POTV configuration for a range of GEO round trip payload weights. Vehicle sizing guidelines observed are as follows:

- a. Operating mode: Manned or unmanned
- b. Safety: Stages have engine out capability
- c. In-orbit refurbishment: Subsystem module replacement
Propellant transfer under low "G"
- d. T/W capability: Initial $\leq 0.1g$
Burnout $\geq 3.0g$
- e. Weight contingency: 25% on dry weight
- f. Flight performance reserves: 2% on total delta V
- g. Meteoroid protection: $P_0 = 0.97$
- h. Launch loads: 3.3g Shuttle and HLLV
- i. Maximum stage diameter: 4.42 M (14.5 ft.) with Shuttle

No. of passengers	Dim "A" length	Gross Wt (tons)
25	6.51m	7.54
50	9.29m	13.28
100	14.85m	24.28

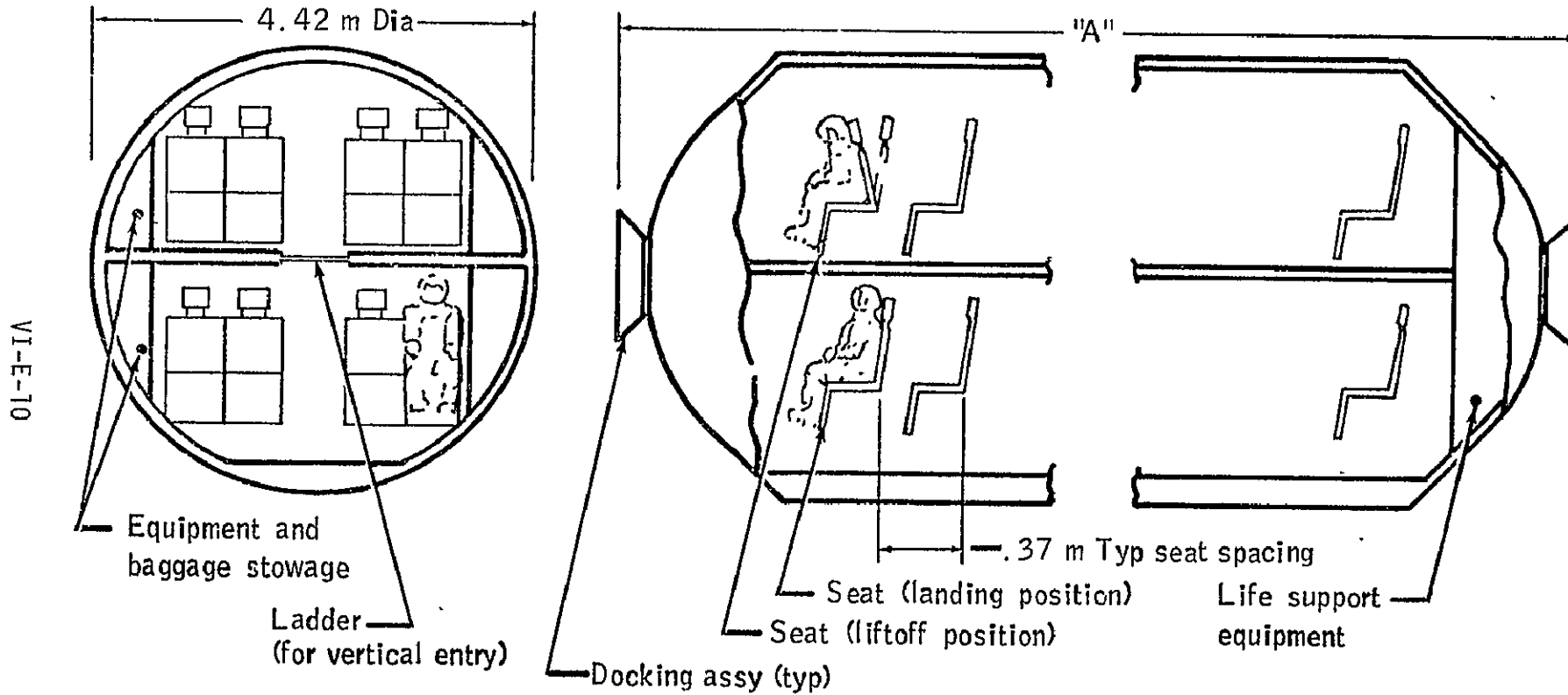


Figure VI-E-2.- Crew rotation passenger module.

Payload density	Dim "A" length	Gross wt * (lbs)
128 kg/m ³	17 m	35MT
144	16 m	34MT
160	13 m	33MT

* Includes 29MT consumables/spares (180 day/25-man resupply)

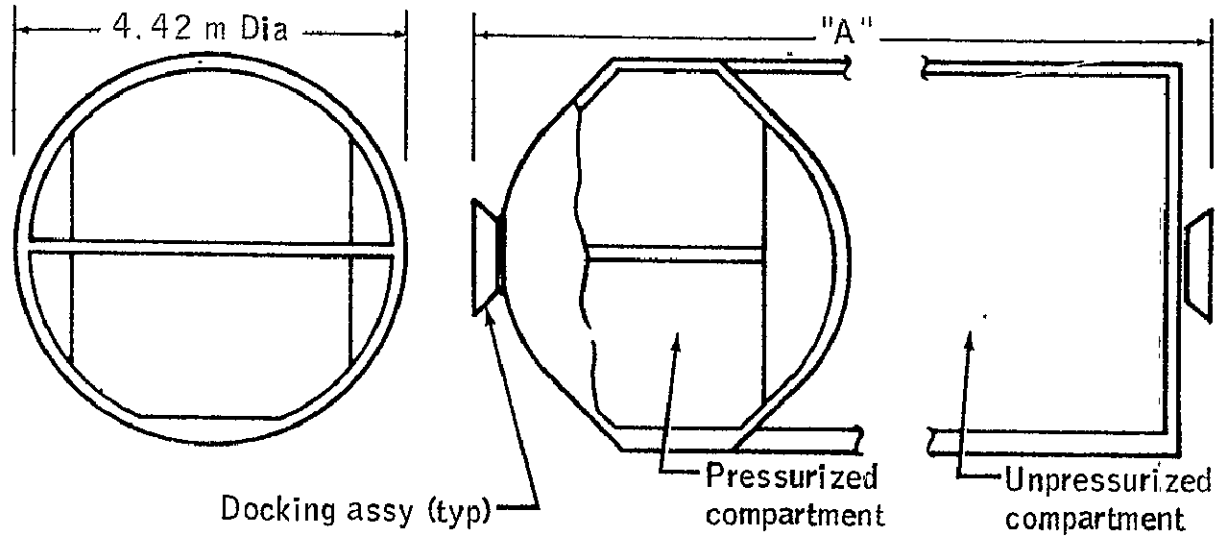


Figure VI-E-3. Resupply module

(Parametric stage mass fraction data were derived from the Boeing FSTSA study.) Results of the sizing study are plotted on Figure VI-E-4. The single stage and common stage are seen to yield similar ignition weights as are the two 1-1/2 stage drop tank options. On the basis of minimum ignition weight, and hence POTV delivery requirements to LEO, the 1-1/2 stage appears to be the most attractive. However, a comprehensive costing and program analysis is required of each option to determine the most cost efficient option. In addition to the POTV options reusable to LEO, POTV options that are refuelable in GEO are viable options during the operational phase when a GEO base exists, provided an economic COTV is available to deliver propellants.

Of particular interest is the common stage option sized for stage 2 refueling at GEO. These results are plotted on Figure VI-E-5 with the previous common stage option refueled at LEO. A factor of over four decrease in vehicle ignition weight is seen over the range of GEO payload capability between the two common stage options. The single stage and 1-1/2 stage options refuelable at GEO were also sized and compared to common stage option with stage 2 refuelable at GEO. Common stage vehicle ignition weights at LEO were seen to be lower than the other two options and with the assumption of stage GEO refueling capability, the common stage is the most desirable option for the operational program phase. In addition, prior to this phase, manned GEO sortie flights probably will be required from LEO. The same common stage vehicle could accommodate the smaller sortie crew module (Figure VI-E-1) round trip from LEO to GEO and return.

POTV REFERENCE CONFIGURATION - COMMON STAGE LO₂/LH₂

On the basis of mission versatility described above, the common stage LO₂/LH₂ option is selected as the POTV reference configuration.

General Vehicle Description - This concept consists of two nearly identical stages used in tandem that provide the required mission delta-V. The first of these stages is unmanned and is used to provide approximately 85% of the delta-V required for departure from LEO on a crew rotation flight. Stage 2 provides the remainder of the boost delta-V as well as the impulse required for injection into the destination orbit and for the return to LEO. Following separation from stage 2, stage 1 is returned unmanned to LEO. Splitting the delta-V as described above, results in the stages having identical propellant capacities. Subsystems design approaches are also common between the stages including the size of the main engine. Taken individually, each of these stages is similar to the single stage concept in terms of subsystem selection and location. At the forward end of the stage 1 are two types of docking provisions. One of these systems is used to connect with stage 2 while the center mounted unit is an international type design that allows docking with systems other than stage 2; examples of these other systems include a tanker for independent servicing or a space station if basing is required while awaiting the return of stage 2.

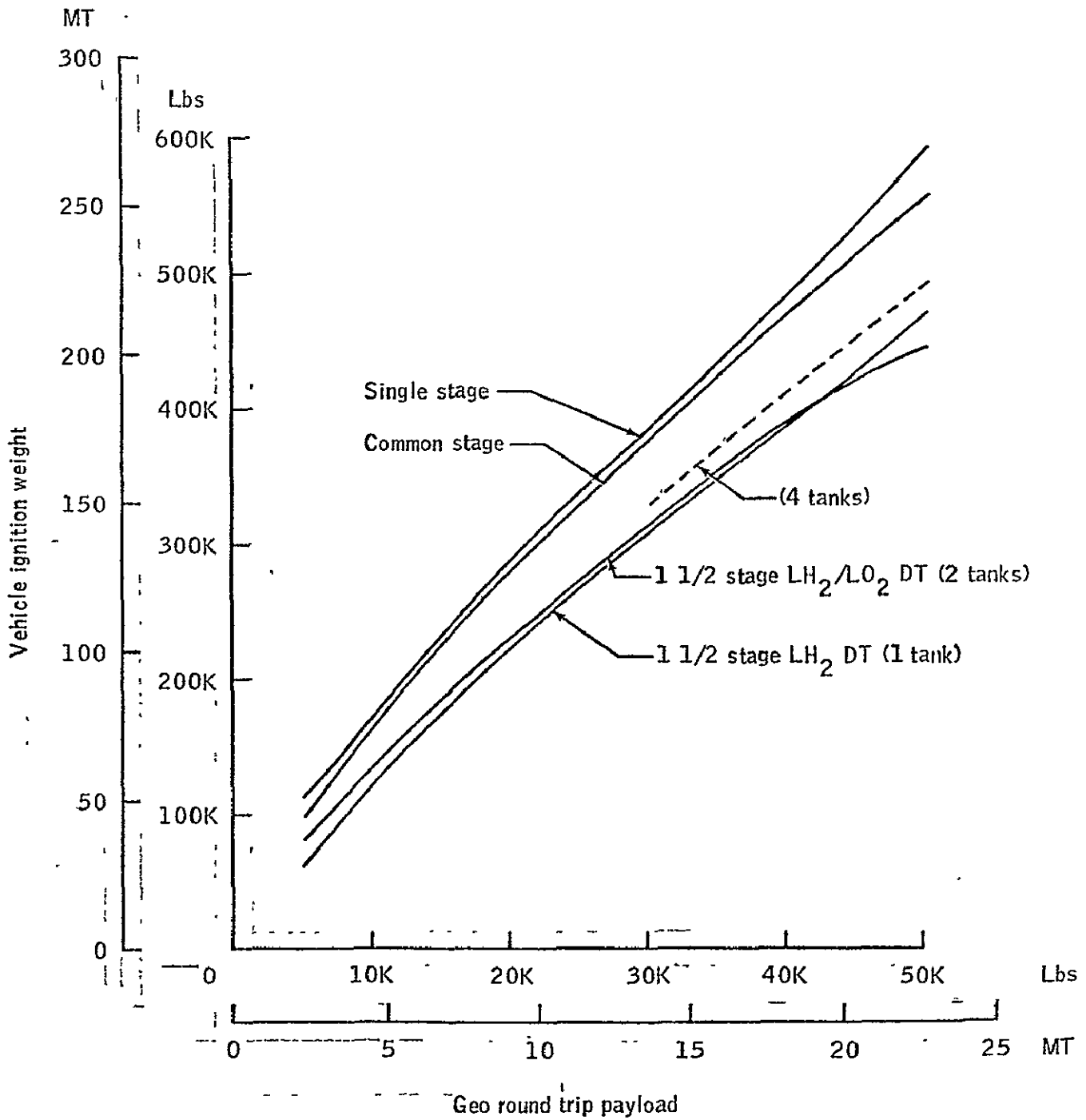


Figure VI-E-4. POTV staging option GEO performance comparison

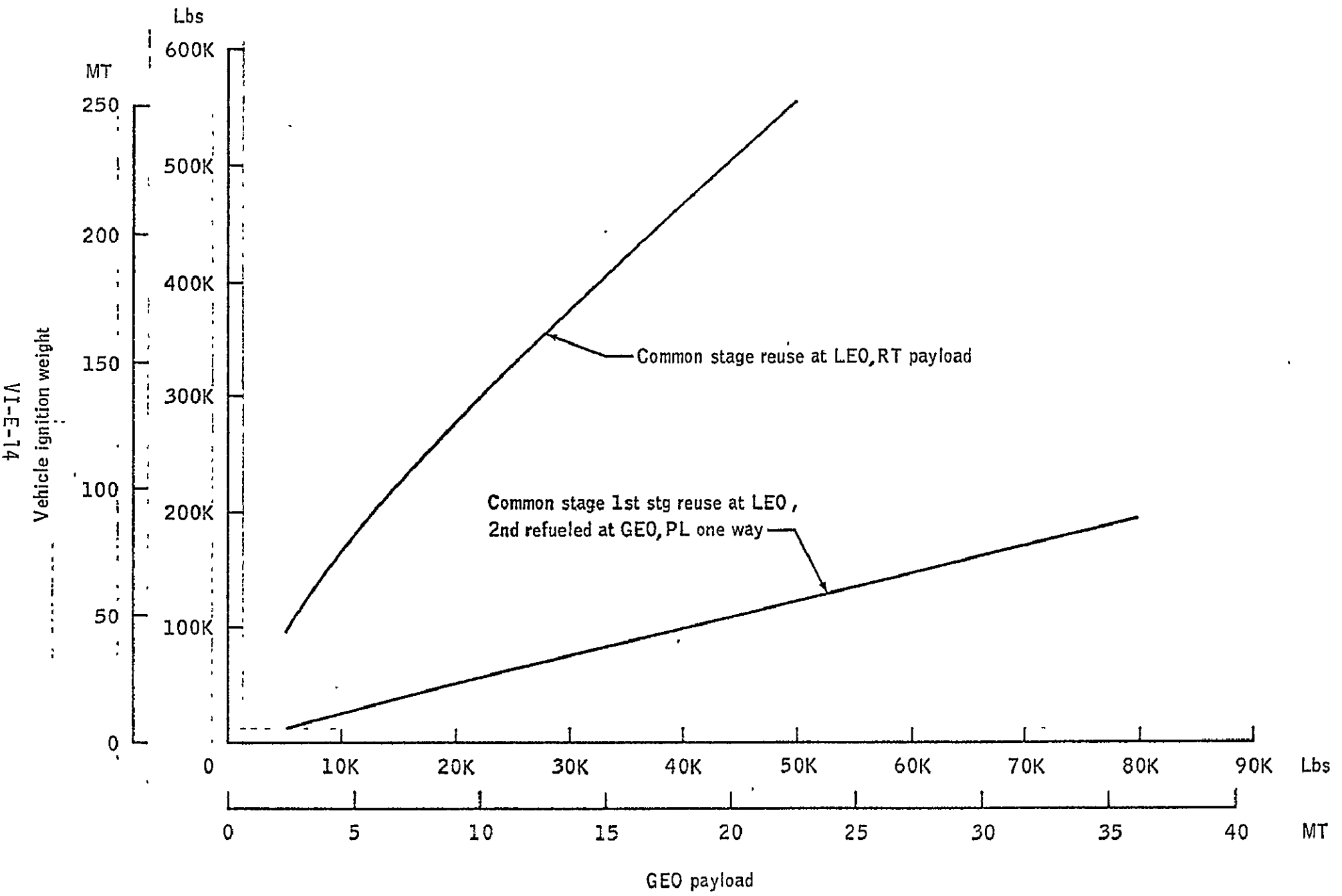


Figure VI-E-5. Common stage mission mode comparison

Stage 2 docking provisions are required at both the forward and aft ends. The forward docking station uses an international type unit for attaching payloads. In addition, this unit accommodates tankers or is used to connect the stage to a space station for basing. The aft docking provisions are used in conjunction with those in the forward section of stage 1 and enable the stages to be connected. Provisions are also included on stage 2 to allow servicing of stage 1 when the two stages are connected, and the tanker is docked at the forward end of stage 2.

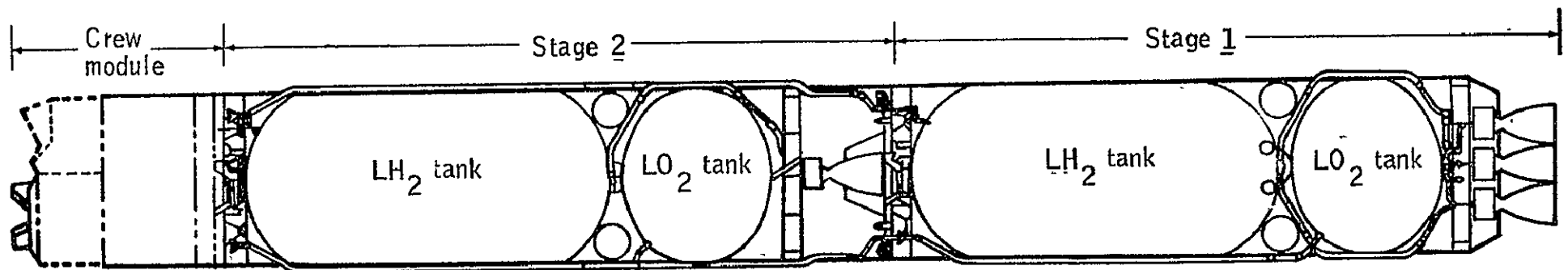
Mission Requirements - The requirements of all three mission types - crew rotation, resupply, and GEO sortie - may be satisfied by the different operating modes of one size of common stage POTV. The fully reusable to LEO operating mode satisfies the manned geosynchronous sortie mission requirements which will appear in the program before a GEO base is available. After a GEO base is available, crew rotation and resupply mission requirements may be satisfied by a common stage whose stage 2 is refueled at the GEO base.

Sizing Method - The common stage vehicle is sized for the GEO sortie mission requirements. The 4-man crew module described earlier (Figure VI-E-1) is flown as the GEO round trip payload with both stages refueled at LEO.

Vehicle Description - The vehicle inboard profile is shown on Figure VI-E-6. The OTV startburn mass is 123 metric tons with a main propellant loading of 106 metric tons. Each stage is 4.42 meters in diameter and 17.06 meters in length (stage 2 length is 15.61 meters with engine nozzles retracted) and are Shuttle compatible and require on-orbit fueling and refueling. The first stage employs four 66,720 newtons (15,000 lbf) thrust engines and the second stage employs two of the same engines. Mass properties are given in Table VI-E-5 for the fully loaded vehicle sized for the sortie mission described earlier.

The vehicle inboard profile for the crew rotation mission is seen on Figure VI-E-7. As described earlier, the crew rotation mission requires stage 2 to be refueled at GEO. A two-man version of the sortie crew module described earlier is assumed to be utilized for manned control of stage 2 and is described by the weights tabulation in Table VI-E-6. On the outbound trip to GEO, the common stage POTV accommodates approximately 20 metric tons of high priority cargo in addition to the 75-man crew rotation passenger module and the 2-man crew control compartment. On the inbound trip, stage 2 returns the crew rotation passenger module and the crew control compartment to LEO.

Single Stage Option - Either stage of the common stage vehicle may be flown autonomously in a single stage mode without the crew module. Payload performance to GEO from LEO has been calculated for stage 2 and is listed below:



Common stage LO₂/LH₂

Life: 30 missions

Payload: 75 passengers + 20 tons (up)
 75 passengers (down)
 (2nd stage GEO refuel)
 ≈\$12 m/ft

Length: 33.28m

Diam: 4.42m

Total weight: 123 tons

Propellant weight: 106 tons

Number of engines at 66 720 newtons each:

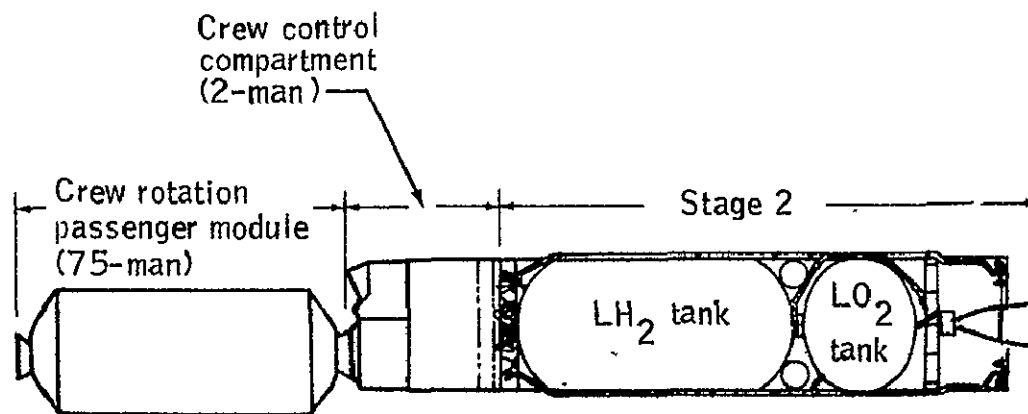
Stage 1: 4 engines

Stage 2: 2 engines

Figure VI-E-6. Personnel orbital transfer vehicle (POTV_L) characteristics

TABLE VI-E-5
 PRELIMINARY WEIGHT STATEMENT
 POTV REFERENCE CONFIGURATION - COMMON STAGE O₂/H₂
 GEO SORTIE MISSION

	Stage 1, lbs	Stage 2, lbs
Dry Mass	(13,210)	(15,210)
Structures and Mechanisms	4,650	4,850
Main Propulsion	3,190	2,270
Thermal Control	1,070	1,180
Auxiliary Propulsion	480	2,630
Avionics	560	560
EPS	620	680
Contingency (25%)	2,640	3,040
Unusable Fluids and EPS Reactants	(860)	(1,340)
LO ₂	370	360
LH ₂	390	380
APS	100	600
Stage Burnout	(14,070)	(16,550)
Inflight Expendables	(117,460)	(122,840)
EPS Reactant	90	420
Boil Off	110	990
Start/Stop Losses	110	180
APS Impulse Propellant	950	5,750
Main Impulse Propellant	116,200	115,500
Stage Ignition lbs (Metric Tons)	131,530 (59.66)	139,390 (63.23)
Vehicle Ignition lbs (Metric Tons)	270,920 (122.60)	



Note: POTV₁ stage 2 refueled at GEO for return to LEO
(propellant weight = 53 metric tons)

Figure VI-E-7. Crew rotation POTV₁ configuration for return from GEO to LEO

TABLE V-E-6

CREW CONTROL MODULE
PRELIMINARY WEIGHT STATEMENT

Primary Structure ⁽¹⁾	1248 kg	2 Crew + 1 Day Reserves	336 kg
Secondary Structure ⁽²⁾	771	Consumables ⁽³⁾	204
Airlock	236	Manned Maneuvering Units ⁽²⁾	<u>181</u>
Mission Support Module	<u>272</u>	Total Variables	721
Total Structure	2527		
Crew Accommodations	400		
Environmental Control	290		
Elect. Power & Distribution	386	Total CM Wt.	5405 kg
Avionics & Console	363	Total Payload to GEO	5405 kg (11,915 lbs)
25% Wt. Growth Contingency	<u>937</u>	Return Payload to LEO	5330 kg (11,750 lbs)
Total Dry Weight	4684		

(1) Control Compt 12.18M³
Crew Quarters 33.81M³

(2) Hatches, Windows, Docking, Arms
(3) 5 Day Mission, 6 Airlock

VI-E-19

Stage expended:	25.7 MT
GEO round trip:	1.2 MT
GEO delivery:	5.4 MT
GEO retrieval:	1.8 MT

For comparison, the MSFC baseline Tug of October 1974 is designed as a reusable single stage containing a usable propellant loading of 23 metric tons has the corresponding payload performance values as listed below:

Stage expended:	10.6 MT
GEO round trip:	.9 MT
GEO Delivery:	3.6 MT
GEO retrieval:	1.5 MT

COST AND SCHEDULE SUMMARY

The cost estimate summary is shown in Table VI-E-7 as provided by Ms. Debbie Webb of the Resources Management Office. Total DDT&E for the two stages is estimated to be \$478M (1976 dollars) and the total first unit cost is estimated to be \$31M.

The nominal development schedule is shown on Figure VI-E-8, as extracted from the Boeing FSTSA study (Phase I Extension Technical Report, December 9, 1975). The schedule includes a fluids transfer technology program to support design and development of on-orbit refueling systems and a stage-to-stage docking/connect system technology program.

(M of 76\$)

	<u>TFU</u>	<u>DDT&E</u>
POTV	<u>31</u>	<u>478</u>
Program Management	0	35
SE&I	0	19
Systems Support	0	39
Stage 1	<u>16</u>	<u>311</u>
Structures	4	44
Propulsion	5	169
TPS	1	6
Avionics	4	84
Electrical Power System	1	3
Inst., Ass. & Co.	2	3
Major Ground Test	0	2
Stage 2	<u>15</u>	<u>74</u>
Structures	4	10
Propulsion	4	44
TPS	1	2
Avionics	4	11
Electrical Power System	1	2
Inst., Ass., & Co.	2	3
Major Ground Test	0	2

Table VI-E-7. COST ESTIMATE SUMMARY
POTV₁ REFERENCE CONFIGURATION
COMMON STAGE LO₂/LH₂

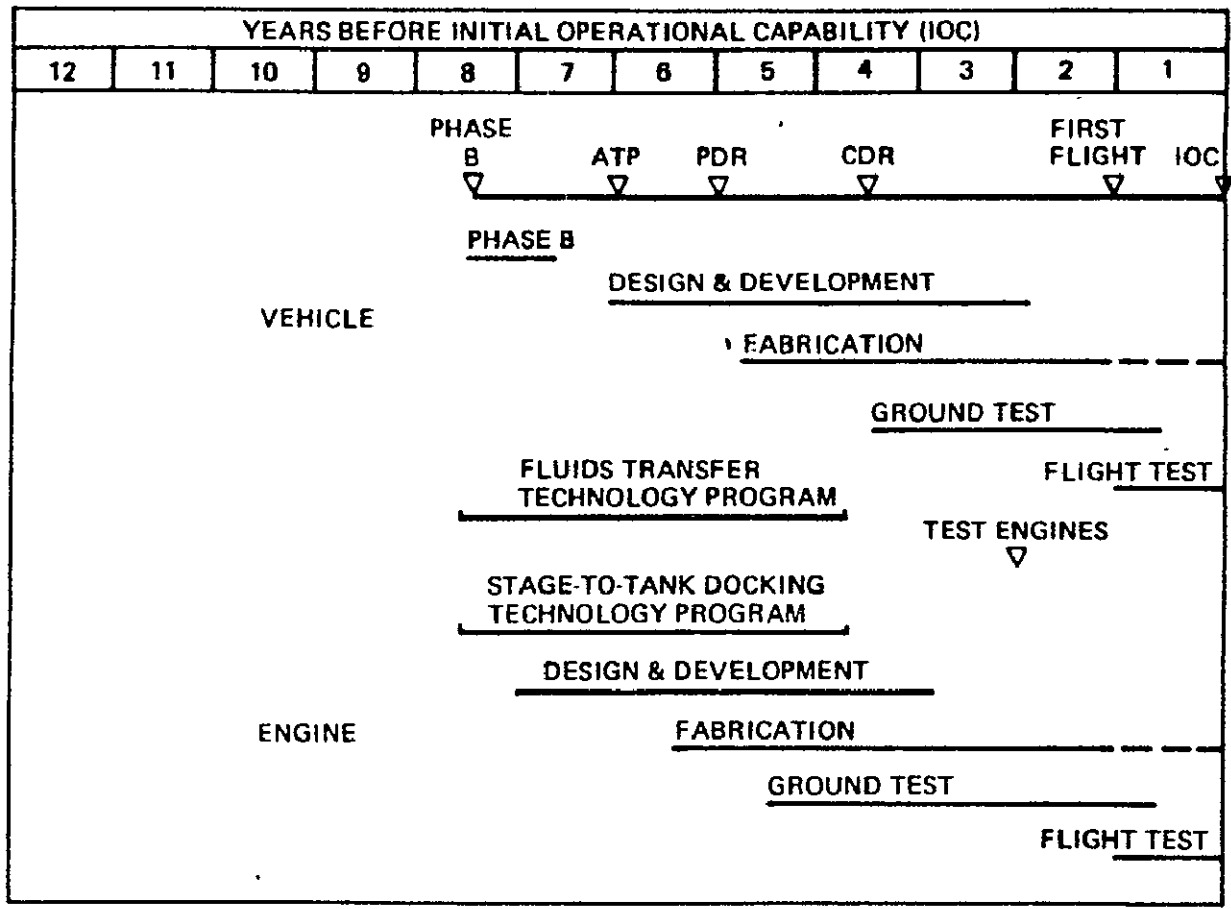


Figure VI-E-8 Common stage O₂/H₂ POTV development schedule

VI. F. Summary of Projected Transportation System Characteristics
(C. Mac Jones, Future Programs Office)

1. Introduction

To understand the space transportation fleet traffic and implications thereof, a space transportation scenario was developed as associated with the SPS implementation scenario. The baseline SPS implementation scenario (Scenario "B") indicates one or more satellites will be brought on-line yearly over a 30-year period such that by the end of 2024, 112 SPS units will be operational at GEO. Figure VI-F-1 presents this baseline SPS implementation schedule. In addition, annual repair of the on-orbit operational SPS units represents a space transportation requirement above the construction-related requirement. The annual repair payload mass has been estimated as 1% of the on-orbit operational SPS mass.

The operational requirements of the transportation system were considered for the three SPS systems options (column-cable/GEO, truss/GEO, and truss/LEO) in order to scope the transportation costs and other parameters for the baseline scenario. Maximum, nominal and minimum estimates of characteristics were made for each option by using all worst case estimates for minimum and characteristics judged "most likely" for nominal.

The space transportation fleet has been characterized by four vehicles:

(a) Heavy Lift Launch Vehicle (HLLV) - unmanned launches of all cargo to LEO.

(b) Cargo Orbital Transfer Vehicle (COTV) - LEO to GEO transfer of all cargo.

(c) Personnel Orbital Transfer Vehicle (POTV) - LEO to GEO and return transfer of all personnel and optional high priority cargo to LEO.

(d) Personnel and Priority Cargo Launch Vehicle (PLV) - manned launches of all personnel and optional high priority cargo to LEO.

These vehicles have been described in detail in earlier sections in discussions of candidate configurations. Detail characteristics of the vehicles used in the scenario are outlined later in this section.

The space transportation scenario logic involving operational aspects of the SPS and characteristics of the space transportation fleet was developed by the Future Programs Office in an illustrative example of the year 2014 of the SPS scenario. This basic logic was evolved into a

	1990	1995	2000	2005	2010	2015	2020	2025
SATELLITES/YR	P	T 1	1 1 1	1 1 2 2 2	2 3 3 3 3	4 4 5 5 5	6 6 6 6 6	6 6 7 7 7
CUM TOTAL			1 2 3 4	5 6 8 10 12	14 17 20 23 26	30 34 39 44 49	55 61 67 73 79	85 91 98 105 112

LEGEND
P=PROTOTYPE OPERATIONAL
T=COMPLETION OF TESTING

FIGURE VI-F-1 Baseline SP5 Implementation Schedule

HP-9810A computer program with typewriter output so that yearly and total SPS program space transportation traffic models with associated costs could be derived more expediently as corresponding scenario data inputs evolved.

Launch Site Consideration

A 28.5° latitude due east launch was assumed for the HLLV's, requiring the OTV's to make the plane change for the equatorial orbit. This is a conservative assumption for performance, since an equatorial launch site offers the advantages of increased Earth rate, a slight increase in altitude because of the Earth's oblateness and, most importantly, the elimination of the plane change requirement which saves approximately 1500 fps of delta V. An additional operational benefit of an equatorial launch site is the opening of the launch window to almost "at will" launch instead of the total of about 3 hours daily available at a 28.5° KSC launch site. Future studies will investigate more thoroughly the technical and other trade-offs for various launch sites as well as the impacts of establishing the SPS in a Lagrangian metastable orbit inclined at approximately 7.3°.

Transportation Fleet Description

Vehicle characteristics for the space transportation fleet were synthesized for input to the scenario computer program. In-house and contractor studies served as background and reference data for developing the detailed vehicle data. Projected ranges of technology (performance, weights, and costs) were used in sizing the minimum cost (MIN), nominal cost (NOM), and maximum cost (MAX) vehicle derivative.

Heavy Lift Launch Vehicle (HLLV) - The HLLV will be utilized for transport of all SPS hardware, OTV hardware and propellants, construction and support bases and consumables, and personnel consumables from Earth to LEO. Eleven candidate launch vehicles have been identified of these basic types: complete winged entry/recovery, complete ballistic entry/recovery, winged entry/recovery with large external hydrogen tank expended. The various costs of development, acquisition and operation are still under study. The minimum cost vehicle has been characterized as a two stage, series burn ballistic entry/recovery unmanned launch vehicle with O₂/propane booster and O₂/H₂ second stage. The maximum cost vehicle has been characterized as a two stage, series burn winged entry/recovery with O₂/RP-1 booster and O₂/H₂ second stage. The following HLLV input data was derived to provide the extremes and is consistent with HLLV study data to date:

	<u>Min</u>	<u>Nom</u>	<u>Max</u>
Payload/flt, tons	900	700	450
Flt cost, \$/flt	20	23	25
Flt turnaround, days	5	6	9

Cargo Orbital Transfer Vehicle (COTV) - The COTV will be utilized for transport of all SPS hardware, GEO bases and consumables, and GEO personnel consumables from LEO to GEO. Again, several candidates have been identified in two basic categories of independent power and dependent power and then in three categories of high thrust chemical propulsion, low thrust electrical propulsion, and combined chemical/electrical propulsion.

For SPS geosynchronous construction, independent power is required of the COTV and based on studies to date, conventional O_2/H_2 high thrust propulsion is selected with a 2-1/2 stage option for vehicle sizing purposes. The range of COTV_G (subscript "G" denoting SPS GEO construction) is described as follows:

	<u>Min</u>	<u>Nom</u>	<u>Max</u>
Payload, MT	250	250	250
Stages	2½	2½	2½
Isp, sec	470	460	455
Mass fraction (λ')	.94	.93	.92
Total inert weight, MT	29	35	43
Prop weight, MT	453	475	494
Expended inert weight, MT	7	9	11
Flt cost, \$M/flt	5	10	20
Flt turnaround, days	5	7	10
Mission life	50	30	20

For SPS LEO construction, dependent power vehicles utilizing electrical propulsion for most of the transfer from LEO to GEO have been selected. Conventional O_2/H_2 chemical propulsion will be required for occultation periods or for transporting the payload plus electrical propulsion module to sunlit altitudes. The extent of this supplemental propulsion is not yet well defined, as departure altitude, data, inclination, desired launch window and thrust/mass ratio all interact to determine the minimum sunlit "handover" altitudes. One SPS concept, the planar photovoltaic array design, may be separated into 30 modules, each of which can provide electrical power to the electrical propulsion stages to avoid excessive structural loads on the array modules, for propulsion units are assumed to be mounted to the corners of each module. Studies of the relative merits of the propulsion options have not indicated a clear preference. Therefore, for vehicle sizing purposes for this scenario, an expendable MPD thermal arcjet propulsion unit with reusable chemical propulsion to 3500 km altitude is assumed for the COTV_L (subscript "L" denoting SPS LEO construction). The range of COTV_L is given as follows:

	<u>Min</u>	<u>Nom</u>	<u>Max</u>
Payload, MT	1000	1000	1000
Electric Propulsion:			
Isp, Sec	4000	3000	2500
Mass fraction (λ)	.6	.6	.6
Inert weight, MT	79	110	138
Prop weight, MT	119	166	207
Expended inert, MT	79	110	138
Chemical Propulsion:			
Isp, Sec	470	460	455
Mass fraction (λ)	.93	.92	.90
Inert weight, MT	43	56	77
Prop weight, MT	572	634	695
Total Vehicle:			
Inert weight, MT	122	166	215
Prop weight, MT	691	800	902
Expended inert, MT	79	110	138
Flt cost, \$M/flt	20	30	70
Flt turnaround, days	5	7	10
Mission Life	20	10	5

Personnel Orbital Transfer Vehicle (POTV) - The POTV will be utilized to transport all personnel from LEO to GEO and return. To minimize passenger exposure to the VanAllen belt radiation, a trip time of less than one day is required. Therefore, conventional high thrust O_2/H_2 chemical propulsion is assumed.

For SPS GEO construction, a passenger module may be carried as part of the payload of the COTV_G. For purposes of this scenario in determining POTV_G GEO trips required, the passenger only capability has been calculated and is limited by the down payload capability of stages. In addition, when the COTV_G is utilized as the POTV_G, the second stage drop tank is not expended at GEO, but is returned with the stage 2 core and hence the down propellant. The range of POTV_G characteristics is given as follows:

	<u>Min</u>	<u>Nom</u>	<u>Max</u>
Passengers	240	230	215
Isp, sec	470	460	455
Mass fraction (λ)	.94	.93	.92
Inert weight, MT	29	35	43
Prop weight, MT	453	475	494
Flt cost, \$M/flt	10	15	25
Flt turnaround, days	5	7	10
Mission life	50	30	20

For SPS LEO construction, the POTV is regarded as a special purpose device due to the long trip times associated with the COTV_L. The number of people traveling to GEO will be less due to the large LEO construction crew and therefore infers a smaller passenger carrying vehicle than the POTV_G. In addition, this common stage O₂/H₂ vehicle takes advantage of the economies of the COTV_L by having its down propellant delivered to GEO. The range of POTV_L is given as follows:

	<u>Min</u>	<u>Nom</u>	<u>Max</u>
Passengers	75	75	75
Isp, sec	470	462	455
Mass fraction (λ')	.89	.89	.88
Inert weight, MT	17	19	23
Prop up, MT	93	106	126
Prop down, MT	47	53	63
Flt cost, \$M/flt	7	12	22
Flt turnaround, days	5	7	10
Mission life	50	30	20

Personnel and Priority Cargo Launch Vehicle (PLV) - The PLV will be utilized for transport of all personnel from Earth to LEO and return. The PLV will be available for small loads of priority cargo, but this capability is not considered in this scenario exercise. Basically, the PLV is an upgraded Shuttle with the two baseline SRB's replaced by a "liquid replacement booster" (LRB) that operates in a series burn mode with the Orbiter/ET. The LRB is reusable following a ballistic entry and parachute/landing rockets water splashdown. The range of PLV characteristics is given as follows and is consistent with in-house studies by Rockwell International and Boeing.

	<u>Min</u>	<u>Nom</u>	<u>Max</u>
Passengers/flt	80	50	40
Flt cost, \$M/flt	8	10	12
Flt turnaround, days	7	11	14

Orbital Propellant Storage/Transfer

For the space transportation scenario, it was assumed that all COTV's and POTV's are based at LEO for refurbishment, refueling, and other flight vehicle turnaround activities. It was also assumed that all OTV propellants are delivered by HLLV to a LEO depot "tank farm" for propellant storage before OTV refueling. There will be propellant losses associated with this storage/transfer activity in terms of daily boiloff, transfer residuals, and chilldown losses. These LEO propellant losses have been estimated as 30% such that for every kilogram of OTV propellant required at LEO, 1.3 kilograms must be delivered to LEO by the HLLV. In the case of the POTV_L, the crew rotation mission requires that the second stage be refueled at GEO; therefore, a more modest tank farm is assumed available at GEO. The total GEO propellant loss has been estimated at

50% such that for every kilogram of propellant required at GEO for POTV_L refueling, 1.5 kilograms must be delivered to LEO by the HLLV, and subsequently, the COTV_L must deliver 1.2 kilograms to the GEO depot tank farm.

Additional study and refinement of requirements is required in this area and will be provided by a proposed JSC FY77 contracted study titled "Orbital Propellant Transfer and Storage Systems for Large Space Programs."

Computer Output Data

Annual and total 30 year program runs were completed for three SPS construction concepts:

- Concept 1 - Column/cable SPS constructed at GEO
- Concept 2 - Truss SPS constructed at GEO
- Concept 3 - Truss SPS constructed at LEO

Year 2024 Totals - The following computer printout tables represent the space transportation activity and costs related to "Construction Only" (Table VI-F-1) and "Repair Only" (Table VI-F-2) of the SPS scenario in the year 2024. This year represents the maximum activity year during the 30 year scenario. Vehicle flights, fleet sizes, personnel involved, and costs are at a peak with construction of seven SPS units and hypothetical repair of 105 SPS units occurring during the year.

TABLE VI-F-1

CONSTRUCTION ONLY

Page 1 of 1

YEAR 2024 TRANSPORTATION TRAFFIC MODEL
(Preliminary Estimates)

	GEO ASSY (1)			LEO ASSY (3)		
	MIN	NOM	MAX	MIN	NOM	MAX
No. of SPS	7.0	7.0	7.0	7.0	7.0	7.0
SPS mass each, tonsX10 ³	48.387	83.582	128.459	51.564	90.123	132.365
GEO man-years/SPS	474	474	474	200	200	200
LEO persnl consum/SPS, tonsX10 ³	1.422	1.422	1.422	0.400	0.400	0.400
GEO Base, tonsX10 ³	0.000	0.000	0.000	0.000	0.000	0.000
LEO man-years/SPS	160	176	230	736	740	766
LEO persnl consum/SPS, tonsX10 ³	0.320	0.352	0.460	2.169	2.177	2.229
LEO Base, tonsX10 ³	0.000	0.000	0.000	0.000	0.000	0.000
Const Base suppt/SPS, tonsX10 ³	1.000	1.000	1.000	1.000	1.000	1.000
LEO prop storage/transfer factor 1.30						
GEO prop storage/transfer factor 1.50						
A. POTV CHARACTERISTICS						
Passengers/flt	240	230	215	75	75	75
Inert weight each, tonsX10 ³	0.029	0.035	0.043	0.017	0.019	0.023
Prop up, tonsX10 ³	0.453	0.475	0.494	0.093	0.106	0.126
Prop down, tonsX10 ³	0.000	0.000	0.000	0.047	0.053	0.063
Flt cost, \$M/flt	10	15	25	7	12	22
Flt turnaround, days	5	7	10	5	7	10
Mission life	50	30	20	50	30	20
B. PLV CHARACTERISTICS						
Passengers/flt	80	50	40	80	50	40
Flt cost, \$M/flt	8	10	12	8	10	12
Flt turnaround, days	7	11	14	7	11	14
C. CQTV CHARACTERISTICS						
Payload/flt, tonsX10 ³	0.250	0.250	0.250	1.000	1.000	1.000
Total inert wt, tonsX10 ³	0.029	0.035	0.043	0.122	0.166	0.215
Expended inert wt, tonsX10 ³	0.007	0.009	0.011	0.079	0.110	0.138
Propellant/flt, tonsX10 ³	0.453	0.475	0.494	0.691	0.800	0.902
Flt cost, \$M/flt	5	10	20	20	30	70
Flt turnaround, days	5	7	10	5	7	10
Mission life	50	30	20	20	10	5
D. HLLV CHARACTERISTICS						
Payload/flt, tons	900	700	450	900	700	450
Flt cost, \$M/flt	20	23	25	20	23	25
Flt turnaround, days	5	6	9	5	6	9

ORIGINAL PAGE IS
OF POOR QUALITY

VI-F-8

YEAR 2024 TRANSPORTATION TRAFFIC MODEL
(Preliminary Estimates)

	GEO ASSY (1)			LEO ASSY (3)		
	MIN	NOM	MAX	MIN	NOM	MAX
No. of SPS/yr	7.0	7.0	7.0	7.0	7.0	7.0
SPS mass each tonsX10 ³	48.387	83.582	128.459	51.564	90.123	132.365
Total SPS mass tonsX10 ³ /yr	338.709	585.074	899.213	360.948	630.861	926.555
A. MANNED SUPPORT TO GEO						
Man trips/yr to GEO & return	6636	6636	6636	2800	2800	2800
Personnel consum, tonsX10 ³ /yr	9.95	9.95	9.95	2.80	2.80	2.80
POTV GEO trips/yr	28	29	31	37	37	37
POTV prop GEOup tonsX10 ³ /yr	12.53	13.70	15.25	3.47	3.96	4.70
POTV prop GEOdwn tonsX10 ³ /yr	0.00	0.00	0.00	1.75	1.98	2.35
COTV trips/yr	40	40	40	5	5	6
COTV prop tonsX10 ³ /yr	18.04	18.91	19.67	3.51	4.30	5.28
COTV flt cost \$M/yr	199	398	796	102	161	410
POTV flt cost \$M/yr	277	433	772	261	448	821
POTV flt turnaround, days	5	7	10	5	7	10
POTV fleet size, units	2	2	2	2	2	2
POTV replacement, units	1	1	2	1	1	2
B. MANNED SUPPORT TO LEO						
LEO man trips/yr	8876	9100	9856	13104	13160	13524
Personnel consum, tons 10 ³ /yr	2.24	2.46	3.22	15.18	15.24	15.60
PLV flts/yr	111	182	246	164	263	338
PLV flt cost \$M/yr	888	1820	2957	1310	2632	4057
PLV flt turnaround, days	7	11	14	7	11	14
PLV fleet size, units	2	6	9	3	8	13
C. GEO CONSTRUCTION SUPPORT						
Const Base, tonsX10 ³ /yr	0.00	0.00	0.00	0.00	0.00	0.00
Equip & consum, tonsX10 ³ /yr	7.00	7.00	7.00	0.00	0.00	0.00
COTV trips/yr	28	28	28	0	0	0
COTV prop tonsX10 ³ /yr	12.68	13.30	13.83	0.00	0.00	0.00
COTV flt cost \$M/yr	140	280	560	0	0	0

VI-F-9

ORIGINAL PAGE IS
OF POOR QUALITY

TABLE VI-F-1 (CONT'D)

CONSTRUCTION ONLY

YEAR 2024 TRANSPORTATION TRAFFIC MODEL
(Preliminary Estimates)

	GEO ASSY (1)			LEO ASSY (3)		
	MIN	NOM	MAX	MIN	NOM	MAX
D. SPS TRANSFER TO GEO						
Total SPS mass tonsX10 ³ /yr	339	585	899	361	631	927
COTV trips/yr	1355	2340	3597	361	631	927
COTV prop tonsX10 ³ /yr	614	1112	1777	249	505	836
COTV flt cost \$M/yr	6774	23403	71937	7219	18926	64859
E. TOTAL COTV REQMT						
COTV flt turnaround, days	5	7	10	5	7	10
Total COTV fleet, units	20	46	101	5	12	26
COTV replacement, units	28	80	183	18	64	186
Total COTV flt cost \$M/yr	7113	24081	73293	7321	19087	65269
F. LEO CONSTRUCTION SUPPORT						
Const Base, tonsX10 ³ /yr	0.00	0.00	0.00	0.00	0.00	0.00
Equip & consum, onesX10 ³ /yr	0.00	0.00	0.00	7.00	7.00	7.00
G. TOTAL CARGO LAUNCH REQMT						
Cargo mass, tonsX10 ³ /yr	1223	2112	3341	753	1406	2225
Payload mass per HLLV, tons	900	700	450	900	700	450
HLLV flts/yr	1359	3017	7425	837	2009	4944
HLLV flt cost \$M/yr	27173	69401	185619	16735	46213	123603
HLLV flt turnaround, days	5	6	9	5	6	9
HLLV fleet size, units	19	50	184	11	33	122
H. TRANSPORTATION COST RECAP						
POTV flt cost \$M/yr	277	433	772	261	448	821
FLV flt cost \$M/yr	888	1820	2957	1310	2632	4057
COTV flt cost \$M/yr	7113	24081	73293	7321	19087	65269
Subtotal	8277	26334	77022	8892	22167	70147
HLLV flt cost \$M/yr	27173	69401	185619	16735	46213	123603
TOTAL TRANSPORTATION COST \$M	35451	95735	262640	25627	68380	193751
Specific cost \$/Kg SPS	104.66	163.63	292.08	71.00	108.39	209.11
Specific cost \$/KWe bus	506.44	1367.65	3752.01	366.10	976.85	2767.87

VI-F-10

YEAR 2024 TRANSPORTATION TRAFFIC MODEL
(Preliminary Estimates)

	GEO ASSY (2)			LEO ASSY		
	MIN	NOM	MAX	MIN	NOM	MAX
No. of SPS	7.0	7.0	7.0	7.0	7.0	7.0
SPS mass each, tonsX10 ³	51.564	90.123	132.365	0.000	0.000	0.000
GEO man-years/SPS	574	574	574	0	0	0
GEO persnl consum/SPS, tonsX10 ³	1.722	1.722	1.722	0.000	0.000	0.000
GEO Base, tonsX10 ⁵	0.000	0.000	0.000	0.000	0.000	0.000
LEO man-years/SPS	160	176	230	0	0	0
LEO persnl consum/SPS, tonsX10 ³	0.320	0.352	0.460	0.000	0.000	0.000
LEO Base, tonsX10 ⁵	0.000	0.000	0.000	0.000	0.000	0.000
Const Base suppt/SPS, tonsX10 ³	1.000	1.000	1.000	0.000	0.000	0.000
LEO prop storage/transfer factor	1.30					
GEO prop storage/transfer factor	1.50					
A. POTV CHARACTERISTICS						
Passengers/flt	240	230	215	0	0	0
Inert weight each, tonsX10 ³	0.029	0.035	0.043	0.000	0.000	0.000
Prop up, tonsX10 ³	0.453	0.475	0.494	0.000	0.000	0.000
Prop down, tonsX10 ³	0.000	0.000	0.000	0.000	0.000	0.000
Flt cost, \$M/flt	10	15	25	0	0	0
Flt turnaround, days	5	7	10	0	0	0
Mission life	50	30	20	50	30	20
B. PLV CHARACTERISTICS						
Passengers/flt	80	50	40	80	50	40
Flt cost, \$M/flt	8	10	12	8	10	12
Flt turnaround, days	7	11	14	7	11	14
C. COTV CHARACTERISTICS						
Payload/flt, tonsX10 ³	0.250	0.250	0.250	0.000	0.000	0.000
Total inert wt, tonsX10 ³	0.029	0.035	0.043	0.000	0.000	0.000
Expended inert wt, tonsX10 ³	0.007	0.009	0.011	0.000	0.000	0.000
Propellant/flt, tonsX10 ³	0.453	0.475	0.494	0.000	0.000	0.000
Flt cost, \$M/flt	5	10	20	0	0	0
Flt turnaround, days	5	7	10	0	0	0
Mission life	50	30	20	0	0	0
D. HLLV CHARACTERISTICS						
Payload/flt, tons	900	700	450	900	700	450
Flt cost, \$M/flt	20	23	25	20	23	25
Flt turnaround, days	5	6	9	5	6	9

VI-F-11

YEAR 2024 TRANSPORTATION TRAFFIC MODEL
(Preliminary Estimates)

VI-F-13

	GEO ASSY (2)			LEO ASSY		
	MIN	NOM	MAX	MIN	NOM	MAX
D. SPS TRANSFER TO GEO						
Total SPS mass tonsX10 ³ /yr	361	631	927	0	0	0
COTV trips/yr	1444	2523	3706	0	0	0
COTV prop tonsX10 ³ /yr	654	1199	1831	0	0	0
COTV flt cost \$M/yr	7219	25234	74124	0	0	0
E. TOTAL COTV REQMT						
COTV flt turnaround, days	5	7	10	0	0	0
Total COTV fleet, units	21	50	104	0	0	0
COTV replacement, units	30	87	189	0	0	0
Total COTV flt cost \$M/yr	7600	25997	75649	0	0	0
F. LEO CONSTRUCTION SUPPORT						
Const Base, tonsX10 ³ /yr	0.00	0.00	0.00	0.00	0.00	0.00
Equip & consum, tonsX10 ³ /yr	0.00	0.00	0.00	0.00	0.00	0.00
G. TOTAL CARGO LAUNCH REQMT						
Cargo mass, tonsX10 ³ /yr	1309	2282	3452	0	0	0
Payload mass per HLLV, tons	900	700	450	900	700	450
HLLV flts/yr	1454	3261	7671	0	0	0
HLLV flt cost \$M/yr	29081	74992	191776	0	0	0
HLLV flt turnaround, days	5	6	9	5	6	9
HLLV fleet size, units	20	54	190	0	0	0
H. TRANSPORTATION COST RECAP						
POTV flt cost \$M/yr	335	524	934	0	0	0
LEV flt cost \$M/yr	1028	2100	3377	0	0	0
COTV flt cost \$M/yr	7600	25997	75649	0	0	0
Subtotal	8962	28621	79960	0	0	0
HLLV flt cost \$M/yr	29081	74992	191776	0	0	0
TOTAL TRANSPORTATION COST \$M	38044	103613	271735	0	0	0
Specific cost \$/Kg SPS	105.40	164.24	293.28	0.00	0.00	0.00
Specific cost \$/Kwe bus	543.48	1480.19	3881.94	0.00	0.00	0.00

ORIGINAL PAGE IS OF POOR QUALITY

REPAIR ONLY

TABLE VI-F-2

YEAR 2024 TRANSPORTATION TRAFFIC MODEL
(Preliminary Estimates)

	GEO ASSY (1)			LEO ASSY (3)		
	MIN	NOM	MAX	MIN	NOM	MAX
No. of SPS operational	105.0	105.0	105.0	105.0	105.0	105.0
SPS mass each, tonsX10 ³	48.387	83.582	128.459	51.564	90.123	132.365
GEO man-years/SPS	12.00	12.00	12.00	12.00	12.00	12.00
GEO persnl consum/SPS, tonsX10 ³	0.02400	0.02400	0.02400	0.02400	0.02400	0.02400
GEO Base, tonsX10 ³	0.000	0.000	0.000	0.000	0.000	0.000
LEO man-years/SPS	0.37	0.53	1.07	0.39	0.43	0.69
LEO persnl consum/SPS, tonsX10 ³	0.00074	0.00106	0.00214	0.00078	0.00086	0.00138
LEO Base, tonsX10 ³	0.000	0.000	0.000	0.000	0.000	0.000
SPS repair suppt, % SPS mass	1.000	1.000	1.000	1.000	1.000	1.000
LEO prop storage/transfer factor	1.30					
GEO prop storage/transfer factor	1.50					
A. POTV CHARACTERISTICS						
Passengers/flt	240	230	215	75	75	75
Inert weight each, tonsX10 ³	0.029	0.035	0.043	0.017	0.019	0.023
Prop up, tonsX10 ³	0.453	0.475	0.494	0.093	0.106	0.126
Prop down, tonsX10 ³	0.000	0.000	0.000	0.047	0.053	0.063
Flt cost, \$M/flt	10	15	25	7	12	22
Flt turnaround, days	5	7	10	5	7	10
Mission life	50	30	20	50	30	20
B. PLV CHARACTERISTICS						
Passengers/flt	80	50	40	80	50	40
Flt cost, \$M/flt	8	10	12	8	10	12
Flt turnaround, days	7	11	14	7	11	14
C. COTV CHARACTERISTICS						
Payload/flt, tonsX10 ³	0.250	0.250	0.250	1.000	1.000	1.000
Total inert wt, tonsX10 ³	0.029	0.035	0.043	0.122	0.166	0.215
Expended inert wt, tonsX10 ³	0.007	0.009	0.011	0.079	0.110	0.138
Propellant/flt, tonsX10 ³	0.453	0.475	0.494	0.691	0.800	0.902
Flt cost, \$M/flt	5	10	20	20	30	70
Flt turnaround, days	5	7	10	5	7	10
Mission life	50	30	20	20	10	5
D. HLLV CHARACTERISTICS						
Payload/flt, tons	900	700	450	900	700	450
Flt cost, \$M/flt	20	23	25	20	23	25
Flt turnaround, days	5	6	9	5	6	9

VI-F-14

YEAR 2024 TRANSPORTATION TRAFFIC MODEL
(Preliminary Estimates)

	GEO ASSY(1)			LEO ASSY(3)		
	MIN	NOM	MAX	MIN	NOM	MAX
No. of SPS operational	105.0	105.0	105.0	105.0	105.0	105.0
SPS mass each tonsX10 ³	48.387	83.582	128.459	51.564	90.123	132.365
Total SPS mass tonsX10 ³ /yr	5080.635	8776.110	13488.195	5414.220	9462.915	13898.325
A. MANNED SUPPORT TO GEO						
Man trips/yr to GEO & return	2520	2520	2520	2520	2520	2520
Personnel consum, tonsX10 ³ /yr	2.52	2.52	2.52	2.52	2.52	2.52
POTV GEO trips/yr	11	11	12	34	34	34
POTV prop GEOup tonsX10 ³ /yr	4.76	5.20	5.79	3.12	3.56	4.23
POTV prop GEOdwn tonsX10 ³ /yr	0.00	0.00	0.00	1.58	1.78	2.12
COTV trips/yr	10	10	10	5	5	5
COTV prop tonsX10 ³ /yr	4.57	4.79	4.98	3.16	3.87	4.76
COTV flt cost \$M/yr	50	101	202	91	145	369
POTV flt cost \$M/yr	105	164	293	235	403	739
POTV flt turnaround, days	5	7	10	5	7	10
POTV fleet size, units	2	2	2	2	2	2
POTV replacement, units	0	0	1	1	1	2
B. MANNED SUPPORT TO LEO						
LEO man trips/yr	2598	2631	2745	2602	2610	2665
Personnel consum, tons 10 ³ /yr	0.08	0.11	0.22	0.08	0.09	0.14
PLV flts/yr	32	53	69	33	52	67
PLV flt cost \$M/yr	260	526	823	260	522	799
PLV flt turnaround, days	7	11	14	7	11	14
PLV fleet size, units	2	2	3	2	2	3
3. GEO CONSTRUCTION SUPPORT						
Const Base, tonsX10 ³ /yr	0.00	0.00	0.00	0.00	0.00	0.00
Equip & consum, tonsX10 ³ /yr	50.81	87.76	134.88	54.14	94.63	138.98
COTV trips/yr	203	351	540	54	95	139
COTV prop tonsX10 ³ /yr	92.06	166.75	266.53	37.41	75.70	125.36
COTV flt cost \$M/yr	1016	3510	10791	1083	2839	9729

VI-F-15

ORIGINAL PAGE IS
OF POOR QUALITY

REPAIR ONLY

TABLE VI-F-2 (CONT'D)
YEAR 2024 TRANSPORTATION TRAFFIC MODEL
(Preliminary Estimates)

	GEO ASSY(1)			MIN	LEO ASSY(3)	
	MIN	NOM	MAX		NOM	MAX
D. SPS TRANSFER TO GEO						
Total SPS mass tonsX10 ³ /yr	0	0	0	0	0	0
COTV trips/yr	0	0	0	0	0	0
COTV prop tonsX10 ³ /yr	0	0	0	0	0	0
COTV flt cost \$M/yr	0	0	0	0	0	0
E. TOTAL COTV REQMT						
COTV flt turnaround, days	5	7	10	5	7	10
Total COTV fleet, units	3	7	15	1	2	4
COTV replacement, units	4	12	27	3	10	29
Total COTV flt cost \$M/yr	1067	3611	10992	1174	2984	10098
F. LEO CONSTRUCTION SUPPORT						
Const Base, tonsX10 ³ /yr	0.00	0.00	0.00	0.00	0.00	0.00
Equip & consum, tonsX10 ³ /yr	0.00	0.00	0.00	0.00	0.00	0.00
G. TOTAL CARGO LAUNCH REQMT						
Cargo mass, tonsX10 ³ /yr	187	321	505	121	221	346
Payload mass per HLLV, tons	900	700	450	900	700	450
HLLV flts/yr	208	458	1123	134	315	768
HLLV flt cost \$M/yr	4152	10534	28078	2687	7249	19211
HLLV flt turnaround, days	5	6	9	5	6	9
HLLV fleet size, units	3	8	28	2	5	19
H. TRANSPORTATION COST RECAP						
POTV flt cost \$M/yr	105	164	293	235	403	739
PLV flt cost \$M/yr	260	526	823	260	522	799
COTV flt cost \$M/yr	1057	3611	10992	1174	2984	10098
Subtotal	1431	4302	12109	1670	3909	11637
HLLV flt cost \$M/yr	4152	10534	28078	2687	7249	19211
TOTAL TRANSPORTATION COST \$M	5583	14836	40186	4357	11158	30848

VI-F-16

TABLE VI-F-2 (CONT'D)
 YEAR 2024 TRANSPORTATION TRAFFIC MODEL
 (Preliminary Estimates)

	GEO ASSY (2)				LEO ASSY	
	KIN	NOM	MAX	MIN	NOM	MAX
No. of SPS operational	105.0	105.0	105.0	105.0	105.0	105.0
SPS mass each, tonsX10 ³	51.564	90.123	132.365	0.000	0.000	0.000
GEO man-years/SPS	12.00	12.00	12.00	0.00	0.00	0.00
GEO persnl consum/SPS, tonsX10 ³	0.02400	0.02400	0.02400	0.00000	0.00000	0.00000
GEO Base, tonsX10 ³	0.000	0.000	0.000	0.000	0.000	0.000
LEO man-years/SPS	0.37	0.53	1.07	0.00	0.00	0.00
LEO persnl consum/SPS, tonsX10 ³	0.00074	0.00106	0.00214	0.00000	0.00000	0.00000
LEO Base, tonsX10 ³	0.000	0.000	0.000	0.000	0.000	0.000
SPS repair suppt, % SPS mass	1.000	1.000	1.000	1.000	1.000	1.000
LEO prop storage/transfer factor	1.30					
GEO prop storage/transfer factor	1.50					
A. POLV CHARACTERISTICS						
Passengers/flt	240	230	215	0	0	0
Inert weight each, tonsX10 ³	0.029	0.035	0.043	0.000	0.000	0.000
Prop up, tonsX10 ³	0.453	0.475	0.494	0.000	0.000	0.000
Prop down, tonsX10 ³	0.000	0.000	0.000	0.000	0.000	0.000
Flt cost, \$M/flt	10	15	25	0	0	0
Flt turnaround, days	5	7	10	0	0	0
Mission life	50	30	20	50	30	20
B. PLV CHARACTERISTICS						
Passengers/flt	80	50	40	80	50	40
Flt cost, \$M/flt	8	10	12	8	10	12
Flt turnaround, days	7	11	14	7	11	14
C. COTV CHARACTERISTICS						
Payload/flt, tonsX10 ³	0.250	0.250	0.250	0.000	0.000	0.000
Total inert wt, tonsX10 ³	0.029	0.035	0.043	0.000	0.000	0.000
Expended inert wt, tonsX10 ³	0.007	0.009	0.011	0.000	0.000	0.000
Propellant/flt, tonsX10 ³	0.453	0.475	0.494	0.000	0.000	0.000
Flt cost, \$M/flt	5	10	20	0	0	0
Flt turnaround, days	5	7	10	0	0	0
Mission life	50	30	20	0	0	0
D. HLLV CHARACTERISTICS						
Payload/flt, tons	900	700	450	900	700	450
Flt cost, \$M/flt	20	23	25	20	23	25
Flt turnaround, days	5	6	9	5	6	9

VI-F-17

ORIGINAL PAGE IS OF POOR QUALITY

REPAIR ONLY

TABLE VI-F-2 (CONT'D)

YEAR 2024 TRANSPORTATION TRAFFIC MODEL
(Preliminary Estimates)

	GEO ASSY (2)			LEO ASSY		
	MIN	NOM	MAX	MIN	NOM	MAX
No. of SPS operational	105.0	105.0	105.0	105.0	105.0	105.0
SPS mass each tonsX10 ³	51.564	90.123	132.365	0.000	0.000	0.000
Total SPS mass tonsX10 ³ /yr	5414.220	9462.915	13898.325	0.000	0.000	0.000
A. MANNED SUPPORT TO GEO						
Man trips/yr to GEO & return	2520	2520	2520	0	0	0
Personnel consum, tonsX10 ³ /yr	2.52	2.52	2.52	0.00	0.00	0.00
ICTV GEO trips/yr	11	11	12	\$	\$	\$\$\$\$\$\$\$\$\$\$\$\$\$\$\$\$
POTV prop GEOup tonsX10 ³ /yr	4.76	5.20	5.79	0.00	0.00	0.00
POTV prop GEOdown tonsX10 ³ /yr	0.00	0.00	0.00	0.00	0.00	0.00
COTV trips/yr	10	10	10	\$	\$	\$\$\$\$\$\$\$\$\$\$\$\$\$\$\$\$
COTV prop tonsX10 ³ /yr	4.57	4.79	4.98	0.00	0.00	0.00
COTV flt cost \$M/yr	50	101	202	0	0	0
ICTV flt cost \$M/yr	105	164	293	0	0	0
POTV flt turnaround, days	5	7	10	0	0	0
POTV fleet size, units	2	2	2	37	2	2
POTV replacment, units	0	0	1	\$	\$	\$\$\$\$\$\$\$\$\$\$\$\$\$\$\$\$
B. MANNED SUPPORT TO LEO						
LEO man trips/yr	2598	2631	2745	0	0	0
Personnel consum, tons 10 ³ /yr	0.08	0.11	0.22	0.00	0.00	0.00
PLV flts/yr	32	53	69	0	0	0
PLV flt cost \$M/yr	260	526	823	0	0	0
PLV flt turnaround, days	7	11	14	7	11	14
PLV fleet size, units	2	2	3	2	2	2
C. GEO CONSTRUCTION SUPPORT						
Const Base, tonsX10 ³ /yr	0.00	0.00	0.00	0.00	0.00	0.00
Equip & consum, tonsX10 ³ /yr	54.14	94.63	138.98	0.00	0.00	0.00
COTV trips/yr	217	379	556	\$	\$	\$\$\$\$\$\$\$\$\$\$\$\$\$\$\$\$
COTV prop tonsX10 ³ /yr	98.11	179.80	274.63	0.00	0.00	0.00
COTV flt cost \$M/yr	1083	3785	11119	0	0	0

-VI-F-18-

REPAIR ONLY

TABLE VI-F-2 (CONT'D)

YEAR 2024 TRANSPORTATION TRAFFIC MODEL
(Preliminary Estimates)

	MIN	GEO ASSY (2) NOM	MAX	MIN	LEO ASSY NOM	MAX
D. SPS TRANSFER TO GEO						
Total SPS mass tonsX10 ³ /yr	0	0	0	0	0	0
COTV trips/yr	0	0	0	0	0	0
COTV prop tonsX10 ³ /yr	0	0	0	0	0	0
COTV flt cost \$M/yr	0	0	0	0	0	0
E. TOTAL COTV REQMT						
COTV flt turnaround, days	5	7	10	0	0	0
Total COTV fleet, units	3	7	16	0	0	0
COTV replacement, units	5	13	28	0	0	0
Total COTV flt cost \$M/yr	1133	3886	11320	0	0	0
F. LEO CONSTRUCTION SUPPORT						
Const Base, tonsX10 ³ /yr	0.00	0.00	0.00	0.00	0.00	0.00
Equip & consum, tonsX10 ³ /yr	0.00	0.00	0.00	0.00	0.00	0.00
G. TOTAL CARGO LAUNCH REQMT						
Cargo mass, tonsX10 ³ /yr	198	344	520	0	0	0
Payload mass per HLLV, tons	900	700	450	900	700	450
HLLV flts/yr	220	492	1156	0	0	0
HLLV flt cost \$M/yr	4403	11318	28903	0	0	0
HLLV flt turnaround, days	5	6	9	5	6	9
HLLV fleet size, units	3	8	29	0	0	0
H. TRANSPORTATION COST RECAP						
POTV flt cost \$M/yr	105	164	293	0	0	0
PLV flt cost \$M/yr	260	526	823	0	0	0
COTV flt cost \$M/yr	1133	3886	11320	0	0	0
Subtotal	1498	4577	12437	0	0	0
HLLV flt cost \$M/yr	4403	11318	28903	0	0	0
TOTAL TRANSPORTATION COST \$M	5901	15895	41340	0	0	0

VI-F-19

Thirty Year Program Totals/Construction Only - The following computer printout tables (Table VI-F-3) represent the total space transportation activity and costs related to "Construction Only" over the 30 year program period. Inputs to this computer run are identical to the year 2024 run except for the total number of SPS units (112) and the mass related to the total number of LEO and GEO base installations (total of 7 construction/operations bases). Fleet size output data for the various vehicles represents average values over the 30 year period. Maximum fleet size values may be determined by referring to the year 2024 output.

TABLE VI-F-3

CONSTRUCTION ONLY

YEAR 30 TRANSPORTATION TRAFFIC MODEL
(Preliminary Estimates)

	GEO ASSY (1)			LEO ASSY (3)		
	MIN	NOM	MAX	MIN	NOM	MAX
No. of SPS	112.0	112.0	112.0	112.0	112.0	112.0
SPS mass each, tonsX10 ³	48.387	83.582	128.459	51.564	90.123	132.365
GEO man-years/SPS	474	474	474	200	200	200
GEO persnl consum/SPS, tonsX10 ³	1.422	1.422	1.422	0.400	0.400	0.400
GEO Base, tonsX10 ³	42.000	42.000	42.000	7.000	7.000	7.000
LEO man-years/SPS	160	176	230	736	740	766
LEO persnl consum/SPS, tonsX10 ³	0.320	0.352	0.460	2.169	2.177	2.229
LEO Base, tonsX10 ³	7.000	7.000	7.000	56.000	56.000	56.000
Const Base suppt/SPS, tonsX10 ³	1.000	1.000	1.000	1.000	1.000	1.000
LEO prop storage/transfer factor 1.30						
GEO prop storage/transfer factor 1.50						
A. POTV CHARACTERISTICS						
Passengers/flt	240	230	215	75	75	75
Inert weight each, tonsX10 ³	0.029	0.035	0.043	0.017	0.019	0.023
Prop up, tonsX10 ³	0.453	0.475	0.494	0.093	0.106	0.126
Prop down, tonsX10 ³	0.000	0.000	0.000	0.047	0.053	0.063
Flt cost, \$M/flt	10	15	25	7	12	22
Flt turnaround, days	5	7	10	5	7	10
Mission life	50	30	20	50	30	20
B. PLV CHARACTERISTICS						
Passengers/flt	80	50	40	80	50	40
Flt cost, \$M/flt	8	10	12	8	10	12
Flt turnaround, days	7	11	14	7	11	14
C. COTV CHARACTERISTICS						
Payload/flt, tonsX10 ³	0.250	0.250	0.250	1.000	1.000	1.000
Total inert wt, tonsX10 ³	0.029	0.035	0.043	0.122	0.166	0.215
Expended inert wt, tonsX10 ³	0.007	0.009	0.011	0.079	0.110	0.138
Propellant/flt, tonsX10 ³	0.453	0.475	0.494	0.691	0.800	0.902
Flt cost, \$M/flt	5	10	20	20	30	70
Flt turnaround, days	5	7	10	5	7	10
Mission life	50	30	20	20	10	5
D. HLLV CHARACTERISTICS						
Payload/flt, tons	900	700	450	900	700	450
Flt cost, \$M/flt	20	23	25	20	23	25
Flt turnaround, days	5	6	9	5	6	9

VI-F-21

YEAR 30 TRANSPORTATION TRAFFIC MODEL
(Preliminary Estimates)

	GEO ASSY (1)			LEO ASSY (3)		
	MIN	NOM	MAX	MIN	NOM	MAX
No. of SPS/yr	112.0	112.0	112.0	112.0	112.0	112.0
SPS mass each tonsX10 ³	48.387	83.582	128.459	51.564	90.123	132.365
Total SPS mass tonsX10 ³ /yr	5419.344	9361.184	14387.408	5775.168	10093.776	14824.880
A. MANNED SUPPORT TO GEO						
Man trips/yr to GEO & return	106176	106176	106176	44800	44800	44800
Personnel consum, tonsX10 ³ /yr	159.26	159.26	159.26	44.80	44.80	44.80
POTV GEO trips/yr	442	462	494	597	597	597
POTV prop GEOup, tonsX10 ³ /yr	200.41	219.28	243.96	55.55	63.32	75.26
POTV prop GEOdown, tonsX10 ³ /yr	0.00	0.00	0.00	28.07	31.66	37.63
COTV trips/yr	637	637	637	81	86	94
COTV prop tonsX10 ³ /yr	288.59	302.60	314.71	56.18	68.77	84.54
COTV flt cost \$M/yr	3185	6371	12741	1626	2579	6561
POTV flt cost \$M/yr	4424	6925	12346	4181	7168	13141
POTV flt turnaround, days	5	7	10	5	7	10
POTV fleet size, units	2	2	2	2	2	2
POTV replacement, units	9	15	25	12	20	30
B. MANNED SUPPORT TO LEO						
LEO man trips/yr	142016	145600	157696	209664	210560	216384
Personnel consum, tons 10 ³ /yr	35.84	39.42	51.52	242.93	243.82	249.65
PLV flts/yr	1775	2912	3942	2621	4211	5410
PLV flt cost \$M/yr	14202	29120	47309	20966	42112	64915
PLV flt turnaround, days	7	11	14	7	11	14
PLV fleet size, units	2	3	5	2	4	7
C. GEO CONSTRUCTION SUPPORT						
Const Base, tonsX10 ³ /yr	42.00	42.00	42.00	7.00	7.00	7.00
Equip & consum, tonsX10 ³ /yr	112.00	112.00	112.00	0.00	0.00	0.00
COTV trips/yr	616	616	616	7	7	7
COTV prop tonsX10 ³ /yr	279.05	292.60	304.30	4.84	5.60	6.31
COTV flt cost \$M/yr	3080	6160	12320	140	210	490

YEAR 30 TRANSPORTATION TRAFFIC MODEL
(Preliminary Estimates)

	GEO ASSY (1)			LEO ASSY (3)		
	MIN	NOM	MAX	MIN	NOM	MAX
D. SPS TRANSFER TO GEO						
Total SPS mass tonsX10 ³ /yr	5419	9361	14387	5775	10094	14825
COTV trips/yr	21677	37445	57550	5775	10094	14825
COTV prop tonsX10 ³ /yr	9820	17786	28430	3991	8075	13372
COTV flt cost \$M/yr	108387	374447	1150993	115503	302813	1037742
E. TOTAL COTV REQMT						
COTV flt turnaround, days	5	7	10	5	7	10
Total COTV fleet, units	10	25	54	3	7	14
COTV replacement, units	459	1290	2940	293	1019	2985
Total COTV flt cost \$M/yr	114652	386978	1176054	117269	305602	1044792
F. LEO CONSTRUCTION SUPPORT						
Const Base, tonsX10 ³ /yr	7.00	7.00	7.00	56.00	56.00	56.00
Squir & consur, tonsX10 ³ /yr	0.00	0.00	0.00	112.00	112.00	112.00
G. TOTAL CARGO LAUNCH REQMT						
Cargo mass, tonsX10 ³ /yr	19707	33941	53607	12063	22516	35597
Payload mass per HLLV, tons	900	700	450	900	700	450
HLLV flts/yr	21896	48486	119126	13403	32165	79105
HLLV flt cost \$M/yr	437929	1115189	2978159	268057	739796	1977622
HLLV flt turnaround, days	5	6	9	5	6	9
HLLV fleet size, units	10	27	98	6	18	65
H. TRANSPORTATION COST RECAP						
POTV flt cost \$M/yr	4424	6925	12346	4181	7168	13141
PLV flt cost \$M/yr	14202	29120	47309	20966	42112	64915
COTV flt cost \$M/yr	114652	386978	1176054	117269	305602	1044792
Subtotal	133278	423022	1235709	142417	354882	1122849
HLLV flt cost \$M/yr	437929	1115189	2978159	268057	739796	1977622
TOTAL TRANSPORTATION COST \$M	571206	1538211	4213868	410474	1094678	3100470
Specific cost \$/Kg SPS	105.40	164.32	292.89	71.08	108.45	209.14
Specific cost \$/Kwe bus	510.01	1373.40	3762.38	366.49	977.39	2768.28

ORIGINAL PAGE IS OF POOR QUALITY VI-F-23

TABLE VI-F-3 (CONT'D)

Page 1 of 1

CONSTRUCTION ONLY

YEAR 30 TRANSPORTATION TRAFFIC MODEL
(Preliminary Estimates)

	GEO ASSY (2)			LEO ASSY		
	MIN	NOM	MAX	MIN	NOM	MAX
No. of SPS	112.0	112.0	112.0	112.0	112.0	112.0
SPS mass each, tonsX10 ³	51.564	90.123	132.365	0.000	0.000	0.000
GEO man-years/SPS	574	574	574	0	0	0
GEO persnl consum/SPS, tonsX10 ³	1.722	1.722	1.722	0.000	0.000	0.000
GEO Base, tonsX10 ³	49.000	49.000	49.000	0.000	0.000	0.000
LEO man-years/SPS	160	176	230	0	0	0
LEO persnl consum/SPS, tonsX10 ³	0.320	0.352	0.460	0.000	0.000	0.000
LEO Base, tonsX10 ³	7.000	7.000	7.000	0.000	0.000	0.000
Const Base suppt/SPS, tonsX10 ³	1.000	1.000	1.000	0.000	0.000	0.000
LEO prop storage/transfer factor	1.30					
GEO prop storage/transfer factor	1.50					
A. POTV CHARACTERISTICS						
Passengers/flt	240	230	215	0	0	0
Inert weight each, tonsX10 ³	0.029	0.035	0.043	0.000	0.000	0.000
Prop up, tonsX10 ³	0.453	0.475	0.494	0.000	0.000	0.000
Prop down, tonsX10 ³	0.000	0.000	0.000	0.000	0.000	0.000
Flt cost, \$M/flt	10	15	25	0	0	0
Flt turnaround, days	5	7	10	0	0	0
Mission life	50	30	20	50	30	20
B. PLV CHARACTERISTICS						
Passengers/flt	80	50	40	80	50	40
Flt cost, \$M/flt	8	10	12	8	10	12
Flt turnaround, days	7	11	14	7	11	14
C. COTV CHARACTERISTICS						
Payload/flt, tonsX10 ³	0.250	0.250	0.250	0.000	0.000	0.000
Total inert wt, tonsX10 ³	0.029	0.035	0.043	0.000	0.000	0.000
Expended inert wt, tonsX10 ³	0.007	0.009	0.011	0.000	0.000	0.000
Propellant/flt, tonsX10 ³	0.453	0.475	0.494	0.000	0.000	0.000
Flt cost, \$M/flt	5	10	20	0	0	0
Flt turnaround, days	5	7	10	0	0	0
Mission life	50	30	20	0	0	0
D. HLLV CHARACTERISTICS						
Payload/flt, tons	900	700	450	900	700	450
Flt cost, \$M/flt	20	23	25	20	23	25
Flt turnaround, days	5	6	9	5	6	9

VI-F-24

YEAR 30 TRANSPORTATION TRAFFIC MODEL
(Preliminary Estimates)

	GEO ASSY (2)			LEO ASSY		
	MIN	NOM	MAX	MIN	NOM	MAX
No. of SPS/yr	112.0	112.0	112.0	112.0	112.0	112.0
SPS mass each tonsX10 ³	51.564	90.123	132.365	0.000	0.000	0.000
Total SPS mass tonsX10 ³ /yr	5775.168	10093.776	14824.880	0.000	0.000	0.000
A. MANNED SUPPORT TO GEO						
Man trips/yr to GEO & return	128576	128576	128576	0	0	0
Personnel consum, tonsX10 ³ /yr	192.86	192.86	192.86	0.00	0.00	0.00
POTV GEO trips/yr	536	559	598	\$	\$	\$
POTV prop GEOup tonsX10 ³ /yr	242.69	265.54	295.43	0.00	0.00	0.00
POTV prop GEOdown tonsX10 ³ /yr	0.00	0.00	0.00	0.00	0.00	0.00
COTV trips/yr	771	771	771	\$	\$	\$
COTV prop tonsX10 ³ /yr	349.47	366.44	381.10	0.00	0.00	0.00
COTV flt cost \$M/yr	3857	7715	15429	0	0	0
POTV flt cost \$M/yr	5357	8385	14951	0	0	0
POTV flt turnaround, days	5	7	10	0	0	0
POTV fleet size, units	2	2	2	1094	2	2
POTV replacement, units	11	19	30	\$	\$	\$
B. MANNED SUPPORT TO LEO						
LEO man trips/yr	164416	168000	180096	0	0	0
Personnel consum, tons 10 ³ /yr	35.84	39.42	51.52	0.00	0.00	0.00
PLV flts/yr	2055	3360	4502	0	0	0
PLV flt cost \$M/yr	16442	33600	54029	0	0	0
PLV flt turnaround, days	7	11	14	7	11	14
PLV fleet size, units	2	3	6	2	2	2
C. GEO CONSTRUCTION SUPPORT						
Const Base, tonsX10 ³ /yr	49.00	49.00	49.00	0.00	0.00	0.00
Equip & consum, tonsX10 ³ /yr	112.00	112.00	112.00	0.00	0.00	0.00
COTV trips/yr	644	644	644	\$	\$	\$
COTV prop tonsX10 ³ /yr	291.73	305.90	318.14	0.00	0.00	0.00
COTV flt cost \$M/yr	3220	6440	12880	0	0	0

VI-F-25

ORIGINAL PAGE IS OF POOR QUALITY

CONSTRUCTION ONLY

TABLE VI-F-3 (CONT'D)

YEAR 30 TRANSPORTATION TRAFFIC MODEL
(Preliminary Estimates)

	GEO ASSY (2)			LEO ASSY		
	MIN	NOM	MAX	MIN	NOM	MAX
D. SPS TRANSFER TO GEO						
Total SPS mass tonsX10 ³ /yr	5775	10094	14825	0	0	0
COTV trips/yr	23101	40375	59300	0	0	0
COTV prop tonsX10 ³ /yr	10465	19178	29294	0	0	0
COTV flt cost \$M/yr	115503	403751	1185990	0	0	0
E. TOTAL COTV REQMT						
COTV flt turnaround, days	5	7	10	0	0	0
Total COTV fleet, units	11	27	55	0	0	0
COTV replacement, units	490	1393	3036	0	0	0
Total COTV flt cost \$M/yr	122581	417906	1214300	0	0	0
F. LEO CONSTRUCTION SUPPORT						
Const Base, tonsX10 ³ /yr	7.00	7.00	7.00	0.00	0.00	0.00
Equip & consum, tonsX10 ³ /yr	0.00	0.00	0.00	0.00	0.00	0.00
G. TOTAL CARGO LAUNCH REQMT						
Cargo mass, tonsX10 ³ /yr	21104	36687	55405	0	0	0
Payload mass per HLLV, tons	900	700	450	900	700	450
HLLV flts/yr	23449	52411	123123	0	0	0
HLLV flt cost \$M/yr	468979	1205442	3078071	0	0	0
HLLV flt turnaround, days	5	6	9	5	6	9
HLLV fleet size, units	11	29	101	0	0	0
H. TRANSPORTATION COST RECAP						
POTV flt cost \$M/yr	5357	8385	14951	0	0	0
PLV flt cost \$M/yr	16442	33600	54029	0	0	0
COTV flt cost \$M/yr	122581	417906	1214300	0	0	0
Subtotal	144380	459891	1283279	0	0	0
HLLV flt cost \$M/yr	468979	1205442	3078071	0	0	0
TOTAL TRANSPORTATION COST \$M	613359	1665333	4361350	0	0	0
Specific cost \$/Kg SPS	106.21	164.99	294.19	0.00	0.00	0.00
Specific cost \$/KWe bus	547.64	1486.90	3894.06	0.00	0.00	0.00

VI-F-26

Thirty Year Program Totals/Repair Only - The following computer printout tables (Table VI-F-4) represent the total space transportation activity and costs related to "Repair Only" over the 30 year program period. Inputs to this computer run are identical to the year 2024 run except for the total number of operational SPS (1173.5) which represents the cumulative number of SPS repaired over the 30 year period. Fleet size output data for the various vehicles represents average values over the 30 year period. Maximum fleet size values may be determined by referring to year 2025 output.

TABLE VI-F-4

Page 1 of 1

REPAIR ONLY

 YEAR 30 TRANSPORTATION TRAFFIC MODEL
 (Preliminary Estimates)

	GEO ASSY (1)			LEO ASSY (3)		
	MIN	NOM	MAX	MIN	NOM	MAX
No. of SPS operational	1173.5	1173.5	1173.5	1173.5	1173.5	1173.5
SPS mass each, tonsX10 ³	48.387	83.582	128.459	51.564	90.123	132.365
GEO man-years/SPS	12.00	12.00	12.00	12.00	12.00	12.00
GEO persnl consum/SPS, tonsX10 ³	0.02400	0.02400	0.02400	0.02400	0.02400	0.02400
GEO Base, tonsX10 ³	0.000	0.000	0.000	0.000	0.000	0.000
LEO man-years/SPS	0.37	0.53	1.07	0.39	0.43	0.69
LEO persnl consum/SPS, tonsX10 ³	0.00074	0.00106	0.00214	0.00078	0.00086	0.00138
LEO Base, tonsX10 ³	0.000	0.000	0.000	0.000	0.000	0.000
SPS repair suppt, % SPS mass	1.000	1.000	1.000	1.000	1.000	1.000
LEO prop storage/transfer factor	1.30					
GEO prop storage/transfer factor	1.50					
A. POTV CHARACTERISTICS						
Passengers/flt	240	230	215	75	75	75
Inert weight each, tonsX10 ³	0.029	0.035	0.043	0.017	0.019	0.023
Prop up, tonsX10 ³	0.453	0.475	0.494	0.093	0.106	0.126
Prop down, tonsX10 ³	0.000	0.000	0.000	0.047	0.053	0.063
Flt cost, \$M/flt	10	15	25	7	12	22
Flt turnaround, days	5	7	10	5	7	10
Mission life	50	30	20	50	30	20
B. PLV CHARACTERISTICS						
Passengers/flt	80	50	40	80	50	40
Flt cost, \$M/flt	8	10	12	8	10	12
Flt turnaround, days	7	11	14	7	11	14
C. COTV CHARACTERISTICS						
Payload/flt, tonsX10 ³	0.250	0.250	0.250	1.000	1.000	1.000
Total inert wt, tonsX10 ³	0.029	0.035	0.043	0.122	0.166	0.215
Expended inert wt, tonsX10 ³	0.007	0.009	0.011	0.079	0.110	0.138
Propellant/flt, tonsX10 ³	0.453	0.475	0.494	0.691	0.800	0.902
Flt cost, \$M/flt	5	10	20	20	30	70
Flt turnaround, days	5	7	10	5	7	10
Mission life	50	30	20	20	10	5
D. HLLV CHARACTERISTICS						
Payload/flt, tons	900	700	450	900	700	450
Flt cost, \$M/flt	20	23	25	20	23	25
Flt turnaround, days	5	6	9	5	6	9

VI-F-28.

YEAR 30 TRANSPORTATION TRAFFIC MODEL
 (Preliminary Estimates)

	GEO ASSY (1)			LEO ASSY (3)		
	MIN	NOM	MAX	MIN	NOM	MAX
No. of SPS Operational	1173.5	1173.5	1173.5	1173.5	1173.5	1173.5
SPS mass each tonsX10 ³	48.387	83.582	128.459	51.564	90.123	132.365
Total SPS mass tonsX10 ³ /yr	56782.145	98083.477	150746.637	60510.354	105759.341	155330.328
A. MANNED SUPPORT TO GEO						
Man trips/yr to GEO & return	28164	28164	28164	28164	28164	28164
Personnel consum, tonsX10 ³ /yr	28.16	28.16	28.16	28.16	28.16	28.16
POTV GEO trips/yr	117	122	131	376	376	376
POTV prop GEOup tonsX10 ³ /yr	53.16	58.16	64.71	34.92	39.81	47.32
POTV prop GEOdwn tonsX10 ³ /yr	0.00	0.00	0.00	17.65	19.90	23.66
COTV trips/yr	113	113	113	51	54	59
COTV prop tonsX10 ³ /yr	51.03	53.51	55.65	35.32	45.23	53.15
COTV flt cost \$M/yr	563	1127	2253	1022	1621	4124
POTV flt cost \$M/yr	1174	1837	3275	2629	4506	8261
POTV flt turnaround, days	5	7	10	5	7	10
POTV fleet size, units	2	2	4	2	7	10
POTV replacement, units	2	4	7	8	13	19
B. MANNED SUPPORT TO LEO						
LEO man trips/yr	29032	29408	30675	29079	29173	29783
Personnel consum, tons 10 ³ /yr	0.87	1.24	2.51	0.92	1.01	1.62
PLV flts/yr	363	588	767	363	583	745
PLV flt cost \$M/yr	2903	5882	9203	2908	5835	8935
PLV flt turnaround, days	7	11	14	7	11	14
PLV fleet size, units	2	2	2	2	2	2
C. GEO CONSTRUCTION SUPPORT						
Const Base, tonsX10 ³ /yr	0.00	0.00	0.00	0.00	0.00	0.00
Equip & consum, tonsX10 ³ /yr	567.82	980.83	1507.47	605.10	1057.59	1553.30
COTV trips/yr	2271	3923	6030	605	1058	1553
COTV prop tonsX10 ³ /yr	1028.89	1863.59	2978.75	418.13	846.07	1401.08
COTV flt cost \$M/yr	11356	39233	120597	12102	31728	108731

VI-F-29

TABLE VI-F-4 (CONT'D)

Page 2 of 2

REPAIR ONLY

YEAR

30 TRANSPORTATION TRAFFIC MODEL
(Preliminary Estimates)

	GEO ASSY (1)			LEO ASSY (3)		
	MIN	NCM	MAX	MIN	NOM	MAX
D. SPS TRANSFER TO GEO						
Total SPS mass tonsX10 ³ /yr	0	0	0	0	0	0
COTV trips/yr	0	0	0	0	0	0
COTV prop tonsX10 ³ /yr	0	0	0	0	0	0
COTV flt cost \$M/yr	0	0	0	0	0	0
E. TOTAL COTV REQMT						
COTV flt turnaround, days	5	7	10	5	7	10
Total COTV fleet, units	1	3	6	0	1	1
COTV replacement, units	48	135	307	33	111	322
Total COTV flt cost \$M/yr	11920	40360	122850	13124	33349	112856
F. LEO CONSTRUCTION SUPPORT						
Const Base, tonsX10 ³ /yr	0.00	0.00	0.00	0.00	0.00	0.00
Equip & consum, tonsX10 ³ /yr	0.00	0.00	0.00	0.00	0.00	0.00
G. TOTAL CARGO LAUNCH REQMT						
Cargo mass, tonsX10 ³ /yr	2088	3583	5648	1352	2465	3863
Payload mass per HLLV, tons	900	700	450	900	700	450
HLLV flts/yr	2320	5118	12551	1502	3522	8584
HLLV flt cost \$M/yr	46400	117725	313782	30033	81008	214605
HLLV flt turnaround, days	5	6	9	5	6	9
HLLV fleet size, units	1	3	10	1	2	7
H. TRANSPORTATION COST RECAP						
POTV flt cost \$M/yr	1174	1837	3275	2629	4506	8261
PLV flt cost \$M/yr	2903	5882	9203	2908	5835	8935
COTV flt cost \$M/yr	11920	40360	122850	13124	33349	112856
Subtotal	15996	48078	135328	18661	43690	130052
HLLV flt cost \$M/yr	46400	117725	313782	30033	81008	214605
TOTAL TRANSPORTATION COST \$M	62397	165804	449110	48694	124697	344657

VI-F-30

TABLE VI-F-4 (CONT'D)

REPAIR ONLY

YEAR 30 TRANSPORTATION TRAFFIC MODEL
(Preliminary Estimates)

	GEO ASSY (2)			LEO ASSY		
	MIN	NOM	MAX	MIN	NOM	MAX
No. of SPS operational	1173.5	1173.5	1173.5	1173.5	1173.5	1173.5
SPS mass each, tonsX10 ³	51.564	90.123	132.365	0.000	0.000	0.000
GEO man-years/SPS	12.00	12.00	12.00	0.00	0.00	0.00
GEO persnl consum/SPS, tonsX10 ³	0.02400	0.02400	0.02400	0.00000	0.00000	0.00000
GEO Base, tonsX10 ³	0.000	0.000	0.000	0.000	0.000	0.000
LEO man-years/SPS	0.37	0.53	1.07	0.00	0.00	0.00
LEO persnl consum/SPS, tonsX10 ³	0.00074	0.00106	0.00214	0.00000	0.00000	0.00000
LEO Base, tonsX10 ³	0.000	0.000	0.000	0.000	0.000	0.000
SPS repair suppt, % SPS mass	1.000	1.000	1.000	1.000	1.000	1.000
LEO prop storage/transfer factor	1.30					
GEO prop storage/transfer factor	1.50					
A. POTV CHARACTERISTICS						
Passengers/flt	240	230	215	0	0	0
Inert weight each, tonsX10 ³	0.029	0.035	0.043	0.000	0.000	0.000
Prop up, tonsX10 ³	0.453	0.475	0.494	0.000	0.000	0.000
Prop down, tonsX10 ³	0.000	0.000	0.000	0.000	0.000	0.000
Flt cost, \$M/flt	10	15	25	0	0	0
Flt turnaround, days	5	7	10	0	0	0
Mission life	50	30	20	50	30	20
B. PLV CHARACTERISTICS						
Passengers/flt	80	50	40	80	50	40
Flt cost, \$M/flt	8	10	12	8	10	12
Flt turnaround, days	7	11	14	7	11	14
C. COTV CHARACTERISTICS						
Payload/flt, tonsX10 ³	0.250	0.250	0.250	0.000	0.000	0.000
Total inert wt, tonsX10 ³	0.029	0.035	0.043	0.000	0.000	0.000
Expended inert wt, tonsX10 ³	0.007	0.009	0.011	0.000	0.000	0.000
Propellant/flt, tonsX10 ³	0.453	0.475	0.494	0.000	0.000	0.000
Flt cost, \$M/flt	5	10	20	0	0	0
Flt turnaround, days	5	7	10	0	0	0
Mission life	50	30	20	0	0	0
D. HLLV CHARACTERISTICS						
Payload/flt, tons	900	700	450	900	700	450
Flt cost, \$M/flt	20	23	25	20	23	25
Flt turnaround, days	5	6	9	5	6	9

VI-F-31

REPAIR ONLY

TABLE VI-F-4 (CONT'D)

YEAR 30 TRANSPORTATION TRAFFIC MODEL
(Preliminary Estimates)

	GEO ASSY (2)			LEO ASSY		
	MIN	NOM	MAX	MIN	NOM	MAX
D. SPS TRANSFER TO GEO						
Total SPS mass tonsX10 ³ /yr	0	0	0	0	0	0
COTV trips/yr	0	0	0	0	0	0
COTV prop tonsX10 ³ /yr	0	0	0	0	0	0
COTV flt cost \$M/yr	0	0	0	0	0	0
E. TOTAL COTV REQMT						
COTV flt turnaround, days	5	7	10	0	0	0
Total COTV fleet, units	1	3	6	0	0	0
COTV replacement, units	51	145	316	0	0	0
Total COTV flt cost \$M/yr	12665	43430	126517	0	0	0
F. LEO CONSTRUCTION SUPPORT						
Const Base, tonsX10 ³ /yr	0.00	0.00	0.00	0.00	0.00	0.00
Equip & consun, tonsX10 ³ /yr	0.00	0.00	0.00	0.00	0.00	0.00
G. TOTAL CARGO LAUNCH REQMT						
Cargo mass, tonsX10 ³ /yr	2214	3850	5814	0	0	0
Payload mass per HLLV, tons	900	700	450	900	700	450
HLLV flts/yr	2460	5500	12920	0	0	0
HLLV flt cost \$M/yr	49205	126489	323004	0	0	0
HLLV flt turnaround, days	5	6	9	5	6	9
HLLV fleet size, units	1	3	11	0	0	0
H. TRANSPORTATION COST RECAP						
POTV flt cost \$M/yr	1174	1837	3275	0	0	0
PLV flt cost \$M/yr	2903	5882	9203	0	0	0
COTV flt cost \$M/yr	12665	43430	126517	0	0	0
Subtotal	16742	51149	138995	0	0	0
HLLV flt cost \$M/yr	49205	126489	323004	0	0	0
TOTAL TRANSPORTATION COST \$M	65947	177637	461998	0	0	0

VI-F-33

Concluding Remarks

The following table was derived from the "nominal" transportation traffic model and shows the average transportation costs for construction of one SPS unit in terms of dollars per KW of electrical energy at the ground distribution network for each option.

	(1) Column/Cable GEO	(2) Truss LEO	(3) Truss GEO
Total HLLV flight cost, \$/KWe	996	1076	661
Total PLV	26	30	37
Total COTV	345	373	273
Total POTV	6	7	6
Total Transportation Cost	1373	1486	977

Conclusions and comments related to this table and previous discussions include:

a. Personnel transportation costs amount to less than 5% of the total and are not expected to become a determining factor between LEO and GEO construction or in basic system feasibility.

b. Costs of operating the heavy lift launch vehicle dominate the transportation costs. These are determined by three factors, which in turn require refinement:

(1) Costs per flight of the optimally-sized launch vehicle (\$/kg to LEO).

(2) Specific mass of the power satellite (kg/KWe)

(3) "Orbit burden factor" ($\frac{\text{kg to LEO}}{\text{kg payload to GEO}}$) consequent to the choice of orbit transfer system.

c. The use of O_2/H_2 chemical OTV's required for GEO assembly rather than payload powered high specific impulse OTV's which may be utilized for LEO assembly imposes 40 to 50% in additional launch costs for transporting the additional OTV propellant. They include the possible use of non-payload powered high specific impulse systems even though early analysis of this option appears to incur higher transportation costs because of the weight, cost, and return requirement of the dedicated power supply.

d. OTV propellant may be reduced by launching HLLV's from an equatorial launch site and thereby deleting the plane change requirement. This opportunity also deserves additional study.

e. The total costs cited above are based upon first estimates of acquisition and operating costs of the transportation elements. These costs will, in fact, be rate-dependent and this fact requires consideration in further studies. Additionally, the costs, particularly for the electric propulsion components, are highly speculative and require significant effort to arrive at.

The transportation costs are a dominant factor in the current uncertainty of the ultimate economic feasibility of solar power from space and requires significant effort to reduce this uncertainty.

Additional analyses of the space transportation scenario output are provided in Section VII Integrated Operations and Section XI Program Costs and Economic Analysis.

VII. INTEGRATED OPERATIONS

C. R. Hicks
Payloads Operations Division

A. Systems Requirements Analysis

The capability to manufacture and construct large solar power stations in space will require a new dimension in space operations where innovative and advanced concepts can produce gains measured in orders of magnitude rather than percentages. The physical requirements for Solar Power Satellites (SPS) call for large microwave transmission antennas on the order of 1 km in diameter and large surfaces on the order of 100 to 200 km². Because of these physical requirements, the location for the manufacture and construction of the SPS will be expanded to include both low-Earth orbital and geosynchronous orbital locations as well as ground-based factory and plant activities. Therefore, space operations will be greatly influenced by the manufacturing and construction concept selected, which in turn will determine requirements for construction time, space equipment, transportation system, ground support system, and personnel and material resources.

The basic elements needed to define and develop an integrated operations and mission management concept for the manufacture, construction, quality control, checkout, operation, and maintenance of a large number of SPS's are: the Solar Power Satellites operating at geosynchronous Earth orbit (GEO); Operational Bases in GEO and low-Earth orbit (LEO), consisting of construction, manufacturing, maintenance, and logistics facilities; a Space Transportation System to transport material, equipment, and personnel between Earth and the operational bases in LEO and GEO; and a Ground Support System consisting of the Communications and Data Network facilities, Launch and Recovery operation facilities, Program Headquarters Mission Control facilities, industrial and warehouse facilities, the ground transportation systems, and the SPS ground receiving stations and operations control facilities; and the materials, equipment, supplies, and personnel resources. A number of these elements are discussed in detail in other sections of this report. A very general SPS operations scenario is shown in figure VII-1 to describe the mission sequence and basic elements of the SPS production and operation system.

B. Program Model

To develop an estimate of the overall program requirements for the creation of a Solar Power Satellite System, this study has assumed an SPS implementation rate that calls for the construction of 112 SPS units (scenario B, sec. III) producing 10 GW power each at the ground over a 30-year time frame from 1995 to 2025. Three alternative construction and assembly concepts, involving two configurations, were evaluated during the study to identify program requirements. These three alternatives are defined as follows.

Concept 1: The "COLUMN/CABLE" SPS configuration constructed and assembled primarily in GEO. Chemical COTV transportation from LEO to GEO.

ORIGINAL PAGE IS
OF POOR QUALITY

VII-2

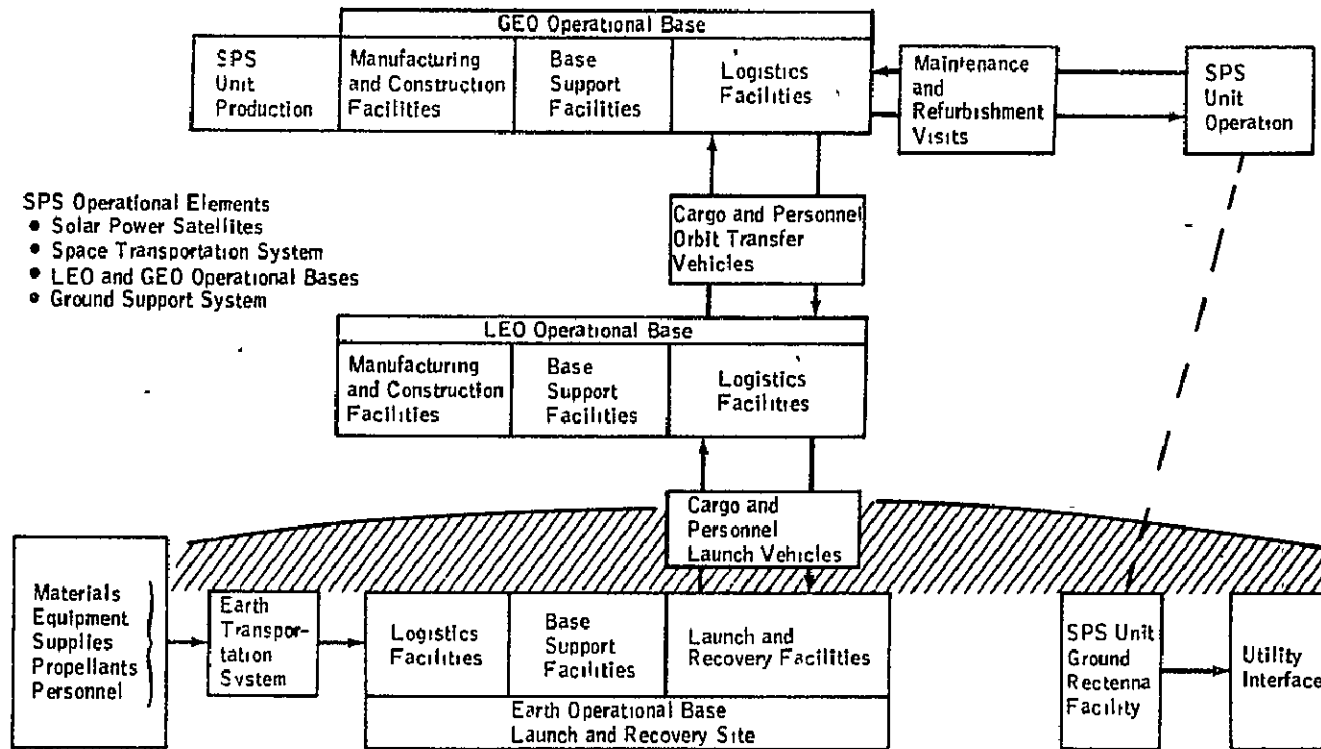


Figure VII-1.- SPS mission scenario.

Concept 2: The "TRUSS" SPS configuration constructed and assembled primarily in GEO. Chemical COTV transportation from LEO to GEO.

Concept 3: The "TRUSS" SPS configuration constructed and partially assembled in LEO with final assembly in GEO. Self-powered transportation from LEO to GEO.

Program models have been developed for each of the preceding concepts to identify the following program requirements for each year.

1. SPS units constructed
2. Total SPS units on line
3. Mass to GEO and LEO
4. Operational base units implemented and total on line
5. Personnel in GEO and LEO for production and maintenance
6. New POTV, COTV, PLV, and HLLV units required
7. Personnel and cargo launch vehicle total flights and flight rate to LEO
8. Personnel and cargo orbital transfer vehicle total flight and flight rate to GEO
9. Personnel and cargo launch and orbital transfer vehicles fleet size

The program models utilize the results of the systems analysis of the basic SPS elements conducted during this study. The guidelines and assumptions are listed in table VII-1. For each construction and configuration concept, a "nominal" weight and size SPS (sec. IV) was used in the calculations. The resulting program models are listed in tables VII-2 to VII-4.

C. Mission Management Concept

In developing a philosophy for an overall mission management concept that can satisfy the basic system requirements and conduct the program model as presented above, the following guidelines have been identified and assumed.

1. Personnel-operated and automated machines for manufacturing and construction tasks in space
2. Operations and control authority delegated throughout the ground- and space-based facilities
3. Program and overall operations and control authority maintained on ground
4. Dedicated synchronous satellite communications relay system

In general, all past space programs and the approaching Shuttle Orbiter, Spacelab, and IUS Space Transportation System (STS) missions can be regarded as ground-based space operations; that is, the complement of

TABLE VII-1.- SPS PROGRAM MODEL INPUTS, ASSUMPTIONS, AND GUIDELINES

Characteristics	Concept		
	1. Column/cable GEO	2. Truss GEO	3. Truss LEO
SPS characteristics			
Number of SPS units, total	112	112	112
SPS 'nominal' unit mass each, M tons X 10 ³	83.582 ^a (81.8)	90.123 ^a (84.4)	90.123 ^a (84.4)
SPS unit mass repair each, M tons X 10 ³ per year	.836	.901	.901
Operational base characteristics			
GEO base mass each, M tons X 10 ³	6.000	7.000	1.000
LEO base mass each, M tons X 10 ³	1.000	1.000	8.000
GEO and LEO base mass repair each, M tons X 10 ³ per year (construction facilities only)	1.000 (GEO)	1.000 (GEO)	1.000 (LEO)
Personnel characteristics			
24 hours/7 days/week operations 3 shifts/day, 4 orbital teams 180-day orbital tour per person			
Construction, base support, and logistics operations			
GEO personnel, total, each new SPS unit per year	474	574	200
LEO personnel, total, each new SPS unit per year	176	176	740
Maintenance operations			
GEO personnel, total, each operational SPS per year	12	12	12
LEO personnel, total, each operational SPS per year	.53	.53	.43
Provisions			
GEO personnel provisions, M tons per person per year	3.0	3.0	2.0
LEO personnel provisions, M tons per person per year	2.0	2.0	3.0

^aNumbers in parentheses are final masses, but the program model was not updated.

TABLE VII-1.- Concluded

Characteristics	Concept		
	1. Column/cable GEO	2. Truss GEO	3. Truss LEO
HLLV characteristics, nominal			
Two-stage ballistic:			
Payload, M tons	700	700	700
Flight turnaround, days	6	6	6
Vehicle life, missions	300	300	300
Flight cost, \$M/flight	23	23	23
PLV characteristics, nominal			
Modified Shuttle:			
Payload, passengers	50	50	50
Flight turnaround, days	11	11	11
Vehicle life, missions	100	100	100
Flight cost, \$M/flight	10	10	10
COTV characteristics, nominal			
	(2-1/2 stage chemical)	(2-1/2 stage chemical)	(Electric/chemical)
Payload, M tons	250	250	1000
Inert weight, M tons	35	35	166
Expended inert weight, M tons	9	9	110
Propellant/flight, M tons	475	475	800
Propellant loss in LEO storage/flight, M tons	143	143	240
Flight duration, days	TBD	TBD	50
Flight turnaround, days	7	7	7
Vehicle life, missions	30	30	10
Flight cost, \$M/flight	10	10	30
POTV characteristics, nominal			
	(passenger module for 2-1/2 stage chemical)	(passenger module for 2-1/2 stage chemical)	(special purpose)
Payload, passengers	230	230	75
Inert weight, M tons	35	35	19
Propellant weight, M tons	475	475	106/up, 53/down
Propellant loss in LEO storage/flight, M tons	143	143	58
Flight turnaround, days	7	7	7
Vehicle life, missions	30	30	30
Flight cost, \$M/flight	15	15	12

ORIGINAL PAGE IS
OF POOR QUALITY

VII-5

TABLE VII-2.- Program Model Summary for "Column/Cable" SPS in Geo

YEAR	SPS UNITS		OPS BASE UNITS IN LEO & GEO		TOTAL PERSONNEL IN SPACE					TOTAL MASS TO SPACE M. TONS X 10 ³	
	PER YR.	TOTAL ON LINE	PER YR.	TOTAL ON LINE	LEO		GEO		TOTAL PER YR.	LEO	GEO
					PROD.	MAINT.	PROD.	MAINT.		PER. YR.	PER. YR.
1995	.5	0	1	1	88		237	0	325	172	49
1996	.5	0	0	1	88		237	0	325	151	43
1997	1	1	0	1	176	1	474	12	663	305	87
1998	1	2	0	1	176	1	474	24	675	308	88
1999	1	3	0	1	176	2	474	36	688	311	89
2000	1	4	0	1	176	2	474	48	690	314	90
2001	1	5	1	1	176	3	474	60	703	323	96
2002	2	6	0	2	352	3	948	72	1375	621	177
2003	2	8	0	2	352	4	948	96	1400	627	179
2004	2	10	0	2	352	5	948	120	1425	634	181
2005	2	12	1	2	352	6	948	144	1450	661	188
2006	3	14	0	3	528	7	1422	168	2125	948	270
2007	3	17	0	3	528	9	1422	204	2163	957	273
2008	3	20	0	3	528	10	1422	240	2200	966	275
2009	3	23	1	3	528	11	1422	276	2237	996	284
2010	4	26	0	4	704	13	1896	312	2925	1286	366
2011	4	30	1	4	704	15	1896	360	2975	1320	376
2012	5	34	0	5	880	17	2370	408	3675	1613	459
2013	5	39	0	5	880	20	2370	468	3738	1628	465
2014	5	44	1	5	880	22	2370	528	3800	1664	474
2015	6	49	0	6	1056	24	2844	588	4512	1960	558
2016	6	55	0	6	1056	27	2844	660	4587	1978	563
2017	6	61	0	6	1056	30	2844	732	4662	1996	569
2018	6	67	0	6	1056	33	2844	804	4737	2015	574
2019	6	73	0	6	1056	36	2844	876	4812	2033	579
2020	6	79	0	6	1056	39	2844	948	4887	2051	584
2021	6	85	1	6	1056	42	2844	1020	4962	2091	595
2022	7	91	0	7	1232	45	3318	1092	5687	2390	680
2023	7	98	0	7	1232	49	3318	1176	5775	2411	686
2024	7	105	0	7	1232	53	3318	1260	5863	2433	692
2025		112		7		56		1344	1400	342	96

VII-6

TABLE VII-2.- Concluded ("Column/Cable"/Geo)

YEAR	POTV FLIGHTS TO GEO				COTV FLIGHTS TO GEO				PLV FLIGHTS TO LEO				HLLV FLIGHTS TO LEO			
	PER YR.	TOTAL	FLEET SIZE	NEW UNITS	PER YR.	TOTAL	FLEET SIZE	NEW UNITS	PER YR.	TOTAL	FLEET SIZE	NEW UNITS	PER YR.	TOTAL	FLEET SIZE	NEW UNITS
1995	2	2	2	2	196	196	4	7	13	13	2	2	245	245	4	4
1996	2	4	2	0	172	368	4	6	13	26	2	0	216	461	4	0
1997	4	8	2	0	347	715	7	11	26	52	2	0	435	896	8	4
1998	4	12	2	0	351	1066	7	12	27	79	2	0	440	1336	8	0
1999	4	16	2	0	354	1420	7	12	28	107	2	0	444	1780	8	0
2000	4	20	2	0	357	1777	7	12	28	135	2	0	448	2228	8	0
2001	5	25	2	0	385	2162	7	13	29	164	2	0	483	2711	8	15
2002	9	34	2	1	709	2871	14	24	55	219	2	1	888	3599	15	0
2003	9	43	2	0	716	3587	14	24	56	275	2	0	897	4496	15	0
2004	10	53	2	0	722	4309	14	25	57	332	2	1	906	5402	15	0
2005	10	63	2	1	753	5062	14	25	58	390	2	0	946	6348	15	0
2006	14	77	2	0	1080	6142	22	36	85	475	3	2	1354	7702	23	23
2007	14	91	2	0	1091	7233	22	37	87	562	3	1	1367	9069	23	0
2008	14	105	2	1	1101	8334	22	37	88	650	3	1	1380	10449	23	0
2009	15	120	2	1	1135	9469	22	38	90	740	3	1	1423	11872	23	0
2010	19	139	2	0	1465	10934	29	49	117	857	4	2	1837	13709	31	31
2011	20	159	2	1	1503	12437	29	50	119	976	4	1	1885	15594	31	0
2012	24	183	2	1	1837	14274	37	62	147	1123	5	2	2303	17897	39	8
2013	25	208	2	1	1854	16128	37	62	150	1273	5	1	2325	20222	39	0
2014	26	234	2	1	1895	18023	37	64	152	1425	5	1	2377	22599	39	0
2015	30	264	2	1	2233	20256	44	75	181	1606	6	2	2800	25399	46	38
2016	31	295	2	1	2253	22509	44	76	184	1790	6	2	2826	28225	46	0
2017	32	327	2	1	2274	24783	44	76	187	1977	6	2	2852	31077	46	11
2018	32	359	2	1	2294	27077	45	77	190	2167	6	2	2878	33955	49	0
2019	33	392	2	1	2315	29392	45	78	193	2360	6	2	2904	36859	49	0
2020	34	426	2	1	2336	31728	45	78	196	2556	6	2	2931	39790	49	38
2021	34	460	2	1	2380	34108	45	80	199	2756	6	2	2987	42777	49	0
2022	39	499	2	1	2721	36829	54	91	228	2984	7	2	3414	46191	57	19
2023	39	538	2	1	2745	39574	54	92	231	3215	7	2	3444	49635	57	0
2024	40	578	2	1	2769	42343	54	93	235	3450	7	2	3475	53110	57	0
2025	12	590	2	0	385	42728	8	13	56	3506	2	0	489	53599	8	0

VII-7

TABLE VII-3.- Program Model Summary for "Truss" SPS in Geo -

YEAR	SPS UNITS		OPS BASE UNITS IN LEO & GEO		TOTAL PERSONNEL IN SPACE					TOTAL MASS TO SPACE M, TONS x 10 ³	
	PER YR.	TOTAL ON LINE	PER YR.	TOTAL ON LINE	LEO		GEO		TOTAL PER. YR.	LEO	GEO
					PROD.	MAINT.	PROD.	MAINT.		PER. YR.	PER. YR.
1995	.5	0	1	1	88	0	287	0	375	187	54
1996	.5	0	0	1	88	0	287	0	375	163	47
1997	1	1	0	1	176	1	574	12	763	329	94
1998	1	2	0	1	176	1	574	24	775	333	95
1999	1	3	0	1	176	2	574	36	788	336	96
2000	1	4	0	1	176	2	574	48	790	339	97
2001	1	5	1	1	176	3	574	60	803	366	105
2002	2	6	0	2	352	3	1148	72	1575	672	191
2003	2	8	0	2	352	4	1148	96	1600	678	193
2004	2	10	0	2	352	5	1148	120	1625	685	195
2005	2	12	1	2	352	6	1148	144	1650	715	204
2006	3	14	0	3	528	7	1722	168	2425	1024	292
2007	3	17	0	3	528	9	1722	204	2463	1034	295
2008	3	20	0	3	528	10	1722	240	2500	1044	297
2009	3	23	1	3	528	11	1722	276	2537	1077	307
2010	4	26	0	4	704	13	2296	312	3325	1389	396
2011	4	30	1	4	704	15	2296	360	3375	1427	406
2012	5	34	0	5	880	17	2870	408	4175	1742	495
2013	5	39	0	5	880	20	2870	468	4238	1758	500
2014	5	44	1	5	880	22	2870	528	4300	1799	512
2015	6	49	0	6	1056	24	3444	588	5122	2117	602
2016	6	55	0	6	1056	27	3444	660	5187	2136	608
2017	6	61	0	6	1056	30	3444	732	5262	2156	614
2018	6	67	0	6	1056	33	3444	804	5337	2176	619
2019	6	73	0	6	1056	36	3444	876	5412	2195	624
2020	6	79	0	6	1056	39	3444	948	5487	2215	630
2021	6	85	1	6	1056	42	3444	1020	5562	2260	643
2022	7	91	0	7	1232	45	4018	1096	6387	2581	734
2023	7	98	0	7	1232	49	4018	1176	6475	2603	741
2024	7	105	0	7	1232	53	4018	1260	6563	2626	747
2025		112		7		56		1344	1400	367	104

8-IIA

TABLE VII-3.- Concluded ("Truss/Geo)

YEAR	POTV FLIGHTS TO GEO				COTV FLIGHTS TO GEO				PLV FLIGHTS TO LEO				HLLV FLIGHTS TO LEO			
	PER YR.	TOTAL	FLEET SIZE	NEW UNITS	PER YR.	TOTAL	FLEET SIZE	NEW UNITS	PER YR.	TOTAL	FLEET SIZE	NEW UNITS	PER YR.	TOTAL	FLEET SIZE	NEW UNITS
1995	2	2	2	2	241		4	8	15	15	2	2	268	268	5	5
1996	2	4	2	0	186		4	6	15	30	2	0	233	501	5	0
1997	5	9	2	0	376		8	13	31	61	2	0	471	972	8	3
1998	5	14	2	0	380		8	13	31	92	2	0	475	1447	8	0
1999	5	19	2	0	383		8	13	32	124	2	1	480	1927	8	0
2000	5	24	2	0	387		8	13	32	156	2	0	485	2412	8	5
2001	6	30	2	1	418		8	14	33	189	2	0	524	2936	9	1
2002	11	41	2	0	765		15	26	63	252	2	1	960	3896	16	7
2003	11	52	2	0	773		15	26	64	316	2	0	969	4865	16	0
2004	11	63	2	1	780		15	26	65	381	2	1	979	5844	16	0
2005	11	74	2	0	815		16	28	66	447	2	1	1022	6866	16	11
2006	16	90	2	1	1166		23	39	97	544	3	2	1463	8329	25	7
2007	17	107	2	0	1177		23	40	98	642	3	1	1477	9809	25	7
2008	17	124	2	1	1188		23	40	100	742	4	2	1491	11297	25	0
2009	17	141	2	1	1227		24	41	112	854	4	1	1540	12837	25	0
2010	22	163	2	1	1582		31	53	133	987	5	2	1985	14822	33	19
2011	23	186	2	1	1625		32	55	135	1122	5	1	2039	16861	33	7
2012	29	215	2	1	1980		39	66	167	1289	5	1	2488	19349	42	16
2013	29	244	2	1	2001		39	67	170	1459	6	2	2512	21861	42	0
2014	29	273	2	1	2048		40	69	172	1631	6	1	2570	24431	42	0
2015	35	308	2	1	2409		47	81	205	1836	7	2	3025	27456	50	27
2016	36	344	2	1	2432		47	82	208	2044	7	2	3053	30509	50	17
2017	36	380	2	1	2454		48	82	211	2255	7	2	3082	33591	51	17
2018	37	417	2	1	2476		48	83	214	2469	7	2	3109	36720	51	0
2019	38	455	2	1	2498		49	84	217	2686	7	2	3137	39857	51	0
2020	38	493	2	1	2521		49	85	220	2906	7	2	3165	43022	53	29
2021	39	532	2	1	2571		50	86	223	3129	7	2	3227	46249	53	7
2022	44	576	2	1	2937		57	98	256	3385	8	3	3687	49936	61	25
2023	45	621	2	1	2963		57	99	259	3644	8	2	3720	53656	61	0
2024	46	667	2	1	2989		58	100	262	3906	8	2	3753	57409	62	0
2025	12	679	2	1	415		8	14	56	3962	2	0	525	57934	9	0

6-11A

TABLE VII-4.- Program Model Summary for "Truss" SPS in Leo

YEAR	SPS UNITS		OPS BASE UNITS IN LEO & GEO		TOTAL PERSONNEL IN SPACE					TOTAL MASS TO SPACE M. TONS X 10 ³	
	PER YR.	TOTAL ON LINE	PER YR.	TOTAL ON LINE	LEO		GEO		TOTAL PER. YR.	LEO	GEO
					PROD.	MAINT.	PROD.	MAINT.		PER. YR.	PER. YR.
1995	.5	0	1	1	370	0	100	0	470	104	46
1996	.5	0	0	1	370	0	100	0	470	101	45
1997	1	1	0	1	740	1	200	12	953	203	91
1998	1	2	0	1	740	1	200	24	965	205	93
1999	1	3	0	1	740	2	200	36	978	207	94
2000	1	4	0	1	740	2	200	48	992	209	95
2001	1	5	1	1	740	3	200	60	1003	214	97
2002	2	6	0	2	1480	3	400	72	1955	415	189
2003	2	8	0	2	1480	4	400	96	1980	419	191
2004	2	10	0	2	1480	5	400	120	2005	423	192
2005	2	12	1	2	1480	6	400	144	2030	429	194
2006	3	14	0	3	2220	7	600	168	2995	632	286
2007	3	17	0	3	2220	9	600	204	3033	639	289
2008	3	20	0	3	2220	10	600	240	3070	645	292
2009	3	23	1	3	2220	11	600	276	3107	653	295
2010	4	26	0	4	2960	13	800	312	4085	859	388
2011	4	30	1	4	2960	15	800	360	4135	869	393
2012	5	34	0	5	3700	17	1000	408	5125	1076	487
2013	5	39	0	5	3700	20	1000	468	5188	1087	492
2014	5	44	1	5	3700	22	1000	528	5250	1099	498
2015	6	49	0	6	4440	24	1200	588	6252	1309	592
2016	6	55	0	6	4440	27	1200	660	6327	1322	598
2017	6	61	0	6	4440	30	1200	732	6402	1334	604
2018	6	67	0	6	4440	33	1200	804	6477	1347	609
2019	6	73	0	6	4440	36	1200	876	6552	1359	615
2020	6	79	0	6	4440	39	1200	948	6627	1372	621
2021	6	85	1	6	4440	42	1200	1020	6702	1387	627
2022	7	91	0	7	5180	45	1400	1092	7717	1597	723
2023	7	98	0	7	5180	49	1400	1176	7805	1612	729
2024	7	105	0	7	5180	53	1400	1260	7893	1627	735
2025		112		7		56		1344	1400	235	106

VII-10

TABLE VII-4.- Concluded ("Truss/Leo)

YEAR	POTV FLIGHTS TO GEO				COTV FLIGHTS TO GEO				PLV FLIGHTS TO LEO				HLLV FLIGHTS TO LEO			
	PER YR.	TOTAL	FLEET SIZE	NEW UNITS	PER YR.	TOTAL	FLEET SIZE	NEW UNITS	PER YR.	TOTAL	FLEET SIZE	NEW UNITS	PER YR.	TOTAL	FLEET SIZE	NEW UNITS
1995	3	3	2	2	46	46	1	5	19	19	2	2	149	149	3	3
1996	3	6	2	0	45	91	1	5	19	38	2	0	146	295	3	0
1997	5	11	2	0	91	182	2	10	38	76	2	0	290	585	5	2
1998	6	17	2	0	93	275	2	10	39	115	2	1	293	878	5	0
1999	6	23	2	0	94	369	2	10	39	154	2	0	296	1174	5	0
2000	6	29	2	0	95	464	2	10	40	194	2	1	299	1473	5	3
2001	7	36	2	1	97	561	2	10	40	234	2	0	305	1778	5	0
2002	13	49	2	0	189	750	4	19	78	312	3	2	592	2370	10	7
2003	14	63	2	1	191	941	4	19	79	391	3	0	598	2968	10	0
2004	14	77	2	0	192	1133	4	19	80	471	3	1	604	3572	10	0
2005	15	92	2	1	194	1329	4	29	81	552	3	0	613	4185	10	3
2006	20	112	2	0	286	1613	6	29	120	672	5	3	903	5088	16	13
2007	21	133	2	1	289	1902	6	29	121	793	5	1	912	6000	16	0
2008	22	155	2	0	292	2194	6	29	123	916	5	1	921	6921	16	0
2009	23	178	2	1	295	2489	6	30	124	1040	5	1	933	7854	16	0
2010	29	207	2	1	388	2877	8	39	163	1203	6	2	1226	9080	21	8
2011	31	238	2	1	393	3270	8	39	165	1368	6	2	1241	10321	21	13
2012	38	276	2	1	487	3757	10	49	205	1573	7	2	1537	11858	26	5
2013	39	315	2	1	492	4249	10	49	207	1780	7	2	1552	13410	26	0
2014	41	356	2	2	498	4747	10	50	210	1990	7	2	1570	14980	26	0
2015	48	404	2	2	592	5339	12	60	250	2240	9	3	1869	16849	31	13
2016	50	454	2	2	598	5937	12	60	253	2493	9	2	1887	18736	31	13
2017	52	506	2	2	604	6541	12	60	256	2749	9	2	1905	20641	34	8
2018	53	559	2	2	609	7150	12	61	259	3008	9	3	1923	22564	34	0
2019	55	614	2	2	615	7765	12	62	262	3270	9	2	1941	24505	34	0
2020	57	671	2	2	621	8386	12	62	265	3535	9	3	1959	26464	34	13
2021	59	730	2	2	627	9013	12	63	268	3803	9	2	1980	28444	34	13
2022	66	796	3	2	723	9736	14	73	308	4111	11	3	2282	30726	39	13
2023	68	864	3	2	729	10465	14	73	312	4423	11	3	2303	33029	39	0
2024	71	935	3	2	735	11200	14	74	315	4738	11	3	2324	35353	39	0
2025	36	971	3	0	106	11306	2	10	56	4794	2	0	336	35689	6	0

VII-11

flight systems is prepared for flight in ground-based facilities and is largely controlled in accordance with plans and procedures developed and managed from ground-based facilities. The development of continuously manned permanent space facilities in LEO and GEO conducting the SPS program model and detailed functions as discussed in sections IV, V, and VI requires that the authority for operations and control of daily ongoing activities must be delegated to the primary operational sites, basically the launch and recovery site, the LEO and GEO operational bases, and the SPS satellite ground rectenna sites.

The mission management concept that has been developed to incorporate this philosophy is illustrated in figure VII-2. This concept applies only to the production/operational phase of implementing the 112 SPS's.

D. Mission Management Functions

The decentralization and assignment of SPS mission management functions are allocated and identified as follows from figure VII-2.

1. Program Headquarters Mission Control

It is envisioned that one element of the basic Ground Support System will be a control function and facility for the overall program management, operations, administration, program planning, resource control, mission planning, etc. type of SPS activities. This control element would also manage and direct all the ground-based manufacturing required, would obtain necessary materials for orbital construction, and in general manage the overall ground support requirements for ensuring that all the basic cargo elements are accounted for and in the system. This control element would also manage the ground transportation operations required to transport cargo elements to the launch site. This element would also manage the overall selection, training, simulation activities, and assignment of all personnel in their respective job functions and tasks. This element would manage the overall orbital construction and assembly operations being conducted on the ground and in LEO and GEO on an overall project basis. The coordination of the Communications and Data Network relay satellites and ground station would be assigned to this element for overall SPS responsibility.

2. Launch and Recovery Control

The second major element of the SPS ground support system is the operations and control of the launch and recovery operations.

The basic function of this control element is to manage all the ground operations involved with the preparation, launch, and return of all personnel and cargo to and from the LEO operational bases and

ORIGINAL PAGE IS
OF POOR QUALITY

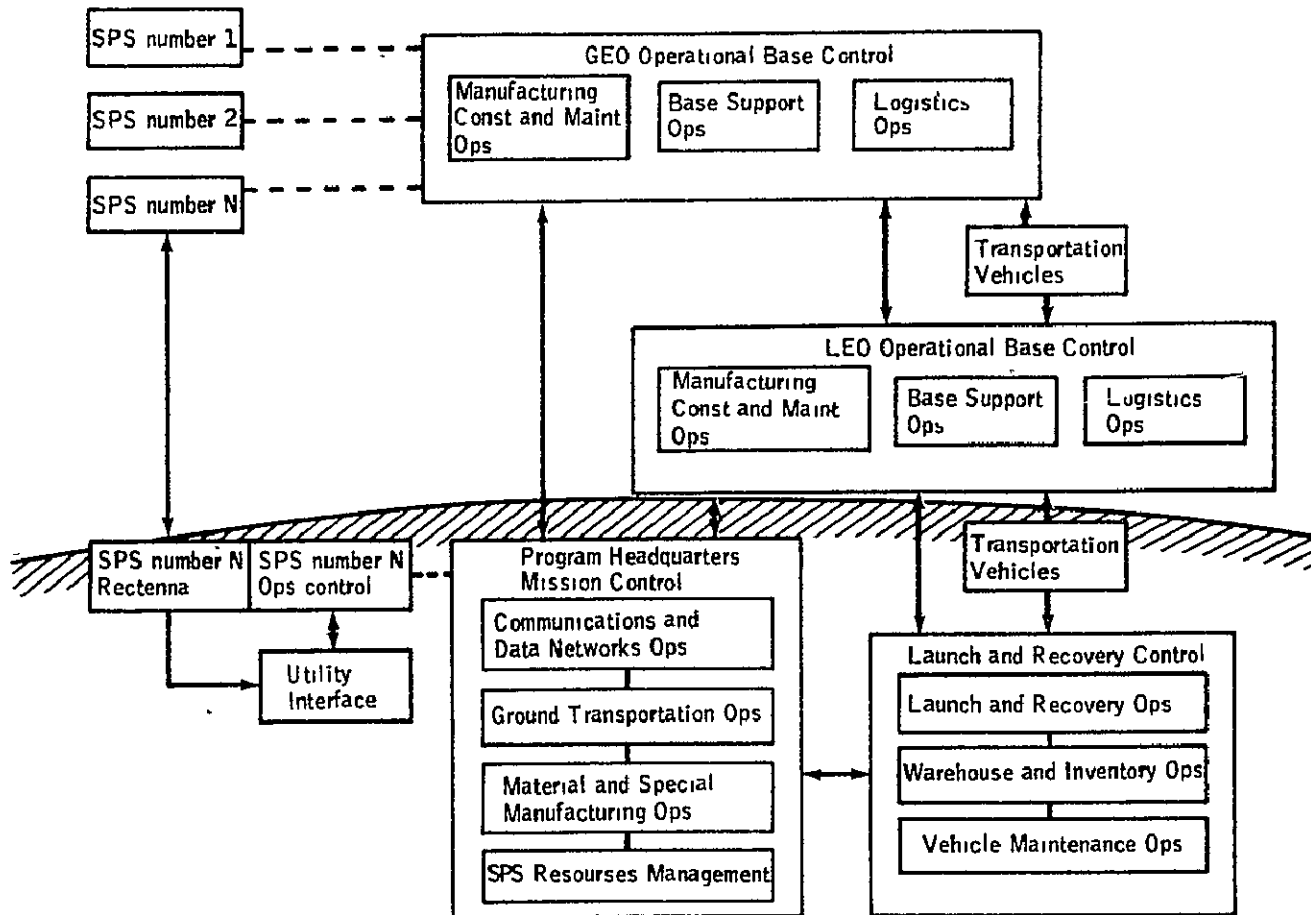


Figure VII-2.- SPS mission management concept.

the maintenance of the cargo launch vehicles (HLLV) and the personnel launch vehicle (PLV). This element will also manage and conduct the training and simulation for all transportation vehicle flight crews.

3. LEO Operational Base Control

The LEO and GEO operational bases utilize the same basic elements for operations and control authority, with the major differences being due to the nature of the functions and tasks required in their respective orbital location for manufacturing and construction operations, logistics operations, and base support operations. Each space operational base (LEO or GEO) is envisioned to manage its own day-to-day activities involved with manufacturing, construction, logistics, and transportation operations and its interfaces with the other major elements in the SPS system.

It is expected that the LEO operational base will be predominantly concerned with logistics and transportation operations because its position in LEO links it directly to the ground and to the GEO operational base. This base will be the primary "space traffic control center" handling all cargo and personnel arriving and departing via the launch vehicles from Earth and then, in turn, acting as a warehouse in space until transferring required cargo and personnel to orbital transfer vehicles (OTV) for departure to the GEO operational base and handling arriving OTV's returning from GEO. It is therefore expected that significant authority for operations and control over all the SPS logistics and transportation operations will be delegated to the LEO operational base.

Because of its ongoing full range of space operation activities and its ready access to the ground, the LEO operational base is the prime candidate for implementing and conducting training and simulation for all new orbital crew personnel.

4. GEO Operational Base Control

The GEO operational base, similar to the LEO operational base, will manage its own day-to-day activities involved with manufacturing, construction, logistics and transportation operations, and its interface with the other major elements in the SPS system.

It is expected that the GEO operational base will be predominantly concerned with the manufacturing, construction, and final checkout and operational go-ahead for each SPS satellite because its position in GEO is the resident operational location for the SPS satellites. Therefore, it is expected that significant authority for operations and control over all the SPS manufacturing, construction, checkout, and maintenance will be delegated to the GEO operational base.

The GEO operational base will also conduct the routine maintenance and "onboard" inspection of all individual SPS satellite units after they are operational by sending resident GEO base crewmembers to visit several SPS units on periodic inspection and maintenance tours. Emergency visits to any SPS unit would also be managed by the GEO base.

5. SPS (Individual Unit) Ground Control

The primary authority for operations and control of each individual SPS unit after it becomes operational will reside with a ground control facility located at the ground rectenna station. The SPS ground control elements for each of the 112 SPS units complete the basic elements comprising the ground-based support system.

It is expected that the SPS control facility will manage the power transmission from the SPS unit in orbit to the rectenna and into the interface with a ground-based utility distribution system. This control facility will monitor the performance and status of the SPS systems and will coordinate as required with the Program Headquarters Mission Control facility for assistance and with the GEO operational base for "revisit" operations.

Position and tracking information for all 112 SPS units will be managed and coordinated by the Program Headquarters Mission Control facility. Potential conflicts or potential in-orbit collisions will be identified and the necessary operations required to correct the situation will be determined and implemented by the Program Headquarters Mission Control and the respective SPS Ground Control facilities of each involved SPS unit.

E. Key Considerations and Areas For Further Investigation

During the development of the SPS program model and the overall mission management concept for SPS operations and control, many new and challenging functions and tasks have been identified that are lacking in technology development and/or analysis in significant depth; therefore, many critical areas requiring operational and design trade-offs cannot be evaluated at this stage of our understanding. However, the following concerns have been selected as having the most significant impact on the SPS design and operations concept during this study effort.

1. Prelaunch, Launch, and Recovery Operations

The Program Model discussed in subsection VII-B implies the magnitude of ground support operations involved in the daily flow of personnel and material, equipment, etc. in various packaged forms, which have to be transported from the original location by some ground transportation element to the launch site, where they are received, unloaded, processed, and stored for assignment to a launch vehicle. (See

also fig. VII-1.) Preparations for launch commence when the launch assignment is made. Recovery operations for returning vehicles are also handled at the launch and recovery facilities. It is recognized that the personnel and facilities involved in the ground operations of the SPS system will be an important element in the operational assessment and cost of the SPS; however, no in-depth analyses of these operational elements have been conducted during this study. Significant attention needs to be devoted to this area in follow-on efforts to this study.

2. Space Manufacturing and Construction Options

This new area of technology and its operational considerations have been discussed in previous sections. However, the concepts and options selected for accomplishing the space manufacturing and construction tasks have "significant" influence on the operational requirements of the SPS system in such areas as operational base manning, crew skill mix, construction sequence and mission activity schedules, simulation and training, etc. Early design, development, test, and evaluation (DDT&E) programs must be directed at developing and demonstrating this new area of space technology.

3. Operational Space Base Control Operations

The magnitude of operational activity required in LEO and GEO to accomplish the implementation and operations of the 112 SPS systems, when considering total personnel operating on Earth and in space; multiple vehicles moving between, to, and from Earth, LEO, and GEO bases; the space manufacturing and construction tasks; and the massive cargo requirements as discussed in previous sections, has led to a mission management concept assigning significant operations and control authority to the space base elements of the SPS system. The implications of basing control, operations, and management functions in space will have philosophical, programmatic, economic, and technical repercussions upon the composition of future space program concepts, particularly when examined in the context of resource requirements, costs, systems definition, and reliable requirements for advanced technology development. In this study, the concept of in-space operational control has only been identified and further analysis is required.

4. Simulation and Training Operations

The operation of space manufacturing and construction equipment will require manned and automated tasks involving a broad range of skill mix activities that have not been exercised or required in past or current space programs. With the involvement of thousands of ground and orbital crew personnel in conjunction with the large and massive space structures and equipment required for SPS production and operations, the area of simulation and training operations and facilities has only been identified in this study and further analysis is required.

5. Safety in SPS Operations

This study has not included a safety analysis associated with the manufacturing, construction, checkout, operations, or with the associated space logistics operations of cargo and personnel transfer, vehicle servicing, refurbishment, maintenance and operations, and propellant storage and servicing tasks. Potentially hazardous situations need to be identified and examined in depth to assess all the natural and induced hazards associated with all mission phases and elements of the SPS system.

VIII. ENVIRONMENTAL CONSIDERATIONS

A. Methodology

Jerry Poradek
Urban Systems Project Office

Introduction

One of the primary concerns for implementation of any power generation system is the concern over the deterioration of the environment which may result from the system implementation. This is as true for solar power satellite, as for a nuclear generation plant, for a coal-burning plant or for any other type of electrical energy generation system. In order to assess the impact on the environment of a power generation system, environmental impact evaluation methodologies have been developed. In the impact evaluation process for the SPS, the following sequence of activities has been defined.

- a. A definition of the type of pollution source.
- b. A definition of the activity which produces the pollution source, such as power plant fabrication, transportation system, etc.
- c. A definition of the pollutants that are involved, whether they be air pollution, water pollution, etc.
- d. A definition of the magnitude of each of the pollutants, based on an individual plant and a scenario of satellites which includes launch dates and the number of satellites to be launched.
- e. A definition of the scope of the pollution effects; that is, where and how do the pollutants affect the environment?
- f. A definition of the magnitude effects.
- g. A definition of possible synergistic effects after the individual effects are identified. Synergistic effects are those effects produced when two or more pollutants interact simultaneously to create an effect of greater magnitude than any of the individual pollutants would without interaction.
- h. A definition of potential cascading effects must be made. Cascade effects are those in series with other effects and are based on previous pollution.
- j. Finally, an assessment of the integrated impact on the environment as a whole.

Approach

Because of the complexity of the task, a step-by-step process of evaluation was defined for this program. Table VIII-A-1 defines the ten steps to be utilized in the evaluation of not only the SPS, but the nuclear and coal-fired generation systems. These steps begin with an identification of the type of power plant, proceed to a breakdown of the plant activities, including all of the pollution-related activities necessary to build and use the plant for 30 years. An attempt at definition of the pollutants and their effects will be made and finally, because the systems are not totally comparable, an interpretation of the overall effect will be made. This program will, by necessity, take several years and require a multiplicity of technical and scientific disciplines. In this document the methodology is defined and several important parameters defined.

Figure VIII-A-1 shows the process methodology from source identification to impact classification. Table VIII-A-2 indicates the types of methodology techniques that can and have been used to evaluate environmental impacts of various large and small programs. The level of detail which the investigation can go is dependent upon the depth of detail available in defining the operational activities, the type and magnitude of the pollutant and the scope effects caused by the pollutant at the given magnitude for individual pollutants, synergistic or cascade conditions. Table VIII-A-2 lists these methodologies. In this program, the intent is to define as complete a network system as possible, but in some areas, especially early in the program, the level of detail of information may allow only ad hoc type evaluations. Table VIII-A-3 indicates the detail of knowledge available for impact assessment and shows a great deal of further investigation is required for the SPS. The flow of methodology for this investigation is given in figure VIII-A-2. Once the activity is defined and the pollutants identified, parallel investigations can be conducted into the definition of pollutant magnitudes and the scope of the effects. The level of knowledge then determines the detail available for the magnitude of single, synergistic and cascade effects and, in turn, the overall impact interpretation. Figures VIII-A-3, VIII-A-4a and VIII-A-4b show a more specific breakdown of the check pattern used in this program.

Because of the complexity and detail required for the environmental analysis, a system of priorities was developed. Priority 1 items are those parameters considered to have a major impact on program results. Priority 2 items are those parameters considered to produce a measurable effect on the results. Priority 3 items will not be determined because they are considered as negligible affect parameters. Figure VIII-A-5a through VIII-A-7b prioritize the specific areas for investigation for each of the power systems, coal fired, nuclear and SPS.

A number of methodologies have been developed to evaluate the impact on the environment of significant systems. These include: (a) Ad hoc techniques which suggest broad areas of possible impact, but go into little or no detail; (b) checklists which are specific lists of environmental parameters to be checked, but which do not establish a direct cause of effect relationship between the physical magnitude of the pollutant and its effect on the surrounding environment; (c) matrix formation, which lists the project activities and lists the potential impacted parameters. The matrix interconnects the activities and the potential impact parameter. It identifies the cause/effect relationship of the activity and the related pollution; (d) Network system, or methodology, which lists the project activities, the impacted parameters, and establishes a cause, condition and effect network. This technique attempts to recognize a cascade of impacts triggered by a project action. The depth of detail or level to which the methodology can be pursued in any project activity or impacted parameter is directly dependent of the detail of information known about that particular parameter or activity. In the case of land-based power plants, such as coal-burning and nuclear plants, the impacts are still being studied, although the project activities and the magnitude of the pollutants are well defined. However, in the solar power satellite, only general project activities have been identified, and in addition, except for the troposphere, very little is known about impact effects on the environment of the pollutants which are generated.

In this evaluation program, three power generation systems are identified and an attempt is made to define each system to about the same level of detail. Coal power generation plants, nuclear power generation plants, and solar power satellite electrical generation plants are evaluated individually for their pollution magnitudes and then are compared as directly as possible. To do this, an attempt is made, where possible, to identify the types of pollution and the activities in the plant operation in such a way that the pollution impacts can be compared directly. The types of pollution are broken down into six areas: land use, air pollution, water pollution or water use, thermal pollution, radiation pollution and noise. The activities, the areas are broken down into two levels. Level I, the pollution that is generated by the actual plant operation and Level II, the pollution which is generated by the support activities such as the plant fabrication, the supply of fuel to the plant, and the removal and disposal of the waste from the plant. In the case, for instance, of supply for a coal-fired plant, the coal brought to the plant must be mined and delivered to the plant. The pollution that can be identified with the processes of mining and transportation of the coal to the plant is the pollution generated by the Level II supply category. The pollution from the coal being burned in the plant would be listed under the Level I pollution.

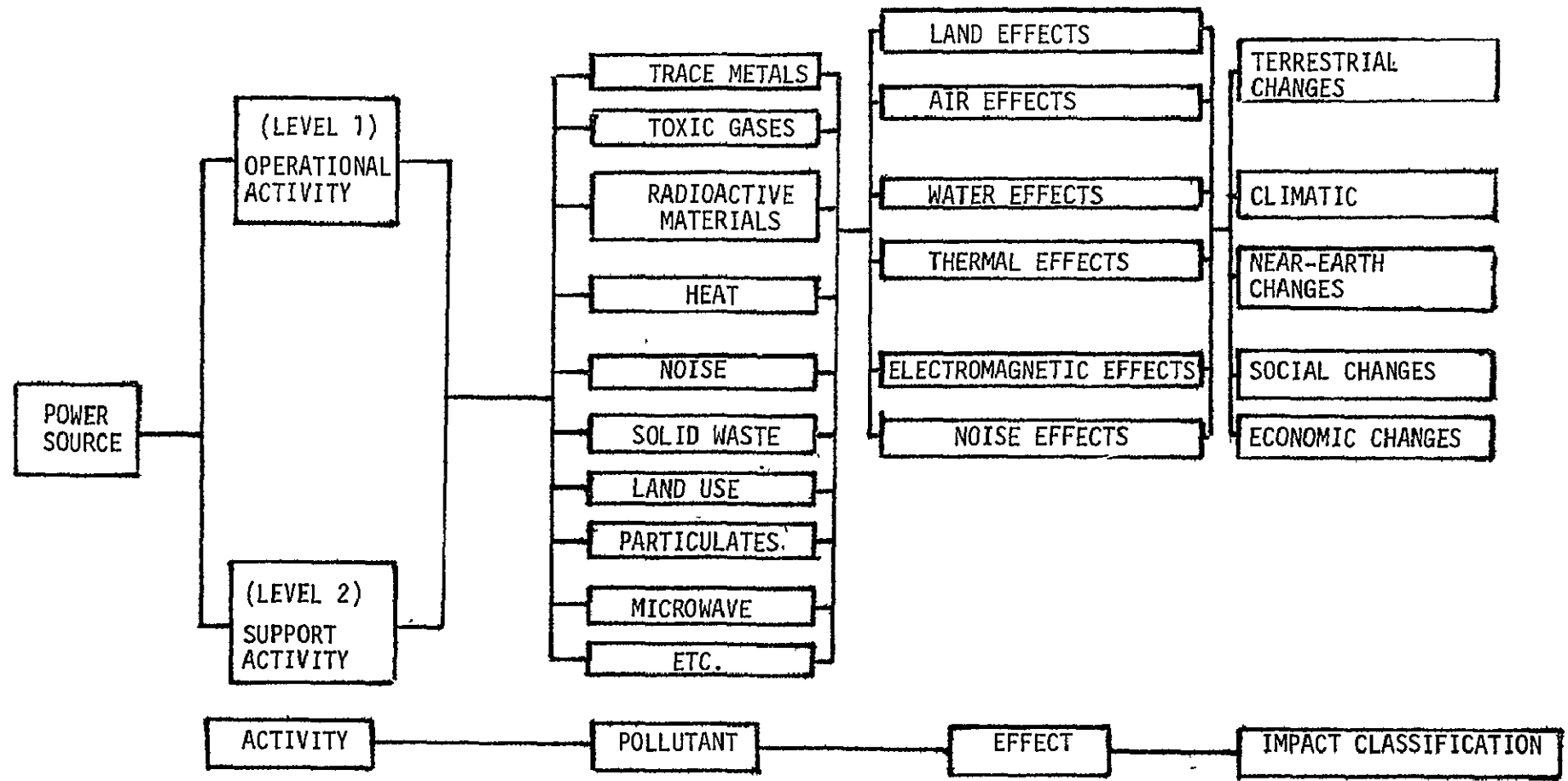
Table VIII-A-1

IMPACT EVALUATION PROCESS

- o Define Type of Pollution Source
- o Define the Activity
- o Define the Pollutant
- o Define the Magnitude of the Pollutant
- o Define the Scope of the Pollution Effects
- o Define the Magnitude of the Effects
- o Define Possible Synergistic Effects
- o Define Cascade Effects
- o Define Impact Classification
- o Interpretation of the Impact on the Environment

6.9

VIII-A-5



METHODOLOGY BREAKDOWN

Figure VIII-A-1

TABLE VIII-A-2

METHODOLOGY LEVELS

AD HOC.....Suggests broad areas of possible impact.
CHECKLISTS.....Specific lists of environmental parameters. Does not establish direct cause-effect relationship.
MATRIX.....List of project activities.
List of potentially impacted parameters.
Matrix interconnects the above lists and identifies cause-effect relationship.
NETWORKS.....List of project activities.
List of impacted parameters.
Establishes cause-condition-effect networks.
Attempts to recognize a cascade of impacts triggered by a project action.

TABLE VIII-A-3

POWER SYSTEMS

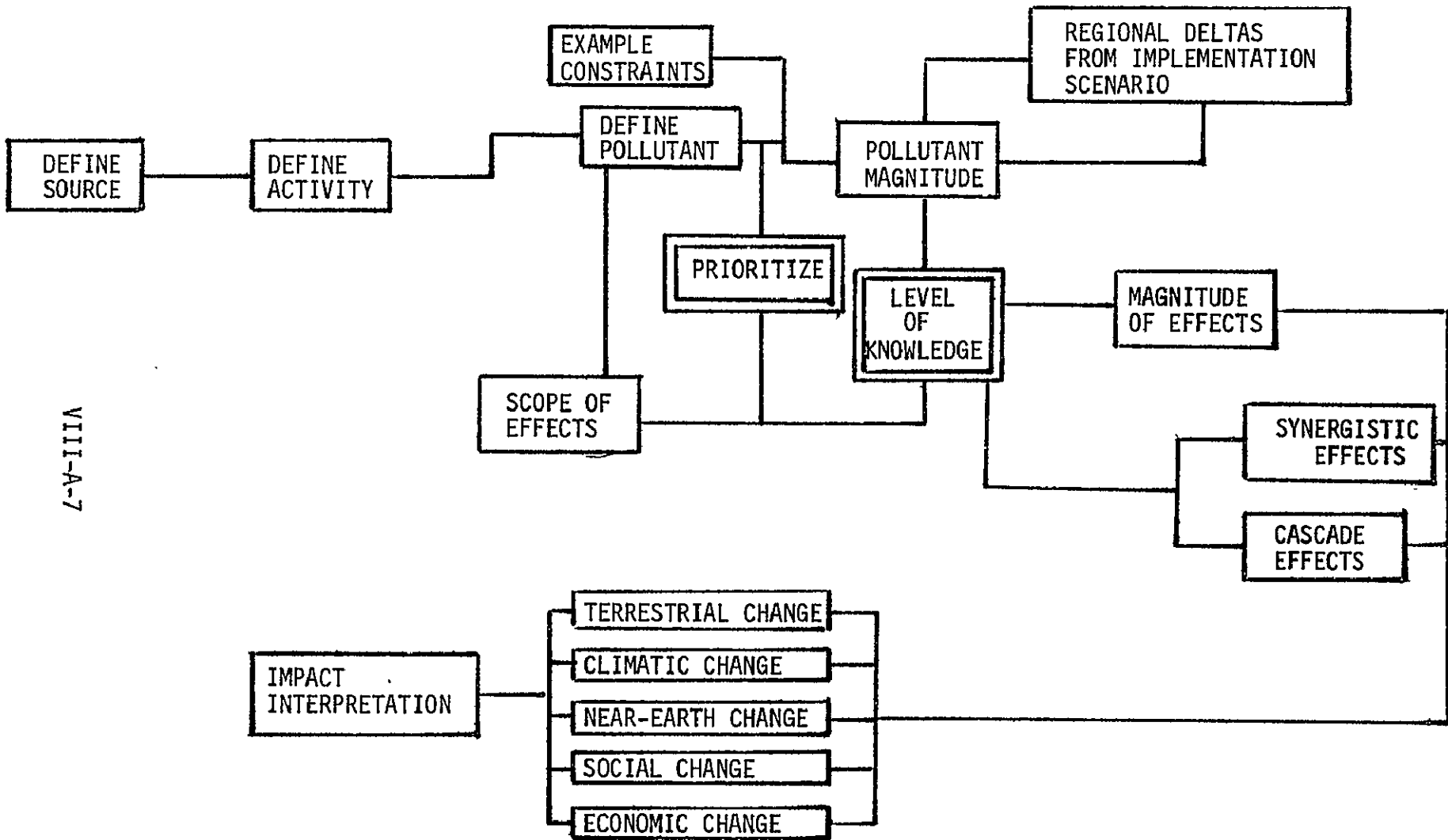
DETAIL OF KNOWLEDGE

LAND-BASED POWER SYSTEM

Activities----- Well defined.
Pollution Parameters-----Reasonably well defined.
Impact Definition-----Variable, but fairly well defined generally. Also, under extensive investigation.

SPS

Activities-----Fair to vague definition.
Pollution Parameters-----Fairly well defined.
Impact Definition-----Variable from fair definition to almost nonexistent with detailed investigations in only a few areas.

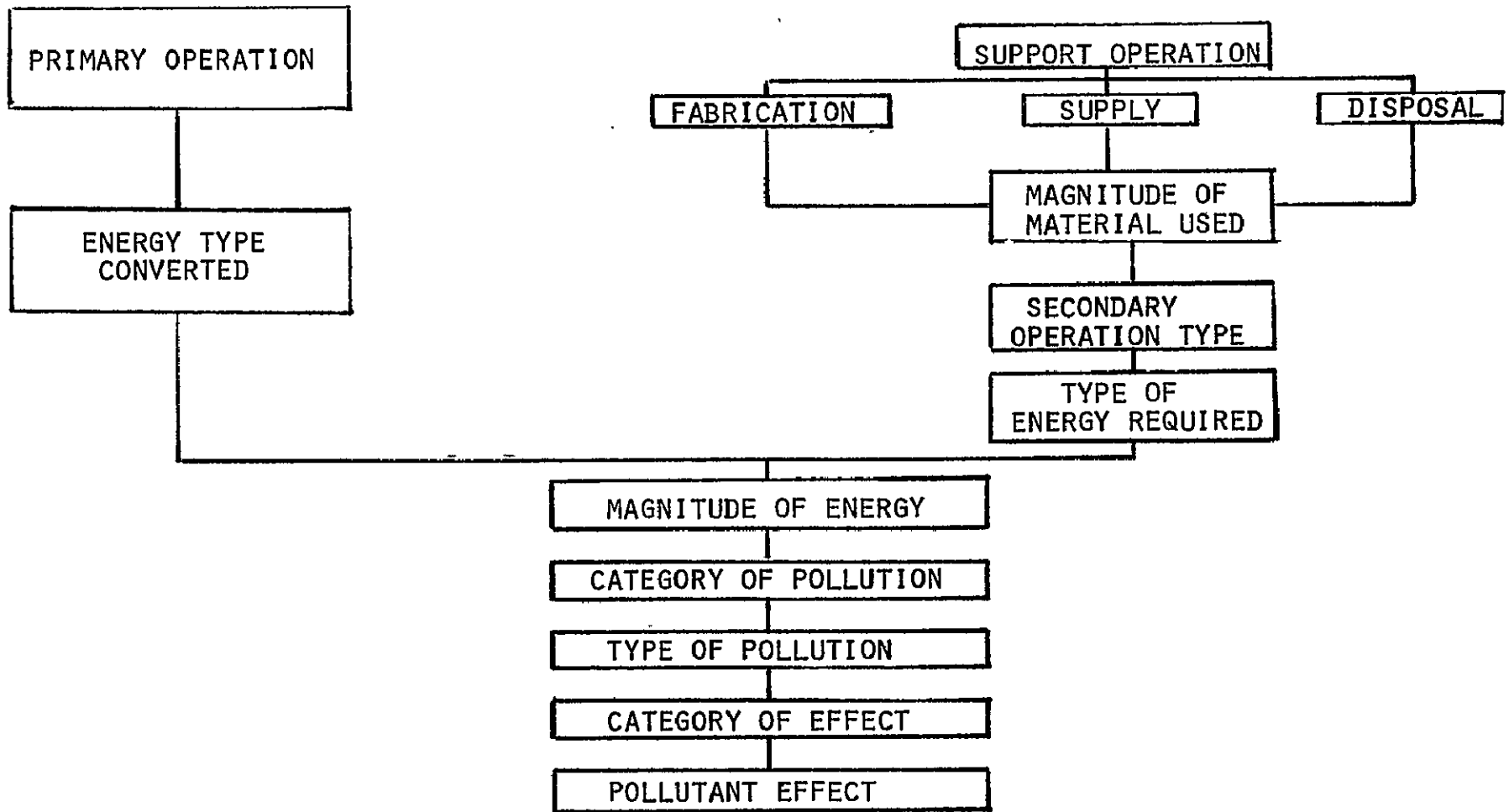


VIII-A-7

METHODOLOGY FLOW PATTERN

Figure VIII-A-2

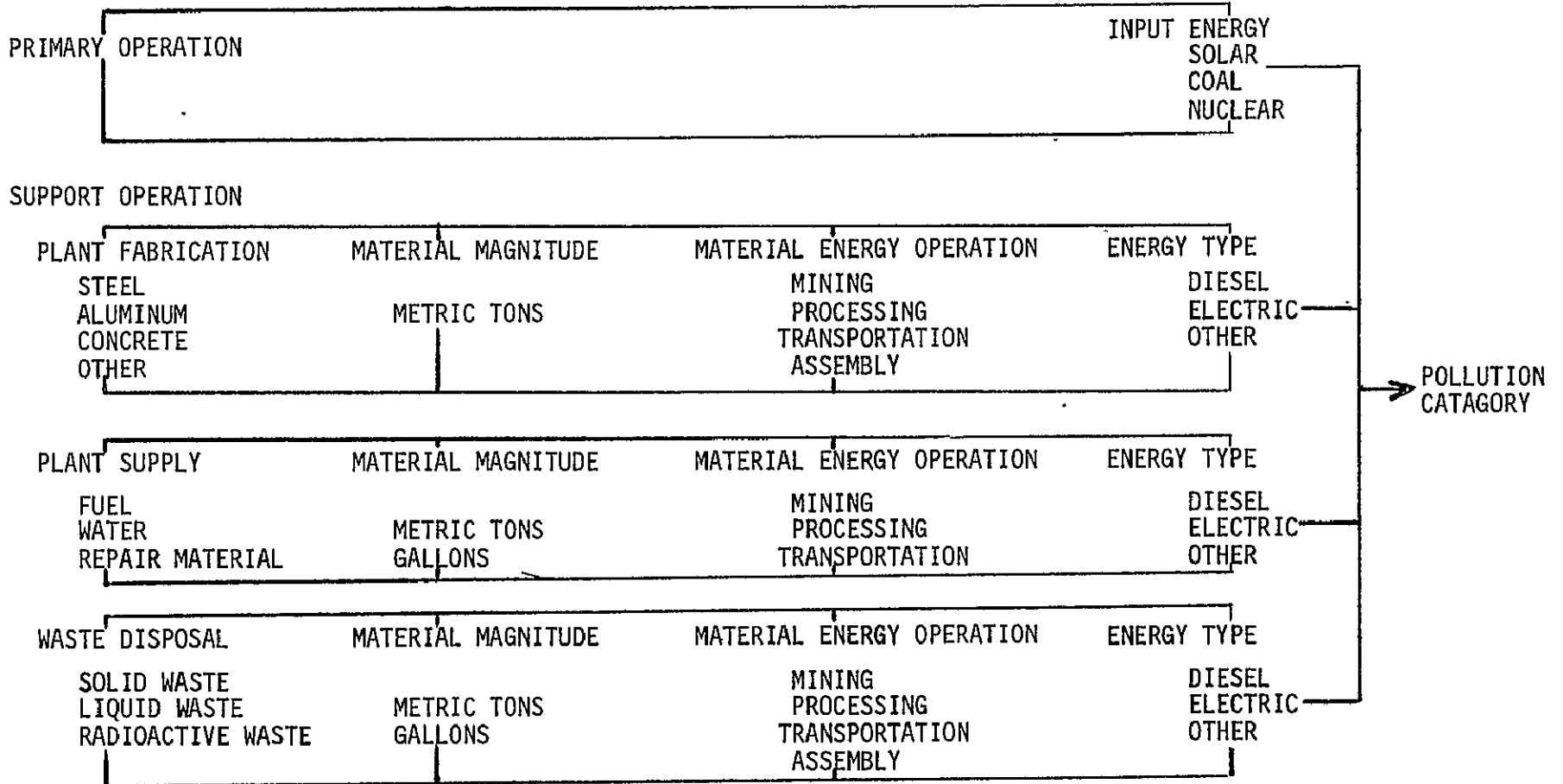
VIII-A-8



POWER PLANT ANALYSES

Figure VIII-A-3

CHECK PATTERN BREAKDOWN



VIII-A-9

FIGURE VIII-A-4a.

CHECK PATTERN BREAKDOWN (CONT)

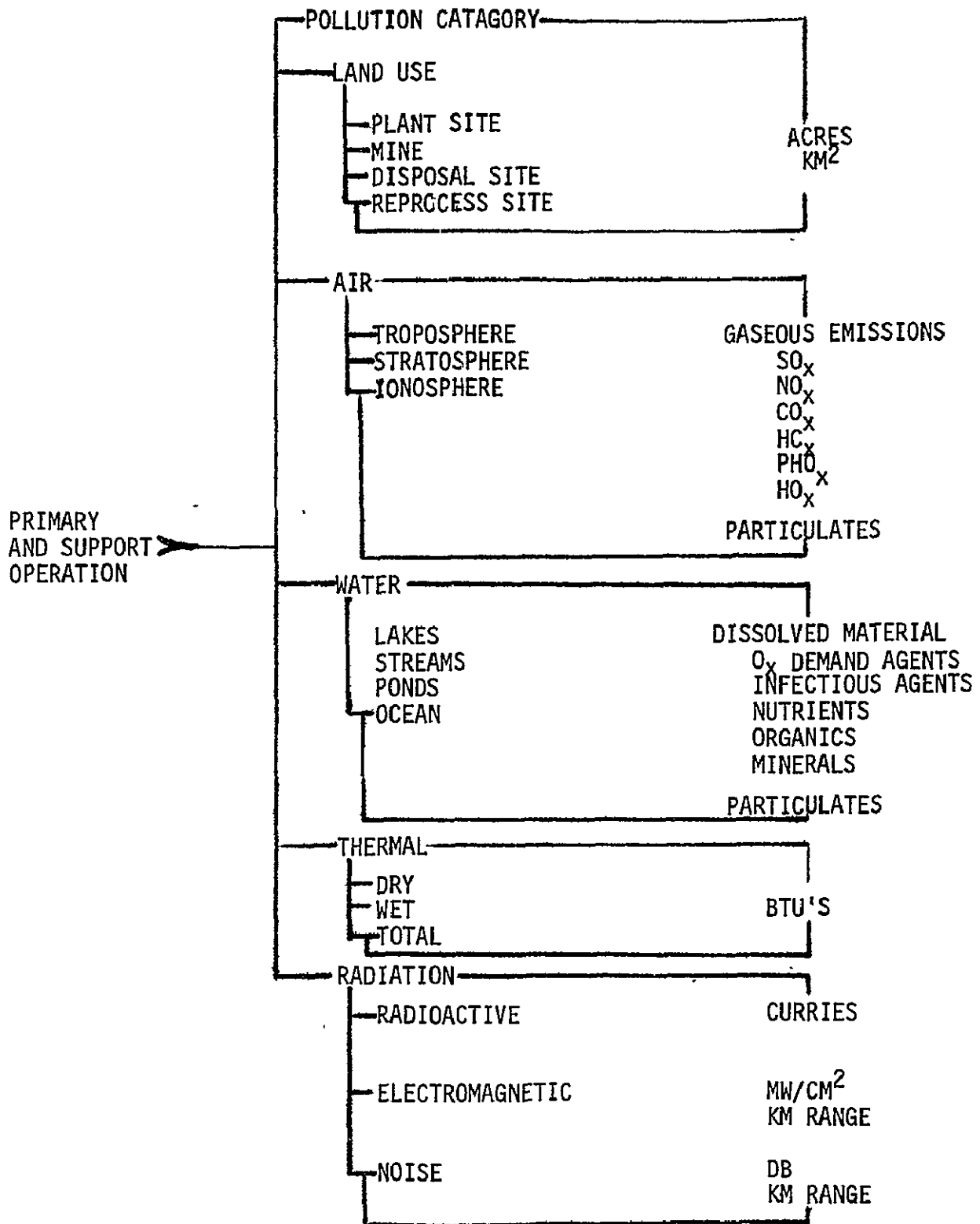
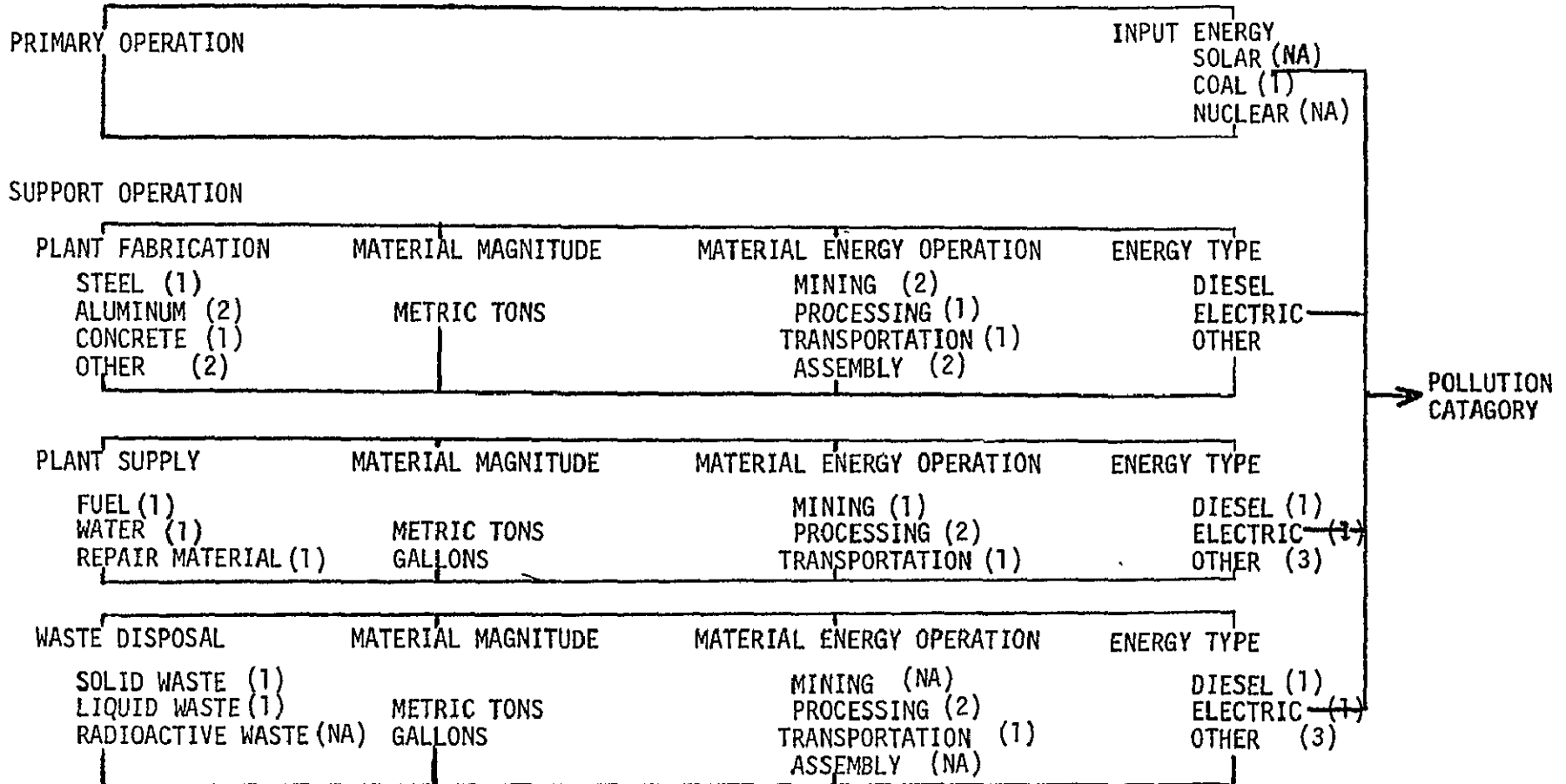


Figure VIII-A-4b.

CHECK PATTERN BREAKDOWN - COAL PLANT PRIORITIES



VIII-A-11

Figure VIII-A-5a.

COAL PLANT PRIORITIES - CHECK PATTERN BREAKDOWN (CONT)

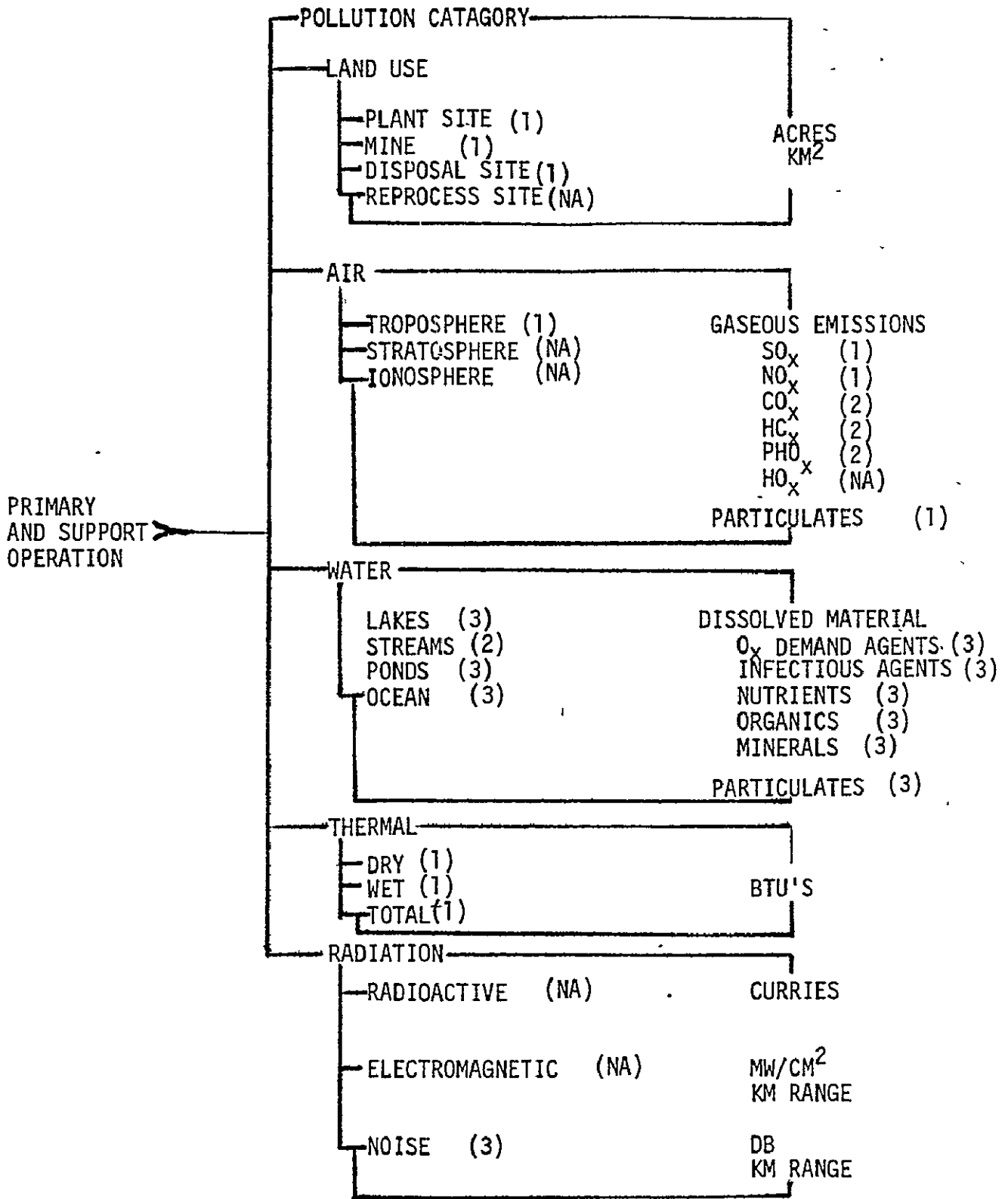


Figure VIII-A-5b.

CHECK PATTERN BREAKDOWN - NUCLEAR PLANT PRIORITIES

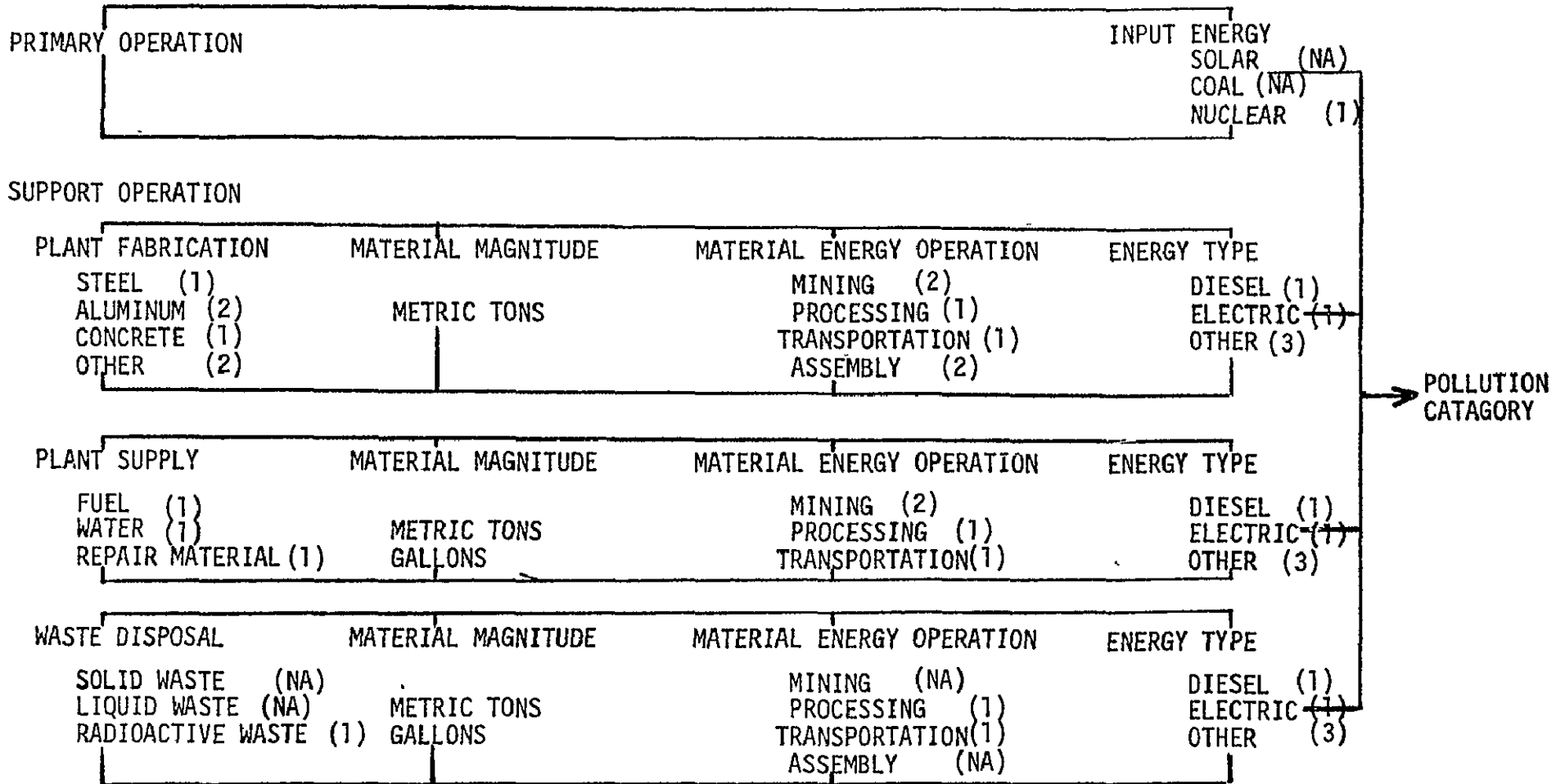


Figure VIII-A-6a.

VIII-A-13

NUCLEAR PLANT PRIORITIES - CHECK PATTERN BREAKDOWN (CONT)

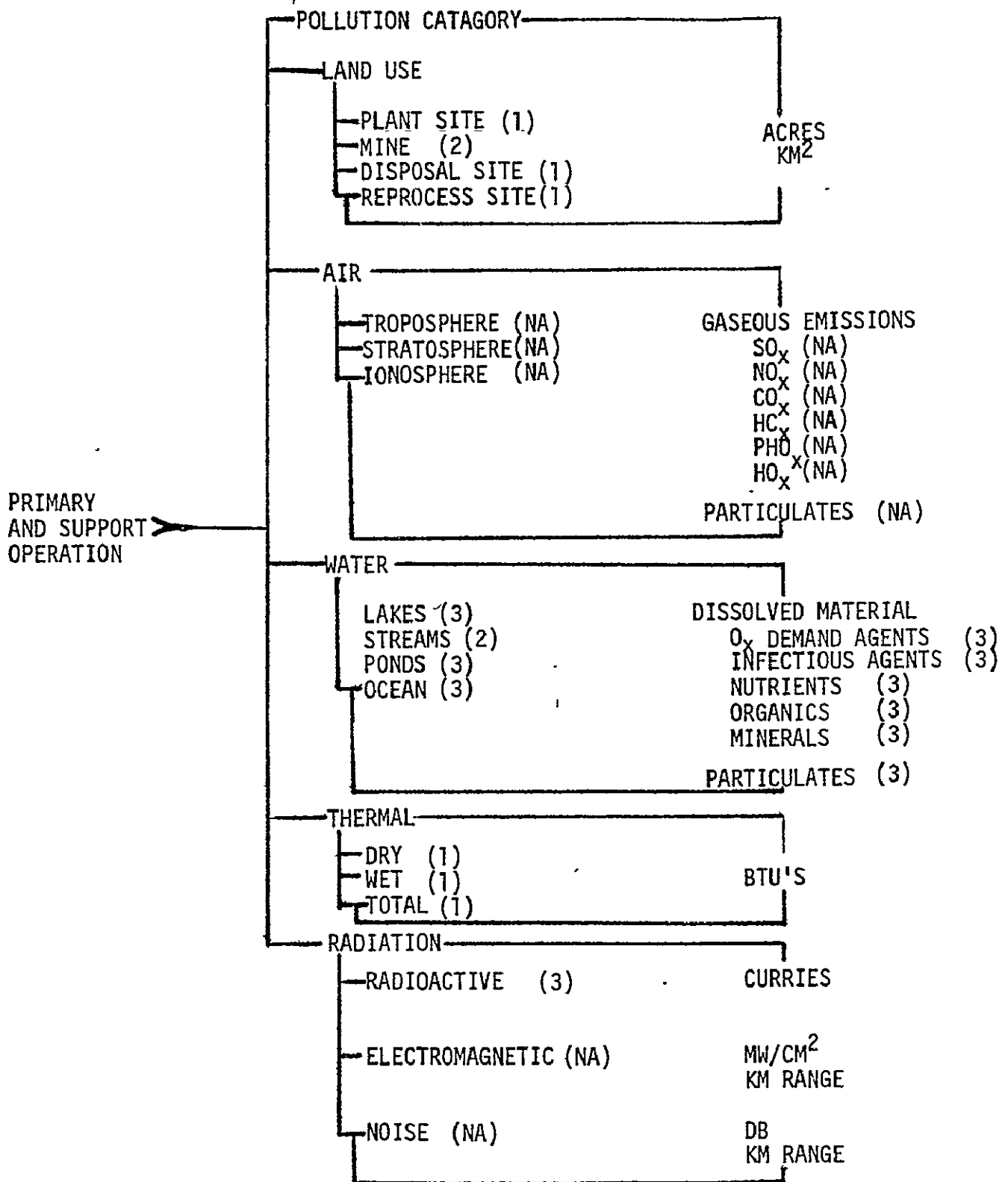
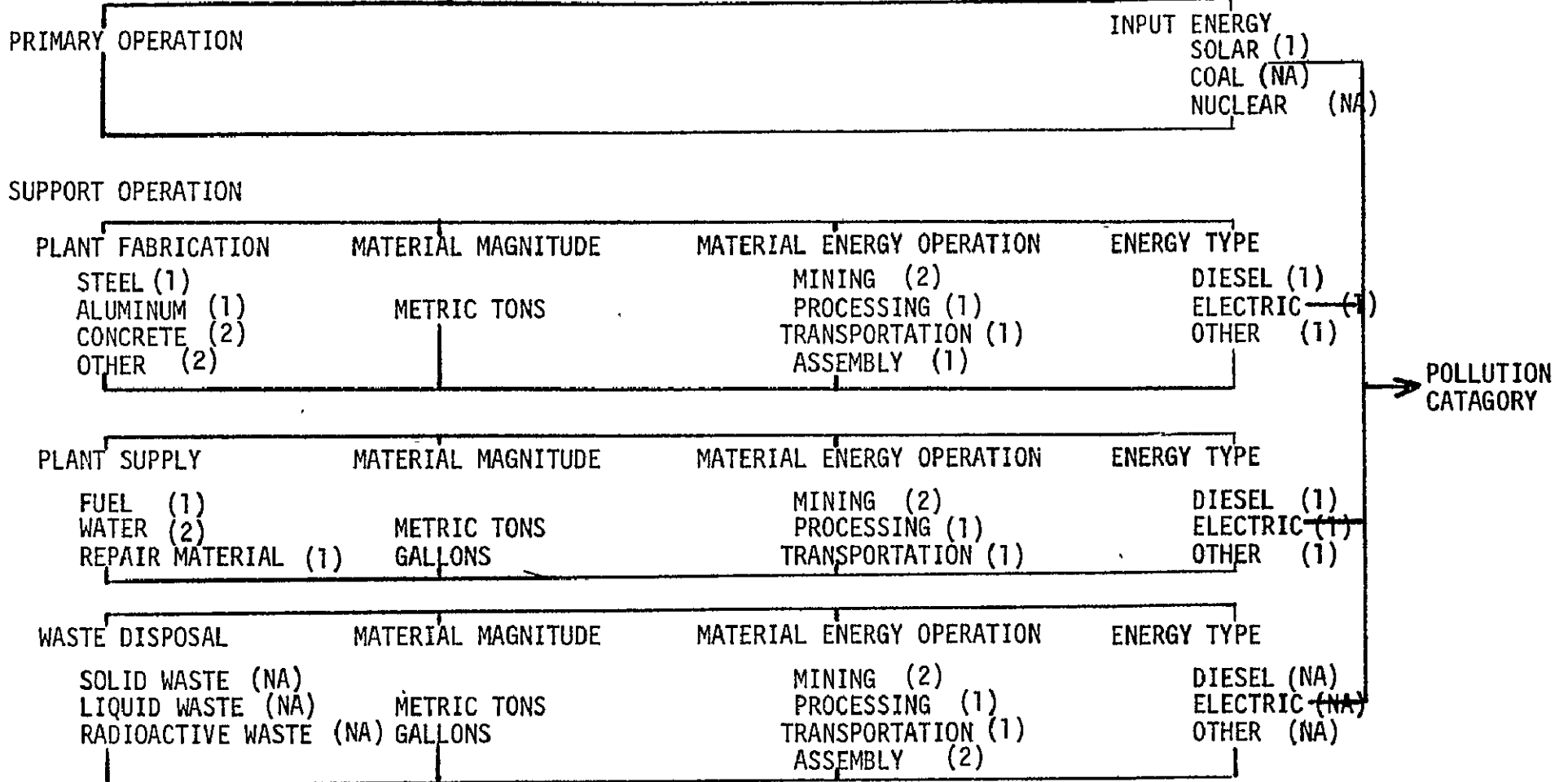


Figure VIII-A-6b.

CHECK PATTERN BREAKDOWN - SOLAR SATELLITE PRIORITIES



WTT-A-15

Figure VIII-A-7a.

SOLAR SATELLITE PRIORITIES -CHECK PATTERN BREAKDOWN (CONT)

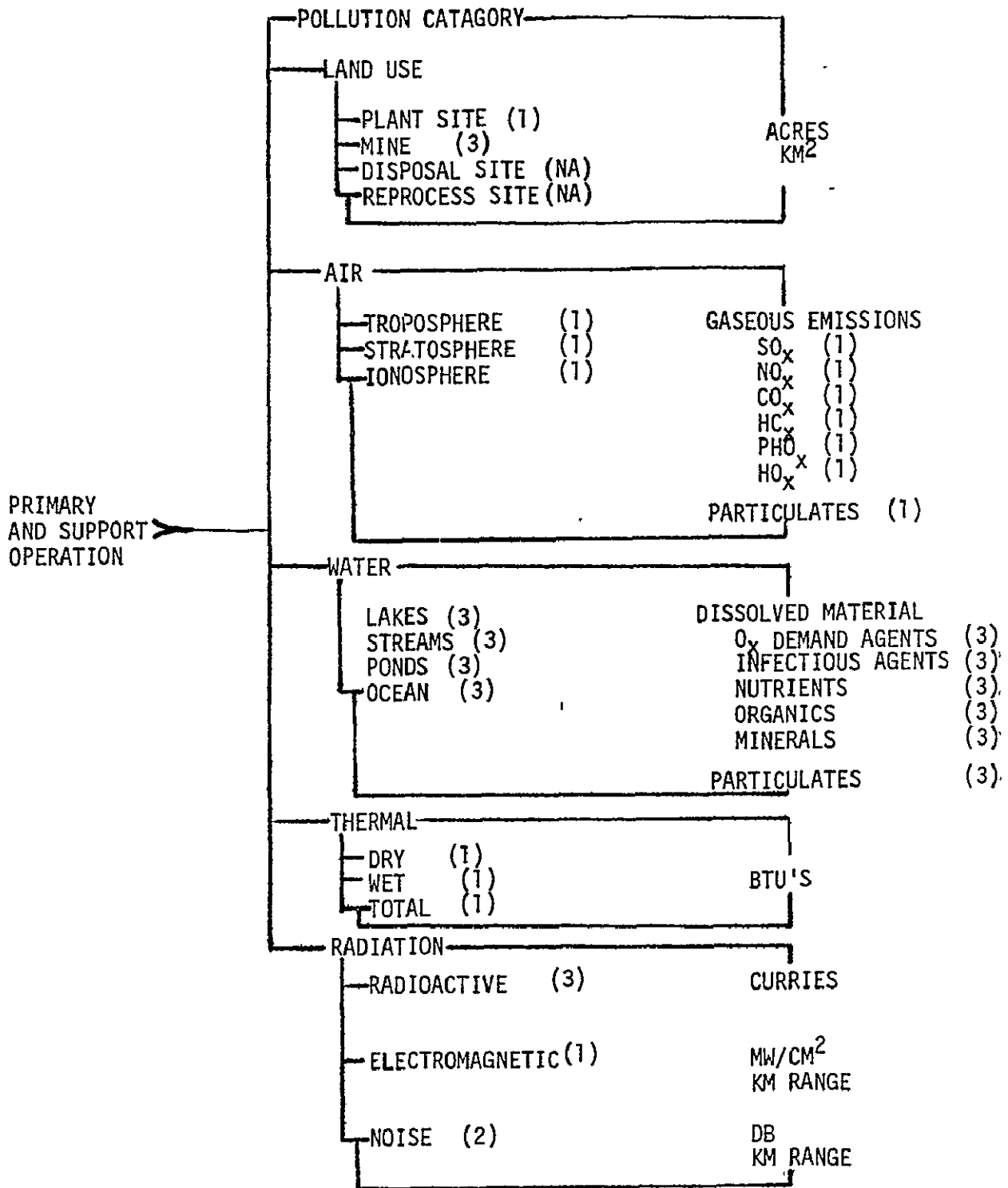


Figure VIII-A-7b.
VIII-A-16

B. ENVIRONMENTAL QUESTIONS

Although the environmental effects of the SPS is categorized as shown in the previous investigation for a direct comparison with coal-fired and nuclear systems, the information required to produce the comparable numbers is gathered in another manner. In order to group the areas of investigated and direct activity in certain areas of expertise the investigation of environmental considerations fell into three areas:

- a. Vehicle Emission
- b. Microwave Beam
- c. Operational Space Environment

For vehicle emissions, both the type of fuel and number of launches can be varied throughout the lifetime of the SPS program. These in turn can change the type and magnitude of the pollutants. Table VIII-B-1 identified the area of investigations required for the determination of environmental impact from launch vehicles.

The situation for microwave beams is somewhat different because the microwave frequency and probable energy level can be fixed, thereby reducing the scope of the investigations. Table VIII-B-2 defines the areas of investigations identified for microwave beam investigations.

An area of investigation peculiar to the SPS, which must be reviewed and defined, is the operational space environment. Because this system operates in an area and environment where other power systems do not operate, namely 36000km above the earth, these environmental problems are not encountered in coal or nuclear systems. All systems have specific areas of environmental concern which are unique to that system. Because of the space environment of the solar collector, this area must be carefully evaluated. Table VIII-B-3 summarizes the specific points of environmental concern which have been identified.

SPS ENVIRONMENTAL SUMMARY

In general, the details of knowledge and the level of concern for these various parameters have been summarized as follows:

TABLE VIII-B-1

VEHICLE EMISSIONS

Troposphere

Type and Magnitude of Pollutants

Type and Magnitude of Impacts

Launch Area Impact

Gas Cloud, Rainout Effects, Etc.

Biomedical Effects

Weather Modification

Meteorological Effects

Ecological Consequences

Stratosphere

Type and Magnitude of Pollutants

Type and Magnitude of Impact

Ozone Depletion

Physical Effect

Biomedical Effect

Weather Modification Assessment

Ionosphere

Type and Magnitude of Pollutants

Type and Magnitude of Impact

"Punch-Out" Effect Assessment

Thermosphere/Magnetosphere

Type and Magnitude of Pollutants

Type and Magnitude of Impact

Disturbances

Surface/Troposphere Interface

Noise

Magnitude

Effects

Seismic

Magnitude

Effects

Vehicle Failure

Effects

TABLE VIII-B-2

MICROWAVE BEAM

Ionospheric/Beam Interaction

Microwave Beam Effects on:

Astronomy

Electronic Systems of:

Satellites

Aircraft

Ground Devices

Radio Communications

Troposphere

Beam Heating

Rectenna Heating

Biological Effects of Microwave Carrier on:

Humans

Animals

Plants

TABLE VIII-B-3

OPERATIONAL SPACE ENVIRONMENT

Ionizing Radiation

- Magnitude Definition
- Biological Effects on Crew
- Equipment Effects
- Dosage and Shielding Assessment

Stray Microwave Radiation at the Satellite

- Scattered
- Reflected
- Parasitic

Magnetosphere Plasma Environment

- Spacecraft Charging
- High Voltage/Plasms Interaction

Meteoroid Environment

- Crew/Habitat Protection
- Equipment and Solar Cell

Space Debris

- SPS and Other Satellites
- Orbital Altitude Effects

(1) Launch Systems

Environmental considerations for the launch systems range from effects on the ground through the exosphere. These effects are mostly the results of the products of combustion of the propellant, and to some degree may be controlled. The following discussion assumes a nominal equilibrium condition of 4700 HLLV launches per year, using an RP-1 fuel with liquid O₂ for the booster.

a. Ground and Tropospheric Effects

Since ground and troposphere effects are localized, they will play a part in the selection of the launch site. Some of these effects will require engineering solutions while others are basic to the concept.

1. Thermal

Each HLLV will burn energy at the rate of 2.3×10^3 G watts; while this lasts for only 168 seconds, it represents a power level greater than all the power stations in the U.S. However, averaged over a year at the nominal launch rate, the equivalent of 25 G watts of power would be continuously released in the troposphere. Heat sources of this magnitude are capable of causing changes in the local weather patterns (reference 1). These changes, while probably not severe, should be considered in site selection.

2. Noise

The amount of noise generated will have an effect on life in the local area, as well as on building structures near the launch site.

3. Run-off of unburnt propellant

Even a small fraction of the HLLV fuel could cause significant local ecological damage if the fuel were not properly contained. This containment should include the unburnt propellant during lift-off.

4. Ground Cloud

Although the ground cloud will probably not contain any toxic compounds, it may contain a considerable amount of particulates swept up from the ground by the exhaust plume.

b. Stratospheric Effects-Ozone Chemistry

Potential launch environmental effects in the stratosphere are the consequence of compounds being emitted which may act as catalysts to the destruction of ozone. Three "families" of catalysts are known to

exist. They are NO_x (NO , NO_2 , or NO_3), HO_x (H , OH , HO_2 , H_2O_2 , or HNO_3), and Cl_x (HCl , Cl , or ClO). Stratospheric mixing ratios of these compounds on the order of a part per billion can be a problem. By scaling the stratospheric deposition rate of the space shuttle to the HLLV, then it can be concluded that a launch frequency of 1 HLLV per year will come to a global equilibrium mixing ratio in about 10 years of 0.1 parts per billion, by volume, (PPBV) of exhaust products. Therefore, 4700 HLLV's per year would produce an equilibrium of 470 PPBV of exhaust products. Thus, the composition of the exhaust products is important.

In order to determine this composition, an RP-1, liquid oxygen fuel was assumed, with a chamber pressure of 4000 psi, an oxygen mass to fuel mass ratio of 2.6, a hydrogen to carbon atom ratio of 1.9423 for the RP-1 fuel, and a combustion temperature of 6900°R. Mr. Sanford Gordon of Lewis Research Center calculated the following combustion products, in a manner similar to that described in reference 2.

<u>Compound</u>	<u>Mole Fraction</u>
CO	0.31
CO ₂	0.17
H	0.020
HCO	0.00007
HO ₂	0.00008
H ₂	0.077
H ₂ O	0.35
H ₂ O ₂	0.00004
O	0.0074
OH	0.050
O ₂	0.013

These products are at the exit plane of the nozzle. They will after burn to a slightly different composition, as shown for the Space Shuttle in references 2 and 3. The main differences will be in the CO and NO_x fractions. As shown in reference 2, essentially all of the CO will after burn to CO_2 . H and OH may also after burn to H_2O , but this calculation has not yet been made. Thus, these compounds may not be significant. However, the NO_x produced by afterburning and plume shock may be significant. Although the amount of NO_x produced in this manner by the Space Shuttle is only about 0.01% to 0.1% of the propellant (ref 4), it could vary significantly for a different configuration. For example,

to vary the initial expanded plume boundary temperature from 1130°K to 2000°K, causes NO_x to increase by a factor of 35. The amount of NO_x produced by afterburning at higher altitudes is a sensitive function of the shock waves produced by the launch vehicle and would have to be studied in detail.

The effects of the major exhaust product, H₂O, is uncertain. An increase in H₂O will lead to an increase in HO_x which is capable of catalytically destroying ozone. However, an increase in HO_x would lead to a decrease in NO_x another catalytical destroyer of ozone. Some unpublished results from the University of Michigan predict a 4% to 5% decrease in ozone from doubling the concentration of H₂O. Thus, although the direction of the net effect of H₂O has not yet been fully established, it should be small.

Should the OH and H not after-burn, it will, in a few days, still become H₂O in the stratosphere. However, in these few days, local effects may result. These local effects could consist of a "corridor" where OH destroys a significant amount of O₃ before going to H₂O or reducing NO₂. This would have to be studied in further detail.

Impurities such as N₂ and S can probably be controlled so that they, within themselves, would not cause much problem. For example, the N₂ impurities in LO₂ used in the Space Shuttle is less than 0.7%, and only a small fraction of this will form NO_x.

Thus, the following table can be constructed to give the contributions to the stratosphere for important minor compounds. This table assumes an equilibrium condition resulting from a launch rate of 4700 HLLV's/year.

Compound	Stratospheric Mixing Ratio PPBV (parts per billion, volume)	Max SPS Contribution, PPBV (see discussion)
H ₂ O	3,000	165
CH ₄	1,000	0
H ₂	500	36
CO	100	0
NO _x	20	<1?
HO _x	1 to 10	.05 to .5*
Cl _x	1	0
CO ₂	320,000	226

*HO_x from H₂O-does not include possible "corridor" effect.

Note that there is not a significantly large percentage increase in any of the minor compounds, although the percentages are approaching these levels. The level of NO_x is probably the most significant, and the most uncertain. More work is needed in this area.

In summary, although stratospheric chemistry may be altered slightly by a large launch rate of HLLV's, the effects should be minimal as long as careful attention is given to the choice of propellant, propellant combustion conditions, and launch vehicle geometry.

c. Ionosphere

An unpredicted effect of releasing large quantities of H_2O and H_2 in the F-region of the ionosphere was measured on May 14, 1973, with the launch of the Skylab Workshop. "The effect was a large and rapid decrease in the total number of ionospheric electrons within a distance of 1000 kilometers of the burning engines of the Saturn V launch vehicle." (reference 5). This hole lasted for several hours. The same effect could be expected from the second stage of the HLLV if this stage were ignited between 200km and 400km; thus, a large launch frequency could cause a significant reduction in ionospheric electrons. This would effect short wave communications and have the positive effect of giving astronomers a new window, as suggested in reference 6. However, the effect will be reduced by avoiding ignition in this region. However, there is a sufficient ion density at the 500 km altitude that this effect should be studied further.

d. Magnetosphere and Space

1. The effects of releasing propellants in the magnetosphere from the orbital transfer vehicle, could possibly cause magnetic sub-storms. The propellant gases would slowly be ionized and become trapped in the Earth's magnetic field. Although this effect is probably insignificant, it should be looked at closer.

2. Space Debris (litter)

The indiscriminate releasing of objects in Earth orbit would lead to a major problem for the solar power station, as well as any other large structures in Earth orbit. For example, if each of the 4700 launches per year left only one object in some indiscriminate orbit, then every 5 months we would inject the equivalent number of objects known to be in low Earth orbit in 1970. This 1970 number leads to about 1 impact per year on a 10 km power station at 200 km, and to 50 impacts per year at 800 km. (reference 7). Thus, not only is it important not to release new objects in space, some old ones will probably have to be retrieved.

Proper management of space debris may solve this problem. For example, objects can be disposed of by putting them into orbits with an apogee less than the altitude of the construction orbit for the power station. Or, selected orbits can be reserved for SPS construction.

(2) Entry Systems

Entry systems are expected to raise two environmental issues: 1. sonic boom and 2. NO_x production in the stratosphere. Both of these issues will require further investigation.

The effects of sonic boom can be minimized by design factors, the location of the recovery site, and changes in the entry path. These considerations should influence the location of the recovery site, so that the sonic boom will occur over unpopulated areas.

A significant amount of NO_x is produced by the shock waves resulting from entry of a spacecraft into the Earth's atmosphere. However, this NO_x is deposited at a sufficiently high altitude that the effect on ozone is reduced. Before an accurate evaluation can be made, more work is required.

If air breathing engines are used to land the spacecraft, NO_x will also be produced. The amount of NO_x will be of the order of, or greater than, the amount deposited by a large passenger jet. However, since most of the fuel is expected to be burned in the troposphere, the net effect of these engines on ozone will probably be less than the passenger jet.

(3) Power Transfer System

The power transfer system consists of the SPS itself, the microwave beam, and the rectenna. Of these, the microwave beam is probably the most significant.

a. Microwave Effects

From previous studies, narrow limits have been imposed on the microwave frequencies and power densities to be used. For this reason, it becomes important to the SPS project to have a thorough understanding of the environmental effects of these microwaves. There are two areas which will require a major amount of work: (1) long and short term effects of microwaves on life. (2) global and local effects of ionospheric heating.

1. Biologic Effects

The effects of microwaves on life may well be the most important environmental questions to be studied. Aside from an abnormal

excursion of the microwave beam, life will routinely be exposed to microwaves in two ways: (1) all life forms that live around the perimeter of the rectenna, receiving a microwave flux that represents a small fraction of the maximum beam intensity (less than 1 mw/cm²). (2) airborne life forms (i.e., birds, bats and insects) which fly through the beam and receive the full beam intensity. Although the experimental data in reference 8 does have some uncertainties in the microwaves flux, the data should be taken as indicative of the types of problems that may be encountered. For example, the data suggest that the survival of some species may be directly effected at maximum beam intensity, while other species may show only slight short-term effects. Therefore, there is the possibility that certain species of airborne life may be effected in the time required to fly across the microwave beam. Although there may be a natural avoidance of microwaves by birds, as exemplified by using microwaves to clear runways of birds, there may also be a natural attraction, such as heat during colder climatic conditions. These possibilities must be looked at in detail.

The effects of microwaves may extend below thermogenic intensities (i.e., below 10 mw/cm²), ranging from decreased weight, slower reflexes, decreased birth rate, and increased abnormal offspring to changes in the rate of transport of K⁺ and Na⁺ ions across membranes, decreased reproductive functions, and changes in immunobiologic resistance (at intensities of 1mw/cm² or less). In addition, there is some controversy regarding a decrease in eye lens translucency of workmen routinely exposed to microwaves. Some authors report no difference between workmen exposed and those not exposed, while others report an increase in the lens aging process. The resolution may be that a definite threshold is required for producing lens opacity; however, it has only been consistently produced in the rabbit. This data contains uncertainties, and at times is contradictory. In order to avoid controversy, it is important that exact safe levels be established. Such work is already being done by the Food and Drug Administration, Bureau of Radiological Health, and the University of Washington. This work should be followed closely, as well as new studies started.

2. Ionospheric Heating - see section IV-A-2

Although only a small fraction of the microwave beam would be absorbed by the ionosphere, the beam could cause measurable changes in the temperature. This would, in turn, lead to changes in the ionosphere chemistry, effecting the ion density, and short wave communications. Although these effects would probably be of insignificant consequence they should be looked at closer. Most previous experiments at ionosphere modification have been at RF frequencies and power densities different than proposed for the SPS (ref. 9); therefore more studies would be required to determine the exact effects on the ionosphere.

3. Radio Interference - see section IV-C-2

Radio noise produced by the microwave beam may cause interference to users of frequencies near that of the beam. These could include radio astronomers, and certain radar and communication frequencies. The extent of that interference will depend on the microwave frequency used as well as the size of the band that can be set aside for energy transmission.

b. SPS Effects

1. Magnetosphere

Each SPS will require a significant amount of propellant in order to maintain attitude and position in orbit. Although this amount will be less than that of the orbital transfer vehicle, it will be consistently released, and should be looked at farther.

2. Reflected and Emitted Light

In addition to microwaves, the SPS will reflect sunlight, and emit thermal, IR, radiation which could interfere with astronomical observations. From Earth, the reflected sunlight will cause an SPS to normally appear as a stellar object, about as bright as the planet Venus. However, if the SPS is allowed to drift a few degrees from its solar attitude, as is expected in order to conserve propellant, then there will be times that light will be specularly reflected to areas on Earth. This would be observed from these areas as a large increase in brightness, to that of a full moon, or brighter. This brightness would last for several minutes to about an hour. Both the intensity and duration of brightness would depend on the "flatness" of the solar cells and mirror surfaces.

c. Rectenna Site

A 10 G watt solar power station can expect to dump about 0.5 G watt of heat into the atmosphere at the 5GW rectenna site. Although this is less than that of a conventional power station, or that of a large city, it should be studied. It has been shown that minor local changes in meteorology take place as a result of heat islands of larger magnitudes. If the effect exist at this lower level, a complete understanding can help to minimize it, or produce desirable results.

(4) Summary of SPS Environmental Effects

The following outline summarizes the SPS environmental effects. Each effect is followed by a "priority number" (1, 2 or 3) to designate its relative level of importance.

I. Launch Systems

A. Ground and Tropospheric Effects

1. Thermal, Weather Modification (2)
2. Noise (3)
3. Run-off of Unburnt Propellant (3)
4. Ground Cloud (3)

B. Stratospheric Effects-Ozone Chemistry

1. NO_x Production (1)
2. H_2O and other emissions (2)

C. Ionosphere - H_2 & H_2O emission (3)

D. Magnetosphere and Space

1. Magnetic Disturbances (3)
2. Space Debris (1)

II. Entry Systems

A. NO_x Production (2)

B. Sonic Boom (1)

III. Power Transfer System

A. Microwave Beam

1. Biologic Effects (1)
2. Ionospheric Heating (1)
3. Radio Interference (2)

B. SPS Effects

1. Magnetosphere Disturbances (3)
2. Reflected and Emitted Light (3)

C. Rectenna Site-Weather Modification (3)

REFERENCES

1. Hanna, Steven R. and Franklin A. Giffond, "Meteorological Effects of Energy Dissipation at Large Power Parks", Bulletin American Meteorological Society, Vol 56, No. 10, Oct 1975, p 1069.
2. Huff, Vearl N., Anthony Fortini, and Sanford Gordon, "Theoretical Performance of JP-4 Fuel and Liquid Oxygen as a Rocket Propellant". NACA RME56D23, September 7, 1956.
3. Stedman, D.H., R. S. Stolarski, R. J. Cicerone, and J. K. Williams, "Studies on Space Shuttle Rocket Exhaust Effluent Chemistry in the Atmosphere", NASA CR-129042, March 1974.
4. Pergament, Harold S. and Roger D. Thorpe, "NO_x Deposited in the Stratosphere by the Space Shuttle", NASA CR-132715, July 1975.
5. Mendillo, Michael, Gerald S. Hawkins, John A. Klobuchar, "A Large-Scale Hole in the Ionosphere Caused by the Launch of Skylab", Science, Vol. 187, pp 343-345, January 31, 1975.
6. Papagiannis, Michael D., Michael Mendillo "Low Frequency Radio Astronomy Through an Artificially Created Ionospheric Window", Nature, Vol. 255, p 42-43, May 1, 1975.
7. McCarter, James W., "Probability of Satellite Collision", NASA TMX-64671, June 8, 1972.
8. Biologic Effects and Health Hazards of Microwave Radiation, Proceedings of an International Symposium, Warsaw, October 15-18, 1973, Polish Medical Publishers, Warsaw, 1974.
9. Non-linear Effects in Electromagnetic Wave Propagation, AGARD Conference Proceedings No. 138, November 12-15, 1973.
10. Glaser, Peter E., "The Satellite Solar Power Station", presented at the Conference on Space Manufacturing Facilities, Princeton University, May 7-9, 1975.

C. Comparisons with Conventional Systems

It is essential in a complex society not only to evaluate the environmental impact of the direct operation of the various types of power plants, but to define the pollution generated from sources needed to build, supply and remove waste material from the power plant for its life cycle. In order to perform this evaluation, the typical amounts of material needed for the plant fabrication must be identified; the types and amounts of energy needed to extract and process the material must be known; and the amount of transport mileage to the plant site and the transportation means is required. With this information, the amount of energy required for a given increment of electrical power generation can then be summed. The pollution associated with this identified type and magnitude of energy can be defined. Adding to this information, the estimates of electrical demand growth through the years can produce a energy and materials use scenario for any basic type of electrical power generation system whether it is fossil fuel, nuclear or solar powered. As part of the SPS study, a computer program for this energy and resources comparison is being developed. Once the magnitude of the pollutants are identified, the effects of such pollution can be better defined.

Table VIII-C-1 is a brief summary of some of the pollution estimated produced from three different type of plants of equal 10 GW electrical output size. This table is a first approximation of the identified pollutants. Many assumptions were made such as average sulfur content of coal, transport distances, and types of transport, etc. These assumptions attempt to approach U. S. averages for the various factors. The factors listed are those for which direct comparisons on magnitudes of pollution can be defined. At this time, no attempt has been made to identify the difference in the effects of these pollutant levels. All values listed are Level I category only.

ENVIRONMENTAL COMPARISON OF 10 GW
POWER PLANT OPERATIONS

	NUCLEAR	COAL	SPS
PRIMARY FUEL	112 MT/YR	42×10^6 MT/YR	3.49×10^6 MT/LAUNCH YEAR ONLY)
WASTE	330 MT/YR	8×10^6 MT/YR ASH 3.6×10^6 MT/YR SLUDGE ⁽²⁾	
AIRBORNE EMISSIONS			
SO ₂		1.5×10^6 MT/YR ⁽¹⁾ $.3 \times 10^6$ MT/YR ⁽²⁾	
NO _x		$.6 \times 10^6$ MT/YR ⁽¹⁾ $.3 \times 10^6$ MT/YR ⁽²⁾	1800 MT (LAUNCH YEAR ONLY)
PARTICULATE		$.8 \times 10^6$ MT/YR ⁽³⁾	
THERMAL LOSS TOTAL	770×10^{12} BTU/YR	700×10^{12} BTU/YR	102×10^{12} BTU (LAUNCH YEAR ONLY) 15×10^{12} BTU/YR (RECTENNA)
WATER EVAPORATED	96.5×10^6 MT/YR	$.96 \times 10^6$ MT/YR	
LAND USE FIXED	40-50 KM ²	3.6 KM ²	64 KM ²
30 YEARS	3.9 KM ²	900 KM ²	200 KM ²

- (1) NO CONTROL
(2) CONTROL (SO₂ OR NO_x)
(3) PRESENT CONTROLS

Table VIII-C-1

IX. Manufacturing Capacity, Natural Resources, Transportation and Energy Considerations

The purpose of this section is to show how critical resources and industrial capacity might be identified, and during the early design period to assess the impact of varying designs and resources and industrial capacity.

A. Requirements

The SPS can be broken down into a number of systems. Each of these systems can be further broken down into a series of subsystems, which can in turn be further broken down to components. The mass of materials making up these components can then be determined. In the early design phases, there are numerous alternates in components and component materials. The first task is to identify these alternate approaches. Figure IXA-1 shows a breakdown of the transmission/receiving system based upon Raytheon's "Microwave Power Transmission Studies" (draft) of December 1975. This study contains numerous alternates to components which have a marked effect on the materials to be used, and the amount of each material. In Figure IXA-1, the most probable configuration has been indicated by solid boxes. Alternates have been indicated by dashed boxes. Designs which have been considered, but appear unlikely to be used are indicated by crossed-out boxes. The nominal design is arbitrarily defined as the solid boxes, and the dashed boxes as design perturbations. The individual pieces which make up the component described by a box can be identified by material, from the Raytheon report.

This information can now be arranged in a matrix in which the rows are component parts and the columns are basic materials required for a SPS. For each box the columns are summed to give the total of each material and the gross weight. A second matrix in which the rows represent the summed outputs above gives the total of each type material and the gross weight for one system configuration. Repeating the process, over all systems give a material summary of the total SPS and is shown in Part 1 of Appendix IX(A). Vehicles and fuel requirements are estimated from the gross weights above, and the results are estimated in Part 2 of the Appendix. Proposed launching assembly schemes are shown in Figure IXA-2.

The alternate boxes can be considered, and alternate matrices constructed. For each column, i. e., variation in material amounts can be established by substituting alternates into the summary and hence, determining ranges of amounts of various materials. No attempt has been made at this point to make range of amounts of materials estimates.

B. Manufacturing Capacity

The following considerations will influence material choices or the need for finding alternate materials:

- a. Estimated total usage rates for the material.
- b. Estimated total amounts of material available.
- c. Estimated cost changes with time.
- d. Estimated cost changes with production rates.
- e. Production facilities capacities for finished product.
- f. Construction of new facilities.
- g. Strategic impact (mostly from abroad).
- h. Energy requirements for fabrication (mine to pad).

To achieve a materials breakdown for this study, detailed materials data from Raytheon, Boeing and in-house studies were used to compile typical material requirements. The data contained in reference IX-1 is used to establish critical materials or indicated manufacturing capacity requirements. Part 4, Section 1 of Appendix IX-(A) summarizes for the materials used in the construction of the SPS, the data required to establish critical materials.

C. Natural Resourcesⁱ

In Part 4, Section 1 of Appendix IX-(A) are shown the estimates of national and world-wide demand for various resources. In Part 4, Section 3 of Appendix IX-(A), the impact of the SPS on these national and world-wide resources and demands are estimated. In general, there are no resources which are critical, but there will be additional manufacturing capacity required for argon, arsenic, gallium, hydrogen, oxygen and silicon.

In Part 4, Section 2 of Appendix IX-(A), an estimate of the energy payback for the major materials of the SPS has been made. Approximately .8 years are required to produce the electrical energy used to manufacture the raw SPS materials. The aluminum requirement for one 10 GW SPS has been estimated at 1.08 million metric tons. About 50 percent of this requirement is for the rectenna. In reference IX-1, the forecast for aluminum demand for cans in the U. S. has been estimated at between 1.4 and 5.0 million short tons per year. The base forecast is 2.3 million tons/year showing that the SPS demand is about the same as the beverage industry. The total average world demand was estimated at 83.2 million tons/year. The total world reserves are estimated at 1.2 billion tons. If the current demand growth rate of about 6 percent continues, the total demand will exceed known reserves of aluminum around 2010 to 2015. It would appear that an alternate material for rectenna construction should be expected to evolve since an overall shortage of aluminum should result from heavy world demands.

D. Surface Transportation

In the preceding section on SPS materials, the transport of material from the launch site to geosynchronous orbit was considered in the materials requirements for the SPS; to complete the picture the logistics of getting the material to the launch site needs to be considered.

To develop a plan for ground transportation, it is necessary to start with raw materials and trace the entire transportation of materials in the manufacturing sequence to the launch site. No accurate detailed attempt is made to do this at this time. However, rough assumptions are made to obtain an insight into the approximate ground transportation requirements in support of SPS manufacturing.

The cost of transportation of raw materials is reflected in the cost of these commodities. For the SPS, it is assumed that on the average, materials will pass through two contractors at different locations. From the final contractor, the material will pass to the launch site. Figure IXD-1 shows typical flow of material from raw material source to launch site using typical transport means. As the logistics are more closely studied, the percentages above can be refined.

The costs of these various means of transportation are well known both in terms of dollars and energy expenditures, and flow rates can easily be established once construction schedules have been established. This, in turn, will establish the warehousing and handling facilities at intermediate points.

As has been shown in the program requirements section of this report, the construction rate could typically grow from one-half an SPS per year to seven SPS's per year in a 30-year period. The total transport requirement based upon the scenario of figure III-2 would grow from 8.6×10^7 metric ton km/year to around 1.2×10^{10} metric ton km/year. Warehouse and transport facilities would be expected to increase by up to a factor of fifteen.

Some information is available to check the realism of our model of ground transportation requirements for the SPS. In reference IX-2, it has been noted that correlation between intercity freight movements and the commodity component of the gross national product is very close. Both items increased at an annual rate of 3 percent from 1979 to 1958, and correlation was almost perfect between the two series on a year-to-year basis. The services component of the gross national product was about 38 percent of the GND in 1960 and is expected to increase to about 40 percent in the year 2000. Table IXD-1 shows the projected metric ton kilometer for goods and construction for the year 2000.

Table IXD-1

Metric ton km of Intercity Freight Vs. Dollars total GNP and Goods and Construction Component of GNP for Year 2000

<u>Transport Medium</u>		<u>Total GNP</u>	<u>Goods & Const GNP Comp</u>
Rail	Lo	.92	1.53
	Med	1.24	2.08
	Hi	1.50	2.51
Truck	Lo	1.20	2.01
	Med	1.30	2.18
	Hi	1.50	2.51
Inland Water Ways	Lo	.60	1.00
	Med	.70	1.17
	Hi	.80	1.34
Oil Pipe Lines	Lo	.654	1.09
	Med	.852	1.42
	Hi	1.00	1.68
*TOTAL	Lo	3.52	5.87
	Med	4.12	6.57
	Hi	4.62	7.71

*Air Tonnage Negligible

Table IXD-2 shows the estimated intercity freight transportation for the year 2000 from reference IX-2.

Table IXD-2

Intercity Freight Transportation Projection for Year 2000

<u>Transport Medium</u>	<u>Billion Metric Ton KM</u>	
Rail	Lo	1266
	Med	2672
	Hi	5355
Truck	Lo	1634
	Med	2803
	Hi	5355
Inland Water Ways	Lo	817
	Med	1510
	Hi	2855

<u>Transport Medium</u>	<u>Billion Metric Ton KM</u>	
Oil Pipe Lines	Lo	886
	Med	1832
	Hi	2855
Air	Lo	3.85
	Med	10.57
	Hi	42.45
TOTAL	Lo	4768
	Med	8839
	Hi	16424

Using table IXD-1 and estimating 1000 to 2000 dollars per KW for the SPS would indicate that for a 10 GE plant, that 3.52×10^{10} to 4.62×10^{10} metric ton KM would be expected to be expended in the construction of an SPS. Figure IXD-1 would yield about 2.25×10^{10} metric ton kilometers indicating that this model is reasonable. This amount less than 1 percent of the total projected for miles for the year 2000 for a single satellite. For the maximum rate of construction (7 per year) it would barely exceed two percent of the lowest projection of total ton miles for the year 2000.

E. Energy Payback

A preliminary study was conducted to assess the energy required for the implementation of an SPS and the time required for the SPS to generate an equivalent amount of energy. Table IX-2 lists the energy intensive materials required for the implementation of an SPS of "nominal" weight and the energy involved in its production. 6.7×10^{10} KW hrs are required in the processing of the material for an SPS. Approximately 80 percent of the total is involved in the production of the necessary propellants and aluminum for the rectenna. Previous comments regarding the use of aluminum for the support structure of the rectenna should be noted.

Table IX-2
Energy Payback 10 GW SPS

ITEM	QUANTITY, Kg	TOTAL ENERGY TO PRODUCE KWH
Rocket Propellant and Gases	3.42×10^{10}	2.78×10^{10}
Rectenna	1.12×10^9	2.70×10^{10}
Other SPS Materials	8.64×10^8	1.20×10^{10}
	Total	6.7×10^{10}

SPS Electrical Energy Output = 8.05×10^{10} KWH/YR

$$\frac{6.7 \times 10^{10} \text{ KWH}}{8.05 \times 10^{10} \text{ KWH/YR}} = 0.83 \text{ Year}$$

The SPS produces 8.1×10^{10} KW/HRS per year; consequently, the 6.7×10^{10} KW/HRS used in implementation of the SPS would be generated or "paid back" in less than ten months. This figure compares favorably with estimates for conventional ground systems which range from 0.2 to 1.0 year for payback.

REFERENCES

- IX-1 Staff, Bureau of Mines, Bureau of Mines Bulletin 650, 1970 Edition, Mineral Facts and Problems, U. S. Government Printing Office, 1970
- IX-2 Hans H. Landsberg, Leonard L. Fischman, and Joseph L. Fisher; Resources in America's Future Patterns of Requirements and Availability, John Hopkins Press, 1963

TABLES

- IXD-1 Metric Ton KM of Intercity Freight Vs. Dollars
Total GNP and Goods and Construction Component of
GNP for the Year 2000
- IXD-2 Intercity Freight Transportation Projection for Year 2000

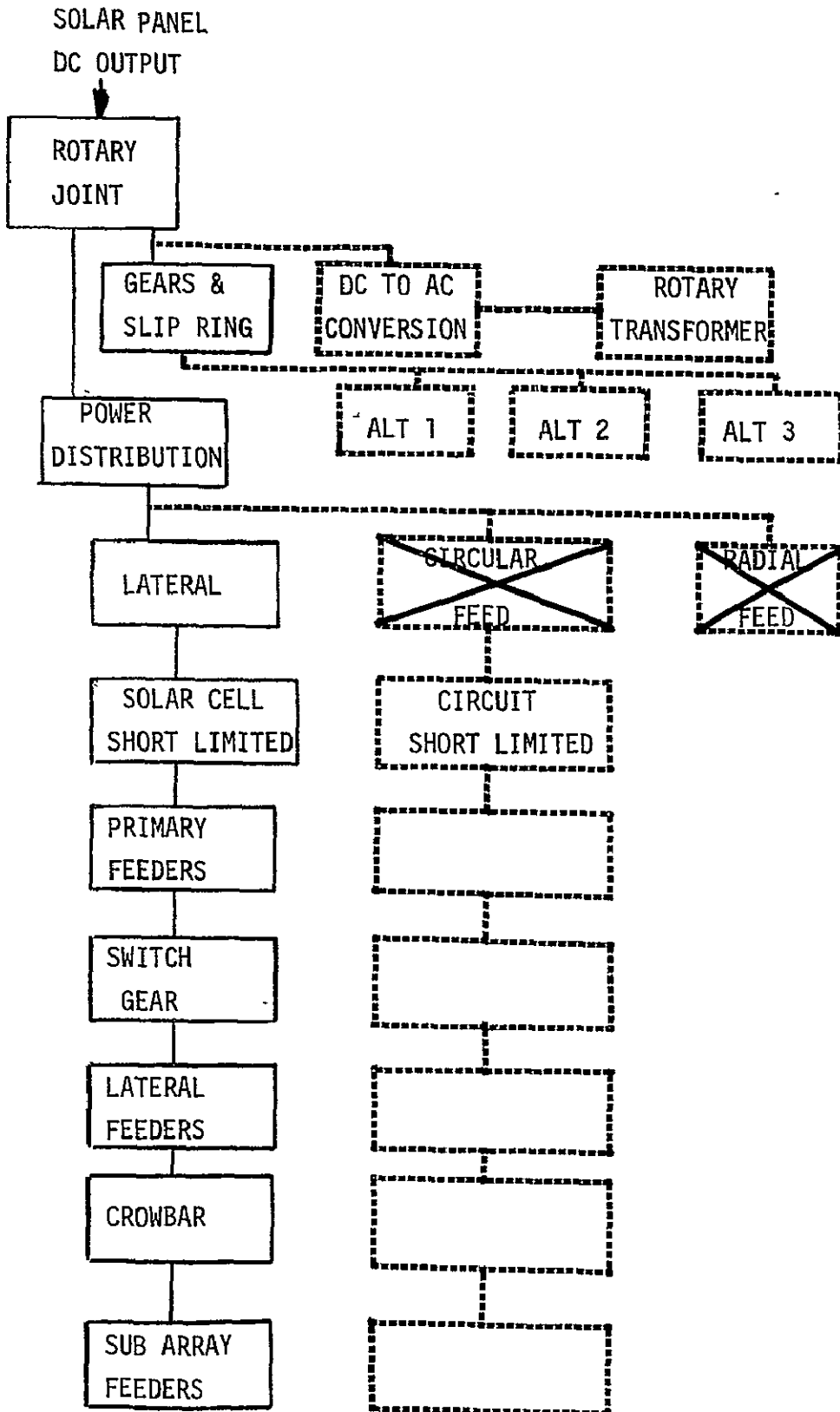


Figure 1XA-1
 CONFIGURATION & CONFIGURATION
 ALTERNATIVES FOR MICROWAVE
 POWER TRANSMISSION SYSTEM

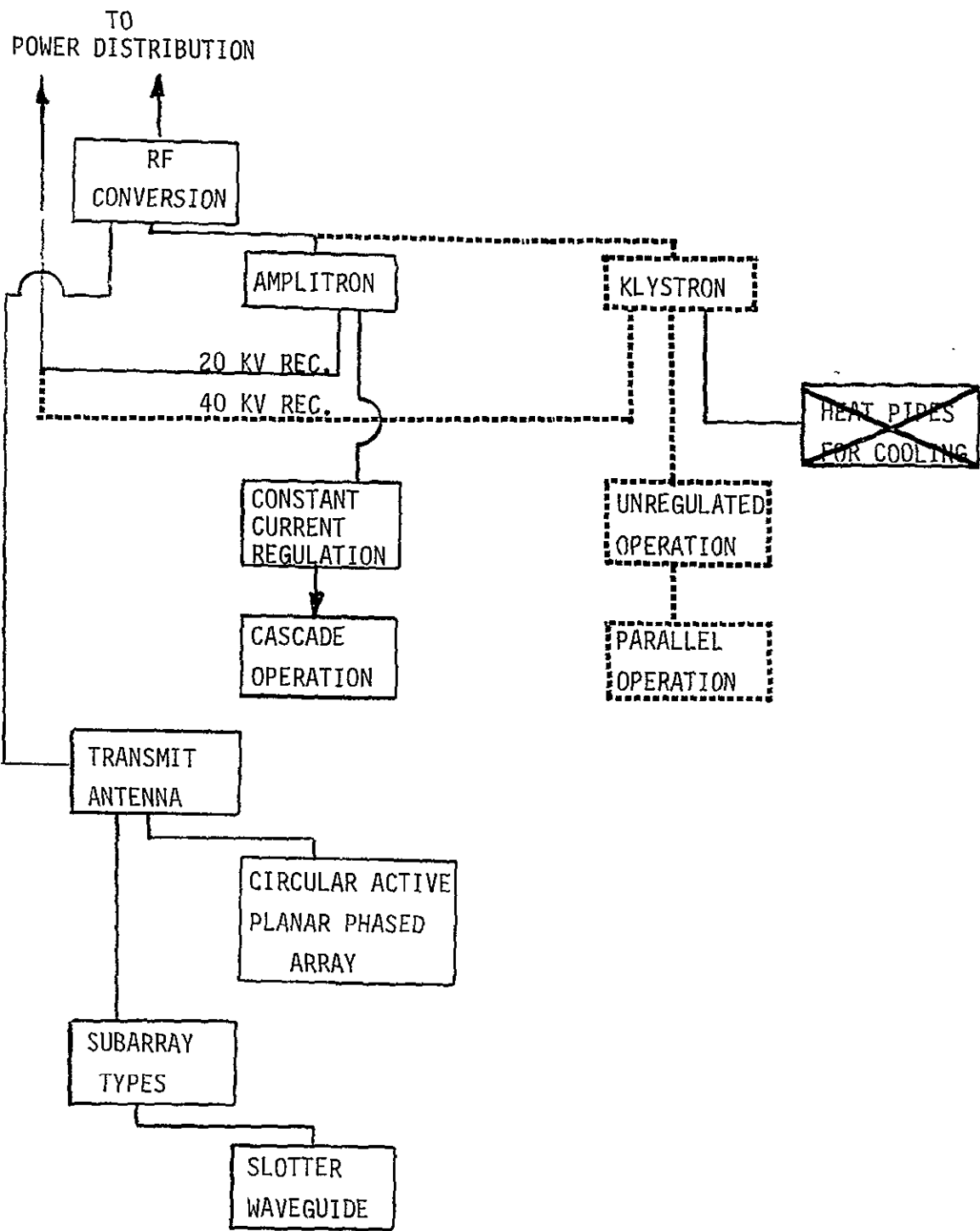


Figure 1XA-1 (CONT)
 CONFIGURATION & CONFIGURATION
 ALTERNATIVES FOR MICROWAVE
 POWER TRANSMISSION SYSTEM

TO
SUBARRAY TYPES

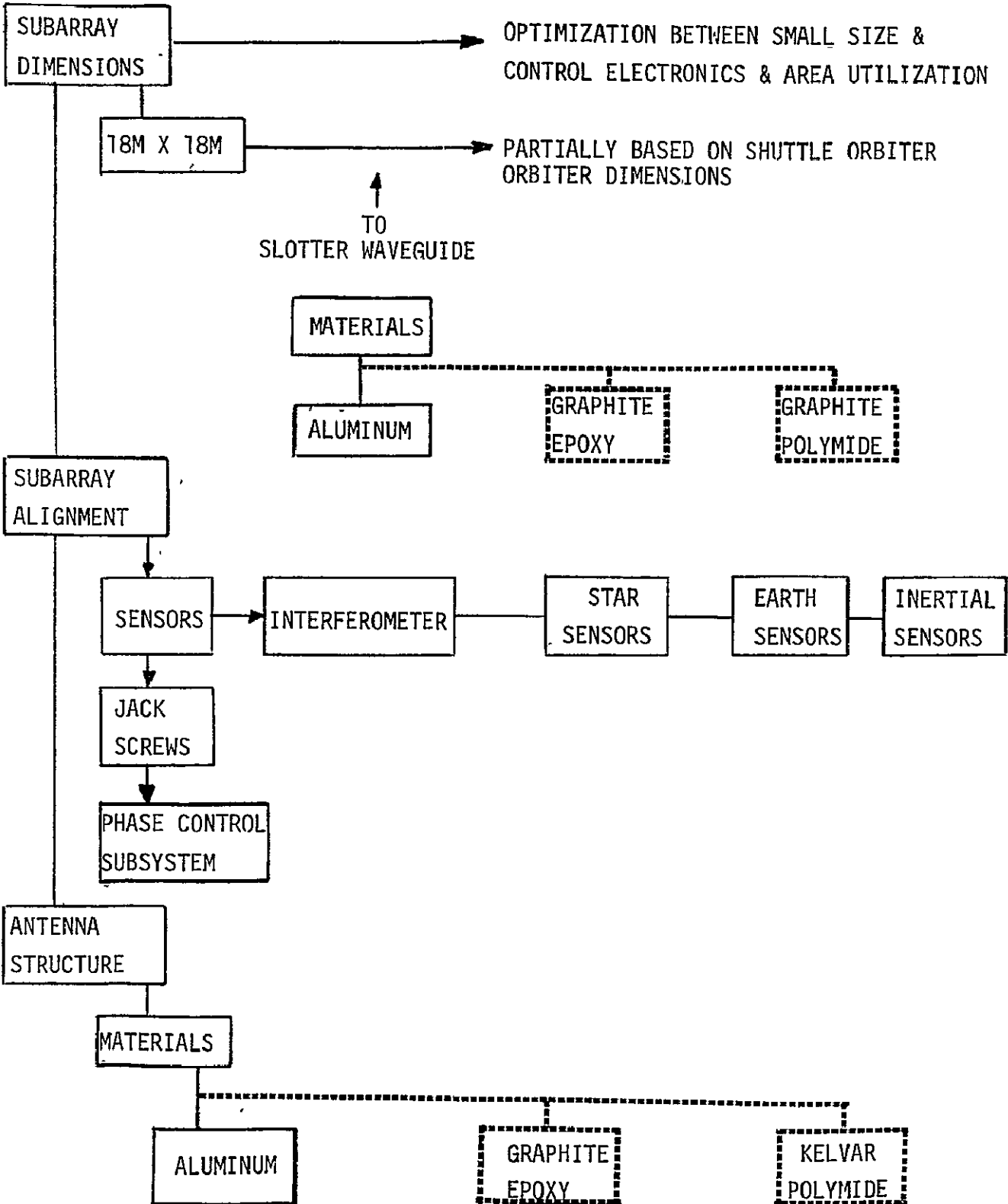


Figure 1XA-1 (CONT)
CONFIGURATION & CONFIGURATION
ALTERNATIVES FOR MICROWAVE
POWER TRANSMISSION SYSTEM

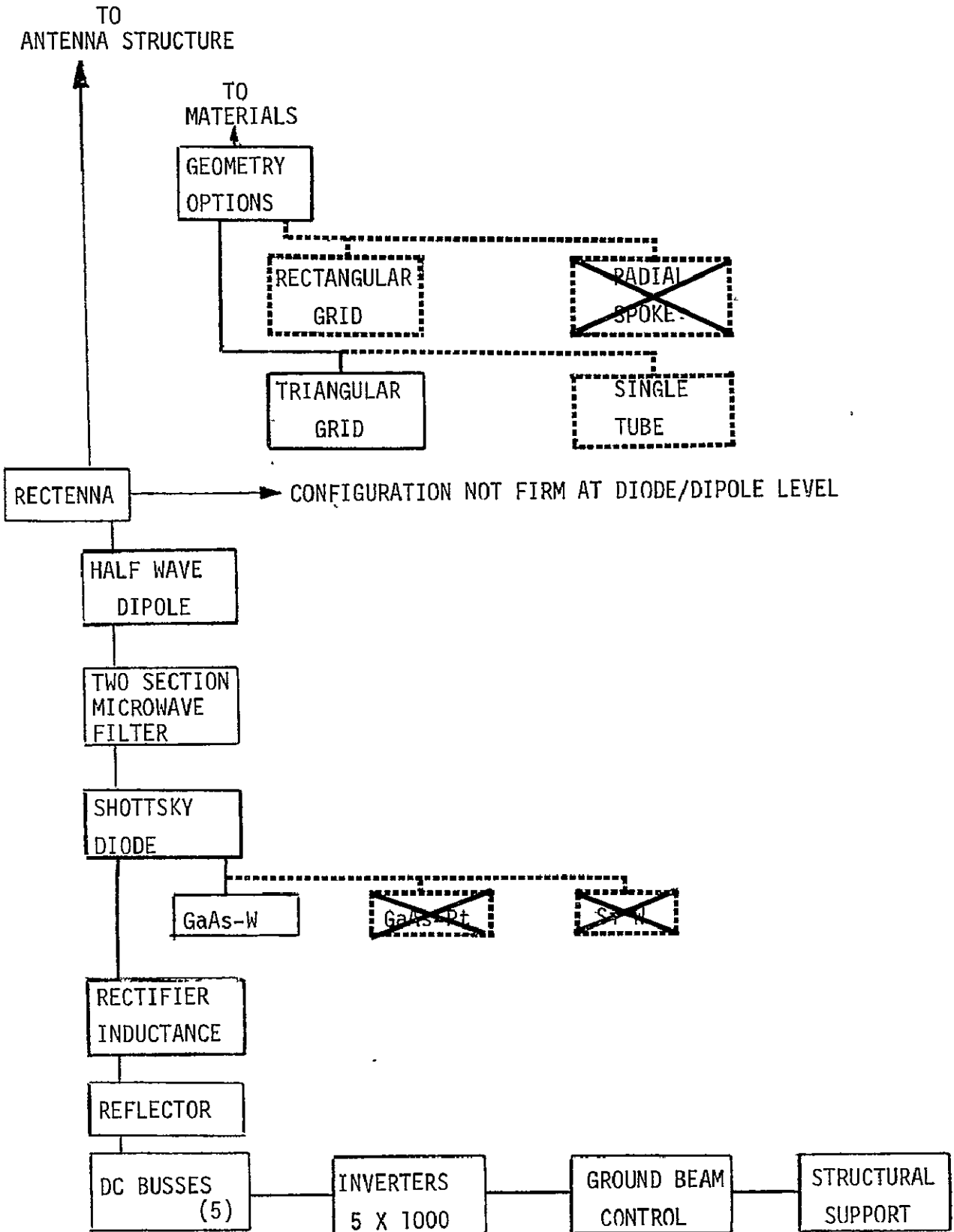


Figure IXA-1 (CONT)
 CONFIGURATION & CONFIGURATION
 ALTERNATIVES FOR MICROWAVE
 POWER TRANSMISSION SYSTEM

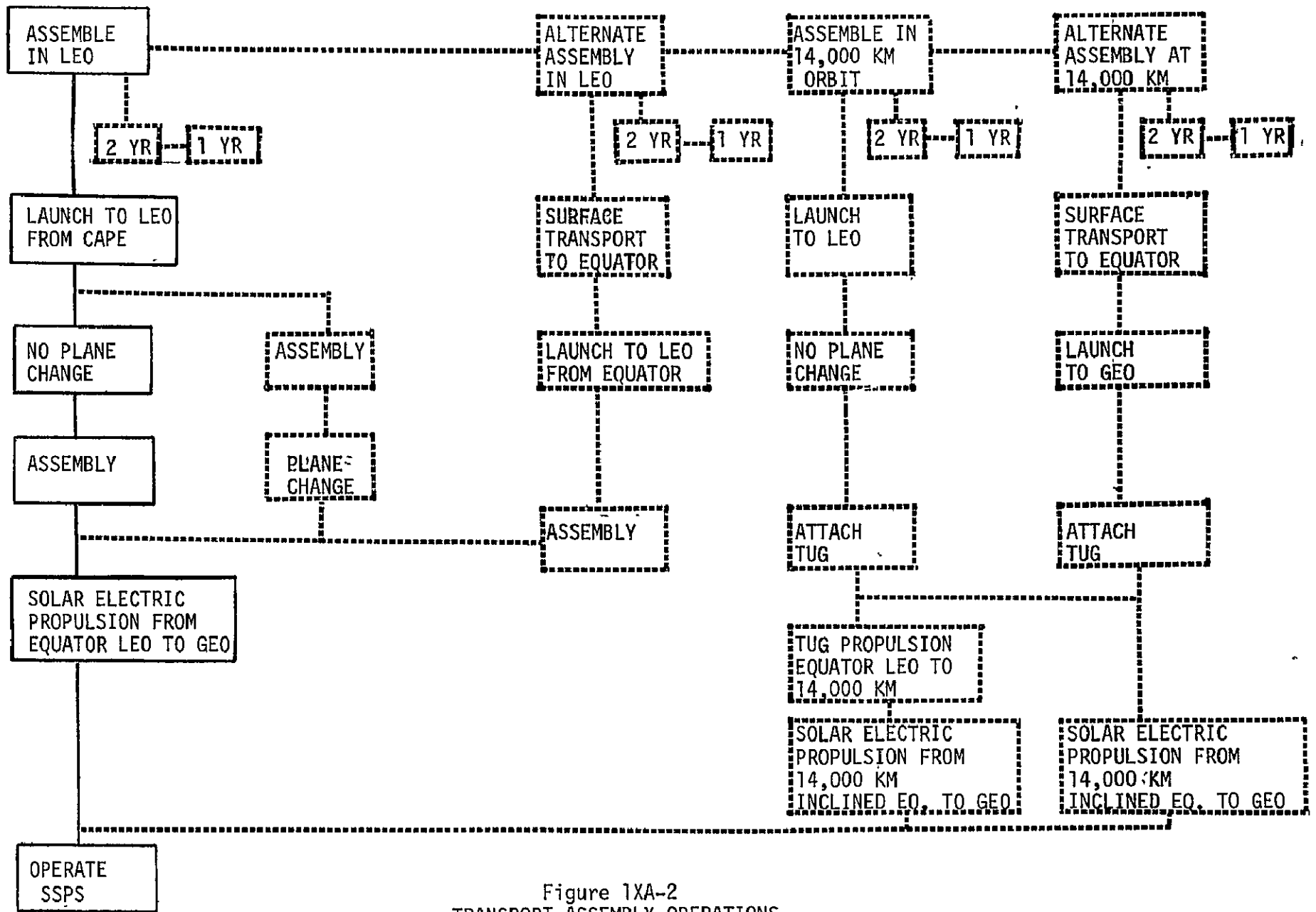


Figure IXA-2
TRANSPORT ASSEMBLY OPERATIONS

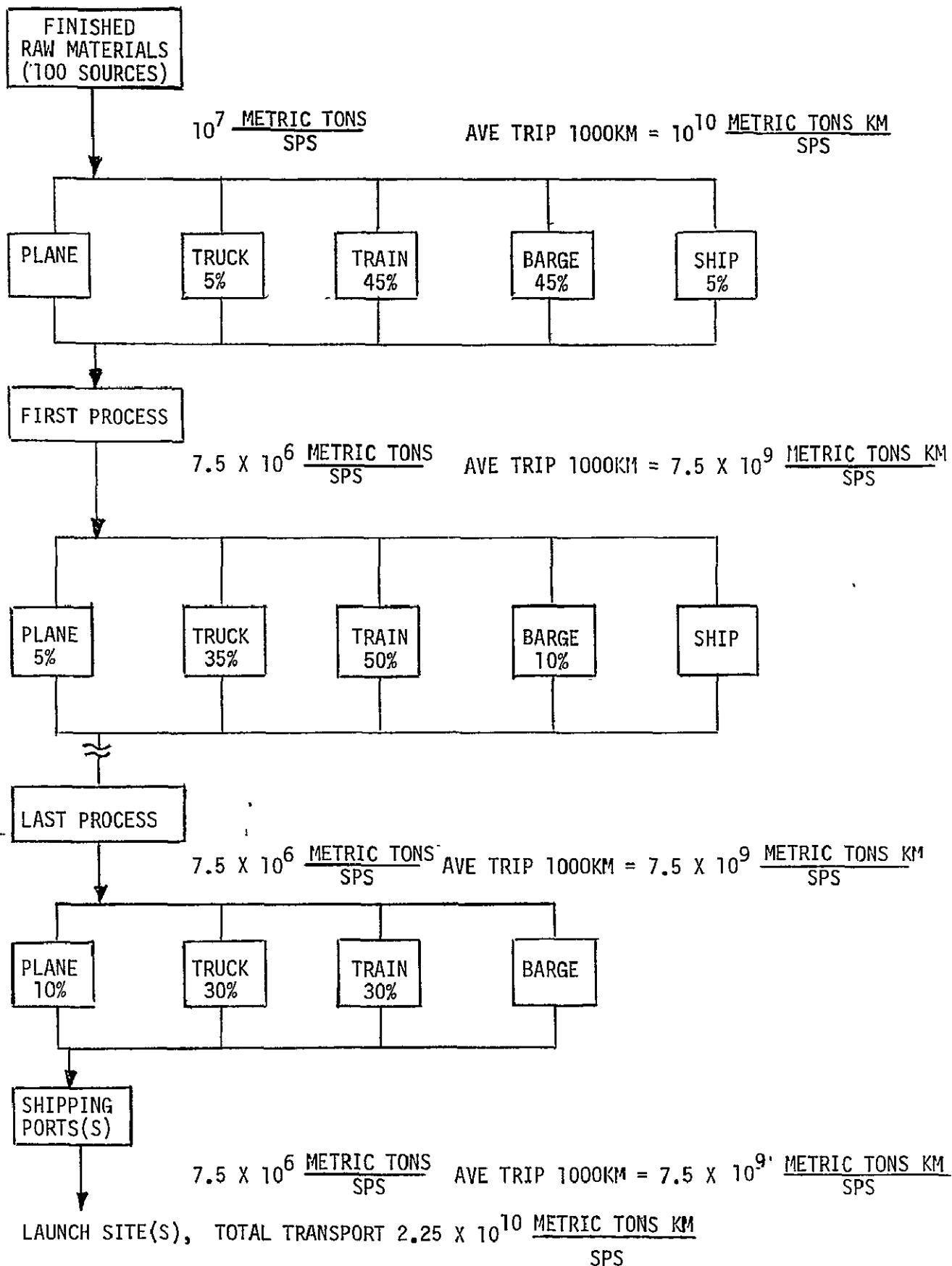


Figure 1XD-1
 TYPICAL GROUND TRANSPORTATION
 FLOW SCENARIO FOR AN SPS IX-14

ORIGINAL PAGE IS
OF POOR QUALITY

PRELIMINARY

SOLAR POWER SATELLITE INFORMATION

PART 1	NONCONSUMABLES	
1.0	MICROWAVE POWER TRANSMISSION SYSTEM	PAGE 1
2.0	SOLAR CELL COLLECTION SYSTEM	PAGE 10
3.0	SOLAR ELECTRIC PROPULSION SYSTEM	PAGE 11
4.0	HEAVY LAUNCH VEHICLE	PAGE 12
5.0	PERSONNEL TO LOW EARTH ORBIT TRANSFER VEHICLE	PAGE 14
6.0	REQUIREMENTS ESTIMATED FOR REMOTE ASSEMBLY LOW-ORBIT	PAGE 15
PART 2	CONSUMABLES	
1.0	VEHICLE FLIGHT DATA	PAGE 16
2.0	CONSUMABLES SUMMARY	PAGE 18
PART 3	TOTAL MATERIALS REQUIREMENT-NON CONSUMABLES MATERIALS SUMMARY	
PART 4	BASIC MATERIALS DEMANDS, SUPPLIES, AND AVAILABILITY	
1.0	BASIC MATERIALS DEMANDS AND SUPPLIES	PAGE 20
2.0	RANK OF MATERIAL USAGE BY WEIGHT	PAGE 23
3.0	SPS MATERIAL USAGE VS NATIONAL AND WORLD DEMANDS, AND RESOURCES	PAGE 25

NOTE: ASSUME ASSEMBLY TIME = 1 YEAR

A P P E N D I X

SECTION IX

ORIGINAL PAGE IS
OF POOR QUALITY

PART 1
NONCONSUMABLES
MATERIAL REQUIREMENTS FOR 56M SPS
1.0 MICROWAVE POWER TRANSMISSION SYSTEM

COMPONENT	STEEL	CU	AG	AL (METRIC TONS)	ELTRNIK (TONS)	RM	TOTAL
1.1 ROTARY JOINT							
1.1.1 AZIMUTH DRIVE							
1.1.1.1 GEARBOX	.109+02	.000	.000	.000	.000	.000	.10900+02
1.1.1.2 MOTORS	.075+01	.219+01	.000	.000	.000	.000	.10940+02
1.1.2 SUPPORT	.193+02	.000	.000	.000	.000	.000	.19300+02
1.1.3 SLIP RING BRUSH	.000	.000	.100+01	.000	.000	.000	.10000+01
1.1.4 ELFV DRIVE	.883+01	.220+01	.000	.000	.000	.000	.11030+02
1.1.5 LUBRICANT GEARS	.000	.000	.000	.000	.000	.100-11	.10000-11
1.1.5 LUBRICANT SLIP RINGS	.000	.000	.000	.000	.000	.100-11	.10000-11
1.1.7 DRIVE	.100+01	.000	.000	.000	.000	.000	.10000+01
1.1 TOTAL	.487+02	.439+01	.100+01	.000	.000	.200-11	.54260+02

NOTE: THE VALUE .100-11, INDICATES TO BE DETERMINED

PART I
NONCONSUMABLES

PAGE 2

COMPONENT	STEEL	CU	AG	AL (METRIC)	ELT/NIX (TONS)	RM	TOTAL
1.2 INPUT POWER DISTRIBUTION							
1.2.1 PRIMARY FEEDERS	.400	.000	.000	.477+02	.000	.000	.47700+02
1.2.2 SECONDARY FEELERS	.700	.000	.000	.160+01	.000	.000	.16000+01
1.2.3 TERTIARY DISTRIBUTION	.000	.000	.000	.700+03	.000	.000	.70000+03
1.2.4 SUB ARWAY DISTRIBUTION	.000	.000	.000	.100+00	.000	.000	.10000+00
1.2.5 SWITCH GEAR	.000	.000	.000	.000	.000	.621+02	.62100+02
1.2.6 CROSS BAR	.000	.000	.000	.000	.301+03	.000	.30100+03
1.2.7 AUXILIARY POWER	.000	.000	.000	.000	.883+02	.000	.88300+02
1.2 TOTAL	.400	.000	.000	.501+02	.389+03	.621+02	.50150+03

NOTE: THE VALUE .100-11, INDICATES TO BE DETERMINED

ORIGINAL PAGE IS
OF POOR QUALITY

PART I
NONCONSUMABLES

COMPONENT	PT	SMCO	CU	GRAPHITE	STEEL (METRIC TONS)	AL	FLTRNJK	TBN	GAASPT	TOTAL
1.3 DC TO RF CONVERSION										
1.3.1 ANODE STRONG										
1.3.1.1 CATHODE	.200+01	.000	.112+02	.000	.000	.000	.000	.000	.000	.13200+02
1.3.1.2 FACTS	.000	.411+03	.000	.000	.000	.000	.000	.000	.000	.41100+03
1.3.1.3 ANODE	.000	.000	.166+03	.000	.000	.000	.000	.000	.000	.16600+03
1.3.1.4 RADIATOR	.000	.000	.000	.166+04	.000	.000	.000	.000	.000	.16600+04
1.3.1.5 POLES	.000	.000	.000	.000	.154+03	.000	.000	.000	.000	.15400+03
1.3.1.6 I/O AND MOTORS	.000	.000	.216+02	.000	.042+02	.000	.000	.000	.000	.10780+03
1.3.1 TOTAL	.200+01	.411+03	.199+03	.166+04	.240+03	.000	.000	.000	.000	.25120+04

NOTE: THE VALUE .100-11, INDICATES TO BE DETERMINED

PART I
NONCONSUMABLES

COMPONENT	AL	STFL	CU	LLTRNIK (METRIC TONS)	PM	TBD	TOTAL
1.4 TRANSMIT ANTENNA							
1.4.1 SLOTTED WAVE GUIDE	.318+04	.000	.000	.000	.000	.000	.31800+04
1.4.2 WAVEGUIDE/STRUCT INTERFACE							
1.4.2.1 SHAFT	.000	.188+03	.000	.000	.000	.000	.18800+03
1.4.2.2 WORM	.000	.356+02	.000	.000	.000	.000	.35600+02
1.4.2.3 MOTOR 80/20	.000	.644+02	.161+02	.000	.000	.000	.80500+02
1.4.2.4 THERMAL ISOLATION	.000	.000	.000	.000	.000	.142+02	.14200+02
1.4.2.5 GEARBOX AND GIMBAL	.000	.618+02	.000	.000	.000	.000	.61800+02
1.4.2.6 LUBRICANT	.000	.000	.000	.000	.000	.100-11	.10000-11
1.4.2.7 CONDUCTORS (MOTORS)	.100-11	.000	.000	.000	.000	.000	.10000-11
1.4.2 TOTAL	.100-11	.350+03	.161+02	.000	.000	.142+02	.38010+03
1.4.3 ATTITUDE CONTROL/ALIGNMENT							
1.4.3.1 COMMUNICATION S. S.	.000	.000	.000	.230+00	.000	.000	.23000+00
1.4.3.2 CPU AND MEMORY	.000	.000	.000	.800+01	.000	.000	.80000+01
1.4.3.3 ATTITUDE SENSORS	.000	.000	.000	.465+00	.000	.000	.46500+00
1.4.3.4 SUBARRAY CONTROL	.000	.000	.000	.182+03	.000	.000	.18200+03
1.4.3.5 SCREW/JACK ACTUATORS	.000	.000	.000	.145+03	.000	.000	.14500+03
1.4.3 TOTAL	.000	.000	.000	.322+03	.000	.000	.32277+03

NOTE: THE VALUE .100-11, INDICATES TO BE DETERMINED.

ORIGINAL PAGE IS
OF POOR QUALITY

PART I
NONCONSUMABLES

PAGE 1

COMPONENT	AL	STEEL	CU	LITRIN RN (METRIC TONS)	TBD	TOTAL
1.4.4 ANTENNA STRUCTURE						
1.4.4.1 SUBARRAY PRIMARY	.137+03	.000	.000	.000	.000	.13770+03
1.4.4.2 SUBARRAY SECONDARY	.470+02	.000	.000	.000	.000	.47000+02
1.4.4.3 SUPPORT STRUCTURE	.106+03	.000	.000	.000	.000	.10600+03
1.4.4.4 YOKE	.540+02	.000	.000	.000	.000	.54000+02
1.4.4.5 COATINGS	.000	.000	.000	.000	.210+02	.21000+02
1.4.4.6 AMPLIFIER ATTACH	.230+02	.000	.000	.000	.000	.23000+02
1.4.4 TOTAL	.367+03	.000	.000	.000	.210+02	.36800+03
1.4 TOTAL	.355+04	.350+03	.161+02	.328+03	.000	.42759+04

NOTE: THE VALUE .100-11, INDICATES TO BE DETERMINED.

PART I
NONCONSUMABLES

PAGE 6

COMPONENT	PT	SMCO	CU	GRPHITE (METRIC	STEEL TONS)	AL	ELTRNIK	TBD	GAASPT	CONCRETE	TOTAL
1.5 RECTLNNA											
1.5.1 RECTIFIER											
1.5.1.1 DIPOLE AND FILTERS	.000	.000	.000	.000	.000	.500+06	.000	.000	.000		.50000+06
1.5.1.2 DIODE	.300-05	.000	.000	.000	.000	.100-12	.000	.000	.600+01		.60000+01
1.5.1.3 REFLECTOR	.000	.000	.000	.000	.000	.100-12	.000	.000	.000		.10000-12
1.5.1.4 D.C. BUSSES	.000	.000	.215+04	.000	.000	.000	.000	.000	.000		.21500+04
1.5.1.5 INVERTERS	.000	.000	.000	.000	.000	.000	.100-11	.000	.000		.10000-11
1.5.1.6 GROUND BEAM CONTROL	.000	.000	.000	.000	.000	.000	.100-11	.000	.000		.10000-11
1.5.1.7 STRUCTURAL SUPPORT	.000	.000	.000	.000	.000	.000	.000	.100-11	.000	.152+07	.15200+07
1.5.1 TOTAL	.300-05	.000	.215+04	.000	.000	.500+06	.200-11	.000	.600+01		.20222+07

NOTES: THE VALUE .100-11 INDICATES TO BE DETERMINED
THE VALUE .100-12 INDICATES INCLUDED IN DIPOLE & FILTERS
SECTION 1.5 IS GROUND EQUIPMENT ONLY

PART 1
NONCONSUMABLES

COMPONENT	MICROWAVE POWER TRANSMISSION SYSTEM - ALTERNATE SYSTEMS							TOTAL
	GRAPHITE	MO	GAASW	W (METRIC TONS)	SI	RM	TBD	
A1.3								
DC TO RF CONVERSION								
A1.3.1								
KLYSTRONS								
A1.3.1.1								
PYROLYTIC GRAPHITE	.431+04	.000	.000	.000	.000	.000	.000	.43100+04
A1.3.1.2								
BASE METALS	.000	.000	.000	.000	.000	.000	.599+03	.59900+03
A1.3.1.3								
HEAT PIPES	.000	.000	.000	.000	.000	.114+04	.000	.11400+04
A1.3.1.4								
GUN ASSEMBLY	.000	.000	.000	.000	.000	.930+01	.000	.90000+01
A1.3.1.5								
SULFONIO	.000	.000	.000	.000	.000	.000	.295+04	.29500+04
A1.3.1.6								
MOLYBDENUM	.000	.152+03	.000	.000	.000	.000	.000	.15200+03
A1.3.1 TOTAL	.431+04	.152+03	.000	.000	.000	.115+04	.355+04	.91600+04

NOTE: THE VALUE .100-11, INDICATES TO BE DETERMINED

PART 1
NONCONSUMABLES

COMPONENT	GRAPHITE	MO	GAASW	W (METRIC TONS)	SI	RM	TND	TOTAL
A1.5 RECTENNA								
A1.5.1.2 (1) (GAAS-W)	.000	.000	.600+01	.300-05	.000	.000	.000	.60000+01
A1.5.1.2 (2) (SI-W)	.037	.000	.700	.300-05	.600+01	.000	.000	.60000+01

NOTE: THE VALUE +100-11, INDICATES TO BE DETERMINED

ORIGINAL PAGE IS
OF POOR QUALITY

PART 1
NONCONSUMABLES

PAGE 9

COMPONENT	MICROWAVE POWER TRANSMISSION SYSTEM - SUMMARY										
	AL	STEEL	CU	AG (METRIC TONS)	PT	SMCO	GRAPHITE	GAAS	FLTRNLY	RM	CONCRETE
1.1 PRIMARY JOINT	.000	.489+02	.439+01	.100+01	.000	.000	.000	.000	.000	.200-11	
1.2 FLIGHT POWER DISTRIBUTION	.501+02	.000	.000	.000	.000	.000	.000	.000	.389+03	.621+02	
1.3 DC TO RF CONVERSION	.000	.240+03	.199+03	.000	.200+01	.411+03	.166+04	.000	.000	.000	
1.4 TRANSMIT ANTENNA	.355+04	.350+03	.161+02	.000	.000	.000	.000	.000	.328+03	.000	
1.1-1.4 FLIGHT TOTAL	.360+04	.639+03	.219+03	.100+01	.200+01	.411+03	.166+04	.000	.717+03	.621+02	
1.5 RECTENNA (GROUND)	.500+06	.000	.215+04	.000	.300-05	.000	.000	.600+01	.200-11	.000	.152+07
1.0 TOTAL	.504+06	.639+03	.237+04	.100+01	.200+01	.411+03	.166+04	.600+01	.717+03	.621+02	

NOTE: THE VALUE .200-11, INDICATES TO BE DETERMINED

PART I
NONCONSUMABLES

PAGE 9A

MICROWAVE POWER TRANSMISSION SYSTEM SUMMARY (CONTINUED)

COMPONENT	TBD	(METRIC TONS)	TOTAL
1.1 ROTARY JOINT	.000		.54260+02
1.2 INPUT POWER DISTRIBUTION	.000		.50150+03
1.3 DC TO RF CONVERSION	.000		.25120+04
1.4 TRANSMIT ANTENNA	.352+02		.42759+04
1.1-1.4 FLIGHT TOTAL	.352+02		.50950+06 7246.
1.5 RECTENNA (GROUND)	.000		.20222+07
1.0 TOTAL	.352+02		.50950+06

NOTE: THE VALUE .100-11, INDICATES TO BE DETERMINED

ORIGINAL PAGE IS
OF POOR QUALITY

PART 1
NONCONSUMABLES

2.0 SOLAR CELL COLLECTION SYSTEM BASE LINE SYSTEM

COMPONENT	SI SS	SL CP	SI AOH	GOLDNOV (METRIC TONS)	CU	BLACK PAINT	AL	MYLAR	AR	TBD	TOTAL
2.1 SOLAR CELL											
2.1.1 SOLAR CELL +1MM	.109+05	.000	.000	.000	.000	.000	.000	.000	.000	.000	.10900+05
2.1.2 FILTER GLASS +1MM	.000	.109+05	.000	.000	.000	.000	.000	.000	.000	.000	.10900+05
2.1.3 BUS BAR	.000	.000	.000	.523+04	.000	.000	.000	.000	.000	.000	.52300+04
2.1.4 INTERCONNECT	.000	.000	.000	.000	.407+04	.000	.000	.000	.000	.000	.40700+04
2.1.5 INFILM COAT	.000	.000	.000	.000	.000	.523+04	.000	.000	.000	.000	.52300+04
2.1.6 ADHESIVE	.000	.000	.479+04	.000	.000	.000	.000	.000	.000	.000	.47900+04
2.1 TOTAL	.109+05	.109+05	.479+04	.523+04	.407+04	.523+04	.000	.000	.000	.000	.41120+05
2.2 POWER DIST. BUS AND SWITCHES	.000	.000	.000	.000	.000	.000	.205+05	.000	.000	.000	.20500+05
2.3 ALUMINIZED MYLAR	.000	.000	.000	.000	.000	.000	.000	.688+04	.000	.000	.68800+04
2.4 STRUCTURAL NON-CONDUCTING	.000	.000	.000	.000	.000	.000	.688+04	.000	.000	.000	.68800+04
2.5 ORIENTATION ENGINES	.000	.000	.000	.000	.000	.000	.000	.000	.000	.100-11	.10000-11
2.6 ORIENTATION PROPELLANT	.000	.000	.000	.000	.000	.000	.000	.000	.177+04	.000	.17700+04
2.0 TOTAL	.109+05	.109+05	.479+04	.523+04	.407+04	.523+04	.274+05	.688+04	.177+04	.100-11	.77070+05

NOTE: THE VALUE .100-11, INDICATES TO BE DETERMINED

PART 1
NONCONSUMABLES

PAGE 11

COMPONENT	3.0 SOLAR ELECTRIC PROPULSION SYSTEM (FOR MPTS AND SCSS ONLY)									
	W	MO	CERMISK	STEEL (METRIC TONS)	CU (TONS)	STSTEEL	AR	ELTRNIX	T8U	TOTAL
3.1 ELECTRIC TSS										
3.1.1 MFD THRUSTERS (10)	.625+02	.625+02	.130+01	.000	.000	.000	.000	.000	.000	.12630+03
3.1.2 CABLING	.000	.000	.000	.003	.660+01	.000	.000	.000	.000	.66090+01
3.1.3 THRUSTER STRUCT AND COOL	.000	.000	.000	.000	.000	.000	.000	.000	.222+02	.22210+02
3.1.4 CONTROL RECTIFIER	.000	.000	.000	.002	.000	.000	.000	.133+02	.000	.13300+02
3.1.5 TRANSFORMER	.000	.000	.000	.200+03	.437+02	.000	.000	.000	.000	.24370+03
3.1.6 ARGON FELD AND CONTROL	.000	.000	.000	.000	.000	.900+00	.000	.000	.000	.90000+00
3.1.7 HEAT REJECTION	.000	.000	.000	.354+02	.000	.000	.000	.000	.000	.35400+02
3.1 TOTAL	.625+02	.625+02	.130+01	.235+03	.503+02	.900+00	.000	.133+02	.222+02	.44840+03
3.2 PROPELLANT TANKAGE										
3.2.1 AR TANKS PLUMBING AND CONT.	.000	.000	.000	.000	.000	.000	.000	.000	.000	.00000
3.3 THRUST MODULE EQUIPMENT										
3.3.1 GIMBAL ASSEMBLY	.000	.000	.000	.180+01	.000	.000	.000	.000	.000	.18000+01
3.3.2 AUX POWER ASSEMBLY	.000	.000	.000	.000	.230+01	.000	.000	.000	.000	.23000+01
3.3.3 INSTRUMENTATION AND CONTROL	.000	.000	.000	.000	.000	.000	.000	.500+00	.000	.50000+00
3.3.4 AC GEN ASSEMBLY	.000	.000	.000	.800+02	.197+02	.000	.000	.000	.000	.99700+02
3.3 TOTAL	.000	.000	.000	.818+02	.220+02	.000	.000	.500+00	.000	.10970+03
3.4 GUIDANCE AND CONTROL	.000	.000	.000	.000	.000	.000	.000	.100-11	.000	.10000-11
3.0 TOTAL	.625+02	.625+02	.130+01	.317+03	.723+02	.900+00	.000	.138+02	.222+02	.55270+03

NOTE: THE VALUE .100-11, INDICATES TO BE DETERMINED

ORIGINAL PAGE IS
OF POOR QUALITY

PART 1
NONCONSUMABLES

4.0 HEAVY LAUNCH VEHICLE

COMPONENT	AL	INSULAT	H2O	CU (METRIC TONS)	STEEL	INCONEL	RCS PRO	OTH PRO	GROWTH	ELTRNIK	TOTAL
4.1											
STRUCTURE											
4.1.1											
FORWARD BODY	.594+02	.000	.000	.000	.000	.000	.000	.000	.000	.000	
4.1.2											
LOX TANK	.562+02	.000	.000	.000	.000	.000	.000	.000	.000	.000	
4.1.3											
LH2 TANK	.900+02	.550+01	.000	.000	.000	.000	.000	.000	.000	.000	
4.1.4											
INTER. TANK STRUCTURE	.590+02	.000	.000	.000	.000	.000	.000	.000	.000	.000	
4.1.5											
LOWER SKIRT	.185+02	.000	.000	.000	.000	.000	.000	.000	.000	.000	
4.1.6											
THRUST SHELL	.256+02	.000	.000	.000	.000	.000	.000	.000	.000	.000	
4.1.7											
BASIC STRUCTURE FRAME	.533+02	.000	.000	.000	.000	.000	.000	.000	.000	.000	
4.1.8											
BASI SHIELD	.247+02	.000	.000	.000	.000	.000	.000	.000	.000	.000	
4.1.9											
RO-1 TANKS	.890+01	.000	.000	.000	.000	.000	.000	.000	.000	.000	
4.1.10											
SECONDARY STRUCTURE	.166+02	.000	.000	.000	.000	.000	.000	.000	.000	.000	
4.1 TOTAL	.412+03	.550+01	.000	.000	.000	.000	.000	.000	.000	.000	
4.2											
INDUCED ENV. PROTECTION	.130+02	.000	.630+02	.000	.000	.000	.000	.000	.000	.000	
4.3											
AUXILLIARY SYSTEMS	.200+01	.000	.000	.100+01	.110+01	.000	.000	.000	.000	.000	
4.4											
PROPULSION											
4.4.1											
ENGINE ACCESSORIES	.980+01	.000	.000	.000	.900+01	.000	.000	.000	.000	.000	
4.4.2											
PROPellant SYSTEM	.440+02	.000	.000	.000	.000	.000	.000	.000	.000	.000	
4.4.3											
ENGINES	.000	.000	.000	.000	.000	.186+03	.000	.000	.000	.000	
4.4 TOTAL	.530+02	.000	.000	.000	.900+01	.186+03	.000	.000	.000	.000	

PART 1
NONCONSUMABLES

PAGE 12A

4.0 HEAVY LAUNCH VEHICLE (CONTINUED)

COMPONENT	TBD	TOTAL
4.1		
STRUCTURE		
4.1.1		
FORWARD BODY	.000	
4.1.2		.59400+02
LOX TANK	.000	.56200+02
4.1.3		
LH2 TANK	.000	.95500+02
4.1.4		
INTER. TANK STRUCTURE	.000	.59000+02
4.1.5		
LOWER SKIRT	.000	.18500+02
4.1.6		
THRUST SHELL	.000	.25600+02
4.1.7		
BASE STRUCTURE FRAME	.000	.53300+02
4.1.8		
BASE SHIELD	.000	.24700+02
4.1.9		
ROCKET TANKS	.000	.89000+01
4.1.10		
SECONDARY STRUCTURE	.000	.16600+02
4.1 TOTAL	.000	.41770+03
4.2		
INDUCED ENV. PROTECTION	.000	.76000+02
4.3		
AUXILIARY SYSTEMS	.000	.41000+01
4.4		
PROPULSION		
4.4.1		
ENGINE ACCESSORIES	.000	.19600+02
4.4.2		
PROPELLANT SYSTEM	.000	.44000+02
4.4.3		
IGNITERS	.000	.18600+03
4.4 TOTAL	.000	.24960+03

PART I
NONCONSUMABLES

COMPONENT	AL	INSULAT	H2O	CU (METRIC TONS)	STEEL	INCONFL	RCS PRO	OTH PRO	GROWTH	ELTRNIK	TOTAL
4.5 PROPULSION RCS	.000	.000	.000	.000	.000	.119+01	.000	.000	.000	.000	.000
4.6 PRIME POWER	.000	.000	.000	.000	.000	.000	.000	.000	.000	.000	.000
4.7 ELEC. CONVERSION AND DIST.	.000	.000	.000	.320+02	.000	.000	.000	.000	.000	.000	.000
4.8 AVIONICS	.000	.000	.000	.000	.000	.000	.000	.000	.000	.200+01	.000
4.9 ENVIRONMENTAL CONTROL	.181+02	.000	.000	.000	.000	.000	.000	.000	.000	.000	.000
4.10 WEIGHT GROWTH	.000	.000	.000	.000	.000	.000	.000	.000	.139+03	.000	.000
4.11 INERT WEIGHTS	.000	.000	.000	.000	.000	.000	.000	.000	.000	.000	.000
4.11.1 RESIDUAL PROPELLANT	.000	.000	.000	.000	.000	.000	.000	.812+02	.000	.000	.000
4.11.2 RESIDUAL COOLANT	.000	.000	.540+02	.000	.000	.000	.000	.000	.000	.000	.000
4.11.3 RESIDUAL RETRO PROPELLANT	.000	.000	.000	.000	.000	.000	.910+01	.000	.000	.000	.000
4.11.4 USEABLE RCS PROPELLANT	.000	.000	.000	.000	.000	.000	.340+01	.000	.000	.000	.000
4.11.5 USEABLE RETRO PROPELLANT	.000	.000	.000	.000	.000	.000	.000	.490+02	.000	.000	.000
4.11.6 USEABLE DEORBIT PROPELLANT	.000	.000	.000	.000	.000	.000	.000	.117+02	.000	.000	.000
4.11 TOTAL	.181+02	.000	.540+02	.320+02	.000	.110+01	.125+02	.152+03	.139+03	.200+01	.000
4.12 ASCENT PROPELLANT	.000	.000	.000	.000	.100	.000	.000	.914+04	.000	.000	.000
4.0 TOTAL	.499+03	.550+01	.117+03	.330+02	.109+02	.187+03	.125+02	.929+04	.139+03	.200+01	.000
ESTIMATE & VEHICLES REQUIRED FOR 56 TSPS	.299+04	.330+02	.702+03	.190+03	.654+02	.112+04	.750+02	.558+04	.814+03	.120+02	.000

PART I
NONCONSUMABLES

COMPONENT	TAD	TOTAL
4.5 PROPULSION RCS	.000	.11000+01
4.6 PRIME POWER	.160+01	.16000+01
4.7 ELEC. CONVERSION AND DIST.	.000	.32000+02
4.8 AVIONICS	.000	.20000+01
4.9 ENVIRONMENTAL CONTROL	.000	.18100+02
4.10 WEIGHT GROWTH	.000	.13900+03
4.11 INERT WEIGHTS	.000	.00000
4.11.1 RESIDUAL PROPELLANTS	.000	.01200+02
4.11.2 RESIDUAL COOLANT	.000	.54000+02
4.11.3 RESIDUAL RETRO PROPELLANT	.000	.91000+01
4.11.4 USABLE RCS PROPELLANT	.000	.34000+01
4.11.5 USABLE RETRO PROPELLANT	.000	.59000+02
4.11.6 USABLE DEORBIT PROPELLANT	.000	.11700+02
4.11 TOTAL	.160+01	.00000
4.12 TOTAL	.000	.91400+04
4.0 TOTAL	.160+01	.10300+05
ESTIMATE 4 VEHICLES E USED FOR 16 VPS	.960+01	.61700+05

ORIGINAL PAGE IS
OF POOR QUALITY

PART 1
NONCONSUMABLES

500 PERSONNEL TO LOW EARTH ORBIT TRANSFER VEHICLE
TO BE DETERMINED

PART 1
NONCONSUMABLES

6.0 REQUIREMENTS ESTIMATE FOR REMOTE ASSEMBLY 10-ORBIT
OF MPTS

ASSEMBLY TIME = 1 MONTH

EQUIPMENT	MASS EA.	GRUMMAN NO.	MASS TO.	RATIOED FOR INCREASED AREA (1.69)		
				NO.	MASS TO.	CONSUMABLE
6.1 RAM SUPPORT MODULE	.5440+01	2	.1089+02	3	.1632+02	
6.2 RAM COM MODULE	.8760+01	2	.1752+02	3	.2628+02	
6.3 REMOTE CONTROL MANIPULATOR	.1830+00	182	.3331+02	308	.5636+02	.621 LB PROP/LB STRUCTURE
6.4 TORS	.2036+01	6	.1227+02	19	.2934+02	
6.5 CONTROL MODULE	.9500+01	1	.9500+01	7	.1900+02	
6.6 MANUFACT. MODULE	.9100+01	8	.7280+02	14	.1274+03	.100-11
6.1-6.6 TOTAL			.1562+03		.2657+03	
6.7 FUEL STORAGE	.1000-11					

THE VALUE .1000-11, INDICATES TO BE DETERMINED

PRINTER FORMAT SHEET

1. PREPARED BY	2. REV REV. NO.	3. REPORT NAME FILE NO.	4. PROG NO.	5. PROJ NO.	6. RELEASED	7. FORM NO.	8. COPIES	9.	10.	11. PAGE OF
----------------	--------------------	----------------------------	-------------	-------------	-------------	-------------	-----------	----	-----	----------------

12. COMMENTS

PART B
CONSUMABLES

1.2 PLTM VEHICLE (SHUTTLE) - GROUND TO UEO (CONFORMS TO PAYLOAD/ORBIT - VEHICLE MATRIX)

PERSONNEL 6

METRIC TONS

PAYLOAD PER VEHICLE

TBD

CONSUMABLES/FLIGHT

GROWTH
FACTOR

CONSERVATION
FACTOR

GRAND TOTAL
CONSUMABLES/FLIGHT

- LOX
- LH2
- JP-1
- N2O4
- MMH
- HG
- LNE
- SOLID ROCKET

- 603.67
- 221.4
- N/A
- 29.43
- 16.00
- TBD
- TBD
- 1054.00

- 1.25
- 1.25
-
- 1.25
-
-
-
- 1.25

- 2.0
- 1.4
-
- 2.0
-
-
-
-

- 1509.18
- 387.45
-
- 73.38
-
-
-
-

PERSONNEL

6

PERSONNEL CONSUMABLES

FOOD

PERSONAL EQUIPMENT

REPLACEMENT PARTS

TURN AROUND TIME

TBD DAYS

AIR FRAME LIFE

TBD FLIGHTS

ENGINE LIFE

TBD FLIGHTS

REFURBISHING MATERIAL

TBD

5.105

7342 x 10⁴

PRINTER FORMAT SHEET

1 PREPARED BY	2 NEW REV'D	3 REPORT NAME FILE NO	4 PROG NO	5 PROJ TO	6 RELEASED	7 FORM NO	8 COPIES	9	10	11 PAGE OF
										PAGE 18
PART 2 CONSUMABLES 2.0 CONSUMABLES SUMMARY										
(NITRATE TONS)										
HHLV - HHLV HOSPITALS TRANSPORT TO LEO										
	SYSTEM	MACS	TRIPS	LOX	LH2	JP-11	NR	HHT	N2O4	SRF
	MPTS	.7344+04	.3235+02	.1623+03	.2896+07	.1280+07				
	ECCS	.7707+05	.3400+02	.2453+07	.4386+06	.1932+06				
	SEPS	.5527+03	.2435+01	.1761+05	.3141+04	.1383+04				
	TOTAL	.8497+05	.2587+04	.1851+08	.3398+07	.1495+07				
SEPS - MATERIALS TRANSPORT TO GEO										
		.8441+05	.1100+01			.4120+05				
SHUTTLE PERSONNEL ASSEMBLY STATION AND SUPPORT TO LEO										
		.5443+00	.1080+03	.6520+05	.2391+05	.1728+04	.3178+04	.1138+06		
	GRAND TOTALS	.6944+06	.2696+04	.1878+08	.3362+07	.1179+07	.4120+05	.1728+04	.3178+04	.1138+06
ESTIMATED NUMBER OF VEHICLES										
	HHLV		6							
	SHUTTLE		16							

ORIGINAL PAGE IS OF POOR QUALITY

PART 3
TOTAL MATERIALS REQUIREMENT - NONCONSUMABLES MATERIALS SUMMARY (METRIC TONS)

MATERIAL	HPTS	SCCS	SEPS	ASSFMB	LEOMTS	GEOMTS	LEOPTS	GLOPTS	PLTTOTAL	GNDTOTAL	GRANDTOTAL
AL	.5036+06	.2738+05			.2995+04				.5340+06	.5000+06	.10340+07
STEEL	.6349+03		.3172+03		.6540+02				.1021+04	.2000	.10215+04
CU	.2377+04	.4079+04	.7230+02		.1980+03				.4710+04	.2100+04	.88496+04
AG	.1577+01								.1000+01	.0000	.10000+01
PT	.2110+01								.2000+01	.3000-05	.70000+01
SMO	.4113+03								.4110+03	.0000	.41100+03
GR. WHITE	.1663+04								.1640+04	.0000	.16600+04
GAAS	.6000+01								.4000+01	.6000+01	.12000+02
ELECT	.7171+03		.1380+02		.1200+02				.7429+03	.2000-11	.74287+03
RM	.6210+02								.6210+02	.0000	.62100+02
CONCRETE										.1520+07	.15200+07
SISS		.1090+05							.1090+05		.10900+05
SLCP		.1090+05							.1090+05		.47700+04
SIADH		.4790+04							.4790+04		.52300+04
GOLKOV		.5230+04							.5230+04		.52300+04
BLK PAINT		.5230+04							.5230+04		.68000+04
HYLAR		.6800+04							.6800+04		.17700+04
AR		.1770+04							.1770+04		.62500+02
W			.0000		.6250+02				.6250+02		.62500+02
MO			.6250+02						.6250+02		.13000+01
CERMISK			.1300+01						.1300+01		.90000+02
STAIN STEEL			.9000+02						.9000+02		.33000+02
INSULAT											.70700+03
H2O					.3300+02				.3300+02		.11276+04
INCOMP					.7520+03				.7020+03		.75000+02
RC3 PRU					.1123+04				.1123+04		.55751+05
OTU PRU					.7100+02				.7500+02		.83100+03
GRU TH					.5575+05				.5575+05		.67000+02
					.8340+03				.8340+03		
TBD	.3520+02	.1000-11	.2220+02		.9600+01				.6700+02	.0000	.67000+02
TOTAL	.5044+06	.7707+05	.5527+03		.6180+05				.6489+06	.2022+07	.26602+07

THE VALUE .11 E-11, INDICATES TO BE DETERMINED

PART 4
 BASIC MATERIALS DEMANDS, SUPPLIES, AND AVAILABILITY
 1.0 BASIC MATERIALS DEMANDS AND SUPPLIES
 (METRIC TONS)

MATERIAL	USED IN 1968	PROJECTED DEMANDS IN YR 2000		TOTAL RESOURCES		CUMULATIVE DEMAND TO YR 2000		REMARKS	
		US	WORLD	US	WORLD	US	WORLD		
AG	H	•1000+06	•2600+04	•5612+76	•13310+37	•65007+11	•00000	•86000+07	•20600+08
	M	•0000	•0000	•5073+76	•11400+37	•00000	•00000	•79000+02	•18500+08
	L	•0000	•0000	•4527+36	•95100+06	•00000	•00000	•72000+07	•16400+08
AL	H	•4200+07	•1000+08	•4000+08	•10200+09	•00000	•13000+10	•40700+09	•12000+10
	M	•0000	•0000	•3000+08	•75400+09	•00000	•00000	•33400+09	•10000+10
	L	•0000	•0000	•2000+07	•40000+08	•00000	•00000	•26200+09	•80000+09
AR	H	•0000	•0000	•0000	•00000	•00000	•00000	•00000	•00000
	M	•0000	•0000	•0000	•00000	•00000	•00000	•00000	•00000
	L	•0000	•0000	•0000	•00000	•00000	•00000	•00000	•00000
AS	H	•2100+05	•4700+05	•4700+05	•17500+06	•17000+07	•38000+07	•10000+08	•22600+07
	M	•0000	•0000	•3760+05	•80000+05	•00000	•00000	•90000+06	•20000+07
	L	•0000	•0000	•2800+05	•71500+05	•00000	•00000	•81000+06	•18800+07
AU	H	•2500+03	•9600+03	•1134+04	•23520+04	•92000+04	•37200+05	•48500+05	•87400+05
	M	•0000	•0000	•9260+03	•22100+04	•00000	•00000	•38200+05	•72600+05
	L	•0000	•0000	•7170+03	•27700+04	•00000	•00000	•27800+05	•57800+05
B	H	•7000+05	•0000	•3500+06	•10500+07	•32600+07	•65200+08	•55000+07	•14900+08
	M	•0000	•0000	•2830+06	•80000+06	•00000	•00000	•50000+07	•13600+08
	L	•0000	•0000	•2150+06	•64700+06	•00000	•00000	•45300+07	•12200+08
CO	H	•6400+04	•2000+05	•1380+05	•39200+05	•25300+05	•21800+08	•10400+06	•99900+06
	M	•0000	•0000	•1120+05	•33100+05	•00000	•00000	•27000+06	•89500+06
	L	•0000	•0000	•8440+04	•27000+05	•00000	•00000	•23600+06	•79000+06
CR	H	•4600+06	•1360+07	•1290+07	•51900+07	•10200+07	•70200+09	•22700+08	•26600+08
	M	•0000	•0000	•1080+06	•44600+07	•00000	•00000	•20400+08	•21700+08
	L	•0000	•0000	•8700+06	•41300+10	•00000	•00000	•18200+08	•20700+08

ORIGINAL PAGE IS
 OF POOR QUALITY

BASIC MATERIALS DEMANDS, SUPPLIES, AND AVAILABILITY

MATERIAL		USED IN 1948		PROJECTED DEMANDS IN YR 2007		TOTAL RESOURCES		CUMULATIVE DEMAND TO YR 2000		REMARKS
		US	WORLD	US	WORLD	US	WORLD	US	WORLD	
CU	H	•2500+07	•7750+07	•1300+08	•44600+09	•77400+08	•27900+08	•11600+09	•40000+09	
	M	•9000	•2000	•1170+08	•33960+09	•00000	•00000	•10100+09	•40000+09	
	L	•0000	•0000	•1060+08	•23390+09	•00000	•00000	•87300+08	•31900+09	
GA	H	•3000+00	•0000	•1150+01	•34000+01	•27000+04	•20000+05	•19100+02	•22000+02	
	M	•1000	•0000	•6000+00	•20500+01	•00000	•00000	•00000	•00000	
	L	•1000+00	•0000	•2300+00	•70000+00	•00000	•00000	•00000	•00000	
HZ	H	•6350+07	•1550+08	•1620+09	•66000+08	•00000	•00000	•00000	•00000	
	M	•7000	•0000	•1740+09	•24100+09	•00000	•00000	•00000	•00000	
	L	•1000	•0000	•4770+08	•41700+09	•00000	•00000	•00000	•00000	
MO	H	•2530+05	•6260+05	•9370+05	•27100+06	•28500+07	•47000+07	•16000+07	•11700+07	
	M	•7000	•8000	•8740+05	•23500+06	•00000	•00000	•15000+07	•30000+07	
	L	•1000	•0000	•6940+05	•19800+06	•00000	•00000	•14000+07	•37000+07	
N	H	•3000	•0000	•0000	•00000	•00000	•00000	•00000	•00000	
	M	•7000	•0000	•0000	•00000	•00000	•00000	•00000	•00000	
	L	•7000	•0000	•0000	•00000	•00000	•00000	•00000	•00000	
NI	H	•1690+06	•4480+06	•5070+04	•15700+07	•18100+06	•60000+08	•10600+08	•28100+07	
	M	•1000	•0000	•4960+06	•13200+07	•00000	•00000	•96000+09	•25900+07	
	L	•0000	•0000	•4050+06	•10850+07	•00000	•00000	•86000+07	•27100+07	
OZ	H	•1048+08	•3420+08	•6760+08	•10080+09	•11300+16	•00000	•62000+09	•23930+10	
	M	•7000	•0000	•5150+08	•13840+09	•00000	•00000	•56000+09	•20760+10	
	L	•1000	•0000	•3530+08	•96630+08	•00000	•00000	•51400+09	•17600+10	
PT	H	•1800+02	•4913+07	•7055+12	•19490+03	•40400+02	•66610+04	•20660+04	•30920+04	
	M	•1000	•0000	•4360+05	•16320+03	•00000	•00000	•18560+04	•27780+04	
	L	•0000	•0000	•3450+04	•13140+03	•00000	•00000	•16470+04	•24640+04	

PART 4

BASIC MATERIALS DEMANDS, SUPPLIES, AND AVAILABILITY

MATERIAL	USED IN	1948		PROJECTED DEMANDS IN YR 2000		TOTAL RESOURCES		CUMULATIVE DEMAND TO YR 2000		REMARKS
		US	WORLD	US	WORLD	US	WORLD	US	WORLD	
SI	H	.5170+02	.0300	.2543+05	.0000	.0000	.0000	.2947+04	.0000	
	M	.0000	.0000	.0000	.0000	.0000	.0000	.2630+04	.0000	
	L	.0000	.0000	.0000	.0000	.0000	.0000	.2293+04	.0000	
TI	H	.4140+06	.1290+07	.0000	.6900+07	.2290+08	.1290+09	.3300+08	.1033+09	
	M	.0000	.0000	.0000	.4910+07	.0000	.0000	.2670+08	.8100+07	
	L	.0000	.0000	.0000	.2950+07	.0000	.0000	.1990+08	.6000+08	
W	H	.7360+04	.3320+05	.0000	.1970+06	.1360+06	.1190+08	.6160+06	.2180+07	
	M	.0000	.0000	.0000	.9110+05	.0000	.0000	.5570+06	.2130+07	
	L	.0000	.0000	.0000	.7570+05	.0000	.0000	.4900+06	.2070+07	
MMH	H	.0000	.0000	.0000	.0000	.0000	.0000	.0000	.0000	
	M	.0000	.0000	.0000	.0000	.0000	.0000	.0000	.0000	
	L	.0000	.0000	.0000	.0000	.0000	.0000	.0000	.0000	
N2O4	H	.0000	.0000	.0000	.0000	.0000	.0000	.0000	.0000	
	M	.0000	.0000	.0000	.0000	.0000	.0000	.0000	.0000	
	L	.0000	.0000	.0000	.0000	.0000	.0000	.0000	.0000	
JP-1	H	.0000	.0000	.0000	.0000	.0000	.0000	.0000	.0000	
	M	.0000	.0000	.0000	.0000	.0000	.0000	.0000	.0000	
	L	.0000	.0000	.0000	.0000	.0000	.0000	.0000	.0000	

ORIGINAL PAGE IS
OF POOR QUALITY

PART 4

BASIC MATERIALS DEMANDS, SUPPLIES, AND AVAILABILITY

2.0 RANK OF MATERIAL USAGE BY WEIGHT

RANK	MATERIAL	AMOUNT (KG)	GROWTH FACTOR PER CENT	TOTAL EST	PER CENT UNITED STATES	PER CENT YR 2000 DEMAND WORLD	PER CENT TOTAL RESERVE	KWH/KG TO PRODUCE	TOTAL ENERGY TO PRODUCE
1	N2	.1250+10	1.25	.1250+11	HI .0000 MEDIUM .0000 LOW .0000	HI .0000 MEDIUM .0000 LOW .0000	.00	.3200+00	.40000+10
2	LOX	.4150+10	1.25	.1000+12	HI .0000 MEDIUM .0000 LOW .0000	HI .0000 MEDIUM .0000 LOW .0000	.00	.3200+00	.32000+10
3	AL	.1080+10	1.10	.1080+10	HI .0000 MEDIUM .0000 LOW .0000	HI .0000 MEDIUM .0000 LOW .0000	.00	.2400+02	.25900+11
4	LH2	.7540+09	1.25	.1320+10	HI .0000 MEDIUM .0000 LOW .0000	HI .0000 MEDIUM .0000 LOW .0000	.00	.15000+00	.19800+11
5	JP-1	.3200+09	1.15	.3200+19	HI .0000 MEDIUM .0000 LOW .0000	HI .0000 MEDIUM .0000 LOW .0000	.00	.23000+01	.73600+09
6	SRF	.1300+09	1.25	.1600+09	HI .0000 MEDIUM .0000 LOW .0000	HI .0000 MEDIUM .0000 LOW .0000	.00	.36000+01	.58000+10

ORIGINAL PAGE IS
OF POOR QUALITY

PART 4

BASIC MATERIALS DEMANDS, SUPPLIES, AND AVAILABILITY

2.0 RANK OF MATERIAL USAGE BY WEIGHT

RANK	MATERIAL	AMOUNT (KG)	GROWTH FACTOR PER CENT	TOTAL EST	PER CENT YR 2000 DEMAND		PER CENT TOTAL RESERVE	M/HFG TO PRODUCE	TOTAL ENERGY TO PRODUCE
					UNITED STATES	WORLD			
7	AR	.4100+08	1.02	.4200+08	HI MEDIUM	HI MEDIUM	.00	.3200+08	.2000+08
8	SISS	.1100+08	1.00	.1100+08	HI MEDIUM	HI MEDIUM	.00	.1500+01	.1650+08
9	SISSc	.1100+08	1.38	.1190+08	HI MEDIUM	HI MEDIUM	.00	.1800+01	.1850+08
10	CU	.6500+07	1.19	.7200+07	HI MEDIUM	HI MEDIUM	.00	.2600+02	.1870+09
11	NYLAR	.1270+08	1.00	.1230+08	HI MEDIUM	HI MEDIUM	.00	.1500+02	.1800+09
12	INCOJEL (X)	.1110+07	1.10	.1200+07	HI MEDIUM	HI MEDIUM	.00	.3000+02	.3600+08

BASIC MATERIALS DEMANDS, SUPPLIES, AND AVAILABILITY

MAT	AMOUNT M-TONS	3.0 SPS MATERIAL USAGE VS NATIONAL AND WORLD DEMANDS AND RESOURCES										CUMULATIVE RESE. FOR 224 STATS.		REMARKS
		PERCENT OF YEAR 2000 DEMAND						PERCENT OF RESERVES		DEM. RANK	RES. RANK			
		US			WORLD			US	WORLD					
HI	MED	LO	HI	MED	LO	US	WORLD							
AL	.108+27	.277+21	.360+21	.549+21	.106+01	.137+01	.220+01	.132+02	.800-01			2956.	8.96	
AG	.100+01	.597+22	.799+22	.110+01	.220+02	.303+02	.410+02	.170+22	.335+03			.38	.07	
AR	.410+05	.737+01	.878+21	.925+21	.398+01	.329+01	.353+01	-.990-12	-.990-12			-999	-999	MANUFACTURING REQUIRED
AS	.311+02	.667+21	.820+21	.110+20	.220+01	.357+01	.430+01	.200+24	.800+25			.0044	.0017	METAL PROD REQUIRED
AU	.300+01	.260+00	.320+00	.420+00	.120+00	.135+00	.145+00	.326+01	.809+02			7.30	1.8	
B														
CO														
CR														
CU	.650+01	.507+01	.555+01	.661+21	.145+01	.191+01	.278+01	.883+02	.239+02			1.86	.51	
GA	.289+22	.245+24	.419+24	.182+25	.850+03	.141+24	.413+04	.100-11	.713+03				7.24	METAL PROD REQUIRED
H2	.754+26	.850+20	.126+21	.276+21	.310+00	.540+00	.198+01	.100-11	.109-11					MANUFACTURING CAPACITY
HO	.130+01	.140+22	.150+22	.190+22	.570+03	.630+03	.650+03	.450+04	.260+04			.01	.005	
HI														
H2														
O2	.100+28	.148+22	.194+22	.283+22	.550+01	.727+21	.104+02	.100-11	-.990-12					MANUFACTURING CAPACITY REQ.
PT	.200+01	.207+21	.370+21	.520+21	.100+01	.127+01	.150+01	.490+01	.300+00					UPPER LIMIT MAY BE EXCEEDED MANUFACTURING CAPACITY REQ.
SI	.110+25	.781+24	.934+24	.115+25	.100-11	.150-11	.100-11	.100-11	.109-11					
W	.625+12	.143+00	.181+00	.246+00	.590+01	.600+01	.830+01	.460+01	.500+02					

NOTE: THE VALUE .1000-11, INDICATES TO BE DETERMINED

X. PROGRAM DEVELOPMENT PLAN

W. S. Beckham
Urban Systems Project Office

A. Program Phasing

The SPS program plan has been divided into four phases as illustrated in figure X-1. The four phases include an initial phase of system definition and exploratory technology followed by a technology advancement phase. These two phases would provide the information required to make a decision in the 1987 time period to proceed with full-scale development of the system. Assuming a positive decision at this time, an initial system might be in operation in the 1995 time period. The subsequent and final phase would be one of commercialization involving multiple SPS's such as identified in the various scenarios described in section III.

B. System Definition and Exploratory Technology Phase

This immediate phase would include improved definition and assessment of satellite power system concepts; transportation, construction, and operational support systems; design, development, test and evaluation (DDT&E), and recurring costs and environmental impact. A further description of activities in these four areas is presented in figure X-2.

More definitive comparisons of the relative merits of space solar power with other systems such as coal, nuclear, and solar terrestrial are also required in the present phase. Detailed areas in which these comparisons should be attained are presented in figure X-3.

This phase will also involve the detailed definition and cost of the subsequent technological advancement phase. Key activities to support this definition will include solar power system studies, space station analyses as related to subscale system evaluation, technology studies, and program analyses.

A number of significant test activities are proposed to be conducted in this initial phase. A partial listing of these tests is included in figure X-4.

C. Technology Advancement Phase

The technology advancement phase (FY80-87) consists of three elements: ground-based developments, space experiments, and a subscale system evaluation in space. The results of these activities must also be integrated into a continuing program and system analysis and evaluation. A more detailed breakdown of activities that will be required in each of the three elements is presented in figure X-5.

X-2

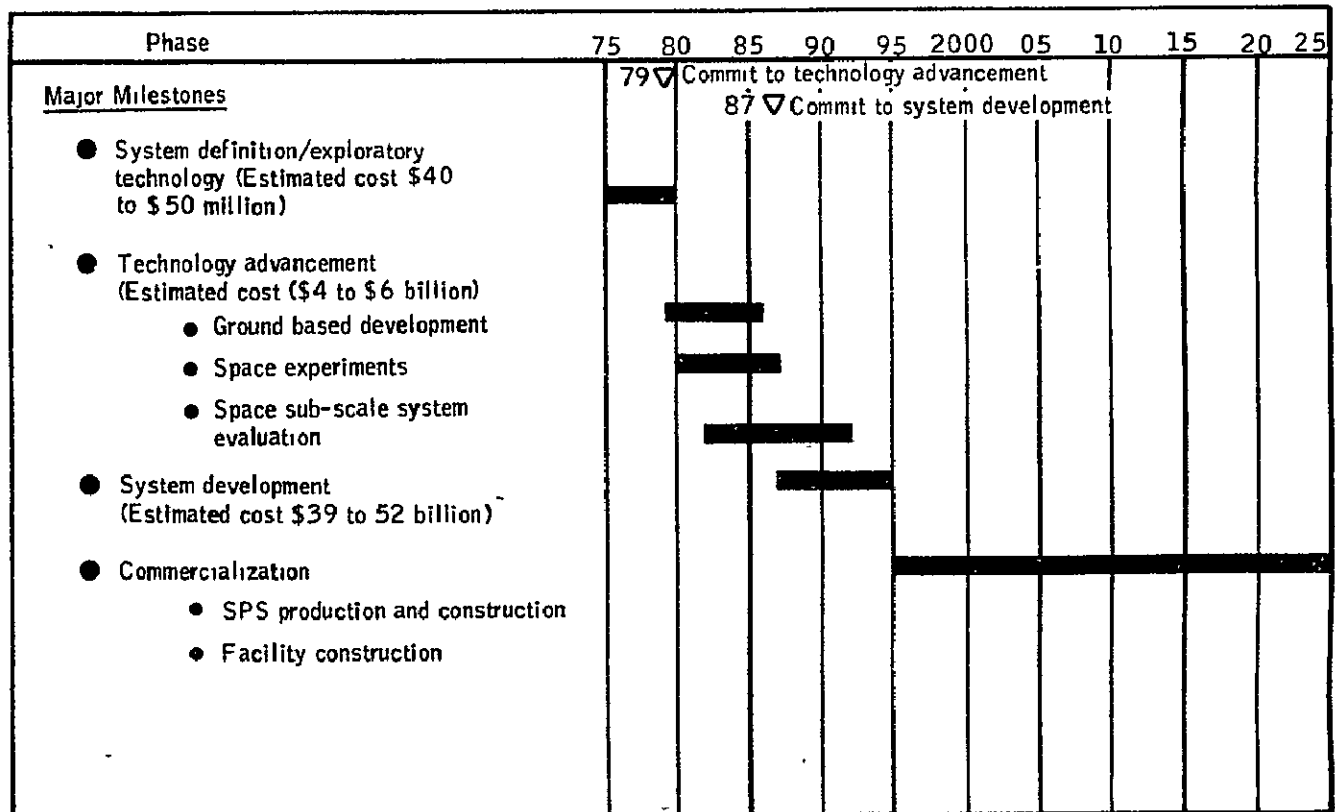


Figure X-1.- Space solar power projected program phasing.

A. SATELLITE POWER SYSTEM CONCEPTS

- o DEFINITIVE COMPARATIVE ANALYSIS AND ASSESSMENT OF THE SEVERAL POWER-GENERATION CONCEPTS
 - SOLAR CELLS (SILICON, GALLIUM ARSENIDE)
 - THERMAL (BRAYTON)
- o RELATIVE MERITS OF LOW-EARTH ORBIT AND GEOSYNCHRONOUS-ORBIT CONSTRUCTION LOCATIONS
- o CONCEPTUAL DESIGN AND ANALYSIS OF A VARIETY OF CONFIGURATIONS
- o DETAILED STRUCTURAL, THERMAL, AND ATTITUDE STABILIZATION AND CONTROL ANALYSES (INCLUDING MODELING AND SIMULATIONS) FOR CONSTRUCTION, MAINTENANCE, AND OPERATION PERIODS
- o IN-DEPTH ANALYSIS AND EVALUATION OF EACH SUBSYSTEM/MAJOR COMPONENT EFFICIENCIES
- o RECTENNA ANALYSES WITH EMPHASIS ON REDUCING COSTS AND CONSTRUCTION ENERGY AND NATURAL RESOURCE REQUIREMENTS
- o DEVELOPMENT AND OPTIMIZATION OF SYSTEM AND DETAILED CONCEPTS FOR SPS-POWER GRID INTERFACE AND OPERATION

B. SUPPORT SYSTEMS

- o CONCEIVE AND EVALUATE TECHNIQUES AND DEVICES FOR CONSTRUCTION, INSPECTION, AND MAINTENANCE OF SATELLITE POWER SYSTEMS, INCLUDING DESIGN CHARACTERISTICS OF A CONSTRUCTION FACILITY WITH ASSOCIATED UTILITY, HABITATION, AND CONTROL FEATURES
- o REFINE STUDIES OF HEAVY LIFT LAUNCH VEHICLES
 - WINGED LAND LANDING VS. BALLISTIC WATER LANDING
 - PAYLOAD/FLEET SIZING
 - OPERATION COST ANALYSIS
 - FACILITY REQUIREMENTS
 - LAUNCH LOCATIONS
- o EVALUATE AND ASSESS ORBITAL TRANSFER MISSION MODES, INCLUDING DESIGN, LIFE, AND COST OF ELECTRICAL, CHEMICAL, AND NUCLEAR PROPULSION SYSTEMS

C. DDT&E AND RECURRING COSTS

- o TOTAL DDT&E COSTS HAVE NOT BEEN DERIVED IN ANY DETAIL. ROUGH ESTIMATES RANGE FROM \$30 TO \$70 BILLION OVER 10- TO 20-YEAR PERIOD. PLANNED STUDIES WOULD TARGET FOR AN ESTIMATE WITH +20 PERCENT ACCURACY
- o PRESENT STUDIES INDICATE AS MUCH AS A FACTOR OF 3 TO 4 (30 TO 110 MILLS/KWH) SPREAD IN ESTIMATES OF THE COST OF COMMERCIAL POWER FROM SOLAR POWER SYSTEMS
- o SYSTEMS STUDIES AND OTHER ACTIVITIES SHOULD REDUCE THIS ESTIMATE SPREAD TO APPROXIMATELY 2 (30 TO 60, 50 TO 100) IN THE NEXT 2 YEARS

Figure X-2.- System definition and exploratory technology phase activities.

D. ENVIRONMENTAL IMPACT

- o PRELIMINARY ASSESSMENT OF THE SYSTEM RESULTS IN MODEST IMPACTS:
AND/OR QUESTIONS TO BE ANSWERED
- o ENVIRONMENT AREAS MAY BE GROUPED AS FOLLOWS:
 - VEHICLE EMISSIONS/OPERATIONS
 - MICROWAVE BEAM
 - EARTH ACTIVITIES
 - SPACE OPERATIONAL ENVIRONMENT
- o WITHIN THE NEXT 2 YEARS, ANALYSES SHOULD PROVIDE INFORMATION
FOR A FIRST-ORDER IMPACT ANALYSIS IN ALL AREAS. TEST DATA RELATED
TO THE BIOLOGICAL EFFECTS OF THE MICROWAVE BEAM ON HUMANS ARE
PROBABLY THE MOST TIME-CRITICAL AREA
- o SUBSEQUENT FIGURES OUTLINE QUESTIONS TO BE TREATED IN EACH
ENVIRONMENTAL AREA

D.1 VEHICLE EMISSIONS/OPERATIONS

- o TROPOSPHERE
 - LAUNCH AREA GAS CLOUD, RAINOUT CONDITIONS, AND
BIOLOGICAL EFFECTS
 - METEOROLOGICAL EFFECTS AND ECOLOGICAL CONSEQUENCES
- o STRATOSPHERE
 - PHYSICAL AND BIOMEDICAL OZONE DEPLETION EFFECTS
 - WEATHER MODIFICATION ASSESSMENT
- o IONOSPHERE
 - ASSESSMENT OF 'PUNCH OUT' EFFECT
- o THERMOSPHERE/
MAGNETOSPHERE
 - PREDICTED DISTRIBUTIONS
- o SONIC BOOM/
LAUNCH NOISE
 - PREDICTED LEVELS
 - POSSIBILITY OF SEISMIC EFFECTS
- o VEHICLE FAILURE
EFFECTS
 - ATMOSPHERE/SURFACE EFFECTS

D.2 MICROWAVE BEAM

- o IONOSPHERE/BEAM INTERACTION
- o EFFECTS ON HUMANS, ANIMALS, PLANTS
- o EFFECTS ON ASTRONOMY, COMMUNICATIONS, ELECTRONIC EQUIPMENT
- o WEATHER EFFECTS AT SURFACE AND IN TROPOSPHERE

Figure X-2.- Continued.

D.3 EARTH ACTIVITIES

- o RESOURCE EXTRACTION, MANUFACTURING, AND TRANSPORTATION EFFECTS
- o LAND USE
 - RECTENNA
 - LAUNCH AND RECOVERY SITES

D.4 OPERATIONAL SPACE ENVIRONMENT

- o IONIZING RADIATION
 - BIOLOGICAL AND EQUIPMENT EFFECTS
 - DOSAGE AND SHIELDING ASSESSMENT
- o MICROWAVE RADIATION
 - REFLECTED/SCATTERED
- o MAGNETOSPHERE PLASMA
 - SPACECRAFT CHARGING
 - HIGH VOLTAGE - PLASMA INTERACTION
- o METEOROIDS
 - CREW/HABITAT
 - EQUIPMENT/SOLAR CELLS
- o SPACE "TRAFFIC"
 - MULTIPLE SPS'S AND THEIR LOGISTICS SUPPORT
 - OTHER SATELLITES

Figure X-2.- Concluded.

REFINE PRESENT PRELIMINARY COMPARISONS IN FOLLOWING AREAS:

- o COST AND RELATED ECONOMIC CONSIDERATIONS
- o TECHNOLOGY REQUIREMENTS
- o ENVIRONMENTAL CONSIDERATIONS
- o SAFETY
- o LOGISTICS IMPLICATIONS
- o NATURAL RESOURCE REQUIREMENTS
- o ENERGY PAYBACK
- o INTERNATIONAL CONSIDERATIONS
- o REGULATORY CONSIDERATIONS
- o INTERFACE WITH PRESENT STRUCTURE

Figure X-3.- The relative merits of space solar power and other systems - coal, nuclear, solar terrestrial.

- o MICROWAVE BEAM - IONOSPHERE INTERACTION TEST
 - ARECIBO AND POSSIBLY NEW OR MODIFIED SYSTEMS
- o DEMONSTRATE PHASED-ARRAY CONCEPT
 - GOLDSTONE
- o COMPLETE LABORATORY PERFORMANCE EVALUATION OF GaAs SOLAR CELLS
- o LABORATORY-SCALE TESTING OF IMPROVED HIGH-RATE SOLAR CELL PRODUCTION TECHNIQUES
- o THERMAL-VACUUM TESTING OF ADVANCED RADIATOR CONCEPTS
- o DESIGN AND TESTING OF PROTOTYPE SPACE FABRICATION DEVICE
- o EVALUATION OF GRAPHITE EPOXY CASTINGS
- o TESTING AND EVALUATION OF MPD AND THERMAL ARC THRUSTERS
- o PRELIMINARY WIND-TUNNEL TESTING OF CONCEPTUAL LAUNCH, REENTRY, AND LANDING CONFIGURATIONS
- o COMPLETE INITIAL TESTS OF BIOLOGICAL EFFECTS OF 'HIGH Z' RADIATION
- o PRELIMINARY TESTS OF MICROWAVE RADIATION ON EQUIPMENT, VEGETATION, AND ANIMALS
- o THERMAL-VACUUM TESTING OF TYPICAL STRUCTURES
- o ADDITIONAL CRITICAL TEST AS IDENTIFIED IN STUDIES

Figure X-4.- Significant test activities, initial phase, July 1976 to July 1978 (partial listing).

<u>TYPICAL ACTIVITIES</u>		
<u>GROUND-BASED DEVELOPMENT</u>	<u>SPACE EXPERIMENTS</u>	<u>SPACE SUBSCALE SYSTEM DEVELOPMENT AND EVALUATION</u>
MICROWAVE POWER TRANSMISSION/ RECEIVING TECHNIQUES	STRUCTURAL ELEMENTS AND FABRICATION TECHNIQUES	CONSTRUCTION/ASSEMBLY OF LARGE SYSTEMS
MICROWAVE GENERATOR DEVELOPMENT	ELECTRONIC/MECHANICAL COMPONENTS	LOGISTICS OF LARGE-SCALE SPACE OPERATIONS
EFFICIENT, LIGHTWEIGHT, LOW- COST SPACE SOLAR CELLS	- ADVANCED SOLAR CELLS - MATERIALS - MICROWAVE GENERATORS - THERMAL CONVERTER COMPONENTS	IN-SPACE PRODUCTIVITY AND ASSEMBLY COSTS
THERMAL CONVERSION SYSTEM, COMPONENT TECHNOLOGY	HIGH-VOLTAGE PLASMA EFFECTS	END-TO-END POWER SYSTEM PERFORMANCE
POWER PROCESSING AND DISTRIBUTION COMPONENTS	ORBITAL TRANSFER THRUSTER FLIGHT EVALUATION	
MATERIALS INVESTIGATION	PROPELLANT TRANSFER	
ORBITAL TRANSFER THRUSTER TECHNOLOGY	EMISSIONS - ATMOSPHERE COMPATIBILITY	
ENVIRONMENT - BIOLOGICAL EFFECTS - IONOSPHERE IMPACTS - RADIOFREQUENCY INTERFERENCE		

Figure X-5.- Technology advancement phase.

Comments pertinent to the activities in this phase are presented in the following paragraphs.

Solar energy conversion.- The most significant contribution to technical and economic feasibility of SPS can be obtained by increase of solar cell array power per unit mass (kilowatts/kilogram) and decrease in cost. It is also expected that solar cell life will play a key role in determining economic feasibility.

Structures.- Although structures appear to be a relatively low weight item in current SPS configurations, it is expected that significant analytical and test efforts will be required to develop and qualify these systems. The main difficulty in this area is the inability to ground test (simulate) the large, lightweight systems.

Microwave conversion and control.- The satisfactory performance of dc/rf power converters is essential to the success of the SPS concept. The key performance parameters are efficiency, lifetime, and noise characteristics. Low component weight is desirable, but it is of secondary importance to conversion efficiency, which directly affects solar array size and weight.

Environmental impact.- The design and performance of SPS is directly influenced by allowable microwave radiation intensity levels on the ground and in the upper atmosphere. It is expected that a major test program will be required to resolve environmental issues and to establish practical but safe design criteria.

Space transportation.- The installed cost of SPS is strongly influenced by space transportation costs. Although the HLLV development appears to be primarily a scale-up and product improvement of existing rocket technology, such as was accomplished in the Saturn V development, significant testing and development will be required to demonstrate low-cost operations and efficient equipment reuse concepts. Development of a suitable low-cost, long-life OTV propulsion system is also mandatory regardless of SPS design configuration.

D. System Development

Detailed plans for the system development phase would be developed during the Technology Advancement phase of the program. The scope of the effort would exceed that required for the Apollo Program, particularly since a continuing commercial phase would be envisaged requiring a large industrial capacity. The ability to accomplish this in the period between 1985 and 1987 will be dependent upon the planning, organization, and long lead-time activities conducted during the preceding phase. The transportation and associated launch and recovery (or landing) facility development will constitute a particularly significant theme of the overall activities of this phase.

E. Program Costs

The program-plan (fig. X-1) shows preliminary estimates of costs by major phase. The initial phase (system definition and exploratory technology) is estimated to cost between \$40 and \$50 million. The major elements in this estimate are as follows:

1. System studies - \$10 to \$14 million
2. Environmental analysis and tests - \$5 to \$6 million
3. Microwave conversion and control - \$10 to \$12 million
4. Structure (thermal and materials) - \$7 to \$9 million
5. Orbit transfer propulsion, exploratory technology - \$7 to \$9 million

Commitment to the technology advancement phase would occur in 1979, assuming favorable results from the initial program phase. The technology advancement phase is estimated to cost \$4 to \$6 billion over a period of about 10 years. The peak annual funding for this phase would be about \$2.0 billion in the 1985-87 time frame. The major cost element of the phase would be the development of techniques and the subsequent construction and evaluation of a subscale system in orbit.

The system development phase (initiated 1987) would involve commitment to a multibillion per year program of 8 to 10 years' duration. The total cost is estimated to be \$45 to \$55 billion, with the major cost elements being development and verification of space transportation systems (\$9 to \$12 billion), solar power satellite systems (\$19 to \$22 billion) and orbital construction facilities (\$16 to \$19 billion).

Expenditures for the final commercialization phase would depend primarily upon SPS unit costs, space transportation costs, and rate of installation. Initial estimates of these costs are given in section XI of this report.

XI. PROGRAM COST AND ECONOMIC ANALYSIS

Tony Redding
Urban Systems Project Office

A. Methodology

The SPS design concepts evaluated involve improved technology in several areas as well as new and vastly expanded space activities over those which have been accomplished to date. The economic analysis and evaluation of SPS are based on projections of capability and technology resulting from a major development program as described in section X. For analytic purposes, it was assumed that the SPS ground-receiving stations (rectennas) would be operated as baseload power sources in a large power grid. This grid would include conventional powerplants (nuclear and fossil fuel) for both baseload and peaking requirements. The general approach adopted was to derive program costs and the associated power production costs for the implementation of 112 10-GW power stations over a period of 30 years beginning in 1995. The program costs were used to determine SPS unit costs. Annual operating and maintenance (O&M) costs were also determined as were the return rates necessary to amortize design, development, test, and evaluation (DDT&E) costs. These costs are then compared with costs of conventional baseload and other future power systems.

B. SPS Costs

The major cost elements of the SPS are as follows:

1. Power Station System - consists of capital cost of Solar Energy Collection System, Microwave Power Transmission System, and the Microwave Reception and Conversion System.
2. Space Transportation System - consists of capital cost and operation cost of HLLV's, COTV's, logistic vehicles (PLV's, POTV's) and associated launch, recovery, and refurbishment facilities.
3. Space Construction System - consists of capital costs of space facilities and equipment for construction and assembly of power station systems, including manpower requirements.
4. Operational Costs - consists of costs of manpower, transportation, consumables, and repair/replacement hardware for sustaining and maintaining operation of the power station system.
5. DDT&E Costs - consists of all nonrecurring research and development funds expended prior to initiation of commercialization (1995).

The preceding cost elements may be expressed in mills/kWh and combined to obtain a total cost of electricity (COE) at the busbar as follows:

$$\text{COE (mills/kWh)} = \text{capital recovery} + \text{O\&M} + \text{DDT\&E}$$

This equation with definition of all terms is shown in figure XI-1.

Capital costs.- The capital cost \overline{CC} of an SPS consists of satellite hardware, satellite construction, space transportation, and ground

system (rectenna) costs. The satellite hardware costs were determined using the cost estimating relationships (CER's) and satellite weight characteristics given in section IV. A range of costs was determined based on satellite weight, satellite configuration and construction location (LEO or GEO), and unit cost of solar cells varying from \$100 to \$500/kW.

The cost of satellite construction was based on requirements delineated in section V. This cost item includes space construction facilities and equipment and space construction personnel.

The space construction facilities are to house construction personnel and equipment and are located in LEO and GEO, as required by the particular construction location and configuration. The costs of these facilities were prorated over the number of satellites constructed because they are reusable. The facilities were estimated at the rate of \$250/kg recurring hardware cost.

The space transportation costs and cost variables are discussed in detail in section VI. The transportation cost per SPS was determined by summing the total space transportation cost for 112 satellites and dividing by 112 to reflect the reusability of launch and orbit transfer vehicles.

The rectenna costs were based primarily upon the recurring costs of diodes, circuits, and the support structure. Unit costs utilized are given in section IV. As indicated in figure XI-1, a plant lifetime of 30 years was assumed in the computation of capital recovery rate. Also, a fixed rate of return of 15 percent for principal, interest, taxes, and insurance was utilized in all cases. The SPS plant factor utilized was 0.92, which is based on an average downtime of 4 weeks/yr for maintenance and repair. This downtime period would include the loss of power during the brief eclipse periods.

O&M costs.- The primary operation of SPS will be conducted from the ground receiving station. It is anticipated that routine, but infrequent, "onboard" monitoring and inspection may also be required. This may be accomplished by a crew that services several SPS's, thus reducing the costs attributable to a single SPS.

As a baseload power system, SPS will be designed to operate at full capacity year round. It is anticipated, however, that scheduled shut-downs of several days' duration will be required annually to replace or repair failed or malfunctioning components (klystron tubes, solar array blanket sections, etc.). In such cases, an HLLV and the selected COTV concept could be scheduled to deliver the hardware. Personnel and consumables would be delivered by the personnel transportation vehicles. Preliminary estimates of annual O&M costs were based on the following assumptions:

Cost of electricity (mills/kWh) = Capital recovery + O&M + DDT&E

$$\text{Capital recovery} = \left[\frac{r}{1 - \left(\frac{1}{r+1}\right)^y} \right] \left(\frac{\overline{CC}}{E} \right) (1000)$$

r = rate of return, 15 percent assumed

y = plant lifetime, 30 years assumed

\overline{CC} = satellite materials + construction + space transportation + rectenna

E = (plant capacity, kW) (plant factor) (hours/yr)

Operation and maintenance

$$\text{O\&M} = \frac{(\text{Manpower} + \text{materials} + \text{space transportation})/\text{yr}}{\text{Annual electrical energy, kWh/yr}}$$

Design, development, test and evaluation

$$\text{DDT\&E} = \frac{\text{Total funding outlay}}{\left(\begin{array}{l} \text{Average no. of SPS's} \\ \text{over first 30 years} \end{array} \right) (E) (30)}$$

Figure XI-1.- Cost equations.

1. Ground O&M staff	48 man-yr/yr/10-GW system
2. On-orbit maintenance/repair	12 man-yr/yr
3. Repair/replacement/maintenance	1 percent of SPS mass/yr (per sec. VII)

DDT&E costs.- The DDT&E cost was based on development cost estimates for the major program elements. The estimates utilized are given in table XI-1. The estimates shown are the cumulative funding requirements from the start of technology advancement through system development (1995). The amortization of these costs over the initial 30 years of SPS operation per scenario B was accomplished using the equation shown at the bottom of figure XI-1. The numerator of the equation (total funding outlay) may include interest on capital expended during the 20-year development program. If a 9-percent interest charge is used, the effect is to increase the actual cost by a factor of about 1.4. However, as will be shown later, the DDT&E amortization cost is a small fraction of the cost of electricity.

Cost summary.- Table XI-2 shows a summary of the cost estimates for the range of design parameters investigated. Note that the total COE ranges from 29 to 115 mills/kWh. The COE for the "nominal" system is 50 to 59 mills/kWh, which consists of 46 to 52 mills/kWh for capital recovery, 3 mills/kWh (6 percent) for O&M, and 1 mill/kWh (2 percent) for amortization of DDT&E. The capital recovery cost breaks down to about 45 percent for space transportation, 40 percent for satellite and construction, and 15 percent for the rectenna. In the highest cost combination (COE = 115 mills/kWh), transportation costs increase to 60 to 70 percent. The satellite capital recovery is 25 to 30 percent and the rectenna only 8 to 10 percent.

The SPS capital cost expressed in \$/kW varies from a low of \$1400/kW to a high of \$5780/kW. This cost is the primary driver in establishing the cost of electricity for the SPS.

This nominal cost system results from an overall SPS efficiency of 5 percent, solar array weight of 0.4 kg/m², \$300/kW for solar cell blankets, and a transportation cost from Earth to GEO of \$108 to \$164/kg. The construction location and satellite configuration are seen to have little effect on COE.

Figure XI-2 illustrates the range of possible cost combinations for the SPS weight range investigated.

TABLE XI-1.- DDT&E COST ESTIMATE SUMMARY

Element	Estimated cost, \$ billion
Power station systems	19.0 to 22.0
HLLV	5.0 to 10.0
COTV	1.0 to 2.0
POTV	1.0 to 1.5
PLV	0.5 to 1.1
Construction facilities and equipment (orbital)	16.0 to 19.0
Total program	42.5 to 55.6

TABLE XI-2.- SUMMARY OF COST ESTIMATES AND RELEVANT PARAMETERS FOR 10-GW SPS

Construction configuration (a)	Parameters						Capital cost, \$/kW	Cost, mills/kWh						
	Efficiency, percent	Size, km ²	Weight, kgX10 ⁶ (b)	Solar array		Transportation, \$/kg		Capital recovery				DDT&E	O&M	Total
				kg/m ²	\$/kW			Rectenna	Satellite	Transportation	Total			
Maximum range														
G-CC	4	183	129 (124)	0.46	500	293	5560	8	27	69	104	1	6	111
G-T	4	183	133 (122)	.46	500	294	5780	8	28	71	107	1	7	115
L-T	4	183	133 (122)	.46	500	209	4660	8	28	51	87	1	6	94
Nominal range														
G-CC	5	144	84 (82)	0.40	300	152	2800	8	19	25	52	1	3	56
G-T	5	144	90 (84)	.40	300	164	3000	8	20	27	55	1	3	59
L-T	5	144	90 (84)	.40	300	108	2500	8	20	18	46	1	3	50
Minimum range														
G-CC	8	96	48 (47)	0.31	100	105	1500	5	11	12	28	1	2	31
G-T	8	96	52 (48)	.31	100	106	1600	5	12	12	29	1	2	32
L-T	8	96	52 (48)	.31	100	71	1400	5	12	9	26	1	2	29

^aG-CC = Construction in geosynchronous Earth orbit, column/cable construction.

G-T = Construction in geosynchronous Earth orbit; truss configuration.

L-T = Construction in low-Earth orbit; truss configuration.

^bNumbers in parentheses are final numbers, but cost model was not changed.

ORIGINAL PAGE IS
OF POOR QUALITY

XI-6

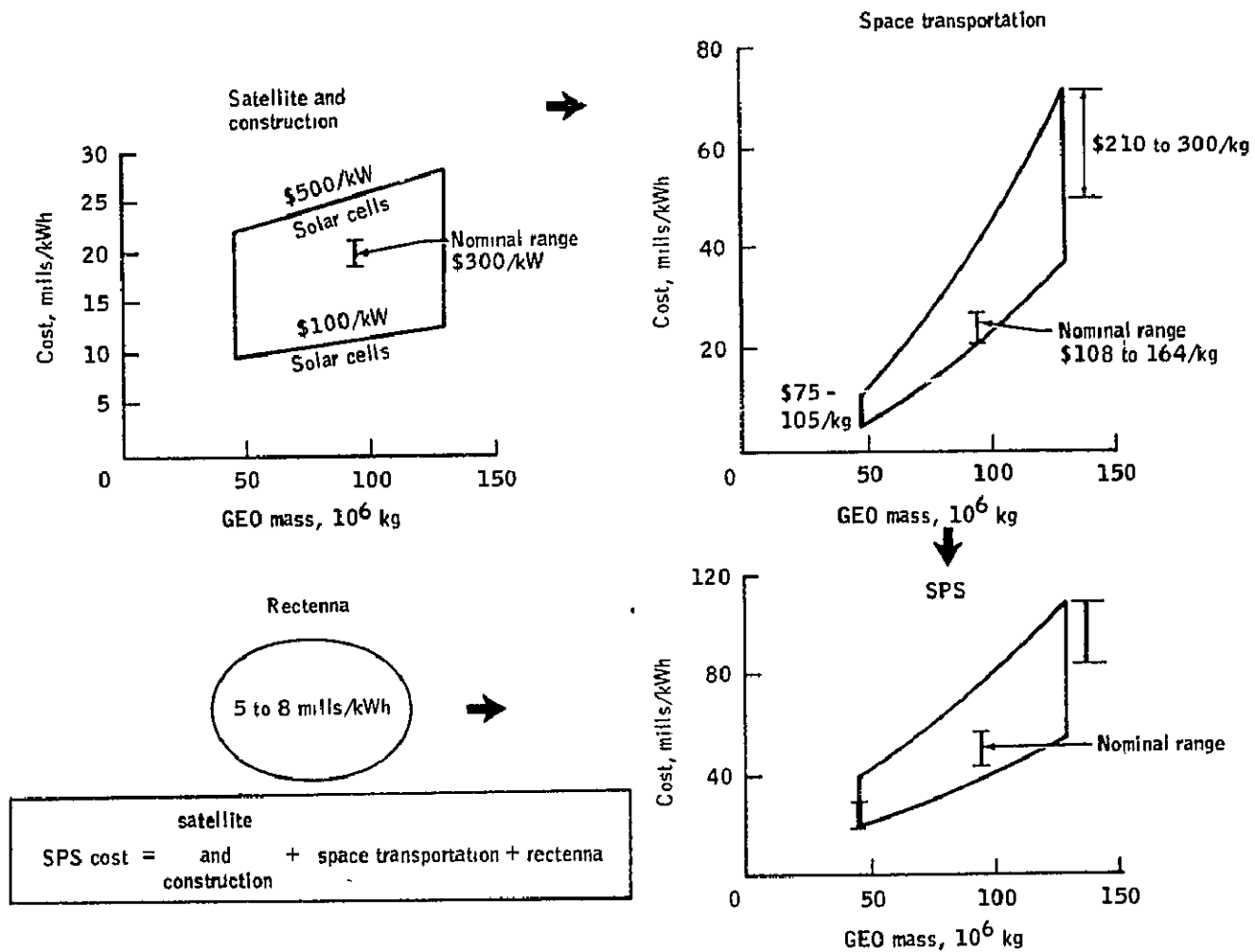


Figure XI-2.- SPS cost parametrics.

C. Comparison With Conventional and Other Advanced Systems

The economic viability of SPS will be dependent upon the costs and economics of alternative conventional and other future power systems.

Figure XI-3 shows a summary of typical power-generation costs for baseload conventional systems and several advanced concepts receiving research and development interest (and funding) at this time. The range of costs shown for each of the conventional systems corresponds to site-specific variations such as local environmental constraints, local labor and materials costs, land and site preparation costs, and fuel cost variations. The cost of coal-fired plants varies greatly depending upon the degree of stack gas scrubbing required and the type of cleanup system utilized. The conventional nuclear systems shown are light water reactors (pressurized water and boiling water). It is expected that the fast breeder reactor (liquid metal cooled) will have a capital cost in the \$800 to \$900/kW range.

The highest cost conventional systems are coal and nuclear, which are becoming the major electrical power sources for the last quarter of this century. As with SPS, the other advanced power systems shown generally have higher capital costs (\$/kW) than the conventional systems, but have zero-to-minimal fuel costs. The technical and economic feasibility of these systems is currently being investigated by ERDA and others. Although not shown in figure XI-3, nuclear fusion is another advanced power-generation system that currently receives significant research and development funding; however, major technological breakthroughs are still required before total system definition may be accomplished.

The range of power-generation costs for the advanced systems is 28 to 55 mills/kWh for the ocean thermal system to 97 to 121 mills/kWh for ground-based solar thermal systems. The solar thermal systems could not be strictly classified as a baseload system because only limited (short-term) energy storage is provided. The wind power-generation system cost is based on the "fuel saver" operational mode wherein the wind system operates in parallel with conventional plants when windspeeds are within a specified range, thus effecting a reduction of fuel consumption in the conventional plants. In this mode of operation, the wind plant annual capacity factor, which is a measure of equipment utilization, is very low (30 to 40 percent at best).

Also shown in the figure is the range of costs estimated for the SPS. The possible SPS costs span the range from a low of 29 mills/kWh for the lightest weight, lowest transportation and unit cost system to 115 mills/kWh for the highest weight, highest transportation and unit cost system. At the low range, the SPS cost is competitive with current conventional systems, and the highest estimated cost is no greater than that of other advanced systems presently receiving research and development support.

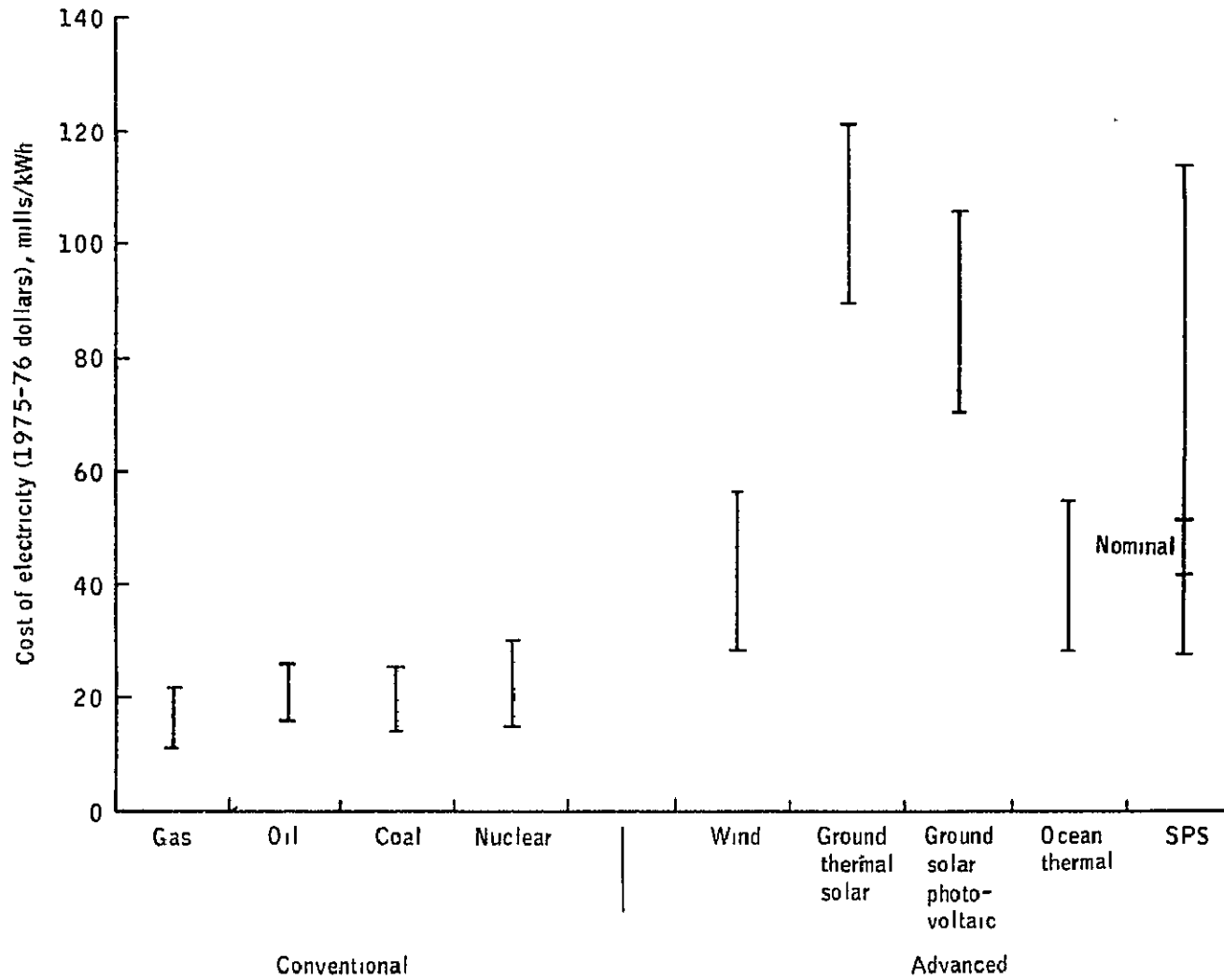


Figure XI-3.- Conventional and advanced power generation system costs.

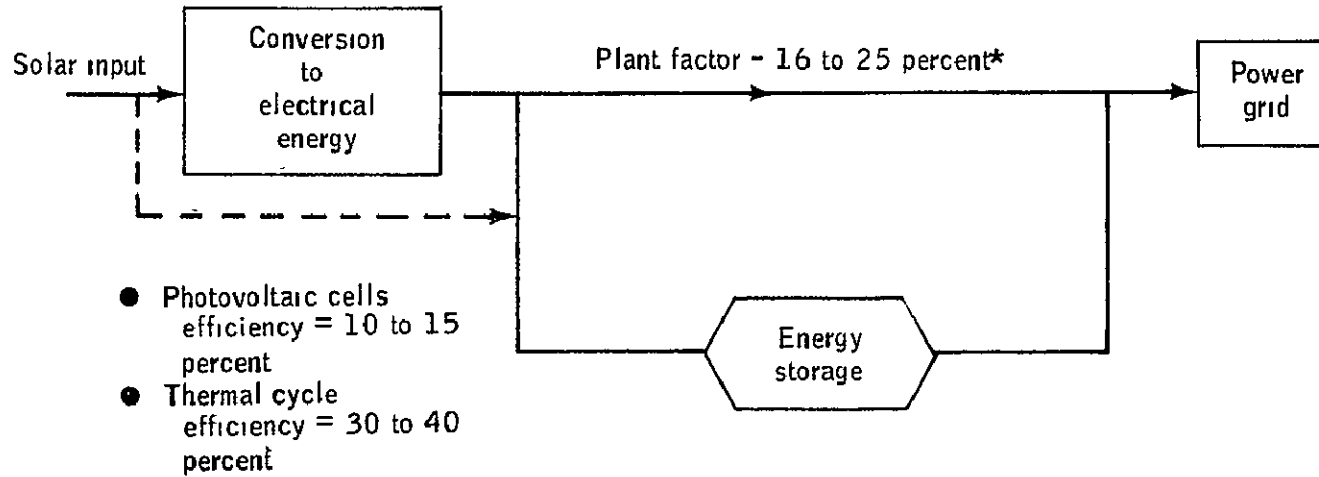
Terrestrial solar power.- A brief design and evaluation study was performed to determine the relative cost of electricity for alternate terrestrial solar power concepts. Figure XI-4 illustrates a generalized energy flow diagram for a terrestrial solar power system. As two example cases, a photovoltaic and a thermal cycle (steam Rankine) were analyzed to determine the cost of electricity for these systems.

The systems were sized to 5 GW to be comparable with a 5-GW SPS rectenna. In both cases, it was assumed that the plants were located in the southwestern region of the United States, where plant factors of as high as 0.16 to 0.25 may be obtainable. Figures XI-5 and XI-6 show the energy flow diagrams for hydro pumped storage and fuel cell/water electrolysis cell (hydrogen) storage terrestrial solar power systems. In the solar thermal case, a hybrid system consisting of a combination solar plant and coal-burning steam powerplant was analyzed. Figures XI-7 and XI-8 show the estimated COE for these cases as a function of storage time. It was assumed that with no storage the plant factor varied from 0.16 to 0.25, which is optimistic for such systems. The terrestrial photovoltaic system was costed based on \$300/kW solar cells operating at 11-percent efficiency.

Note on figure XI-8 that the nominal SPS cost (50 to 60 mills/kWh) is lower than the solar thermal terrestrial system by a substantial margin. The hybrid solar - coal plant has about half the cost of electricity of the SPS, but it saves only 13 percent in thermal energy (coal), whereas the SPS is a 100-percent substitution for the coal.

Figure XI-9 shows the estimated land requirements for the two cases mentioned above together with SPS land requirement. The terrestrial photovoltaic system requires about three times the land area of the solar thermal system because of its lower conversion efficiency.

ORIGINAL PAGE IS
OF POOR QUALITY



- Photovoltaic cells efficiency = 10 to 15 percent
- Thermal cycle efficiency = 30 to 40 percent

Hybrid

- Fossil
- Nuclear

- Batteries
- Thermal/chemical
- Pumped storage
- Flywheels
- Water electrolysis/fuel cell

*Southwest locations

Figure XI-4.- Terrestrial solar power.

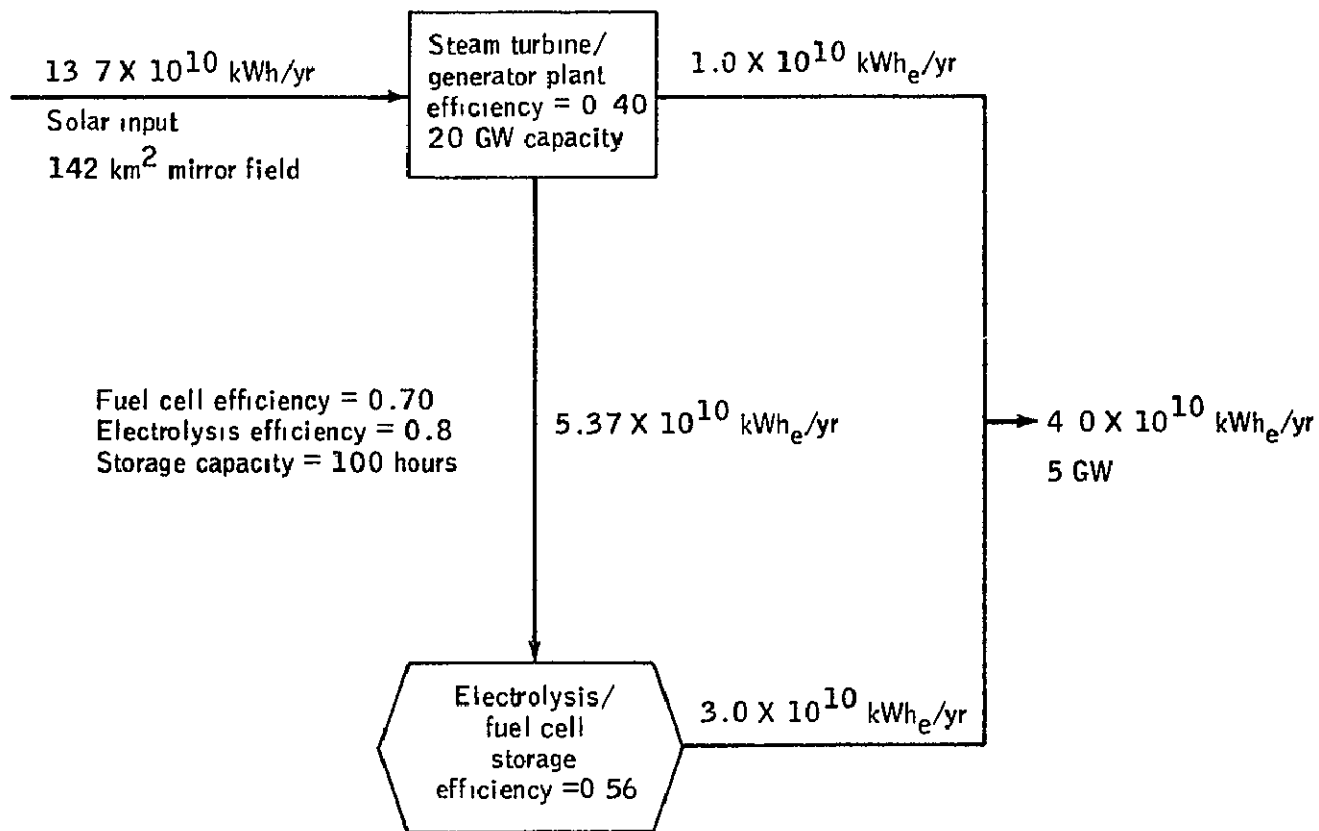


Figure XI-5.- The 5-GW solar power tower concept with electrolysis cell/fuel cell energy storage.

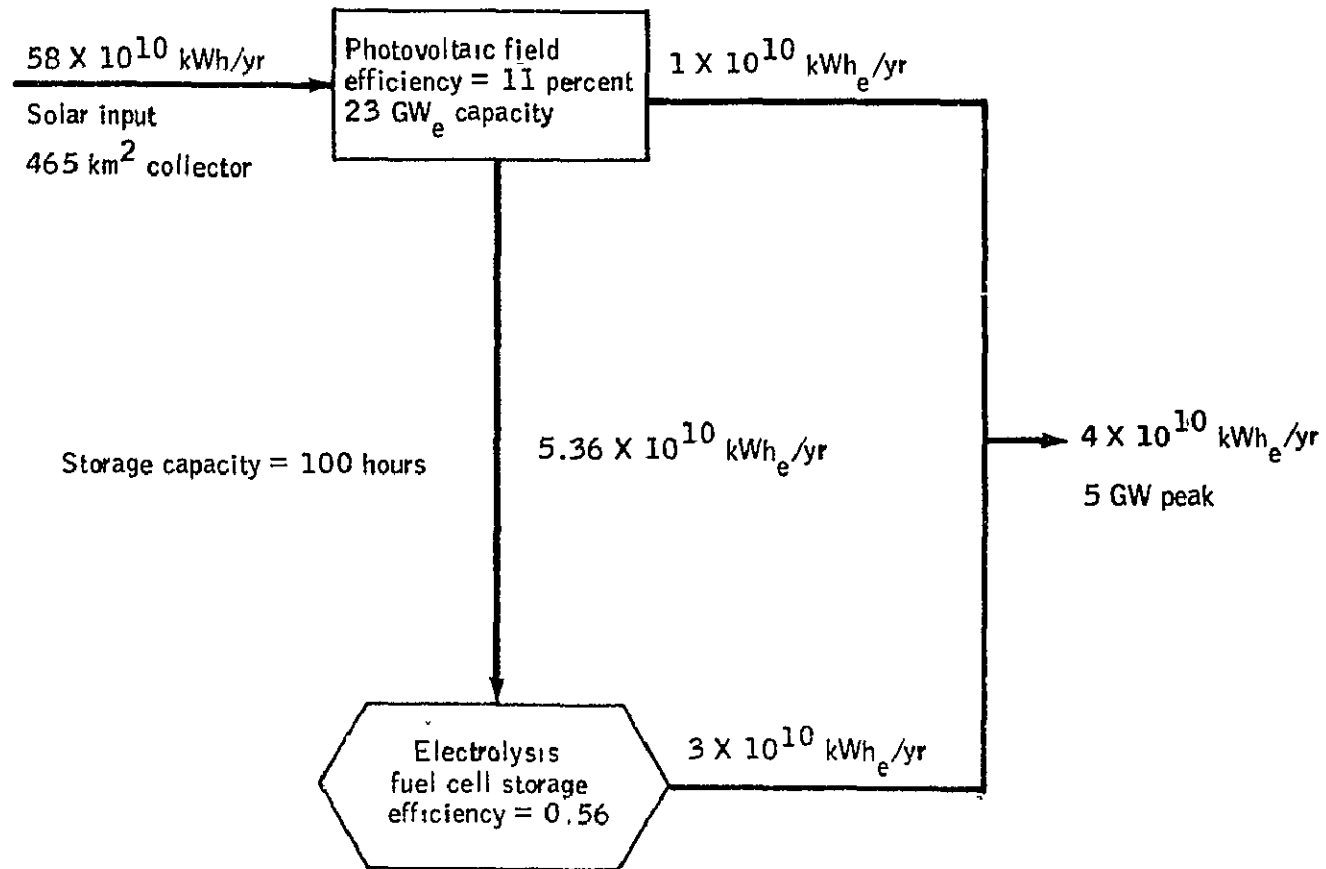


Figure XI-6.- The 5-GW solar photovoltaic-fuel cell/electrolysis cell system.

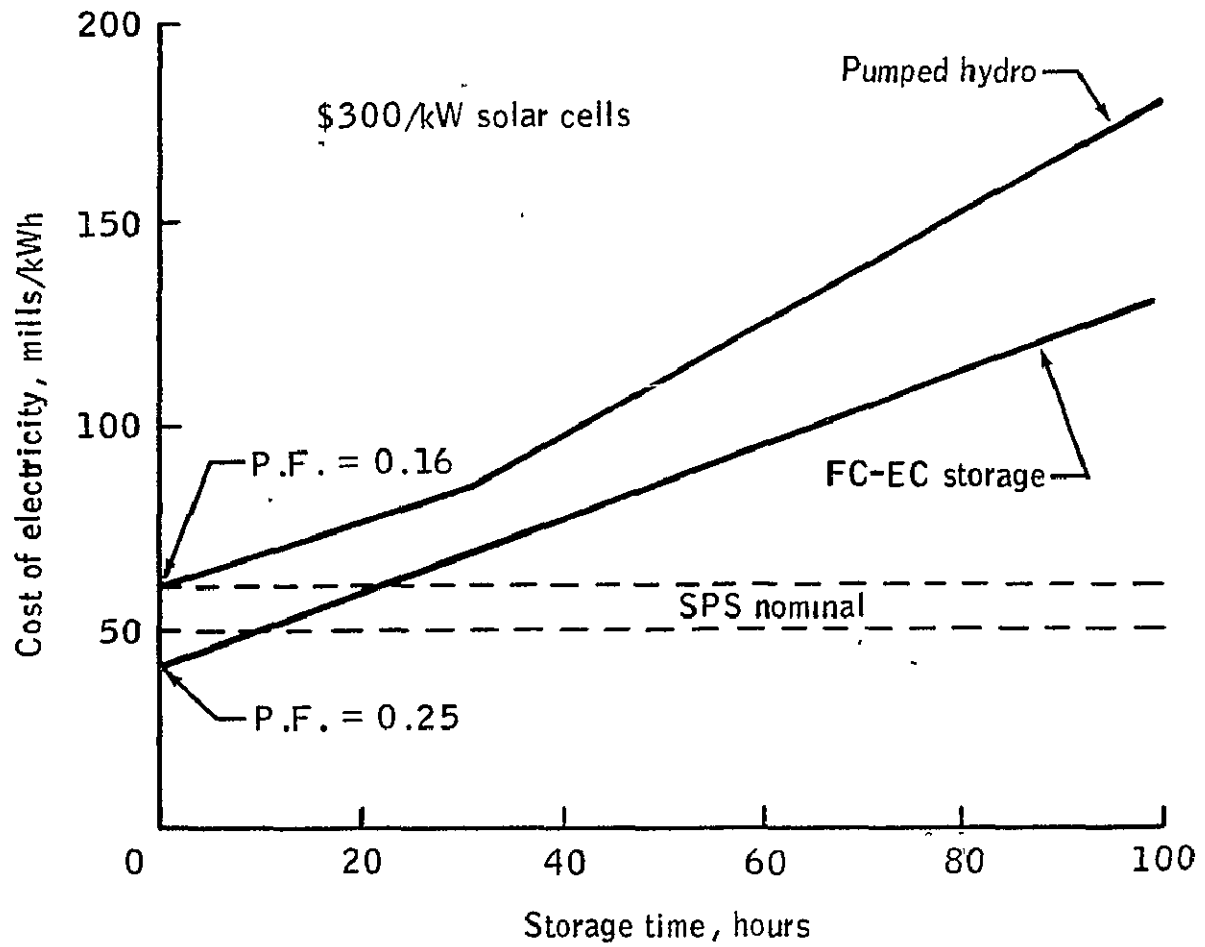


Figure XI-7.- Terrestrial solar photovoltaic power cost for 5-GW plant.

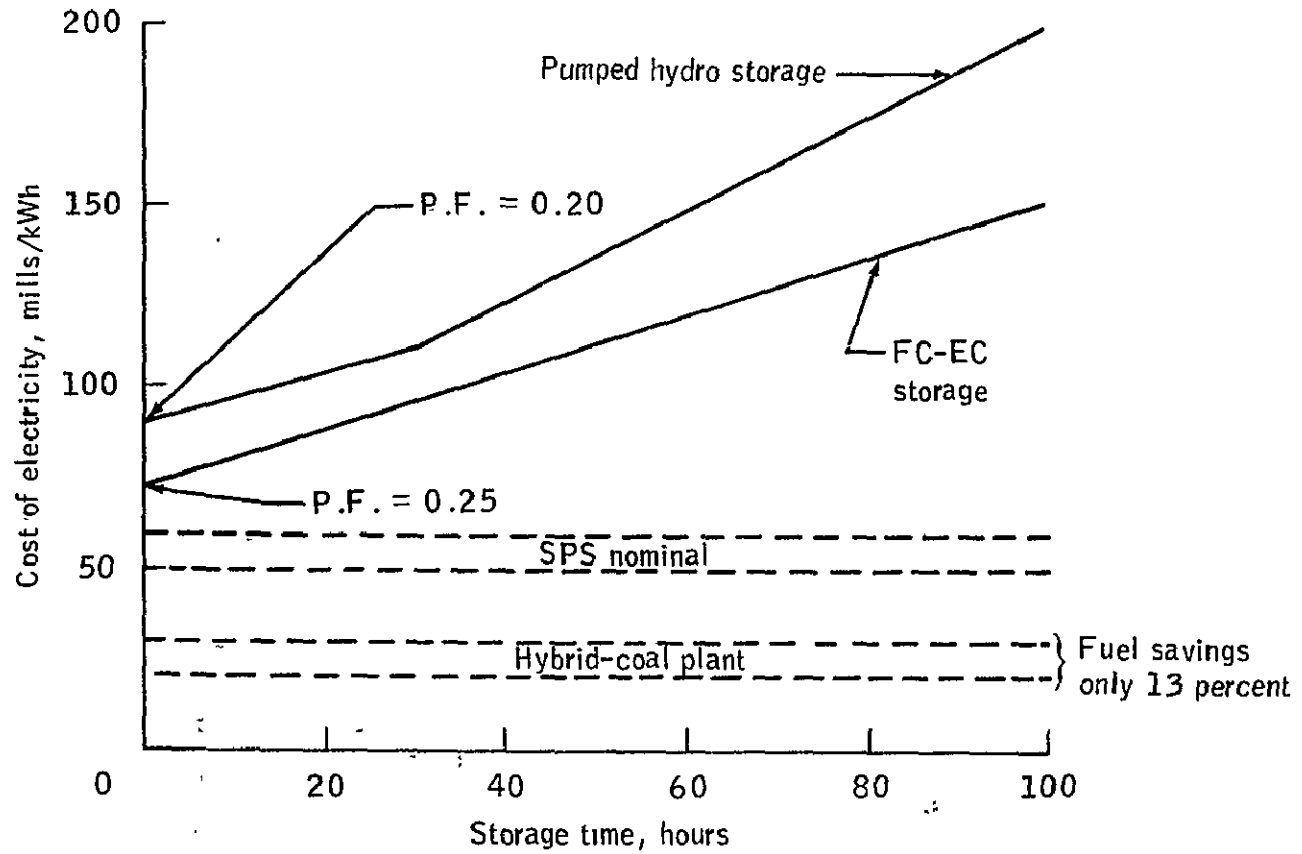


Figure XI-8.- Terrestrial solar thermal power cost for 5-GW power tower concept.

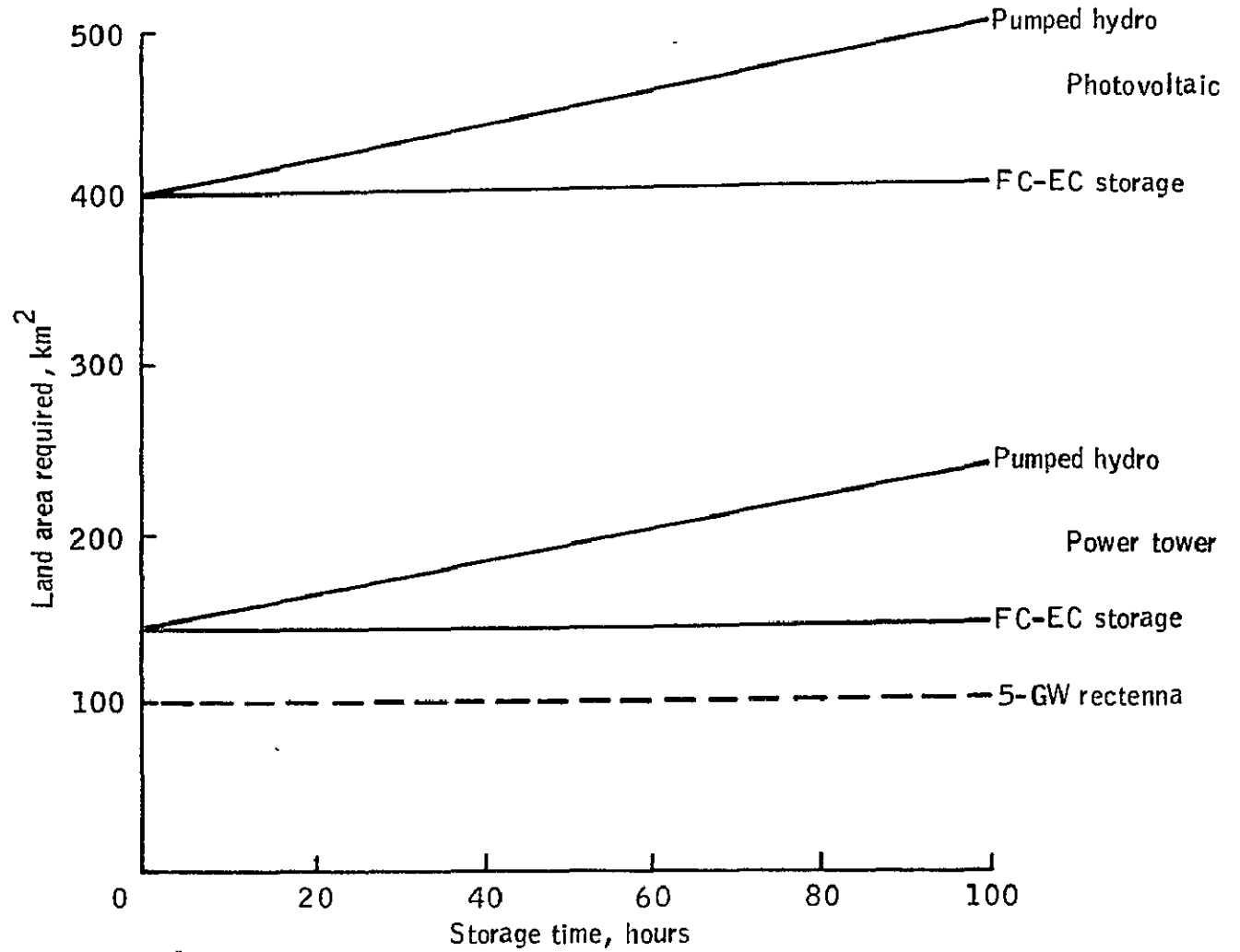


Figure XI-9.- Land area requirements for 5-GW plant.

D. Summary Remarks

Preliminary SPS cost and economic analyses indicate the following:

1. The SPS appears to be an economically viable electrical power generation system for the early 2000 time period. The cost to produce electricity is 29 to 115 mills/kWh based on a 15-percent rate of return on capital investment and a 0.92 plant capacity factor. The COE based on nominal system characteristics (weight, efficiencies, transportation, etc.) is 50 to 60 mills/kWh. These costs are in the competitive range with the 28 to 121 mills/kWh for other advanced systems of current interest and, at the lowest values, compete with conventional coal and nuclear costs (15 to 29 mills/kWh).

2. The highest cost component in the SPS concepts investigated is the solar cell blankets, comprising up to 81 percent of the SPS capital cost. Figure XI-10 shows this relationship together with the relative cost contribution of the other components.

3. DDT&E costs represent a substantial investment (up to \$50 billion); however, when this cost is amortized over the 30-year implementation period (112 power stations), the amortization cost is only 2 percent of the COE.

4. SPS O&M costs are 2 to 7 mills/kWh, which do not appear excessive based on initial estimates.

5. Concept 3 (truss structure, LEO construction, electric COTV) results in the lowest cost design; however, further analysis is required because of the very preliminary nature of this study.

6. The assumptions used in the "nominal" cases (50 to 60 mills/kWh) are worthy of mention because they represent a set of assumptions that are believed to be attainable and do not represent any extreme breakthroughs in technology. For instance, the silicon solar cell for this nominal design case was 10.4 percent efficient at the operating temperature of 100° C. The cost of the array was \$300/kW (ERDA goals: \$500/kW in 1985 and \$100 to \$300/kW in the year 2000)¹ and the basic cell was 4 mils thick. The total system end-to-end efficiency was 5.4 percent, which represented a total satellite weight of 84 000 metric tons. The transportation cost used was \$164/kg to GEO compared to the projected current Shuttle cost of \$550/kg to LEO.

Appendix A provides a more detail discussion of terrestrial solar power systems. Appendix B provides a description of the methodology utilized for SPS cost sensitivity analysis and discussions of preliminary results. Total costs given in Appendix B should not be compared with the costs given in the text of Section XI since the latter is based on specific design concepts, whereas the Appendix B gives generalized results that indicate parametric trends only.

¹Reference ERDA 48, vol. II.

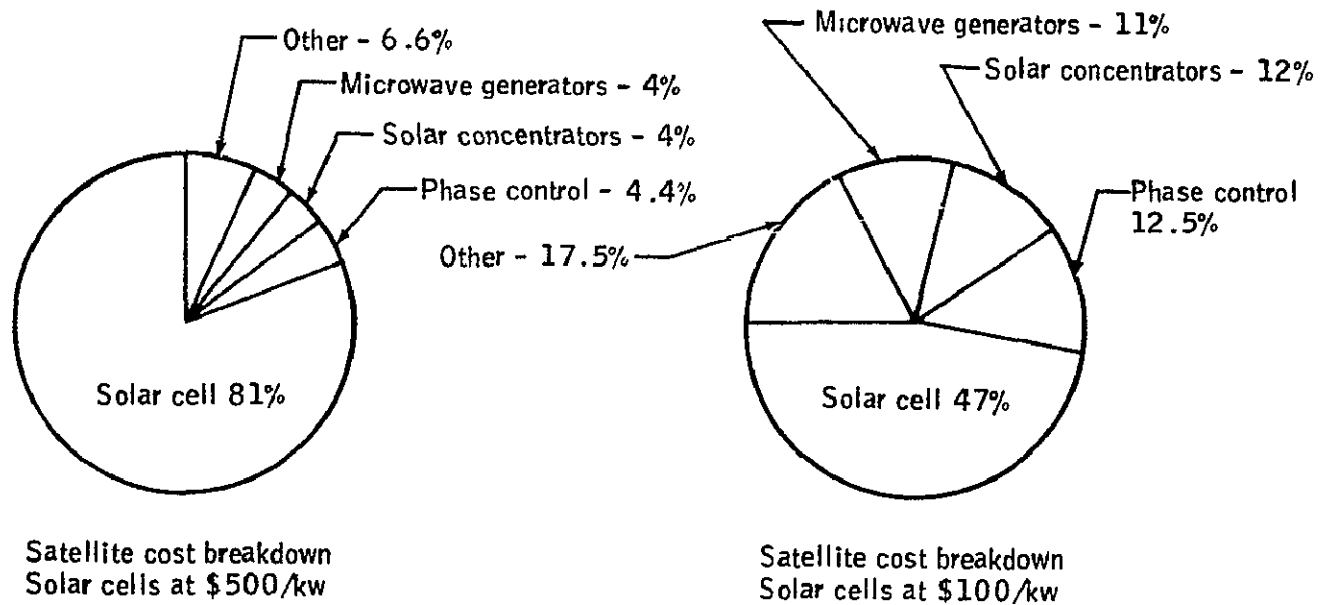


Figure XI-10.- Satellite cost breakdown.

Terrestrial Solar Power

Terrestrial solar plants generally fall into categories of thermal, photovoltaic, wind-powered, or ocean thermal gradient. Numerous other designs have been considered for the transformation of solar energy into electrical energy. Many devices have been built and proven workable, although often impractical. A few small systems have been developed to a level that comparisons with conventional systems can be reasonably estimated. Also, several large systems have been built into pilot plants for similar comparisons. These large solar plants such as the Soviet Union's Solar Technical Laboratory (Ref. 1) near the Turkish border, the University of Genoa's facility in Italy and the Solar Energy Laboratory at Odeillo, France have been operational for sufficient periods so that operational data is available. Another large pilot plant has been designed by The Martin-Marietta for location in central Arizona. A prototype to this is currently under construction at Sandia Labs, New Mexico. Those system designs which appear to have the greatest potential for large total capacity electrical power generation are being comparatively analyzed by the Jet Propulsion Laboratory (JPL) for the NASA Office of Energy Programs (Ref. 2). A more comprehensive analysis by JPL and others is summarized for each of the terrestrial solar power plant categories.

Basically solar thermal-electric power plants are classified as central receiver or distributed collector types.

a. The central receiver plant uses large mirrors or arrays of many mirrors with tracking mechanisms (heliostats) so that the solar energy is reflected onto a centrally located receiver. This allows large concentrations of energy at the receiver for producing a high temperature carrier fluid. Obviously, mirror arrangement, size and type (flat or focusing) provide a variety of variables for optimizing the collector field. Similarly, the type of tracking mechanisms and the design of the receivers, heat exchangers, storage facility, turbine/generator sets and heat rejection systems suggest a detailed tradeoff analysis.

b. The distributed collectors generally use parabolic dish collector surfaces which reflect and focus the solar energy with the assistance of tracking mechanisms onto individual receivers. The receivers can be coupled in parallel to produce large quantities of high temperature transport fluid (generally steam). However, a small heat engine such as a Brayton cycle engine can be located in the focal area for immediate mechanical to electrical energy conversion. Distributed collectors offer numerous variations as suggested by their intended function, including the generation of large quantities of electrical energy.

c. The most competitive terrestrial solar thermal-electric power plant is a central receiver configuration as reported by JPL. Figure XIA-1 is a summary of this analysis and it can be seen energy cost of the central receiver designs are generally less than that of the distributed receivers. The least cost configuration analyzed is the central receiver system with a six-hour storage capability and a wet-type heat rejection. The selection of the wet-type heat rejection is the most cost effective, assuming a sufficiency of water for evaporative cooling. It is realized that this may not be the case in some otherwise logical locations for central receivers. The low of 92 mills/KWe HR is over 11 percent less than the best distributed collector system studied.

The design of the central receiver power plant determined most cost effective is shown in Figure XIA-2. This is a 100 MWe plant with a storage capacity of 70 MWe for 6 hours and a load factor of 0.54. The land area required for this size and type of plant is about 1.13 sq. miles or 2.94 km². Nearly 0.9 KM² or 30 percent represents collector area. The caloria-rock thermal storage system is optimally sized for 6 hours to help smooth the energy input to the generator, therefore allowing a uniform output during the generating period.

The 92 mills/KWe HR energy cost associated with the selected 100 MWe central receiver plant is based on the total capital and annual operating costs in 1975 dollars averaged over an effective 30 year plant lifetime using 10.5 percent interest rates and a 6 percent long-term inflation factor. Details of this economic methodology are described in Ref. 3.

a. Capital costs include the direct costs of the heliostats, receiver, tower, piping, energy conversion equipment, land costs and improvements. These are summed to provide a total construction cost. Since the heliostat represents the biggest single cost, using a "high-side" of \$91.4/m² results in \$807/KWe or nearly 44 percent of the total "on-line" capital outlay of \$1843/KWe (\$184.3 million total construction cost of the 100 MWe plant with a 6 hour @ 70 MWe storage system). Based on the averaging techniques mentioned above, this represents a 43.3 mills/KWH energy cost for capital investment.

b. The variable costs associated with this plant are primarily O&M and are taken into account only after the system is in full operation. These costs include salaries, preventative and corrective maintenance, associated materials, insurance, profits and taxes. For the candidate plant, these costs total 49.1 mills/KWH or 53 percent of the total annualized life-cycle energy cost.

Advantages and Disadvantages

Most of the advantages and disadvantages of the terrestrial based solar-thermal-electrical generating plant are obvious, therefore, for sake of brevity, some of the major subjects are listed as follows.

G-10

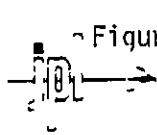


Figure XIA-1 **SUMMARY OF SOLAR THERMAL-ELECTRIC POWER PLANTS**

ORIGINAL PAGE IS OF POOR QUALITY

XI.A-3

HRS STORAGE ¹ COOLING ²	CENTRAL RECEIVER ³				DISTRIBUTED COLLECTORS									
					STEAM		CHEMICAL			SMALL HEAT ENGINE ⁷				
	0/D	6/D	6/W	12 W	SAT	SUPER	CHEM ⁵	CHEM ⁶	THERMAL	BRAYTON	STIRLING	0	6	0
RATED POWER, MWe	100	100	100	100	100	100	500	100	100	1000	1000	1000	1000	
TOTAL CONSTRUCTION COST, \$/KWe	1640	2180	1840	2450	2774	2830	2130	2420	2760	1600	2540	1260	2184	
ENERGY COST, MILLS/KWeHR	121	108	92	97	135	137	108	120	133	177	128	104	113	
LOAD FACTOR	0.39	0.54	0.54	0.69	0.54	0.54	0.54	0.54	0.54	0.39	0.54	0.39	0.54	
OVERALL EFFICIENCY, %	19.7	16.9	19.7	19.2	16.8	17.3	22	18.7	18.7	19.2	18.6	24.7	22.9	

¹HOURS OF STORAGE NORMALLY AT 70% RATED CAPACITY; CALORIA-ROCK STORAGE AT 30 \$/KWeH UNLESS NOTED

²COOLING D IS DRY AT 5 in. Hg CONDENSER DESIGN POINT
W IS WET AT 2 in. Hg CONDENSER DESIGN POINT

³HELIOSTAT COSTS 91.4 \$/M²

⁴4.2 HRS AT 100 MWe

⁵TURBINE INLET CONDITIONS ARE 1050 F, 2000 psi, STORAGE AT 100% RATED

⁶TURBINE INLET CONDITIONS ARE 950 F, 1250 psi, STORAGE AT 100% RATED

⁷REDOX BATTERY STORAGE AT 32.5 \$/KWeH AND 75% THROUGHPUT EFFICIENCY

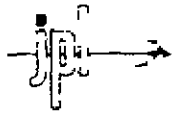
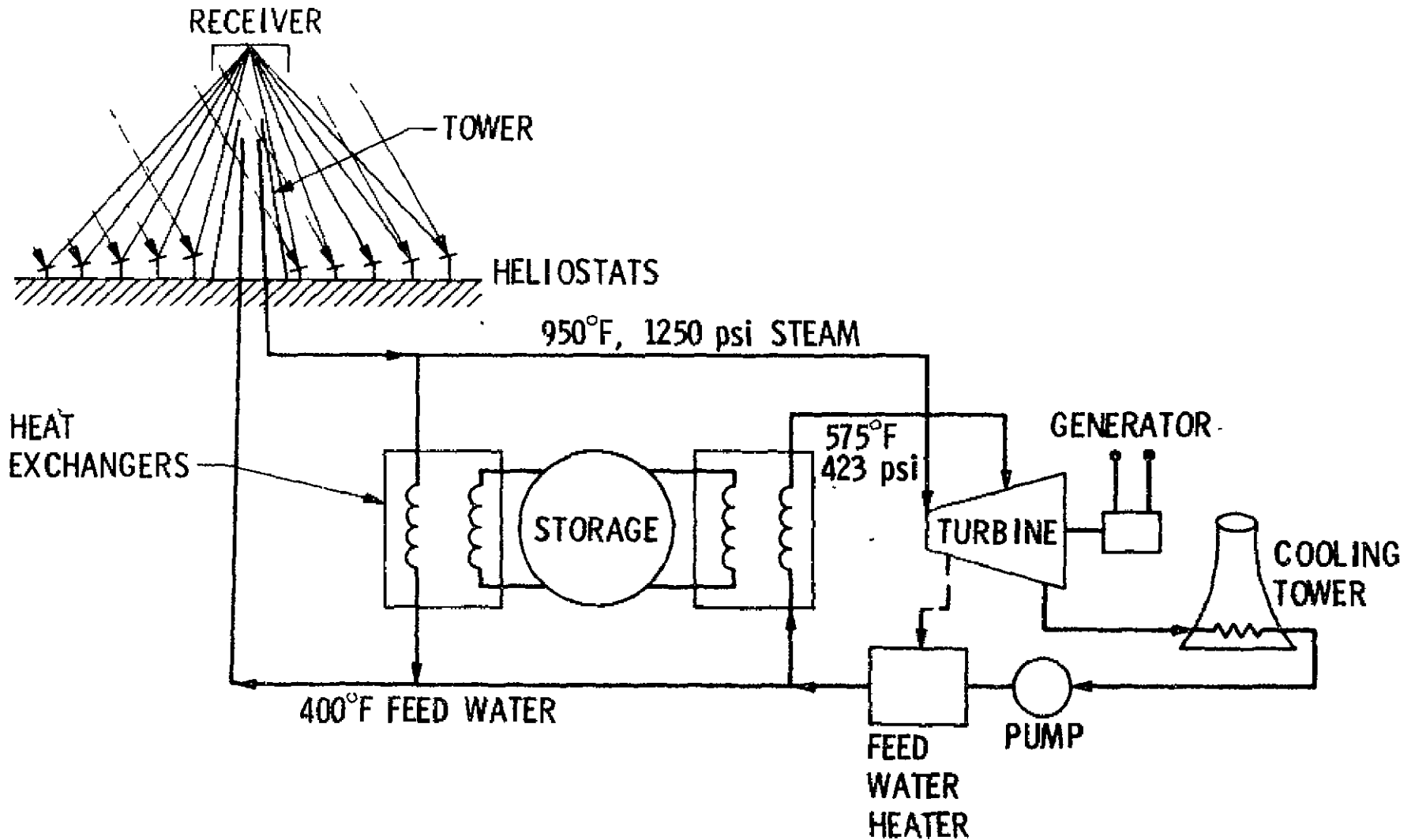


Figure XIA-2 **CENTRAL RECEIVER
SOLAR THERMAL-ELECTRIC POWER PLANT**

XI.A-4



a. Advantages:

1. Non-depletable source of energy.
2. Dependable source of energy in many locations.
3. Requires a minimum of technology advancement.
4. Non-polluting energy.

b. Disadvantages:

1. High initial costs before any return realized.
2. Intermittent power source due to day-night cycle and weather
3. Large land areas involved.
4. High solar influx and low cost land areas generally are distant from land centers.

Utilization of significant amounts of solar power through photovoltaics is a relatively recent endeavor. The production of solar cells in the U.S. started in 1957 and until the past few years, has been directed almost entirely towards our space program. About four years ago, a major effort was started to reduce the high costs associated with space requirements to provide solar cells for a wide variety of terrestrial applications. From an initial \$500/watt in 1958 to less than 10 percent of that amount currently, good progress is evident. Obviously, this level must be reduced several more factors of 10 to be competitive in the near future. Since 1971, the solar energy budget reflects the growing emphasis on this energy source and photovoltaic conversion has accounted for 15-20 percent of that total each year. Figure XIA-3 shows planning milestones for the Solar Photovoltaic Conversion (SPC) program by ERDA as presented in July 1975 at the First ERDA SPC Conference. It is apparent that this relatively young program has many alternatives to pursue, therefore listing design specifics in this briefing would be meaningless.

In 1973, representatives of the NSF/RANN photovoltaic energy conversion program presented the following estimates at the 10th IEEE Photovoltaic Specialists Conference:

"The estimated electric power cost for a 1 kw average residential photovoltaic system using \$0.50/peak watts arrays is 7¢/kwh, based on a 20-year lifetime, 14 percent overall system conversion efficiency, and a 15.5 percent cost of capital over a 20-year period. The electric power costs drop to 1.6¢/kwh with the use of \$0.1/peak watt arrays. These \$0.1/peak watt arrays are projected to produce power at 1.8¢/kwh for a 10 MW central station."

From Figure XIA-3 the \$0.50/peak watt (peak watt is the output on a clear day for a solar array normal to the incident sunlight) is projected to be feasible in 1980. This relates to 7¢/kwh or 70 mils/kwh, not a competitive energy cost in the 1980's by most projections, but possibly competitive by the year 2000. The more optimistic \$0.1/peak watt array estimated achievable by 1990 could produce power at 18 mils/kwh, a very competitive rate. Figure XIA-4 shows another evaluation of photovoltaic as performed by TRW for ERDA (Ref. 4). This, too, shows favorable competition of both solar approaches to conventional electrical power generation well before the year 2000. This analysis was based on a 30-year plant life, 13 percent investment index and a 5 percent escalation rate.

Recent efforts by JPL for ERDA using what is expected to become a standardized economic methodology as defined in Ref. 3* and the best estimates of photovoltaic near-term technology to construct a baseload electric generating plant operational in 1990 produces the following chart.

*1975 dollars, 30-year plant life, 10.5 percent interest rate and 6 percent inflation.

	FY	75	76	77	78	79	80	81	82	83	84	85
1. Systems & applicat. BG & analysis Demonstrations				Prel design spec		Detail design spec						
			45kW	170kW	285kW	600kW	1MW	2MW	4MW	7MW	10MW	
2. Low-cost silicon arrays Tech development Large-scale prod						\$5000/kW estab	\$500/kW feas demo		\$2000/kW estab		\$1000/kW estab	\$500/kW
			170kW delv	150 kW delv	270kW delv	500kW delv	1MW delv	2MW delv	3MW delv	4MW delv		
3. Concentrator systems					\$5000/kW estab		\$2000/kW estab		\$1000/kW estab			\$250/kW estab
			Test fac oper			Solar cell perf spec						
5. Research & develop							10% eff thin-film demo				\$100 to \$300/kW thin film feas demo	
				Eval tasks init	Prelim subsyst tests	Cand subsys selected		Dev & proto-test comp		Hard ware devlpd		
7. Assmt of goals							Plant ownership deter					

Source: ERDA semiannual solar photovoltaic conversion program conference proceedings July/1975

Figure XI-A-3.- Planning milestones for solar photovoltaic conversion program.

ORIGINAL PAGE IS OF POOR QUALITY

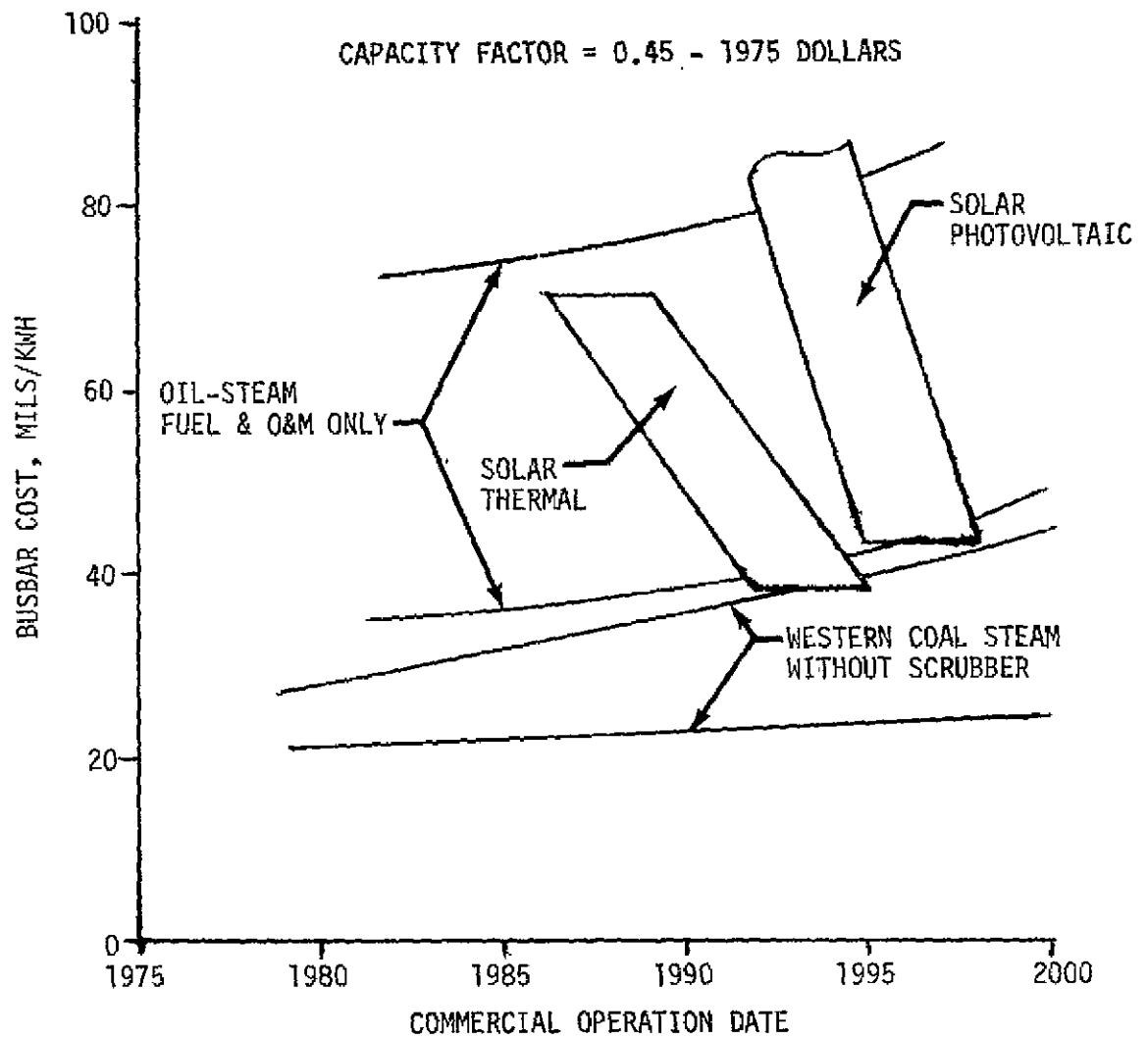


Figure XIA-4 SOLAR THERMAL & PHOTOVOLTAIC ENERGY CONVERSION PROJECTION
INTERMEDIATE PLANT OPERATION

PHOTOVOLTAIC EFFICIENCY

	<u>11 Percent</u>	<u>19 Percent</u>
HRS Storage	6	6
Rated Power, MWe	100	100
Construction Cost, \$/kwe	2130	1365
Energy Cost Mills/KW Hr.	106	72
Load Factor	0.54	0.54
Overall Efficiency	5.5	9.5

This chart is produced assuming concentration ratios of 2:1 and the basic cell efficiencies are temperature corrected. Again, it is apparent the energy cost of 72 to 106 mills/KWe HR is beyond the period's competition, but if the projected optimizations are achieved near schedule, large use of photovoltaic electric power production will closely follow. This is also the conclusion of other studies (Ref. 4).

A summary of some of the more obvious advantages and disadvantages of large scale Terrestrial Solar Photovoltaic electric power generation over other solar plants are listed below:

a. Advantages

1. Direct conversion of solar energy to electrical energy without mechanical parts.
2. No thermal heat rejection required, therefore no pollution potential.
3. Unlike most concentrator systems, solar cells work on diffused as well as direct sunlight, allowing wider use throughout the country.
4. Collectors systems are very scalable and disperse well to the energy users.

b. Disadvantages

1. Major advances in manufacturing technology necessary before cells can become competitive for large scale electrical power generation.
2. The low efficiencies dictate large land areas required for large amounts of electrical power.

In contrast to photovoltaics, solar power utilization through the harnessing of the wind's energy has been performed for many centuries. This has remained a small scale effort until the recent energy developments of the past decade, however. A variety of proposals concerning large scale electrical power generation by giant windmills have been published in the past few years. Very limited experience exists for the large units proposed in each study, however. Some operational experience exists such as that provided by European scientists on a 70 KW windmill generator capable of supplying five families with electrical power built on the German island of Sylt in 1973, another 70 KW windmill erected in 1942 at Gedser, Denmark and the huge 1250 KW prototype built near Rutland, Vermont in 1941-45. It was estimated that production models of that power plant would have cost \$191/KW in 1945 compared to \$125/KW for conventional plants, so the project was terminated. A number of federal agencies have granted contracts for windmill research. The NASA and NSF have invested nearly one million dollars for construction (recently completed) of a 100 KW windmill generator near Sandusky, Ohio. This initial system will test components and subsystems and will be used to collect performance data to aid in designing other wind generators of many sizes.

Consistent with establishing performance data of large wind-driven electrical generators, a recently completed study by Lockheed Aircraft Corporation has been presented showing logical locations for large numbers of the wind turbines throughout the United States. Surveying long-term weather reports from 768 weather stations, the team concluded that 20,000 square miles of open land was available with sufficient wind velocities. An average wind velocity of 12 mph is considered a practical minimum. The best areas in the country for windpower are the Pacific northwest, the southwest, the Great Plains and the northeast.

Since the tapping of this energy source in major quantities is only recently receiving major emphasis in this country, optimizing experience and therefore the discussion of definite design alternatives are premature at this time.

Most economic analyses dealing with large scale use of wind power have been very superficial. More rigorous studies funded by ERDA are in work. The preliminary results of one ERDA funded study by TRW are shown in Figure XIA-5. The fuel saver mode presented indicates no storage is involved. Storage could be added to a wind conversion plant to replace intermediate plants, however, statistics for calm intervals are not yet compiled, making design difficult. Valid conclusions are apparent from the information presented, nevertheless. Using the 18 mph design wind plant shown, it can be seen that a site with only 60 days of appropriate wind is needed to best the oil/steam generation plant and 110 days to be advantageous over the midwest coal/steam conventional plants. The cost balance shifts increasingly in favor of wind conversion with time, since fossil fuel costs escalate in real dollars in most economic projections.

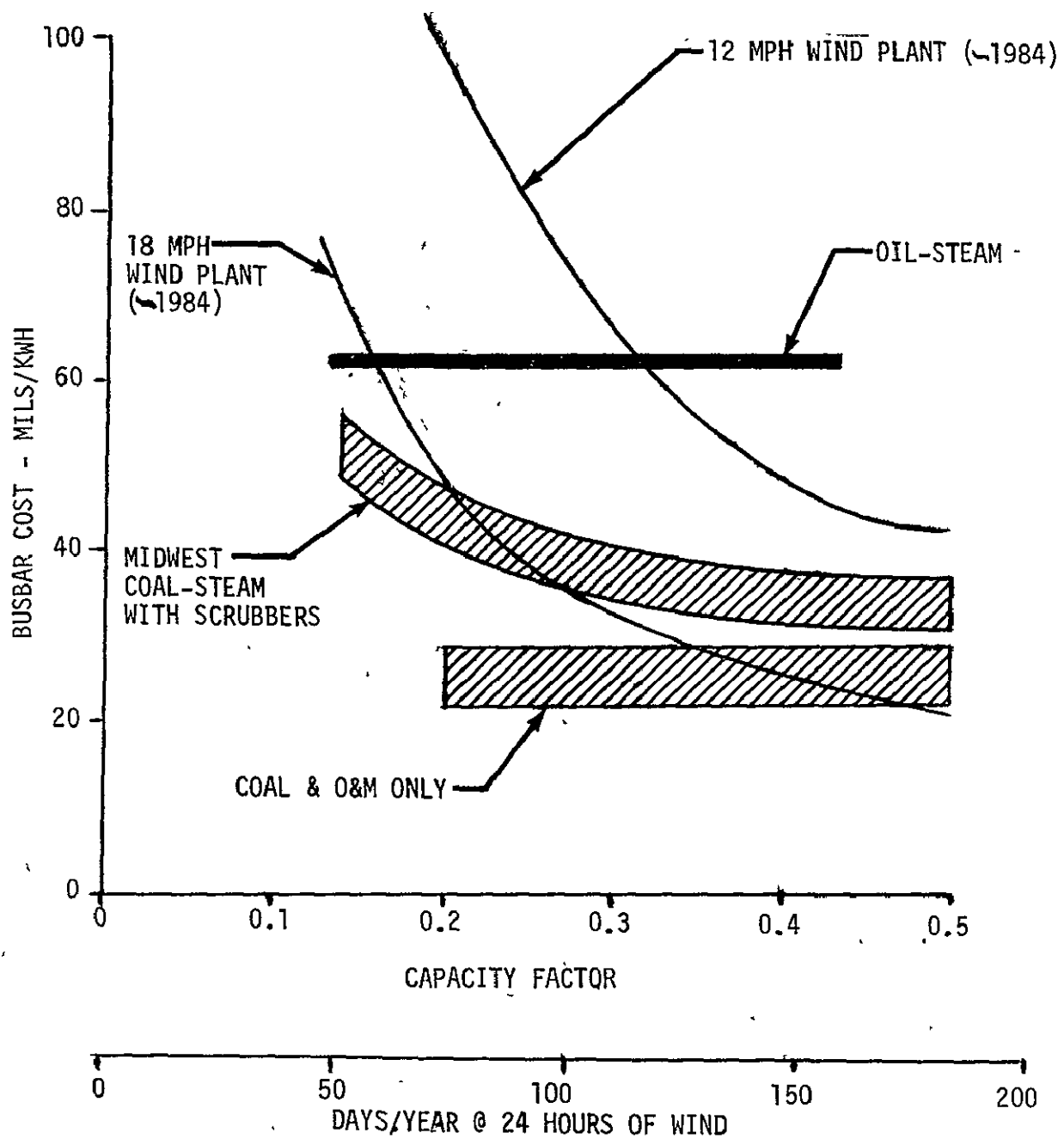


Figure XIA-5 WIND ENERGY CONVERSION COST COMPARISON
FUEL SAVER MODE

Some of the major considerations for implementation of wind conversion systems over other solar powered systems are listed below;

a. Advantages

1. Wind-powered systems produce no air or water pollution and little noise.
2. Adapts to mechanical storage systems such as flywheels, compressed air and pumped storage.
3. Wind power is frequently available throughout the 24-hour period while direct solar energy is limited to daytime.
4. With mass production, construction time should be much quicker to bring wind power on-line than conventional and other solar energy types.

b. Disadvantages

1. Changing weather patterns, both short and long term, limit wind powerplants in base and intermediate load modes.
2. Only very large structures will be practical since (a.) wind velocity is diminished within about 200 feet of the ground, (b.) terrain roughness causes turbulence resulting in nonuniformity of performance and (c.) rotor power output is not only a function of the wind velocity, but of the rotor's airstream diameter.
3. Size limits location.

Investigation into the ocean thermal gradient as a potential electrical energy source is only at a feasibility study stage, no prototypes are near detail design stage, let alone construction. Although the theoretical aspects of this power source may not provide major drawbacks to this constant energy source, the design uniqueness does. The systems major components are a cold water pipe which brings cold water up from the ocean depths to cool the working fluid in a condensing heat exchanger and boiler feed pumps. The much warmer, near surface water, warms the working fluid to the boiler heat exchanger, turbine and generator set. The entire system must be constructed on a floating platform and, despite major improvements in underwater and off-shore technology, many areas must be greatly advanced for this application. The relatively low temperature differences involved dictate low Carnot efficiencies, therefore the equipment such as transfer pipe, heat exchangers and turbines must be huge and the flow rates extremely large in order to reach an economical output.

Assuming the ocean thermal plant can achieve the very preliminary estimates of cost, schedule and reliability goals set by ERDA, a TRW study shown in Figure XIA-6 compares the energy production cost of several conventional plants and an ocean thermal plant, all used for base load operation. Based on 1975 dollars, 13 percent investment index, 5 percent escalation and a 30-year plant life, it can be seen that the ocean thermal system is competitive with the coal-steam and light water reactors by 1990. The high capacity factor (0.85) assigned the ocean thermal points out the expected high utilization of the system.

Obviously, the major advantage of any solar energy system is its utilization of a free, nondepletable source of energy. Some major advantages and disadvantages of the ocean thermal system compared to the solar terrestrial systems are listed below:

a. Advantages

1. Not dependent on daylight hours
2. Many locations provide minimum seasonal effects
3. Locations do not require land investments
4. No pollution

b. Disadvantages

1. Large depths for workable temperature differences
2. Large equipment sizes
3. Off-shore construction handicap
4. Transmission distances significant
5. Location and operation may be under maritime law jurisdiction

CAPACITY FACTOR = 0.70 EXCEPT OCEAN THERMAL = 0.85
1975 DOLLARS

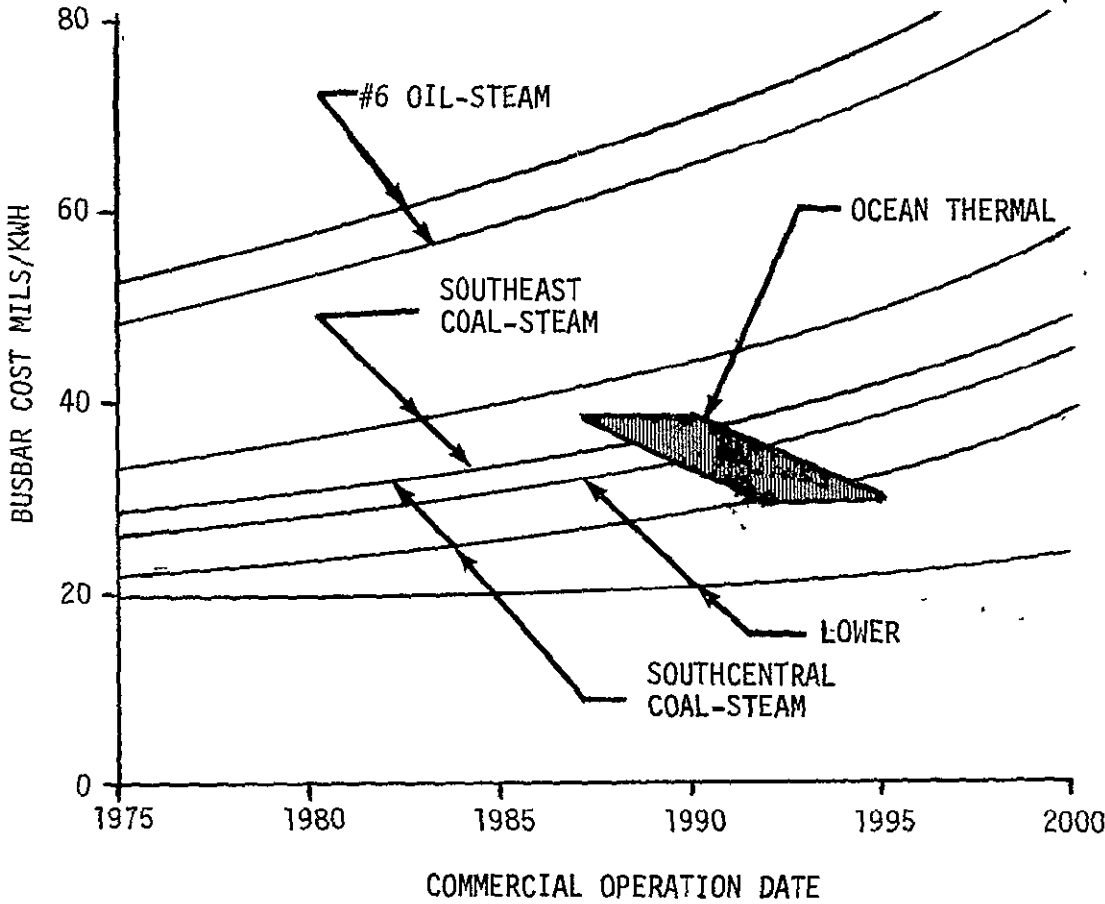


Figure XIA-6 OCEAN THERMAL GRADIENT ENERGY CONVERSION PROJECTION
BASE PLANT OPERATION

REFERENCES

1. Solar Energy - Rau
2. Comparative Assessment of Orbital and Terrestrial Central Power Systems - Program Review published March 1976 - JPL
3. Baseline Economic Analysis for Solar and Conventional Control Power plants - 900-727 November 1975 - JPL
4. Solar Energy Options for Electrical Utilities - April 1976 - TRW
5. "Preliminary Technology Assessment Satellite Power System Concepts," William B. Lenoir and Roy E. Currie, Jr., February 1975.

Cost Sensitivity Analysis

In order to evaluate the sensitivity of various parameters upon the SPS cost, a set of cost equations were used as presented in a Lewis Research Center in-house study based on concepts developed by Raytheon. The electric generation cost equations were taken from Reference 5. The cost equations and various parameters required in the calculations are defined as follows:

Total Capital Cost per Satellite Power System

$$\text{Cost} = C_{bs} + C_{wg} + C_t + C_{pc} + C_{at} + C_{rec} + C_{pwr} + C_{atpwr} \\ + C_{xmtdis} + C_{gnddis} + C_{xcmd}$$

The component costs are specified in the following:

COST EQUATIONS

1. Backup Structure Cost, C_{bs} (Antenna Support Structure)

$$C_{bs} = UC_{bs} \cdot UW_{bs} \cdot A_t + W_{jt} \cdot UC_{bs}$$

Where:

UC_{bs} = Cost of backup structure, \$/kg

UW_{bs} = Weight of backup structure, kg/m²

A_t = Area of transmittal antenna, m²

W_{jt} = Total weight of rotary joint, kg

2. Waveguide Cost, C_{wg}

$$C_{wg} = UC_{wg} \cdot A_t$$

Where:

UC_{wg} = Unit cost of waveguide, \$/m²

3. DC-RF Converter Cost, C_t

$$C_t = UC_t \cdot P_{rdc} / (N_r \cdot N_{rf} \cdot N_{bm})$$

Where:

UC_t = Unit cost of converter, \$/kw

P_{rdc} = Total delivered ground power, kw

N_r = Rectenna collection and conversion efficiency

N_{rf} = R_f link efficiency including effects of atmosphere, scattering losses, and pointing errors.

N_{bm} = Beam efficiency or fraction of available power intercepted by rectenna.

4. Phase Control Cost, C_{pc}

$$C_{pc} = UC_{pc} \cdot A_t/A_{sae}$$

Where:

UC_{pc} = Unit cost of phase control, \$/subarray

A_{sae} = Area of electrical subarray

5. Pointing Control Cost, C_{pt}

$$C_{pt} = UC_{pt} \cdot A_t/A_{sam}$$

Where:

UC_{pt} = Unit Cost of pointing, \$/subarray

A_{sam} = Area of mechanical subarray

6. Assembly and Transportation of Transmitting Antenna, C_{at}

$$C_{at} = (UC_{to} + UC_{tg} + UC_a + UC_{tl}) + W_{mpts}$$

Where:

UC_{to} = Unit cost of transport to LEO, \$/kg

UC_{tg} = Unit cost of transport to GEO, \$/kg

UC_a = Unit orbital assembly cost, \$/kg

UC_{tl} = Unit land transport cost, \$/kg

W_{mpts} = Total system weight, kg

$$W_{mpts} = W_{bs} + W_{wg} + W_t + W_{pc} + W_{pt} + W_{xmtdis} + W_{xcmd}$$

Where:

$W_{bs} = U_{wbs} \cdot A_t + W_{jt}$ (backup structure weight)

$W_{wg} = UW_{wg} \cdot A_t$ (waveguide weight)

$W_{pc} = UW_{pc} \cdot A_t/A_{sae}$ (phase control weight)

$W_{pt} = UW_{pt} \cdot A_t/A_{sam}$ (pointing control weight)

$W_{xmtdis} = UW_{xmtdis} \cdot \sqrt{P_{rdc}/N_{dc}}$ (distribution system weight)

$W_t = UW_t \cdot P_{rdc}/(N_r N_{rf} N_{bm})$ (converter weight)

W_{xcmd} = total weight of transmitter command control system, kg

and:

UW_{wg} = Unit weight of waveguide, kg/m^2

UW_{pc} = Unit weight of phase control system, $kg/subarray$

UW_{pt} = Unit weight of pointing control, $kg/subarray$

UW_{xmtdis} = Coefficient of distribution system weight, $kg/(kw)^{1/2}$

UW_t = Unit weight of converter, kg/kw

N_{dc} = DC-DC system efficiency

7. Rectenna Cost, C_{rec}

$$C_{rec} = UC_{rec} \cdot A_r + UC_{prep} \cdot A_r / S_{in} \emptyset + (4/\pi) \cdot UC_{1nd} \cdot A_r \cdot (SLR)^2 / S_{in} \emptyset + C_{gcmd}$$

Where:

UC_{rec} = Unit cost of rectenna, $$/m^2$

A_r = Beam area normal to beam axis at receiving site, m^2

UC_{prep} = Unit preparation cost of land, $$/m^2$

\emptyset = Incidence angle of beam, degrees

UC_{1nd} = Unit cost of land, $$/m^2$

S_{1r} = Ratio of fence diameter to rectenna diameter

C_{gcmd} = Cost of ground command and pilot signal microwave system

8. Prime Power System Cost, C_{pwr}

$$C_{pwr} = UC_{pwr} \cdot P_{rdc} / N_{dc}$$

Where:

UC_{pwr} = Unit cost of prime power, $$/kw$

9. Assembly and transport of prime power, CAT_{pwr}

$$CAT_{pwr} = (UC_{to} + UC_{tg} + UC_a + UC_{tl}) \cdot UW_{pwr} \cdot P_{rdc} / N_{dc}$$

Where:

UW_{pwr} = Unit weight of prime power, kg/kw

10. DC Distribution on Transmitting Antenna Cost, C_{xmtdis}

$$C_{xmtdis} = UC_{xmtdis} \cdot \sqrt{P_{rdc} / N_{dc}}$$

Where:

UC_{xmtdis} = coefficient of distribution system cost $$/ (kw)^{1/2}$

11. DC Collection and Conversion at Rectenna Cost, C_{gnddis}

$$C_{gnddis} = UC_{gnddis} \cdot \sqrt{P_{rdc}}$$

Where:

$$UC_{gnddis} = \text{unit cost of distribution system, } \$/(\text{kw})^{1/2}$$

12. Transmitter Command Control System Cost, C_{xcmd}

Electric Generation Cost, m , (mills/kwh)

$$m = (C \cdot \frac{P_e}{E} + N) \times 1000$$

Where:

$$P_e = (1 + i)^{n-1} \cdot \text{Cost}$$

P_e is the effective total capital cost of plant at start of operation and includes effects of interest, cost of capital during construction, n years, and assumes uniform payments of cost/ n per year during construction.

Cost = Total Capital Cost of Plant

E = Nominal kwh/year to busbar

N = Annual operating costs

i = Interest rate during construction

$$c = \frac{r}{1 - \frac{(1)}{1+r} y} \quad (\text{Capitalization Factor})$$

r = Required rate of return for interest, taxes and insurance

y = Plant lifetime, years

A key parameter for SPS implementation is the length of time to construct the satellite and make it operational. The proposed implementation scenarios allow one year for construction of a satellite; however, as more information becomes available on construction in space, this time may expand. Figure XIB-1 illustrates the effect of length of construction time on electric generation cost as a function of transportation and assembly cost. As an example, the cost of electrical power generation increases from 28 mils/kwh for a one year construction period to 40 mils/kwh for 5 years. This data was for transportation cost of \$100/kg and prime power cost of \$300/kw. The conclusion is that maintaining the construction period at one year is a considerable cost saving.

The prime power system cost sensitivity was evaluated up to \$500/kw. The increase in electric generation cost was linear and ranged from 15 mils/kwh at \$50/kw to 31 mils/kwh at \$500/kw for a \$60/kg transportation cost. Similar trends for \$100/kg and \$250/kg are shown in Figure XIB-2.

The electric generation costs for SPS, with no transportation and assembly costs included, are shown in Figure XIB-3 as a function of prime power cost. The generation cost ranges from 9 mils/kwh to 24 mils/kwh as prime power cost varies from \$50/kw to \$500/kw. Using the data of Figures XIB-3 and XIB-4 the equations are derived for electric generation cost:

Definitions:

- MILS_b = Electric Generation Cost (Baseline Weight), MILS/kwh
- MILS_g = Electric Generation Cost (50% Weight Growth), MILS/kwh
- C_b = Electric Generation (No Transportation Cost), MILS/kwh
- TRAN = Transportation Cost, \$/kg
- MILS_b = (.105) TRAN + C
- MILS_g = (.158) TRAN + C

The equations can be used as in the following example:

- Assume transportation cost \$100/kg
- Assume prime power cost \$300/kg
- From Fig. Prime Power Cost, C = 17.5
- MILS_b = (.105) (100) + 17.5 = 28 mils/kwh
- MILS_g = (.158) (100) + 17.5 = 33.3 mils/kwh

The required rate of return for taxes, interest, and insurance was varied up to 20 percent to assess its significance upon the electric generation cost. The transportation cost was held constant at \$100/kg and

prime power cost was \$300/kw. The electric generation cost increased from 12 mils/kwh at 5 percent to 36.4 mils/kwh at 20 percent, an increase of 200 percent. As shown in Figure XIB-5 the critical nature of ownership upon this rate of return value and hence the cost of electricity is immediately apparent and must be addressed to assure the most economically sound approach to the problem.

Plant factor was varied from 80 to 100 percent fixed transportation cost of \$100/kg and prime power cost of \$300/kw. The resulting electric generation cost is shown in Figure XIB-6. If the plant factor is reduced from 100 to 80 percent, the generation cost is increased by 25 percent.

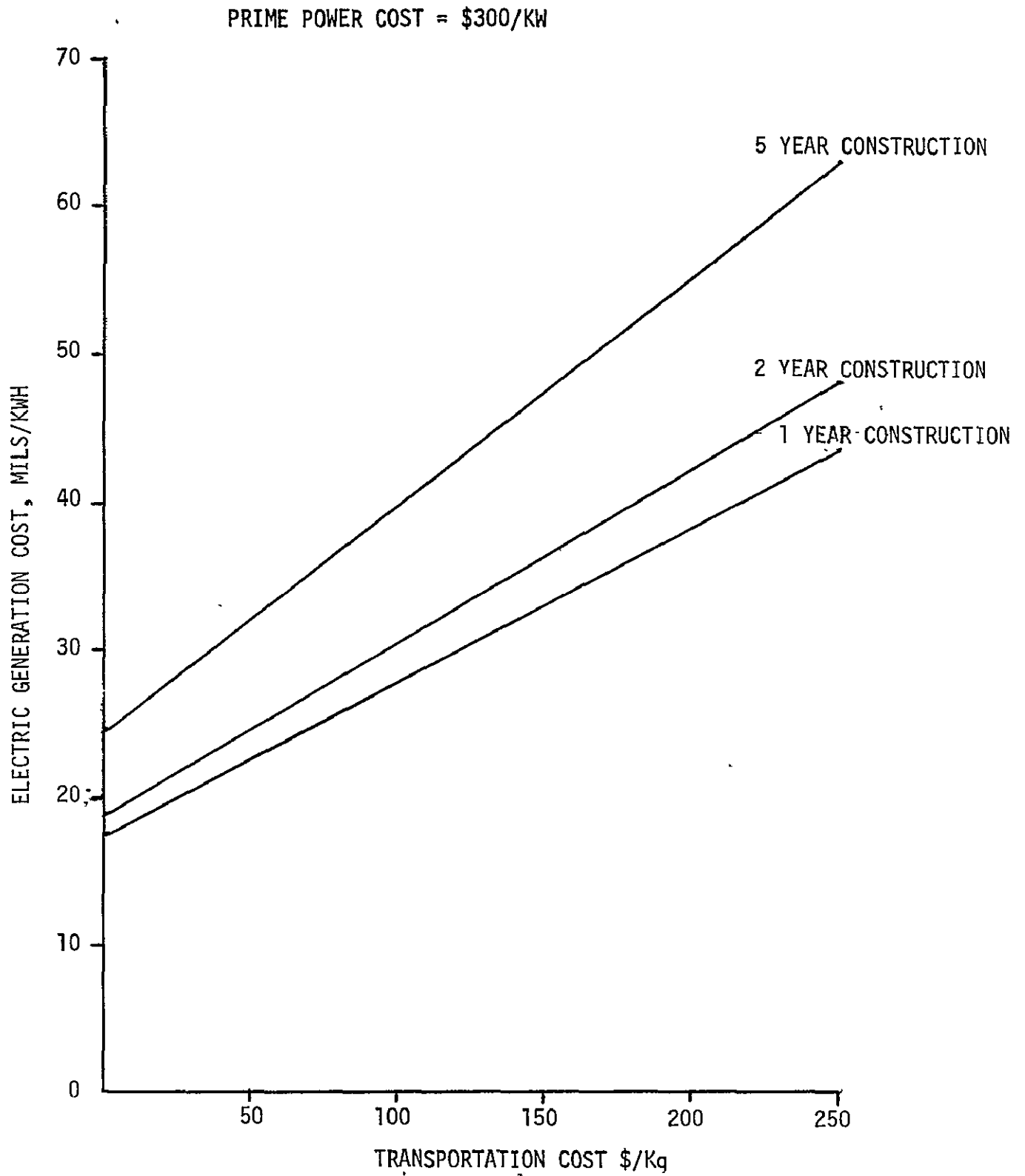


Figure XIB-1 EFFECT OF CONSTRUCTION TIME ON ELECTRICAL GENERATION COST

1 YEAR CONSTRUCTION

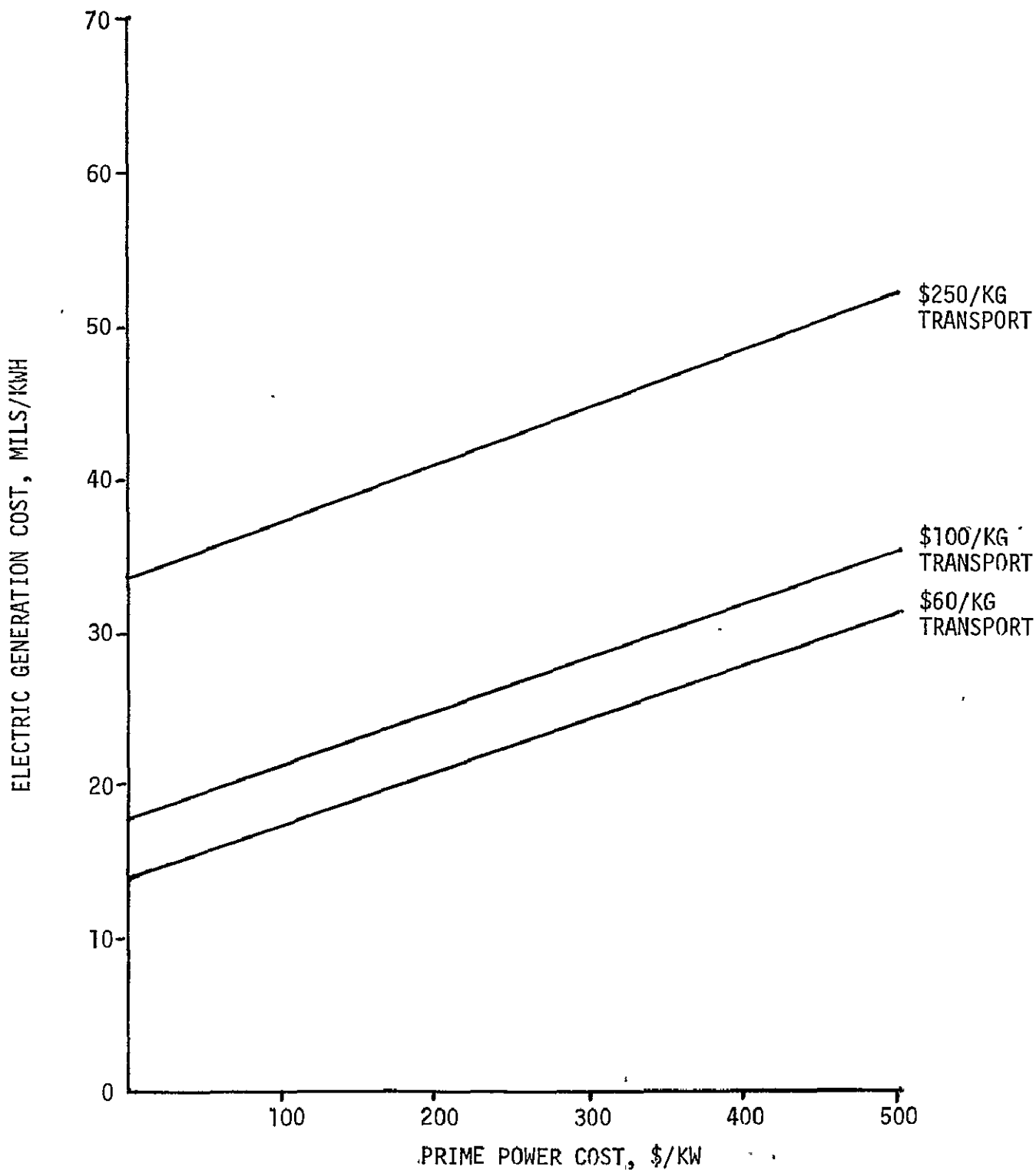


Figure XIB-2 EFFECT OF PRIME POWER SYSTEM COST ON ELECTRIC GENERATION COST FOR VARIATIONS IN TRANSPORTATION AND ASSEMBLY COST

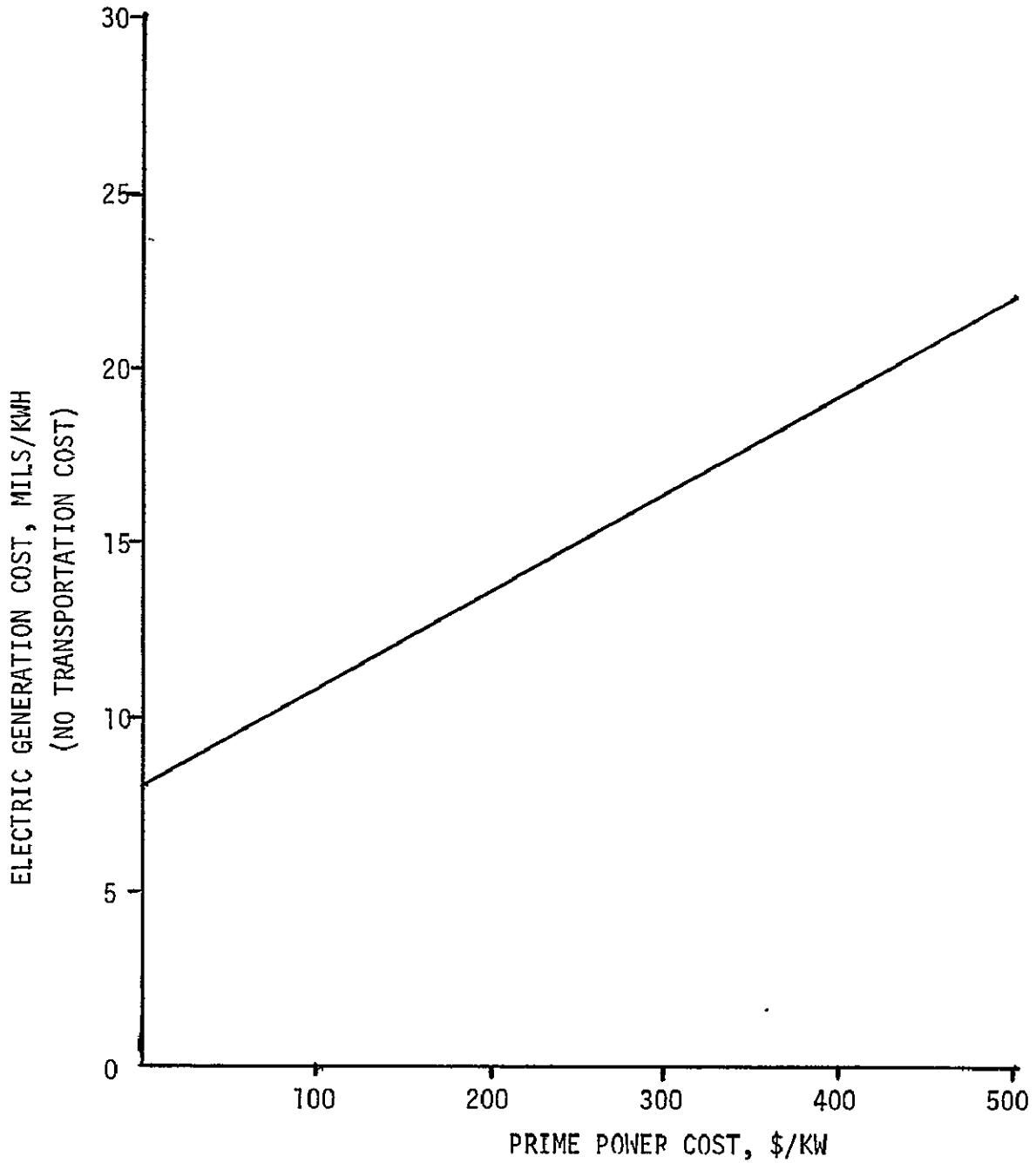


Figure XIB-3 EFFECT OF PRIME POWER COST ON ELECTRIC GENERATION COST, WITH NO TRANSPORTATION AND ASSEMBLY COST

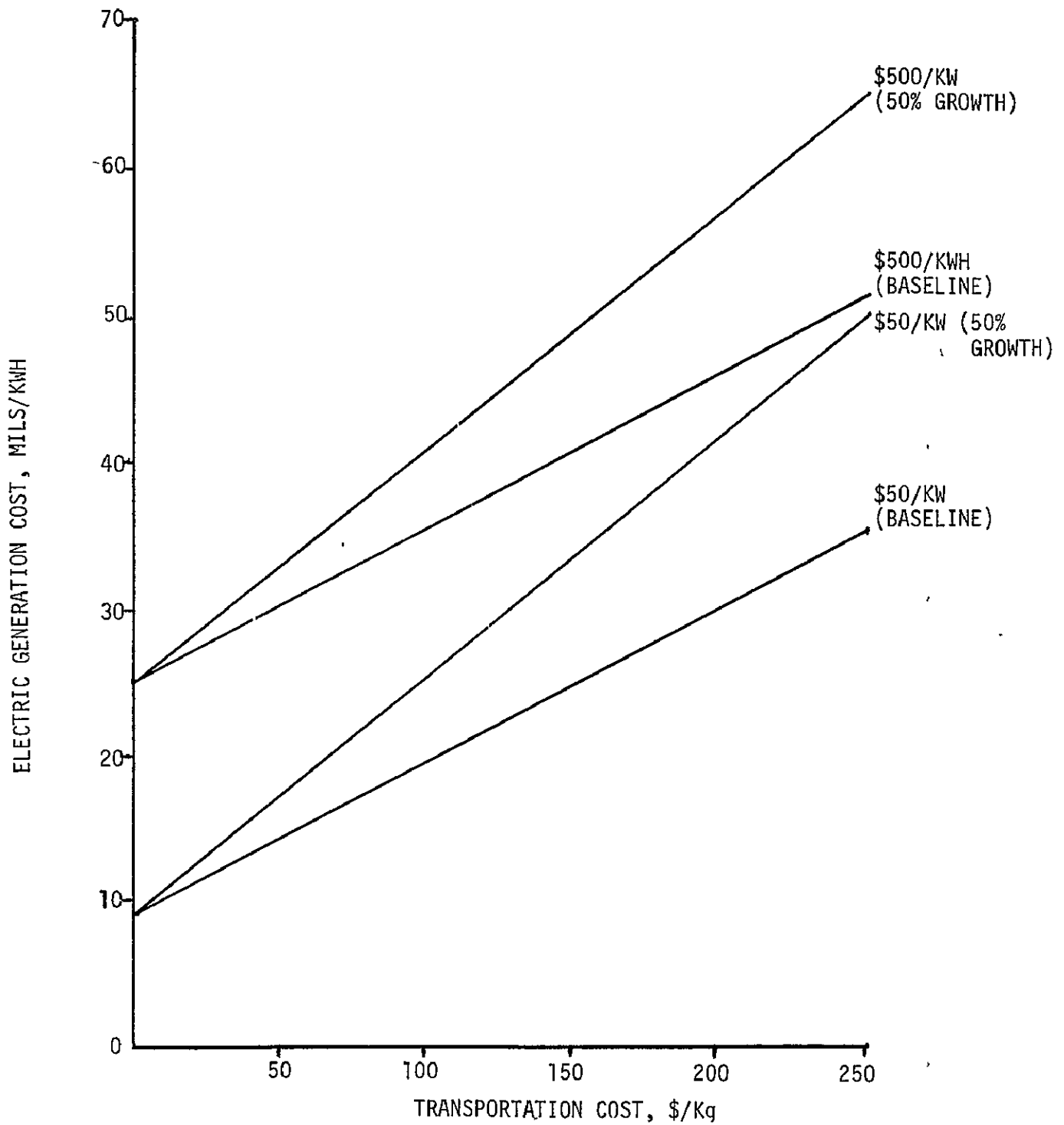


Figure XIB-4 ELECTRIC GENERATION COST FOR VARIATIONS IN PRIME POWER COST, SYSTEM WEIGHT AND TRANSPORTATION COST

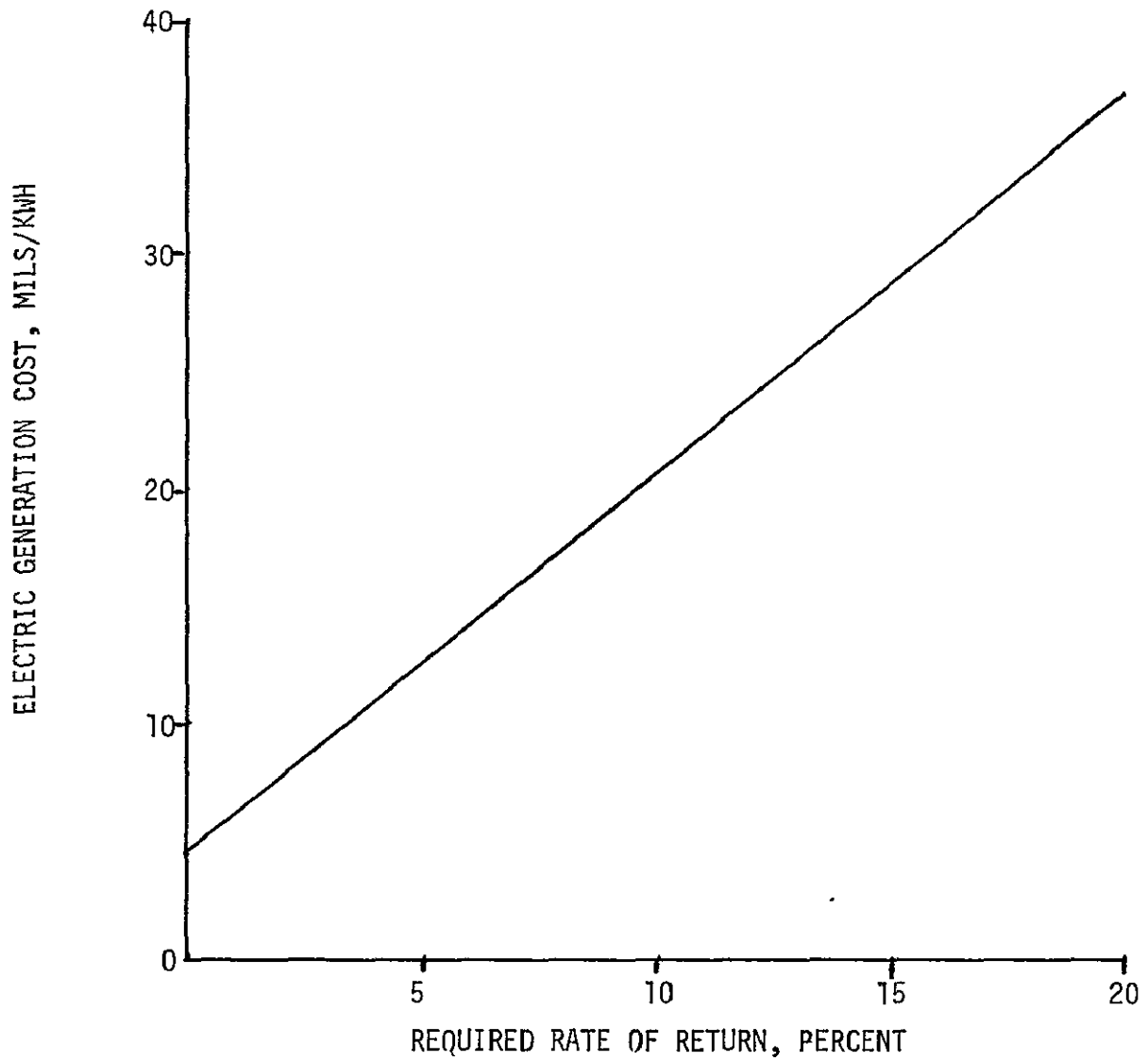


Figure XIB-5 ELECTRIC GENERATION COST AS A FUNCTION OF REQUIRED RATE OF RETURN

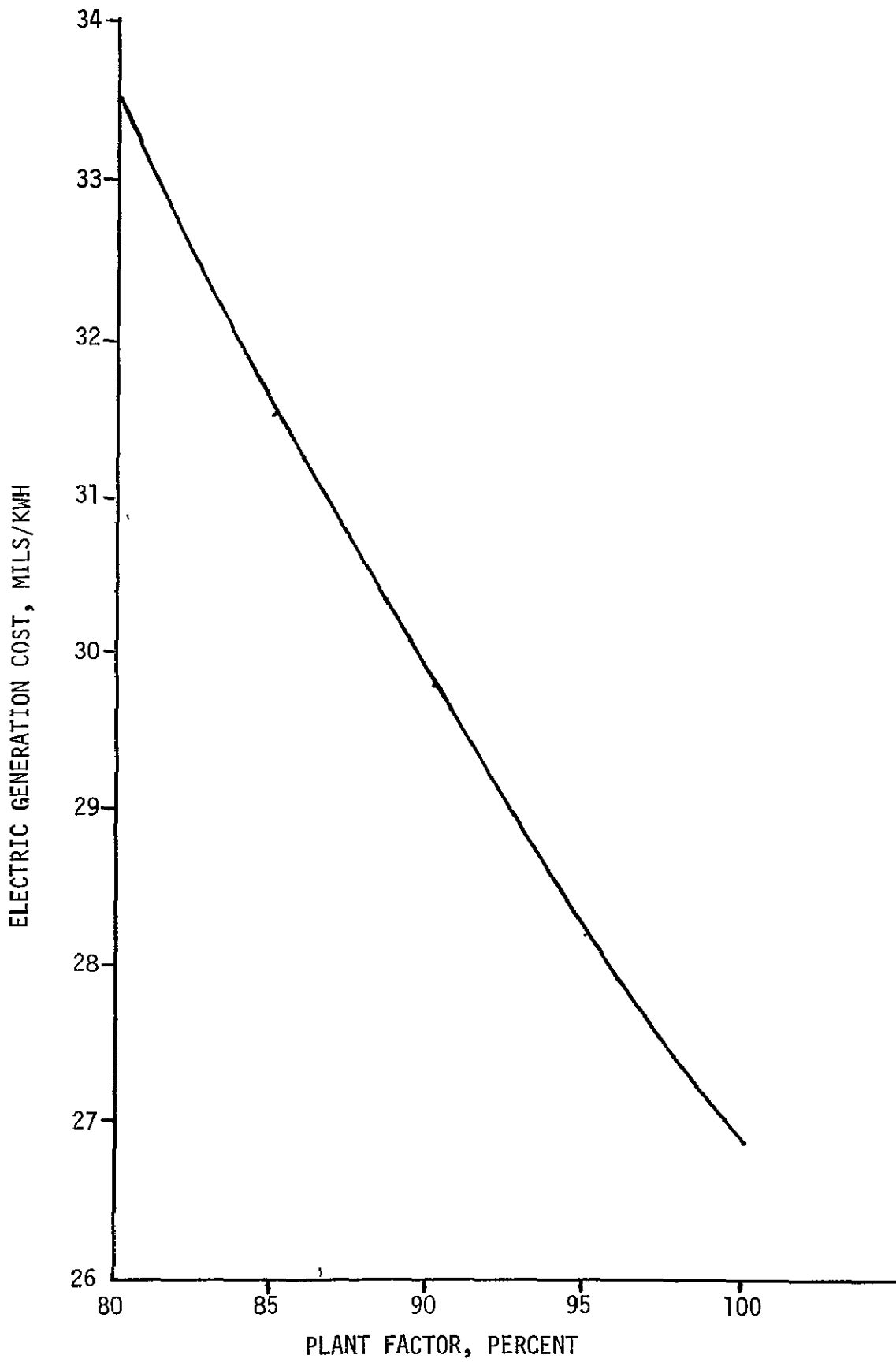


Figure XIB-6 ELECTRIC GENERATION COST AS A FUNCTION OF PLANT FACTOR